Apêndice E

Dados Geotécnicos e Interpretação das Investigações de Campo e Laboratório

Dezembro de 2019

A versão oficial deste Apêndice é a versão em língua inglesa. Em caso de qualquer contradição ou divergência de interpretação entre a versão traduzida e a versão em língua inglesa deste Apêndice, prevalecerá a versão em língua inglesa.

ÍNDICE

1 INTRODUÇÃO 1
1.1 Geral 1
1.2 Resumo das Constatações 1
2 PROGRAMA 1 – PROGRAMA DE AMOSTRAGEM A GRANEL 2
2.1 Locais de Amostragem a Granel 2
3 PROGRAMA 2 – PROGRAMA DE INVESTIGAÇÃO DE CAMPO 8
3.1 Escopo da Investigação de Campo 8
3.2 Ensaio de Permeâmetro de Guelph 9
3.3 Ensaios de Tensiômetro 10
3.4 Ensaios de Densidade por Cone de Areia 11
3.5 Monitoramento do Fluxo através do Vale Atual 12
3.6 Sondagem e Amostragem dos Solos da Fundação 14
4 ENSAIOS DE ÍNDICES FÍSICOS EM LABORATÓRIO 15
4.1 Escopo 15
4.2 Granulometria 15
4.3 Gravidade específica 19
4.4 Teor de umidade 19
4.5 Limites de Atterberg 20
4.6 Difração de Raios-X 21
4.7 Microscópio Eletrônico de Varredura 23
4.8 Ensaios Adicionais de MEV 24
4.9 Curvas Características de Água no Solo 25
5 ENSAIOS AVANÇADOS DE LABORATÓRIO 26
5.1 Amostras Reconstituídas 26
5.2 Ensaio de compressão triaxial 27
5.2.1 Escopo 27
5.2.2 Procedimento para Ensaio Triaxial Padrão com Deformação Controlada 28
5.2.3 Procedimento para Ensaio Triaxial com Carga Controlada 29
5.2.4 Resultados dos Ensaios Padrão com Deformação Controlada, CID, CIU, e CAU 31
5.2.5 Resultadosdos Ensaios Com Carga Controlada 42
5.2.6 Resultados do Ensaio com Carga Controlada com *Creep* 42
5.3 Ensaio com *Bender Element* 47
5.3.1 Escopo 47
5.3.2 Procedimento 47

5.3.3 Resultados 48
5.4 Ensaios de Cisalhamento Direto Simples 50
5.4.1 Escopo 50
5.4.2 Procedimento 50
5.4.3 Resultados dos Ensaios 50
6 PARÂMETROS DOS ENSAIOS DE CAMPO E DE LABORATÓRIO USADOS NA ANÁLISE DE DEFORMAÇÃO 54
6.1 Geral 54
6.2 Dados de Entrada do Modelo Mohr-Coulomb 55
6.2.1 Parâmetros Drenados 55
6.3 Parâmetros para S*train-Weakening* 57
6.3.1 Parâmetros drenados 57
6.3.2 Parâmetros não drenados 59
6.4 Dados de Entrada do Modelo de Estado Crítico 63
6.4.1 Parâmetro de Acoplamento Volumétrico, N 63
6.4.2 Parâmetro de Dilatação, χ_{tc} 63
6.4.3 Elasticidade, G_{max} 65
6.4.4 Endurecimento, H0, Hψ 66
6.5 Parâmetro de Estado 67
6.6 Resumo dos Parâmetros 67
7 INTERPRETAÇÃO DOS DADOS DE ENSAIOS CPTU E V_S 68
7.1 Geral 68
7.2 Processamento dos Dados dos Ensaios de CPTu 69
7.3 Delineamento de Rejeitos 70
7.4 Estimativa de Resistência de Pico e Liquefeita Usando Dados de Ensaios de CPTu 70
7.5 Estimativa de Parâmetros de Estado Usando Dados dos Ensaios de CPTu 71
7.5.1 Método Robertson (2009) 72
7.5.2 Método de Plewes et al. (1992) 72
7.5.3 Método de expansão da cavidade – Jefferies e Been (2016) 73
7.5.4 Resultados 73
7.6 Avaliação da Cimentação a Partir dos Dados de Ensaios de CPTu 75
7.7 Comparação de Dados de Ensaios de CPTu e Dados de Ensaios de FVT 76

LISTA DE FIGURAS

Figura 1: Vista de locais de amostragem sobrepostos em uma imagem pré-rompimento da Barragem I 4
Figura 2: Vista de locais de amostragem sobrepostos em uma imagem pós-rompimento da Barragem I 4

Figura 3: Lamas amostradas no local S1 5
Figura 4: Lamas amostradas no local S2 5
Figura 5: Rejeitos grossos amostrados no local S6a (imagem à esquerda) e S6b (imagem à direita) 6
Figura 6: Exemplo de camadas observadas em rejeitos grossos 6
Figura 7: Solo residual compactado amostrado no local S7 7
Figura 8: Curvas granulométricas de amostras de rejeitos grossos 16
Figura 9: Curvas granulométricasde amostras de rejeitos finos 16
Figura 10: Curvas granulométricasde amostras de lamas 17
Figura 11: Curvas granulométricasde aterros de berma compactados (solo residual) 17
Figura 12: Curvas granulométricasde aterros de berma compactados (rejeitos) 18
Figura 13: Curvas granulométricasde amostras de solo residual 18
Figura 14: Imagem de MEV da amostra 1, saco 2 (lamas), passante pela peneira nº 200 23
Figura 15: Imagem de MEV da amostra 3, saco 2 (rejeitos grossos), retida na peneira nº 40 24
Figura 16: Imagem de MEV de amostra de rejeitos grossos mostrando aderência de óxido de ferro 25
Figura 17: Gradações reconstituídas de rejeitos finos, grossos e médios 27
Figura 18: Configuração do ensaio triaxial: (a) Pedra porosa modificada; (b) Colocação da amostra por compactação úmida, (c) Configuração final da amostra 29
Figura 19: Curvas CSL de todas as três gradações de rejeitos testadas 32
Figura 20: Gráfico de CSL para gradações de rejeitos médios testadas 33
Figura 21: Gráfico de CSL para gradações de rejeitos grossos testadas 34
Figura 22: Gráfico de CSL para gradações de rejeitos finos testadas 35
Figura 23: Trajetórias de tensão nos ensaios CID e CIU nas gradações de rejeitos médios 37
Figura 24: Trajetórias de tensão nos ensaios CID e CIU nas gradações de rejeitos grossos 38
Figura 25: Trajetórias de tensão nos ensaios CID e CIU nas gradações de rejeitos finos 39
Figura 26: Resultados de ensaios triaxiais anisotrópicos não drenados com deformação controlada (CAU, $K_0 = 0,5$) 41

Figura 27: Comparação de TX14 e TXDW01 43

Figura 28: Comparação dos resultados dos ensaios triaxiais com deformação controlada e carga controlada 44

Figura 29: Resultados do ensaio CAU com carga controlada(TXDW03) – K_0 = 0,5 e 0,4 ... 45

Figura 30: Resultados do ensaio CAU com carga controlada (TXDW03) – K_0 = 0,4 para 0,3 46

Figura 31: Relações de velocidade de onda de cisalhamento normalizada versus índice de vazios para: a) todos os dados, b) gradações médias e grossas e c) gradação fina 49

Figura 32: Resultados dos ensaios de DSS (DSS01) – Material da fundação do solo residual 53

Figura 33: Relação entre o módulo volumétrico (K) e o parâmetro de estado (ψ) 56

Figura 34: Relação entre o módulo de cisalhamento (G) e o parâmetro de estado (ψ) para análise drenada 56

Figura 35: Relação entre o ângulo de atrito de pico e o parâmetro de estado (ψ) para análise drenada 57

Figura 36: Relação entre deformação específica plástica com perda de resistência pós-pico ($\varepsilon_{P\text{-}SL}$) e parâmetro de estado (ψ) para análise drenada 58

Figura 37: Relação entre deformação específica plástica à resistência residual (ε_{P-R}) e parâmetro de estado (ψ) para análise drenada 59

Figura 38: Relação entre módulo de cisalhamento (G) e parâmetro de estado (ψ) para análise não drenada 60

Figura 39: Relação entre Su (pico)/*p'* e parâmetro de estado (ψ) para análise não drenada .. 60

Figura 40: Relação entre Su (residual)/*p'* e parâmetro de estado (ψ)para análise não drenada 61

Figura 41: Relação entre deformação específica plástica com perda de resistência pós-pico ($\varepsilon_{P\text{-}SL}$) e parâmetro de estado (ψ) para análise não drenada 62

Figura 42: Relação entre deformação específica plástica e resistência residual (ε_{P-R}) e parâmetro de estado (ψ) para análise não drenada 62

Figura 43: Dilatação – Relação da razão de tensão para a gradação de rejeitos médios 63

Figura 44: Dilatação – Relação de parâmetros de estado para gradações de rejeitos médios 64

Figura 45: Comparação de curvas de tensão-deformação de amostras testadas com a mesma tensão efetiva média, mas com estados cada vez mais densos 65
Figura 46: Tendência de G_{max} dos dados do dilatômetro sísmico (V_s) 66
Figura 47: Planta de localização dos ensaios de CPTu 69
Figura 48: Distribuição de parâmetros de estado (ψ) para rejeitos grossos 74
Figura 49: Distribuição de parâmetros de estado (ψ) para rejeitos finos 74
Figura 50: Gráfico Q_{tn} vs I_G para identificar solos com microestrutura 76
Figura 51: Resultado do ensaio de FVT – VT-16-11 (profundidade 22,5 m) 77
Figura 52: Resultado do ensaio de FVT – VT-16-12 (profundidade 9,0 m) 77

LISTA DE TABELAS

Tabela 1: Detalhes da amostra 8
Tabela 2: Resultados dos ensaios de permeâmetro de Guelph (condutividade hidráulica, K_{sat}) 10
Tabela 3: Resultados do ensaio de tensiômetro 11
Tabela 4: Resultados dos ensaios de densidade pelo método do cone de areia 12
Tabela 5: Medições de vazão 13
Tabela 6: Detalhes dos furos de sondagem conforme construídos 14
Tabela 7: Resultados dos ensaios de gravidade específica 19
Tabela 8: Resumo dos resultados dos ensaios de teor de umidade 20
Tabela 9: Resultados dos ensaios de limite de Atterberg 21
Tabela 10: Resultados da DRX 22
Tabela 11: Resumo dos ensaios de SWCC 25
Tabela 12: Gradações de amostras representativas 26
Tabela 13: Resumo dos ensaios triaxiais 30
Tabela 14: Resumo dos ensaios de elementos flexores 48
Tabela 15: Tabela resumida dos ensaios de DSS 50
Tabela 16: Resumo dos ensaios de DSS 52
Tabela 17: Resumo dos parâmetros selecionados a partir dos ensaios de laboratório 67
Tabela 18: Critérios de delineação de rejeitos 70

LIST OF ANNEXES

Annex 1: Field Investigation Data

Annex 2: Summary of Tests

Annex 3: Index Test Data

Annex 4: X-Ray Diffraction Report

Annex 5: Scanning Electron Microscopy Images

Annex 6: Scanning Electron Microscopy Testing Report

Annex 7: Soil-Water Characteristic Curves

Annex 8: Advanced Testing Data

Annex 9: CPTu Plots, V_s Plots & Histograms

1 INTRODUÇÃO

1.1 Geral

Este Apêndice analisa os dados de campo e de laboratório da Barragem I da Mina Córrego do Feijão ("Barragem I") da Vale SA ("Vale") em Brumadinho, Brasil, para determinar dados de entrada das análises necessárias como parte da investigação do rompimento da Barragem I. Alguns desses parâmetros foram determinados a partir de dados coletados antes do rompimento, como dados dos ensaios cone de penetração (CPTu). Outros parâmetros exigiram a coleta de dados adicionais, que o Painel obteve em duas campanhas em junho e julho de 2019 e de ensaios de laboratório. Este Apêndice resume os dados adicionais que foram coletados, bem como as interpretações feitas. Este Apêndice deve ser lido conjuntamente com o Apêndice B, que resume os dados disponíveis coletados antes do rompimento.

Este Apêndice é composto de duas partes: (i) uma parte factual que resume as investigações de campo pós-rompimento e os ensaios de laboratório concluídos como parte da investigação do Painel; e (ii) uma seção interpretativa, na qual os principais parâmetros geotécnicos são determinados a partir de dados atuais e preexistentes de campo e laboratório.

1.2 Resumo das Constatações

As principais constatações relevantes para a caracterização de rejeitos para uso na avaliação de possíveis mecanismos e gatilhos de rompimento estão resumidas abaixo:

- Verificou-se que os rejeitos continham uma alta porcentagem de ferro na forma de hematita, goethita e magnetita.

- Os dados de ensaios triaxiais constataram que os rejeitos desenvolveram uma resposta incomum durante o cisalhamento. Por exemplo, amostras de rejeitos fofos desenvolveram um ângulo de atrito de pico maior que o ângulo de atrito do estado crítico. Amostras de rejeitos densos desenvolveram uma maior dilatação do que o normal para outros rejeitos ou solos naturais.

- Esta alta dilatação das amostras de rejeitos densos levou a uma curva de tensão-deformação muito íngreme, com um pico de resistência não drenada que é maior do que seria estimado a partir de relações empíricas e uma resistência residual não drenada (ou liquefeita) que é mais baixa do que a sugerida pelas relações empíricas.

- Embora o pico de resistência dos rejeitos tenha sido considerado mais alto do que o esperado, também foi observado que muito pouca deformação específica (<1%) é necessária para exceder o pico de resistência.

- Esta reação de comportamento frágil também é observável nos dados dos ensaios de palheta de campo coletados antes do rompimento da Barragem I e nos dados laboratoriais apresentados no Apêndice B.

- Acredita-se que esta alta resistência de pico e reação de comportamento frágil sejam um reflexo da leve cimentação que foi inferida pela primeira vez a partir dos dados do CPTu e velocidade da onda de cisalhamento (V_s) e está relacionada à mineralogia e oxidação dos rejeitos com alto teor de ferro.

2 PROGRAMA 1 – PROGRAMA DE AMOSTRAGEM A GRANEL

2.1 Locais de Amostragem a Granel

As amostras deformadas foram coletadas manualmente pela Klohn Crippen Berger Ltd. (KCB) em vários locais da área ocupada pela barragem durante uma visita ao local realizada em 4 de junho de 2019. As amostras foram coletadas com a intenção de serem representativas dos tipos de rejeitos represados na instalação e do solo residual usado na construção de algumas das bermas de contenção. As amostras foram escavadas com pá e colocadas em baldes de plástico em cada local de amostragem mostrado sobre uma imagem pré-rompimento da Barragem I na Figura 1 e em uma imagem pós-rompimento da Barragem I na Figura 2. Os locais da amostra são mostrados em branco nessas figuras. Fotografias representativas dos locais das amostras são mostradas na Figura 3 a Figura 7 e um resumo dos detalhes e coordenadas das amostras estão listados na Tabela 1.

Como as amostras tinham como intenção serem usadas em um programa de ensaios de laboratório no qual as amostras seriam reconstituídas em densidades pré-determinadas, as amostras foram coletadas em vários locais, representativos da variedade de rejeitos e materiais de construção de barragens. Estas amostras foram classificadas de acordo com o seguinte esquema desenvolvido para os materiais descritos neste Apêndice, com base em sua gradação e localização dentro do represamento, em bermas de contenção ou na fundação:

- Rejeitos grossos – A gradação é predominantemente do tamanho de areia nas plotagens de granulometria.

- Rejeitos Finos – A gradação é predominantemente do tamanho de silte em gráficos de granulometria.

- Lamas – Qualquer material que esteja a montante do contorno das lamas definido no Apêndice F e foi determinado através de fotografia aérea e interpretação dos ensaios de CPTu.

- Aterro de berma compactado (rejeitos) – berma de contenção composta por rejeitos compactados.

- Aterro de berma compactado (solo residual) – Berma de contenção composta por solo residual compactado.

- Solo residual/coluvionar – Solo nativo abaixo ou adjacente à Barragem I.

Algumas observações feitas durante a coleta das amostras foram:

- As exposições das amostras de lamas (S1 e S2) não mostraram estrutura perceptível, exceto para laminações finas que refletiam a deposição sequencial, de modo que amostras a granel foram retiradas de dois locais.

- Os rejeitos grossos apresentaram camadas distintas (em uma escala de 10s de centímetros (cm)). Foram coletadas amostras a granel dos materiais nos locais S3, S4, S5 e S6. No local S6, duas subamostras também foram coletadas em leitos individuais, em um esforço para identificar a variação no tamanho dos grãos nestes dois leitos exemplares. Estas amostras foram classificadas como rejeitos grossos porque eram predominantemente grossos; no entanto, elas continham camadas finas suficientes para que este material pudesse ser subamostrado, a fim de limitar a faixa de gradações de rejeitos na praia de rejeitos em ensaios triaxiais posteriores.

As amostras de rejeitos grossos foram coletadas de superfícies expostas de rejeitos intactos que representam praias de rejeitos de alteamentos anteriores abaixo da berma final.

Todas as amostras foram fechadas hermeticamente em sacos plásticos e, em seguida, colocadas em baldes de 10 galões e enviadas ao laboratório da KCB em Vancouver para testes. Os resultados dos ensaios-índice e laboratoriais avançados realizados nestas amostras estão resumidos nas seções 4 e 5 deste Apêndice.



Figura 1: Vista de locais de amostragem sobrepostos em uma imagem pré-rompimento da Barragem I



Figura 2: Vista de locais de amostragem sobrepostos em uma imagem pós-rompimento da Barragem I



Figura 3: Lamas amostradas no local S1



Figura 4: Lamas amostradas no local S2



Figura 5: Rejeitos grossos amostrados no local S6a (imagem à esquerda) e S6b (imagem à direita)



Figura 6: Exemplo de camadas observadas em rejeitos grossos



Figura 7: Solo residual compactado amostrado no local S7

Tabela 1: Detalhes da amostra

ID do local	Nº da amostra – Tipo de rejeitos	Coordenadas UTM (SIRGAS 2000, Zona 23S)	Comentários	Peso aprox. (kg)
S1	saco 1 – lamas	590,542 E, 7775217 N	Balde 1 de 10	20
	saco 2 – lamas		Balde 1 de 10	
	saco 3 – lamas		Balde 2 de 10	15
	saco 4 – lamas		Balde 2 de 10	
S2	saco 1 – lamas	592285 E, 7775206 N	Balde 3 de 10	15
	saco 2 – lamas		Balde 3 de 10	
S3	saco 1 – rejeitos grossos	591792 E, 7775188 N	Balde 4 de 10	25
	saco 2 – rejeitos grossos		Balde 4 de 10	
S4	saco 1 – rejeitos grossos	591798 E, 7775203 N	Balde 5 de 10	20
	saco 2 – rejeitos grossos		Balde 5 de 10	
	saco 3 – rejeitos grossos		Balde 6 de 10	10
S5	saco 1 – rejeitos grossos	591791 E, 7775196 N	Balde 7 de 10	25
	saco 2 – rejeitos grossos		Balde 7 de 10	
S6a	saco 1 – rejeitos grossos	591804 E, 7775194 N	Balde 8 de 10	20
	saco 2 – rejeitos grossos		Balde 8 de 10	
S6b	saco 1 – rejeitos grossos	591804 E, 7775194 N	Balde 9 de 10	10
	saco 2 – rejeitos grossos		Balde 9 de 10	
	saco 3 – rejeitos grossos		Balde 9 de 10	
S7	saco 1 – aterro de berma compactada (solo residual)	591788 E, 7775211 N	Balde 10 de 10	10
	saco 2 – aterro de berma compactada (solo residual)		Balde 10 de 10	

3 PROGRAMA 2 – PROGRAMA DE INVESTIGAÇÃO DE CAMPO

3.1 Escopo da Investigação de Campo

Uma investigação de campo foi solicitada pelo Painel de Especialistas para preencher as lacunas de dados que haviam sido identificadas. Esta investigação foi concluída em julho de 2019. Os ensaios/atividades de campo realizados como parte desta investigação foram:

- Ensaios de permeâmetro de Guelph para medir a condutividade hidráulica próximo da superfície in situ, dos rejeitos e tipos de aterros de bermas compactadas.
- Ensaios de tensiômetro para medir a sucção in situ nos locais dos ensaios de permeâmetro de Guelph.
- Ensaios de cone de areia para medir a densidade in situ nos locais dos ensaios de permeâmetro de Guelph.

- Medições de vazão nos córregos que fluem através do atual vale da Barragem I, a fim de fornecer uma estimativa aproximada da água que penetra na instalação a partir do solo natural durante esta época do ano.

- Perfuração/amostragem do solo natural sob a barragem para coletar amostras intactas.

As localizações dos furos de ensaio/perfuração são mostradas na Figura 1 do Anexo 1.

Amostras deformadas foram coletadas em todos os permeâmetros de Guelph e locais de ensaio de densidade in situ e foram entregues após a conclusão do programa de campo no laboratório da KCB em Vancouver para ensaios de índices físicos. Os resultados dos ensaios de índices físicos são apresentados na Seção 4.

3.2 Ensaio de Permeâmetro de Guelph

No total, 16 ensaios foram realizados na Barragem I e bermas remanescentes, conforme mostrado na Figura 2 do Anexo 1. Dos 16 ensaios, cinco foram realizados em rejeitos finos, cinco em aterros compactados da berma (rejeitos), quatro em aterros compactados da berma (solo residual) e dois em lamas. Os ensaios foram realizados em áreas intactas da barragem remanescente e apenas os locais mostrados na Figura 2 do Anexo 1 encontravam-se acessíveis. Não havia áreas intactas de rejeitos grossos acessíveis. Os ensaios foram conduzidos de acordo com a norma ASTM[1] D5126-16. Uma configuração típica do ensaio é mostrada na Figura 3 do Anexo 1.

Os resultados dos ensaios que resumem as condutividades hidráulicas saturadas (K_{sat}) calculados a partir dos ensaios de permeâmetro de Guelph são mostrados na Tabela 2.

[1] A ASTM é uma organização internacional de normas que desenvolve normas técnicas voluntárias para vários materiais, produtos, sistemas e serviços. https://www.astm.org/

Tabela 2: Resultados dos ensaios de permeâmetro de Guelph (condutividade hidráulica, K_{sat})

Tipos de material	ID do permeâmetro de Guelph	[3]Condutividade hidráulica, Ksat (cm/s)
Rejeitos finos	GP-02B	$2,5x10^{-4}$
	GP-08	$7,7x10^{-4}$
	GP-12	$6,2x10^{-4}$
Aterro de berma compactado (rejeitos)	GP-03	$5,6x10^{-5}$
	GP-10	$3,1x10^{-4}$
	GP-06	[1]$3,2x10^{-3}$
	GP-16	$3,9x10^{-3}$
Aterro de berma compactado (solo residual)	GP-07	[1]$1,4x10^{-4}$
	GP-05	[1]$9,1x10^{-6}$
	GP-09	$2,5x10^{-5}$
	GP-11	$4,5x10^{-4}$
	[2]GP-14	$6,2x10^{-4}$
Lamas	GP-01	$3,1x10^{-5}$
	GP-04B	[1]$2,3x10^{-4}$
	GP-13	$4,9x10^{-5}$
	GP-15	$1,2x10^{-4}$

OBSERVAÇÕES:

[1]Condições de regime permanente não estabelecidas durante o ensaio. Os resultados fornecidos representam a condutividade hidráulica calculada no final do ensaio.

[2]As condutividades hidráulicas medidas indicam que o material está dentro da faixa de aterro de berma compactado (solo residual). No entanto, os resultados do ensaio de granulometria e a descrição visual das notas de campo indicam que a gradação é mais semelhante ao aterro de berma compactado (rejeitos). Como resultado, GP-14 e DT-12 (o local correspondente do ensaio de densidade de substituição de areia) foram classificados como aterros de berma compactados (rejeitos e solo residual).

[3]As medições de condutividade hidráulica utilizaram o "Single Head Method 1 & 2" descrito no manual de instruções de operação da SoilMoisture.

3.3 Ensaios de Tensiômetro

Os ensaios de tensiômetro foram realizados a 1,5 m de cada local de ensaio de permeâmetro de Guelph (se as condições do solo permitiram), em 13 locais (mostrados na Figura 2 do Anexo 1). O tensiômetro foi deixado no chão durante todo o ensaio do permeâmetro de Guelph ou até que o indicador se estabilizasse para permitir uma leitura. No caso do GP-04, a ponta de cerâmica quebrou durante o ensaio e o ensaio não pôde ser realizado.

Um resumo dos resultados do ensaio do tensiômetro é mostrado na Tabela 3.

Tabela 3: Resultados do ensaio de tensiômetro

ID do ensaio de permeâmetro de Guelph	Leitura do tensiômetro (kPa)	ID do ensaio de permeâmetro de Guelph	Leitura do tensiômetro (kPa)
GP-01[1]	-	GP-10	10
GP-02[1]	-	GP-11	15
GP-03	15-10	GP-12	15
GP-04	-	GP-13	10
GP-05	22-21	GP-14	20
GP-06	12-10	GP-15	13
GP-07	13	GP-16	22
GP-08	10-15		
GP-09	20		

OBSERVAÇÕES:
[1]Devido a interrupções logísticas no início do Programa 2, os ensaios de tensiômetros não puderam ser realizados em GP-01 e 02.

3.4 Ensaios de Densidade por Cone de Areia

Os ensaios de densidade pelo método de cone de areia foram conduzidos a 1,5 m dos 14 locais de ensaio de permeâmetro de Guelph, conforme mostrado na Figura 4 do Anexo 1 (apenas um ensaio de densidade foi realizado adjacente a GP-04A e GP-04B). Dos 14 ensaios, quatro foram realizados em rejeitos finos, cinco em aterros compactados das bermas (rejeitos), quatro em aterros compactados das bermas (solo residual) e dois em lamas. Os ensaios foram conduzidos de acordo com a norma ASTM D1556/D1556M e com a norma brasileira NBR [2] 7185:2016. As configurações típicas do ensaio são mostradas nas figuras 5 e 6 do Anexo 1.

Um resumo dos pesos específicos calculados a partir dos ensaios de densidade pelo método do cone deareia é mostrado na Tabela 4.

[2] As normas NBR (Normas Brasileiras Regulamentadoras) são normas técnicas publicadas pela Associação Brasileira de Normas Técnicas (ABNT). https://www.abnt.org.br/

Tabela 4: Resultados dos ensaios de densidade pelo método do cone de areia

Material	ID do ensaio	Peso especícifo úmido (kN/m³)	Peso específico seco (kN/m³)
Rejeitos finos	DT-06	21,5	19,4
	DT-10	19,6	16,4
Aterro de berma compactado (solo residual)	DT-03	17,0	13,8
	DT-05	20,3	17,0
	DT-07	17,8	14,0
	DT-09	15,1	12,0
	[1]DT-12	15,0	24,1
Aterro de berma compactado (rejeitos)	DT-04	24,9	23,7
	DT-08	24,7	17,1
	DT-13	19,3	13,0
	DT-15	24,0	23,2
Lamas	DT-01	22,8	17,8
	DT-02	20,5	17,0
	DT-11	16,4	13,7
	DT-14	18,4	16,2

OBSERVAÇÕES:

[1]As densidades úmidas medidas indicam que o material está dentro da faixa de material de aterro de berma compactado (solo residual). No entanto, os resultados do ensaio de granulometria indicam que a gradação é mais semelhante ao aterro compactado das bermas (rejeitos). Como resultado, DT-12 e GP-14 (o local correspondente do ensaio de permeâmetro de Guelph) foram classificados como aterro compactado das bermas (rejeitos e solo residual).

3.5 Monitoramento do Fluxo através do Vale Atual

As medições de fluxo superficial foram feitas em nove locais em três riachos observados no atual vale da Barragem I, mostradas na Figura 7 do Anexo 1, que pareciam captar a maior parte do fluxo dos remanescentes atuais da barragem. Os remanescentes da barragem tinham aparência visual seca e não foi observado fluxo significativo dos rejeitos na ombreira esquerda, longe do local conhecido de córregos preexistentes. Consequentemente, usou-se a premissa de que a maior parte da água que flui por meio destes riachos se originou das nascentes conhecidas antes da construção da Barragem I. As vazões foram medidas através da criação de um Weir artesanal, se necessário, usando rejeitos do solo adjacente ao riacho e registrando a quantidade de tempo necessária para encher um balde de 3,6 L usando a água que flui através da soleira. Esta foi uma abordagem relativamente básica e fornece apenas uma medida aproximada da vazão. As configurações típicas para estes ensaios são mostradas nas Figuras 8 e 9 do Anexo 1. As medições de vazão começaram em 5 de julho de 2019 e foram realizadas quase que diariamente pelos 18 dias restantes do programa de investigação de campo. Foram realizadas medições de vazão pela manhã e à noite, totalizando 60 medições.

Um resumo das medições de vazão é apresentado na Tabela 5.

Tabela 5: Medições de vazão

Data	Vazão (L/s)																
	Córrego 1					Córrego 2					Córrego 3					Total	
	ID do local	Ao leste (m)	Ao norte (m)	Leitura manhã (L/s)	Leitura noite (L/s)	ID do local	Ao leste (m)	Ao norte (m)	Leitura manhã (L/s)	Leitura noite (L/s)	ID do local	Ao leste (m)	Ao norte (m)	Leitura manhã (L/s)	Leitura noite (L/s)	Leitura manhã (L/s)	Leitura noite (L/s)
05-jul-19	-	-	-	-	-	-	-	-	-	-	3A	591861	7774951	1,46	-		
06-jul-19	-	-	-	-	-	-	-	-	-	-	3B	591868	7774979	0,97	1,87		
07-jul-19	-	-	-	-	-	-	-	-	-	-	3C	591866	7774972	1,80	1,26		
08-jul-19	-	-	-	-	-	-	-	-	-	-	3D	519896	7774988	1,50	0,96		
09-jul-19	-	-	-	-	-	-	-	-	-	-	3E	591911	7774999	1,34	1,48		
10-jul-19	-	-	-	-	-	-	-	-	-	-	3F	591908	7774978	0,89	1,24		
11-jul-19	-	-	-	-	-	-	-	-	-	-				0,91	-		
12-jul-19	-	-	-	-	-	-	-	-	-	-				-	-		
13-jul-19	-	-	-	-	-	-	-	-	-	-				0,96	-		
14-jul-19	-	-	-	-	-	-	-	-	-	-	3G	591942	7775012	0,88	0,93	**0,88**	**0,93**
15-jul-19	1A	591812	7774972	0,04	0,06	2A	591868	7775002	0,22	0,33				0,96	0,80	**1,21**	**1,19**
16-jul-19				0,08	0,10				0,32	0,40				0,47	1,22	**0,86**	**1,72**
17-jul-19				0,11	0,13				0,16	0,46				0,98	1,61	**1,26**	**2,20**
18-jul-19				0,12	0,11				0,38	0,33				1,56	1,46	**2,06**	**1,90**
19-jul-19				0,11	0,12				0,21	0,25				0,83	1,38	**1,15**	**1,75**
20-jul-19				0,10	-				0,15	-				1,01	-	**1,25**	**-**
21-jul-19				0,08	0,10				0,28	0,32				0,89	1,11	**1,26**	**1,54**
22-jul-19				0,11	0,12				0,21	0,21				1,13	1,08	**1,45**	**1,40**
Média				*0,09*	*0,11*	*Média*			*0,24*	*0,33*	*Média*			*1,09*	*1,26*	**1,42**	**1,70**

3.6 Sondagem e Amostragem dos Solos da Fundação

Quatro furos de sondagem foram realizados como parte da investigação de campo de julho de 2019, localizados conforme mostrado na Figura 10 do Anexo 1. A perfuração foi avançada usando uma sonda rotativa hidráulica montada em esteira (mostrada nas Figuras 11 e 12 do Anexo 1), com água sendo usada como lubrificante de perfuração. A metodologia de sondagem foi:

- Sonda posicionada em cada local de furo de sondagem usando um GPS portátil.
- Perfurações em intervalos de 1 m de profundidade, extraindo e registrando o testemunho (ver Figuras 13 e 14 do Anexo 1).
- Ensaios de penetração padrão (SPTs) realizados em intervalos de 1 m de profundidade no aterro compactado acima da fundação (ver Figuras 15 e 16 do Anexo 1).
- Coleta de amostras em tubos Shelby usando um amostrador de pistão hidráulico nos solos da fundação. Foram coletadas 12 amostras. A amostragem foi finalizada quando a recuperação foi inferior a 50%. Os tubos Shelby foram coletados de todos os furos de sondagem, exceto BH-03, pois o solo natural não foi alcançado neste local. Uma vez recuperadas as amostras, elas foram mantidas na posição vertical. As extremidades das amostras de tubos foram vedadas com cera após a extração do furo de sondagem (ver exemplo na Figura 17 do Anexo 1). Os tubos Shelby foram então transportados para o laboratório da KCB em Vancouver em uma caixa de madeira, em conformidade com a norma ASTM D4220-14 (veja a Figura 18 do Anexo 1).

Os registros de furos de sondagem, incluindo os locais, são apresentados no Anexo 1. Um resumo dos detalhes dos furos de sondagem é apresentado na Tabela 6. Devido à precisão limitada do dispositivo GPS portátil usado em campo, as coordenadas dos locais dos furos de ensaio devem ser consideradas aproximadas.

Tabela 6: Detalhes dos furos de sondagem conforme construídos

ID do local	Ao leste (m)	Ao norte (m)	[1]Elevação estimada do solo (m)	Data de conclusão
BH-01	591793	7774986,0	863,7	17 de julho de 2019
BH-02	591793,4	7774932,6	857,8	19 de julho de 2019
BH-03	591689,2	7774982,9	870,7	23 de julho de 2019
BH-04	591797,0	7774937,8	859,0	23 de julho de 2019

OBSERVAÇÃO:
[1]Elevação do solo estimada a partir do GPS portátil no momento da perfuração e usando os dados LiDAR de 2019.

4 ENSAIOS DE ÍNDICES FÍSICOS EM LABORATÓRIO

4.1 Escopo

Os tipos, procedimentos e número de ensaios realizados são apresentados no Anexo 2. Esta seção descreve os resultados dos ensaios de índices físicos em todos os tipos de material. Os objetivos básicos do programa foram caracterizar as propriedades do ensaio-índice de cada tipo de material para comparação com os dados pré-existentes e confirmar a representatividade das amostras.

Os ensaios de índices físicos foram realizados em amostras coletadas como parte do Programa 1 e 2 (consulte as Seções 2 e 3). Os locais das amostras são mostrados no Anexo 1.

Os ensaios de índices físicos realizados nas amostras de solo incluíram ensaios de granulometria, ensaios de gravidade específica, determinação do teor de umidade e ensaios de limite de Atterberg. Ensaios adicionais incluíram análise por difração de raios X (DRX) e imagens por microscopia eletrônica de varredura (MEV). Os seguintes resultados dos ensaios-índice são detalhados no Anexo 3.

4.2 Granulometria

Um total de 44 ensaios de granulometria foram realizados em amostras coletadas dos Programas 1 e 2. Estes ensaios foram realizados de acordo com a norma ASTM D422. Os seguintes ensaios de granulometria foram realizados:

- 12 ensaios em rejeitos grossos
- dois ensaios em rejeitos finos
- 10 ensaios em lamas
- seis ensaios em aterros de berma compactados (solo residual)
- seis ensaios em aterros de berma compactados (rejeitos)
- oito ensaios em materiais de fundação coletados de amostras com tubo Shelby

Os resultados são mostrados na Figura 8 a Figura 13.

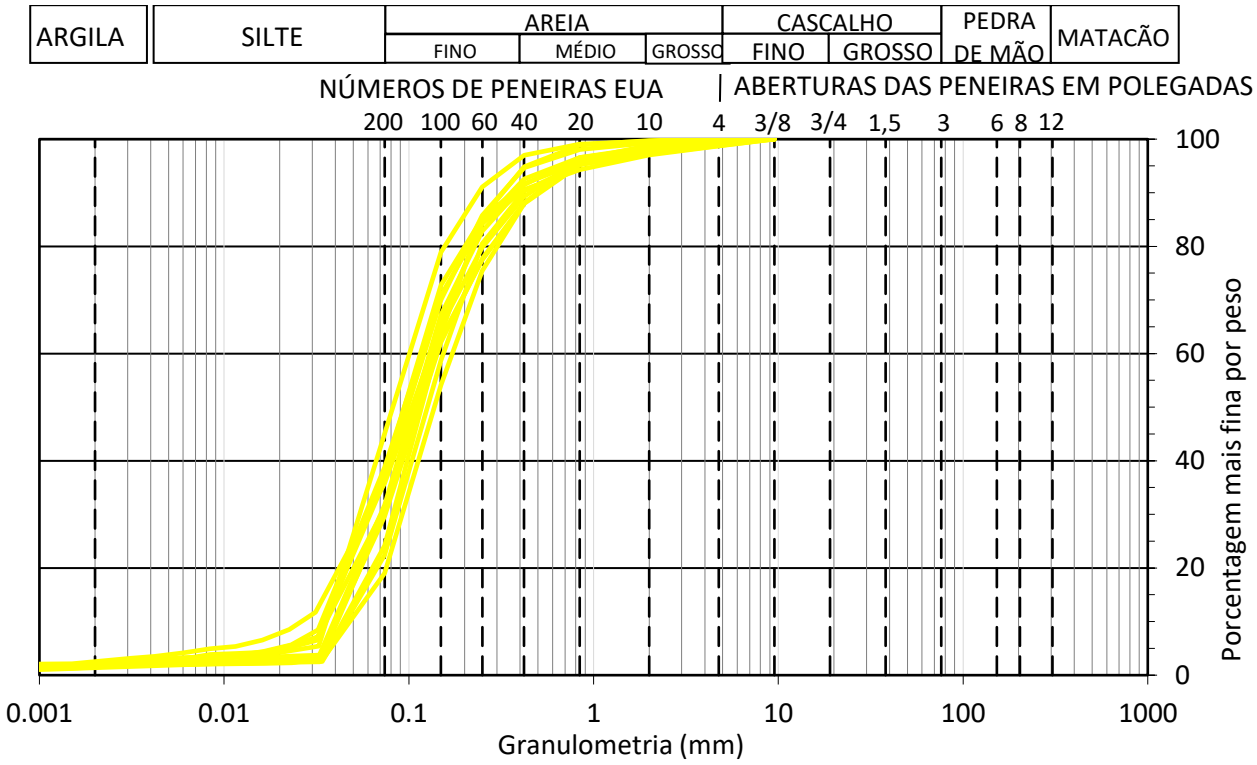


Figura 8: Curvas granulométricas de amostras de rejeitos grossos

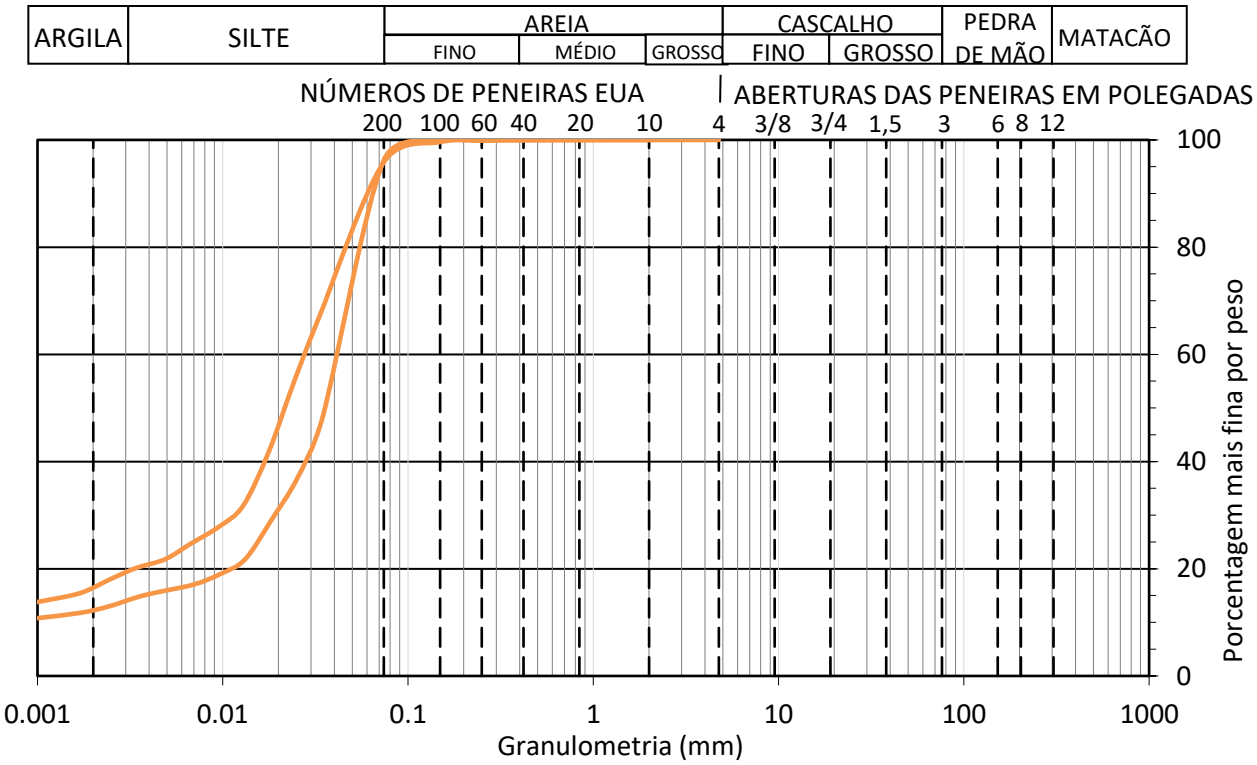


Figura 9: Curvas granulométricas de amostras de rejeitos finos

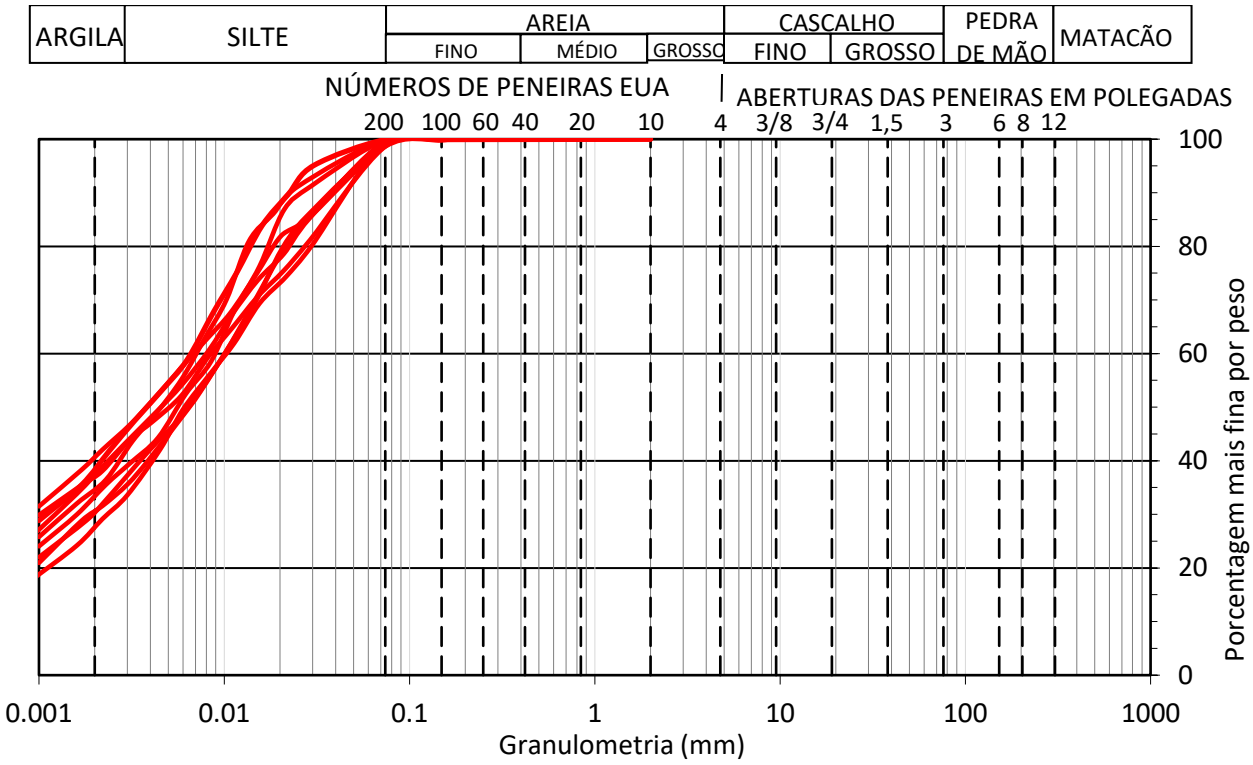


Figura 10: Curvas granulométricas de amostras de lamas

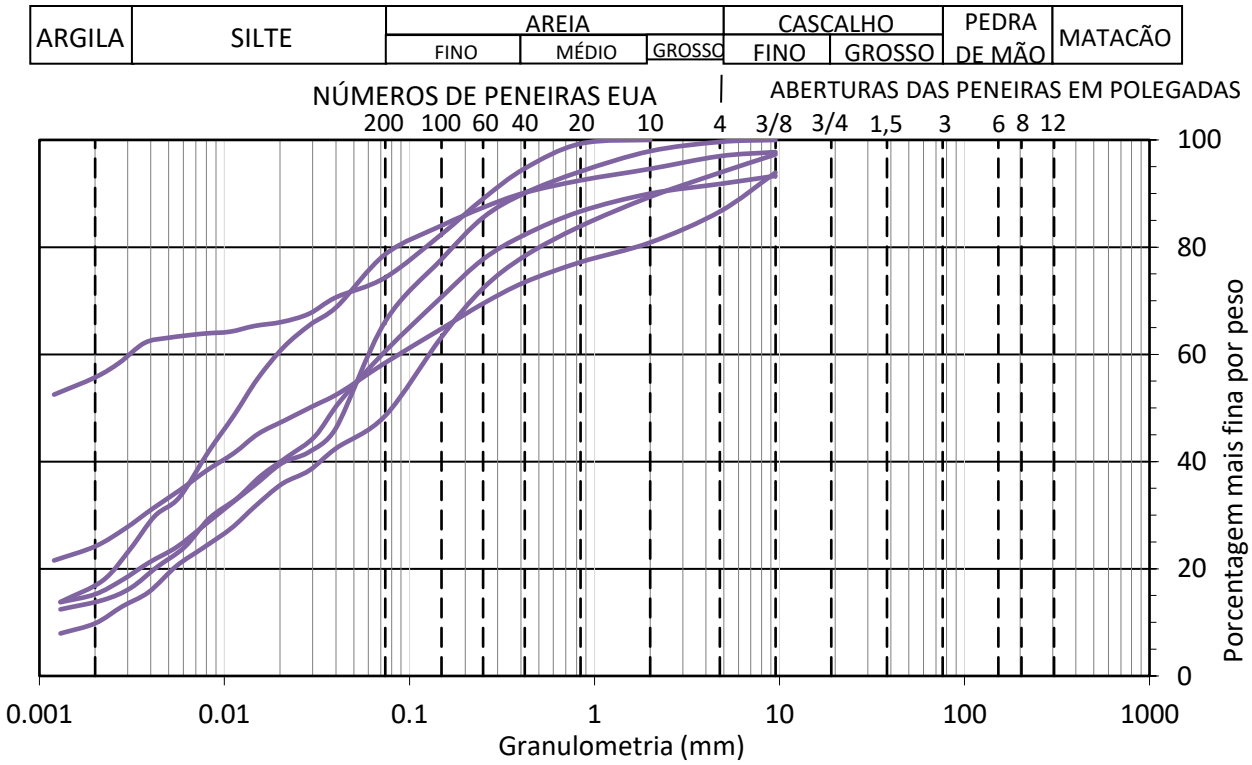


Figura 11: Curvas granulométricas de aterros de berma compactados (solo residual)

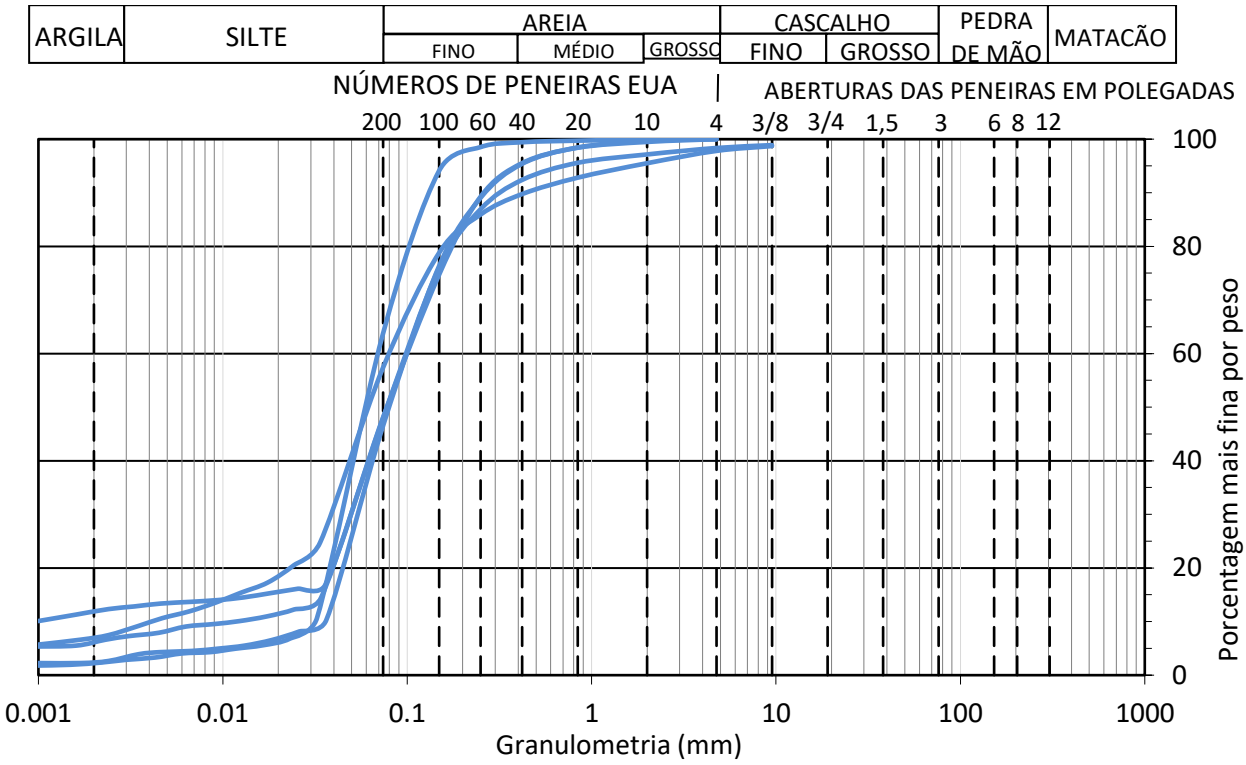


Figura 12: Curvas granulométricas de aterros de berma compactados (rejeitos)

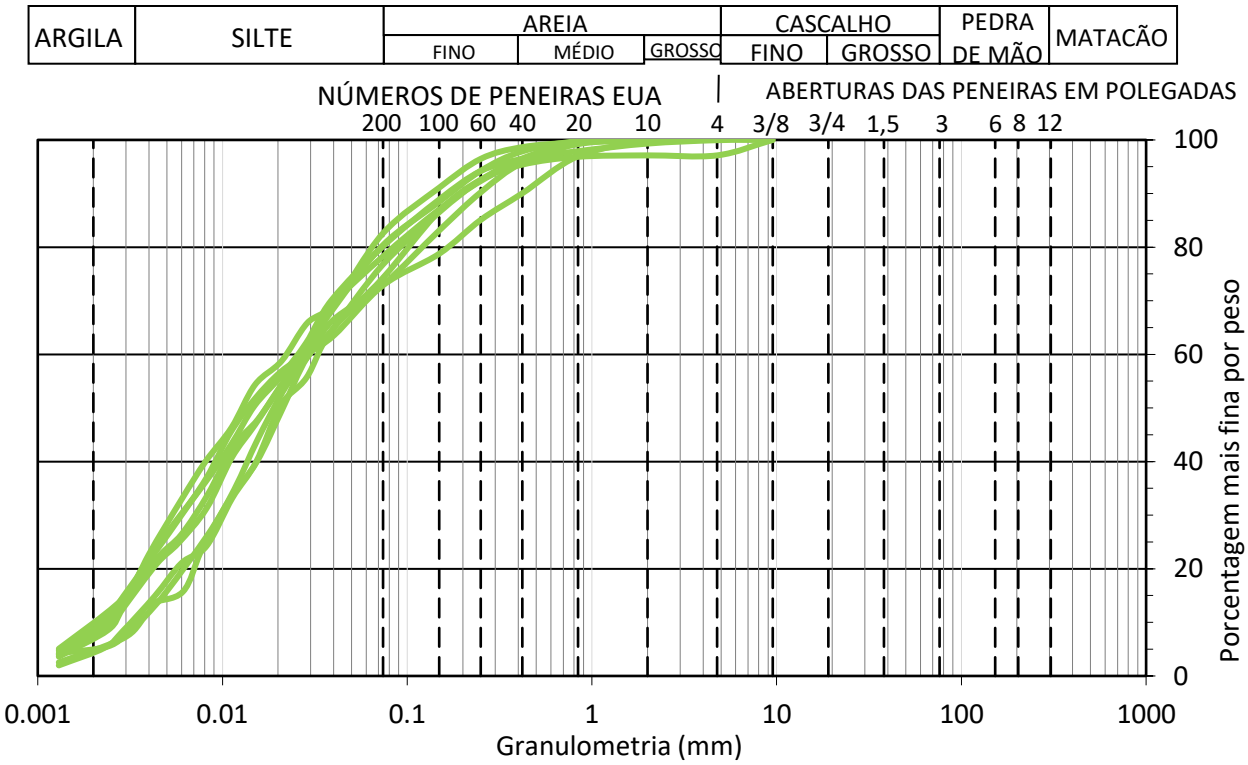


Figura 13: Curvas granulométricas de amostras de solo residual

4.3 Gravidade específica

Foram realizados 29 ensaios de gravidade específica nas amostras coletadas no Programa 1, incluindo 17 em rejeitos grossos, nove em lamas e três em aterros compactados das bermas (solo residual). Foram realizados 14 ensaios de gravidade específica nas amostras coletadas durante o Programa 2, incluindo quatro em aterros compactados das bermas (rejeitos), dois em rejeitos finos, quatro em aterros compactados das bermas (solo residual) e quatro em lamas. Nove ensaios de gravidade específica foram realizados nos materiais da fundação coletados de amostras de furos de sondagem do Programa 2. Os resultados destes ensaios estão resumidos na Tabela 7.

Estes ensaios foram conduzidos de acordo com a norma ASTM D854.

Tabela 7: Resultados dos ensaios de gravidade específica

Material	Programa de gravidade específica média 1	Programa de gravidade específica média 2
Rejeitos grossos	4,89 (4,64-4,99)	-
Rejeitos finos	-	3,89 (3,87-3,90)
Lamas	4,00 (3,92-4,07)	3,91 (3,61-4,32)
Berma compactada (solo residual)	3,14 (3,12-3,16)	2,75 (2,67-2,86)
Berma compactada (rejeitos)	-	4,39 (4,10-4,93)
Solo da fundação	-	2,81 (2,79-2,83)

OBSERVAÇÕES:
[1]Os valores mostrados entre parênteses indicam a faixa de resultados (mín-máx).

4.4 Teor de umidade

Foram realizados 24 ensaios em amostras coletadas no Programa 1 para determinar o teor de umidade das amostras de rejeitos finos e grossos, lamas e bermas compactadas nos remanescentes da barragem. Foram realizados 31 ensaios em amostras coletadas no Programa 2 para determinar o teor de umidade dos rejeitos finos, lamas, aterro compactado das bermas (rejeitos) e aterro compactado das bermas (solo residual) nos locais dos ensaios de permeâmetro de Guelph. Seis ensaios foram realizados em materiais de fundação coletados de amostras de furos de sondagem no Programa 2. Os resultados destes ensaios estão resumidos na Tabela 8.

Estes ensaios foram conduzidos de acordo com a norma ASTM D2216.

Tabela 8: Resumo dos resultados dos ensaios de teor de umidade

Material	Teor médio de umidade (%) Programa 1[2]	Teor médio de umidade (%) Programa 2[2]
Rejeitos grossos	10,2 (5,6-14,8)	-
Rejeitos finos	-	19,5 (10,6-31,4)
Lamas	25,9 (22,0-33,7)	24,1 (13,1-36,5)
Berma compactada (solo residual)	19,8 (18,2-22,3)	24,6 (17,1-33,8)
Berma compactada (rejeitos)	-	8,7 (3,4-15,4)
Solo da fundação	-	38,9 (28,3-43,5)

OBSERVAÇÕES:
[1]Os valores mostrados entre parênteses indicam a faixa de resultados (mín-máx).
[2]O método de secagem por ar foi usado.

4.5 Limites de Atterberg

Foram realizados 16 ensaios de limite de Atterberg em amostras coletadas durante o Programa 1; oito em amostras de lamas coletadas na extensão a montante da Barragem I e oito em aterros de berma compactados (solo residual). Foram realizados 18 ensaios de limite de Atterberg em amostras coletadas durante o Programa 2. As faixas de Limite de Liquidez (WL), Limite de Plasticidade (PL) e índice de plasticidade de rejeitos finos de programas de ensaios anteriores, conforme resumido no Apêndice B, são de 18 a 30%, 14 a 23% e 4 a 7%, respectivamente. Os resultados dos ensaios de laboratório dos rejeitos finos geralmente estão de acordo com os resultados anteriores.

Além disso, oito ensaios de limite de Atterberg foram realizados em materiais da fundação (solo residual) coletados durante o Programa 2.

Estes ensaios foram conduzidos de acordo com a norma ASTM D4318 e os resultados estão resumidos na Tabela 9.

Tabela 9: Resultados dos ensaios de limite de Atterberg

Material	Resultados médios dos ensaios dos limites de Atterberg Programa 1			Resultados médios dos ensaios dos limites de Atterberg Programa 2		
	WL	WP	PI	WL	WP	PI
Rejeitos grossos	-	-	-	-	-	-
Rejeitos finos	-	-	-	21 (19-22)	17 (16-18)	4 (3-4)
Lamas	44 (34-49)	26 (22-31)	18 (12-22)	42 (15-53)	24 (11-30)	18 (4-26)
Berma compactada (solo residual)	34 (30-36)	25 (23-26)	10 (7-11)	52 (35-66)	31 (25-38)	20 (9-28)
Berma compactada (rejeitos)	-	-	-	20 (16-29)	16 (14-18)	4 (1-11)
Solo da fundação	-	-	-	60 (54-68)	41 (33-56)	18 (10-29)

OBSERVAÇÕES:
[1]Os valores mostrados entre parênteses indicam a faixa de resultados (mín-máx).
[2]As amostras GP-01/DT-01 e GP-04B/DT-02, coletadas na praia da ombreira oeste, inicialmente foram direcionadas aos rejeitos finos, mas foram posteriormente reclassificadas como lamas, com base nos resultados dos ensaios de campo e ensaios de índices físicos. Isto é compatível com as imagens de satélite da Barragem I, discutidas no Apêndice F, nas quais o lago de decantaçãoestava consistentemente mais próxima da crista da barragem a oeste em comparação a leste.

4.6 Difração de Raios-X

As análises de DRX foram realizadas na Universidade de British Columbia (UBC) em amostras de lamas e rejeitos grossos coletadas durante o Programa 1. Os resultados de DRX são apresentados no Anexo 4. Os ensaios tiveram como objetivo identificar a mineralogia das lamas e dos rejeitos grossos. Quatro ensaios de DRX foram realizados; dois em amostras de lamas e dois em amostras de rejeitos grossos.

Todas as amostras eram predominantemente hematita (lamas aproximadamente 40% a 50%; rejeitos grossos aproximadamente 80% a 90%). As lamas também tiveram uma porcentagem significativa de goethita (~ 30%) e uma porcentagem maior de caulinita (~ 5% a 10%), quartzo (~ 5%), talco (~ 2% a 3%) e bayerita (~ 2 % a 3%) que os rejeitos grossos. Os rejeitos grossos continham entre aproximadamente 5% e 10% de magnetita. Também foram realizados quatro ensaios de DRX em amostras de rejeitos finos do Programa 2. Os resultados da análise de fase quantitativa são apresentados na Tabela 10 e mostram mineralogia semelhante às amostras de lama do Programa 1, sendo as principais exceções a ocorrência de menos goethita (~10% a 20%) e mais quartzo (~ 12% a 29%).

As amostras de rejeitos grossos do Programa 1 em junho de 2019 foram representativas dos rejeitos profundos retidos pela barragem, enquanto as amostras do Programa 2 em julho de 2019 foram representativas dos rejeitos de superfície. A mineralogia das amostras coletadas nos Programas 1 e 2 está dentro da faixa de amostragem e ensaio anteriores em outros locais ao longo da bacia, conforme resumido na Figura 5-32 no Apêndice B.

Tabela 10: Resultados da DRX

Mineral	Fórmula ideal	Programa 1				Programa 2			
		N.º 1 amostra 1 saco 2 raios-x (lamas)	**N.º 2 amostra 1 saco 4 raios-x (lamas)**	**N.º 3 amostra 3 saco 2 raios-x (rejeitos grossos)**	**N.º 4 amostra 5 saco 1 raios-x (rejeitos grossos)**	**DT-01 (rejeitos finos)**	**DT-02 (rejeitos finos)**	**DT-06 (rejeitos finos)**	**DT10 (rejeitos finos)**
Hematita	α-Fe_2O_3	50,1	44,4	87,7	86,8	43,1	54,1	50,3	44,3
Goethita	A-$Fe^{3+}O(OH)$	32,0	34,0	3,4	3,0	20,7	15,3	10,2	13,7
Magnetita	Fe_3O_4	0,4	0,4	6,5	7,6	1,9	1,5	1,3	1,3
Quartzo	SiO_2	5,4	6,6	1,6	1,5	14,9	12	28,5	21,8
Caulinita	$Al_2Si_2O_5(OH)_4$	6,2	8,9	0,6	0,6	11,6	10,9	6,4	13,5
Talco	$Mg_3Si_4O10(OH)_2$	2,7	2,3	-	-	3,1	2	1,4	1,1
Gibbsita	$Al(OH)_3$	0,9	1,0	0,3	0,4	3	2,2	1,4	3
Bayerita	$Al(OH)_3$	2,2	2,4	-	-	1,7	2	0,5	1,4
Total		100,0	100,0	100,0	100,0	100,0	100,0	100,0	100,0

4.7 Microscópio Eletrônico de Varredura

Amostras de lamas e rejeitos grossos foram submetidas a imagens de microscopia eletrônica de varredura (MEV) na UBC, usando um microscópio eletrônico Philips XL30. A coleta de imagens foi concluída em duas amostras de lamas e duas de rejeitos grossos coletadas durante o Programa 1, a fim de avaliar qualitativamente a estrutura das partículas, a angularidade e outros parâmetros a nível microscópico. Estes ensaios mostraram que a forma das partículas dos rejeitos grossos e lamas é semelhante. Ambos contêm partículas tipicamente subangulares a angulares, geralmente com uma superfície porosa.

Exemplos destas imagens de MEV podem ser vistos na Figura 14 e Figura 15. Veja no Anexo 5 todas as imagens.

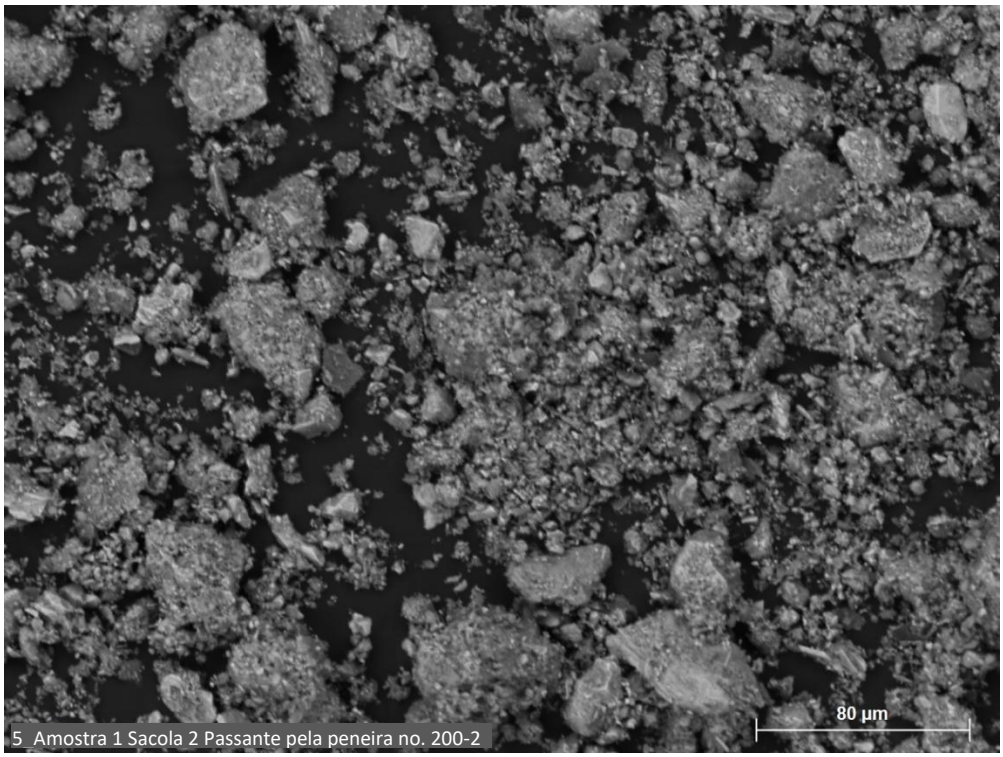


Figura 14: Imagem de MEV da amostra 1, saco 2 (lamas), passante pela peneira nº 200

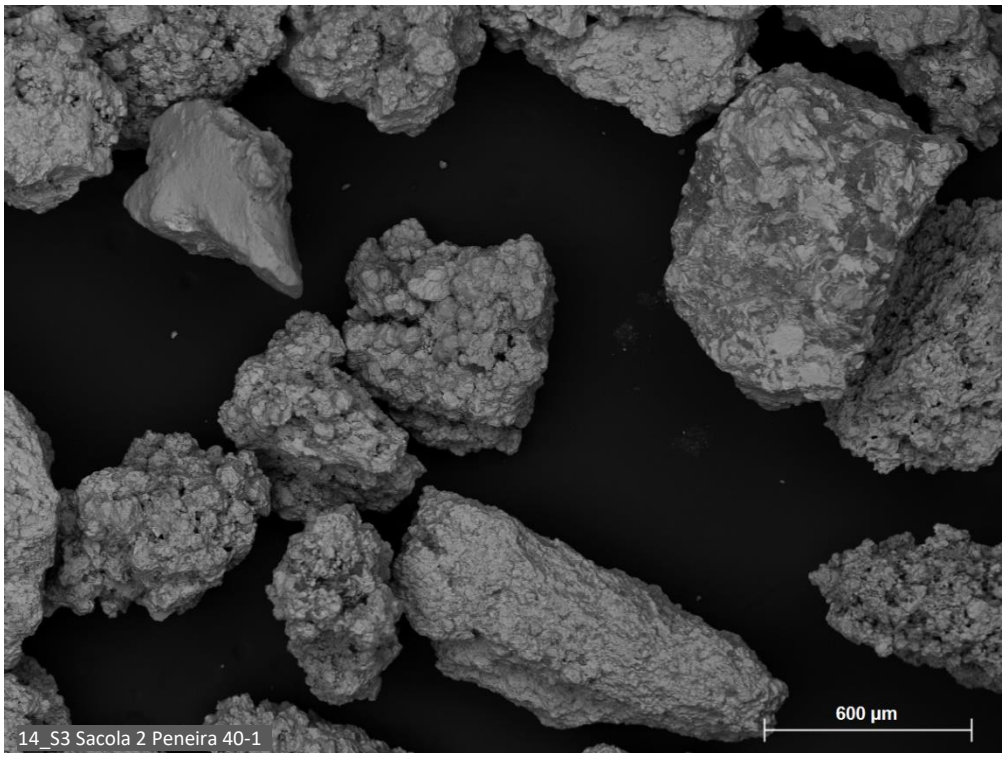


Figura 15: Imagem de MEV da amostra 3, saco 2 (rejeitos grossos), retida na peneira nº 40

4.8 Ensaios Adicionais de MEV

Conforme discutido mais adiante nas Seções 5 e 6, um componente adicional da resistência ao cisalhamento pôde ser observado em ensaios de laboratório, o que foi atribuído à cimentação de partículas inferida a partir dos dados da V_S. Para entender melhor esta aderência, ensaios de MEV adicionais foram realizados na Universidade de Queensland (UQ) na Austrália.

Amostras de lamas e misturas de rejeitos grossos, algumas das quais foram submetidas a ensaios triaxiais anteriores, foram submetidas ao MEV de elétrons secundários (SE) e de elétrons retroespalhados (BSE) em uma escala de micrômetros (µm) (um aumento na escala de 10 a 100 vezes comparados ao MEV usado na UBC). Demonstrou-se que partículas de óxido de ferro granuladas e do tamanho de argila agem como cimentos, formando partículas finas no caso das lamas, aderindo partículas menores (10s de µm) a partículas maiores (100s de µm) e unindo partículas menores. Estes cimentos podem ser responsáveis pelo componente adicional de resistência observado nos ensaios triaxiais.

Os resultados dos ensaios de MEV realizados na UQ estão resumidos no Anexo 6.

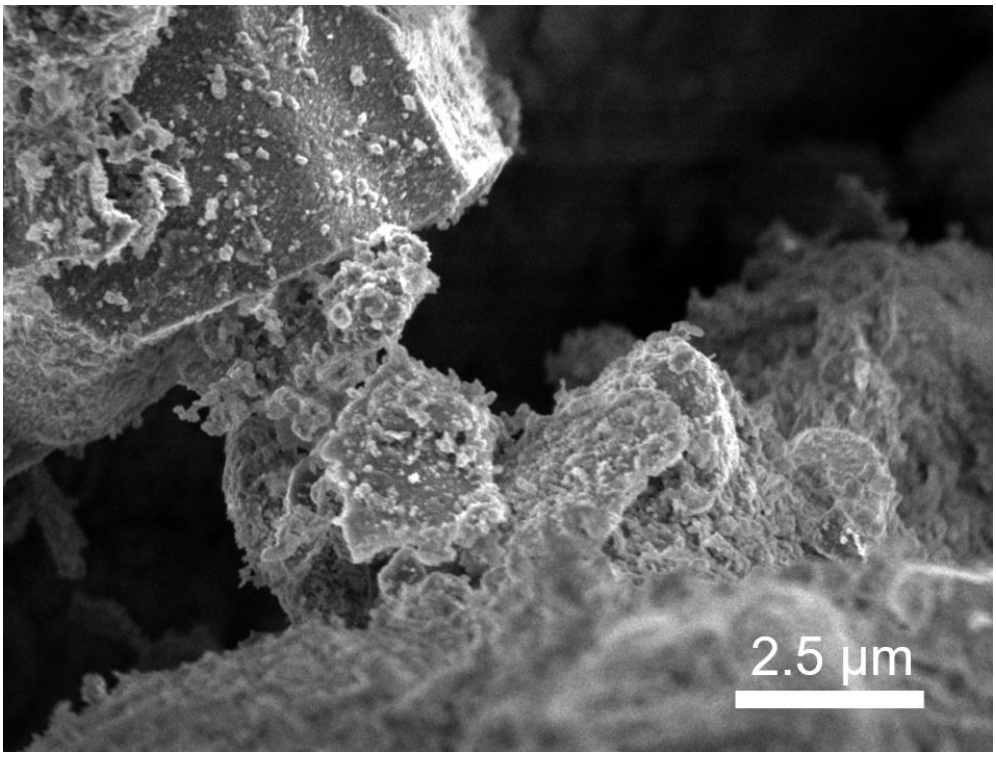


Figura 16: Imagem de MEV de amostra de rejeitos grossos mostrando aderência de óxido de ferro

4.9 Curvas Características de Água no Solo

O ensaio de permeabilidade não-saturada foi realizado pelo Centro de Pesquisa Geotécnica da Universidade de Alberta para desenvolver curvas características de água no solo (SWCCs) para várias gradações de rejeitos. As SWCCs foram realizadas usando dois métodos: (i) célula Tempe e (ii) dispositivo HYPROP 2. Os ensaios foram realizados em amostras coletadas durante o Programa 2 e em uma amostra reconstituída de rejeitos grossos. Um resumo dos ensaios de SWCC realizados é mostrado na Tabela 11 e discutido mais detalhadamente no Anexo 7.

Tabela 11: Resumo dos ensaios de SWCC

Material	ID da amostra	Método da célula de Tempe	Método HYPROP 2
Lamas	DT-01	X	
	DT-02	X	X
Rejeitos finos	DT-06	X	X
	DT-10	X	
Rejeitos grossos (amostra reconstituída – gradação média)	AG A03255A01	X	X
Aterro de bermas compactado (rejeitos/solo residual)	GP-03/09	X	X
Aterro de bermas compactado (rejeitos/solo residual)	GP-14	X	X

5 ENSAIOS AVANÇADOS DE LABORATÓRIO

Esta seção descreve os resultados de ensaios avançados de laboratório realizados em amostras de rejeitos reconstituídos. Os tipos, procedimentos e números dos ensaios estão detalhados no Anexo 2. O objetivo deste programa de ensaio foi desenvolver parâmetros de engenharia para uso em análises pelo Painel.

5.1 Amostras Reconstituídas

As amostras reconstituídas foram preparadas a partir das amostras deformadas de rejeitos grossos, coletadas no Programa 1. Isto envolveu combinar as amostras deformadas, peneirá-las e depois separá-las por tamanhos de grãos componentes. Estes componentes individuais foram então recombinados nas proporções necessárias e misturados completamente, a fim de reproduzir qualquer uma das gradações representativas discutidas abaixo. A gradação das amostras reconstituídas foi confirmada através de outro ensaio de granulometria antes e após o ensaio. Os resultados dos ensaios de granulometria para todos os ensaios avançados realizados em amostras de rejeitos reconstituídos, são fornecidos no Anexo 8.

Um dos principais parâmetros de interesse durante este programa foi a inclinação da linha de estado crítico (CSL) para várias gradações de rejeitos. Devido ao potencial impacto dos finos na CSL, foi decidido desenvolver CSLs para gradações representativas. Em um primeiro momento, a gradação média dos rejeitos dos ensaios laboratoriais previamente realizados no local foi usada como gradação representativa. Para avaliar o impacto das variações do teor de finos na CSL, amostras representativas do percentil 20 (grosso) e percentil 80 (fino) dos ensaios laboratoriais anteriores também foram reconstituídas e testadas. Tabela 12 resume as gradações representativas testadas. Como comparação, as curvas de gradação reconstituídas foram sobrepostas às curvas granulométricas históricas, resumidas no Apêndice B, conforme mostrado na Figura 17. A comparação mostra que as gradações reconstituídas estão em geral alinhadas com as gradações de amostras históricas de rejeitos.

Tabela 12: Gradações de amostras representativas

Tamanho da abertura da peneira (mm)	Nº da Peneira EUA	Porcentagem mais fina (%) – média	Porcentagem mais fina (%) – fina	Porcentagem mais fina (%) – grossa
9,51	3/8 polegadas	100,0	100	100
4,76	4	100,0	100	99,2
2	10	99,0	100	96,8
0,841	20	97,0	100	91,2
0,42	40	92,5	100	79,2
0,25	60	84,5	100	67,2
0,149	100	72,0	88	55
0,074	200	51,5	71,2	32,8

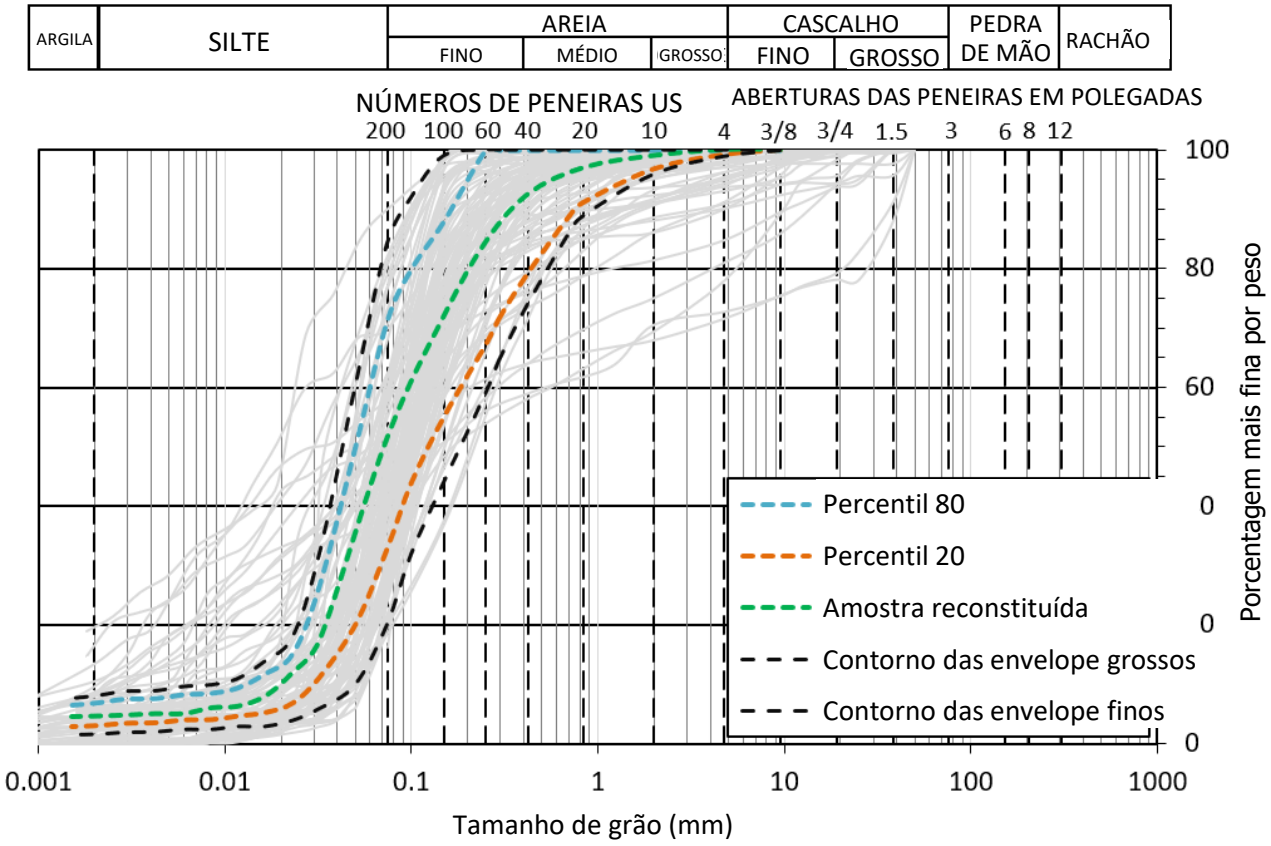


Figura 17: Gradações reconstituídas de rejeitos finos, grossos e médios

5.2 Ensaio de compressão triaxial

5.2.1 Escopo

Foram realizados 35 ensaios triaxiais, incluindo:

- 22 ensaios padrão isotropicamente adensados drenados (CID) com deformação controlada;
- dois ensaios padrão isotropicamente adensados não drenados (CIU) com deformação controlada;
- oito ensaios padrão anisotropicamente adensados não drenados (CAU) com deformação controlada;
- um ensaio anisotropicamente adensado não drenado com carga controlada (CAU-DL);
- um ensaio anisotropicamente adensado controlado não drenado com carga controlada (CAU-DL) e *creep*; e
- um ensaio anisotropicamente adensado drenado com carga controlada (CAU-DL).

Os ensaios foram realizados em amostras reconstituídas fofas e densas das três gradações representativas (fina, grossa e média). As amostras foram testadas com tensões efetivas médias iniciais (p') variando de 40 quilopascais (kPa) a 1500 kPa.

O principal objetivo do programa de ensaio triaxial era determinar a linha de estado crítico (CSL) das diversas gradações representativas de rejeitos. Ensaios adicionais foram realizados em amostras significativamente densas da CSL, a fim de desenvolver parâmetros de dilatação, e uma série de ensaios de compressão triaxial não drenada foi realizada, de modo a avaliar tendências em picos e forças residuais não drenadas.

5.2.2 Procedimento para Ensaio Triaxial Padrão com Deformação Controlada

Os ensaios triaxiais padrão com deformação controlada foram conduzidos de acordo com as normas ASTM D4767-11 (CIU/CAU) e ASTM D7181-11 (CID/CAD). As amostras reconstituídas foram adensadas até o nível de tensão efetiva média necessária. Esta fase de adensamento foi seguida pela fase de cisalhamento em condições drenadas ou não drenadas (CID/CAD ou CIU/CAU), utilizando carregamento com deformação controlada. Os ensaios iniciais se voltaram aos índices de vazios iniciais dos estados fofos e densos, usando os índices de vazios medidos em amostragems anteriores. Os índices de vazios iniciais para amostras destinadas a estarem fofas e densas foram tomados como os percentis 80 e 20 da faixa histórica, respectivamente, de amostras com gradação semelhante à da média. Depois que um conjunto inicial de ensaios triaxiais foi realizado para determinar a CSL, isto, combinado com o parâmetro de estado estimado dos ensaios de CPTu pré-rompimento, permitiu ao Painel especificar índices de vazios para o restante dos ensaios de laboratório.

As amostras foram preparadas por compactação úmida, de acordo com o procedimento descrito por Jefferies e Been (2016).[3] Além disso, as amostras foram preparadas em 11 camadas horizontais e a variação de volume foi medida ao longo de todo o ensaio (veja a Figura 18). Uma análise granulométrica com lavagem foi realizada em cada amostra antes de cada ensaio triaxial. Após a conclusão dos ensaios triaxiais, as amostras, juntamente com as placas superior e inferior, foram congeladas para uma determinação precisa do teor de umidade. Este teor de umidade foi então usado para calcular o índice de vazios final, assumindo condições totalmente saturadas que foram comparadas com o índice de vazios acompanhado durante os ensaios. Após os ensaios, a gradação de cada amostra triaxial foi testada novamente para avaliar se ocorreu o esmagamento de grãos. Os resultados dos ensaios são apresentados no Anexo 8.

[3] Jefferies, M., & Been, K. (2016). *Soil liquefaction: A critical state approach* (2nd ed.). London: Taylor & Francis.

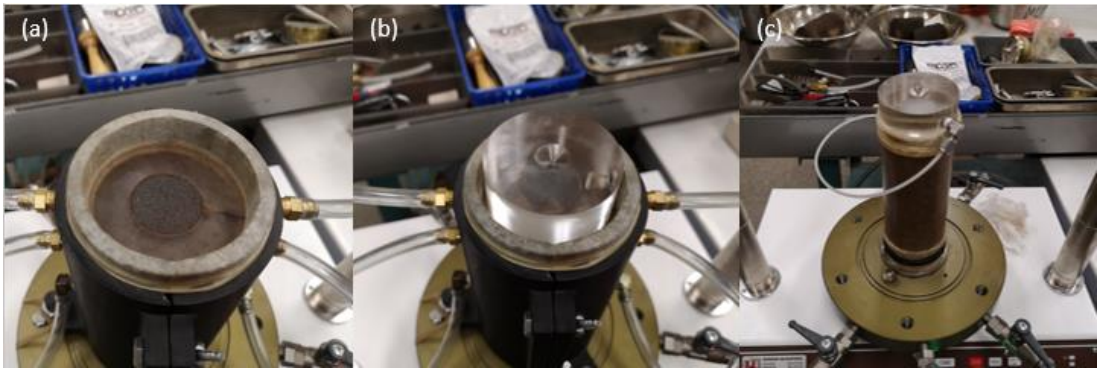


Figura 18: Configuração do ensaio triaxial: (a) Pedra porosa modificada; (b) Colocação da amostra por compactação úmida, (c) Configuração final da amostra

5.2.3 Procedimento para Ensaio Triaxial com Carga Controlada

As amostras dos ensaios triaxiais com carga controlada foram preparadas da mesma maneira que as amostras dos ensaios triaxiais padrão, a fim de obter um índice de vazios inicial uniforme. Após a saturação, as amostras foram adensadas anisotropicamente até a meta da tensão efetiva média (p') e tensão de desvio (q). No final da fase de adensamento anisotrópico, a carga vertical foi substituída por um peso morto e todas as bombas foram colocadas em controle manual. A carga vertical foi aumentada, adicionando-se sacos de areia de 500 g nos quatro baldes de plástico presos à estrutura de carregamento, e o incremento real de carga foi medido pela célula de carga. Para o ensaio drenado (CAD-DL), quando o deslocamento e o volume da amostra pararam de mudar, foi adicionado outro incremento de carga. Para o ensaio não drenado (CAU-DL), a taxa de carregamento foi ajustada para aproximadamente 1 kPa/min.

O ensaio final com carga controlada foi adensado anisotropicamente e drenado da mesma maneira que os dois ensaios anteriores, mas, em vez de aumentar a carga após a consolidação, a carga foi mantida constante e os deslocamentos na amostra foram monitorados. Este ensaio final foi denominado como um ensaio anisotropicamente adensado com carga controlada, não drenado, com *creep* (CAU-DL-C). Este ensaio CAU-DL-C foi realizado em etapas e a carga foi mantida constante após o adensamento até um coeficiente de tensão lateral (K_0) de 0,5 e 0,4. O ensaio foi encerrado após a amostra se romper durante o adensamento anisotrópico de K_0 = 0,4 a 0,3.

Tabela 13 resume os diferentes ensaios triaxiais realizados.

Tabela 13: Resumo dos ensaios triaxiais

Material	Nº do ensaio	Índice de vazios adensado	Pressão de adensamento (kPa)	Tipo de ensaio	Teor de finos (%)	
					Antes do ensaio	Após o ensaio
Amostras médias reconstituídas	TX01	0,87	1500	CID	51,9	54,5
	TX02	1,0	200	CID	51,6	50,7
	TX03	0,9	1000	CID	51,6	52,7
	TX04	0,97	500	CIU	51,3	49,9
	TX05	0,68	500	CID	51,9	50,9
	TX06	0,84	1500	CID	51,3	53,9
	TX07	0,84	2000	CIU	51,6	50,6
	TX08	0,9	40	CID	52,1	51,1
	TX09	0,82	100	CID	50,9	48,8
	TX18	0,79	100	CID	48,6	-
	TX19	0,76	100	CID	48,6	50,2
	TX20	0,66	500	CID	48,6	50,0
	TX21	0,72	500	CID	49,7	50,0
	TX30	0,83	196	CAU, K_0=0,5	50,4	51,1
	TX31	0,76	198	CAU, K_0=0,5	50,4	51,3
	TX32	0,81	200	CAU, K_0=0,5	50,4	51,3
Amostras finas reconstituídas	TX10	0,96	50	CID	71,3	68,3
	TX11	0,97	100	CID	71,4	72,3
	TX12	0,85	500	CID	71,5	73,8
	TX13	0,85	1000	CID	71,3	70,8
	TX22	0,91	200	CID	68,7	69,2
	TX23	0,87	200	CID	69,0	68,7
	TX24	0,84	356	CID	68,8	68,5
	TX26	0,99	198	CAU, K_0=0,5	66,7	68,9
	TX27	0,92	198	CAU, K_0=0,5	72,9	71,2
	TX28	0,82	198	CAU, K_0=0,5	72,9	70,9
	TX29	0,82	200	CAU, K_0=0,5	70,6	71,2
Amostras grossas reconstituídas	TX14	0,96	50	CID	32,9	30,0
	TX15	0,79	100	CID	32,3	28,9
	TX16	0,75	500	CID	32,3	29,4
	TX17	0,81	1000	CID	32,9	32,6
	TX25	0,88	198	CAU, K_0=0,5	28,0	28,7
	TXDW01	0,91[4]	86	CAD-DL, K_0=0,5	29,4	27,6
	TXDW02	0,88	150	CAU-DL, K_0=0,5	28,0	30,2
	TXDW03	0,87	75	CAU-DL-C, K_0 = 0,5 e 0,4	34,1	32,1

OBSERVAÇÕES:

[1]Índice de vazios antes do adensamento dos rejeitos fofos, estimado a partir dos resultados dos ensaios de índice de vazios medidos, resumidos no Apêndice B. Considerado o percentil 80 das amostras com gradação semelhante às das amostras de 4 de junho.

[2]Índice de vazios antes do adensamento dos rejeitos densos. Estimado a partir dos resultados dos ensaios de índice de vazios medidos, resumidos no Apêndice B. Considerado o percentil 20 das amostras com gradação semelhante às das amostras de 4 de junho.
[3]Tipo de ensaio: Ensaio não drenado adensado isotropicamente (CIU), ensaio drenado adensado isotropicamente (CID), ensaio não drenado adensado anisotropicamente (CAU), ensaio drenado adensado anisotropicamente (CAD).
[4]A amostra se rompeu durante o adensamento anisotrópico.

5.2.4 Resultados dos Ensaios Padrão com Deformação Controlada, CID, CIU, e CAU

Os resultados dos ensaios de compressão triaxial estão resumidos no Anexo 8. Estes resultados foram plotados, a fim de mostrar a variação do índice de vazios (*e*) versus tensão efetiva média (*p′*) e a tensão de desvio (*q*) versus *p′*. Foram produzidos gráficos para as três gradações representativas de rejeitos (fino, grosso e médio).

Linha de estado crítico (CSL)

A CSL é definida como a relação entre *e* e *p′* para uma determinada unidade de solo, em uma condição em que o solo sofrerá cisalhamento com volume constante e tensão constante de cisalhamento. Conforme mostrado na Figura 20 a Figura 22, foi selecionada uma relação de lei de potência não-linear como a melhor representação da CSL para as três gradações de rejeitos representativas. A relação curvada da CSL para todas as três gradações de rejeitos representativas (fina, grossa e média) foi representada pela seguinte equação:

Equação 5-1: $$e = A - B\left(\frac{p'}{p_{ref}}\right)^{C}$$

Em que:

- *p′* – Tensão efetiva média (kPa)
- p_{ref} – Condição de tensão de referência, tomada como 100 kPa
- *A* – Selecionado como 1,29, 1,19 e 1,22 para as gradações de rejeitos fino, grosso e médio, respectivamente
- *B* – Selecionado como 0,34 para todas as gradações de rejeitos
- *C* – Selecionado como 0,11 para todas as gradações de rejeitos

Uma relação linear alternativa para a CSL também foi calculada e pode ser representada pela seguinte equação:

Equação 5-2: $$e = \Gamma - \lambda_e \ln(p')$$

Em que:

- *p′* – Tensão efetiva média (kPa)

- Γ – índice de vazios na CSL a um p' de 1 kPa
- λ_e – inclinação da CSL

Γ para as gradações de rejeitos fino, grosso e médio foi calculado como Γ = 1,12, 1,01 e 1,04, respectivamente. λ_e para as gradações de rejeitos fino, grosso e médio foi calculado como 0,039.

Todas as três curvas de CSL foram plotadas em um gráfico para fazer comparações entre as CSLs de cada gradação (veja a Figura 19). Vale ressaltar que a inclinação da CSL foi a mesma para toda a faixa de gradações de rejeitos testadas.

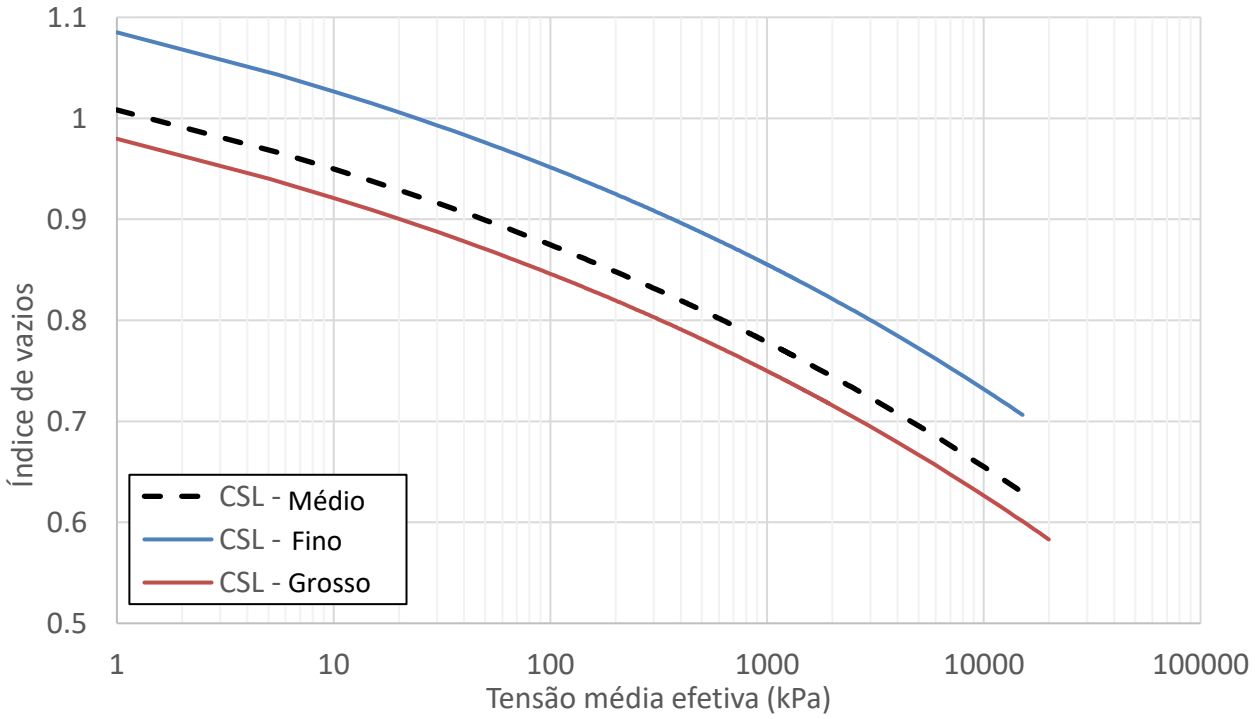


Figura 19: Curvas CSL de todas as três gradações de rejeitos testadas

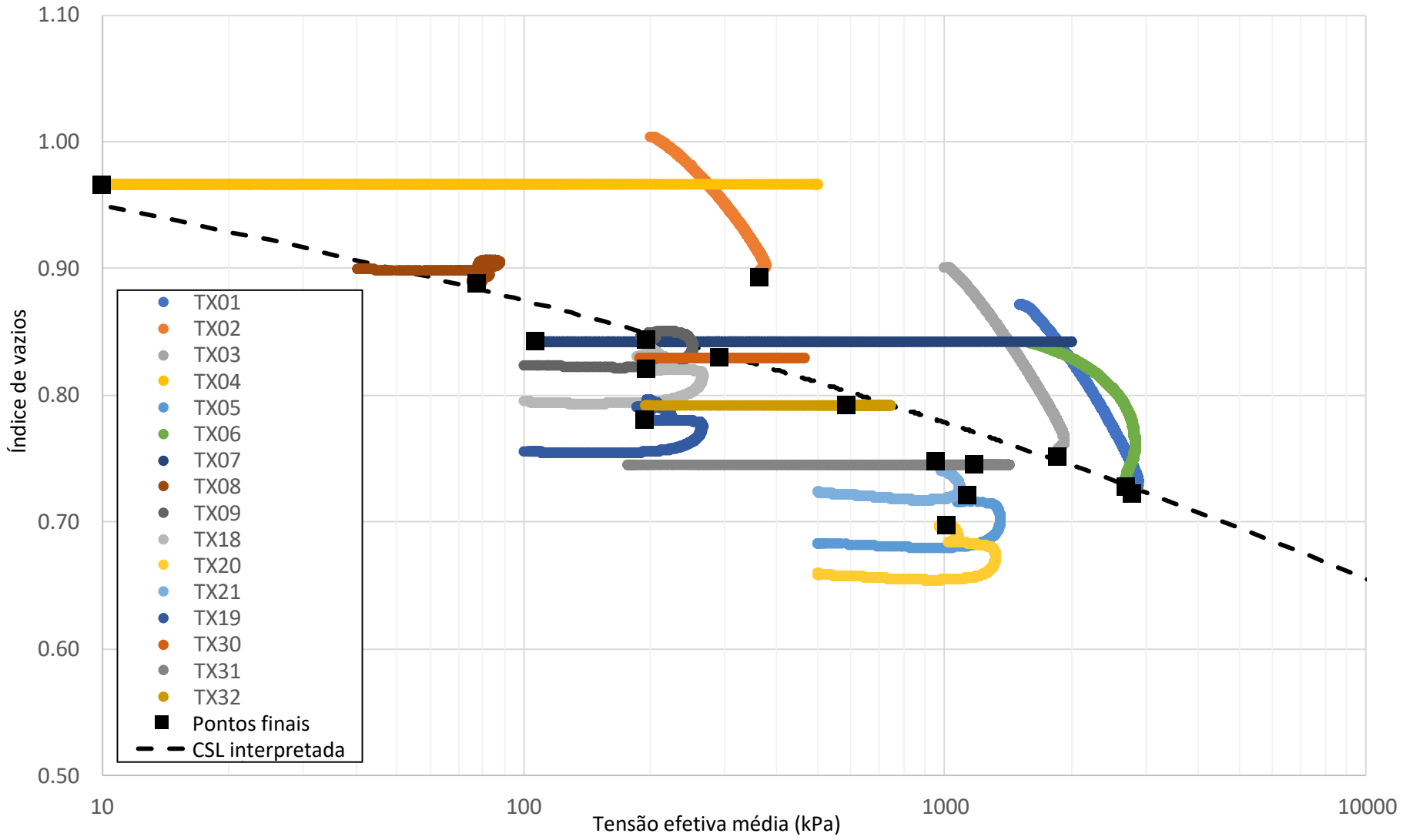


Figura 20: Gráfico de CSL para gradações de rejeitos médios testadas

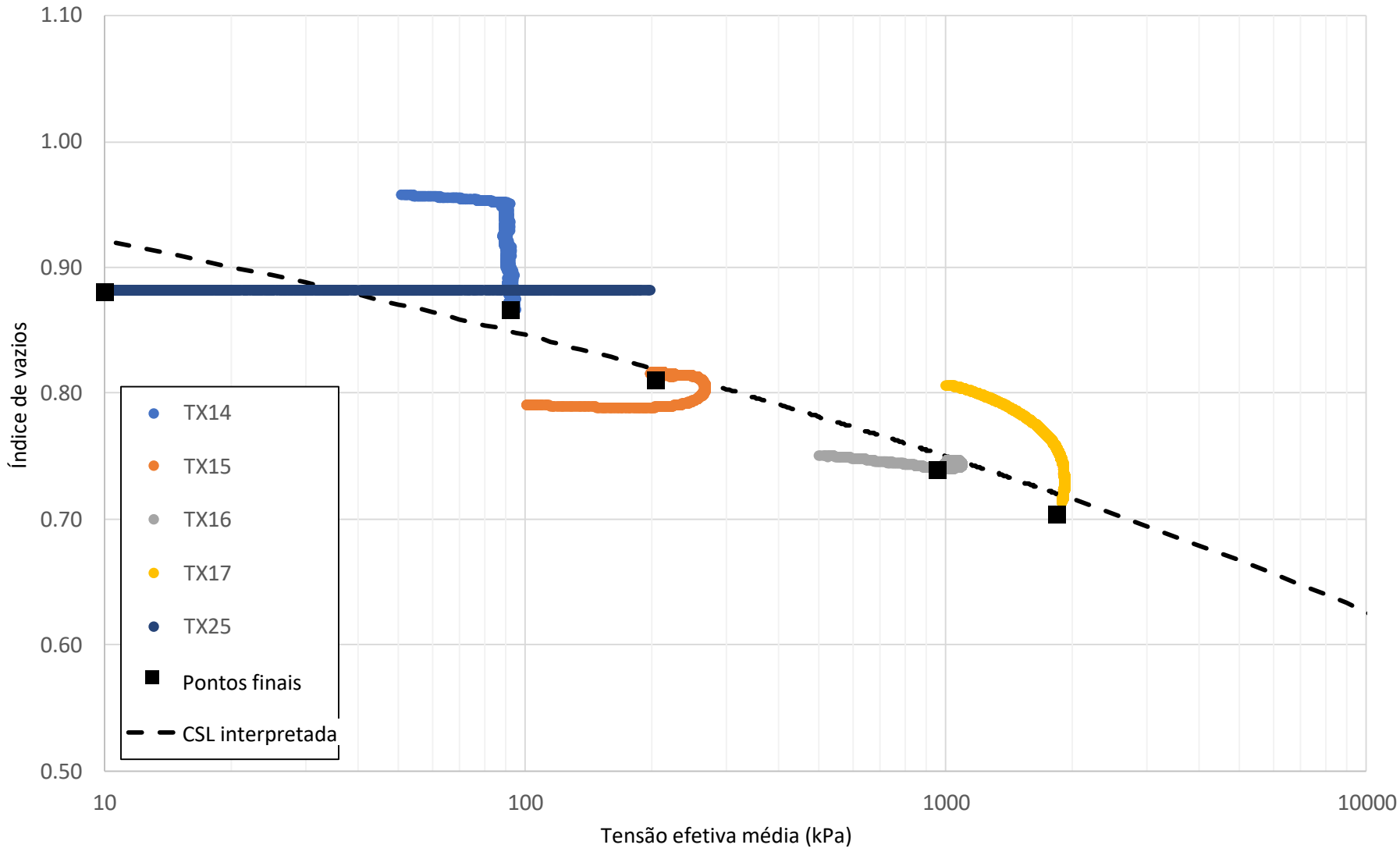


Figura 21: Gráfico de CSL para gradações de rejeitos grossos testadas

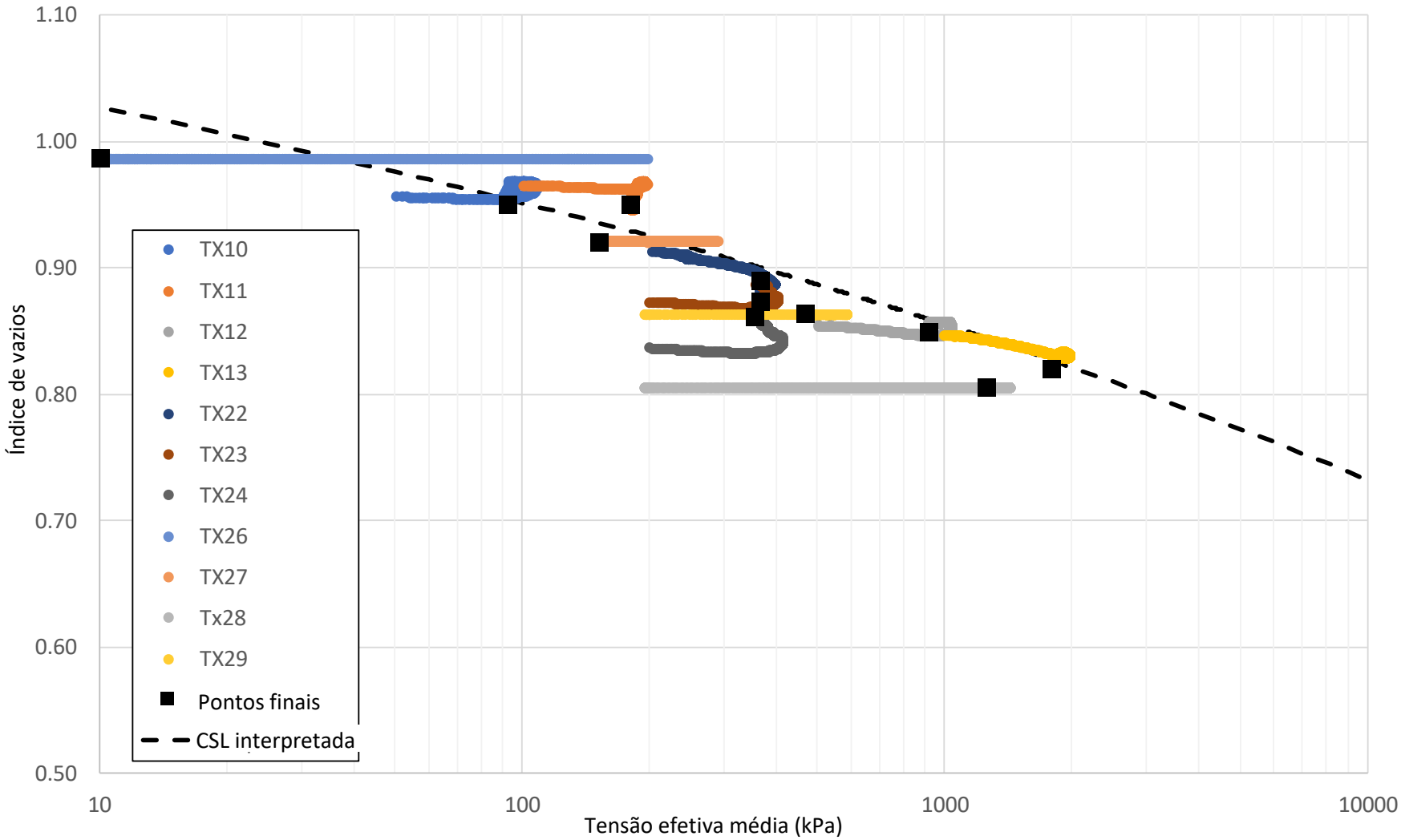


Figura 22: Gráfico de CSL para gradações de rejeitos finos testadas

Ângulo de atrito do estado crítico

As trajetórias de tensão para as três gradações de rejeitos representativas testadas são mostrados na Figura 23 a Figura 25 em um gráfico de *q* versus *p'*. O gradiente de uma linha traçada através dos pontos extremos destas trajetórias de tensão é chamado de razão de atrito do estado crítico (M_{tc}) e variou entre 1,35 e 1,39. Os ângulos equivalentes de atrito do estado crítico (ϕ'_c) para as gradações de rejeitos finos, grossos e médios testados são 34°, 34° e 33°, respectivamente. A faixa de valores de M_{tc} foi confirmada usando o intercepto da linha detendência em um gráfico da razão de tensão máxima (*q*/*p'*) versus dilatação mínima, que produziu o mesmo valor. Este gráfico é mostrado na Figura 43.

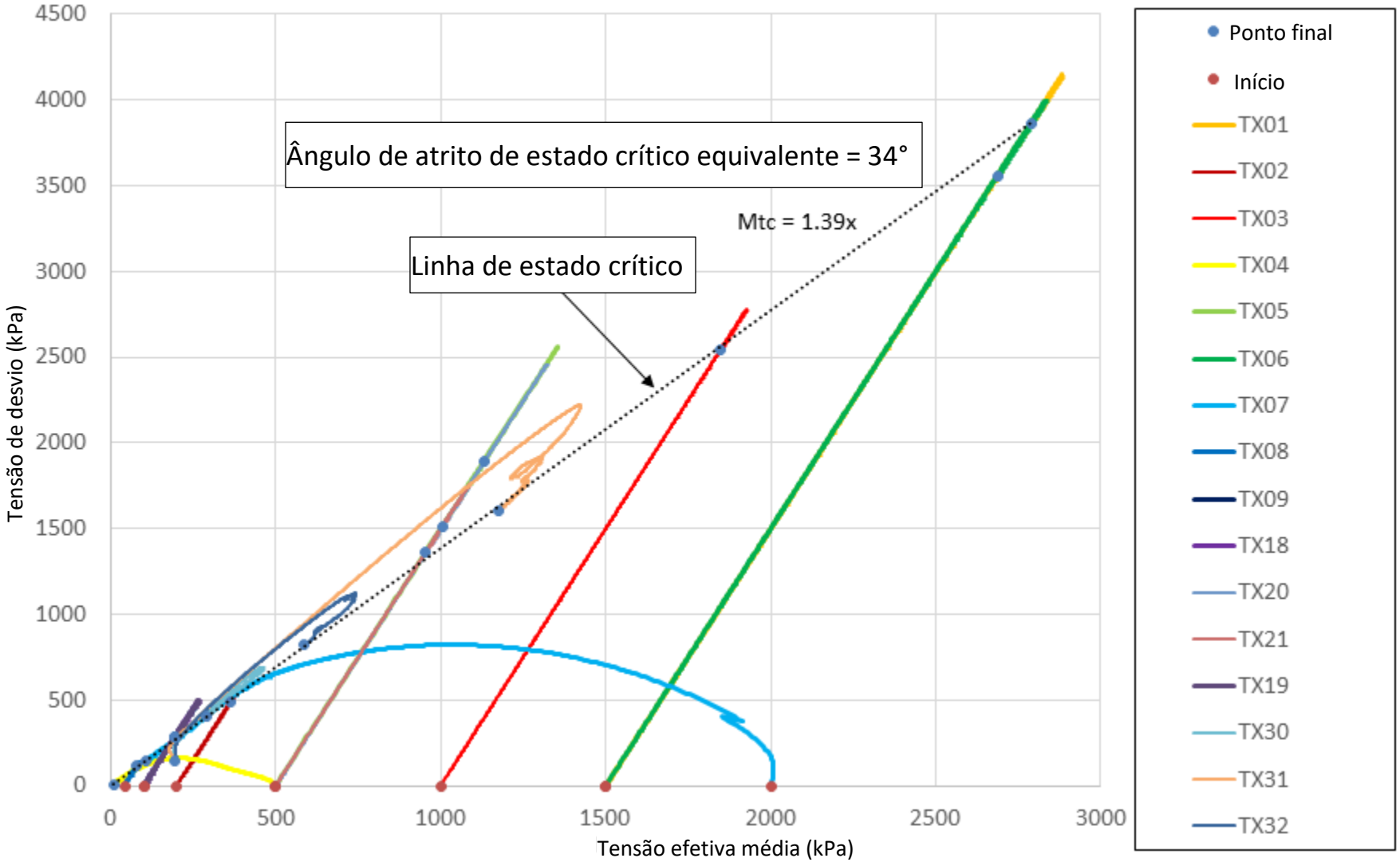


Figura 23: Trajetórias de tensão nos ensaios CID e CIU nas gradações de rejeitos médios

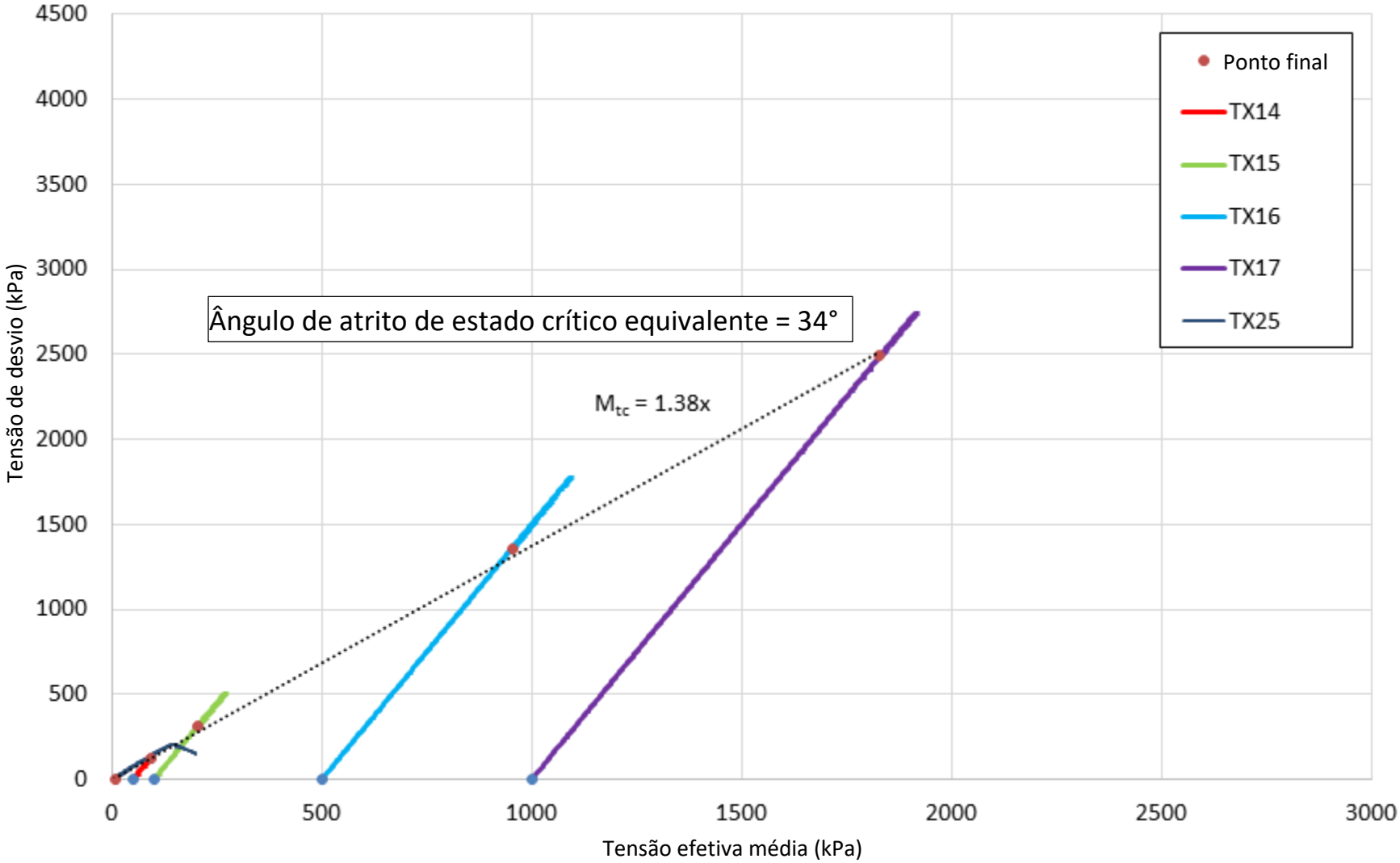


Figura 24: Trajetórias de tensão nos ensaios CID e CIU nas gradações de rejeitos grossos

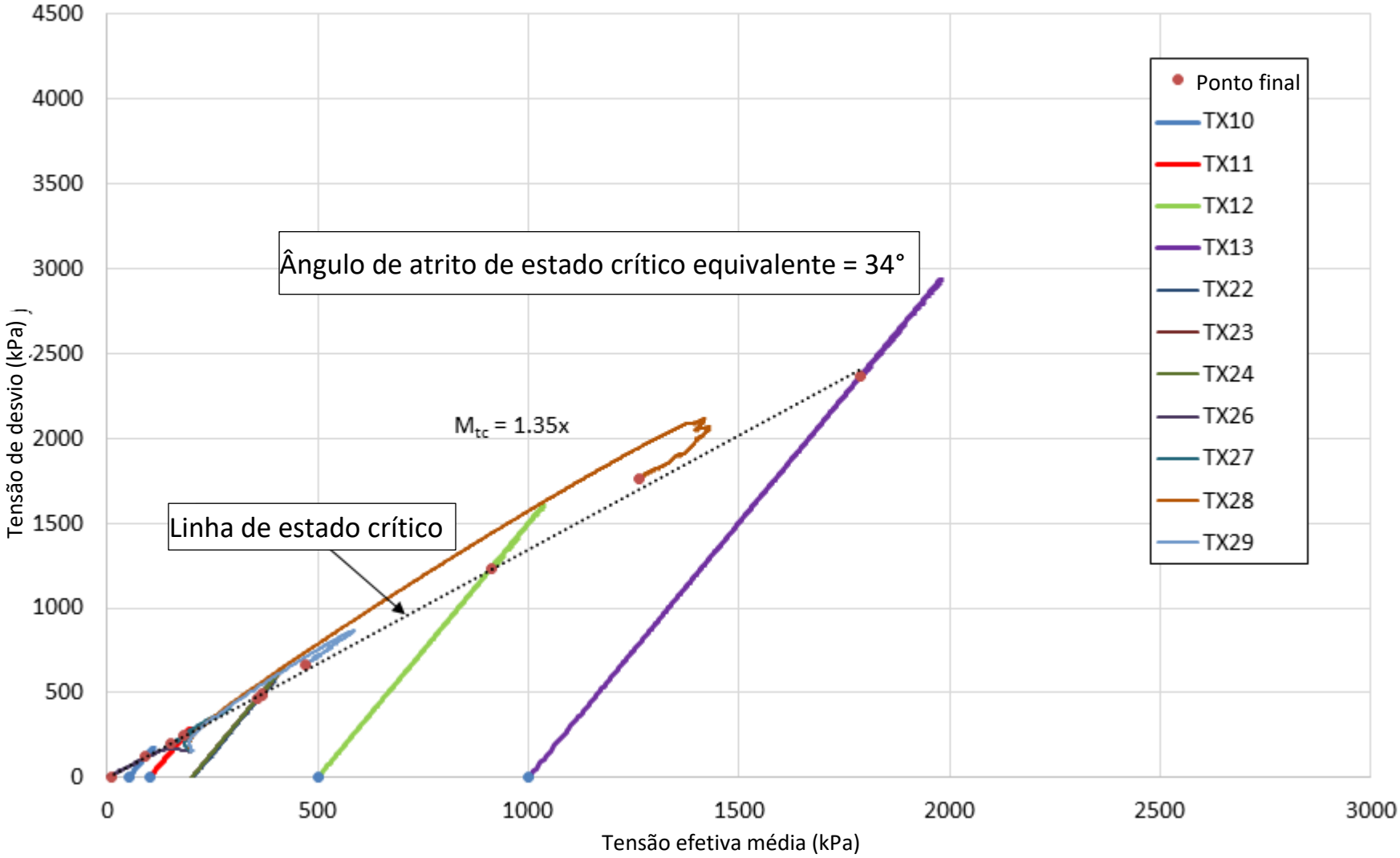


Figura 25: Trajetórias de tensão nos ensaios CID e CIU nas gradações de rejeitos finos

Resultados dos ensaios CAU

Oito ensaios triaxiais anisotropicamente adensados não drenados (CAU) foram realizados nas gradações de rejeitos finos, grossos e médios para avaliar a resposta não drenada das amostras em vários parâmetros de estado. Todas as amostras foram adensadas anisotropicamente para uma tensão efetiva média de 200 kPa e um K_0 de 0,5 antes de iniciar o carregamento não drenado. As amostras de gradação fina, grossa e média foram preparadas para um índice de vazios adensado que variou entre 0,76 e 0,99.

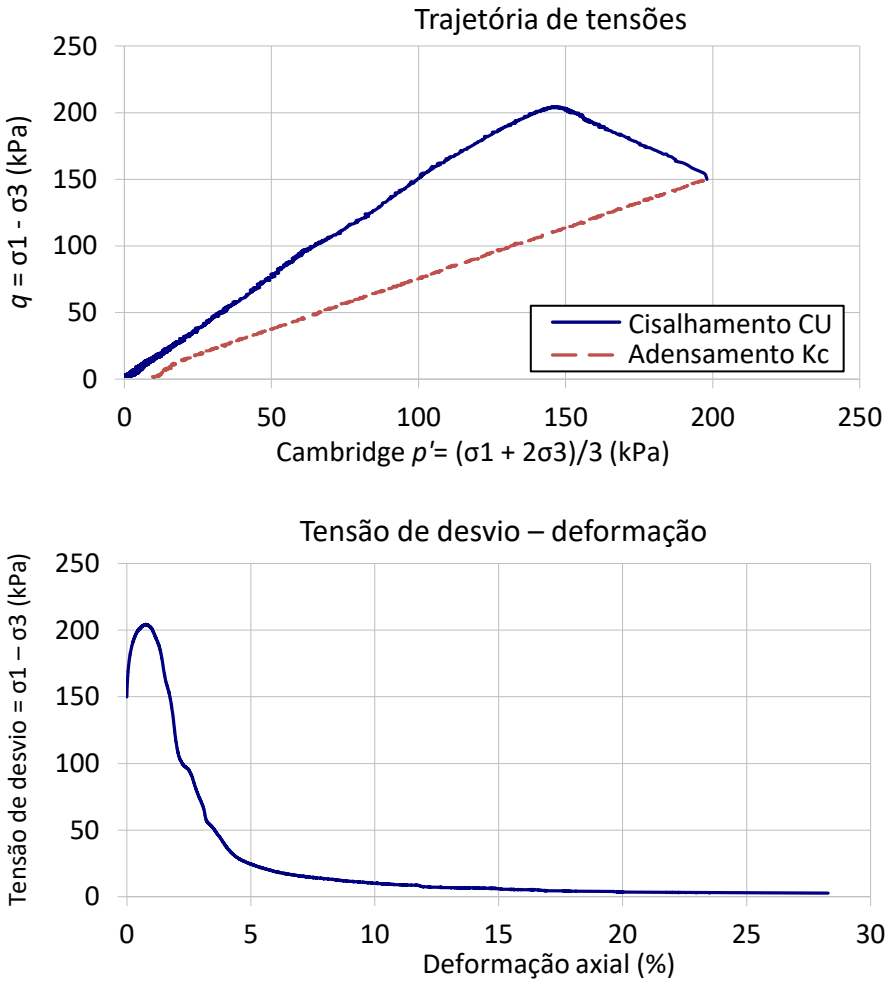
Os resultados de duas amostras fofas (ψ= +0,07), uma gradação de rejeitos finos e uma gradação de rejeitos grossos são comparados na Figura 26. Ambas as amostras geraram uma reação de comportamento extremamente frágil durante o carregamento não drenado. As amostras romperam nas deformações axiais de 0,3% e 0,8% para as gradações finas e grossas, respectivamente. As tensões de pico e desvio residual para as gradações finas foram de 167,3 kPa e 1,8 kPa, respectivamente. Para as gradações grossas, as tensões de pico e desvio residual foram de 204,4 kPa e 2,7 kPa, respectivamente. Isto equivale a razões de resistência de pico e residual (S_u/p') de 0,42 a 0,51 (equivalente a S_u/σ'_v = 0,28 a 0,34) e 0,005 a 0,01, respectivamente. As resistências de pico são significativamente mais altas que as estimativas empíricas baseadas em dados de ensaios de CPTu, como as de Olson e Stark (2003)[4], e as resistências residuais (ou liquefeitas) são significativamente menores que as estimativas empíricas, como as de Robertson (2010).[5]

Os resultados dos ensaios confirmaram que as gradações fina e grossa se comportam de maneira semelhante durante o cisalhamento não drenado.

[4] Olson, S., & Stark, T.D. (2003). Yield strength ratio and liquefaction analysis of slopes and embankments. *American Society of Civil Engineers Journal of Geotechnical and Geoenvironmental Engineering*, *129*(8), 727-737.

[5] Robertson, P.K. (2010). Evaluation of flow liquefaction and liquefied strength using the cone penetration test. *American Society of Civil Engineers Journal of Geotechnical Engineering*, *136*(6), 842-853.

Gradação grossa (TX25)



Gradação fina (TX26)

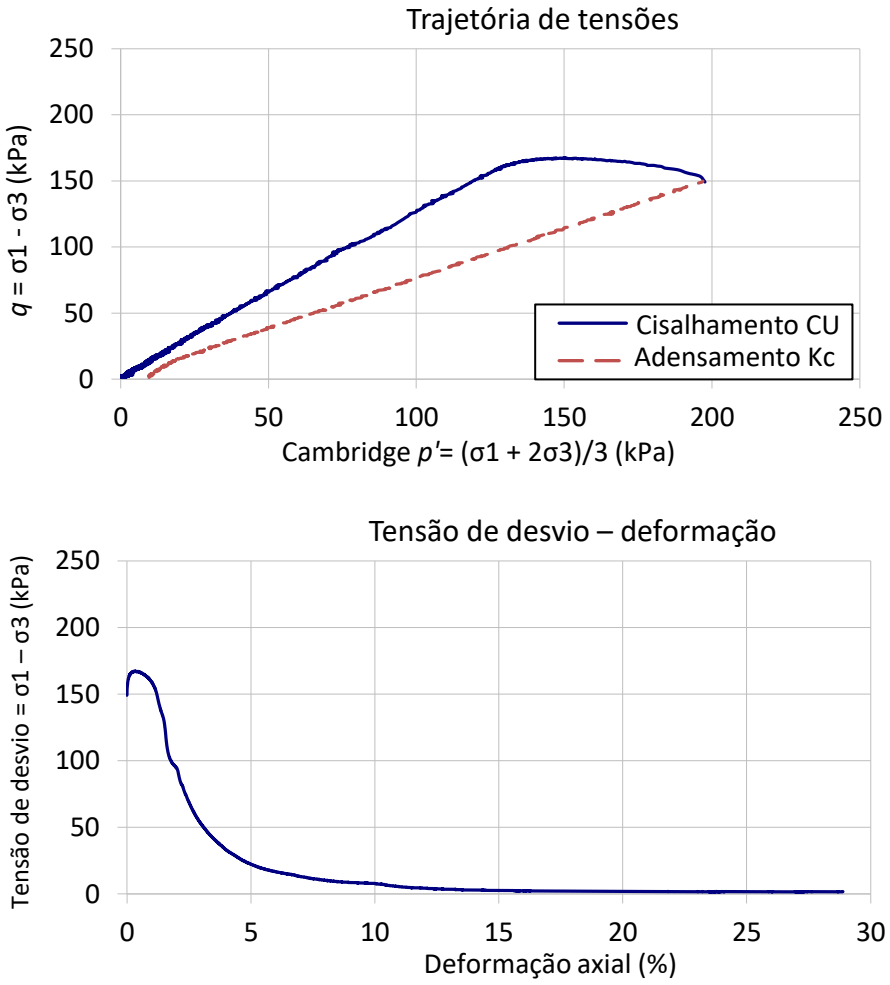


Figura 26: Resultados de ensaios triaxiais anisotrópicos não drenados com deformação controlada (CAU, K_0 = 0,5)

5.2.5 Resultadosdos Ensaios Com Carga Controlada

Dois ensaios com carga controlada foram realizados para comparação com os ensaios com deformação controlada. Ambos ensaios foram realizados na gradação de rejeitos grossos. O primeiro ensaio (TXDW01) foi realizado como um ensaio drenado e foi destinado a replicar o ensaio TX14, que era um ensaio CID com deformação controlada realizado com uma tensão efetiva média inicial de 50 kPa e um parâmetro de estado de +0,09. Este ensaio mostrou uma redução abrupta no volume em torno de 1% de deformação específica, com uma tensão efetiva média constante (p') de aproximadamente 90 kPa e tensão de desvio (q) de aproximadamente 120 kPa (veja a Figura 21). O objetivo do ensaio com carga controlada equivalente foi verificar se esta redução volumétrica levaria à geração de poro-pressão e perda de resistência sob uma carga constante. O ensaio com carga controlada equivalente foi adensado anisotropicamente para tensões próximas àquelas em que houve ruptura em TX14; no entanto, a amostra se rompeu rapidamente em p'= 86 kPa e q = 110 kPa (veja a Figura 27).

O segundo ensaio com carga controlada (TXDW02) foi realizado para comparação com o ensaio CAU com deformação controlada (TX25) realizado com uma tensão efetiva média inicial de 200 kPa e um K_0 de 0,5. Exceto na aplicação de carga do peso morto, o TXDW02 foi realizado exatamente da mesma maneira que o TX25. O TXDW02 sofreu ruptura em uma deformação específica axial de 0,7% e gerou um pico q de 220,8 kPa (veja a Figura 28). Isto equivale a uma razão de resistência de pico (S_u/p') de 0,55. A razão de resistência residual desta amostra não pôde ser medida porque a ruptura ocorreu de maneira rápida e levou à ruptura completa da amostra. Estes resultados são semelhantes aos do ensaio por deformação controlada equivalente (TX25), ilustrando a consistência geral entre os métodos de ensaio.

5.2.6 Resultados do Ensaio com Carga Controlada com *Creep*

O ensaio de carga controlada com *creep* (CAU-DL-C – consulte a seção 5.2.3) foi realizado para avaliar o potencial de acúmulo de deformação com o tempo em que uma amostra de rejeitos fofos é carregada em vários níveis de tensão. Isto foi investigado carregando a amostra nos valores K_0 atribuídos e mantendo a carga aplicada constante. Durante a primeira etapa deste ensaio, a amostra foi carregada para um K_0 de 0,5 com uma tensão efetiva média (p') de 100 kPa e uma tensão de desvio (q) de 74 kPa. A amostra foi então mantida nestes valores de p' e q com as válvulas de drenagem abertas por 4.012 minutos. Durante este período, a amostra acumulou 0,05% de deformação específica axial.

A segunda etapa do ensaio envolveu diminuir o K_0 para 0,4 no mesmo valor de p', aumentando o q para 100 kPa. A amostra foi então mantida nestes valores de p' e q por 2.539 minutos; desta vez com as válvulas de drenagem fechadas. A amostra acumulou 0,13% de deformação específica axial durante este período. As válvulas de drenagem foram então reabertas e a amostra foi adensada anisotropicamente até uma meta de K_0 de 0,3. A amostra sofreu ruptura durante este adensamento anisotrópico em um K_0 de 0,33. Como o ensaio estava sendo realizado usando um equipamento de carga controlada, esta ruptura da amostra levou ao rápido acúmulo de deformação e o ensaio não pôde continuar.

Resultados com deformação controlada (CID – TX14) – estágio de cisalhamento

Resultados com carga controlada (TXDW01) – Somente estágio de adensamento anisotrópico

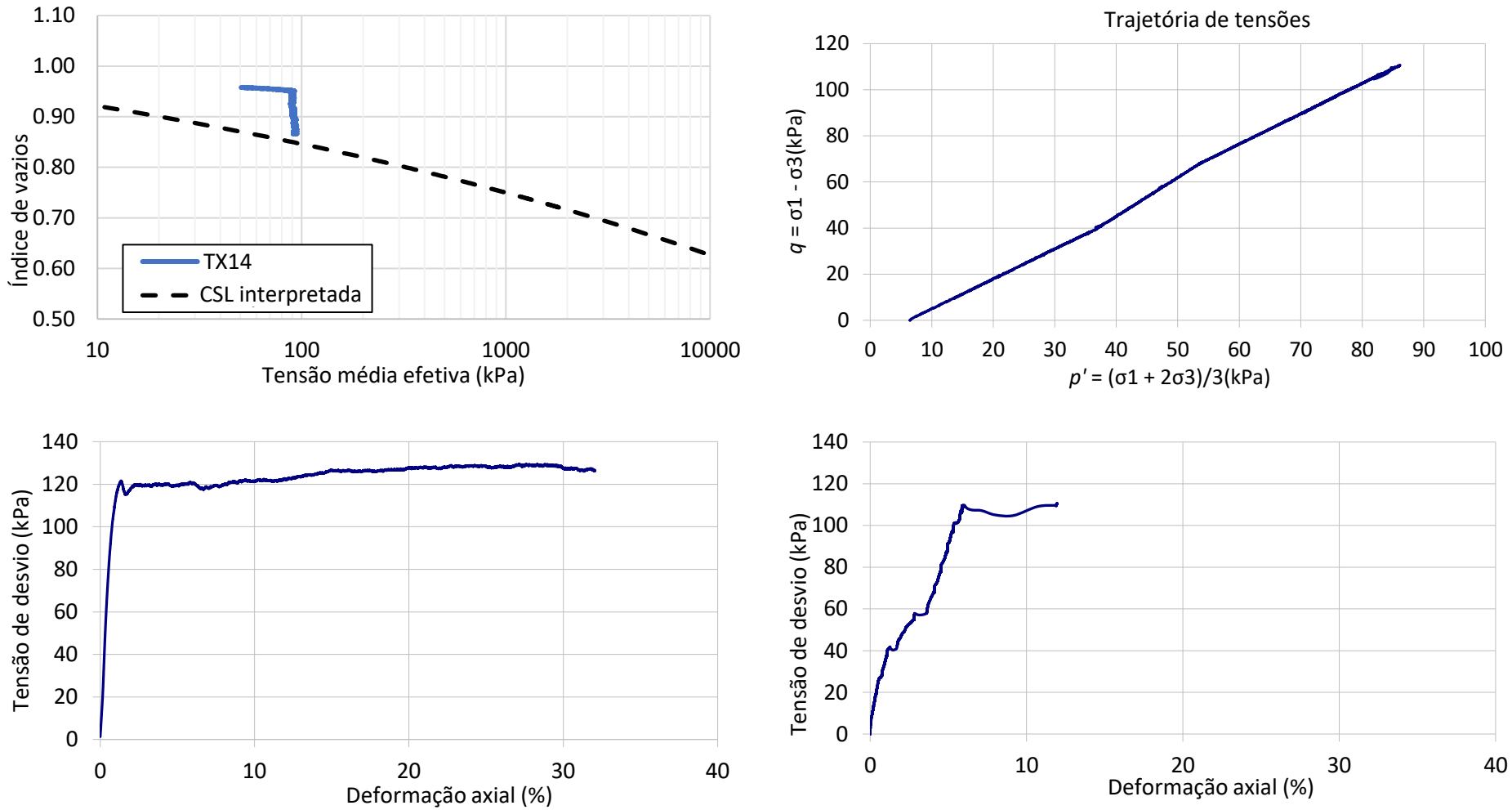
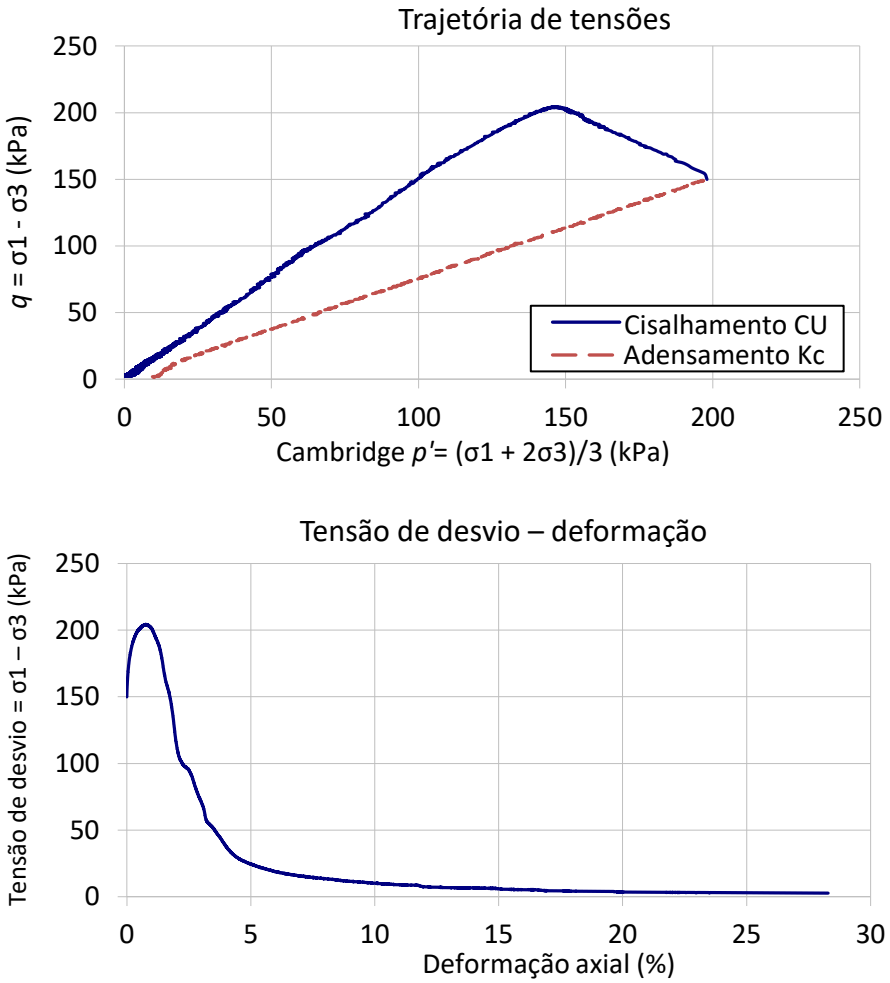


Figura 27: Comparação de TX14 e TXDW01

Resultados do ensaio CAU com carga controlada (TXDW03)



Resultados do ensaio CAU com carga controlada (TXDW02)

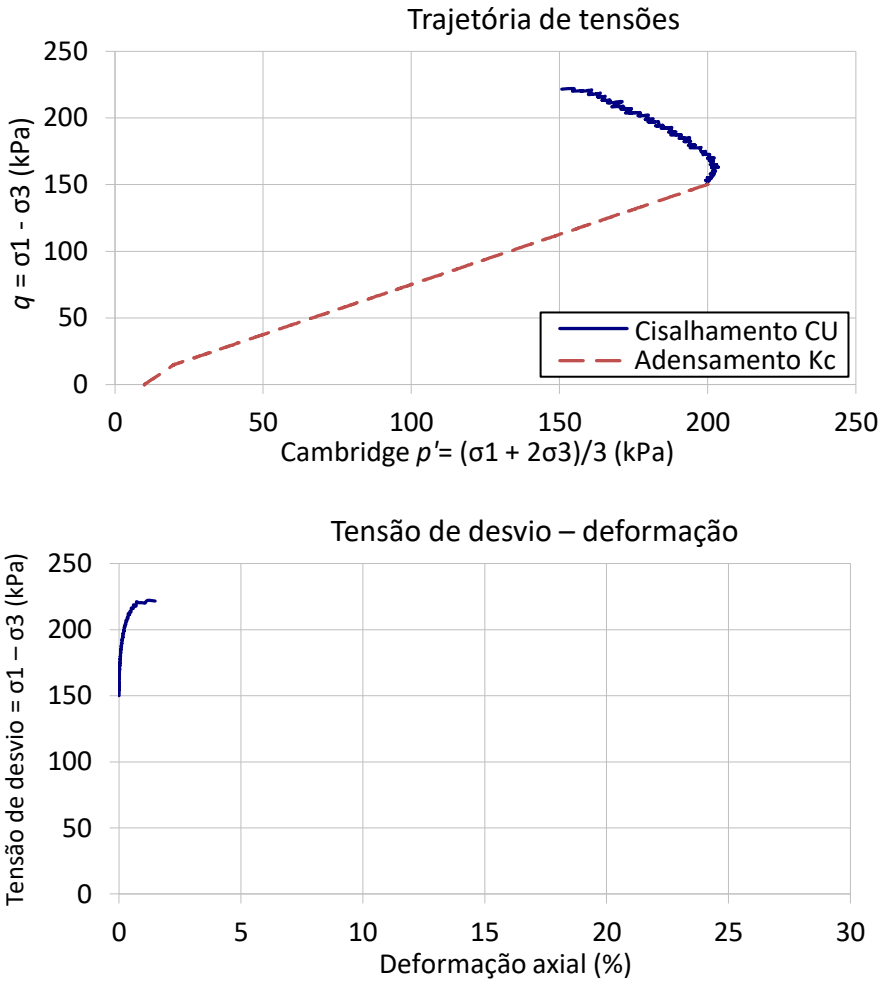
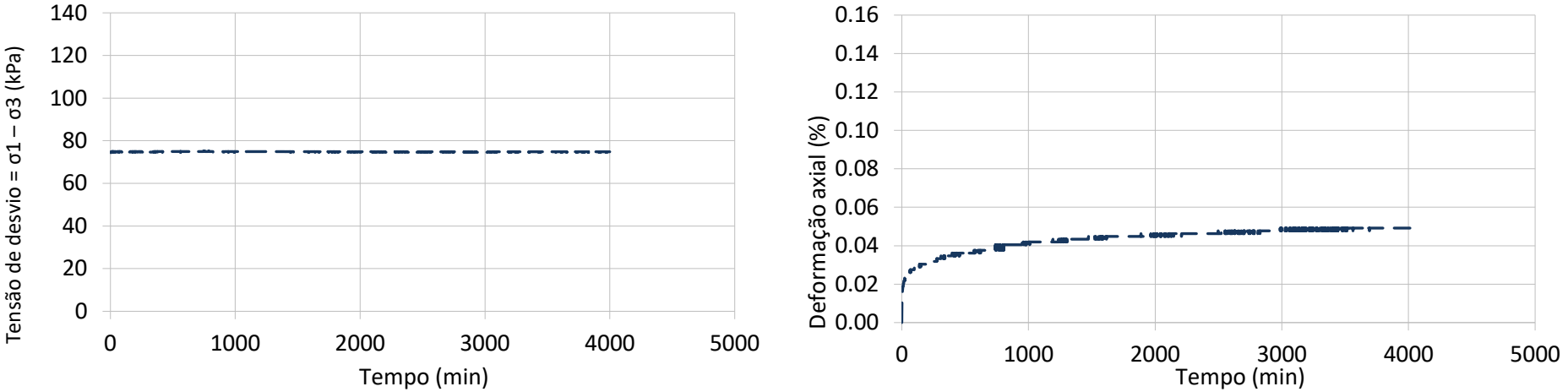


Figura 28: Comparação dos resultados dos ensaios triaxiais com deformação controlada e carga controlada

Coeficiente de tensão lateral (K_0) = 0,5



Coeficiente de tensão lateral (K_0) = 0,4

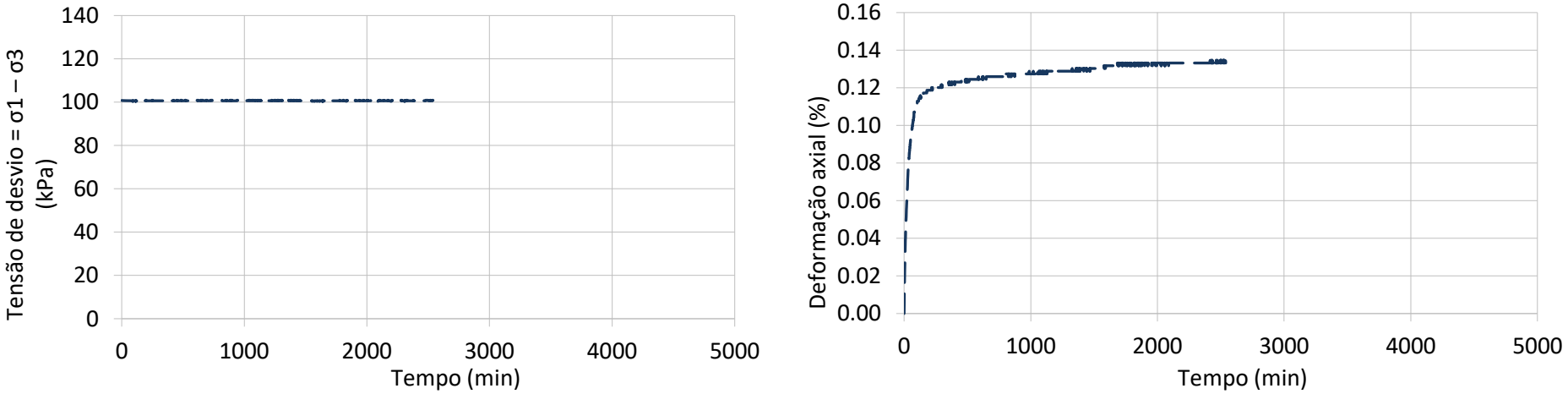


Figura 29: Resultados do ensaio CAU com carga controlada(TXDW03) – K_0 = 0,5 para 0,4

Coeficiente de tensão lateral (K_0) = 0,4 a 0,3

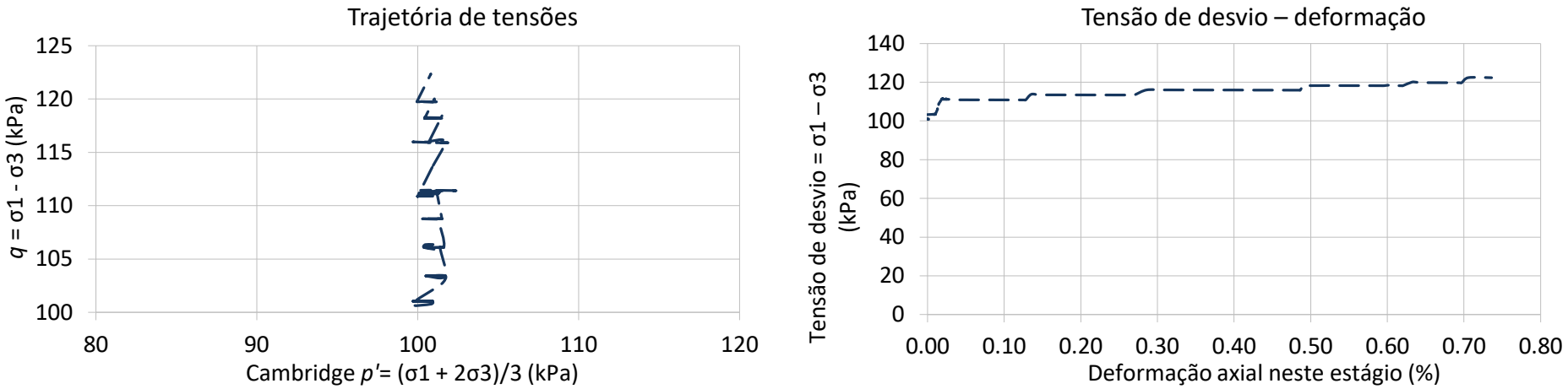


Figura 30: Resultados do ensaio CAU com carga controlada (TXDW03) – K_0 = 0,4 e 0,3

5.3 Ensaio com *Bender Element*

5.3.1 Escopo

Os ensaios com *bender element* foram realizados em amostras separadas, isotropicamente adensadas, para os ensaios triaxiais descritos na Seção 5.2, durante todo o estágio de adensamento dos ensaios, para determinar uma relação entre e, p' e V_s.

5.3.2 Procedimento

No momento, não existe um padrão internacionalmente aceito para o ensaio com *bender elements*. O ensaio foi realizado seguindo as recomendações descritas em "Interpretataion of International Parallel Test on the Measurement of G_{max} using Bender Elements" (Yamashita et al. 2009).[6]

O sistema LoadTrac-II/FlowTrac-II da Geocomp com sistema WaVeMe incorporado foi usado para adensar os corpos de prova e medir o tempo de deslocamento da onda, a fim de obter velocidades de onda de cisalhamento em diferentes estágios de adensamento. O sistema WaVeMe consiste em placas piezo-cerâmicas, conhecidas como sensores P e S, normalmente denominadas com *bender elements*. Um sinal elétrico foi aplicado aos sensores transmissores, a fim de distorcer o corpo de prova e induzir um potencial de tensão para produzir um sinal. O potencial de entrada e saída foi gravado continuamente e o tempo de deslocamento foi determinado.

O tempo de chegada da onda S foi medido usando uma única onda S em diferentes frequências, variando de 5 kHz a 15 kHz, conforme recomendado por Yamashita et al. (2009).

As velocidades das ondas de cisalhamento foram calculadas usando a seguinte fórmula:

Equação 5-3:
$$V_s = \frac{H_t}{T_s}$$

Em que:

- H_t = Distância entre as duas pontas do elemento flexor, que depende da altura da amostra em diferentes incrementos da carga de adensamento.
- T_s = tempo de chegada da onda S, determinada usando o método do domínio de tempo.

O tempo de viagem da onda S foi determinado usando a distância entre as duas pontas do elemento flexor (e a altura da amostra) em diferentes incrementos da carga de adensamento.

[6] Yamashita, S., Kawaguchi, T., Nakata, Y., Mikami, T., Fujiwara, T., & Shibuya, S. (2009). Interpretation of international parallel test on the measurement of G_{max} using bender elements. *Soils and Foundations*, *49*(4), 631-650.

O módulo de cisalhamento (G_{max}) foi calculado usando a seguinte fórmula:

Equação 5-4: $$G_{max} = \rho * V_s^2$$

Em que:

- ρ = Densidade a cada incremento de carga de adensamento.

5.3.3 Resultados

Os ensaios com *bender elements* foram realizados em gradações de rejeitos fofos e densos (fino, grosso e médio), adensados a 1500 kPa. As amostras foram colocadas em um índice de vazios, e_i, variando de 0,7 a 1,2. Um resumo dos ensaios completos dos elementos flexores é apresentado na Tabela 14. Os resultados dos ensaios estão detalhados no Anexo 8.

Tabela 14: Resumo dos ensaios de elementos flexores

Material	Nº do ensaio	Índice inicial de vazios	Pressão de adensamento (kPa)
Gradação média	TXBD01	1,2	50, 100, 200, 400, 600, 800, 1000, 1200, 1500
	TXBD02	0,9	50, 100, 200, 400, 600, 800, 1000, 1200, 1500
	TXBD03	1,0	50, 100, 200, 400, 600, 800, 1000, 1200, 1500
	TXBD08	0,8	50, 100, 200, 400, 600, 800, 1000, 1200, 1500
Gradação fina	TXBD04	1,1	50, 100, 200, 400, 600, 800, 1000, 1200, 1500
	TXBD05	0,9	50, 100, 200, 400, 600, 800, 1000, 1200, 1500
	TXBD10	0,7	50, 100, 200, 400, 600, 800, 1000, 1200, 1500
Gradação grossa	TXBD06	1,1	50, 100, 200, 400, 600, 800, 1000, 1200, 1500
	TXBD07	0,9	50, 100, 200, 400, 600, 800, 1000, 1200, 1500
	TXBD09	0,7	50, 100, 200, 400, 600, 800, 1000, 1200, 1500

Os dados foram plotados como velocidade de onda de cisalhamento normalizada (V_{s1}) versus índice de vazios, usando a abordagem de Cunning et al. (1995),[7] a fim de desenvolver relações de índices de vazios, velocidade de onda de cisalhamento e tensão efetiva média que poderiam ser usadas para estimar o índice de vazios in situ a partir dos resultados do V_s. Verificou-se que os dados de gradação grossa e média podiam ser ajustados com a mesma relação, ao passo que uma relação diferente foi desenvolvida para os dados de gradação fina.

[7] Cunning, J.C., Robertson, P.K., & Sego, D.C. (1995). Shear wave velocity to evaluate in situ state of cohesionless Soils. *Canadian Geotechnical Journal*, *32*, 848-858.

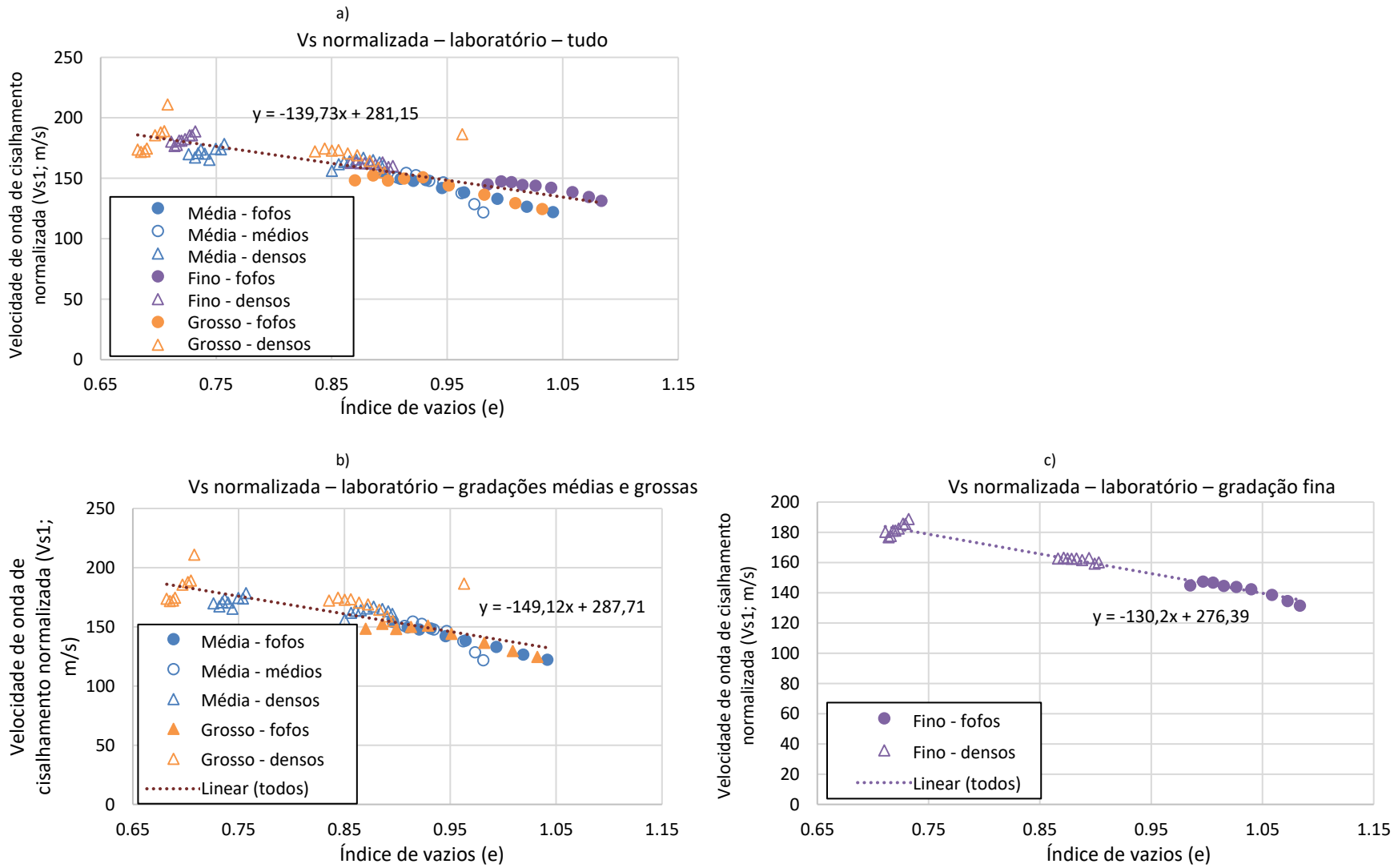


Figura 31: Relações de velocidade de onda de cisalhamento normalizada versus índice de vazios para: a) todos os dados, b) gradações médias e grossas e c) gradação fina

5.4 Ensaios de Cisalhamento Direto Simples

5.4.1 Escopo

Seis ensaios de cisalhamento direto simples (DSS) com carregamento monotônico foram realizados em amostras de tubos Shelby dos solos da fundação, coletados no Programa 2, a fim de medir o pico de resistência ao cisalhamento não drenado e rigidez. Cada tubo Shelby foi escaneado usando aparelho de raios-X para produzir uma imagem do material dentro do tubo. Isto serviu para verificar se o material sofreu deformação no processo de sondagem ou transporte. Estas imagens também foram usadas para determinar seções de amostras que seriam usadas para os ensaios DSS. As imagens dos raios-X são mostradas no Anexo 8. Os corpos de prova foram cisalhadas com um máximo de 20% de deformação específica de cisalhamento antes de reverter a direção de cisalhamento e completar um ciclo de cisalhamento na direção oposta. Os corpos de prova foram cisalhados a uma taxa de 5%/h.

5.4.2 Procedimento

Os ensaios de DSS foram realizados de acordo com a norma ASTM D6528. Todo o cisalhamento foi realizado sem drenagem, mantendo o volume da amostra constante. Isto foi feito alterando a carga vertical automaticamente, de modo que a altura da amostra permanecesse constante. Os corpos de prova DSS foram adensados com pressões de confinamento de 350 kPa, 370 kPa, 520 kPa e 800 kPa. Estas pressões de confinamento foram selecionadas para serem maiores que a tensão efetiva vertical a que o solo estava sujeito nestes locais antes do rompimento da barragem.

Um resumo das amostras usadas para os ensaios DSS é mostrado na Tabela 15.

Tabela 15: Tabela resumida dos ensaios de DSS

Número da amostra	Pressões de confinamento (kPa)	Elevação aproximada da amostra (m)
BH-01 Tubo Shelby 01	520	860,0
BH-01 Tubo Shelby 02	520	859,2
BH-02 Tubo Shelby 01	800	854,2
BH-02 Tubo Shelby 02	800	853,1
BH-04 Tubo Shelby 01	350	855,2
BH-04 Tubo Shelby 02	370	853,5

5.4.3 Resultados dos Ensaios

Um resumo dos resultados dos ensaios de DSS é apresentado na Tabela 16 e os resultados estão detalhados no Anexo 8. Os resultados dos ensaios selecionados estão ilustrados na Figura 32. A razão de pico de resistência ao cisalhamento não drenado variou de 0,29 a 0,43. O pico foi tipicamente atingido acima de 10% da deformação específica de cisalhamento e não houve perda significativa de resistência

no ciclo inicial de cisalhamento. Estes resultados sugerem que os solos da fundação (solo residual) não desenvolveram um comportamento frágil durante o cisalhamento não drenado.

Tabela 16: Resumo dos ensaios de DSS

ID do ensaio	Teor de umidade		Índice de vazios		Deformação específica axial após adensamento (%)	Tensão efetiva vertical, σ'_{vc} (kPa)	Resistência de pico ao cisalhamento não drenado (kPa)	Relação de poro-pressão em excesso máxima, $\Delta U/\sigma'_{vc}$	Taxa de tensão máxima não drenada, τ/σ'_{vc}
	Inicial, W_i (%)	Final, W_f (%)	Na colocação, e_i	Índice de vazios final, e_0 (1)					
DSS01 BH-01	35	37	1,06	1,17	8	520	175	386	0,34
DSS02 BH-01	38	40	1,21	1,15	7	520	184	406	0,35
DSS03 BH-02	43	43	1,31	1,40	10	800	221	657	0,28
DSS04 BH-02	29	29	0,96	0,85	9	800	199	630	0,25
DSS05 BH-04	36	42	1,25	1,21	5	350	154	272	0,44
DSS06 BH-04	30	30	0,94	0,91	9	370	131	303	0,35

OBSERVAÇÃO:
[1]Os índices de vazios após o adensamento foram calculados usando medidas de altura

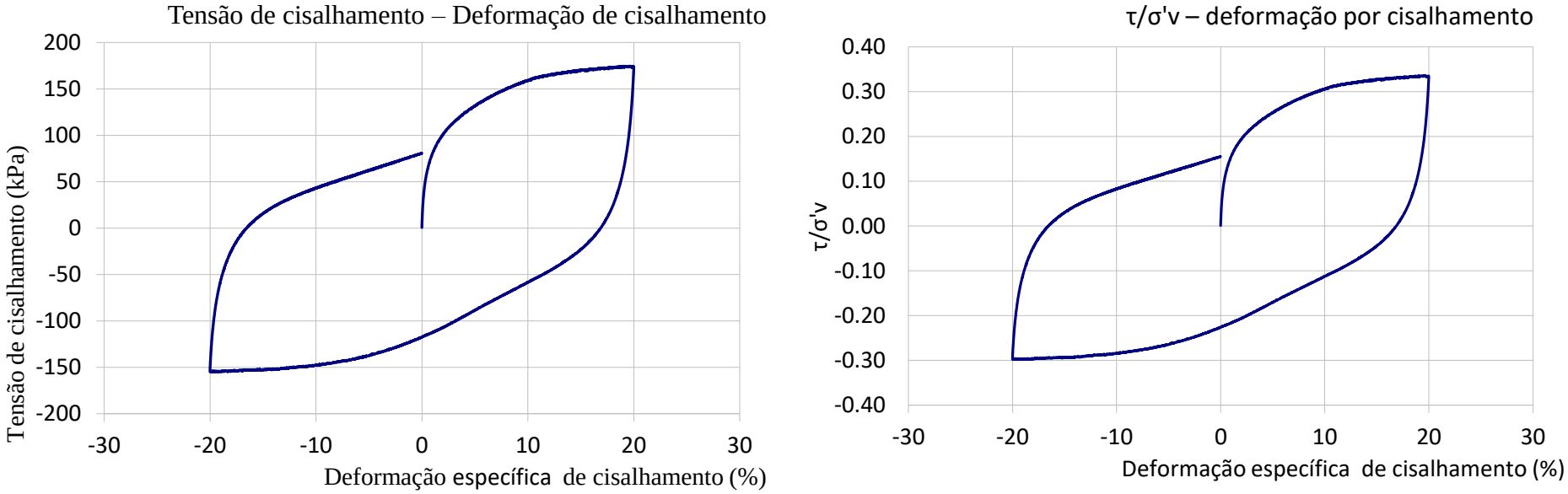


Figura 32: Resultados dos ensaios de DSS (DSS01) – Material da fundação do solo residual

6 PARÂMETROS DOS ENSAIOS DE CAMPO E DE LABORATÓRIO USADOS NA ANÁLISE DE DEFORMAÇÃO

6.1 Geral

Os parâmetros foram calculados a partir dos dados de campo e de laboratório, com o objetivo principal de concluir as análises de deformação e estabilidade destinadas a simular as condições anteriores ao rompimento da barragem e testar possíveis mecanismos e gatilhos de rompimento. As análises são discutidas no Apêndice H. Os parâmetros necessários para as várias análises foram:

- Análises de deformação de Mohr-Coulomb – Módulos de elasticidade, pico de resistência ao cisalhamento drenada, resistência ao cisalhamento não drenada e resistência ao cisalhamento residual não drenada. Estes foram derivados de dados de ensaios triaxiais. Os valores dos módulos atribuídos foram informados pelo parâmetro de estado estimado dos rejeitos derivados do ensaio de CPTu.

    - Este modelo foi utilizado para as análises iniciais de deformação bidimensional (2D) e tridimensional (3D).

- Análises de deformação por *strain-weakening* – Os parâmetros foram os mesmos que os exigidos para as análises de Mohr-Coulomb, exceto que, nestas análises, as resistências de pico e residual são especificadas na mesma análise, assim como a deformação relativa necessária para a transição de pico para residual. A deformação na qual ocorre a perda de resistência pós-pico e a deformação na resistência residual foram informadas pelo parâmetro de estado estimado dos rejeitos, derivados dos ensaios de CPTu.

Este modelo foi utilizado para as análises finais de deformação bidimensional (2D) e tridimensional (3D). As tendências desenvolvidas para os parâmetros deste modelo foram consideradas a melhor representação da resposta do solo.

- Análises de deformação de estado crítico (usando o modelo constitutivo NorSand) – Propriedades de estado crítico, parâmetros de dilatação, densidade in situ (ou parâmetro de estado) e módulos de elasticidade. Os parâmetros de estado crítico e de dilatação foram derivados dos dados triaxiais. O parâmetro de estado in situ foi estimado a partir dos dados dos ensaios de CPTu e os módulos de elasticidade foram estimados a partir dos dados dos *bender elements* e do V_s.

Este modelo foi utilizado para análises de sensibilidade nas análises de deformação bidimensionais (2D). Ele também foi utilizado para análises de expansão de cavidade esférica como parte da interpretação dos ensaios de CPTu.

- Análises de estabilidade – Resistências ao cisalhamento não drenadas, de pico e liquefeitas, derivadas de dados de ensaios triaxiais e comparadas com dados de ensaios de CPTu.

As abordagens para derivar estes parâmetros e os resultados obtidos são descritos nas seções a seguir.

6.2 Dados de Entrada do Modelo Mohr-Coulomb

Os módulos de elastacidade e os parâmetros de resistência selecionados para as análises de Mohr-Coulomb foram calculados como módulos secantes a partir dos dados dos ensaios de compressão triaxial drenada. Simulações dos ensaios triaxiais foram concluídas usando o software de diferenças finitas FLAC, versão 8.0, em um elemento como uma verificação para confirmar que os módulos e resistências ao cisalhamento calculados estavam produzindo resultados representativos. Os ensaios em um elemento realizados como parte deste trabalho são mostrados no Anexo 8.

6.2.1 Parâmetros Drenados

Um módulo de Young secante (E) foi calculado em 50% do pico de tensão, e uma razão de Poisson drenada (ν) de 0,2 foi assumida para todos os rejeitos (a análise não foi sensível a este parâmetro). Os módulos de cisalhamento (G) e volumétrico (K) foram calculados a partir destes resultados para inserção nas análises.

Foram desenvolvidas relações de K e G versus parâmetro de estado. Para generalizar as relações, os valores do módulo foram normalizados pela tensão efetiva médio. Estas relações são mostradas na Figura 33 e Figura 34.

Também foi desenvolvida uma relação de ângulo de atrito de pico (ϕ') versus parâmetro de estado para uso nas análises. Esta avaliação identificou uma característica incomum dos rejeitos nesta investigação. É típico que amostras fofas desenvolvam um ângulo de atrito de pico igual ao ângulo de atrito de estado crítico; no entanto, para as amostras testadas, o ângulo de atrito de pico era tipicamente quase dois graus mais alto que o ângulo de atrito de estado crítico de 34°, discutido na Seção 5.2.4. Isto é interpretado como um reflexo da cimentação presente nestes rejeitos, devido a seu alto teor de ferro e à oxidação do ferro.

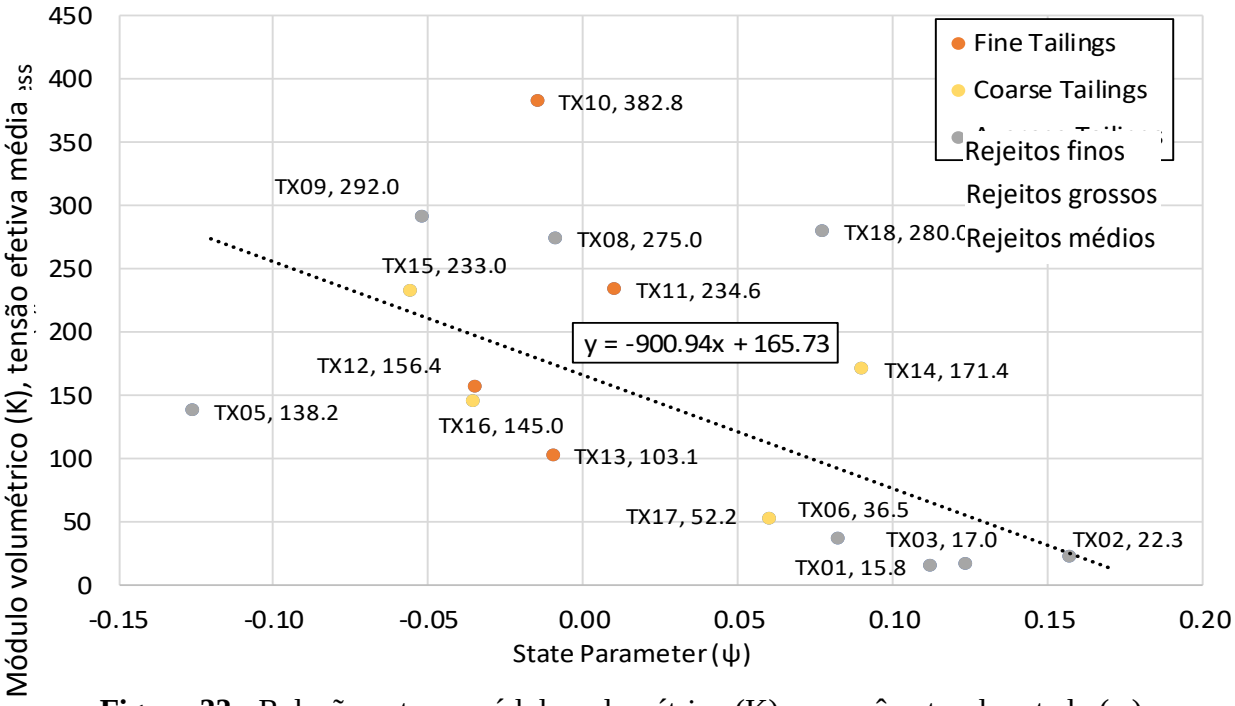


Figura 33: Relação entre o módulo volumétrico (K) e o parâmetro de estado (ψ)

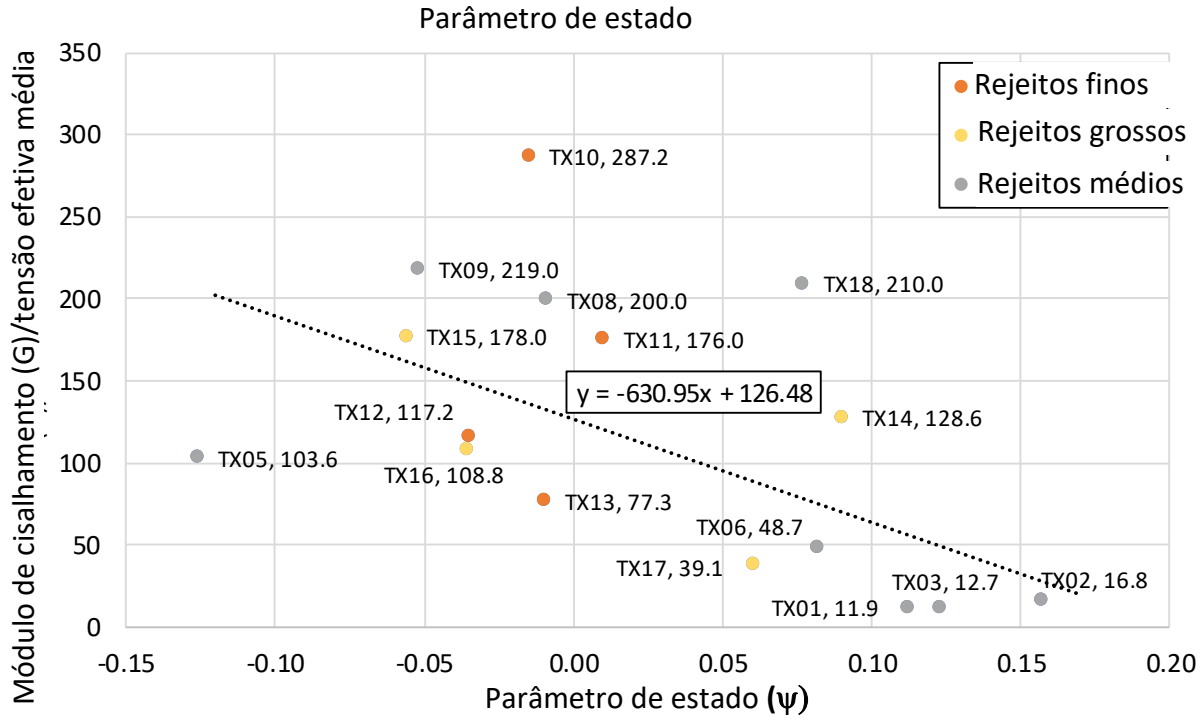


Figura 34: Relação entre o módulo de cisalhamento (G) e o parâmetro de estado (ψ) para análise drenada

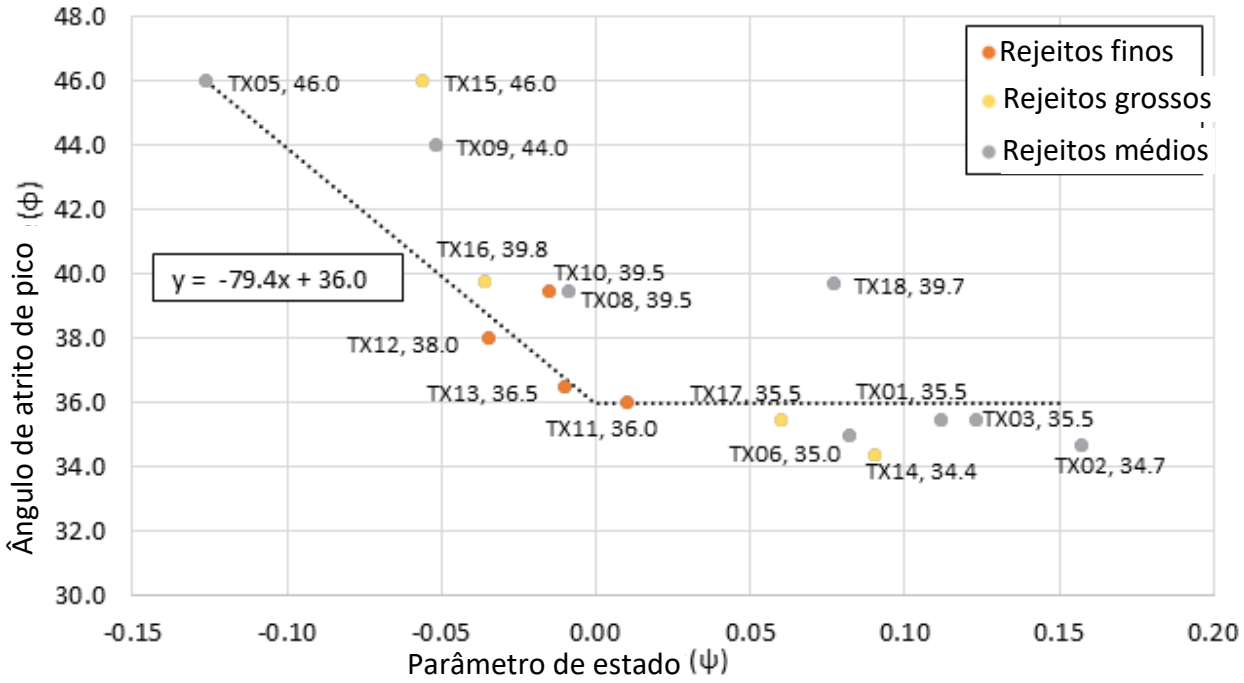


Figura 35: Relação entre o ângulo de atrito de pico e o parâmetro de estado (ψ) para análise drenada

6.3 Parâmetros para *Strain-Weakening*

6.3.1 Parâmetros drenados

As análises de *strain-weakening* foram concluídas para captar a perda de resistência que ocorre durante o cisalhamento drenado ou não drenado dos rejeitos. Para modelar a resposta por *strain-weakening*, a quantidade de deformação plástica (ou seja, deformação específica após o pico de resistência ter sido alcançado) até que ocorra perda de resistência ($\varepsilon_{P\text{-}SL}$) foi calculada a partir dos ensaios triaxiais, juntamente com a quantidade de deformação específica até que a resistência residual seja alcançada (ε_{P-R}). Simulações numéricas dos ensaios triaxiais foram realizadas em um elemento, usando estes valores para verificar se eles estavam captando o comportamento pós-pico dos ensaios adequadamente. Os ensaios de elementos realizados como parte deste trabalho são mostrados no Anexo 8.

Para entrada de dados nas análises de deformação específicas subsequentes, foram desenvolvidas relações de $\varepsilon_{P\text{-}SL}$ e ε_{P-R} versus parâmetro de estado. Estas relações são mostradas na Figura 33 e Figura 34.

As amostras que foram adensadas para um estado fofo, geralmente apresentaram uma resposta dúctil, ao passo que as amostras adensadas para um estado denso geralmente mostraram uma

resposta de comportamento mais frágil. Valores de $\varepsilon_{P\text{-}SL}$ e ε_{P-R} para amostras fofas foram geralmente mais altos que os das amostras densas.

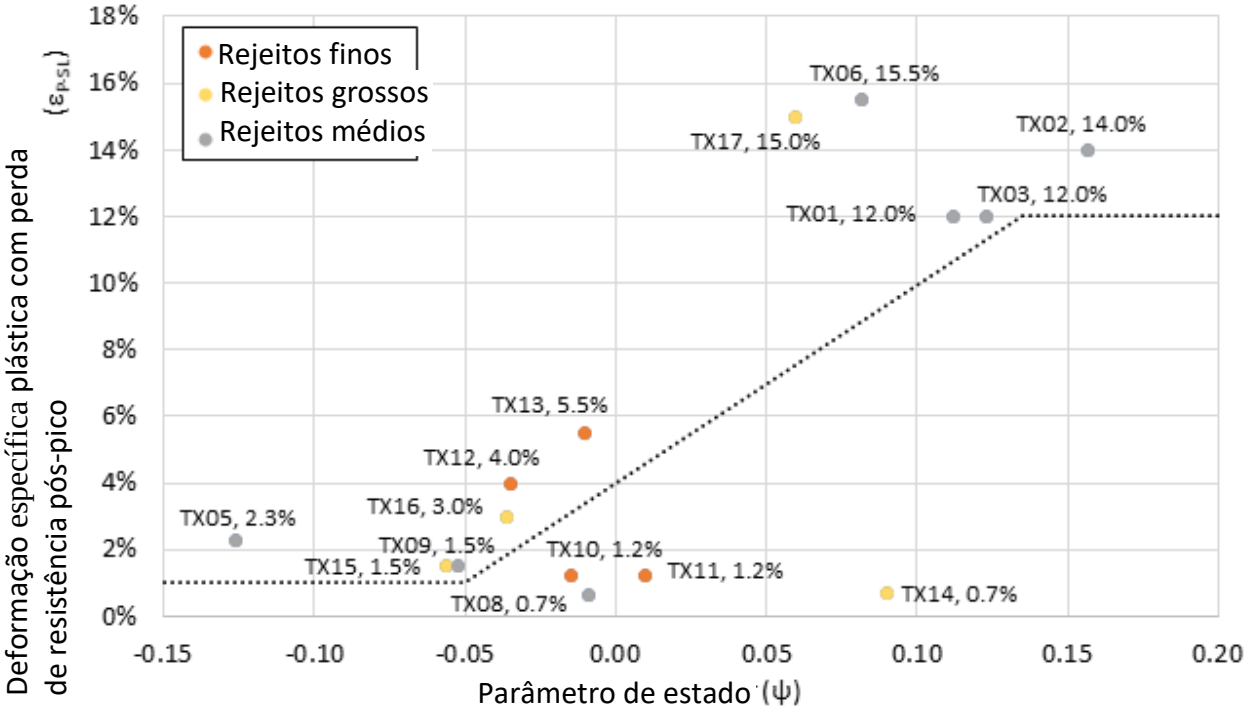


Figura 36: Relação entre deformação específica plástica com perda de resistência pós-pico ($\varepsilon_{P\text{-}SL}$) e parâmetro de estado (ψ) para análise drenada

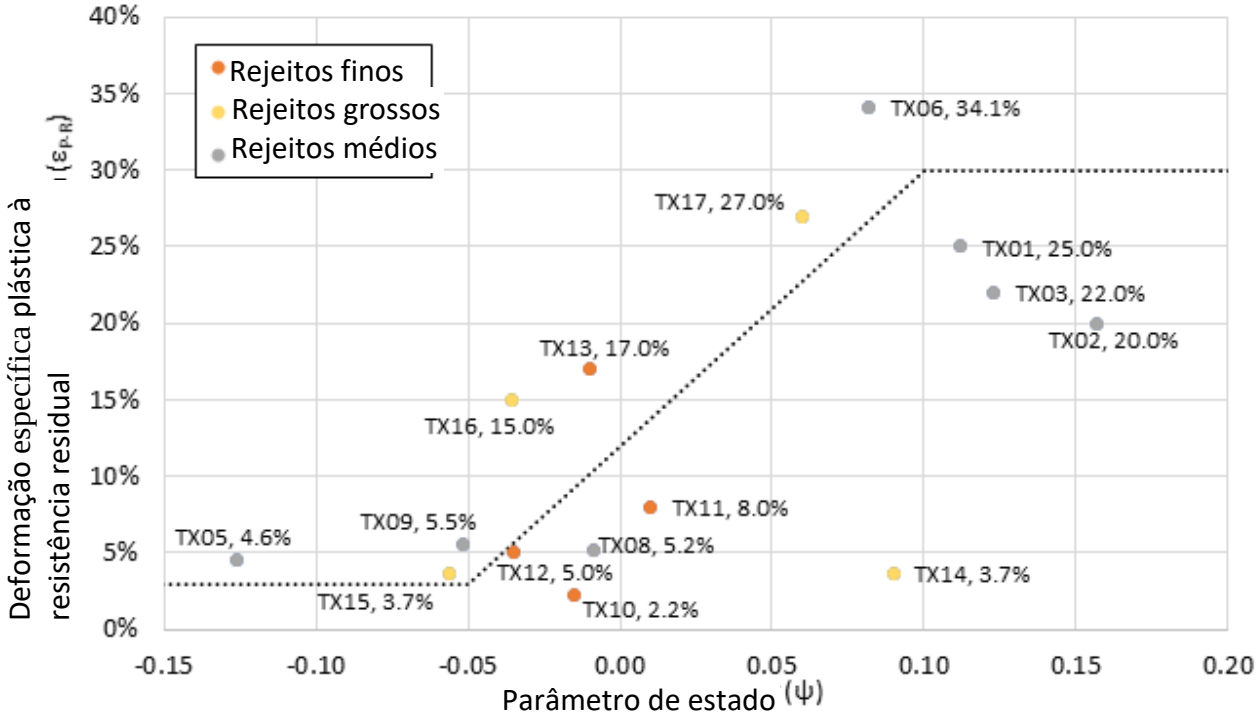


Figura 37: Relação entre deformação específica plástica à resistência residual (ε_{P-R}) e parâmetro de estado (ψ) para análise drenada

6.3.2 Parâmetros não drenados

As razões de resistência não drenada para todos os rejeitos foram calculadas em 50% da tensão de desvio de pico e em ν de 0,49. G foi calculado a partir destes resultados para inserção nas análises.

Foram desenvolvidas relações, correlacionando G e razões de resistência ao cisalhamento não drenada de pico e residual, com o parâmetro de estado para inserção nas análises. G foi normalizado, sendo dividido pela tensão efetiva média. K foi calculado a partir de G e ν usando:

Equação 6-1:

$$K = \frac{2G(1+\nu)}{3(1-(2\nu))}$$

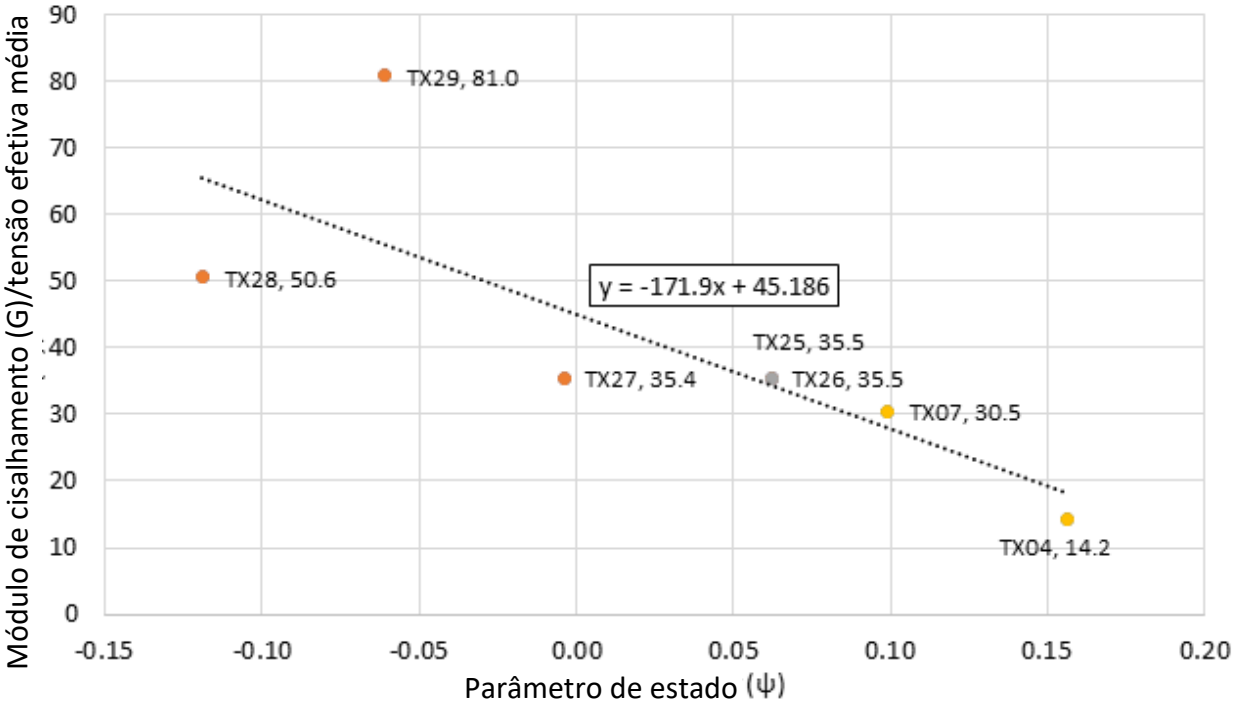


Figura 38: Relação entre módulo de cisalhamento (G) e parâmetro de estado (ψ) para análise não drenada

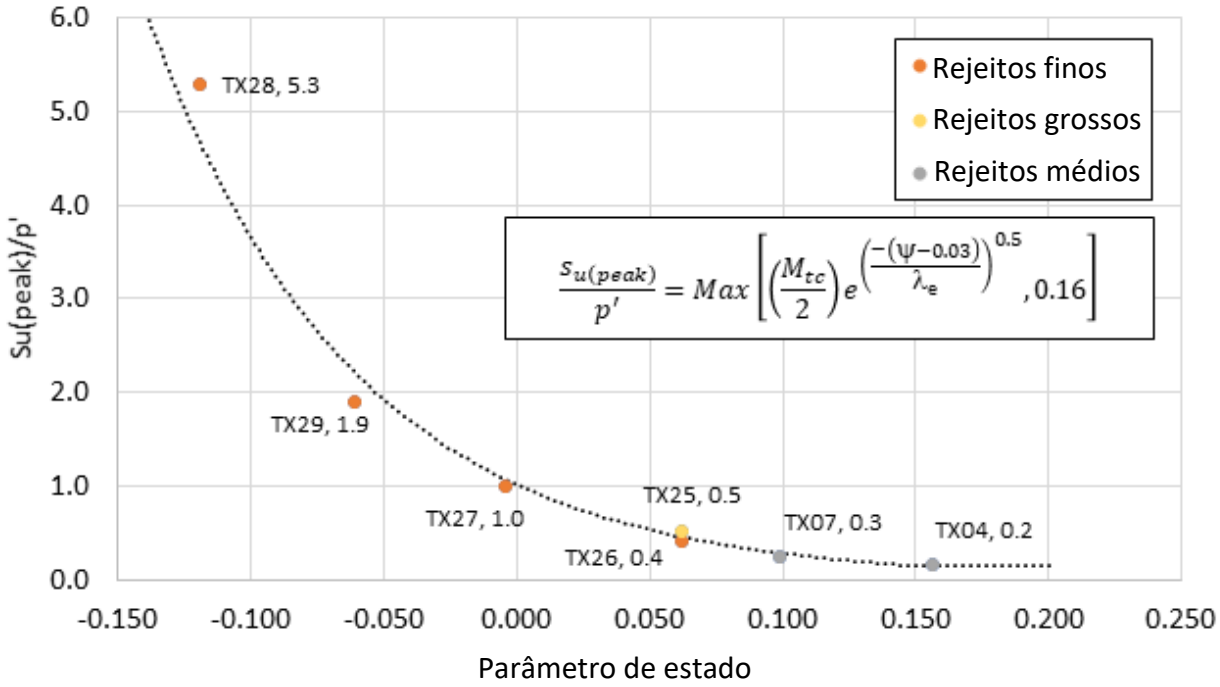


Figura 39: Relação entre Su (pico)/*p'* e parâmetro de estado (ψ) para análise não drenada

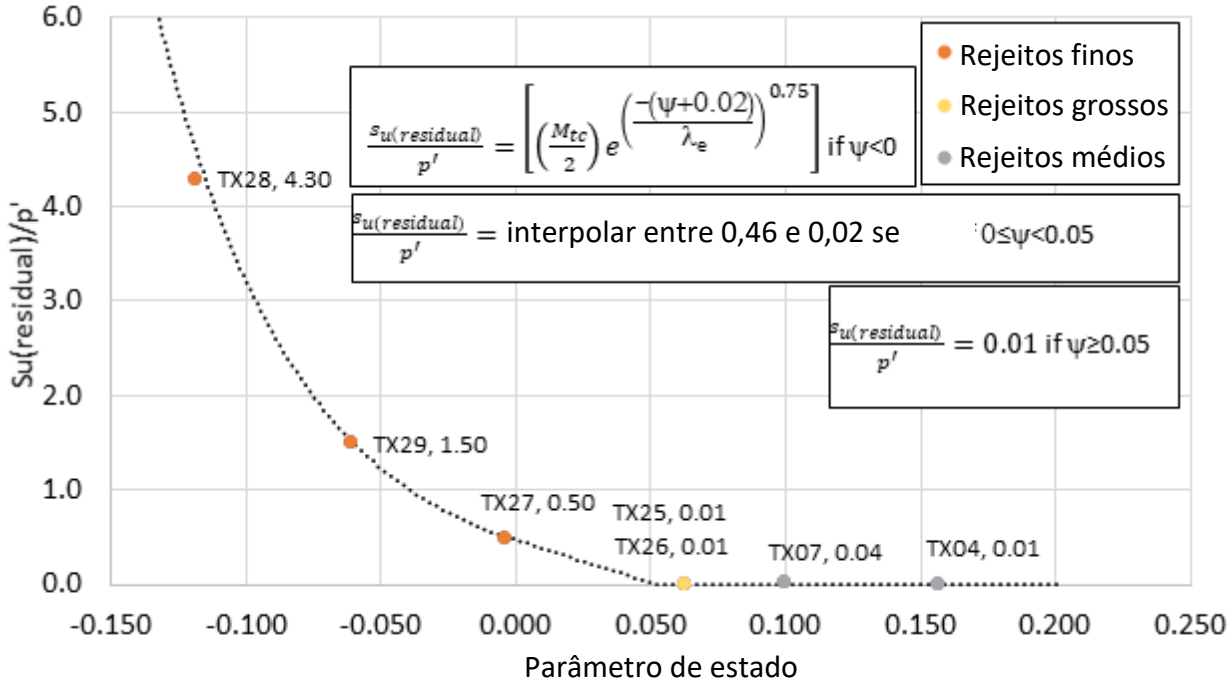


Figura 40: Relação entre Su (residual)/*p'* e parâmetro de estado (ψ)para análise não drenada

A fim de modelar uma resposta do tipo *strain-weakening* dos ensaios de compressão triaxial não drenada, foram desenvolvidas linhas de tendências, correlacionando a deformação específica plástica à deformação específica pós-pico ($\varepsilon_{P\text{-}SL}$) e a deformação específica plástica à resistência residual (ε_{P-R}), a fim de indicar o parâmetro de estado, da maneira descrita para os ensaios de compressão triaxial drenada. Estes parâmetros foram então verificados usando análises de ensaios de elementos, fornecidas no Anexo 8.

As relações $\varepsilon_{P\text{-}SL}$ e ε_{P-R} versus ψ são mostradas na Figura 41 e Figura 42.

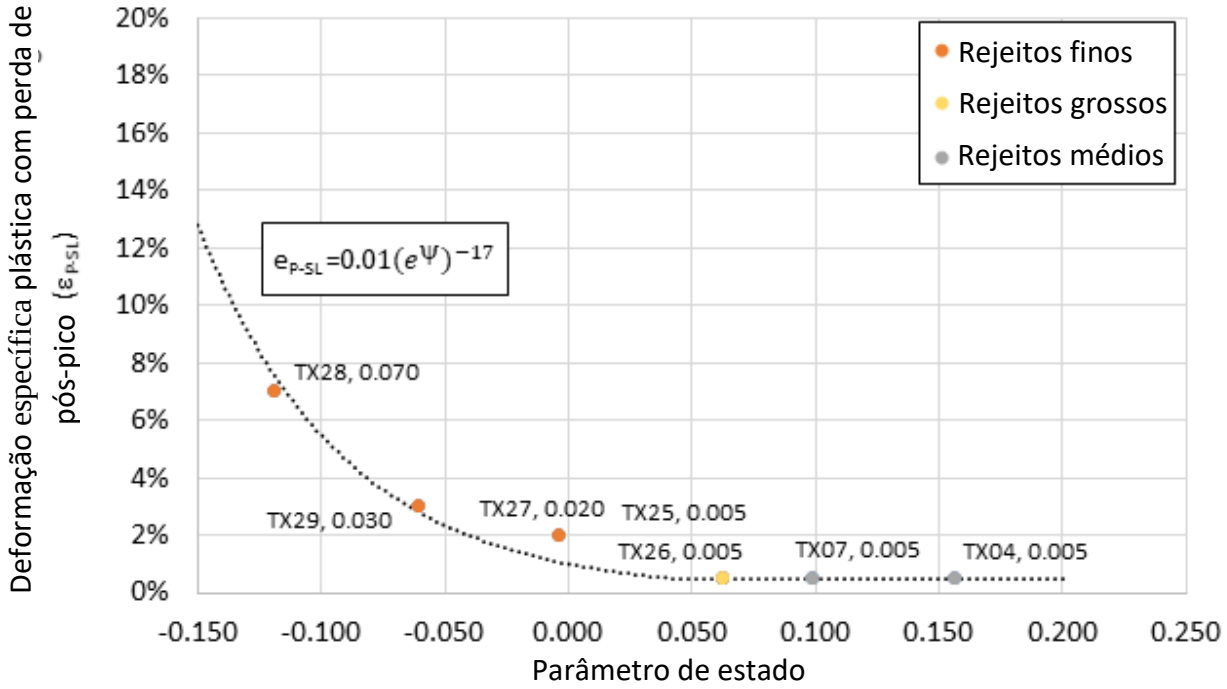


Figura 41: Relação entre deformação específica plástica com perda de resistência pós-pico (ε_{P-SL}) e parâmetro de estado (ψ) para análise não drenada

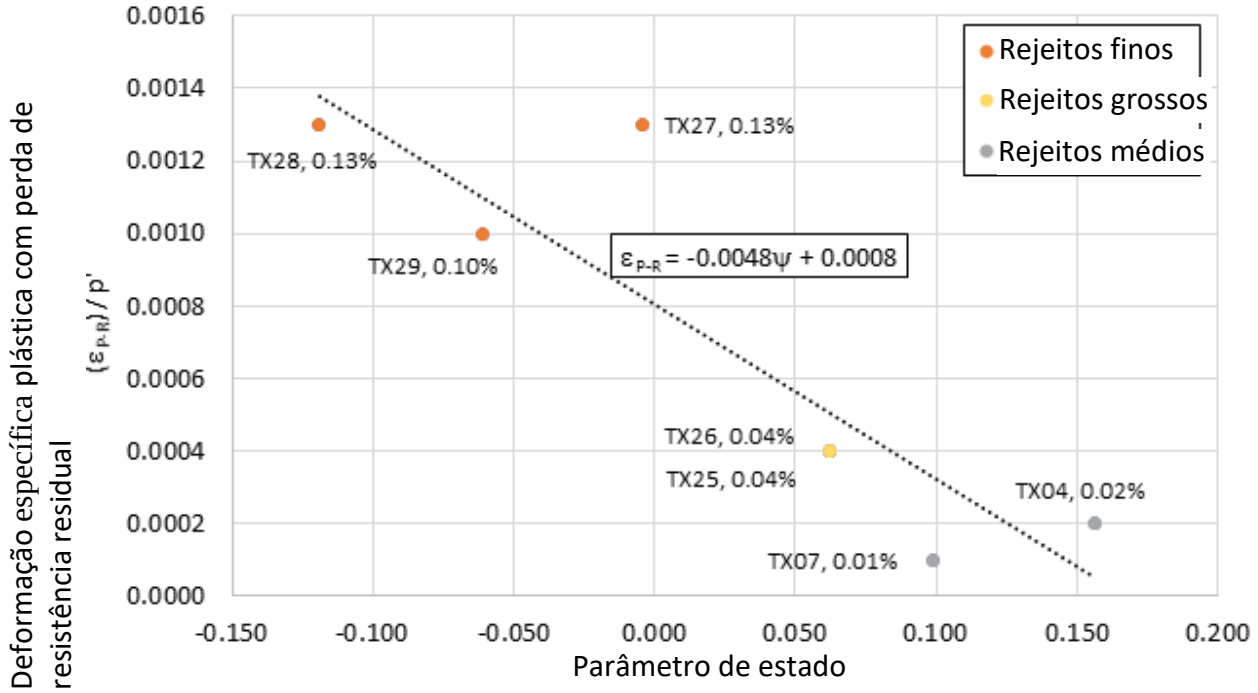


Figura 42: Relação entre deformação específica plástica e resistência residual (ε_{P-R}) e parâmetro de estado (ψ) para análise não drenada

6.4 Dados de Entrada do Modelo de Estado Crítico

Os valores de CSL e M usados nas análises foram os discutidos na Seção 5.2.4. Os outros parâmetros são discutidos abaixo.

6.4.1 Parâmetro de Acoplamento Volumétrico, N

Os parâmetros de dilatação foram derivados a partir de ensaios triaxiais, realizados nas gradações de rejeitos finos, grossos e médios das amostras. O gráfico de dilatação sob tensão na Figura 43 foi usado para determinar o parâmetro de acoplamento volumétrico, N. A inclinação da linha na Figura 43 é igual a (1-N), gerando um valor de N=0,27. A intersecção da linha de tendência na Figura 43 pode ser usada como um método alternativo para calcular o valor de M_{tc}, geralmente chamado de método Bishop. Este valor de 1,31 é semelhante aos valores calculados a partir do final dos pontos de ensaio no gráfico de *q* versus *p'*, tratados na Seção 5.2.4 e equivale a um ângulo de atrito de estado crítico de 34°, compatível com os valores discutidos anteriormente.

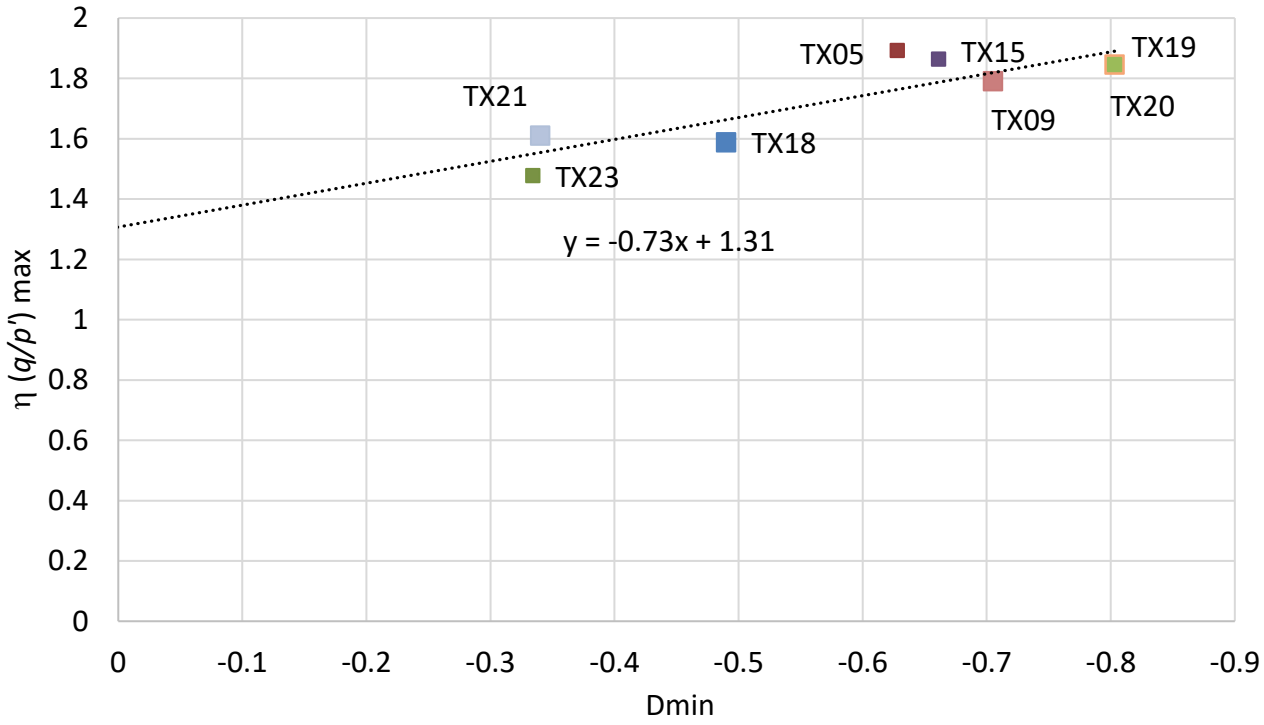


Figura 43: Dilatação – Relação da razão de tensão para a gradação de rejeitos médios

6.4.2 Parâmetro de Dilatação, χ_{tc}

O parâmetro χ_{tc} é a inclinação da linha de tendência para a dilatação mínima (igual à dilatação na razão de tensão de pico) versus o parâmetro de estado na razão de tensão de pico. Figura 44 mostra que este parâmetro é mais alto que o normal, além de ser variável. No tocante à resposta incomum

vista no ângulo de atrito de pico tratado anteriormente, esta resposta é presumida como sendo o resultado da cimentação dos rejeitos. Durante as análises posteriores dos ensaios de elementos, dos resultados dos ensaios triaxiais, usando o modelo constitutivo NorSand, as análises de sensibilidade foram concluídas usando diferentes valores deste parâmetro para determinar seu efeito nos resultados. Como resultado destas análises de sensibilidade, um valor de 6 foi selecionado para uso nas análises. Este alto valor de χ_{tc} levou à instabilidade numérica e análises de sensibilidade foram por fim concluídas para este parâmetro, nas análises em larga escala.

Esta variabilidade na dilatação foi investigada no programa de ensaio triaxial, completando-se três ensaios da gradação de rejeitos médios na mesma tensão efetiva média inicial (100 kPa), em parâmetros de estado cada vez mais densos. Os resultados da Figura 45 mostram uma dilatação reduzida (ou seja, pico da curva tensão-deformação) em um parâmetro de estado de -0,08, se comparado à amostra mais fofa com um parâmetro de estado de -0,05.

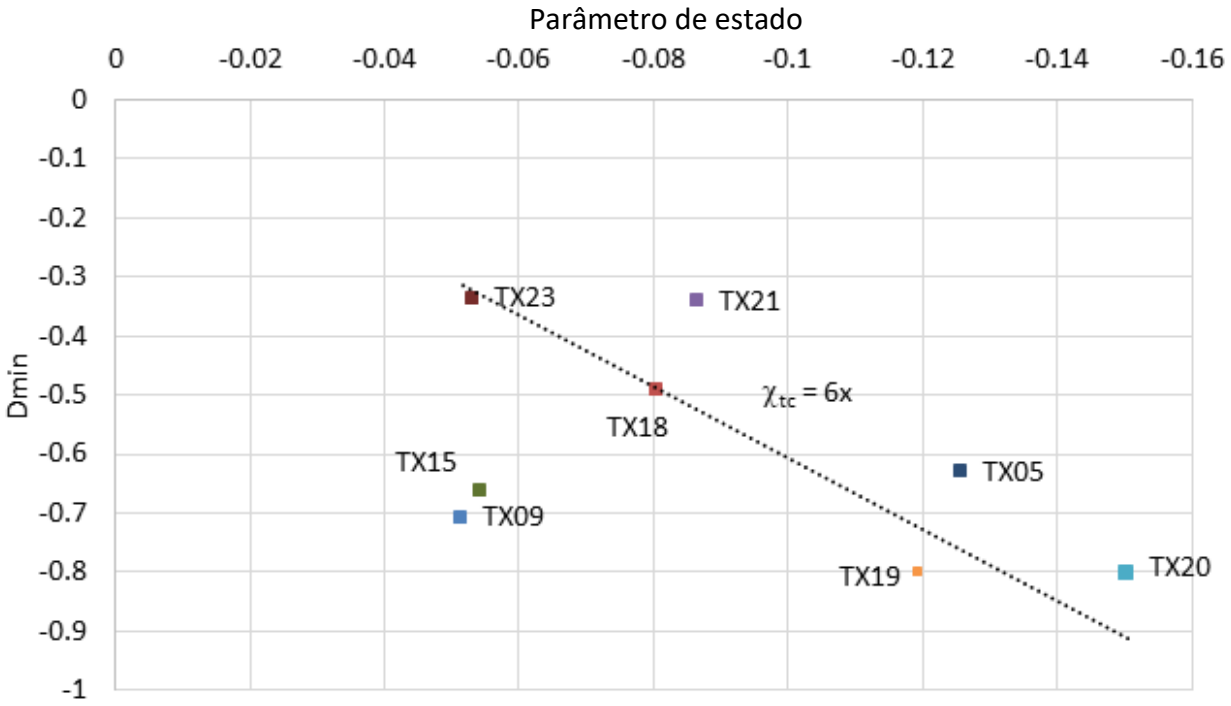


Figura 44: Dilatação – Relação de parâmetros de estado para gradações de rejeitos médios

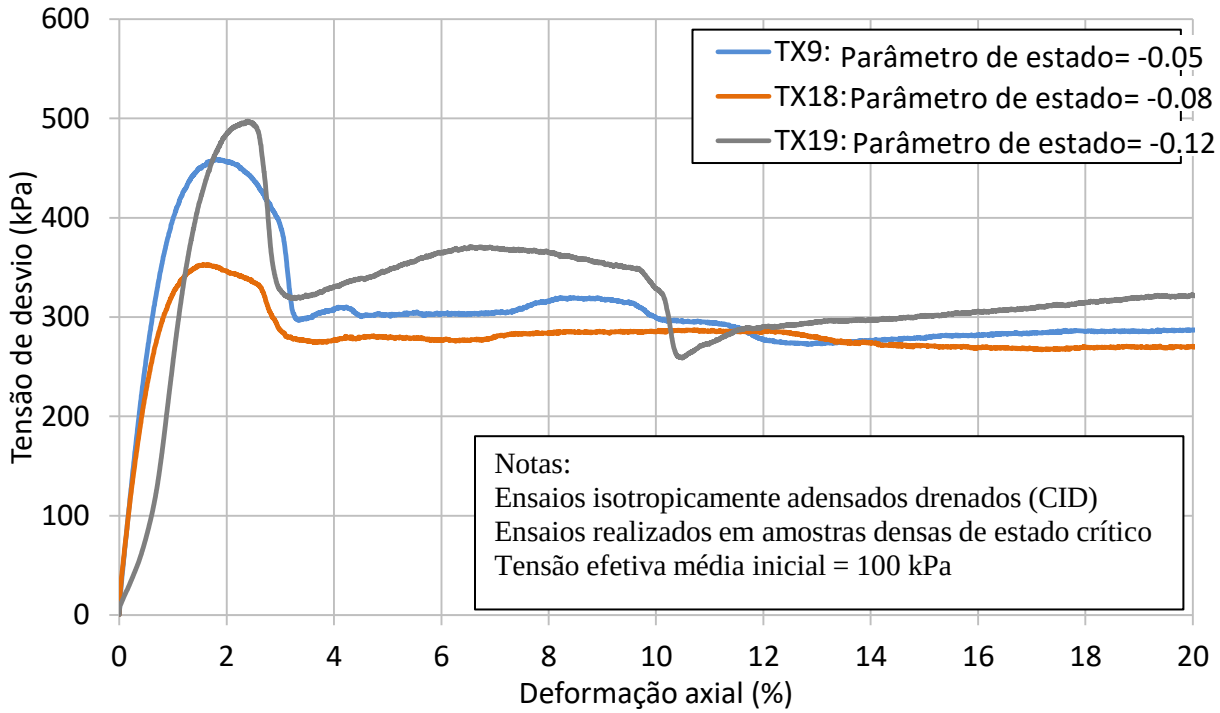


Figura 45: Comparação de curvas de tensão-deformação de amostras testadas com a mesma tensão efetiva média, mas com estados cada vez mais densos

6.4.3 Elasticidade, G_{max}

Foi utilizada nas análises a tendência do módulo de cisalhamento com pequena deformação (G_{max}), com o valor de *p'* determinado a partir do *bender element* e dados do campo de V_s. O valor de G_{max} foi derivado a partir da V_S usando a seguinte fórmula:

Equação 6-2:

$$G_{max}(MPa) = \frac{v_s(^m/_s)^2}{10^6} x \rho_{massa}(^{kg}/_{m^3})$$

Todos os resultados de G_{max} foram plotados em função do respectivo valor de *p'*, na Figura 46. Foi encontrada uma tendência razoável usando a seguinte relação (veja a Equação 6-3).

Equação 6-3:

$$G_{max} = 100\left(\frac{p'}{pref}\right)^{0,5}, em\ que\ p_{ref} = 100\ kPa$$

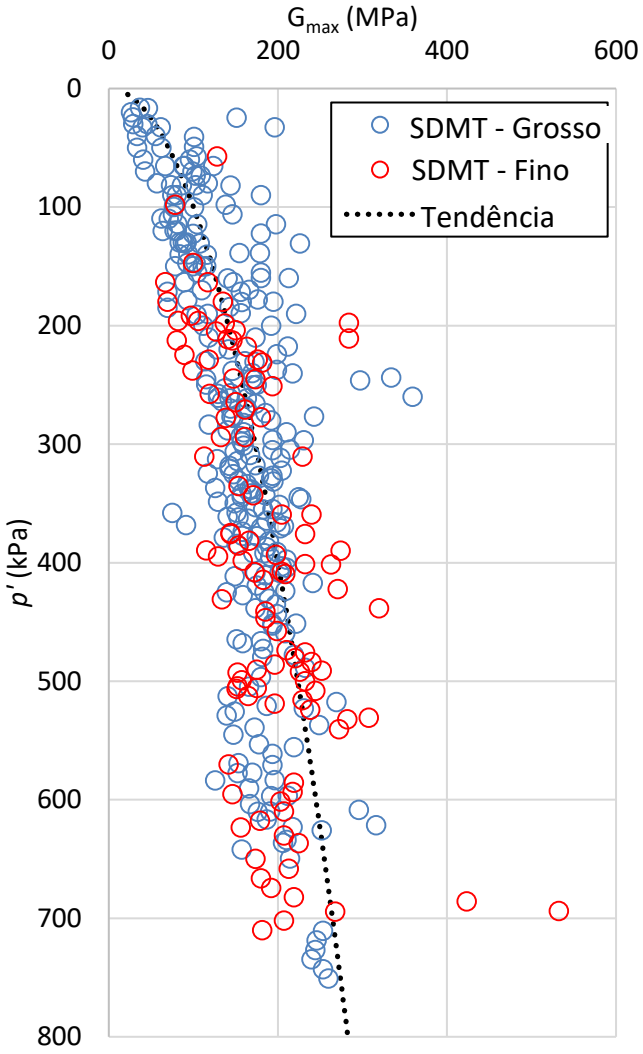


Figura 46: Tendência de G_{max} dos dados do dilatômetro sísmico (V_s)

6.4.4 Endurecimento, H0, Hψ

O módulo de endurecimento plástico foi determinado pela *Iterative Forward Modeling* (IFM) do resultado dos ensaios triaxiais. O objetivo dessa calibração não foi obter o melhor ajuste para cada ensaio individual, e sim obter o melhor ajuste geral para todos os ensaios. No processo de calibração, inicialmente foram utilizados valores constantes de H. Uma vez obtidos bons ajustes, foi desenvolvida uma relação entre o parâmetro de estado inicial e H e os ensaios foram reajustados usando esta relação. A tendência derivada para o endurecimento foi de H_0=160 e H_ψ=1037.

Equação 6-4: $$\boldsymbol{H = H_0 - H_\Psi}$$

Em que,

- H = módulo de endurecimento plástico;
- H_0= intercepto de módulo (relação H versus Ψ); e
- H_ψ= gradiente de módulo.

6.5 Parâmetro de Estado

O parâmetro de estado usado nas análises foi determinado a partir dos dados dos ensaios de CPTu, conforme discutido na Seção 7.5.

6.6 Resumo dos Parâmetros

As propriedades de materiais usadas nas análises estão resumidas na Tabela 17.

Tabela 17: Resumo dos parâmetros selecionados a partir dos ensaios de laboratório

Propriedades	Rejeitos finos/médios/grossos
Parâmetros drenados de Mohr-Coulomb	
Módulo de cisalhamento/*p'*	$G = -631\psi+126,5$
Módulo volumétrico/*p'*	$K = -900,9\psi+165,7$
Ângulo de atrito de pico	Se $\psi < 0$, $\phi' = -79,4\psi + 36°$; Se $\psi > 0$, $\phi' = 36°$
***Strain-weakening* – parâmetros drenados**	
Deformação específica de pico (ε_{P-SL})	Se $\psi \leq -0,05$, $\varepsilon_{P-SL}= 0,01$; Se $-0,05 \leq \psi \leq 0,14$, $\varepsilon_{P-SL}= 0,59\psi + 0.040$; Se $\psi \geq 0,14$, $\varepsilon_{P-SL}= 0,12$
Deformação específica residual (ε_{P-R})	Se $\psi \leq -0,05$, $\varepsilon_{P-R}= 0,03$; Se $-0,05 \leq \psi \leq 0,1$, $\varepsilon_{P-R}= 1,8\psi + 0.12$; Se $\psi \geq 0,1$, $\varepsilon_{P-R}= 0,13$
Ângulo de atrito residual	$\phi' = 34°$
***Strain Weakening* – parâmetros não drenados**	
Módulo de cisalhamento	$G = -171,9x\psi+45,2$
Módulo volumétrico	$K=(2G(1+\nu))/(3(1-2\nu))$
Razão de Poisson (ν)	0,49
Resistência de pico ao cisalhamento não drenado	$s_{u(peak)}/p' = \text{Max}\ ((M_{tc}/2)*\exp(-(\psi+\psi_{offset})/\lambda_e)^{0.5}, 0,16)$; $\psi_{offset} = -0,03$
Resistência residual ao cisalhamento não drenado	Se $\psi < 0$, $s_{u(residual)}/p' = \text{Max}\ ((M_{tc}/2)*\exp(-(\psi+\psi_{offset})/\lambda_e)^{0.75}, 0,01)$; Se $\psi \geq 0.05$, $s_{u(residual)}/p'=0,01$; $\psi_{offset} = +0,02$
Deformação específica de pico (ε_{P-SL})	$\varepsilon_{P-SL}=0,01e(\psi)-17$
Deformação específica residual (ε_{P-R})/p'	$\varepsilon_{P-R} = -0,0048\psi+0,0008$
Parâmetros do modelo de estado crítico (NorSand)	

Γ	1,12/1,04/1,02
λ_e	0,039
Parâmetro de CSL curvada A	1,29/1,22/1,19
Parâmetro de CSL curvada B	0,34
Parâmetro de CSL curvada C	0,11
M_{tc}	1,38
N	0,27
X_{tc}	6
G_{max}	$G_{max} = 100x(p'/pref)^{0,5}$
H_0	160
$H\psi$	1037
Γ	1,12/1,04/1,02
Parâmetros do modelo de solo CH	
E_{ref}	800
ν	0,4
Rf	0,99
n	0,15
c	0
ϕ	*p'* <370kPa = 22,5; *p'* > 800 = 17; interpolar para *p'* intermediário

7 INTERPRETAÇÃO DOS DADOS DE ENSAIOS CPTU E V_S

7.1 Geral

Como parte deste estudo, foi realizada uma análise dos dados disponíveis do ensaio de CPTu. Isso incluiu a delimitação do material de rejeitos na barragem em tipos de rejeitos semelhantes (ou seja, rejeitos finos e grossos e lamas, conforme discutido na Seção 7.3). Uma descrição de como o delineamento foi desenvolvido em duas dimensões (2D) e três dimensões (3D) é apresentada no Apêndice F. Esta seção descreve o processo usado para calcular parâmetros de resistência não drenada e parâmetros de estado a partir dos dados dos ensaios de CPTu. Os dados brutos dos ensaios de CPTu disponíveis para esta investigação incluíram 28 ensaios de CPTu e nove ensaios de velocidade da onda de cisalhamento (V_s) realizados como parte de investigações geotécnicas em 2005, 2016 e 2018 (conforme resumido no Apêndice B). A Figura 47 mostra os locais dos ensaios de CPTu na Barragem I.

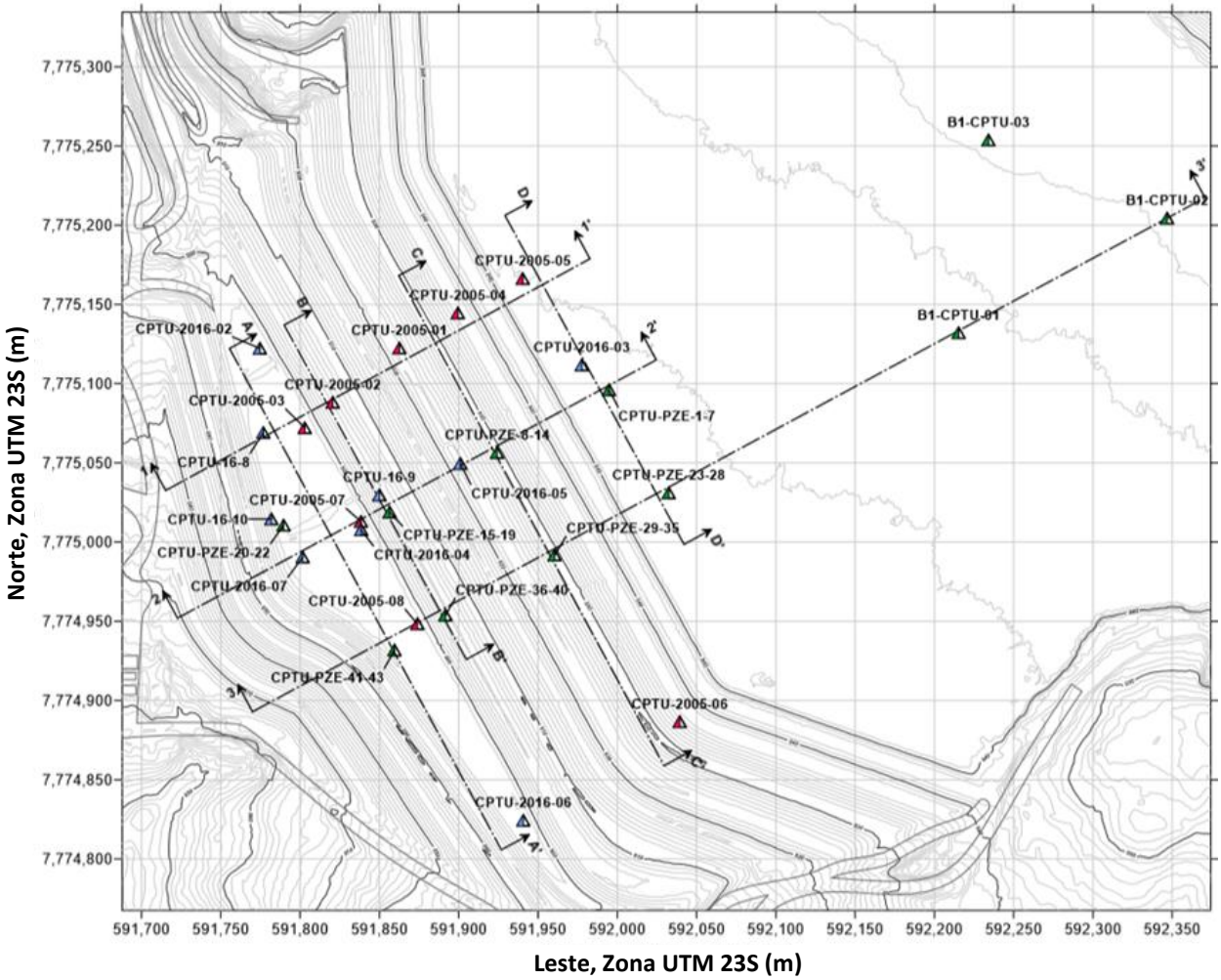


Figura 47: Planta de localização dos ensaios de CPTu[8]

7.2 Processamento dos Dados dos Ensaios de CPTu

A metodologia usada para processar os dados dos ensaios de CPTu foi composta pelas seguintes etapas:

- Foram processados os dados brutos dos ensaios de CPTu, que incluíram resistência de ponta do cone (qc), atrito lateral (fs) e poro-pressão dinâmica (u2);
- Foram processados os dados brutos do ensaio de dissipação da poro-pressão (PPDT) para estimar a profundidade da linha freática e o gradiente hidráulico;
- Foi calculada a resistência de extremidade corrigida (qt), a taxa de atrito (Rf), o parâmetro de estado (ψ), o índice de tipo de comportamento do solo (Ic), a poro-pressão estática (u),

[8] Apêndice B, Figura 2-1b.

a resistência de extremidade equivalente da areia limpa (Qtn,cs), as razões de resistência pós-liquefação ($Su_{(LIQ)}/\sigma'_v$), as razões de resistência de pico não drenada ($Su_{(peak)}/\sigma'_v$) e o teor aparente de finos (%), para cada ensaio de CPTu e foram plotados os resultados em função da elevação.

Os gráficos dos perfis dos ensaios de CPTu são apresentados no Anexo 9.

7.3 Delineamento de Rejeitos

Uma análise dos dados dos ensaio de CPTu, apresentados no Anexo 9, indicou que os rejeitos retidos pela Barragem I poderiam ser subdivididos em três materiais: rejeitos grossos, rejeitos finos e lamas, na área da praia de rejeitos, na qual os rejeitos finos e grossos foram os mais relevantes para a rompimento, estando mais próximos da face da Barragem I. Os de rejeitos finos e grossos se desenvolveram agrupando regiões da Barragem I com resistências e tipos de comportamento em ensaios de CPTu similares. Os contornos entre estas regiões foram delineados com base nos critérios da Tabela 18 e são mostrados nos perfis de ensaios de CPTu para cada CPTu incluído no Anexo 9. De maneira geral, observou-se que as camadas de rejeitos grossos apresentaram menor teor aparente de finos, maior resistência na ponta (mas ainda eram suscetíveis à liquefação estática, conforme Robertson (2010)) e um índice de tipo de comportamento do solo ≤ 2,6. Observou-se que as camadas de rejeitos finos apresentam maior teor aparente de finos, menor resistência na ponta e um índice de tipo de comportamento do solo > 2,6.

Tabela 18: Critérios de delineação de rejeitos

[1]Tipo de material dos rejeitos	Índice de materiais, I_c	Teor de finos aparentes (%)
Rejeitos grossos	≤ 2,6	≤ 50%
Rejeitos finos	> 2,6	> 50%

OBSERVAÇÃO:
[1]Usou-se a premissa de que um terceiro tipo de material de rejeitos, as lamas, existisse a montante do local da praia, com base nos dados de ensaios de CPTu coletados (B1-CPTu-01, 02, 03) dentro da bacia, que exibia resistências muito baixas.
[2]As camadas de rejeitos finos também foram distinguíveis usando uma resistência de ponta mais baixa em comparação com os rejeitos grossos.

7.4 Estimativa de Resistência de Pico e Liquefeita Usando Dados de Ensaios de CPTu

A razão de resistência de pico ao cisalhamento não drenado, $s_{u(peak)}/\sigma'_{v0}$, foi calculada usando a seguinte fórmula desenvolvida por Olson e Stark (2003).

Equação 7-1: $\frac{s_{u(peak)}}{\sigma'_{v0}} = \mathbf{0,205 + 0,0143}(q_{c1})$; Desde que: $q_{c1} \lesssim \mathbf{6,5\ MPa}$

A razão de resistência liquefeita ao cisalhamento não drenado, $s_{u(liq)}/\sigma'_{v0}$, foi calculada usando a seguinte relação, desenvolvida por Robertson (2010).

Equação 7-2: $\frac{s_{u(liq)}}{\sigma'_{v0}} = \frac{0{,}02199 - 0{,}0003124 \cdot Q_{tn,cs}}{1 - 0{,}02676 \cdot Q_{tn,cs} + 0{,}0001783 \cdot Q_{tn,cs}^2}$; Desde que:

$$\begin{cases} Q_{tn,cs} \leq 70 \\ 0{,}03 \leq \frac{s_{u(liq)}}{\sigma'_{v0}} \leq tan\varphi' \end{cases}$$

Usando estas relações, foi calculado um intervalo de valores para rejeitos finos e grossos. Para desenvolver um conjunto de valores representativos de cada unidade de rejeitos, foram produzidos histogramas dos dados, conforme mostrado no Anexo 9. Os valores de resistência foram comparados com as resistências não drenadas medidas nos ensaios triaxiais. Observou-se que a resistência de pico dos ensaios triaxiais foi significativamente maior que a resistência de pico não drenada estimada a partir destas relações empíricas e que a resistência liquefeita foi menor nos ensaios triaxiais do que as sugeridas por essas relações. Isto é considerado um reflexo da diferente mineralogia destes rejeitos, se comparados com os solos usados para desenvolver as correlações empíricas dos ensaios de CPTu, e da cimentação dos rejeitos, que não é captada nestas relações empíricas. Como resultado, foi dada preferência aos dados do ensaio triaxial, a fim de atribuir as resistências de pico e liquefeita dos rejeitos. As tendências de resistência de pico e residual não drenada descritas na Seção 6.2 foram usadas nas análises.

7.5 Estimativa de Parâmetros de Estado Usando Dados dos Ensaios de CPTu

Diversos métodos estão disponíveis para calcular o parâmetro de estado in situ a partir dos dados dos ensaios de CPTu. Os métodos de Robertson (2009),[9] Plewes et al. (1992)[10] e Jefferies e Been (2016) foram utilizados nesta avaliação. Os métodos de Robertson (2009) e Plewes et al. (1992) são empíricos e não exigem ensaios laboratoriais ou análises numéricas, mas dependem de relações desenvolvidas a partir de um banco de dados de solos arenosos compostos de sílica. O método desenvolvido por Jefferies e Been (2016) é uma abordagem mais específica do local, com base em simulações numéricas, e incorpora dados de ensaios-índice e de laboratório.

Esta seção discute os três métodos examinados para caracterizar o parâmetro de estado in situ de rejeitos finos e grossos.

[9] Robertson, P.K. (2009). Interpretation of cone penetration tests – a unified approach. *Canadian Geotechnical Journal*, *46*(11), 1337-1355.

[10] Plewes, H.D., Davies, M.P., & Jefferies, M.G. (1992). CPT based screening procedure for evaluating liquefaction susceptibility. Proceedings from *The 45th Canadian Geotechnical Conference*, 41-49. Richmond, BC: BiTech Publishers Ltd.

7.5.1 Método Robertson (2009)

O método Robertson (2009) usa a resistência corrigida na ponta (qt) e atrito lateral (f) dos dados dos ensaios de CPTu para calcular uma resistência normalizada no cone (Q_{tn}) usando a Equação 7-3.

Equação 7-3: $$\boldsymbol{Q_{tn} = \left[\left(\frac{q_t - \sigma_v}{p_a}\right)\right]\left(\frac{p_a}{\sigma'_v}\right)^n}$$

Em que,

- σ_v= tensão vertical total in situ
- σ'_v= tensão vertical efetiva total in situ
- p_a= pressão atmosférica
- n= componente de tensão ($n \leq 1$)

A resistência de cone normalizada (Q_{tn}) é ajustada, a fim de contabilizar o teor de finos, mineralogia e plasticidade, usando o fator de correção K_c, de modo a calcular um valor de areia limpa equivalente ($Q_{tn,cs}$), conforme mostrado na Equação 7-4.

Equação 7-4: $$\boldsymbol{Q_{tn,cs} = K_c Q_{tn}}$$

Em que,

- K_c= 1,0, se $I_c \leq 1{,}64$
- $K_c = 5{,}581 I_c^3 - 0{,}403 I_c^4 - 21{,}63 I_c^2 + 33{,}75 I_c - 17{,}88$, se $I_c > 1{,}64$

O parâmetro de estado in situ (ψ) é então calculado, através da Equação 7-5.

Equação 7-5: $$\boldsymbol{\psi = 0{,}56 - 0{,}33 \log\left(Q_{tn,cs}\right)}$$

7.5.2 Método de Plewes et al. (1992)

O método de Plewes et al. (1992) normaliza o valor de q_t, usando a tensão efetiva média e a poro-pressão dinâmica e o relaciona com (ψ) através da, Equação 7-8, Equação 7-9 e Equação 7-9.

Equação 7-6: $$\boldsymbol{Q_p\left(1 - B_q\right) + 1 = \bar{k}\, exp(-\bar{m}\psi)}$$

Equação 7-7: $$\boldsymbol{B_q = \frac{(u - u_0)}{(q_t - \sigma'_{v0})}}$$

Equação 7-8: $$\boldsymbol{\frac{\bar{k}}{M_{tc}} = 3 + \frac{0{,}85}{\lambda_{10}}}$$

Equação 7-9: $$\bar{m} = 11,9 - 13,3\lambda_{10}$$

Em que,

- Q_p=resistência no cone normalizada
- B_q= razão de poro-pressão
- M_{tc}= razão de atrito crítica
- λ_{10}= inclinação da linha de estado crítico
- $\bar{k}$ e $\bar{m}$= parâmetros semi-empíricos para estimar o valor de ψ

Embora o método forneça relações empíricas para estimar λ_{10} e M_{tc}, ele também indica que o desenvolvimento da CSL do solo, através de ensaios triaxiais em amostras de solo intactas ou reconstituídas, pode ser usado para refinar estimativas de λ_{10} e M_{tc} e assim fornecer uma estimativa de (ψ) que é mais específica para o solo. O cálculo de (ψ) foi realizado usando um valor de λ_{10} de 0,09 e um valor de M_{tc} de 1,38, conforme discutido na Seção 6.4.1.

7.5.3 Método de expansão da cavidade – Jefferies e Been (2016)

O método Jefferies e Been (2016) usa os parâmetros de estado crítico discutidos na Seção 6.4.1 em simulações numéricas de expansão da cavidade esférica, o que é tratado como análogo ao ensaio de CPTu. Estas simulações são usadas para desenvolver valores específicos de $\bar{k}$ e $\bar{m}$ para cada local (consulte o método de Plewes, et al. (1992)), a fim de calcular ψ a partir dos dados dos ensaios de CPTu. Estas análises usaram o modelo constitutivo NorSand com os dados de entrada discutidos na Seção 6 e resumidos na Tabela 17.

7.5.4 Resultados

Usando os três métodos descritos acima, as estimativas de (ψ) foram calculadas para rejeitos finos e grossos em cada local de ensaio de CPTu, conforme mostrado no Anexo 9. Foram produzidos histogramas dos dados, conforme mostrado no Anexo 9. Os histogramas são sobrepostos para os rejeitos grossos e finos na Figura 48 e Figura 49, que também mostram as distribuições destes dados usados nas análises (consulte o Apêndice H). O método de Robertson (2009) não foi utilizado para os rejeitos finos, porque o uso da correção do teor de finos nessa relação não foi considerado adequado, em virtude da similaridade na inclinação da CSL para os rejeitos grossos e finos.

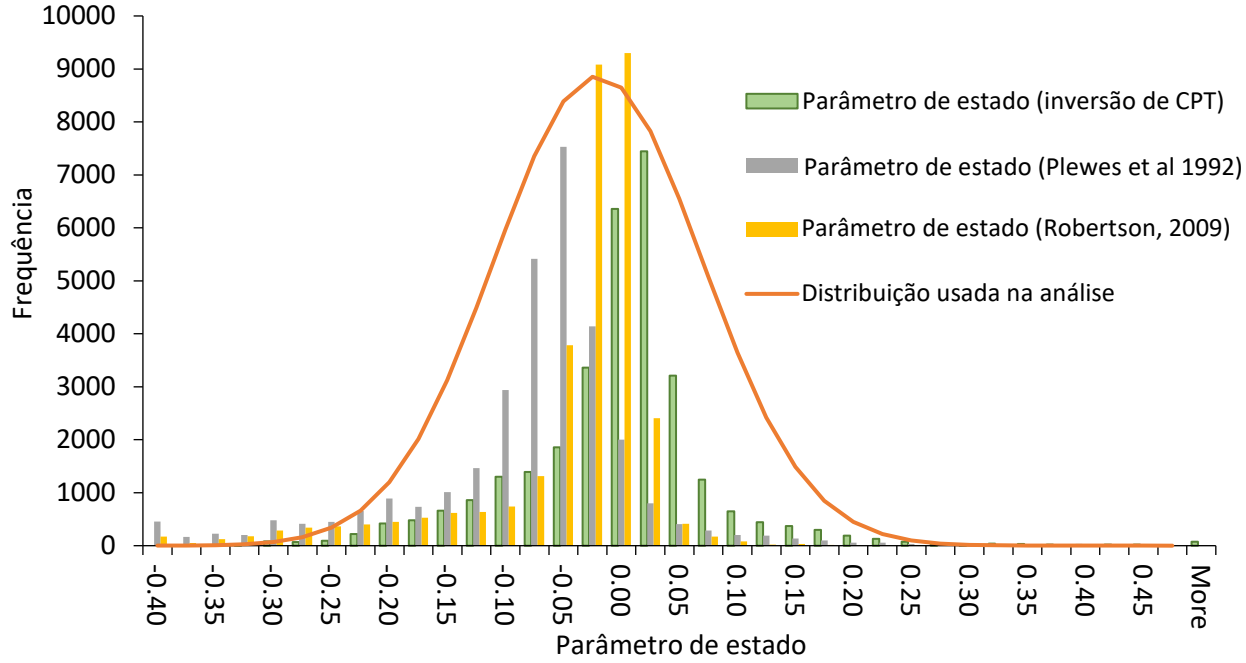


Figura 48: Distribuição de parâmetros de estado (ψ) para rejeitos grossos

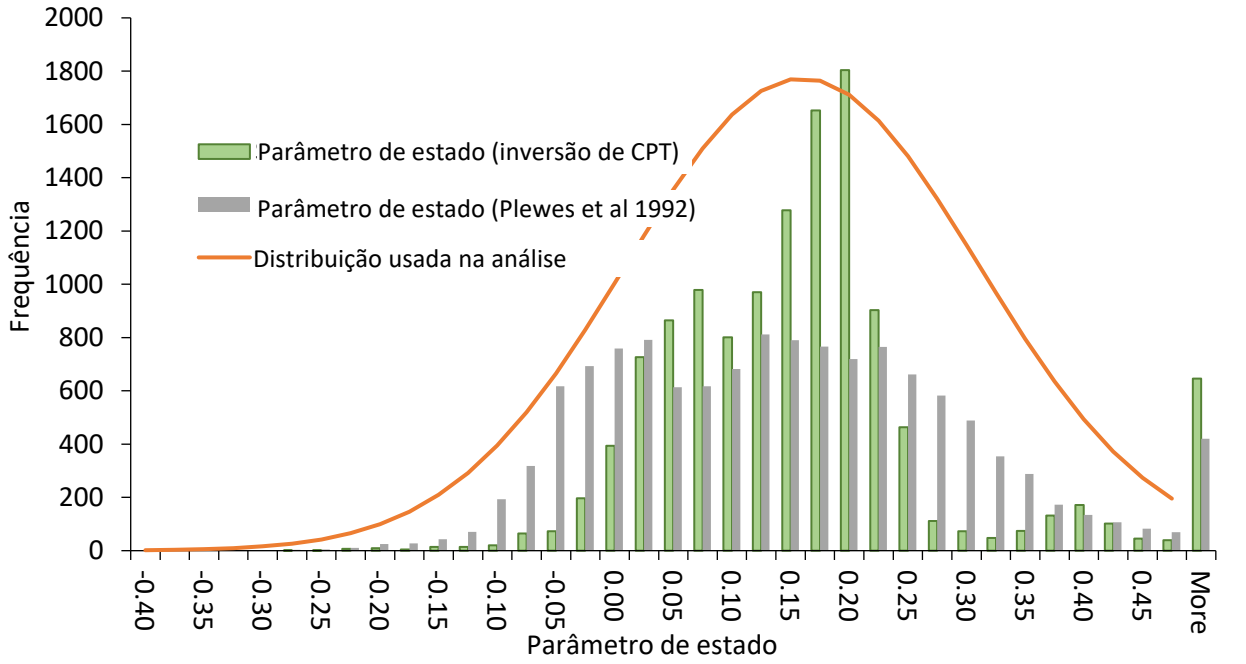


Figura 49: Distribuição de parâmetros de estado (ψ) para rejeitos finos

No geral, os resultados indicam que os três métodos estimam uma faixa semelhante de parâmetro de estado para rejeitos grossos.

Para rejeitos finos, os métodos de Plewes et al. (1992) e Jefferies e Been (2016) estimaram uma faixa semelhante de ψ; no entanto, a distribuição do método de Plewes et al. (1992) foi mais uniforme. Ambos os métodos mostraram que o ψ de rejeitos finos foi significativamente maior do que nos rejeitos grossos.

Devido à variação de ψ em todos os rejeitos e entre os métodos de análise, as distribuições de ψ, mostradas na Figura 48 eFigura 49, foram usadas nas análises em vez de selecionar um "estado característico" destes intervalos. Consulte o Apêndice H para saber como isso foi usado nas análises. Estas distribuições abrangem o intervalo de ψ calculado a partir dos vários métodos.

7.6 Avaliação da Cimentação a Partir dos Dados de Ensaios de CPTu

Robertson (2016) [11] desenvolveu uma relação entre Q_{tn} e o índice de rigidez em pequenas deformações I_G, a fim de rastrear os dados dos ensaios de CPTu e SMDT no tocante aos sinais de aderência. Esta relação, denominada índice de pequenas deformações normalizado modificado (K_G^*), foi usada para identificar sinais de cimentação entre os rejeitos finos e grossos. Solos com K_G^*> 330 tendem a ter cimentação significativa com valores mais altos de K_G^*, indicando uma maior presença de cimentação. Conforme indicado nos gráficos dos ensaios de CPTu no Anexo 9, foram identificados sinais de cimentação entre os rejeitos finos e grossos, com valores de K_G^* tipicamente plotados para o limite inferior dos solos cimentados (veja o exemplo na Figura 50). Este resultado é compatível com as conclusões dos ensaios de MEV realizados na UQ, conforme discutido na Seção 4.8.

[11] Robertson, P.K. (2018). Cone penetration test (CPT) based soil behaviour type (SBT) classification system – an update. *Canadian Geotechnical Journal*, *53*(12), 1910-1927.

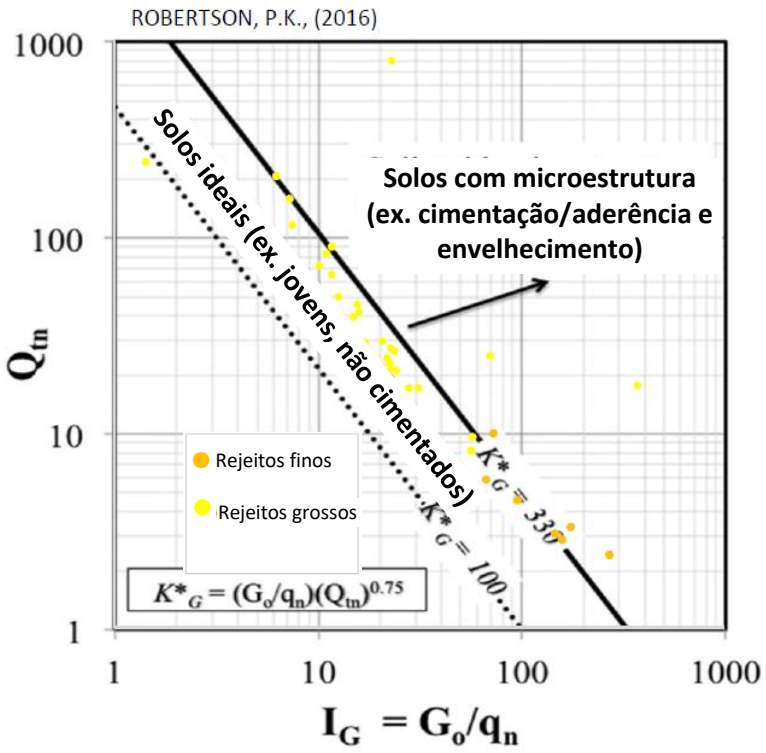


Figura 50: Gráfico Q_{tn} vs I_G para identificar solos com microestrutura

7.7 Comparação de Dados de Ensaios de CPTu e Dados de Ensaios de FVT

Os ensaios de palhetas de campo (FVT) foram realizados anteriormente na Barragem I, conforme discutido no Apêndice B. Como parte destes ensaios, foram medidas as resistências de cisalhamento não drenadas de pico, residuais e remoldadas, bem como as curvas de tensão-deformação. Estes parâmetros de resistência não foram usados diretamente nas análises desta investigação, mas as curvas tensão-deformação destes ensaios foram usadas como prova para corroborar que uma rápida perda de resistência se desenvolve nestes materiais, o que é compatível com as cimentações observadas descritas anteriormente e os resultados dos ensaios triaxiais de laboratório tratados na Seção 5.2. Figura 51 e a Figura 52 apresentam exemplos de curvas de tensão-deformação de ensaios de FVT em rejeitos finos e grossos, respectivamente.

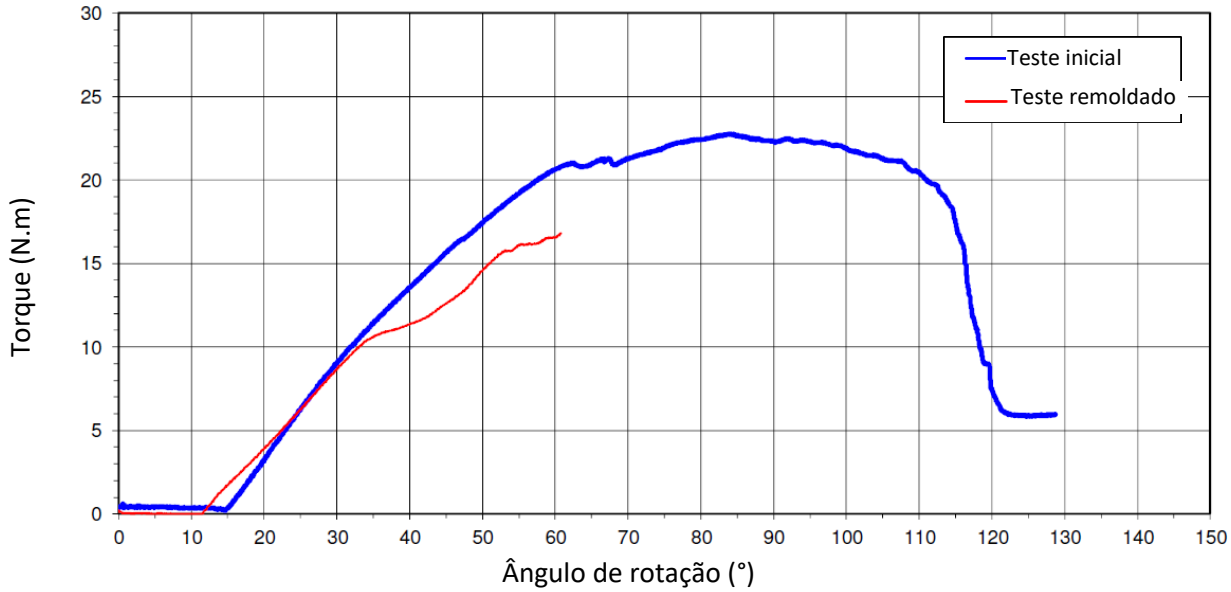


Figura 51: Resultado do ensaio de FVT – VT-16-11 (profundidade 22,5 m)

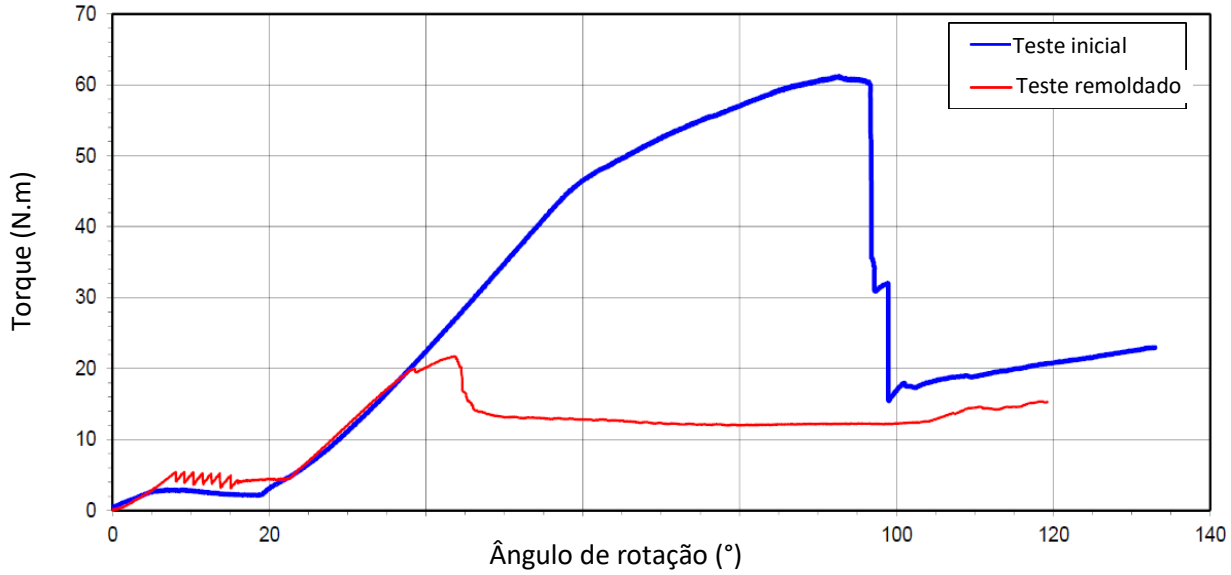


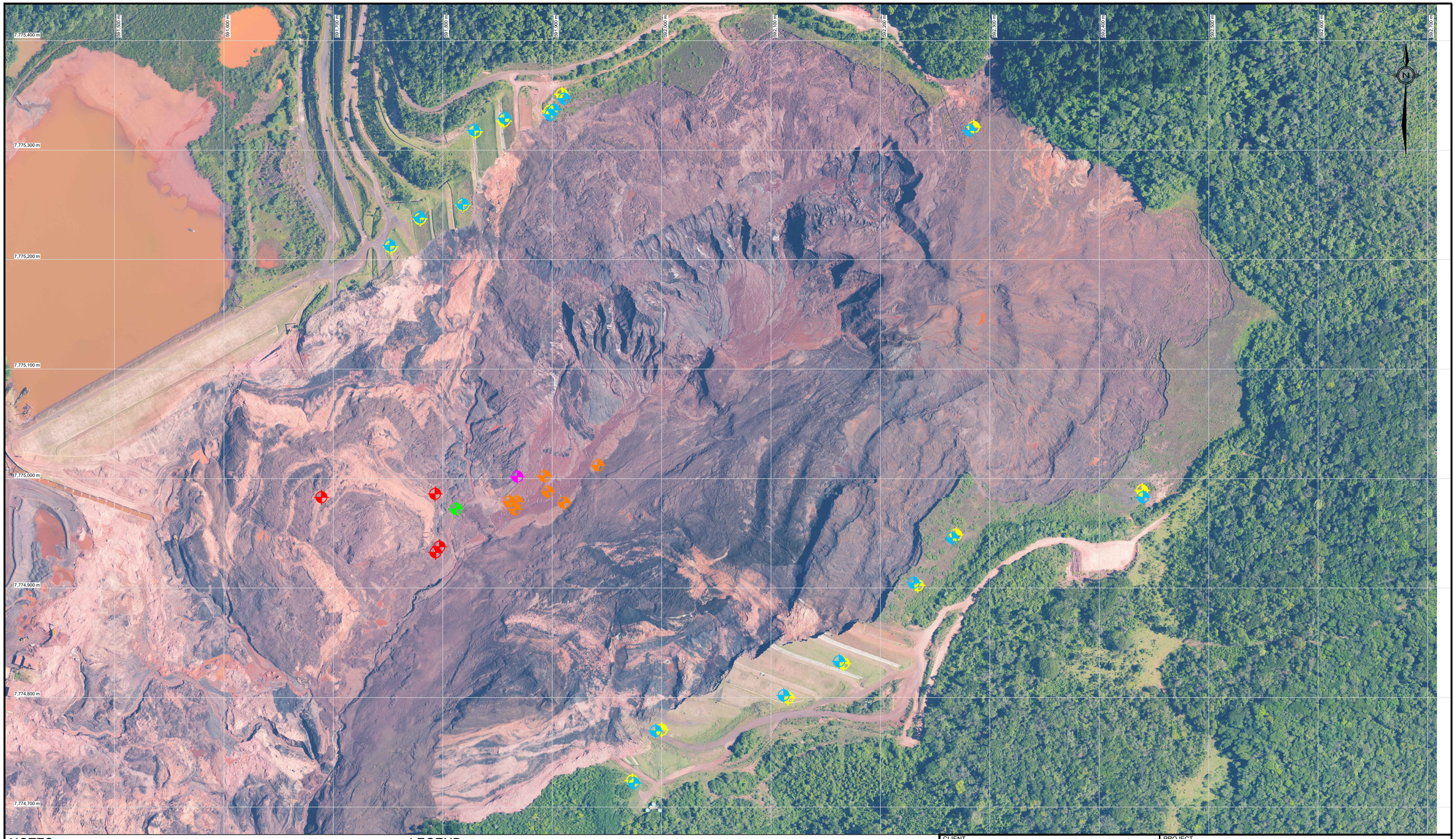
Figura 52: Resultado do ensaio de FVT – VT-16-12 (profundidade 9,0 m)

Appendix E

Annex 1 – Field Investigation Data

December 2019

Field Investigations



NOTES:

1. DRAWING COORDINATES ARE BASED ON UTM ZONE 23S GRID SYSTEM. ALL COORDINATES ARE IN METERS.
2. LOCATIONS OF FLOW MEASUREMENTS ARE APPROXIMATE AND ARE BASED ON A HANDHELD GPS DEVICE.

LEGEND:

- BOREHOLE LOCATION
- GUELPH PERMEAMETER MEASUREMENT LOCATION
- DENSITY TEST MEASUREMENT LOCATION
- STREAM 1 MEASUREMENT LOCATION
- STREAM 2 MEASUREMENT LOCATION
- STREAM 3 MEASUREMENT LOCATION

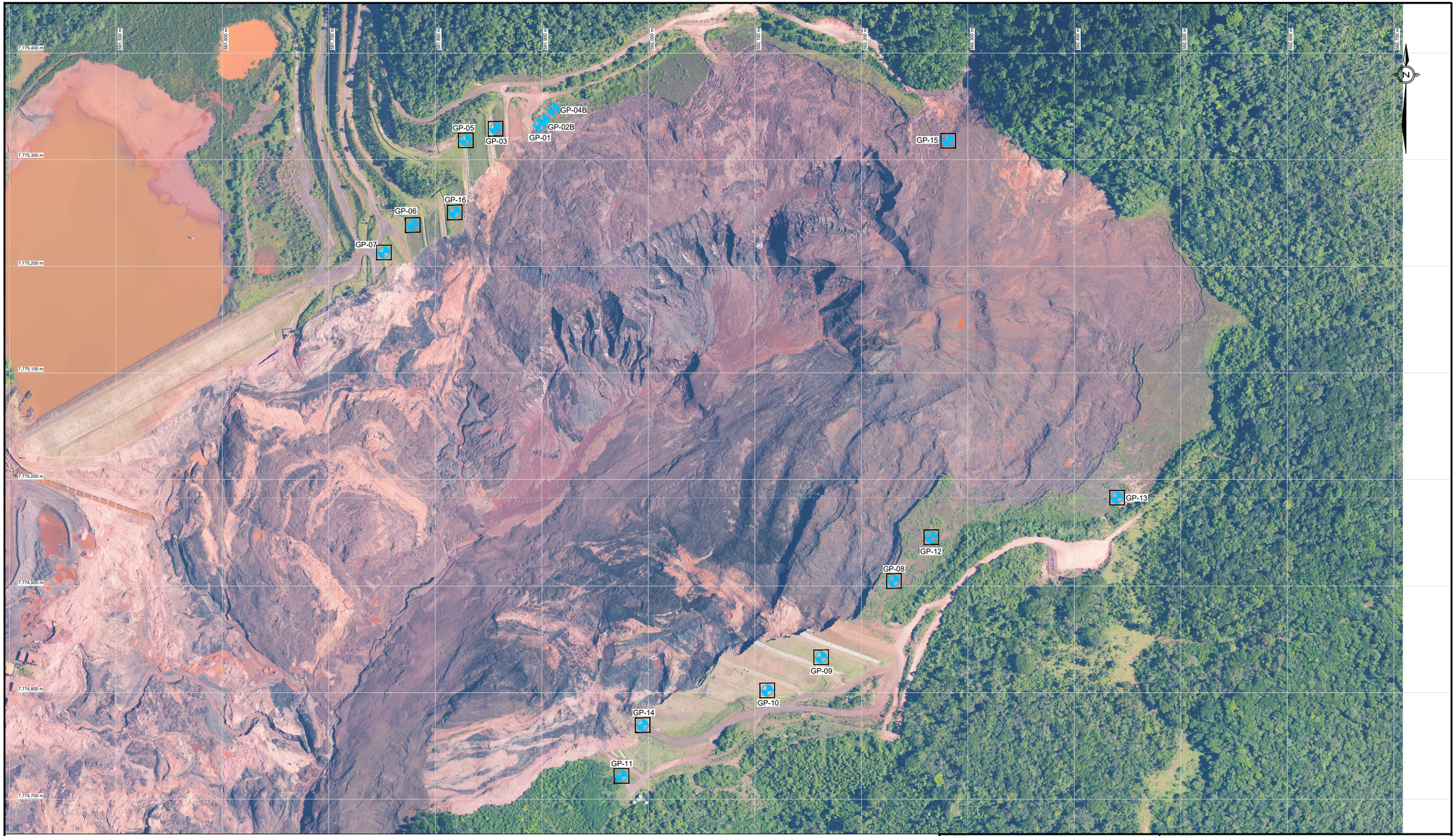
CLIENT

PROJECT
REPORT OF THE EXPERT PANEL ON THE TECHNICAL CAUSES OF THE FAILURE OF FEIJAO DAM 1

TITLE
FIELD INVESTIGATION TEST LOCATIONS

SCALE	PROJECT No.	FIG. No.
N.T.S	0	1

KCB-FG-B-L



NOTES:

1. DRAWING COORDINATES ARE BASED ON UTM ZONE 23S GRID SYSTEM. ALL COORDINATES ARE IN METERS.

LEGEND:

- GUELPH PERMEAMETER TEST LOCATIONS
- TENSIOMETER TEST LOCATIONS

CLIENT

PROJECT
REPORT OF THE EXPERT PANEL ON THE TECHNICAL CAUSES OF THE FAILURE OF FEIJAO DAM 1

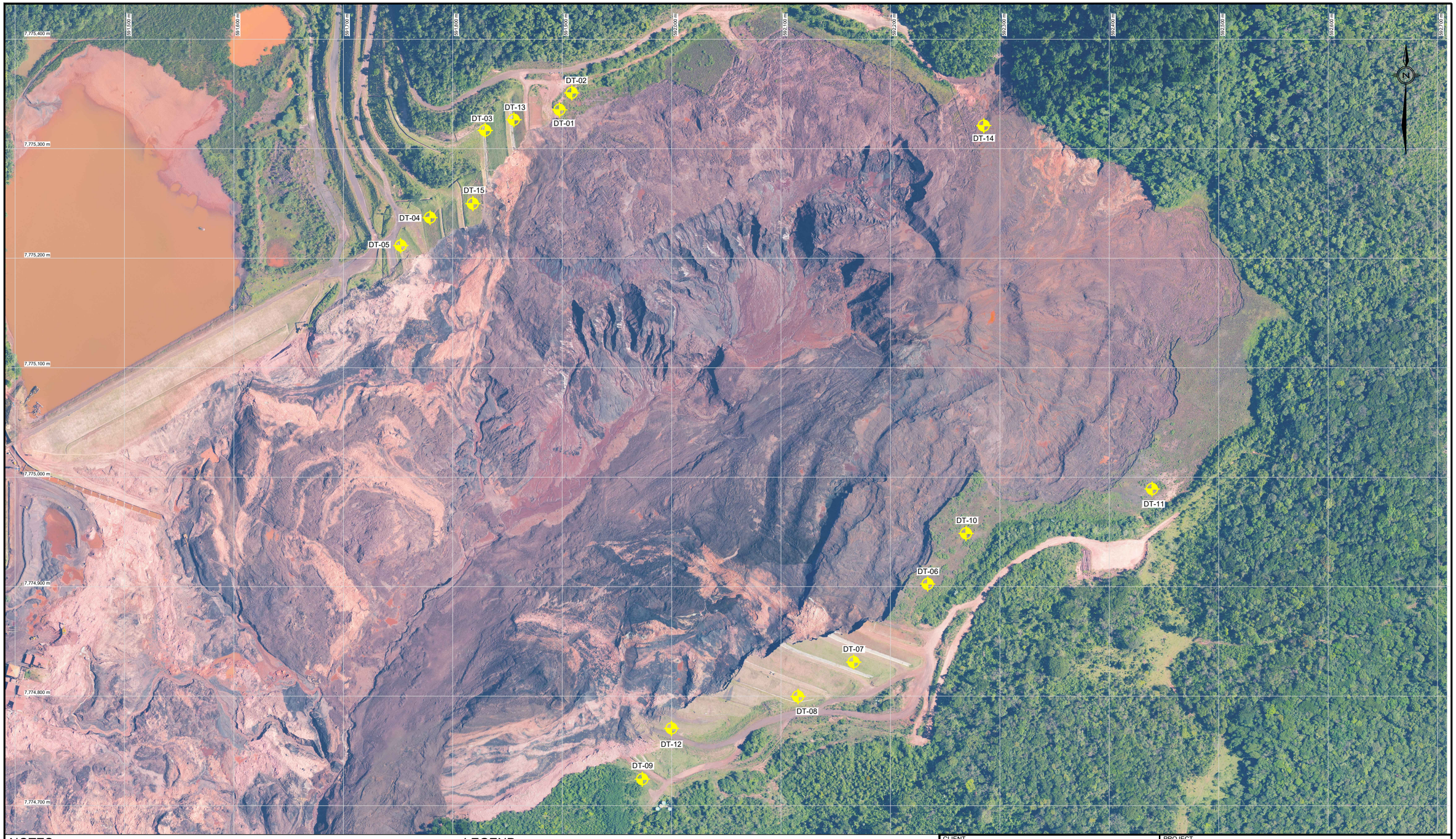
TITLE
GUELPH PERMEAMETER & TENSIOMETER TEST LOCATIONS

SCALE	PROJECT No.	FIG. No.
N.T.S	0	2

KCB-FIG-84



Figure 3 **Guelph Permeameter Test at Location GP-01 (July 2, 2019)**



NOTES:

1. DRAWING COORDINATES ARE BASED ON UTM ZONE 23S GRID SYSTEM. ALL COORDINATES ARE IN METERS.

LEGEND:

DENSITY TEST LOCATIONS

CLIENT

PROJECT
REPORT OF THE EXPERT PANEL ON THE TECHNICAL CAUSES OF THE FAILURE OF FEIJAO DAM 1

TITLE
SAND-REPLACEMENT DENSITY TEST LOCATIONS

SCALE	PROJECT No.	FIG. No.
N.T.S	0	4

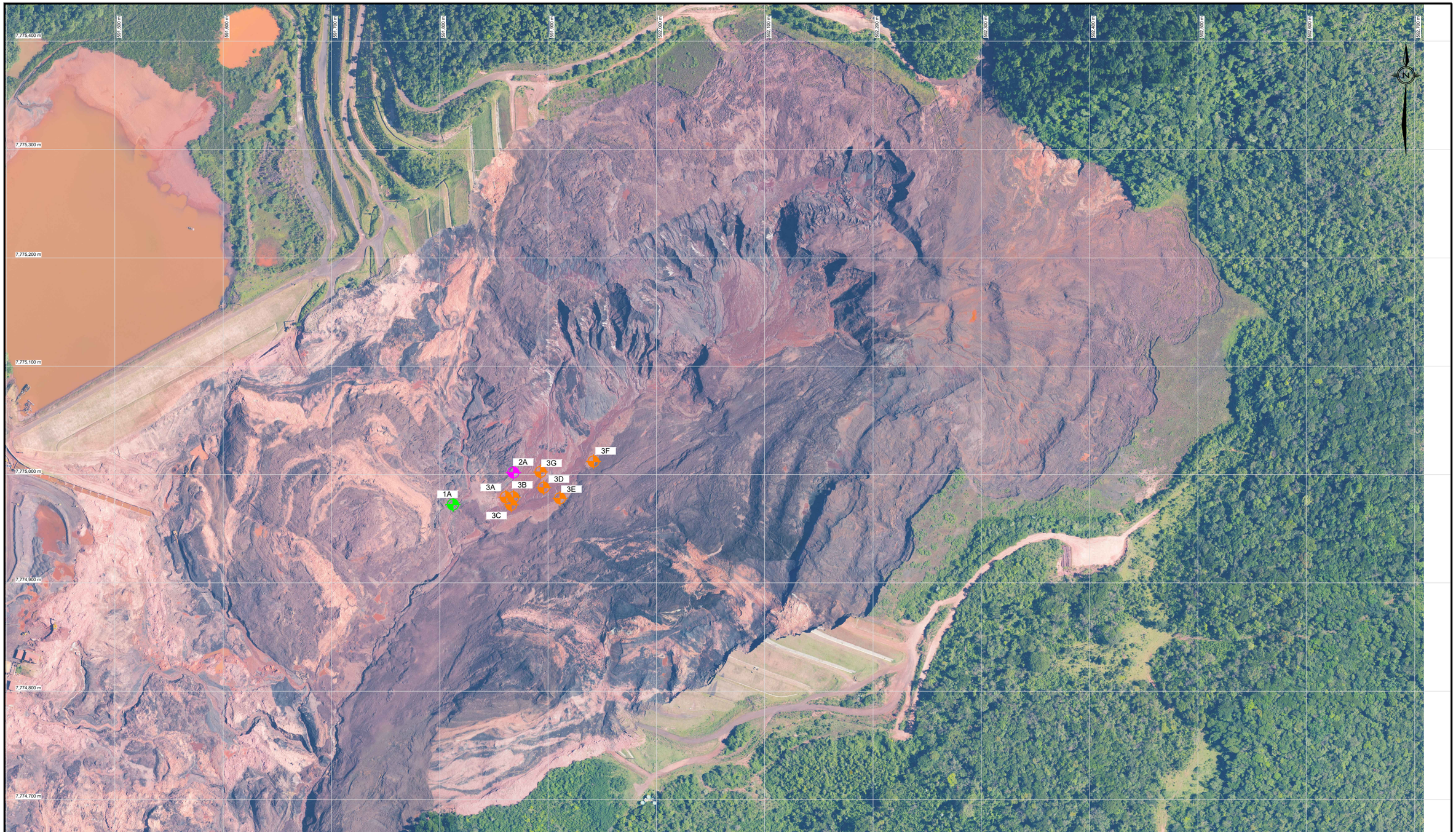
KCB-F-IG-84-L



Figure 5 **Sand Replacement Test DT-01 (July 4, 2019)**



Figure 6 **Sand Replacement Test DT-07 (July 9, 2019)**



NOTES:

1. DRAWING COORDINATES ARE BASED ON UTM ZONE 23S GRID SYSTEM. ALL COORDINATES ARE IN METERS.
2. LOCATIONS OF FLOW MEASUREMENTS ARE APPROXIMATE AND ARE BASED ON A HANDHELD GPS DEVICE.

LEGEND:

- STREAM 1 FLOW RATE LOCATIONS
- STREAM 2 FLOW RATE LOCATIONS
- STREAM 3 FLOW RATE LOCATIONS

CLIENT

PROJECT
REPORT OF THE EXPERT PANEL ON THE TECHNICAL CAUSES OF THE FAILURE OF FEIJAO DAM 1

TITLE
FLOW RATE MEASUREMENT LOCATIONS

SCALE	PROJECT No.	FIG. No.
N.T.S	0	7

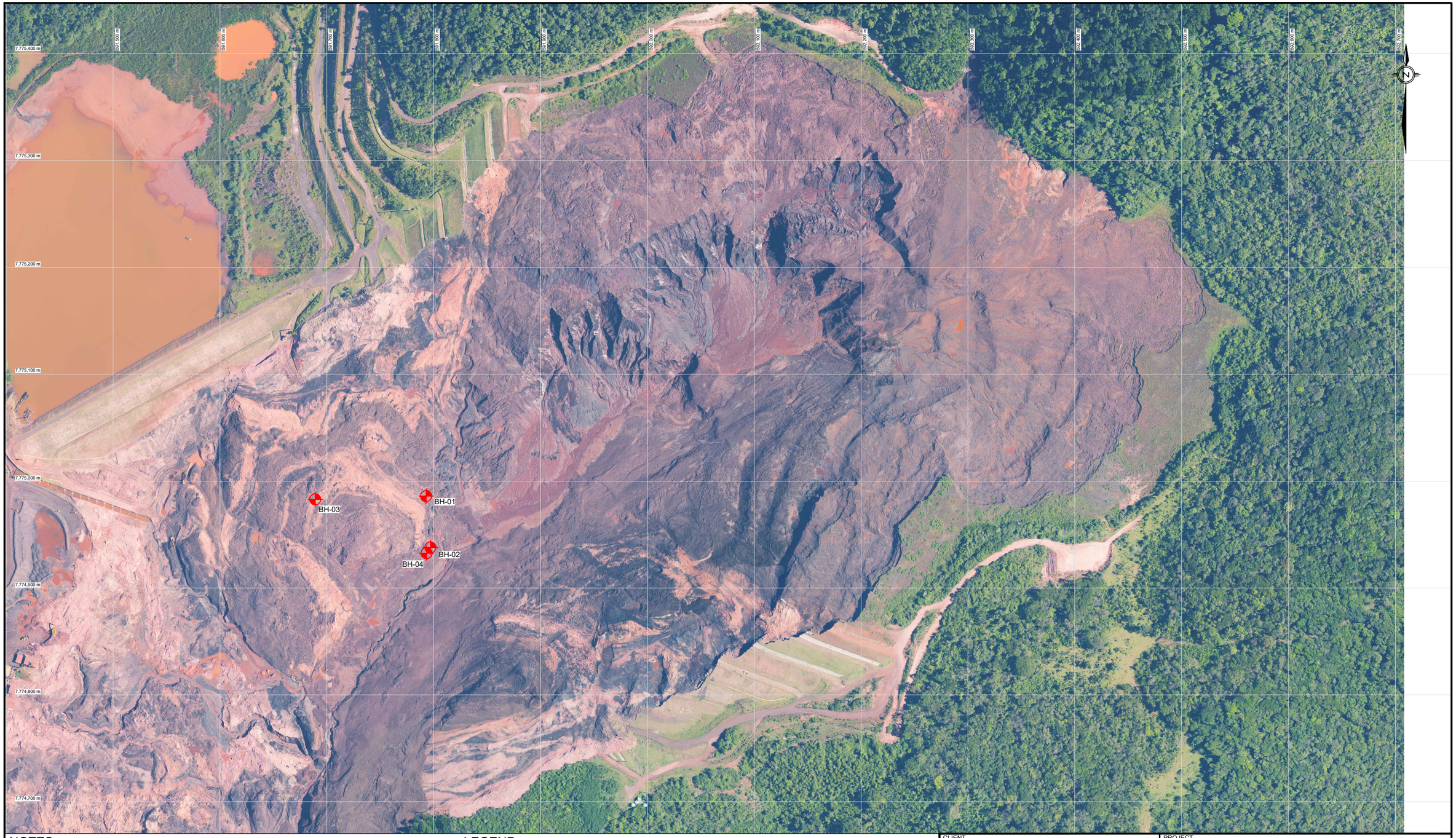
KGI-FIG-B4-



Figure 8 **Flow Rate Measurement at Stream 2 (July 18, 2019)**



Figure 9 **Flow Rate Measurement at Stream 3 (July 18, 2019)**



NOTES:

1. DRAWING COORDINATES ARE BASED ON UTM ZONE 23S GRID SYSTEM. ALL COORDINATES ARE IN METERS.

LEGEND:

BOREHOLE LOCATIONS

CLIENT

PROJECT
REPORT OF THE EXPERT PANEL ON THE TECHNICAL CAUSES OF THE FAILURE OF FEIJAO DAM 1

TITLE
BOREHOLE LOCATIONS

SCALE	PROJECT No.	FIG. No.
N.T.S	0	10

KGS-FIG-BHL



Figure 11 **Rotary Drilling Rig Observed at Site on June 4, 2019**



Figure 12 **Rotary Drilling Rig Used at Borehole Sites**



Figure 13 **Collected Core Samples of Compacted Fill at BH-01 (3 m to 6 m)**



Figure 14 **Collected Core Samples of Compacted Fill at BH-01 (6 m to 9 m)**



Figure 15 **Standard Penetration Testing (SPT) at BH-01**



Figure 16 **Collected SPT Samples at BH-01**



Figure 17 **Sealing of a Shelby Tube Using Wax**



Figure 18 Packaged Shelby Tube Samples

Borehole Logs

BOREHOLE LOG BH-01

STARTED: 2019/07/11 **FINISHED:** 2019/07/17

DRILL METHOD: Mud Rotary

GROUND ELEV. (m): 863.70

COORDINATES (m): N 7774986 E 591793

DEPTH (m)	SPT BLOWS	SAMPLE TYPE	SAMPLE No.	SYMBOL	DESCRIPTION OF MATERIALS
		Grab	BH01/01		SILT (MH); sandy (fine to medium grained, trace coarse grained), trace clay, high plasticity, firm to stiff, moisture content is less than the plastic limit, brownish yellow to yellowish red, moderate cementation, homogeneous. [FILL]
1	5, 10				From 1.0 m to 1.45 m: SPT-01
		Grab	BH01/02		
		Grab	BH01/03		At 1.65 m: 350 mm zone; trace sand (coarse grained, less than 4.1 mm, subangular to subrounded).
2	67				At 2.0 m: SPT-02 Refused
					NO RECOVERY [DRILLER DISTURBED]
		Grab	BH01/04		2.50 / 861.20 At 2.3 m: 200 mm zone; GRAVEL (fine to coarse grained, less than 55 mm, subangular to subrounded), well graded, moist, homogeneous.
3	6, 9				3.00 / 860.70 SILT(MH); sandy (fine grained), trace clay, trace gravel (fine grained, less than 5 mm, angular to subangular), high plasticity, firm to stiff, moisture content is less than the plastic limit, brownish yellow to yellowish red, homogeneous. [FILL]
		Shelby	BH01/05		SILT (MH); sandy (fine grained), trace clay, high plasticity, firm to stiff, moisture content is less than the plastic limit, light brown to brownish yellow (some yellowish red veins less than 1 mm thick, possibly biotite oxidation), moderate cementation, homogeneous. [FOUNDATION]
4		Grab	BH01/06		
		Shelby	BH01/07		At 3.0 m to 3.45 m: SPT-03 At 3.5 m: SHELBY 01
5		Grab	BH01/08		At 3.88 m: trace sand (fine to medium grained), high plastic, some greenish grey zones (less than 2 mm thick), some light brown to reddish brown zones (less than 2 mm thick), trace light grey veins (less than 1 mm thick).
		Shelby	BH01/09		At 4.5 m: SHELBY 02 NO RECOVERY [DRILLER DISTURBED]
		Grab	BH01/10		At 5.5 m: SHELBY 03
6		Grab	BH01/11		
7		Grab	BH01/12		
8		Grab	BH01/13		
9		Grab	BH01/14		
10					

Su - kPa: 20 60 100 140 180

VANE PEAK ◆ REMOLD ◇ FIELD LAB ■ □ ▲UC/2 △P.PEN

★ % FINES ● SPT N

W_P% W% W_L%

20 40 60 80

Continued Next Page

PROJECT NO.:

PROJECT: APPENDIX E

LOCATION: Feijão Dam 01, Toe of slope

LOGGED BY: HS (0m-18m) **CHECKED BY: JMD**

SHEET 1 OF 2

BOREHOLE LOG_SPT A03355A01_VSA_BH_LOGS.GPJ KCBL_CALGARY.GDT 19-12-5

BOREHOLE LOG BH-01

STARTED: 2019/07/11 **FINISHED:** 2019/07/17
DRILL METHOD: Mud Rotary
GROUND ELEV. (m): 863.70
COORDINATES (m): N 7774986 E 591793

Su - kPa: 20 60 100 140 180
VANE PEAK ◆ FIELD ■ LAB ▲ UC/2
REMOLD ◇ □ △ P.PEN
★ % FINES ● SPT N
W_P% W% W_L%
20 40 60 80

DEPTH (m)	SPT BLOWS	SAMPLE TYPE	SAMPLE No.	SYMBOL	DESCRIPTION OF MATERIALS
11		Grab	BH01/15		
		Grab	BH01/16		
12		Grab	BH01/17		
13		Grab	BH01/18		
14		Grab	BH01/19		
					14.80
15		Grab	BH01/20		848.90 SILT (MH); some sand (fine grained, trace coarse grained), trace gravel (fine grained, less than 5mm, subangular to angular), trace clay, high plasticity, poorly graded, stiff to very stiff, light brown to light grey, moisture content is less than plastic limit, moderate to low cementation, homogeneous. [FOUNDATION]
16		Grab	BH01/21		At 16.2m to 17.0 m: Low plasticity.
17		Grab	BH01/22		
18					18.00 845.70 End of Hole at: 18 m
19					
20					

PROJECT NO.:
PROJECT: APPENDIX E
LOCATION: Feijão Dam 01, Toe of slope
LOGGED BY: HS (0m-18m) **CHECKED BY: JMD**
SHEET 2 OF 2

BOREHOLE LOG_SPT A03355A01_VSA_BH_LOGS.GPJ KCBL_CALGARY.GDT 19-12-5

BOREHOLE LOG BH-02

STARTED: 2019/07/18 **FINISHED:** 2019/07/19

DRILL METHOD: Mud Rotary

GROUND ELEV. (m): 857.80

COORDINATES (m): N 7774932.55 E 591793.43

DEPTH (m)	SPT BLOWS	SAMPLE TYPE	SAMPLE No.	SYMBOL	DESCRIPTION OF MATERIALS
		Grab	BH02/01		SILT (MH); sandy (fine to medium grained), trace gravel (fine grained, subangular to subrounded, less than 5 mm), trace clay, high plastic, firm to stiff, reddish brown to dark brown and dark grey, moisture content is less than the plastic limit, moderate cemenation, homogeneous. [FILL]
1	4, 5	Grab	BH02/02		From 1.0 m to 1.45 m: SPT-01
2	3, 5	Grab	BH02/03		From 2.0 m to 2.45 m: SPT-02
					2.70
					855.10 SILT (MH); some sand (fine to medium grained, trace coarse grained), trace clay, high plastic, firm to stiff, light brown to brownish yellow, light grey zones (less than 1 mm thick), greenish grey zones (less than 1 mm thick), dark grey zones (less than 1 mm thick), weak cementation, moisture content is less than the plastic limit, homogeneous. [FOUNDATION]
3		Grab	BH02/04		
		Shelby	BH02/05		At 3.5 m: SHELBY 01
4		Grab	BH02/06		
		Shelby	BH02/07		At 4.5 m: SHELBY 02
5		Grab	BH02/08		
		Shelby	BH02/09		At 5.5 m: SHELBY 03
6		Grab	BH02/10		At 6.5 m: 500 mm zone; some sand (fine to medium grained, poorly graded).
		Shelby	BH02/11		At 6.5 m: SHELBY 04
7		Grab	BH02/12		At: 6.95 m: some sand (fine to medium grained).
		Shelby	BH02/13		At 7.5 m: SHELBY 05
8		Grab	BH02/14		
		Shelby	BH02/15		At: 8.5 m SHELBY 06
9		Grab	BH02/16		
		Shelby	BH02/17		
10					10.00

Continued Next Page

Su - kPa: 20 60 100 140 180

VANE PEAK ◆ FIELD ■ LAB ▲ UC/2
REMOLD ◇ □ △ P.PEN

★ % FINES ● SPT N

W_P% W% W_L%

20 40 60 80

PROJECT NO.:

PROJECT: APPENDIX E

LOCATION: Feijão Dam 01, Toe of slope

LOGGED BY: HS (0m-10.5m) CHECKED BY: JMD

BOREHOLE LOG_SPT A03355A01_VSA_BH_LOGS.GPJ KCBL_CALGARY.GDT 19-12-5

BOREHOLE LOG BH-02

STARTED: 2019/07/18 **FINISHED:** 2019/07/19

DRILL METHOD: Mud Rotary

GROUND ELEV. (m): 857.80

COORDINATES (m): N 7774932.55 E 591793.43

DEPTH (m)	SPT BLOWS	SAMPLE TYPE	SAMPLE No.	SYMBOL	DESCRIPTION OF MATERIALS
		Grab	BH02/18		847.80
					End of Hole at: 10.5 m
11					
12					
13					
14					
15					
16					
17					
18					
19					
20					

Su - kPa

20 60 100 140 180

VANE PEAK ◆ FIELD ■ LAB ▲ UC/2

REMOLD ◇ FIELD □ LAB △ P.PEN

★ % FINES ● SPT N

W_P% W% W_L%

× – – – – o – – – – ×

20 40 60 80

PROJECT NO.:

PROJECT: APPENDIX E

LOCATION: Feijão Dam 01, Toe of slope

LOGGED BY: HS (0m-10.5m) **CHECKED BY: JMD**

SHEET 2 OF 2

BOREHOLE LOG_SPT A03355A01_VSA_BH_LOGS.GPJ KCBL_CALGARY.GDT 19-12-5

BOREHOLE LOG BH-03

STARTED: 2019/07/22 **FINISHED:** 2019/07/23

DRILL METHOD: Mud Rotary

GROUND ELEV. (m): 870.70

COORDINATES (m): N 7774982.91 E 591689.16

DEPTH (m)	SPT BLOWS	SAMPLE TYPE	SAMPLE No.	SYMBOL	DESCRIPTION OF MATERIALS
		Grab	BH03/01		SILT (MH); sandy (fine to medium grained, trace coarse grained), trace clay, high plasticity, firm to stiff, moisture content is less than plastic limit, brownish yellow to yellowish red, weak cementation, homogeneous. [FILL]
1	3, 5	Grab	BH03/02		From 1.0 m to 1.45 m: SPT-01
2	3, 4	Grab	BH03/03		From 2.0 m to 2.45 m: SPT-02
3	6, 5	Grab	BH03/04		From 3.0 m to 3.45 m: SPT-03
4	21, 11	Grab	BH03/05		At 4.0 m: trace gravel (fine grained, less than 6 mm, subrounded to subangular). From 4.0 m to 4.45 m: SPT-04
5	6, 7	Grab	BH03/06		From 5.0 m to 5.45 m: SPT-05
6	7, 7	Grab	BH03/07		From 6.0 m to 6.45 m: SPT-06
7	11, 12	Grab	BH03/08		From 7.0 m to 7.45 m: SPT-07
8	13, 14	Grab	BH03/09		8.00 / 862.70 SILT (MH); some sand (medium to coarse grained), some gravel (coarse grained, less than 75 mm, Ironstone), trace clay, high plastic, reddish brown to dark brown, driller disturbed (cutting head damaged during drilling). [FILL] At 8.0 m to 8.45 m: SPT-08
9					9.00 / 861.70 End of Hole at: 9 m
10					

Su - kPa: 20 60 100 140 180

VANE PEAK ◆ FIELD ■ LAB ▲ UC/2
REMOLD ◇ □ △ P.PEN

★ % FINES ● SPT N

W_P% W% W_L%

20 40 60 80

PROJECT NO.:

PROJECT: APPENDIX E

LOCATION: Feijão Dam 01, Toe of slope

LOGGED BY: HS (0m-9m) **CHECKED BY: JMD**

SHEET 1 OF 1

BOREHOLE LOG_SPT A03355A01_VSA_BH_LOGS.GPJ KCBL_CALGARY.GDT 19-12-5

BOREHOLE LOG BH-04

STARTED: 2019/07/23 **FINISHED:** 2019/07/23

DRILL METHOD: Mud Rotary

GROUND ELEV. (m): 859.00

COORDINATES (m): N 7774937.82 E 591797.01

DEPTH (m)	SPT BLOWS	SAMPLE TYPE	SAMPLE No.	SYMBOL	DESCRIPTION OF MATERIALS
0		Grab	BH04/01		SILT (MH); sandy (fine to medium grained, trace coarse grained), trace clay, high plastic, firm to stiff, moisture content is less than the plastic limit, reddish brown to dark brown to dark grey, moderate cementation, homogeneous. [FILL]
3.50					
855.50		Grab	BH04/02		SILT (MH); some sand (fine to medium grained, trace coarse grained), trace clay, high plastic, firm to stiff, light brown to brownish yellow, light grey zones (less than 1 mm thick), greenish grey zones (less than 1 mm thick), dark grey zones (less than 1 mm thick), weak cementation, moist, homogeneous. [FOUNDATION]
4		Shelby	BH04/03		
		Grab	BH04/04		At 3.7 m: SHELBY 01
5					NO RECOVERY: Failed Shelby sample, overdrilled to 5.3 m.
		Shelby	BH04/04		At 5.3 m: SHELBY 02A
5.65					
853.35					End of Hole at: 5.65 m
6					
7					
8					
9					
10					

Su - kPa

20 60 100 140 180

VANE PEAK ◆ FIELD ■ LAB ▲ UC/2

REMOLD ◇ □ △ P.PEN

★ % FINES ● SPT N

W_P% W% W_L%

× – – – – o – – – – ×

20 40 60 80

PROJECT NO.:

PROJECT: APPENDIX E

LOCATION: Feijão Dam 01, Toe of slope

LOGGED BY: HS (0m-5.65) **CHECKED BY: JMD**

SHEET 1 OF 1

Appendix E

Annex 2 – Summary of Tests

December 2019

Table 1 Summary Table of Test Type and Procedures

Test Type	Laboratory	Standard	Additional Reference	Number of Tests									
				Coarse Tailings	Fine Tailings	Slimes	Compacted Berm (Residual Soil)	Compacted Berm (Tailings)	Foundation Material	Average Gradation	Coarse Gradation	Fine Gradation	Total
Washed Sieve	KCB V	ASTM D422-63(2007)e2		12	2	2	6	6	8	39	22	28	125
Hydrometer	KCB V	ASTM D422-63(2007)e2		12	2	10	6	6	8	39	22	28	133
Specific Gravity	KCB V	ASTM D854-14		17	2	13	7	4	9	-	-	-	52
Water Content	KCB V	ASTM D2216-19		12	8	15	14	10	6	-	-	-	65
Atterberg Limit	KCB V	ASTM D4318-17e1		-	2	14	16	4	12	-	-	-	48
X-ray Diffraction	University of British Columbia	N/A		2	-	2	-	-	-		-	-	4
Scanning Electron Microscope (SEM)	University of British Columbia and University of Queensland	N/A		2	-	3	-	-	-	2	-	-	7
Triaxial Compression	KCB V	ASTM D4767-11(CIU) ASTM D7181-11(CIU)		-	-	-	-	-	-	16	7	12	35
Direct Simple Shear Test	KCB V	ASTM D6528-17		-	-	-	-	-	6	-	-	-	6
Bender Element Tests	KCB V	N/A	Yamashita et al. 2009	-	-	-	-	-	-	4	3	3	10

Appendix E

Annex 3 – Index Test Data

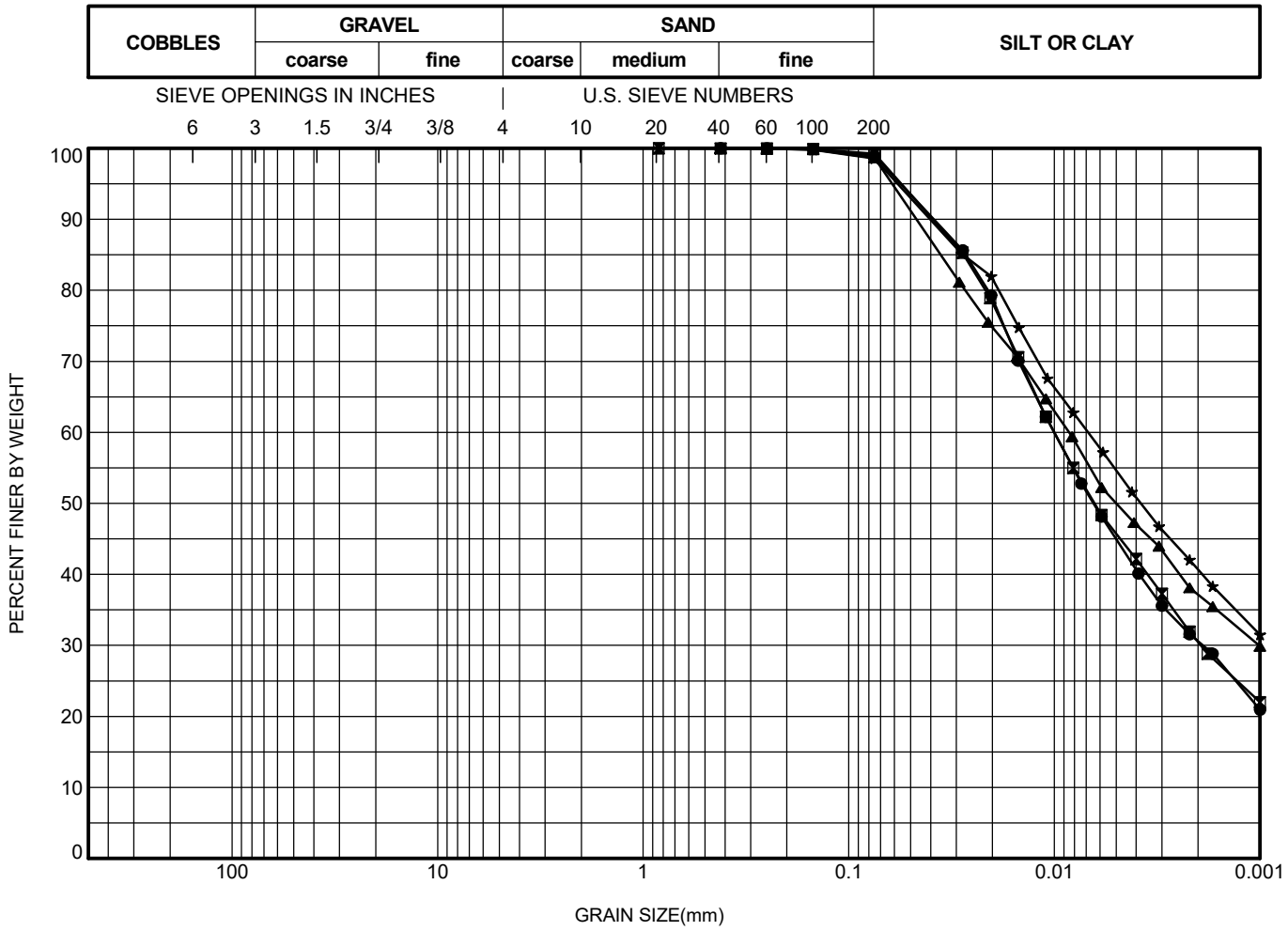
December 2019

Program 1

Particle Size Distribution
Specific Gravity Tests
Moisture Content
Atterberg Limit Test

Particle Size Distribution

GRAIN SIZE DISTRIBUTION



	HOLE	DEPTH (m)	D85	D60	D50	D15	D10	CU	%GRAVEL	%SAND	%FINES
●	S 1	0.00							0.0	1.1	98.9
⊠	S 1	0.00							0.0	0.8	99.2
▲	S 1	0.00							0.0	1.4	98.6
★	S 1	0.00							0.0	1.4	98.6

	HOLE	SAMPLE	DEPTH (m)	W%	W_L	W_P	PI	REMARKS / SAMPLE DESCRIPTION
●	S 1	Bag 1	0.00		43	26	17	Slimes. Pail 1
⊠	S 1	Bag 2	0.00		41	25	16	Slimes. Pail 1
▲	S 1	Bag 3	0.00		43	24	20	Slimes. Pail 2
★	S 1	Bag 4	0.00		46	26	20	Slimes. Pail 2

CU = COEFFICIENT OF UNIFORMITY = D60/D10 **PARTICLE SIZES, e.g. D85, in mm** **Tested by Wet Sieving Method (ASTM D1140 & D422)**

PROJECT NO.: A03355A01

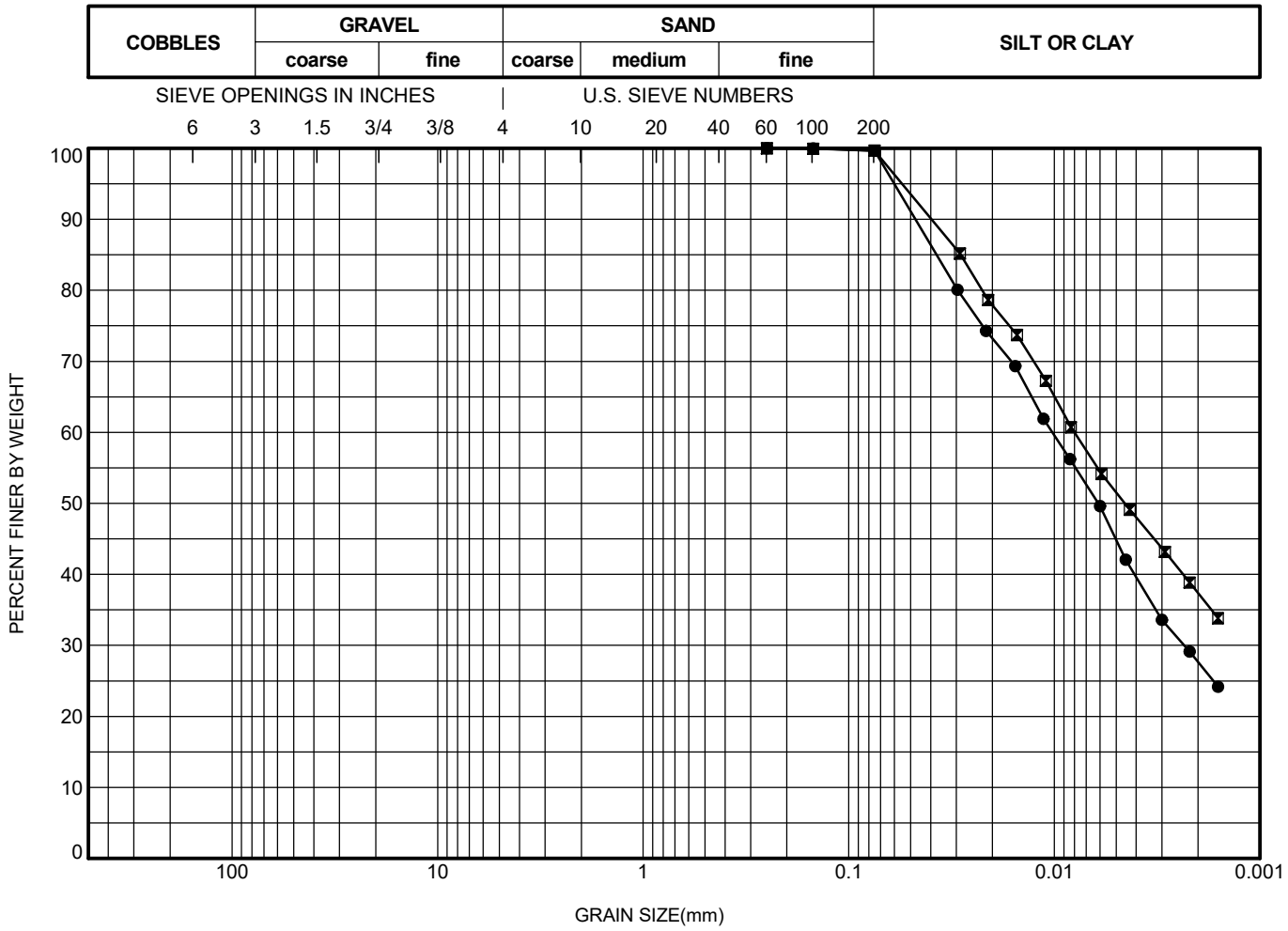
PROJECT:

LOCATION:

FIGURE:

DRAWN BY: HM **CHECKED BY:** JG

GRAIN SIZE DISTRIBUTION



	HOLE	DEPTH (m)	D85	D60	D50	D15	D10	CU	%GRAVEL	%SAND	%FINES
●	S 2	0.00							0.0	0.4	99.6
⊠	S 2	0.00							0.0	0.3	99.7

	HOLE	SAMPLE	DEPTH (m)	W%	W_L	W_P	PI	REMARKS / SAMPLE DESCRIPTION
●	S 2	Bag 1	0.00		48	31	17	Slimes. Pail 3
⊠	S 2	Bag 2	0.00		49	27	22	Slimes. Pail 3

CU = COEFFICIENT OF UNIFORMITY = D60/D10 **PARTICLE SIZES, e.g. D85, in mm** **Tested by Wet Sieving Method (ASTM D1140 & D422)**

PROJECT NO.: A03355A01

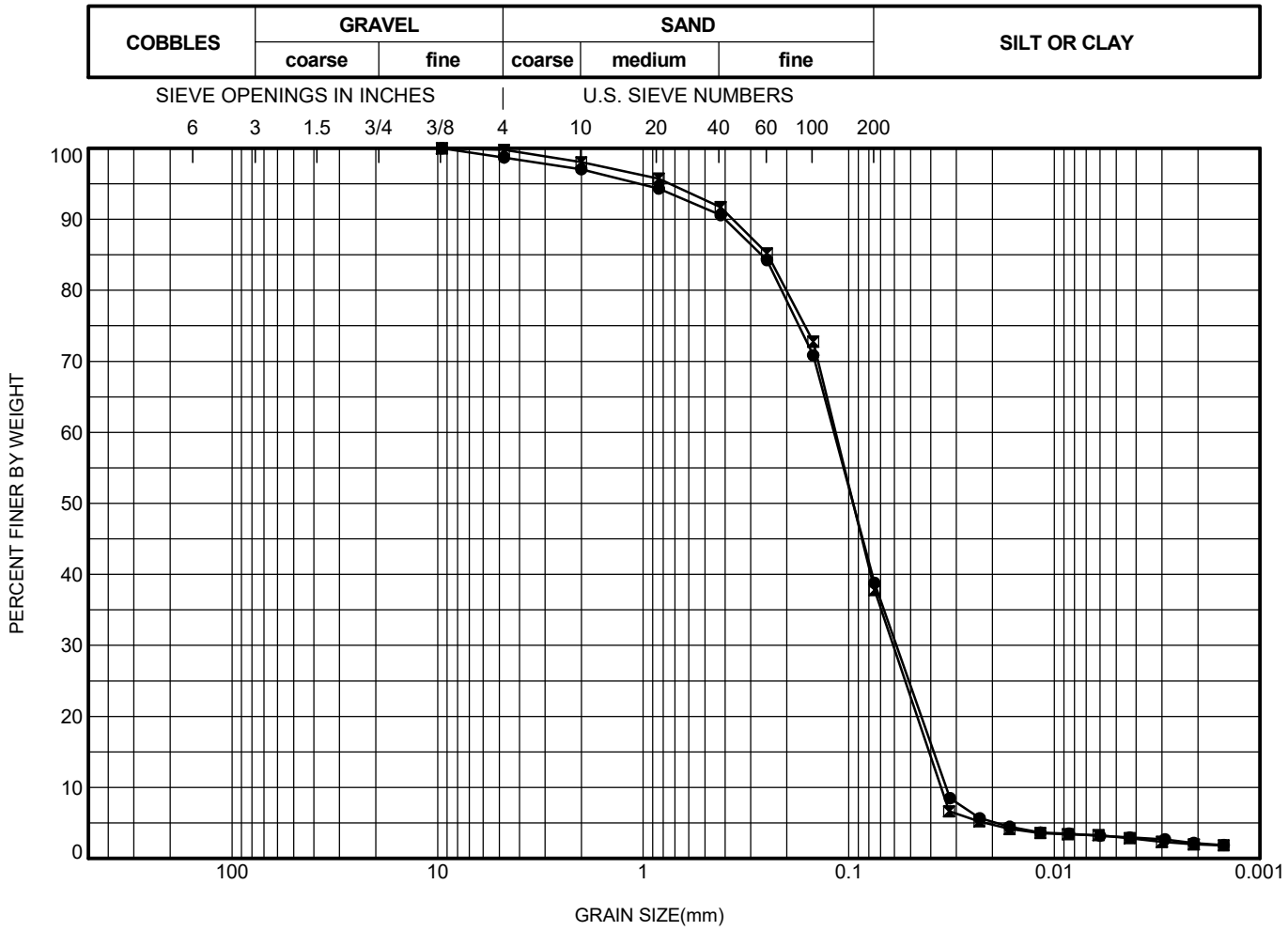
PROJECT:

LOCATION:

FIGURE:

DRAWN BY: HM **CHECKED BY:** JG

GRAIN SIZE DISTRIBUTION



	HOLE	DEPTH (m)	D85	D60	D50	D15	D10	CU	%GRAVEL	%SAND	%FINES
●	S 3	0.00	0.266	0.118	0.095				1.3	59.9	38.8
⊠	S 3	0.00	0.248	0.116	0.095				0.2	62.0	37.8

	HOLE	SAMPLE	DEPTH (m)	W%	W_L	W_P	PI	REMARKS / SAMPLE DESCRIPTION
●	S 3	Bag 1	0.00					Beach tailings. Pail 4
⊠	S 3	Bag 2	0.00					Beach tailings. Pail 4

CU = COEFFICIENT OF UNIFORMITY = D60/D10 **PARTICLE SIZES, e.g. D85, in mm** **Tested by Wet Sieving Method (ASTM D1140 & D422)**

PROJECT NO.: A03355A01

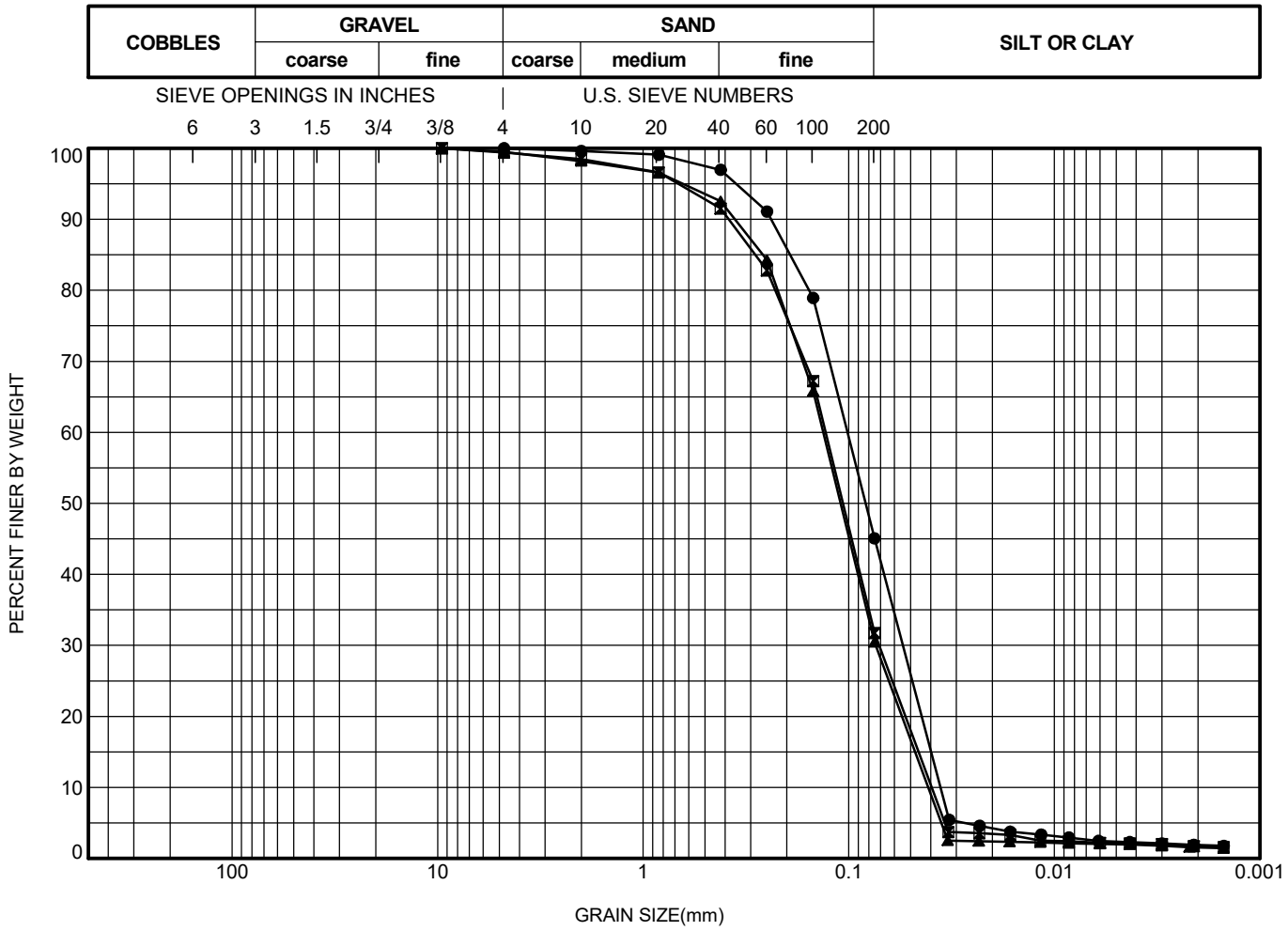
PROJECT:

LOCATION:

FIGURE:

DRAWN BY: HM **CHECKED BY:** JG

GRAIN SIZE DISTRIBUTION



	HOLE	DEPTH (m)	D85	D60	D50	D15	D10	CU	%GRAVEL	%SAND	%FINES
●	S 4	0.00	0.193	0.102	0.083				0.0	54.9	45.1
⊠	S 4	0.00	0.285	0.130	0.107				0.6	67.7	31.7
▲	S 4	0.00	0.261	0.133	0.110				0.5	69.0	30.5

	HOLE	SAMPLE	DEPTH (m)	W%	W_L	W_P	PI	REMARKS / SAMPLE DESCRIPTION
●	S 4	Bag 1	0.00					Beach tailings. Pail 5
⊠	S 4	Bag 2	0.00					Beach tailings. Pail 5
▲	S 4	Bag 3	0.00					Beach tailings. Pail 6

CU = COEFFICIENT OF UNIFORMITY = D60/D10 **PARTICLE SIZES, e.g. D85, in mm** **Tested by Wet Sieving Method (ASTM D1140 & D422)**

PROJECT NO.: A03355A01

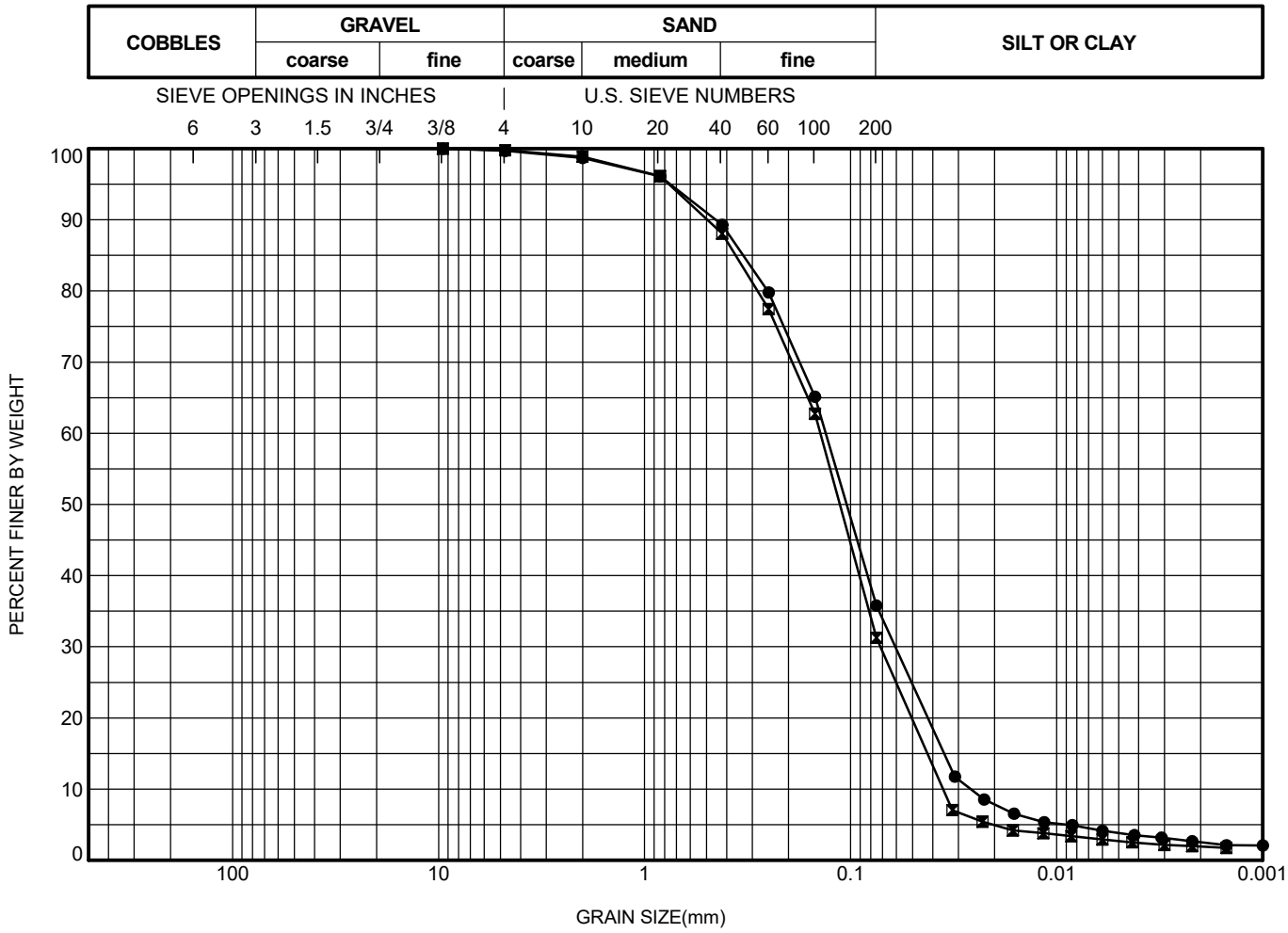
PROJECT:

LOCATION:

FIGURE:

DRAWN BY: HM **CHECKED BY:** JG

GRAIN SIZE DISTRIBUTION



	HOLE	DEPTH (m)	D85	D60	D50	D15	D10	CU	%GRAVEL	%SAND	%FINES
●	S 5	0.00	0.332	0.132	0.105				0.3	63.9	35.8
⊠	S 5	0.00	0.362	0.140	0.113				0.2	68.5	31.3

	HOLE	SAMPLE	DEPTH (m)	W%	W_L	W_P	PI	REMARKS / SAMPLE DESCRIPTION
●	S 5	Bag 1	0.00					Beach tailings. Pail 7
⊠	S 5	Bag 2	0.00					Beach tailings. Pail 7

CU = COEFFICIENT OF UNIFORMITY = D60/D10 **PARTICLE SIZES, e.g. D85, in mm** **Tested by Wet Sieving Method (ASTM D1140 & D422)**

PROJECT NO.: A03355A01

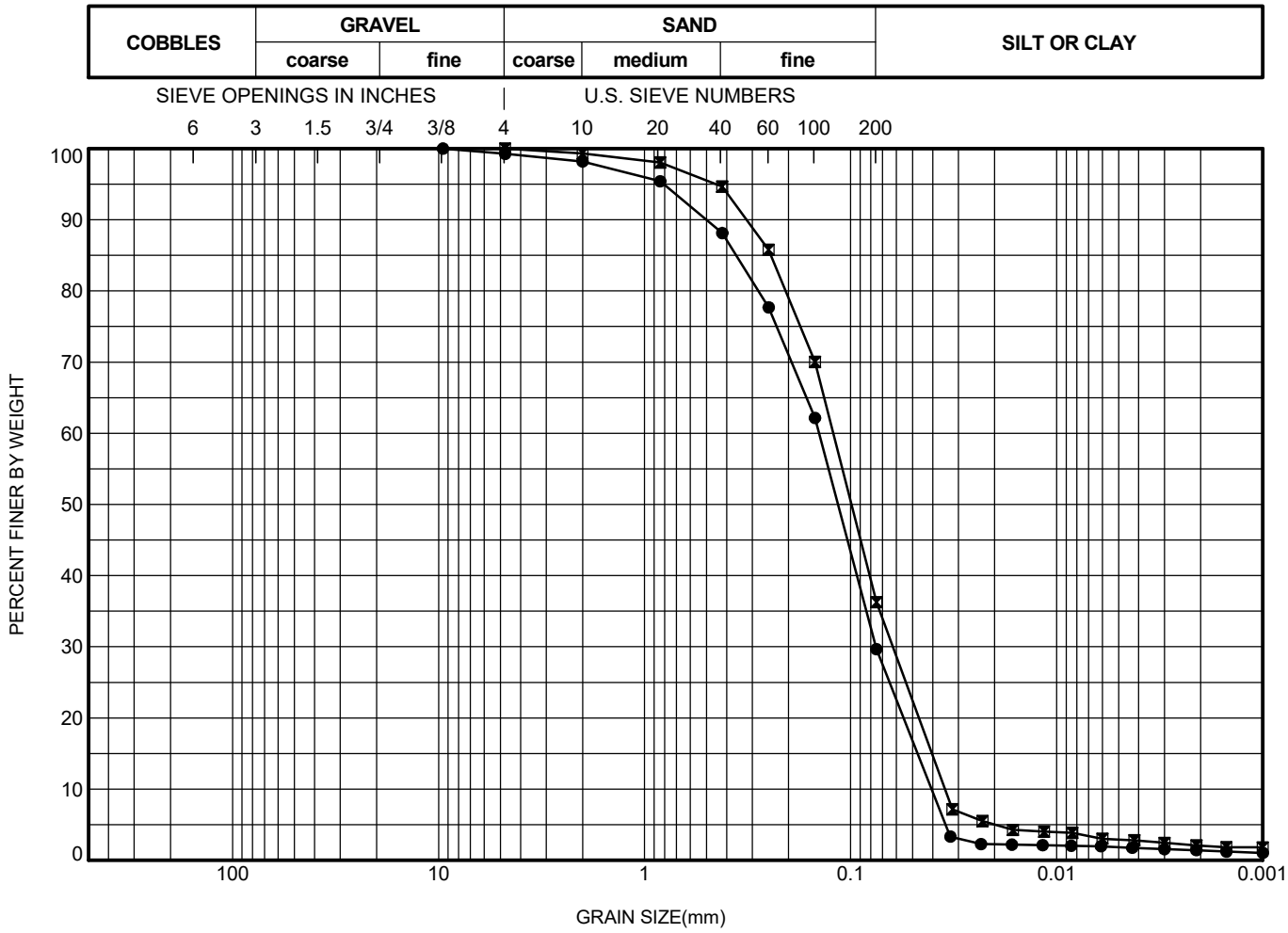
PROJECT:

LOCATION:

FIGURE:

DRAWN BY: HM **CHECKED BY:** JG

GRAIN SIZE DISTRIBUTION



	HOLE	DEPTH (m)	D85	D60	D50	D15	D10	CU	%GRAVEL	%SAND	%FINES
●	S 6	0.00	0.359	0.142	0.115				0.7	69.6	29.7
⊠	S 6	0.00	0.244	0.122	0.099				0.0	63.7	36.3

	HOLE	SAMPLE	DEPTH (m)	W%	W_L	W_P	PI	REMARKS / SAMPLE DESCRIPTION
●	S 6	Bag 1	0.00					Beach tailings. Pail 8
⊠	S 6	Bag 2	0.00					Beach tailings. Pail 8

CU = COEFFICIENT OF UNIFORMITY = D60/D10 **PARTICLE SIZES, e.g. D85, in mm** **Tested by Wet Sieving Method (ASTM D1140 & D422)**

PROJECT NO.: A03355A01

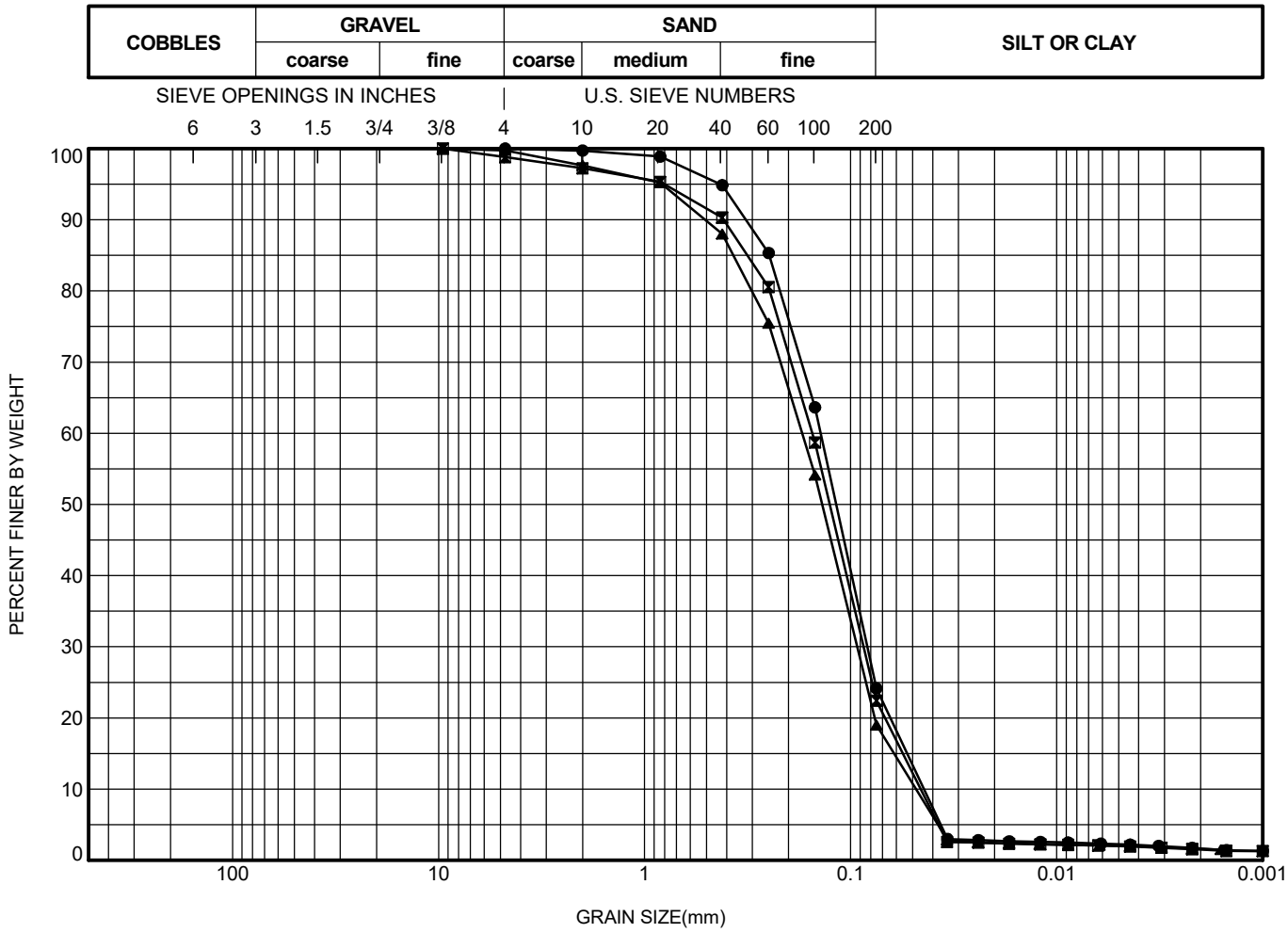
PROJECT:

LOCATION:

FIGURE:

DRAWN BY: HM **CHECKED BY:** JG

GRAIN SIZE DISTRIBUTION



	HOLE	DEPTH (m)	D85	D60	D50	D15	D10	CU	%GRAVEL	%SAND	%FINES
●	S 6b	0.00	0.248	0.140	0.118				0.0	75.9	24.1
⊠	S 6b	0.00	0.317	0.154	0.126				1.2	76.4	22.4
▲	S 6b	0.00	0.371	0.172	0.138				0.2	80.8	19.0

	HOLE	SAMPLE	DEPTH (m)	W%	W_L	W_P	PI	REMARKS / SAMPLE DESCRIPTION
●	S 6b	Bag 1	0.00					Beach tailings. Pail 9
⊠	S 6b	Bag 2	0.00					Beach tailings. Pail 9
▲	S 6b	Bag 3	0.00					Beach tailings. Pail 9

CU = COEFFICIENT OF UNIFORMITY = D60/D10 **PARTICLE SIZES, e.g. D85, in mm** **Tested by Wet Sieving Method (ASTM D1140 & D422)**

PROJECT NO.: A03355A01

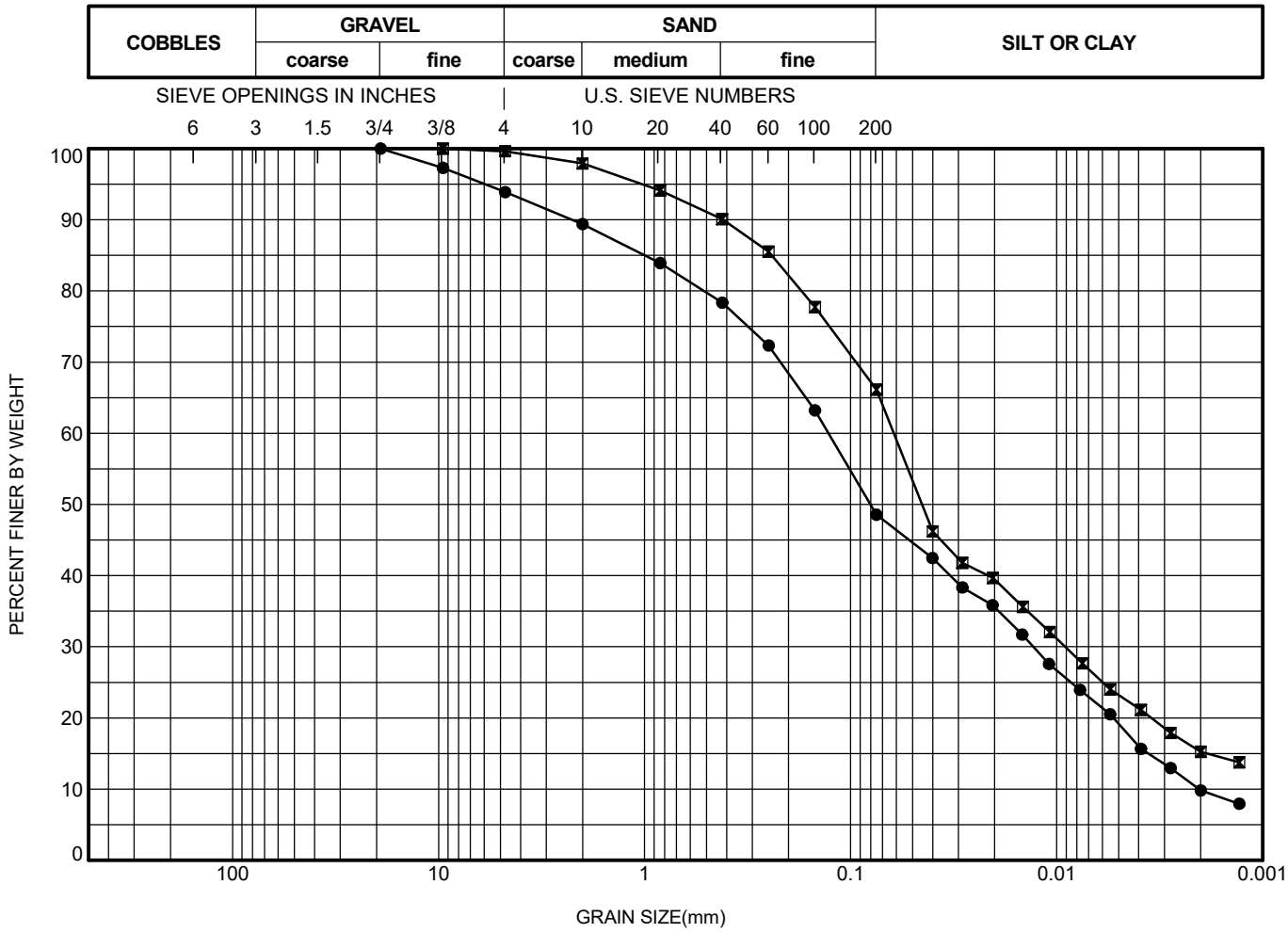
PROJECT:

LOCATION:

FIGURE:

DRAWN BY: HM **CHECKED BY:** JG

GRAIN SIZE DISTRIBUTION



	HOLE	DEPTH (m)	D85	D60	D50	D15	D10	CU	%GRAVEL	%SAND	%FINES
●	S 7	0.00	0.998	0.128	0.080				6.1	45.3	48.6
⊠	S 7	0.00	0.241						0.4	33.5	66.1

	HOLE	SAMPLE	DEPTH (m)	W%	W_L	W_P	PI	REMARKS / SAMPLE DESCRIPTION
●	S 7	Bag 1	0.00		30	23	7	Residual Soil. Pail 10. Dried at 45C/dried 45C
⊠	S 7	Bag 2	0.00		35	25	10	Residual Soil Pail 10. Natural/ dried 45C

CU = COEFFICIENT OF UNIFORMITY = D60/D10 **PARTICLE SIZES, e.g. D85, in mm** **Tested by Wet Sieving Method (ASTM D1140 & D422)**

PROJECT NO.: A03355A01

PROJECT:

LOCATION:

FIGURE:

DRAWN BY: HM **CHECKED BY:** JG

Specific Gravity Tests

SPECIFIC GRAVITY OF SOIL SOLIDS (ASTM-D854)

Hole Number	S1			S1		
Sample Number	Bag 1			Bag 3		
Depth (m)						
Sample Description	Slimes			Slimes		
Flask No.	11	SG-6	SG-10	SG-5	KL-2	SG-9
Volume of Flask @ 20° C ml	500	500	500	500	500	500
Method of Air removal	boiling	boiling	boiling	boiling	boiling	boiling
De-airing Period hr	2	2	2	2	2	2
Test temperature ° C	22.2	22.1	22.1	22.1	22.1	22.1
Mass of Flask+Water (M_a) g	678.58	670.54	669.95	672.12	675.50	667.84
Mass of Flask+Water+Soil (M_b) g	726.58	718.98	718.20	720.29	723.74	716.26
Mass of Dish/Flask+Soil	244.03	236.38	236.08	238.15	241.46	234.09
Mass of Dish/Flask	180.38	172.18	171.94	173.90	177.06	169.66
Mass of Dry Soil (M_o) g	63.65	64.20	64.14	64.25	64.40	64.43
Correction factor (K) @ Test Temperature	0.99952	0.99954	0.99954	0.99954	0.99954	0.99954
Specific Gravity of Solids @ 20° C	**4.065**	**4.072**	**4.035**	**3.994**	**3.983**	**4.023**
Average Specific Gravity of Solids @ 20° C		**4.06**			**4.00**	

Hole Number	S2					
Sample Number	Bag 1					
Depth (m)						
Sample Description	Slimes					
Flask No.	10	12	SG-2			
Volume of Flask @ 20° C ml	500	500	500			
Method of Air removal	boiling	boiling	boiling			
De-airing Period hr	2	2	2			
Test temperature ° C	22.5	22.6	22.5			
Mass of Flask+Water (M_a) g	679.64	680.38	671.54			
Mass of Flask+Water+Soil (M_b) g	729.12	733.56	719.38			
Mass of Dish/Flask+Soil	247.53	253.35	237.46			
Mass of Dish/Flask	181.51	182.10	173.27			
Mass of Dry Soil (M_o) g	66.02	71.25	64.19			
Correction factor (K) @ Test Temperature	0.99945	0.99943	0.99945			
Specific Gravity of Solids @ 20° C	**3.989**	**3.941**	**3.924**			
Average Specific Gravity of Solids @ 20° C		**3.95**				

Specific Gravity of Solids @ 20° C = $(K \times M_o)/(M_o + M_a - M_b)$

PROJECT#:	A03355A01			
PROJECT:				
LOCATION:				
DATE:	2019-06-12			
TESTED BY:	HM	CHECKED BY:	JG	

SPECIFIC GRAVITY OF SOIL SOLIDS (ASTM-D854)

Hole Number	S3			S4		
Sample Number	Bag 1			Bag 1		
Depth (m)						
Sample Description	Beach Tailings			Beach Tailings		
Flask No.	SG-4	12	SG-7	8	KL-3	SG-2
Volume of Flask @ 20° C ml	500	500	500	500	500	500
Method of Air removal	boiling	boiling	boiling	boiling	boiling	boiling
De-airing Period hr	2	2	2	2	2	2
Test temperature ° C	22.3	22.4	22.4	22.4	22.5	22.4
Mass of Flask+Water (M_a) g	670.67	680.41	667.77	678.62	675.78	671.54
Mass of Flask+Water+Soil (M_b) g	751.38	761.22	749.12	742.66	740.36	732.03
Mass of Dish/Flask+Soil	273.98	283.69	271.46	260.50	258.14	249.11
Mass of Dish/Flask	172.56	182.11	169.41	180.44	177.35	173.26
Mass of Dry Soil (M_o) g	101.42	101.58	102.05	80.06	80.79	75.85
Correction factor (K) @ Test Temperature	0.99950	0.99948	0.99948	0.99904	0.99945	0.99948
Specific Gravity of Solids @ 20° C	**4.895**	**4.888**	**4.927**	**4.993**	**4.981**	**4.936**
Average Specific Gravity of Solids @ 20° C	**4.90**			**4.97**		

Hole Number	S4			S5		
Sample Number	Bag 3			Bag 2		
Depth (m)						
Sample Description	Beach Tailings			Beach Tailings		
Flask No.	10	SG-3	SG-11	SG-8	SG-12	1
Volume of Flask @ 20° C ml	500	500	500	500	500	500
Method of Air removal	boiling	boiling	boiling	boiling	boiling	boiling
De-airing Period hr	2	2	2	2	2	2
Test temperature ° C	22.4	22.5	22.5	22.6	22.6	22.6
Mass of Flask+Water (M_a) g	679.66	672.25	670.38	670.60	670.59	667.22
Mass of Flask+Water+Soil (M_b) g	751.81	743.83	743.12	748.75	751.88	749.18
Mass of Dish/Flask+Soil	273.47	265.04	264.15	270.24	274.34	271.38
Mass of Dish/Flask	181.52	173.92	172.18	172.38	172.53	168.77
Mass of Dry Soil (M_o) g	91.95	91.12	91.97	97.86	101.81	102.61
Correction factor (K) @ Test Temperature	0.99948	0.99943	0.99945	0.99943	0.99943	0.99943
Specific Gravity of Solids @ 20° C	**4.642**	**4.661**	**4.780**	**4.962**	**4.959**	**4.966**
Average Specific Gravity of Solids @ 20° C	**4.69**			**4.96**		

Specific Gravity of Solids @ 20° C = $(K \times M_o)/(M_o + M_a - M_b)$

PROJECT#:	A03355A01			
PROJECT:				
LOCATION:				
DATE:	2019-06-12			
TESTED BY:	HM	CHECKED BY:	JG	

SPECIFIC GRAVITY OF SOIL SOLIDS (ASTM-D854)

Hole Number		S6			S6b		
Sample Number		Bag 2			Bag 2		
Depth (m)							
Sample Description		Beach Tailings			Beach Tailings		
Flask No.		SG-4	SG-6	SG-5	3	KL-3	
Volume of Flask @ 20° C	ml	500	500	500	500	500	
Method of Air removal		boiling	boiling	boiling	boiling	boiling	
De-airing Period	hr	2	2	2	2	2	
Test temperature	° C	23.1	22.6	22.6	22.5	23.1	
Mass of Flask+Water (M_a)	g	670.59	670.47	672.06	671.43	675.72	
Mass of Flask+Water+Soil (M_b)	g	744.70	748.15	747.04	741.86	749.88	
Mass of Dish/Flask+Soil		265.30	269.40	267.77	261.65	270.85	
Mass of Dish/Flask		172.56	172.16	173.90	172.69	177.35	
Mass of Dry Soil (M_o)	g	92.74	97.24	93.87	88.96	93.50	
Correction factor (K) @ Test Temperature		0.99931	0.99943	0.99943	0.99948	0.99924	
Specific Gravity of Solids @ 20° C		**4.975**	**4.969**	**4.966**	**4.798**	**4.831**	
Average Specific Gravity of Solids @ 20° C			**4.97**			**4.81**	

Hole Number							
Sample Number							
Depth (m)							
Sample Description							
Flask No.							
Volume of Flask @ 20° C	ml						
Method of Air removal							
De-airing Period	hr						
Test temperature	° C						
Mass of Flask+Water (M_a)	g						
Mass of Flask+Water+Soil (M_b)	g						
Mass of Dish/Flask+Soil							
Mass of Dish/Flask							
Mass of Dry Soil (M_o)	g						
Correction factor (K) @ Test Temperature							
Specific Gravity of Solids @ 20° C							
Average Specific Gravity of Solids @ 20° C							

Specific Gravity of Solids @ 20° C = $(K \times M_o)/(M_o + M_a - M_b)$

PROJECT#:	A03355A01			
PROJECT:				
LOCATION:				
DATE:	2019-06-12			
TESTED BY:	HM	CHECKED BY:	JG	

SPECIFIC GRAVITY OF SOIL SOLIDS (ASTM-D854)

Hole Number		S7					
Sample Number		Bag 1					
Depth (m)							
Sample Description							
Flask No.		8	SG-3	SG-7			
Volume of Flask @ 20° C	ml	500	500	500			
Method of Air removal		boiling	boiling	boiling			
De-airing Period	hr	2	2	2			
Test temperature	° C	22.6	22.7	22.7			
Mass of Flask+Water (M_a)	g	678.62	672.24	667.75			
Mass of Flask+Water+Soil (M_b)	g	721.07	714.61	706.02			
Mass of Dish/Flask+Soil		242.94	235.88	225.49			
Mass of Dish/Flask		180.47	173.93	169.43			
Mass of Dry Soil (M_o)	g	62.47	61.95	56.06			
Correction factor (K) @ Test Temperature		0.99943	0.99941	0.99941			
Specific Gravity of Solids @ 20° C		**3.119**	**3.162**	**3.149**			
Average Specific Gravity of Solids @ 20° C			**3.14**				

Hole Number							
Sample Number							
Depth (m)							
Sample Description							
Flask No.							
Volume of Flask @ 20° C	ml						
Method of Air removal							
De-airing Period	hr						
Test temperature	° C						
Mass of Flask+Water (M_a)	g						
Mass of Flask+Water+Soil (M_b)	g						
Mass of Dish/Flask+Soil							
Mass of Dish/Flask							
Mass of Dry Soil (M_o)	g						
Correction factor (K) @ Test Temperature							
Specific Gravity of Solids @ 20° C							
Average Specific Gravity of Solids @ 20° C							

Specific Gravity of Solids @ 20° C = $(K \times M_o)/(M_o + M_a - M_b)$

PROJECT#:	A03355A01			
PROJECT:				
LOCATION:				
DATE:	2019-06-12			
TESTED BY:	HM	CHECKED BY:	JG	

Moisture Content

WATER CONTENT OF SOIL
(ASTM D2216)

Hole Number	Sample Number	Depth (m)	Wet Weight + Tare (g)	Dry Weight + Tare (g)	Tare (g)	Water Weight (g)	Total Dry Weight (g)	Water Content (%)	Notes
S1	Bag 1		160.06	144.90	84.39	15.16	60.51	**25.05**	
S1	Bag 1		228.49	201.55	90.15	26.94	111.40	**24.18**	
S1	Bag 2		252.88	222.70	85.92	30.18	136.78	**22.06**	
S1	Bag 3		233.76	205.06	87.73	28.70	117.33	**24.46**	
S1	Bag 4		289.64	253.21	105.13	36.43	148.08	**24.60**	
S2	Bag 1		288.93	237.89	86.47	51.04	151.42	**33.71**	
S2	Bag 2		273.25	233.78	88.91	39.47	144.87	**27.25**	

PROJECT No.:	A03355A01
PROJECT NAME:	
LOCATION:	
DATE:	2019/06/17
TESTED BY:	HM, JG CHECKED BY: JG

WATER CONTENT OF SOIL
(ASTM D2216)

Hole Number	Sample Number	Depth (m)	Wet Weight + Tare (g)	Dry Weight + Tare (g)	Tare (g)	Water Weight (g)	Total Dry Weight (g)	Water Content (%)	Notes
S3	Bag 1		251.30	233.80	85.30	17.50	148.50	11.78	
S3	Bag 2		216.23	204.64	88.24	11.59	116.40	9.96	
S4	Bag 1		230.14	219.25	86.29	10.89	132.96	8.19	
S4	Bag 2		299.04	271.46	84.46	27.58	187.00	14.75	
S4	Bag 3		285.01	259.91	86.76	25.10	173.15	14.50	
S5	Bag 1		288.28	278.42	103.55	9.86	174.87	5.64	
S5	Bag 2		282.46	273.56	120.18	8.90	153.38	5.80	
S6	Bag 1		281.70	258.23	90.74	23.47	167.49	14.01	
S6	Bag 2		302.33	285.71	102.38	16.62	183.33	9.07	
S6B	Bag 1		235.88	224.85	113.20	11.03	111.65	9.88	
S6B	Bag 2		302.65	283.89	118.42	18.76	165.47	11.34	
S6B	Bag 3		338.22	323.21	134.27	15.01	188.94	7.94	

PROJECT No.:	A03355A01
PROJECT NAME:	
LOCATION:	
DATE:	2019/06/17
TESTED BY:	HM, JG CHECKED BY: JG

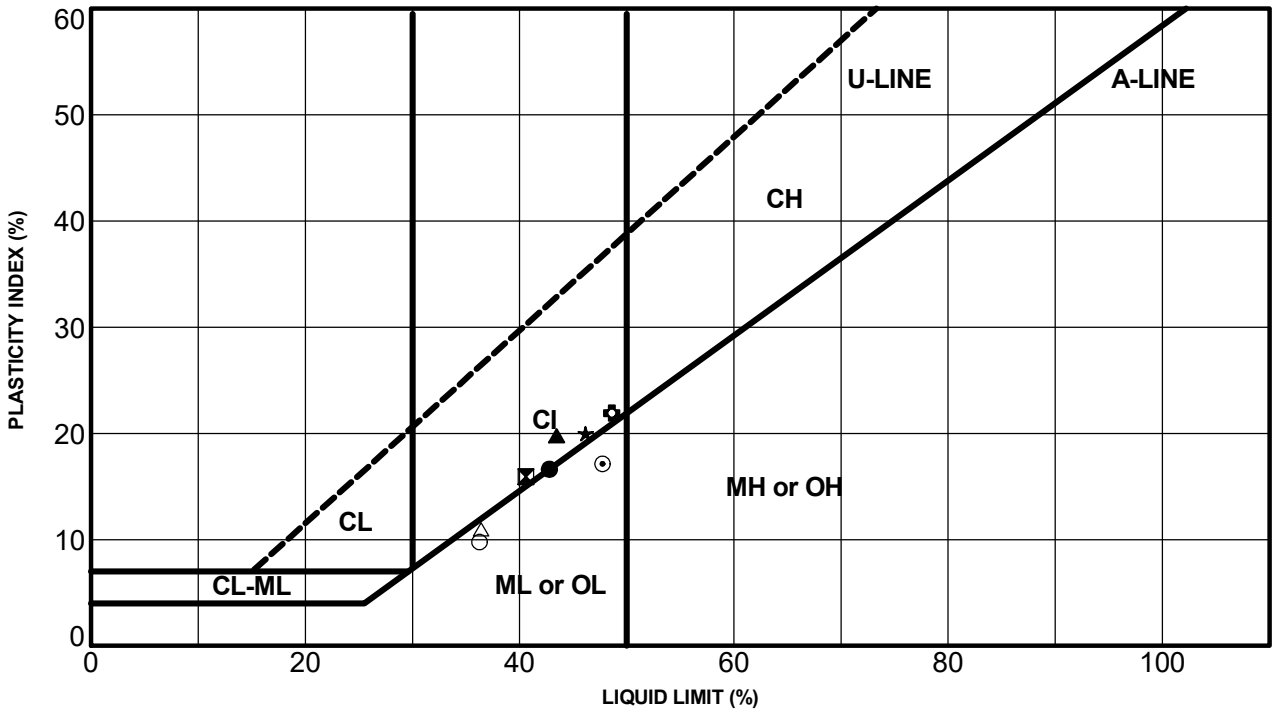
WATER CONTENT OF SOIL
(ASTM D2216)

Hole Number	Sample Number	Test Number	Wet Weight + Tare (g)	Dry Weight + Tare (g)	Tare (g)	Water Weight (g)	Total Dry Weight (g)	Water Content (%)	Notes
S7	Bag1	WC 1	316.15	308.70	268.82	7.45	39.88	**18.68**	WC @ 110 °C
S7	Bag1	WC 2	213.98	198.68	114.00	15.30	84.68	**18.07**	WC @ 45 °C
S7	Bag 1	WC 2	213.98	198.68	114.00	15.30	84.68	**18.07**	13th of June
S7	Bag 1	WC 2	213.98	198.66	114.00	15.32	84.66	**18.10**	14th of June
S7	Bag 1	WC 2	213.98	198.65	114.00	15.33	84.65	**18.11**	15th of June
S7	Bag 1	WC 2	213.98	198.62	114.00	15.36	84.62	**18.15**	16th of June
S7	Bag 1	WC 2	213.98	198.62	114.00	15.36	84.62	**18.15**	17th of June
S7	Bag2	WC 1	356.92	342.79	279.41	14.13	63.38	**22.29**	WC @ 110 °C
S7	Bag2	WC 2	261.20	238.11	123.62	23.09	114.49	**20.17**	WC @ 45 °C
S7	Bag 2	WC 2	261.20	238.11	123.62	23.09	114.49	**20.17**	13th of June
S7	Bag 2	WC 2	261.20	238.10	123.62	23.10	114.48	**20.18**	14th of June
S7	Bag 2	WC 2	261.20	238.10	123.62	23.10	114.48	**20.18**	15th of June
S7	Bag 2	WC 2	261.20	238.10	123.62	23.10	114.48	**20.18**	16th of June
S7	Bag 2	WC 2	261.20	238.10	123.62	23.10	114.48	**20.18**	17th of June

PROJECT No.:	A03355A01
PROJECT NAME:	
LOCATION:	
DATE:	2019/06/17
TESTED BY:	HM, JG CHECKED BY: JG

Atterberg Limit Tests

PLASTICITY CHART



	HOLE	SAMPLE	DEPTH (m)	W_L	W_P	PI	% FINES	REMARKS/SAMPLE DESCRIPTION
●	S 1	Bag 1	0.0	43	26	17	98.9	Slimes. Pail 1
⧓	S 1	Bag 2	0.0	41	25	16	99.2	Slimes. Pail 1
▲	S 1	Bag 3	0.0	43	24	20	98.6	Slimes. Pail 2
★	S 1	Bag 4	0.0	46	26	20	98.6	Slimes. Pail 2
⊙	S 2	Bag 1	0.0	48	31	17	99.6	Slimes. Pail 3
✿	S 2	Bag 2	0.0	49	27	22	99.7	Slimes. Pail 3
○	S 7	Bag 1	0.0	36	26	10		Residual Soil. Pail 10. Natural/dried 110C
△	S 7	Bag 2	0.0	36	25	11		Residual Soil Pail 10. Natural/ dried 110C

PROJECT NO.: A03355A01

PROJECT:

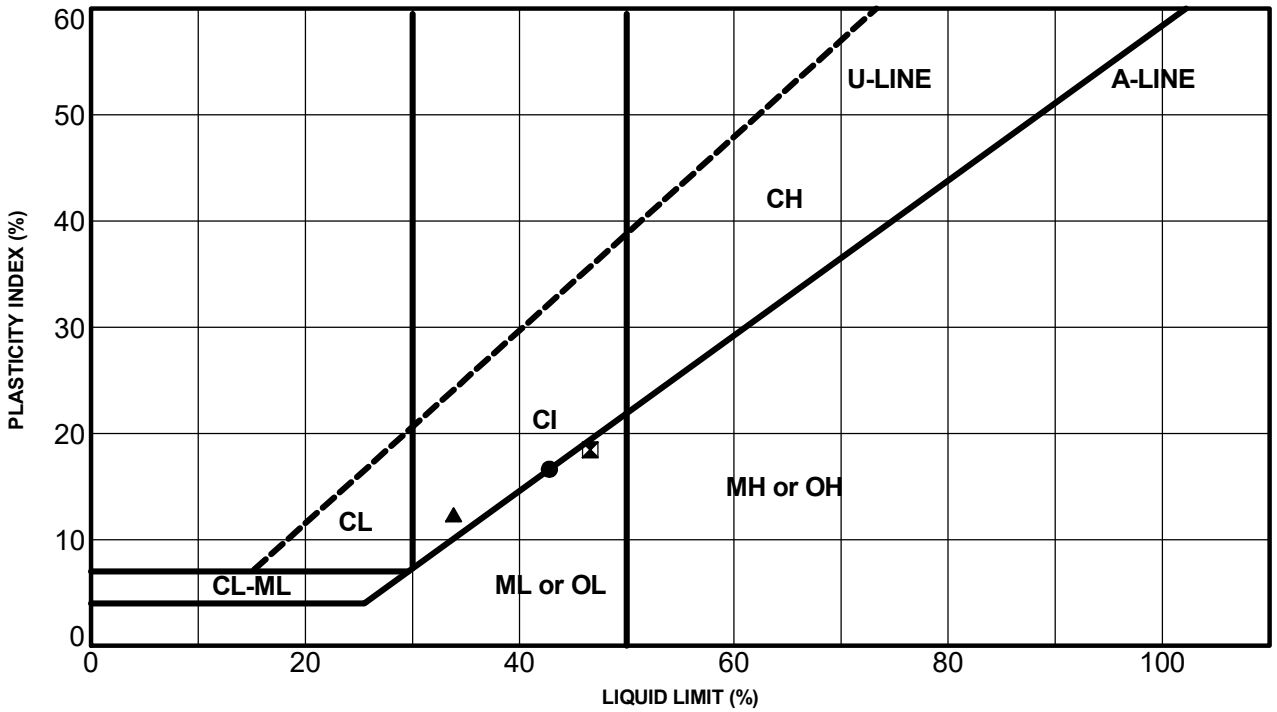
LOCATION:

FIGURE:

DRAWN BY: HM **CHECKED BY:** JG

KC_ATTERBERG-SI A03355A01 ORIGINAL SAMPLES.GPJ SIEVE.GDT 19-11-21

PLASTICITY CHART

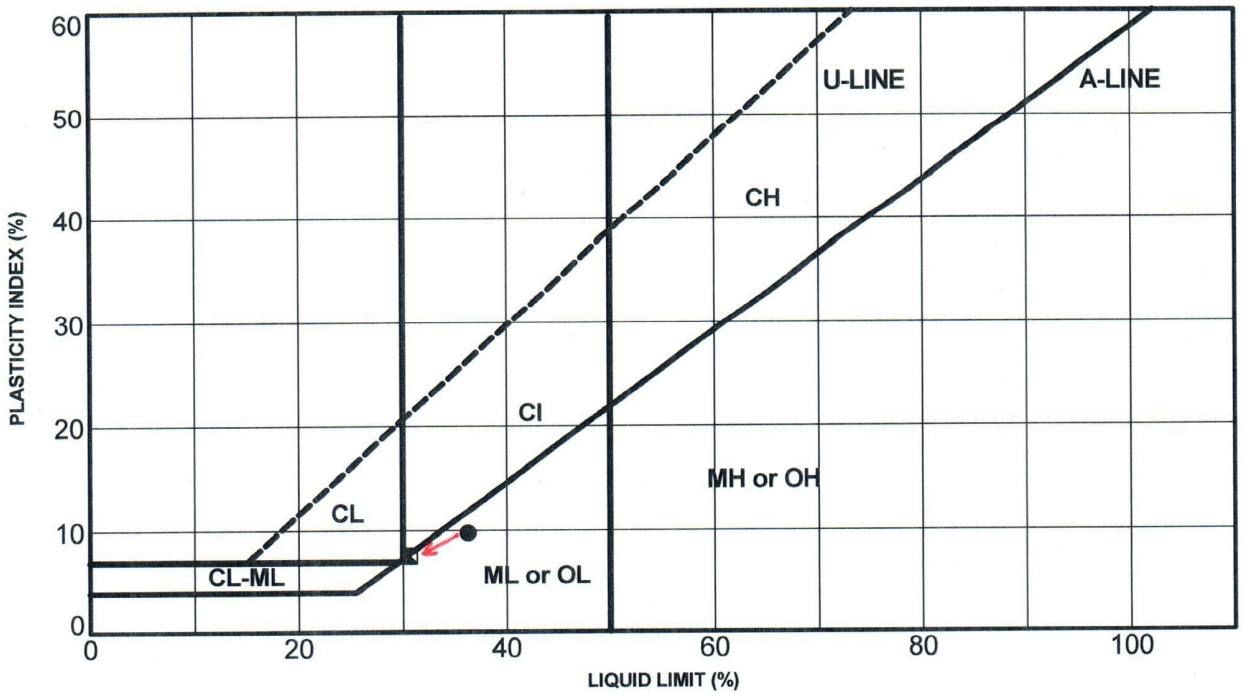


	HOLE	SAMPLE	DEPTH (m)	W_L	W_P	PI	% FINES	REMARKS/SAMPLE DESCRIPTION
●	S 1	Bag 1	0.0	43	26	17	98.9	Slimes. Pail 1
⧓	S 1	Bag 1	0.0	47	28	18		Dark Slimes. Pail 1
▲	S 1	Bag 1	0.0	34	22	12		Orange Slimes. Pail 1

KC_ATTERBERG-SI A03355A01 ORIGINAL SAMPLES.GPJ SIEVE.GDT 19-11-21

PROJECT NO.: A03355A01
PROJECT:
LOCATION:
FIGURE:
DRAWN BY: HM **CHECKED BY:** JG

PLASTICITY CHART

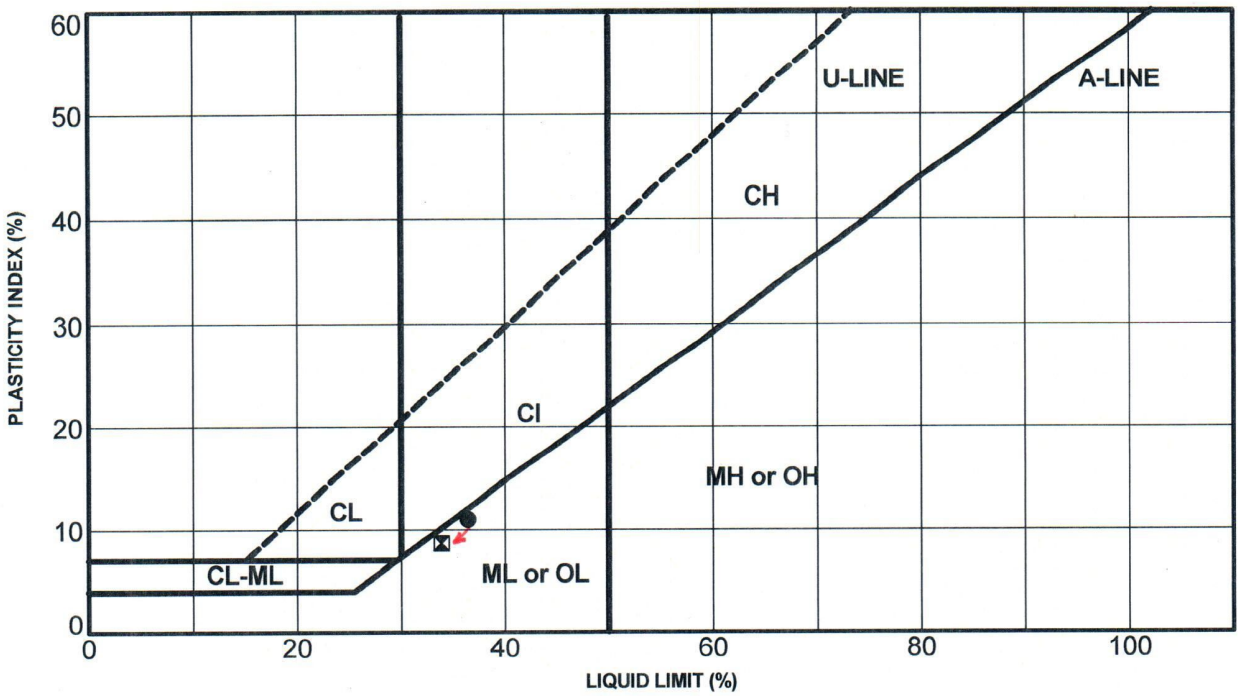


	HOLE	SAMPLE	DEPTH (m)	W_L	W_P	PI	% FINES	REMARKS/SAMPLE DESCRIPTION
●	S 7	Bag 1	0.0	36	26	10		Residual Soil. Pail 10. Natural/dried 110C
⊠	S 7	Bag 1	0.0	31	23	8		Residual Soil. Pail 10. Dried at 45C/dried 110C

PROJECT NO.:	A03355A01
PROJECT:	VSA - Confidential
LOCATION:	
FIGURE:	
DRAWN BY: HM	CHECKED BY: JG

KCB_ATTERBERG-SI CONF T19046.GPJ SIEVE.GDT 20-6-19

PLASTICITY CHART



	HOLE	SAMPLE	DEPTH (m)	W_L	W_P	PI	% FINES	REMARKS/SAMPLE DESCRIPTION
●	S 7	Bag 2	0.0	36	25	11		Residual Soil Pail 10. Natural/ dried 110C
⊠	S 7	Bag 2	0.0	34	25	9		Residual Soil Pail 10 dried at 45C/ dried 110C

PROJECT NO.:	A03355A01
PROJECT:	VSA - Confidential
LOCATION:	
FIGURE:	
DRAWN BY: HM	CHECKED BY: JG

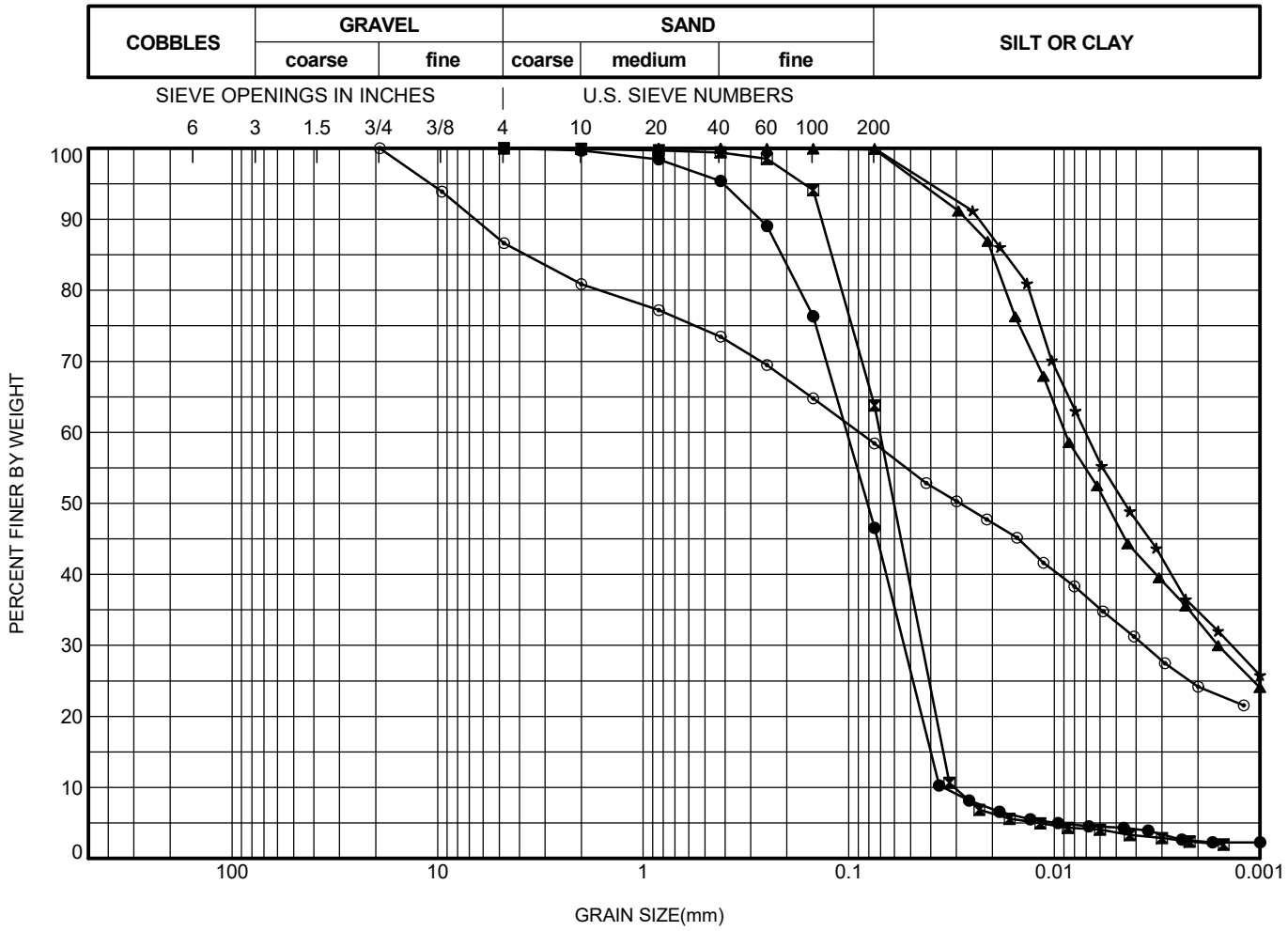
KCB_ATTERBERG-SI CONF T19046.GPJ SIEVE.GDT 20-6-19

Program 2

Particle Size Distribution
Specific Gravity Tests
Moisture Content
Atterberg Limit Test

Particle Size Distribution

GRAIN SIZE DISTRIBUTION



	HOLE	DEPTH (m)	D85	D60	D50	D15	D10	CU	%GRAVEL	%SAND	%FINES
●	DT04	0.00	0.212	0.102	0.081				0.0	53.4	46.6
⊠	DT08	0.00	0.121						0.0	36.2	63.8
▲	GP01	0.00							0.0	0.2	99.8
★	GP04B	0.00							0.0	0.0	100.0
⊙	GP05	0.00	3.716	0.089					13.4	28.2	58.4

	HOLE	SAMPLE	DEPTH (m)	W%	W_L	W_P	PI	REMARKS / SAMPLE DESCRIPTION
●	DT04	BS01	0.00					
⊠	DT08	BS01	0.00					
▲	GP01	BS01	0.00		48	29	20	
★	GP04B	BS01	0.00		53	27	26	
⊙	GP05	BS01	0.00		35	26	9	Air dried sample

CU = COEFFICIENT OF UNIFORMITY = D60/D10 **PARTICLE SIZES, e.g. D85, in mm** **Tested by Wet Sieving Method (ASTM D1140 & D422)**

PROJECT NO.: A03355A01

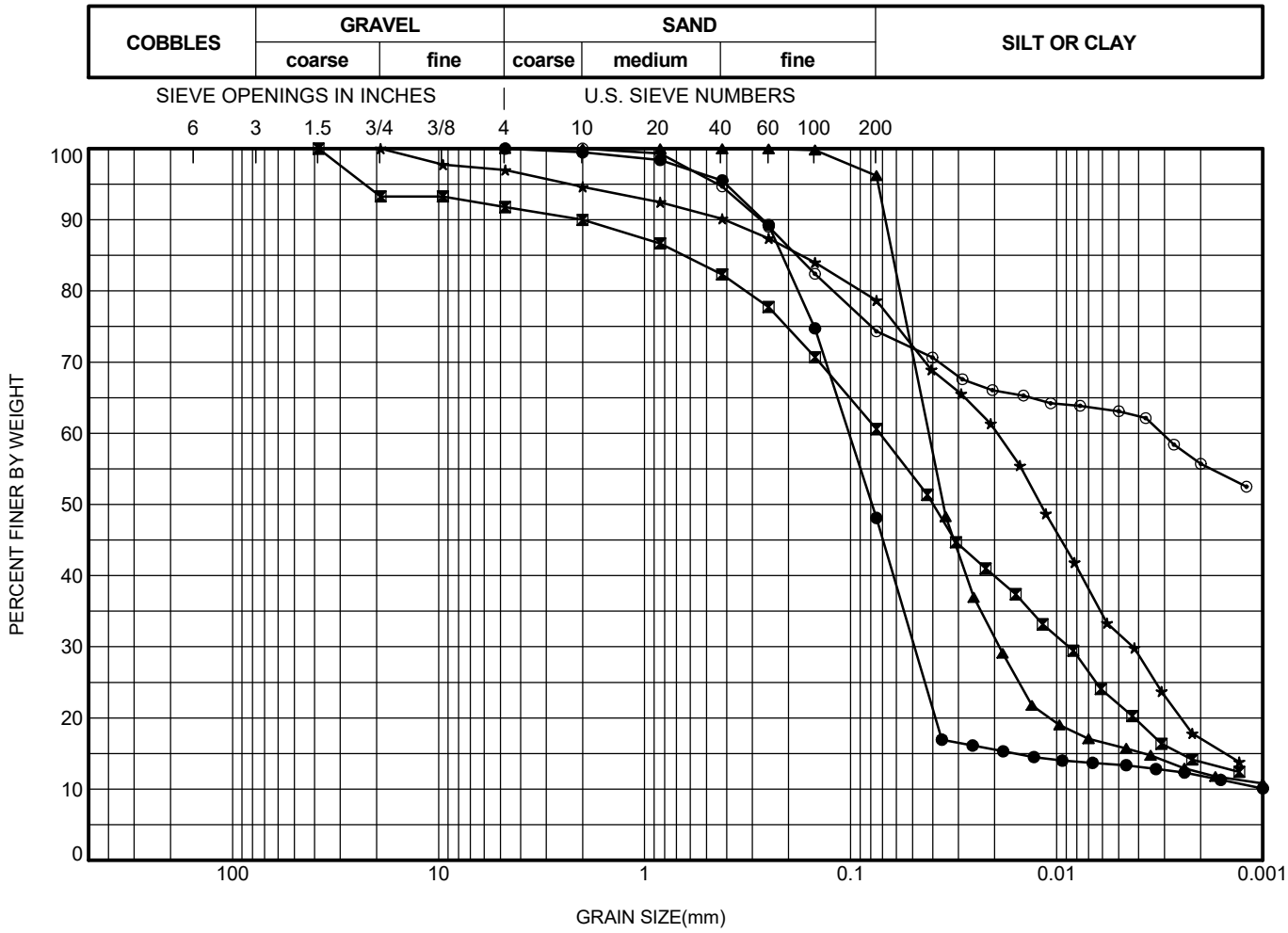
PROJECT:

LOCATION:

FIGURE:

DRAWN BY: AX **CHECKED BY:** JG

GRAIN SIZE DISTRIBUTION



	HOLE	DEPTH (m)	D85	D60	D50	D15	D10	CU	%GRAVEL	%SAND	%FINES
●	GP06	0.00	0.215	0.102	0.079				0.0	51.9	48.1
⊠	GP07	0.00	0.643						8.2	31.2	60.6
▲	GP08	0.00							0.0	3.8	96.2
★	GP09	0.00	0.173						3.0	18.3	78.7
⊙	GP11	0.00	0.183						0.0	25.7	74.3

	HOLE	SAMPLE	DEPTH (m)	W%	W_L	W_P	PI	REMARKS / SAMPLE DESCRIPTION
●	GP06	BS01	0.00		16	15	1	
⊠	GP07	BS01	0.00		42	27	15	Air dried sample
▲	GP08	BS01	0.00		19	16	3	
★	GP09	BS01	0.00		62	37	25	Air dried sample
⊙	GP11	BS01	0.00					

CU = COEFFICIENT OF UNIFORMITY = D60/D10 **PARTICLE SIZES, e.g. D85, in mm** **Tested by Wet Sieving Method (ASTM D1140 & D422)**

PROJECT NO.: A03355A01

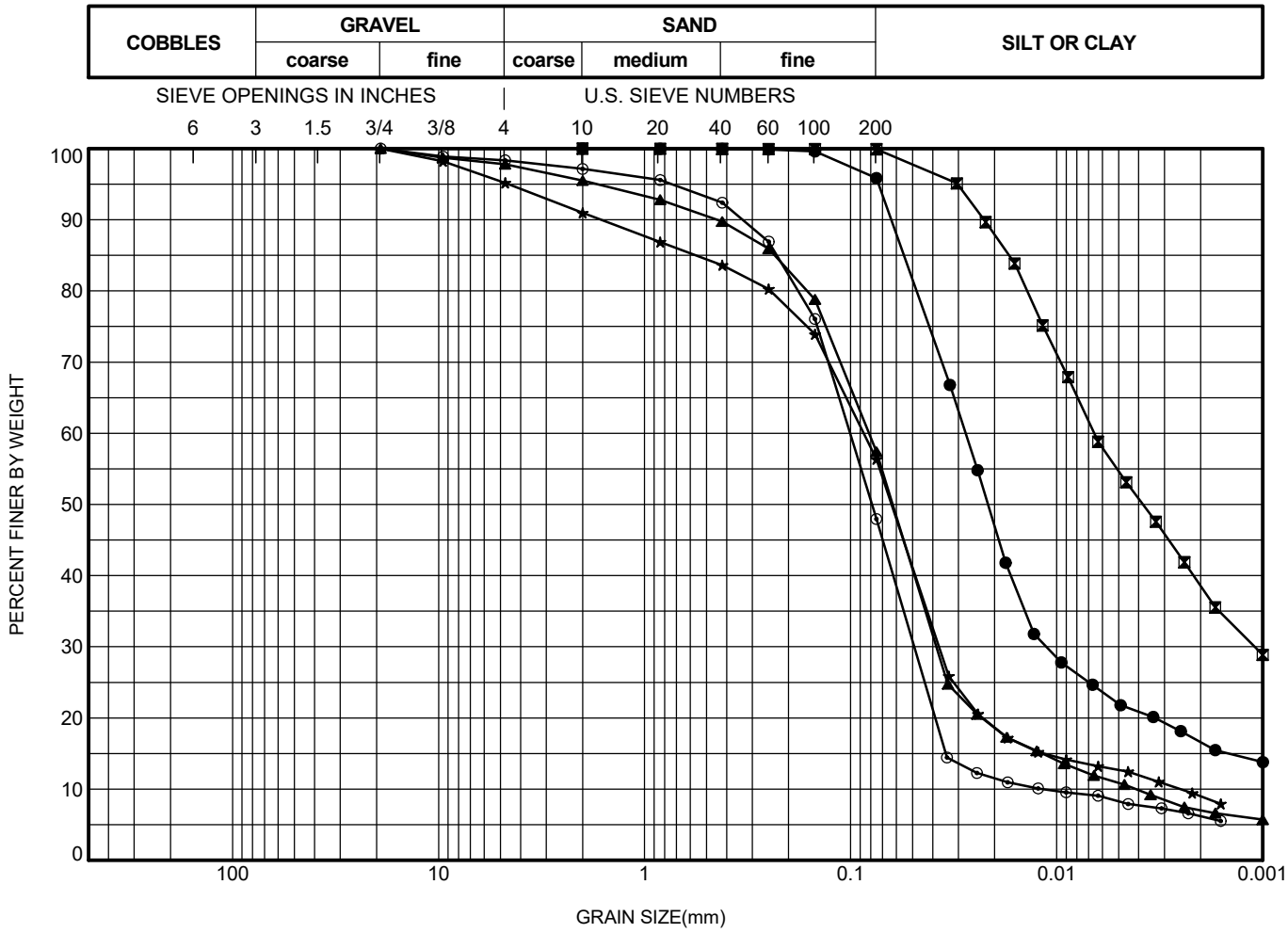
PROJECT:

LOCATION:

FIGURE:

DRAWN BY: AX **CHECKED BY:** JG

GRAIN SIZE DISTRIBUTION



	HOLE	DEPTH (m)	D85	D60	D50	D15	D10	CU	%GRAVEL	%SAND	%FINES
●	GP12	0.00							0.0	4.2	95.8
⊠	GP13	0.00							0.0	0.1	99.9
▲	GP14	0.00	0.234	0.082					2.2	40.4	57.4
★	GP15	0.00	0.563	0.087					4.8	38.8	56.3
⊙	GP16	0.00	0.228	0.101	0.079				1.7	50.4	48.0

	HOLE	SAMPLE	DEPTH (m)	W%	W_L	W_P	PI	REMARKS / SAMPLE DESCRIPTION
●	GP12	BS01	0.00		22	18	4	
⊠	GP13	BS01	0.00		49	27	22	
▲	GP14	BS01	0.00		18	15	3	
★	GP15	BS01	0.00		15	11	4	
⊙	GP16	BS01	0.00		16	14	2	

CU = COEFFICIENT OF UNIFORMITY = D60/D10 **PARTICLE SIZES, e.g. D85, in mm** **Tested by Wet Sieving Method (ASTM D1140 & D422)**

PROJECT NO.: A03355A01

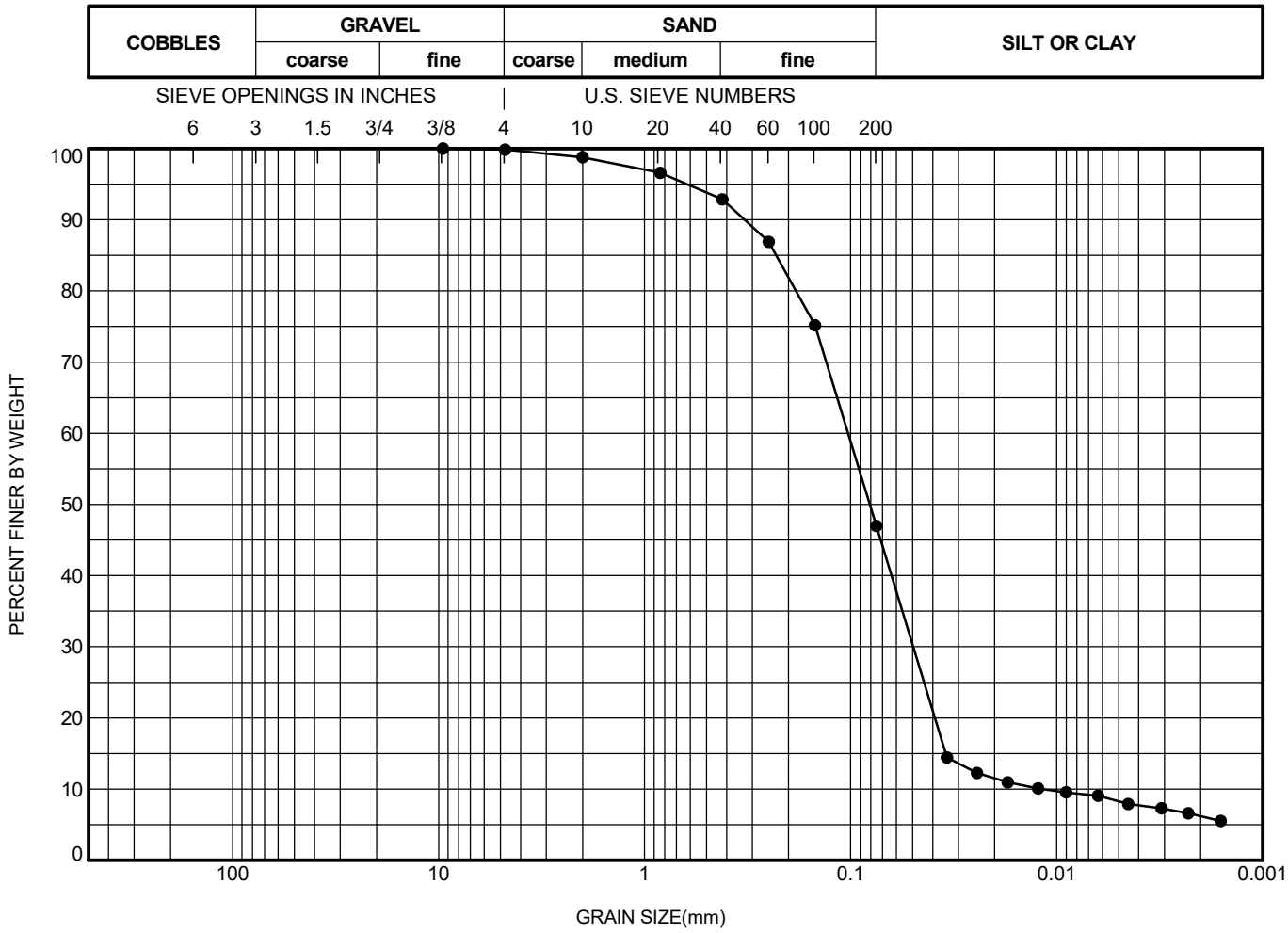
PROJECT:

LOCATION:

FIGURE:

DRAWN BY: AX **CHECKED BY:** JG

GRAIN SIZE DISTRIBUTION



	HOLE	DEPTH (m)	D85	D60	D50	D15	D10	CU	%GRAVEL	%SAND	%FINES
●	GP16	0.00	0.230	0.103	0.081				0.1	52.9	47.0

	HOLE	SAMPLE	DEPTH (m)	W%	W_L	W_P	PI	REMARKS / SAMPLE DESCRIPTION
●	GP16	BS01	0.00					attempt 2

CU = COEFFICIENT OF UNIFORMITY = D60/D10 **PARTICLE SIZES, e.g. D85, in mm** **Tested by Wet Sieving Method (ASTM D1140 & D422)**

PROJECT NO.: A03355A01

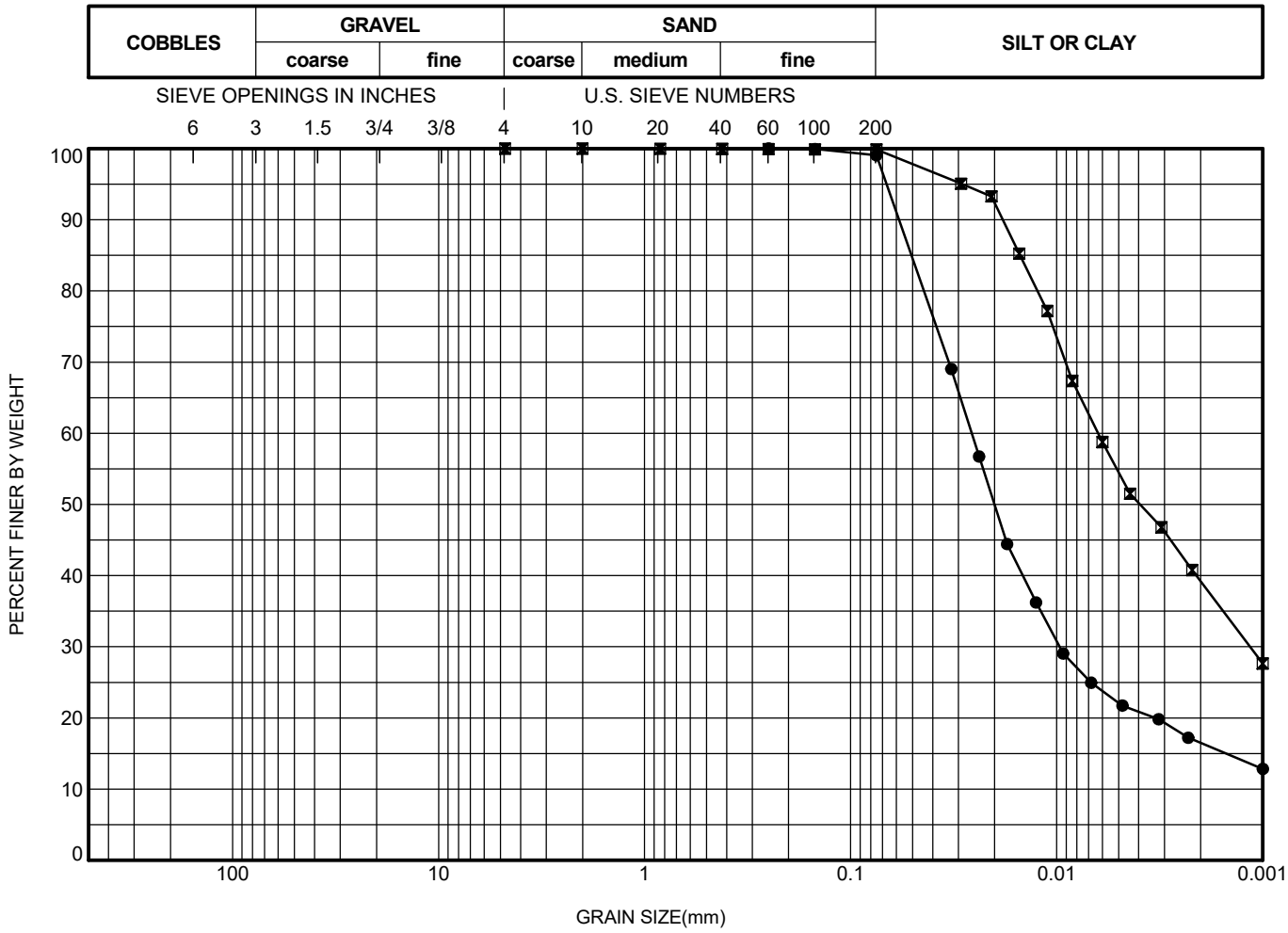
PROJECT:

LOCATION:

FIGURE:

DRAWN BY: AX **CHECKED BY:** JG

GRAIN SIZE DISTRIBUTION



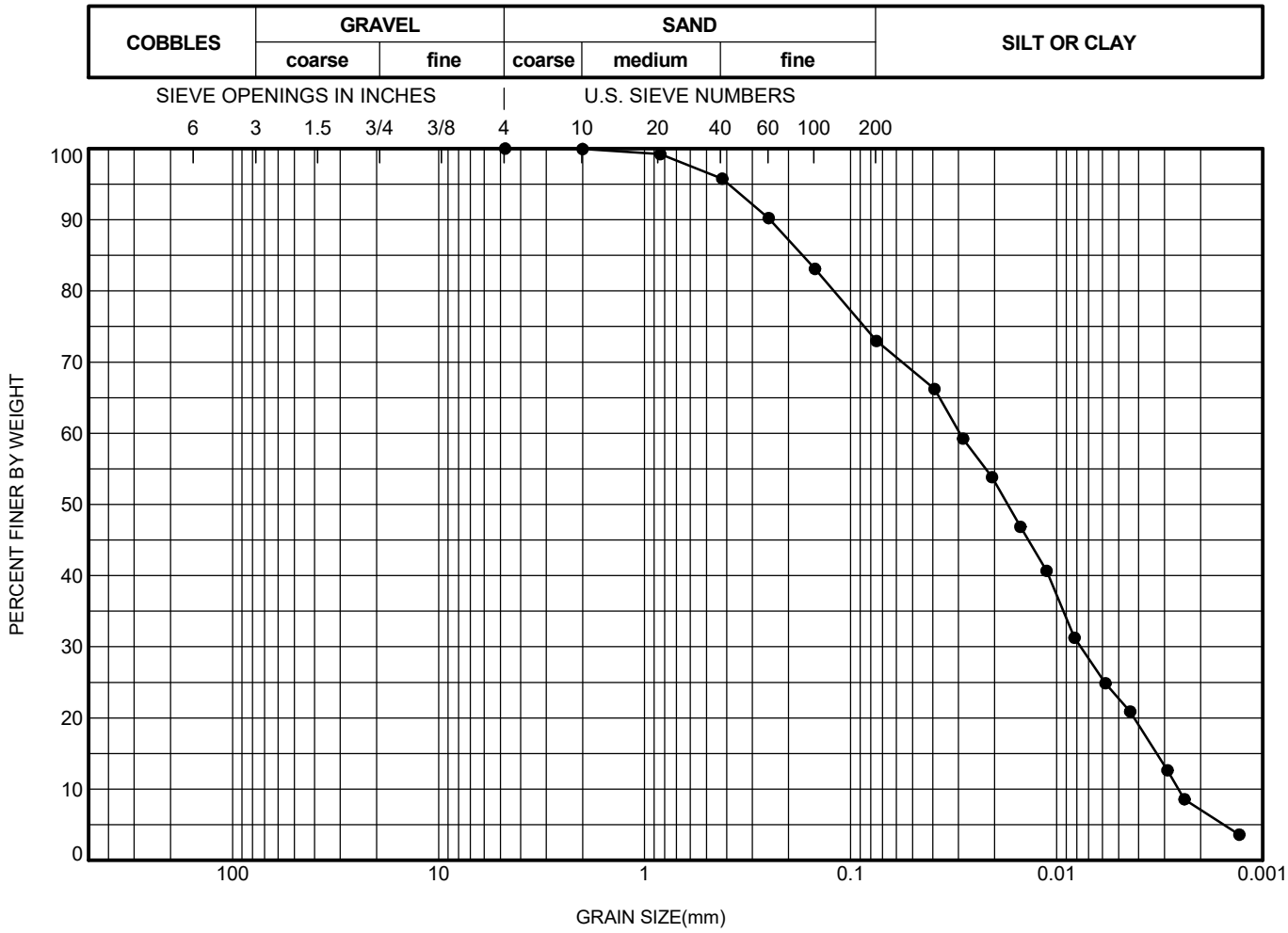
	HOLE	DEPTH (m)	D85	D60	D50	D15	D10	CU	%GRAVEL	%SAND	%FINES
●	Slimes 1	0.00							0.0	0.9	99.1
⊠	Slimes 2	0.00							0.0	0.1	99.9

	HOLE	SAMPLE	DEPTH (m)	W%	W_L	W_P	PI	REMARKS / SAMPLE DESCRIPTION
●	Slimes 1		0.00		34	22	11	Pail 13
⊠	Slimes 2		0.00		52	30	22	Pail 14

CU = COEFFICIENT OF UNIFORMITY = D60/D10 **PARTICLE SIZES, e.g. D85, in mm** **Tested by Wet Sieving Method (ASTM D1140 & D422)**

PROJECT NO.: A03355A01
PROJECT:
LOCATION: Brazil
FIGURE:
DRAWN BY: AX **CHECKED BY:** BY

GRAIN SIZE DISTRIBUTION



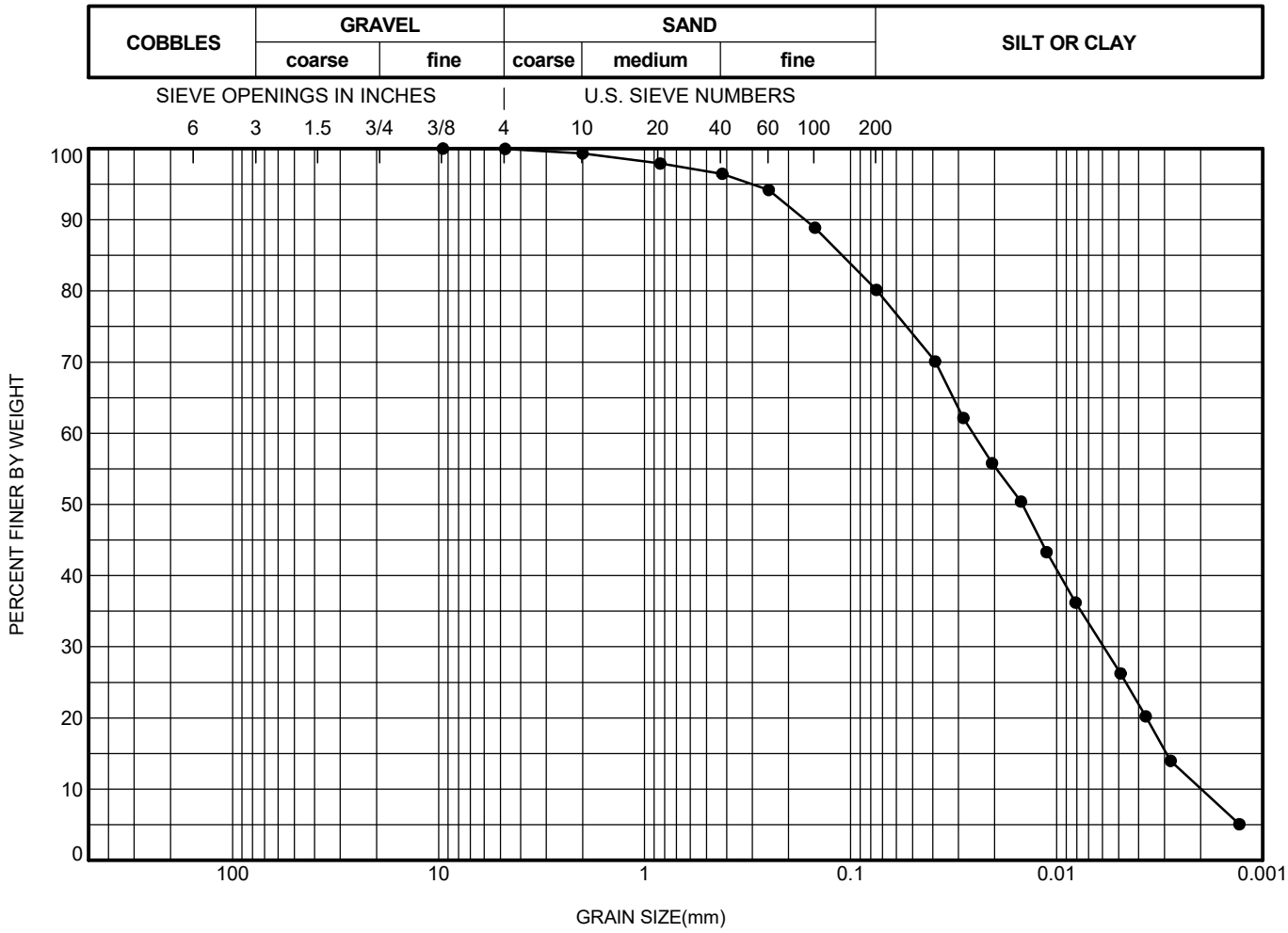
	HOLE	DEPTH (ft)	D85	D60	D50	D15	D10	CU	%GRAVEL	%SAND	%FINES
●	BH-01	3.50	0.171						0.0	27.0	73.0

	HOLE	SAMPLE	DEPTH (ft)	W%	W_L	W_P	PI	REMARKS / SAMPLE DESCRIPTION
●	BH-01	01	3.50		56	36	20	Air Dried

CU = COEFFICIENT OF UNIFORMITY = D60/D10 **PARTICLE SIZES, e.g. D85, in mm** **Tested by Wet Sieving Method (ASTM D1140 & D422)**

PROJECT NO.: A03355A01
PROJECT:
LOCATION: Brazil
FIGURE:
DRAWN BY: AX **CHECKED BY:** BY

GRAIN SIZE DISTRIBUTION



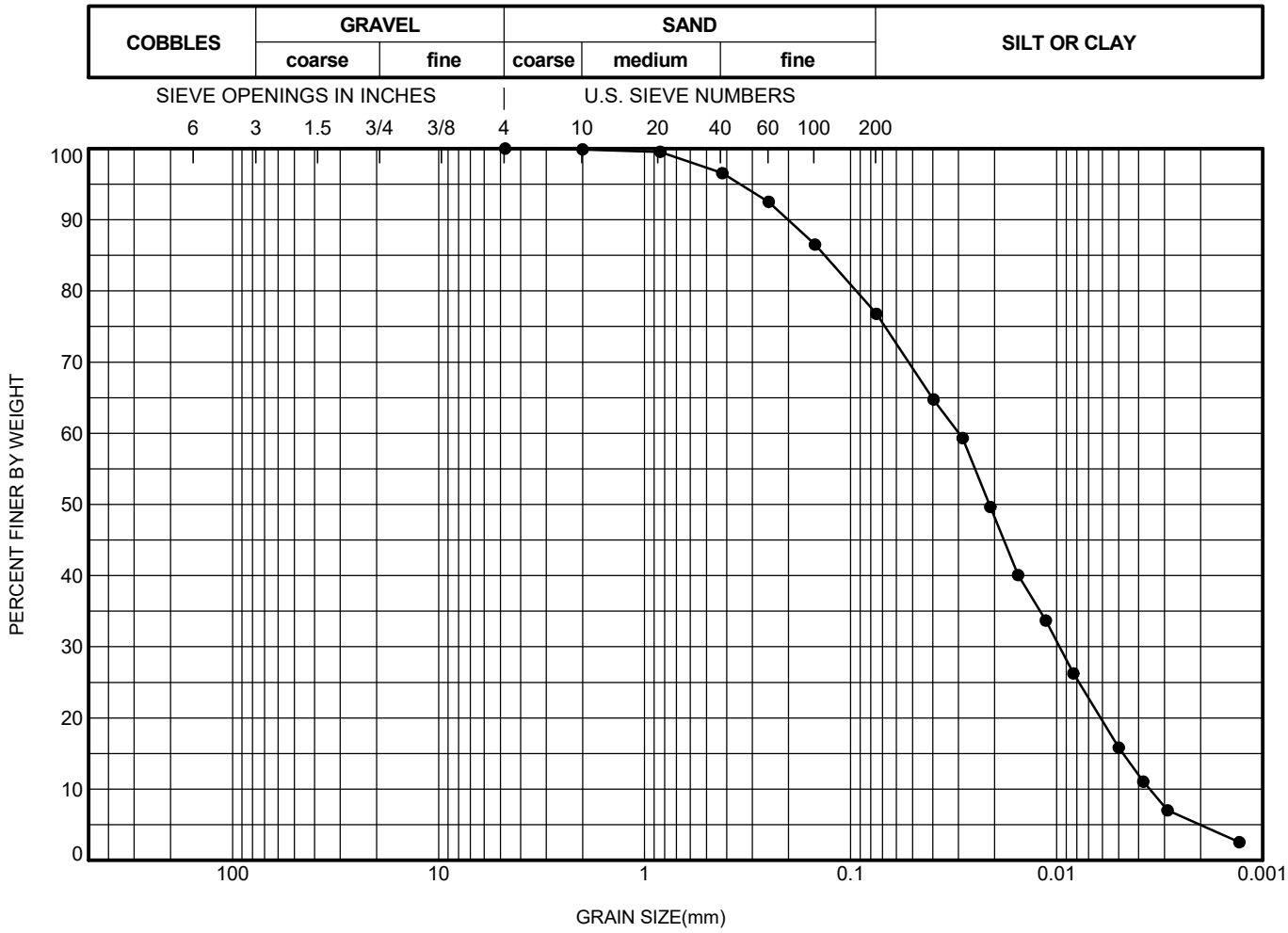
	HOLE	DEPTH (ft)	D85	D60	D50	D15	D10	CU	%GRAVEL	%SAND	%FINES
●	BH-01	4.50	0.110						0.0	19.8	80.1

	HOLE	SAMPLE	DEPTH (ft)	W%	W_L	W_P	PI	REMARKS / SAMPLE DESCRIPTION
●	BH-01	02	4.50		59	42	17	Air Dried

CU = COEFFICIENT OF UNIFORMITY = D60/D10 **PARTICLE SIZES, e.g. D85, in mm** **Tested by Wet Sieving Method (ASTM D1140 & D422)**

PROJECT NO.: A03355A01
PROJECT:
LOCATION: Brazil
FIGURE:
DRAWN BY: AX **CHECKED BY:** BY

GRAIN SIZE DISTRIBUTION



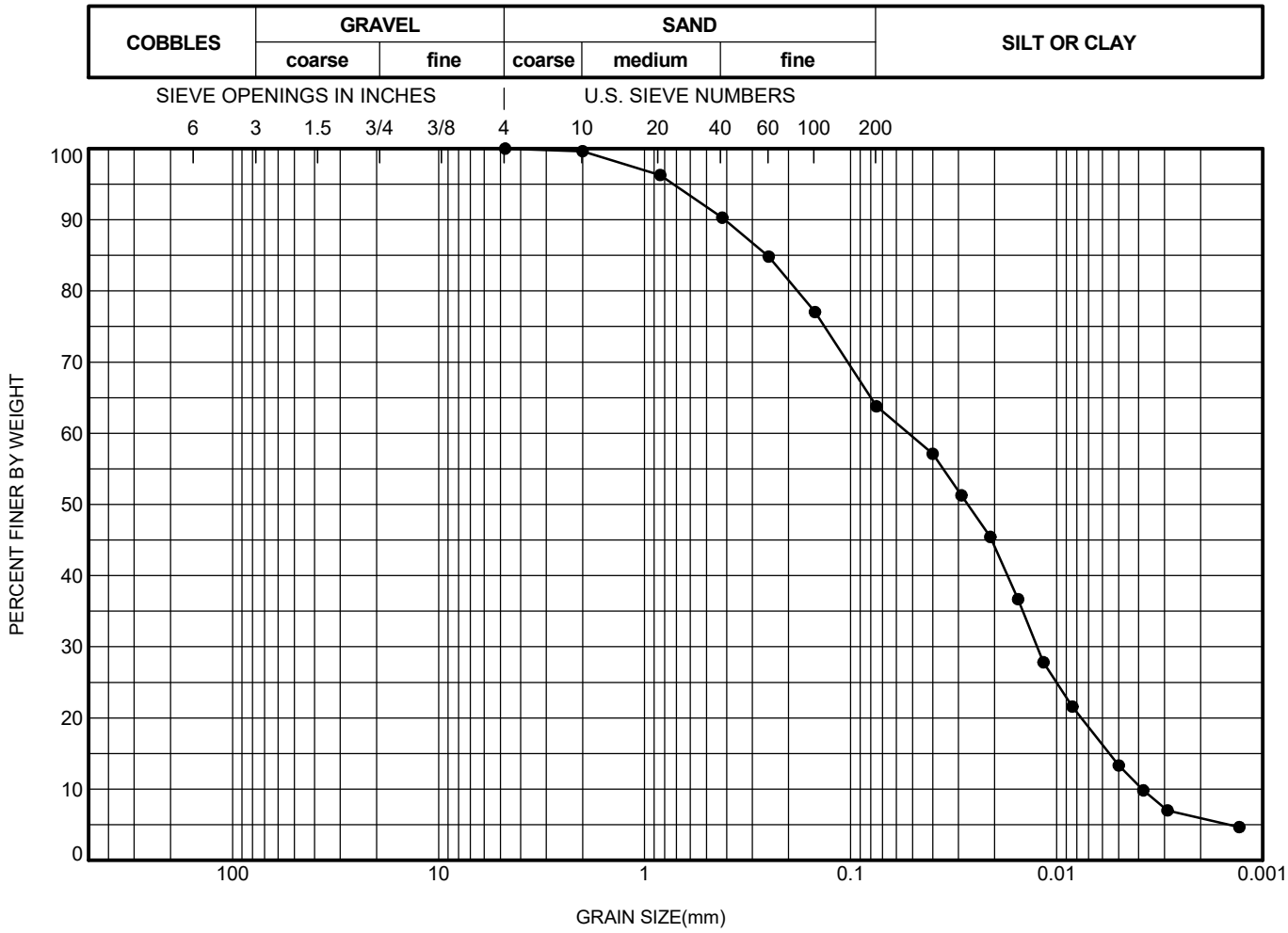
	HOLE	DEPTH (ft)	D85	D60	D50	D15	D10	CU	%GRAVEL	%SAND	%FINES
●	BH-02	3.50	0.134						0.0	23.2	76.8

	HOLE	SAMPLE	DEPTH (ft)	W%	W_L	W_P	PI	REMARKS / SAMPLE DESCRIPTION
●	BH-02	01	3.50		58	48	10	Air Dried

CU = COEFFICIENT OF UNIFORMITY = D60/D10 **PARTICLE SIZES, e.g. D85, in mm** **Tested by Wet Sieving Method (ASTM D1140 & D422)**

PROJECT NO.: A03355A01
PROJECT:
LOCATION: Brazil
FIGURE:
DRAWN BY: AX **CHECKED BY:** BY

GRAIN SIZE DISTRIBUTION



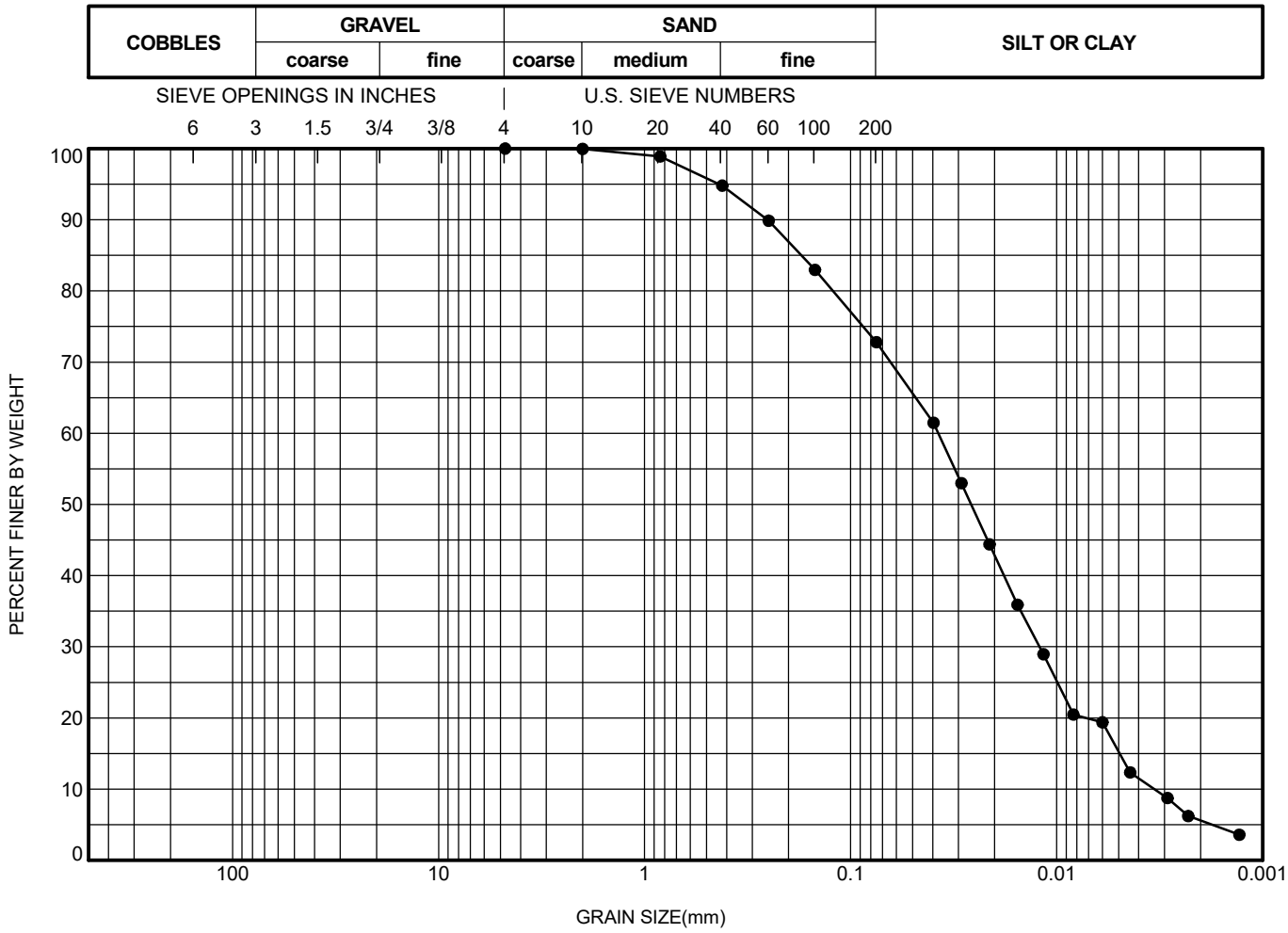
	HOLE	DEPTH (ft)	D85	D60	D50	D15	D10	CU	%GRAVEL	%SAND	%FINES
●	BH-02	0.00	0.254						0.0	36.2	63.8

	HOLE	SAMPLE	DEPTH (ft)	W%	W_L	W_P	PI	REMARKS / SAMPLE DESCRIPTION
●	BH-02	02	0.00		52	37	15	Air Dried

CU = COEFFICIENT OF UNIFORMITY = D60/D10 **PARTICLE SIZES, e.g. D85, in mm** **Tested by Wet Sieving Method (ASTM D1140 & D422)**

PROJECT NO.: A03355A01
PROJECT:
LOCATION: Brazil
FIGURE:
DRAWN BY: AX **CHECKED BY:** BY

GRAIN SIZE DISTRIBUTION



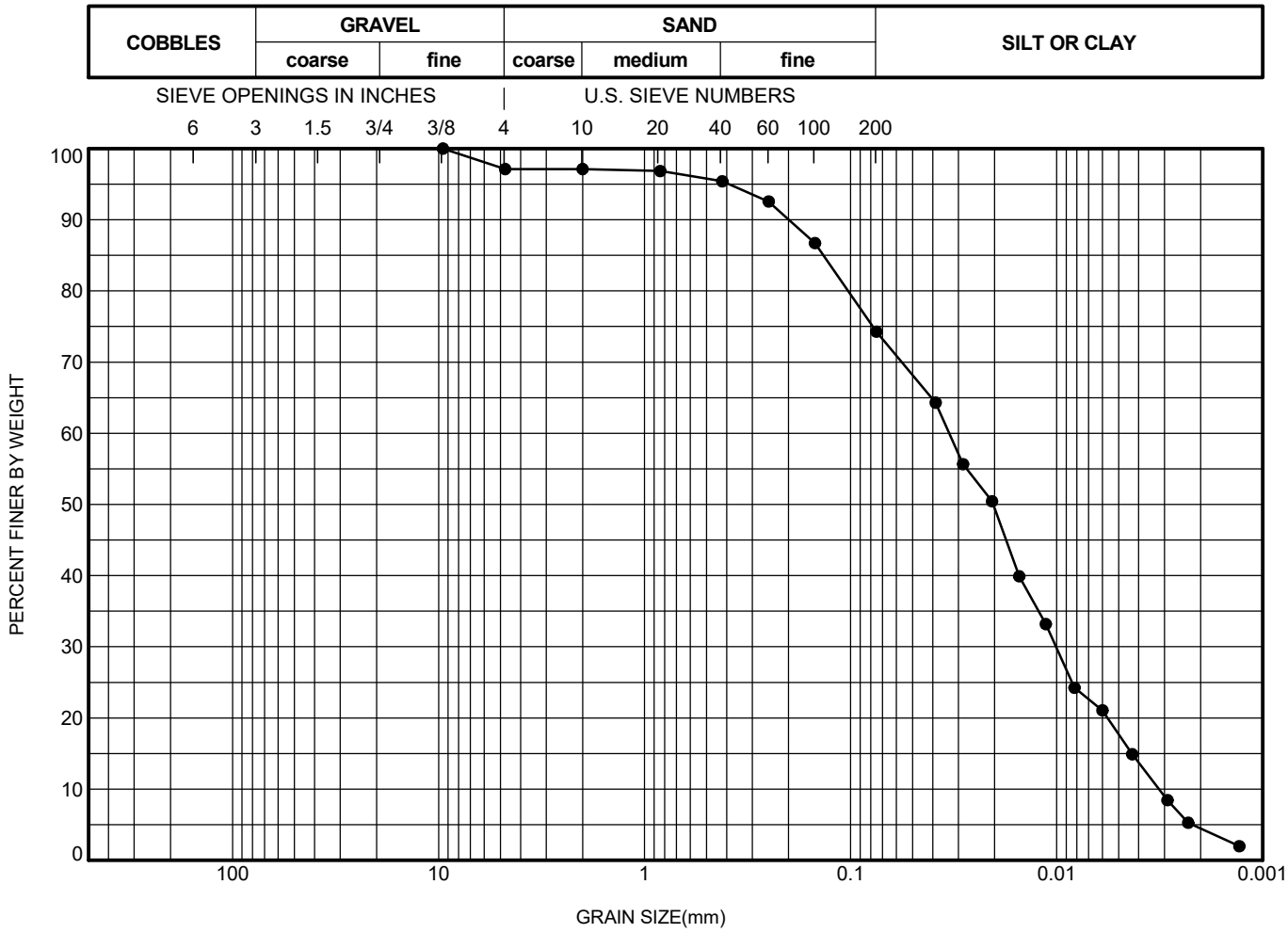
	HOLE	DEPTH (ft)	D85	D60	D50	D15	D10	CU	%GRAVEL	%SAND	%FINES
●	BH-04	0.00	0.174						0.0	27.2	72.8

	HOLE	SAMPLE	DEPTH (ft)	W%	W_L	W_P	PI	REMARKS / SAMPLE DESCRIPTION
●	BH-04	01	0.00		59	50	9	Air Dried

CU = COEFFICIENT OF UNIFORMITY = D60/D10 **PARTICLE SIZES, e.g. D85, in mm** **Tested by Wet Sieving Method (ASTM D1140 & D422)**

PROJECT NO.: A03355A01
PROJECT:
LOCATION: Brazil
FIGURE:
DRAWN BY: AX **CHECKED BY:** BY

GRAIN SIZE DISTRIBUTION



	HOLE	DEPTH (ft)	D85	D60	D50	D15	D10	CU	%GRAVEL	%SAND	%FINES
●	BH-04	5.30	0.136						2.9	22.8	74.3

	HOLE	SAMPLE	DEPTH (ft)	W%	W_L	W_P	PI	REMARKS / SAMPLE DESCRIPTION
●	BH-04	02	5.30		55	38	17	Air Dried

CU = COEFFICIENT OF UNIFORMITY = D60/D10 **PARTICLE SIZES, e.g. D85, in mm** **Tested by Wet Sieving Method (ASTM D1140 & D422)**

PROJECT NO.: A03355A01

PROJECT:

LOCATION: Brazil

FIGURE:

DRAWN BY: AX **CHECKED BY:** BY

Specific Gravity Tests

SPECIFIC GRAVITY OF SOIL SOLIDS (ASTM-D854)

Hole Number	DT-04	GP-1
Sample Number	BS-01	BS-01
Depth (m)		
Sample Description	More sandy than other samples	

Flask No.	KL-2	SG9
Volume of Flask @ 20° C ml	500	500
Method of Air removal	boiling	boiling
De-airing Period hr	2	2
Test temperature ° C	22.6	22.6
Mass of Flask+Water (M_a) g	675.44	667.80
Mass of Flask+Water+Soil (M_b) g	742.07	711.38
Mass of Dish/Flask+Soil	260.64	227.83
Mass of Dish/Flask	177.05	169.67
Mass of Dry Soil (M_o) g	83.59	58.16
Correction factor (K) @ Test Temperature	0.99943	0.99943
Specific Gravity of Solids @ 20° C	**4.926**	**3.987**
Average Specific Gravity of Solids @ 20° C	**4.93**	**3.99**

Hole Number	GP-4B	GP-5
Sample Number	BS-01	BS-01
Depth (m)		
Sample Description		Residual

Flask No.	SG6	12
Volume of Flask @ 20° C ml	500	500
Method of Air removal	boiling	boling
De-airing Period hr	2	2
Test temperature ° C	22.9	22.6
Mass of Flask+Water (M_a) g	670.42	680.38
Mass of Flask+Water+Soil (M_b) g	707.29	720.22
Mass of Dish/Flask+Soil	222.53	243.40
Mass of Dish/Flask	172.15	182.10
Mass of Dry Soil (M_o) g	50.38	61.30
Correction factor (K) @ Test Temperature	0.99936	0.99943
Specific Gravity of Solids @ 20° C	**3.727**	**2.855**
Average Specific Gravity of Solids @ 20° C	**3.73**	**2.85**

Specific Gravity of Solids @ 20° C = $(K \times M_o)/(M_o + M_a - M_b)$

PROJECT#:	A03355A01			
PROJECT:				
LOCATION:	Brazil			
DATE:	2019-08-17			
TESTED BY:	HM	CHECKED BY:	JG	

SPECIFIC GRAVITY OF SOIL SOLIDS (ASTM-D854)

Hole Number	GP-6	GP-7
Sample Number	BS-01	BS-01
Depth (m)		
Sample Description		Residual
Flask No.	SG10	SG7
Volume of Flask @ 20° C ml	500	500
Method of Air removal	boiling	boiling
De-airing Period hr	2	2
Test temperature ° C	22.6	22.7
Mass of Flask+Water (M_a) g	669.89	667.74
Mass of Flask+Water+Soil (M_b) g	720.15	702.58
Mass of Dish/Flask+Soil	238.39	224.21
Mass of Dish/Flask	171.93	169.42
Mass of Dry Soil (M_o) g	66.46	54.79
Correction factor (K) @ Test Temperature	0.99943	0.99941
Specific Gravity of Solids @ 20° C	**4.100**	**2.745**
Average Specific Gravity of Solids @ 20° C	**4.10**	**2.74**

Hole Number	GP-8	GP-9
Sample Number	BS-01	BS-01
Depth (m)		
Sample Description		Residual
Flask No.	SG4	11
Volume of Flask @ 20° C ml	500	500
Method of Air removal	boling	boiling
De-airing Period hr	2	2
Test temperature ° C	22.5	22.6
Mass of Flask+Water (M_a) g	670.66	678.51
Mass of Flask+Water+Soil (M_b) g	718.67	715.71
Mass of Dish/Flask+Soil	237.32	238.88
Mass of Dish/Flask	172.57	180.36
Mass of Dry Soil (M_o) g	64.75	58.52
Correction factor (K) @ Test Temperature	0.99945	0.99943
Specific Gravity of Solids @ 20° C	**3.866**	**2.743**
Average Specific Gravity of Solids @ 20° C	**3.87**	**2.74**

Specific Gravity of Solids @ 20° C = $(K \times M_o)/(M_o + M_a - M_b)$

PROJECT#:	A03355A01			
PROJECT:				
LOCATION:	Brazil			
DATE:	2019-08-17			
TESTED BY:	HM	CHECKED BY:	JG	

SPECIFIC GRAVITY OF SOIL SOLIDS (ASTM-D854)

Hole Number	GP-11	GP-12
Sample Number	BS-01	BS-01
Depth (m)		
Sample Description		
Flask No.	SG3	3
Volume of Flask @ 20° C ml	500	500
Method of Air removal	boiling	boling
De-airing Period hr	2	2
Test temperature ° C	22.6	22.6
Mass of Flask+Water (M_a) g	672.24	671.41
Mass of Flask+Water+Soil (M_b) g	707.89	716.46
Mass of Dish/Flask+Soil	230.93	233.24
Mass of Dish/Flask	173.92	172.68
Mass of Dry Soil (M_o) g	57.01	60.56
Correction factor (K) @ Test Temperature	0.99943	0.99943
Specific Gravity of Solids @ 20° C	**2.667**	**3.902**
Average Specific Gravity of Solids @ 20° C	**2.67**	**3.90**

Hole Number	GP-13	GP-14
Sample Number	BS-01	BS-01
Depth (m)		
Sample Description		
Flask No.	KL-3	10
Volume of Flask @ 20° C ml	500	500
Method of Air removal	boiling	boiling
De-airing Period hr	2	2
Test temperature ° C	22.6	22.6
Mass of Flask+Water (M_a) g	675.77	679.65
Mass of Flask+Water+Soil (M_b) g	722.81	729.53
Mass of Dish/Flask+Soil	242.42	247.34
Mass of Dish/Flask	177.35	181.53
Mass of Dry Soil (M_o) g	65.07	65.81
Correction factor (K) @ Test Temperature	0.99943	0.99943
Specific Gravity of Solids @ 20° C	**3.607**	**4.129**
Average Specific Gravity of Solids @ 20° C	**3.61**	**4.13**

Specific Gravity of Solids @ 20° C = $(K \times M_o)/(M_o + M_a - M_b)$

PROJECT#:	A03355A01			
PROJECT:				
LOCATION:	Brazil			
DATE:	2019-08-17			
TESTED BY:	HM	CHECKED BY:	JG	

SPECIFIC GRAVITY OF SOIL SOLIDS (ASTM-D854)

Hole Number	GP-15			GP-16		
Sample Number	BS-01			BS-01		
Depth (m)						
Sample Description						
Flask No.		SG12			1	
Volume of Flask @ 20° C ml		500			500	
Method of Air removal		boiling			boiling	
De-airing Period hr		2			2	
Test temperature ° C		22.6			22.6	
Mass of Flask+Water (M_a) g		670.59			667.22	
Mass of Flask+Water+Soil (M_b) g		719.70			716.61	
Mass of Dish/Flask+Soil		236.41			232.66	
Mass of Dish/Flask		172.53			168.77	
Mass of Dry Soil (M_o) g		63.88			63.89	
Correction factor (K) @ Test Temperature		0.99943			0.99943	
Specific Gravity of Solids @ 20° C		**4.323**			**4.404**	
Average Specific Gravity of Solids @ 20° C		**4.32**			**4.40**	

Hole Number						
Sample Number						
Depth (m)						
Sample Description						
Flask No.						
Volume of Flask @ 20° C ml						
Method of Air removal						
De-airing Period hr						
Test temperature ° C						
Mass of Flask+Water (M_a) g						
Mass of Flask+Water+Soil (M_b) g						
Mass of Dish/Flask+Soil						
Mass of Dish/Flask						
Mass of Dry Soil (M_o) g						
Correction factor (K) @ Test Temperature						
Specific Gravity of Solids @ 20° C						
Average Specific Gravity of Solids @ 20° C						

Specific Gravity of Solids @ 20° C = $(K \times M_o)/(M_o + M_a - M_b)$

PROJECT#:	A03355A01			
PROJECT:				
LOCATION:	Brazil			
DATE:	2019-08-17			
TESTED BY:	HM	CHECKED BY:	JG	

Moisture Content

WATER CONTENT OF SOIL
(ASTM D2216)

Hole Number	Sample Number	Depth (m)	Wet Weight + Tare (g)	Dry Weight + Tare (g)	Tare (g)	Water Weight (g)	Total Dry Weight (g)	Water Content (%)	Notes
DT01	BS01		482.19	392.68	73.45	89.51	319.23	**28.0**	
DT02	BS01		328.81	288.34	86.46	40.47	201.88	**20.0**	
DT03	BS01		476.04	398.28	71.71	77.76	326.57	**23.8**	
DT04	BS01		303.80	296.75	90.77	7.05	205.98	**3.4**	
DT05	BS01		289.81	255.78	80.32	34.03	175.46	**19.4**	
DT06	BS01		286.29	267.23	87.73	19.06	179.50	**10.6**	
DT07	BS01		605.72	495.22	86.79	110.50	408.43	**27.1**	
DT08	BS01		245.31	239.08	85.29	6.23	153.79	**4.1**	
DT09	BS01		360.48	310.62	118.39	49.86	192.23	**25.9**	
DT10	BS01		258.52	233.32	102.36	25.20	130.96	**19.2**	
DT11	BS01		353.45	312.15	103.55	41.30	208.60	**19.8**	
DT12	BS01		323.53	290.92	78.71	32.61	212.21	**15.4**	
DT13	BS01		322.38	295.20	79.10	27.18	216.10	**12.6**	
DT14	BS01		286.24	222.83	88.47	63.41	134.36	**47.2**	
DT15	BS01		362.69	354.54	114.53	8.15	240.01	**3.4**	
GP01	BS01		220.33	188.98	103.08	31.35	85.90	**36.5**	
GP02A	BS01		272.14	232.37	105.64	39.77	126.73	**31.4**	
GP02B	BS01		237.00	212.78	88.92	24.22	123.86	**19.6**	
GP03	BS01		240.57	225.01	109.18	15.56	115.83	**13.4**	
GP04A	BS01		370.88	326.90	109.20	43.98	217.70	**20.2**	
GP04B	BS01		288.98	235.52	79.76	53.46	155.76	**34.3**	
GP05	BS01		225.90	197.19	79.02	28.71	118.17	**24.3**	
GP06	BS01		262.53	254.49	76.57	8.04	177.92	**4.5**	
GP07	BS01		291.30	263.20	99.34	28.10	163.86	**17.1**	
GP08	BS01		342.34	309.73	93.22	32.61	216.51	**15.1**	
GP09	BS01		210.57	174.76	68.67	35.81	106.09	**33.8**	
GP10	BS01		304.61	282.61	111.19	22.00	171.42	**12.8**	
GP11	BS01		291.26	250.49	90.22	40.77	160.27	**25.4**	
GP12	BS01		291.89	257.47	90.80	34.42	166.67	**20.7**	
GP13	BS01		274.28	247.67	90.25	26.61	157.42	**16.9**	
GP14	BS01		328.83	310.04	90.28	18.79	219.76	**8.6**	

PROJECT No.:	A03355A01
PROJECT NAME:	
LOCATION:	
DATE:	2019-08-12
TESTED BY:	AX CHECKED BY: JG

WATER CONTENT OF SOIL
(ASTM D2216)

Hole Number	Sample Number	Depth (m)	Wet Weight + Tare (g)	Dry Weight + Tare (g)	Tare (g)	Water Weight (g)	Total Dry Weight (g)	Water Content (%)	Notes
GP15	BS01		223.41	209.03	99.64	14.38	109.39	**13.1**	
GP16	BS01		366.60	356.86	79.48	9.74	277.38	**3.5**	

PROJECT No.:	A03355A01
PROJECT NAME:	
LOCATION:	
DATE:	2019-08-12
TESTED BY:	AX CHECKED BY: JG

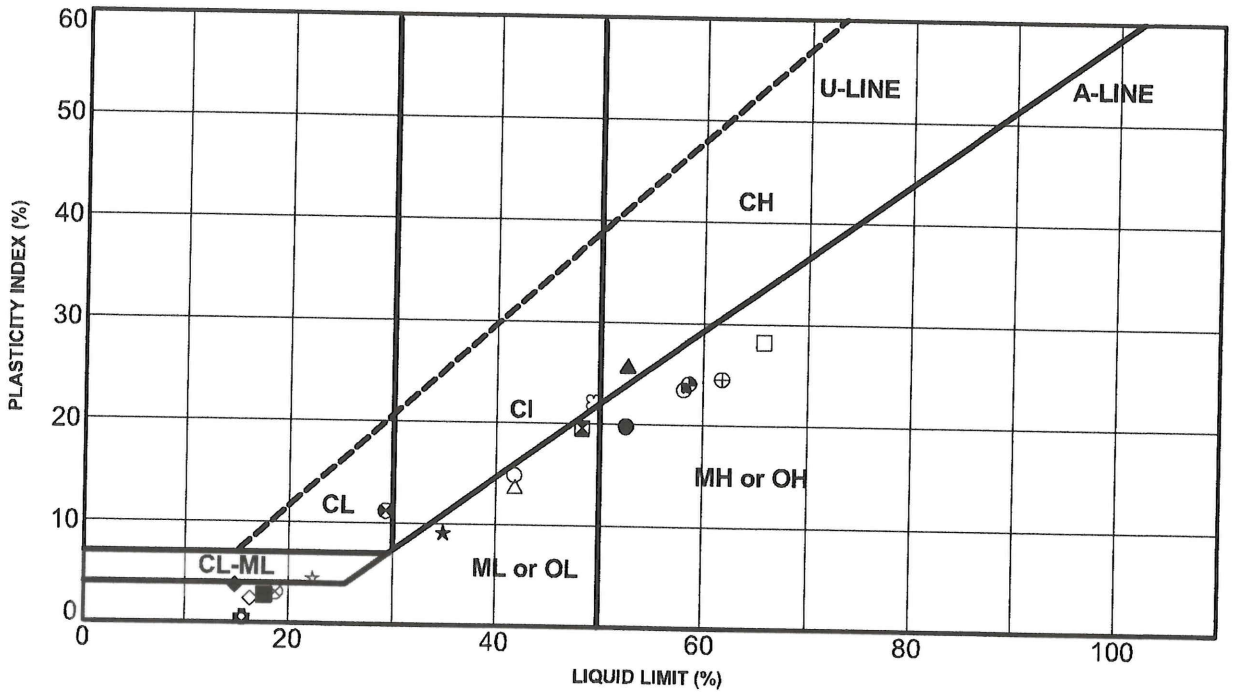
WATER CONTENT OF SOIL
(ASTM D2216)

Hole Number	Sample Number	Depth (m)	Wet Weight + Tare (g)	Dry Weight + Tare (g)	Tare (g)	Water Weight (g)	Total Dry Weight (g)	Water Content (%)	Notes
BH01	Shelby 1	3.5	273.11	234.29	129.78	38.82	104.51	**37.1**	
BH01	Shelby 2	4.5	277.18	238.29	145.12	38.89	93.17	**41.7**	
BH02	Shelby 1	3.5	304.56	247.17	115.09	57.39	132.08	**43.5**	
BH02	Shelby 2		294.80	249.21	87.88	45.59	161.33	**28.3**	
BH04	Shelby 1		289.59	242.53	129.19	47.06	113.34	**41.5**	
BH04	Shelby 2	5.3	206.95	167.01	69.74	39.94	97.27	**41.1**	

PROJECT No.:	A03355A01
PROJECT NAME:	
LOCATION:	Brazil
DATE:	2019-10-04
TESTED BY:	HM CHECKED BY: BY

4 Atterberg Limit Tests

PLASTICITY CHART



	HOLE	SAMPLE	DEPTH (m)	W_L	W_P	PI	% FINES	REMARKS/SAMPLE DESCRIPTION
●	DT03	BS01	0.0	53	33	20		
⊠	GP01	BS01	0.0	48	29	20	99.8	
▲	GP04B	BS01	0.0	53	27	26	100.0	
★	GP05	BS01	0.0	35	26	9	58.4	Air dried sample
⊙	GP05	BS01	0.0	58	35	23		Prepared immediately
✿	GP06	BS01	0.0	16	15	1	48.1	
○	GP07	BS01	0.0	42	27	15	60.6	Air dried sample
△	GP07	BS01	0.0	42	28	14		Prepared immediately
⊗	GP08	BS01	0.0	19	16	3	96.2	
⊕	GP09	BS01	0.0	62	37	25	78.7	Air dried sample
□	GP09	BS01	0.0	66	38	28		Prepared immediately
⊗	GP10	BS01	0.0	29	18	11		
◒	GP11	BS01	0.0	59	35	24	67.4	
☆	GP12	BS01	0.0	22	18	4	95.8	
⊠	GP13	BS01	0.0	49	27	22	99.9	
■	GP14	BS01	0.0	18	15	3	57.4	
◆	GP15	BS01	0.0	15	11	4	56.3	
◇	GP16	BS01	0.0	16	14	2	48.0	

PROJECT NO.: A03355A01

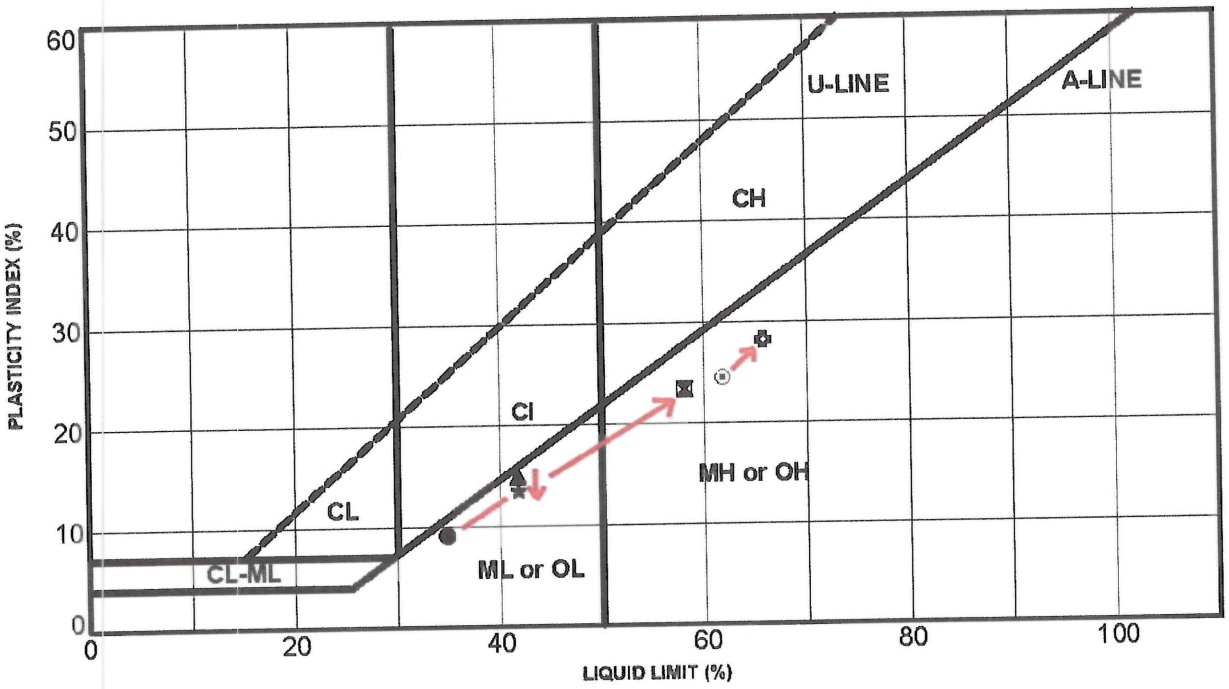
PROJECT:

LOCATION:

FIGURE:

DRAWN BY: AX CHECKED BY: JG

PLASTICITY CHART

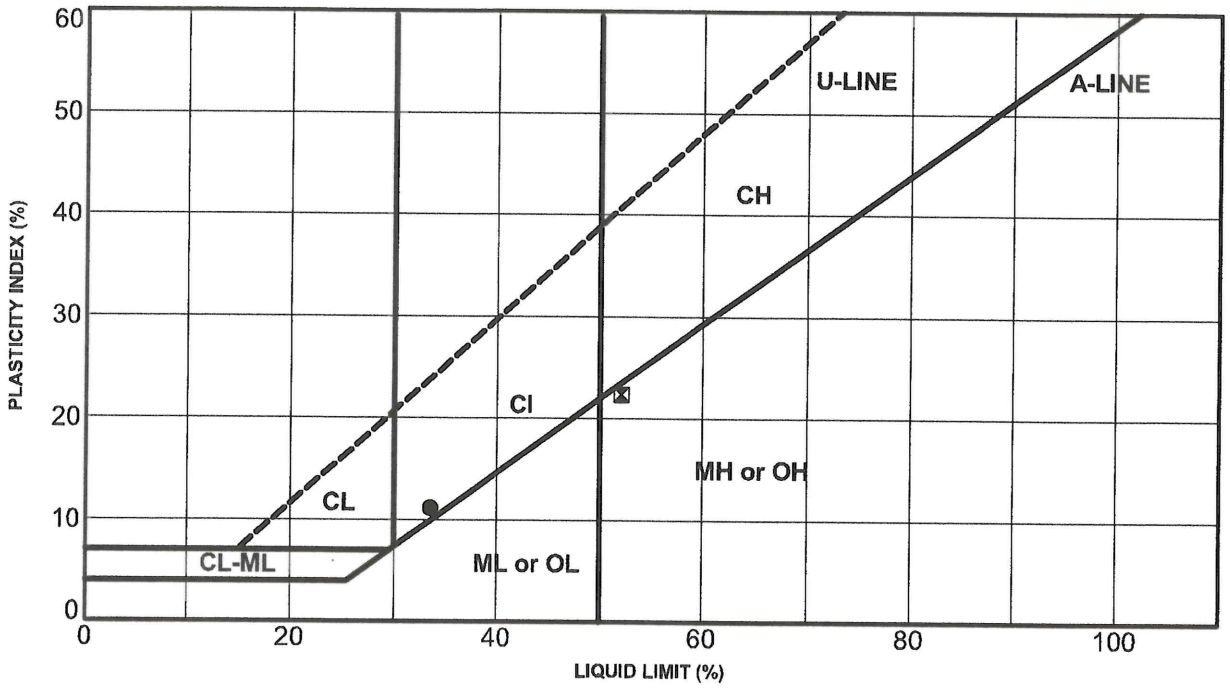


	HOLE	SAMPLE	DEPTH (ft)	W_L	W_P	PI	% FINES	REMARKS/SAMPLE DESCRIPTION
●	GP05	BS01	0.0	35	26	9		Air dried sample
⊠	GP05	BS01	0.0	58	35	23		Prepared immediately
▲	GP07	BS01	0.0	42	27	15		Air dried sample
★	GP07	BS01	0.0	42	28	14		Prepared immediately
⊙	GP09	BS01	0.0	62	37	25		Air dried sample
✿	GP09	BS01	0.0	66	38	28		Prepared immediately

PROJECT NO.:	A03355A01
PROJECT:	
LOCATION:	
FIGURE:	
DRAWN BY: AX	CHECKED BY: JG

KC_ATTERBERG-IMP_CONF T19065.GPJ SIEVE.GDT 19-9-27

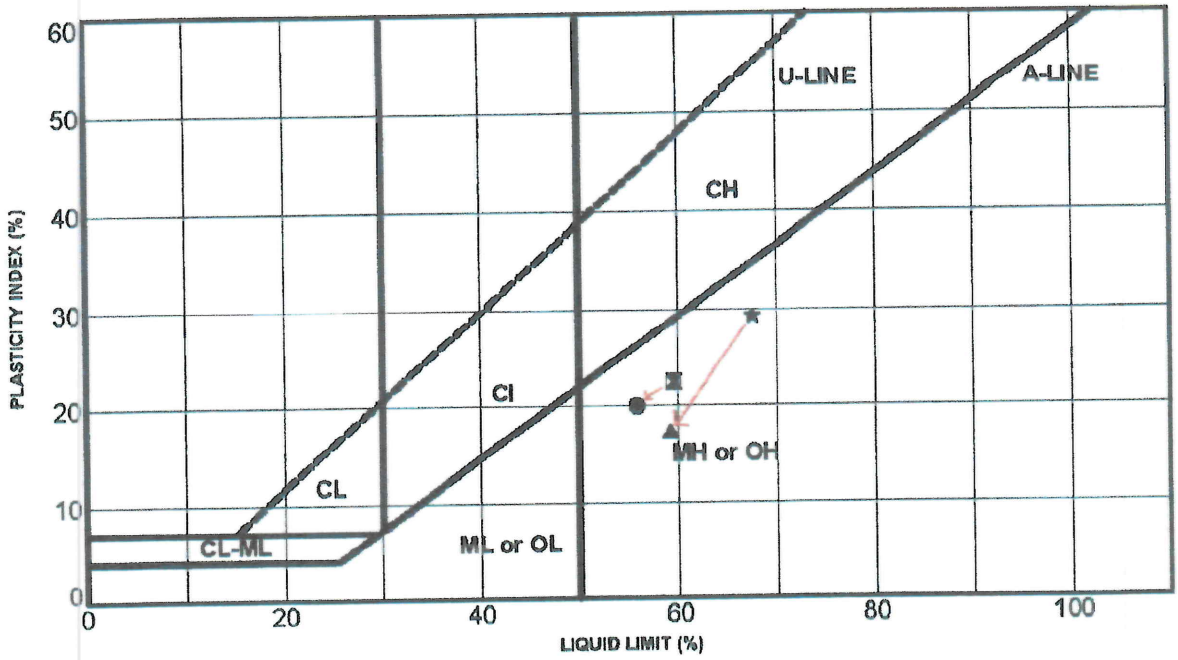
PLASTICITY CHART



	HOLE	SAMPLE	DEPTH (m)	W_L	W_P	PI	% FINES	REMARKS/SAMPLE DESCRIPTION
●	Slimes 1		0.0	34	22	11	99.1	Pail 13
⊠	Slimes 2		0.0	52	30	22	99.9	Pail 14

	PROJECT NO.: A03355A01
	PROJECT:
	LOCATION: Brazil
	FIGURE:
	DRAWN BY: AX CHECKED BY: BY

PLASTICITY CHART

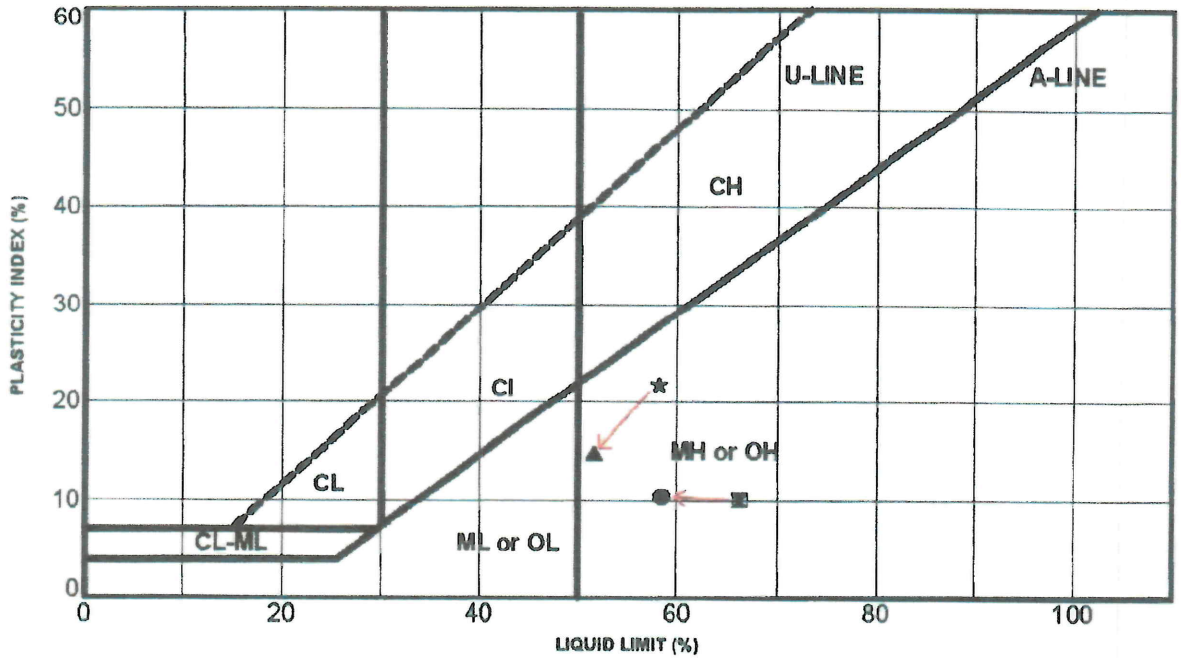


	HOLE	SAMPLE	DEPTH (m)	W_L	W_P	PI	% FINES	REMARKS/SAMPLE DESCRIPTION
●	BH-01	01	3.5	56	36	20	73.0	Air Dried
⊠	BH-01	01	3.5	60	37	22	67.9	Natural
▲	BH-01	02	4.5	59	42	17	80.1	Air Dried
★	BH-01	02	4.5	68	38	29	82.6	Natural

PROJECT NO.:	A03355A01
PROJECT:	
LOCATION:	Brazil
FIGURE:	
DRAWN BY:	AX
CHECKED BY:	BY

KO_ATTERBERG SI A03355A01 BZ 1190F2.GPJ SIEVE.GDT 19-10-4

PLASTICITY CHART

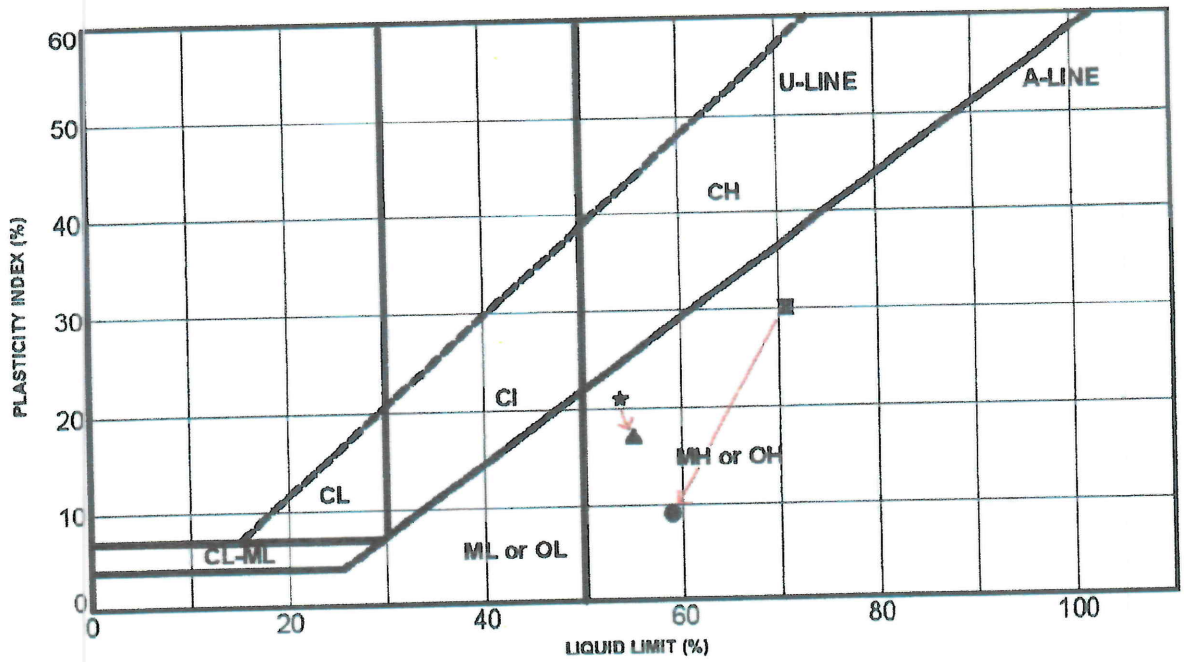


	HOLE	SAMPLE	DEPTH (m)	W_L	W_P	PI	% FINES	REMARKS/SAMPLE DESCRIPTION
●	BH-02	01	3.5	58	48	10	76.8	Air Dried
⊠	BH-02	01	3.5	66	56	10	71.2	Natural
▲	BH-02	02	4.5	52	37	15	63.8	Air Dried
★	BH-02	02	4.5	58	36	22	53.3	Natural

PROJECT NO.: A03355A01
PROJECT:
LOCATION: Brazil
FIGURE:
DRAWN BY: AX CHECKED BY: BY

KC ATTERBERG-SI A03355A01 BLT1907.2.GPJ SIEVE.GDT 19-10-4

PLASTICITY CHART



	HOLE	SAMPLE	DEPTH (m)	W_L	W_P	PI	% FINES	REMARKS/SAMPLE DESCRIPTION
●	BH-04	01	3.0	59	50	9	72.8	Air Dried
⊠	BH-04	01	3.0	71	41	30	73.2	Natural
▲	BH-04	02	5.3	55	38	17	74.3	Air Dried
★	BH-04	02	5.3	54	33	21	74.1	Natural

PROJECT NO.: A03355A01
PROJECT:
LOCATION: Brazil
FIGURE:
DRAWN BY: AX CHECKED BY: BY

KC_ATTERBERG-SI A03355A01 BZ 190722.GPJ SIEVE.GDT 19-10-4

Appendix E

Annex 4 – X-Ray Diffraction Report

December 2019

University of British Columbia X-Ray Diffraction Report

QUANTITATIVE PHASE ANALYSIS OF 4 POWDER SAMPLES USING THE RIETVELD METHOD AND X-RAY POWDER DIFFRACTION DATA

Project: A03355A01

Klohn Crippen Berger
#500 – 2955 Virtual Way
Vancouver, BC V5M 4X6

Jacob Kabel, B.Sc.
Elisabetta Pani, Ph.D.
Edith Czech, M.Sc.
Jenny Lai, B.Sc.
Lan Kato, B.A.

Dept. of Earth, Ocean & Atmospheric Sciences
The University of British Columbia
6339 Stores Road
Vancouver, BC V6T 1Z4

July 18, 2019

EXPERIMENTAL METHOD

The samples of **Project A03355A01** were reduced to the optimum grain-size range for quantitative X-ray analysis (<10 μm) by grinding under ethanol in a vibratory McCrone Micronizing Mill for 10 minutes. Continuous-scan X-ray powder-diffraction data were collected over a range 3-80°2θ with CoKα radiation on a Bruker D8 Advance Bragg-Brentano diffractometer equipped with an Fe filter foil, 0.6 mm (0.3°) divergence slit, incident- and diffracted-beam Soller slits and a LynxEye-XE detector. The long fine-focus Co X-ray tube was operated at 35 kV and 40 mA, using a take-off angle of 6°.

RESULTS

The X-ray diffractograms were analyzed using the International Centre for Diffraction Database PDF-4 using Search-Match software by Bruker. X-ray powder-diffraction data of the samples were refined with Rietveld program Topas 4.2 (Bruker AXS). The results of quantitative phase analysis by Rietveld refinements are given in Table 1. These amounts represent the relative amounts of crystalline phases normalized to 100%. The Rietveld refinement plots are shown in Figures 1-4.

Table 1. Results of quantitative phase analysis (wt.%) – Project A03355A01

Mineral	Ideal Formula	#1 Sample 1 Bag2 X-Ray	#2 Sample 1 Bag4 X-Ray	#3 Sample 3 Bag2 X-Ray	#4 Sample 5 Bag1 X-Ray
Hematite	α-Fe_2O_3	50.1	44.4	87.7	86.8
Goethite	α-$Fe^{3+}O(OH)$	32.0	34.0	3.4	3.0
Magnetite	Fe_3O_4	0.4	0.4	6.5	7.6
Quartz	SiO_2	5.4	6.6	1.6	1.5
Kaolinite	$Al_2Si_2O_5(OH)_4$	6.2	8.9	0.6	0.6
Talc	$Mg_3Si_4O_{10}(OH)_2$	2.7	2.3		
Gibbsite	$Al(OH)_3$	0.9	1.0	0.3	0.4
Bayerite	$Al(OH)_3$	2.2	2.4		
Total		100.0	100.0	100.0	100.0

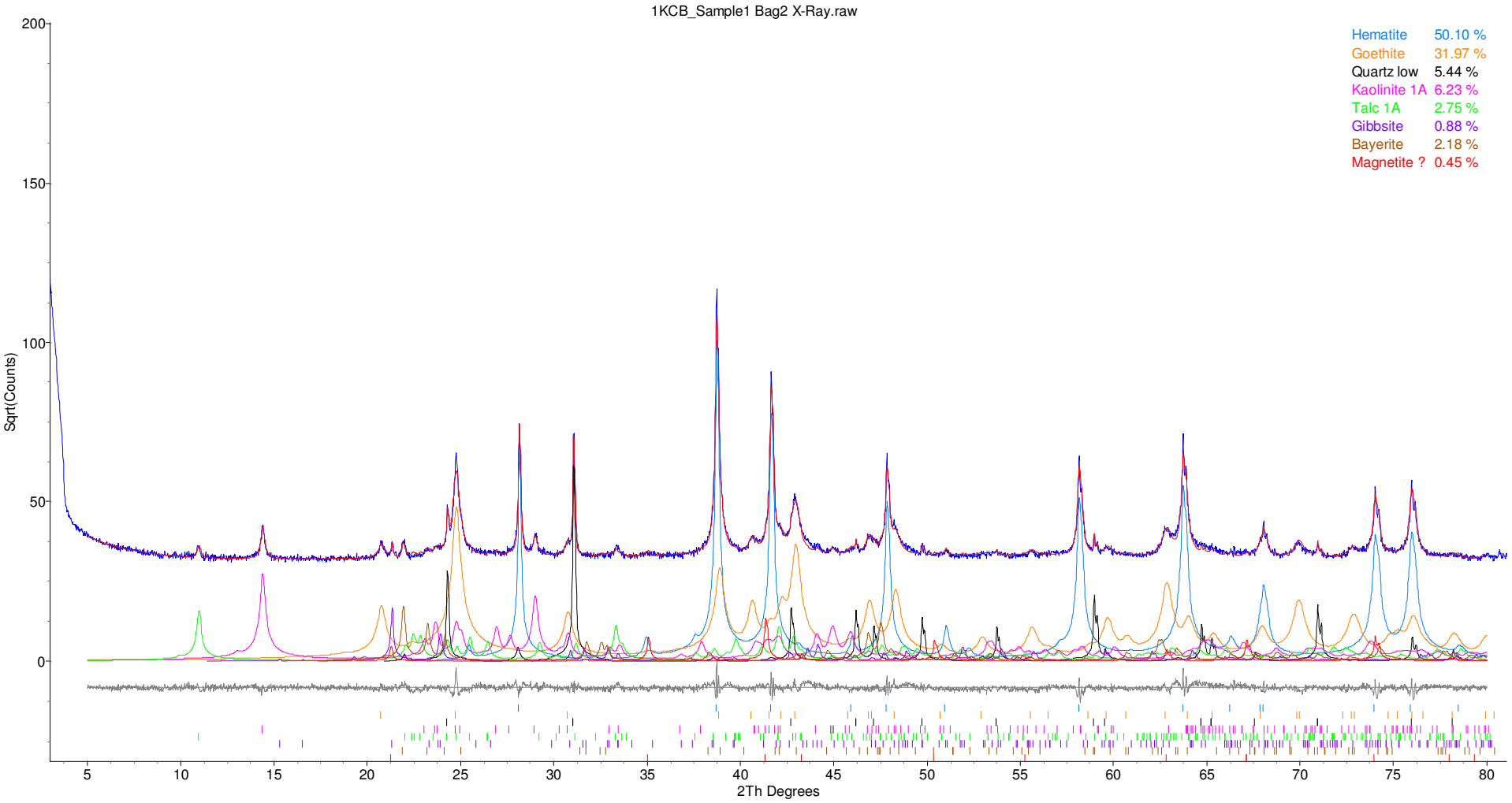


Figure 1. Rietveld refinement plot of **Sample 1 Bag2 X-Ray** (blue line - observed intensity at each step; red line - calculated pattern; solid grey line below - difference between observed and calculated intensities; vertical bars - positions of all Bragg reflections). Coloured lines are individual diffraction patterns of all phases.

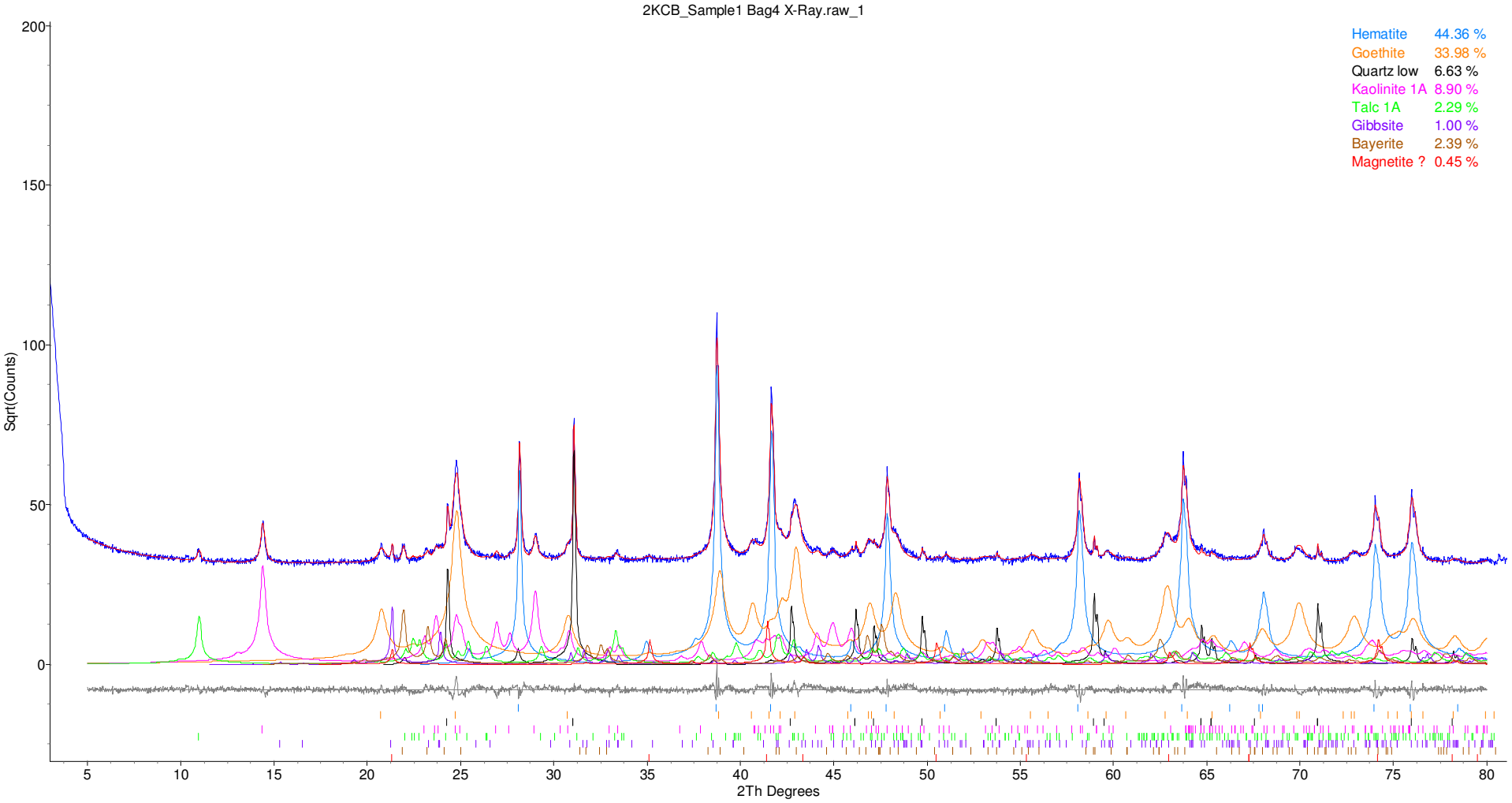


Figure 2. Rietveld refinement plot of **Sample 1 Bag4 X-Ray** (blue line - observed intensity at each step; red line - calculated pattern; solid grey line below - difference between observed and calculated intensities; vertical bars - positions of all Bragg reflections). Coloured lines are individual diffraction patterns of all phases.

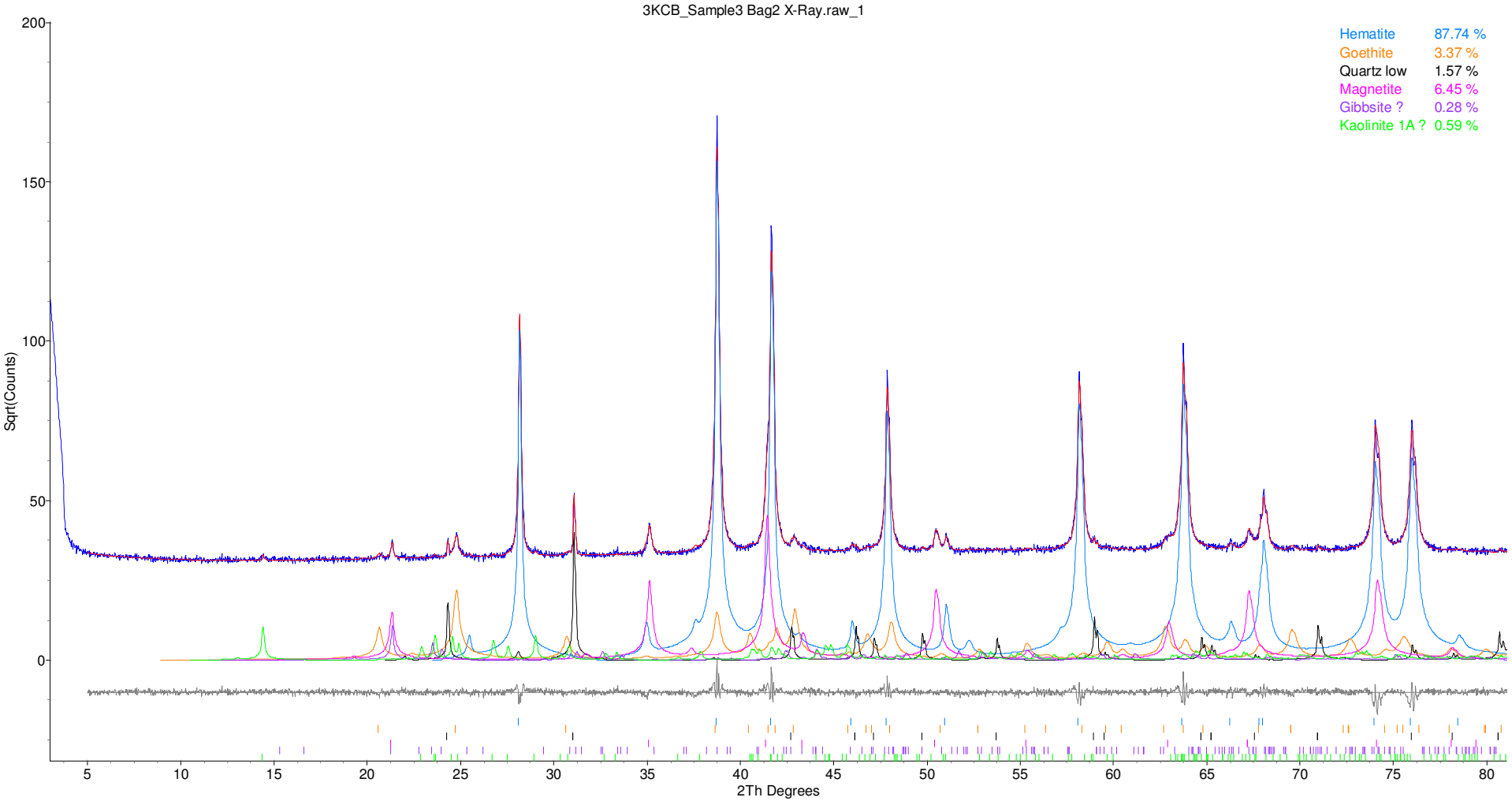


Figure 3. Rietveld refinement plot of **Sample 3 Bag2 X-Ray** (blue line - observed intensity at each step; red line - calculated pattern; solid grey line below - difference between observed and calculated intensities; vertical bars - positions of all Bragg reflections). Coloured lines are individual diffraction patterns of all phases.

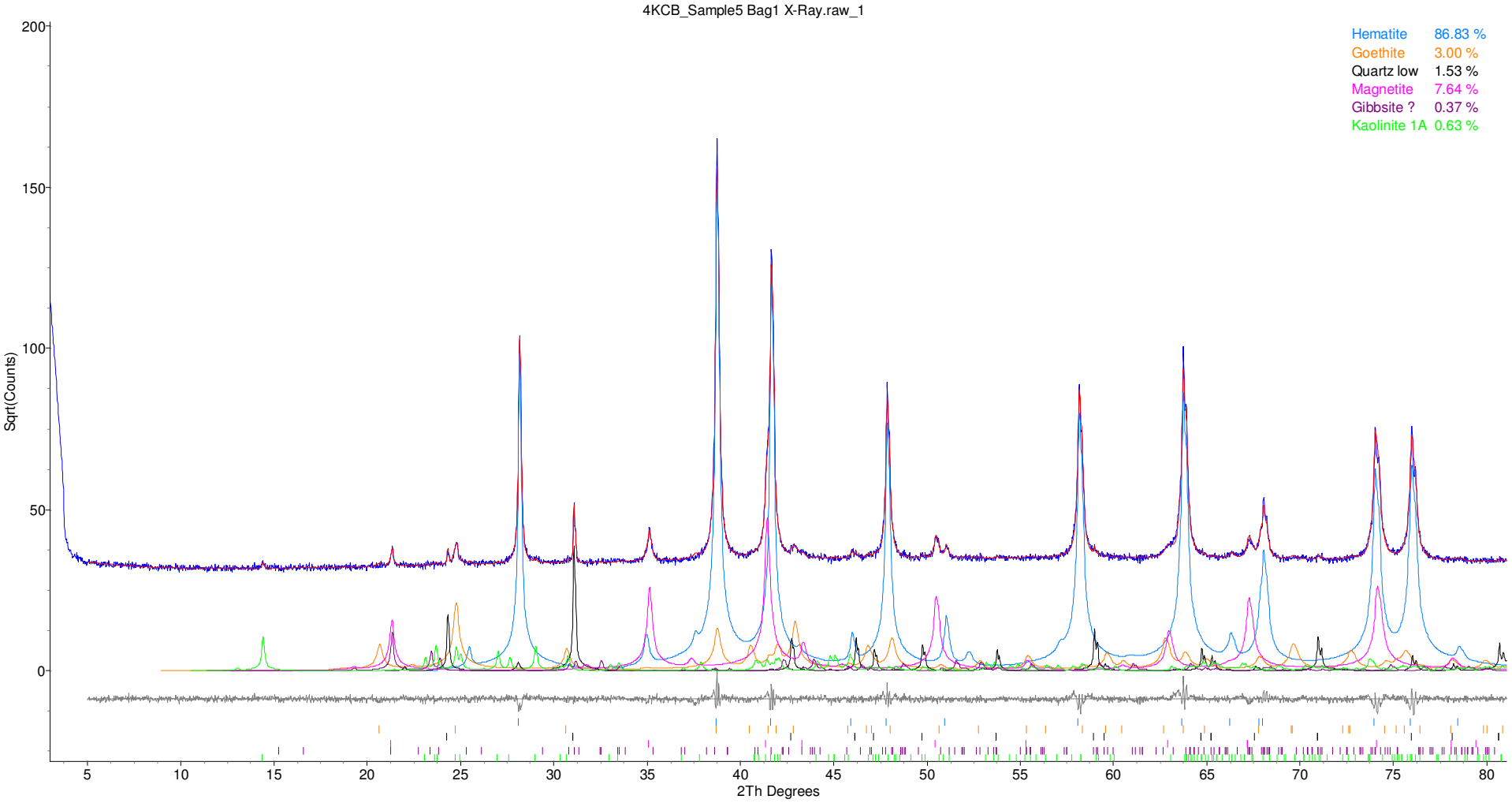
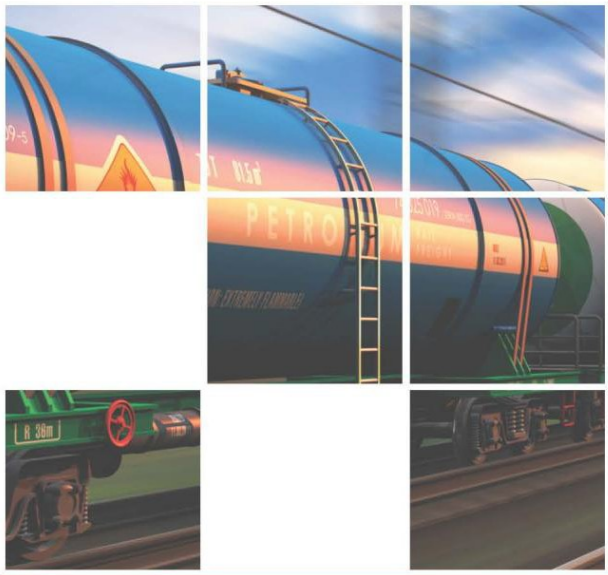
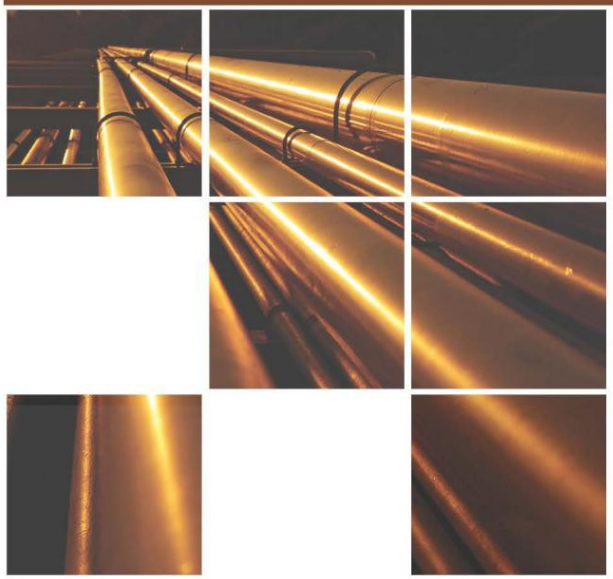


Figure 4. Rietveld refinement plot of **Sample 5 Bag1 X-Ray** (blue line - observed intensity at each step; red line - calculated pattern; solid grey line below - difference between observed and calculated intensities; vertical bars - positions of all Bragg reflections). Coloured lines are individual diffraction patterns of all phases.

University of Alberta X-Ray Diffraction Report



BULK X-RAY DIFFRACTION (XRD) ANALYSIS USING RIETVELD METHOD OF FOUR SAMPLES



Company: UNIVERSITY OF ALBERTA

Work Order No: 19A20079

Date: October, 2019



AGAT Geology Department
3801 – 21st Street N.E.
Calgary, Alberta T2E 6T5

AGAT Laboratories

BULK XRD ANALYSIS USING RIETVELD METHOD

Introduction: Four samples identified as '**BT-01, DT-02, DT-06, and DT-10**' were received by the AGAT Laboratories Geology Department for bulk X-Ray Diffraction (XRD) analysis using Rietveld Method.

Sample Preparation: Each sample was homogenized carefully considering nature of materials and a subsample (~ 100 grams) was crushed with a vibratory disc mill (RS200; Retsch) to reduce the size of materials. The crushed subsample was homogenized again and approximately 3 grams was taken for micronizing using a planetary ball mill.

X-Ray Data Collection and Analysis:

Diffractometer Name:	XPERT PRO X-RAY DIFFRACTOMETER
Instrumental Parameters:	Radiation Source – Copper (Cu)
	Generator settings - 40 mA, 45 kV
	Start position [°2θ] - 4
	End position [°2θ] - 80
	Step size [°2θ] - 0.03
	Scan step time [s] – 0.5
Data Analysis:	ICDD PDF-4 Mineral 2019 powder diffraction database
	X'PERT HighScore for mineral identification
	TOPAS for quantitative phase analysis (QPA) using Rietveld Method
Detection Limit:	0.5 – 1.0 % depending on the type and nature of sample

Quantitative Phase Analysis: Using HighScore program, the different mineral phases of the XRD patterns were identified. Once the mineral phases were identified, Rietveld refinements were performed by importing the trace pattern into TOPAS 5. This program (TOPAS 5) is used for Rietveld analysis to quantify the mineralogy. Four refined diffractograms are attached with this report as appendix. The quantitative mineral phases of four samples are given in the Tables 1-4.

Sample 1 – DT-01; Date Sampled- October 08, 2019

Results: The XRD results (**Table 1**) show that this sample consists mainly of oxides (hematite and magnetite) with lesser amounts of hydroxides (goethite, gibbsite, and bayerite), tectosilicate (quartz), and phyllosilicates (kaolinite and talc) minerals.

Table 1: Results of quantitative mineral analysis (relative weight %) of X-ray diffraction data for sample 1 (**DT-01**) using Rietveld method

Mineral Name	Compound Name	Standard Chemical Formula	Mineral Concentration, wt.%
Hematite	Iron oxide	Fe_2O_3	**43.1**
Goethite	Iron oxide hydroxide	FeO(OH)	**20.7**
Quartz	Silicon oxide	SiO_2	**14.9**
Kaolinite	Aluminum silicate hydroxide	$Al_2Si_2O_5(OH)_4$	**11.6**
Talc steatite soapstone	Magnesium silicate hydrate	$Mg_3(Si_4O_{10})(OH)_2$	**3.1**
Gibbsite	Aluminum hydroxide	$Al(OH)_3$	**3.0**
Magnetite	Iron oxide	Fe_3O_4	**1.9**
Bayerite	Aluminum hydroxide	Al(OH)3	**1.7**
		Total:	**100**

Sample 2 – DT-02; Date Sampled- October 08, 2019

Results: The XRD results (**Table 2**) show that this sample consists mainly of oxides (hematite and magnetite) with lesser amounts of hydroxides (goethite, gibbsite, and bayerite), tectosilicate (quartz), and phyllosilicates (kaolinite and talc) minerals.

Table 2: Results of quantitative mineral analysis (relative weight %) of X-ray diffraction data for sample 2 (**DT-02**) using Rietveld method

Mineral Name	Compound Name	Standard Chemical Formula	Mineral Concentration, wt.%
Hematite	Iron oxide	Fe_2O_3	**54.1**
Goethite	Iron oxide hydroxide	FeO(OH)	**15.3**
Quartz	Silicon oxide	SiO_2	**12.0**
Kaolinite	Aluminum silicate hydroxide	$Al_2Si_2O_5(OH)_4$	**10.9**
Gibbsite	Aluminum hydroxide	$Al(OH)_3$	**2.2**
Bayerite	Aluminum hydroxide	Al(OH)3	**2.0**
Talc steatite soapstone	Magnesium silicate hydrate	$Mg_3(Si_4O_{10})(OH)_2$	**2.0**
Magnetite	Iron oxide	Fe_3O_4	**1.5**
		Total:	**100**

Sample 3 – DT-06; Date Sampled- October 08, 2019

Results: The XRD results (**Table 3**) show that this sample consists mainly of oxides (hematite and magnetite) with lesser amounts of tectosilicate (quartz), hydroxides (goethite, gibbsite, and bayerite), and phyllosilicates (kaolinite and talc) minerals.

Table 3: Results of quantitative mineral analysis (relative weight %) of X-ray diffraction data for sample 3 (**DT-06**) using Rietveld method

Mineral Name	Compound Name	Standard Chemical Formula	Mineral Concentration, wt.%
Hematite	Iron oxide	Fe_2O_3	**50.3**
Quartz	Silicon oxide	SiO_2	**28.5**
Goethite	Iron oxide hydroxide	FeO(OH)	**10.2**
Kaolinite	Aluminum silicate hydroxide	$Al_2Si_2O_5(OH)_4$	**6.4**
Gibbsite	Aluminum hydroxide	$Al(OH)_3$	**1.4**
Talc steatite soapstone	Magnesium silicate hydrate	$Mg_3(Si_4O_{10})(OH)_2$	**1.4**
Magnetite	Iron oxide	Fe_3O_4	**1.3**
Bayerite	Aluminum hydroxide	Al(OH)3	**0.5**
		Total:	**100**

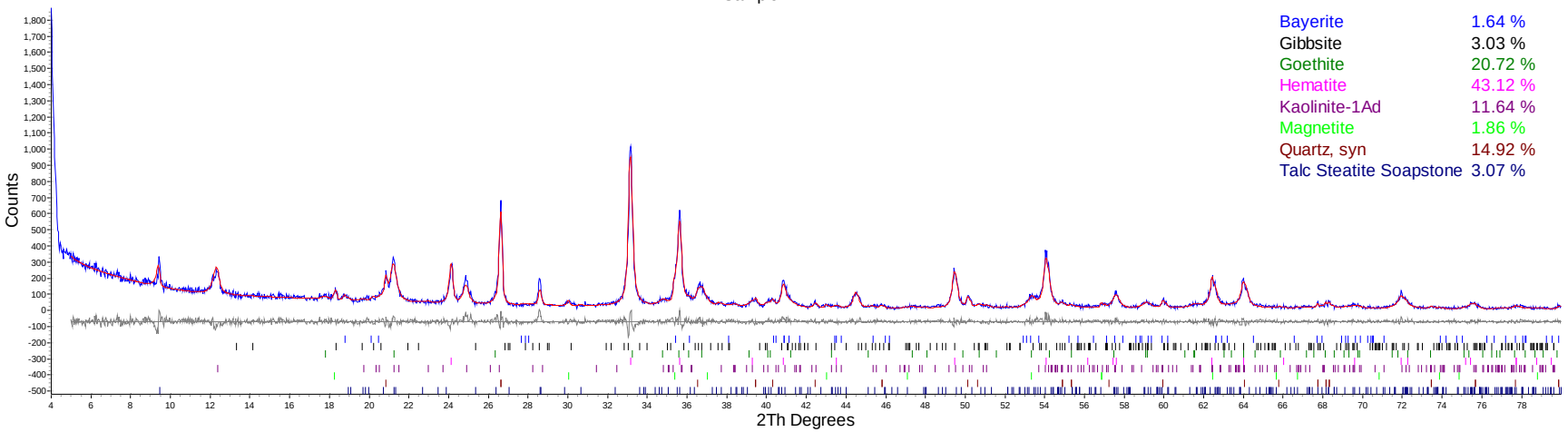
Sample 4 – DT-10; Date Sampled- October 08, 2019

Results: The XRD results (**Table 4**) show that this sample consists mainly of oxides (hematite and magnetite) with lesser amounts of tectosilicate (quartz), hydroxides (goethite, gibbsite, and bayerite), and phyllosilicates (kaolinite and talc) minerals.

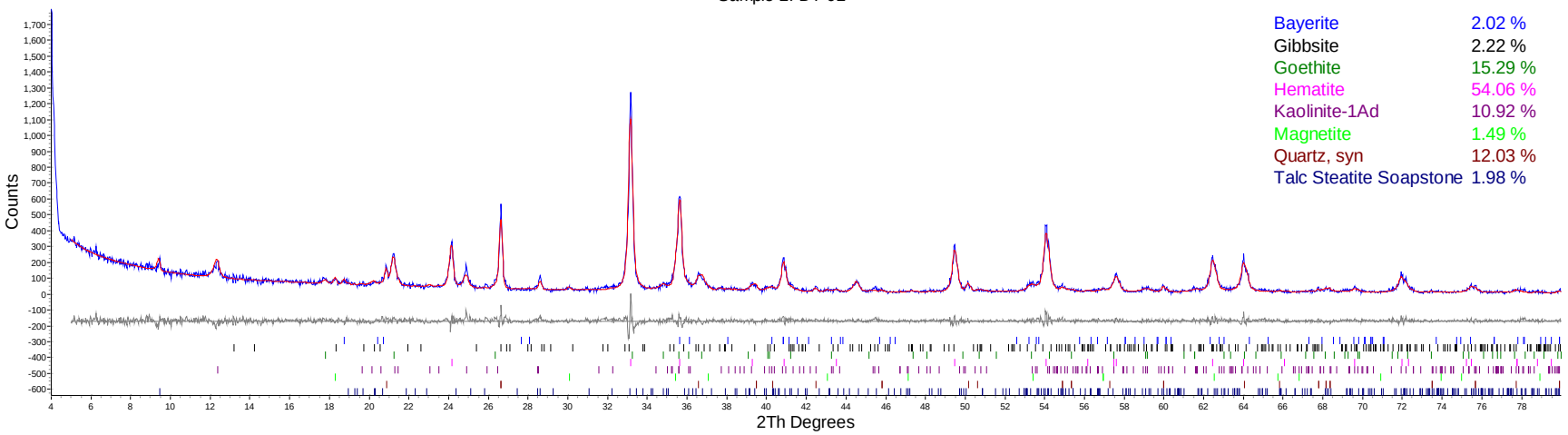
Table 4: Results of quantitative mineral analysis (relative weight %) of X-ray diffraction data for sample 4 (**DT-10**) using Rietveld method

Mineral Name	Compound Name	Standard Chemical Formula	Mineral Concentration, wt.%
Hematite	Iron oxide	Fe_2O_3	**44.3**
Quartz	Silicon oxide	SiO_2	**21.8**
Goethite	Iron oxide hydroxide	FeO(OH)	**13.7**
Kaolinite	Aluminum silicate hydroxide	$Al_2Si_2O_5(OH)_4$	**13.5**
Gibbsite	Aluminum hydroxide	$Al(OH)_3$	**3.0**
Bayerite	Aluminum hydroxide	Al(OH)3	**1.4**
Magnetite	Iron oxide	Fe_3O_4	**1.3**
Talc steatite soapstone	Magnesium silicate hydrate	$Mg_3(Si_4O_{10})(OH)_2$	**1.1**
		Total:	**100**

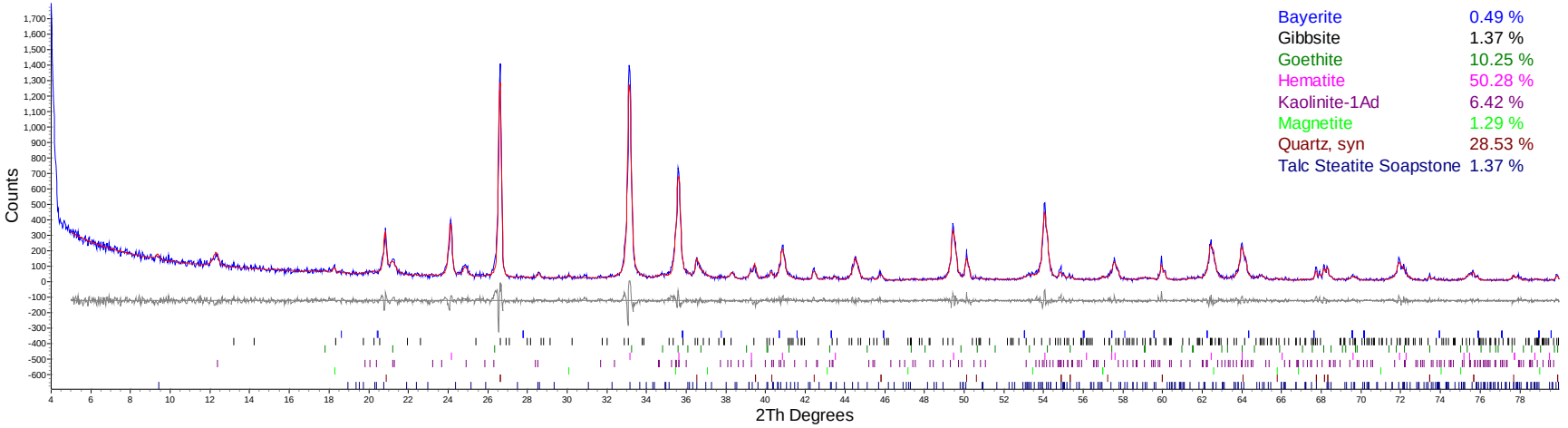
Sample 1: DT-1


Counts
2Th Degrees
Bayerite 1.64 %
Gibbsite 3.03 %
Goethite 20.72 %
Hematite 43.12 %
Kaolinite-1Ad 11.64 %
Magnetite 1.86 %
Quartz, syn 14.92 %
Talc Steatite Soapstone 3.07 %

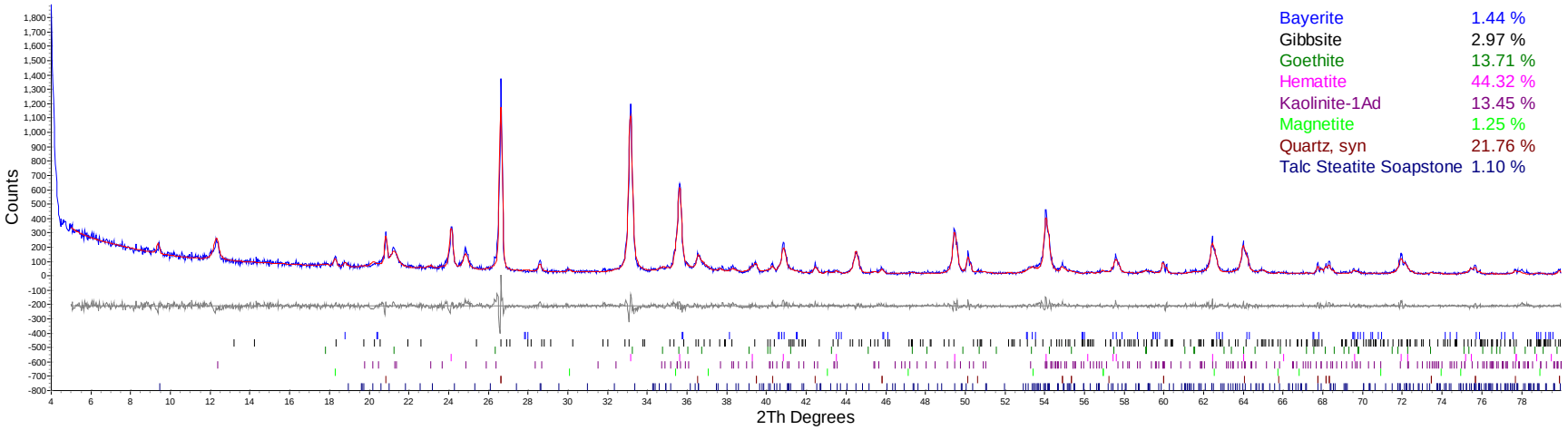
Sample 2: DT-02



Sample 3: DT-06



Sample 4: DT-10

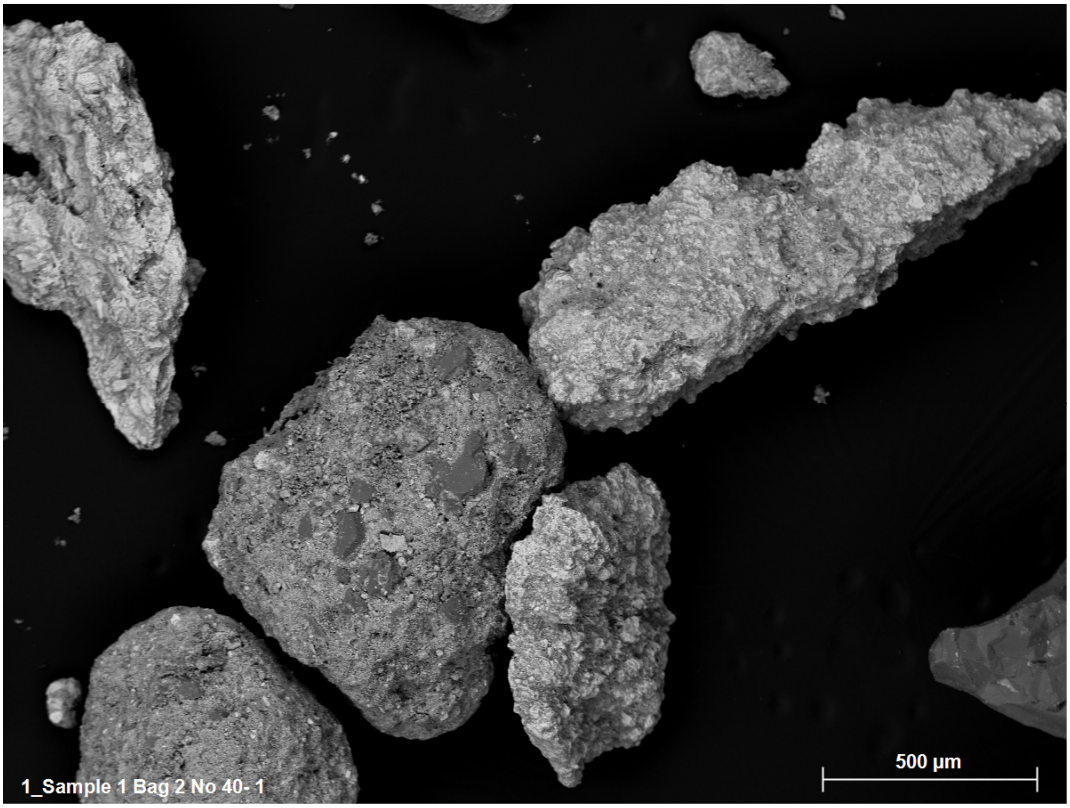


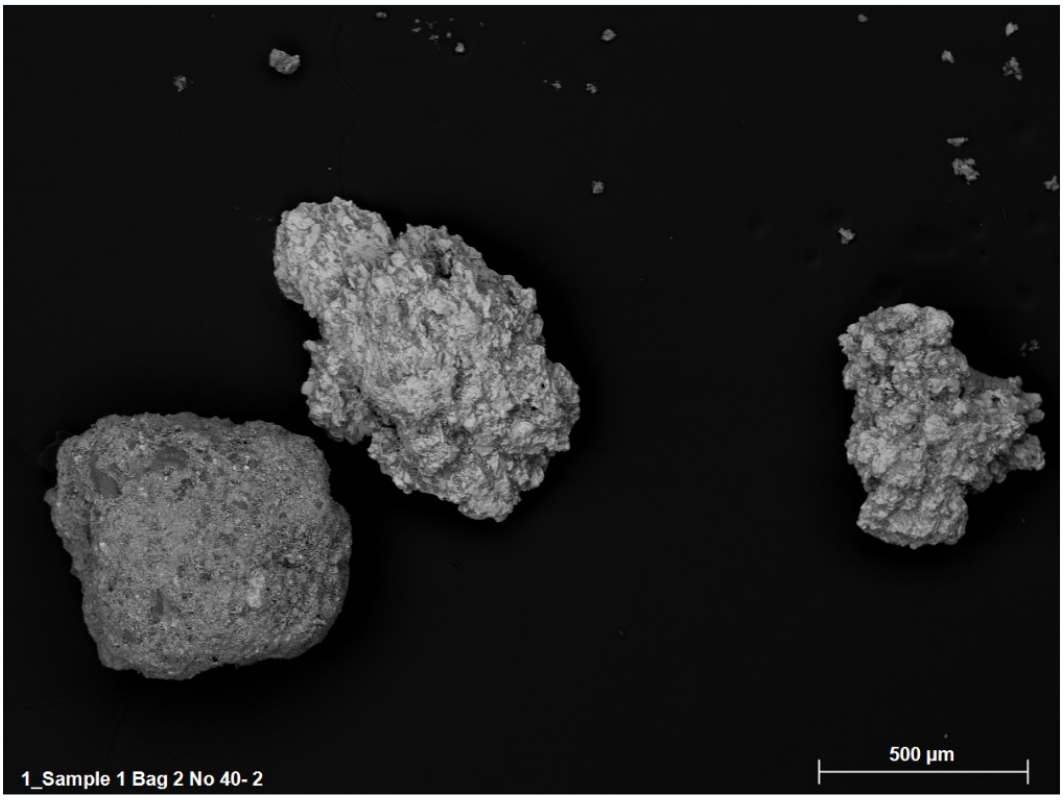
Appendix E

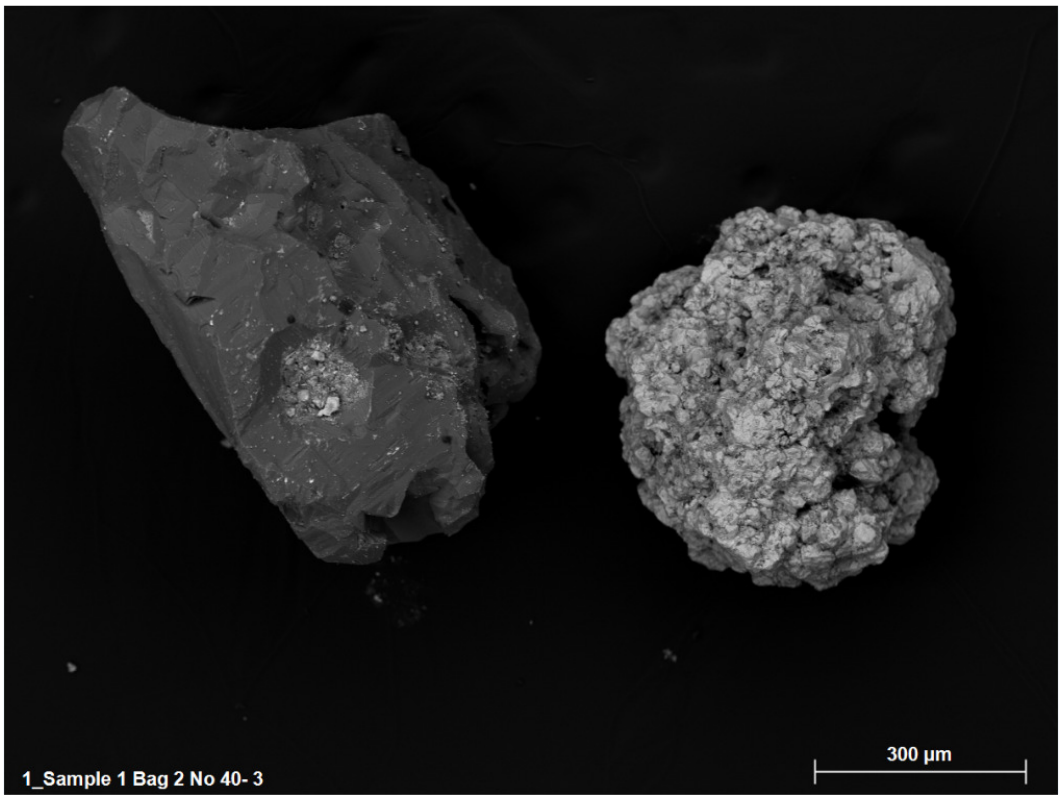
Annex 5 – Scanning Electron Microscopy Images

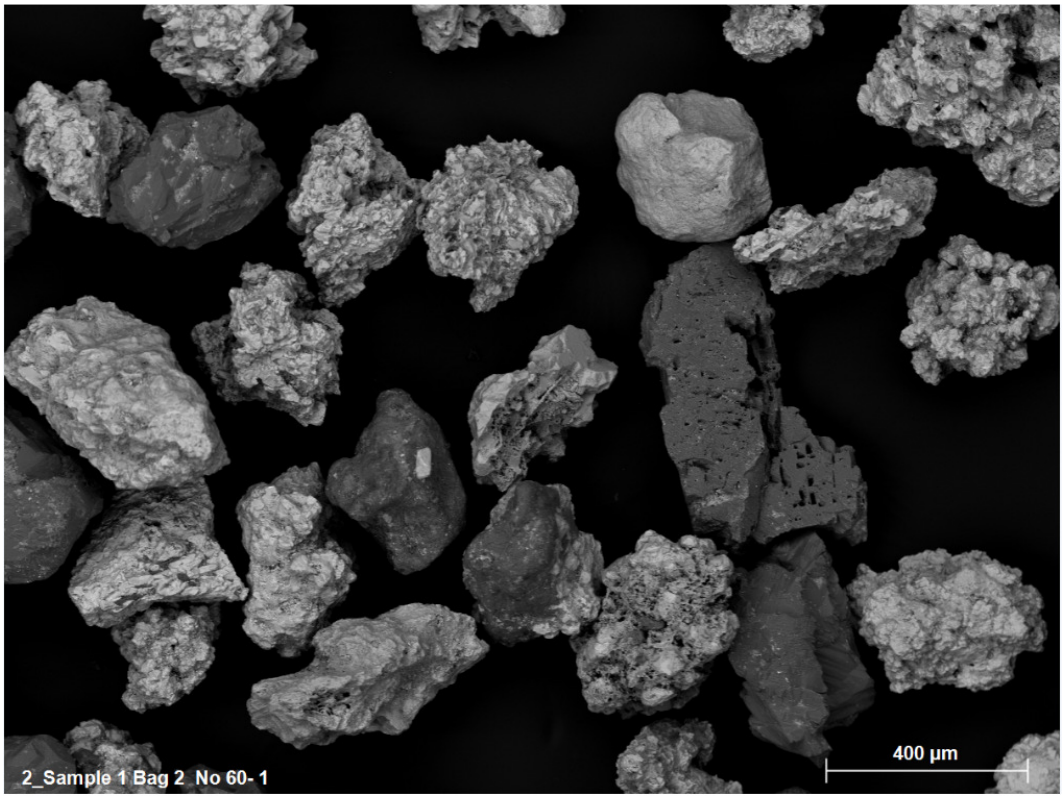
December 2019

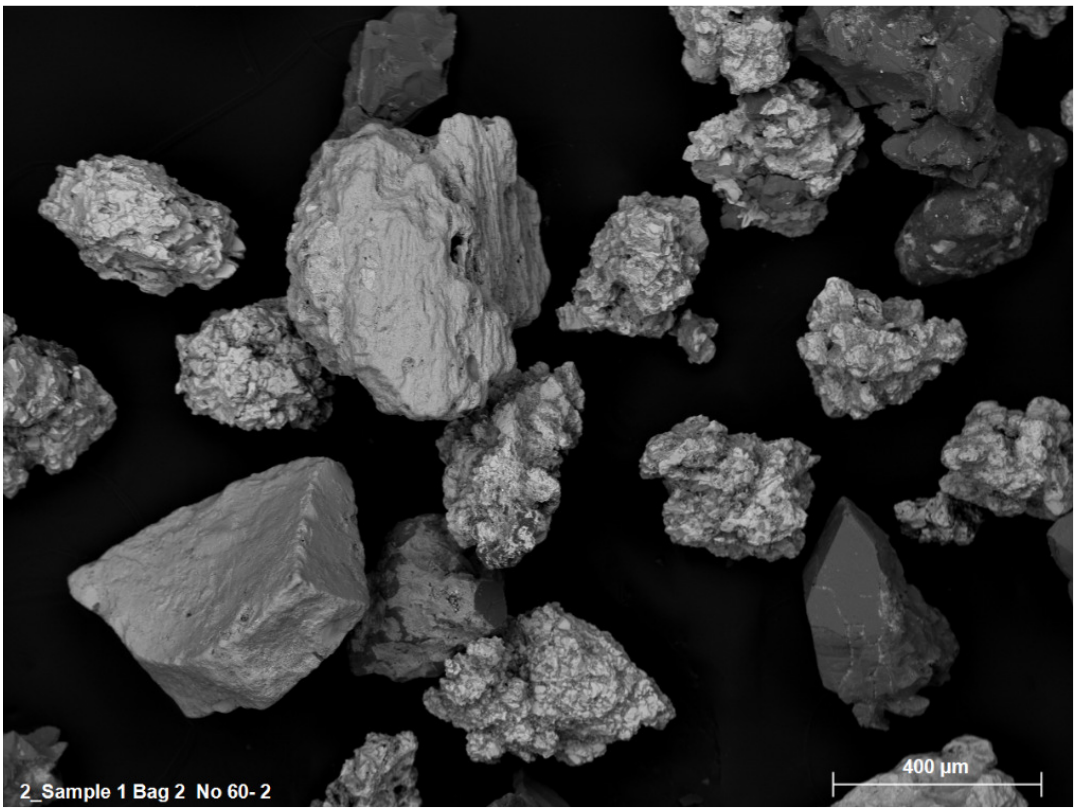
University of British Columbia Scanning Electron Microscope (SEM) Imaging

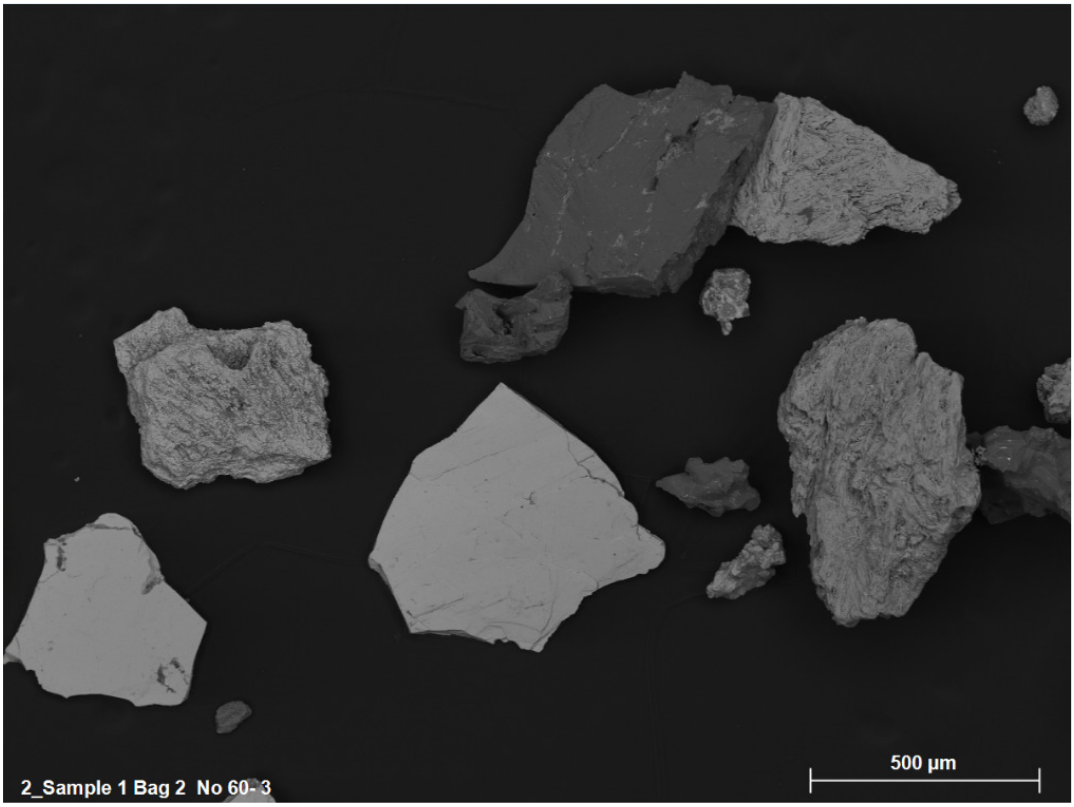

500 µm
1_Sample 1 Bag 2 No 40- 1

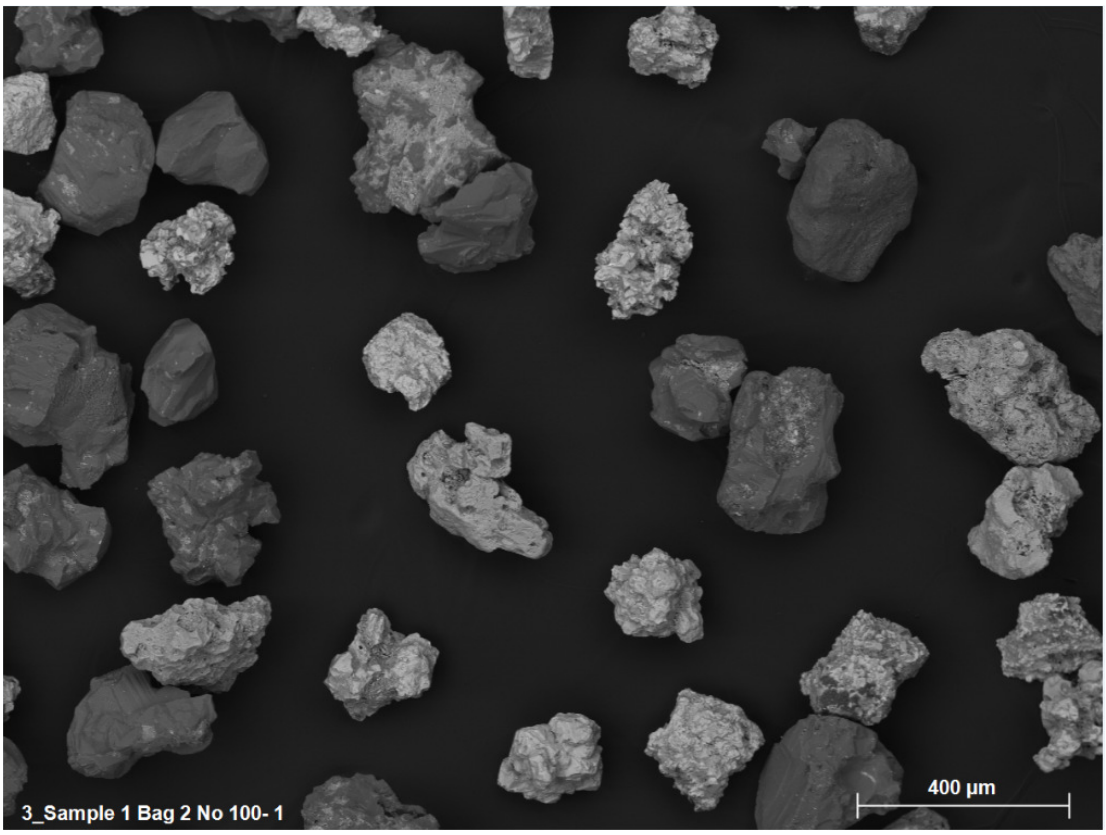

500 µm
1_Sample 1 Bag 2 No 40- 2

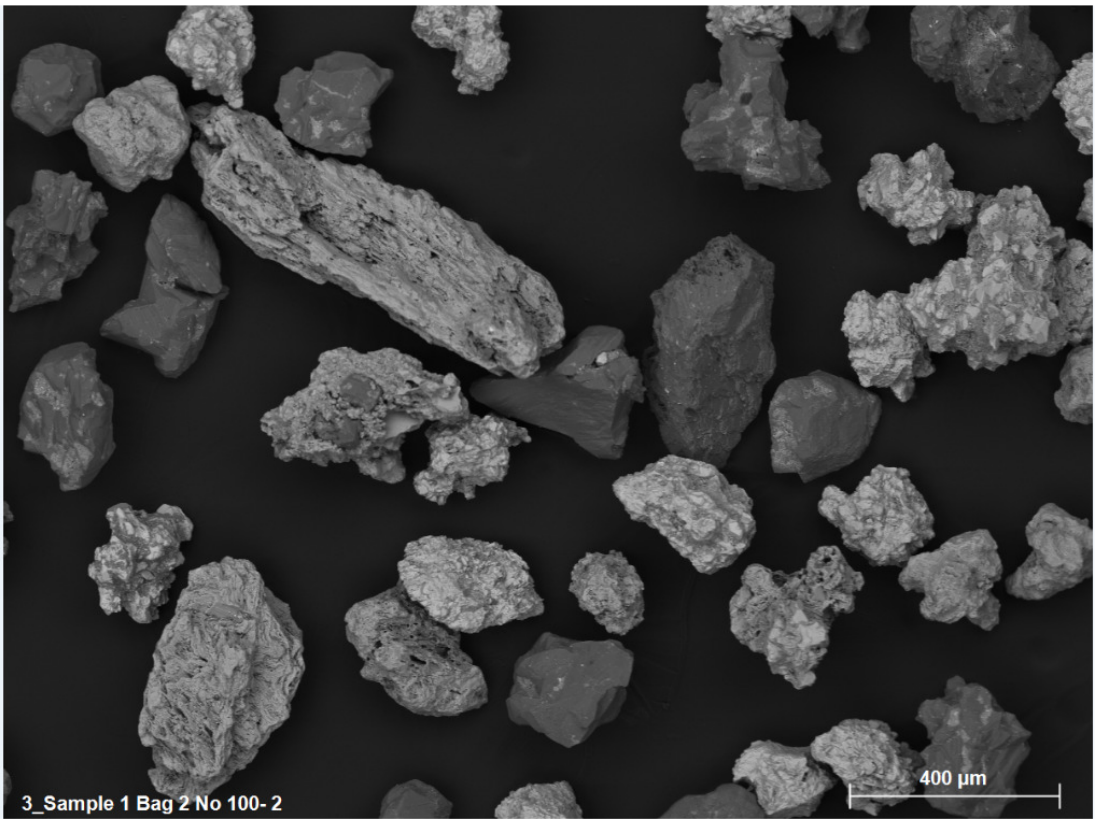

1_Sample 1 Bag 2 No 40- 3
300 µm

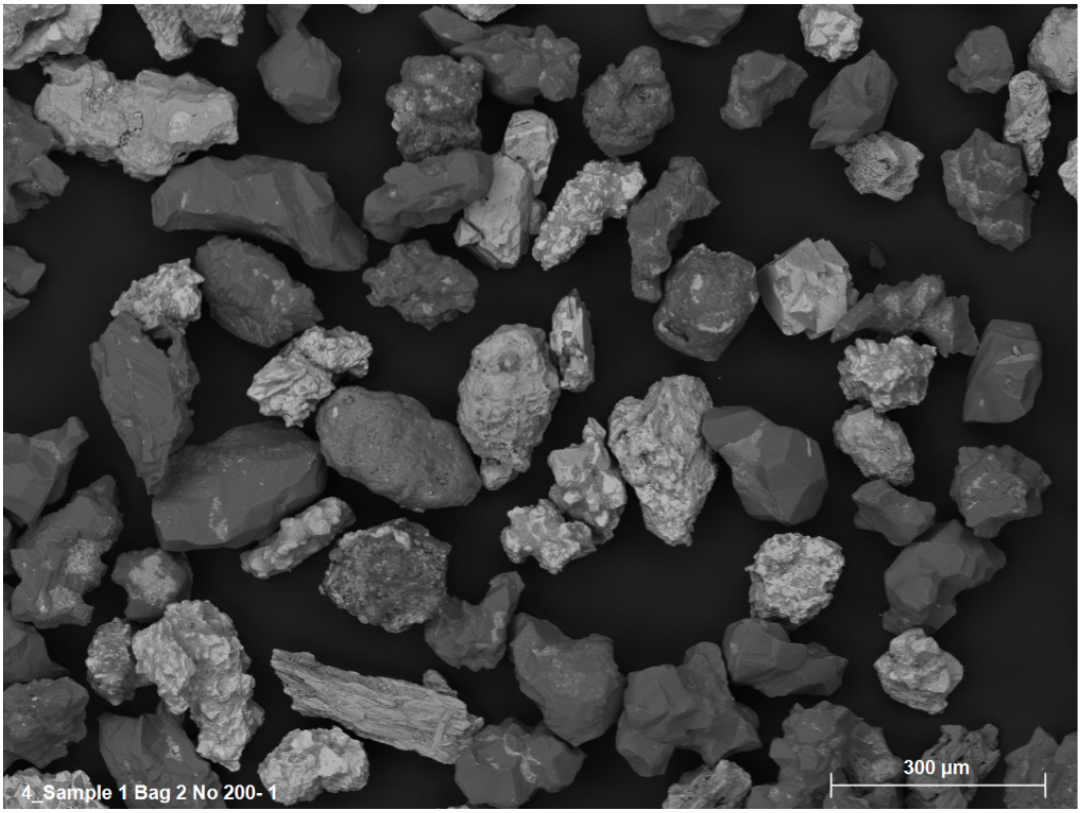

2_Sample 1 Bag 2 No 60- 1
400 µm

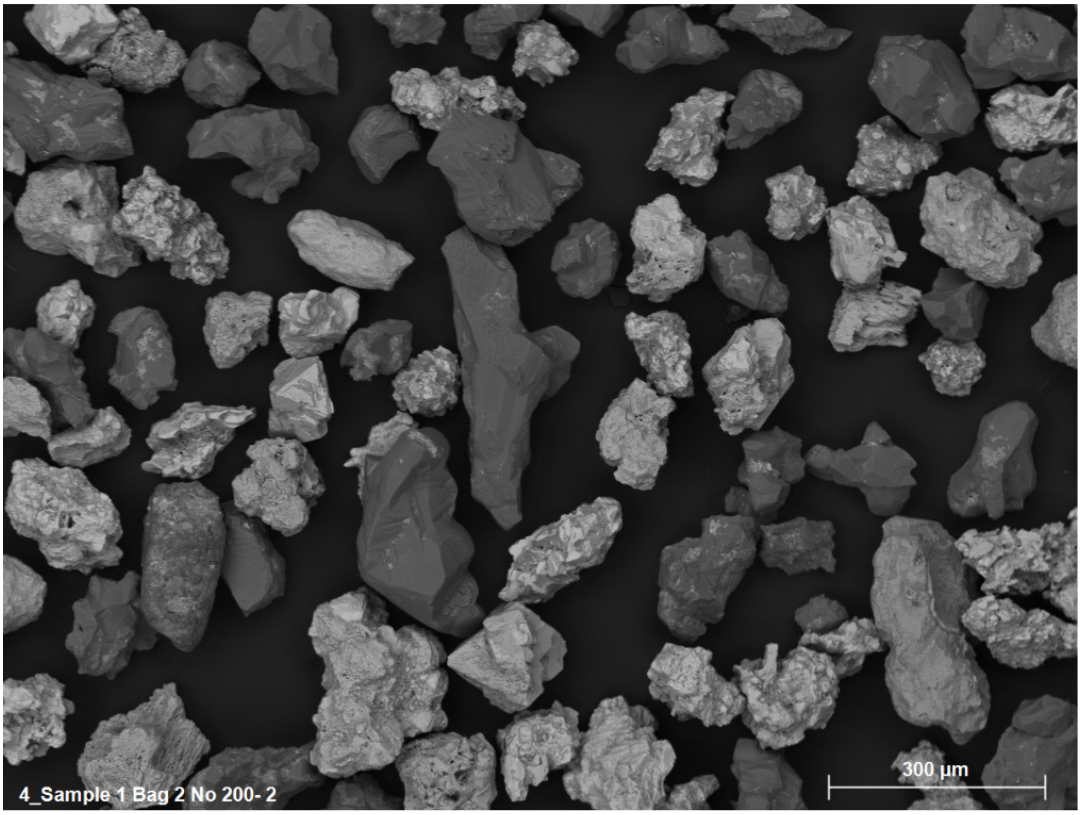

400 µm
2_Sample 1 Bag 2 No 60- 2

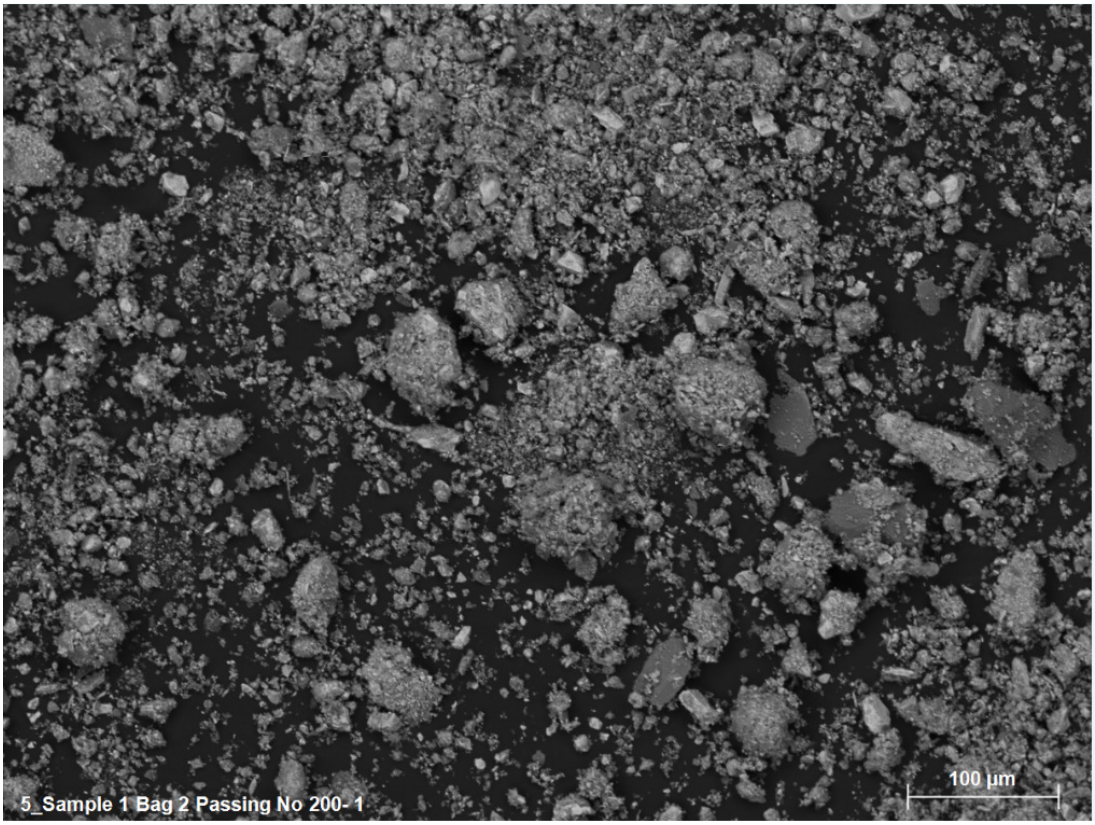

500 µm
2_Sample 1 Bag 2 No 60- 3

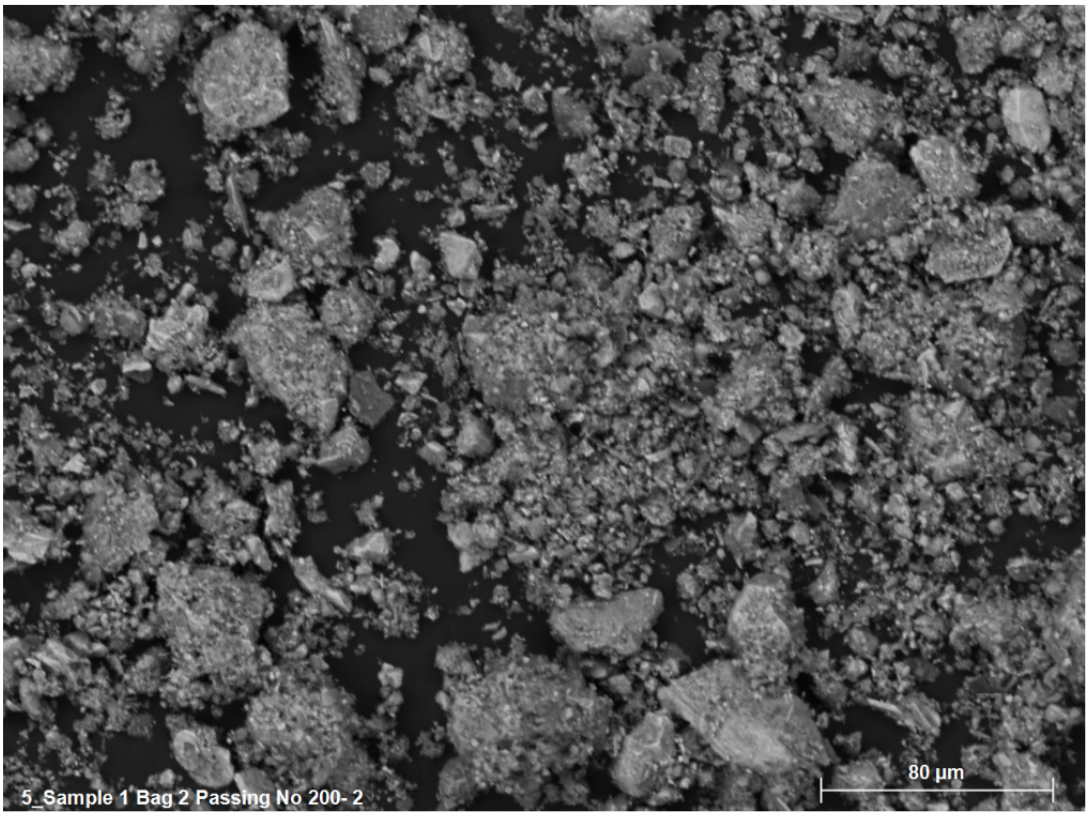

400 µm
3_Sample 1 Bag 2 No 100- 1

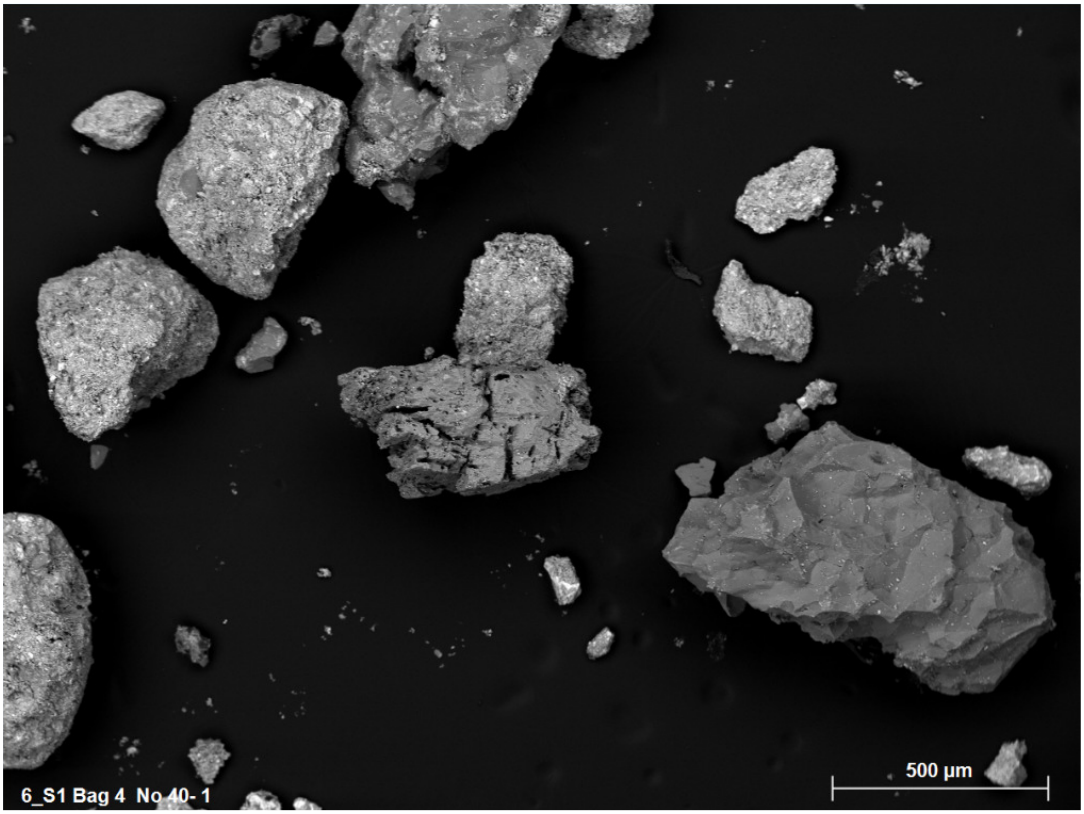

400 µm
3_Sample 1 Bag 2 No 100- 2

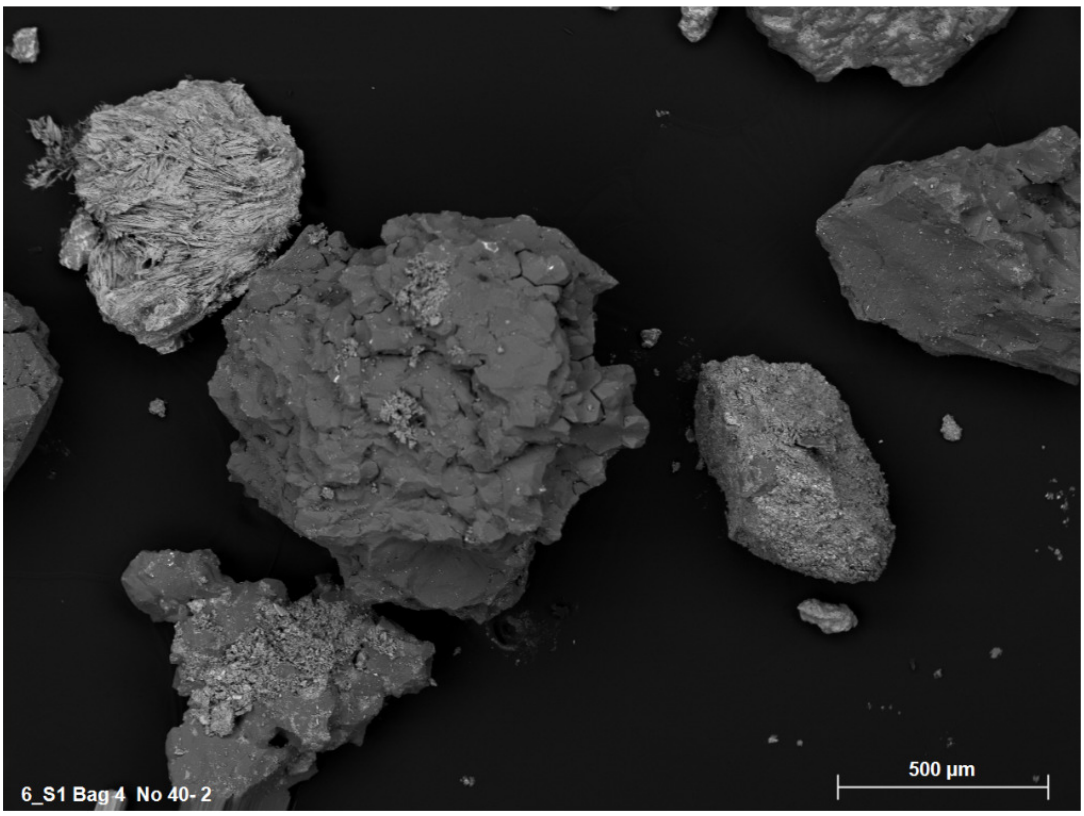

300 µm
4_Sample 1 Bag 2 No 200- 1

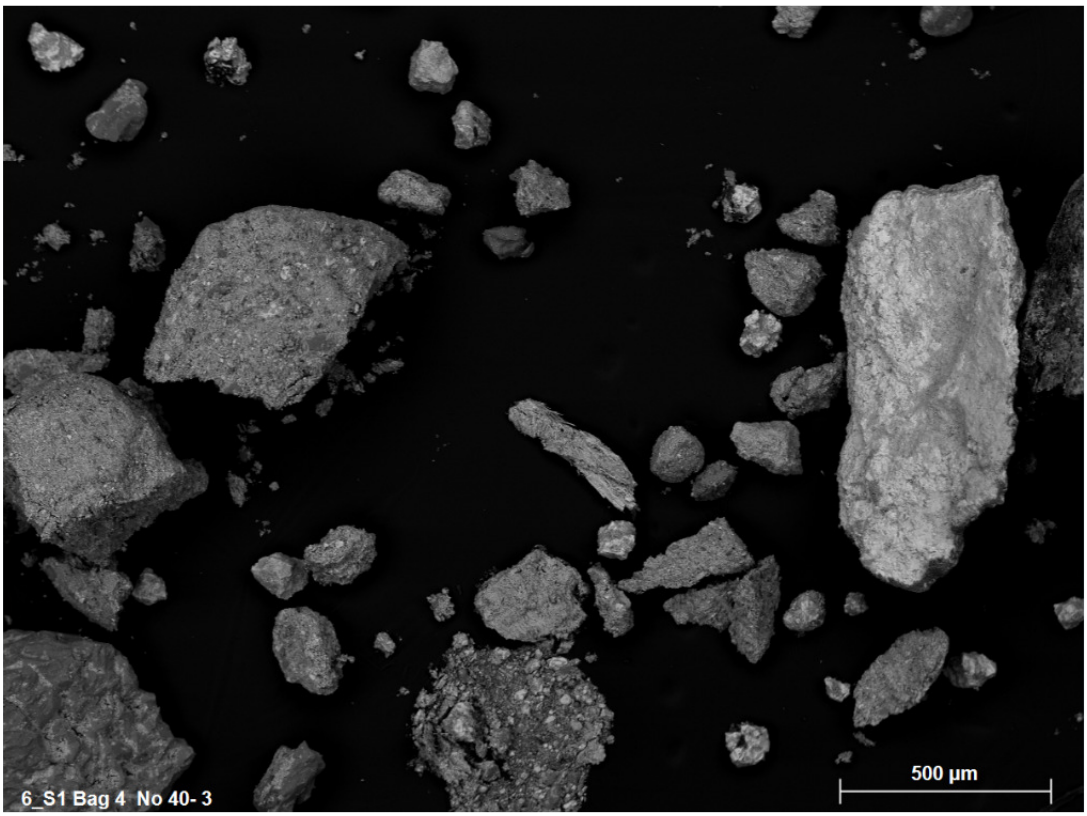

300 µm
4_Sample 1 Bag 2 No 200- 2

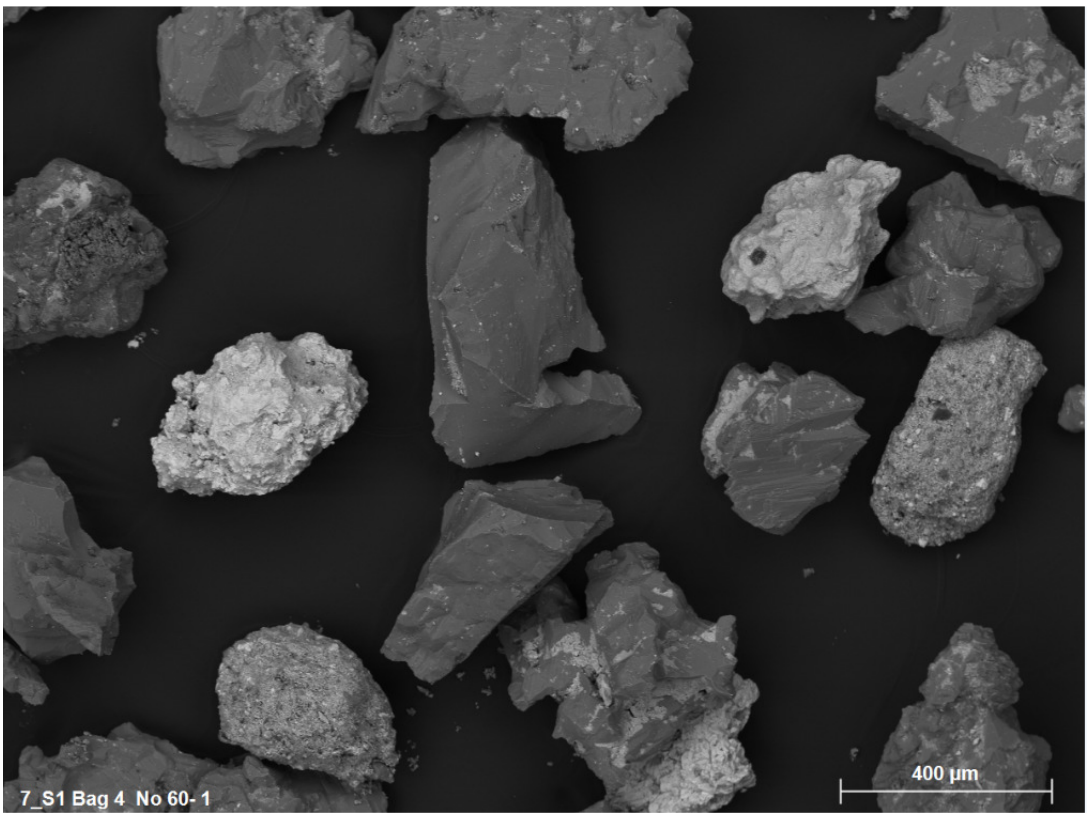

5_Sample 1 Bag 2 Passing No 200- 1
100 µm

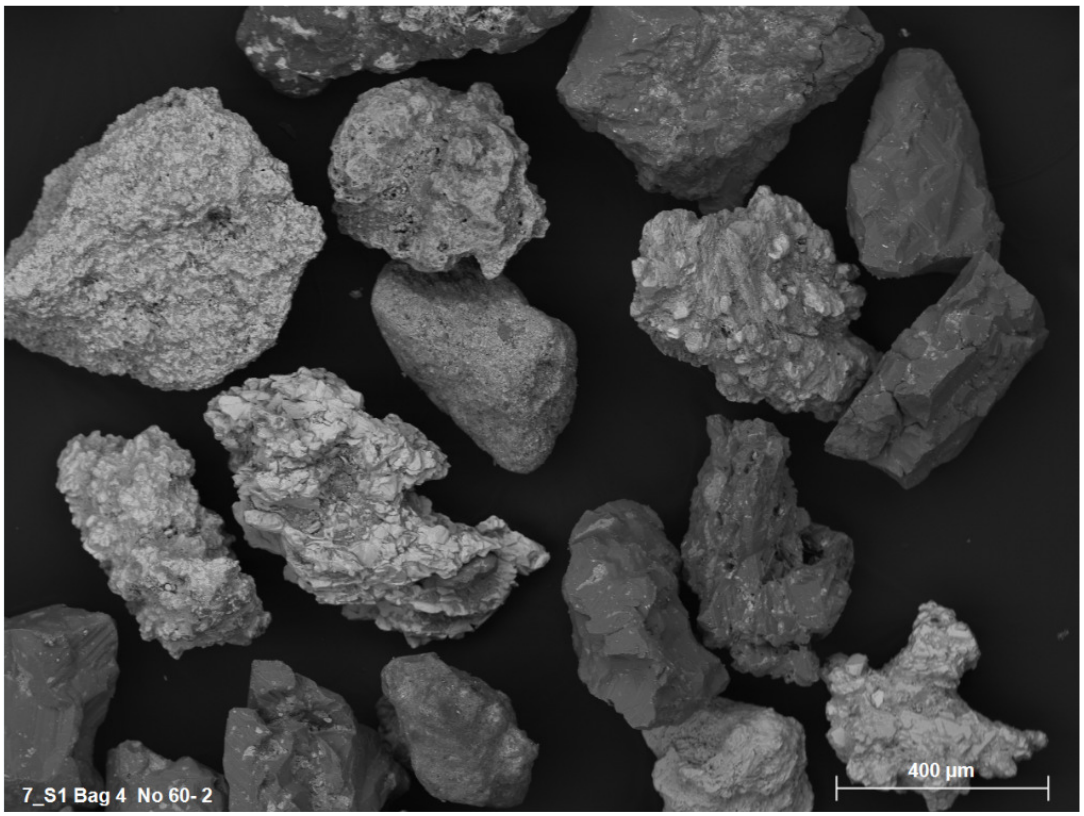

5_Sample 1 Bag 2 Passing No 200- 2
80 µm

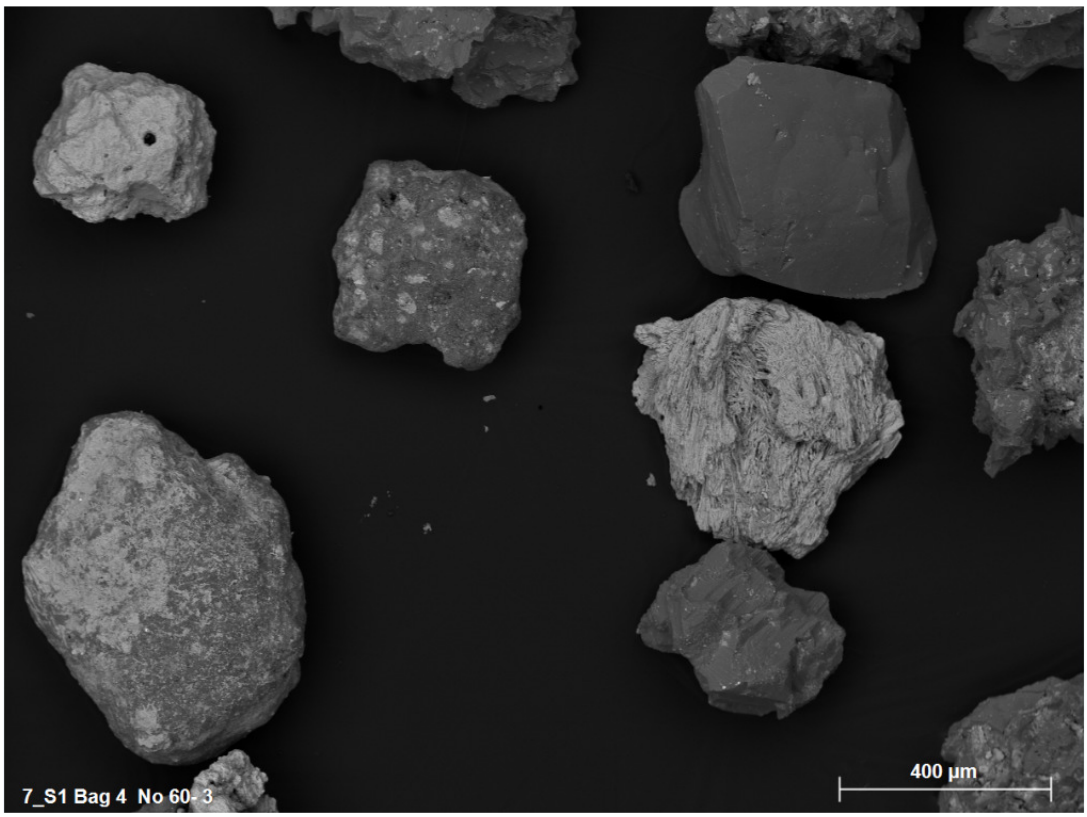

500 µm
6_S1 Bag 4 No 40- 1

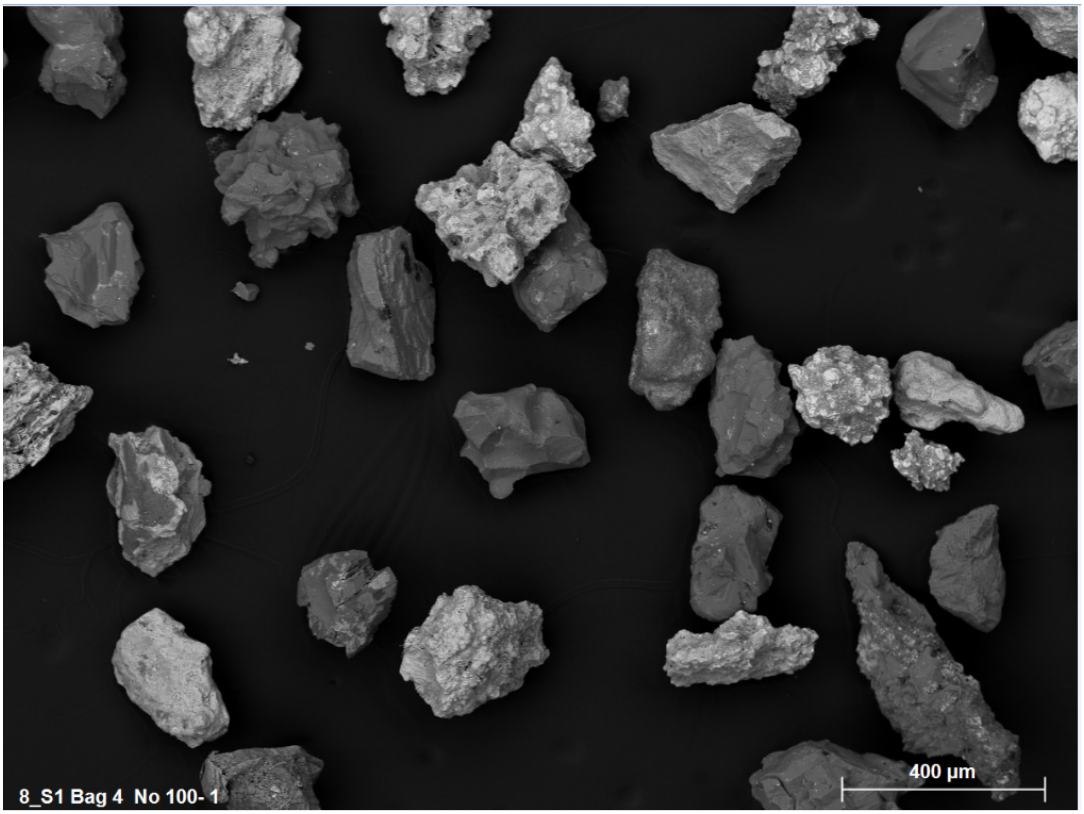

500 µm
6_S1 Bag 4 No 40- 2

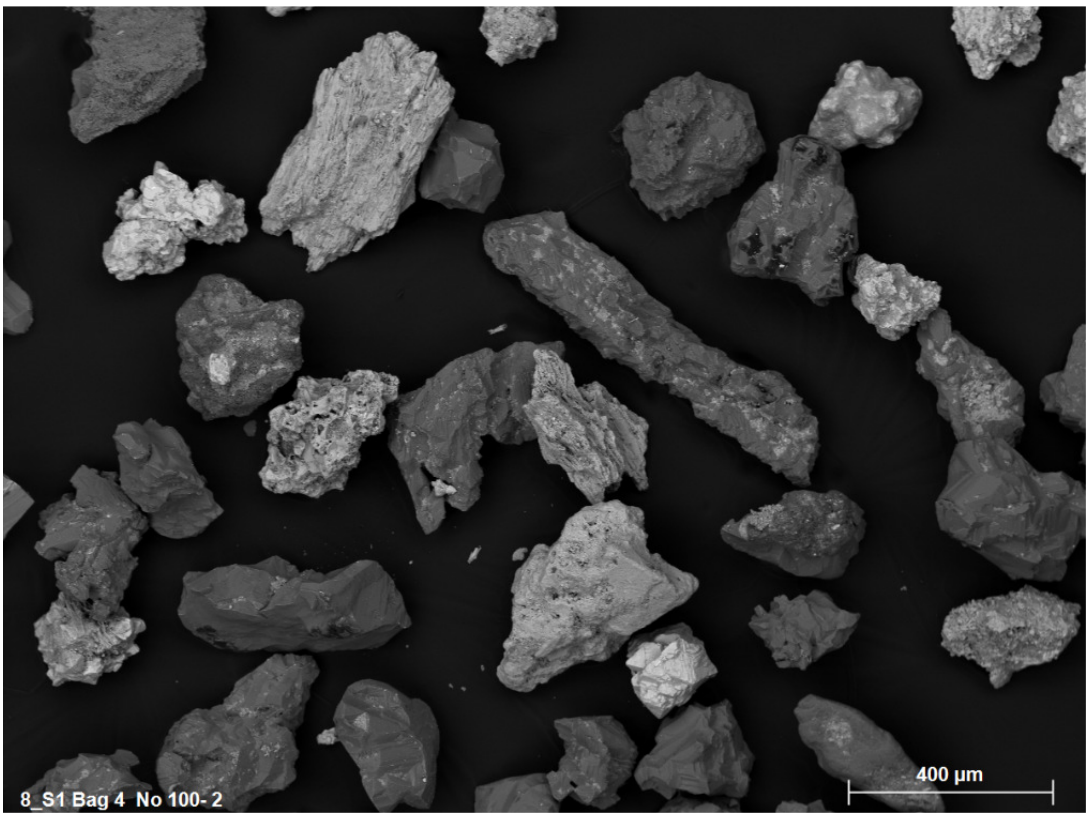

6_S1 Bag 4 No 40- 3
500 µm

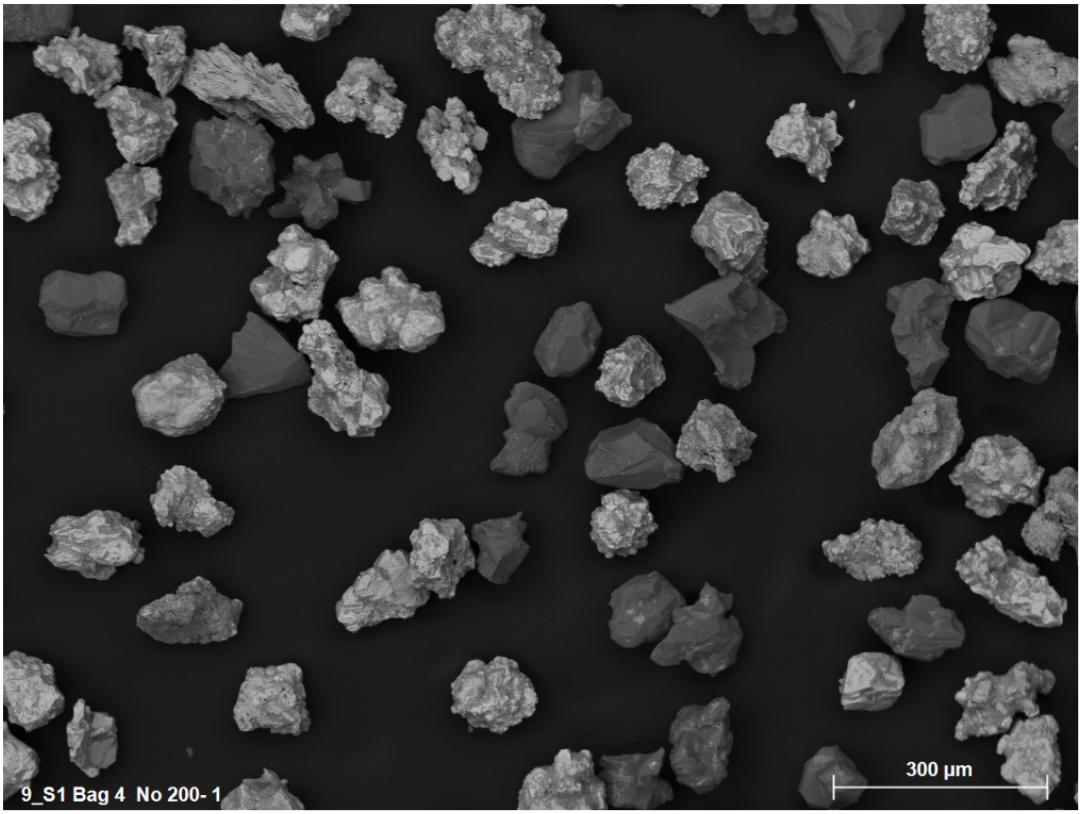

7_S1 Bag 4 No 60- 1
400 µm

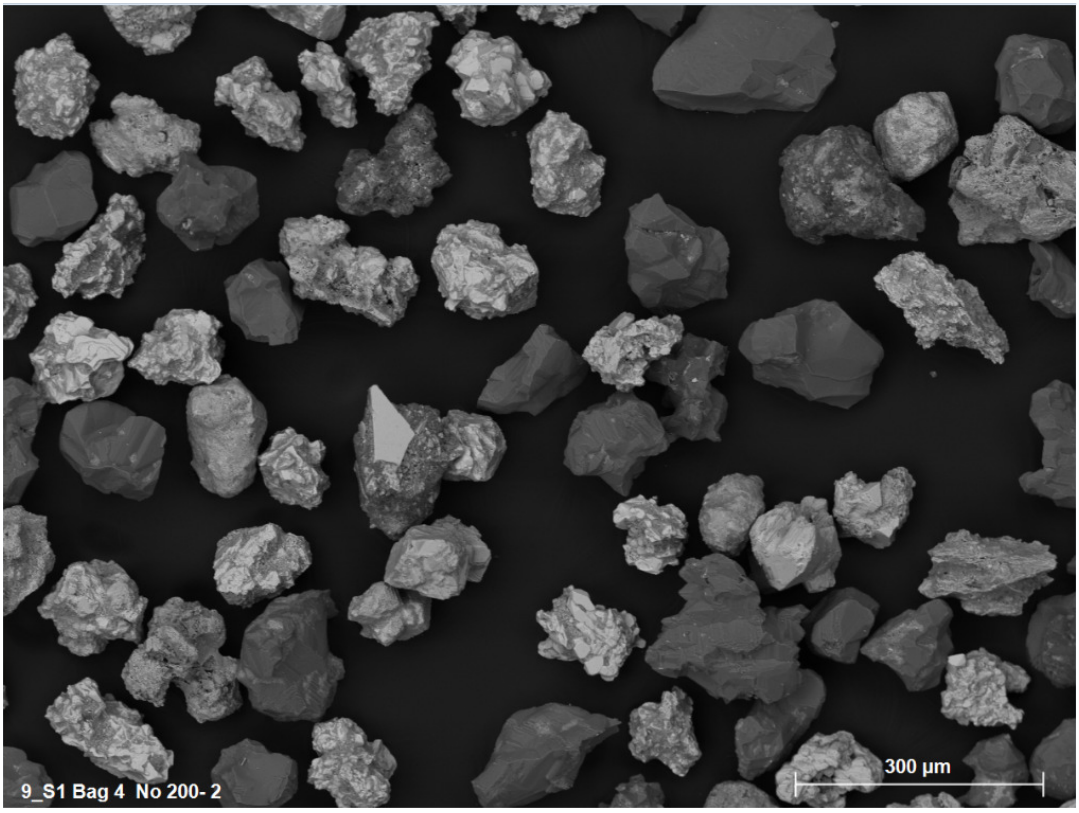

7_S1 Bag 4 No 60- 2
400 µm

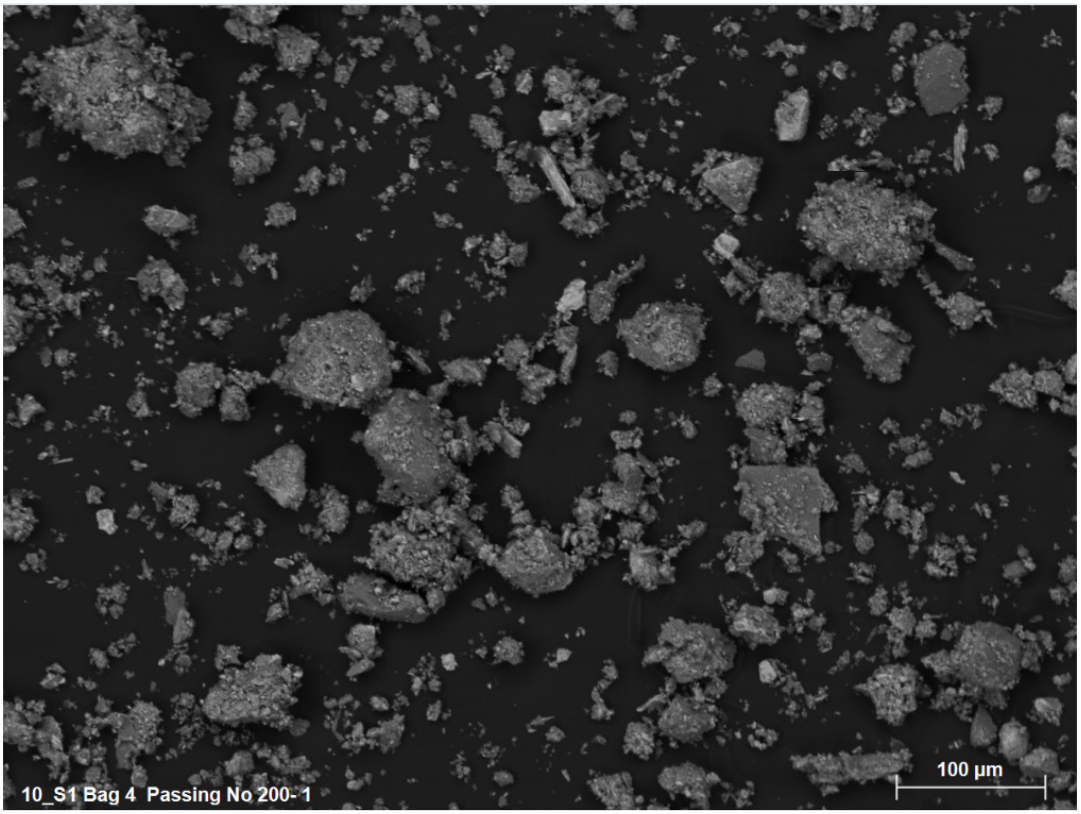

7_S1 Bag 4 No 60- 3
400 µm

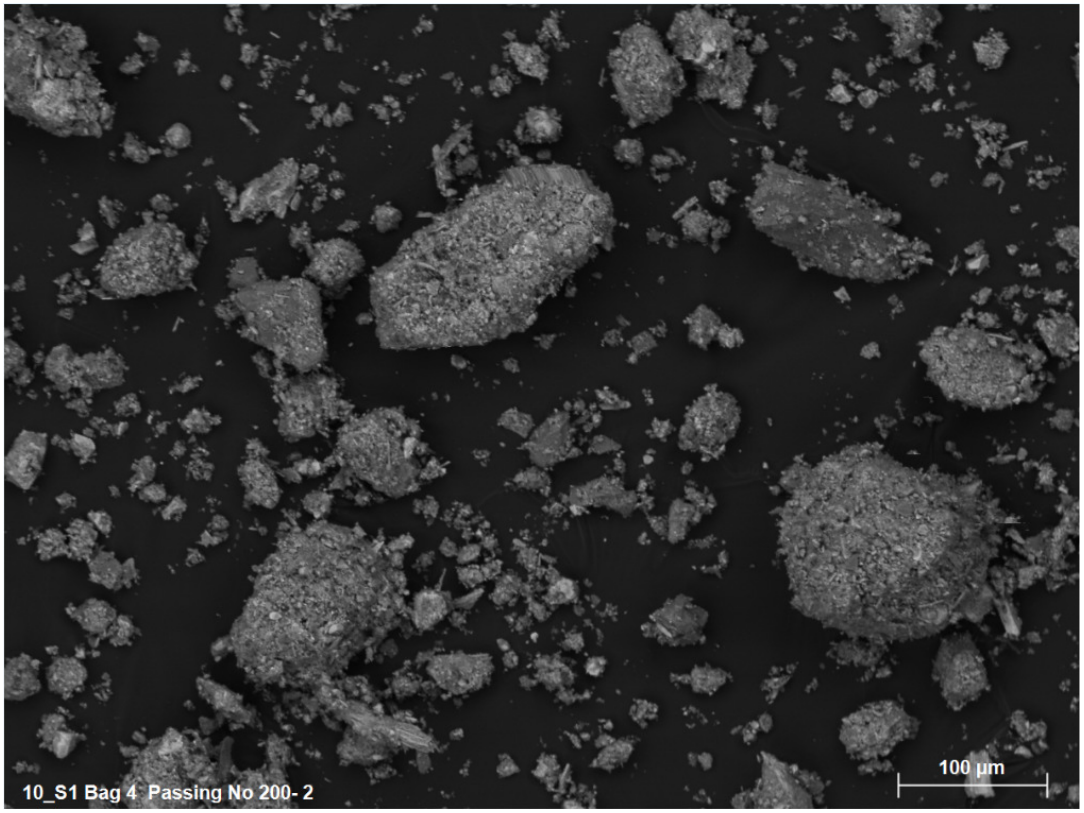

8_S1 Bag 4 No 100- 1
400 µm

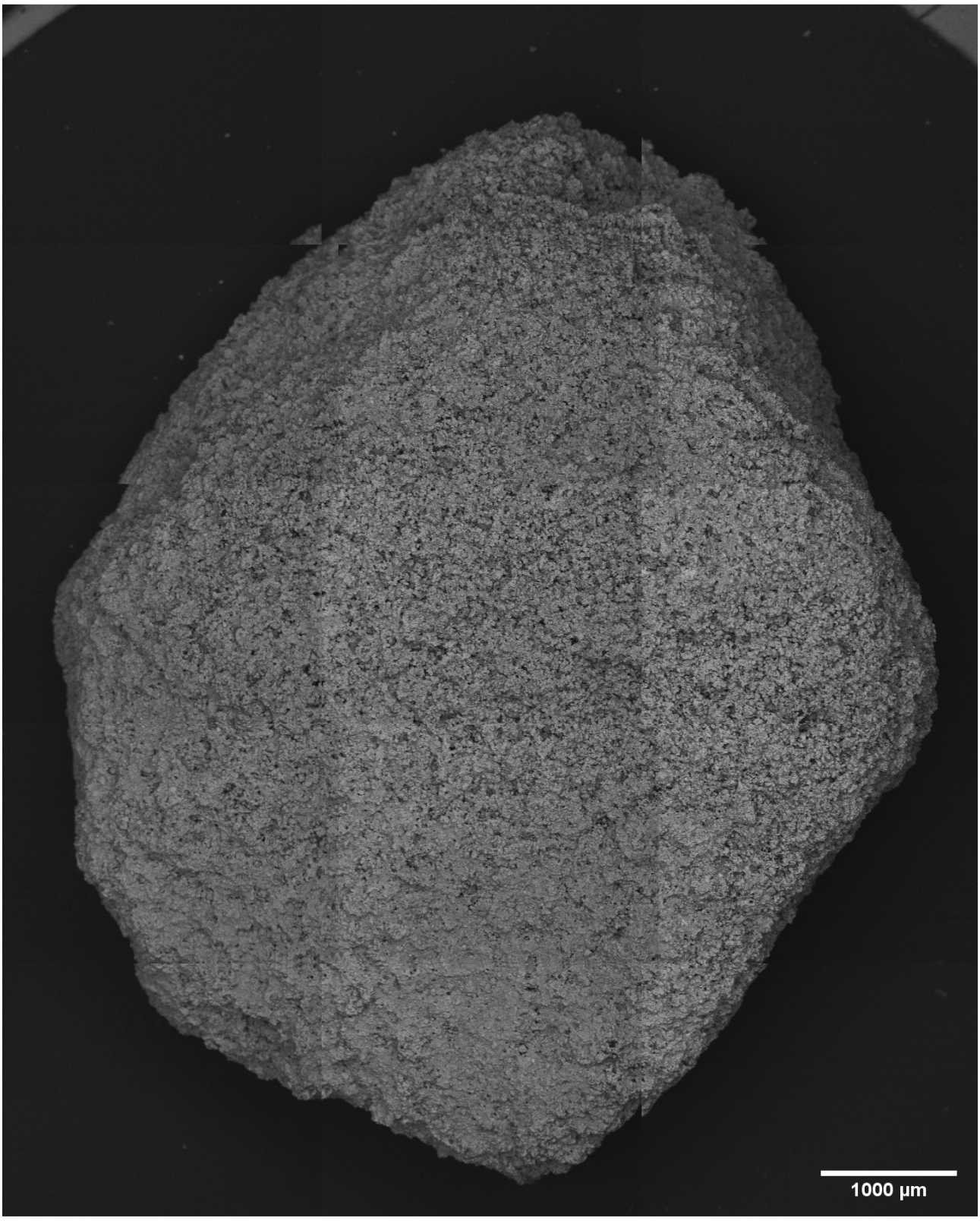

8_S1 Bag 4 No 100- 2
400 µm

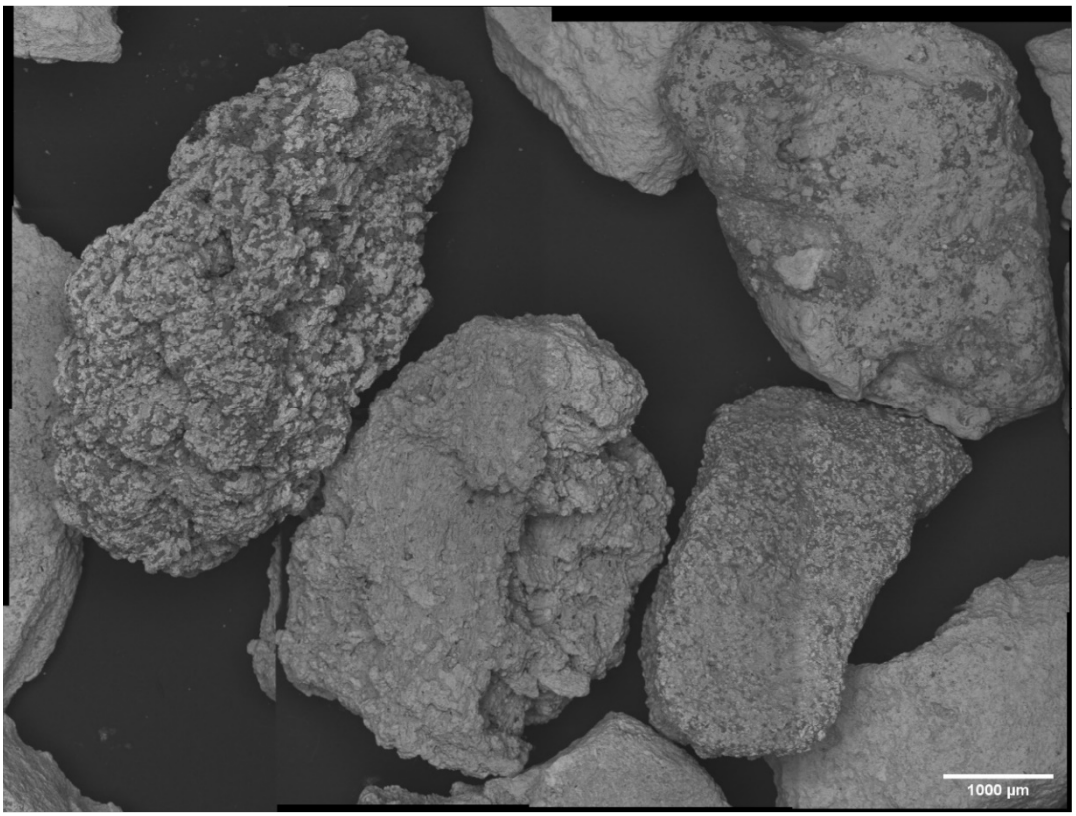

9_S1 Bag 4 No 200- 1
300 µm

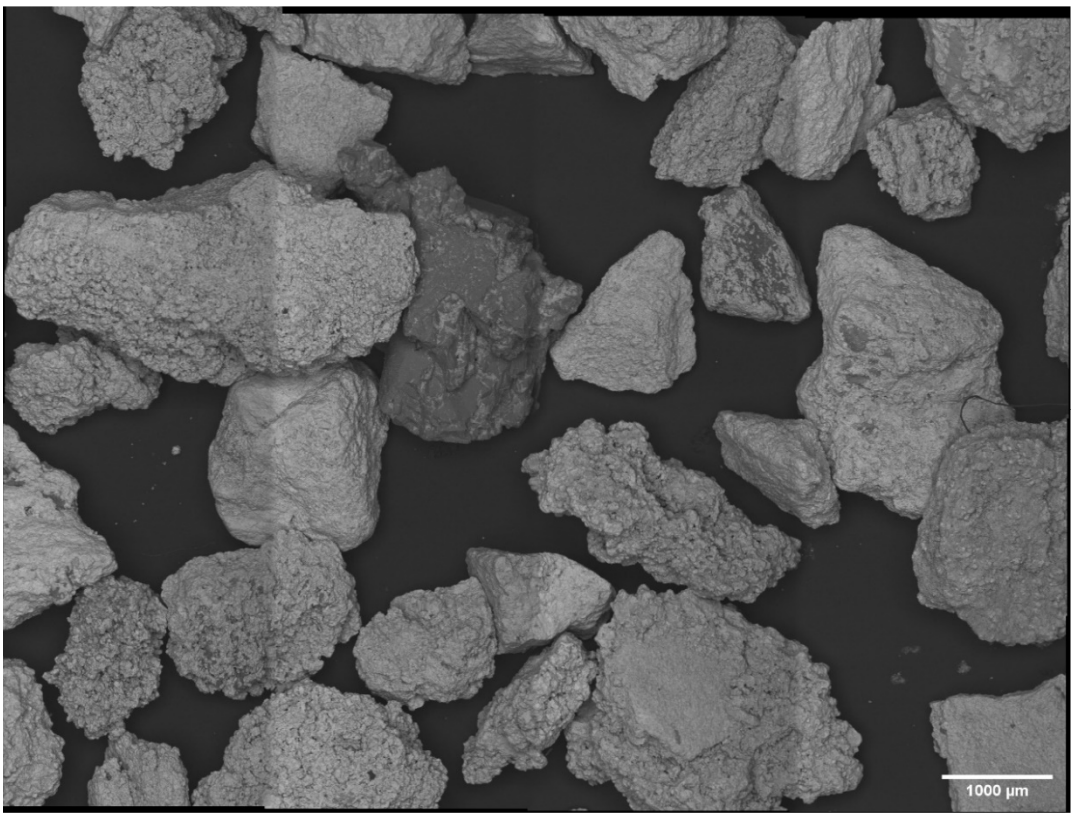

9_S1 Bag 4 No 200- 2
300 µm

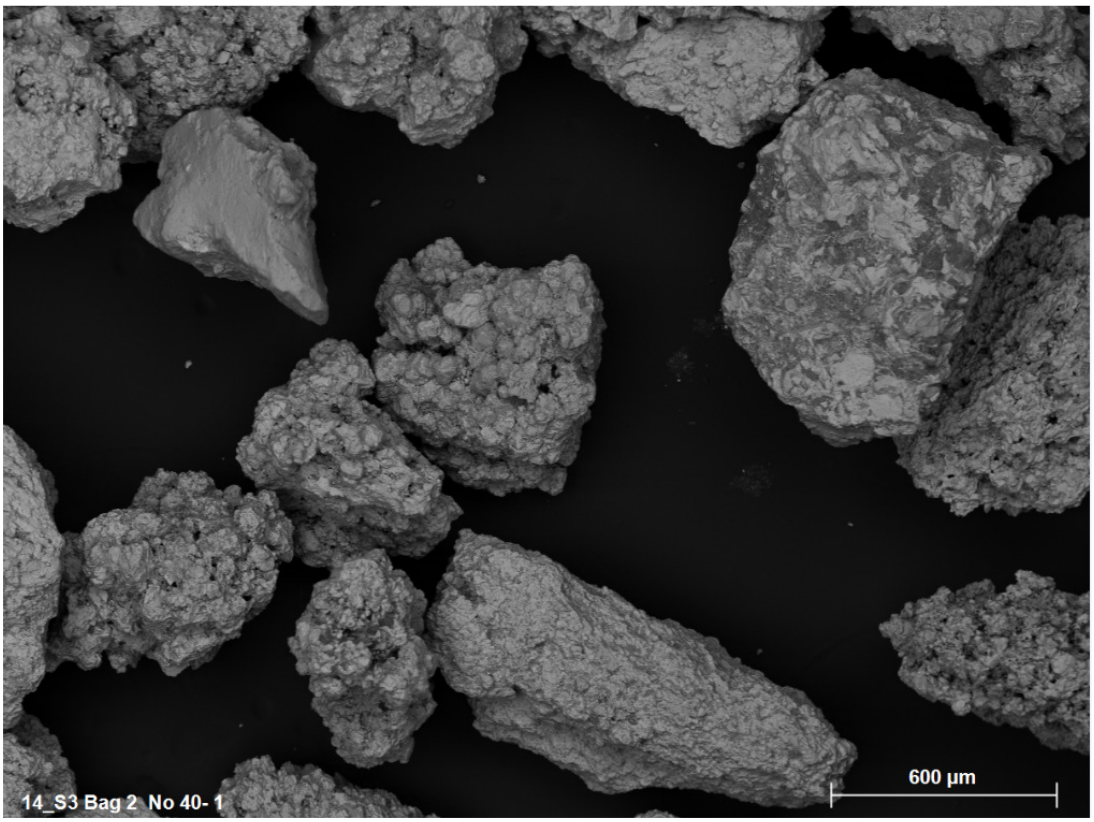

100 µm
10_S1 Bag 4 Passing No 200- 1

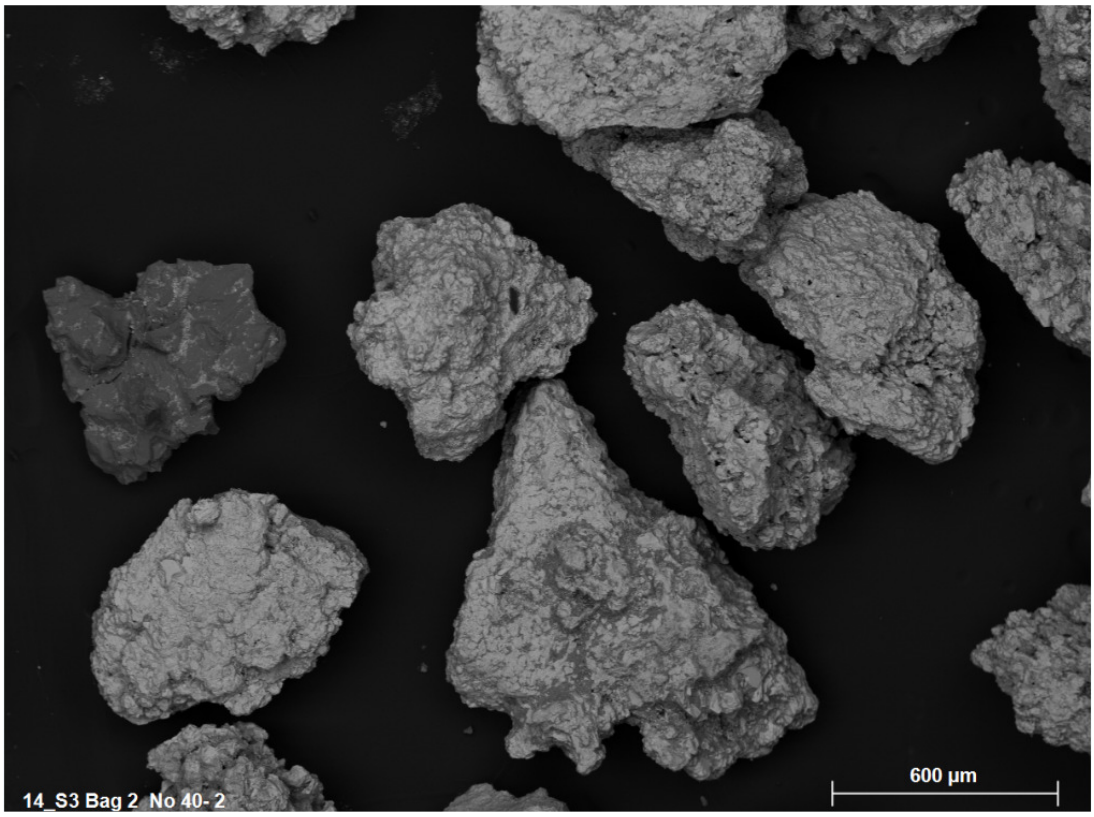

100 µm
10_S1 Bag 4 Passing No 200- 2

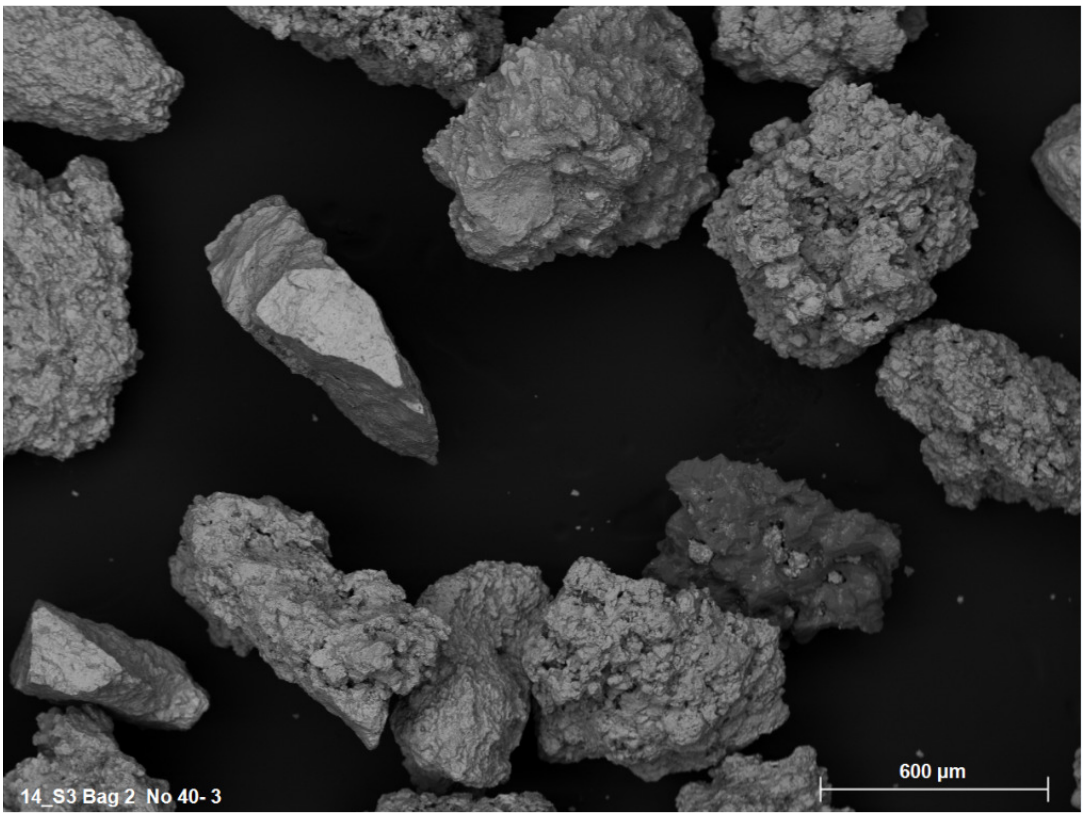

1000 µm

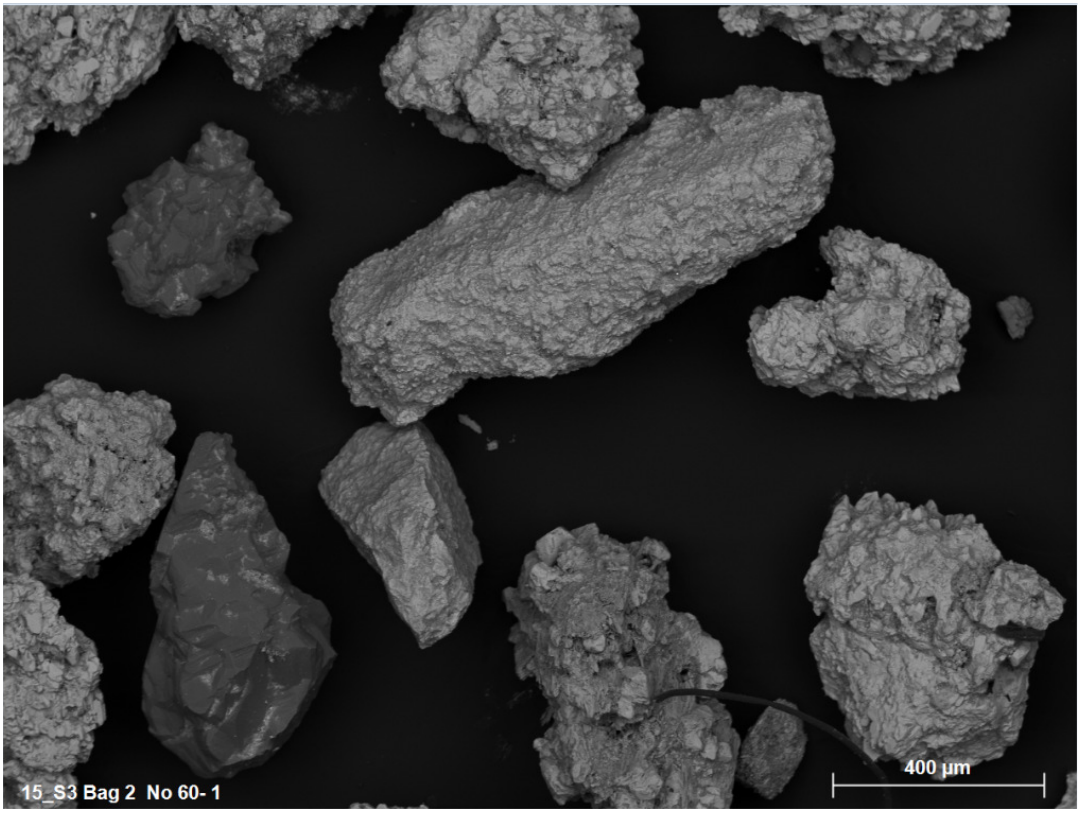

1000 µm

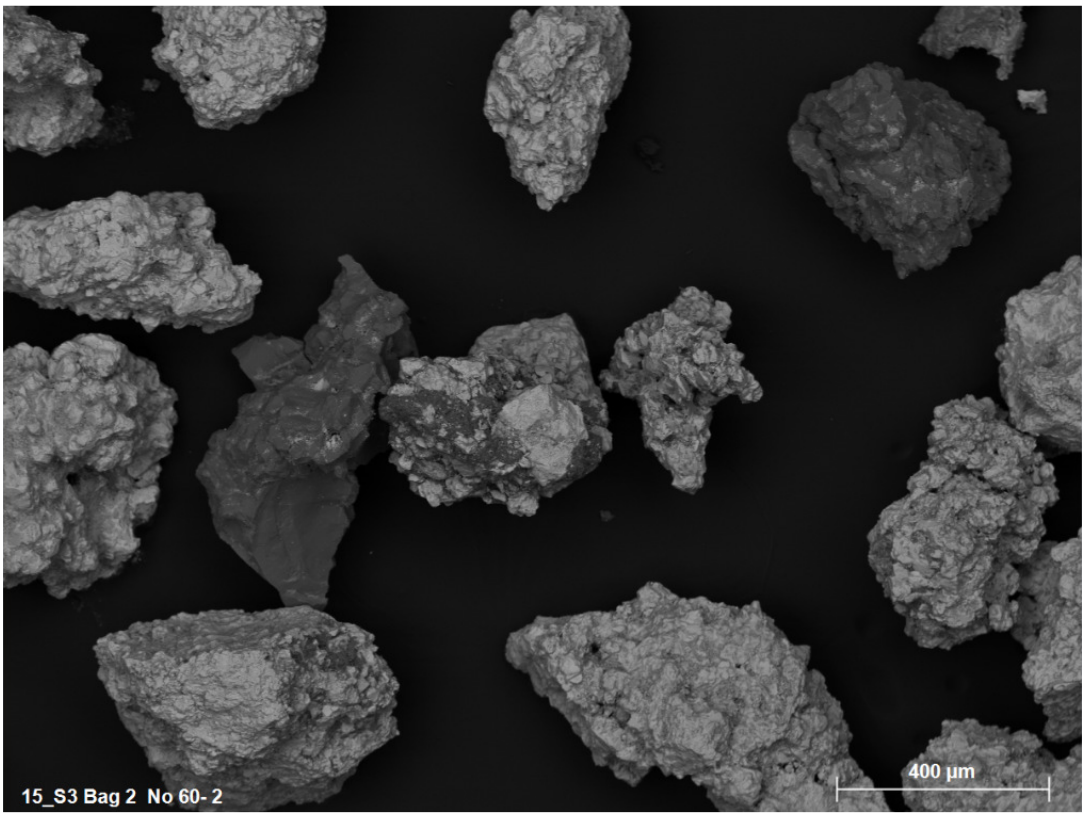

1000 µm

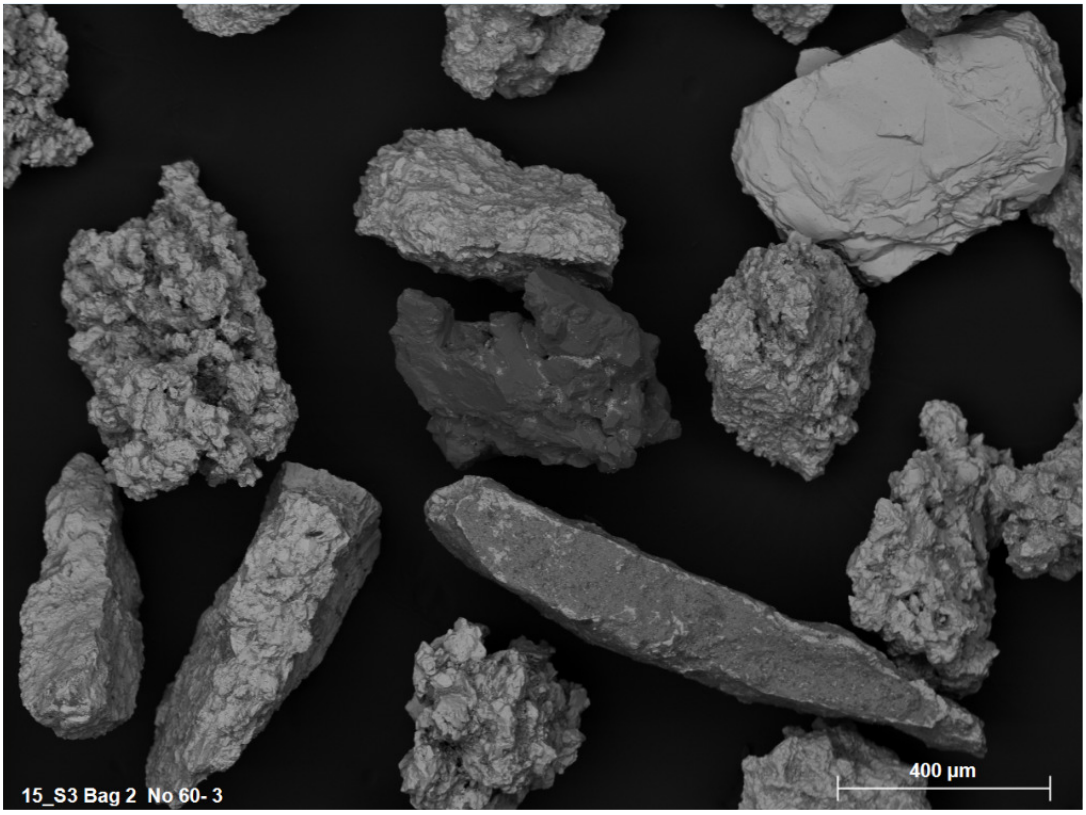

600 µm
14_S3 Bag 2 No 40- 1

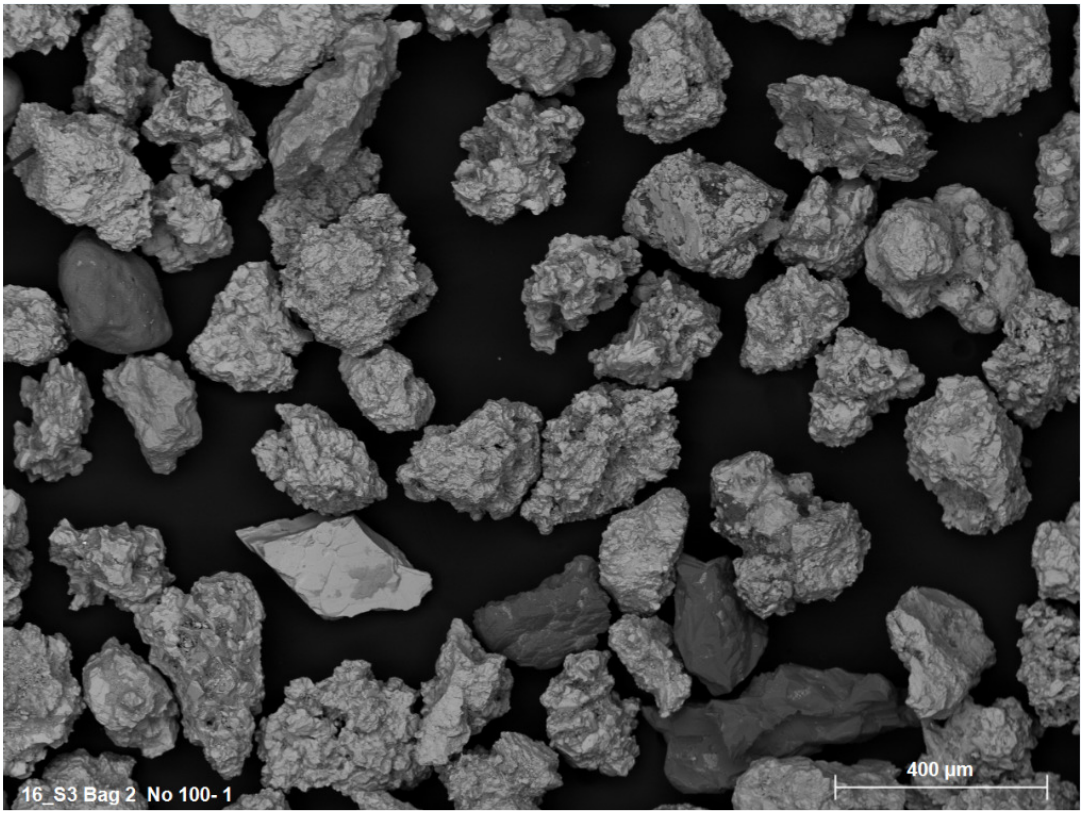

600 µm
14_S3 Bag 2 No 40- 2

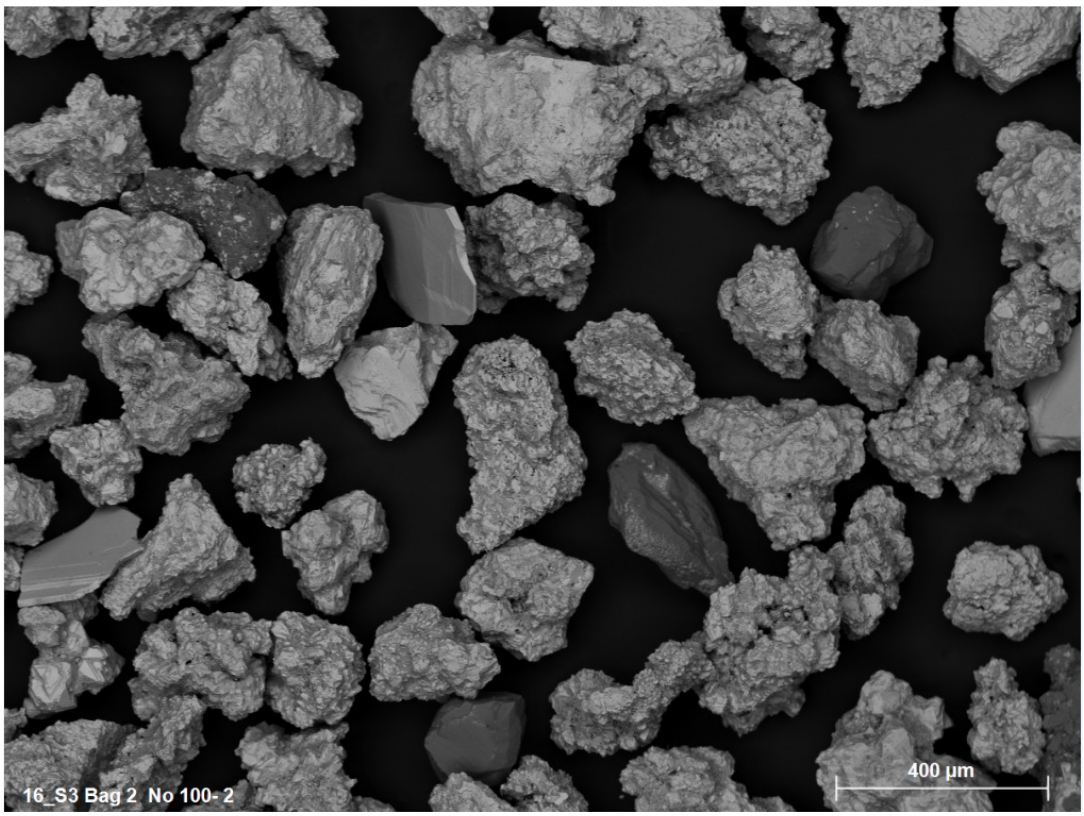

600 µm
14_S3 Bag 2 No 40- 3

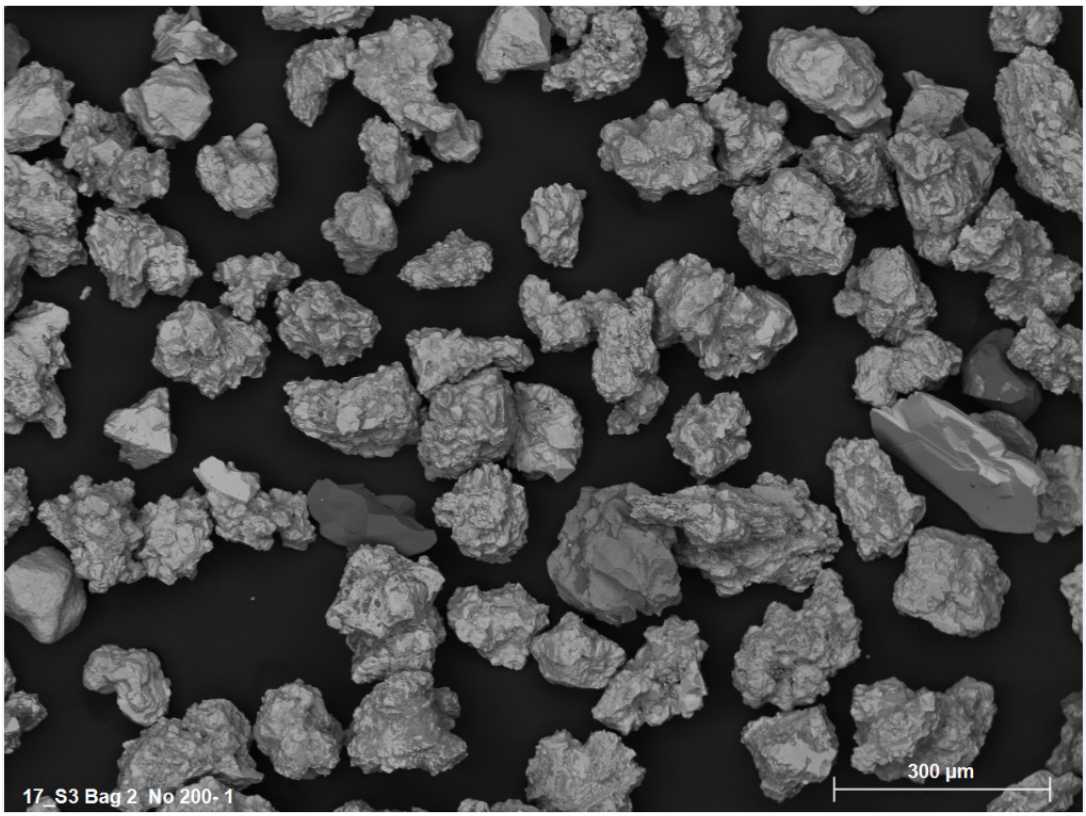

400 µm
15_S3 Bag 2 No 60- 1

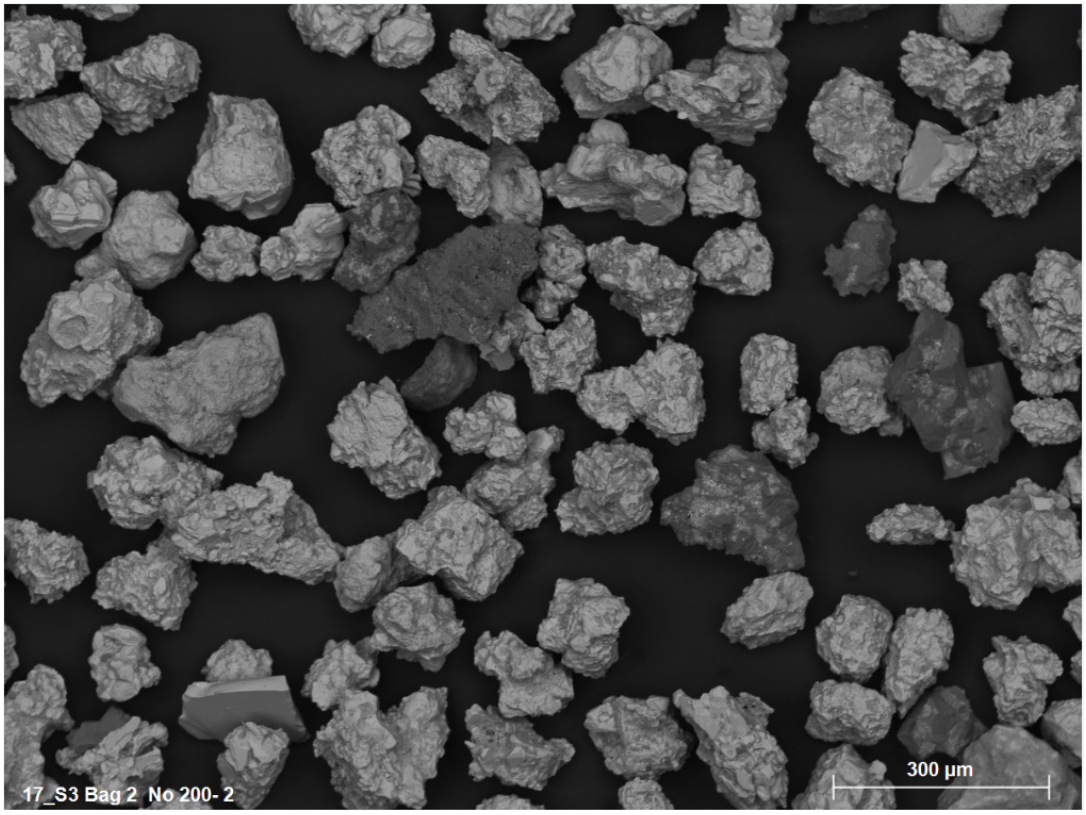

15_S3 Bag 2 No 60- 2
400 µm

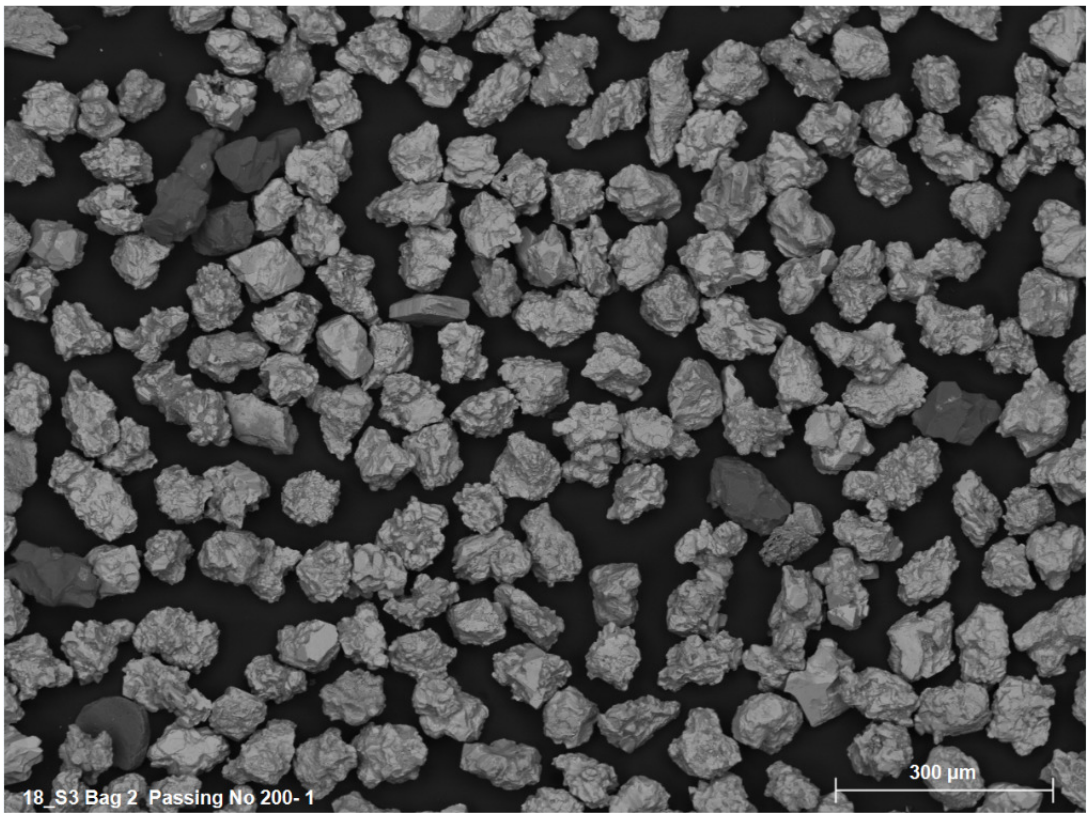

15_S3 Bag 2 No 60- 3
400 µm

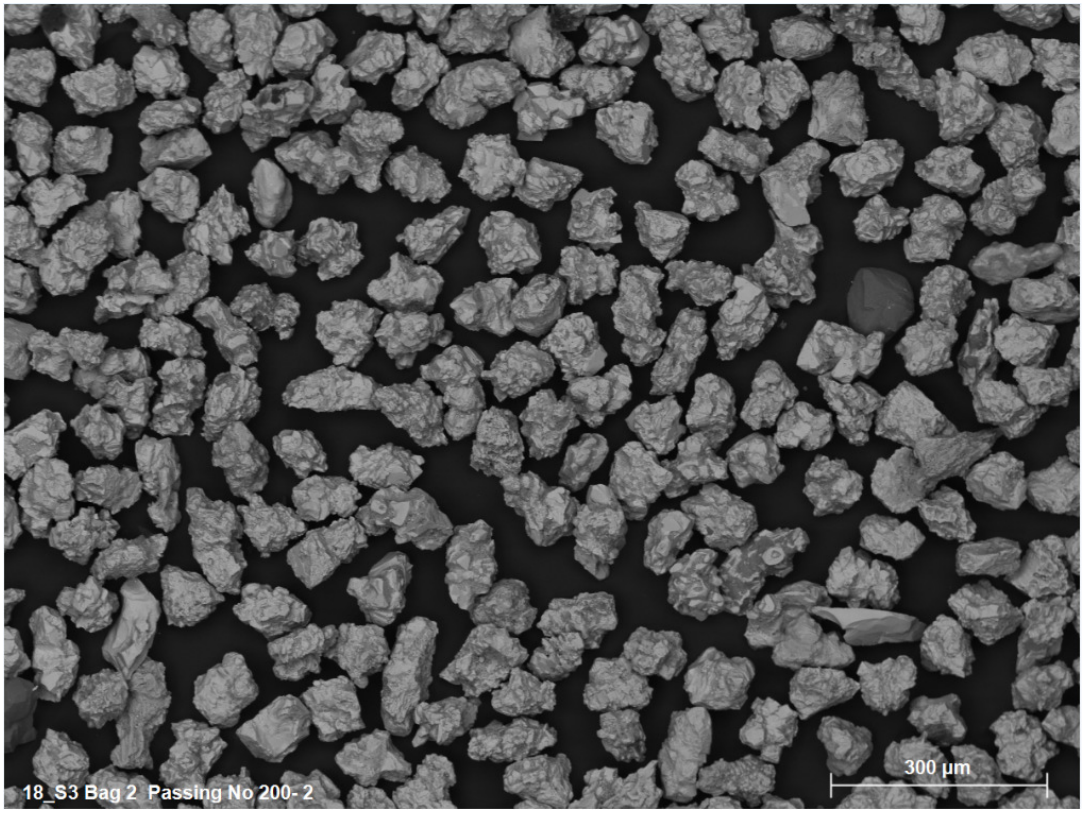

16_S3 Bag 2 No 100- 1
400 µm

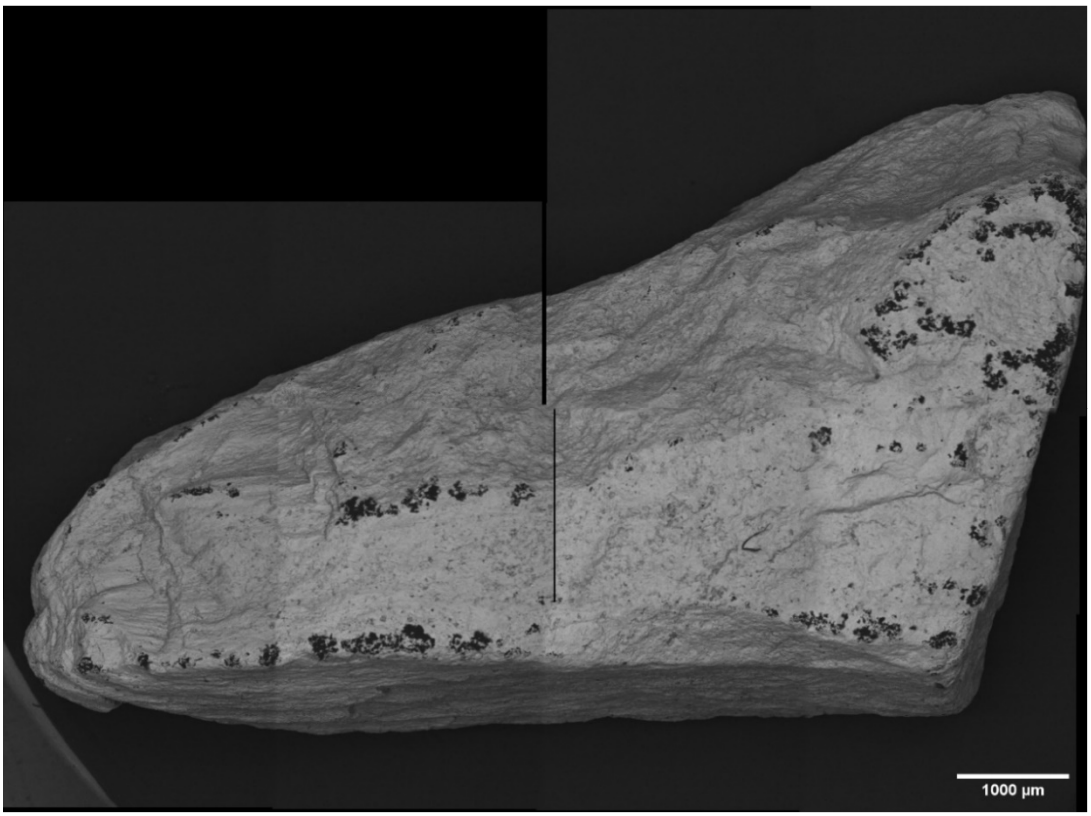

16_S3 Bag 2 No 100- 2
400 µm

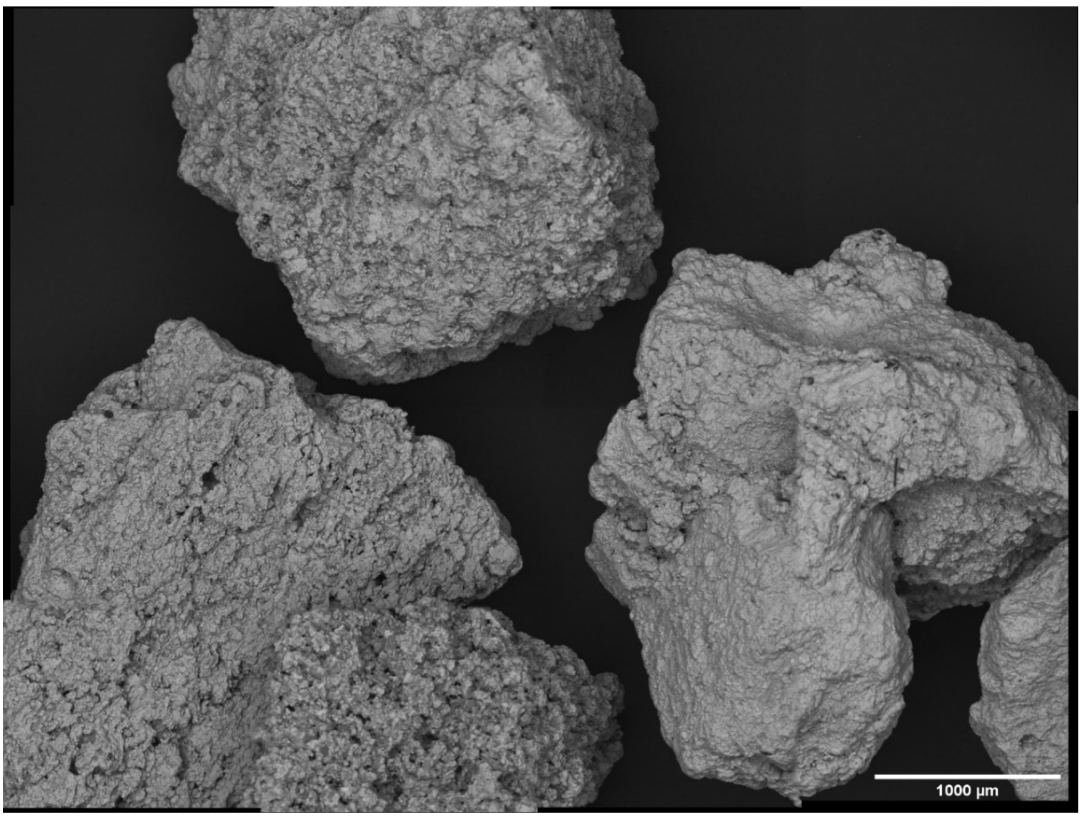

17_S3 Bag 2 No 200- 1
300 µm

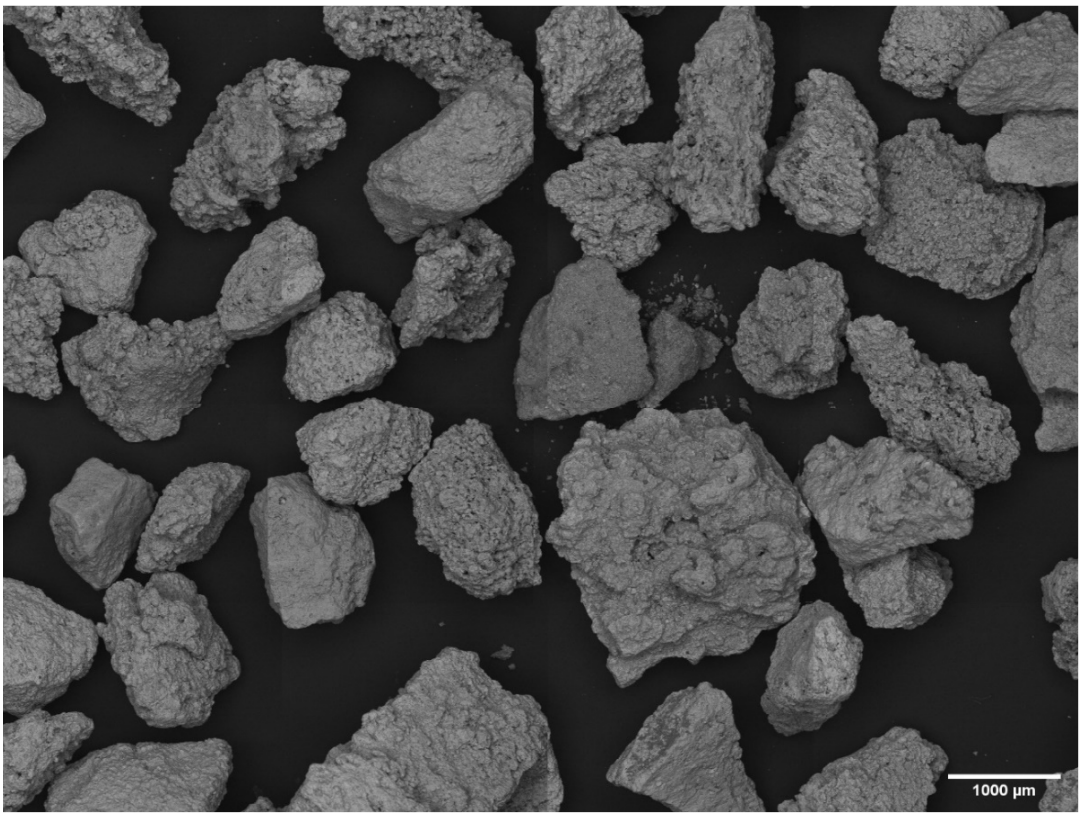

17_S3 Bag 2 No 200- 2
300 µm

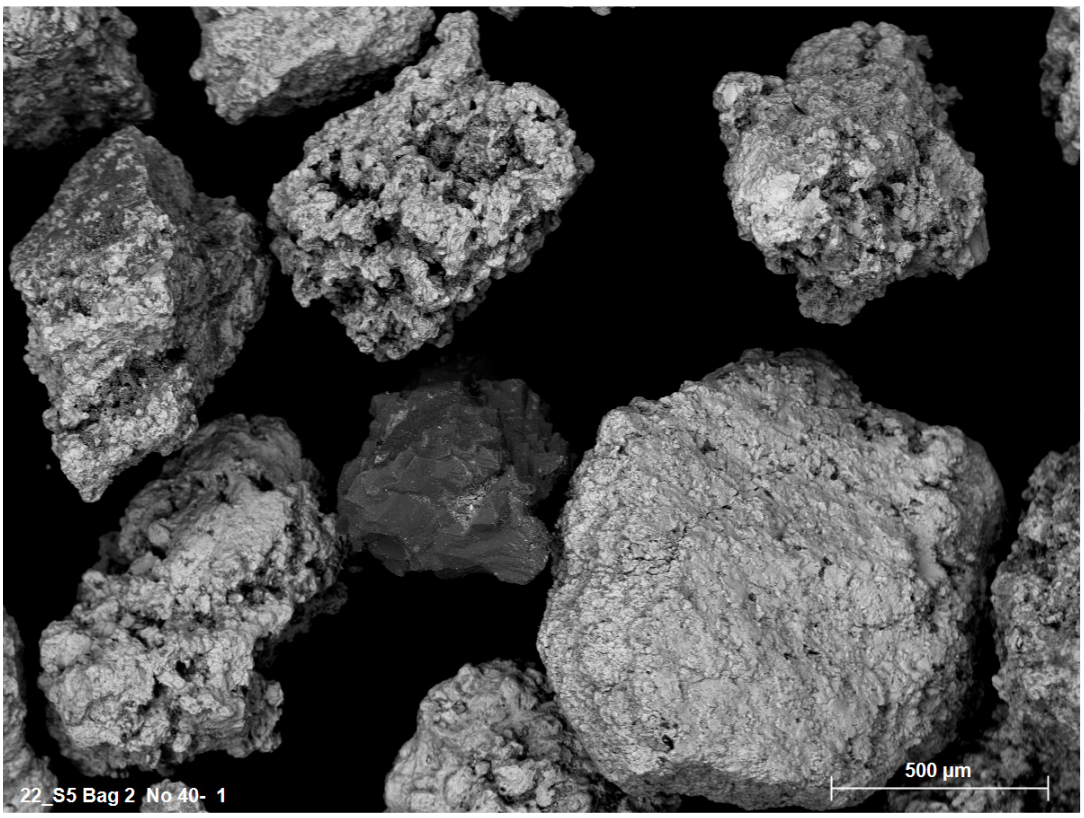

300 µm
18_S3 Bag 2 Passing No 200- 1

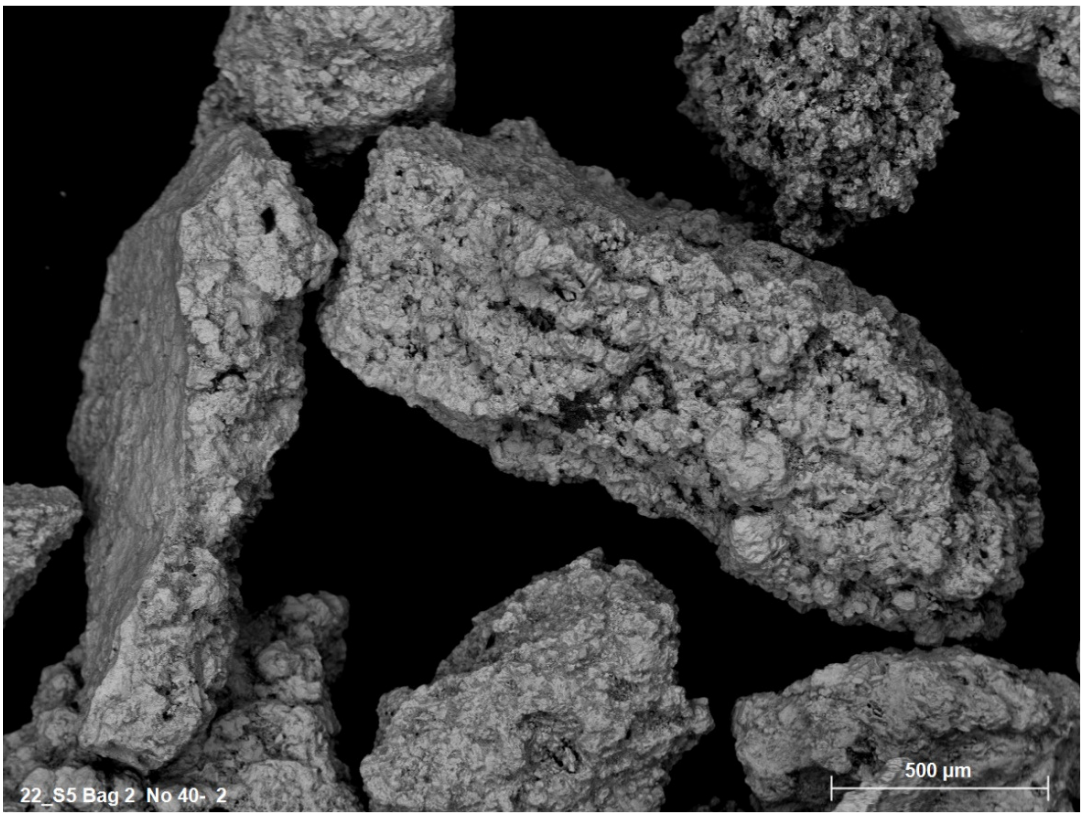

300 µm
18_S3 Bag 2 Passing No 200- 2

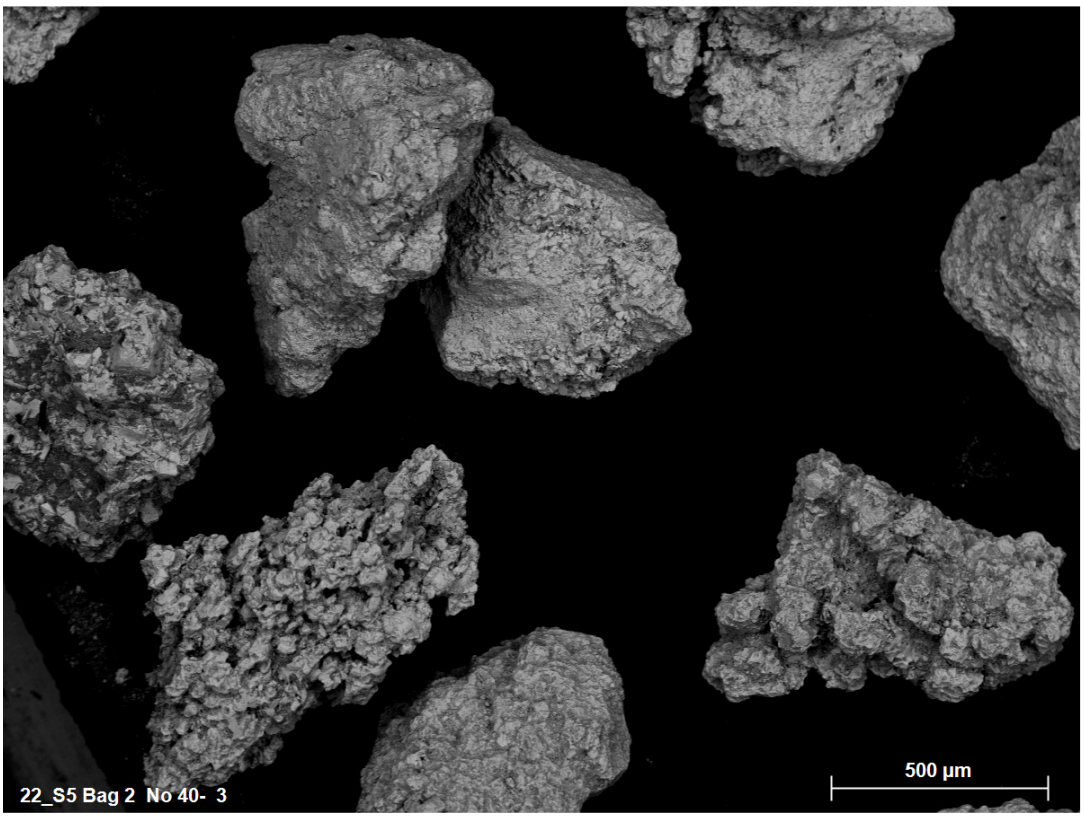

1000 µm

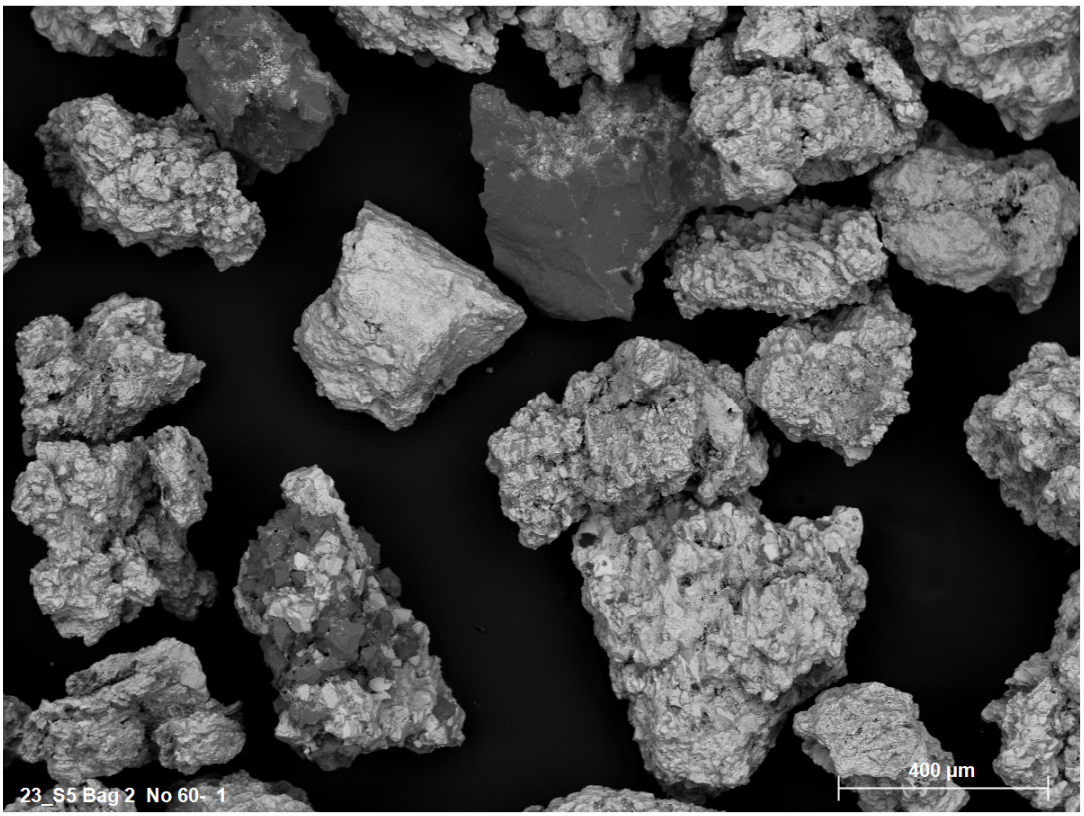

1000 µm

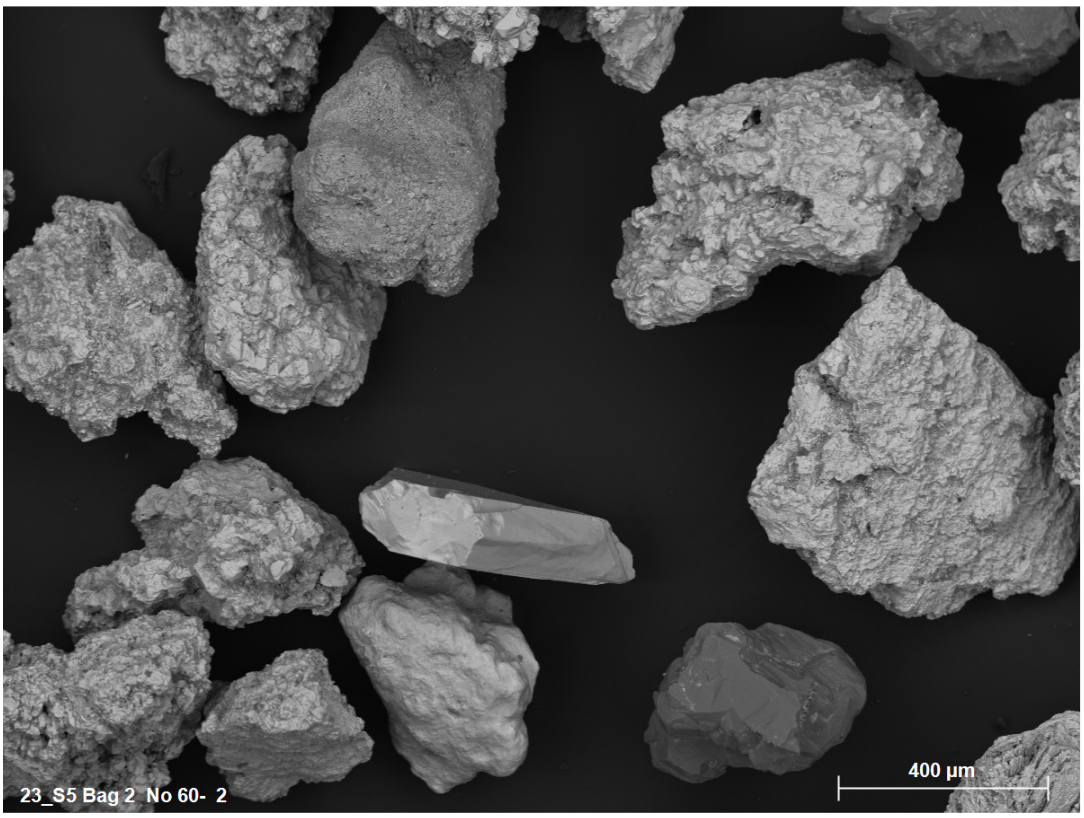

1000 µm

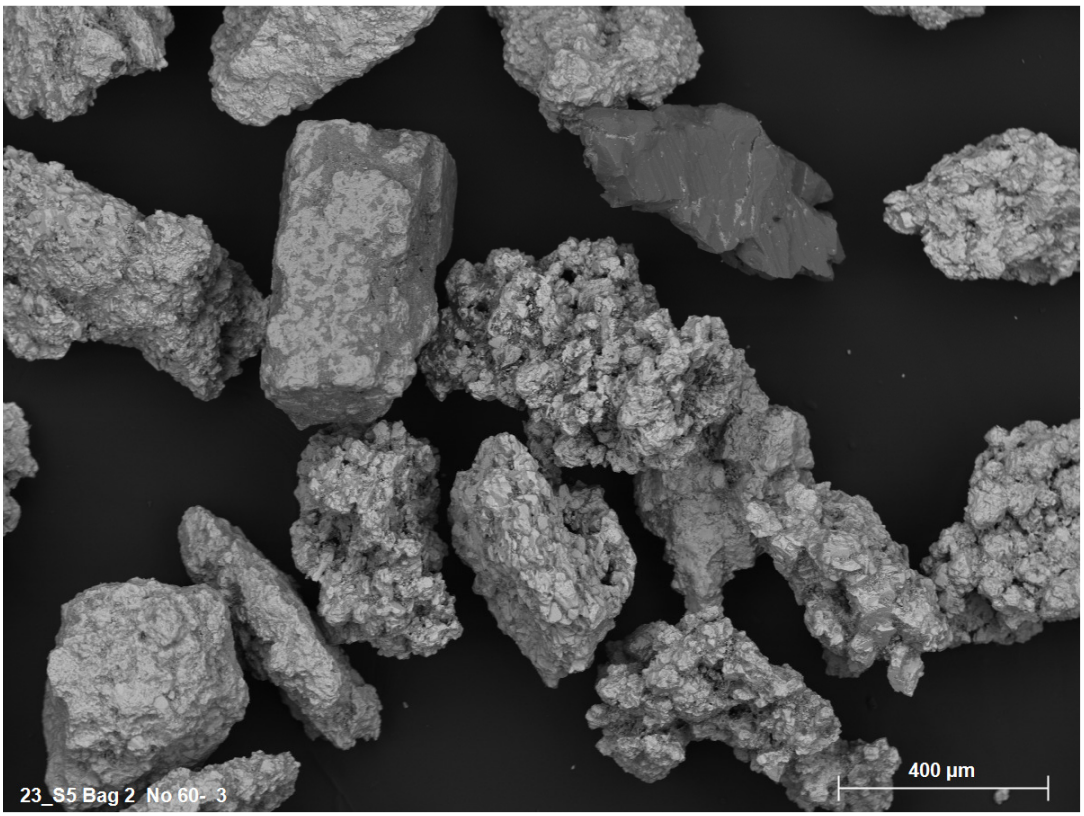

500 µm
22_S5 Bag 2 No 40- 1

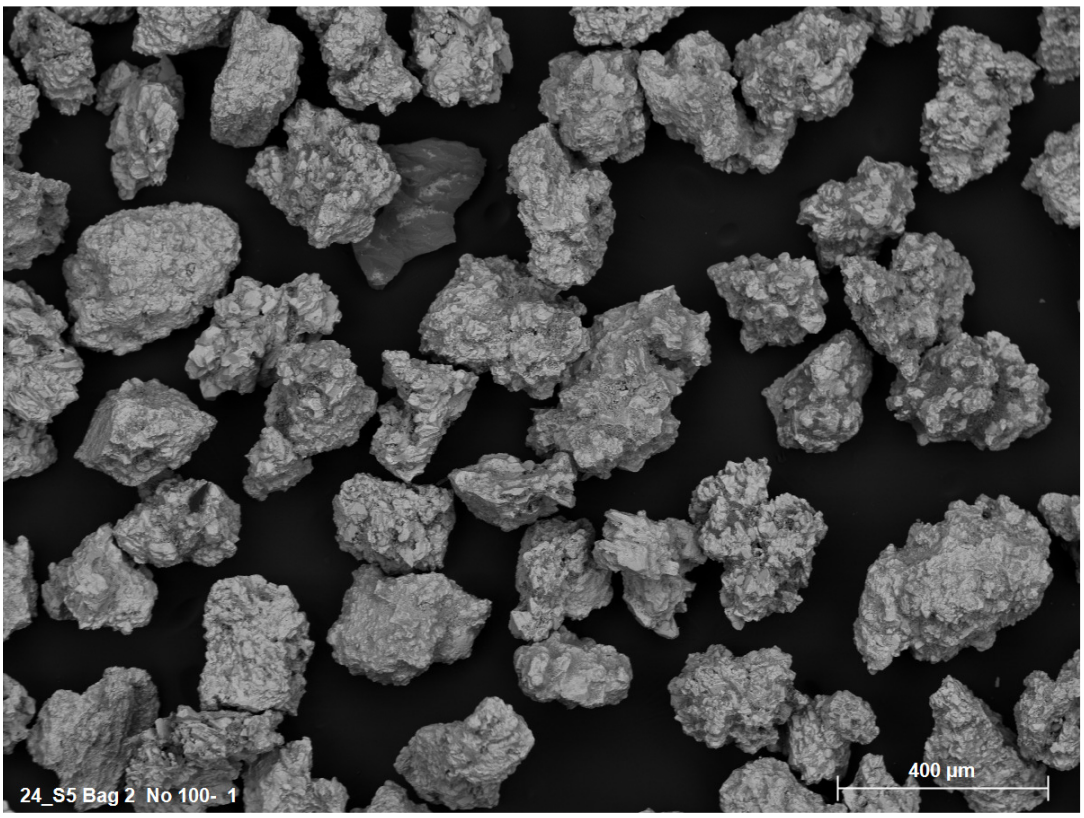

22_S5 Bag 2 No 40- 2
500 µm

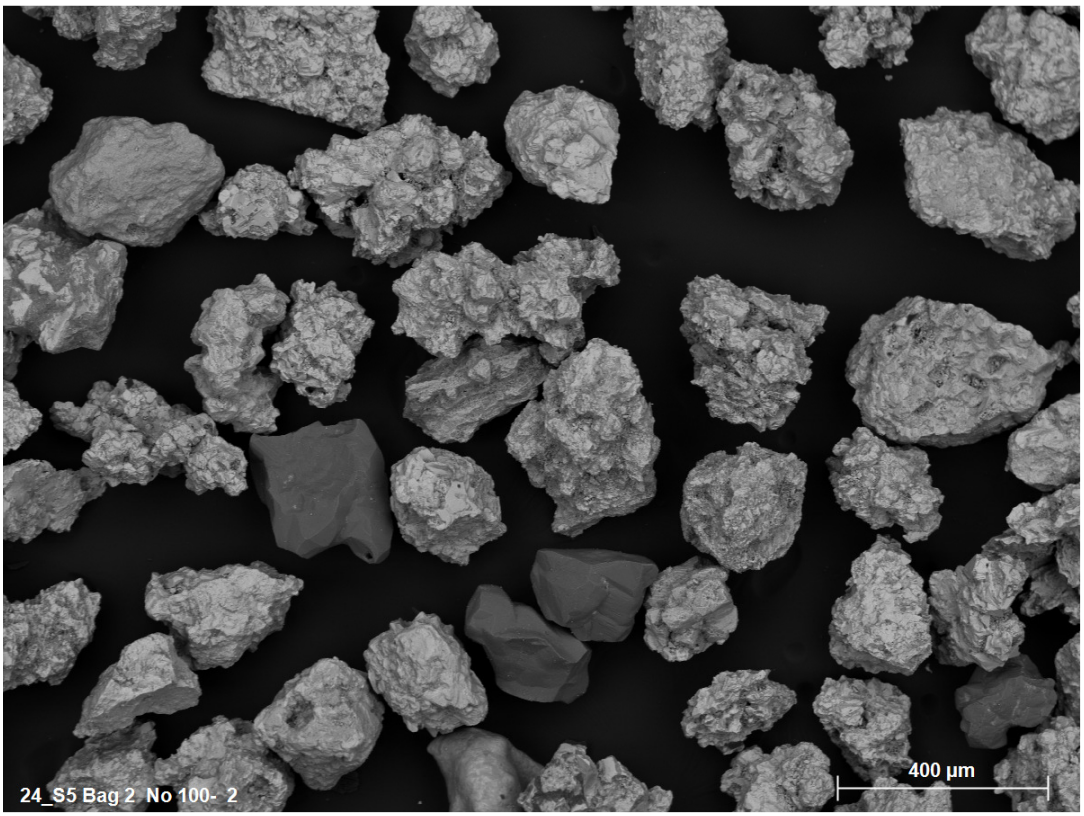

22_S5 Bag 2 No 40- 3
500 µm

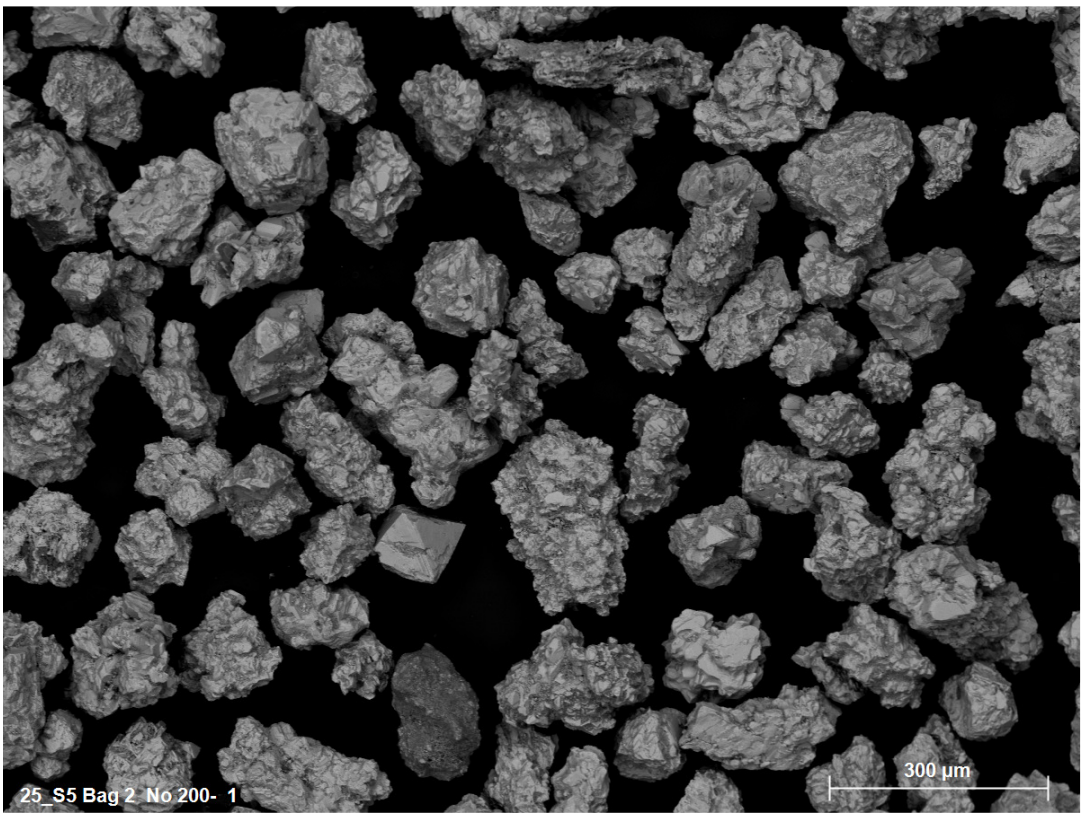

400 µm
23_S5 Bag 2 No 60- 1

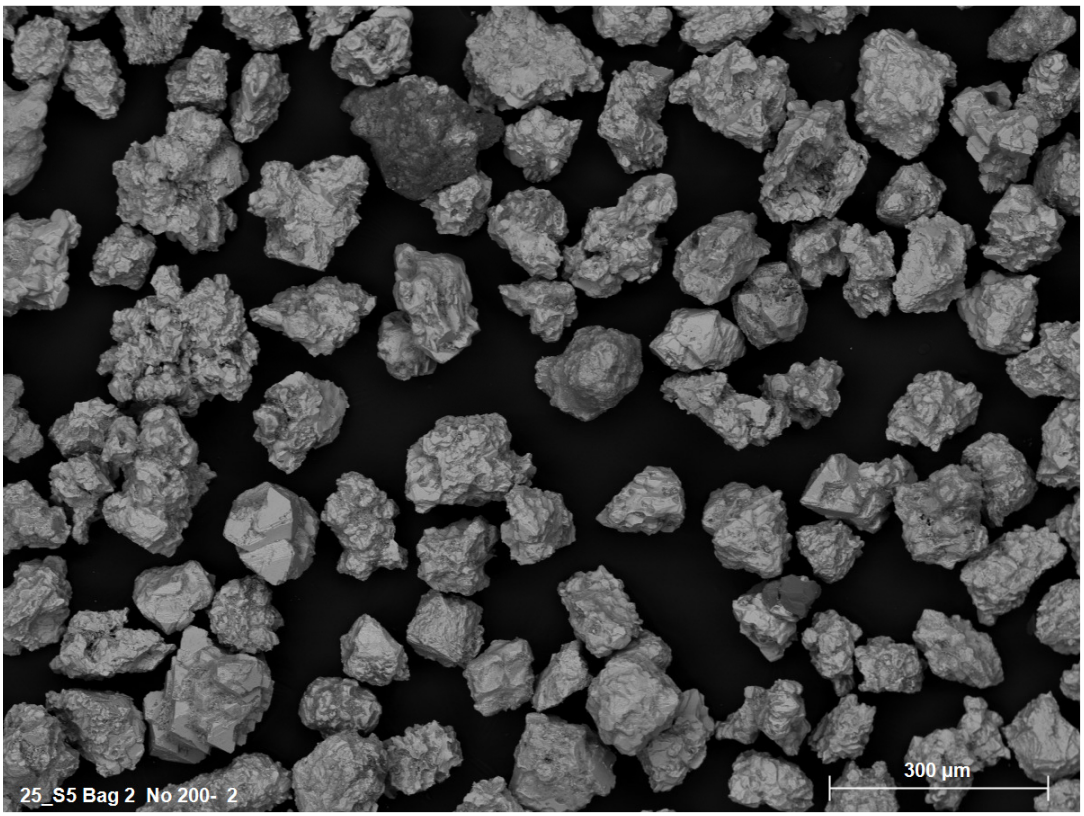

400 µm
23_S5 Bag 2 No 60- 2

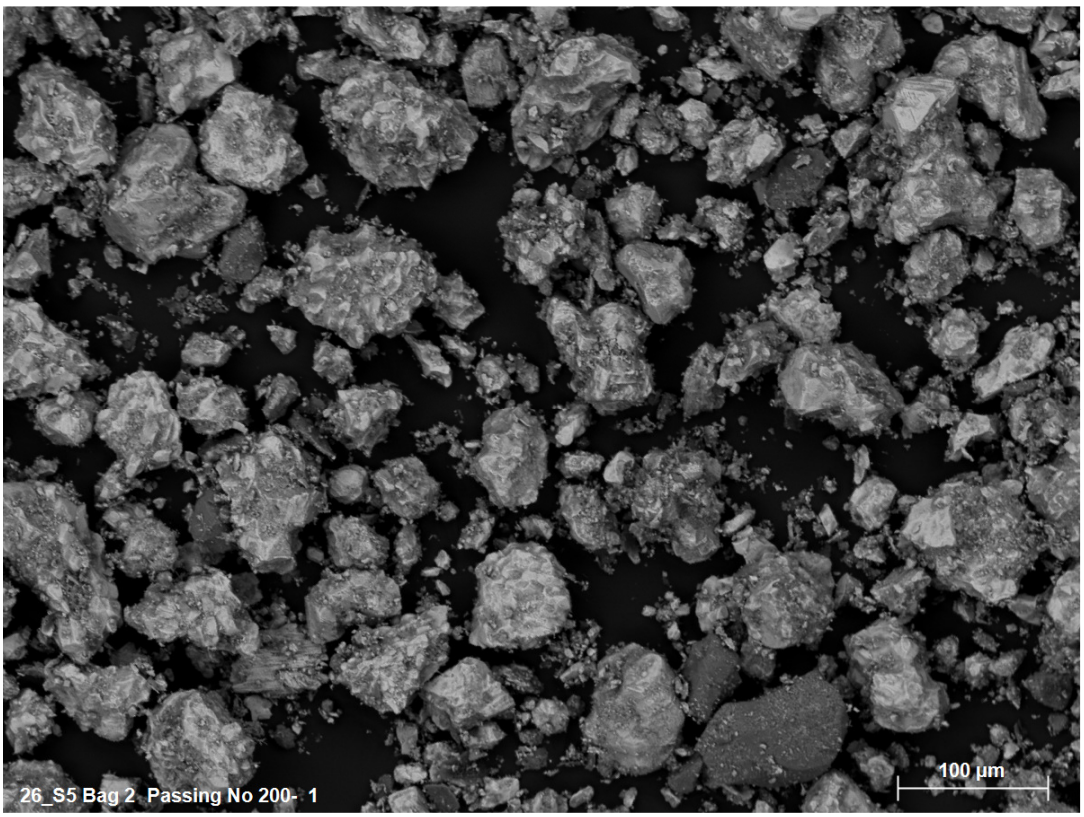

400 µm
23_S5 Bag 2 No 60- 3

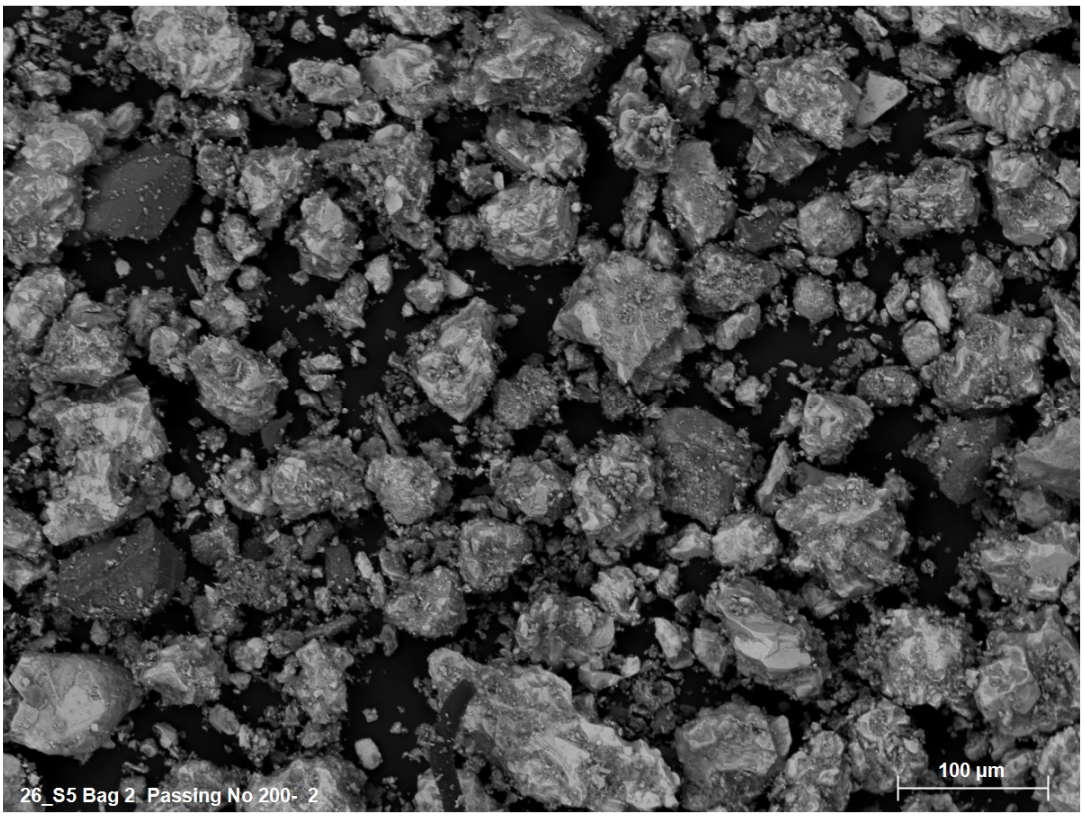

400 µm
24_S5 Bag 2 No 100- 1


24_S5 Bag 2 No 100- 2
400 µm


25_S5 Bag 2 No 200- 1
300 µm


25_S5 Bag 2 No 200- 2
300 µm


26_S5 Bag 2 Passing No 200- 1
100 µm


26_S5 Bag 2 Passing No 200- 2
100 µm

Appendix E

Annex 6 – Scanning Electron Microscopy Testing Report

December 2019

University of Queensland Scanning Electron Microscope (SEM) Testing Report

THE UNIVERSITY OF QUEENSLAND
AUSTRALIA

Professor Gordon Southam
School of Earth & Environmental Sciences
The University of Queensland
St.Lucia, QLD 4072
Tel: +617 3365 8505
Fax: +617 3365 6899
Email: g.southam@uq.edu.au

CRICOS PROVIDER NUMBER 00025B

November 2019

Attention: Klohn Crippen Berger

Re: Laboratory Testing to Evaluate Cementation (Bonding) in Tailings Samples

Introduction

Additional laboratory testing was carried out by the University of Queensland (Australia) in order to better understand the physical nature of the tailings samples described below, and their characteristics of cementation (bonding), in order to evaluate whether such characteristics is a function of particle size, or can be attributed to the process of sample preparation and strength testing.

Samples Tested

Samples were received from the Klohn Crippen and Berger (KCB) laboratory in Vancouver, Canada. The samples were comprised of:

1. Slimes
2. Untested Average Gradation (a mixture of Fine and Coarse Tailings after sample preparation [drying and sieving], but before strength testing)
3. Tested Average Gradation (a similar mixture of Fine and Coarse Tailings after sample preparation [drying and sieving] and strength testing)

The photograph of the Slimes sample (Figure 1) shows an agglomerated lump that could physically be broken to a fine powder consisting of particles typically ≤ 10 µm in size. In contrast, the untested and tested Average Gradations were a mixture of mm- to µm-sized particles.



Figure 1. Photograph of Slimes sample

Testing Methodology – Scanning Electron Microscopy (SEM)

Sub-samples of each of the three supplied samples were dried in a 40°C oven overnight (the oven temperature was limited to avoid excessive alteration of the samples), vacuum embedded in plastic, and polished to sub-μm-size for Back Scattered Electron (BSE) SEM. The dried sub-samples proved difficult to embed in plastic, and were first examined using Secondary Electron SEM (SE-SEM).

For the BSE-SEM examination, each sub-sample was re-embedded in plastic, re-polished, degassed at 50°C overnight and coated with 10 nm iridium using a Quorum Q150T sputter coater prior to examination using a JEOL7100 SEM in BSE-mode with an accelerating voltage of 15 kV.

Results

SE-SEM imaging of the Slimes sub-sample highlighted the consolidated nature (Fig. 1 and Fig. 2a) of this fine-grained, ≤10-μm-sized material (Fig. 2b). At high resolution (Fig. 2c and d), sub-μm-scale thin films of secondary iron oxides were observed coating the μm- to 10-μm-sized particles.

BSE-SEM imaging showed the Slimes to be a generally homogenous (Fig. 3), comprising predominantly iron oxides, with minor clay and quartz. X-Ray diffraction (XRD) analysis of the Slimes revealed that the Slimes comprised 40 to 50% hematite, about 30% goethite, 5 to 10% kaolinite, about 5% quartz, and other minor minerals.[1] At high magnification, the 10's of μm-sized particles were enclosed within the sub-μm clay-sized matrix.

The untested and tested Average Gradation sub-samples could not be differentiated using SEM imaging. Both were observed to comprise both individual particles and bonded particles (Fig. 4). In both samples, fine-grained μm clay-sized particles acted as cements, bonding smaller (10's of μm-sized) particles to larger (100's of μm-sized) particles (Fig. 4A and C), and bonding smaller particles together (Fig. 4B and D). Although less dominant, clay minerals also played a role in bonding these particles (Fig. 5). XRD analysis of the Fine Tailings revealed that they comprised 40 to 55% hematite, 10 to 20% goethite, 1 to 2% magnetite, 10 to 30% quartz, 5 to 15% kaolinite, and other minor minerals.[2] XRD analysis of the Coarse Tailings revealed that they comprised 80 to 90% hematite, 5 to 10% magnetite, about 3% goethite, 1 to 2% quartz, and <1% kaolinite and other minerals.[3]

[1] See Annex E4.
[2] See Annex E4.
[3] See Annex E4.

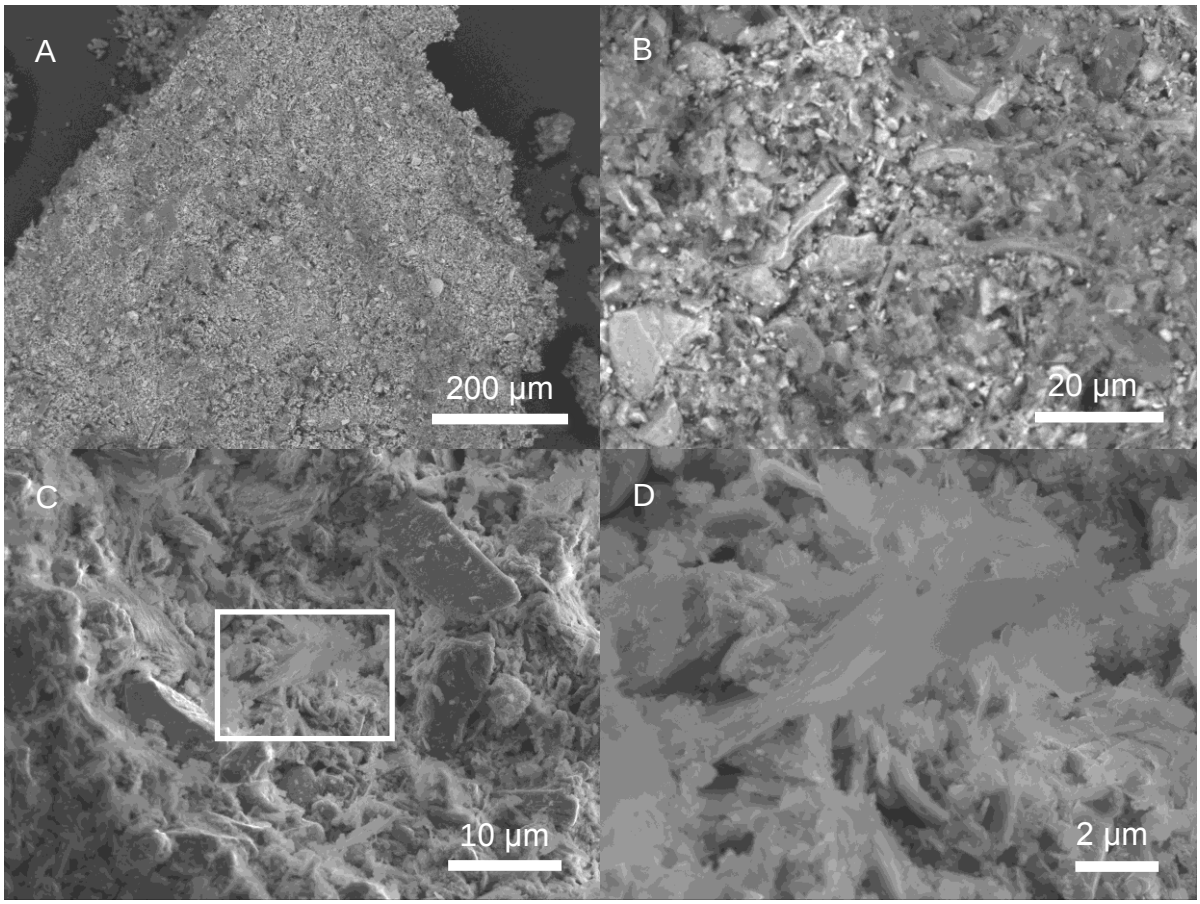


Figure 2. Representative SE-SEM micrographs of the Slimes sub-sample highlighting the fine-grained nature of the agglomerated material (images A and B), and the presence of thin films of platy, secondary iron oxide coatings (images C and D). The box in image C corresponds to image D, highlighting one of these coatings.

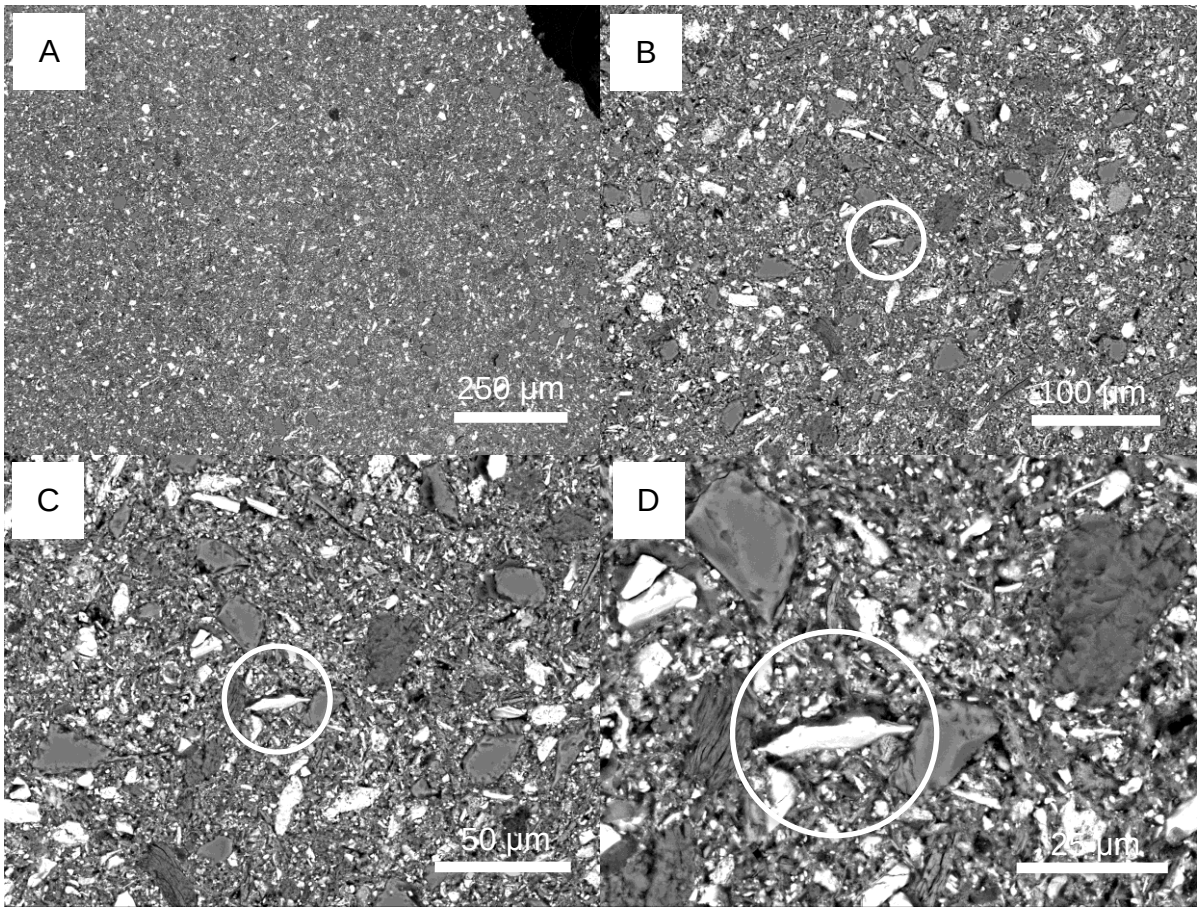


Figure 3. A focal series of representative BSE-SEM micrographs of the Slimes sub-sample, demonstrating the generally homogenous distribution of fine-gained particles. The circles in images B to D highlight the same iron oxide particle. In image D, the three main materials that comprise the sample are clearly visible: iron oxide (bright material; e.g., the circled grain), quartz (light grey, 'solid' with conchoidal fractures), and the layered clay minerals (darkest grey-scale material).

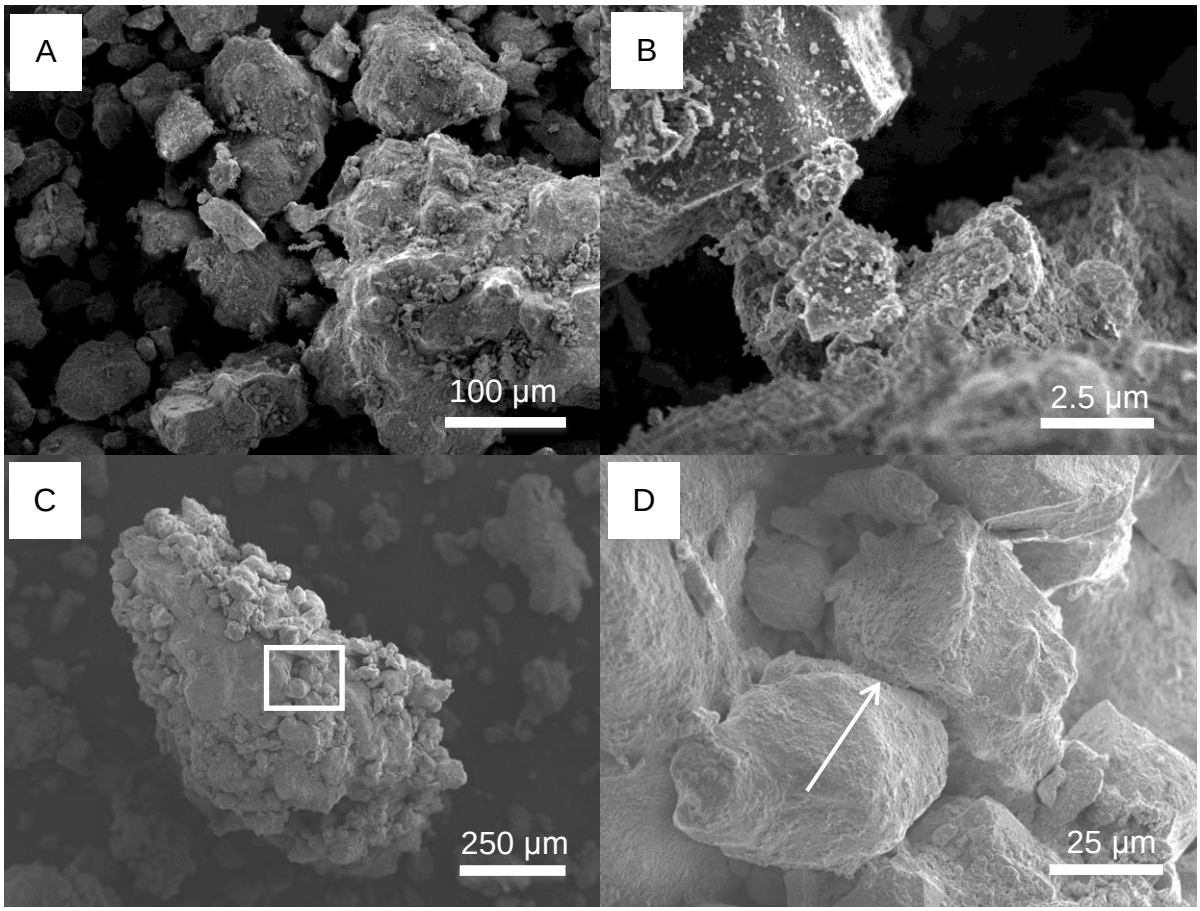


Figure 4. Representative SE-SEM micrographs of untested (images A and B) and tested (images C and D) Average Gradation sub-samples showing fine particles bonded to, and cross-linking, larger particles (images A and C versus image B), in which fine-grained clay-sized particles appear to act like a column of cement linking two smaller particles. The finer-grained particles in image C are iron oxide nodules, and these are in turn bonded to the larger particle by iron oxide cement. The box in image C corresponds to image D, highlighting small iron oxide nodules that are bonded by coatings of µm-scale clay-sized iron oxide cement (arrow).

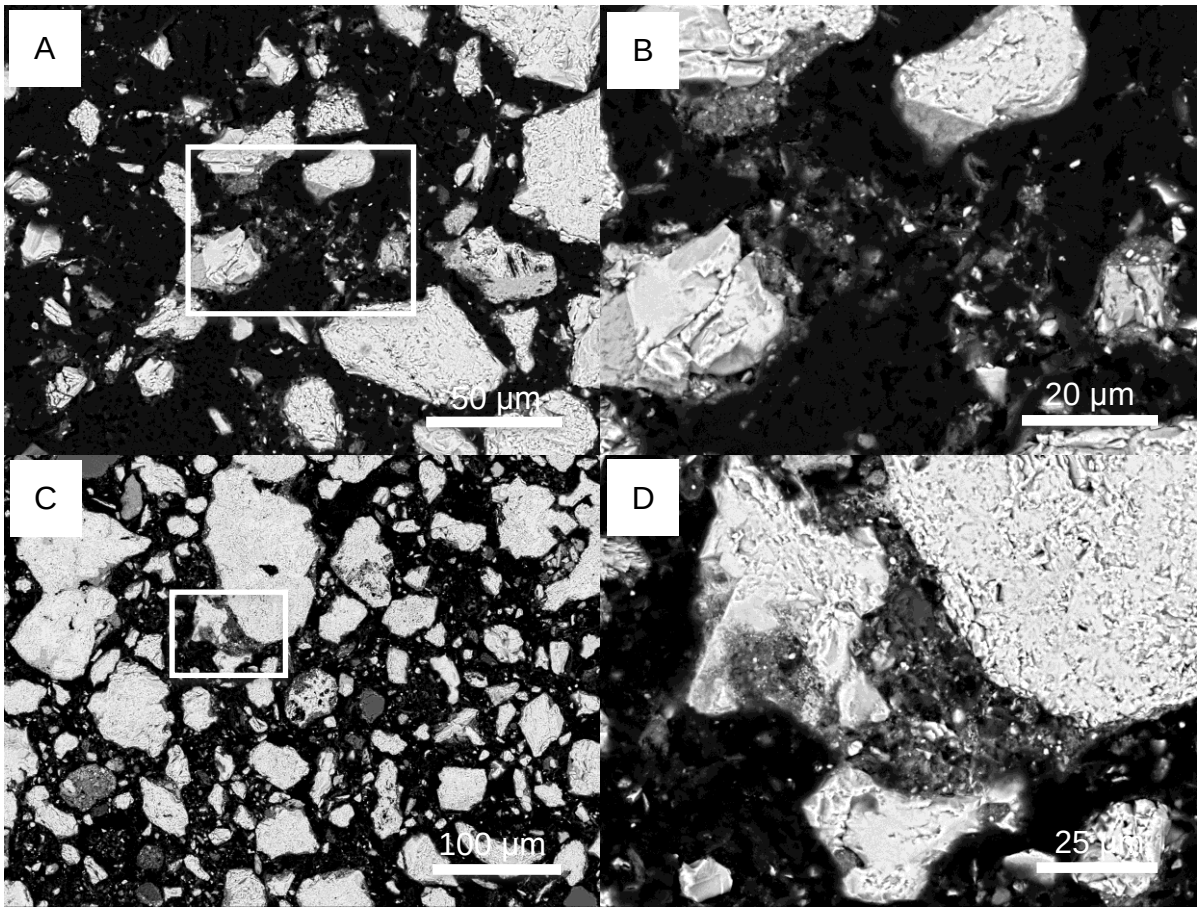


Figure 5. Representative BSE-SEM micrographs of untested (images A and B) and tested (images C and D) Average Gradation sub-samples. The boxes in images A and C correspond to the images in B and D, respectively. Note the distribution of µm-scale iron oxide, quartz and clay-sized particles between the 10's to 100's of µm-scale clasts, in particular, the iron oxide clasts in image D, which have bonded to one other via finer-grained particles.

Discussion and Interpretation

The purpose of the testing was to better understand the physical nature of the iron ore tailings, and their cementation (bonding) in particular, as a function of particle size, and as a result of sample preparation and strength testing. Further, it was also intended to investigate whether sample preparation and strength testing resulted in a loss of bonding between particles and hence a loss of strength.

Thin films of secondary iron oxides were observed on the Slimes, but were not observed in the untested and tested Average Gradation samples. The likely explanation for this is the very much greater surface area per unit volume of the finer-grained Slimes, which provided more opportunity for secondary iron oxide formation and bonding. Although they were not observed in the Average Gradation samples, based on their observation and structure in the Slimes sample, any secondary iron oxide thin films present in undisturbed Fine and Coarse Tailings may have been destroyed by sampling, sample preparation and testing.

The widespread occurrence of clay-sized iron oxides in the Average Gradation samples suggests that they may be responsible for the transient strength of the Average Gradation samples. The clay-sized iron oxides are a constant in all three samples, coating, linking and bonding larger particles to one another.



Dr. Gordon Southam

BSc Microbiology, PhD Microbiology

Appendix E

Annex 7 – Soil-Water Characteristic Curves

December 2019

University of Alberta Soil Water Characteristic Report

Final Report

for

Soil Water Characteristic Curve Measurements

Prepared for

Klohn Crippen Berger

by

Dr. Louis K. Kabwe
University of Alberta Geotechnical Center

November 26, 2019

1. INTRODUCTION

This report presents detailed data for twelve (12) measured soil-water characteristic curves (SWCC). The tables and figures in the main body of the report summarize the results for each of the tests. The tables and figures are briefly discussed. Also given are figures that compare the test results of the two methods used: i) the Tempe cell and ii) the HYPROP 2 device.
In summary, the results show the air entry values (AEV) for the samples tested ranged from 3 to 40 kPa. These are characteristic of sand and silt. Results also show that the two methods used yield comparable results.

2. BACKGROUND

The SWCC has become a valuable tool for the estimation of unsaturated soil property functions in geotechnical engineering practices (Fredlund and Rahardjo, 1993; Fredlund, 2002). The SWCC is used to describe the relationship between the amount of water in the soil and the corresponding values of matric suction ($u_a - u_w$). The SWCC is commonly measured using the Tempe pressure plate cell for soils with low to moderate AEVs up to 500 kPa and can require several weeks to complete, depending on soil type. The newly developed HYPROP 2 device (METER Environment, 2018) takes only days to generate a SWCC in the wet range (up to 300 kPa) and it does this automatically. The objective of this testing program was to measure the SWCC of various samples using the Tempe cell and HYPROP 2 devices.

3. DEVICES AND TEST PROCEDURES

3.1 Apparatuses

Two devices were used in this testing program: a Tempe pressure cell apparatus and a new HYPROP 2 device (METER Environment, 2018). The Tempe cell apparatus is shown in Figure 1 and the HYPROP 2 device is shown in Figure 2. The Tempe cell device is made up of three main components (see Figure 1): i) the bottom part fitted with a 500 kPa (5 bar) ceramic high air entry disc and an outlet for water from the sample, ii) an acrylic cylinder (7 cm in diameter x 9 cm high) to hold the sample, and iii) a top cap fitted with an inlet for air pressure supply. The HYPROP 2 device (see Figure 2) comprises a bottom part fitted with two mini-tensiometers to measure water potential and a cell (8 cm in diameter x 5 cm high) to hold the sample and a balance for weighing the sample.



Figure 1. Tempe Cell Components and Measurement Set Up

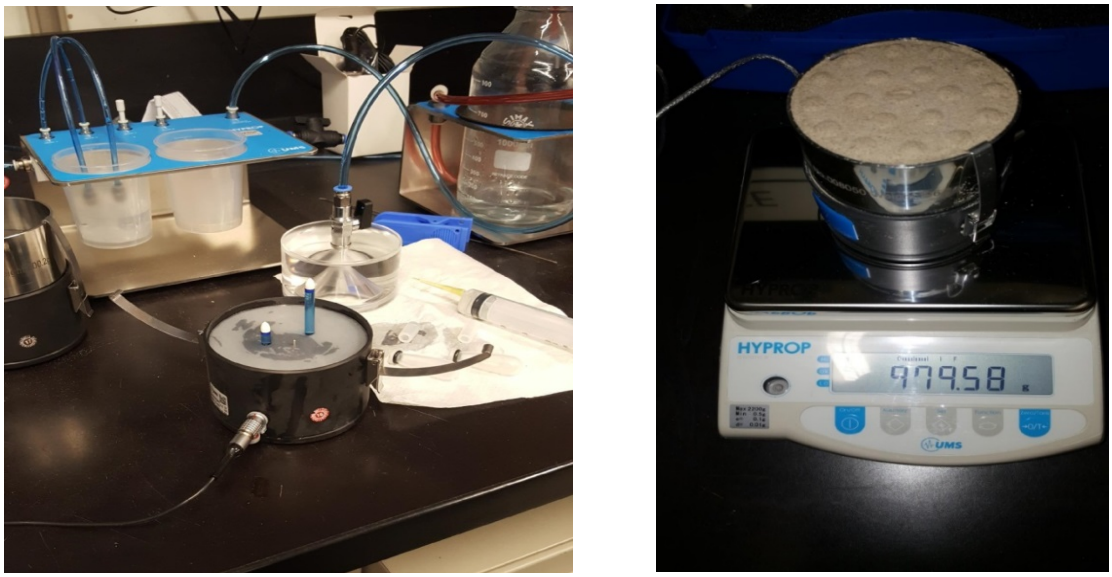


Figure 2. HYPROP 2 Components and Measurement Set Up

3.2 Tempe Cell Test Procedure

The SWCC was measured following the standard method recommended by Fredlund and Rahardjo (1993). Once a saturated sample is confined in a Tempe cell (Figure 1), the air pressure is applied over the sample through the inlet on top of the cap and porewater released from the sample is collected at the base of the cell. The change in mass of the sample is monitored by weighing the overall mass of the soil specimen until the mass change stops, and it is assumed that equilibrium

is reached. At this stage, the applied air pressure is equal to the soil suction. Higher air pressure steps are applied until the maximum suction is reached. At the end of the test, the sample is removed from the cell and the final water content is determined by oven-drying. This water content together with the previous changes in weight are used to back-calculate the water contents corresponding to each suction value. The matric suction is then plotted against corresponding water contents to give the SWCC.

3.3 HYPROP 2 Test Procedure

Before measurement, a saturated sample is confined in a measuring cell and two precision mini-tensiometers are inserted in the sample to measure water potential at different levels within the saturated soil sample while the sample rests on a laboratory balance. The HYPROP 2 is set up to run automatically. The HYPROP-Fit software detects the balance, and the measuring head automatically assigns measuring values to the tensions. Over time, the sample dries, and the instrument measures the changing water potential and the changing sample weight simultaneously. Moisture content is calculated from the weight measurements, and the instrument plots' changes in water potential correlated to changes in moisture content. HYPROP 2 generates a SWCC of soil samples in 3 to 9 days.

4. SAMPLES

Samples tested were received in plastic bags. The amount of material in each bag ranged from 200 g to 6.5 Kg. The samples for Tempe cell tests were dried in an oven at 105 ^{o}C, prior to the tests. Samples for HYPROP 2 testing were used directly from their storage bags. All the tests were carried out in the Unsaturated Soil Mechanics Laboratory of the University of Alberta Geotechnical Centre.

Table 4.1. Summary of Samples Selected for Testing

Sample Name	**Sample Mass (g)**	**Tempe Cell**	**Hyprop**
DT-01	3400	X	
DT-02	5400	X	X
DT-06	5260	X	X
DT-10	4100	X	
GP-03/09	680	X	X
GP-14	770	X	X
AG A03255A01		X	X

5. SUMMARY OF TESTS RESULTS

5.1 SWCCs Measured using the Tempe Cell

5.1.1 Testing Status

Table 5.1. Summary of Test Status using the Tempe Cell

Sample ID	**SWCC**	**Notes**
DT-01	Completed	Fine Tailings
DT-02	Completed	Fine Tailings
DT-06	Completed	Fine Tailings
DT-10	Completed	Fine Tailings
AG A03255A01	Completed	Coarse Tailings
GP-03/09	Completed	Loose Residual Topsoil
GP-14	Completed	Loose Residual Topsoil

AG: Average Gradation

5.1.2 Summary of Tempe Cell Test Results

Table 5.2. Summary of Tempe Cell SWCC Properties

Sample ID	**AEV (kPa)**
DT-01	~ 15
DT-02	~ 20
DT-06	~ 40
DT-10	~ 15
AG A03255A01	~ 9
GP-03/09	~ 3
GP-14	~6

AEV = Air Entry Value

In summary, the AEV of the samples tested and completed using the Tempe cell ranged from 3 to 40 kPa, which are characteristic of sand and silt. Figure 3 shows the measured SWCCs completed using the Tempe cell method.

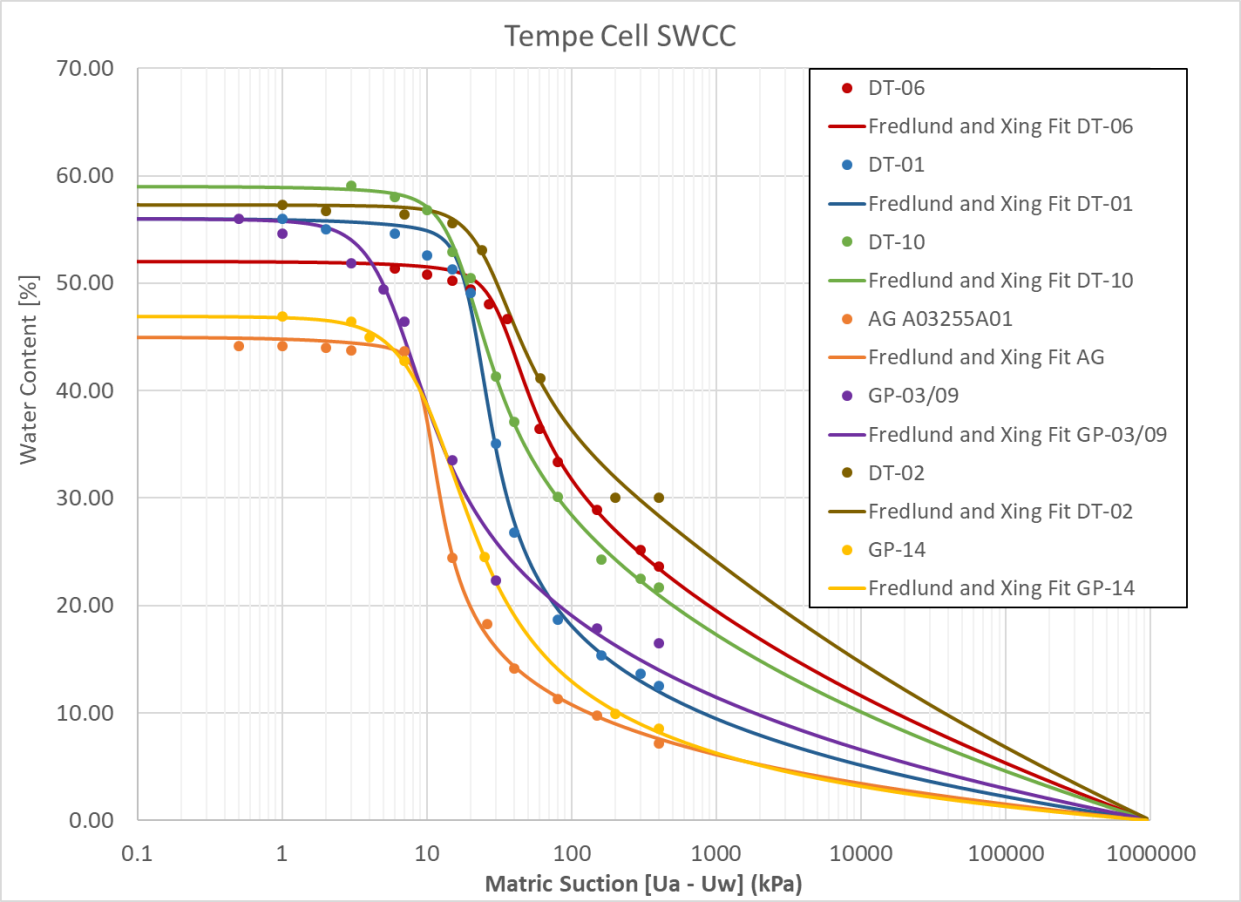


Figure 3. SWCC Plots Measured using the Tempe Cell

5.2 SWCCs Measured using the HYPROP 2 Device

5.2.1 Testing Status

Table 5.3. Summary of Test Status using HYPROP 2 Device

Sample ID	**SWCC**	**Notes**
DT-02	Completed	
DT-06	Completed	Power loss during test
AG A03255A01	Completed	
GP-03/09	Completed	
GP-14	Completed	

AG: Average Gradation

5.2.2 Summary of Test Results

Table 5.4. Summary of HYPROP SWCC Properties

Sample ID	AEV (kPa)
DT-02	~30
DT-06	~40
AG A03255A01	~ 8
GP-03/09	~ 4
GP-14	~ 3

In summary, the AEV of the samples tested and completed up to date using the HYPROP 2 device ranged from 3 to 40 kPa, which are characteristic of sand and silt. Figure 4 shows the completed measured SWCCs using the HYPROP 2 method.

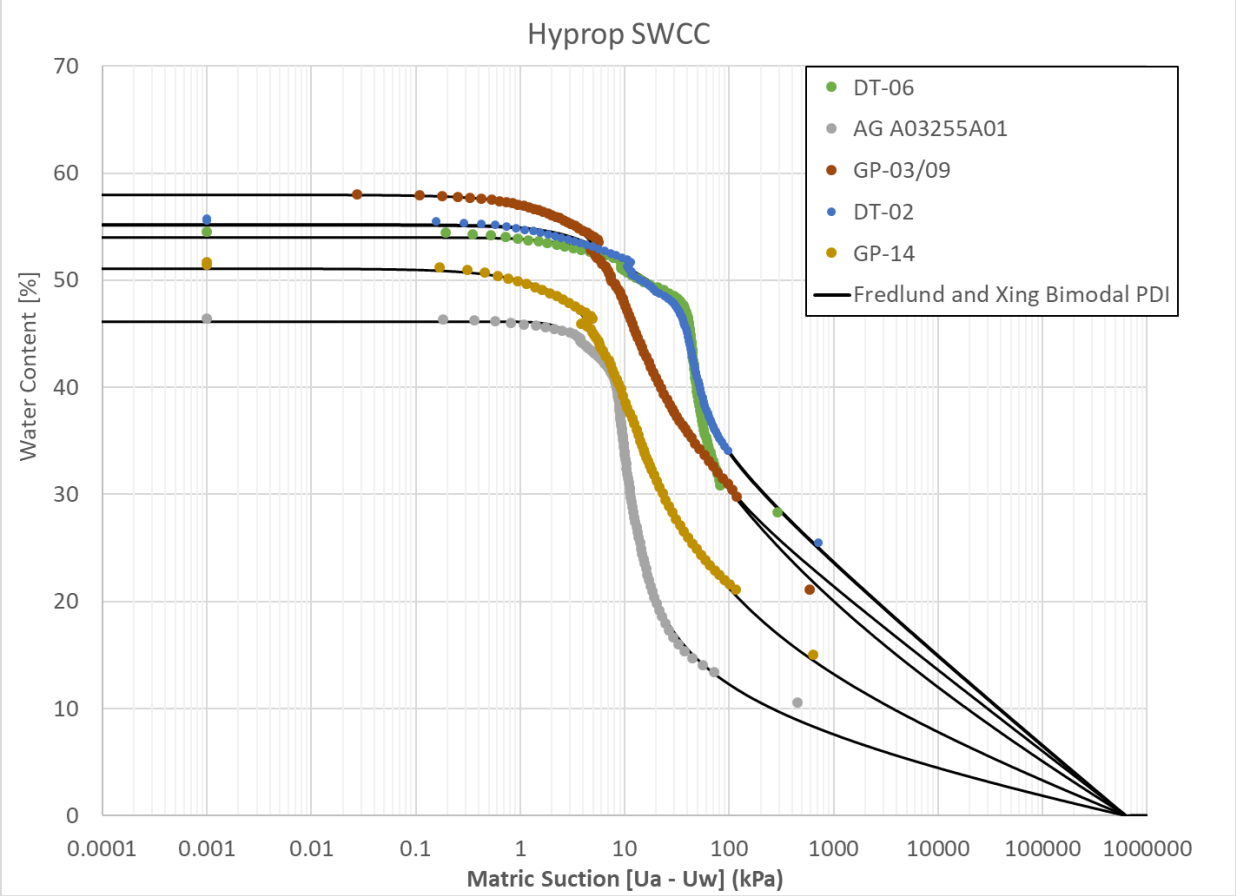


Figure 4. SWCC Plots Measured using the HYPROP 2 Device

5.3 Comparison between the Tempe Cell and HYPROP 2 Tests Results

The following figures display the HYPROP 2 data for each test separately, along with Tempe cell data. It is interesting to note that the Tempe cell and HYPROP 2 device yield comparable results in Figures 5 to 9.

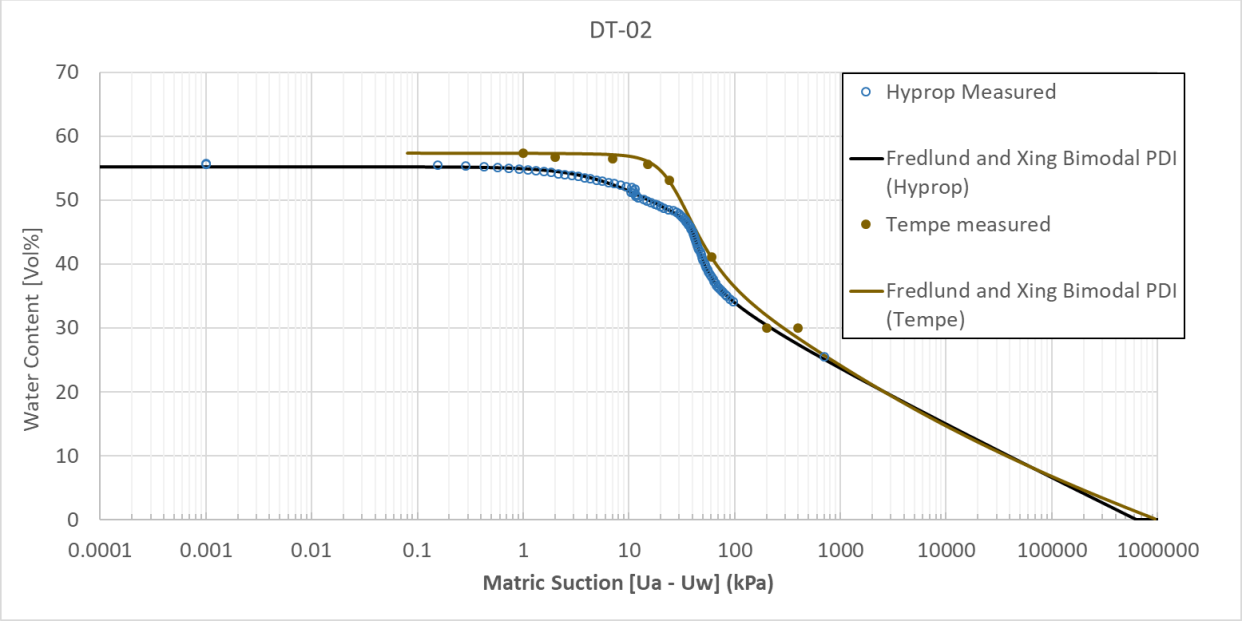


Figure 5. SWCC Data for DT-02

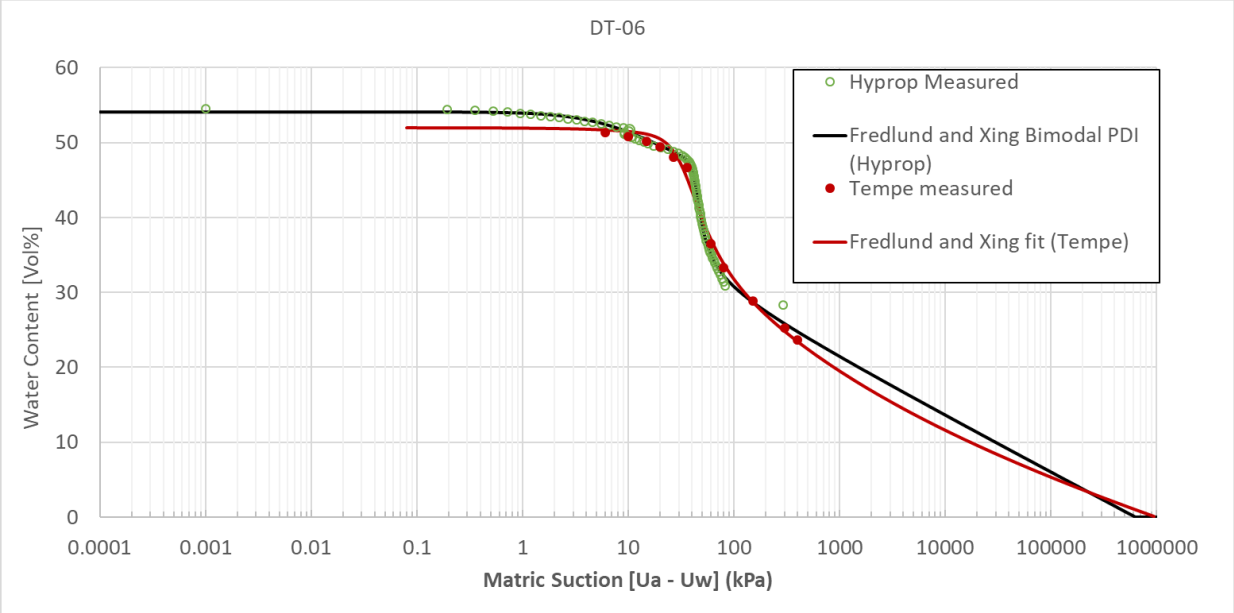


Figure 6. SWCC Data for DT-06

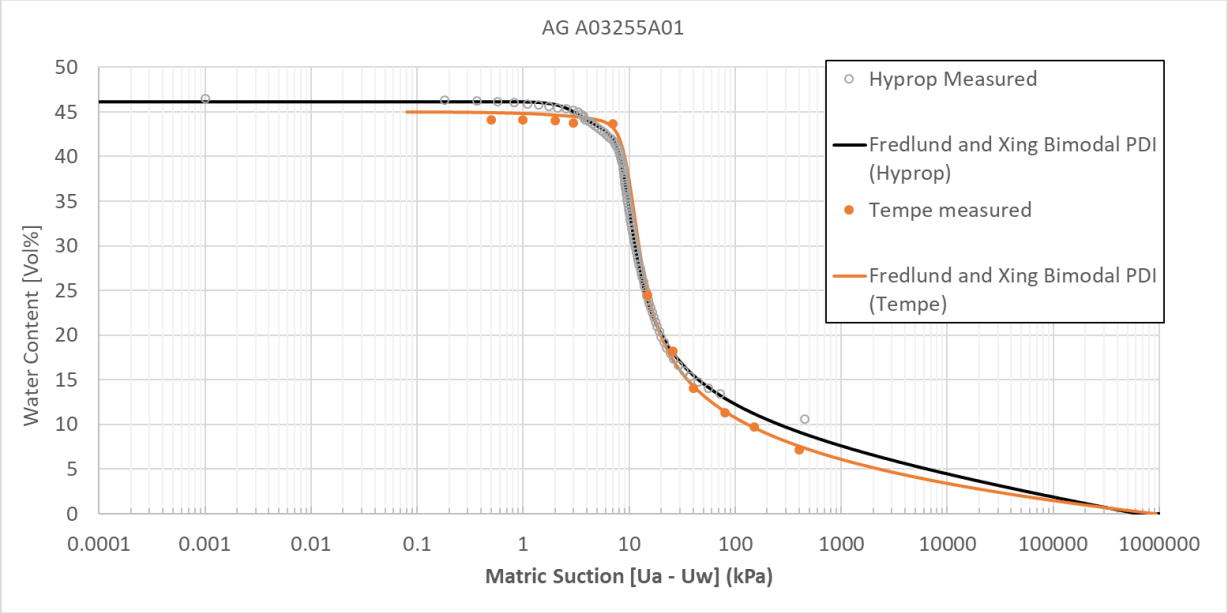


Figure 7. SWCC Data for AG A03255A01

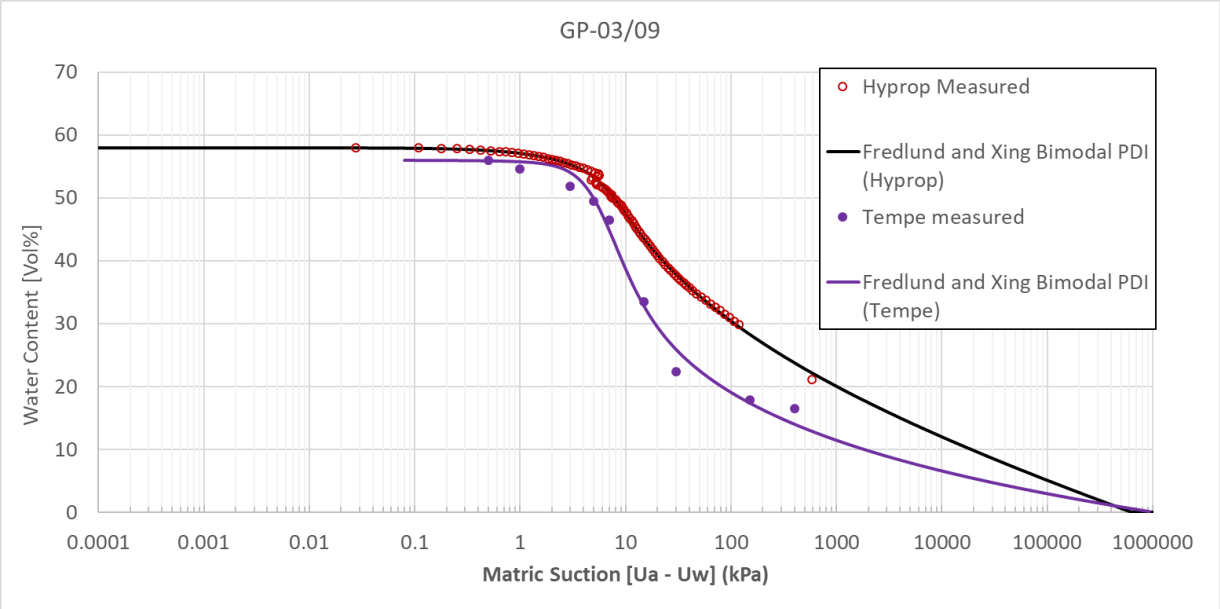


Figure 8. SWCC Data for GP-03/09

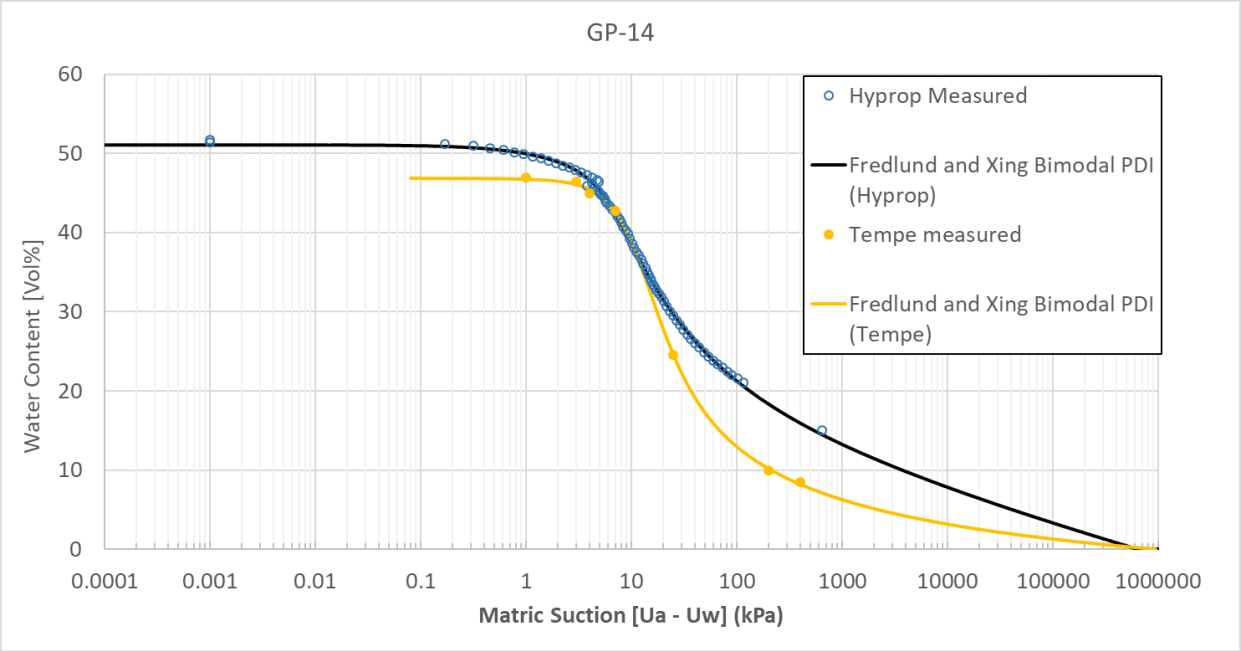


Figure 9. SWCC Data for GP-14

5.4 Summary

A total of 12 SWCCs curves have been completed. Five SWCCs have been completed with the HYPROP 2 Device and seven SWCCs have been completed using the Tempe Cell method.

6. REFERENCES

Fredlund, D.G. 2002. Use of soil water characteristic curve in the implementation of unsaturated soil mechanics. UNSAT 2002. Proceedings of the Third International Conference on Unsaturated Soils, Recife, Brazil, March 10-13, pp. 887-904.

Fredlund. D.G. and Rahardjo, H. 1993. Soil mechanics for unsaturated soils. John Wiley and Sons New York, N.Y.

HYPROP 2 User Manual v **2018**/3. METER Environment.

APPENDIX

Table A.1. Summary of Samples Received

SAMPLE NAME	MASS (kg)
DT-01	3.4
DT-02	5.4
DT-03	3.6
DT-04	6.44
DT-05	3.7
DT-06	5.26
DT-07	3.3
DT-08	5.04
DT-09	3.1
DT-10	4.1
DT-11	3.1
DT-12	2.5
DT-13	4.2
GP-01	0.17
GP-02-A	0.4
GP-02-B	0.27
GP-03	0.44
GP-04-A	0.8
GP-04-B	0.84
GP-05	0.16
GP-06	1.39
GP-07	0.64
GP-08	1.39
GP-09	0.24
GP-10	0.41
GP-11	0.61
GP-12	0.73
GP-13	1.17
GP-14	0.77
GP-15	0.36
GP-16	1.44

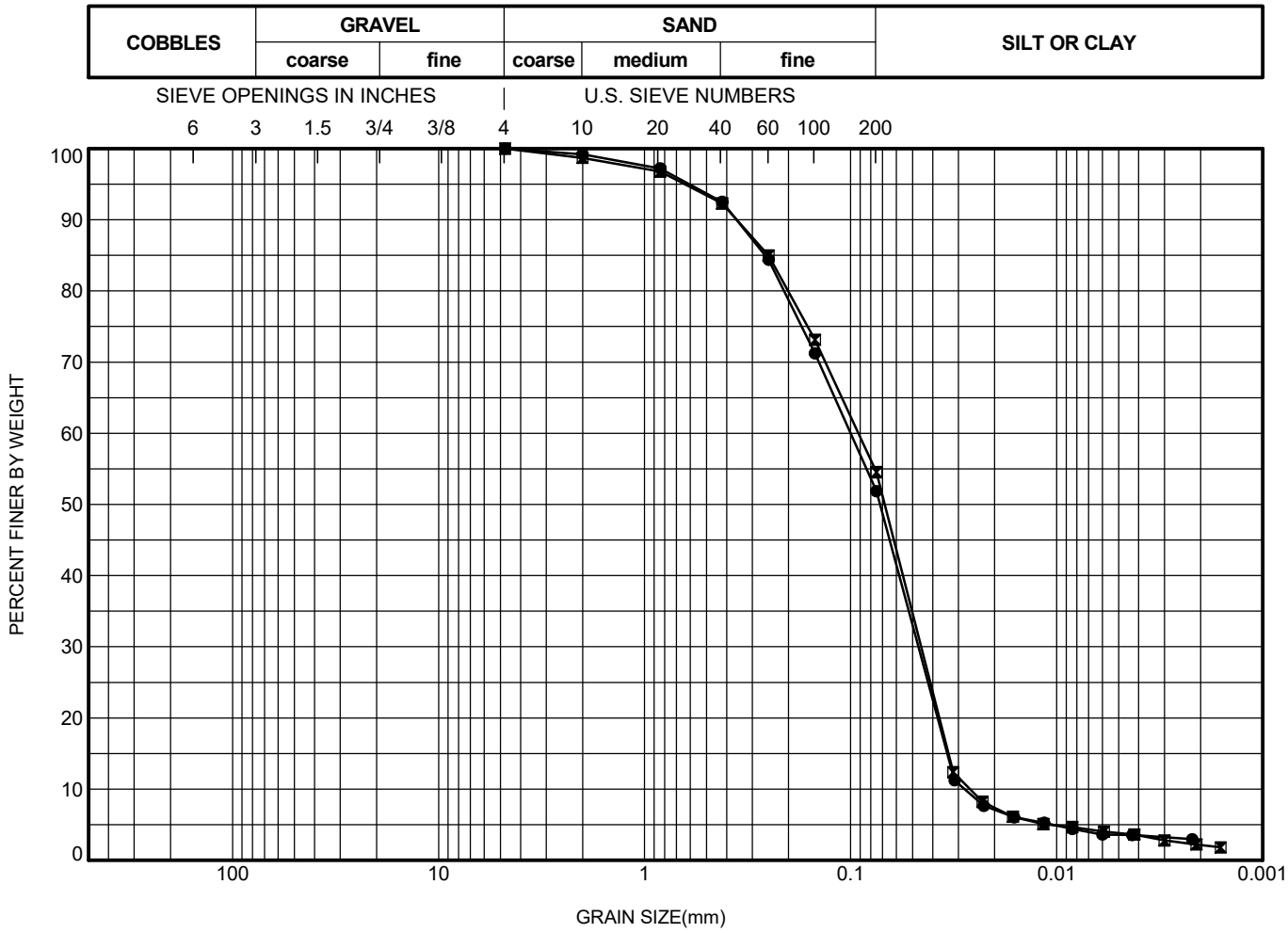
Appendix E

Annex 8 – Advanced Testing Data

December 2019

Particle Size Distribution of Triaxial Gradients

GRAIN SIZE DISTRIBUTION



	HOLE	DEPTH (m)	D85	D60	D50	D15	D10	CU	%GRAVEL	%SAND	%FINES
●	TX01-CID	0.00	0.260	0.100					0.0	48.1	51.9
⊠	TX01-CID	0.00	0.251	0.092					0.0	45.5	54.5

	HOLE	SAMPLE	DEPTH (m)	W%	W_L	W_P	PI	REMARKS / SAMPLE DESCRIPTION
●	TX01-CID	Average	0.00					Before Testing (TX01/TX05)
⊠	TX01-CID	Average	0.00					After Testing

CU = COEFFICIENT OF UNIFORMITY = D60/D10 **PARTICLE SIZES, e.g. D85, in mm** **Tested by Wet Sieving Method (ASTM D1140 & D422)**

PROJECT NO.: A03355A01

PROJECT:

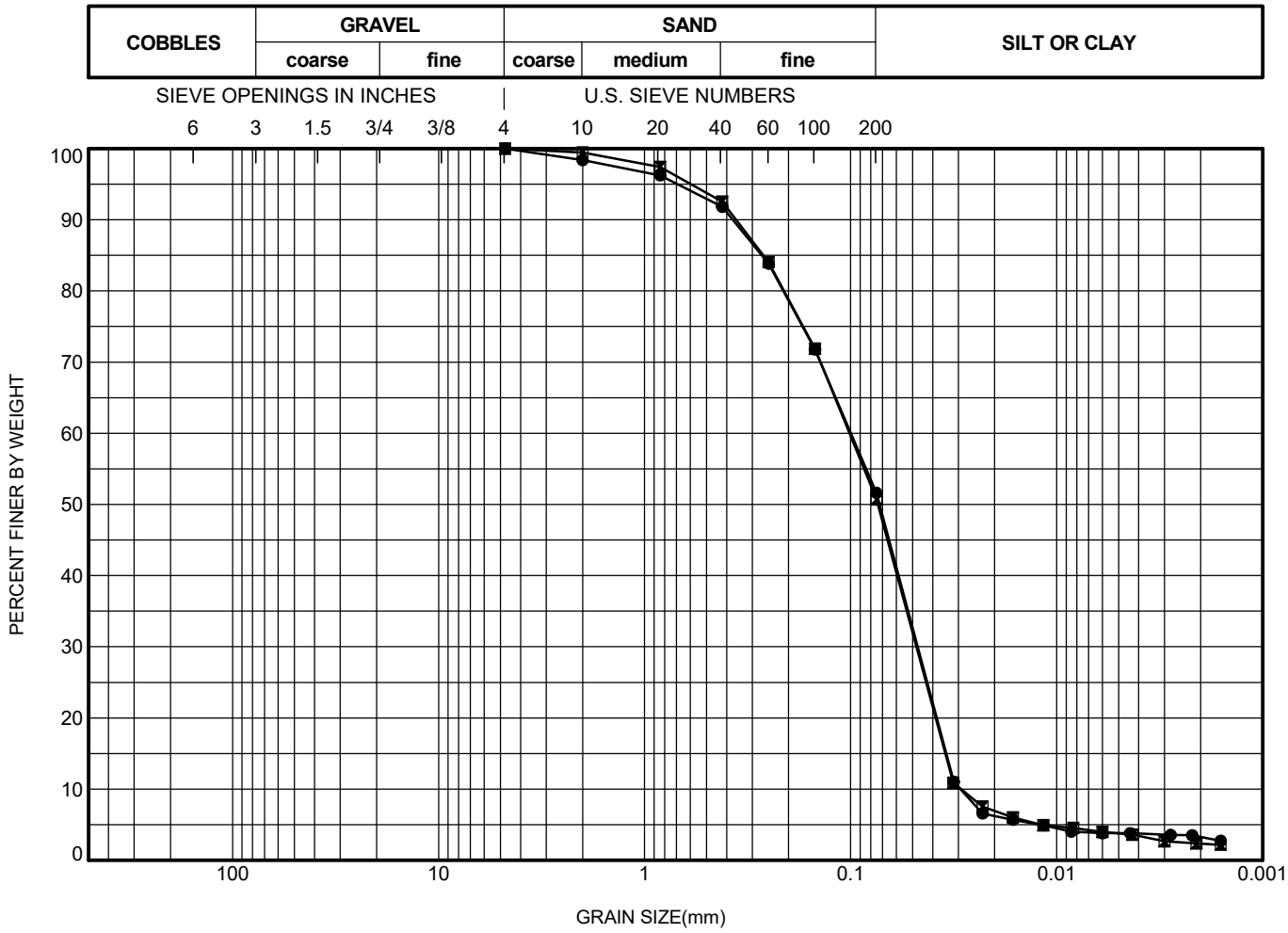
LOCATION:

FIGURE:

DRAWN BY: AX **CHECKED BY:** BY

KC_GRAIN_SIZE-SI A03355A01 TRIAXIAL TESTS PSDS.GPJ SIEVE.GDT 19-11-20

GRAIN SIZE DISTRIBUTION



	HOLE	DEPTH (m)	D85	D60	D50	D15	D10	CU	%GRAVEL	%SAND	%FINES
●	TX02-CID	0.00	0.270	0.100					0.0	48.4	51.6
⊠	TX02-CID	0.00	0.265	0.101					0.0	49.3	50.7

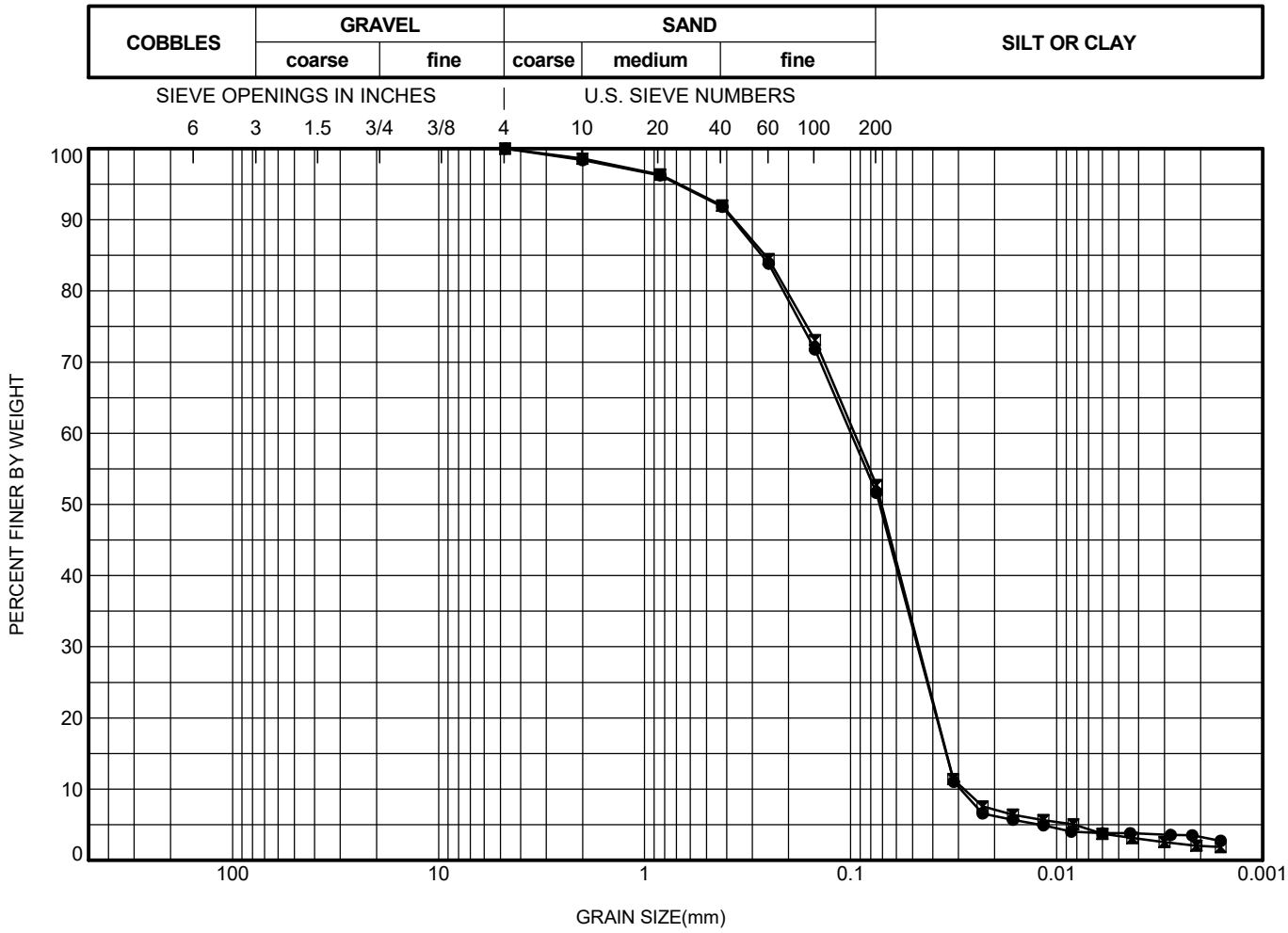
	HOLE	SAMPLE	DEPTH (m)	W%	W_L	W_P	PI	REMARKS / SAMPLE DESCRIPTION
●	TX02-CID	Average	0.00					Before Testing (TX02/TX03/TXBE01)
⊠	TX02-CID	Average	0.00					After Testing

CU = COEFFICIENT OF UNIFORMITY = D60/D10 **PARTICLE SIZES, e.g. D85, in mm** **Tested by Wet Sieving Method (ASTM D1140 & D422)**

PROJECT NO.: A03355A01
PROJECT:
LOCATION:
FIGURE:
DRAWN BY: AX **CHECKED BY:** BY

KC_GRAIN_SIZE-SI A03355A01 TRIAXIAL TESTS PSDS.GPJ SIEVE.GDT 19-11-20

GRAIN SIZE DISTRIBUTION



	HOLE	DEPTH (m)	D85	D60	D50	D15	D10	CU	%GRAVEL	%SAND	%FINES
●	TX03-CID	0.00	0.270	0.100					0.0	48.4	51.6
⊠	TX03-CID	0.00	0.260	0.096					0.0	47.3	52.7

	HOLE	SAMPLE	DEPTH (m)	W%	W_L	W_P	PI	REMARKS / SAMPLE DESCRIPTION
●	TX03-CID	Average	0.00					Before Testing (TX02/TX03/TXBE01)
⊠	TX03-CID	Average	0.00					After Testing

CU = COEFFICIENT OF UNIFORMITY = D60/D10 **PARTICLE SIZES, e.g. D85, in mm** **Tested by Wet Sieving Method (ASTM D1140 & D422)**

PROJECT NO.: A03355A01

PROJECT:

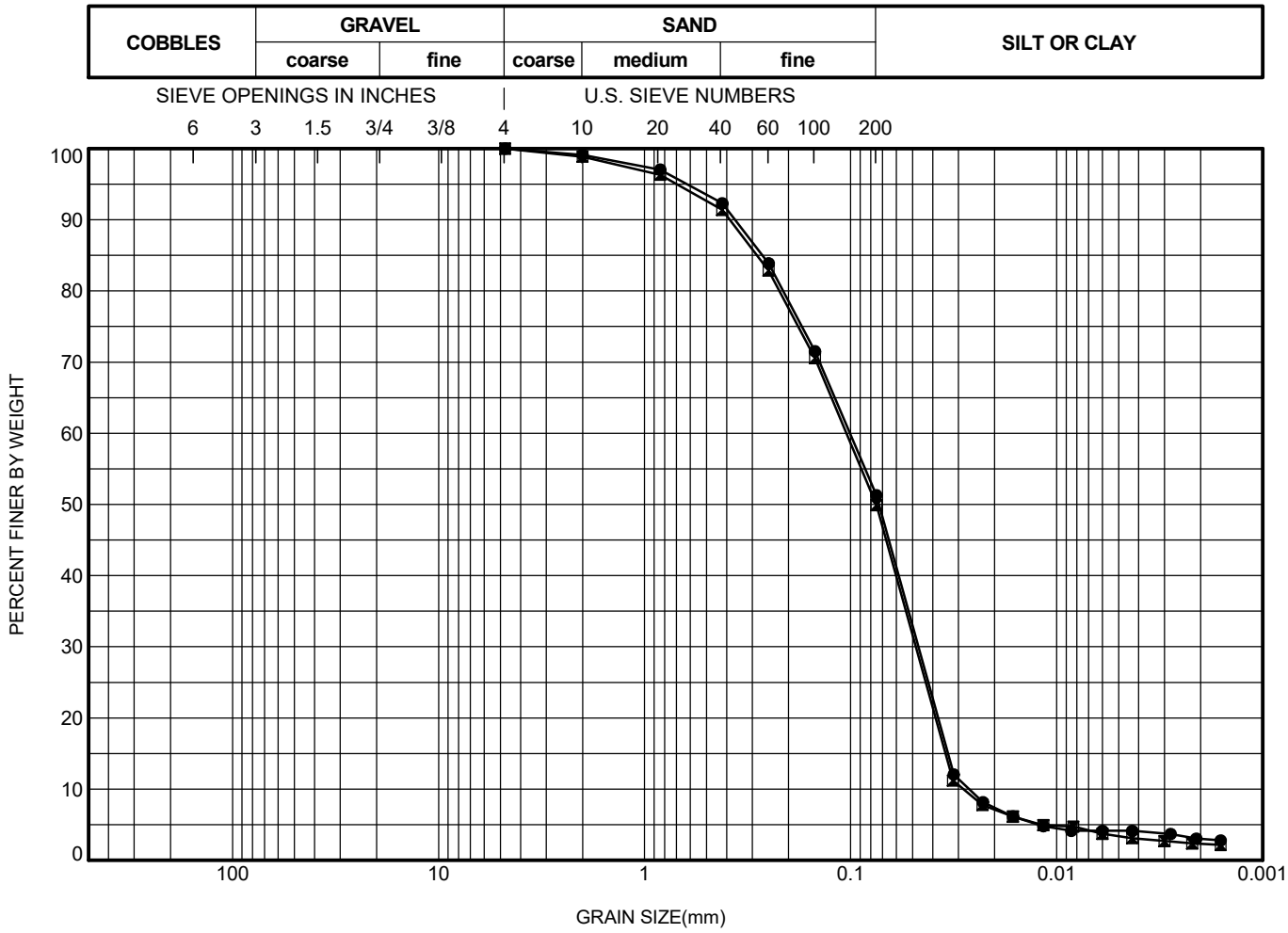
LOCATION:

FIGURE:

DRAWN BY: AX **CHECKED BY:** BY

KC_GRAIN_SIZE-SI A03355A01 TRIAXIAL TESTS PSDS.GPJ SIEVE.GDT 19-11-20

GRAIN SIZE DISTRIBUTION



	HOLE	DEPTH (m)	D85	D60	D50	D15	D10	CU	%GRAVEL	%SAND	%FINES
●	TX04-CIU	0.00	0.268	0.101					0.0	48.7	51.3
☒	TX04-CIU	0.00	0.285	0.105	0.075				0.0	50.1	49.9

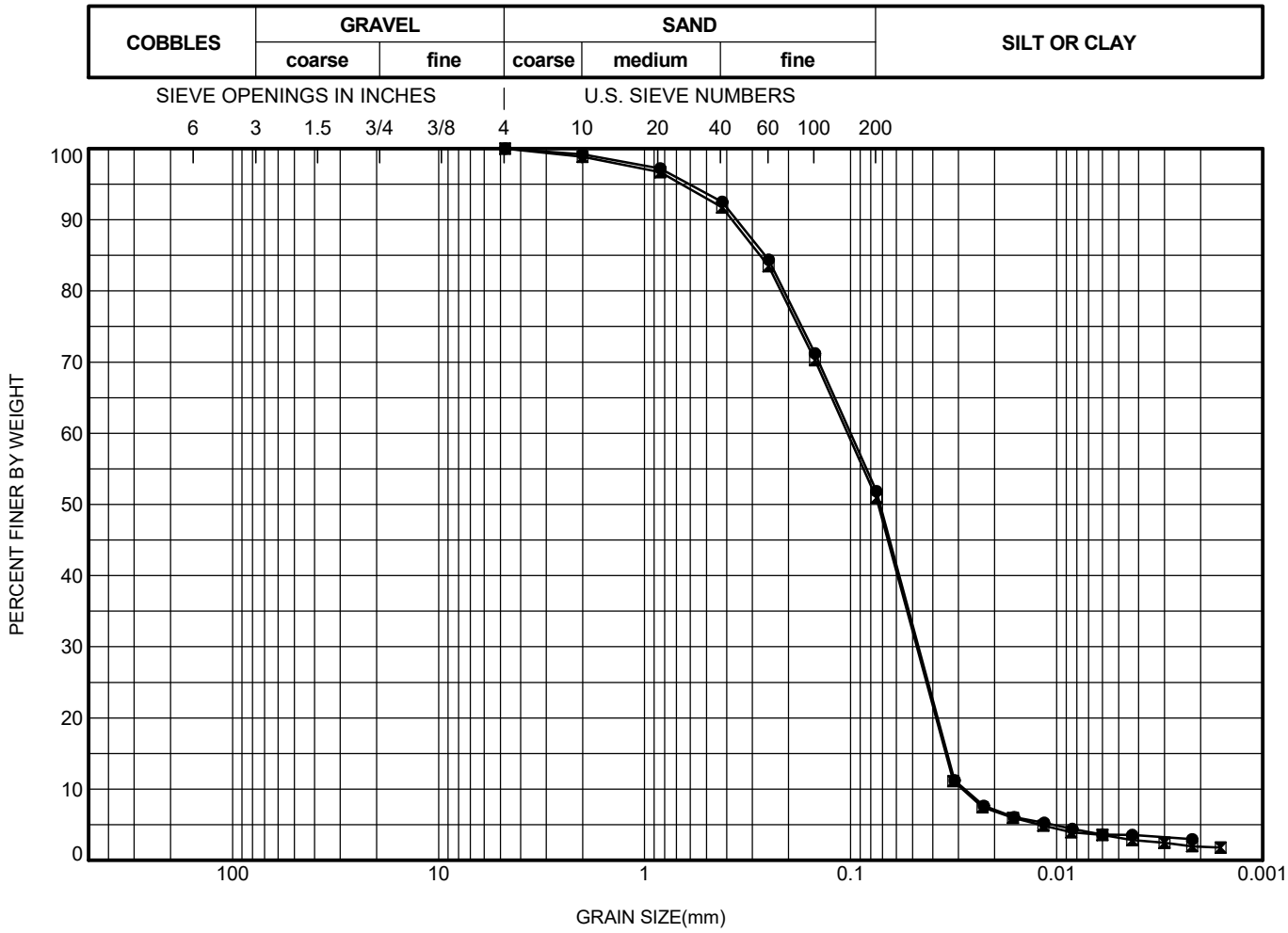
	HOLE	SAMPLE	DEPTH (m)	W%	W_L	W_P	PI	REMARKS / SAMPLE DESCRIPTION
●	TX04-CIU	Average	0.00					Before Testing (TX04/TX06/TXBE02)
☒	TX04-CIU	Average	0.00					After Testing

CU = COEFFICIENT OF UNIFORMITY = D60/D10 **PARTICLE SIZES, e.g. D85, in mm** **Tested by Wet Sieving Method (ASTM D1140 & D422)**

PROJECT NO.: A03355A01
PROJECT:
LOCATION:
FIGURE:
DRAWN BY: AX **CHECKED BY:** BY

KC_GRAIN_SIZE-SI A03355A01 TRIAXIAL TESTS PSDS.GPJ SIEVE.GDT 19-11-20

GRAIN SIZE DISTRIBUTION



	HOLE	DEPTH (m)	D85	D60	D50	D15	D10	CU	%GRAVEL	%SAND	%FINES
●	TX05-CID	0.00	0.260	0.100					0.0	48.1	51.9
⊠	TX05-CID	0.00	0.275	0.104					0.0	49.1	50.9

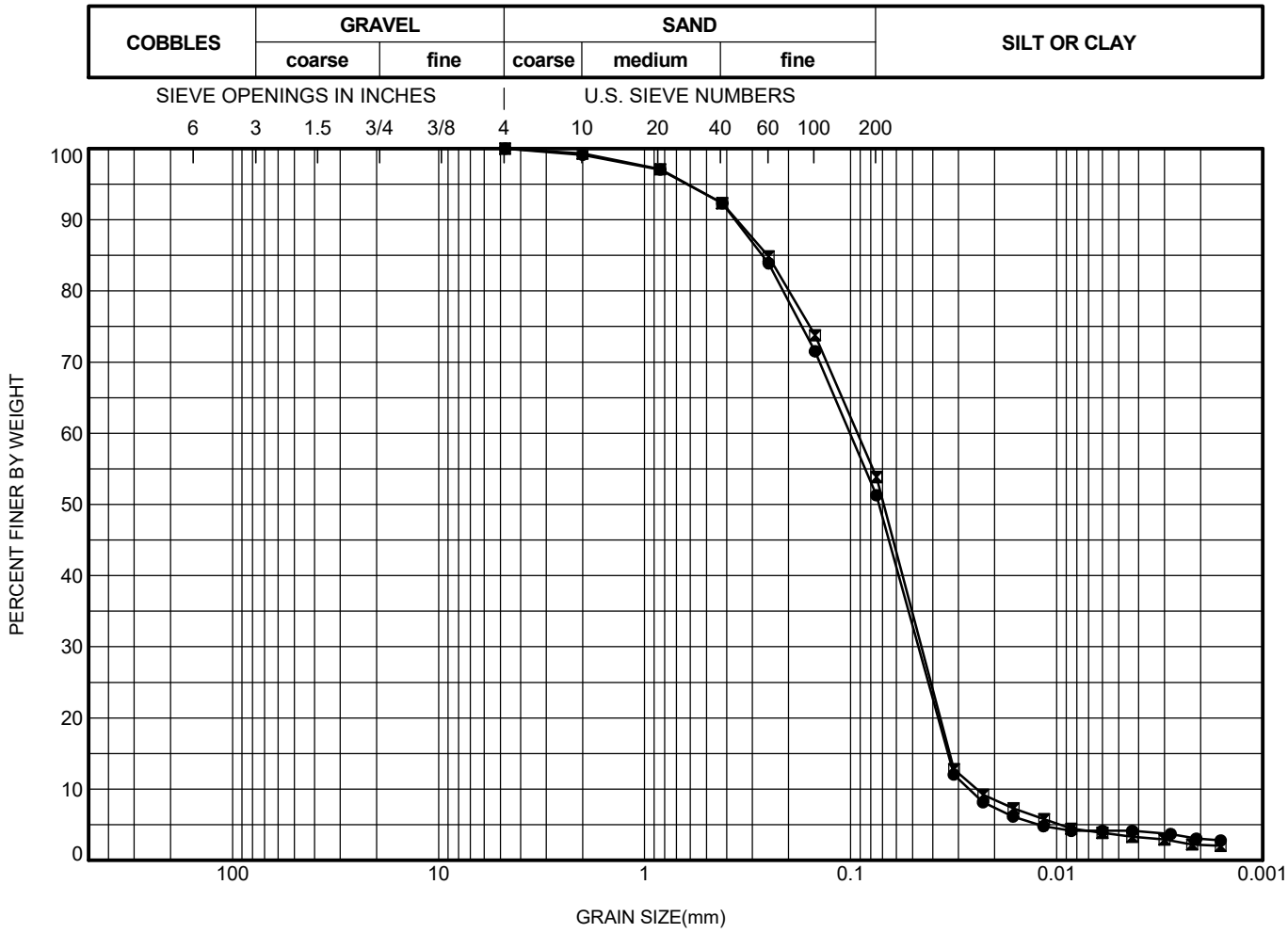
	HOLE	SAMPLE	DEPTH (m)	W%	W_L	W_P	PI	REMARKS / SAMPLE DESCRIPTION
●	TX05-CID	Average	0.00					Before Testing (TX01/TX05)
⊠	TX05-CID	Average	0.00					After Testing

CU = COEFFICIENT OF UNIFORMITY = D60/D10 **PARTICLE SIZES, e.g. D85, in mm** **Tested by Wet Sieving Method (ASTM D1140 & D422)**

PROJECT NO.: A03355A01
PROJECT:
LOCATION:
FIGURE:
DRAWN BY: AX **CHECKED BY:** BY

KC_GRAIN_SIZE-SI A03355A01 TRIAXIAL TESTS PSDS.GPJ SIEVE.GDT 19-11-20

GRAIN SIZE DISTRIBUTION



	HOLE	DEPTH (m)	D85	D60	D50	D15	D10	CU	%GRAVEL	%SAND	%FINES
●	TX06-CID	0.00	0.268	0.101					0.0	48.7	51.3
⊠	TX06-CID	0.00	0.253	0.093					0.0	46.1	53.9

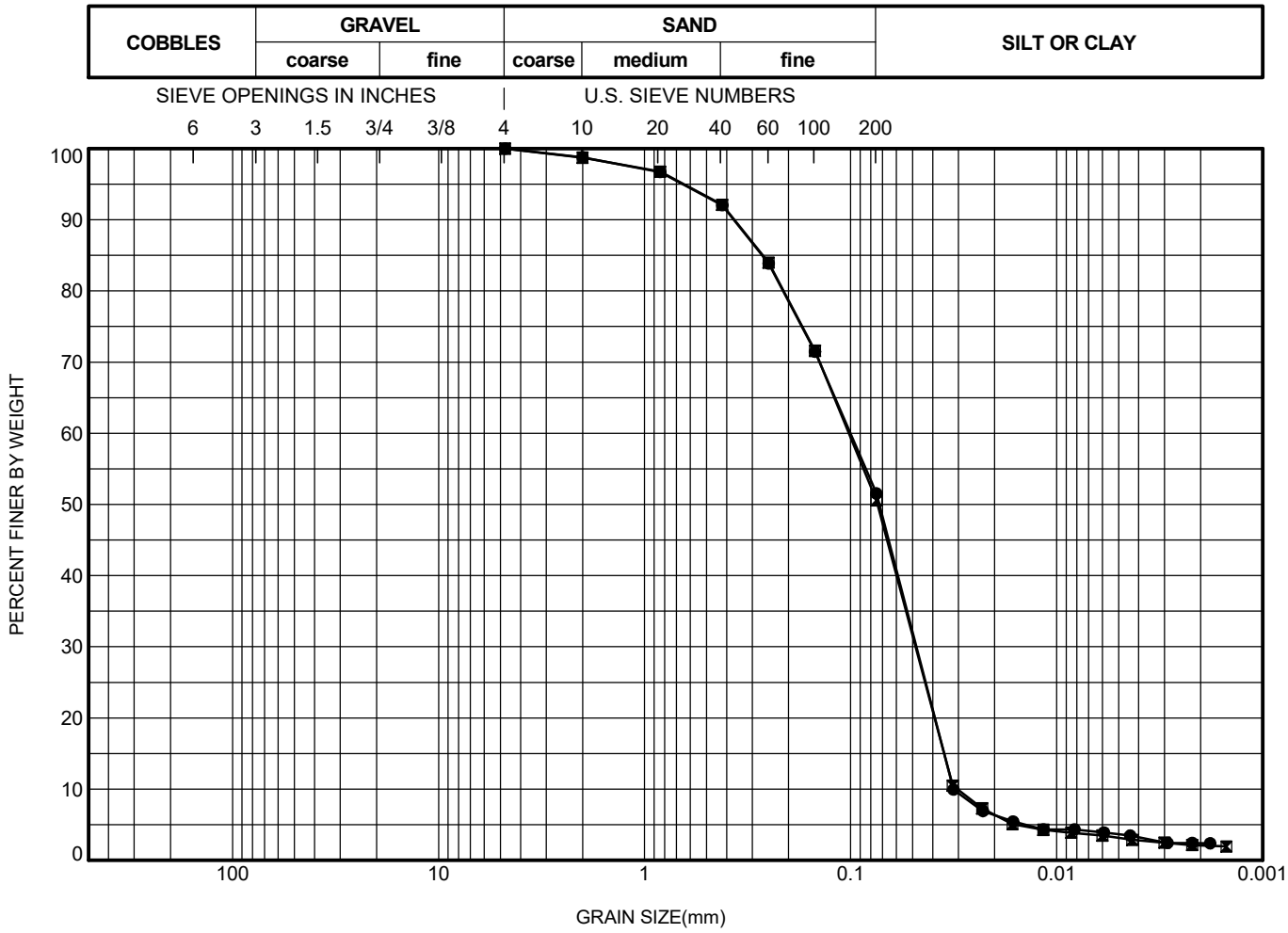
	HOLE	SAMPLE	DEPTH (m)	W%	W_L	W_P	PI	REMARKS / SAMPLE DESCRIPTION
●	TX06-CID	Average	0.00					Before Testing (TX04/TX06/TXBE02)
⊠	TX06-CID	Average	0.00					After Testing

CU = COEFFICIENT OF UNIFORMITY = D60/D10 **PARTICLE SIZES, e.g. D85, in mm** **Tested by Wet Sieving Method (ASTM D1140 & D422)**

PROJECT NO.: A03355A01
PROJECT:
LOCATION:
FIGURE:
DRAWN BY: AX **CHECKED BY:** BY

KC_GRAIN_SIZE-SI A03355A01 TRIAXIAL TESTS PSDS.GPJ SIEVE.GDT 19-11-20

GRAIN SIZE DISTRIBUTION



	HOLE	DEPTH (m)	D85	D60	D50	D15	D10	CU	%GRAVEL	%SAND	%FINES
●	TX07-CIU	0.00	0.269	0.100					0.0	48.4	51.6
⊠	TX07-CIU	0.00	0.267	0.102					0.0	49.4	50.6

	HOLE	SAMPLE	DEPTH (m)	W%	W_L	W_P	PI	REMARKS / SAMPLE DESCRIPTION
●	TX07-CIU	Average	0.00					Before Testing (TX07/TXBE03)
⊠	TX07-CIU	Average	0.00					After Testing

CU = COEFFICIENT OF UNIFORMITY = D60/D10 **PARTICLE SIZES, e.g. D85, in mm** **Tested by Wet Sieving Method (ASTM D1140 & D422)**

PROJECT NO.: A03355A01

PROJECT:

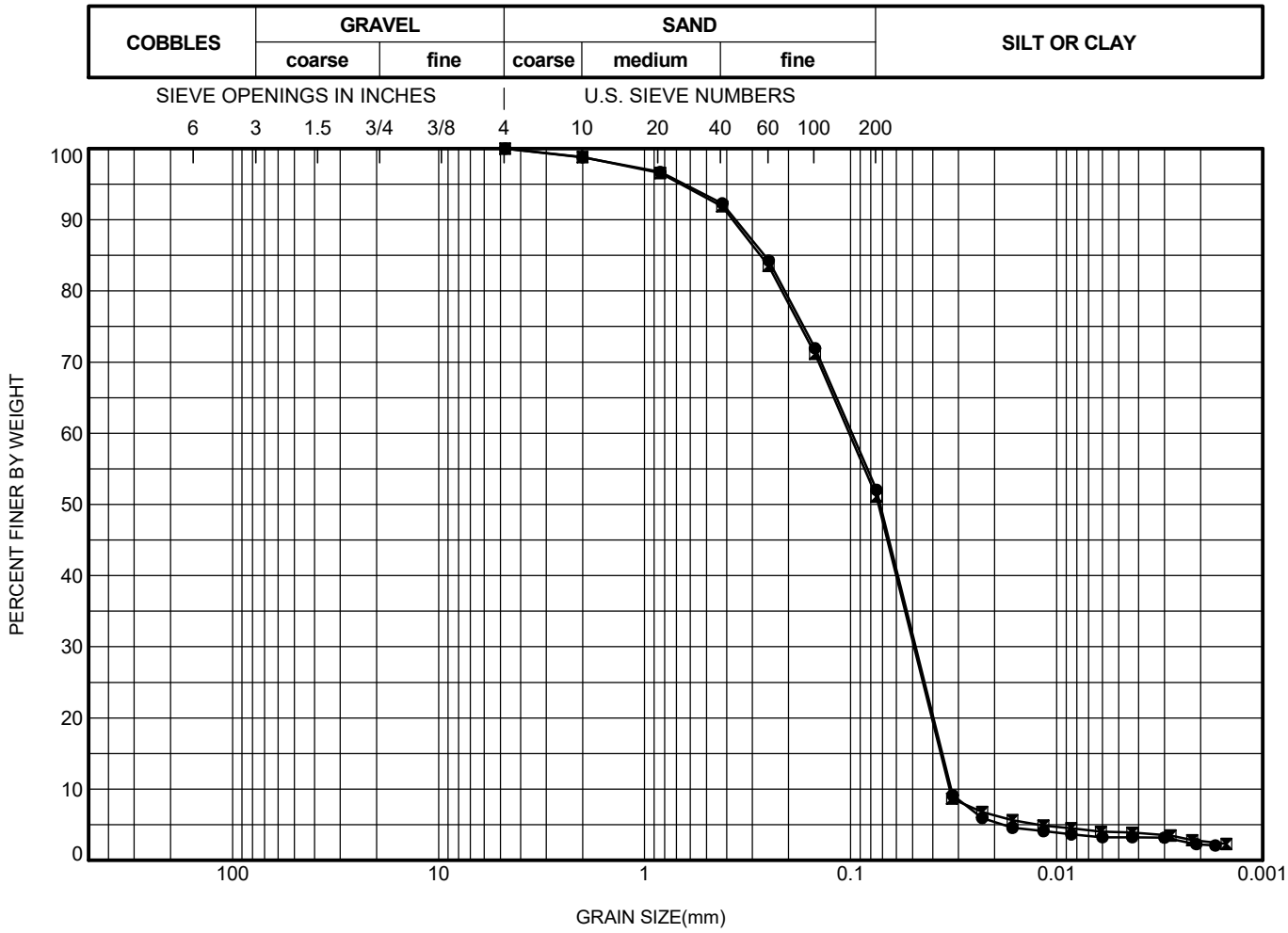
LOCATION:

FIGURE:

DRAWN BY: AX **CHECKED BY:** BY

KC_GRAIN_SIZE-SI A03355A01 TRIAXIAL TESTS PSDS.GPJ SIEVE.GDT 19-11-20

GRAIN SIZE DISTRIBUTION



	HOLE	DEPTH (m)	D85	D60	D50	D15	D10	CU	%GRAVEL	%SAND	%FINES
●	TX08-CID	0.00	0.262	0.099					0.0	47.9	52.1
☒	TX08-CID	0.00	0.274	0.102					0.0	48.9	51.1

	HOLE	SAMPLE	DEPTH (m)	W%	W_L	W_P	PI	REMARKS / SAMPLE DESCRIPTION
●	TX08-CID	Average	0.00					Before Testing
☒	TX08-CID	Average	0.00					After Testing

CU = COEFFICIENT OF UNIFORMITY = D60/D10 **PARTICLE SIZES, e.g. D85, in mm** **Tested by Wet Sieving Method (ASTM D1140 & D422)**

PROJECT NO.: A03355A01

PROJECT:

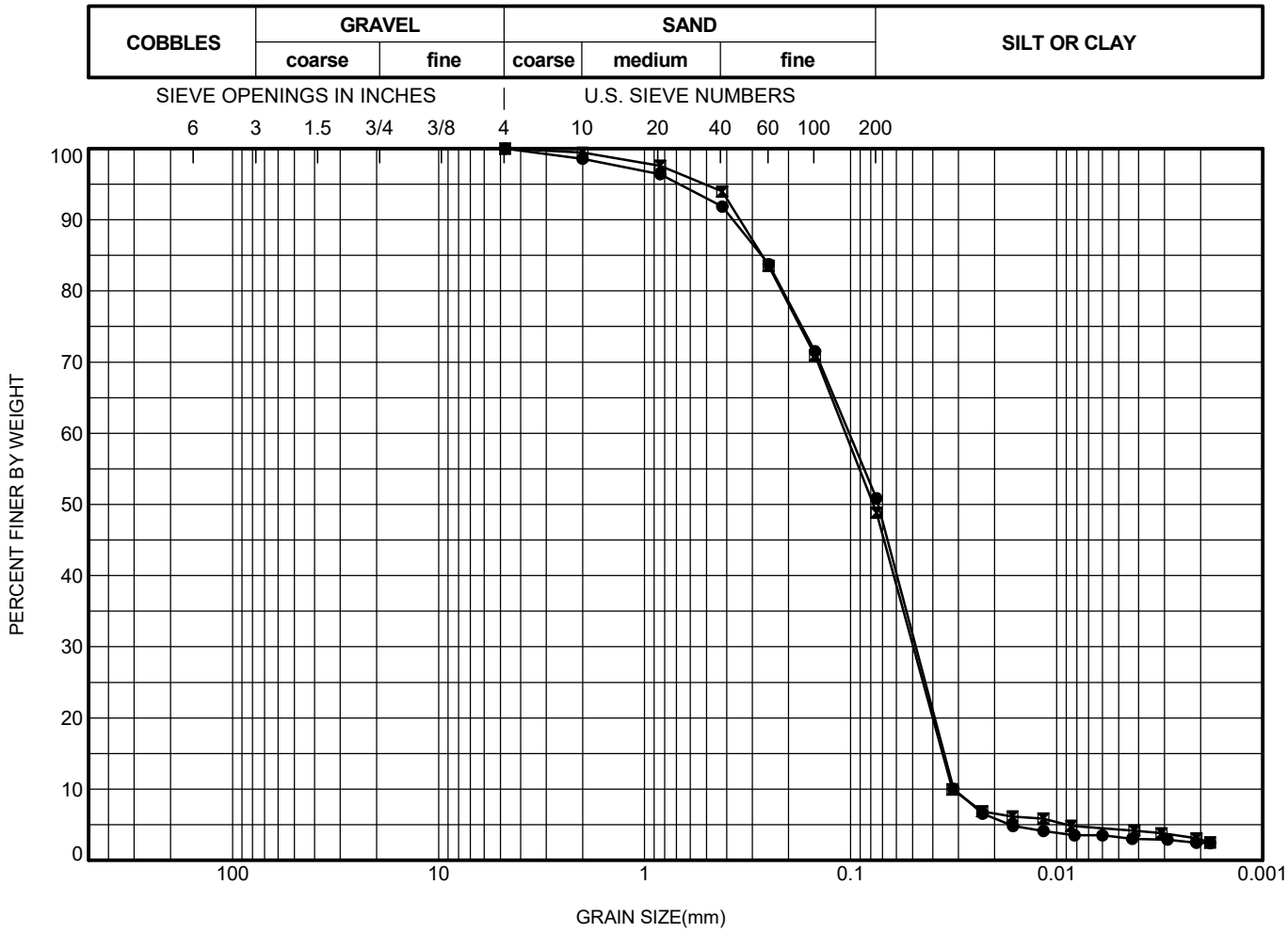
LOCATION:

FIGURE:

DRAWN BY: AX **CHECKED BY:** BY

KC_GRAIN_SIZE-SI A03355A01 TRIAXIAL TESTS PSDS.GPJ SIEVE.GDT 19-11-20

GRAIN SIZE DISTRIBUTION



	HOLE	DEPTH (m)	D85	D60	D50	D15	D10	CU	%GRAVEL	%SAND	%FINES
●	TX09-CID	0.00	0.271	0.102					0.0	49.1	50.9
☒	TX09-CID	0.00	0.269	0.106	0.078				0.0	51.2	48.8

	HOLE	SAMPLE	DEPTH (m)	W%	W_L	W_P	PI	REMARKS / SAMPLE DESCRIPTION
●	TX09-CID	Average	0.00					Before Testing
☒	TX09-CID	Average	0.00					After Testing

CU = COEFFICIENT OF UNIFORMITY = D60/D10 **PARTICLE SIZES, e.g. D85, in mm** **Tested by Wet Sieving Method (ASTM D1140 & D422)**

PROJECT NO.: A03355A01

PROJECT:

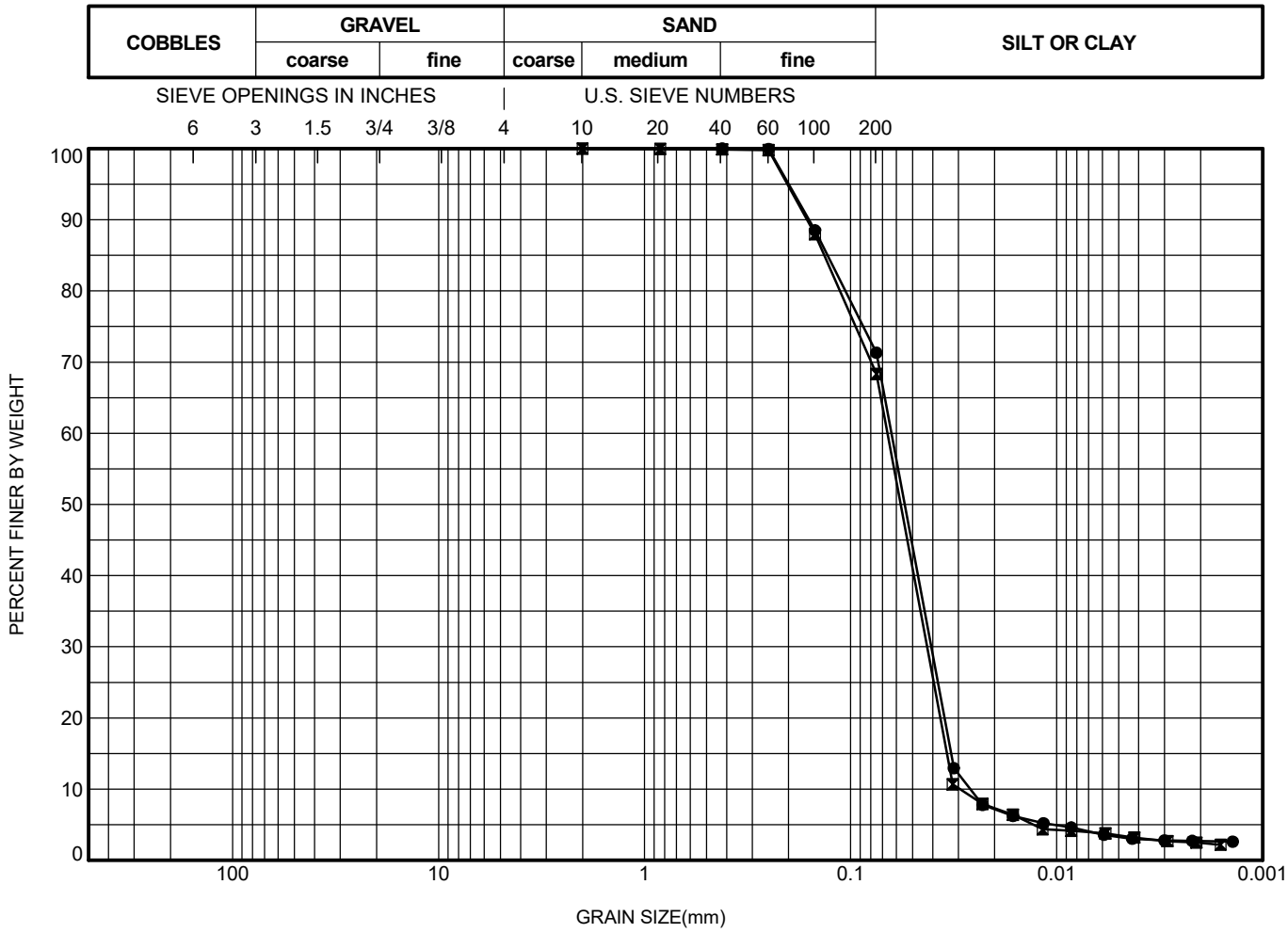
LOCATION:

FIGURE:

DRAWN BY: AX **CHECKED BY:** BY

KC_GRAIN_SIZE-SI A03355A01 TRIAXIAL TESTS PSDS.GPJ SIEVE.GDT 19-11-20

GRAIN SIZE DISTRIBUTION



	HOLE	DEPTH (m)	D85	D60	D50	D15	D10	CU	%GRAVEL	%SAND	%FINES
●	TX10-CID	0.00	0.130						0.0	28.7	71.3
⊠	TX10-CID	0.00	0.134						0.0	31.7	68.3

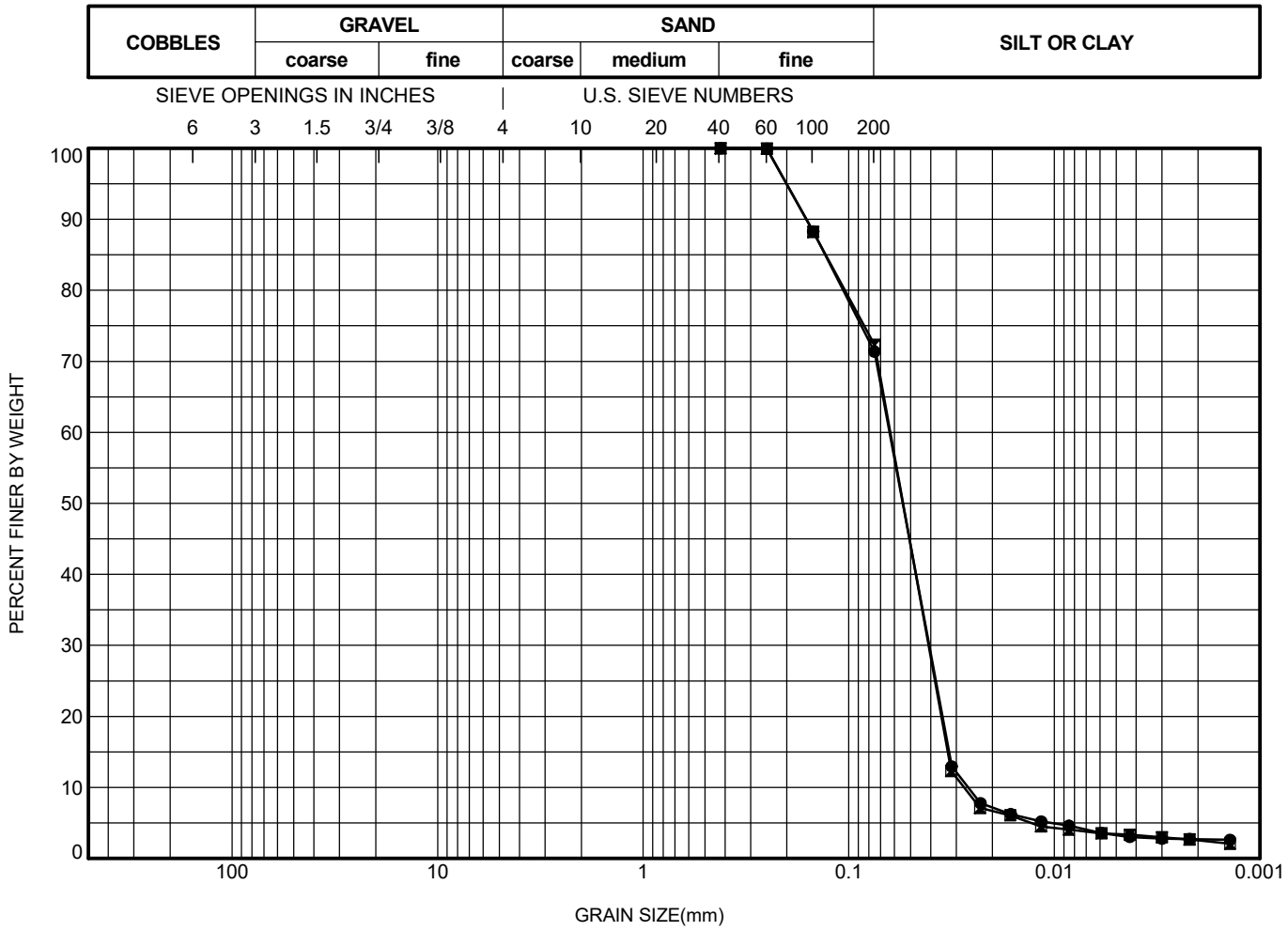
	HOLE	SAMPLE	DEPTH (m)	W%	W_L	W_P	PI	REMARKS / SAMPLE DESCRIPTION
●	TX10-CID	Fine	0.00					Before Testing (TX10/TX11)
⊠	TX10-CID	Fine	0.00					After Testing

CU = COEFFICIENT OF UNIFORMITY = D60/D10 **PARTICLE SIZES, e.g. D85, in mm** **Tested by Wet Sieving Method (ASTM D1140 & D422)**

PROJECT NO.: A03355A01
PROJECT:
LOCATION:
FIGURE:
DRAWN BY: AX **CHECKED BY:** BY

KC_GRAIN_SIZE-SI A03355A01 TRIAXIAL TESTS PSDS.GPJ SIEVE.GDT 19-11-20

GRAIN SIZE DISTRIBUTION



	HOLE	DEPTH (m)	D85	D60	D50	D15	D10	CU	%GRAVEL	%SAND	%FINES
●	TX11-CID	0.00	0.130						0.0	28.6	71.4
☒	TX11-CID	0.00	0.130						0.0	27.7	72.3

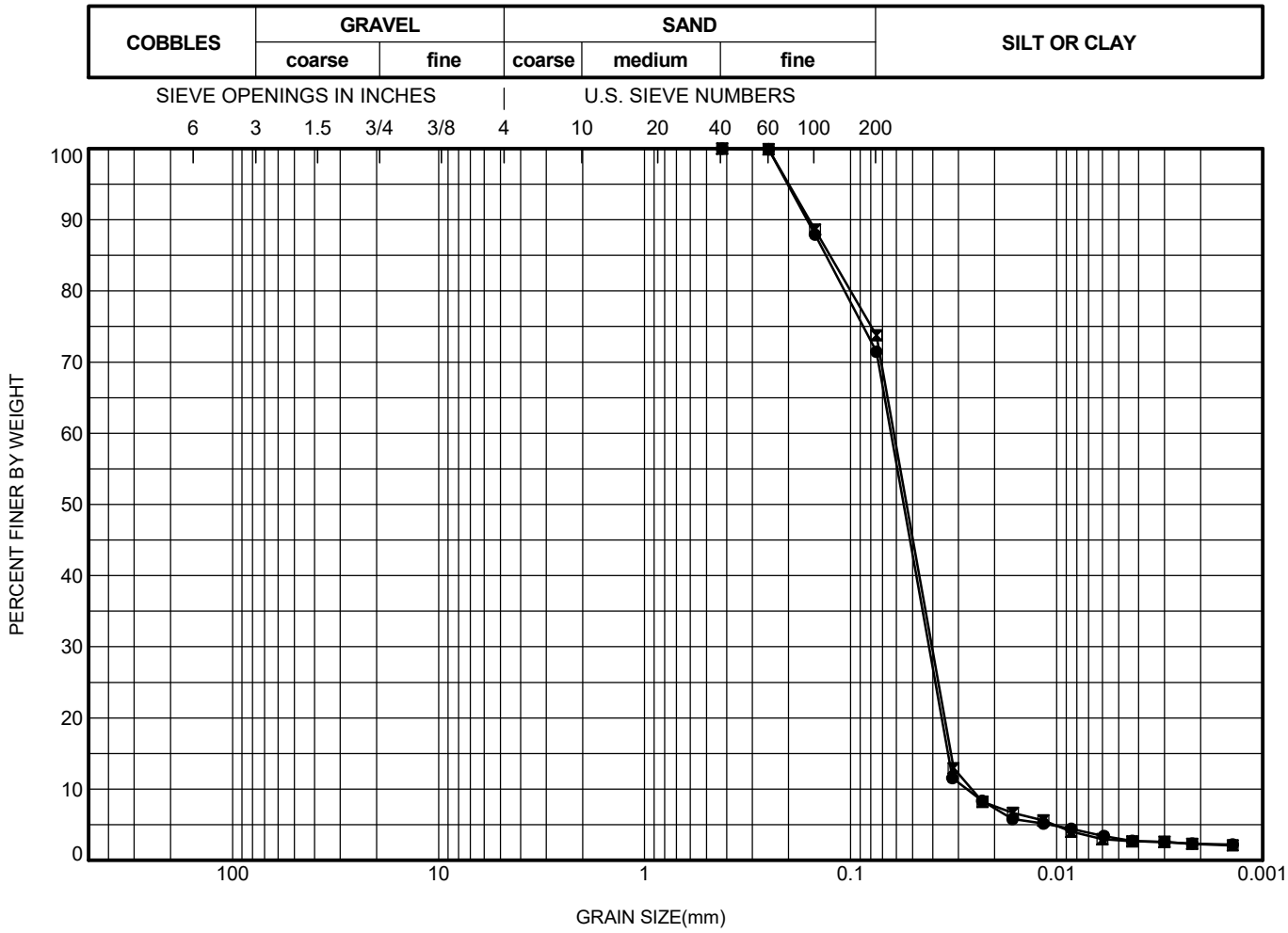
	HOLE	SAMPLE	DEPTH (m)	W%	W_L	W_P	PI	REMARKS / SAMPLE DESCRIPTION
●	TX11-CID	Fine	0.00					Before Testing (TX10/TX11)
☒	TX11-CID	Fine	0.00					After Testing

CU = COEFFICIENT OF UNIFORMITY = D60/D10 **PARTICLE SIZES, e.g. D85, in mm** **Tested by Wet Sieving Method (ASTM D1140 & D422)**

PROJECT NO.: A03355A01
PROJECT:
LOCATION:
FIGURE:
DRAWN BY: AX **CHECKED BY:** BY

KC_GRAIN_SIZE-SI A03355A01 TRIAXIAL TESTS PSDS.GPJ SIEVE.GDT 19-11-20

GRAIN SIZE DISTRIBUTION



	HOLE	DEPTH (m)	D85	D60	D50	D15	D10	CU	%GRAVEL	%SAND	%FINES
●	TX12-CID	0.00	0.132						0.0	28.5	71.5
☒	TX12-CID	0.00	0.126						0.0	26.2	73.8

	HOLE	SAMPLE	DEPTH (m)	W%	W_L	W_P	PI	REMARKS / SAMPLE DESCRIPTION
●	TX12-CID	Fine	0.00					Before Testing (TX12/TXBE05)
☒	TX12-CID	Fine	0.00					After Testing

CU = COEFFICIENT OF UNIFORMITY = D60/D10 **PARTICLE SIZES, e.g. D85, in mm** **Tested by Wet Sieving Method (ASTM D1140 & D422)**

PROJECT NO.: A03355A01

PROJECT:

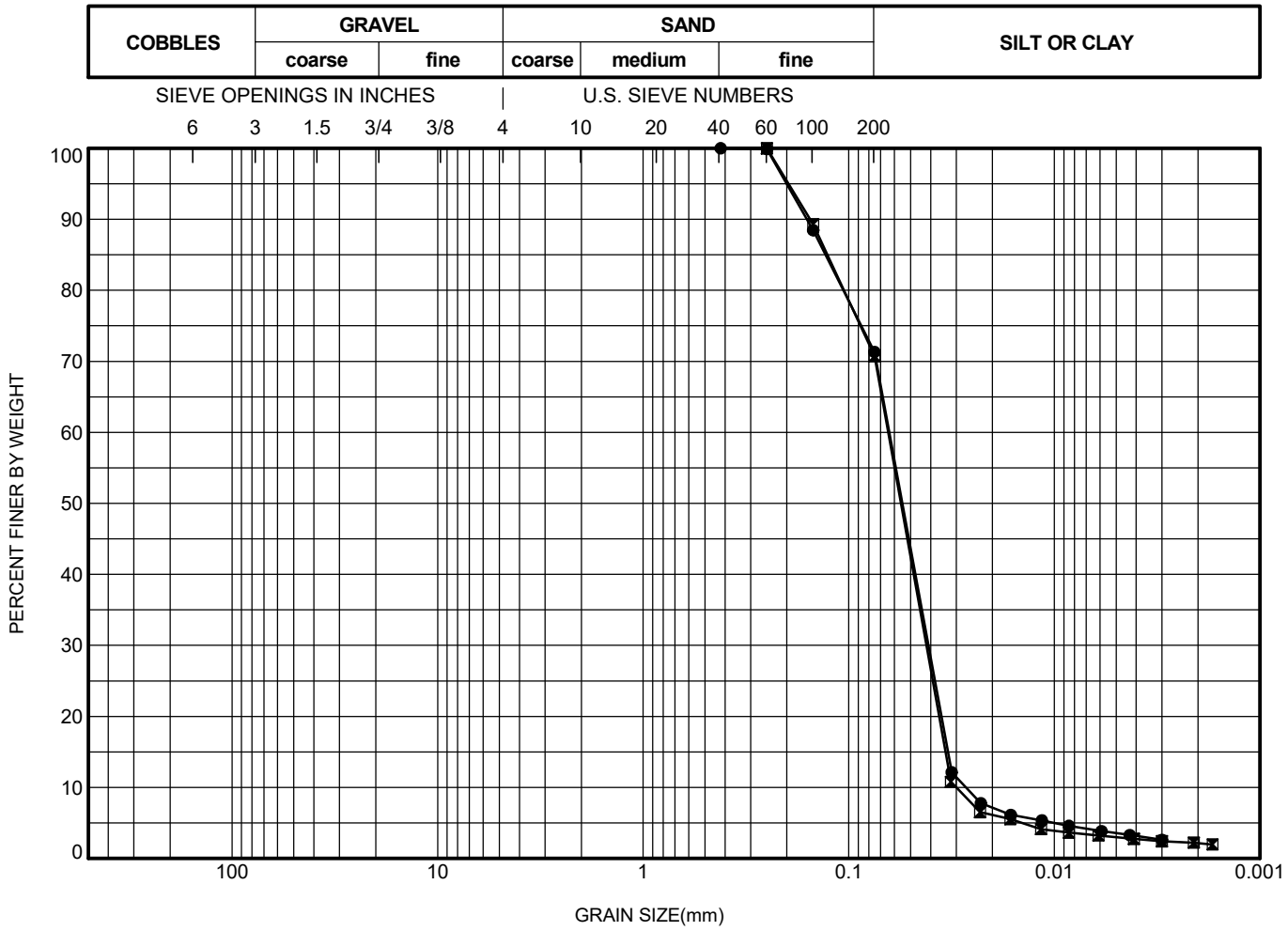
LOCATION:

FIGURE:

DRAWN BY: AX **CHECKED BY:** BY

KC_GRAIN_SIZE-SI A03355A01 TRIAXIAL TESTS PSDS.GPJ SIEVE.GDT 19-11-20

GRAIN SIZE DISTRIBUTION



	HOLE	DEPTH (m)	D85	D60	D50	D15	D10	CU	%GRAVEL	%SAND	%FINES
●	TX13-CID	0.00	0.130						0.0	28.7	71.3
⊠	TX13-CID	0.00	0.127						0.0	29.2	70.8

	HOLE	SAMPLE	DEPTH (m)	W%	W_L	W_P	PI	REMARKS / SAMPLE DESCRIPTION
●	TX13-CID	Fine	0.00					Before Testing (TX13/TXBE04)
⊠	TX13-CID	Fine	0.00					After Testing

CU = COEFFICIENT OF UNIFORMITY = D60/D10 **PARTICLE SIZES, e.g. D85, in mm** **Tested by Wet Sieving Method (ASTM D1140 & D422)**

PROJECT NO.: A03355A01

PROJECT:

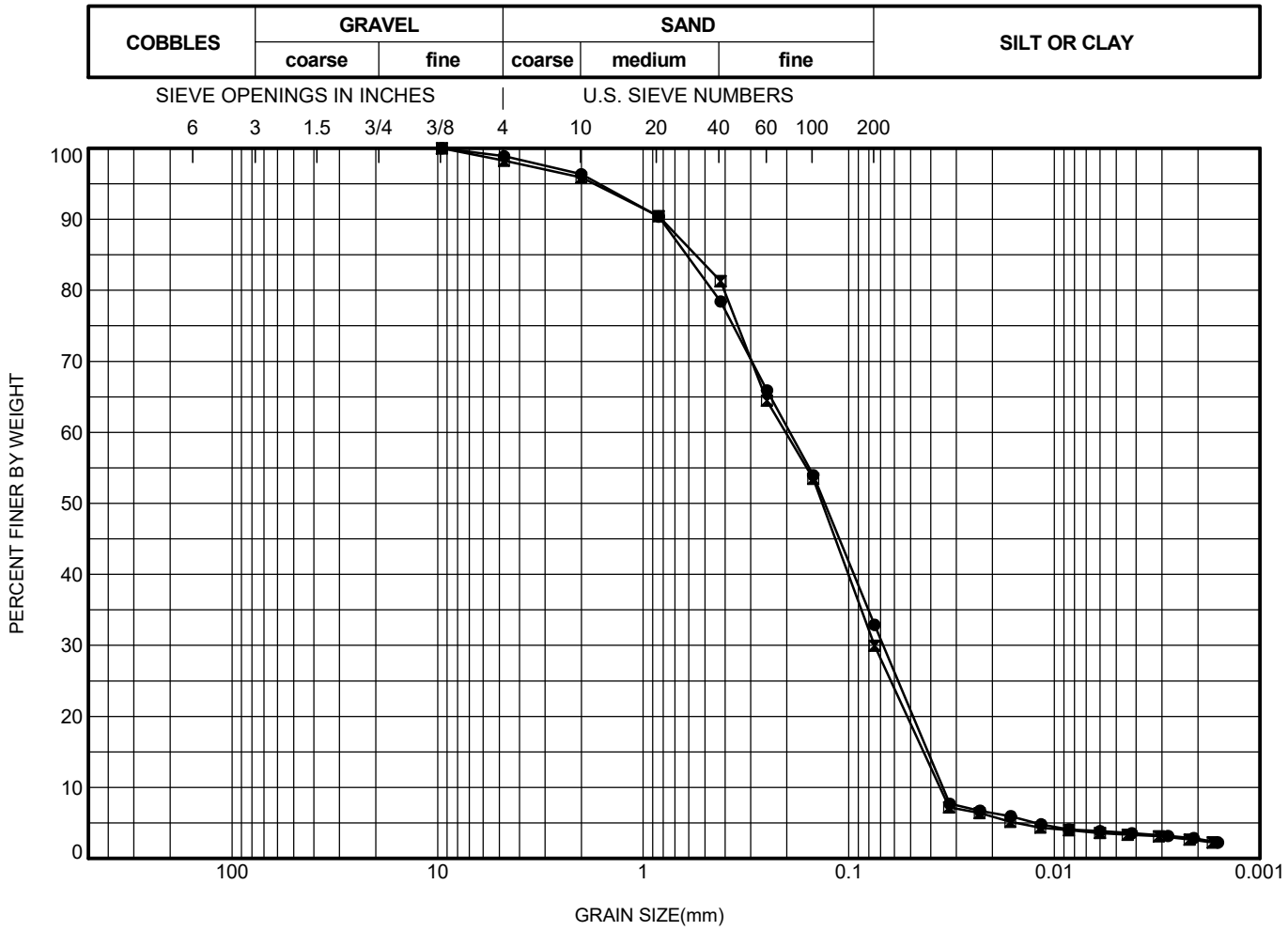
LOCATION:

FIGURE:

DRAWN BY: AX **CHECKED BY:** BY

KC_GRAIN_SIZE-SI A03355A01 TRIAXIAL TESTS PSDS.GPJ SIEVE.GDT 19-11-20

GRAIN SIZE DISTRIBUTION



	HOLE	DEPTH (m)	D85	D60	D50	D15	D10	CU	%GRAVEL	%SAND	%FINES
●	TX14-CID	0.00	0.615	0.194	0.131				1.1	66.0	32.9
⊠	TX14-CID	0.00	0.556	0.203	0.135				1.7	68.3	30.0

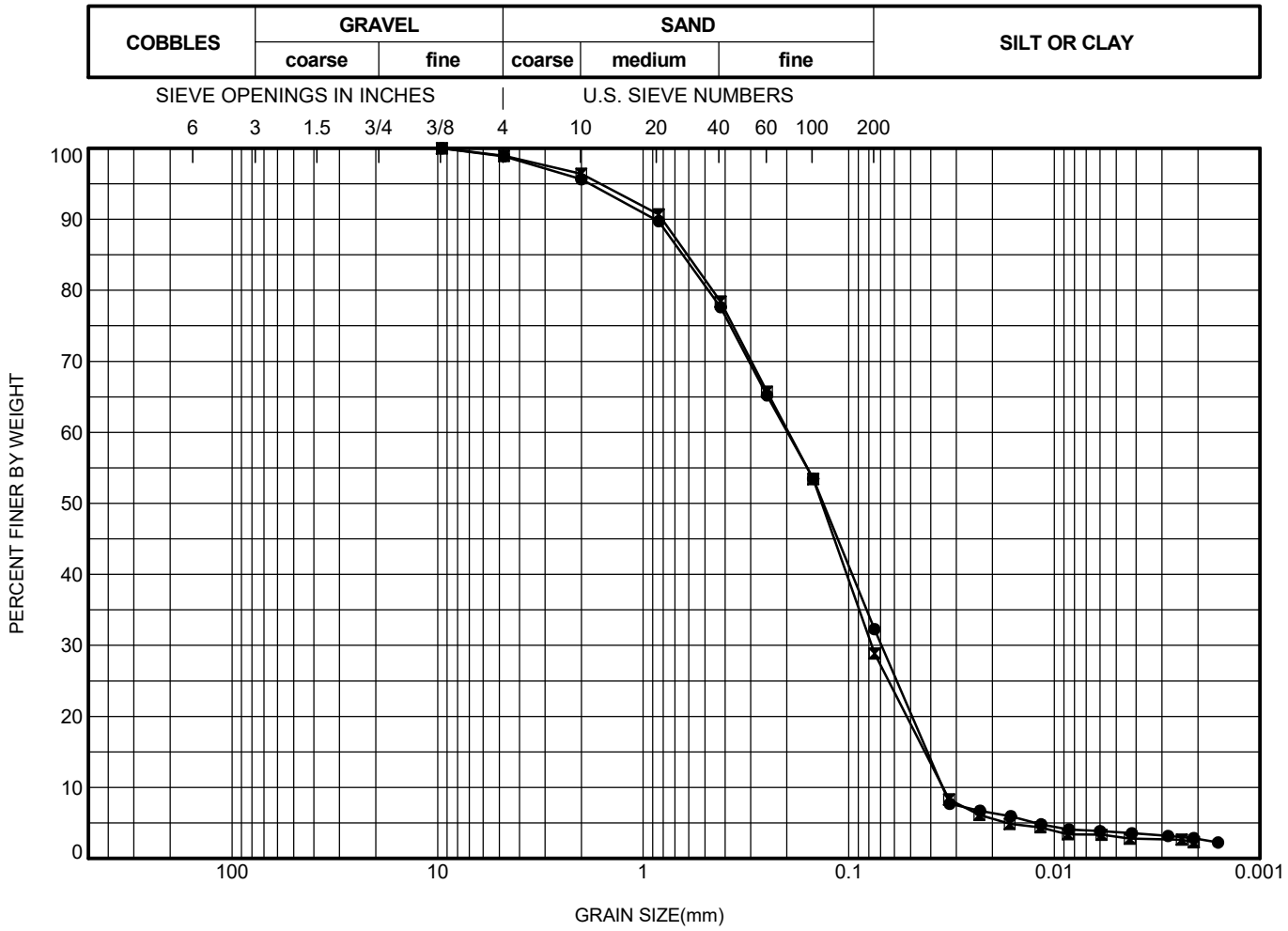
	HOLE	SAMPLE	DEPTH (m)	W%	W_L	W_P	PI	REMARKS / SAMPLE DESCRIPTION
●	TX14-CID	Coarse	0.00					Before Testing (TX14/TX17)
⊠	TX14-CID	Coarse	0.00					After Testing

CU = COEFFICIENT OF UNIFORMITY = D60/D10 **PARTICLE SIZES, e.g. D85, in mm** **Tested by Wet Sieving Method (ASTM D1140 & D422)**

PROJECT NO.: A03355A01
PROJECT:
LOCATION:
FIGURE:
DRAWN BY: AX **CHECKED BY:** BY

KC_GRAIN_SIZE-SI A03355A01 TRIAXIAL TESTS PSDS.GPJ SIEVE.GDT 19-11-20

GRAIN SIZE DISTRIBUTION



	HOLE	DEPTH (m)	D85	D60	D50	D15	D10	CU	%GRAVEL	%SAND	%FINES
●	TX15-CID	0.00	0.641	0.199	0.133				1.1	66.6	32.3
⊠	TX15-CID	0.00	0.610	0.196	0.135				1.1	70.1	28.9

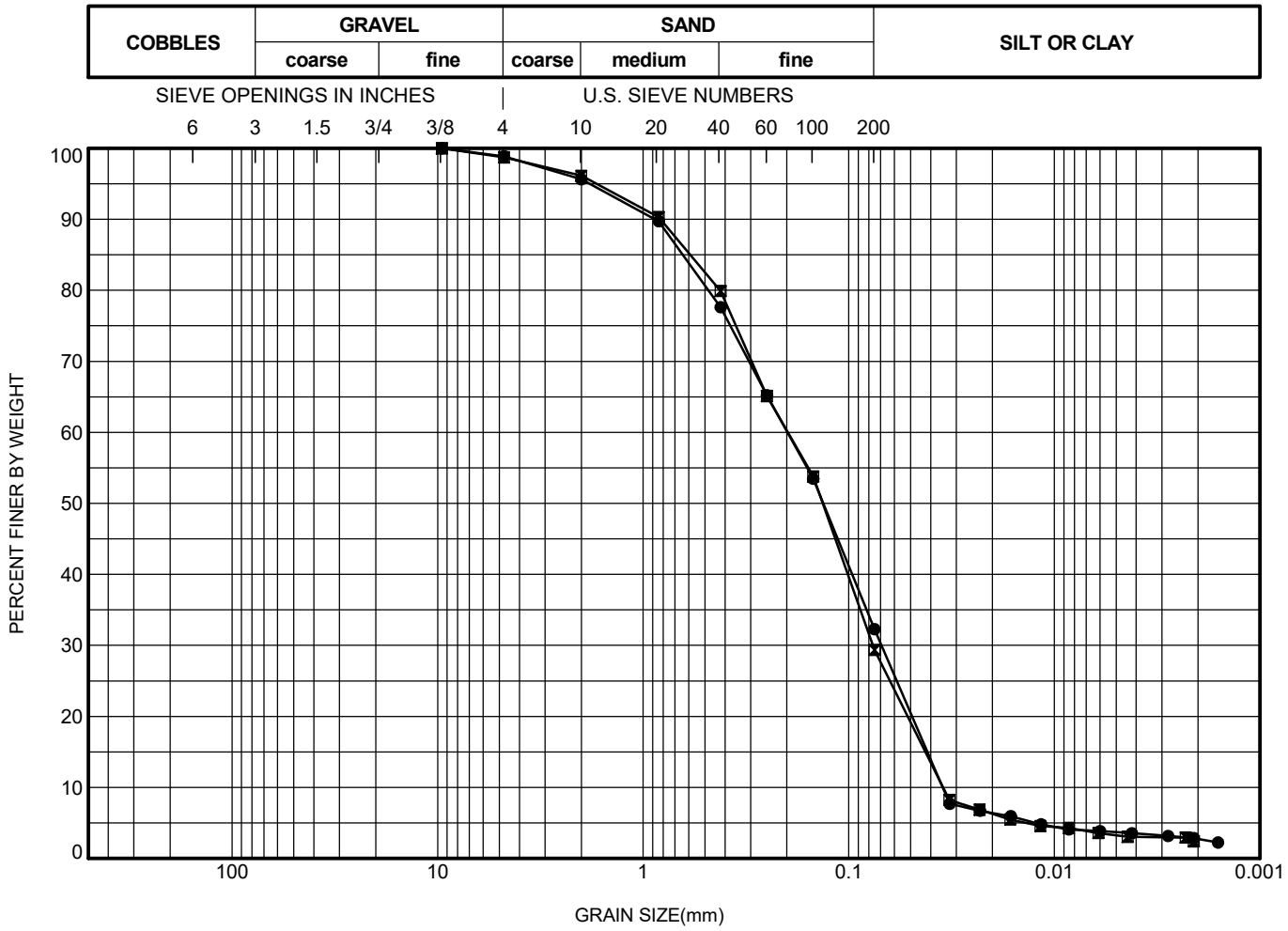
	HOLE	SAMPLE	DEPTH (m)	W%	W_L	W_P	PI	REMARKS / SAMPLE DESCRIPTION
●	TX15-CID	Coarse	0.00					Before Testing (TX15/TX16)
⊠	TX15-CID	Coarse	0.00					After Testing

CU = COEFFICIENT OF UNIFORMITY = D60/D10 **PARTICLE SIZES, e.g. D85, in mm** **Tested by Wet Sieving Method (ASTM D1140 & D422)**

PROJECT NO.: A03355A01
PROJECT:
LOCATION:
FIGURE:
DRAWN BY: AX **CHECKED BY:** BY

KC_GRAIN_SIZE-SI A03355A01 TRIAXIAL TESTS PSDS.GPJ SIEVE.GDT 19-11-20

GRAIN SIZE DISTRIBUTION



	HOLE	DEPTH (m)	D85	D60	D50	D15	D10	CU	%GRAVEL	%SAND	%FINES
●	TX16-CID	0.00	0.641	0.199	0.133				1.1	66.6	32.3
⊠	TX16-CID	0.00	0.590	0.198	0.134				1.3	69.4	29.4

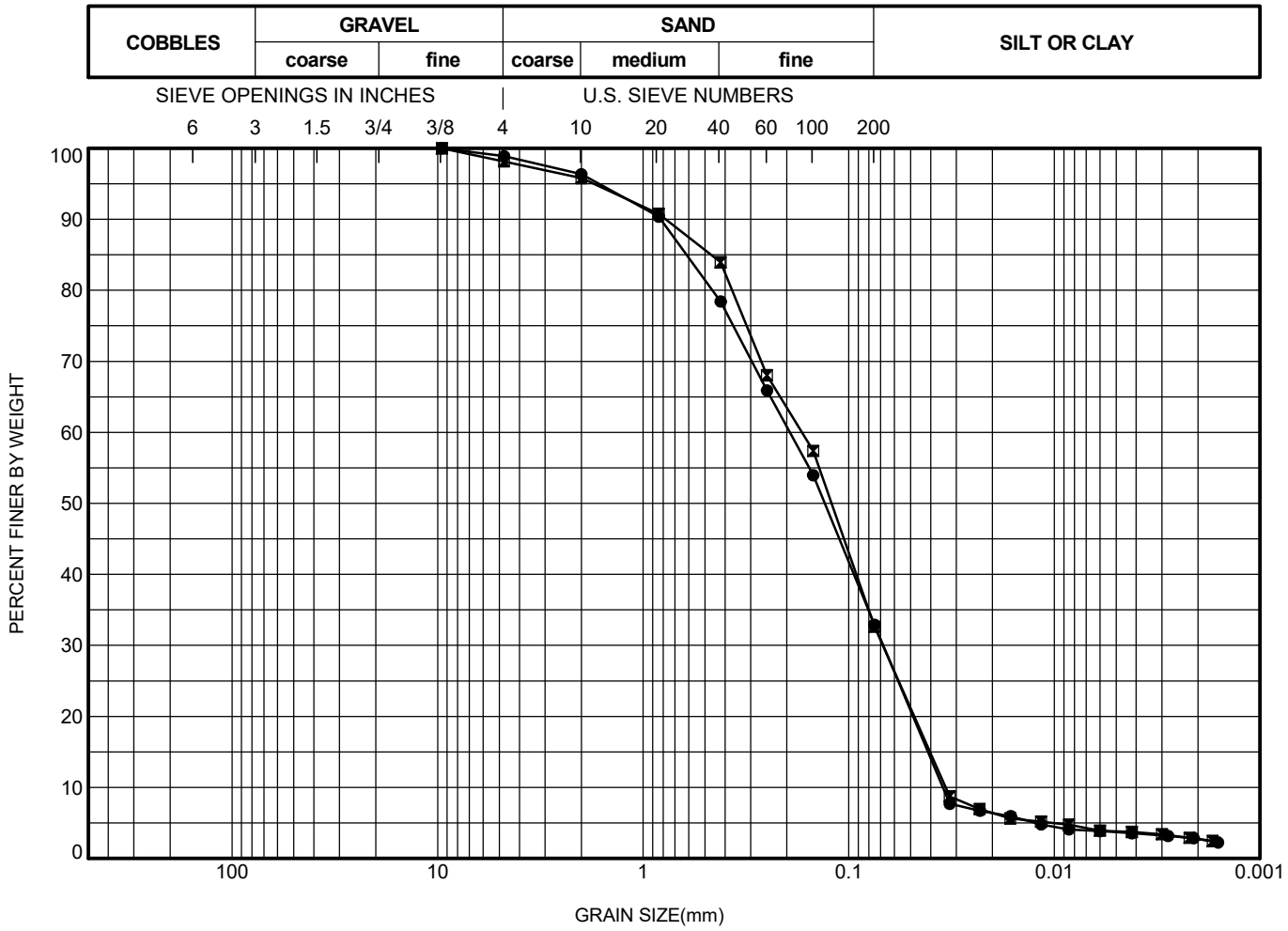
	HOLE	SAMPLE	DEPTH (m)	W%	W_L	W_P	PI	REMARKS / SAMPLE DESCRIPTION
●	TX16-CID	Coarse	0.00					Before Testing (TX15/TX16)
⊠	TX16-CID	Coarse	0.00					After Testing

CU = COEFFICIENT OF UNIFORMITY = D60/D10 **PARTICLE SIZES, e.g. D85, in mm** **Tested by Wet Sieving Method (ASTM D1140 & D422)**

PROJECT NO.: A03355A01
PROJECT:
LOCATION:
FIGURE:
DRAWN BY: AX **CHECKED BY:** BY

KC_GRAIN_SIZE-SI A03355A01 TRIAXIAL TESTS PSDS.GPJ SIEVE.GDT 19-11-20

GRAIN SIZE DISTRIBUTION



	HOLE	DEPTH (m)	D85	D60	D50	D15	D10	CU	%GRAVEL	%SAND	%FINES
●	TX17-CID	0.00	0.615	0.194	0.131				1.1	66.0	32.9
⊠	TX17-CID	0.00	0.467	0.169	0.121				1.8	65.5	32.6

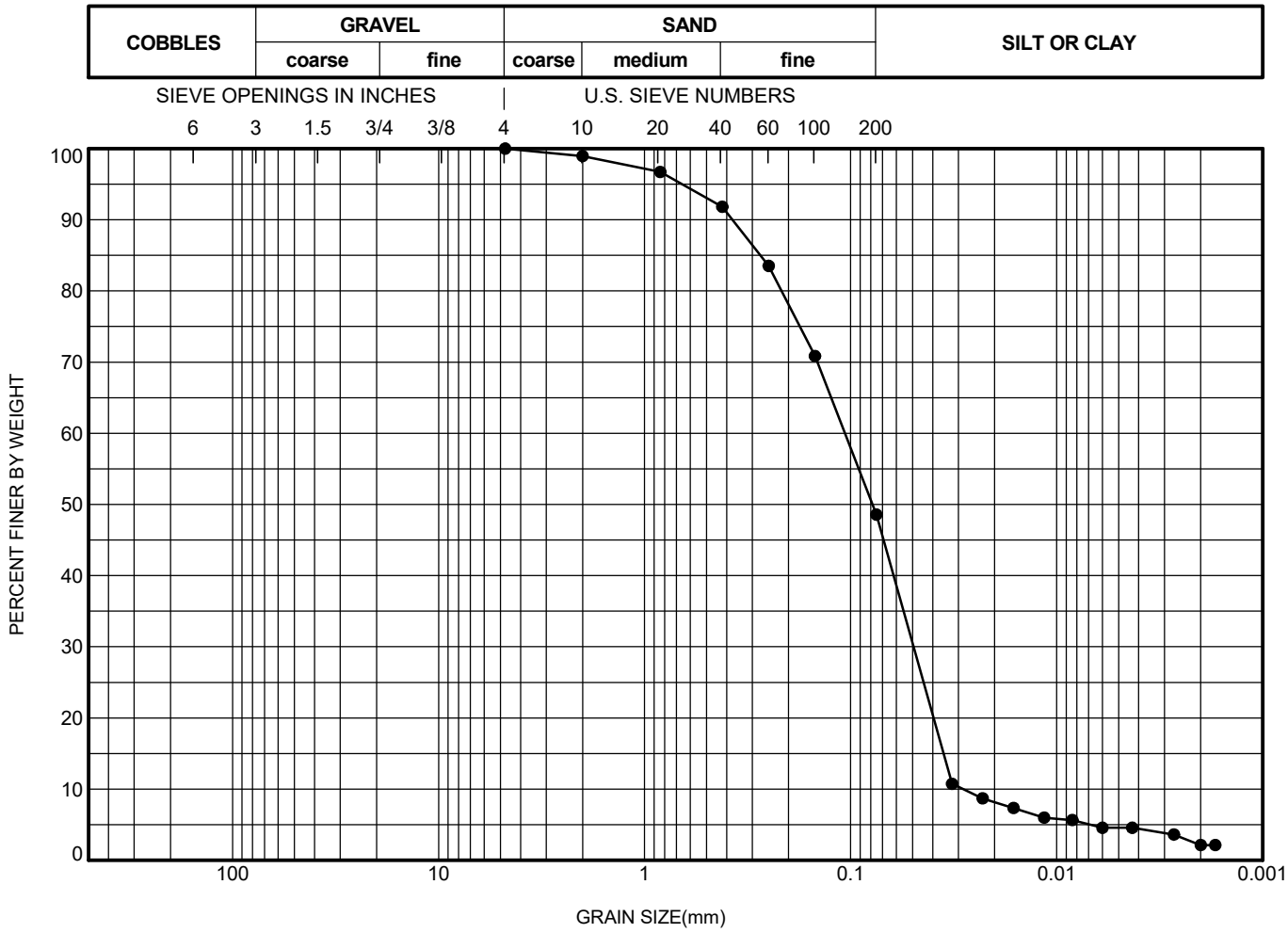
	HOLE	SAMPLE	DEPTH (m)	W%	W_L	W_P	PI	REMARKS / SAMPLE DESCRIPTION
●	TX17-CID	Coarse	0.00					Before Testing (TX14/TX17)
⊠	TX17-CID	Coarse	0.00					After Testing

CU = COEFFICIENT OF UNIFORMITY = D60/D10 **PARTICLE SIZES, e.g. D85, in mm** **Tested by Wet Sieving Method (ASTM D1140 & D422)**

PROJECT NO.: A03355A01
PROJECT:
LOCATION:
FIGURE:
DRAWN BY: AX **CHECKED BY:** BY

KC_GRAIN_SIZE-SI A03355A01 TRIAXIAL TESTS PSDS.GPJ SIEVE.GDT 19-11-20

GRAIN SIZE DISTRIBUTION



	HOLE	DEPTH (m)	D85	D60	D50	D15	D10	CU	%GRAVEL	%SAND	%FINES
●	TX18-CID	0.00	0.274	0.107	0.078				0.0	51.4	48.6

	HOLE	SAMPLE	DEPTH (m)	W%	W_L	W_P	PI	REMARKS / SAMPLE DESCRIPTION
●	TX18-CID	Average	0.00					Before Testing (TX18/TX19/TX20)

CU = COEFFICIENT OF UNIFORMITY = D60/D10 **PARTICLE SIZES, e.g. D85, in mm** **Tested by Wet Sieving Method (ASTM D1140 & D422)**

PROJECT NO.: A03355A01

PROJECT:

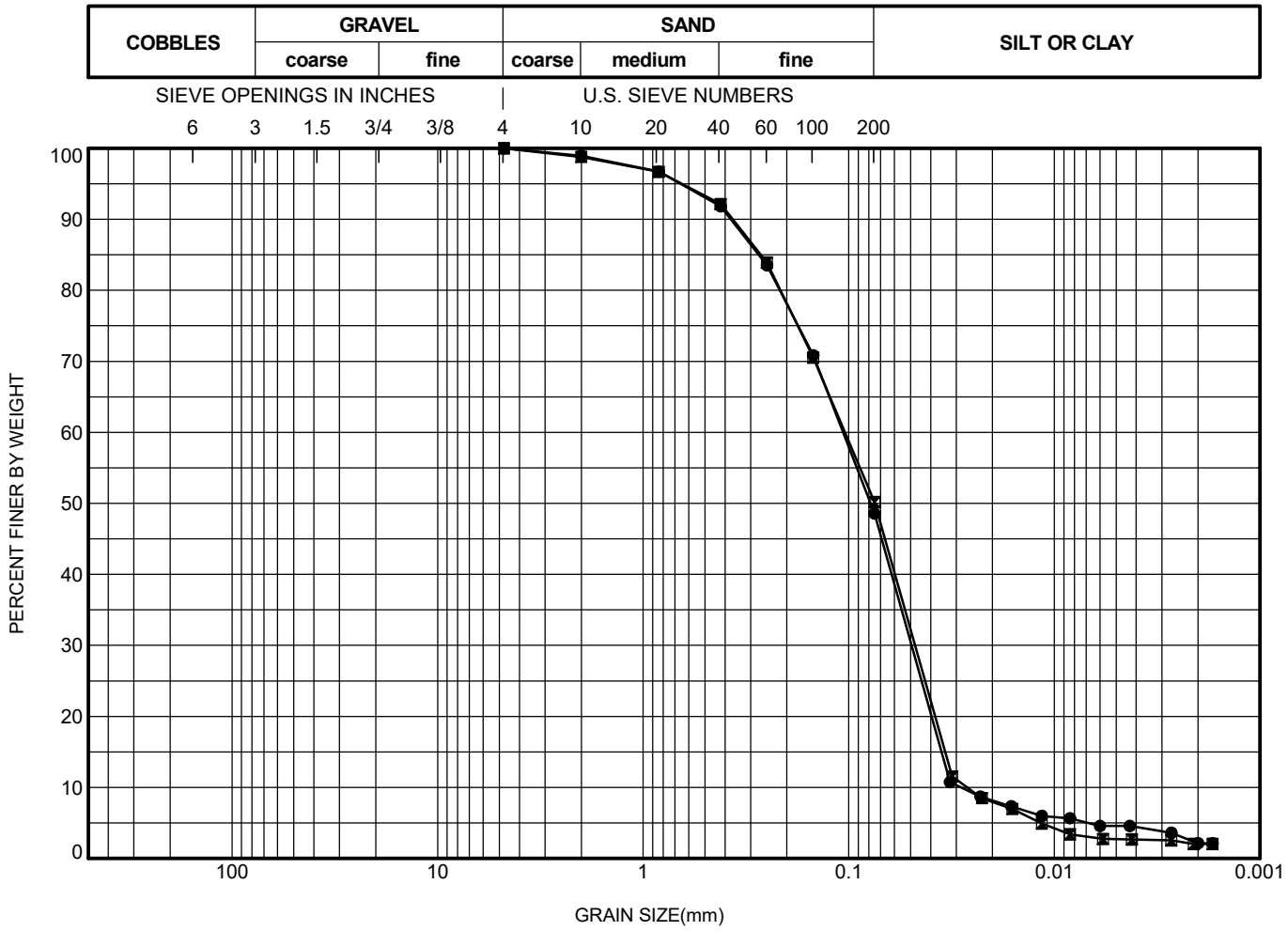
LOCATION:

FIGURE:

DRAWN BY: AX **CHECKED BY:** BY

KC_GRAIN_SIZE-SI A03355A01 TRIAXIAL TESTS PSDS.GPJ SIEVE.GDT 19-11-20

GRAIN SIZE DISTRIBUTION



	HOLE	DEPTH (m)	D85	D60	D50	D15	D10	CU	%GRAVEL	%SAND	%FINES
●	TX19-CID	0.00	0.274	0.107	0.078				0.0	51.4	48.6
☒	TX19-CID	0.00	0.268	0.104					0.0	49.8	50.2

	HOLE	SAMPLE	DEPTH (m)	W%	W_L	W_P	PI	REMARKS / SAMPLE DESCRIPTION
●	TX19-CID	Average	0.00					Before Testing (TX18/TX19/TX20)
☒	TX19-CID	Average	0.00					After Testing

CU = COEFFICIENT OF UNIFORMITY = D60/D10 **PARTICLE SIZES, e.g. D85, in mm** **Tested by Wet Sieving Method (ASTM D1140 & D422)**

PROJECT NO.: A03355A01

PROJECT:

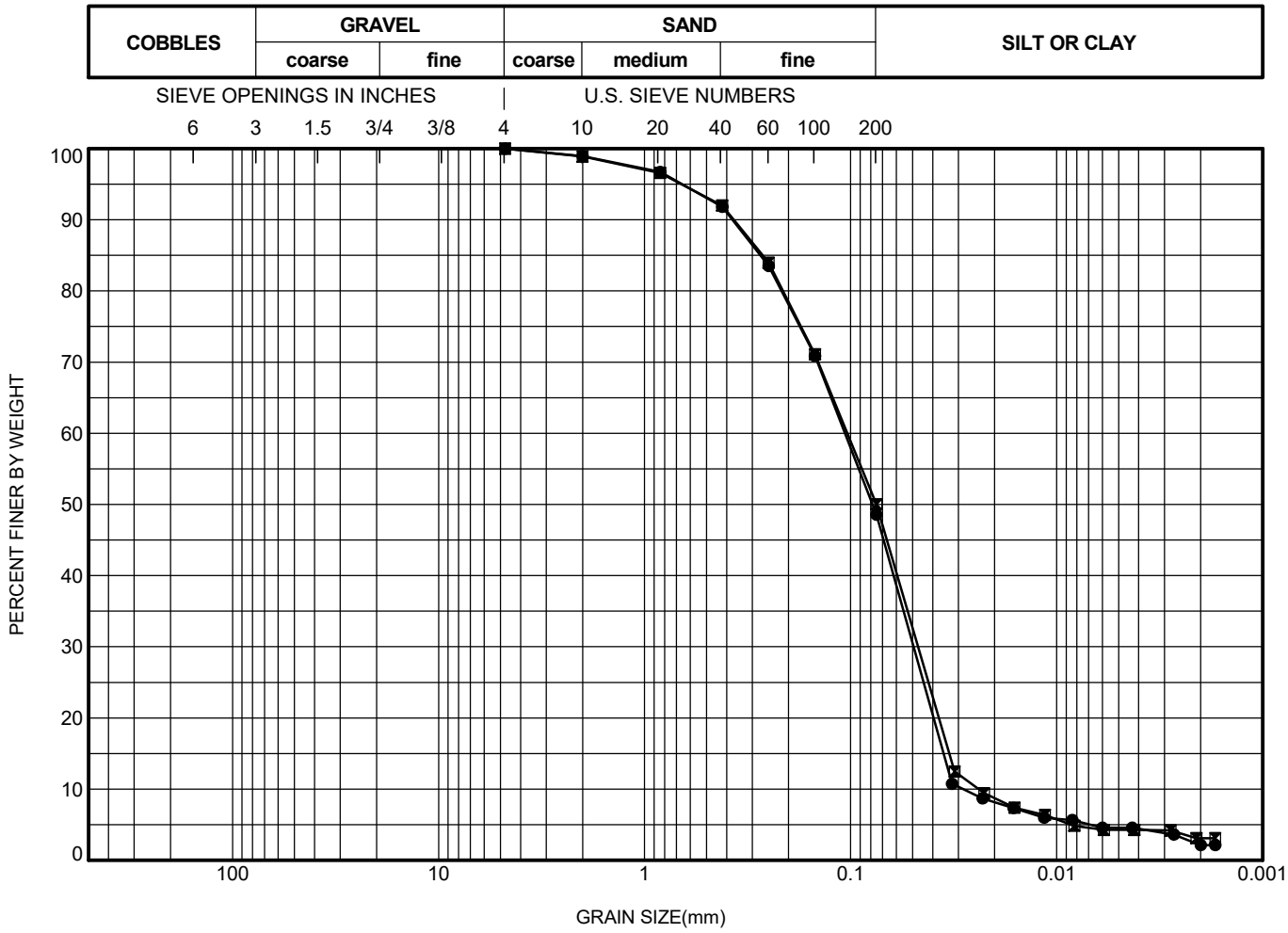
LOCATION:

FIGURE:

DRAWN BY: AX **CHECKED BY:** BY

KC_GRAIN_SIZE-SI A03355A01 TRIAXIAL TESTS PSDS.GPJ SIEVE.GDT 19-11-20

GRAIN SIZE DISTRIBUTION



	HOLE	DEPTH (m)	D85	D60	D50	D15	D10	CU	%GRAVEL	%SAND	%FINES
●	TX20-CID	0.00	0.274	0.107	0.078				0.0	51.4	48.6
⊠	TX20-CID	0.00	0.267	0.104					0.0	50.0	50.0

	HOLE	SAMPLE	DEPTH (m)	W%	W_L	W_P	PI	REMARKS / SAMPLE DESCRIPTION
●	TX20-CID	Average	0.00					Before Testing (TX18/TX19/TX20)
⊠	TX20-CID	Average	0.00					After Testing

CU = COEFFICIENT OF UNIFORMITY = D60/D10 **PARTICLE SIZES, e.g. D85, in mm** **Tested by Wet Sieving Method (ASTM D1140 & D422)**

PROJECT NO.: A03355A01

PROJECT:

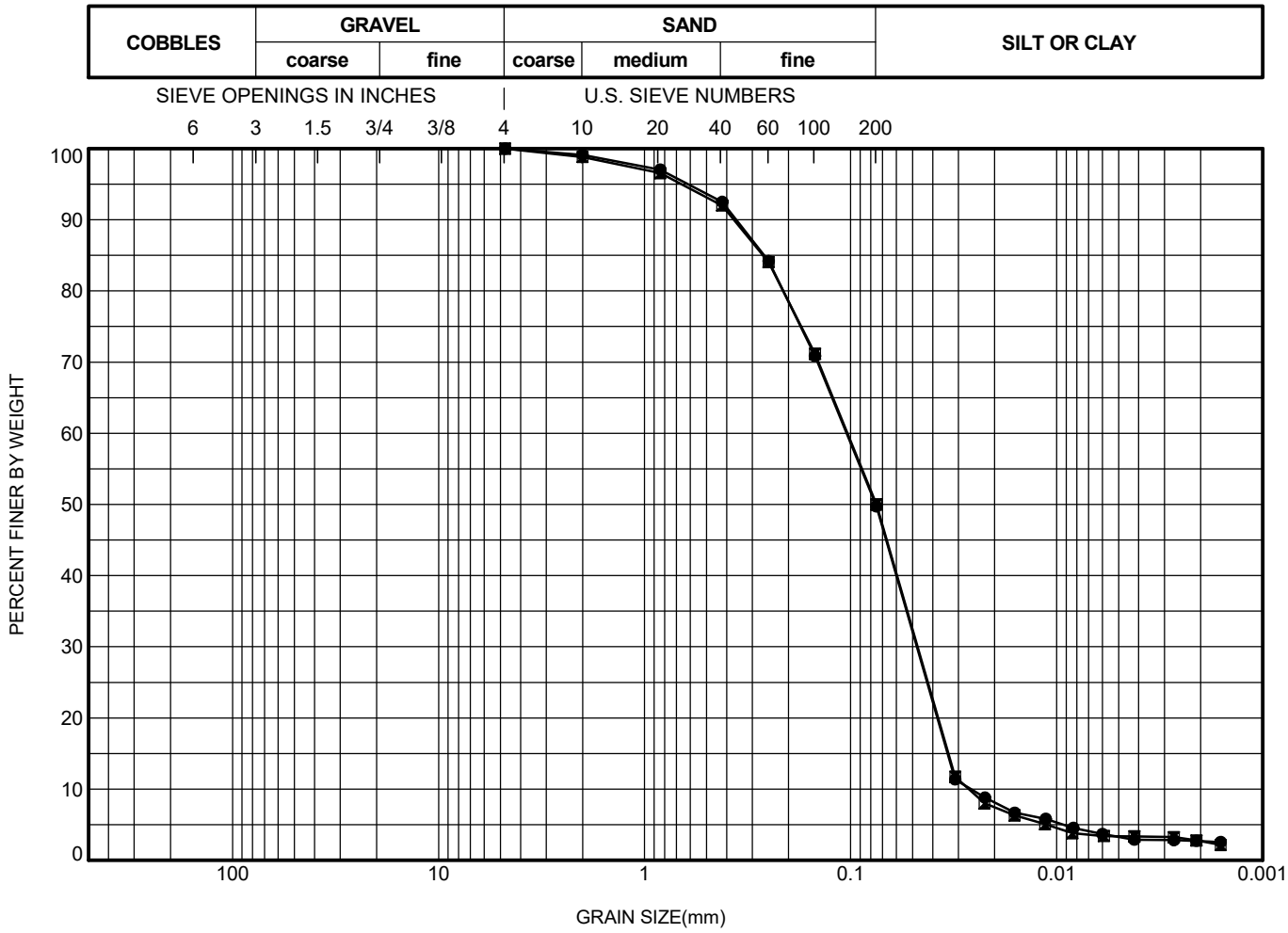
LOCATION:

FIGURE:

DRAWN BY: AX **CHECKED BY:** BY

KC_GRAIN_SIZE-SI A03355A01 TRIAXIAL TESTS PSDS.GPJ SIEVE.GDT 19-11-20

GRAIN SIZE DISTRIBUTION



	HOLE	DEPTH (m)	D85	D60	D50	D15	D10	CU	%GRAVEL	%SAND	%FINES
●	TX21-CID	0.00	0.263	0.105	0.076				0.0	50.3	49.7
☒	TX21-CID	0.00	0.266	0.104	0.075				0.0	50.0	50.0

	HOLE	SAMPLE	DEPTH (m)	W%	W_L	W_P	PI	REMARKS / SAMPLE DESCRIPTION
●	TX21-CID	Average	0.00					Before Testing
☒	TX21-CID	Average	0.00					After Testing

CU = COEFFICIENT OF UNIFORMITY = D60/D10 **PARTICLE SIZES, e.g. D85, in mm** **Tested by Wet Sieving Method (ASTM D1140 & D422)**

PROJECT NO.: A03355A01

PROJECT:

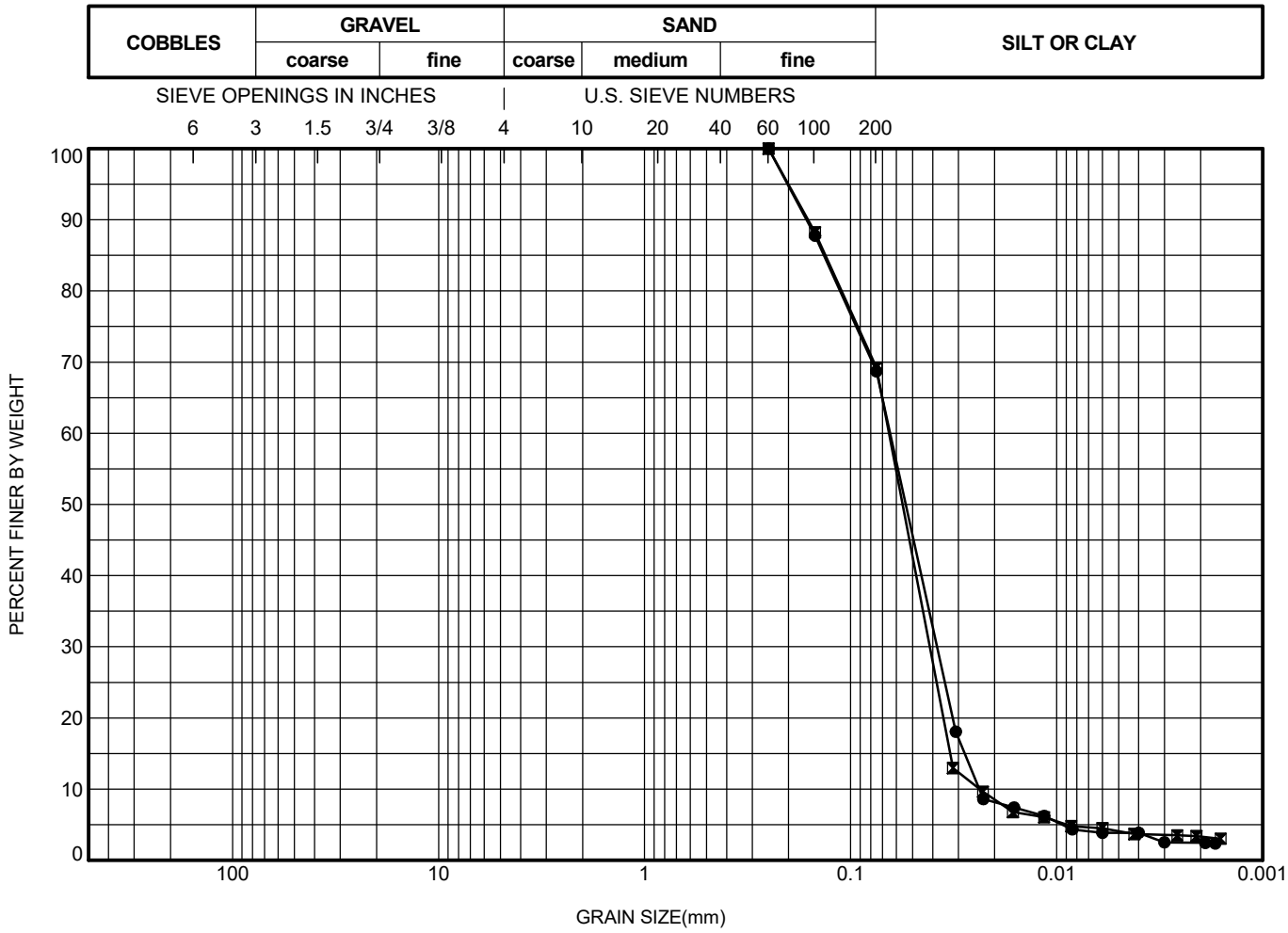
LOCATION:

FIGURE:

DRAWN BY: AX **CHECKED BY:** BY

KC_GRAIN_SIZE-SI A03355A01 TRIAXIAL TESTS PSDS.GPJ SIEVE.GDT 19-11-20

GRAIN SIZE DISTRIBUTION



	HOLE	DEPTH (m)	D85	D60	D50	D15	D10	CU	%GRAVEL	%SAND	%FINES
●	TX22-CID	0.00	0.135						0.0	31.3	68.7
⊠	TX22-CID	0.00	0.133						0.0	30.8	69.2

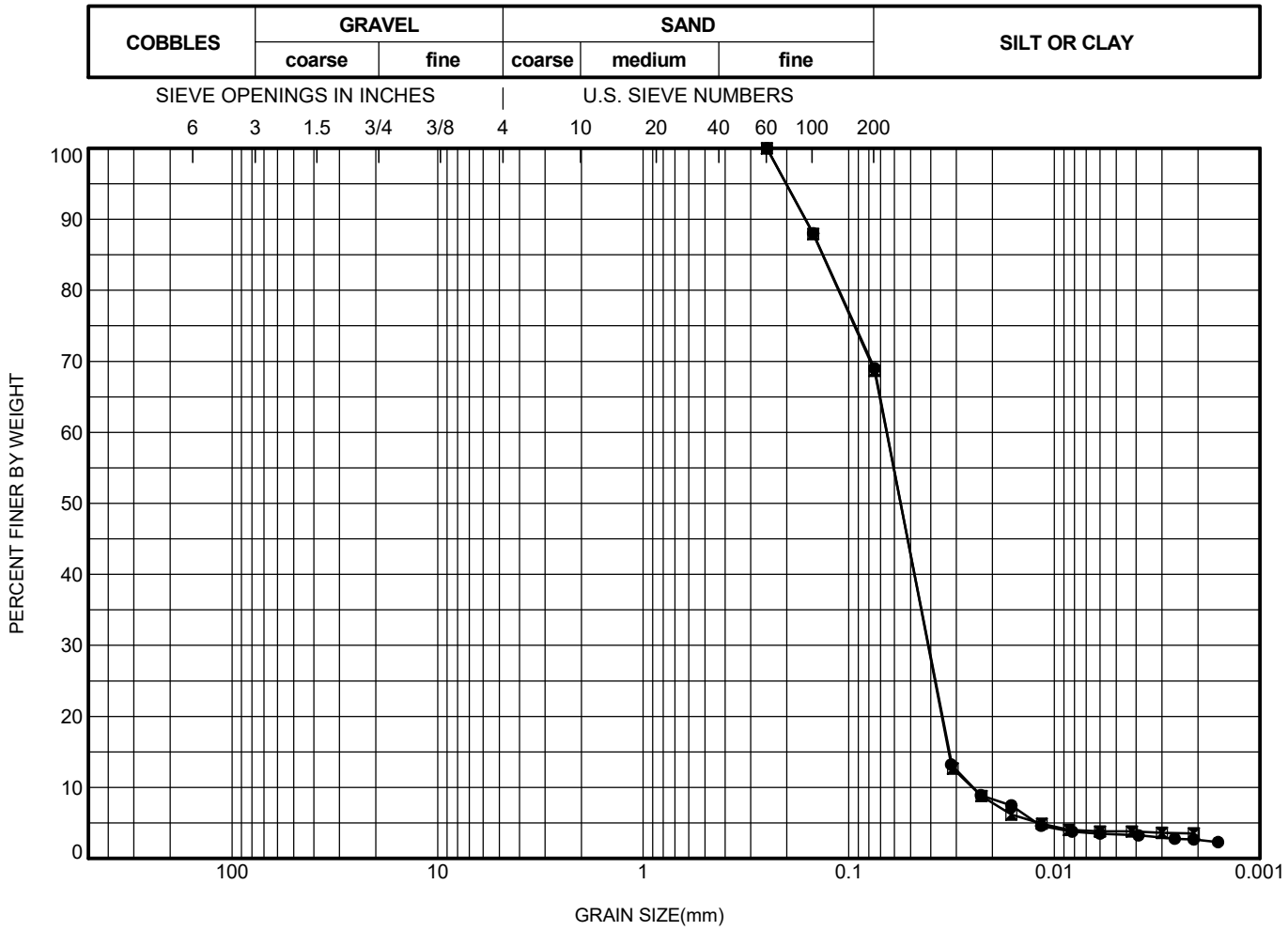
	HOLE	SAMPLE	DEPTH (m)	W%	W_L	W_P	PI	REMARKS / SAMPLE DESCRIPTION
●	TX22-CID	Fine	0.00					Before Testing
⊠	TX22-CID	Fine	0.00					After Testing

CU = COEFFICIENT OF UNIFORMITY = D60/D10 **PARTICLE SIZES, e.g. D85, in mm** **Tested by Wet Sieving Method (ASTM D1140 & D422)**

PROJECT NO.: A03355A01
PROJECT:
LOCATION:
FIGURE:
DRAWN BY: AX **CHECKED BY:** BY

KC_GRAIN_SIZE-SI A03355A01 TRIAXIAL TESTS PSDS.GPJ SIEVE.GDT 19-11-20

GRAIN SIZE DISTRIBUTION



	HOLE	DEPTH (m)	D85	D60	D50	D15	D10	CU	%GRAVEL	%SAND	%FINES
●	TX23-CID	0.00	0.134						0.0	31.0	69.0
⊠	TX23-CID	0.00	0.134						0.0	31.3	68.7

	HOLE	SAMPLE	DEPTH (m)	W%	W_L	W_P	PI	REMARKS / SAMPLE DESCRIPTION
●	TX23-CID	Fine	0.00					Before Testing
⊠	TX23-CID	Fine	0.00					After Testing

CU = COEFFICIENT OF UNIFORMITY = D60/D10 **PARTICLE SIZES, e.g. D85, in mm** **Tested by Wet Sieving Method (ASTM D1140 & D422)**

PROJECT NO.: A03355A01

PROJECT:

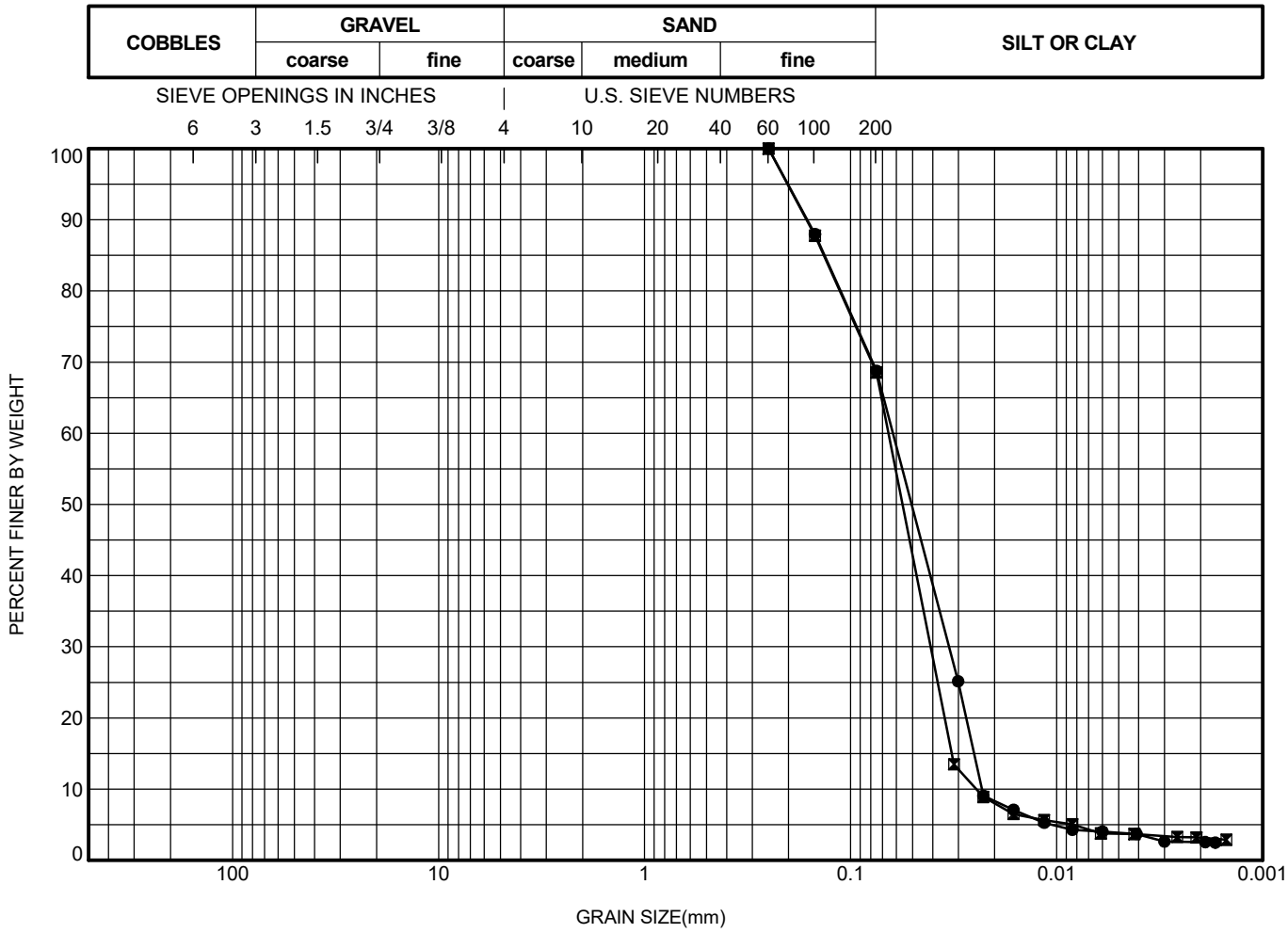
LOCATION:

FIGURE:

DRAWN BY: AX **CHECKED BY:** BY

KC_GRAIN_SIZE-SI A03355A01 TRIAXIAL TESTS PSDS.GPJ SIEVE.GDT 19-11-20

GRAIN SIZE DISTRIBUTION



	HOLE	DEPTH (m)	D85	D60	D50	D15	D10	CU	%GRAVEL	%SAND	%FINES
●	TX24-CID	0.00	0.134						0.0	31.2	68.8
⊠	TX24-CID	0.00	0.135						0.0	31.5	68.5

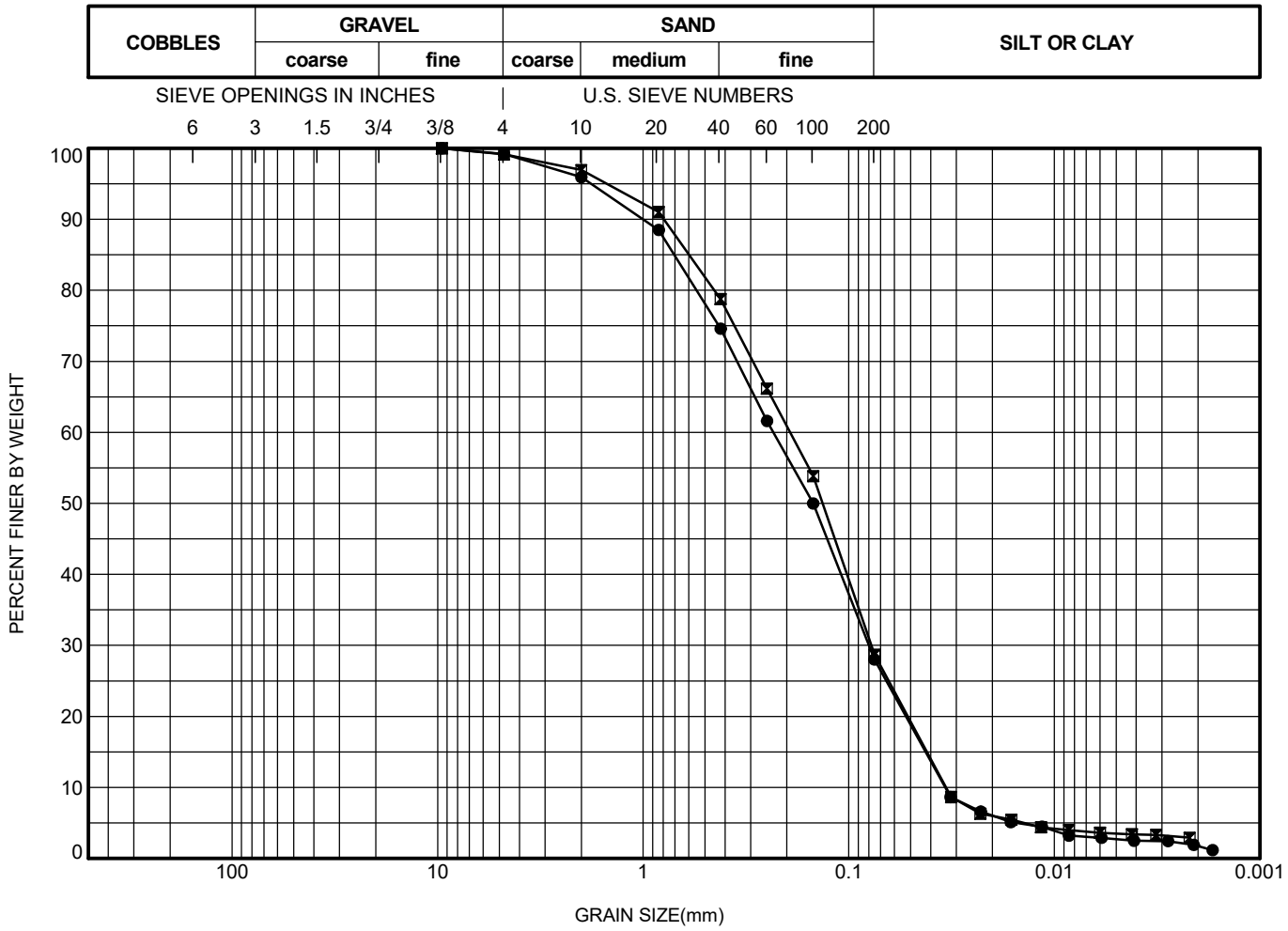
	HOLE	SAMPLE	DEPTH (m)	W%	W_L	W_P	PI	REMARKS / SAMPLE DESCRIPTION
●	TX24-CID	Fine	0.00					Before Testing
⊠	TX24-CID	Fine	0.00		13	13	NP	After Testing

CU = COEFFICIENT OF UNIFORMITY = D60/D10 **PARTICLE SIZES, e.g. D85, in mm** **Tested by Wet Sieving Method (ASTM D1140 & D422)**

PROJECT NO.: A03355A01
PROJECT:
LOCATION:
FIGURE:
DRAWN BY: AX **CHECKED BY:** BY

KC_GRAIN_SIZE-SI A03355A01 TRIAXIAL TESTS PSDS.GPJ SIEVE.GDT 19-11-20

GRAIN SIZE DISTRIBUTION



	HOLE	DEPTH (m)	D85	D60	D50	D15	D10	CU	%GRAVEL	%SAND	%FINES
●	TX25-CAU	0.00	0.705	0.233	0.149				0.8	71.2	28.0
⊠	TX25-CAU	0.00	0.597	0.193	0.134				0.9	70.4	28.7

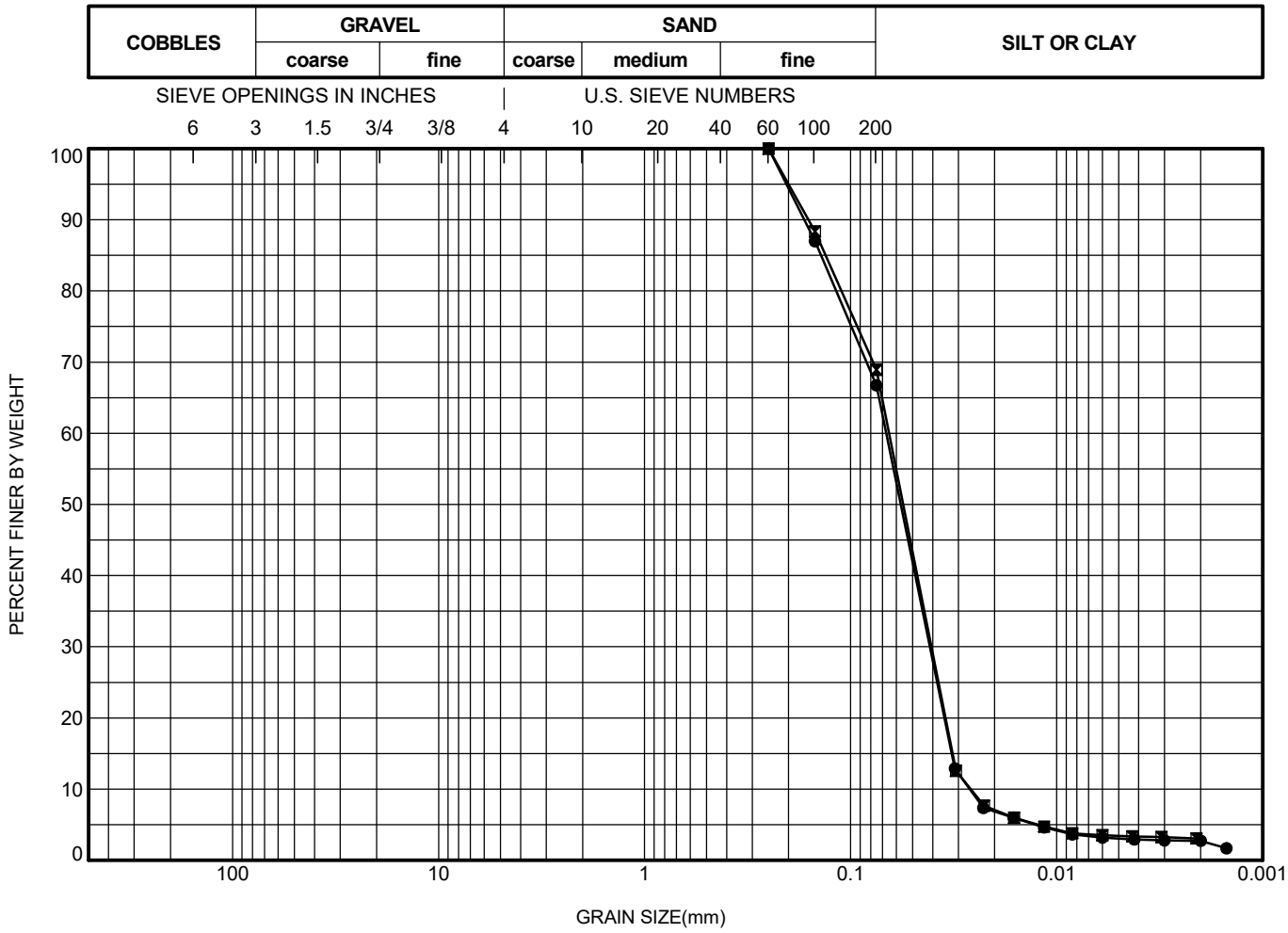
	HOLE	SAMPLE	DEPTH (m)	W%	W_L	W_P	PI	REMARKS / SAMPLE DESCRIPTION
●	TX25-CAU	Coarse	0.00					Before Testing (TX25/TXDW02)
⊠	TX25-CAU	Coarse	0.00					After Testing

CU = COEFFICIENT OF UNIFORMITY = D60/D10 **PARTICLE SIZES, e.g. D85, in mm** **Tested by Wet Sieving Method (ASTM D1140 & D422)**

PROJECT NO.: A03355A01
PROJECT:
LOCATION:
FIGURE:
DRAWN BY: AX **CHECKED BY:** BY

KC_GRAIN_SIZE-SI A03355A01 TRIAXIAL TESTS PSDS.GPJ SIEVE.GDT 19-11-20

GRAIN SIZE DISTRIBUTION



	HOLE	DEPTH (m)	D85	D60	D50	D15	D10	CU	%GRAVEL	%SAND	%FINES
●	TX26-CAU	0.00	0.139						0.0	33.3	66.7
⊠	TX26-CAU	0.00	0.132						0.0	31.1	68.9

	HOLE	SAMPLE	DEPTH (m)	W%	W_L	W_P	PI	REMARKS / SAMPLE DESCRIPTION
●	TX26-CAU	Fine	0.00					Before Testing
⊠	TX26-CAU	Fine	0.00					After Testing

CU = COEFFICIENT OF UNIFORMITY = D60/D10 **PARTICLE SIZES, e.g. D85, in mm** **Tested by Wet Sieving Method (ASTM D1140 & D422)**

PROJECT NO.: A03355A01

PROJECT:

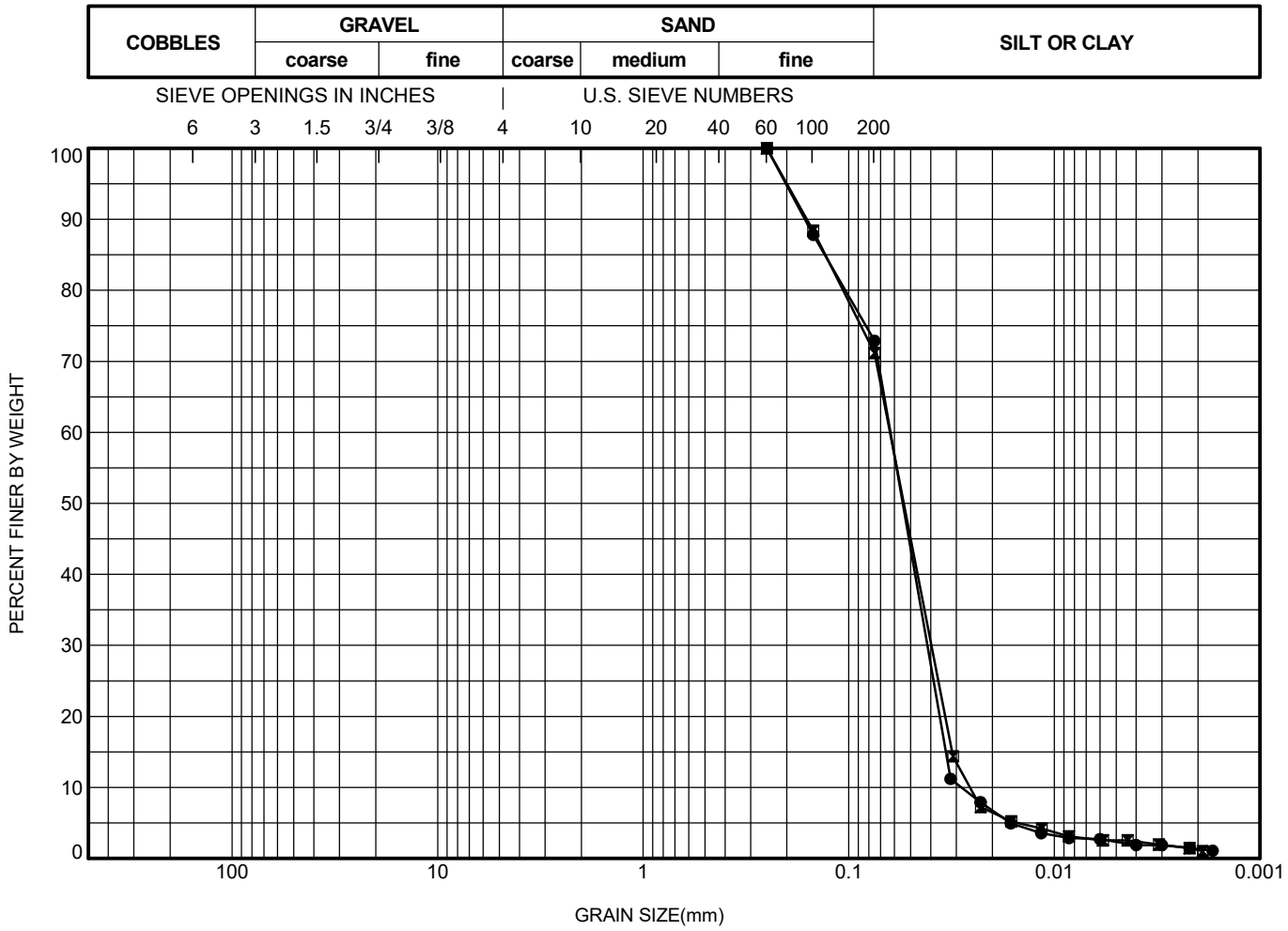
LOCATION:

FIGURE:

DRAWN BY: AX **CHECKED BY:** BY

KC_GRAIN_SIZE-SI A03355A01 TRIAXIAL TESTS PSDS.GPJ SIEVE.GDT 19-11-20

GRAIN SIZE DISTRIBUTION



	HOLE	DEPTH (m)	D85	D60	D50	D15	D10	CU	%GRAVEL	%SAND	%FINES
●	TX27-CAU	0.00	0.131						0.0	27.1	72.9
⊠	TX27-CAU	0.00	0.130						0.0	28.8	71.2

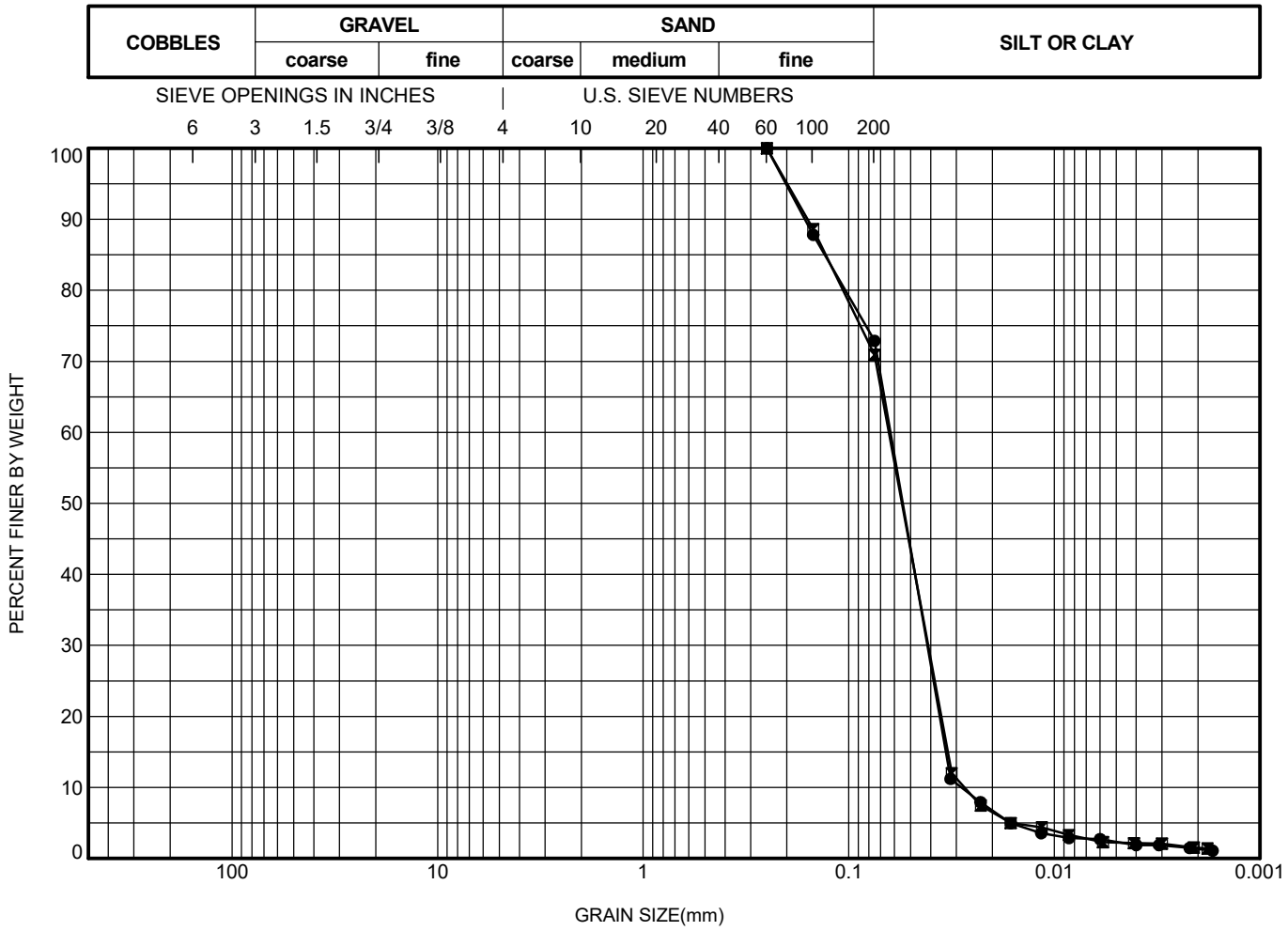
	HOLE	SAMPLE	DEPTH (m)	W%	W_L	W_P	PI	REMARKS / SAMPLE DESCRIPTION
●	TX27-CAU	Fine	0.00					Before Testing (TX27/TX28)
⊠	TX27-CAU	Fine	0.00					After Testing

CU = COEFFICIENT OF UNIFORMITY = D60/D10 **PARTICLE SIZES, e.g. D85, in mm** **Tested by Wet Sieving Method (ASTM D1140 & D422)**

PROJECT NO.: A03355A01
PROJECT:
LOCATION:
FIGURE:
DRAWN BY: AX **CHECKED BY:** BY

KC_GRAIN_SIZE-SI A03355A01 TRIAXIAL TESTS PSDS.GPJ SIEVE.GDT 19-11-20

GRAIN SIZE DISTRIBUTION



	HOLE	DEPTH (m)	D85	D60	D50	D15	D10	CU	%GRAVEL	%SAND	%FINES
●	TX28-CAU	0.00	0.131						0.0	27.1	72.9
⊠	TX28-CAU	0.00	0.130						0.0	29.1	70.9

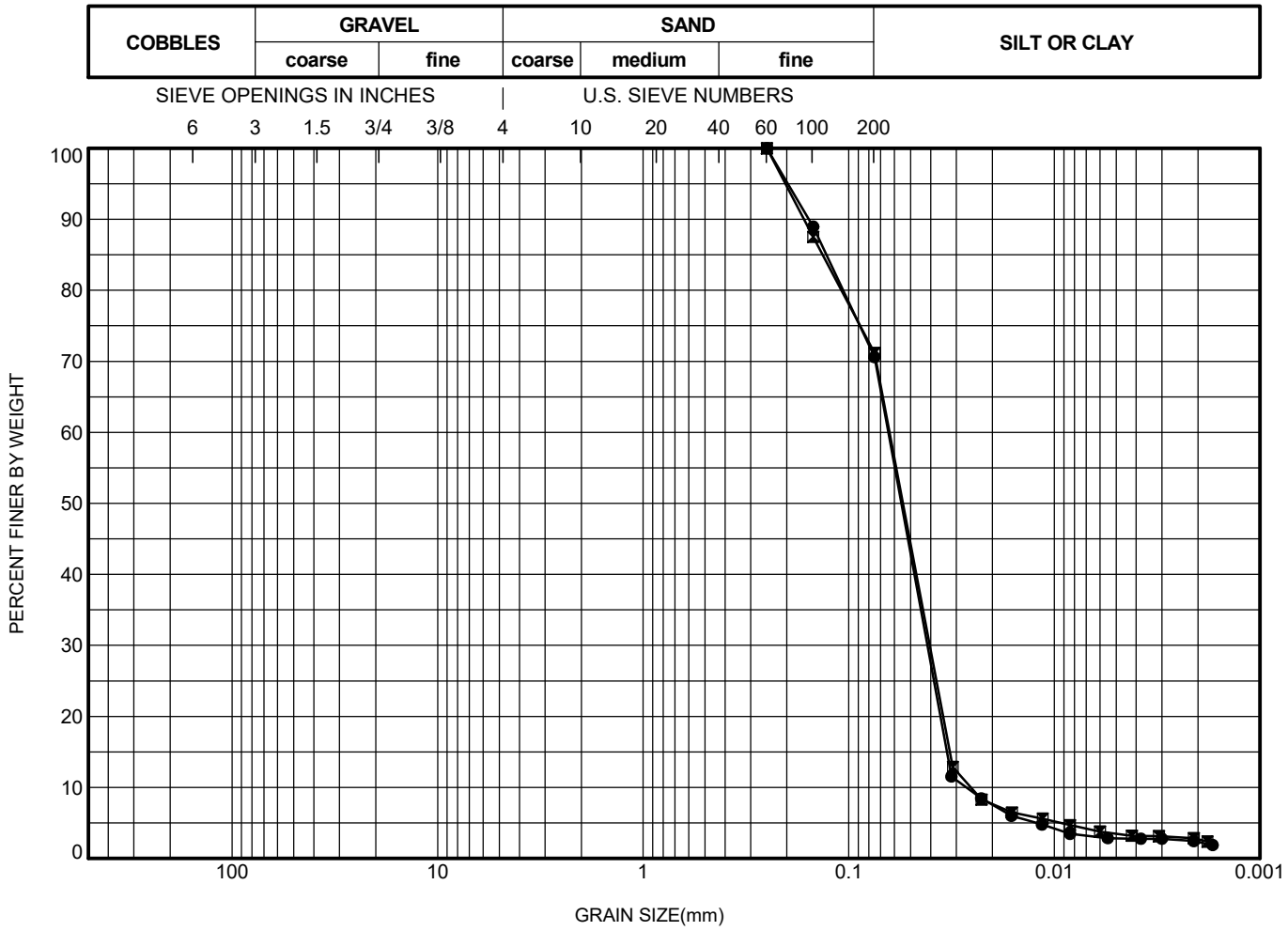
	HOLE	SAMPLE	DEPTH (m)	W%	W_L	W_P	PI	REMARKS / SAMPLE DESCRIPTION
●	TX28-CAU	Fine	0.00					Before Testing (TX27/TX28)
⊠	TX28-CAU	Fine	0.00					After Testing

CU = COEFFICIENT OF UNIFORMITY = D60/D10 **PARTICLE SIZES, e.g. D85, in mm** **Tested by Wet Sieving Method (ASTM D1140 & D422)**

PROJECT NO.: A03355A01
PROJECT:
LOCATION:
FIGURE:
DRAWN BY: AX **CHECKED BY:** BY

KC_GRAIN_SIZE-SI A03355A01 TRIAXIAL TESTS PSDS.GPJ SIEVE.GDT 19-11-20

GRAIN SIZE DISTRIBUTION



	HOLE	DEPTH (m)	D85	D60	D50	D15	D10	CU	%GRAVEL	%SAND	%FINES
●	TX29-CAU	0.00	0.128						0.0	29.4	70.6
⊠	TX29-CAU	0.00	0.134						0.0	28.8	71.2

	HOLE	SAMPLE	DEPTH (m)	W%	W_L	W_P	PI	REMARKS / SAMPLE DESCRIPTION
●	TX29-CAU	Fine	0.00					Before Testing (TX29/TXBE10)
⊠	TX29-CAU	Fine	0.00					After Testing

CU = COEFFICIENT OF UNIFORMITY = D60/D10 **PARTICLE SIZES, e.g. D85, in mm** **Tested by Wet Sieving Method (ASTM D1140 & D422)**

PROJECT NO.: A03355A01

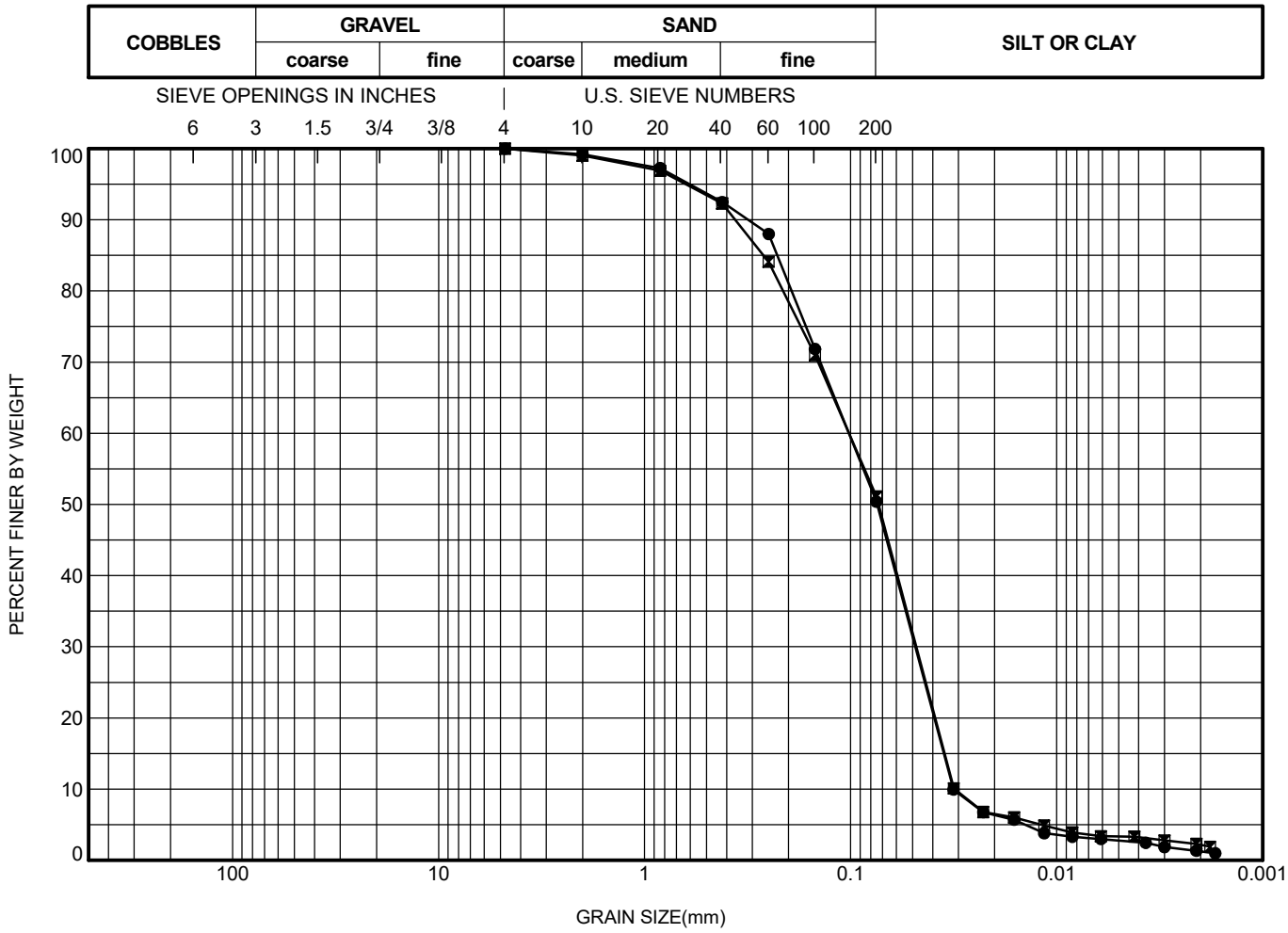
PROJECT:

LOCATION:

FIGURE:

DRAWN BY: AX **CHECKED BY:** BY

GRAIN SIZE DISTRIBUTION



	HOLE	DEPTH (m)	D85	D60	D50	D15	D10	CU	%GRAVEL	%SAND	%FINES
●	TX30-CAU	0.00	0.227	0.102					0.0	49.6	50.4
⊠	TX30-CAU	0.00	0.265	0.102					0.0	48.9	51.1

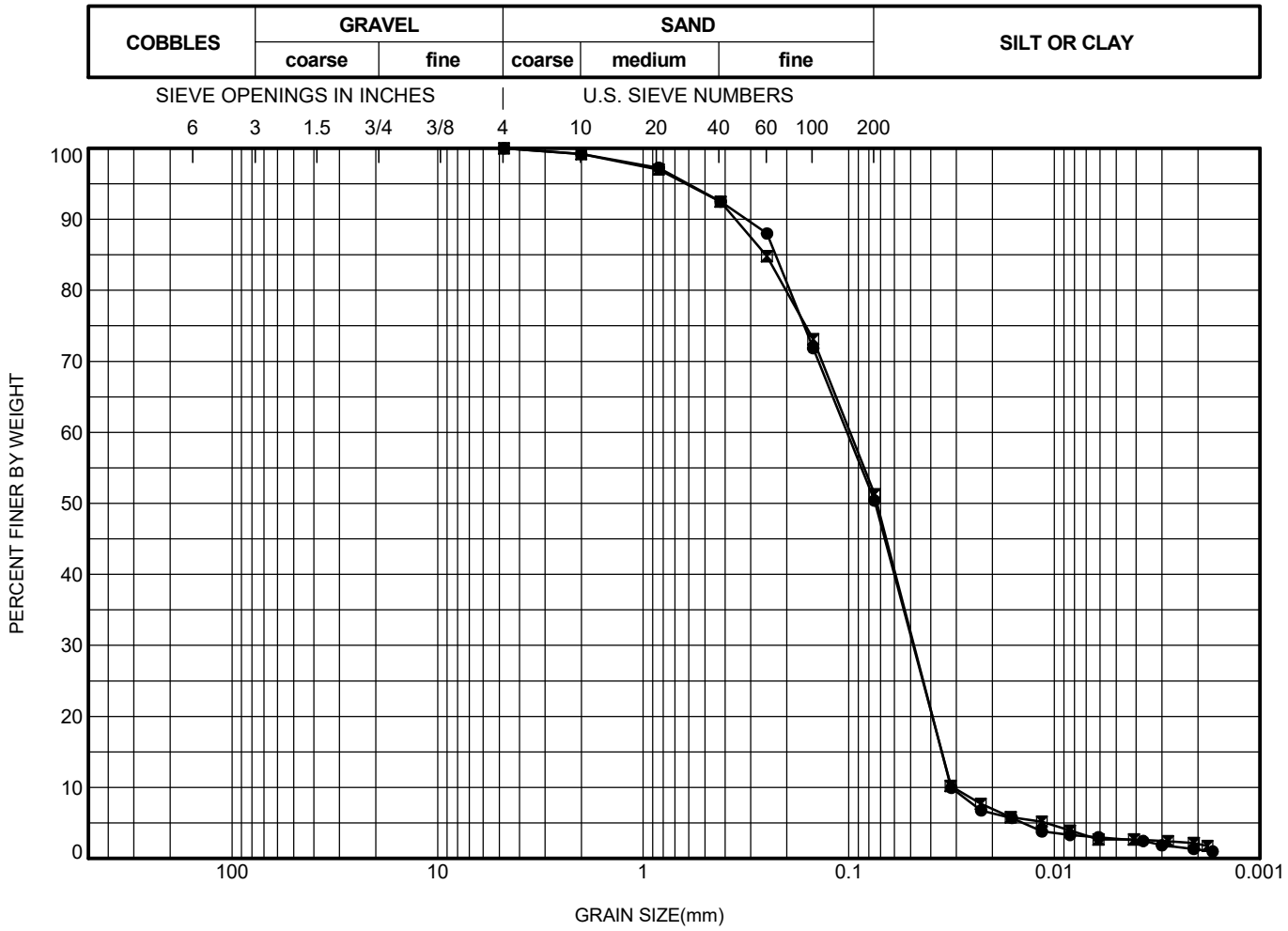
	HOLE	SAMPLE	DEPTH (m)	W%	W_L	W_P	PI	REMARKS / SAMPLE DESCRIPTION
●	TX30-CAU	Average	0.00					Before Testing (TX30/TX31/TX32)
⊠	TX30-CAU	Average	0.00					After Testing

CU = COEFFICIENT OF UNIFORMITY = D60/D10 **PARTICLE SIZES, e.g. D85, in mm** **Tested by Wet Sieving Method (ASTM D1140 & D422)**

PROJECT NO.: A03355A01
PROJECT:
LOCATION:
FIGURE:
DRAWN BY: AX **CHECKED BY:** BY

KC_GRAIN_SIZE-SI A03355A01 TRIAXIAL TESTS PSDS.GPJ SIEVE.GDT 19-11-20

GRAIN SIZE DISTRIBUTION



	HOLE	DEPTH (m)	D85	D60	D50	D15	D10	CU	%GRAVEL	%SAND	%FINES
●	TX31-CAU	0.00	0.227	0.102					0.0	49.6	50.4
☒	TX31-CAU	0.00	0.253	0.099					0.0	48.7	51.3

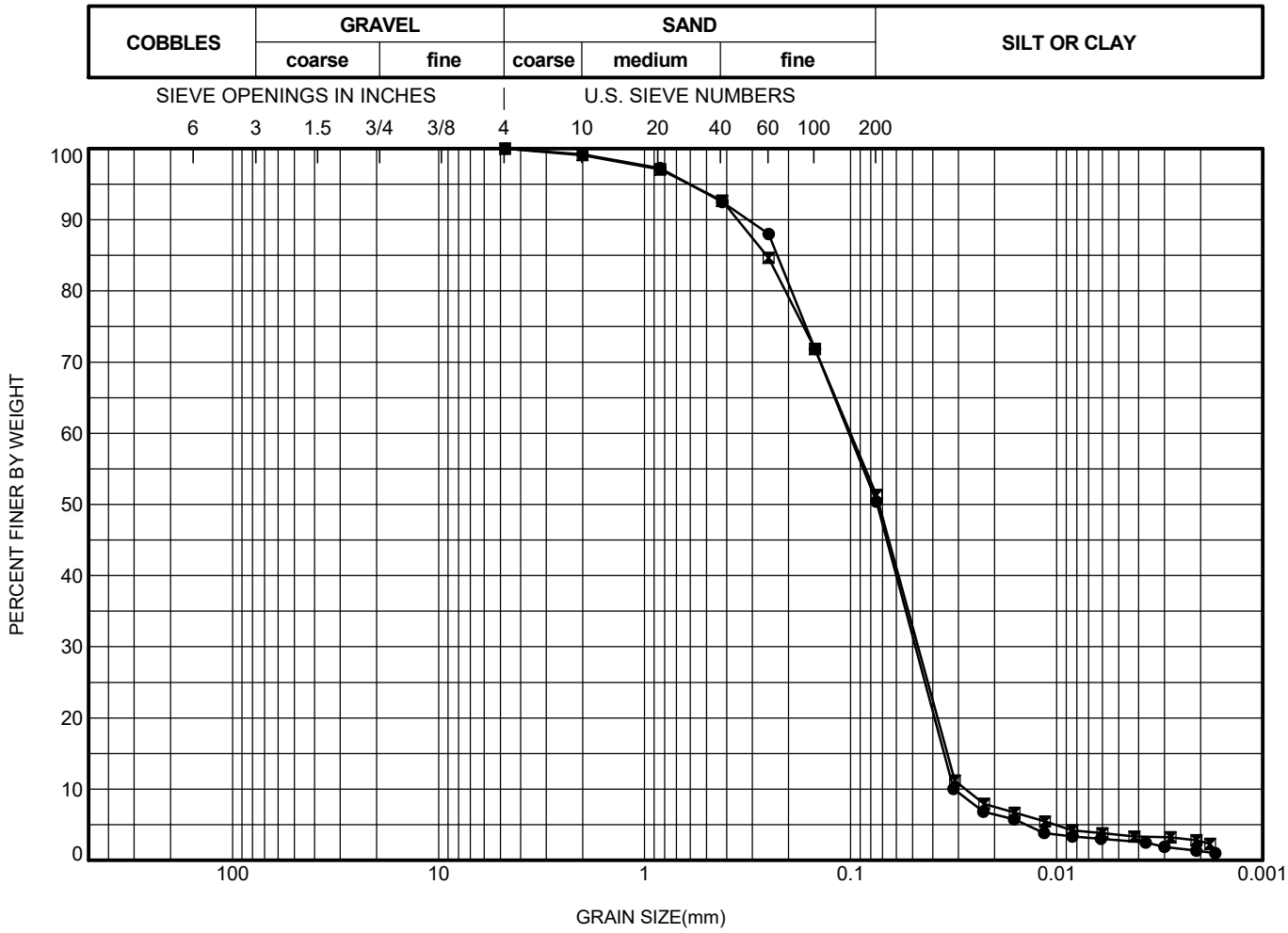
	HOLE	SAMPLE	DEPTH (m)	W%	W_L	W_P	PI	REMARKS / SAMPLE DESCRIPTION
●	TX31-CAU	Average	0.00					Before Testing (TX30/TX31/TX32)
☒	TX31-CAU	Average	0.00					After Testing

CU = COEFFICIENT OF UNIFORMITY = D60/D10 **PARTICLE SIZES, e.g. D85, in mm** **Tested by Wet Sieving Method (ASTM D1140 & D422)**

PROJECT NO.: A03355A01
PROJECT:
LOCATION:
FIGURE:
DRAWN BY: AX **CHECKED BY:** BY

KC_GRAIN_SIZE-SI A03355A01 TRIAXIAL TESTS PSDS.GPJ SIEVE.GDT 19-11-20

GRAIN SIZE DISTRIBUTION



	HOLE	DEPTH (m)	D85	D60	D50	D15	D10	CU	%GRAVEL	%SAND	%FINES
●	TX32-CAU	0.00	0.227	0.102					0.0	49.6	50.4
⊠	TX32-CAU	0.00	0.256	0.100					0.0	48.7	51.3

	HOLE	SAMPLE	DEPTH (m)	W%	W_L	W_P	PI	REMARKS / SAMPLE DESCRIPTION
●	TX32-CAU	Average	0.00					Before Testing (TX30/TX31/TX32)
⊠	TX32-CAU	Average	0.00					After Testing

CU = COEFFICIENT OF UNIFORMITY = D60/D10 **PARTICLE SIZES, e.g. D85, in mm** **Tested by Wet Sieving Method (ASTM D1140 & D422)**

PROJECT NO.: A03355A01

PROJECT:

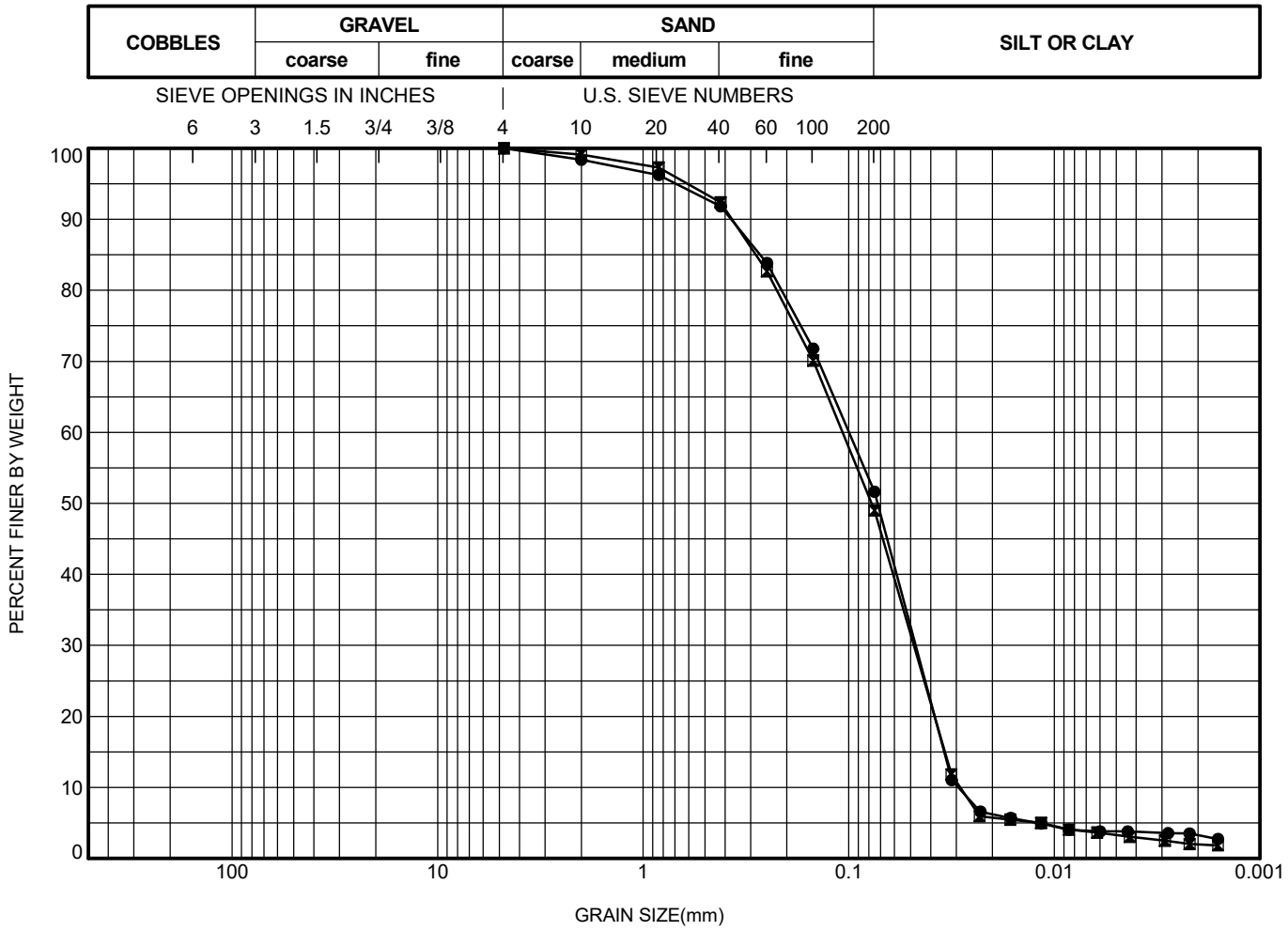
LOCATION:

FIGURE:

DRAWN BY: AX **CHECKED BY:** BY

KC_GRAIN_SIZE-SI A03355A01 TRIAXIAL TESTS PSDS.GPJ SIEVE.GDT 19-11-20

GRAIN SIZE DISTRIBUTION



	HOLE	DEPTH (m)	D85	D60	D50	D15	D10	CU	%GRAVEL	%SAND	%FINES
●	TXBE01	0.00	0.270	0.100					0.0	48.4	51.6
☒	TXBE01	0.00	0.283	0.107	0.077				0.0	51.0	49.0

	HOLE	SAMPLE	DEPTH (m)	W%	W_L	W_P	PI	REMARKS / SAMPLE DESCRIPTION
●	TXBE01	Average	0.00					Before Testing (TX02/TX03/TXBE01)
☒	TXBE01	Average	0.00					After Testing

CU = COEFFICIENT OF UNIFORMITY = D60/D10 **PARTICLE SIZES, e.g. D85, in mm** **Tested by Wet Sieving Method (ASTM D1140 & D422)**

PROJECT NO.: A03355A01

PROJECT:

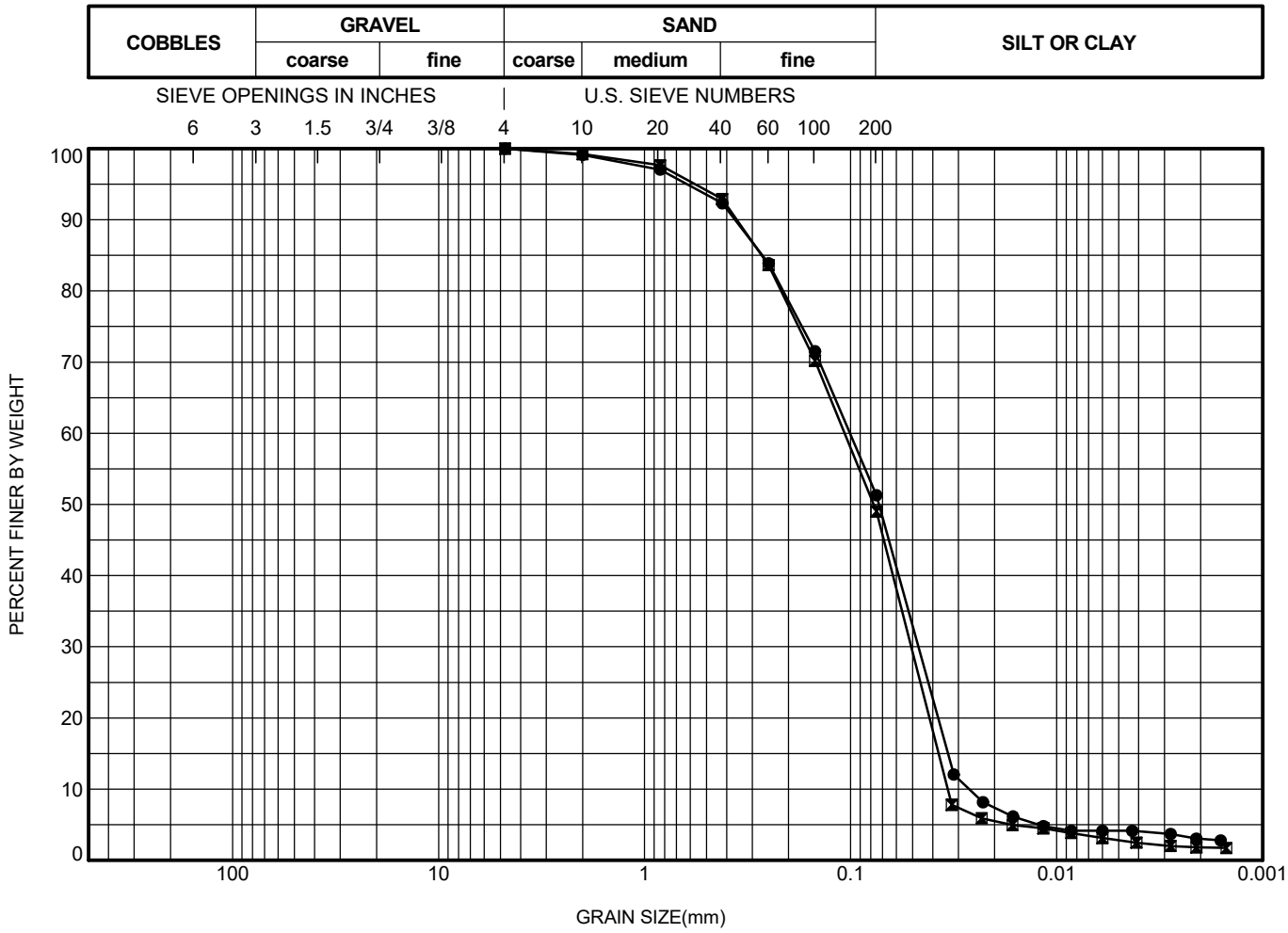
LOCATION:

FIGURE:

DRAWN BY: AX **CHECKED BY:** BY

KC_GRAIN_SIZE-SI A03355A01 TRIAXIAL TESTS PSDS.GPJ SIEVE.GDT 19-11-20

GRAIN SIZE DISTRIBUTION



	HOLE	DEPTH (m)	D85	D60	D50	D15	D10	CU	%GRAVEL	%SAND	%FINES
●	TXBE02	0.00	0.268	0.101					0.0	48.7	51.3
⊠	TXBE02	0.00	0.270	0.107	0.077				0.0	51.0	49.0

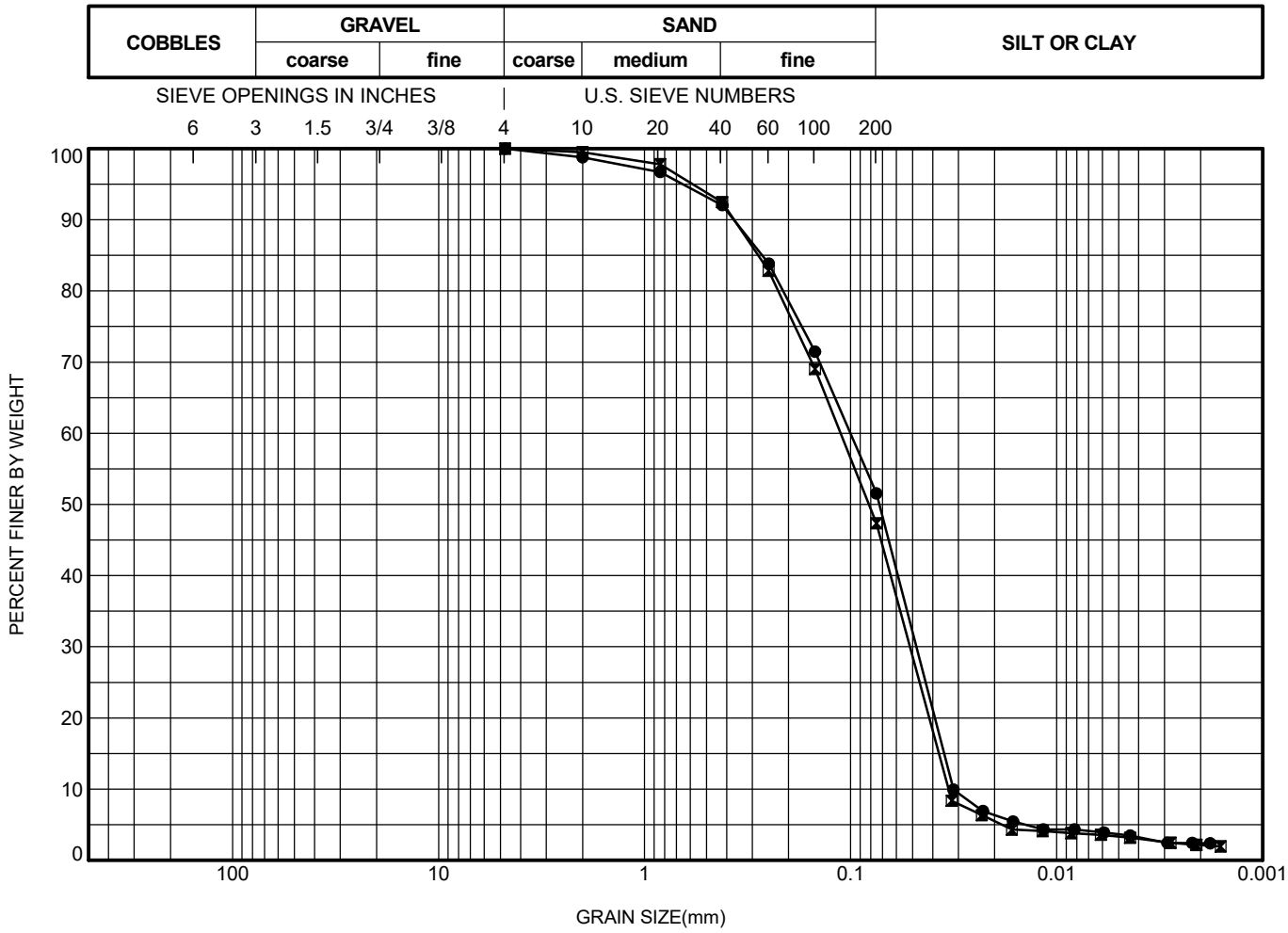
	HOLE	SAMPLE	DEPTH (m)	W%	W_L	W_P	PI	REMARKS / SAMPLE DESCRIPTION
●	TXBE02	Average	0.00					Before Testing (TX04/TX06/TXBE02)
⊠	TXBE02	Average	0.00					After Testing

CU = COEFFICIENT OF UNIFORMITY = D60/D10 **PARTICLE SIZES, e.g. D85, in mm** **Tested by Wet Sieving Method (ASTM D1140 & D422)**

PROJECT NO.: A03355A01
PROJECT:
LOCATION:
FIGURE:
DRAWN BY: AX **CHECKED BY:** BY

KC_GRAIN_SIZE-SI A03355A01 TRIAXIAL TESTS PSDS.GPJ SIEVE.GDT 19-11-20

GRAIN SIZE DISTRIBUTION



	HOLE	DEPTH (m)	D85	D60	D50	D15	D10	CU	%GRAVEL	%SAND	%FINES
●	TXBE03	0.00	0.269	0.100					0.0	48.4	51.6
☒	TXBE03	0.00	0.281	0.112	0.082				0.0	52.6	47.4

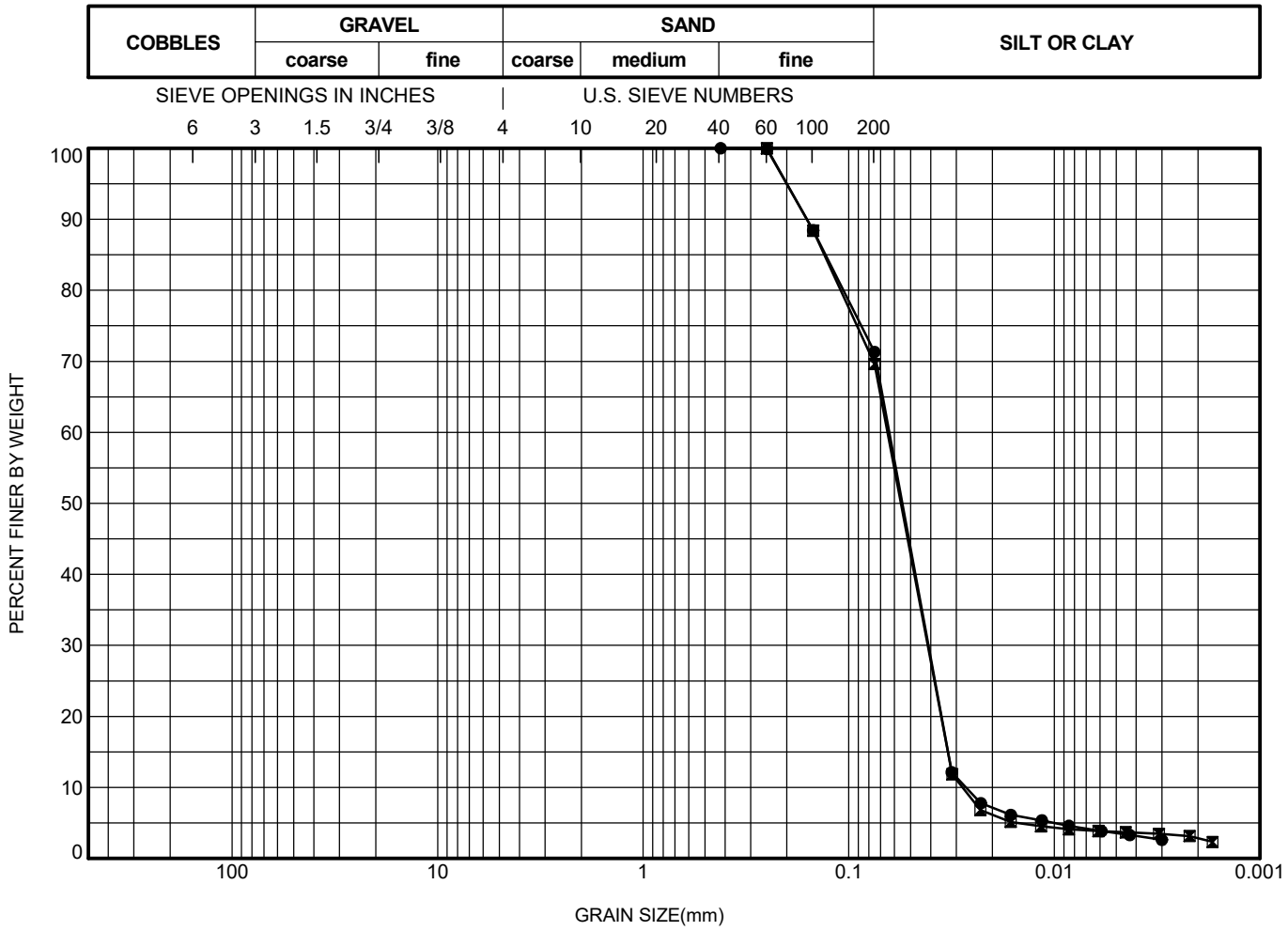
	HOLE	SAMPLE	DEPTH (m)	W%	W_L	W_P	PI	REMARKS / SAMPLE DESCRIPTION
●	TXBE03	Average	0.00					Before Testing (TX07/TXBE03)
☒	TXBE03	Average	0.00					After Testing

CU = COEFFICIENT OF UNIFORMITY = D60/D10 **PARTICLE SIZES, e.g. D85, in mm** **Tested by Wet Sieving Method (ASTM D1140 & D422)**

PROJECT NO.: A03355A01
PROJECT:
LOCATION:
FIGURE:
DRAWN BY: AX **CHECKED BY:** BY

KC_GRAIN_SIZE-SI A03355A01 TRIAXIAL TESTS PSDS.GPJ SIEVE.GDT 19-11-20

GRAIN SIZE DISTRIBUTION



	HOLE	DEPTH (m)	D85	D60	D50	D15	D10	CU	%GRAVEL	%SAND	%FINES
●	TXBE04	0.00	0.130						0.0	28.7	71.3
⊠	TXBE04	0.00	0.132						0.0	30.4	69.6

	HOLE	SAMPLE	DEPTH (m)	W%	W_L	W_P	PI	REMARKS / SAMPLE DESCRIPTION
●	TXBE04	Fine	0.00					Before Testing (TX13/TXBE04)
⊠	TXBE04	Fine	0.00					After Testing

CU = COEFFICIENT OF UNIFORMITY = D60/D10 **PARTICLE SIZES, e.g. D85, in mm** **Tested by Wet Sieving Method (ASTM D1140 & D422)**

PROJECT NO.: A03355A01

PROJECT:

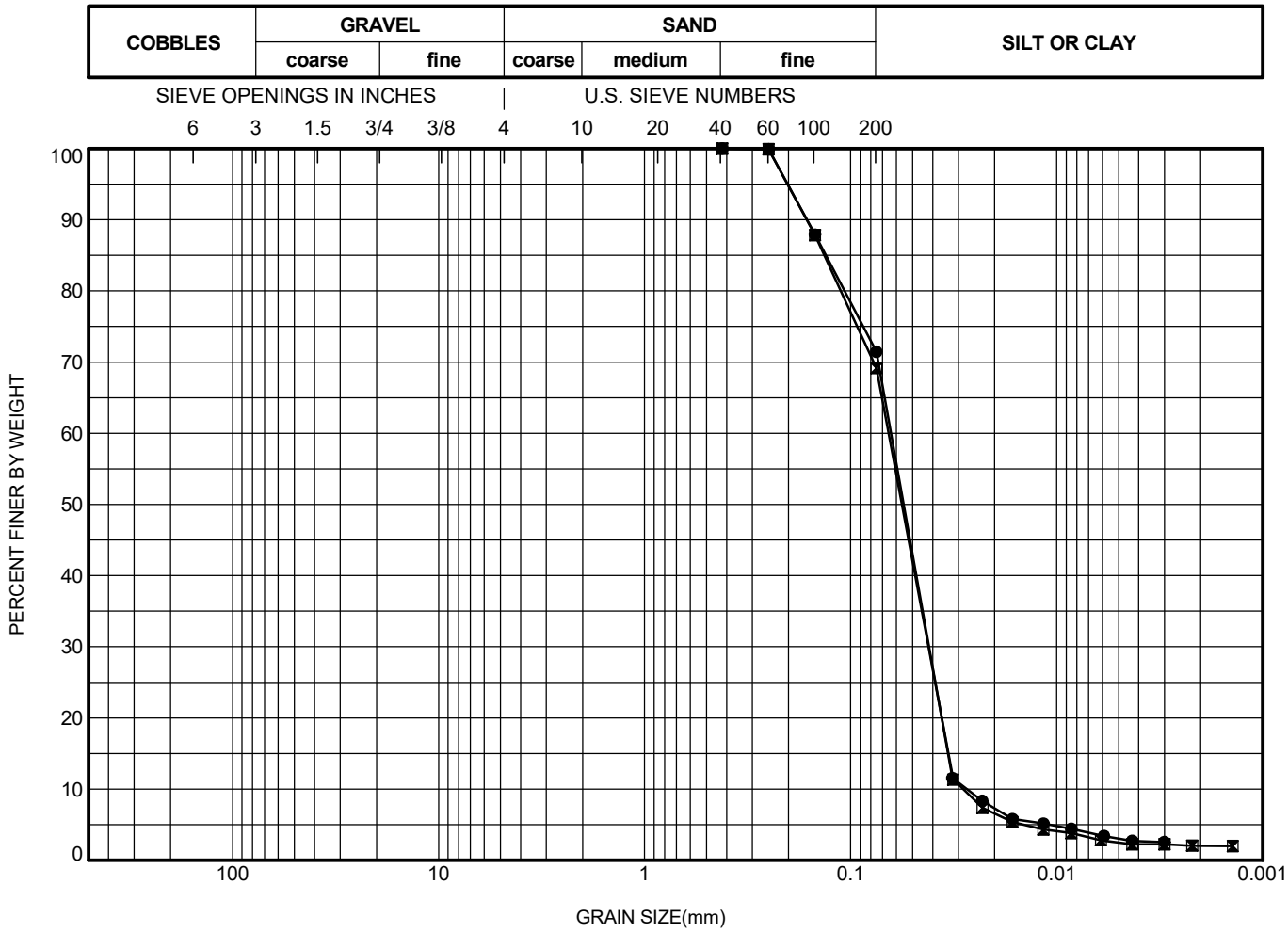
LOCATION:

FIGURE:

DRAWN BY: AX **CHECKED BY:** BY

KC_GRAIN_SIZE-SI A03355A01 TRIAXIAL TESTS PSDS.GPJ SIEVE.GDT 19-11-20

GRAIN SIZE DISTRIBUTION



	HOLE	DEPTH (m)	D85	D60	D50	D15	D10	CU	%GRAVEL	%SAND	%FINES
●	TXBE05	0.00	0.132						0.0	28.5	71.5
⊠	TXBE05	0.00	0.134						0.0	30.8	69.2

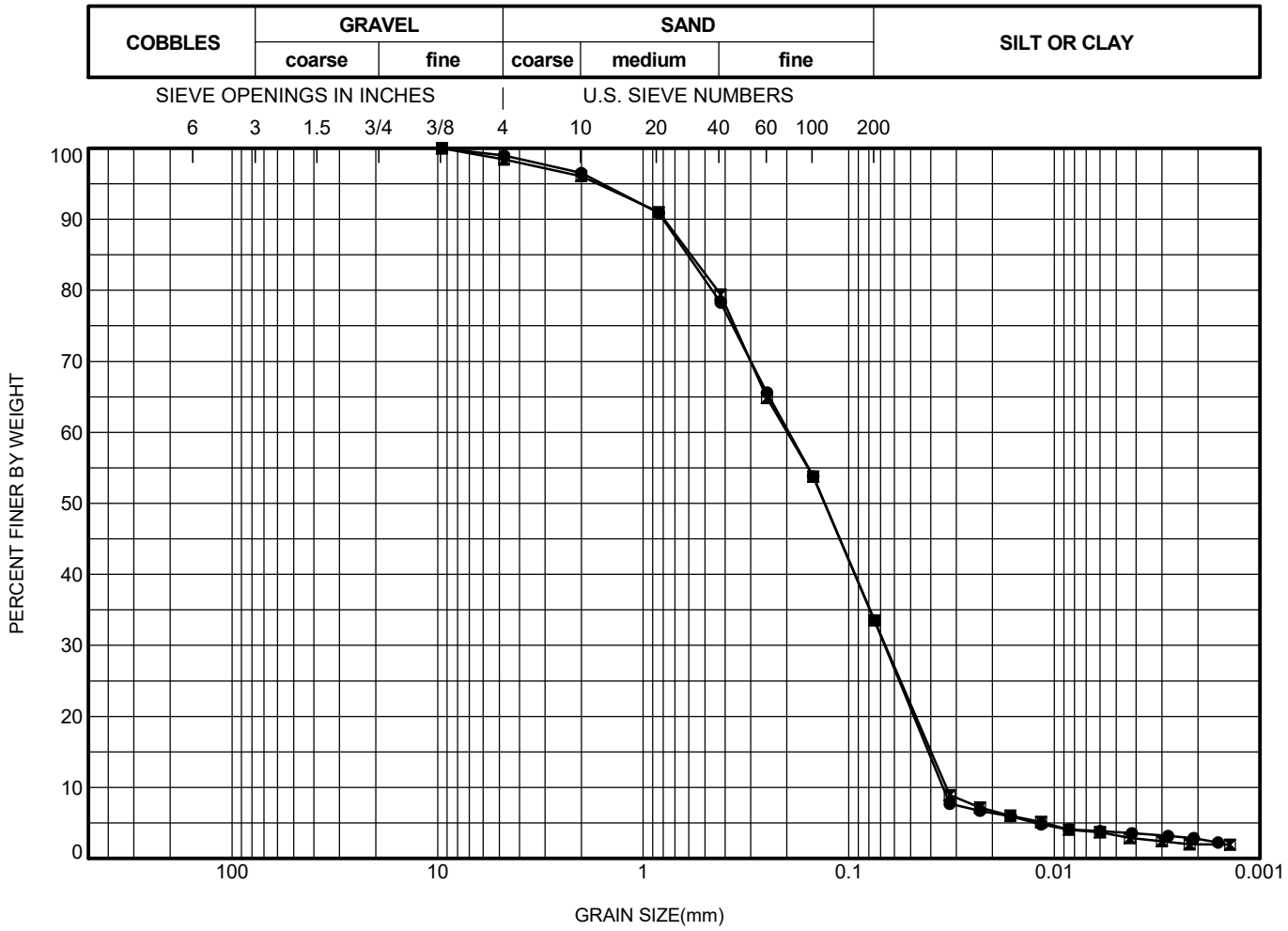
	HOLE	SAMPLE	DEPTH (m)	W%	W_L	W_P	PI	REMARKS / SAMPLE DESCRIPTION
●	TXBE05	Fine	0.00					Fine (TX12/TXBE05)
⊠	TXBE05	Fine	0.00					Fine

CU = COEFFICIENT OF UNIFORMITY = D60/D10 **PARTICLE SIZES, e.g. D85, in mm** **Tested by Wet Sieving Method (ASTM D1140 & D422)**

PROJECT NO.: A03355A01
PROJECT:
LOCATION:
FIGURE:
DRAWN BY: AX **CHECKED BY:** BY

KC_GRAIN_SIZE-SI A03355A01 TRIAXIAL TESTS PSDS.GPJ SIEVE.GDT 19-11-20

GRAIN SIZE DISTRIBUTION



	HOLE	DEPTH (m)	D85	D60	D50	D15	D10	CU	%GRAVEL	%SAND	%FINES
●	TXBE06	0.00	0.608	0.196	0.131				1.0	65.5	33.5
⊠	TXBE06	0.00	0.587	0.199	0.131				1.6	64.9	33.5

	HOLE	SAMPLE	DEPTH (m)	W%	W_L	W_P	PI	REMARKS / SAMPLE DESCRIPTION
●	TXBE06	Coarse	0.00					Before Testing (TXBE06/TXBE07)
⊠	TXBE06	Coarse	0.00					After Testing

CU = COEFFICIENT OF UNIFORMITY = D60/D10 **PARTICLE SIZES, e.g. D85, in mm** **Tested by Wet Sieving Method (ASTM D1140 & D422)**

PROJECT NO.: A03355A01

PROJECT:

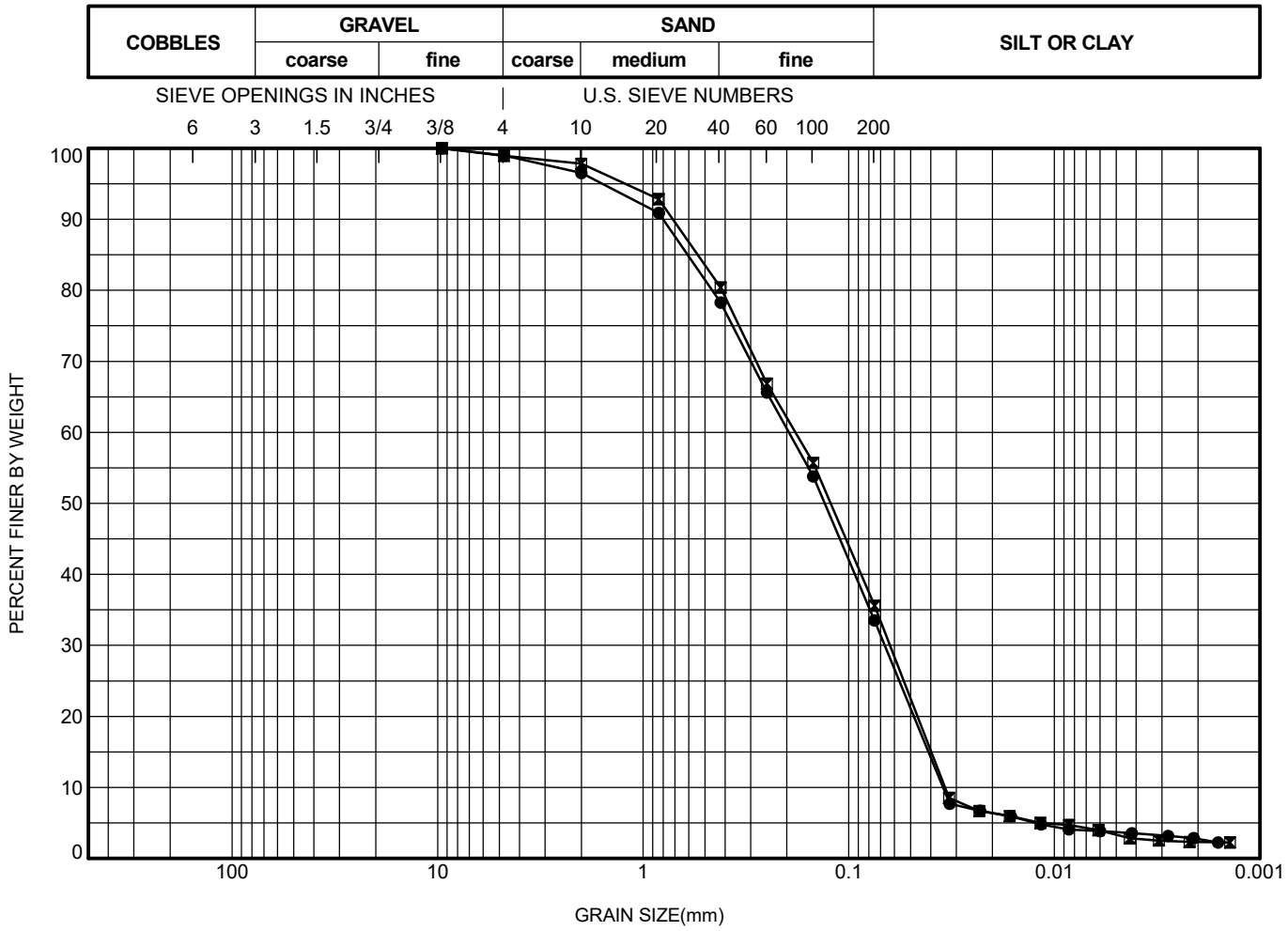
LOCATION:

FIGURE:

DRAWN BY: AX **CHECKED BY:** BY

KC_GRAIN_SIZE-SI A03355A01 TRIAXIAL TESTS PSDS.GPJ SIEVE.GDT 19-11-20

GRAIN SIZE DISTRIBUTION



	HOLE	DEPTH (m)	D85	D60	D50	D15	D10	CU	%GRAVEL	%SAND	%FINES
●	TXBE07	0.00	0.608	0.196	0.131				1.0	65.5	33.5
☒	TXBE07	0.00	0.543	0.182	0.123				1.1	63.3	35.6

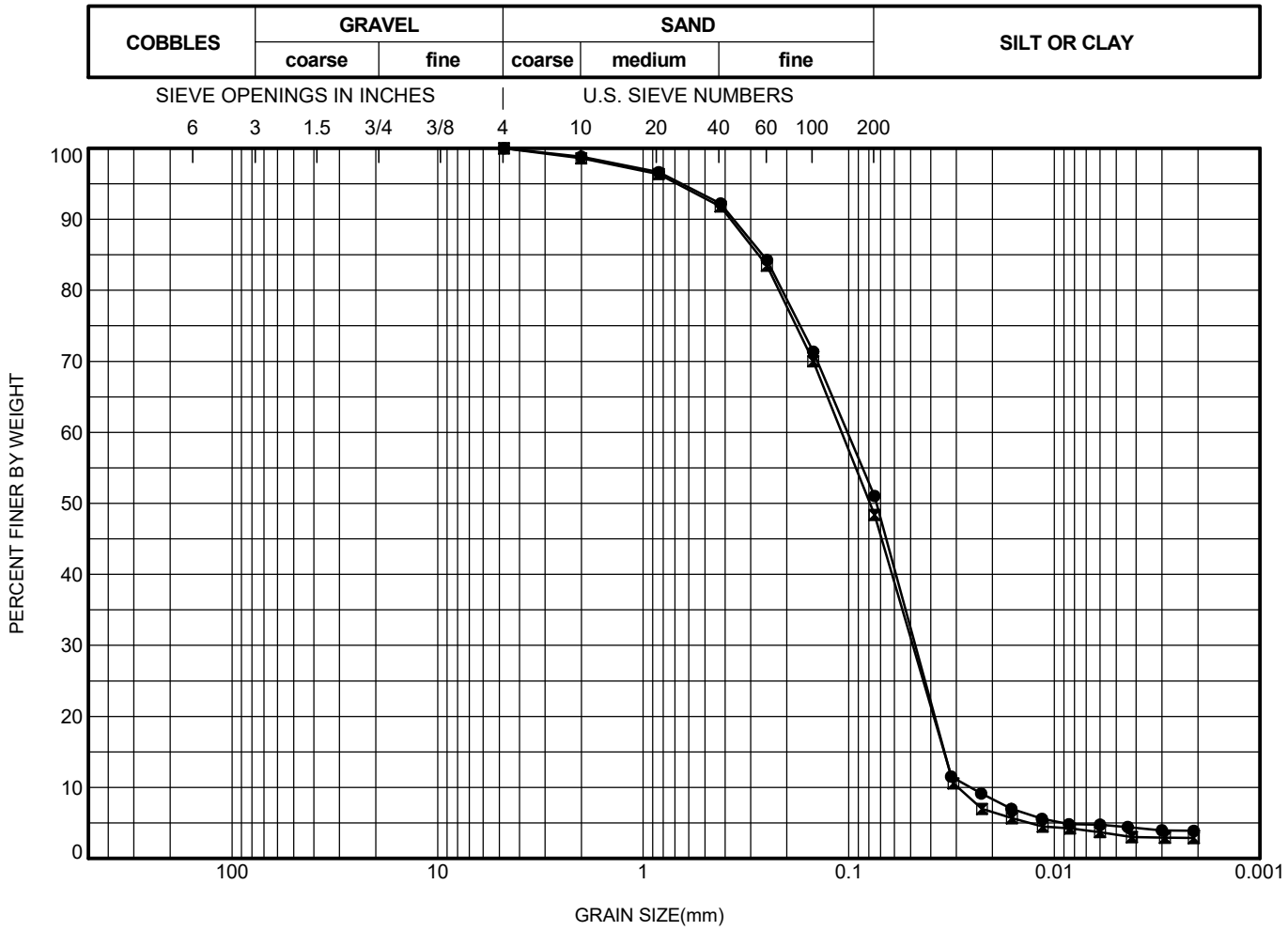
	HOLE	SAMPLE	DEPTH (m)	W%	W_L	W_P	PI	REMARKS / SAMPLE DESCRIPTION
●	TXBE07	Coarse	0.00					Before Testing (TXBE06/TXBE07)
☒	TXBE07	Coarse	0.00					After Testing

CU = COEFFICIENT OF UNIFORMITY = D60/D10 **PARTICLE SIZES, e.g. D85, in mm** **Tested by Wet Sieving Method (ASTM D1140 & D422)**

PROJECT NO.: A03355A01
PROJECT:
LOCATION:
FIGURE:
DRAWN BY: AX **CHECKED BY:** BY

KC_GRAIN_SIZE-SI A03355A01 TRIAXIAL TESTS PSDS.GPJ SIEVE.GDT 19-11-20

GRAIN SIZE DISTRIBUTION



	HOLE	DEPTH (m)	D85	D60	D50	D15	D10	CU	%GRAVEL	%SAND	%FINES
●	TXBE08	0.00	0.262	0.102					0.0	49.0	51.0
⊠	TXBE08	0.00	0.275	0.108	0.079				0.0	51.6	48.4

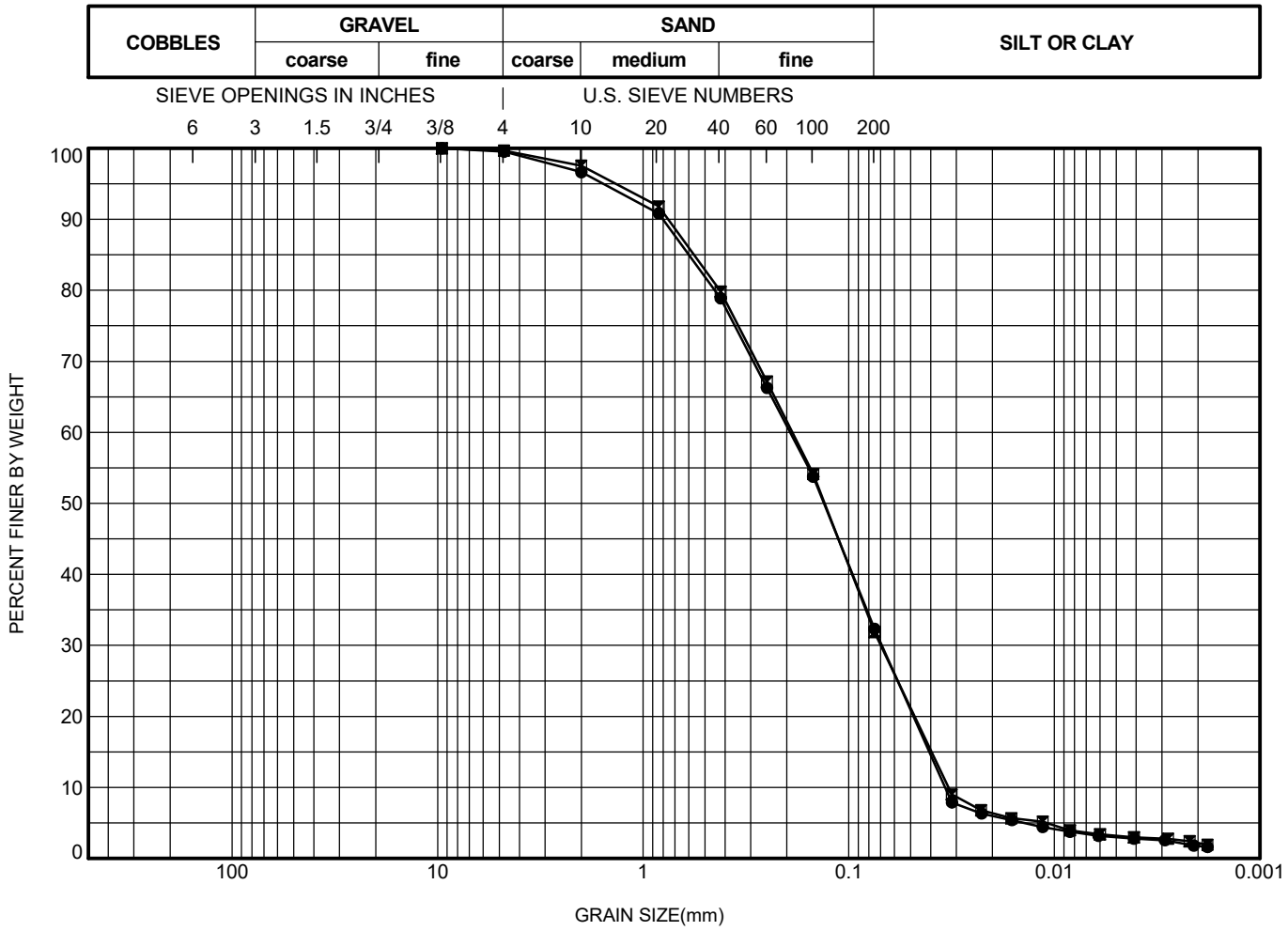
	HOLE	SAMPLE	DEPTH (m)	W%	W_L	W_P	PI	REMARKS / SAMPLE DESCRIPTION
●	TXBE08	Average	0.00					Before Testing
⊠	TXBE08	Average	0.00					After Testing

CU = COEFFICIENT OF UNIFORMITY = D60/D10 **PARTICLE SIZES, e.g. D85, in mm** **Tested by Wet Sieving Method (ASTM D1140 & D422)**

PROJECT NO.: A03355A01
PROJECT:
LOCATION:
FIGURE:
DRAWN BY: AX **CHECKED BY:** BY

KC_GRAIN_SIZE-SI A03355A01 TRIAXIAL TESTS PSDS.GPJ SIEVE.GDT 19-11-20

GRAIN SIZE DISTRIBUTION



	HOLE	DEPTH (m)	D85	D60	D50	D15	D10	CU	%GRAVEL	%SAND	%FINES
●	TXBE09	0.00	0.599	0.193	0.132				0.5	67.2	32.3
☒	TXBE09	0.00	0.566	0.188	0.131				0.3	67.8	31.9

	HOLE	SAMPLE	DEPTH (m)	W%	W_L	W_P	PI	REMARKS / SAMPLE DESCRIPTION
●	TXBE09	Coarse	0.00					Before Testing
☒	TXBE09	Coarse	0.00					After Testing

CU = COEFFICIENT OF UNIFORMITY = D60/D10 **PARTICLE SIZES, e.g. D85, in mm** **Tested by Wet Sieving Method (ASTM D1140 & D422)**

PROJECT NO.: A03355A01

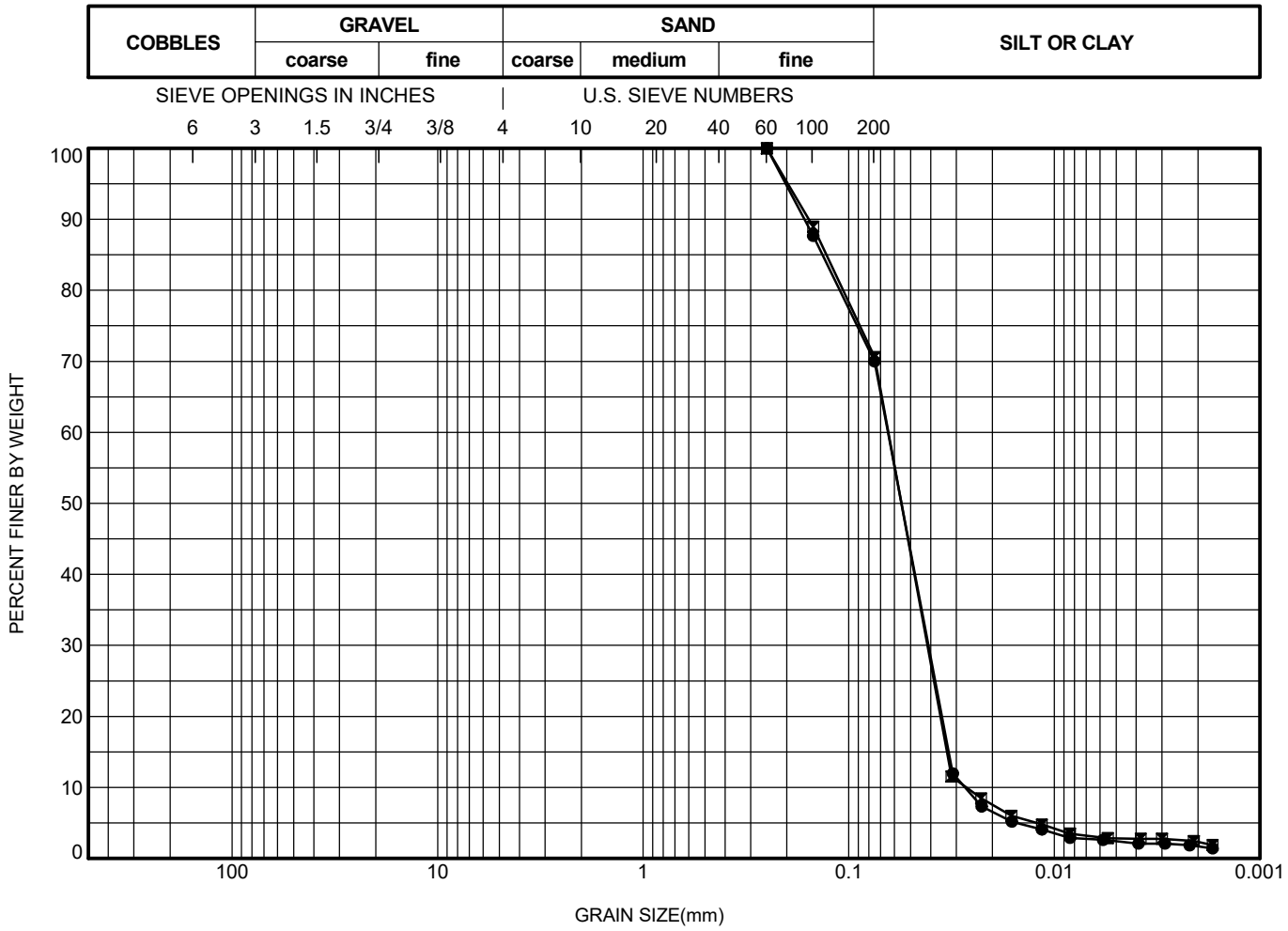
PROJECT:

LOCATION:

FIGURE:

DRAWN BY: AX **CHECKED BY:** BY

GRAIN SIZE DISTRIBUTION



	HOLE	DEPTH (m)	D85	D60	D50	D15	D10	CU	%GRAVEL	%SAND	%FINES
●	TXBE10	0.00	0.134						0.0	30.0	70.0
☒	TXBE10	0.00	0.128						0.0	29.4	70.6

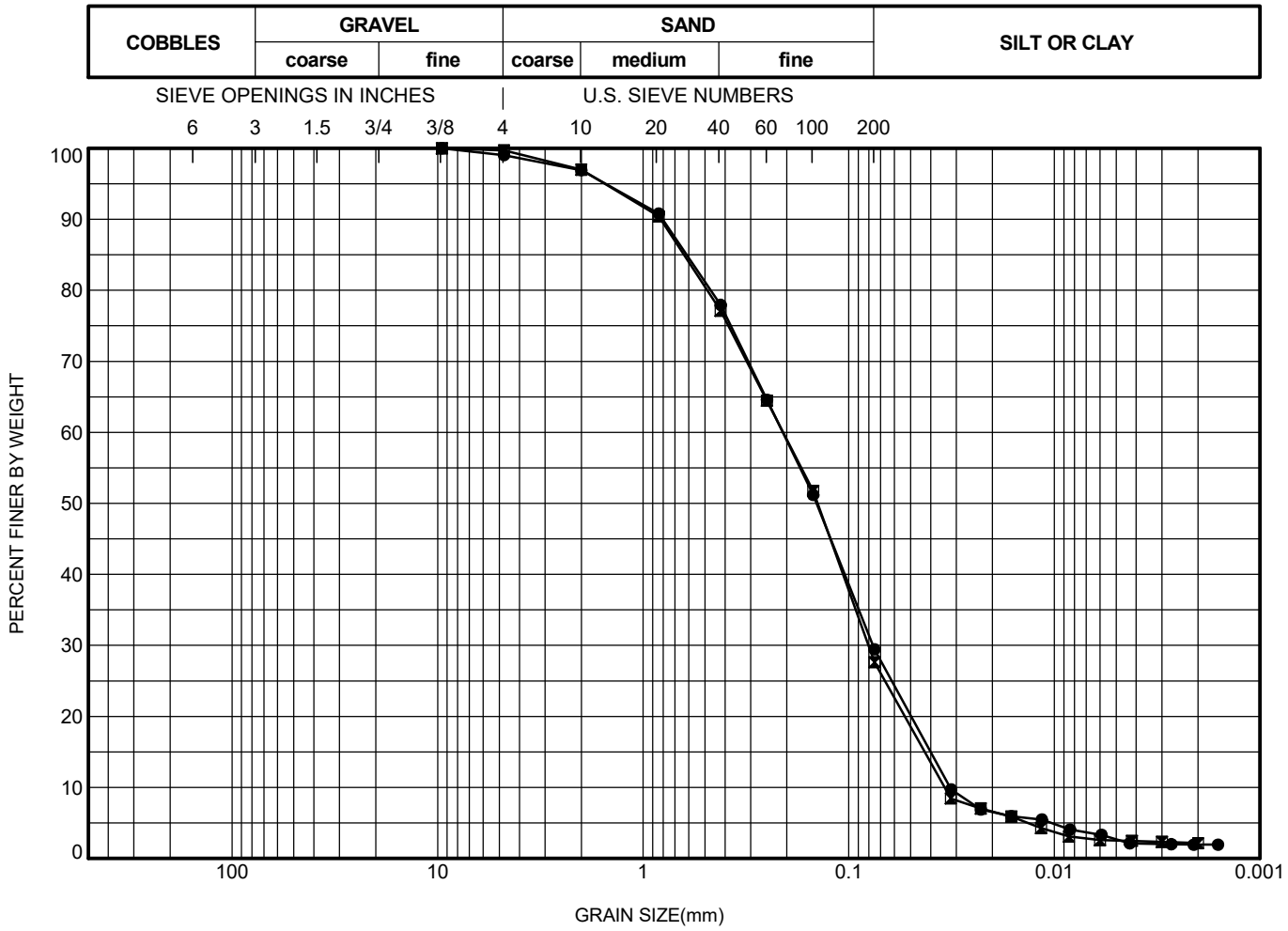
	HOLE	SAMPLE	DEPTH (m)	W%	W_L	W_P	PI	REMARKS / SAMPLE DESCRIPTION
●	TXBE10	Fine	0.00					Before Testing (TX29/TXBE10)
☒	TXBE10	Fine	0.00					After Testing

CU = COEFFICIENT OF UNIFORMITY = D60/D10 **PARTICLE SIZES, e.g. D85, in mm** **Tested by Wet Sieving Method (ASTM D1140 & D422)**

PROJECT NO.: A03355A01
PROJECT:
LOCATION:
FIGURE:
DRAWN BY: AX **CHECKED BY:** BY

KC_GRAIN_SIZE-SI A03355A01 TRIAXIAL TESTS PSDS.GPJ SIEVE.GDT 19-11-20

GRAIN SIZE DISTRIBUTION



	HOLE	DEPTH (m)	D85	D60	D50	D15	D10	CU	%GRAVEL	%SAND	%FINES
●	TXDW01	0.00	0.614	0.209	0.144				1.0	69.6	29.4
⊠	TXDW01	0.00	0.633	0.209	0.142				0.3	72.1	27.6

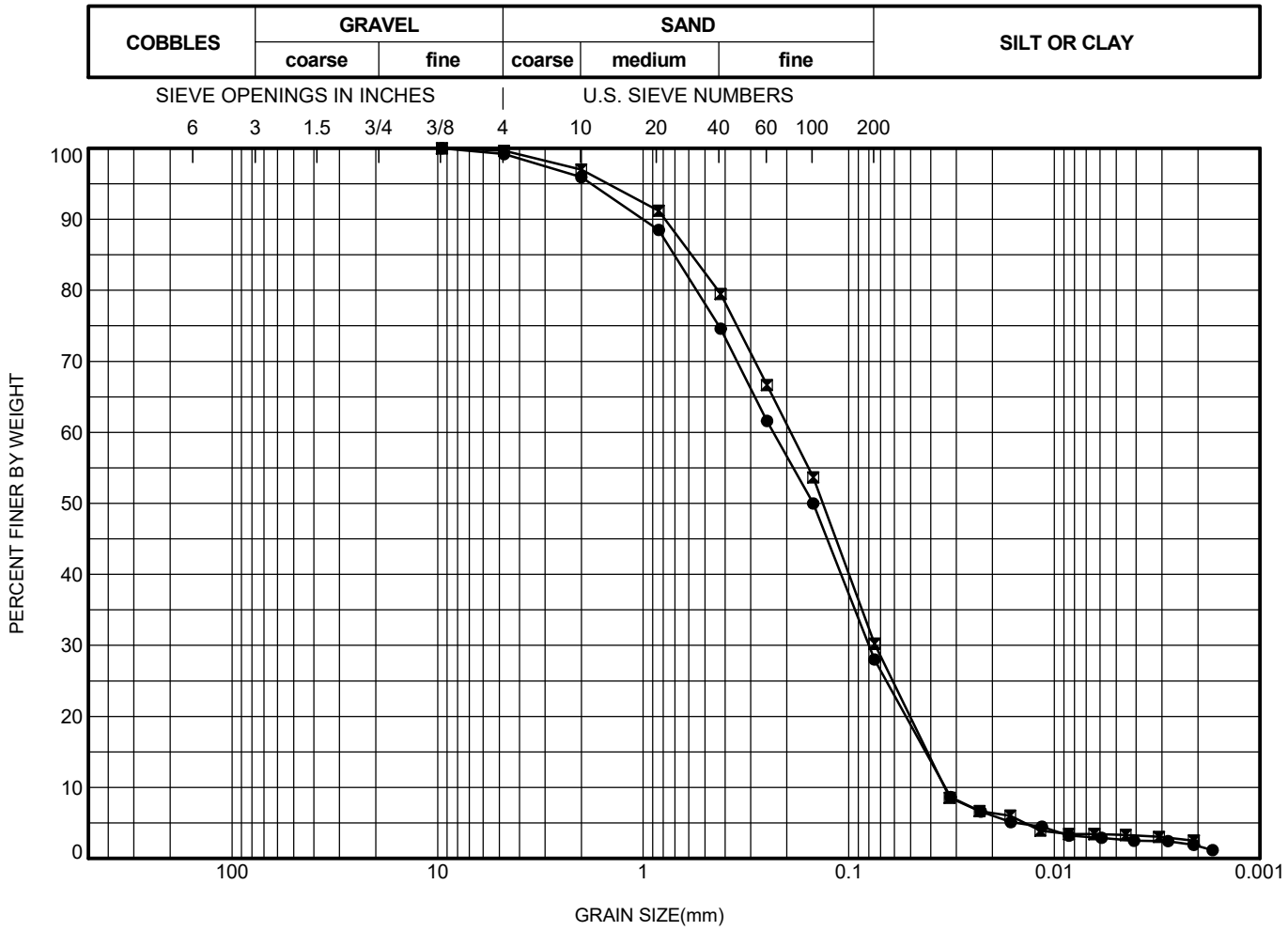
	HOLE	SAMPLE	DEPTH (m)	W%	W_L	W_P	PI	REMARKS / SAMPLE DESCRIPTION
●	TXDW01		0.00					Before Testing
⊠	TXDW01		0.00					After Testing

CU = COEFFICIENT OF UNIFORMITY = D60/D10 **PARTICLE SIZES, e.g. D85, in mm** **Tested by Wet Sieving Method (ASTM D1140 & D422)**

PROJECT NO.: A03355A01
PROJECT:
LOCATION:
FIGURE:
DRAWN BY: AX **CHECKED BY:** BY

KC_GRAIN_SIZE-SI A03355A01 TRIAXIAL TESTS PSDS.GPJ SIEVE.GDT 19-11-20

GRAIN SIZE DISTRIBUTION



	HOLE	DEPTH (m)	D85	D60	D50	D15	D10	CU	%GRAVEL	%SAND	%FINES
●	TXDW02	0.00	0.705	0.233	0.149				0.8	71.2	28.0
⊠	TXDW02	0.00	0.582	0.192	0.134				0.4	69.4	30.2

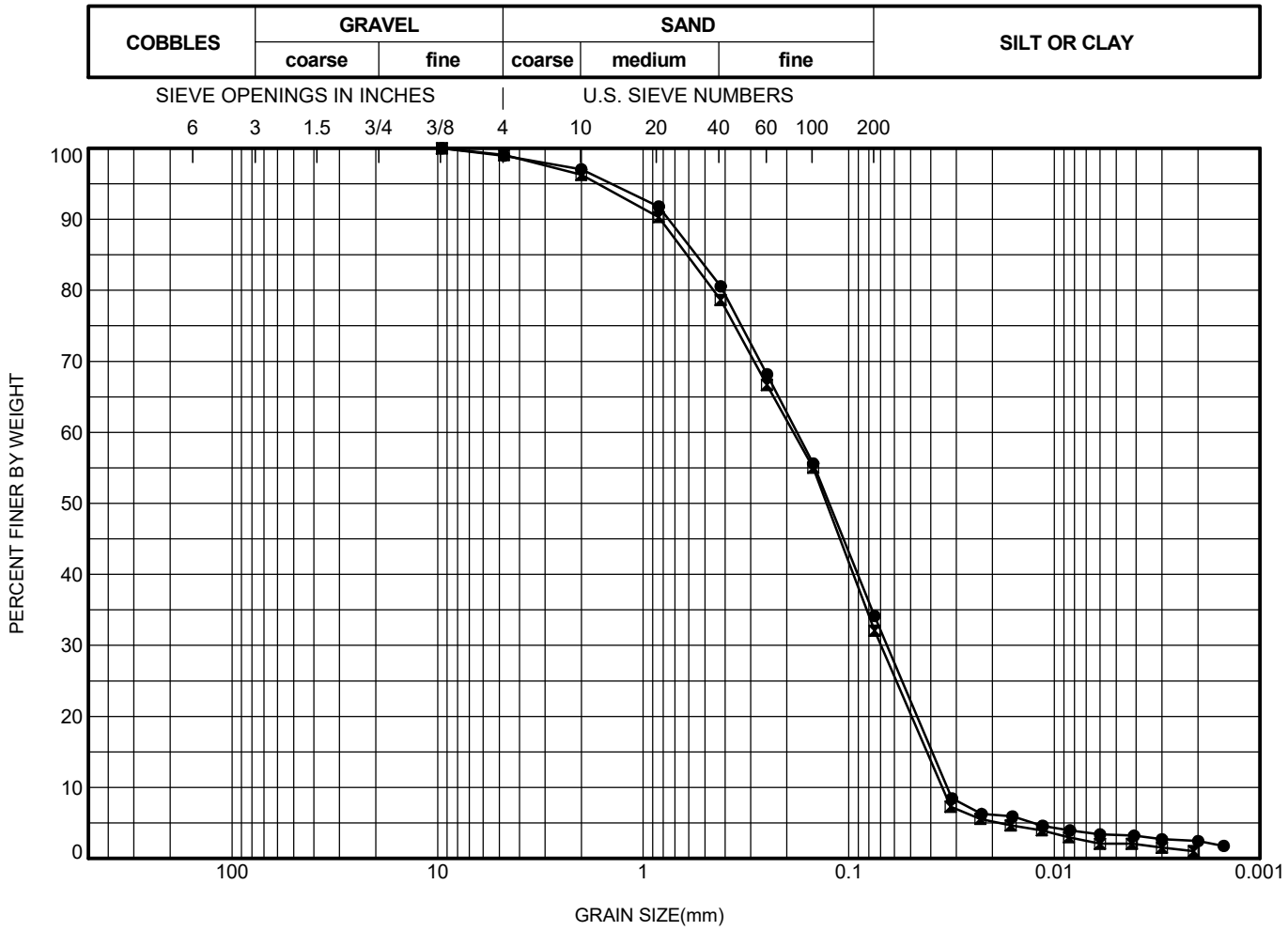
	HOLE	SAMPLE	DEPTH (m)	W%	W_L	W_P	PI	REMARKS / SAMPLE DESCRIPTION
●	TXDW02		0.00					Before Testing (TX25/TXDW02)
⊠	TXDW02		0.00					After Testing

CU = COEFFICIENT OF UNIFORMITY = D60/D10 **PARTICLE SIZES, e.g. D85, in mm** **Tested by Wet Sieving Method (ASTM D1140 & D422)**

PROJECT NO.: A03355A01
PROJECT:
LOCATION:
FIGURE:
DRAWN BY: AX **CHECKED BY:** BY

KC_GRAIN_SIZE-SI A03355A01 TRIAXIAL TESTS PSDS.GPJ SIEVE.GDT 19-11-20

GRAIN SIZE DISTRIBUTION



	HOLE	DEPTH (m)	D85	D60	D50	D15	D10	CU	%GRAVEL	%SAND	%FINES
●	TXDW03	0.00	0.552	0.179	0.125				1.0	64.8	34.1
⊠	TXDW03	0.00	0.613	0.186	0.128				1.0	67.0	32.1

	HOLE	SAMPLE	DEPTH (m)	W%	W_L	W_P	PI	REMARKS / SAMPLE DESCRIPTION
●	TXDW03		0.00					Before Testing
⊠	TXDW03		0.00					After Testing

CU = COEFFICIENT OF UNIFORMITY = D60/D10 **PARTICLE SIZES, e.g. D85, in mm** **Tested by Wet Sieving Method (ASTM D1140 & D422)**

PROJECT NO.: A03355A01
PROJECT:
LOCATION:
FIGURE:
DRAWN BY: AX **CHECKED BY:** BY

KC_GRAIN_SIZE-SI A03355A01 TRIAXIAL TESTS PSDS.GPJ SIEVE.GDT 19-11-20

Individual Triaxial Test Results

Triaxial CD Test - Summary

(ASTM D7181)

PROJECT NO. : A03355A01 DATE : 2019-07-24

PROJECT : TESTED BY: BY

SAMPLE : Average CHECKED BY: JG

TEST NO. : TX 01 - CID

SPECIMEN INFORMATION	UNITS	Initial	Vacuum	Saturation / B-value	End of 1st Consolidation	End of 2nd Consolidation	End of 3rd Consolidation	End of 4th Consolidation	End of 5th Consolidation	End of 6th Consolidation	At Failure	End of Shear
Specimen Height	mm	140.08	140.08	139.55	139.16	138.88	138.44	137.86	137.10	135.29	107.40	94.13
Specimen Diameter	mm	69.80	69.62	67.51	66.78	66.46	66.15	65.83	65.47	65.27	70.41	75.03
Area	cm^2	38.26	38.07	35.79	35.03	34.70	34.37	34.04	33.66	33.46	38.94	44.21
Volume	cm^3	536.01	533.25	499.46	487.46	481.86	475.86	469.28	461.53	452.72	418.21	416.15
Wet Weight	g	1270.48	1270.48	1464.58	1452.58	1446.98	1440.98	1434.40	1426.65	1417.84	1383.33	1381.27
Water Content	%	5.17	5.17	21.24	20.24	19.78	19.28	18.74	18.10	17.37	14.51	14.34
Dry Weight	g	1208.03	1208.03	1208.03	1208.03	1208.03	1208.03	1208.03	1208.03	1208.03	1208.03	1208.03
Wet Density	g/cm^3	2.370	2.383	2.932	2.980	3.003	3.028	3.057	3.091	3.132	3.308	3.319
Dry Density	g/cm^3	2.254	2.265	2.419	2.478	2.507	2.539	2.574	2.617	2.668	2.889	2.903
Specific Gravity of Solids (assumed)	-	4.97	4.97	4.97	4.97	4.97	4.97	4.97	4.97	4.97	4.97	4.97
Solids Volume	cm^3	243.063	243.063	243.063	243.063	243.063	243.063	243.063	243.063	243.063	243.063	243.063
Void Volume	cm^3	292.951	290.191	256.398	244.400	238.795	232.802	226.218	218.464	209.660	175.146	173.088
Water Volume	cm^3	62.455	62.455	256.555	244.557	238.952	232.959	226.375	218.621	209.817	175.303	173.245
Void Ratio (e)	-	1.205	1.194	1.055	1.005	0.982	0.958	0.931	0.899	0.863	0.721	0.712
Saturation Ratio (Sr)	%	21.32	21.52	100.06	100.06	100.07	100.07	100.07	100.07	100.08	100.09	100.09
Effective Confining Stress	kPa				50	100	200	400	800	1500		

Shearing (CU)		
Skempton's B Parameter		0.99
Back Pressure before shearing	kPa	499.0
Confining Stress (σ_3') before shearing	kPa	1500
Shear Strain Rate	mm / min	0.033

At Maximum Stress Ratio		
Axial Stain	%	**20.60**
Deviator Stress	kPa	**4179.4**
Φ '	º	35.6
c' (assumed)	kPa	**0**

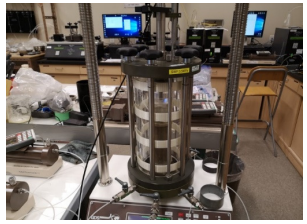
At Maximum Deviator Stress:		
Axial Stain	%	**20.60**
Deviator Stress	kPa	**4179.4**
Φ '	º	35.6
c' (assumed)	kPa	0

Note: *using cambridge method*

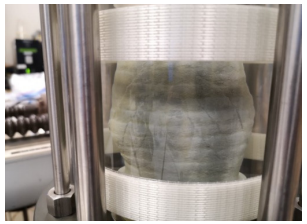
Photos:

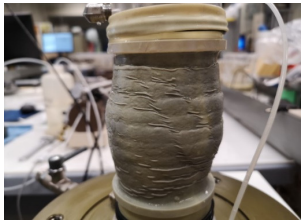
Before Test





After Test

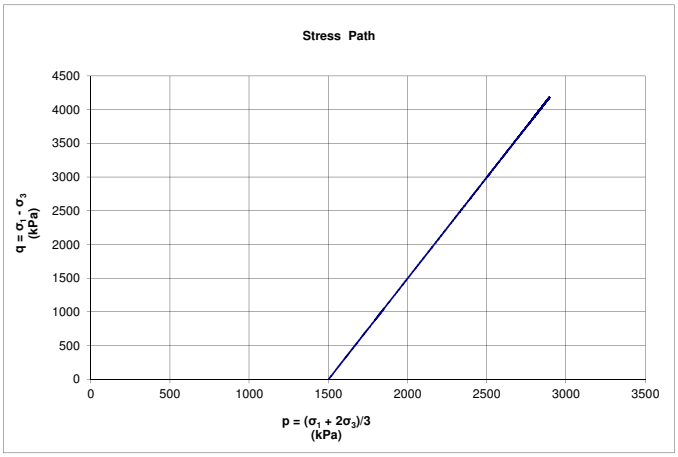


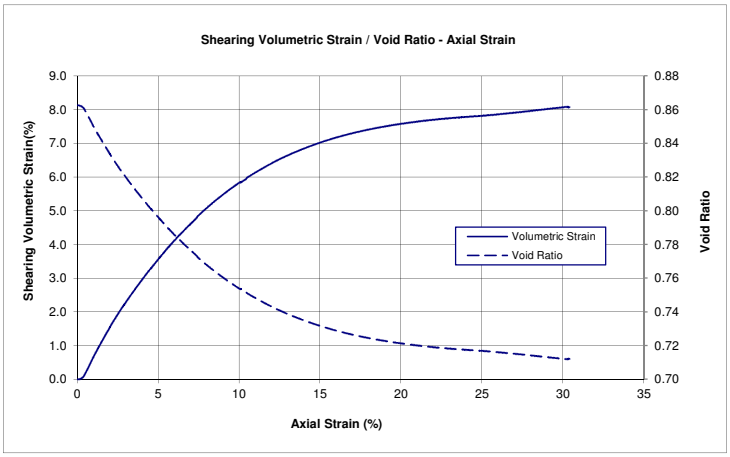


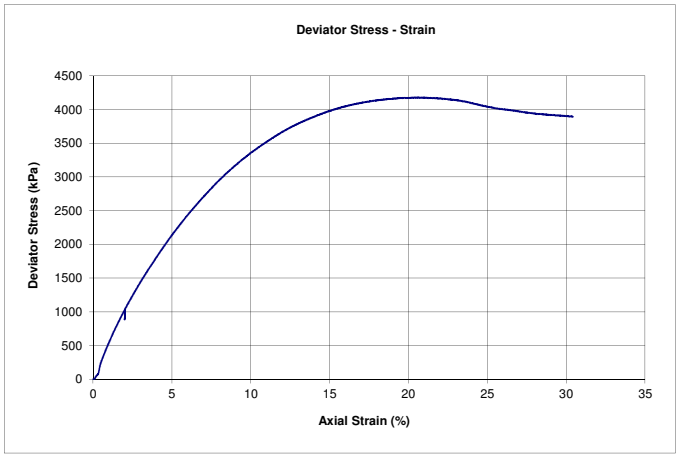
Triaxial CD Test - Charts

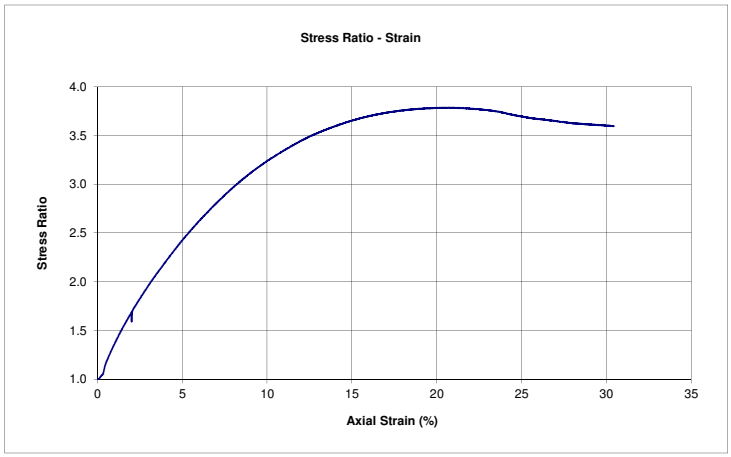
(ASTM D7181)

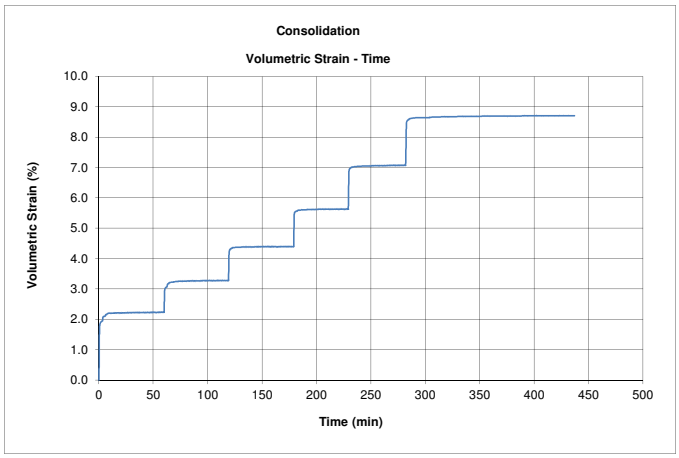
PROJECT NO. :	A03355A01	DATE :	2019-07-24
PROJECT :		TEST BY:	BY
SAMPLE :	Average	CHECKED BY:	JG
TEST NO. :	TX 01 - CID		

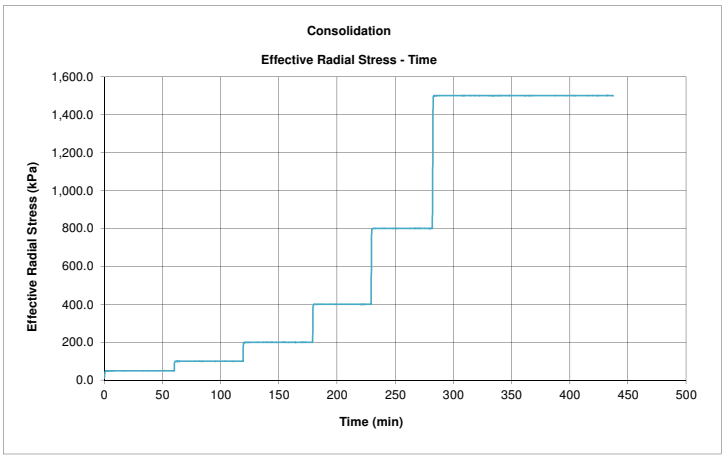












Triaxial CD Test - Summary

(ASTM D7181)

PROJECT NO. : A03355A01
PROJECT :
SAMPLE : Average
TEST NO. : TX 02 - CID

DATE : 2019-07-29
TESTED BY: BY
CHECKED BY: JG

SPECIMEN INFORMATION	UNITS	Initial	Vacuum	Saturation / B-value	End of 1st Consolidation	End of 2nd Consolidation	End of 3rd Consolidation	At Failure	End of Shear	
Specimen Height	mm	139.89	139.49	137.41	135.95	135.39	134.75	109.93	88.31	
Specimen Diameter	mm	69.80	69.40	66.94	66.46	66.20	65.92	71.09	79.13	
Area	cm^2	38.26	37.83	35.19	34.69	34.42	34.13	39.70	49.18	
Volume	cm^3	535.29	527.66	483.52	471.58	466.05	459.90	436.36	434.31	
Wet Weight	g	1215.22	1215.22	1406.90	1394.97	1389.43	1383.28	1359.74	1357.69	
Water Content	%	5.13	5.13	21.71	20.68	20.20	19.67	17.63	17.46	
Dry Weight	g	1155.92	1155.92	1155.92	1155.92	1155.92	1155.92	1155.92	1155.92	
Wet Density	g/cm^3	2.270	2.303	2.910	2.958	2.981	3.008	3.116	3.126	
Dry Density	g/cm^3	2.159	2.191	2.391	2.451	2.480	2.513	2.649	2.662	
Specific Gravity of Solids (assumed)	-	4.97	4.97	4.97	4.97	4.97	4.97	4.97	4.97	
Solids Volume	cm^3	232.580	232.580	232.580	232.580	232.580	232.580	232.580	232.580	
Void Volume	cm^3	302.708	295.078	250.938	239.003	233.470	227.321	203.778	201.732	
Water Volume	cm^3	59.299	59.299	250.979	239.044	233.511	227.362	203.819	201.773	
Void Ratio (e)	-	1.302	1.269	1.079	1.028	1.004	0.977	0.876	0.867	
Saturation Ratio (Sr)	%	19.59	20.10	100.02	100.02	100.02	100.02	100.02	100.02	
Effective Confining Stress	kPa				50	100	200			

Shearing (CU)		
Skempton's B Parameter		0.98
Back Pressure before shearing	kPa	400.0
Confining Stress (σ_3') before shearing	kPa	200
Shear Strain Rate	mm / min	0.035

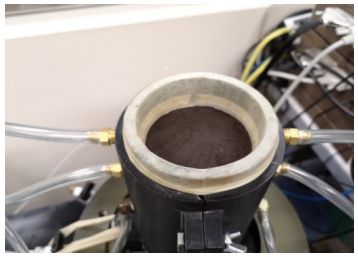
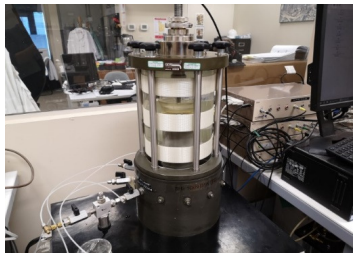
At Maximum Deviator Stress:		
Axial Stain	%	**18.42**
Deviator Stress	kPa	**533.9**
Φ '	º	34.9
c' (assumed)	kPa	**0**

At Maximum Stress Ratio		
Axial Stain	%	**18.82**
Deviator Stress	kPa	**532.4**
Φ '	º	35.0
c' (assumed)	kPa	0

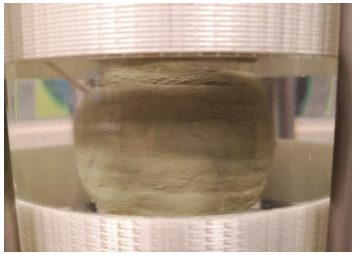
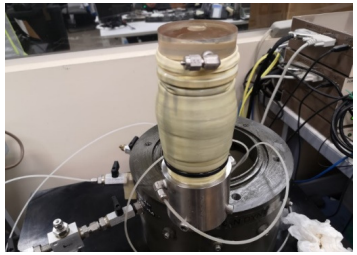
Note: *using cambridge method*

Photos:

Before Test

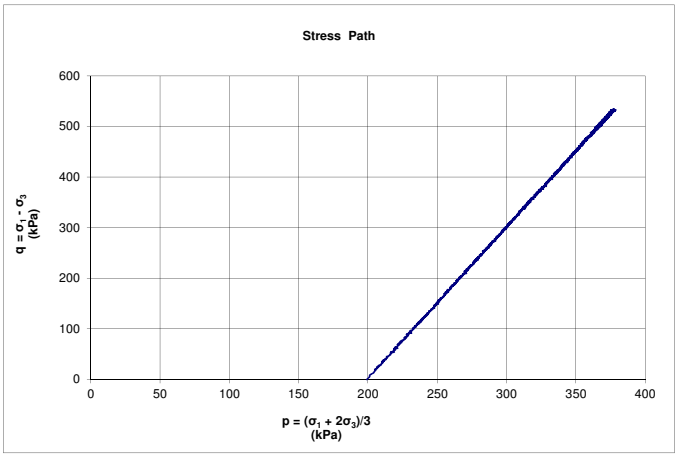
After Test

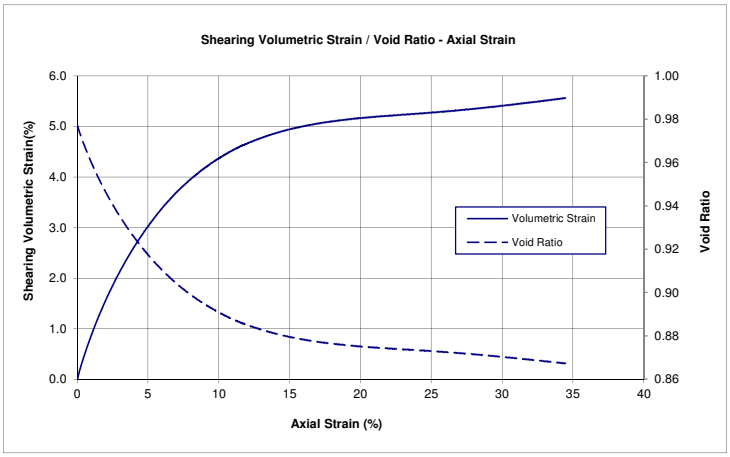



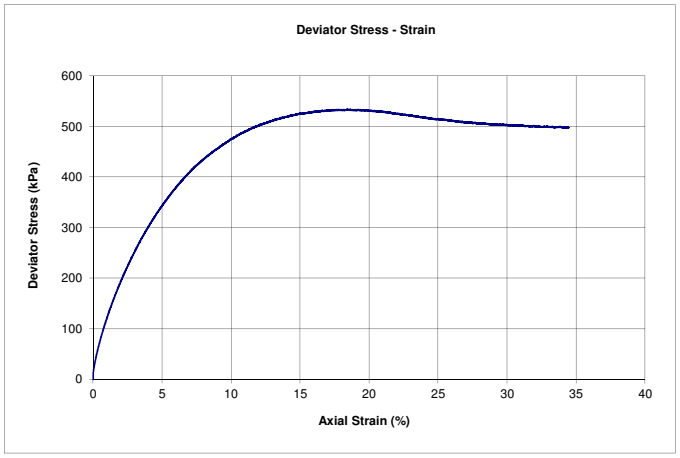
Triaxial CD Test - Charts

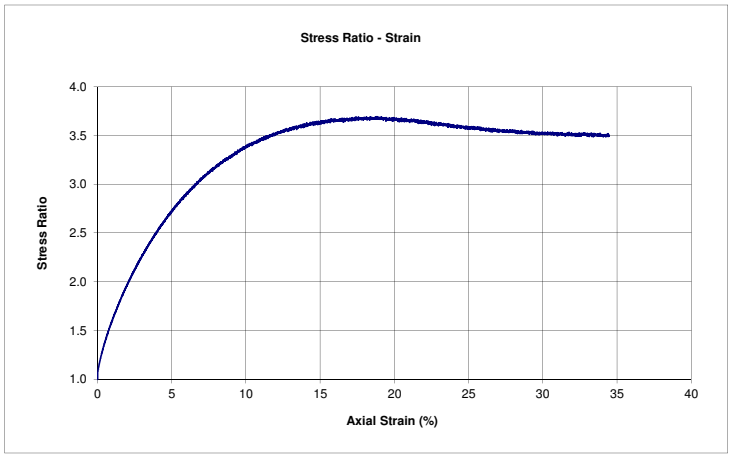
(ASTM D7181)

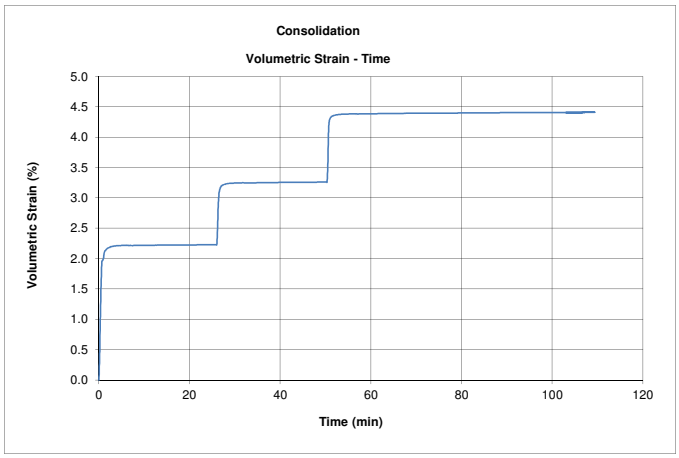
PROJECT NO. :	A03355A01	DATE :	2019-07-29
PROJECT :		TEST BY:	BY
SAMPLE :	Average	CHECKED BY:	JG
TEST NO. :	TX 02 - CID		

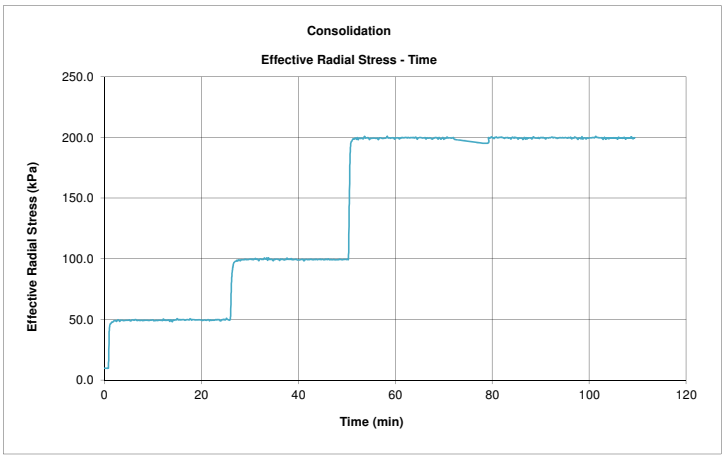












Triaxial CD Test - Summary

(ASTM D7181)

PROJECT NO. : A03355A01 DATE : 2019-07-29

PROJECT : TESTED BY: BY

SAMPLE : Average CHECKED BY: JG

TEST NO. : TX 03 - CID

SPECIMEN INFORMATION	UNITS	Initial	Vacuum	Saturation / B-value	End of 1st Consolidation	End of 2nd Consolidation	End of 3rd Consolidation	End of 4th Consolidation	End of 5th Consolidation	End of 6th Consolidation	At Failure	End of Shear
Specimen Height	mm	140.01	139.46	138.34	137.28	136.73	136.15	135.50	134.84	134.28	108.69	89.86
Specimen Diameter	mm	69.80	69.59	66.34	65.61	65.31	64.97	64.61	64.31	64.08	68.61	75.19
Area	cm^2	38.26	38.04	34.56	33.81	33.50	33.15	32.79	32.48	32.25	36.97	44.40
Volume	cm^3	535.75	530.44	478.11	464.12	458.01	451.40	444.31	438.02	433.00	401.85	399.02
Wet Weight	g	1190.38	1190.38	1382.74	1368.76	1362.64	1356.03	1348.94	1342.65	1337.64	1306.49	1303.65
Water Content	%	5.12	5.12	22.11	20.87	20.33	19.75	19.12	18.57	18.12	15.37	15.12
Dry Weight	g	1132.40	1132.40	1132.40	1132.40	1132.40	1132.40	1132.40	1132.40	1132.40	1132.40	1132.40
Wet Density	g/cm^3	2.222	2.244	2.892	2.949	2.975	3.004	3.036	3.065	3.089	3.251	3.267
Dry Density	g/cm^3	2.114	2.135	2.369	2.440	2.472	2.509	2.549	2.585	2.615	2.818	2.838
Specific Gravity of Solids (assumed)	-	4.97	4.97	4.97	4.97	4.97	4.97	4.97	4.97	4.97	4.97	4.97
Solids Volume	cm^3	227.847	227.847	227.847	227.847	227.847	227.847	227.847	227.847	227.847	227.847	227.847
Void Volume	cm^3	307.900	302.589	250.259	236.276	230.160	223.552	216.463	210.168	205.157	174.005	171.169
Water Volume	cm^3	57.979	57.979	250.339	236.356	230.240	223.632	216.543	210.248	205.237	174.085	171.249
Void Ratio (e)	-	1.351	1.328	1.098	1.037	1.010	0.981	0.950	0.922	0.900	0.764	0.751
Saturation Ratio (Sr)	%	18.83	19.16	100.03	100.03	100.03	100.04	100.04	100.04	100.04	100.05	100.05
Effective Confining Stress	kPa				50	100	200	400	700	1000		

Shearing (CU)		
Skempton's B Parameter		0.99
Back Pressure before shearing	kPa	300.0
Confining Stress (σ_3') before shearing	kPa	1000
Shear Strain Rate	mm / min	0.04

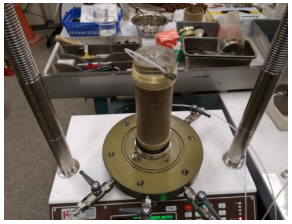
At Maximum Deviator Stress:		
Axial Stain	%	**19.06**
Deviator Stress	kPa	**2781.2**
Φ '	º	35.6
c' (assumed)	kPa	**0**

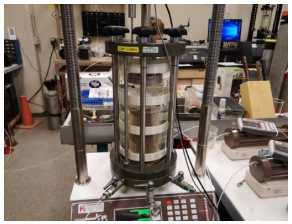
At Maximum Stress Ratio		
Axial Stain	%	**19.35**
Deviator Stress	kPa	**2779.8**
Φ '	º	35.6
c' (assumed)	kPa	0

Note: *using cambridge method*

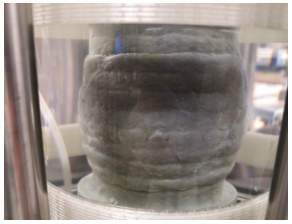
Photos:

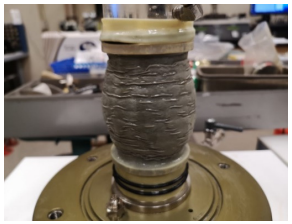
Before Test





After Test

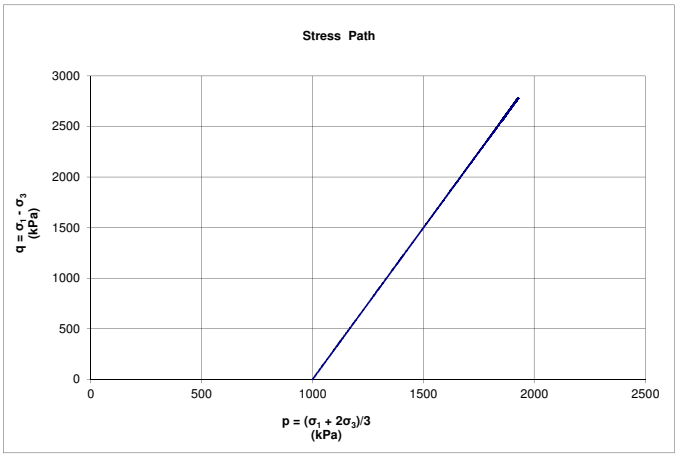


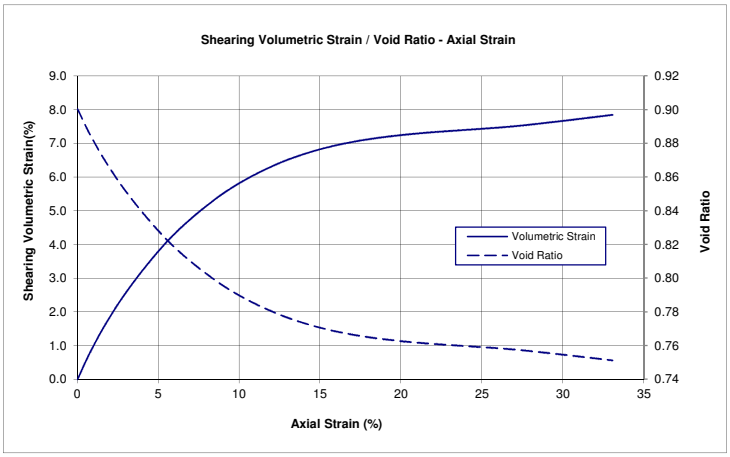


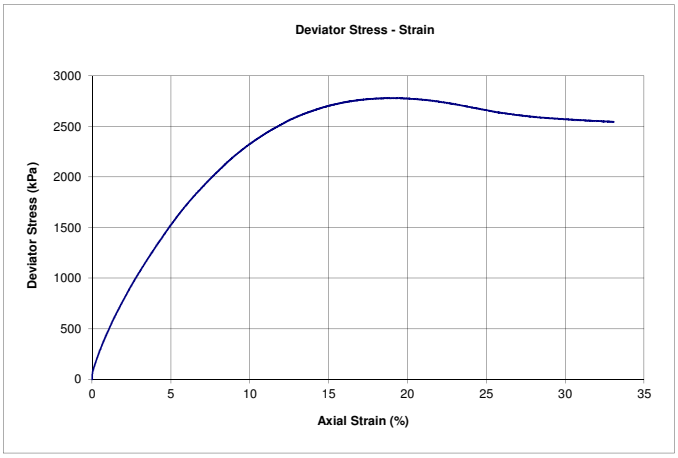
Triaxial CD Test - Charts

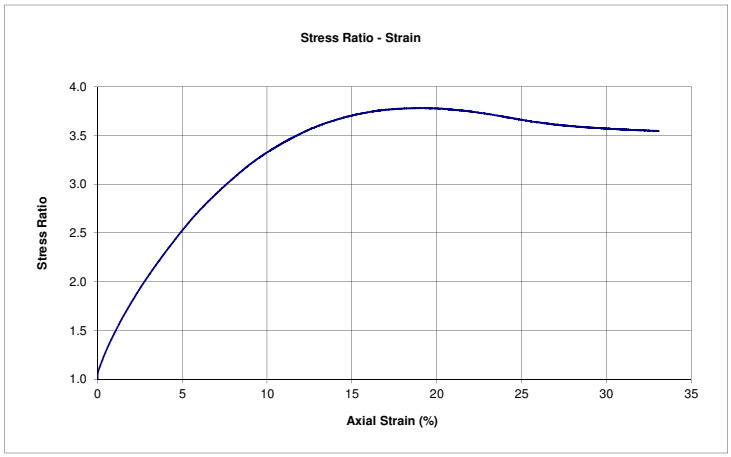
(ASTM D7181)

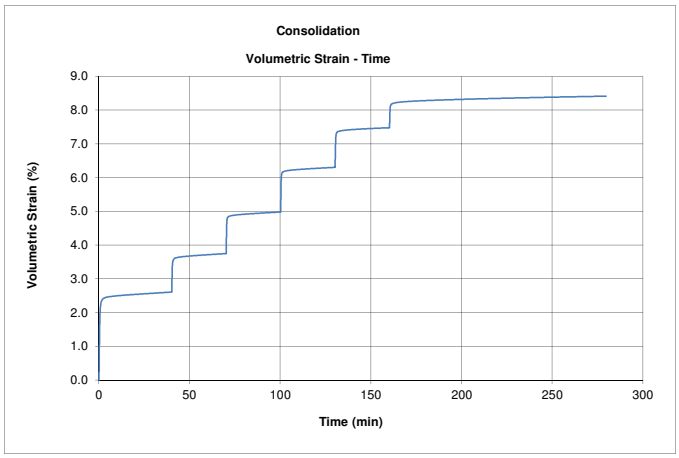
PROJECT NO. :	A03355A01	DATE :	2019-07-29
PROJECT :		TEST BY:	BY
SAMPLE :	Average	CHECKED BY:	JG
TEST NO. :	TX 03 - CID		

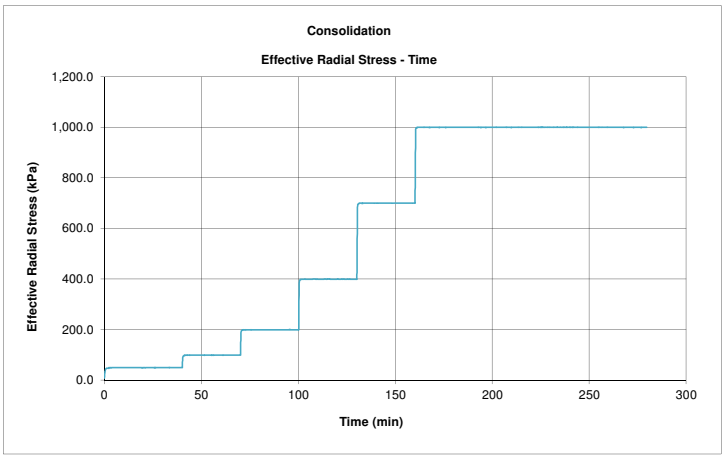












Triaxial CIU Test - Summary

(ASTM D4767)

PROJECT NO. : A03355A01 DATE : 2019-08-01

PROJECT : TESTED BY: BY

SAMPLE : Average CHECKED BY: JG

TEST NO. : TX04 - CIU

SPECIMEN INFORMATION	UNITS	Initial	Vacuum	Saturation	B-value	End of 1st Consolidation	End of 2nd Consolidation	End of 3rd Consolidation	End of 4th Consolidation	End of 5th Consolidation	At Maximum Deviator Stress	End of Shear
Specimen Height	mm	139.96	139.85	139.85	138.65	137.00	136.41	135.75	135.15	134.76	133.23	98.31
Specimen Diameter	mm	69.80	69.45	66.59	66.88	66.45	66.19	65.91	65.67	65.49	65.86	76.67
Area	cm^2	38.26	37.88	34.83	35.13	34.68	34.41	34.12	33.87	33.68	34.07	46.17
Volume	cm^3	535.56	529.78	487.10	487.10	475.16	469.39	463.22	457.81	453.91	453.91	453.91
Wet Weight	g	1215.82	1215.82	1409.82	1411.80	1399.86	1394.08	1387.91	1382.50	1378.61	1378.61	1378.61
Water Content	%	5.06	5.06	21.82	21.99	20.96	20.46	19.93	19.46	19.13	19.13	19.13
Dry Weight	g	1157.26	1157.26	1157.26	1157.26	1157.26	1157.26	1157.26	1157.26	1157.26	1157.26	1157.26
Wet Density	g/cm^3	2.270	2.295	2.894	2.898	2.946	2.970	2.996	3.020	3.037	3.037	3.037
Dry Density	g/cm^3	2.161	2.184	2.376	2.376	2.435	2.465	2.498	2.528	2.550	2.550	2.550
Specific Gravity of Solids	-	4.97	4.97	4.97	4.97	4.97	4.97	4.97	4.97	4.97	4.97	4.97
Solids Volume	cm^3	232.850	232.850	232.850	232.850	232.850	232.850	232.850	232.850	232.850	232.850	232.850
Void Volume	cm^3	302.706	296.932	254.252	254.252	242.315	236.536	230.369	224.960	221.062	221.062	221.062
Water Volume	cm^3	58.557	58.557	252.557	254.532	242.595	236.816	230.649	225.240	221.342	221.342	221.342
Void Ratio (e)	-	1.300	1.275	1.092	1.092	1.041	1.016	0.989	0.966	0.949	0.949	0.949
Saturation Ratio (Sr)	%	19.34	19.72	99.33	100.11	100.12	100.12	100.12	100.12	100.13	100.13	100.13
Effective Confining Stress	kPa					50	100	200	350	500		

Shearing (CU)		
Skempton's B Parameter		0.99
Back Pressure before shearing	kPa	400.0
Confining Stress (σ_3') before shearing	kPa	500
Shear Strain Rate	mm / min	0.04

Note: *using cambridge method*

At Maximum Deviator Stress:		
Axial Stain	%	1.14
Deviator Stress	kPa	163.7
Φ '	º	20.3
c' (assumed)	kPa	0

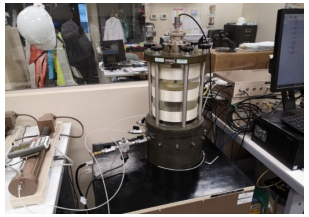
At Maximum Stress Ratio		
Axial Stain	%	10.00
Deviator Stress	kPa	34.9
Φ '	º	33.7
c' (assumed)	kPa	0

(selected at 10% axial strain)

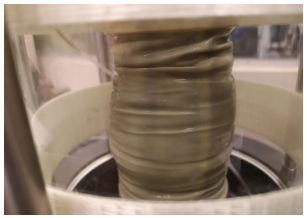
Test Photos:

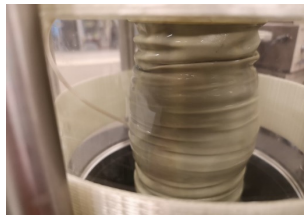
Before Test





After Test

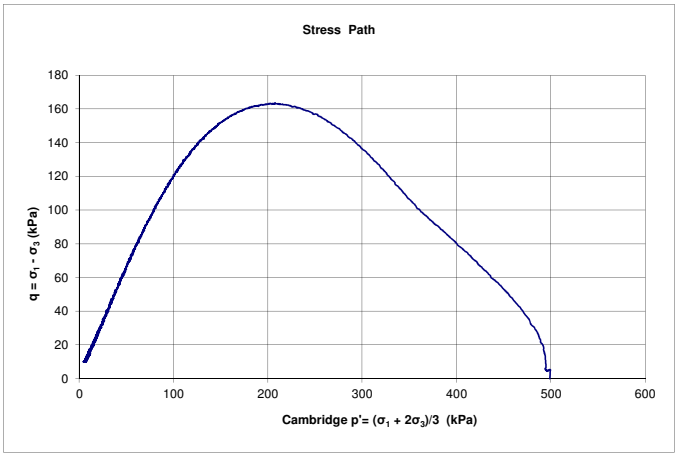


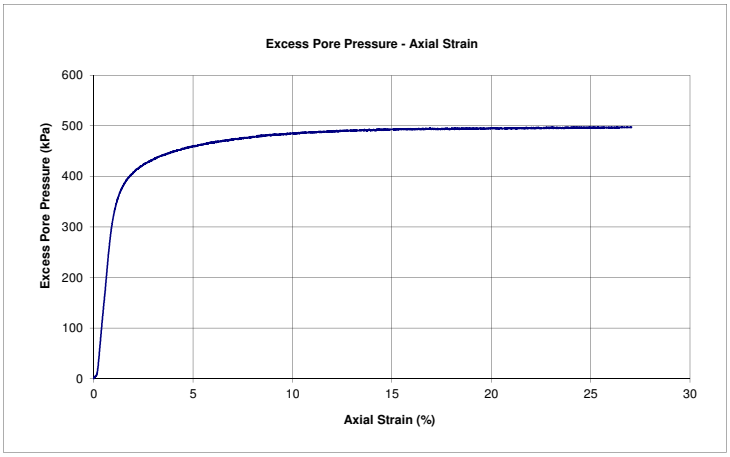


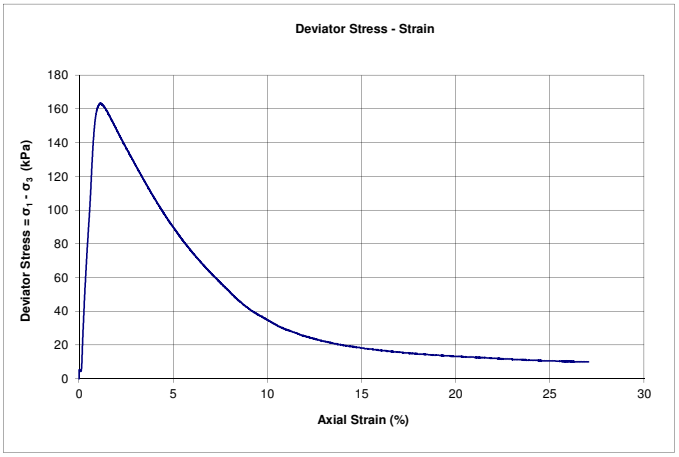
Triaxial CIU Test - Charts

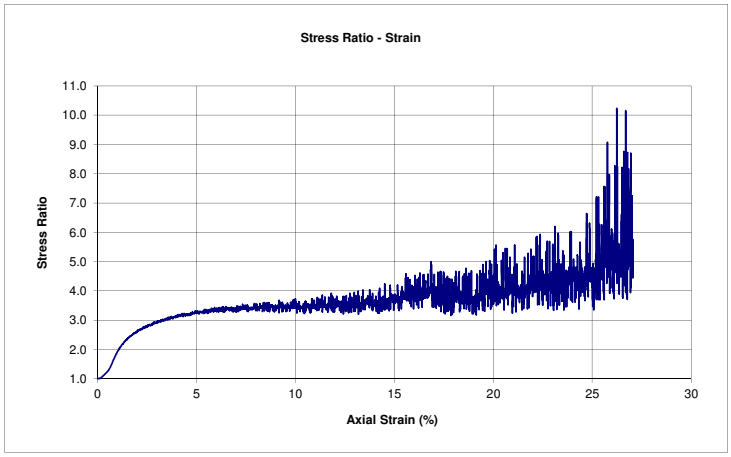
(ASTM D4767)

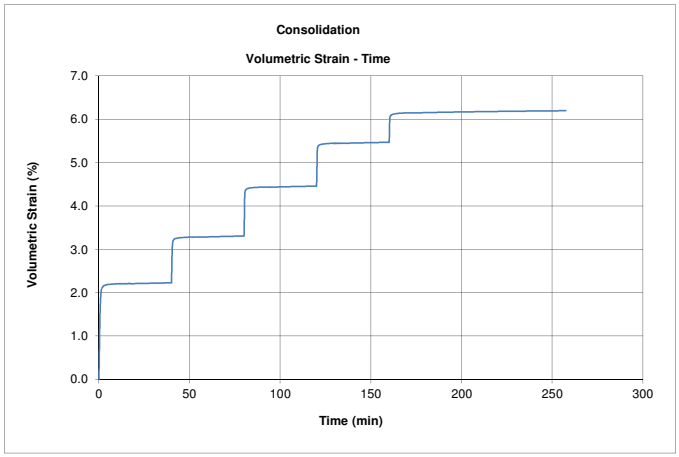
PROJECT NO. :	A03355A01	DATE :	2019-08-01
PROJECT :		TEST BY:	BY
SAMPLE :	Average	CHECKED BY:	JG
TEST NO. :	TX04 - CIU		

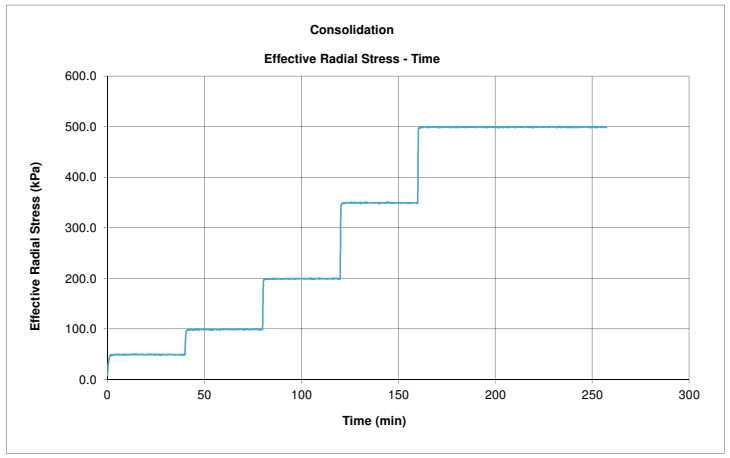












Triaxial CD Test - Summary

(ASTM D7181)

PROJECT NO. : A03355A01
PROJECT :
SAMPLE : Average
TEST NO. : TX05 - CID

DATE : 2019-07-25
TESTED BY: BY
CHECKED BY: JG

SPECIMEN INFORMATION	UNITS	Initial	Vacuum	Saturation	B value	End 1st Cons	End 2nd Cons	End 3rd Cons	End 4th Cons	End 5th Cons	at Failure	End of Shear
Specimen Height	mm	142.60	142.60	142.60	142.56	142.51	142.47	142.40	142.33	142.27	136.86	119.82
Specimen Diameter	mm	70.15	70.15	70.09	70.08	70.01	69.98	69.94	69.90	69.87	71.63	77.00
Area	cm^2	38.65	38.65	38.58	38.57	38.50	38.46	38.42	38.37	38.34	40.29	46.57
Volume	cm^3	551.144	551.144	550.125	549.904	548.632	547.918	547.035	546.150	545.465	551.469	557.968
Wet Weight	g	1749.69	1749.69	1823.69	1835.76	1834.49	1833.77	1832.89	1832.01	1831.32	1837.32	1843.82
Water Content	%	8.82	8.82	13.42	14.17	14.09	14.05	13.99	13.94	13.90	14.27	14.67
Dry Weight	g	1607.88	1607.88	1607.88	1607.88	1607.88	1607.88	1607.88	1607.88	1607.88	1607.88	1607.88
Wet Density	g/cm^3	3.175	3.175	3.315	3.338	3.344	3.347	3.351	3.354	3.357	3.332	3.305
Dry Density	g/cm^3	2.917	2.917	2.923	2.924	2.931	2.935	2.939	2.944	2.948	2.916	2.882
Specific Gravity of Solids	-	4.97	4.97	4.97	4.97	4.97	4.97	4.97	4.97	4.97	4.97	4.97
Solids Volume	cm^3	323.516	323.516	323.516	323.516	323.516	323.516	323.516	323.516	323.516	323.516	323.516
Void Volume	cm^3	227.627	227.627	226.608	226.388	225.116	224.402	223.519	222.634	221.949	227.953	234.451
Water Volume	cm^3	141.815	141.815	215.815	227.885	226.612	225.898	225.015	224.130	223.445	229.449	235.948
Void Ratio (e)	-	0.704	0.704	0.700	0.700	0.696	0.694	0.691	0.688	0.686	0.705	0.725
Saturation Ratio (Sr)	%	62.30	62.30	95.24	100.66	100.66	100.67	100.67	100.67	100.67	100.66	100.64
Effective Confining Stress	kPa					50	100	200	350	500		

Shearing		
Skempton's B Parameter		0.98
Back Pressure before shearing	kPa	355.6
Confining Stress (σ_3') before shearing	kPa	500
Shear Strain Rate	% / min	0.033

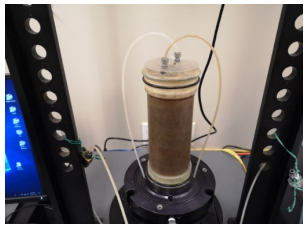
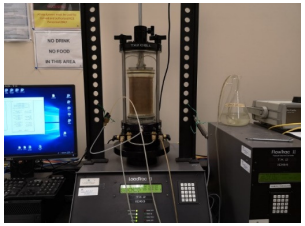
At Max. Deviator Stress:		
Axial Stain (%)	%	**3.80**
Deviator Stress	kPa	**2569.2**
Φ ' (Cambridge)	º	**46.0**
c'	kPa	**0.0**

At Max. Obliquity:		
Axial Stain (%)	%	**3.88**
Deviator Stress	kPa	**2568.0**
Φ ' (Cambridge)	º	**46.0**
c'	kPa	**0.0**

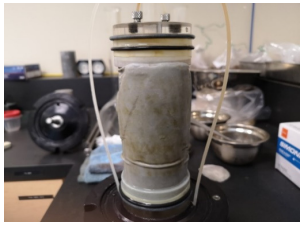
Note: *using cambridge method*

Photos:

Before Test

After Test

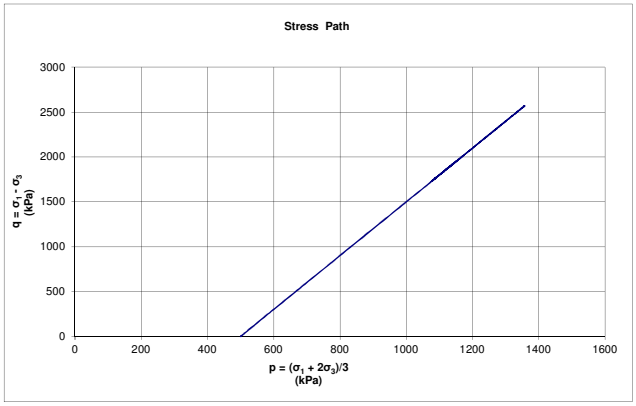



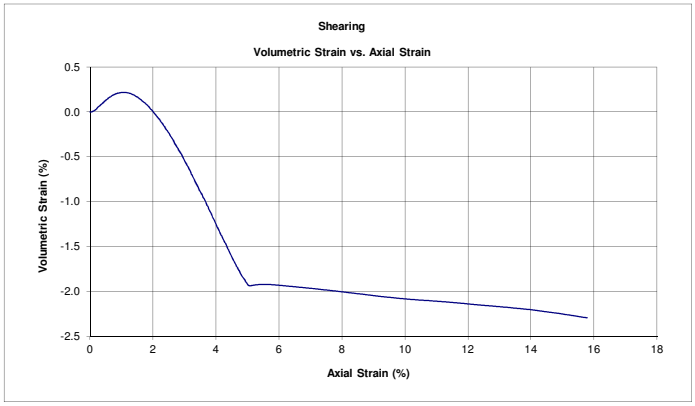
Triaxial CD Test - Charts

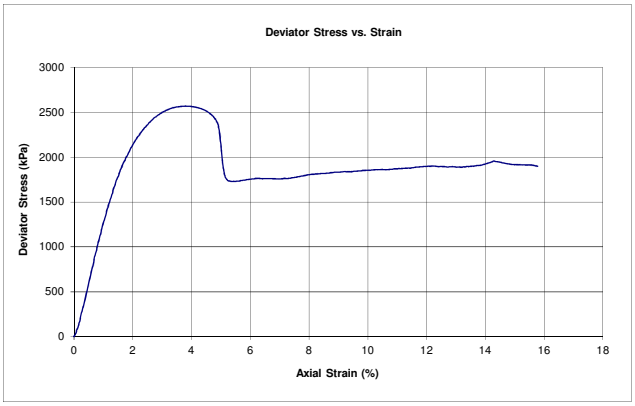
(ASTM D7181)

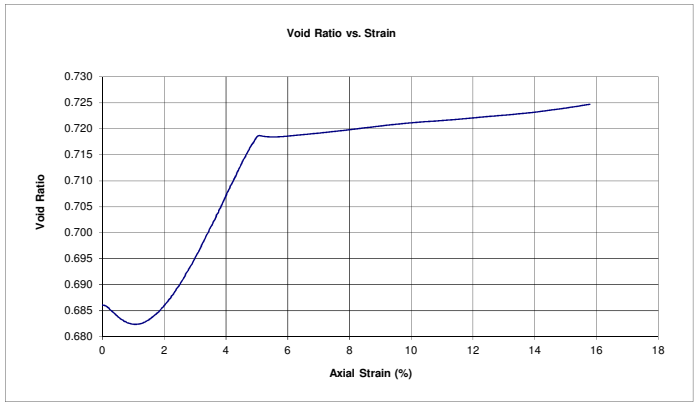
PROJECT NO. : A03355A01
PROJECT :
SAMPLE : Average
TEST NO. : TX05 - CID

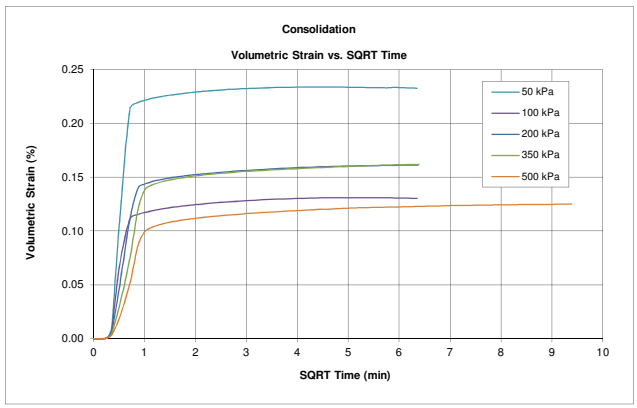
DATE : 2019-07-25
TEST BY: BY
CHECKED BY: JG

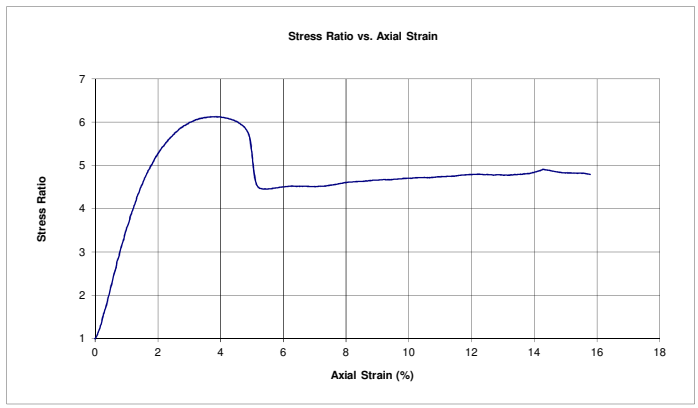












Triaxial CD Test - Summary

(ASTM D7181)

PROJECT NO. : A03355A01 DATE : 2019-07-31

PROJECT : TESTED BY: BY

SAMPLE : Batch 6 CHECKED BY:

TEST NO. : TX 06 - CD

SPECIMEN INFORMATION	UNITS	Initial	Vacuum	Saturation / B-value	End of 1st Consolidation	End of 2nd Consolidation	End of 3rd Consolidation	End of 4th Consolidation	End of 5th Consolidation	End of 6th Consolidation	At Failure	End of Shear
Specimen Height	mm	140.17	140.17	139.71	139.63	139.56	139.47	139.33	139.09	138.73	119.19	115.13
Specimen Diameter	mm	69.81	69.76	69.82	69.71	69.63	69.55	69.44	69.28	69.08	72.86	73.54
Area	cm^2	38.28	38.22	38.29	38.17	38.08	37.99	37.87	37.70	37.48	41.70	42.48
Volume	cm^3	536.51	535.74	534.94	532.95	531.49	529.79	527.62	524.40	519.94	496.99	489.09
Wet Weight	g	1531.25	1531.25	1660.90	1658.91	1657.44	1655.75	1653.57	1650.36	1645.89	1622.95	1615.04
Water Content	%	8.71	8.71	17.91	17.77	17.67	17.55	17.39	17.17	16.85	15.22	14.66
Dry Weight	g	1408.56	1408.56	1408.56	1408.56	1408.56	1408.56	1408.56	1408.56	1408.56	1408.56	1408.56
Wet Density	g/cm^3	2.854	2.858	3.105	3.113	3.119	3.125	3.134	3.147	3.166	3.266	3.302
Dry Density	g/cm^3	2.625	2.629	2.633	2.643	2.650	2.659	2.670	2.686	2.709	2.834	2.880
Specific Gravity of Solids (assumed)	-	4.97	4.97	4.97	4.97	4.97	4.97	4.97	4.97	4.97	4.97	4.97
Solids Volume	cm^3	283.413	283.413	283.413	283.413	283.413	283.413	283.413	283.413	283.413	283.413	283.413
Void Volume	cm^3	253.100	252.331	251.529	249.535	248.073	246.377	244.203	240.990	236.522	213.578	205.673
Water Volume	cm^3	122.686	122.686	252.336	250.342	248.880	247.184	245.010	241.797	237.329	214.385	206.480
Void Ratio (e)	-	0.893	0.890	0.888	0.880	0.875	0.869	0.862	0.850	0.835	0.754	0.726
Saturation Ratio (Sr)	%	48.47	48.62	100.32	100.32	100.33	100.33	100.33	100.33	100.34	100.38	100.39
Effective Confining Stress	kPa				50	100	200	400	800	1500		

Shearing (CU)		
Skempton's B Parameter		0.99
Back Pressure before shearing	kPa	500.0
Confining Stress (σ_3') before shearing	kPa	1500
Shear Strain Rate	mm / min	0.04

At Maximum Deviator Stress:		
Axial Stain	%	**14.08**
Deviator Stress	kPa	**4000.2**
Φ '	º	34.9
c' (assumed)	kPa	**0**

At Maximum Stress Ratio		
Axial Stain	%	**14.25**
Deviator Stress	kPa	**3998.4**
Φ '	º	34.9
c' (assumed)	kPa	0

Note: *using cambridge method*

Photos:

Before Test





After Test

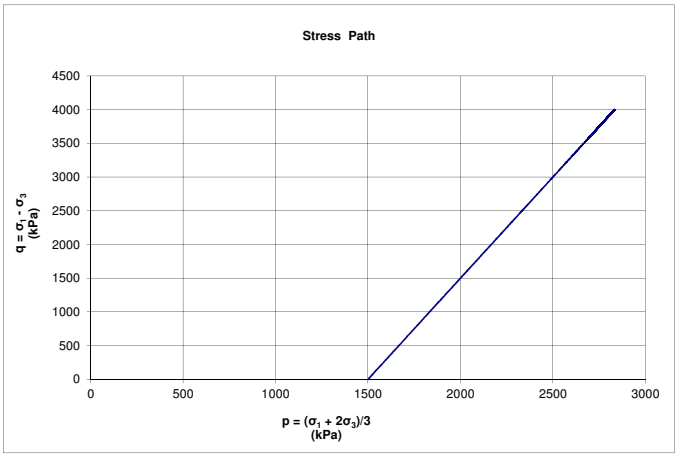


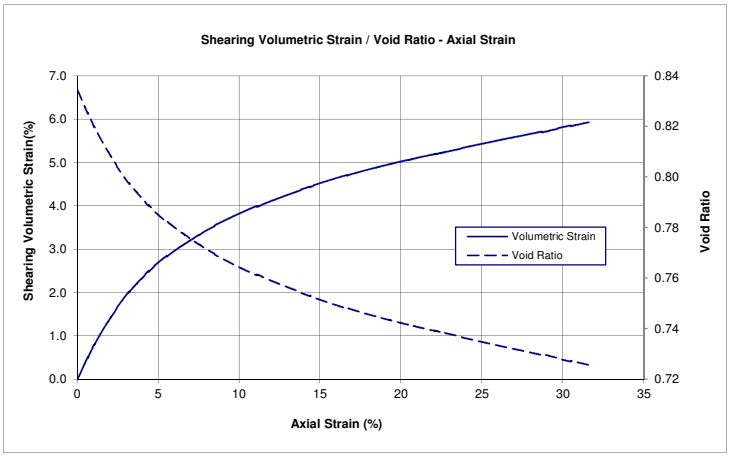


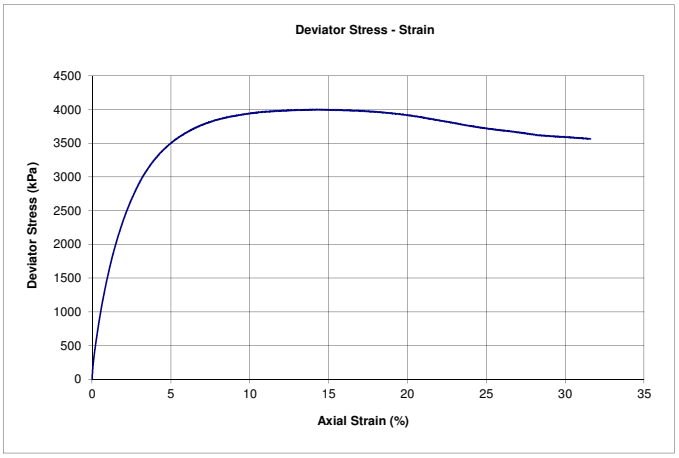
Triaxial CD Test - Charts

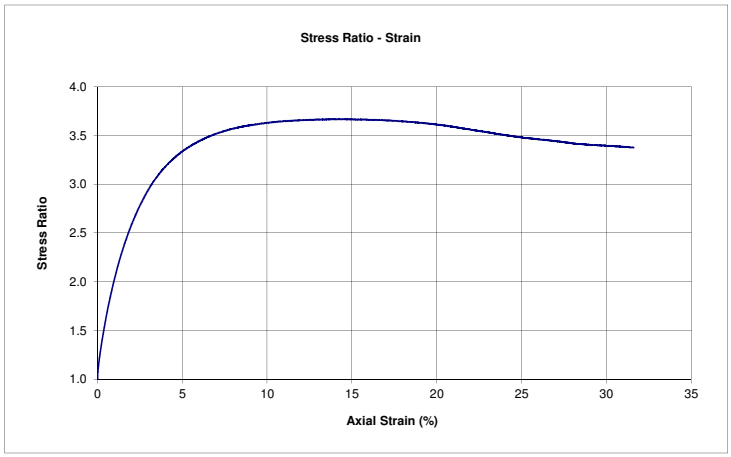
(ASTM D7181)

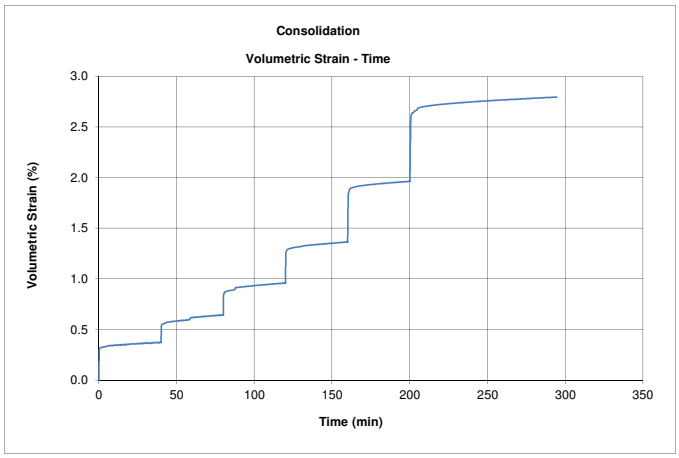
PROJECT NO. :	A03355A01	DATE :	2019-07-31
PROJECT :		TEST BY:	BY
SAMPLE :	Batch 6	CHECKED BY:	
TEST NO. :	TX 06 - CD		

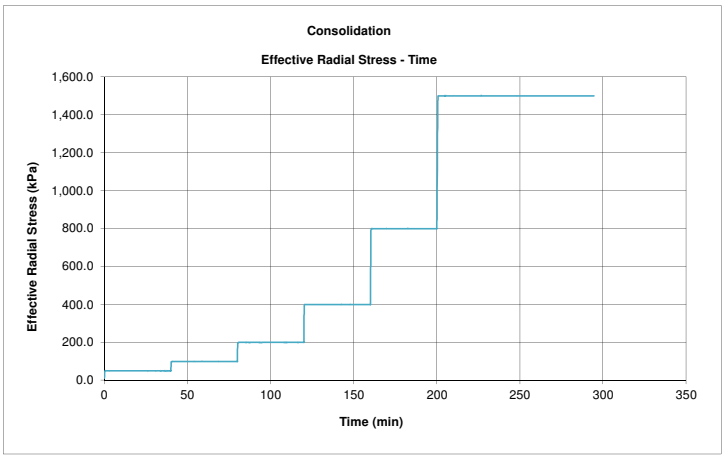












Triaxial CIU Test - Summary

(ASTM D4767)

PROJECT NO. : A03355A01 DATE : 2019-08-02

PROJECT : TESTED BY: BY

SAMPLE : Average CHECKED BY: JG

TEST NO. : TX07 - CIU

SPECIMEN INFORMATION	UNITS	Initial	Vacuum	Saturation / B Value	End of 1st Consolidation	End of 2nd Consolidation	End of 3rd Consolidation	End of 4th Consolidation	End of 5th Consolidation	End of 6th Consolidation	End of 7th Consolidation	At Maximum Deviator Stress
Specimen Height	mm	139.93	139.25	138.66	137.65	137.30	136.81	136.24	135.48	134.54	134.00	131.23
Specimen Diameter	mm	69.80	69.69	68.12	67.56	67.22	66.85	66.46	66.04	65.60	65.24	65.92
Area	cm^2	38.26	38.14	36.45	35.85	35.48	35.10	34.69	34.26	33.80	33.43	34.13
Volume	cm^3	535.44	531.16	505.34	493.43	487.20	480.21	472.56	464.11	454.73	447.93	447.93
Wet Weight	g	1268.03	1268.03	1472.22	1460.31	1454.08	1447.09	1439.44	1430.99	1421.61	1414.81	1414.81
Water Content	%	4.90	4.90	21.79	20.81	20.29	19.71	19.08	18.38	17.60	17.04	17.04
Dry Weight	g	1208.80	1208.80	1208.80	1208.80	1208.80	1208.80	1208.80	1208.80	1208.80	1208.80	1208.80
Wet Density	g/cm^3	2.368	2.387	2.913	2.960	2.985	3.013	3.046	3.083	3.126	3.159	3.159
Dry Density	g/cm^3	2.258	2.276	2.392	2.450	2.481	2.517	2.558	2.605	2.658	2.699	2.699
Specific Gravity of Solids	-	4.97	4.97	4.97	4.97	4.97	4.97	4.97	4.97	4.97	4.97	4.97
Solids Volume	cm^3	243.219	243.219	243.219	243.219	243.219	243.219	243.219	243.219	243.219	243.219	243.219
Void Volume	cm^3	292.222	287.942	262.122	250.210	243.979	236.989	229.339	220.892	211.507	204.714	204.714
Water Volume	cm^3	59.231	59.231	263.421	251.509	245.278	238.288	230.638	222.191	212.806	206.013	206.013
Void Ratio (e)	-	1.201	1.184	1.078	1.029	1.003	0.974	0.943	0.908	0.870	0.842	0.842
Saturation Ratio (Sr)	%	20.27	20.57	100.50	100.52	100.53	100.55	100.57	100.59	100.61	100.63	100.63
Effective Confining Stress	kPa				50	100	200	400	800	1500	2000	

Shearing (CU)		
Skempton's B Parameter		0.99
Back Pressure before shearing	kPa	400.0
Confining Stress (σ_3') before shearing	kPa	2000
Shear Strain Rate	mm / min	0.04

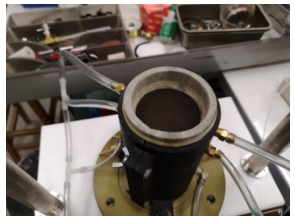
At Maximum Deviator Stress:		
Axial Stain	%	0.58
Deviator Stress	kPa	822.3
Φ '	º	20.3
c' (assumed)	kPa	0

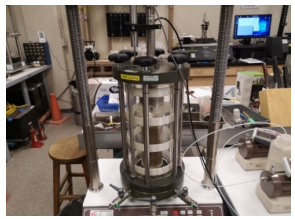
At Maximum Stress Ratio		
Axial Stain	%	9.45
Deviator Stress	kPa	444.0
Φ '	º	35.3
c' (assumed)	kPa	0

Note: *using cambridge method*

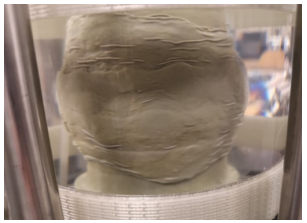
Test Photos:

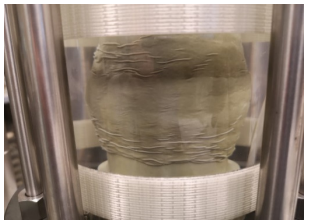
Before Test





After Test

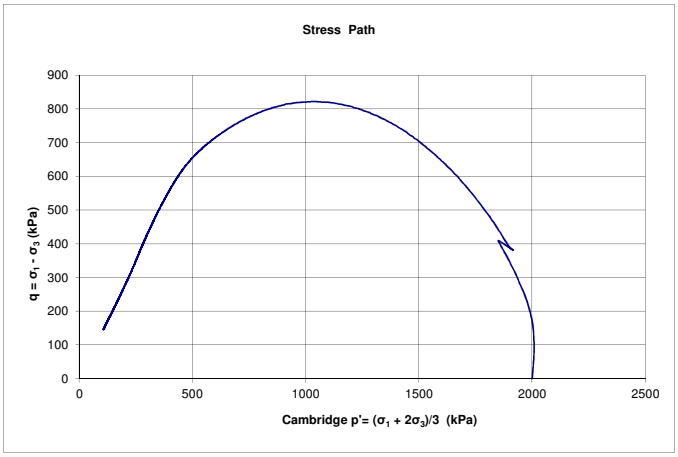


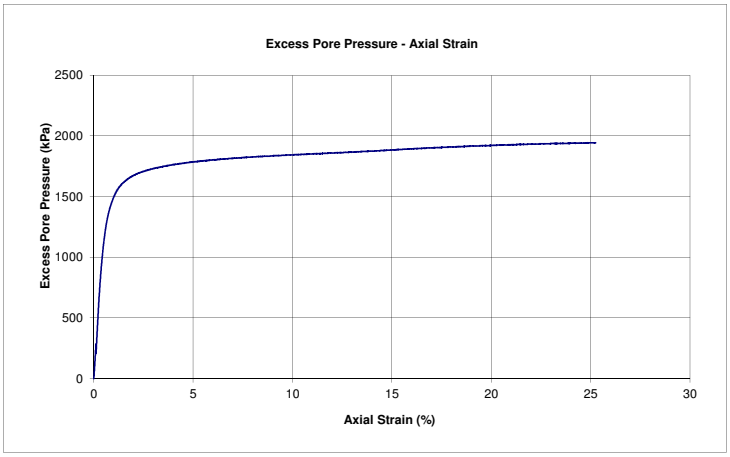


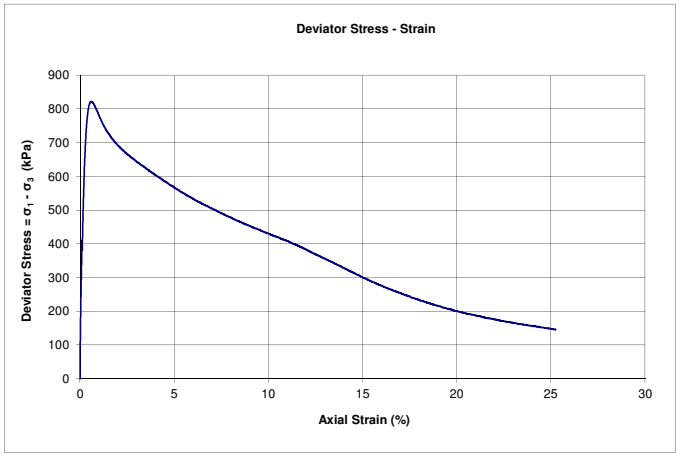
Triaxial CIU Test - Charts

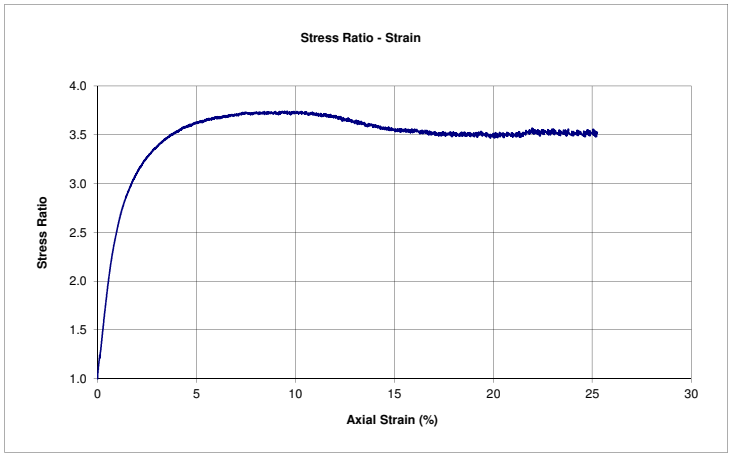
(ASTM D4767)

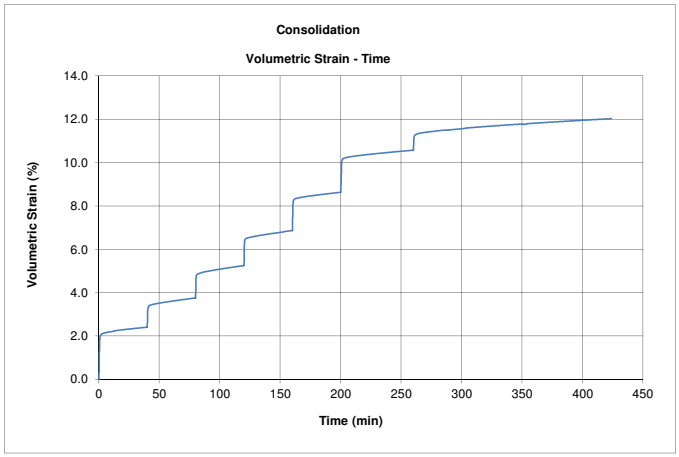
PROJECT NO. :	A03355A01	DATE :	2019-08-02
PROJECT :		TEST BY:	BY
SAMPLE :	Average	CHECKED BY:	JG
TEST NO. :	TX07 - CIU		

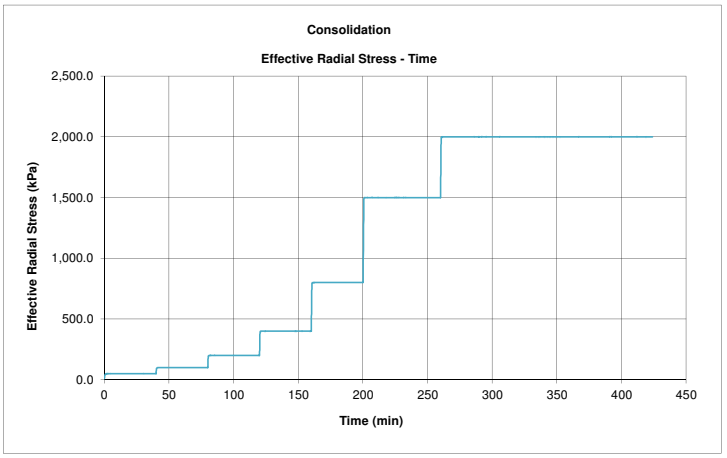












Triaxial CD Test - Summary

(ASTM D7181)

PROJECT NO. : A03355A01
PROJECT :
SAMPLE : Average
TEST NO. : TX 08 - CID

DATE : 2019-08-16
TESTED BY: BY
CHECKED BY: JG

SPECIMEN INFORMATION	UNITS	Initial	Vacuum	Saturation	B-value	End of 1st Consolidation	At Maximum Deviator Stress	End of Shear		
Specimen Height	mm	140.14	140.14	140.14	140.14	140.05	138.19	99.94		
Specimen Diameter	mm	69.90	69.79	69.77	69.78	69.65	70.22	82.23		
Area	cm^2	38.37	38.25	38.24	38.24	38.10	38.73	53.10		
Volume	cm^3	537.78	536.09	535.85	535.85	533.64	535.23	530.72		
Wet Weight	g	1510.55	1510.55	1645.65	1651.61	1649.41	1650.99	1646.49		
Water Content	%	8.15	8.15	17.82	18.25	18.09	18.21	17.88		
Dry Weight	g	1396.72	1396.72	1396.72	1396.72	1396.72	1396.72	1396.72		
Wet Density	g/cm^3	2.809	2.818	3.071	3.082	3.091	3.085	3.102		
Dry Density	g/cm^3	2.597	2.605	2.607	2.607	2.617	2.610	2.632		
Specific Gravity of Solids (assumed)	-	4.97	4.97	4.97	4.97	4.97	4.97	4.97		
Solids Volume	cm^3	281.030	281.030	281.030	281.030	281.030	281.030	281.030		
Void Volume	cm^3	256.752	255.061	254.816	254.816	252.612	254.197	249.694		
Water Volume	cm^3	113.832	113.832	248.932	254.894	252.690	254.275	249.772		
Void Ratio (e)	-	0.914	0.908	0.907	0.907	0.899	0.905	0.888		
Saturation Ratio (Sr)	%	44.34	44.63	97.69	100.03	100.03	100.03	100.03		
Effective Confining Stress	kPa					40				

Shearing (CU)		
Skempton's B Parameter		0.99
Back Pressure before shearing	kPa	500.0
Confining Stress (σ_3') before shearing	kPa	40
Shear Strain Rate	mm / min	0.035

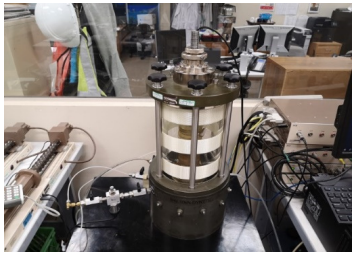
At Maximum Deviator Stress:		
Axial Stain	%	**1.33**
Deviator Stress	kPa	**139.0**
Φ '	º	39.2
c' (assumed)	kPa	**0**

At Maximum Stress Ratio		
Axial Stain	%	**1.23**
Deviator Stress	kPa	**138.5**
Φ '	º	39.3
c' (assumed)	kPa	0

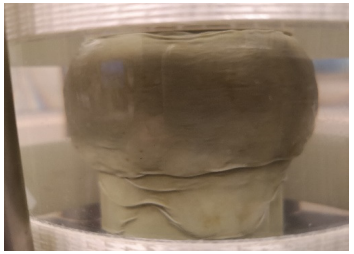
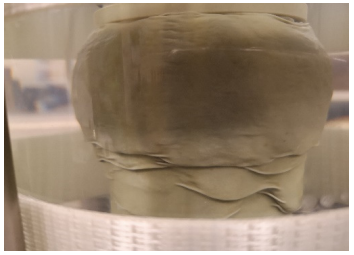
Note: *using cambridge method*

Photos:

Before Test

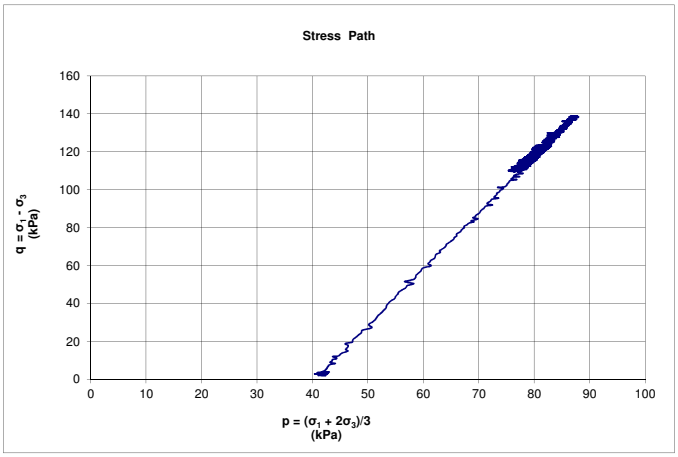
After Test

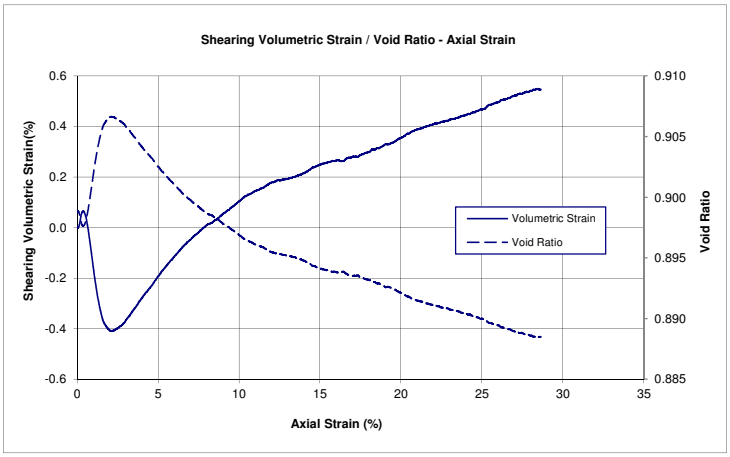



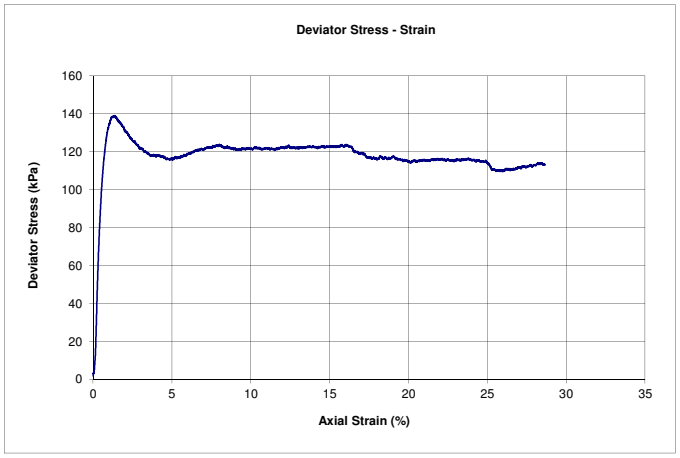
Triaxial CD Test - Charts

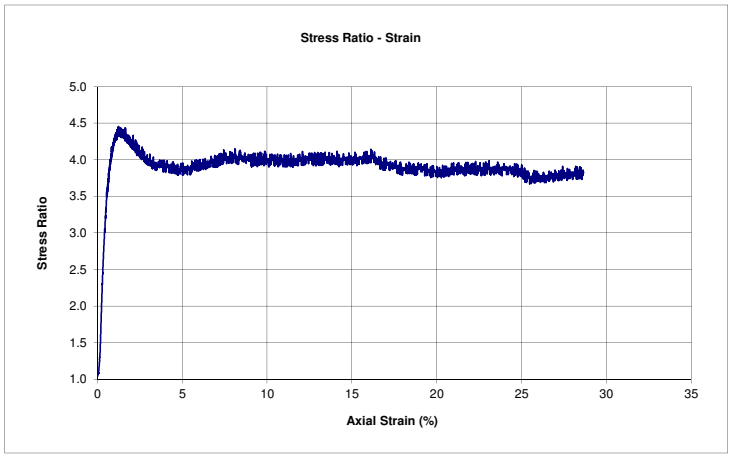
(ASTM D7181)

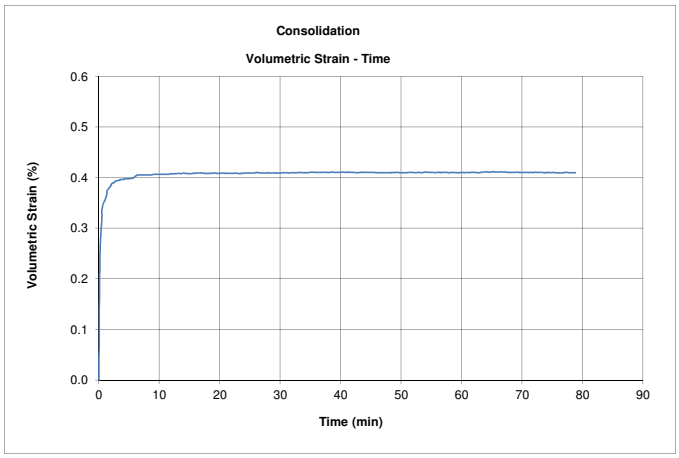
PROJECT NO. :	A03355A01	DATE :	2019-08-16
PROJECT :		TEST BY:	BY
SAMPLE :	Average	CHECKED BY:	JG
TEST NO. :	TX 08 - CID		

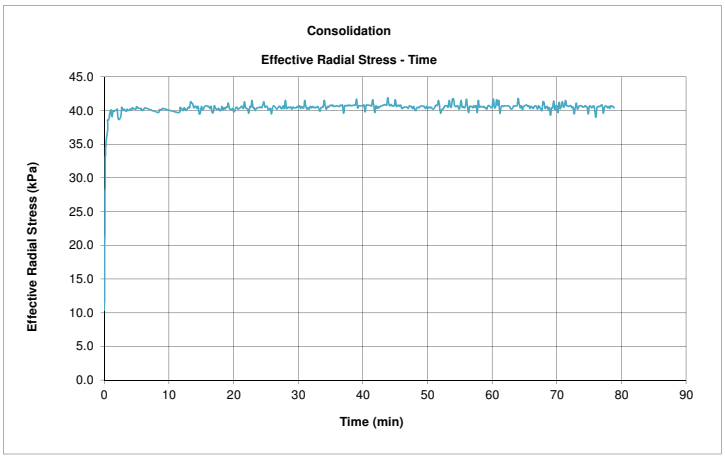












Triaxial CD Test - Summary

(ASTM D7181)

PROJECT NO. : A03355A01
PROJECT :
SAMPLE : Batch 4
TEST NO. : TX 09 - CD

DATE : 2019-08-15
TESTED BY: BY
CHECKED BY:

SPECIMEN INFORMATION	UNITS	Initial	Vacuum	Saturation / B-value	End of 1st Consolidation	End of 2nd Consolidation	At Failure	End of Shear		
Specimen Height	mm	140.03	139.56	139.21	139.15	139.10	136.58	97.07		
Specimen Diameter	mm	69.90	69.93	70.08	69.91	69.78	70.68	83.99		
Area	cm^2	38.37	38.41	38.57	38.39	38.24	39.24	55.40		
Volume	cm^3	537.36	536.02	536.94	534.16	531.94	535.94	537.77		
Wet Weight	g	1567.86	1567.86	1699.68	1696.90	1694.68	1698.68	1700.51		
Water Content	%	7.85	7.85	16.92	16.73	16.57	16.85	16.97		
Dry Weight	g	1453.74	1453.74	1453.74	1453.74	1453.74	1453.74	1453.74		
Wet Density	g/cm^3	2.918	2.925	3.165	3.177	3.186	3.170	3.162		
Dry Density	g/cm^3	2.705	2.712	2.707	2.722	2.733	2.712	2.703		
Specific Gravity of Solids (assumed)	-	4.97	4.97	4.97	4.97	4.97	4.97	4.97		
Solids Volume	cm^3	292.503	292.503	292.503	292.503	292.503	292.503	292.503		
Void Volume	cm^3	244.857	243.513	244.441	241.655	239.436	243.440	245.268		
Water Volume	cm^3	114.119	114.119	245.940	243.154	240.935	244.939	246.767		
Void Ratio (e)	-	0.837	0.833	0.836	0.826	0.819	0.832	0.839		
Saturation Ratio (Sr)	%	46.61	46.86	100.61	100.62	100.63	100.62	100.61		
Effective Confining Stress	kPa				50	100				

Shearing (CU)		
Skempton's B Parameter		0.99
Back Pressure before shearing	kPa	499.0
Confining Stress (σ_3') before shearing	kPa	100
Shear Strain Rate	mm / min	0.04

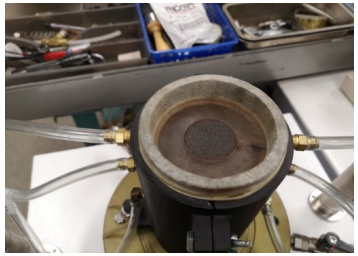
At Maximum Deviator Stress:		
Axial Stain	%	**1.81**
Deviator Stress	kPa	**460.8**
Φ '	º	44.2
c' (assumed)	kPa	**0**

At Maximum Stress Ratio		
Axial Stain	%	**1.82**
Deviator Stress	kPa	**460.2**
Φ '	º	44.2
c' (assumed)	kPa	0

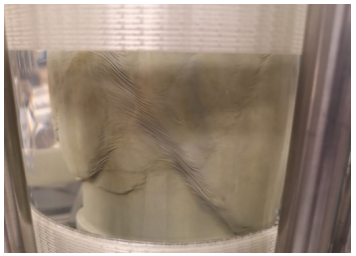
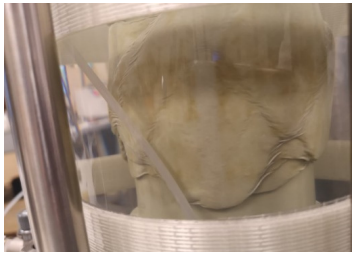
Note: *using cambridge method*

Photos:

Before Test



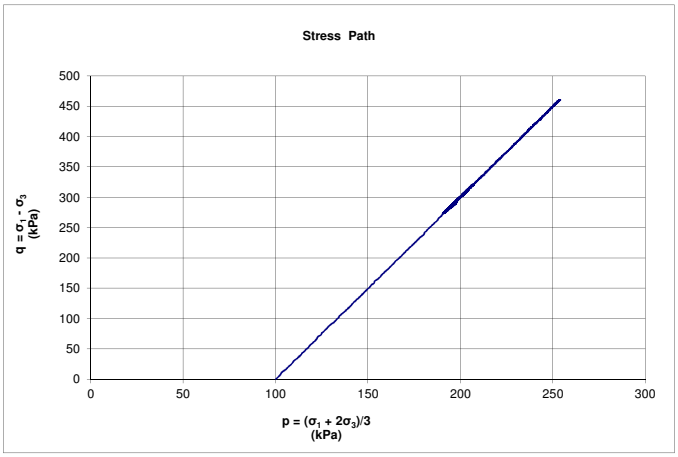

After Test

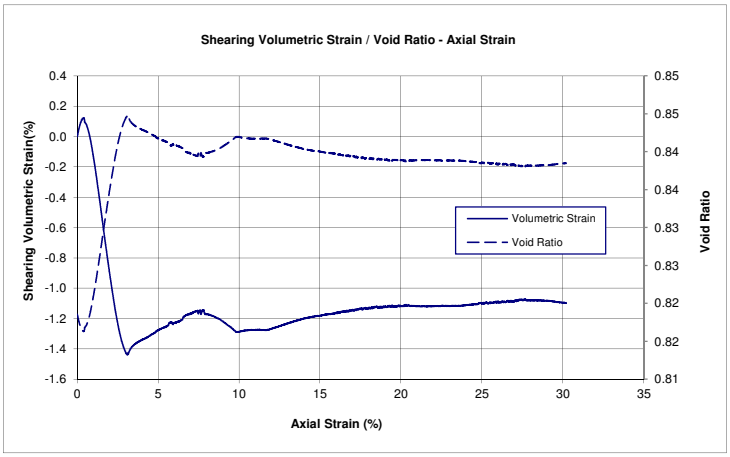



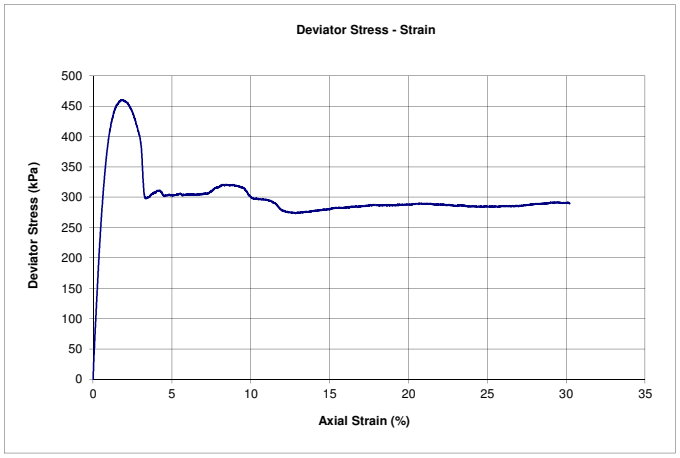
Triaxial CD Test - Charts

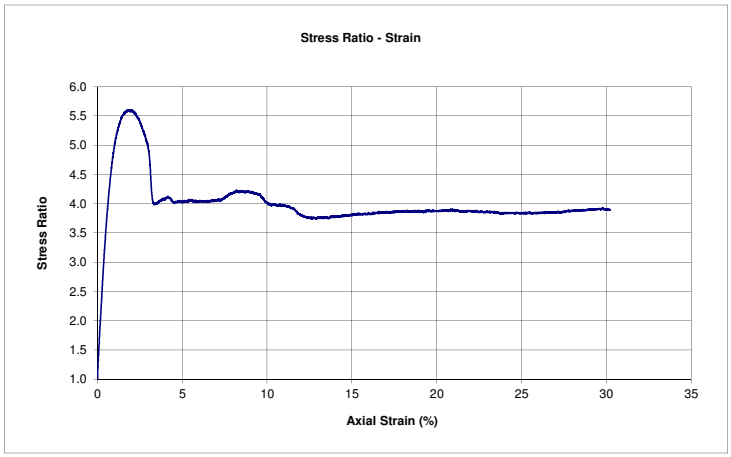
(ASTM D7181)

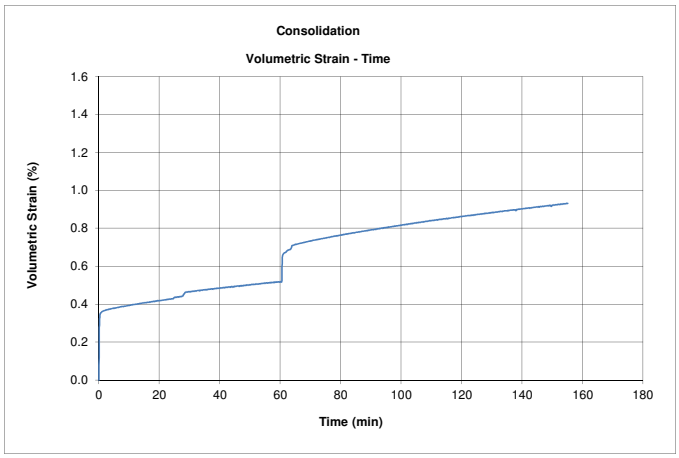
PROJECT NO. :	A03355A01	DATE :	2019-08-15
PROJECT :		TEST BY:	BY
SAMPLE :	Batch 4	CHECKED BY:	
TEST NO. :	TX 09 - CD		

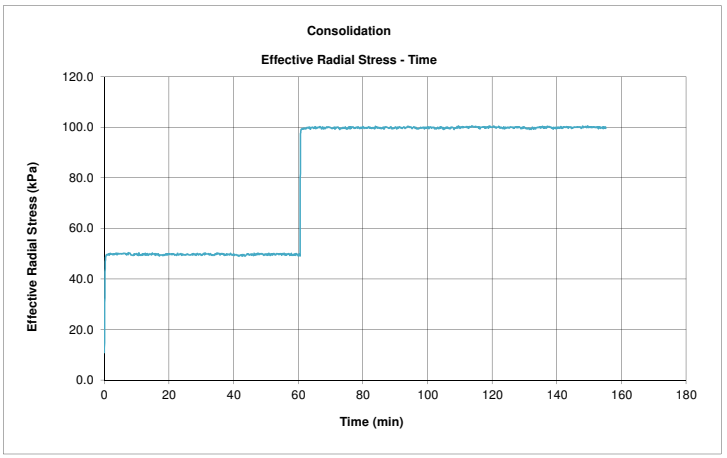












Triaxial CD Test - Summary

(ASTM D7181)

PROJECT NO. : A03355A01 DATE : 2019-08-21

PROJECT : TESTED BY: BY

SAMPLE : Fine Gradation CHECKED BY: JG

TEST NO. : TX 10 - CID

SPECIMEN INFORMATION	UNITS	Initial	Vacuum	Saturation	B-value	End of 1st Consolidation	At Maximum Deviator Stress	End of Shear		
Specimen Height	mm	139.94	139.82	139.82	139.57	139.46	137.45	97.79		
Specimen Diameter	mm	69.80	69.80	69.77	69.77	69.70	70.36	83.17		
Area	cm^2	38.26	38.26	38.24	38.23	38.15	38.88	54.33		
Volume	cm^3	535.48	535.02	534.64	533.64	532.08	534.37	531.32		
Wet Weight	g	1454.05	1454.05	1579.15	1610.67	1609.11	1611.40	1608.35		
Water Content	%	7.80	7.80	17.07	19.41	19.30	19.47	19.24		
Dry Weight	g	1348.84	1348.84	1348.84	1348.84	1348.84	1348.84	1348.84		
Wet Density	g/cm^3	2.715	2.718	2.954	3.018	3.024	3.016	3.027		
Dry Density	g/cm^3	2.519	2.521	2.523	2.528	2.535	2.524	2.539		
Specific Gravity of Solids (assumed)	-	4.96	4.96	4.96	4.96	4.96	4.96	4.96		
Solids Volume	cm^3	271.944	271.944	271.944	271.944	271.944	271.944	271.944		
Void Volume	cm^3	263.536	263.076	262.693	261.693	260.139	262.427	259.373		
Water Volume	cm^3	105.210	105.210	230.310	261.828	260.274	262.562	259.508		
Void Ratio (e)	-	0.969	0.967	0.966	0.962	0.957	0.965	0.954		
Saturation Ratio (Sr)	%	39.92	39.99	87.67	100.05	100.05	100.05	100.05		
Effective Confining Stress	kPa					40				

Shearing (CU)		
Skempton's B Parameter		0.98
Back Pressure before shearing	kPa	498.0
Confining Stress (σ_3') before shearing	kPa	50
Shear Strain Rate	mm / min	0.04

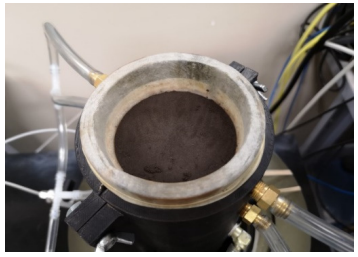
At Maximum Deviator Stress:		
Axial Stain	%	**1.44**
Deviator Stress	kPa	**172.2**
Φ '	º	39.1
c' (assumed)	kPa	**0**

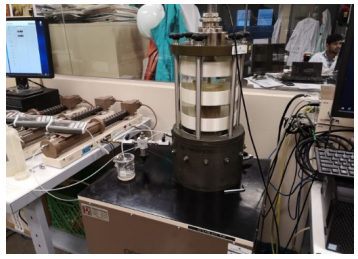
At Maximum Stress Ratio		
Axial Stain	%	**1.35**
Deviator Stress	kPa	**171.4**
Φ '	º	39.5
c' (assumed)	kPa	0

Note: *using cambridge method*

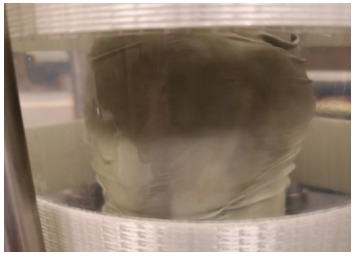
Photos:

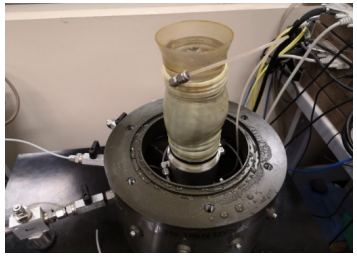
Before Test





After Test

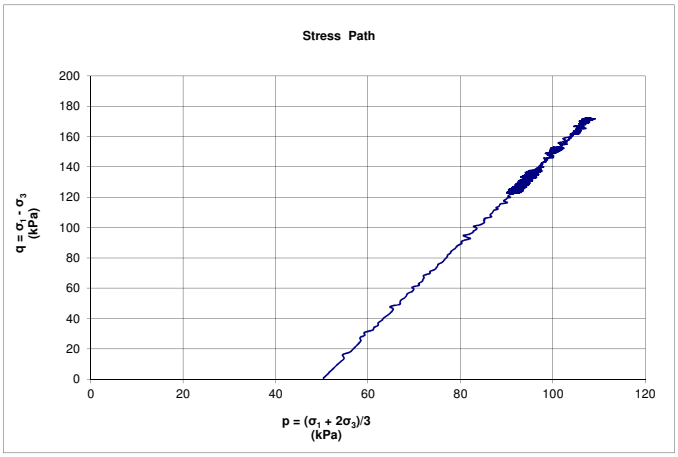


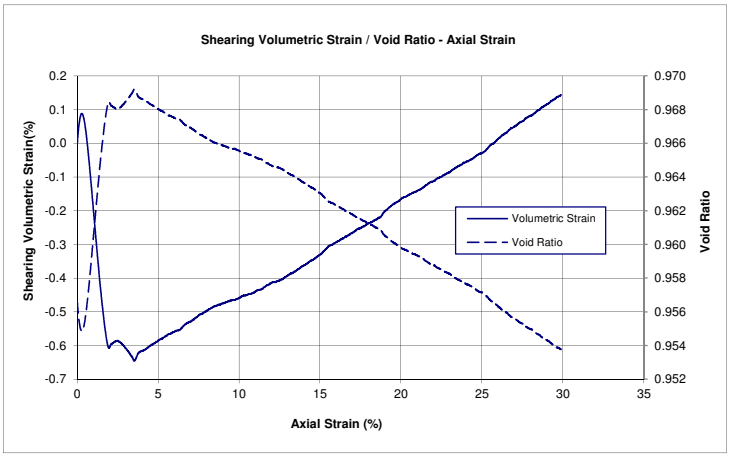


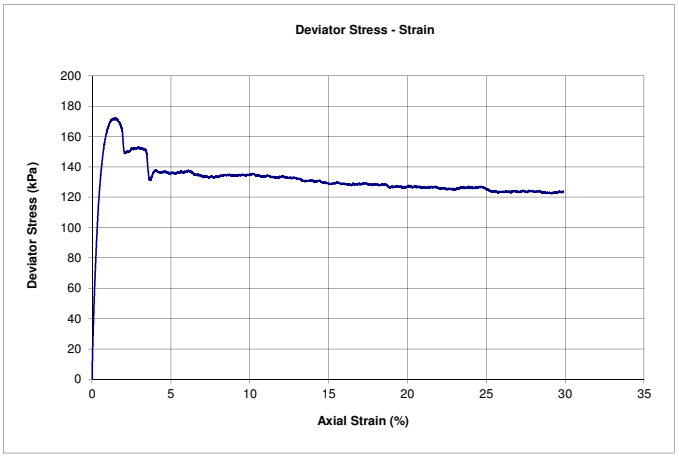
Triaxial CD Test - Charts

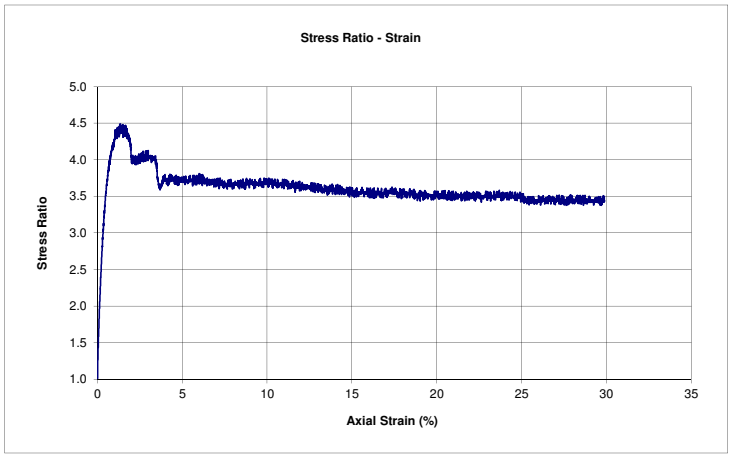
(ASTM D7181)

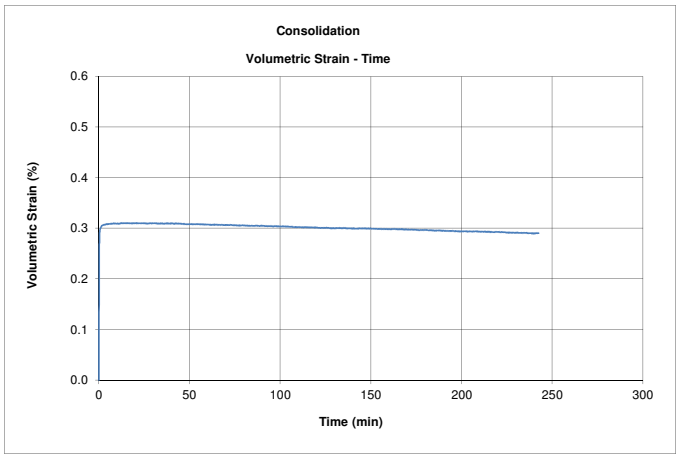
PROJECT NO. :	A03355A01	DATE :	2019-08-21
PROJECT :		TEST BY:	BY
SAMPLE :	Fine Gradation	CHECKED BY:	JG
TEST NO. :	TX 10 - CID		

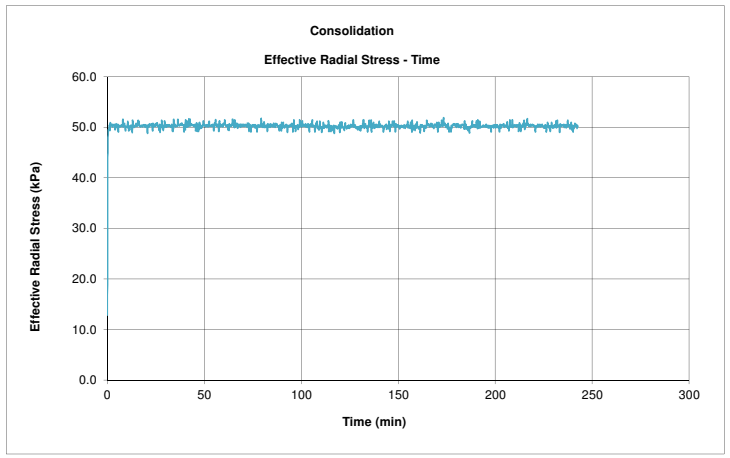












Triaxial CD Test - Summary

(ASTM D7181)

PROJECT NO. : A03355A01
PROJECT :
SAMPLE : Fine Gradation
TEST NO. : TX 11 - CD

DATE : 2019-08-26
TESTED BY: BY
CHECKED BY: JG

SPECIMEN INFORMATION	UNITS	Initial	Vacuum	Saturation	B-Value	End of 1st Consolidation	End of 2nd Consolidation	At Failure	End of Shear	
Specimen Height	mm	140.34	140.34	140.34	140.20	140.13	140.08	137.70	97.47	
Specimen Diameter	mm	70.00	70.00	69.91	69.80	69.70	69.64	70.25	83.07	
Area	cm^2	38.48	38.48	38.39	38.27	38.16	38.09	38.77	54.19	
Volume	cm^3	540.09	540.09	538.70	536.50	534.69	533.53	533.79	528.21	
Wet Weight	g	1453.94	1453.94	1604.94	1611.29	1609.48	1608.32	1608.57	1603.00	
Water Content	%	8.01	8.01	19.23	19.70	19.56	19.48	19.50	19.08	
Dry Weight	g	1346.12	1346.12	1346.12	1346.12	1346.12	1346.12	1346.12	1346.12	
Wet Density	g/cm^3	2.692	2.692	2.979	3.003	3.010	3.014	3.014	3.035	
Dry Density	g/cm^3	2.492	2.492	2.499	2.509	2.518	2.523	2.522	2.548	
Specific Gravity of Solids (assumed)	-	4.96	4.96	4.96	4.96	4.96	4.96	4.96	4.96	
Solids Volume	cm^3	271.394	271.394	271.394	271.394	271.394	271.394	271.394	271.394	
Void Volume	cm^3	268.697	268.697	267.307	265.107	263.300	262.134	262.392	256.813	
Water Volume	cm^3	107.824	107.824	258.824	265.173	263.366	262.200	262.458	256.879	
Void Ratio (e)	-	0.990	0.990	0.985	0.977	0.970	0.966	0.967	0.946	
Saturation Ratio (Sr)	%	40.13	40.13	96.83	100.02	100.02	100.03	100.03	100.03	
Effective Confining Stress	kPa					50	100			

Shearing (CU)		
Skempton's B Parameter		0.99
Back Pressure before shearing	kPa	500.0
Confining Stress (σ_3') before shearing	kPa	100
Shear Strain Rate	mm / min	0.04

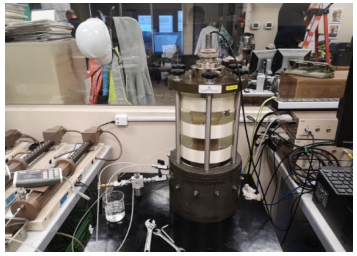
At Maximum Deviator Stress:		
Axial Stain	%	**1.70**
Deviator Stress	kPa	**287.2**
Φ '	º	36.0
c' (assumed)	kPa	**0**

At Maximum Stress Ratio		
Axial Stain	%	**1.72**
Deviator Stress	kPa	**287.0**
Φ '	º	36.2
c' (assumed)	kPa	0

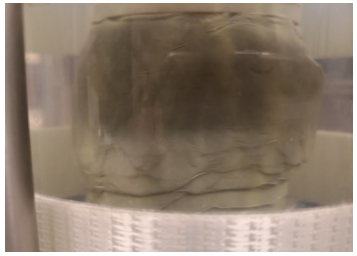
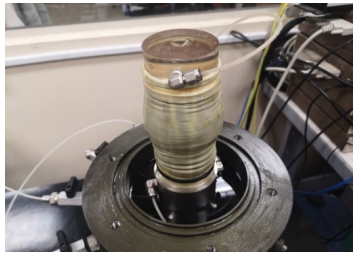
Note: *using cambridge method*

Photos:

Before Test

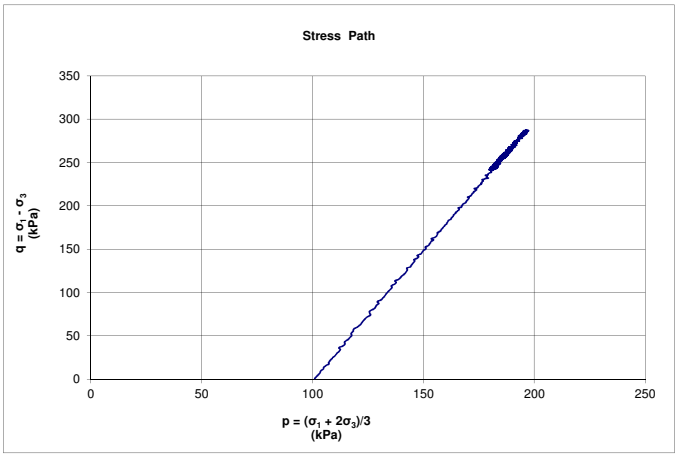
After Test

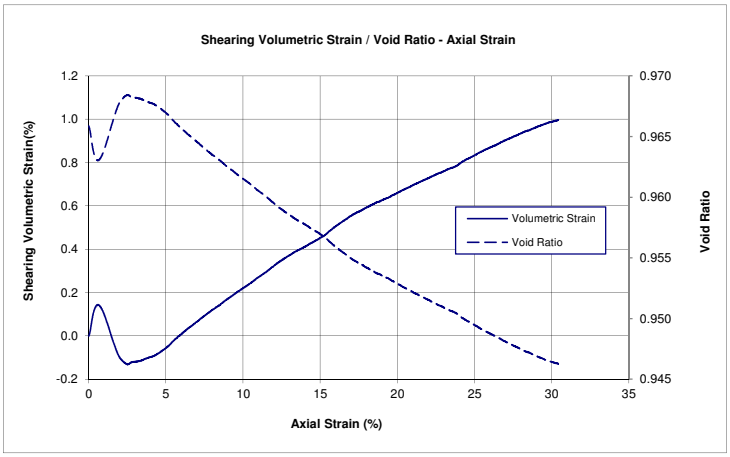



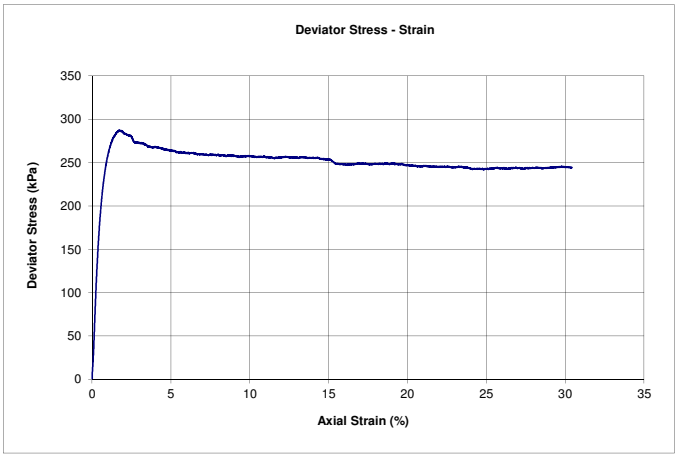
Triaxial CD Test - Charts

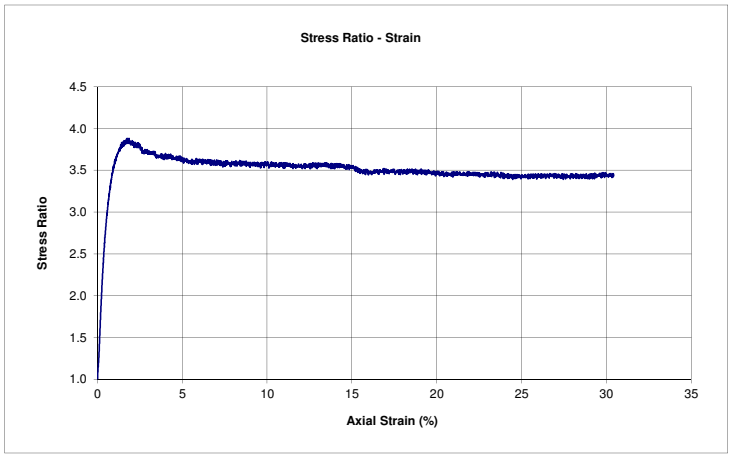
(ASTM D7181)

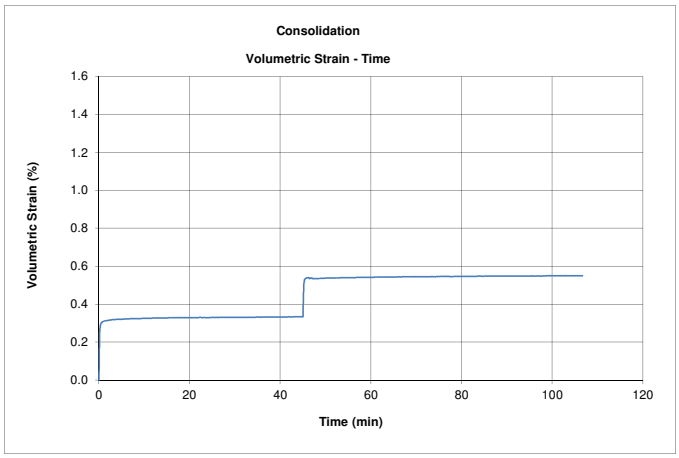
PROJECT NO. :	A03355A01	DATE :	2019-08-26
PROJECT :		TEST BY:	BY
SAMPLE :	Fine Gradation	CHECKED BY:	JG
TEST NO. :	TX 11 - CD		

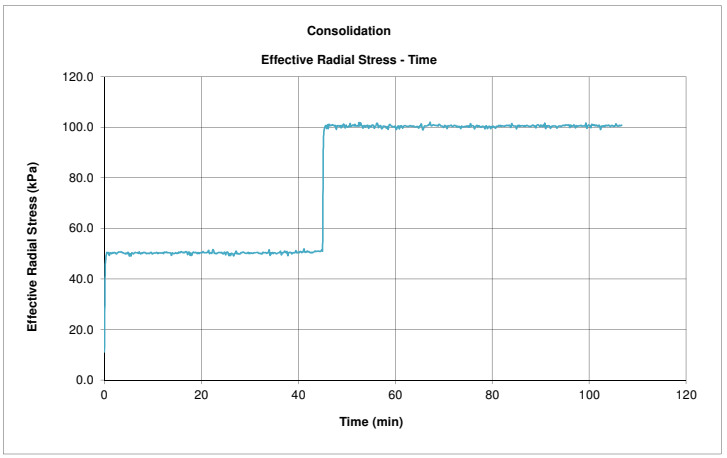












Triaxial CD Test - Summary

(ASTM D7181)

PROJECT NO. : A03355A01 DATE : 2019-08-26

PROJECT : TESTED BY: BY

SAMPLE : Fine Gradation CHECKED BY: JG

TEST NO. : TX 12 - CID

SPECIMEN INFORMATION	UNITS	Initial	Vacuum	Saturation	B-value	End of 1st Consolidation	End of 2nd Consolidation	End of 3rd Consolidation	End of 4th Consolidation	End of 5th Consolidation	At Failure	End of Shear
Specimen Height	mm	140.12	140.12	140.12	139.77	139.68	139.63	139.56	139.47	139.39	134.09	96.79
Specimen Diameter	mm	69.90	69.90	69.90	69.89	69.78	69.73	69.67	69.61	69.56	70.90	83.46
Area	cm^2	38.37	38.37	38.37	38.36	38.24	38.19	38.13	38.05	38.00	39.48	54.71
Volume	cm^3	537.71	537.71	537.71	536.21	534.17	533.28	532.09	530.72	529.69	529.38	529.56
Wet Weight	g	1513.44	1513.44	1644.04	1653.02	1650.98	1650.09	1648.90	1647.53	1646.50	1646.19	1646.37
Water Content	%	7.95	7.95	17.27	17.91	17.76	17.70	17.61	17.51	17.44	17.42	17.43
Dry Weight	g	1401.98	1401.98	1401.98	1401.98	1401.98	1401.98	1401.98	1401.98	1401.98	1401.98	1401.98
Wet Density	g/cm^3	2.815	2.815	3.058	3.083	3.091	3.094	3.099	3.104	3.108	3.110	3.109
Dry Density	g/cm^3	2.607	2.607	2.607	2.615	2.625	2.629	2.635	2.642	2.647	2.648	2.647
Specific Gravity of Solids (assumed)	-	4.91	4.91	4.91	4.91	4.91	4.91	4.91	4.91	4.91	4.91	4.91
Solids Volume	cm^3	285.536	285.536	285.536	285.536	285.536	285.536	285.536	285.536	285.536	285.536	285.536
Void Volume	cm^3	252.169	252.169	252.169	250.669	248.636	247.743	246.549	245.187	244.150	243.842	244.019
Water Volume	cm^3	111.458	111.458	242.058	251.034	249.001	248.108	246.914	245.552	244.515	244.207	244.384
Void Ratio (e)	-	0.883	0.883	0.883	0.878	0.871	0.868	0.863	0.859	0.855	0.854	0.855
Saturation Ratio (Sr)	%	44.20	44.20	95.99	100.15	100.15	100.15	100.15	100.15	100.15	100.15	100.15
Effective Confining Stress	kPa					50	100	200	350	500		

Shearing (CU)		
Skempton's B Parameter		0.99
Back Pressure before shearing	kPa	500.0
Confining Stress (σ_3') before shearing	kPa	500
Shear Strain Rate	mm / min	0.04

At Maximum Deviator Stress:		
Axial Stain	%	**3.81**
Deviator Stress	kPa	**1609.6**
Φ '	º	38.1
c' (assumed)	kPa	**0**

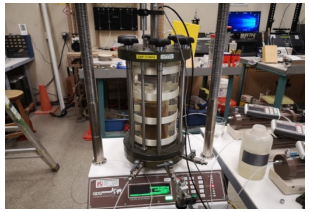
At Maximum Stress Ratio		
Axial Stain	%	**3.63**
Deviator Stress	kPa	**1609.1**
Φ '	º	38.1
c' (assumed)	kPa	0

Note: *using cambridge method*

Photos:

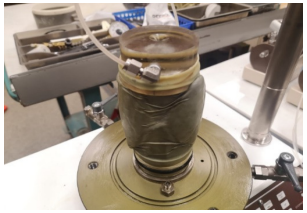
Before Test





After Test

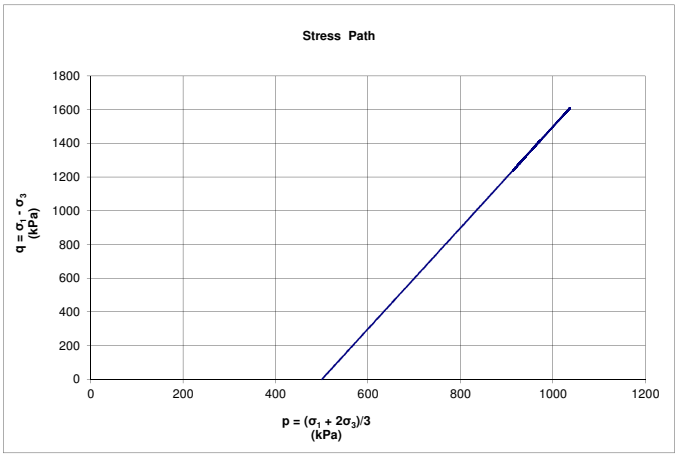


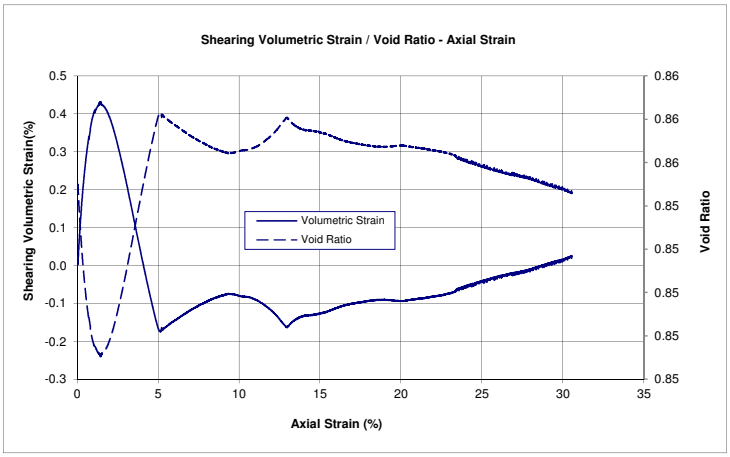


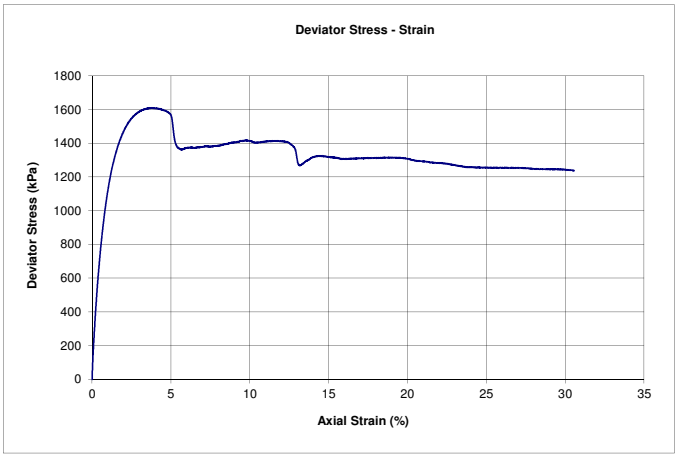
Triaxial CD Test - Charts

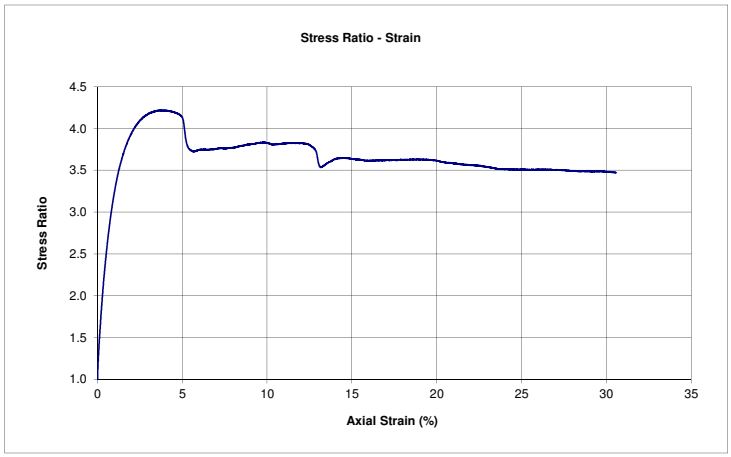
(ASTM D7181)

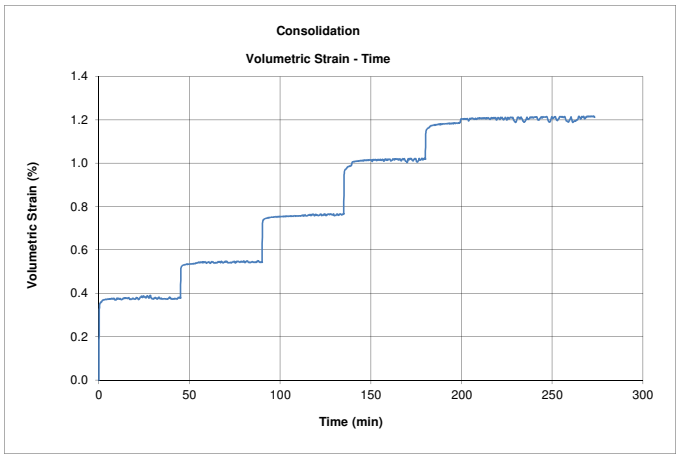
PROJECT NO. :	A03355A01	DATE :	2019-08-26
PROJECT :		TEST BY:	BY
SAMPLE :	Fine Gradation	CHECKED BY:	JG
TEST NO. :	TX 12 - CID		

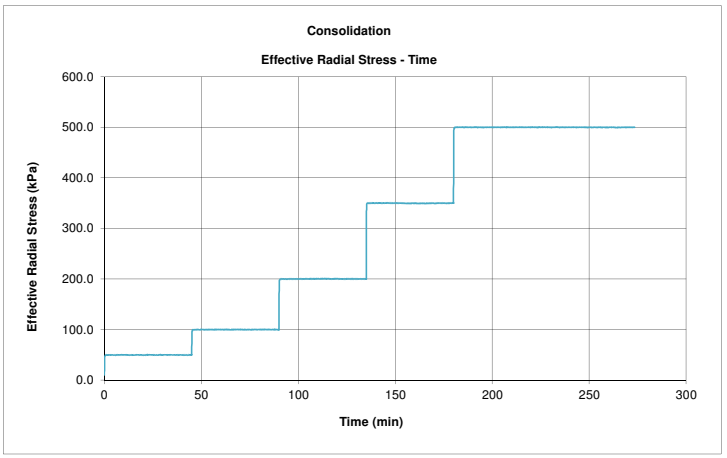












Triaxial CD Test - Summary

(ASTM D7181)

PROJECT NO. : A03355A01 DATE : 2019-08-20

PROJECT : TESTED BY: BY

SAMPLE : Fine Gradation CHECKED BY: JG

TEST NO. : TX 13 - CID

SPECIMEN INFORMATION	UNITS	Initial	Vacuum	Saturation / B-value	End of 1st Consolidation	End of 2nd Consolidation	End of 3rd Consolidation	End of 4th Consolidation	End of 5th Consolidation	End of 6th Consolidation	At Failure	End of Shear
Specimen Height	mm	140.00	139.88	139.49	139.40	139.34	139.25	139.14	139.00	138.88	130.81	95.60
Specimen Diameter	mm	69.90	69.93	69.96	69.88	69.84	69.79	69.73	69.65	69.58	71.38	83.26
Area	cm^2	38.37	38.41	38.44	38.35	38.31	38.26	38.19	38.10	38.02	40.02	54.45
Volume	cm^3	537.24	537.25	536.25	534.62	533.82	532.76	531.29	529.61	528.03	523.49	520.51
Wet Weight	g	1530.80	1530.80	1668.80	1667.17	1666.37	1665.31	1663.84	1662.17	1660.58	1656.04	1653.07
Water Content	%	7.94	7.94	17.67	17.56	17.50	17.42	17.32	17.20	17.09	16.77	16.56
Dry Weight	g	1418.20	1418.20	1418.20	1418.20	1418.20	1418.20	1418.20	1418.20	1418.20	1418.20	1418.20
Wet Density	g/cm^3	2.849	2.849	3.112	3.118	3.122	3.126	3.132	3.138	3.145	3.163	3.176
Dry Density	g/cm^3	2.640	2.640	2.645	2.653	2.657	2.662	2.669	2.678	2.686	2.709	2.725
Specific Gravity of Solids (assumed)	-	4.96	4.96	4.96	4.96	4.96	4.96	4.96	4.96	4.96	4.96	4.96
Solids Volume	cm^3	285.926	285.926	285.926	285.926	285.926	285.926	285.926	285.926	285.926	285.926	285.926
Void Volume	cm^3	251.318	251.319	250.319	248.689	247.892	246.834	245.364	243.688	242.100	237.563	234.586
Water Volume	cm^3	112.605	112.605	250.603	248.973	248.176	247.118	245.648	243.972	242.384	237.847	234.870
Void Ratio (e)	-	0.879	0.879	0.875	0.870	0.867	0.863	0.858	0.852	0.847	0.831	0.820
Saturation Ratio (Sr)	%	44.81	44.81	100.11	100.11	100.11	100.12	100.12	100.12	100.12	100.12	100.12
Effective Confining Stress	kPa				50	100	200	400	700	1000		

Shearing (CU)		
Skempton's B Parameter		0.99
Back Pressure before shearing	kPa	500.0
Confining Stress (σ_3') before shearing	kPa	1000
Shear Strain Rate	mm / min	0.04

At Maximum Deviator Stress:		
Axial Stain	%	**5.81**
Deviator Stress	kPa	**2930.8**
Φ '	º	36.5
c' (assumed)	kPa	**0**

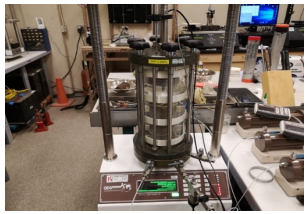
At Maximum Stress Ratio		
Axial Stain	%	**5.64**
Deviator Stress	kPa	**2928.2**
Φ '	º	36.5
c' (assumed)	kPa	0

Note: *using cambridge method*

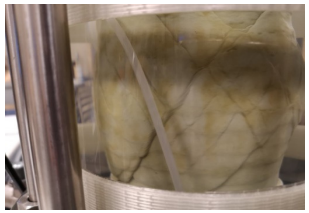
Photos:

Before Test





After Test

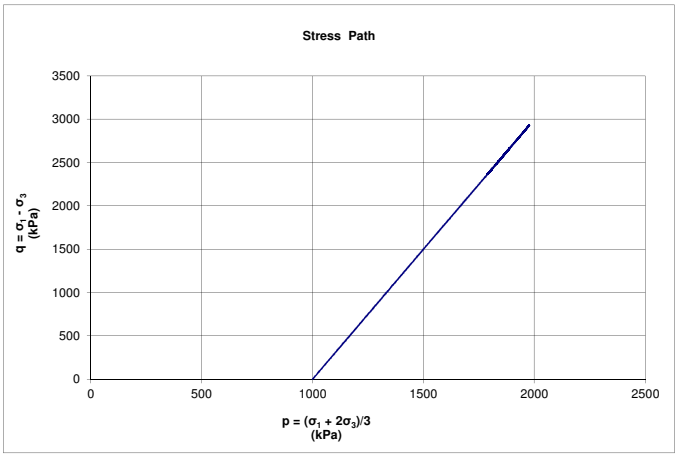


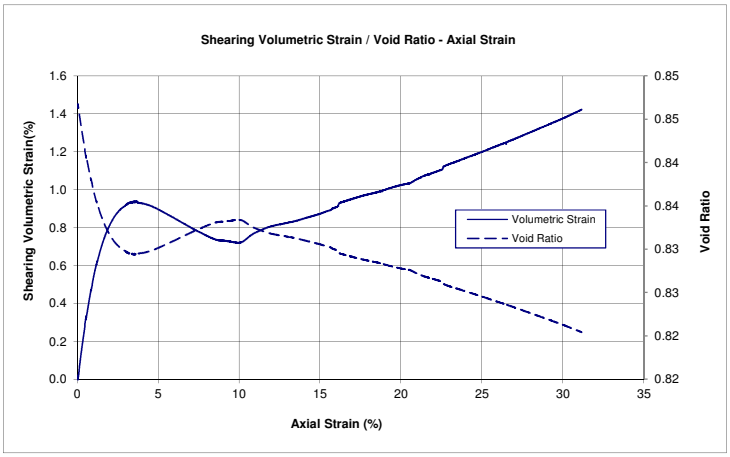


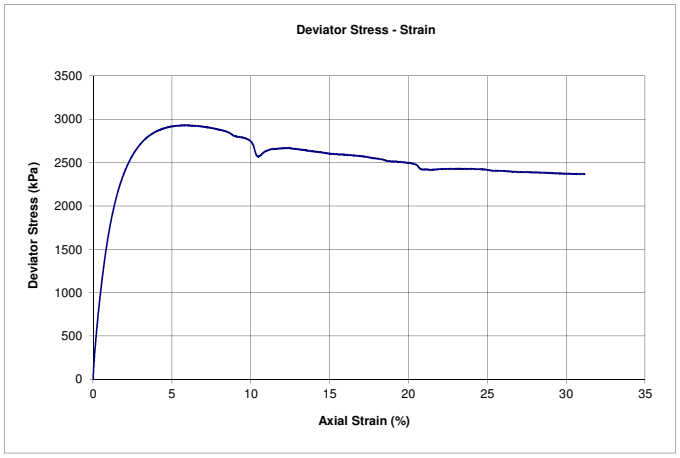
Triaxial CD Test - Charts

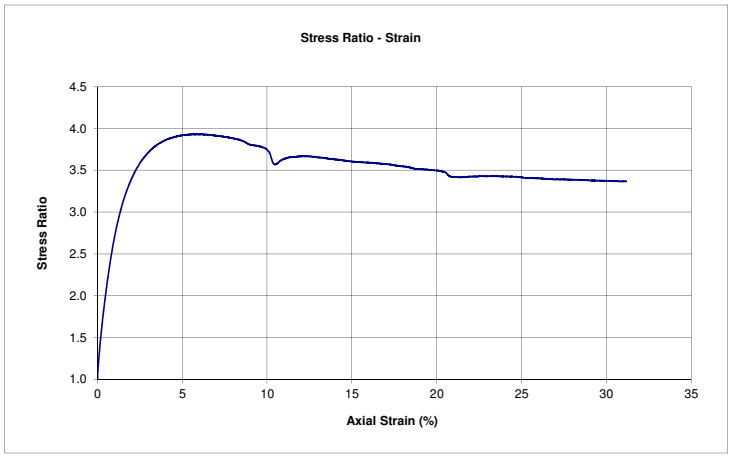
(ASTM D7181)

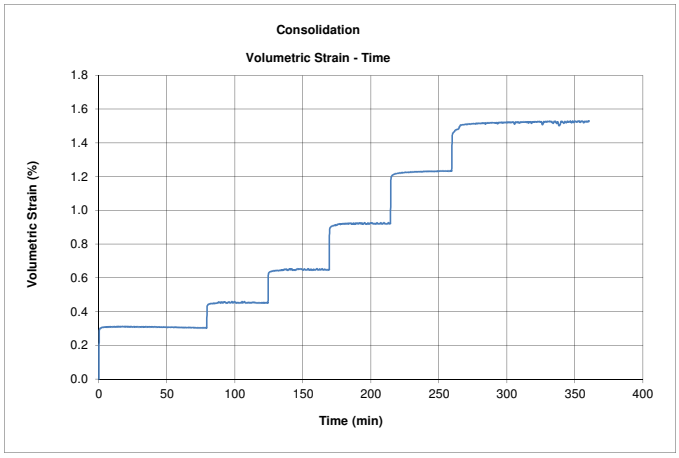
PROJECT NO. :	A03355A01	DATE :	2019-08-20
PROJECT :		TEST BY:	BY
SAMPLE :	Fine Gradation	CHECKED BY:	JG
TEST NO. :	TX 13 - CID		

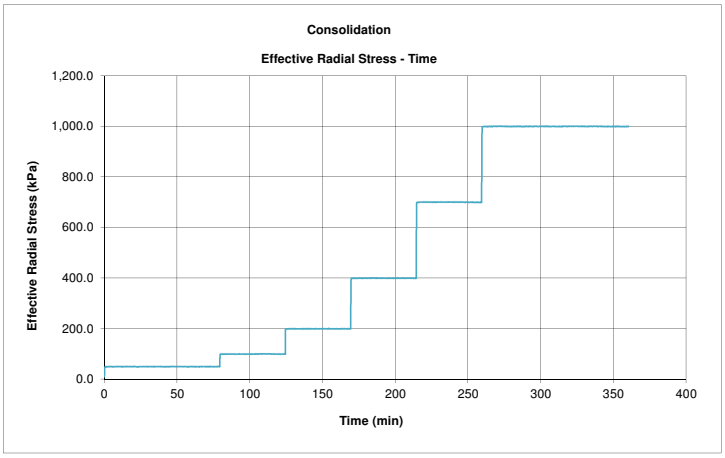












Triaxial CD Test - Summary

(ASTM D7181)

PROJECT NO. : A03355A01
PROJECT :
SAMPLE : Coarse Gradation
TEST NO. : TX 14 - CID

DATE : 2019-08-23
TESTED BY: BY
CHECKED BY: JG

SPECIMEN INFORMATION	UNITS	Initial	Vacuum	Saturation	B-value	End of 1st Consolidation	At Maximum Deviator Stress	End of Shear		
Specimen Height	mm	140.15	140.15	140.15	140.05	139.99	100.36	95.10		
Specimen Diameter	mm	69.81	69.81	69.78	69.67	69.46	80.18	82.28		
Area	cm^2	38.28	38.28	38.24	38.12	37.90	50.49	53.17		
Volume	cm^3	536.44	536.44	535.91	533.91	530.50	506.69	505.63		
Wet Weight	g	1437.60	1437.60	1587.40	1593.68	1590.28	1566.47	1565.41		
Water Content	%	8.05	8.05	19.31	19.78	19.53	17.74	17.66		
Dry Weight	g	1330.50	1330.50	1330.50	1330.50	1330.50	1330.50	1330.50		
Wet Density	g/cm^3	2.680	2.680	2.962	2.985	2.998	3.092	3.096		
Dry Density	g/cm^3	2.480	2.480	2.483	2.492	2.508	2.626	2.631		
Specific Gravity of Solids (assumed)	-	4.91	4.91	4.91	4.91	4.91	4.91	4.91		
Solids Volume	cm^3	270.977	270.977	270.977	270.977	270.977	270.977	270.977		
Void Volume	cm^3	265.460	265.460	264.929	262.929	259.522	235.715	234.656		
Water Volume	cm^3	107.105	107.105	256.905	263.189	259.782	235.975	234.916		
Void Ratio (e)	-	0.980	0.980	0.978	0.970	0.958	0.870	0.866		
Saturation Ratio (Sr)	%	40.35	40.35	96.97	100.10	100.10	100.11	100.11		
Effective Confining Stress	kPa					50				

Shearing (CU)		
Skempton's B Parameter		0.98
Back Pressure before shearing	kPa	500.0
Confining Stress (σ_3') before shearing	kPa	50
Shear Strain Rate	mm / min	0.04

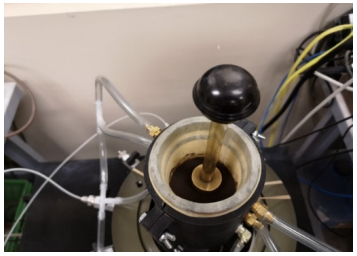
At Maximum Deviator Stress:		
Axial Stain	%	**28.31**
Deviator Stress	kPa	**129.6**
Φ '	º	34.2
c' (assumed)	kPa	**0**

At Maximum Stress Ratio		
Axial Stain	%	**26.76**
Deviator Stress	kPa	**128.3**
Φ '	º	34.6
c' (assumed)	kPa	0

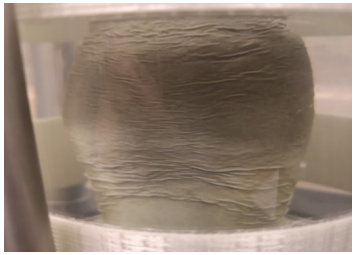
Note: *using cambridge method*

Photos:

Before Test



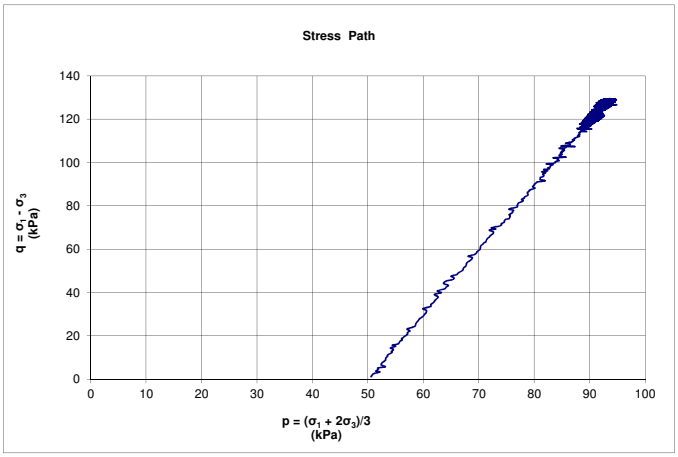

After Test

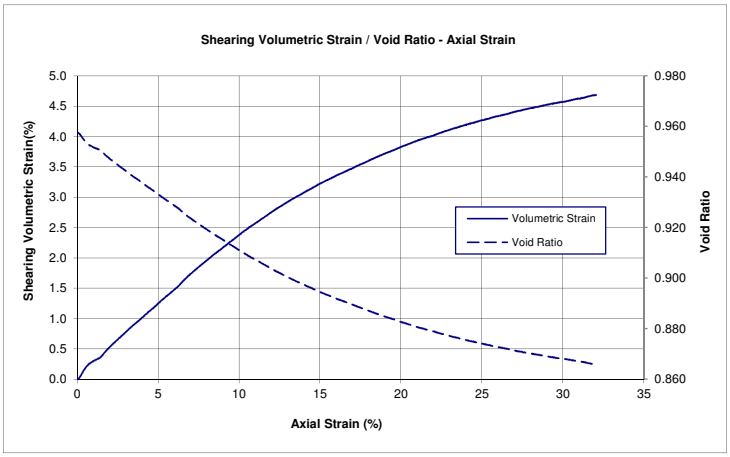


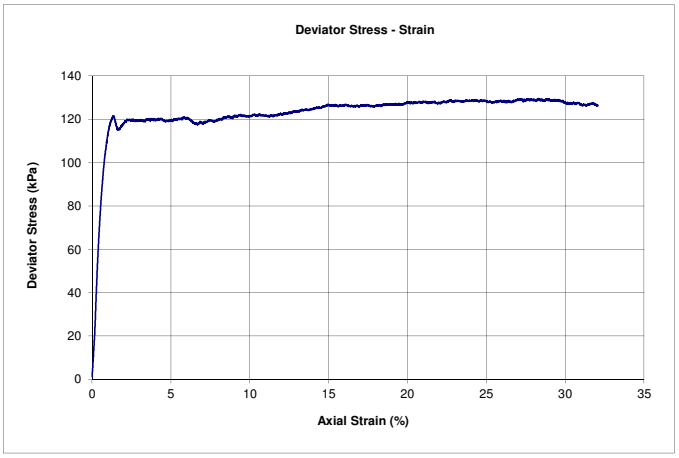

Triaxial CD Test - Charts

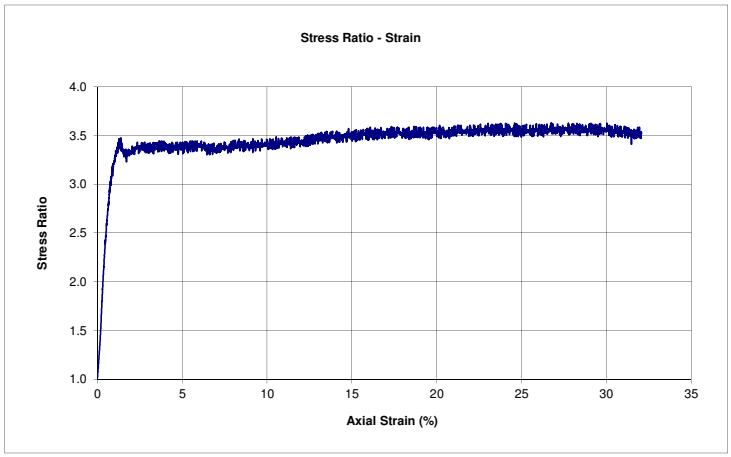
(ASTM D7181)

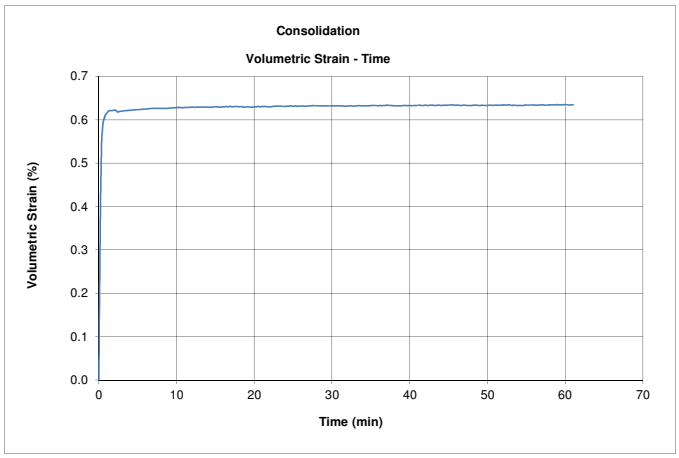
PROJECT NO. :	A03355A01	DATE :	2019-08-23
PROJECT :		TEST BY:	BY
SAMPLE :	Coarse Gradation	CHECKED BY:	JG
TEST NO. :	TX 14 - CID		

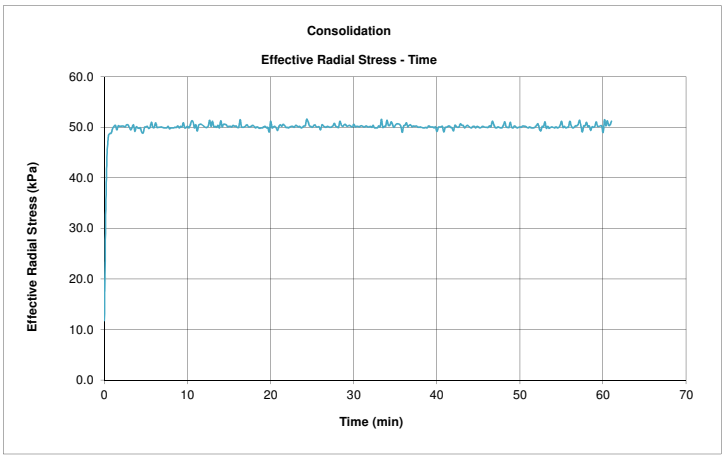












Triaxial CD Test - Summary

(ASTM D7181)

PROJECT NO. : A03355A01 DATE : 2019-08-28

PROJECT : TESTED BY: BY

SAMPLE : Coarse Gradation CHECKED BY: JG

TEST NO. : TX 15 - CID

SPECIMEN INFORMATION	UNITS	Initial	Vacuum	Saturation	B-Value	End of 1st Consolidation	End of 2nd Consolidation	At Failure	End of Shear	
Specimen Height	mm	140.15	140.05	140.05	139.95	139.88	139.81	137.05	98.56	
Specimen Diameter	mm	69.90	69.92	69.90	69.83	69.70	69.65	70.60	83.45	
Area	cm^2	38.37	38.40	38.37	38.29	38.16	38.10	39.15	54.69	
Volume	cm^3	537.820	537.744	537.396	535.896	533.729	532.663	536.534	539.079	
Wet Weight	g	1577.12	1577.12	1685.92	1699.03	1696.86	1695.80	1699.67	1702.21	
Water Content	%	8.00	8.00	15.45	16.35	16.20	16.13	16.39	16.57	
Dry Weight	g	1460.30	1460.30	1460.30	1460.30	1460.30	1460.30	1460.30	1460.30	
Wet Density	g/cm^3	2.932	2.933	3.137	3.170	3.179	3.184	3.168	3.158	
Dry Density	g/cm^3	2.715	2.716	2.717	2.725	2.736	2.741	2.722	2.709	
Specific Gravity of Solids (assumed)	-	4.91	4.91	4.91	4.91	4.91	4.91	4.91	4.91	
Solids Volume	cm^3	297.413	297.413	297.413	297.413	297.413	297.413	297.413	297.413	
Void Volume	cm^3	240.408	240.332	239.984	238.484	236.317	235.251	239.122	241.667	
Water Volume	cm^3	116.824	116.824	225.624	238.735	236.568	235.502	239.373	241.918	
Void Ratio (e)	-	0.808	0.808	0.807	0.802	0.795	0.791	0.804	0.813	
Saturation Ratio (Sr)	%	48.59	48.61	94.02	100.11	100.11	100.11	100.10	100.10	
Effective Confining Stress	kPa					50	100			

Shearing (CU)		
Skempton's B Parameter		0.99
Back Pressure before shearing	kPa	500.0
Confining Stress (σ_3') before shearing	kPa	100
Shear Strain Rate	mm / min	0.04

At Maximum Deviator Stress:		
Axial Stain	%	**1.98**
Deviator Stress	kPa	**504.0**
Φ '	º	45.7
c' (assumed)	kPa	**0**

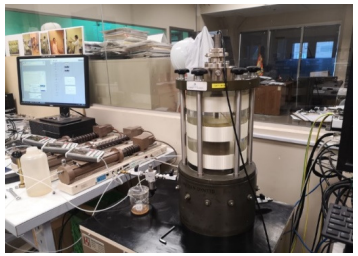
At Maximum Stress Ratio		
Axial Stain	%	**2.05**
Deviator Stress	kPa	**503.1**
Φ '	º	45.9
c' (assumed)	kPa	0

Note: *using cambridge method*

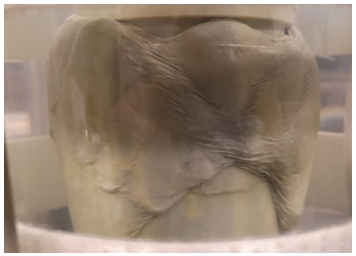
Photos:

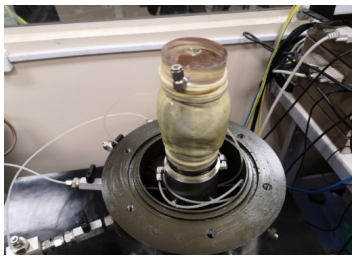
Before Test





After Test

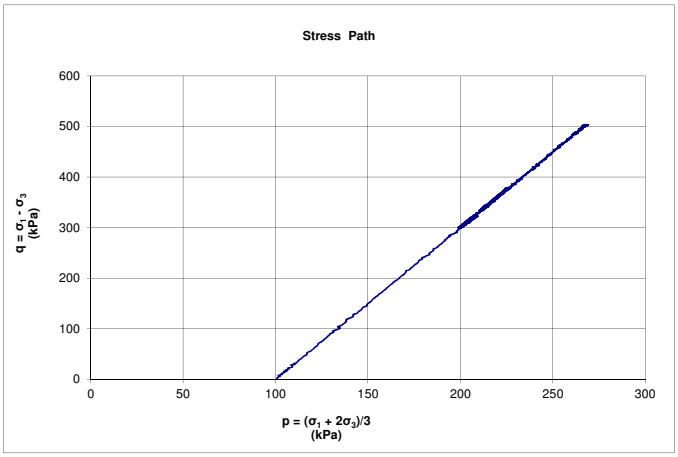


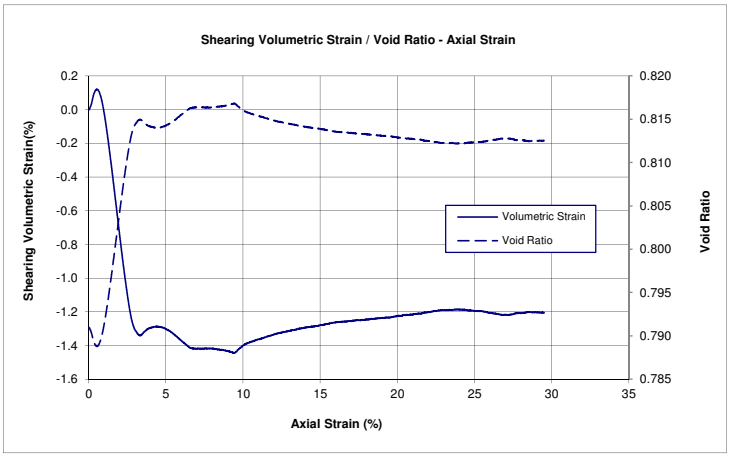


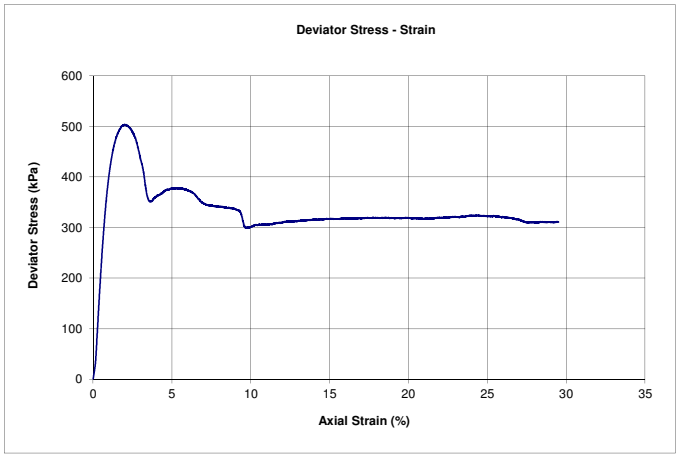
Triaxial CD Test - Charts

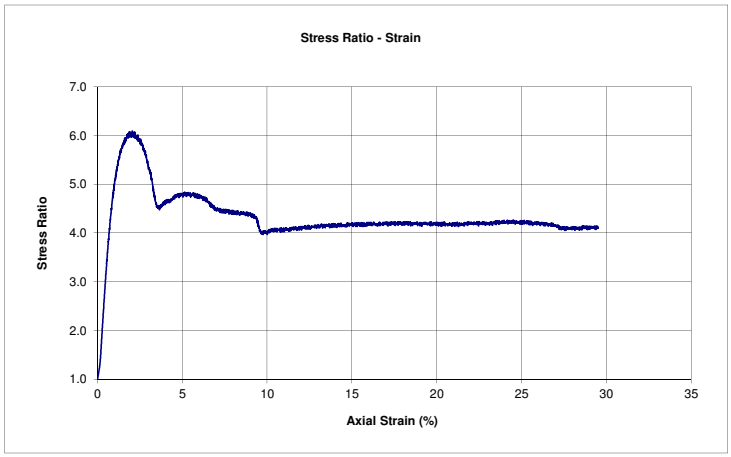
(ASTM D7181)

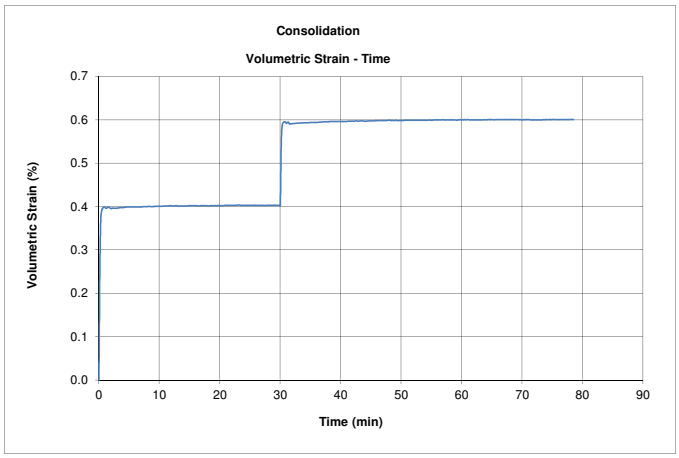
PROJECT NO. :	A03355A01	DATE :	2019-08-28
PROJECT :		TEST BY:	BY
SAMPLE :	Coarse Gradation	CHECKED BY:	JG
TEST NO. :	TX 15 - CID		

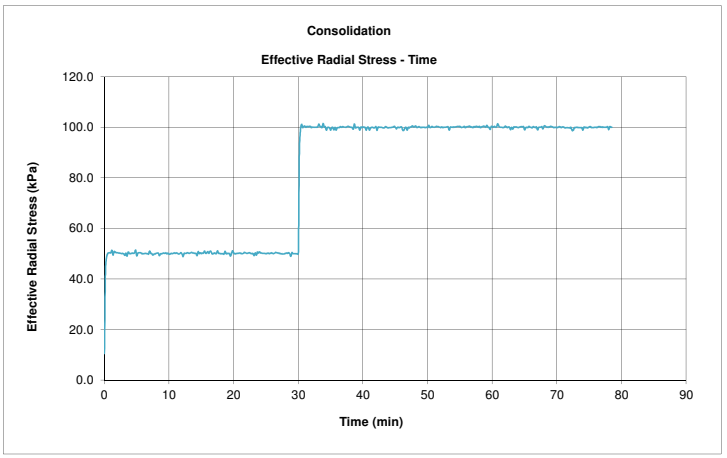












Triaxial CD Test - Summary

(ASTM D7181)

PROJECT NO. : A03355A01 DATE : 2019-08-28

PROJECT : TESTED BY: BY

SAMPLE : Coarse Gradation CHECKED BY: JG

TEST NO. : TX 16 - CID

SPECIMEN INFORMATION	UNITS	Initial	Vacuum	Saturation	B-value	End of 1st Consolidation	End of 2nd Consolidation	End of 3rd Consolidation	End of 4th Consolidation	End of 5th Consolidation	At Failure	End of Shear
Specimen Height	mm	140.24	140.24	140.24	139.95	139.85	139.78	139.68	139.58	139.49	134.27	97.75
Specimen Diameter	mm	69.90	69.90	69.88	69.95	69.86	69.82	69.76	69.69	69.64	70.84	82.93
Area	cm^2	38.37	38.37	38.35	38.43	38.33	38.28	38.22	38.15	38.08	39.42	54.02
Volume	cm^3	536.59	538.17	537.84	537.84	536.08	535.10	533.80	532.42	531.23	529.27	528.07
Wet Weight	g	1609.08	1609.08	1714.68	1725.71	1723.94	1722.96	1721.66	1720.28	1719.09	1717.13	1715.93
Water Content	%	7.98	7.98	15.07	15.81	15.69	15.62	15.53	15.44	15.36	15.23	15.15
Dry Weight	g	1490.16	1490.16	1490.16	1490.16	1490.16	1490.16	1490.16	1490.16	1490.16	1490.16	1490.16
Wet Density	g/cm^3	2.999	2.990	3.188	3.209	3.216	3.220	3.225	3.231	3.236	3.244	3.249
Dry Density	g/cm^3	2.777	2.769	2.771	2.771	2.780	2.785	2.792	2.799	2.805	2.816	2.822
Specific Gravity of Solids (assumed)	-	4.91	4.91	4.91	4.91	4.91	4.91	4.91	4.91	4.91	4.91	4.91
Solids Volume	cm^3	303.496	303.496	303.496	303.496	303.496	303.496	303.496	303.496	303.496	303.496	303.496
Void Volume	cm^3	233.097	234.670	234.348	234.348	232.584	231.602	230.303	228.922	227.734	225.773	224.574
Water Volume	cm^3	118.915	118.915	224.515	235.540	233.776	232.794	231.495	230.114	228.926	226.965	225.766
Void Ratio (e)	-	0.768	0.773	0.772	0.772	0.766	0.763	0.759	0.754	0.750	0.744	0.740
Saturation Ratio (Sr)	%	51.02	50.67	95.80	100.51	100.51	100.51	100.52	100.52	100.52	100.53	100.53
Effective Confining Stress	kPa					50	100	200	350	500		

Shearing (CU)		
Skempton's B Parameter		0.99
Back Pressure before shearing	kPa	500.0
Confining Stress (σ_3') before shearing	kPa	500
Shear Strain Rate	mm / min	0.04

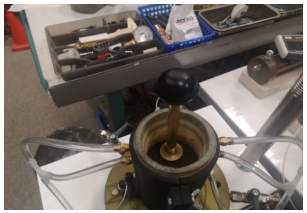
At Maximum Deviator Stress:		
Axial Stain	%	**3.74**
Deviator Stress	kPa	**1775.5**
Φ '	º	39.8
c' (assumed)	kPa	**0**

At Maximum Stress Ratio		
Axial Stain	%	**3.87**
Deviator Stress	kPa	**1774.0**
Φ '	º	39.8
c' (assumed)	kPa	0

Note: *using cambridge method*

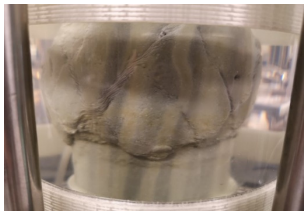
Photos:

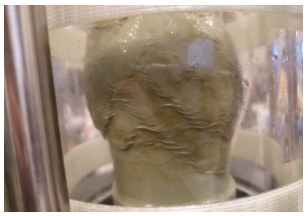
Before Test





After Test

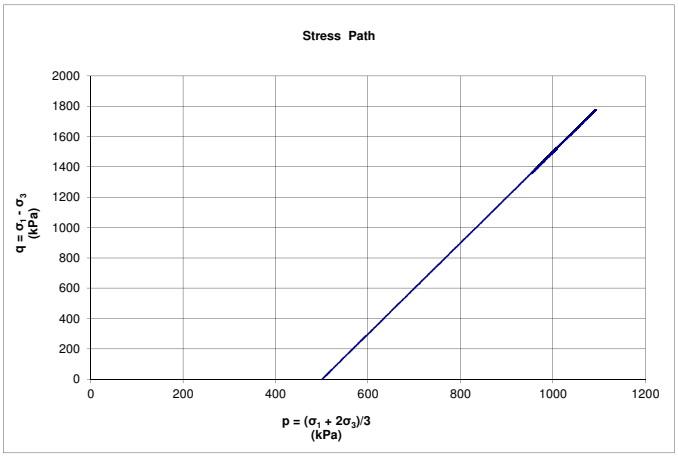


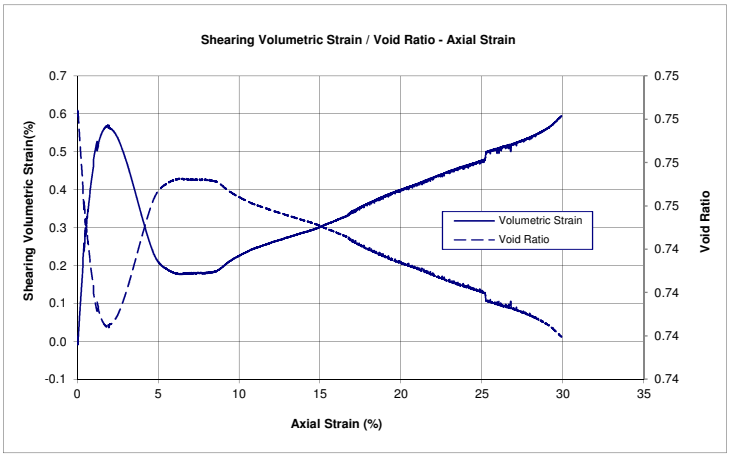


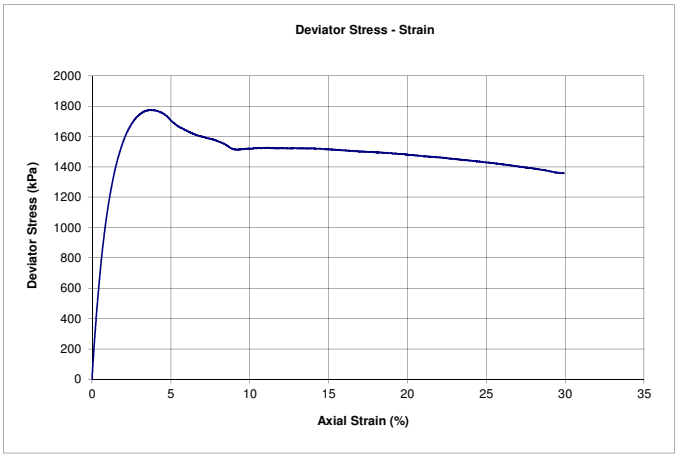
Triaxial CD Test - Charts

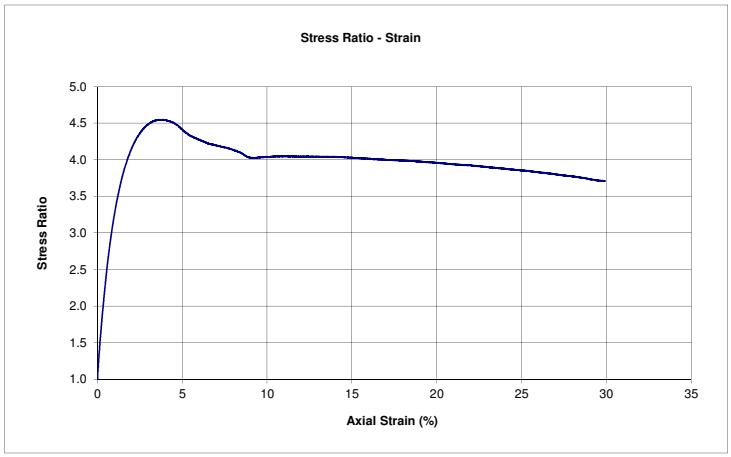
(ASTM D7181)

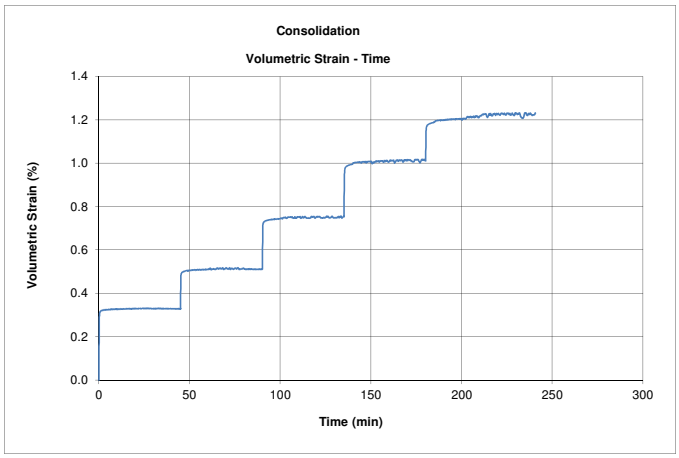
PROJECT NO. :	A03355A01	DATE :	2019-08-28
PROJECT :		TEST BY:	BY
SAMPLE :	Coarse Gradation	CHECKED BY:	JG
TEST NO. :	TX 16 - CID		

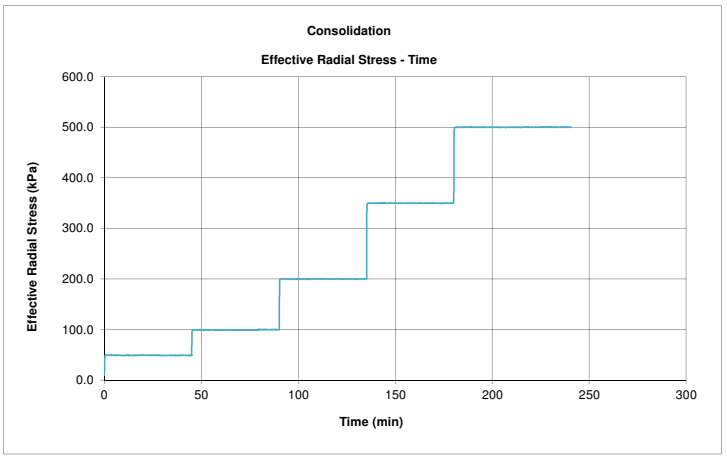












Triaxial CD Test - Summary

(ASTM D7181)

PROJECT NO. : A03355A01 DATE : 2019-08-22

PROJECT : TESTED BY: BY

SAMPLE : Coarse Gradation CHECKED BY: JG

TEST NO. : TX 17 - CID

SPECIMEN INFORMATION	UNITS	Initial	Vacuum	Saturation / B-value	End of 1st Consolidation	End of 2nd Consolidation	End of 3rd Consolidation	End of 4th Consolidation	End of 5th Consolidation	End of 6th Consolidation	At Failure	End of Shear
Specimen Height	mm	140.12	139.64	139.30	139.22	139.15	139.06	138.90	138.69	138.49	118.20	95.58
Specimen Diameter	mm	69.90	69.72	69.54	69.41	69.34	69.26	69.14	69.00	68.88	72.94	80.53
Area	cm^2	38.37	38.18	37.98	37.84	37.77	37.68	37.54	37.39	37.26	41.79	50.93
Volume	cm^3	537.71	533.11	529.11	526.74	525.54	523.91	521.45	518.56	516.06	493.90	486.80
Wet Weight	g	1513.44	1513.44	1646.44	1644.07	1642.87	1641.25	1638.78	1635.89	1633.39	1611.23	1604.13
Water Content	%	7.89	7.89	17.37	17.20	17.12	17.00	16.83	16.62	16.44	14.86	14.36
Dry Weight	g	1402.76	1402.76	1402.76	1402.76	1402.76	1402.76	1402.76	1402.76	1402.76	1402.76	1402.76
Wet Density	g/cm^3	2.815	2.839	3.112	3.121	3.126	3.133	3.143	3.155	3.165	3.262	3.295
Dry Density	g/cm^3	2.609	2.631	2.651	2.663	2.669	2.677	2.690	2.705	2.718	2.840	2.882
Specific Gravity of Solids (assumed)	-	4.91	4.91	4.91	4.91	4.91	4.91	4.91	4.91	4.91	4.91	4.91
Solids Volume	cm^3	285.695	285.695	285.695	285.695	285.695	285.695	285.695	285.695	285.695	285.695	285.695
Void Volume	cm^3	252.010	247.412	243.412	241.041	239.844	238.219	235.753	232.862	230.360	208.205	201.104
Water Volume	cm^3	110.678	110.678	243.676	241.305	240.108	238.483	236.017	233.126	230.624	208.469	201.368
Void Ratio (e)	-	0.882	0.866	0.852	0.844	0.840	0.834	0.825	0.815	0.806	0.729	0.704
Saturation Ratio (Sr)	%	43.92	44.73	100.11	100.11	100.11	100.11	100.11	100.11	100.11	100.13	100.13
Effective Confining Stress	kPa				50	100	200	400	700	1000		

Shearing (CU)		
Skempton's B Parameter		0.99
Back Pressure before shearing	kPa	500.0
Confining Stress (σ_3') before shearing	kPa	1000
Shear Strain Rate	mm / min	0.04

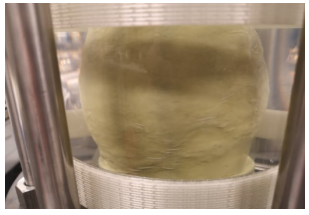
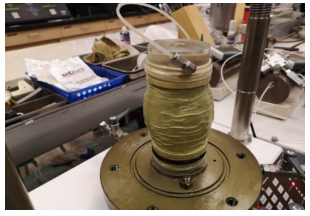
At Maximum Deviator Stress:		
Axial Stain	%	**14.65**
Deviator Stress	kPa	**2744.0**
Φ '	º	35.3
c' (assumed)	kPa	**0**

At Maximum Stress Ratio		
Axial Stain	%	**14.89**
Deviator Stress	kPa	**2743.4**
Φ '	º	35.3
c' (assumed)	kPa	0

Note: *using cambridge method*

Photos: Before Test After Test

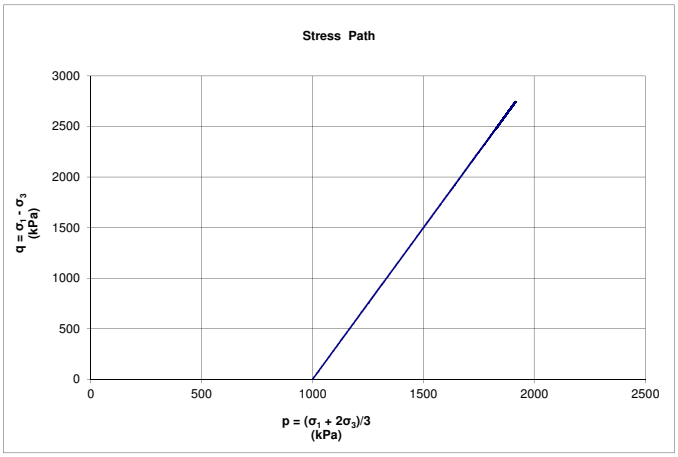


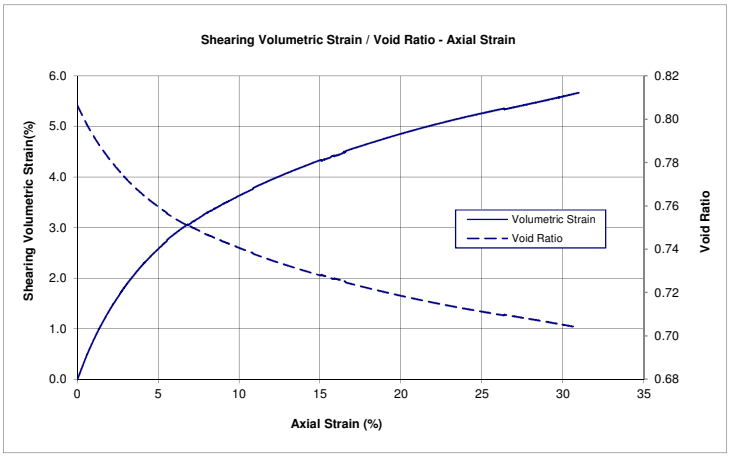



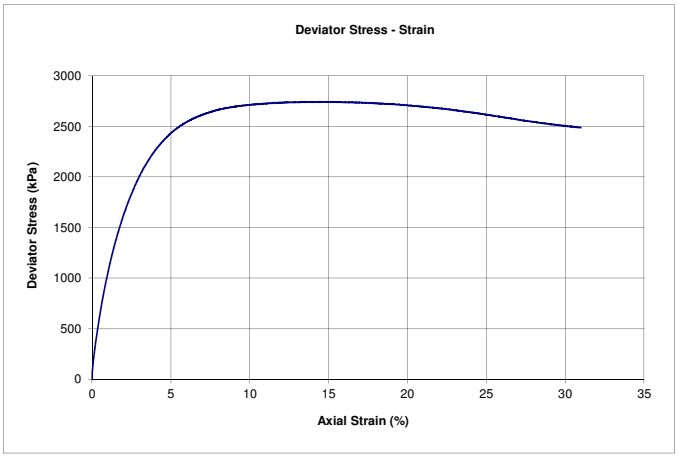
Triaxial CD Test - Charts

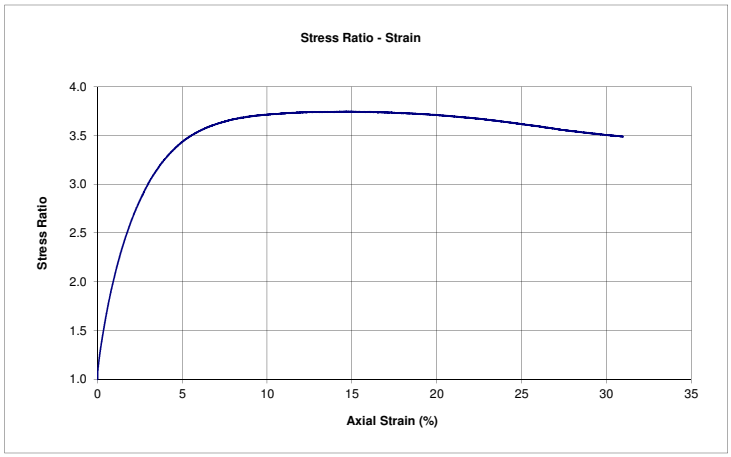
(ASTM D7181)

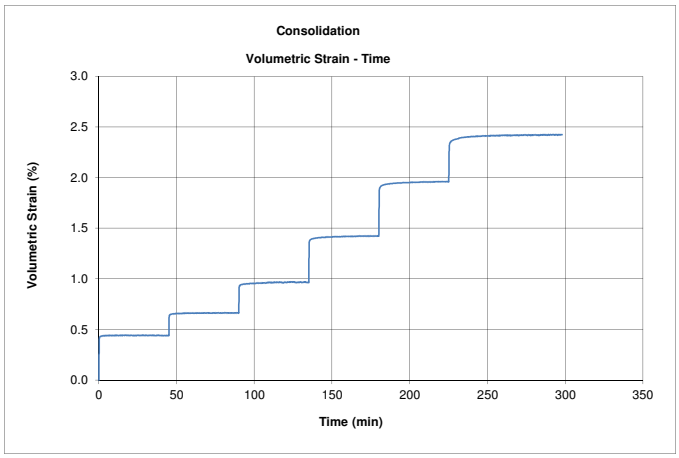
PROJECT NO. :	A03355A01	DATE :	2019-08-22
PROJECT :		TEST BY:	BY
SAMPLE :	Coarse Gradation	CHECKED BY:	JG
TEST NO. :	TX 17 - CID		

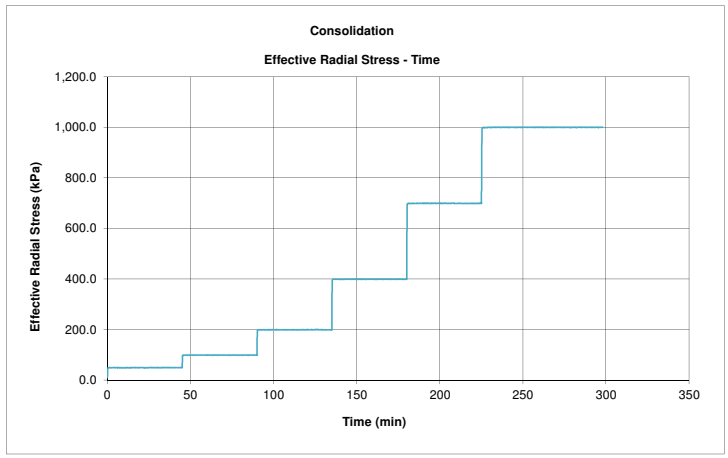












Triaxial CD Test - Summary

(ASTM D7181)

PROJECT NO. : A03355A01
PROJECT :
SAMPLE : Average
TEST NO. : TX 18 - CD

DATE : 2019-09-12
TESTED BY: AX
CHECKED BY: JG

SPECIMEN INFORMATION	UNITS	Initial	Vacuum	Saturation	B-Value	End of 1st Consolidation	End of 2nd Consolidation	At Failure	End of Shear	
Specimen Height	mm	140.19	140.19	140.19	140.05	139.98	139.93	136.72	90.74	
Specimen Diameter	mm	69.80	69.80	69.71	69.62	69.51	69.44	70.36	86.48	
Area	cm^2	38.26	38.26	38.17	38.06	37.94	37.87	38.88	58.74	
Volume	cm^3	536.436	536.436	535.046	533.046	531.146	529.946	531.586	533.006	
Wet Weight	g	1588.90	1588.90	1698.00	1700.00	1698.10	1696.90	1698.54	1699.96	
Water Content	%	8.75	8.75	16.22	16.35	16.22	16.14	16.25	16.35	
Dry Weight	g	1461.06	1461.06	1461.06	1461.06	1461.06	1461.06	1461.06	1461.06	
Wet Density	g/cm^3	2.962	2.962	3.174	3.189	3.197	3.202	3.195	3.189	
Dry Density	g/cm^3	2.724	2.724	2.731	2.741	2.751	2.757	2.748	2.741	
Specific Gravity of Solids (assumed)	-	4.97	4.97	4.97	4.97	4.97	4.97	4.97	4.97	
Solids Volume	cm^3	293.975	293.975	293.975	293.975	293.975	293.975	293.975	293.975	
Void Volume	cm^3	242.460	242.460	241.070	239.070	237.170	235.970	237.610	239.030	
Water Volume	cm^3	127.843	127.843	236.943	238.943	237.043	235.843	237.483	238.903	
Void Ratio (e)	-	0.825	0.825	0.820	0.813	0.807	0.803	0.808	0.813	
Saturation Ratio (Sr)	%	52.73	52.73	98.29	99.95	99.95	99.95	99.95	99.95	
Effective Confining Stress	kPa					50	100			

Shearing (CU)		
Skempton's B Parameter		0.99
Back Pressure before shearing	kPa	390.0
Confining Stress (σ_3') before shearing	kPa	100
Shear Strain Rate	mm / min	0.04

At Maximum Deviator Stress:		
Axial Stain	%	**1.57**
Deviator Stress	kPa	**354.4**
Φ '	º	39.6
c' (assumed)	kPa	**0**

At Maximum Stress Ratio		
Axial Stain	%	**1.57**
Deviator Stress	kPa	**354.4**
Φ '	º	39.6
c' (assumed)	kPa	0

Note: *using cambridge method*

Photos:

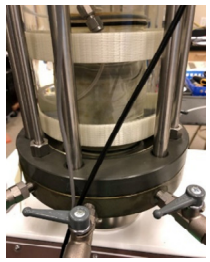
Before Test





After Test

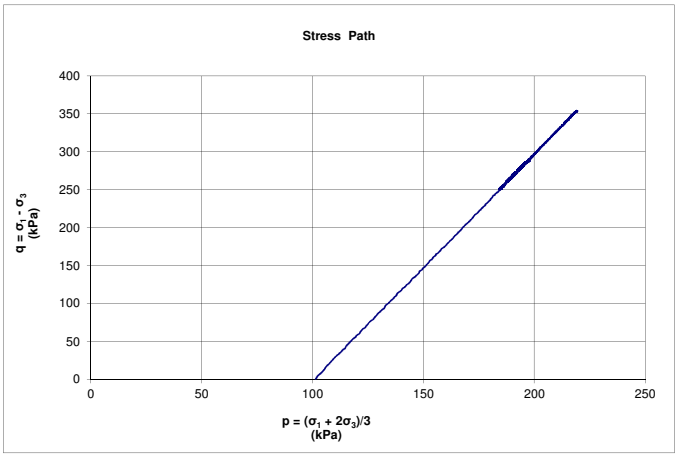


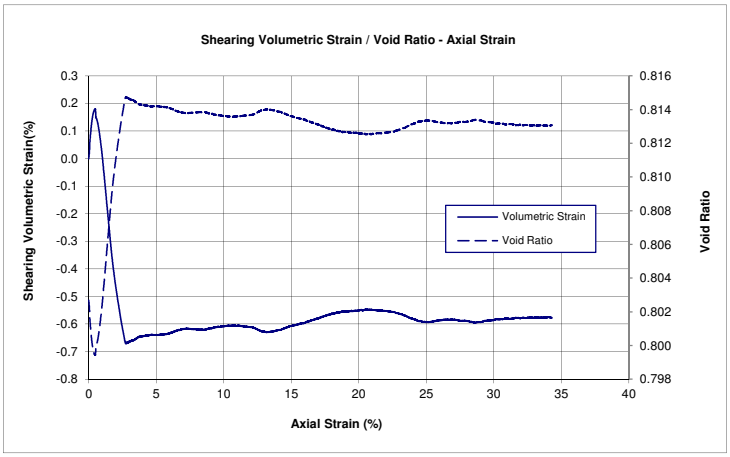


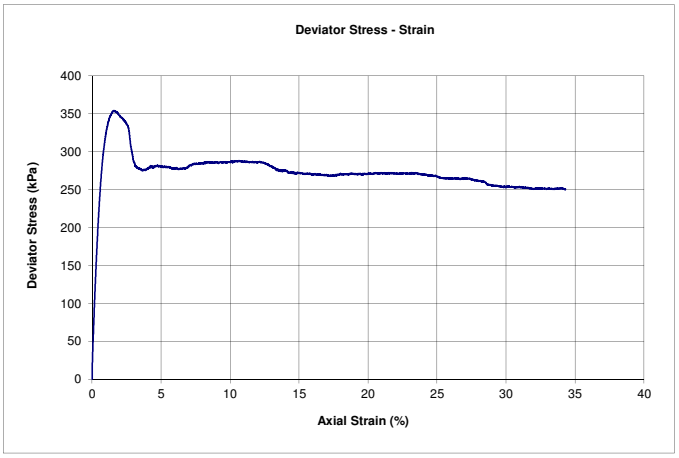
Triaxial CD Test - Charts

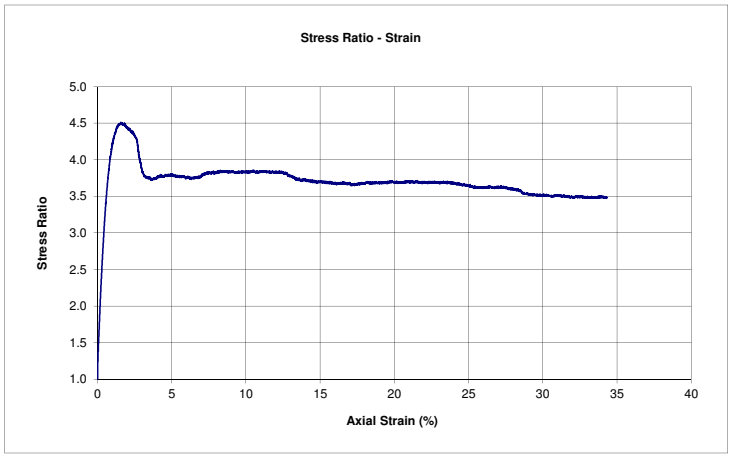
(ASTM D7181)

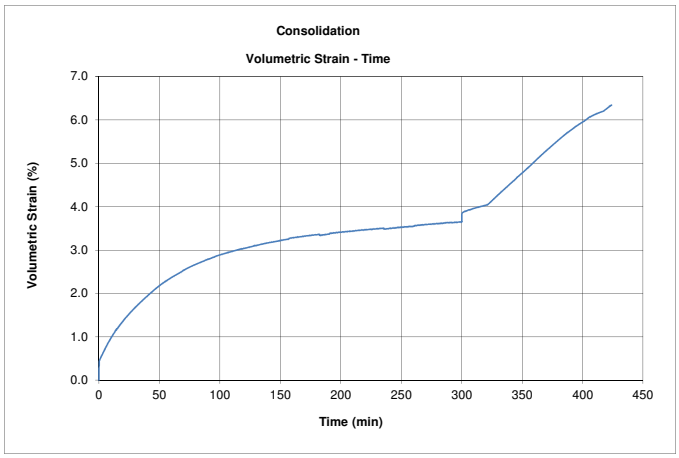
PROJECT NO. :	A03355A01	DATE :	2019-09-12
PROJECT :		TEST BY:	AX
SAMPLE :	Average	CHECKED BY:	JG
TEST NO. :	TX 18 - CD		

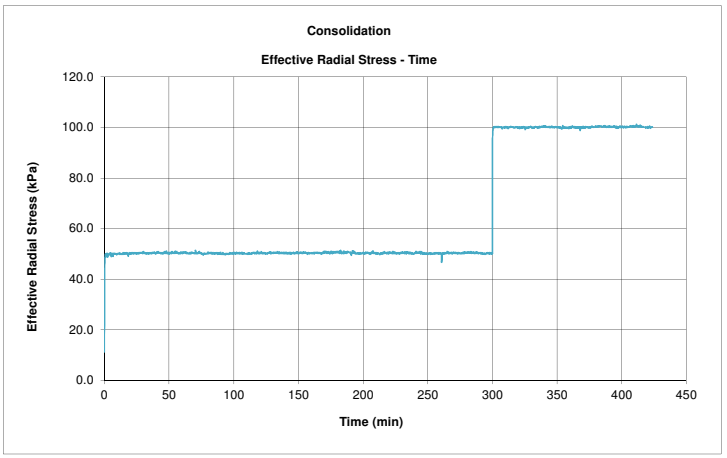












Triaxial CD Test - Summary

(ASTM D7181)

PROJECT NO. : A03355A01
PROJECT :
SAMPLE : Average
TEST NO. : TX 19 - CID

DATE : 2019-09-16
TESTED BY: AX
CHECKED BY: JG

SPECIMEN INFORMATION	UNITS	Initial	Vacuum	Saturation	B-Value	End of 1st Consolidation	End of 2nd Consolidation	At Failure	End of Shear	
Specimen Height	mm	140.54	140.54	140.54	140.40	140.33	140.28	137.07	91.09	
Specimen Diameter	mm	70.00	70.00	69.91	69.95	69.84	69.77	70.99	87.20	
Area	cm^2	38.48	38.48	38.39	38.43	38.31	38.24	39.58	59.71	
Volume	cm^3	540.861	540.861	539.471	539.471	537.571	536.371	542.541	543.931	
Wet Weight	g	1634.35	1634.35	1738.35	1745.09	1743.19	1741.99	1748.16	1749.55	
Water Content	%	8.26	8.26	15.15	15.60	15.47	15.39	15.80	15.89	
Dry Weight	g	1509.65	1509.65	1509.65	1509.65	1509.65	1509.65	1509.65	1509.65	
Wet Density	g/cm^3	3.022	3.022	3.222	3.235	3.243	3.248	3.222	3.216	
Dry Density	g/cm^3	2.791	2.791	2.798	2.798	2.808	2.815	2.783	2.775	
Specific Gravity of Solids (assumed)	-	4.96	4.96	4.96	4.96	4.96	4.96	4.96	4.96	
Solids Volume	cm^3	304.365	304.365	304.365	304.365	304.365	304.365	304.365	304.365	
Void Volume	cm^3	236.496	236.496	235.106	235.106	233.206	232.006	238.176	239.566	
Water Volume	cm^3	124.697	124.697	228.697	235.432	233.532	232.332	238.502	239.892	
Void Ratio (e)	-	0.777	0.777	0.772	0.772	0.766	0.762	0.783	0.787	
Saturation Ratio (Sr)	%	52.73	52.73	97.27	100.14	100.14	100.14	100.14	100.14	
Effective Confining Stress	kPa					50	100			

Shearing (CU)		
Skempton's B Parameter		0.99
Back Pressure before shearing	kPa	390.0
Confining Stress (σ_3') before shearing	kPa	100
Shear Strain Rate	mm / min	0.04

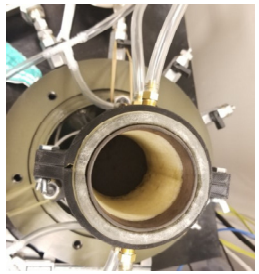
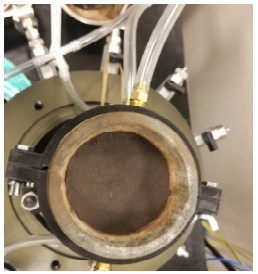
At Maximum Deviator Stress:		
Axial Stain	%	**2.39**
Deviator Stress	kPa	**496.0**
Φ '	º	45.3
c' (assumed)	kPa	**0**

At Maximum Stress Ratio		
Axial Stain	%	**2.45**
Deviator Stress	kPa	**494.2**
Φ '	º	45.5
c' (assumed)	kPa	0

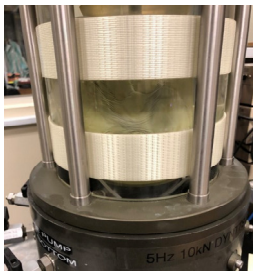
Note: *using cambridge method*

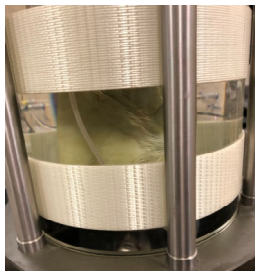
Photos:

Before Test


After Test

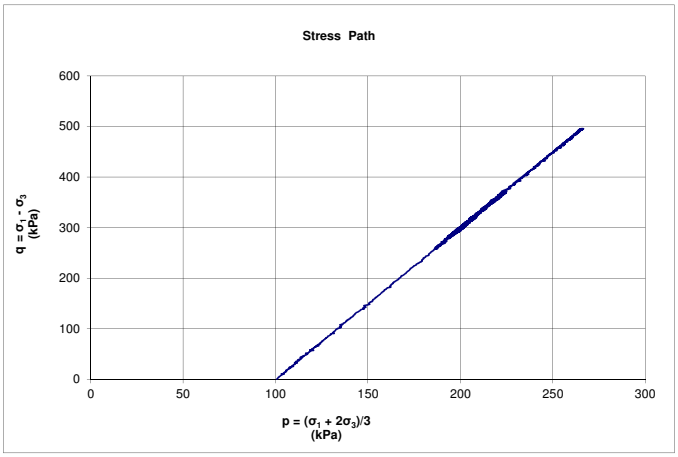


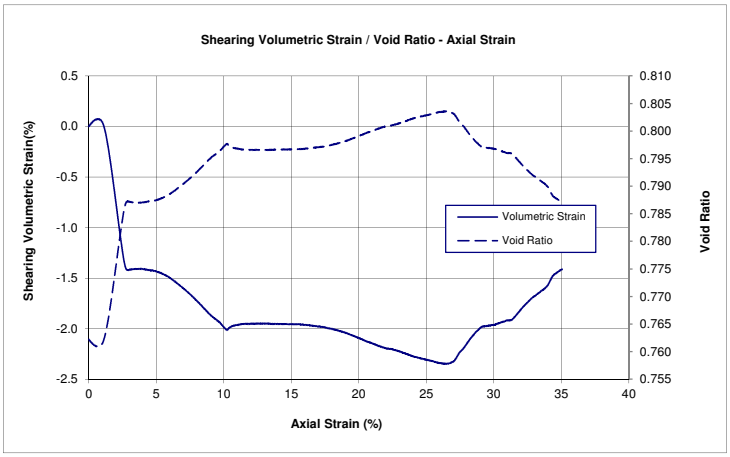


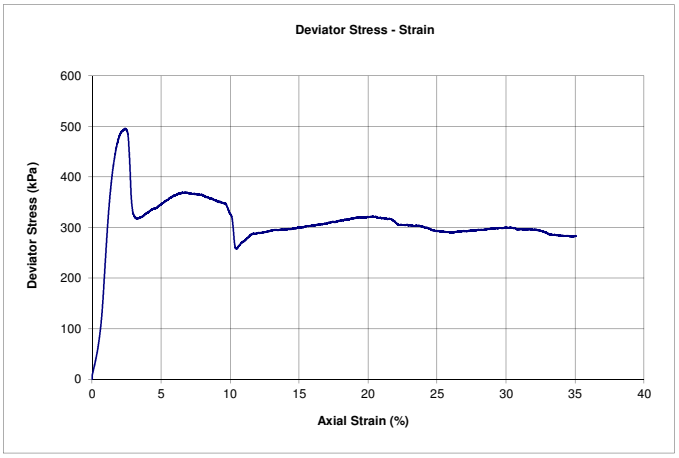
Triaxial CD Test - Charts

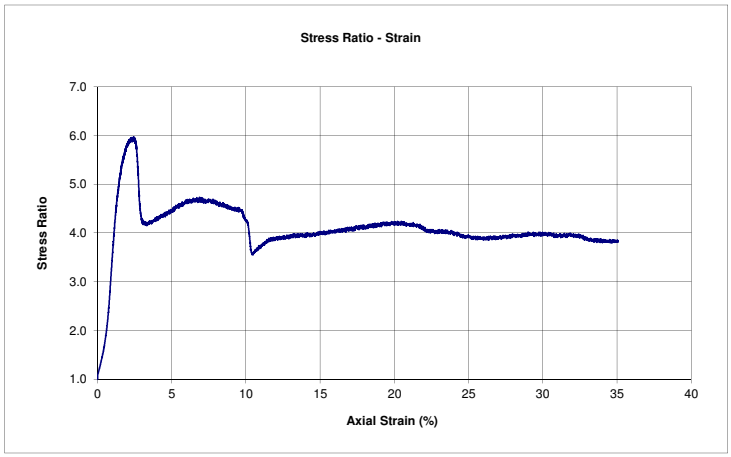
(ASTM D7181)

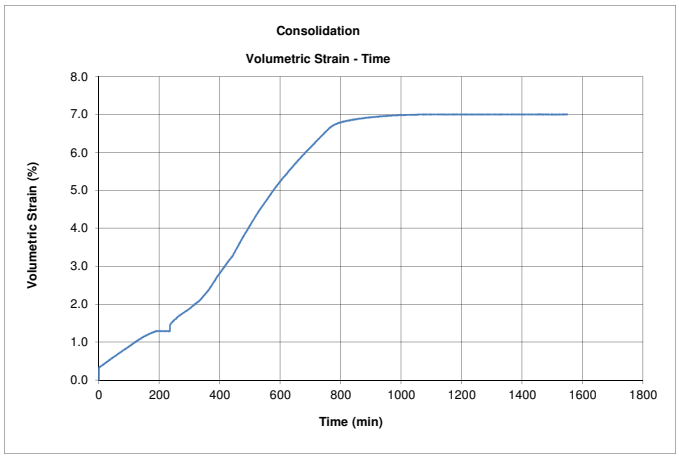
PROJECT NO. :	A03355A01	DATE :	2019-09-16
PROJECT :		TEST BY:	AX
SAMPLE :	Average	CHECKED BY:	JG
TEST NO. :	TX 19 - CID		

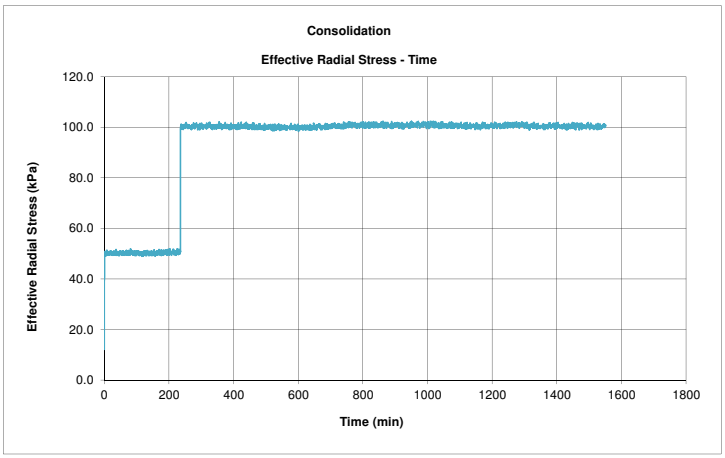












Triaxial CD Test - Summary

(ASTM D7181)

PROJECT NO. : A03355A01 DATE : 2019-09-19

PROJECT : TESTED BY: AX

SAMPLE : Average CHECKED BY: JG

TEST NO. : TX 20 - CID

SPECIMEN INFORMATION	UNITS	Initial	Vacuum	Saturation	B-value	End of 1st Consolidation	End of 2nd Consolidation	End of 3rd Consolidation	End of 4th Consolidation	End of 5th Consolidation	At Failure	End of Shear
Specimen Height	mm	140.12	140.12	140.12	140.10	140.07	140.00	139.83	139.83	139.83	134.10	104.11
Specimen Diameter	mm	70.15	70.15	70.15	70.02	69.98	69.92	69.90	69.84	69.79	71.56	81.79
Area	cm^2	38.65	38.65	38.65	38.51	38.46	38.40	38.38	38.31	38.26	40.22	52.54
Volume	cm^3	541.558	541.558	541.558	539.558	538.745	537.626	536.654	535.737	534.924	539.29	547.00
Wet Weight	g	1712.44	1712.44	1799.44	1800.44	1799.63	1798.51	1797.54	1796.62	1795.81	1800.18	1807.89
Water Content	%	7.90	7.90	13.38	13.44	13.39	13.32	13.26	13.20	13.15	13.43	13.91
Dry Weight	g	1587.06	1587.06	1587.06	1587.06	1587.06	1587.06	1587.06	1587.06	1587.06	1587.06	1587.06
Wet Density	g/cm^3	3.162	3.162	3.323	3.337	3.340	3.345	3.350	3.354	3.357	3.338	3.305
Dry Density	g/cm^3	2.931	2.931	2.931	2.941	2.946	2.952	2.957	2.962	2.967	2.943	2.901
Specific Gravity of Solids (assumed)	-	4.97	4.97	4.97	4.97	4.97	4.97	4.97	4.97	4.97	4.97	4.97
Solids Volume	cm^3	319.328	319.328	319.328	319.328	319.328	319.328	319.328	319.328	319.328	319.328	319.328
Void Volume	cm^3	222.230	222.230	222.230	220.230	219.417	218.298	217.326	216.409	215.596	219.966	227.676
Water Volume	cm^3	125.378	125.378	212.378	213.378	212.565	211.446	210.474	209.557	208.744	213.114	220.824
Void Ratio (e)	-	0.696	0.696	0.696	0.690	0.687	0.684	0.681	0.678	0.675	0.689	0.713
Saturation Ratio (Sr)	%	56.42	56.42	95.57	96.89	96.88	96.86	96.85	96.83	96.82	96.88	96.99
Effective Confining Stress	kPa					50	100	200	350	500		

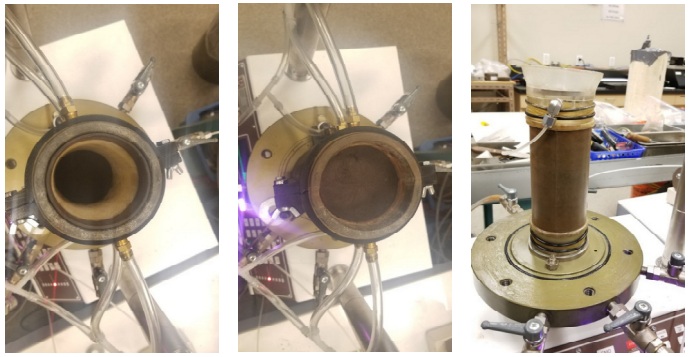
Shearing (CU)		
Skempton's B Parameter		0.99
Back Pressure before shearing	kPa	390.0
Confining Stress (σ_3') before shearing	kPa	500
Shear Strain Rate	mm / min	0.04

At Maximum Deviator Stress:		
Axial Stain	%	**4.09**
Deviator Stress	kPa	**2444.5**
Φ '	º	45.2
c' (assumed)	kPa	**0**

At Maximum Stress Ratio		
Axial Stain	%	**4.01**
Deviator Stress	kPa	**2443.3**
Φ '	º	45.2
c' (assumed)	kPa	0

Note: *using cambridge method*

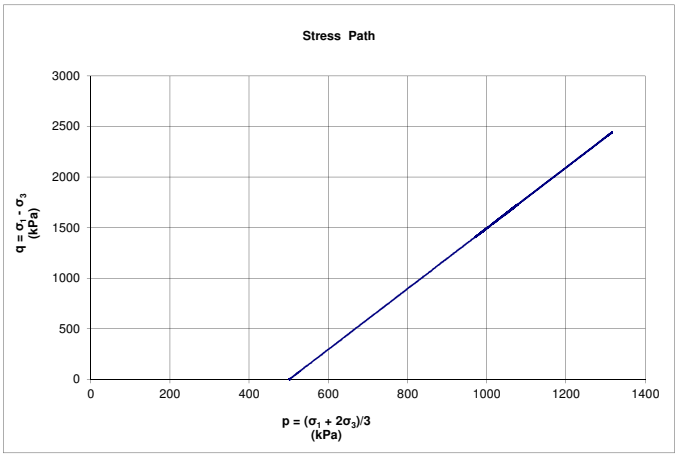
Photos: Before Test After Test

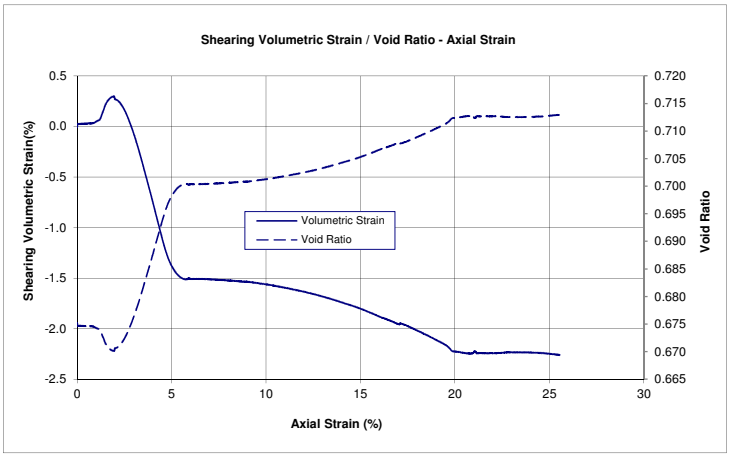


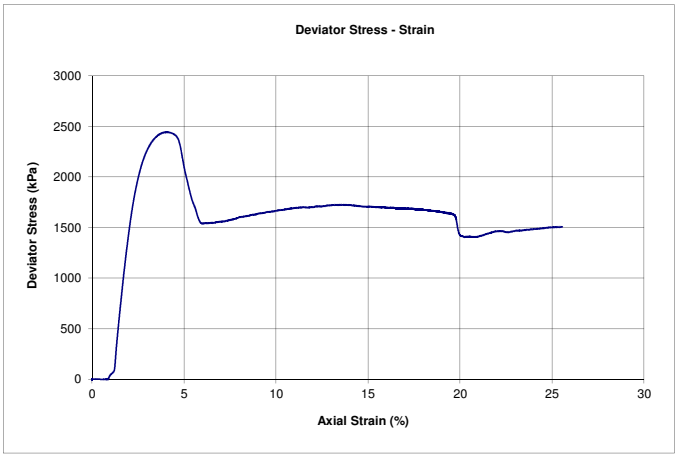
Triaxial CD Test - Charts

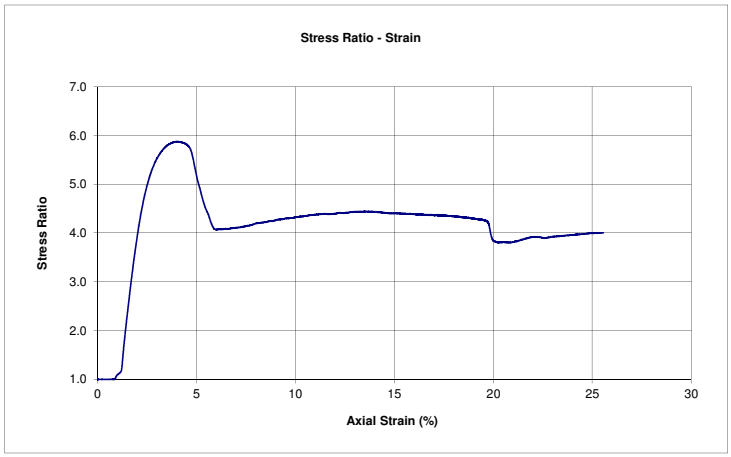
(ASTM D7181)

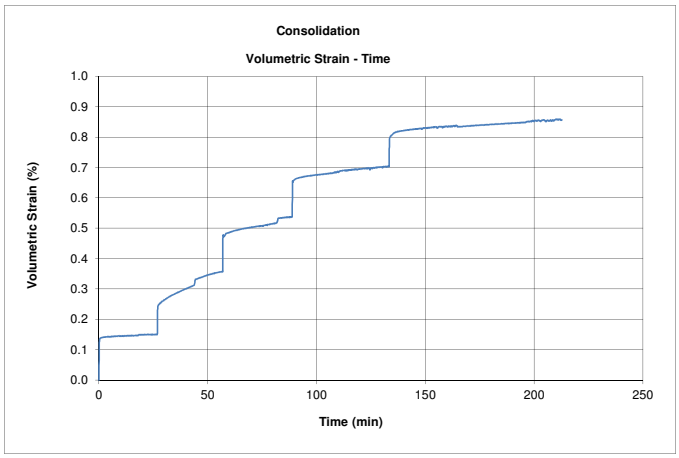
PROJECT NO. :	A03355A01	DATE :	2019-09-19
PROJECT :		TEST BY:	AX
SAMPLE :	Average	CHECKED BY:	JG
TEST NO. :	TX 20 - CID		

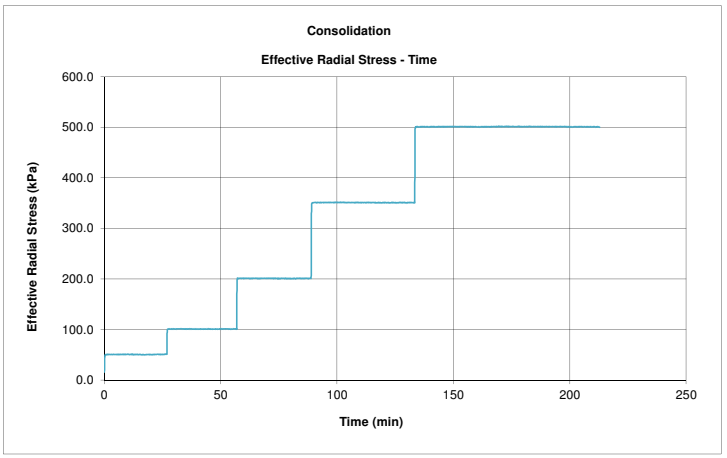












Triaxial CD Test - Summary

(ASTM D7181)

PROJECT NO. : A03355A01 DATE : 2019-09-19

PROJECT : TESTED BY: AX

SAMPLE : Average CHECKED BY: JG

TEST NO. : TX 21 - CID

SPECIMEN INFORMATION	UNITS	Initial	Vacuum	Saturation	B-value	End of 1st Consolidation	End of 2nd Consolidation	End of 3rd Consolidation	End of 4th Consolidation	End of 5th Consolidation	At Failure	End of Shear
Specimen Height	mm	140.23	140.23	139.19	139.17	139.14	139.11	139.05	138.98	138.92	133.71	103.94
Specimen Diameter	mm	70.07	70.07	70.33	70.09	70.05	69.98	69.93	69.89	69.85	71.28	81.33
Area	cm^2	38.56	38.56	38.85	38.59	38.53	38.46	38.41	38.36	38.32	39.90	51.95
Volume	cm^3	540.748	540.748	540.748	536.968	536.155	535.036	534.064	533.147	532.334	533.53	539.96
Wet Weight	g	1636.56	1636.56	1717.36	1732.36	1731.72	1731.15	1730.52	1729.91	1729.45	1730.65	1737.08
Water Content	%	7.77	7.77	13.09	14.08	14.04	14.00	13.96	13.92	13.89	13.97	14.39
Dry Weight	g	1518.57	1518.57	1518.57	1518.57	1518.57	1518.57	1518.57	1518.57	1518.57	1518.57	1518.57
Wet Density	g/cm^3	3.026	3.026	3.176	3.226	3.230	3.236	3.240	3.245	3.249	3.244	3.217
Dry Density	g/cm^3	2.808	2.808	2.808	2.828	2.832	2.838	2.843	2.848	2.853	2.846	2.812
Specific Gravity of Solids (assumed)	-	4.97	4.97	4.97	4.97	4.97	4.97	4.97	4.97	4.97	4.97	4.97
Solids Volume	cm^3	305.547	305.547	305.547	305.547	305.547	305.547	305.547	305.547	305.547	305.547	305.547
Void Volume	cm^3	235.201	235.201	235.201	231.421	230.608	229.489	228.517	227.600	226.787	227.987	234.417
Water Volume	cm^3	117.993	117.993	198.793	213.793	213.152	212.582	211.948	211.345	210.886	212.086	218.514
Void Ratio (e)	-	0.770	0.770	0.770	0.757	0.755	0.751	0.748	0.745	0.742	0.746	0.767
Saturation Ratio (Sr)	%	50.17	50.17	84.52	92.38	92.43	92.63	92.75	92.86	92.99	93.03	93.22
Effective Confining Stress	kPa					50	100	200	350	500		

Shearing (CU)		
Skempton's B Parameter		0.93
Back Pressure before shearing	kPa	430.0
Confining Stress (σ_3') before shearing	kPa	500
Shear Strain Rate	mm / min	0.04

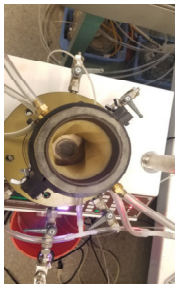
At Maximum Deviator Stress:		
Axial Stain	%	**3.74**
Deviator Stress	kPa	**1741.3**
Φ '	º	39.4
c' (assumed)	kPa	**0**

At Maximum Stress Ratio		
Axial Stain	%	**3.79**
Deviator Stress	kPa	**1740.2**
Φ '	º	39.4
c' (assumed)	kPa	0

Note: *using cambridge method*

Photos:

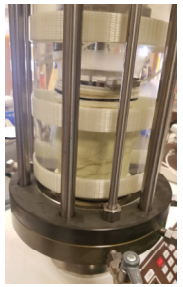
Before Test

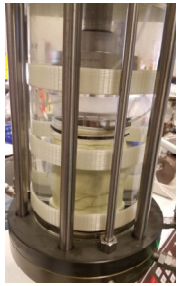






After Test

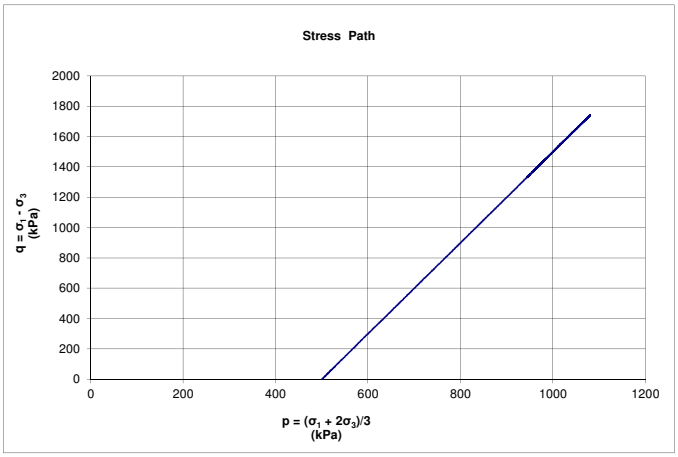


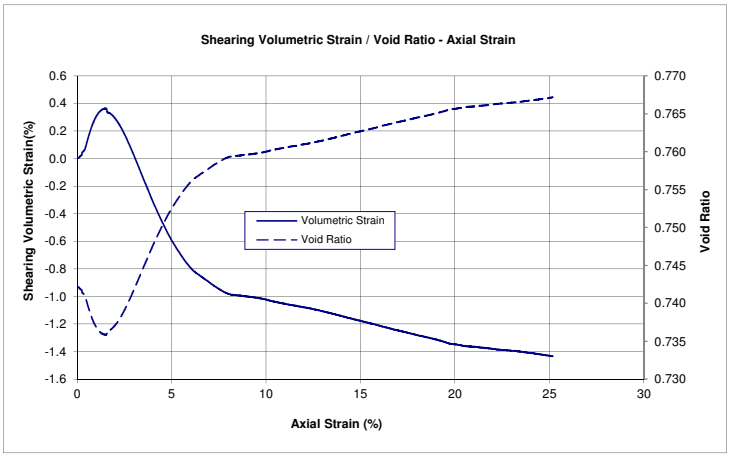


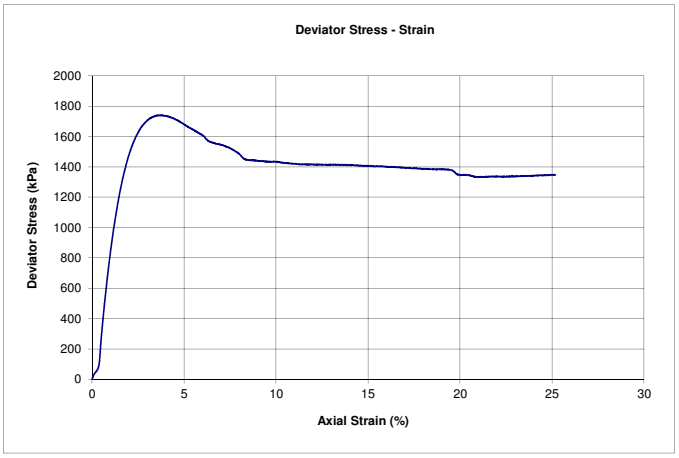
Triaxial CD Test - Charts

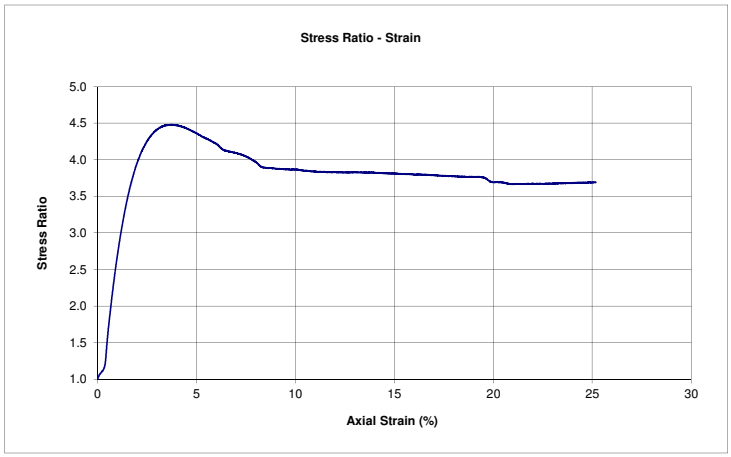
(ASTM D7181)

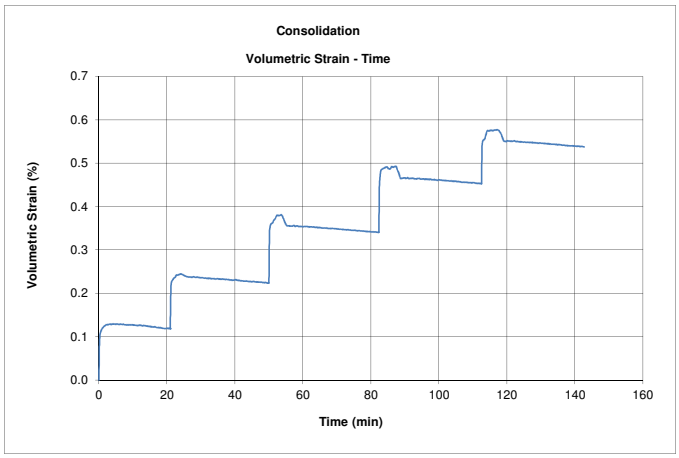
PROJECT NO. :	A03355A01	DATE :	2019-09-19
PROJECT :		TEST BY:	AX
SAMPLE :	Average	CHECKED BY:	JG
TEST NO. :	TX 21 - CID		

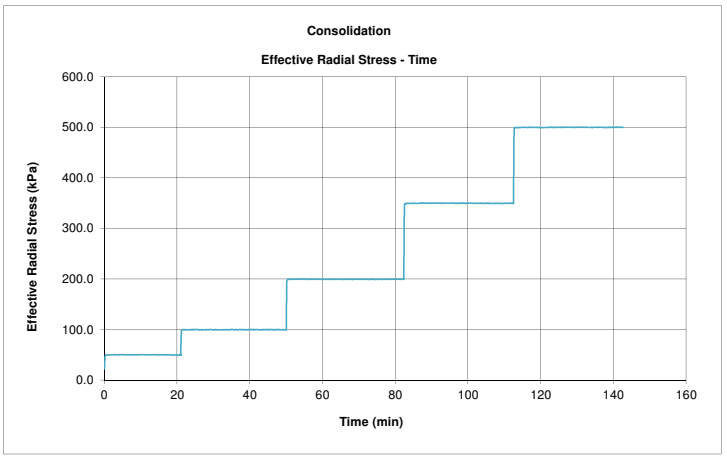












Triaxial CD Test - Summary

(ASTM D7181)

PROJECT NO. : A03355A01 DATE : 2019-09-19

PROJECT : TESTED BY: AX

SAMPLE : Fine CHECKED BY: JG

TEST NO. : TX 22 - CID

SPECIMEN INFORMATION	UNITS	Initial	Vacuum	Saturation / B-value	End of 1st Consolidation	End of 2nd Consolidation	End of 3rd Consolidation	At Failure	End of Shear	
Specimen Height	mm	140.18	140.18	139.81	139.61	139.50	139.34	125.66	90.46	
Specimen Diameter	mm	70.05	70.05	70.14	70.03	69.93	69.79	73.00	85.72	
Area	cm^2	38.54	38.54	38.64	38.51	38.41	38.25	41.85	57.71	
Volume	cm^3	540.25	540.25	540.25	537.71	535.80	533.05	525.92	522.09	
Wet Weight	g	1431.33	1431.33	1613.68	1611.14	1609.23	1606.49	1599.35	1595.53	
Water Content	%	4.87	4.87	18.23	18.04	17.90	17.70	17.18	16.90	
Dry Weight	g	1364.86	1364.86	1364.86	1364.86	1364.86	1364.86	1364.86	1364.86	
Wet Density	g/cm^3	2.649	2.649	2.987	2.996	3.003	3.014	3.041	3.056	
Dry Density	g/cm^3	2.526	2.526	2.526	2.538	2.547	2.560	2.595	2.614	
Specific Gravity of Solids (assumed)	-	4.96	4.96	4.96	4.96	4.96	4.96	4.96	4.96	
Solids Volume	cm^3	275.174	275.174	275.174	275.174	275.174	275.174	275.174	275.174	
Void Volume	cm^3	265.073	265.073	265.073	262.532	260.624	257.880	250.742	246.918	
Water Volume	cm^3	66.469	66.469	248.819	246.279	244.369	241.629	234.491	230.667	
Void Ratio (e)	-	0.963	0.963	0.963	0.954	0.947	0.937	0.911	0.897	
Saturation Ratio (Sr)	%	25.08	25.08	93.87	93.81	93.76	93.70	93.52	93.42	
Effective Confining Stress	kPa				50	100	200			

Shearing (CU)		
Skempton's B Parameter		0.93
Back Pressure before shearing	kPa	386.0
Confining Stress (σ_3') before shearing	kPa	200
Shear Strain Rate	mm / min	0.035

At Maximum Deviator Stress:		
Axial Stain	%	**9.82**
Deviator Stress	kPa	**568.8**
Φ '	º	35.6
c' (assumed)	kPa	**0**

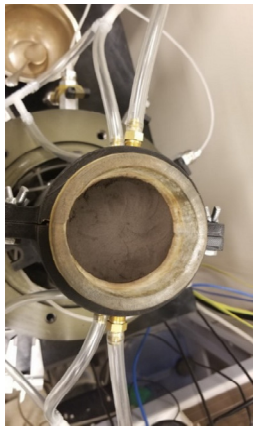
At Maximum Stress Ratio		
Axial Stain	%	**9.51**
Deviator Stress	kPa	**567.6**
Φ '	º	35.7
c' (assumed)	kPa	0

Note: *using cambridge method*

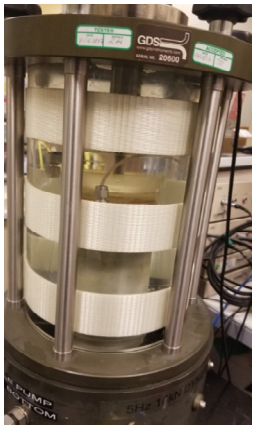
Photos:

Before Test





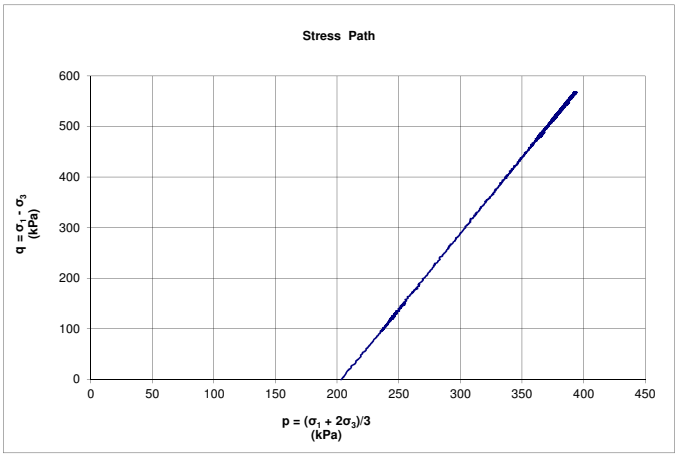
After Test

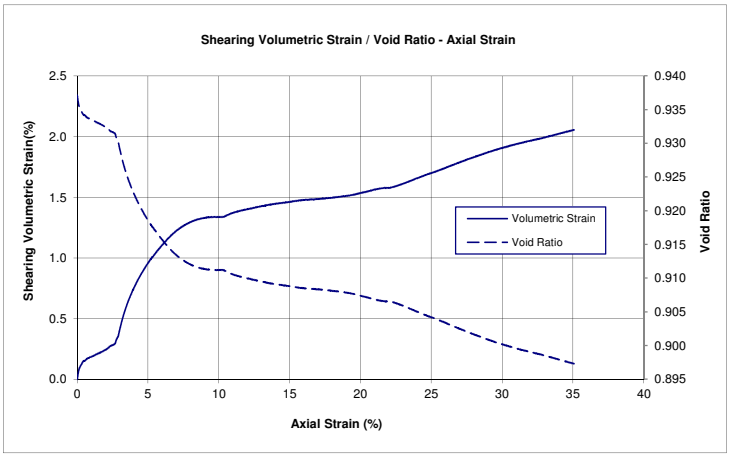


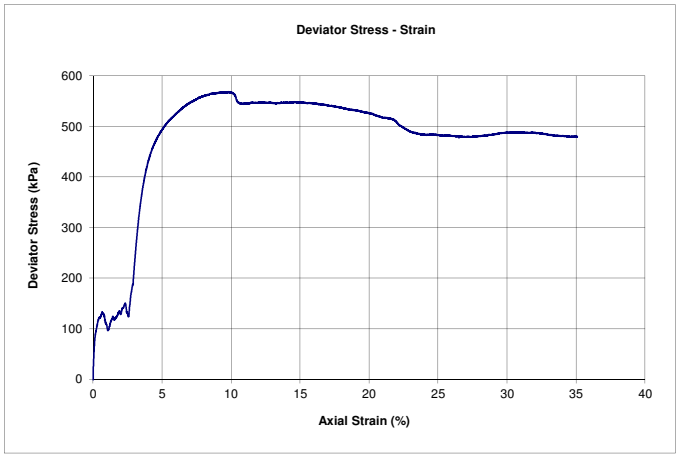
Triaxial CD Test - Charts

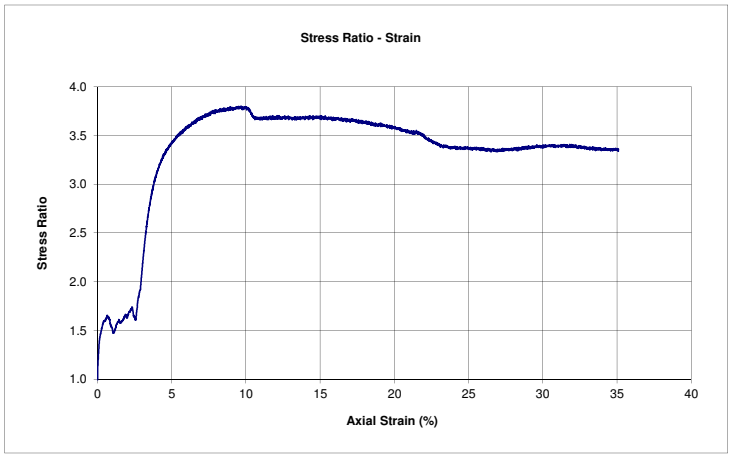
(ASTM D7181)

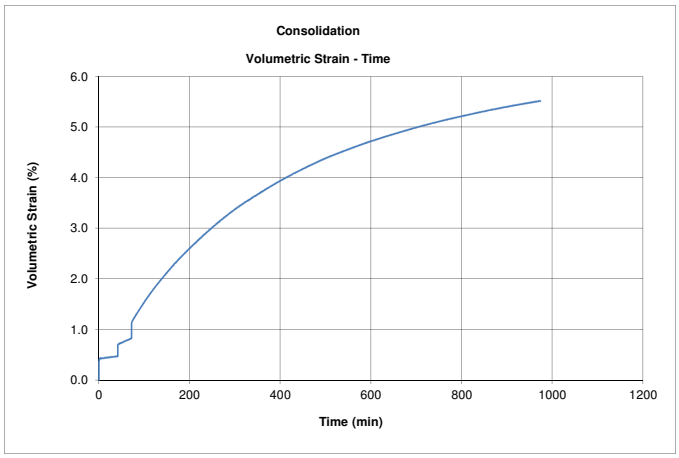
PROJECT NO. :	A03355A01	DATE :	2019-09-19
PROJECT :		TEST BY:	AX
SAMPLE :	Fine	CHECKED BY:	JG
TEST NO. :	TX 22 - CID		

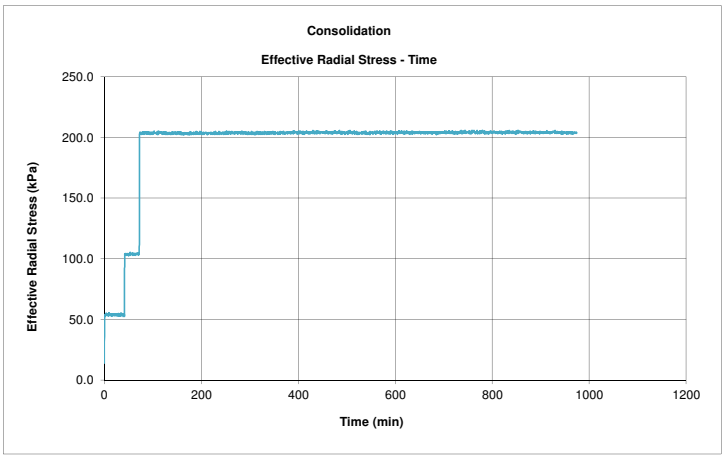












Triaxial CD Test - Summary

(ASTM D7181)

PROJECT NO. : A03355A01 DATE : 2019-10-07

PROJECT : TESTED BY: AX

SAMPLE : Fine Gradation CHECKED BY: JG

TEST NO. : TX 23 - CID

SPECIMEN INFORMATION	UNITS	Initial	Vacuum	Saturation	B-value	End of 1st Consolidation	End of 2nd Consolidation	End of 3rd Consolidation	At Failure	End of Shear
Specimen Height	mm	140.28	139.90	139.81	139.32	139.22	139.15	139.04	135.04	94.92
Specimen Diameter	mm	69.90	69.86	69.85	69.97	69.92	69.88	69.83	70.89	84.82
Area	cm^2	38.37	38.33	38.32	38.46	38.39	38.35	38.30	39.47	56.51
Volume	cm^3	538.32	536.25	535.75	535.75	534.54	533.68	532.47	533.03	536.36
Wet Weight	g	1532.31	1532.31	1660.21	1661.82	1660.62	1659.75	1658.54	1659.10	1662.43
Water Content	%	8.70	8.70	17.77	17.89	17.80	17.74	17.65	17.69	17.93
Dry Weight	g	1409.67	1409.67	1409.67	1409.67	1409.67	1409.67	1409.67	1409.67	1409.67
Wet Density	g/cm^3	2.846	2.857	3.099	3.102	3.107	3.110	3.115	3.113	3.099
Dry Density	g/cm^3	2.619	2.629	2.631	2.631	2.637	2.641	2.647	2.645	2.628
Specific Gravity of Solids (assumed)	-	4.96	4.96	4.96	4.96	4.96	4.96	4.96	4.96	4.96
Solids Volume	cm^3	284.207	284.207	284.207	284.207	284.207	284.207	284.207	284.207	284.207
Void Volume	cm^3	254.112	252.039	251.542	251.542	250.336	249.473	248.265	248.818	252.152
Water Volume	cm^3	122.641	122.641	250.541	252.152	250.946	250.083	248.875	249.428	252.762
Void Ratio (e)	-	0.894	0.887	0.885	0.885	0.881	0.878	0.874	0.875	0.887
Saturation Ratio (Sr)	%	48.26	48.66	99.60	100.24	100.24	100.24	100.25	100.25	100.24
Effective Confining Stress	kPa					50	100	200		

Shearing (CU)		
Skempton's B Parameter		0.98
Back Pressure before shearing	kPa	500.0
Confining Stress (σ_3') before shearing	kPa	200
Shear Strain Rate	mm / min	0.04

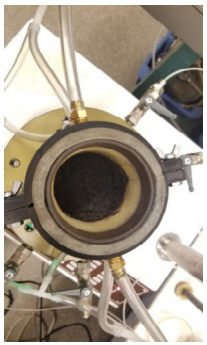
At Maximum Deviator Stress:		
Axial Stain	%	**2.88**
Deviator Stress	kPa	**609.6**
Φ '	º	38.1
c' (assumed)	kPa	**0**

At Maximum Stress Ratio		
Axial Stain	%	**2.99**
Deviator Stress	kPa	**608.7**
Φ '	º	38.1
c' (assumed)	kPa	**0**

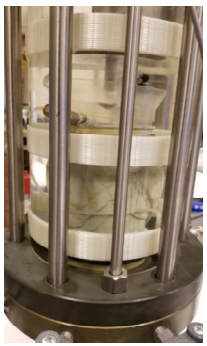
Note: *using cambridge method*

Photos:

Before Test

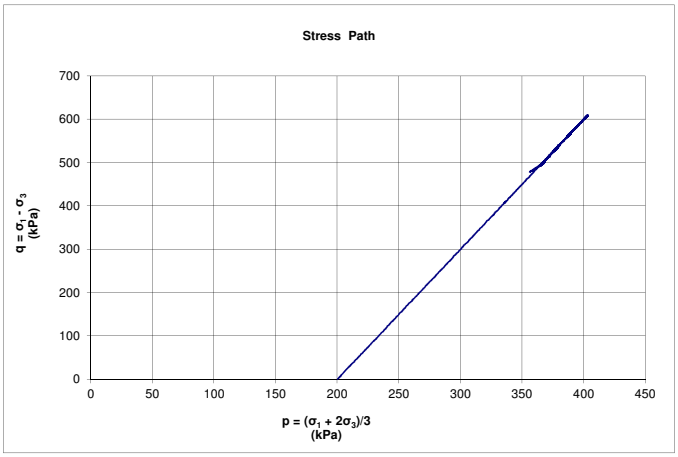

After Test

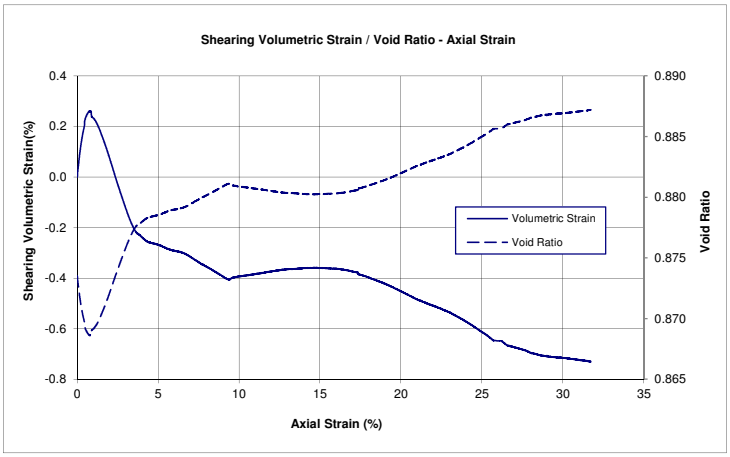



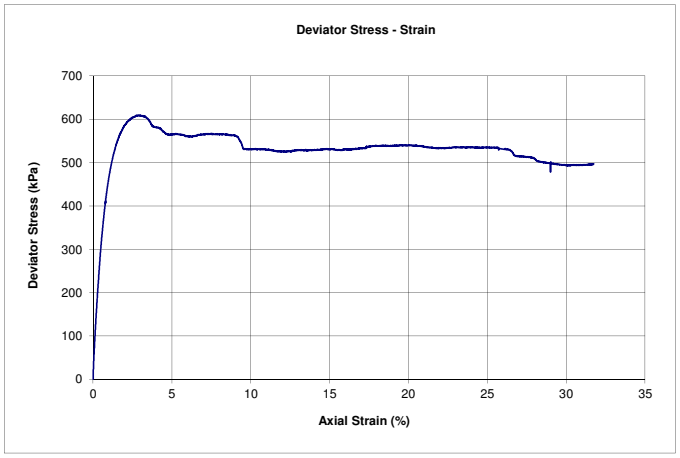
Triaxial CD Test - Charts

(ASTM D7181)

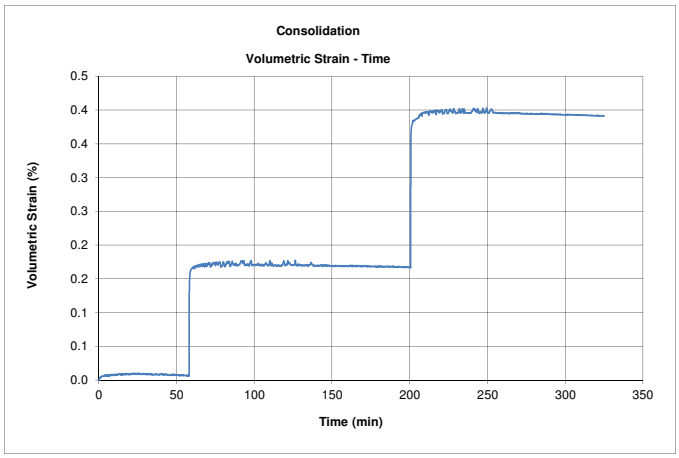
PROJECT NO. :	A03355A01	DATE :	2019-10-07
PROJECT :		TEST BY:	AX
SAMPLE :	Fine Gradation	CHECKED BY:	JG
TEST NO. :	TX 23 - CID		

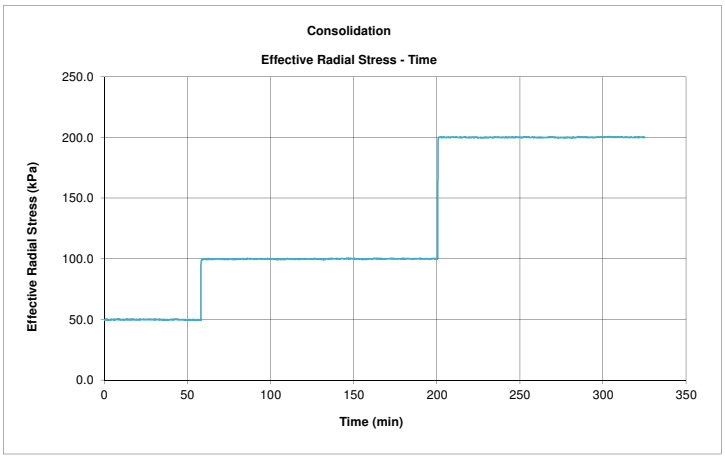












Triaxial CD Test - Summary

(ASTM D7181)

PROJECT NO. : A03355A01 DATE : 2019-10-04

PROJECT : TESTED BY: AX

SAMPLE : Fine Gradation CHECKED BY: JG

TEST NO. : TX 24 - CID

SPECIMEN INFORMATION	UNITS	Initial	Vacuum	Saturation	B-value	End of 1st Consolidation	End of 2nd Consolidation	End of 3rd Consolidation	At Failure	End of Shear
Specimen Height	mm	141.69	141.69	141.69	139.12	139.00	138.90	138.77	135.52	91.12
Specimen Diameter	mm	69.98	69.98	69.95	70.49	70.43	70.40	70.36	71.30	87.39
Area	cm^2	38.46	38.46	38.43	39.03	38.96	38.93	38.88	39.93	59.98
Volume	cm^3	544.98	544.98	544.48	543.00	541.58	540.66	539.48	541.11	546.58
Wet Weight	g	1570.56	1570.56	1691.06	1695.70	1694.28	1693.37	1692.19	1693.82	1699.29
Water Content	%	8.80	8.80	17.15	17.47	17.37	17.31	17.23	17.34	17.72
Dry Weight	g	1443.53	1443.53	1443.53	1443.53	1443.53	1443.53	1443.53	1443.53	1443.53
Wet Density	g/cm^3	2.882	2.882	3.106	3.123	3.128	3.132	3.137	3.130	3.109
Dry Density	g/cm^3	2.649	2.649	2.651	2.658	2.665	2.670	2.676	2.668	2.641
Specific Gravity of Solids (assumed)	-	4.96	4.96	4.96	4.96	4.96	4.96	4.96	4.96	4.96
Solids Volume	cm^3	291.034	291.034	291.034	291.034	291.034	291.034	291.034	291.034	291.034
Void Volume	cm^3	253.941	253.941	253.441	251.961	250.541	249.628	248.447	250.078	255.546
Water Volume	cm^3	127.031	127.031	247.531	252.172	250.752	249.839	248.658	250.289	255.757
Void Ratio (e)	-	0.873	0.873	0.871	0.866	0.861	0.858	0.854	0.859	0.878
Saturation Ratio (Sr)	%	50.02	50.02	97.67	100.08	100.08	100.08	100.08	100.08	100.08
Effective Confining Stress	kPa					50	100	200		

Shearing (CU)		
Skempton's B Parameter		0.98
Back Pressure before shearing	kPa	540.0
Confining Stress (σ_3') before shearing	kPa	200
Shear Strain Rate	mm / min	0.04

At Maximum Deviator Stress:		
Axial Stain	%	**2.34**
Deviator Stress	kPa	**636.9**
Φ '	º	37.9
c' (assumed)	kPa	**0**

At Maximum Stress Ratio		
Axial Stain	%	**2.34**
Deviator Stress	kPa	**636.9**
Φ '	º	37.9
c' (assumed)	kPa	**0**

Note: *using cambridge method*

Photos:

Before Test





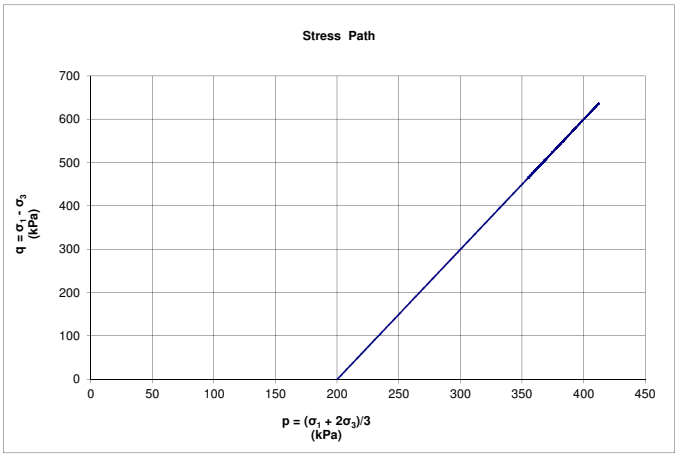
After Test

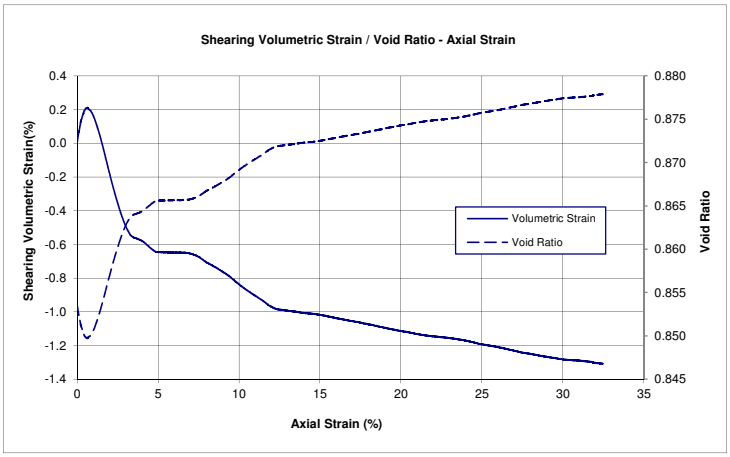


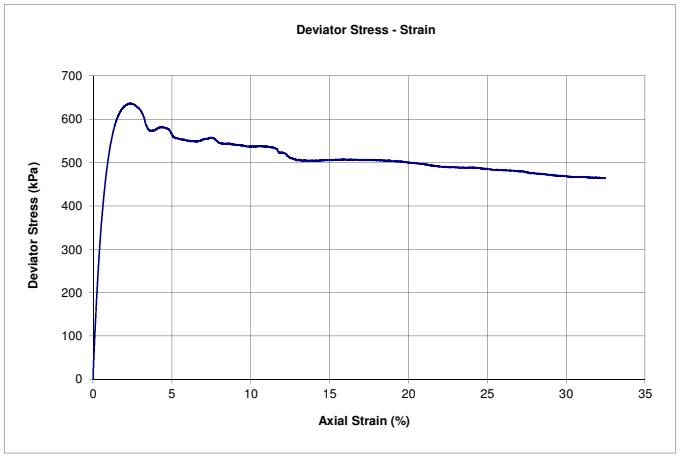
Triaxial CD Test - Charts

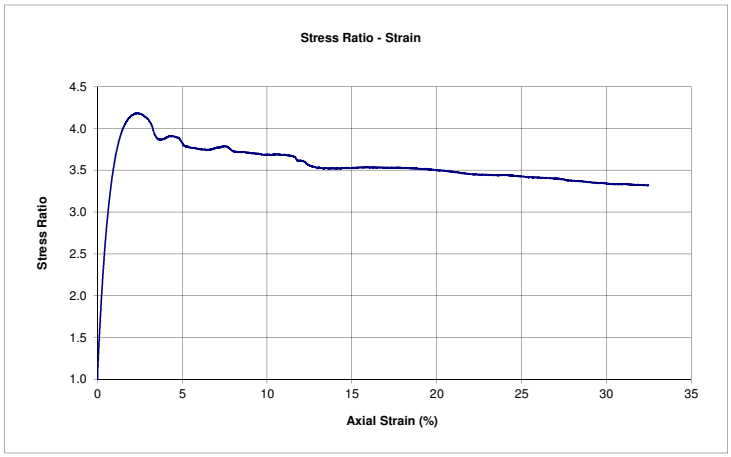
(ASTM D7181)

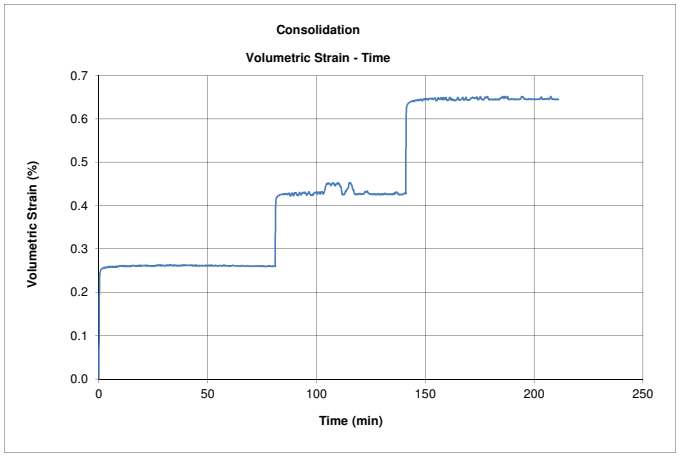
PROJECT NO. :	A03355A01	DATE :	2019-10-04
PROJECT :		TEST BY:	AX
SAMPLE :	Fine Gradation	CHECKED BY:	JG
TEST NO. :	TX 24 - CID		

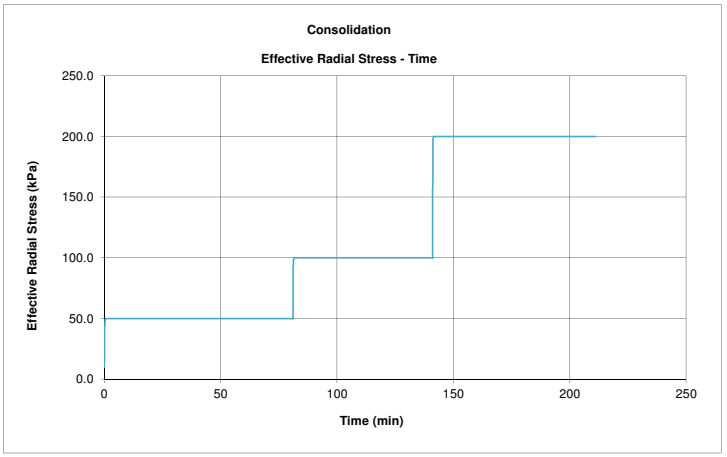












Triaxial CAU Test - Summary

(ASTM D4767)

PROJECT NO. : A03355A01 DATE : 2019-10-01

PROJECT : TESTED BY: BY

SAMPLE : Coarse Gradation CHECKED BY: JG

Details: Anisotropic consolidation, Kc = 0.5, p' = 200 kPa, strain control

SPECIMEN INFORMATION	UNITS	Initial	Vacuum	Saturation	B-value	End of Anisotropic Consolidation*	At Maximum Deviator Stress	End of Shear		
Specimen Height	mm	139.98	140.18	140.18	139.74	138.59	137.54	99.39		
Specimen Diameter	mm	69.80	69.70	69.51	69.56	69.39	69.65	81.94		
Area	cm^2	38.26	38.16	37.95	38.00	37.81	38.10	52.73		
Volume	cm^3	535.63	534.86	532.02	531.02	524.06	524.06	524.06		
Wet Weight	g	1432.50	1432.50	1616.70	1619.75	1612.79	1612.79	1612.79		
Water Content	%	4.79	4.79	18.26	18.49	17.98	17.98	17.98		
Dry Weight	g	1367.02	1367.02	1367.02	1367.02	1367.02	1367.02	1367.02		
Wet Density	g/cm^3	2.674	2.678	3.039	3.050	3.077	3.078	3.078		
Dry Density	g/cm^3	2.552	2.556	2.569	2.574	2.609	2.609	2.609		
Specific Gravity of Solids	-	4.91	4.91	4.91	4.91	4.91	4.91	4.91		
Solids Volume	cm^3	278.415	278.415	278.415	278.415	278.415	278.415	278.415		
Void Volume	cm^3	257.217	256.446	253.603	252.603	245.646	245.642	245.642		
Water Volume	cm^3	65.480	65.480	249.680	252.729	245.772	245.768	245.768		
Void Ratio (e)	-	0.924	0.921	0.911	0.907	0.882	0.882	0.882		
Saturation Ratio (Sr)	%	25.46	25.53	98.45	100.05	100.05	100.05	100.05		
Effective Confining Stress (σ_3')	kPa					150				

** Anisotropic consolidation at 0.01%/min strain rate*

Shearing (CAU)		
Skempton's B Parameter		0.99
Back Pressure before shearing	kPa	499.0
Confining Stress (σ_3') before shearing	kPa	150
Shear Strain Rate	mm / min	0.03

At Maximum Deviator Stress:		
Axial Stain	%	0.75
Deviator Stress	kPa	204.4
Φ '	º	34.3
c' (assumed)	kPa	0

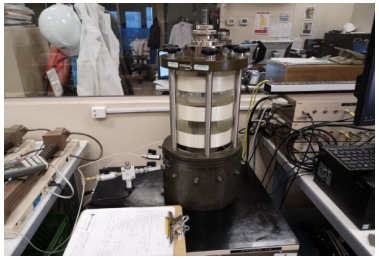
At Maximum Stress Ratio		
Axial Stain	%	-
Deviator Stress	kPa	-
Φ '	º	-
c' (assumed)	kPa	-

Note: *using cambridge method*

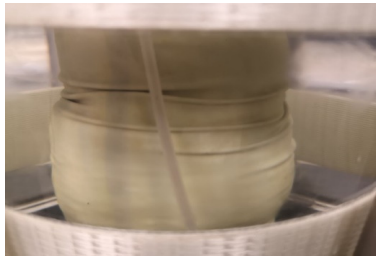
Test Photos:

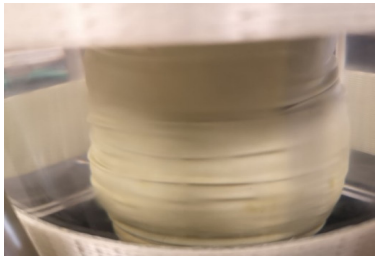
Before Test





After Test

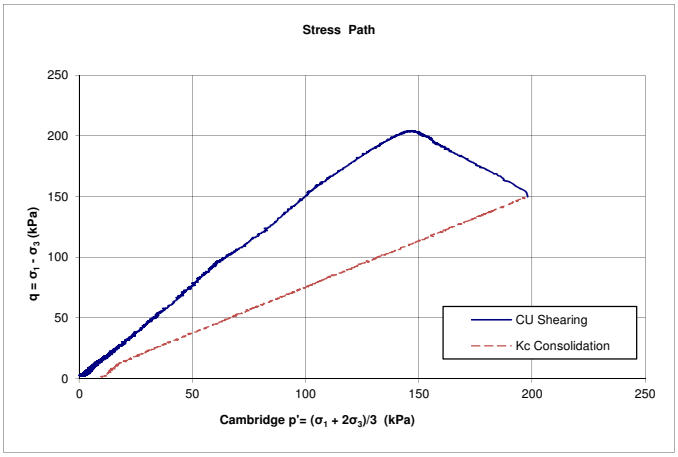


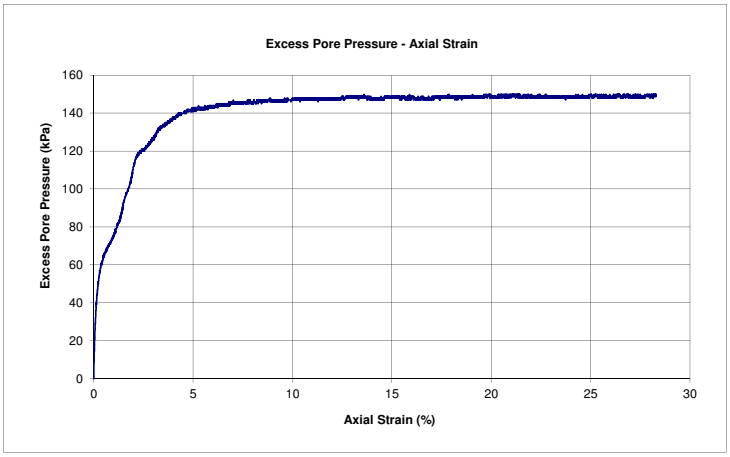


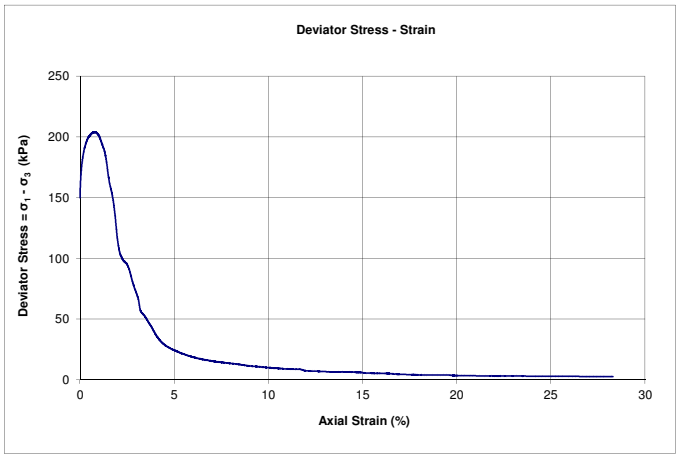
Triaxial CU Test - Charts

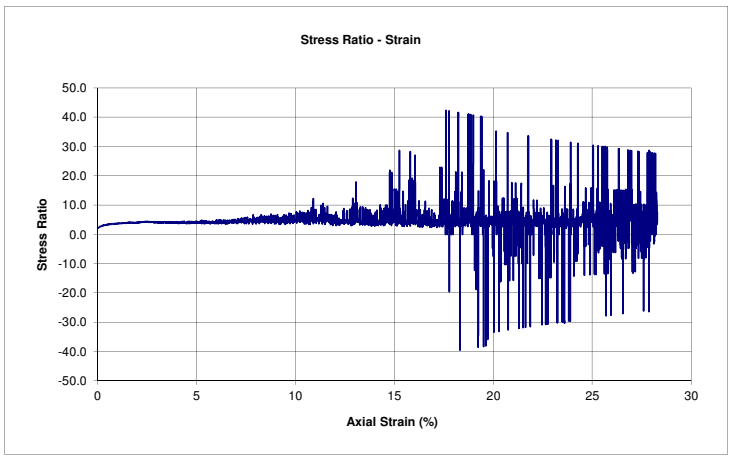
(ASTM D4767)

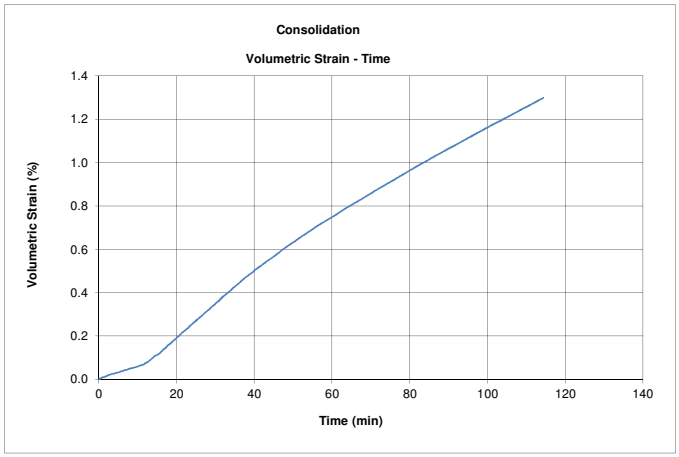
PROJECT NO. :	A03355A01	DATE :	2019-10-01
PROJECT :		TEST BY:	BY
SAMPLE :	Coarse Gradation	CHECKED BY:	JG
Details:	Anisotropic consolidation, Kc = 0.5, p' = 200 kPa, strain control		

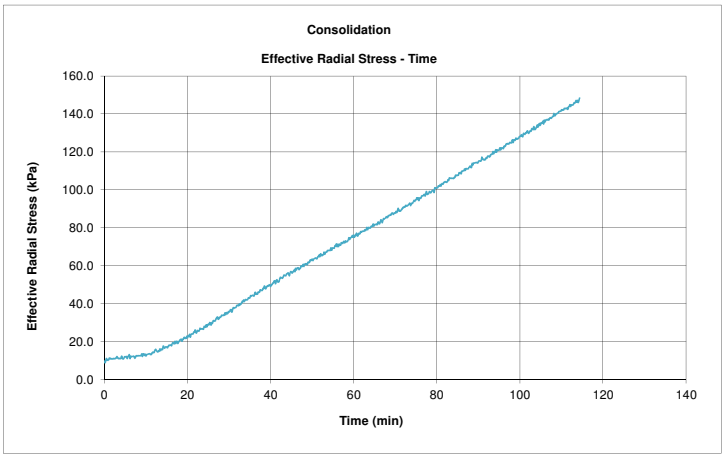












Triaxial CAU Test - Summary

(ASTM D4767)

PROJECT NO. : A03355A01 DATE : 2019-10-10

PROJECT : TESTED BY: BY

SAMPLE : Fine Gradation CHECKED BY: JG

Details: Anisotropic consolidation, Kc = 0.5, p' = 200 kPa, strain control

SPECIMEN INFORMATION	UNITS	Initial	Vacuum	Saturation	B-value	End of Anisotropic Consolidation*	At Maximum Deviator Stress	End of Shear		
Specimen Height	mm	139.90	139.55	139.55	139.00	137.27	136.83	97.62		
Specimen Diameter	mm	69.80	69.71	69.47	69.56	69.45	69.56	82.35		
Area	cm^2	38.26	38.17	37.90	38.00	37.88	38.00	53.26		
Volume	cm^3	535.33	532.61	528.89	528.19	519.96	519.94	519.94		
Wet Weight	g	1402.47	1402.47	1559.17	1564.54	1556.30	1556.29	1556.29		
Water Content	%	8.05	8.05	20.12	20.54	19.90	19.90	19.90		
Dry Weight	g	1297.98	1297.98	1297.98	1297.98	1297.98	1297.98	1297.98		
Wet Density	g/cm^3	2.620	2.633	2.948	2.962	2.993	2.993	2.993		
Dry Density	g/cm^3	2.425	2.437	2.454	2.457	2.496	2.496	2.496		
Specific Gravity of Solids	-	4.96	4.96	4.96	4.96	4.96	4.96	4.96		
Solids Volume	cm^3	261.690	261.690	261.690	261.690	261.690	261.690	261.690		
Void Volume	cm^3	273.636	270.921	267.201	266.501	258.268	258.253	258.253		
Water Volume	cm^3	104.488	104.488	261.188	266.554	258.321	258.306	258.306		
Void Ratio (e)	-	1.046	1.035	1.021	1.018	0.987	0.987	0.987		
Saturation Ratio (Sr)	%	38.18	38.57	97.75	100.02	100.02	100.02	100.02		
Effective Confining Stress (σ_3')	kPa					150				

** Anisotropic consolidation at 0.01%/min strain rate*

Shearing (CAU)		
Skempton's B Parameter		0.98
Back Pressure before shearing	kPa	500.0
Confining Stress (σ_3') before shearing	kPa	150
Shear Strain Rate	mm / min	0.04

At Maximum Deviator Stress:		
Axial Stain	%	0.32
Deviator Stress	kPa	167.3
Φ '	º	28.1
c' (assumed)	kPa	0

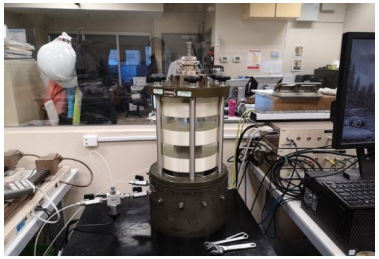
At Maximum Stress Ratio		
Axial Stain	%	-
Deviator Stress	kPa	-
Φ '	º	-
c' (assumed)	kPa	-

Note: *using cambridge method*

Test Photos:

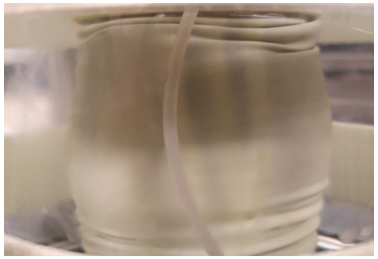
Before Test





After Test

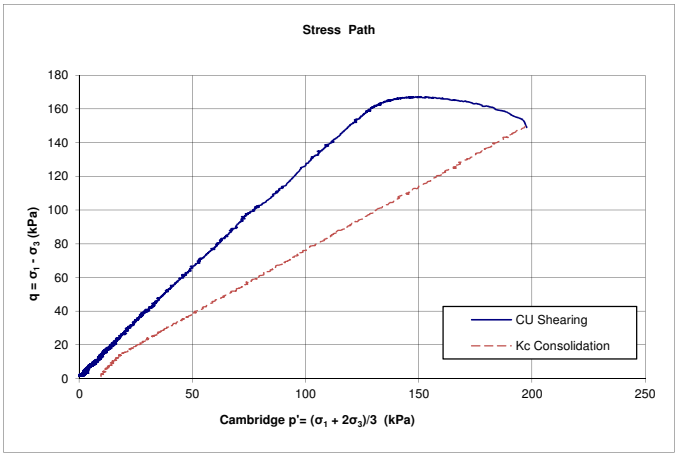


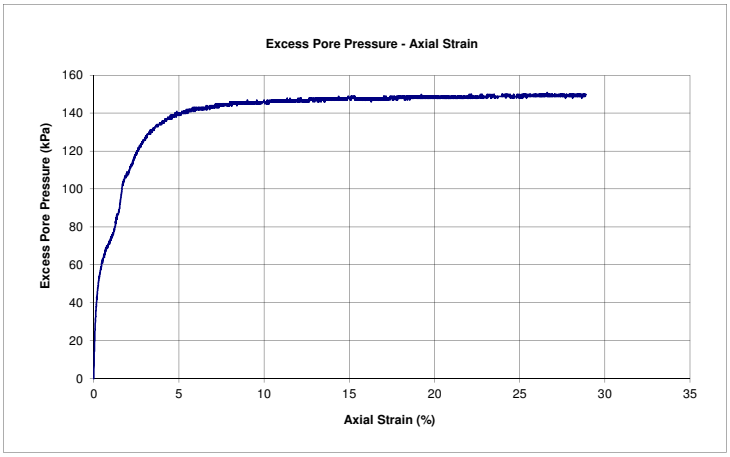


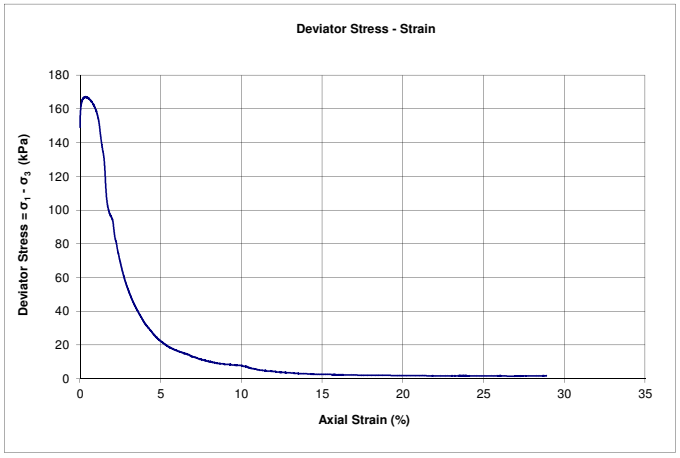
Triaxial CU Test - Charts

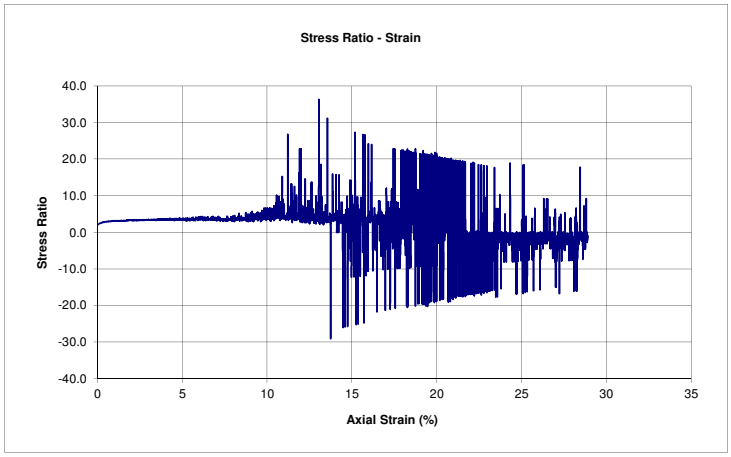
(ASTM D4767)

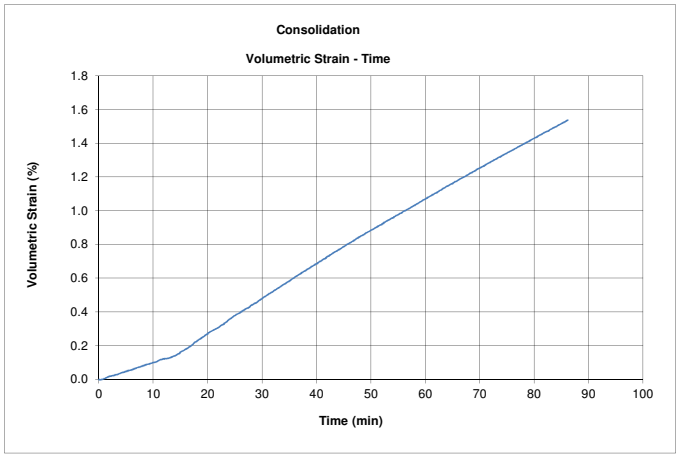
PROJECT NO. :	A03355A01	DATE :	2019-10-10
PROJECT :		TEST BY:	BY
SAMPLE :	Fine Gradation	CHECKED BY:	JG
Details:	Anisotropic consolidation, Kc = 0.5, p' = 200 kPa, strain control		

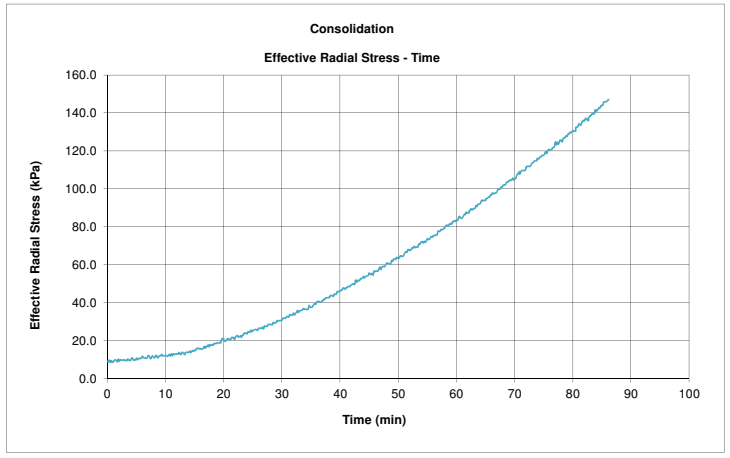












Triaxial CAU Test - Summary

(ASTM D4767)

PROJECT NO. : A03355A01 DATE : 2019-11-06

PROJECT : TESTED BY: BY

SAMPLE : Fine Gradation CHECKED BY: JG

Details: Anisotropic consolidation, Kc = 0.5, p' = 200 kPa, strain control

SPECIMEN INFORMATION	UNITS	Initial	Vacuum	Saturation	B-value	End of Anisotropic Consolidation*	At Maximum Deviator Stress	End of Shear		
Specimen Height	mm	140.85	140.85	140.85	140.74	139.06	99.23	99.23		
Specimen Diameter	mm	70.18	70.18	69.99	69.94	70.01	82.88	82.88		
Area	cm^2	38.68	38.68	38.47	38.41	38.49	53.94	53.94		
Volume	cm^3	544.85	544.85	541.85	540.65	535.28	535.28	535.28		
Wet Weight	g	1453.73	1453.73	1639.13	1644.27	1638.91	1638.91	1638.91		
Water Content	%	5.18	5.18	18.59	18.97	18.58	18.58	18.58		
Dry Weight	g	1382.14	1382.14	1382.14	1382.14	1382.14	1382.14	1382.14		
Wet Density	g/cm^3	2.668	2.668	3.025	3.041	3.062	3.062	3.062		
Dry Density	g/cm^3	2.537	2.537	2.551	2.556	2.582	2.582	2.582		
Specific Gravity of Solids	-	4.96	4.96	4.96	4.96	4.96	4.96	4.96		
Solids Volume	cm^3	278.656	278.656	278.656	278.656	278.656	278.656	278.656		
Void Volume	cm^3	266.189	266.189	263.189	261.989	256.626	256.625	256.625		
Water Volume	cm^3	71.595	71.595	256.995	262.137	256.774	256.773	256.773		
Void Ratio (e)	-	0.955	0.955	0.944	0.940	0.921	0.921	0.921		
Saturation Ratio (Sr)	%	26.90	26.90	97.65	100.06	100.06	100.06	100.06		
Effective Confining Stress (σ_3')	kPa					150				

** Anisotropic consolidation at 0.01%/min strain rate*

Shearing (CAU)		
Skempton's B Parameter		0.99
Back Pressure before shearing	kPa	600.0
Confining Stress (σ_3') before shearing	kPa	150
Shear Strain Rate	mm / min	0.04

At Maximum Deviator Stress:		
Axial Stain	%	2.01
Deviator Stress	kPa	408.6
Φ '	º	34.9
c' (assumed)	kPa	0

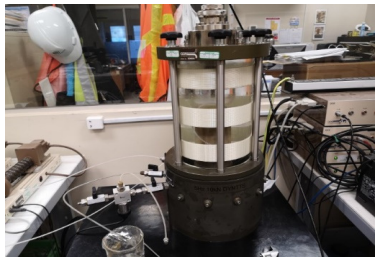
At Maximum Stress Ratio		
Axial Stain	%	6.61
Deviator Stress	kPa	358.2
Φ '	º	35.2
c' (assumed)	kPa	0

Note: *using cambridge method*

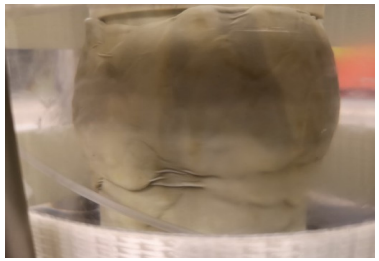
Test Photos:

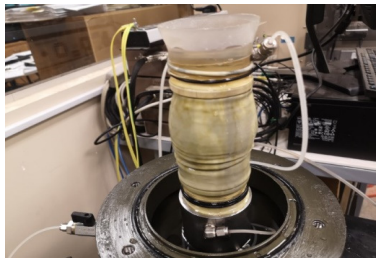
Before Test





After Test

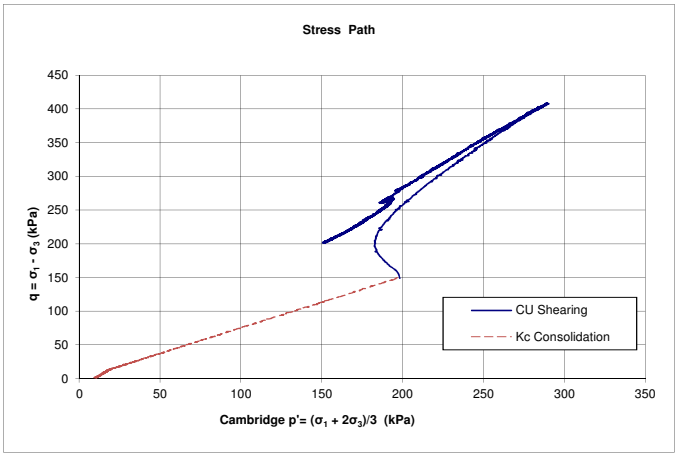


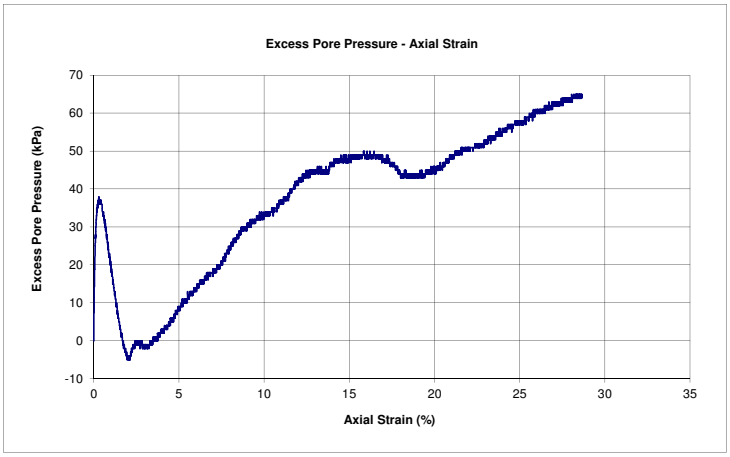


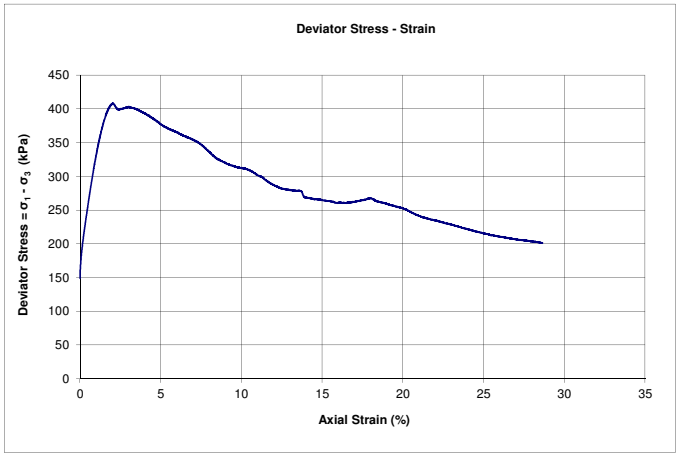
Triaxial CU Test - Charts

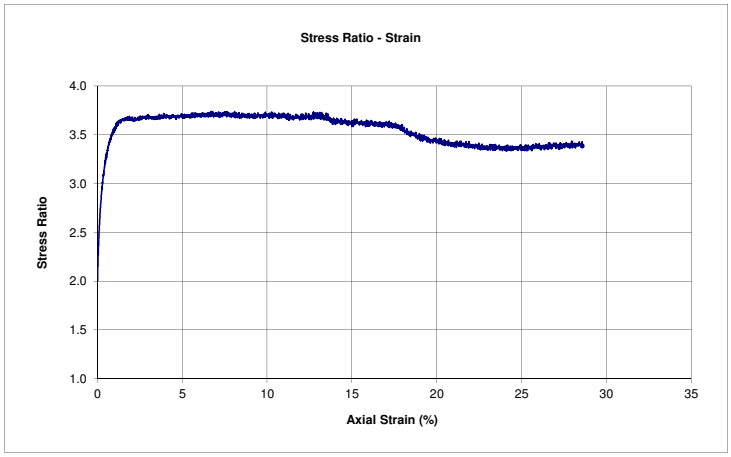
(ASTM D4767)

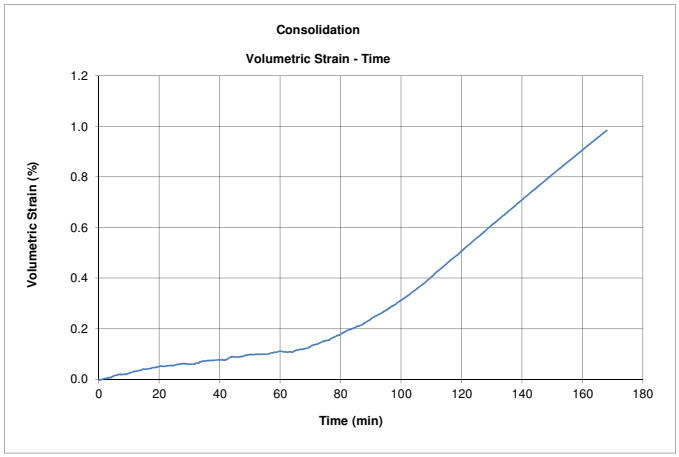
PROJECT NO. :	A03355A01	DATE :	2019-11-06
PROJECT :		TEST BY:	BY
SAMPLE :	Fine Gradation	CHECKED BY:	JG
Details:	Anisotropic consolidation, Kc = 0.5, p' = 200 kPa, strain control		

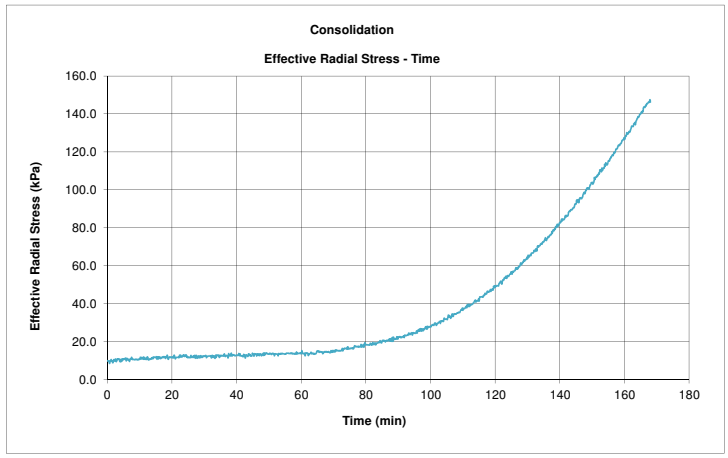












Triaxial CAU Test - Summary

(ASTM D4767)

PROJECT NO. : A03355A01 DATE : 2019-11-06

PROJECT : TESTED BY: BY

SAMPLE : Fine Gradation CHECKED BY: JG

Details: Anisotropic consolidation, Kc = 0.5, p' = 200 kPa, strain control

SPECIMEN INFORMATION	UNITS	Initial	Vacuum	Saturation	B-value	End of Anisotropic Consolidation*	At Maximum Deviator Stress	End of Shear		
Specimen Height	mm	139.93	139.93	139.93	139.63	139.18	129.97	97.65		
Specimen Diameter	mm	70.16	70.16	70.16	70.16	70.08	72.52	83.66		
Area	cm^2	38.66	38.66	38.66	38.66	38.57	41.30	54.97		
Volume	cm^3	540.98	540.98	540.98	539.78	536.81	536.81	536.81		
Wet Weight	g	1545.07	1545.07	1708.67	1713.64	1710.67	1710.67	1710.67		
Water Content	%	5.09	5.09	16.22	16.56	16.35	16.35	16.35		
Dry Weight	g	1470.24	1470.24	1470.24	1470.24	1470.24	1470.24	1470.24		
Wet Density	g/cm^3	2.856	2.856	3.158	3.175	3.187	3.187	3.187		
Dry Density	g/cm^3	2.718	2.718	2.718	2.724	2.739	2.739	2.739		
Specific Gravity of Solids	-	4.96	4.96	4.96	4.96	4.96	4.96	4.96		
Solids Volume	cm^3	296.418	296.418	296.418	296.418	296.418	296.418	296.418		
Void Volume	cm^3	244.560	244.560	244.560	243.360	240.391	240.390	240.390		
Water Volume	cm^3	74.835	74.835	238.435	243.408	240.439	240.438	240.438		
Void Ratio (e)	-	0.825	0.825	0.825	0.821	0.811	0.811	0.811		
Saturation Ratio (Sr)	%	30.60	30.60	97.50	100.02	100.02	100.02	100.02		
Effective Confining Stress (σ_3')	kPa					150				

** Anisotropic consolidation at 0.01%/min strain rate*

Shearing (CAU)		
Skempton's B Parameter		0.99
Back Pressure before shearing	kPa	600.0
Confining Stress (σ_3') before shearing	kPa	150
Shear Strain Rate	mm / min	0.04

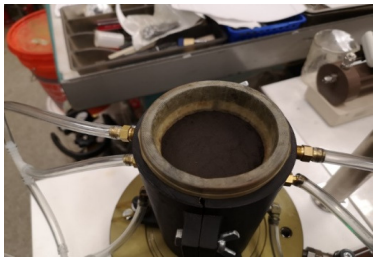
At Maximum Deviator Stress:		
Axial Stain	%	6.62
Deviator Stress	kPa	2106.0
Φ '	º	36.6
c' (assumed)	kPa	0

At Maximum Stress Ratio		
Axial Stain	%	1.54
Deviator Stress	kPa	1120.3
Φ '	º	38.9
c' (assumed)	kPa	0

Note: *using cambridge method*

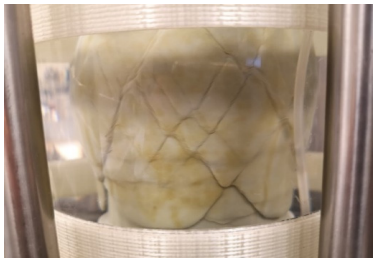
Test Photos:

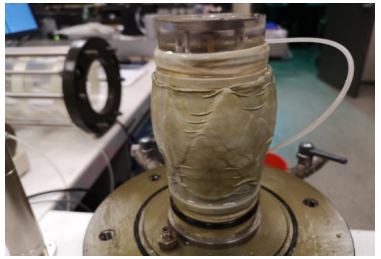
Before Test





After Test

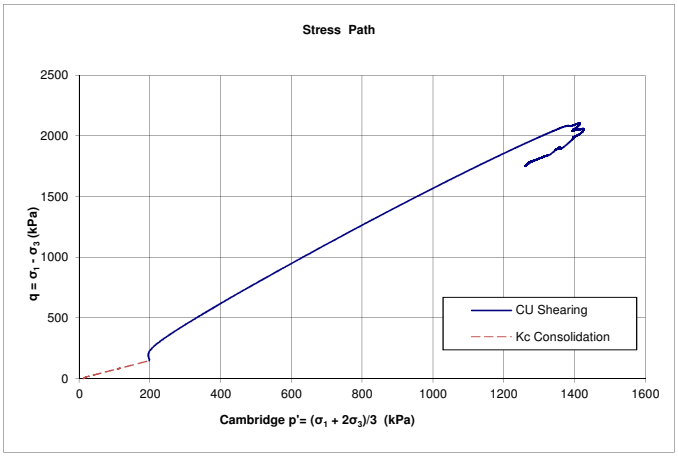


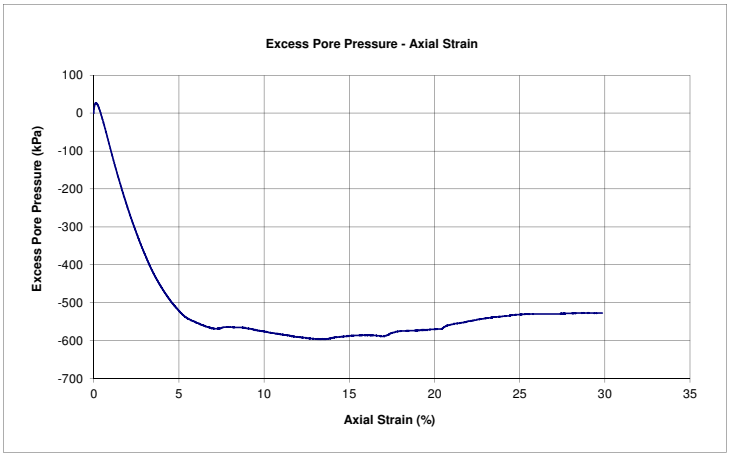


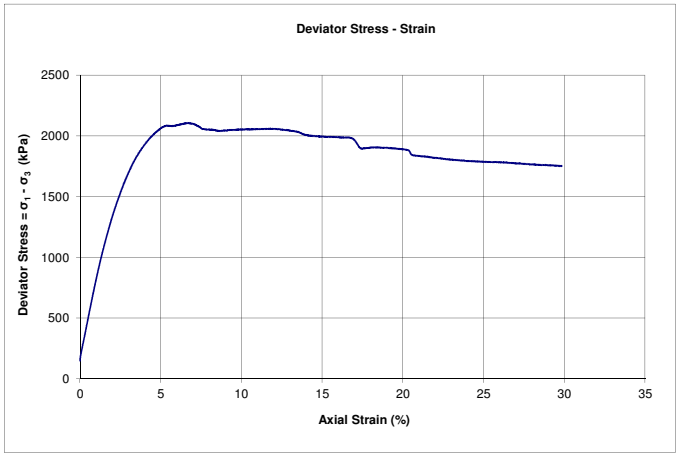
Triaxial CU Test - Charts

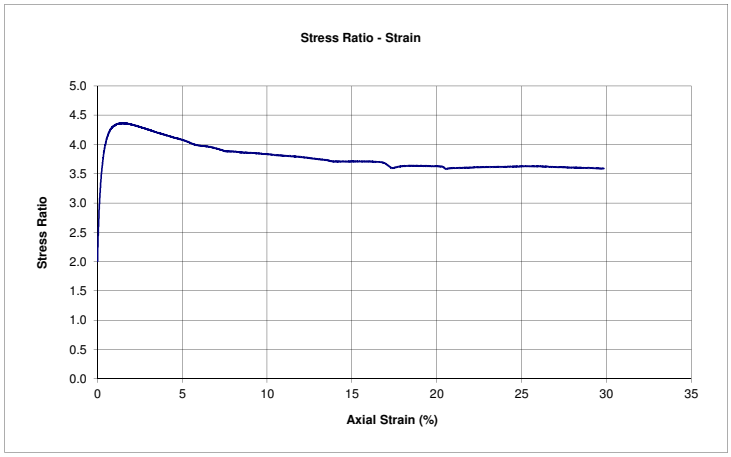
(ASTM D4767)

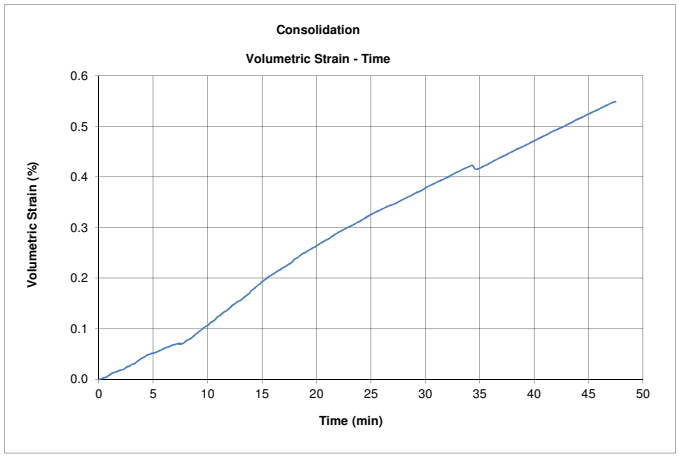
PROJECT NO. :	A03355A01	DATE :	2019-11-06
PROJECT :		TEST BY:	BY
SAMPLE :	Fine Gradation	CHECKED BY:	JG
Details:	Anisotropic consolidation, Kc = 0.5, p' = 200 kPa, strain control		

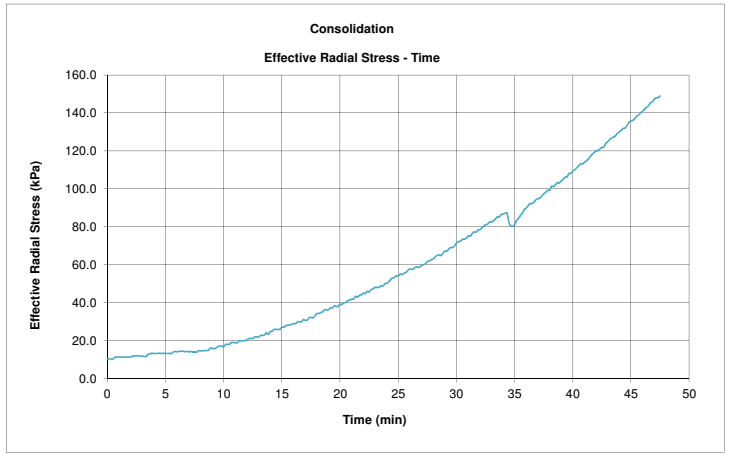












Triaxial CAU Test - Summary

(ASTM D4767)

PROJECT NO. : A03355A01 DATE : 2019-11-06

PROJECT : TESTED BY: BY

SAMPLE : Fine Gradation CHECKED BY: JG

Details: Anisotropic consolidation, Kc = 0.5, p' = 200 kPa, strain control

SPECIMEN INFORMATION	UNITS	Initial	Vacuum	Saturation	B-value	End of Anisotropic Consolidation*	At Maximum Deviator Stress	End of Shear		
Specimen Height	mm	140.86	140.86	140.86	140.80	140.06	133.48	95.29		
Specimen Diameter	mm	69.90	69.91	69.83	69.78	69.76	71.45	84.57		
Area	cm^2	38.37	38.39	38.29	38.24	38.22	40.10	56.17		
Volume	cm^3	540.55	540.70	539.39	538.39	535.25	535.25	535.25		
Wet Weight	g	1496.88	1496.88	1673.38	1675.61	1672.47	1672.47	1672.47		
Water Content	%	5.09	5.09	17.48	17.64	17.42	17.42	17.42		
Dry Weight	g	1424.38	1424.38	1424.38	1424.38	1424.38	1424.38	1424.38		
Wet Density	g/cm^3	2.769	2.768	3.102	3.112	3.125	3.125	3.125		
Dry Density	g/cm^3	2.635	2.634	2.641	2.646	2.661	2.661	2.661		
Specific Gravity of Solids	-	4.96	4.96	4.96	4.96	4.96	4.96	4.96		
Solids Volume	cm^3	287.173	287.173	287.173	287.173	287.173	287.173	287.173		
Void Volume	cm^3	253.372	253.527	252.217	251.217	248.079	248.079	248.079		
Water Volume	cm^3	72.501	72.501	249.001	251.230	248.093	248.092	248.092		
Void Ratio (e)	-	0.882	0.883	0.878	0.875	0.864	0.864	0.864		
Saturation Ratio (Sr)	%	28.61	28.60	98.73	100.01	100.01	100.01	100.01		
Effective Confining Stress (σ_3')	kPa					150				

** Anisotropic consolidation at 0.01%/min strain rate*

Shearing (CAU)		
Skempton's B Parameter		0.98
Back Pressure before shearing	kPa	499.7
Confining Stress (σ_3') before shearing	kPa	150
Shear Strain Rate	% / min	0.03

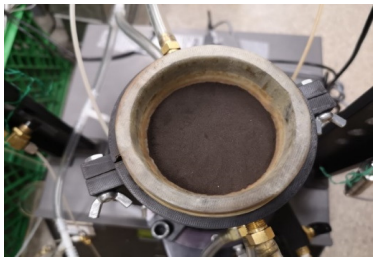
At Maximum Deviator Stress:		
Axial Stain	%	4.70
Deviator Stress	kPa	870.3
Φ '	º	36.4
c' (assumed)	kPa	0

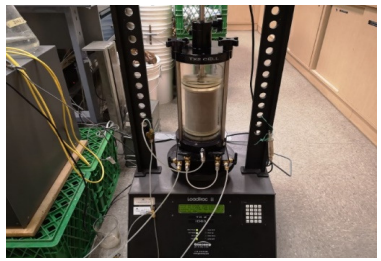
At Maximum Stress Ratio		
Axial Stain	%	2.03
Deviator Stress	kPa	709.7
Φ '	º	37.1
c' (assumed)	kPa	0

Note: *using cambridge method*

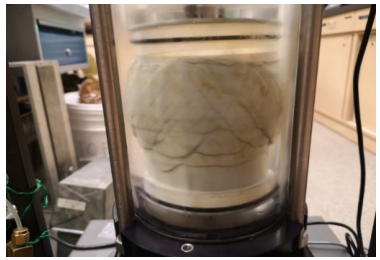
Test Photos:

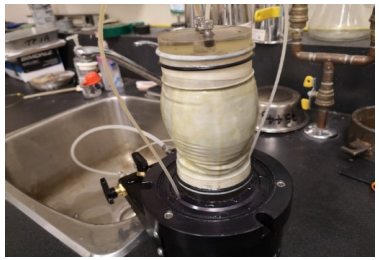
Before Test





After Test

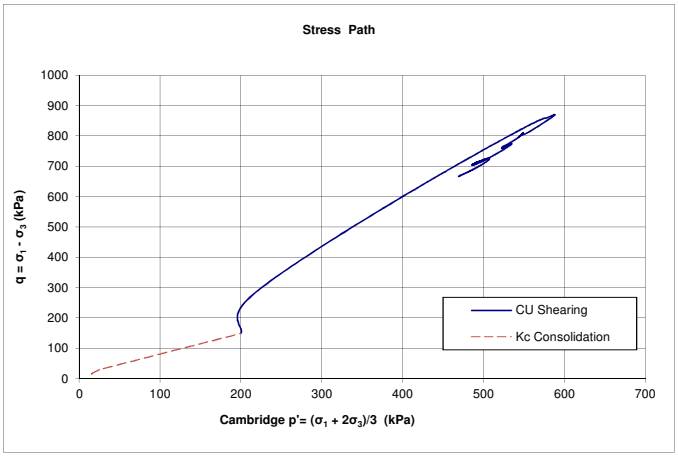


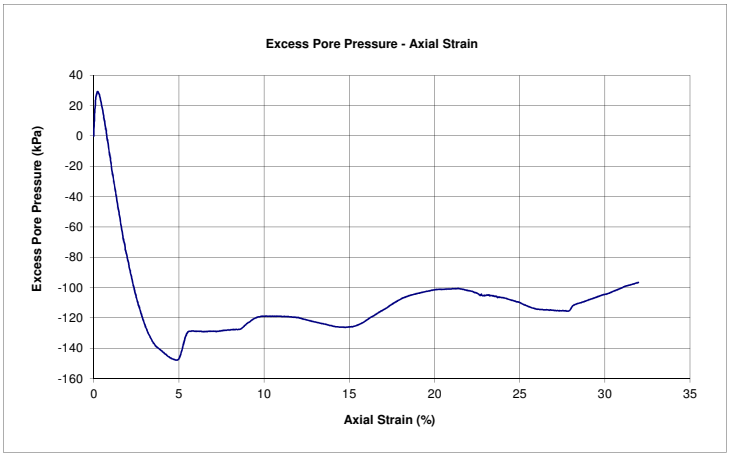


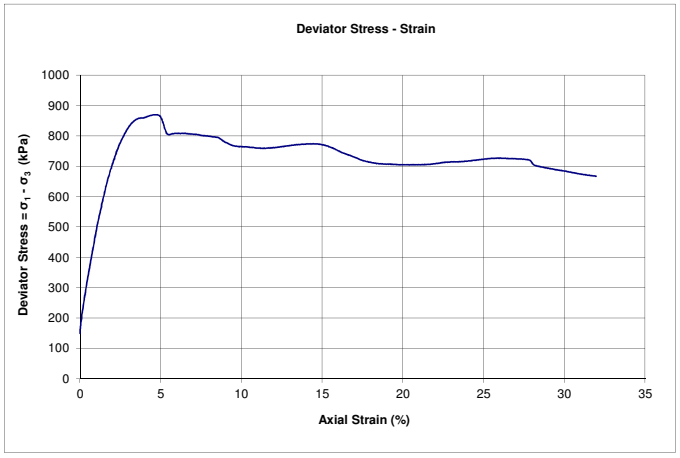
Triaxial CU Test - Charts

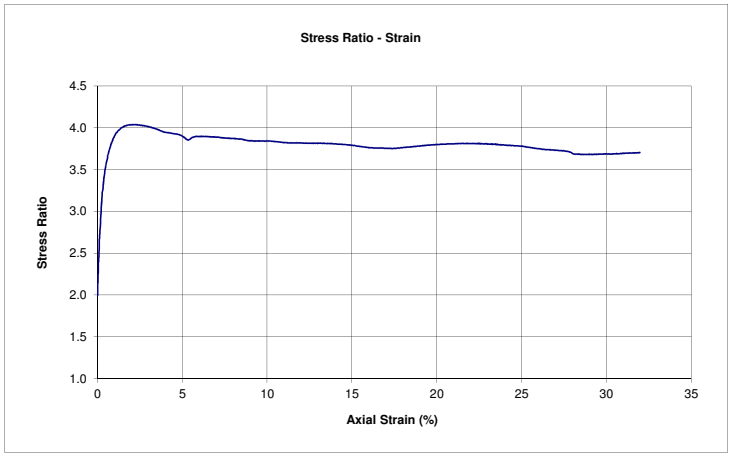
(ASTM D4767)

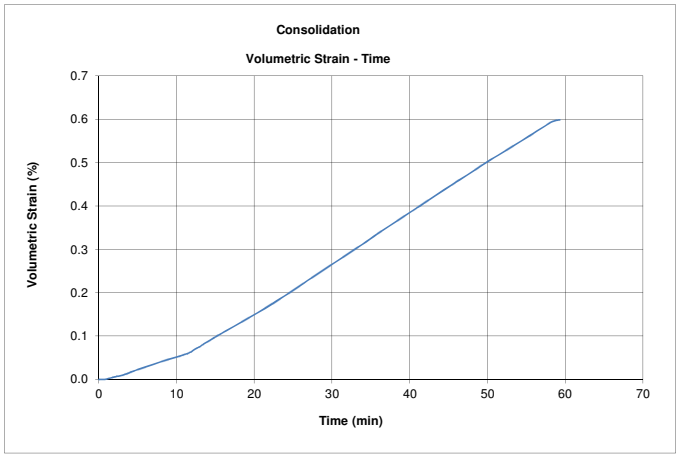
PROJECT NO. :	A03355A01	DATE :	2019-11-06
PROJECT :		TEST BY:	BY
SAMPLE :	Fine Gradation	CHECKED BY:	JG
Details:	Anisotropic consolidation, Kc = 0.5, p' = 200 kPa, strain control		

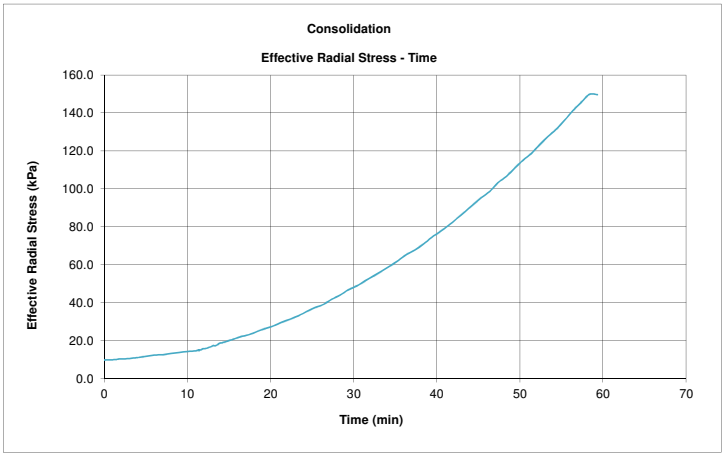












Triaxial CAU Test - Summary

(ASTM D4767)

PROJECT NO. : A03355A01 DATE : 2019-11-07

PROJECT : TESTED BY: BY

SAMPLE : Average Gradation CHECKED BY: JG

Details: Anisotropic consolidation, Kc = 0.5, p' = 200 kPa, strain control

SPECIMEN INFORMATION	UNITS	Initial	Vacuum	Saturation	B-value	End of Anisotropic Consolidation*	At Maximum Deviator Stress	End of Shear		
Specimen Height	mm	140.06	140.74	140.74	140.32	139.72	132.94	96.27		
Specimen Diameter	mm	69.90	69.72	69.64	69.70	69.60	71.35	83.85		
Area	cm^2	38.37	38.18	38.09	38.16	38.05	39.99	55.22		
Volume	cm^3	537.48	537.31	536.13	535.43	531.59	531.59	531.59		
Wet Weight	g	1533.01	1533.01	1679.61	1689.12	1685.29	1685.28	1685.28		
Water Content	%	6.15	6.15	16.30	16.96	16.69	16.69	16.69		
Dry Weight	g	1444.19	1444.19	1444.19	1444.19	1444.19	1444.19	1444.19		
Wet Density	g/cm^3	2.852	2.853	3.133	3.155	3.170	3.170	3.170		
Dry Density	g/cm^3	2.687	2.688	2.694	2.697	2.717	2.717	2.717		
Specific Gravity of Solids	-	4.97	4.97	4.97	4.97	4.97	4.97	4.97		
Solids Volume	cm^3	290.582	290.582	290.582	290.582	290.582	290.582	290.582		
Void Volume	cm^3	246.893	246.725	245.545	244.845	241.012	241.006	241.006		
Water Volume	cm^3	88.818	88.818	235.418	244.930	241.097	241.091	241.091		
Void Ratio (e)	-	0.850	0.849	0.845	0.843	0.829	0.829	0.829		
Saturation Ratio (Sr)	%	35.97	36.00	95.88	100.03	100.04	100.04	100.04		
Effective Confining Stress (σ_3')	kPa					150				

** Anisotropic consolidation at 0.01%/min strain rate*

Shearing (CAU)		
Skempton's B Parameter		0.99
Back Pressure before shearing	kPa	600.0
Confining Stress (σ_3') before shearing	kPa	150
Shear Strain Rate	mm / min	0.04

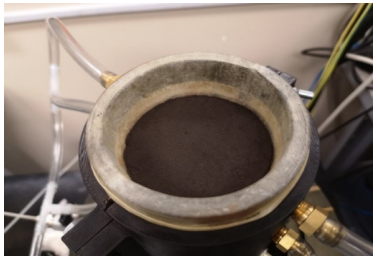
At Maximum Deviator Stress:		
Axial Stain	%	4.86
Deviator Stress	kPa	692.0
Φ '	º	37.0
c' (assumed)	kPa	0

At Maximum Stress Ratio		
Axial Stain	%	1.98
Deviator Stress	kPa	623.8
Φ '	º	37.8
c' (assumed)	kPa	0

Note: *using cambridge method*

Test Photos:

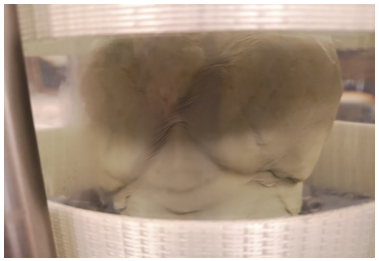
Before Test





After Test

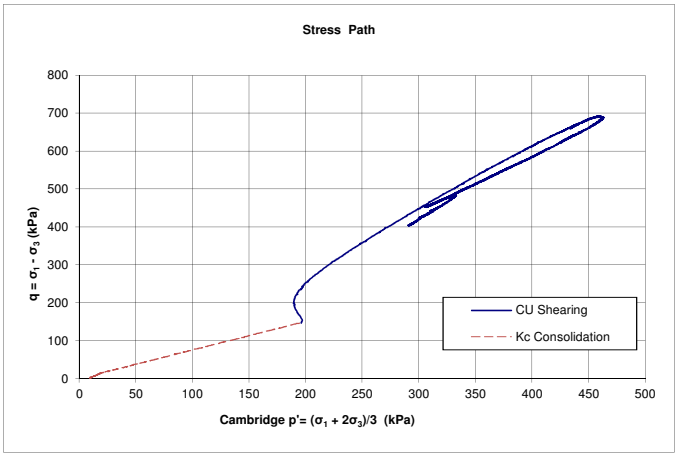


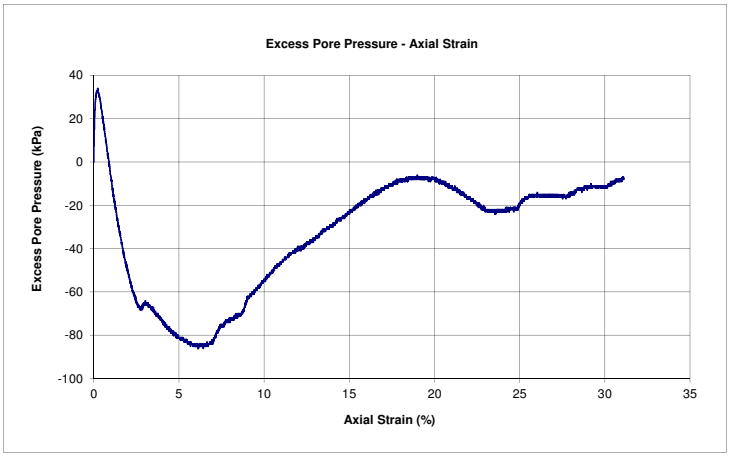


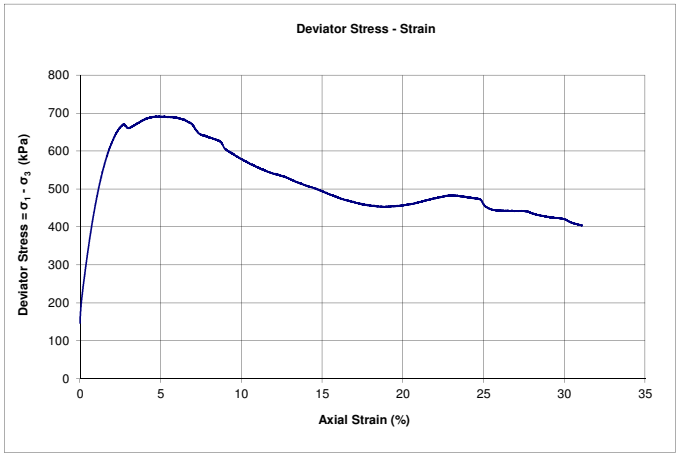
Triaxial CU Test - Charts

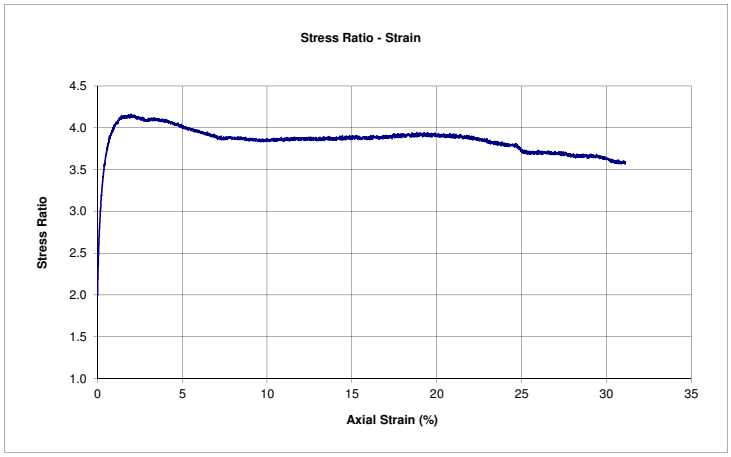
(ASTM D4767)

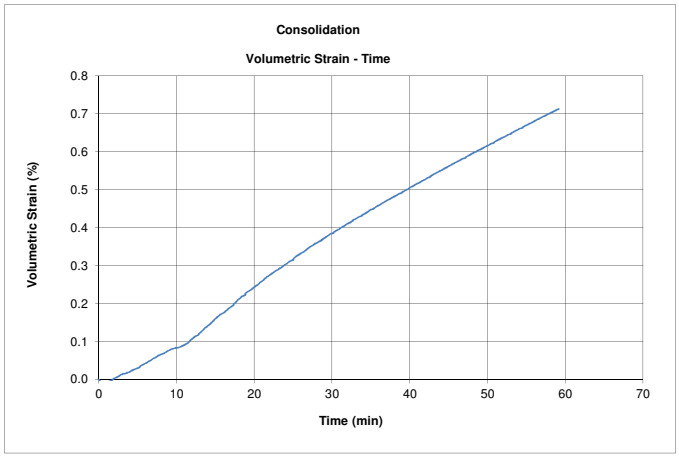
PROJECT NO. :	A03355A01	DATE :	2019-11-07
PROJECT :		TEST BY:	BY
SAMPLE :	Average Gradation	CHECKED BY:	JG
Details:	Anisotropic consolidation, Kc = 0.5, p' = 200 kPa, strain control		

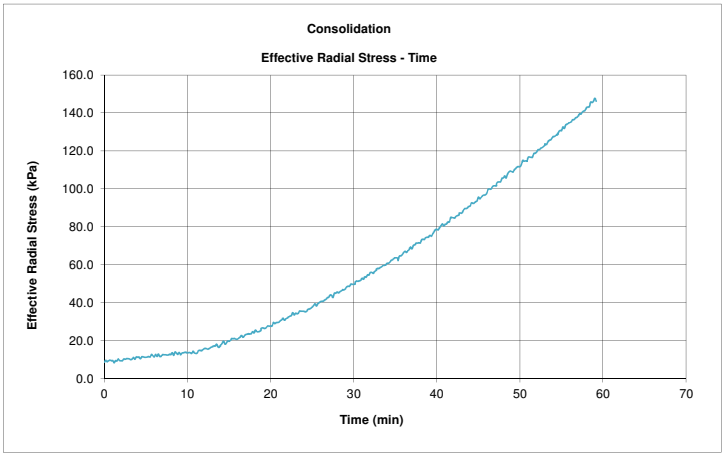












Triaxial CAU Test - Summary

(ASTM D4767)

PROJECT NO. : A03355A01 DATE : 2019-11-07

PROJECT : TESTED BY: AX/BY

SAMPLE : Average Gradation CHECKED BY: JG

Details: Anisotropic consolidation, Kc = 0.5, p' = 200 kPa, strain control

SPECIMEN INFORMATION	UNITS	Initial	Vacuum	Saturation	B-value	End of Anisotropic Consolidation*	At Maximum Deviator Stress	End of Shear		
Specimen Height	mm	141.94	141.94	141.94	141.93	141.37	135.08	97.08		
Specimen Diameter	mm	69.90	69.87	69.68	69.68	69.52	71.12	83.89		
Area	cm^2	38.37	38.34	38.13	38.13	37.96	39.72	55.27		
Volume	cm^3	544.69	544.22	541.22	541.22	536.57	536.57	536.57		
Wet Weight	g	1615.21	1615.21	1753.21	1762.00	1757.35	1757.35	1757.35		
Water Content	%	5.70	5.70	14.73	15.31	15.00	15.00	15.00		
Dry Weight	g	1528.11	1528.11	1528.11	1528.11	1528.11	1528.11	1528.11		
Wet Density	g/cm^3	2.965	2.968	3.239	3.256	3.275	3.275	3.275		
Dry Density	g/cm^3	2.805	2.808	2.823	2.823	2.848	2.848	2.848		
Specific Gravity of Solids	-	4.97	4.97	4.97	4.97	4.97	4.97	4.97		
Solids Volume	cm^3	307.466	307.466	307.466	307.466	307.466	307.466	307.466		
Void Volume	cm^3	237.223	236.756	233.756	233.756	229.108	229.108	229.108		
Water Volume	cm^3	87.102	87.102	225.102	233.891	229.243	229.243	229.243		
Void Ratio (e)	-	0.772	0.770	0.760	0.760	0.745	0.745	0.745		
Saturation Ratio (Sr)	%	36.72	36.79	96.30	100.06	100.06	100.06	100.06		
Effective Confining Stress (σ_3')	kPa					150				

** Anisotropic consolidation at 0.01%/min strain rate*

Shearing (CAU)		
Skempton's B Parameter		0.99
Back Pressure before shearing	kPa	598.0
Confining Stress (σ_3') before shearing	kPa	150
Shear Strain Rate	mm / min	0.04

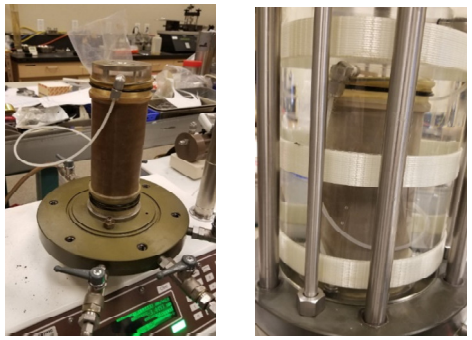
At Maximum Deviator Stress:		
Axial Stain	%	4.45
Deviator Stress	kPa	2224.6
Φ '	º	38.3
c' (assumed)	kPa	0

At Maximum Stress Ratio		
Axial Stain	%	1.74
Deviator Stress	kPa	1316.8
Φ '	º	37.3
c' (assumed)	kPa	0

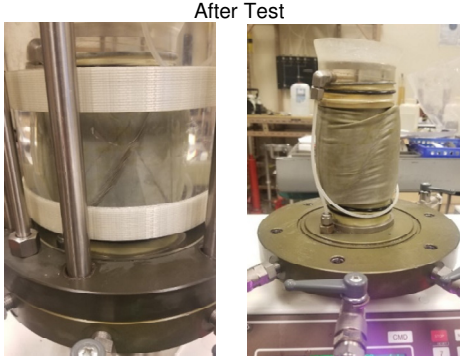
Note: *using cambridge method*

Test Photos:

Before Test



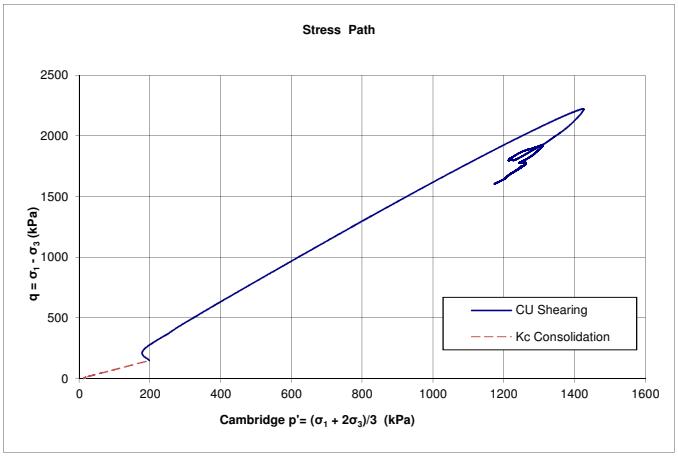
After Test

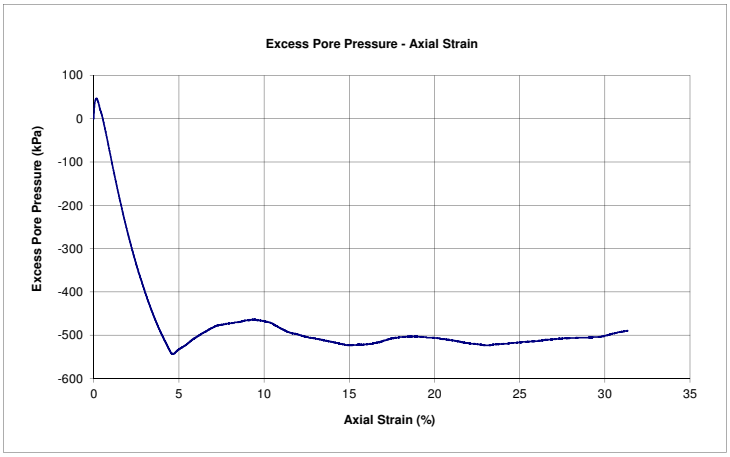


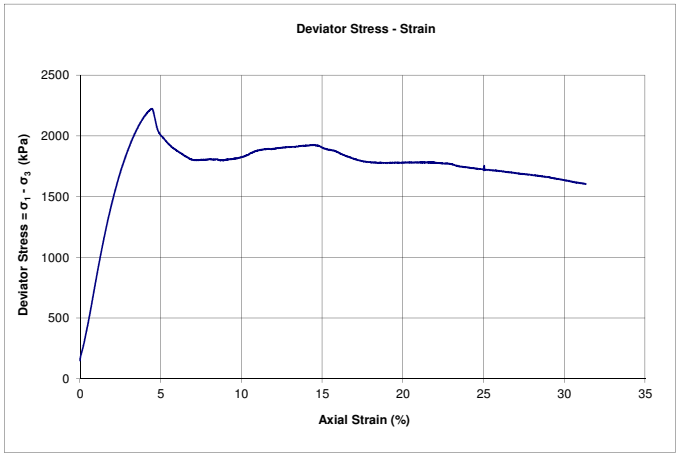
Triaxial CU Test - Charts

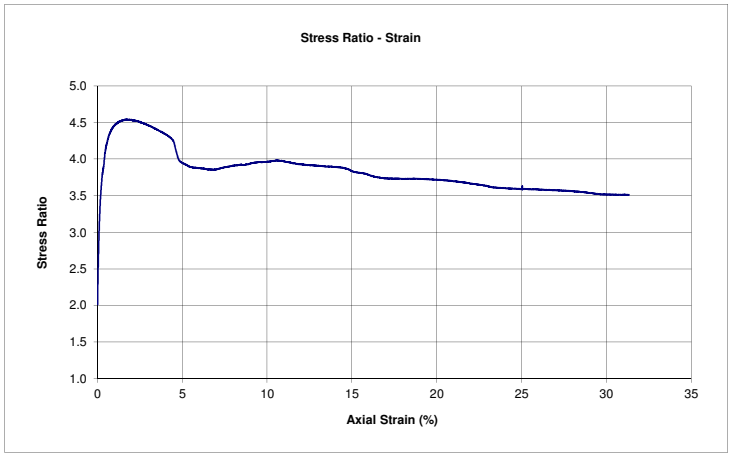
(ASTM D4767)

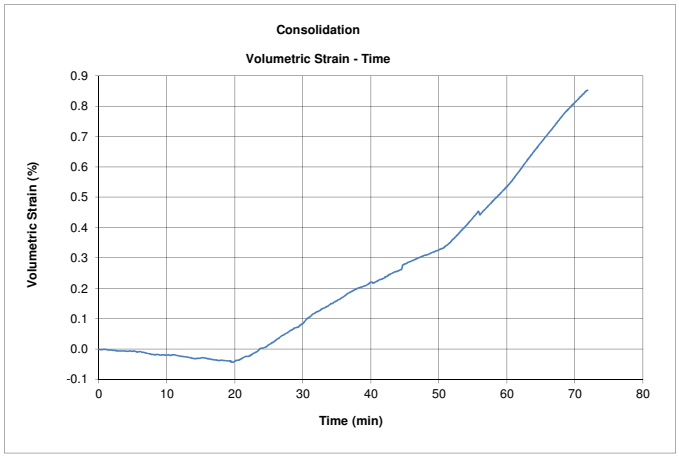
PROJECT NO. :	A03355A01	DATE :	2019-11-07
PROJECT :		TEST BY:	AX/BY
SAMPLE :	Average Gradation	CHECKED BY:	JG
Details:	Anisotropic consolidation, Kc = 0.5, p' = 200 kPa, strain control		

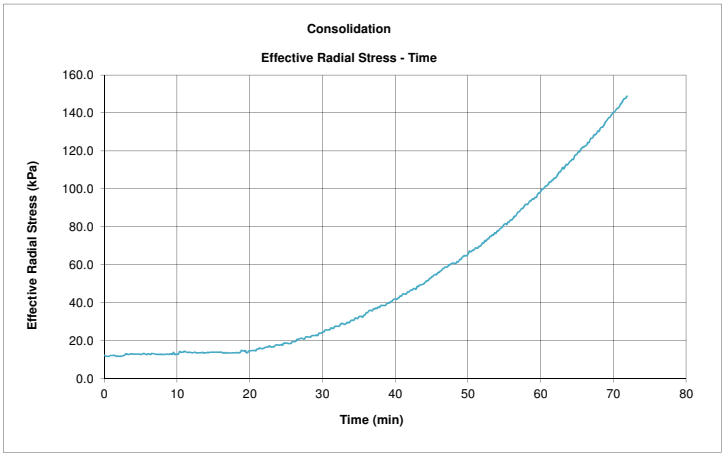












Triaxial CAU Test - Summary

(ASTM D4767)

PROJECT NO. : A03355A01 DATE : 2019-11-08

PROJECT : TESTED BY: AX / BY

SAMPLE : Average Gradation CHECKED BY: JG

Details: Anisotropic consolidation, Kc = 0.5, p' = 200 kPa, strain control

SPECIMEN INFORMATION	UNITS	Initial	Vacuum	Saturation	B-value	End of Anisotropic Consolidation*	At Maximum Deviator Stress	End of Shear		
Specimen Height	mm	141.13	141.13	141.13	141.10	140.33	130.38	96.86		
Specimen Diameter	mm	69.99	69.99	69.86	69.77	69.73	72.34	83.93		
Area	cm^2	38.47	38.47	38.33	38.23	38.19	41.10	55.33		
Volume	cm^3	542.98	542.98	540.97	539.37	535.90	535.90	535.90		
Wet Weight	g	1565.99	1565.99	1723.49	1726.72	1723.25	1723.25	1723.25		
Water Content	%	5.36	5.36	15.96	16.17	15.94	15.94	15.94		
Dry Weight	g	1486.32	1486.32	1486.32	1486.32	1486.32	1486.32	1486.32		
Wet Density	g/cm^3	2.884	2.884	3.186	3.201	3.216	3.216	3.216		
Dry Density	g/cm^3	2.737	2.737	2.747	2.756	2.773	2.773	2.773		
Specific Gravity of Solids	-	4.97	4.97	4.97	4.97	4.97	4.97	4.97		
Solids Volume	cm^3	299.059	299.059	299.059	299.059	299.059	299.059	299.059		
Void Volume	cm^3	243.918	243.918	241.916	240.316	236.846	236.846	236.846		
Water Volume	cm^3	79.667	79.667	237.167	240.394	236.925	236.925	236.925		
Void Ratio (e)	-	0.816	0.816	0.809	0.804	0.792	0.792	0.792		
Saturation Ratio (Sr)	%	32.66	32.66	98.04	100.03	100.03	100.03	100.03		
Effective Confining Stress (σ_3')	kPa					150				

** Anisotropic consolidation at 0.01%/min strain rate*

Shearing (CAU)		
Skempton's B Parameter		0.98
Back Pressure before shearing	kPa	503.6
Confining Stress (σ_3') before shearing	kPa	150
Shear Strain Rate	% / min	0.03

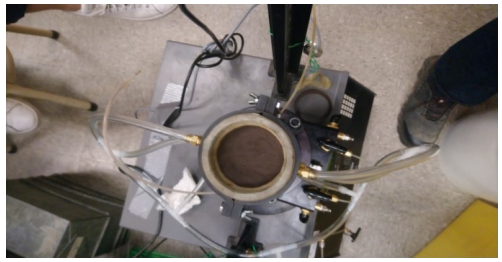
At Maximum Deviator Stress:		
Axial Stain	%	7.09
Deviator Stress	kPa	1125.8
Φ '	º	37.2
c' (assumed)	kPa	0

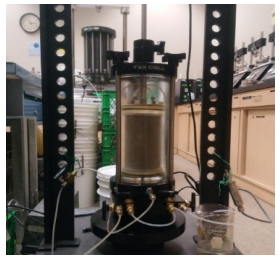
At Maximum Stress Ratio		
Axial Stain	%	1.70
Deviator Stress	kPa	721.5
Φ '	º	38.2
c' (assumed)	kPa	0

Note: *using cambridge method*

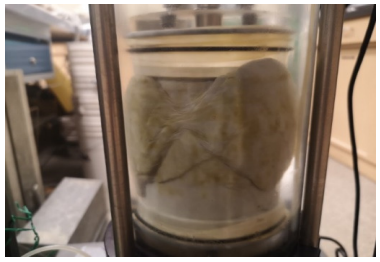
Test Photos:

Before Test





After Test

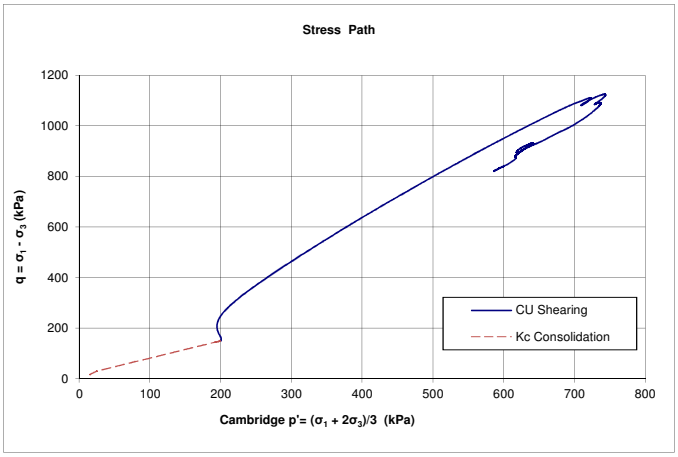


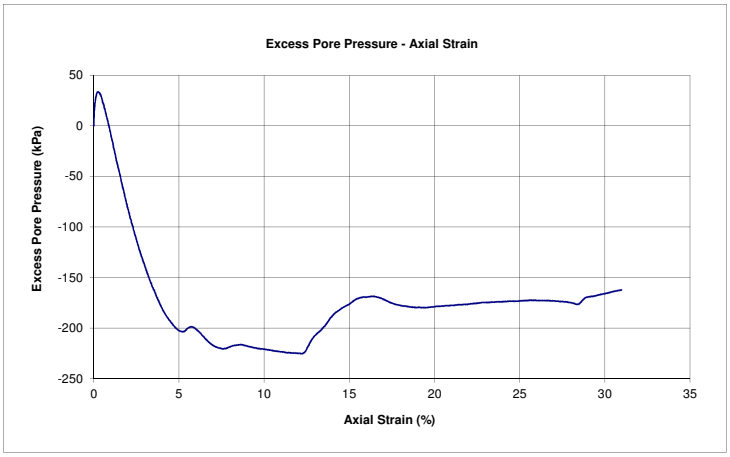


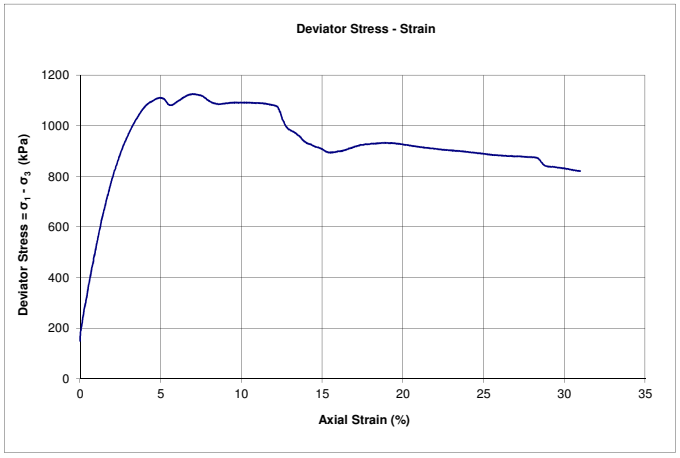
Triaxial CU Test - Charts

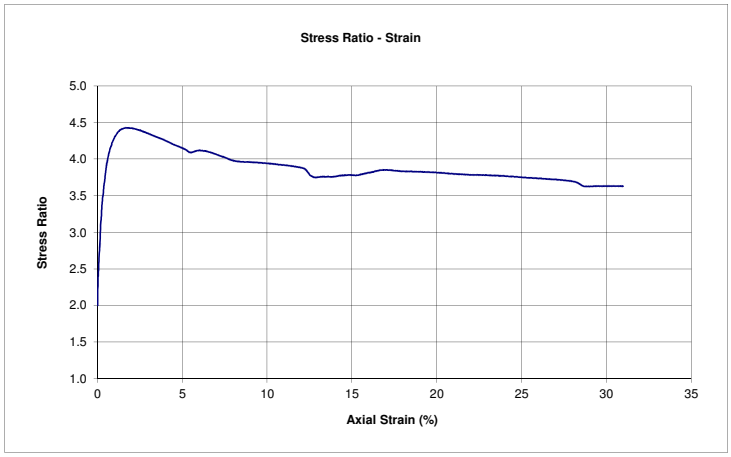
(ASTM D4767)

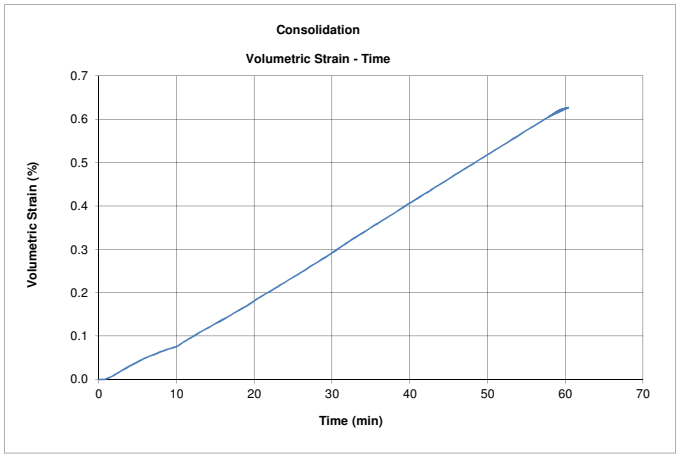
PROJECT NO. :	A03355A01	DATE :	2019-11-08
PROJECT :		TEST BY:	AX / BY
SAMPLE :	Average Gradation	CHECKED BY:	JG
Details:	Anisotropic consolidation, Kc = 0.5, p' = 200 kPa, strain control		

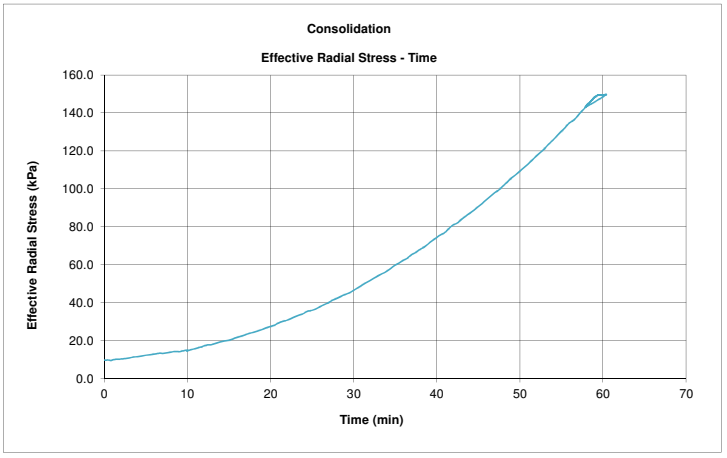












Triaxial CD Test - Summary

(ASTM D7181)

PROJECT NO. : A03355A01
PROJECT :
SAMPLE : Average
TEST NO. : TXDW01 - Anisotropic Consolidation

DATE : 2019-09-16
TESTED BY: AX/JG
CHECKED BY: JG

SPECIMEN INFORMATION	UNITS	Initial	vacuum	flushing	Sat/B value	1AC/End
Specimen Height	mm	140.51	140.82	140.82	140.82	132.01
Specimen Diameter	mm	69.80	69.46	69.44	69.17	70.40
Area	cm^2	38.26	37.89	37.88	37.58	38.93
Volume	cm^3	537.660	533.610	533.360	529.210	513.940
Wet Weight	g	1385.16	1385.16	1567.16	1572.73	1557.46
Water Content	%	4.85	4.85	18.63	19.05	17.89
Dry Weight	g	1321.09	1321.09	1321.09	1321.09	1321.09
Wet Density	g/cm^3	2.576	2.596	2.938	2.972	3.030
Dry Density	g/cm^3	2.457	2.476	2.477	2.496	2.571
Specific Gravity of Solids	-	4.91	4.91	4.91	4.91	4.91
Solids Volume	cm^3	269.061	269.061	269.061	269.061	269.061
Void Volume	cm^3	268.600	264.549	264.299	260.149	244.879
Water Volume	cm^3	64.073	64.073	246.073	251.638	236.368
Void Ratio (e)	-	0.998	0.983	0.982	0.967	0.910
Saturation Ratio (Sr)	%	23.85	24.22	93.10	96.73	96.52
Effective Confining Stress	kPa		Anisotropic Consolidation			p'=86KPa; q=110KPa

Stress Path*		
Skempton's B Parameter		0.98
Back Pressure before shearing	kPa	325.0
Confining Stress (s3') before shearing	kPa	6
Stress Rate	kPa / min	0.03

* one way drainage

Photos:

Before Test





After Test

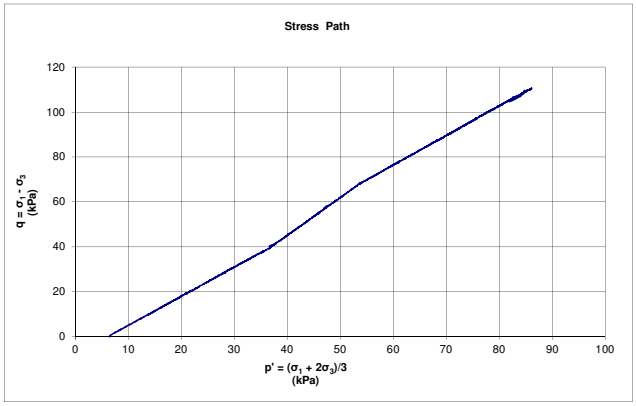


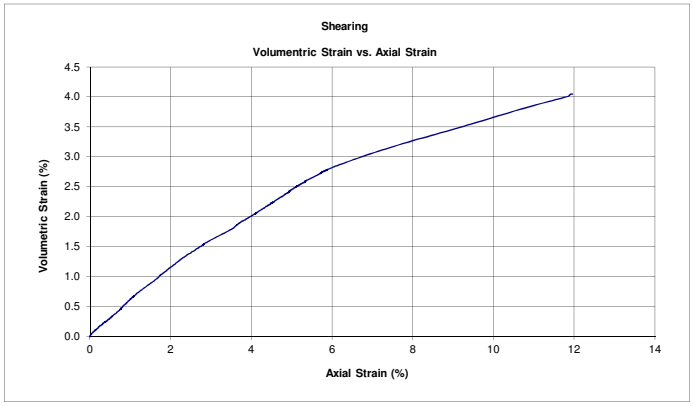
Triaxial CD Test - Charts

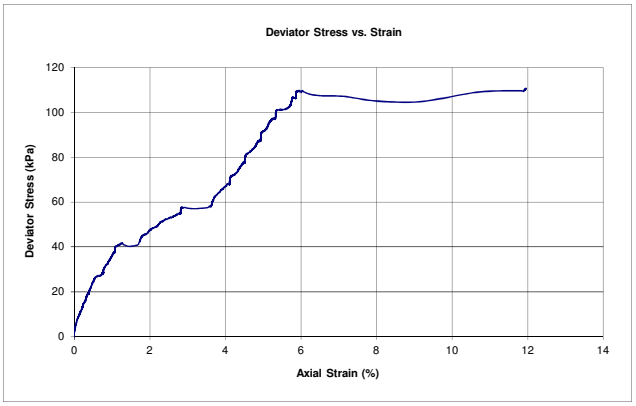
(ASTM D7181)

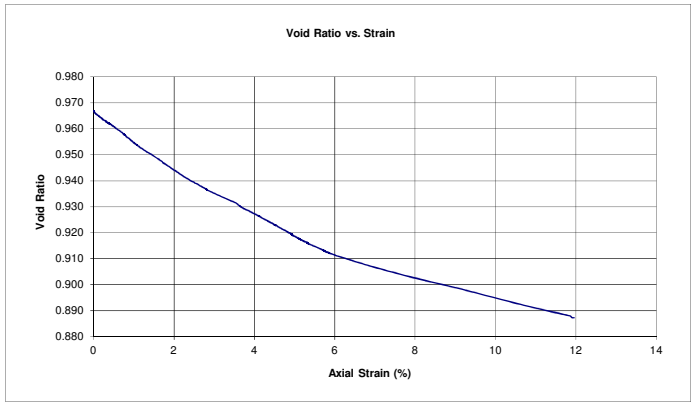
PROJECT NO. : A03355A01
PROJECT :
SAMPLE : Average
TEST NO. : TXDW01 - Anisotropic Consolidation

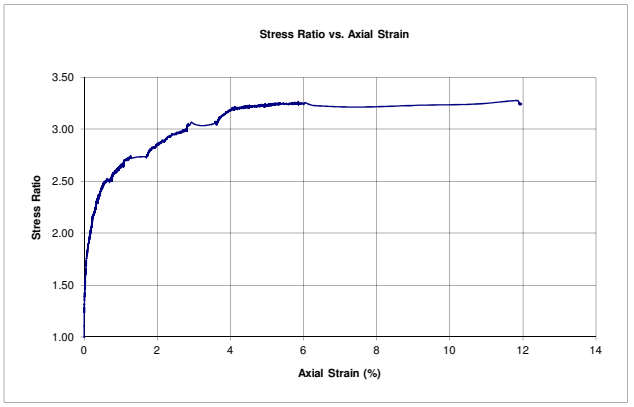
DATE : 2019-09-16
TEST BY: AX/JG
CHECKED BY: JG

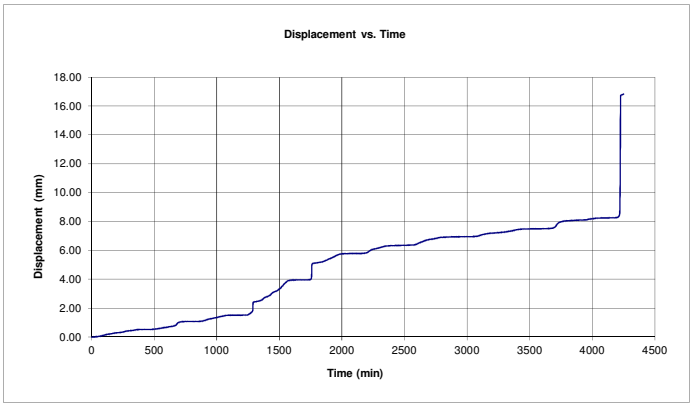












Triaxial CAU Test - Summary

(ASTM D4767)

PROJECT NO. : A03355A01 DATE : 2019-10-02

PROJECT : TESTED BY: BY

SAMPLE : Coarse Gradation CHECKED BY: JG

Details: Anisotropic consolidation, Kc = 0.5, p' = 200 kPa, stress control

SPECIMEN INFORMATION	UNITS	Initial	Vacuum	Saturation	B-value	End of Anisotropic Consolidation*	At Maximum Deviator Stress	End of Shear		
Specimen Height	mm	139.88	139.69	139.69	139.30	137.90	135.87	92.44		
Specimen Diameter	mm	69.80	69.70	69.56	69.56	69.50	70.02	84.88		
Area	cm^2	38.26	38.16	38.00	38.00	37.94	38.51	56.59		
Volume	cm^3	535.25	532.99	530.82	529.32	523.15	523.15	523.15		
Wet Weight	g	1431.48	1431.48	1611.48	1617.05	1610.88	1610.88	1610.88		
Water Content	%	4.80	4.80	17.98	18.39	17.93	17.93	17.93		
Dry Weight	g	1365.92	1365.92	1365.92	1365.92	1365.92	1365.92	1365.92		
Wet Density	g/cm^3	2.674	2.686	3.036	3.055	3.079	3.079	3.079		
Dry Density	g/cm^3	2.552	2.563	2.573	2.581	2.611	2.611	2.611		
Specific Gravity of Solids	-	4.91	4.91	4.91	4.91	4.91	4.91	4.91		
Solids Volume	cm^3	278.191	278.191	278.191	278.191	278.191	278.191	278.191		
Void Volume	cm^3	257.059	254.801	252.627	251.127	244.959	244.959	244.959		
Water Volume	cm^3	65.564	65.564	245.564	251.130	244.962	244.962	244.962		
Void Ratio (e)	-	0.924	0.916	0.908	0.903	0.881	0.881	0.881		
Saturation Ratio (Sr)	%	25.51	25.73	97.20	100.00	100.00	100.00	100.00		
Effective Confining Stress (σ_3')	kPa					150				

** Anisotropic consolidation at 0.01%/min strain rate*

Shearing (CAU)		
Skempton's B Parameter		0.98
Back Pressure before shearing	kPa	723.5
Confining Stress (σ_3') before shearing	kPa	150
Shear Stress Rate	kPa / min	<1

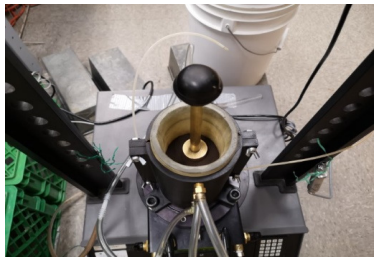
At Maximum Deviator Stress:		
Axial Stain	%	1.17
Deviator Stress	kPa	222.1
Φ '	º	35.4
c' (assumed)	kPa	0

At Maximum Stress Ratio		
Axial Stain	%	1.48
Deviator Stress	kPa	221.6
Φ '	º	36.2
c' (assumed)	kPa	0

Note: *using cambridge method*

Test Photos:

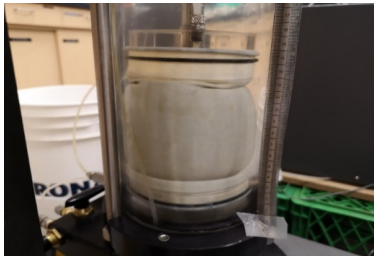
Before Test





After Test

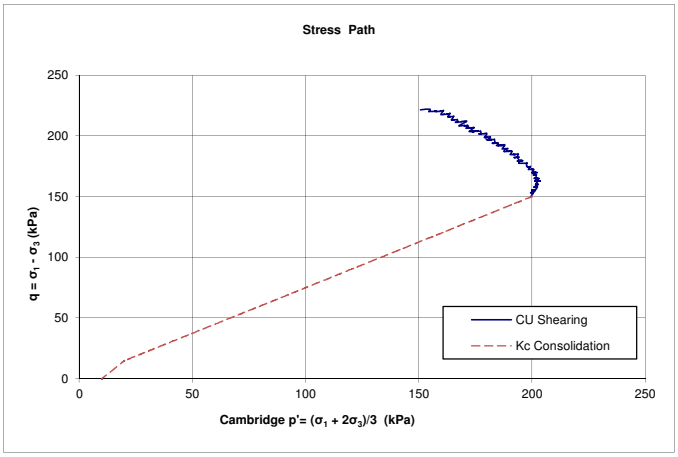


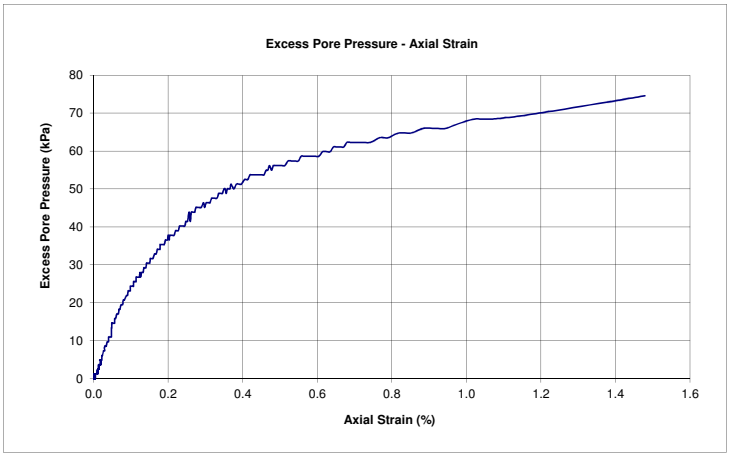


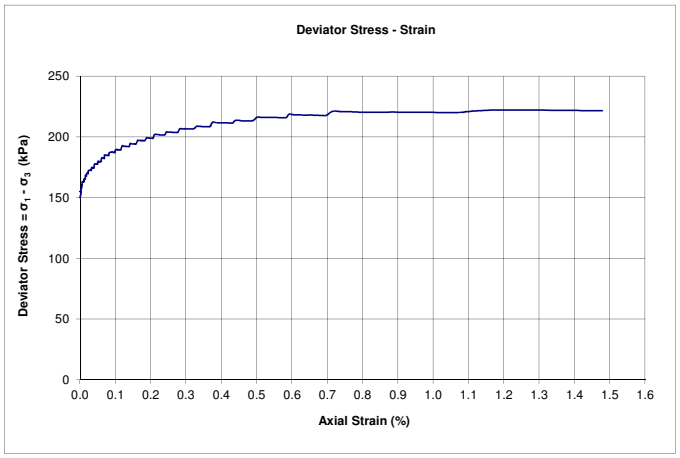
Triaxial CU Test - Charts

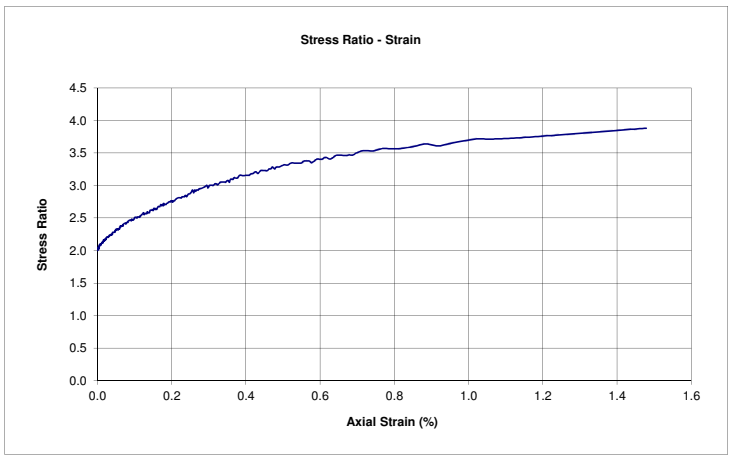
(ASTM D4767)

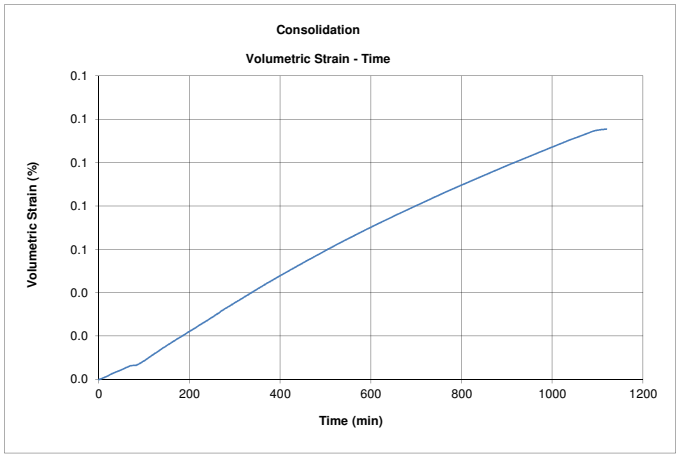
PROJECT NO. :	A03355A01	DATE :	2019-10-02
PROJECT :		TEST BY:	BY
SAMPLE :	Coarse Gradation	CHECKED BY:	JG
Details:	Anisotropic consolidation, Kc = 0.5, p' = 200 kPa, stress control		

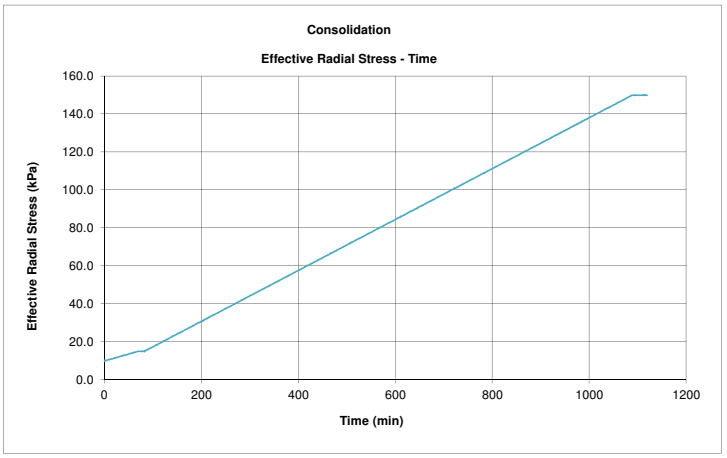












Triaxial CAU - Summary

PROJECT NO. : A03355A01 DATE : 2019-10-14

PROJECT : TESTED BY: AX / BY

SAMPLE : Coarse Gradation CHECKED BY: JG

Details: Anisotropic consolidation, Kc = 0.5, p' = 100 kPa, stress control

						Multi-Stage Anisotropic Consolidation				
SPECIMEN INFORMATION	**UNITS**	**Initial**	**Vacuum**	**Saturation**	**B-value**	**Stress Controled Consolidation***	**Constant Dead Weights Load Drained**	**Dead Weight Loading at Constant p'**	**Constant Dead Weights Load Undrained**	****Dead Weight Loading at Constant p'**
Specimen Height	mm	140.28	140.28	140.28	140.22	138.29	138.15	137.76	137.57	136.56
Specimen Diameter	mm	69.80	69.65	69.32	69.19	69.30	69.39	69.45	69.50	69.65
Area	cm^2	38.26	38.10	37.74	37.60	37.72	37.82	37.88	37.93	38.11
Volume	cm^3	536.63	534.48	529.35	527.29	521.69	522.42	521.86	521.86	520.35
Wet Weight	g	1439.57	1439.57	1609.07	1616.07	1610.47	1611.20	1610.64	1610.64	1609.13
Water Content	%	5.29	5.29	17.69	18.20	17.79	17.84	17.80	17.80	17.69
Dry Weight	g	1367.24	1367.24	1367.24	1367.24	1367.24	1367.24	1367.24	1367.24	1367.24
Wet Density	g/cm^3	2.683	2.693	3.040	3.065	3.087	3.084	3.086	3.086	3.092
Dry Density	g/cm^3	2.548	2.558	2.583	2.593	2.621	2.617	2.620	2.620	2.628
Specific Gravity of Solids	-	4.91	4.91	4.91	4.91	4.91	4.91	4.91	4.91	4.91
Solids Volume	cm^3	278.461	278.461	278.461	278.461	278.461	278.461	278.461	278.461	278.461
Void Volume	cm^3	258.166	256.015	250.891	248.832	243.231	243.958	243.404	243.404	241.894
Water Volume	cm^3	72.327	72.327	241.827	248.827	243.226	243.953	243.399	243.399	241.889
Void Ratio (e)	-	0.927	0.919	0.901	0.894	0.873	0.876	0.874	0.874	0.869
Saturation Ratio (Sr)	%	28.02	28.25	96.39	100.00	100.00	100.00	100.00	100.00	100.00
Effective Confining Stress (σ3')	kPa					75	75	66	66	60
Kc (σ3' / σ1')						1.0 to 0.5	0.5	0.5 to 0.4	0.4	0.33

Skempton's B Parameter		0.98
Back Pressure	kPa	725.0
Stress Rate	kPa / min	~1

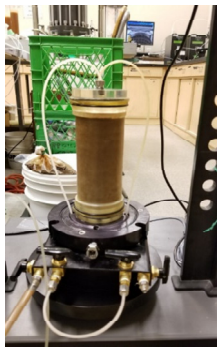
** Sample failed at Kc=0.33

Note: *using cambridge method*

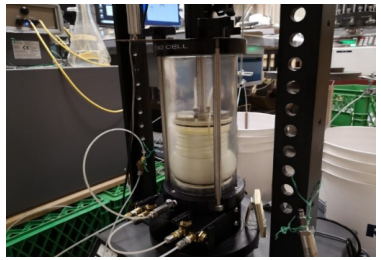
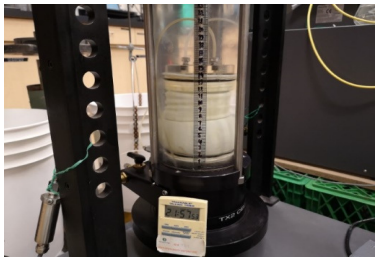
Test Photos:

Before Test



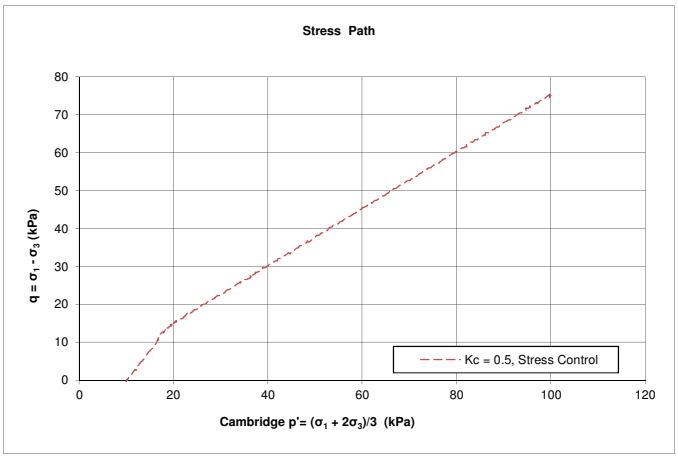


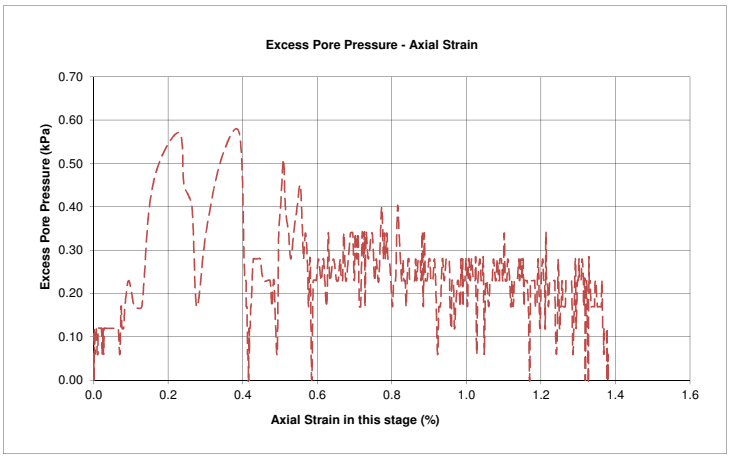
After Test

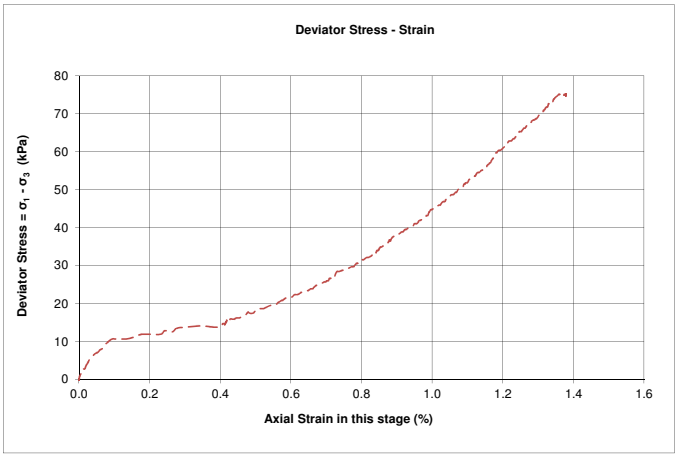



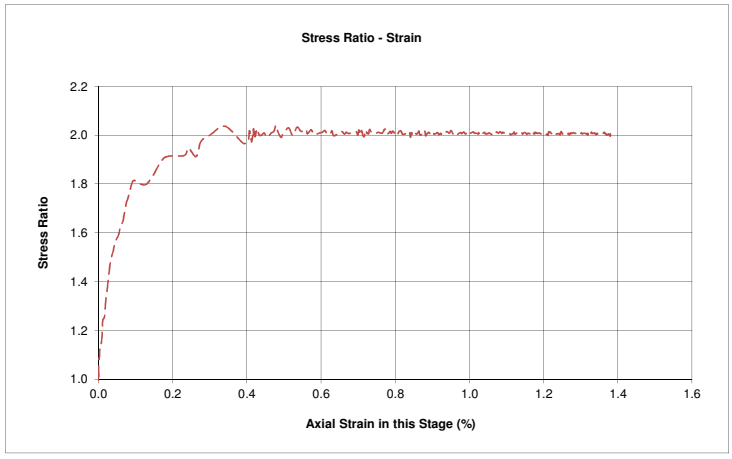
Triaxial CAU Test - Stress Control Anisotropic Consolidation, Kc = 0.5

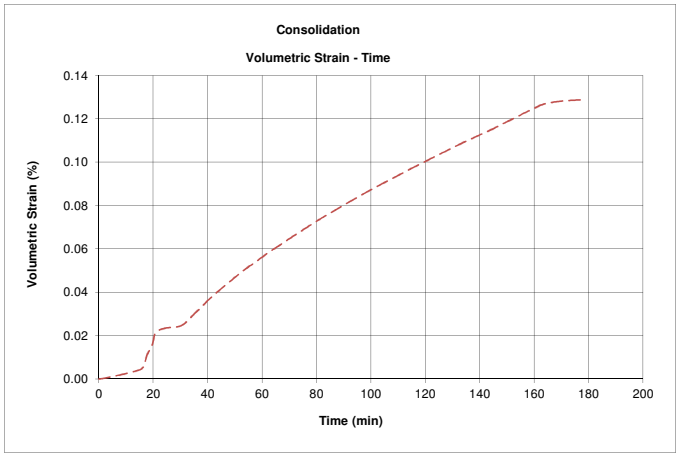
PROJECT NO. :	A03355A01	DATE :	2019-10-14
PROJECT :		TEST BY:	BY
SAMPLE :	Coarse Gradation	CHECKED BY:	JG
Details:	Kc = 0.5, p' = 100 kPa, Stress rate = 1 kPa / min		

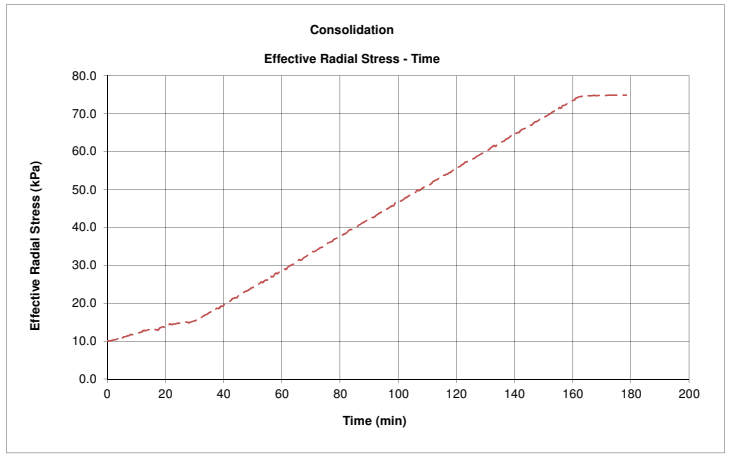






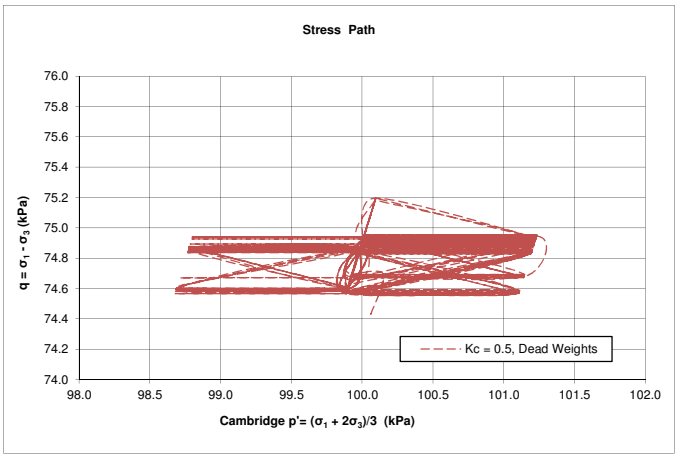


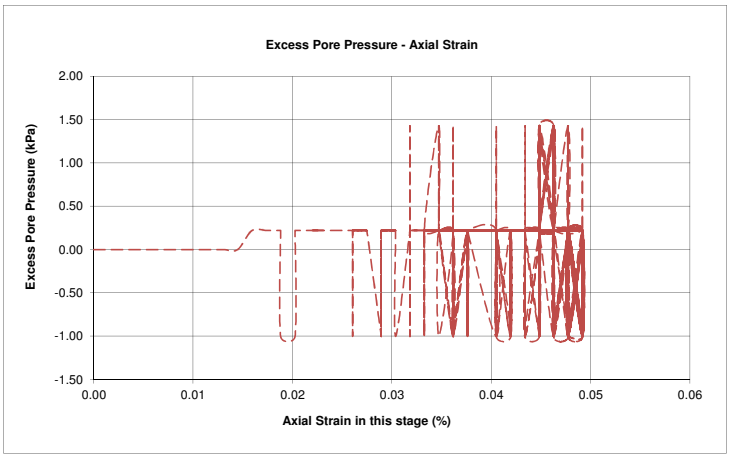


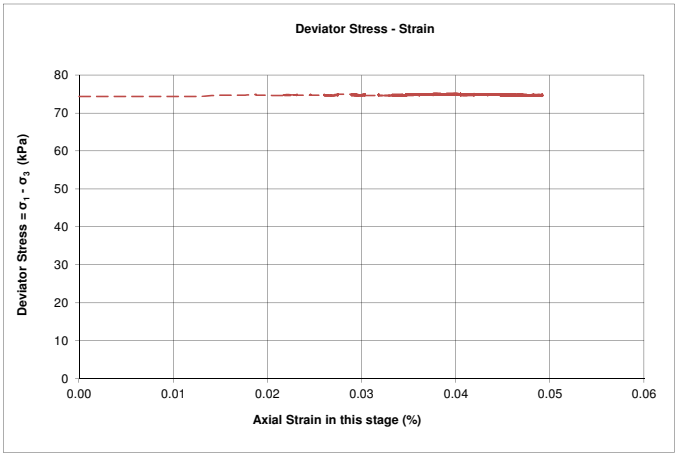


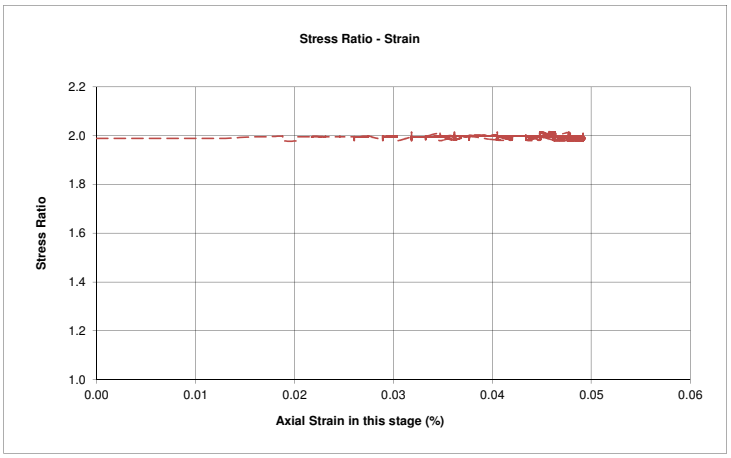
Triaxial Test - Dead Weights Constant Load at Kc = 0.5 (drained)

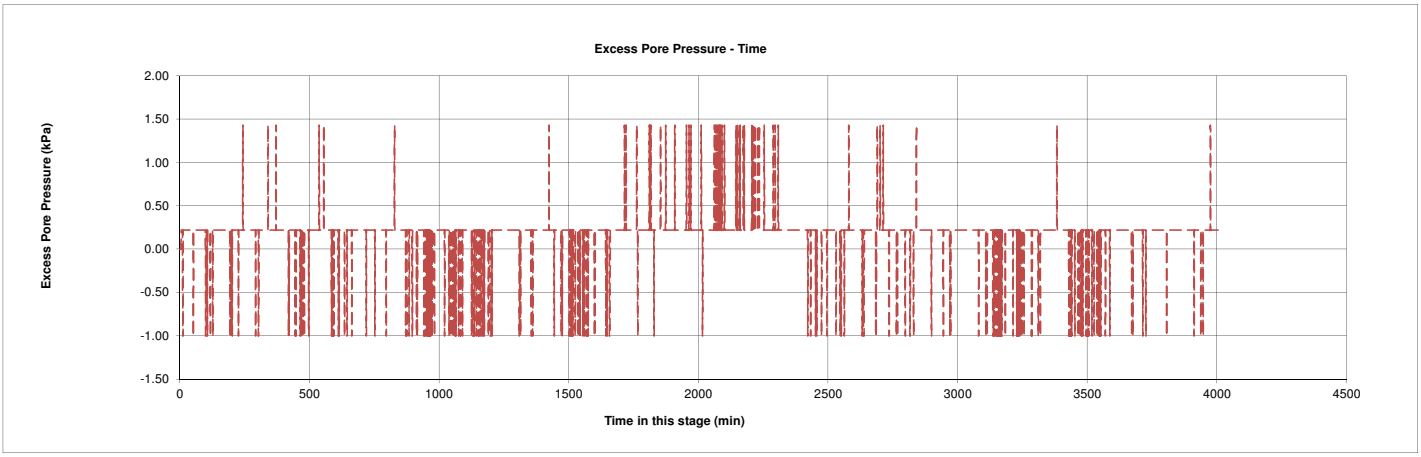
PROJECT NO. :	A03355A01	DATE :	2019-10-14
PROJECT :		TEST BY:	BY
SAMPLE :	Coarse Gradation	CHECKED BY:	JG
Details:	Anisotropic consolidation, Kc = 0.5, p' = 100 kPa, stress control		





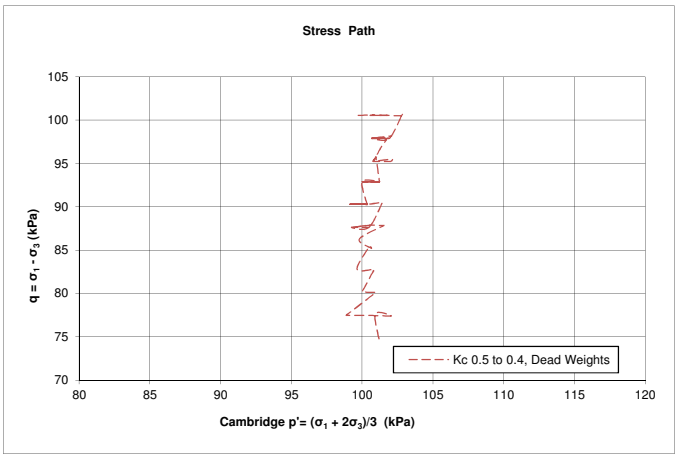


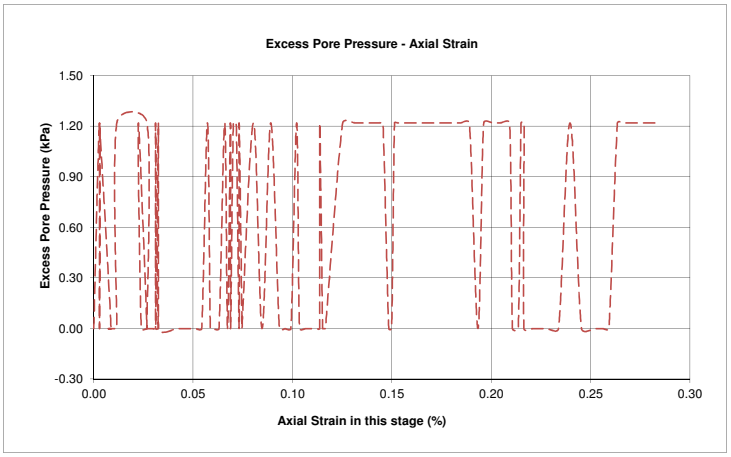


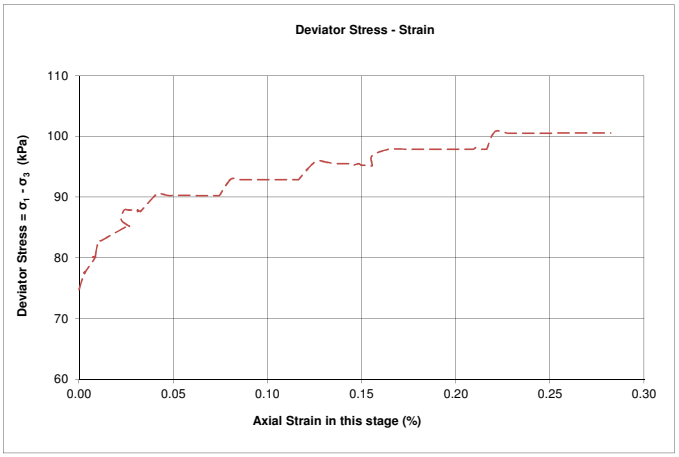


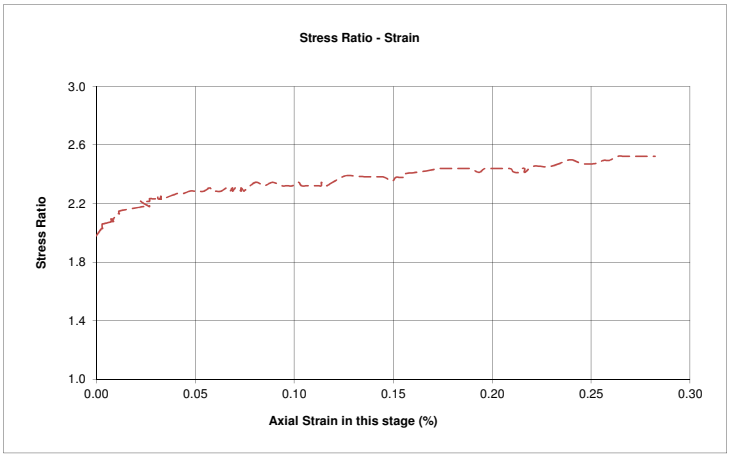
Triaxial CAU Test - Dead Weights Anisotropic Consolidation

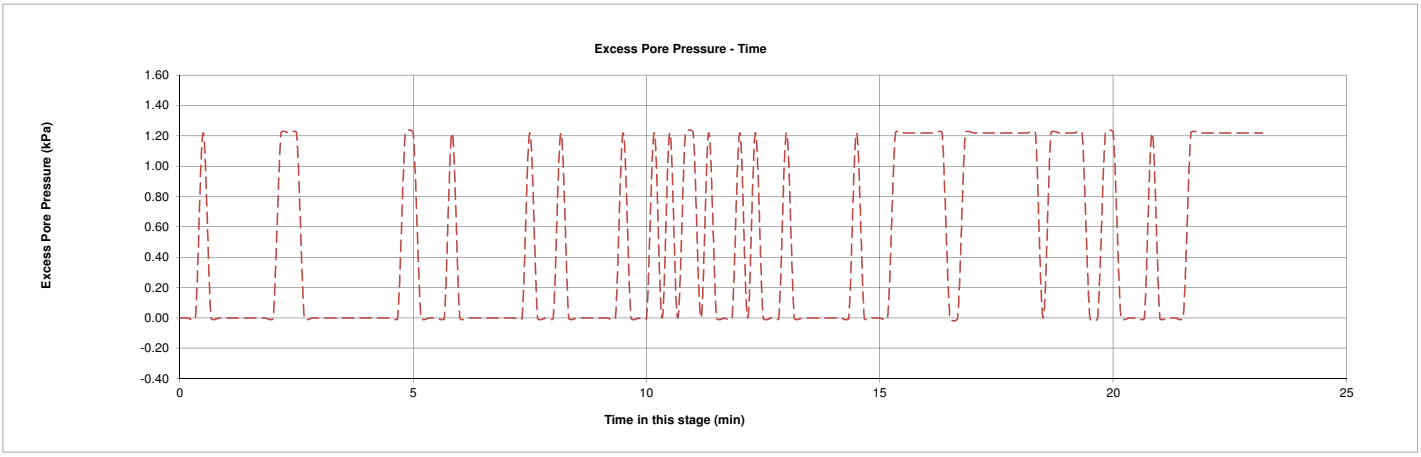
PROJECT NO. :	A03355A01	DATE :	2019-10-14
PROJECT :		TEST BY:	BY
SAMPLE :	Coarse Gradation	CHECKED BY:	JG
Details:	Dead weights loading Kc from 0.5 to 0.4, Constant p' = 100 kPa, Stress rate is around 1 kPa per minute		





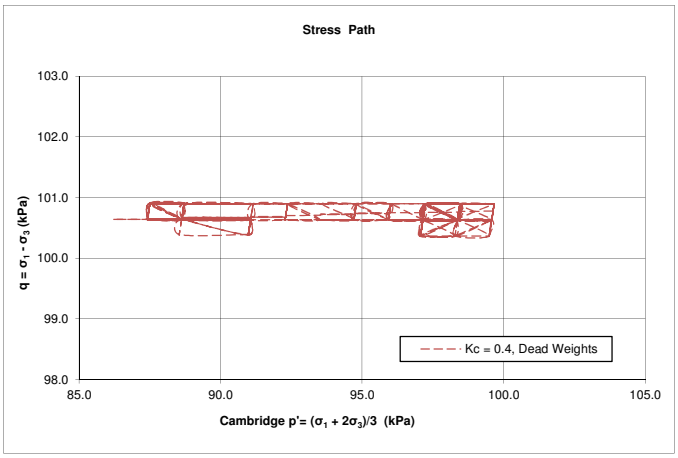


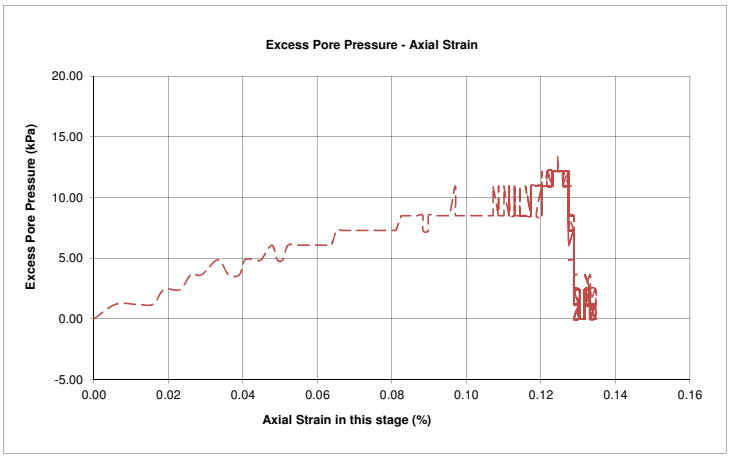


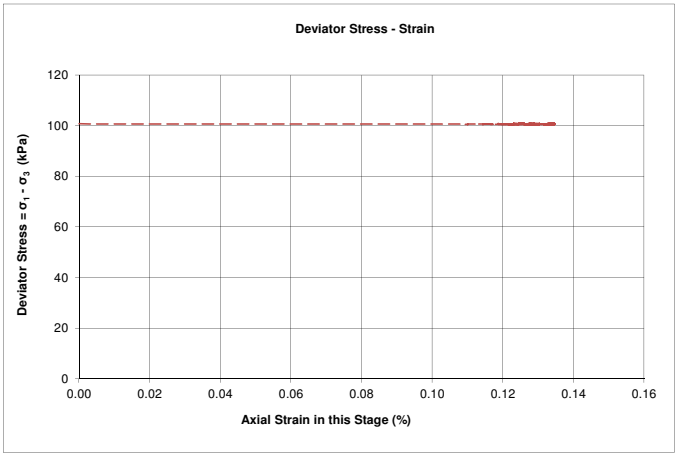


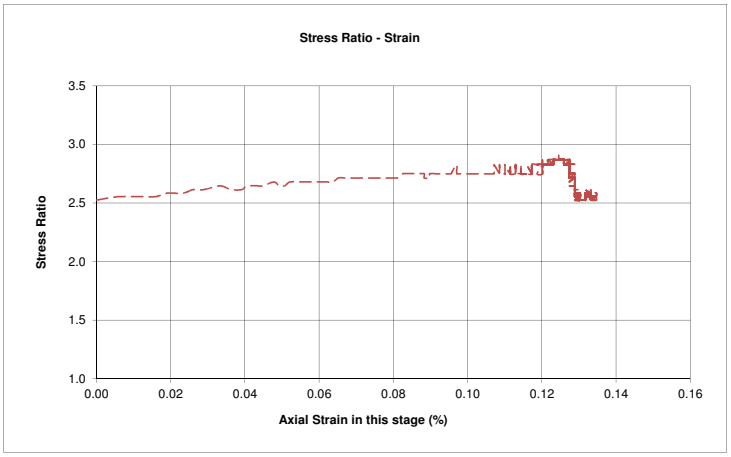
Triaxial Test - Dead Weights Constant Load at Kc = 0.4 (drained)

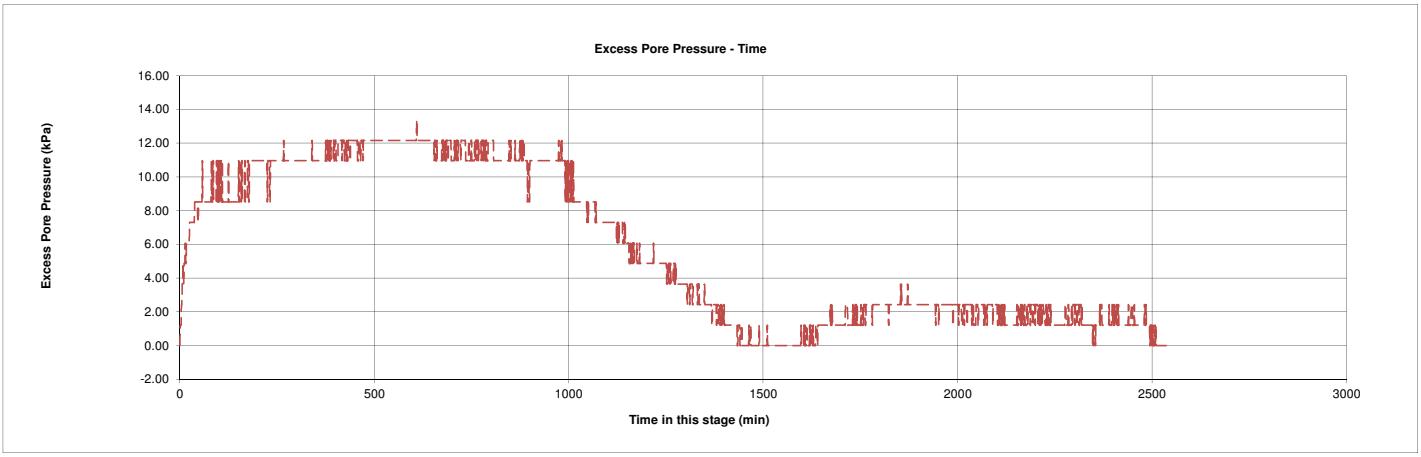
PROJECT NO. :	A03355A01	DATE :	2019-10-14
PROJECT :		TEST BY:	BY
SAMPLE :	Coarse Gradation	CHECKED BY:	JG
Details:	Kc = 0.4, constant dead weight load, undrained		





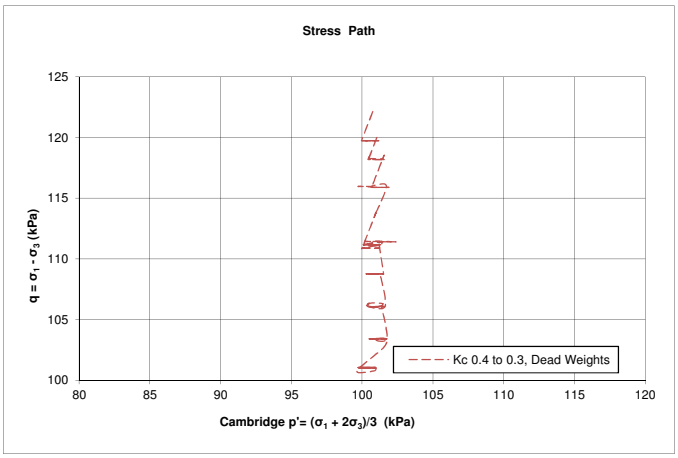


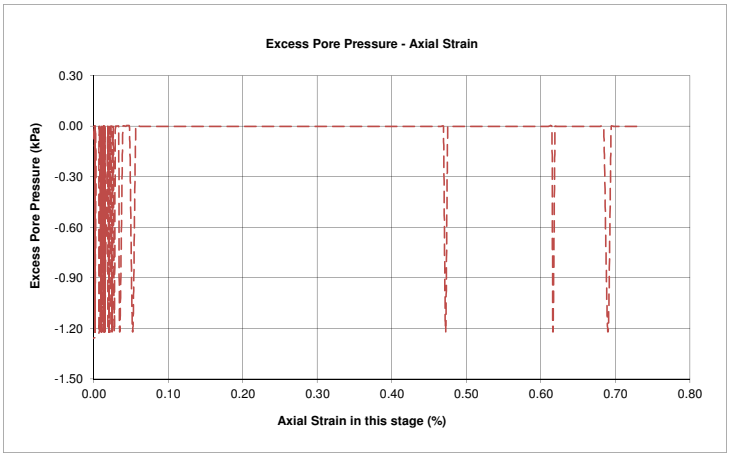


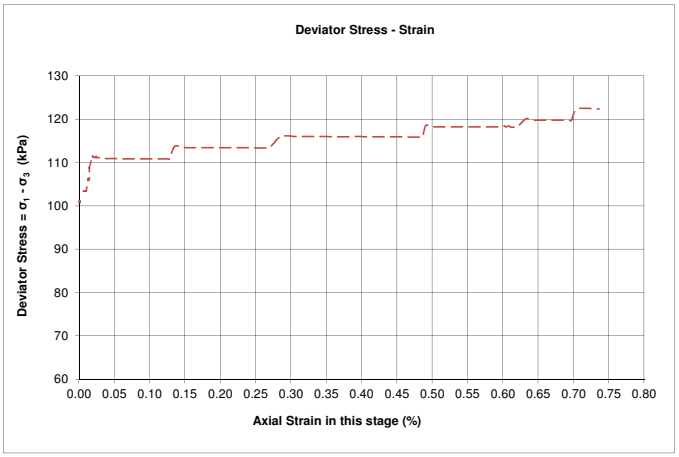


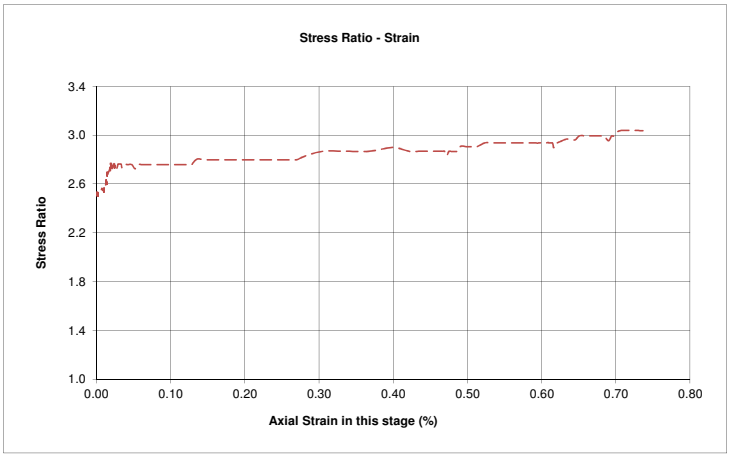
Triaxial CAU Test - Dead Weights Anisotropic Consolidation

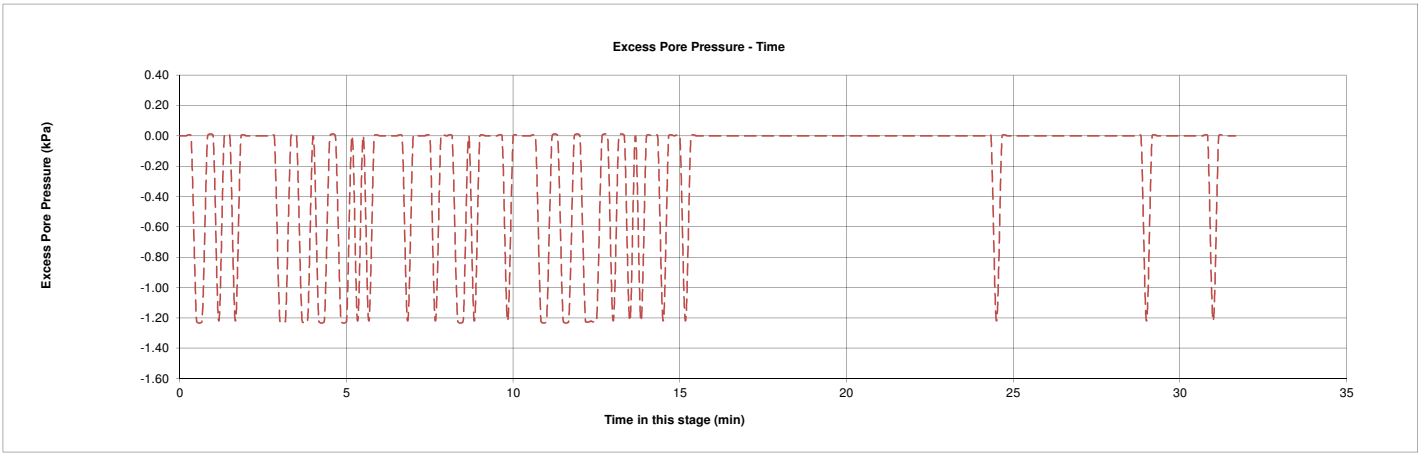
PROJECT NO. :	A03355A01	DATE :	2019-10-14
PROJECT :		TEST BY:	BY
SAMPLE :	Coarse Gradation	CHECKED BY:	JG
Details:	Dead weights loading Kc from 0.4 to 0.3, Constant p' = 100 kPa, Stress rate is around 1 kPa per minute (sample failed at Kc=0.33)		











Individual Bender Element Results

Triaxial Bender Element Test - Summary

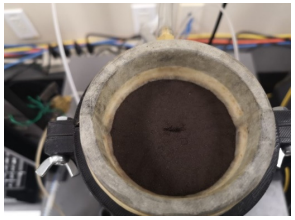
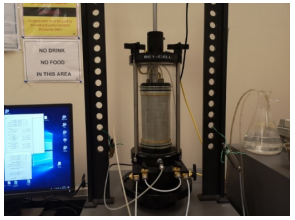
PROJECT NO. A03355A01
PROJECT :
SAMPLE : Average
TEST NO. : TXBD01 e=1.2

DATE : 2019-07-30
TESTED BY: BY
CHECKED BY: JG

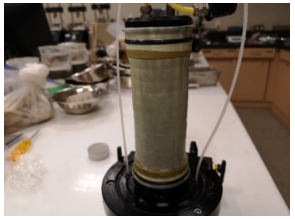
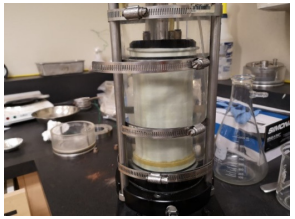
SPECIMEN INFORMATION	UNITS	Initial	Vacuum	Saturation	B value	End 1st Cons	End 2nd Cons	End 3rd Cons	End 4th Cons	End 5th Cons	End 6th Cons	End 7th Cons	End 8th Cons	End 9th Cons
Specimen Height	mm	138.93	138.93	138.93	138.38	137.62	137.18	136.66	135.95	135.47	135.02	134.75	134.45	134.10
Specimen Diameter	mm	69.80	69.65	67.81	67.84	67.37	67.09	66.79	66.48	66.27	66.14	66.02	65.90	65.77
Area	cm^2	38.26	38.10	36.12	36.15	35.64	35.35	35.04	34.71	34.50	34.36	34.23	34.11	33.97
Volume	cm^3	531.614	529.332	501.752	500.252	490.503	484.992	478.850	471.891	467.305	463.911	461.295	458.635	455.577
Wet Weight	g	1261.01	1261.01	1457.01	1458.57	1448.82	1443.31	1437.17	1430.21	1425.62	1422.23	1419.61	1416.95	1413.89
Water Content	%	5.12	5.12	21.46	21.59	20.78	20.32	19.80	19.22	18.84	18.56	18.34	18.12	17.86
Dry Weight	g	1199.59	1199.59	1199.59	1199.59	1199.59	1199.59	1199.59	1199.59	1199.59	1199.59	1199.59	1199.59	1199.59
Wet Density	g/cm^3	2.372	2.382	2.904	2.916	2.954	2.976	3.001	3.031	3.051	3.066	3.077	3.090	3.104
Dry Density	g/cm^3	2.257	2.266	2.391	2.398	2.446	2.473	2.505	2.542	2.567	2.586	2.600	2.616	2.633
Specific Gravity of Solids	-	4.97	4.97	4.97	4.97	4.97	4.97	4.97	4.97	4.97	4.97	4.97	4.97	4.97
Solids Volume	cm^3	241.366	241.366	241.366	241.366	241.366	241.366	241.366	241.366	241.366	241.366	241.366	241.366	241.366
Void Volume	cm^3	290.248	287.966	260.386	258.886	249.136	243.625	237.484	230.525	225.939	222.545	219.929	217.268	214.211
Water Volume	cm^3	61.419	61.419	257.419	258.978	249.229	243.718	237.576	230.617	226.032	222.637	220.021	217.361	214.303
Void Ratio (e)	-	1.203	1.193	1.079	1.073	1.032	1.009	0.984	0.955	0.936	0.922	0.911	0.900	0.887
Saturation Ratio (Sr)	%	21.16	21.33	98.86	100.04	100.04	100.04	100.04	100.04	100.04	100.04	100.04	100.04	100.04
Effective Confining Stress	kPa					50	100	200	400	600	800	1000	1200	1500
Mean Shear Wave Velocity	m/s					**102.76**	**126.58**	**158.23**	**195.73**	**222.38**	**249.96**	**263.02**	**278.49**	**344.99**
Mean Shear Modulus	Mpa					**31.19**	**47.68**	**75.15**	**116.11**	**150.87**	**191.55**	**212.90**	**239.62**	**369.38**

Photos:

Before Test

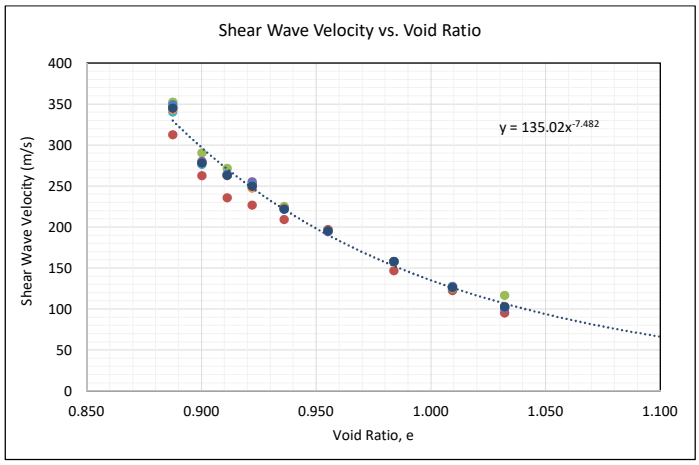
After Test

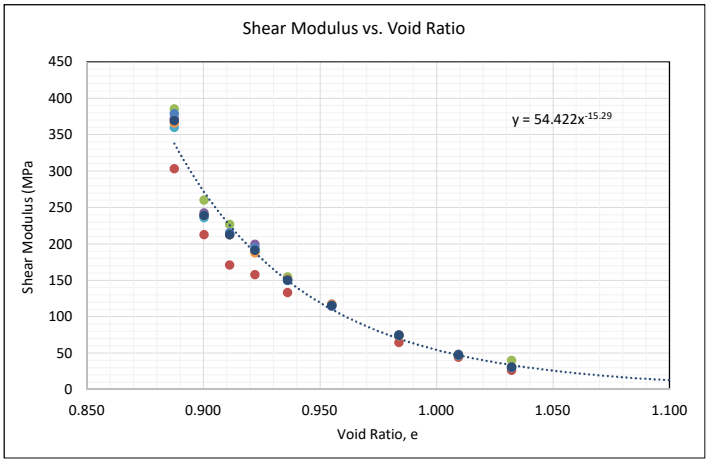



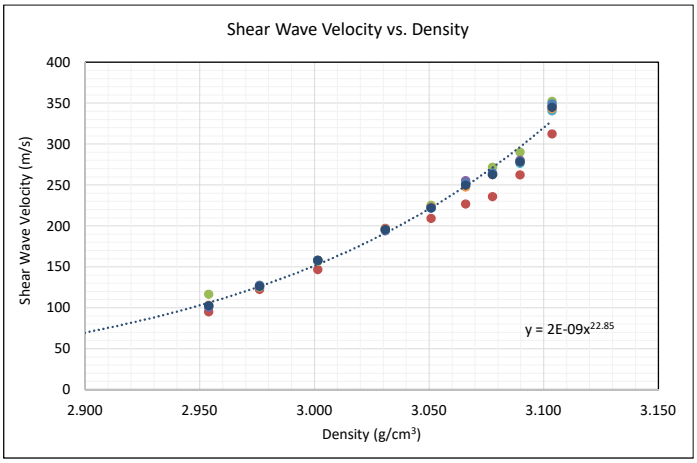
Triaxial Bender Element Test - Charts

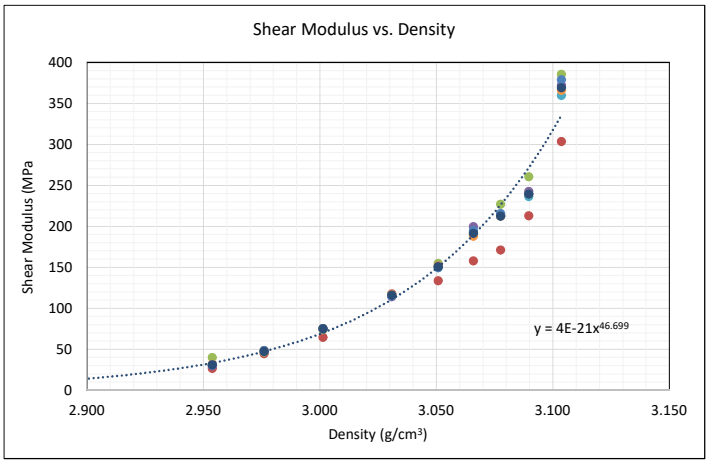
PROJECT NO. : A03355A01
PROJECT :
SAMPLE : Average
TEST NO. : TXBD01 e=1.2

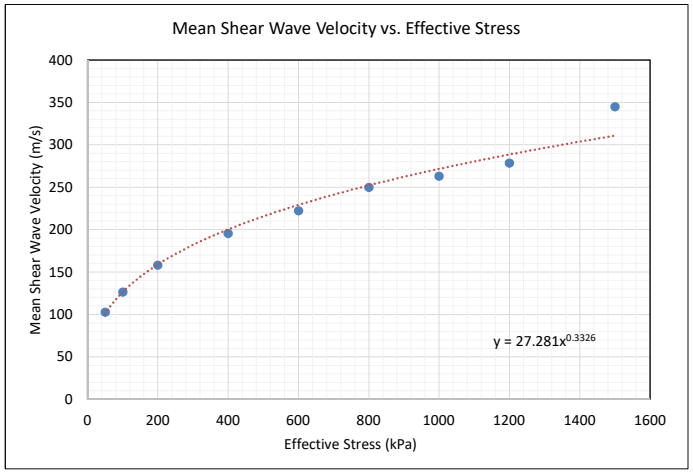
DATE : 2019-07-30
TEST BY: BY
CHECKED BY: JG

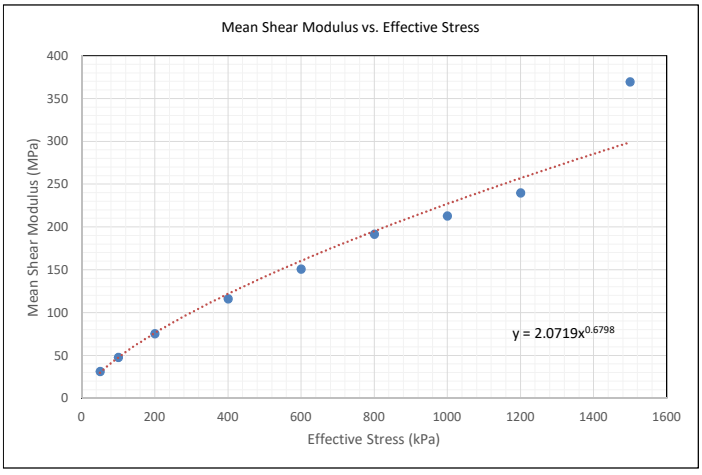












Triaxial Bender Element Test - Summary

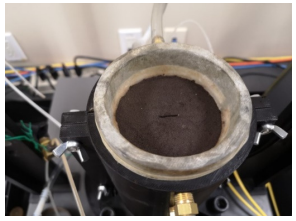
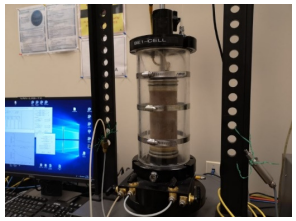
PROJECT NO. A03355A01
PROJECT :
SAMPLE : Average
TEST NO. : TXBD01 e=0.9

DATE : 2019-08-02
TESTED BY: BY
CHECKED BY: JG

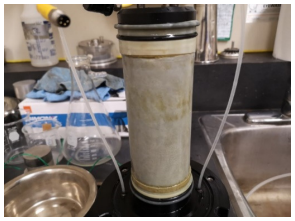
SPECIMEN INFORMATION	UNITS	Initial	Vacuum	Saturation	B value	End 1st Cons	End 2nd Cons	End 3rd Cons	End 4th Cons	End 5th Cons	End 6th Cons	End 7th Cons	End 8th Cons	End 9th Cons
Specimen Height	mm	139.14	138.96	138.96	138.91	138.91	138.85	138.75	138.58	138.45	138.33	138.22	138.13	138.00
Specimen Diameter	mm	69.90	69.90	69.84	69.85	69.78	69.73	69.65	69.54	69.45	69.38	69.32	69.26	69.17
Area	cm^2	38.37	38.37	38.31	38.32	38.24	38.18	38.10	37.98	37.88	37.80	37.74	37.67	37.58
Volume	cm^3	533.945	533.254	532.344	532.344	531.243	530.205	528.624	526.304	524.515	522.939	521.648	520.320	518.621
Wet Weight	g	1515.67	1515.67	1640.80	1647.57	1646.47	1645.43	1643.85	1641.53	1639.74	1638.17	1636.87	1635.55	1633.85
Water Content	%	8.79	8.79	17.77	18.26	18.18	18.10	17.99	17.82	17.70	17.58	17.49	17.39	17.27
Dry Weight	g	1393.21	1393.21	1393.21	1393.21	1393.21	1393.21	1393.21	1393.21	1393.21	1393.21	1393.21	1393.21	1393.21
Wet Density	g/cm^3	2.839	2.842	3.082	3.095	3.099	3.103	3.110	3.119	3.126	3.133	3.138	3.143	3.150
Dry Density	g/cm^3	2.609	2.613	2.617	2.617	2.623	2.628	2.636	2.647	2.656	2.664	2.671	2.678	2.686
Specific Gravity of Solids	-	4.97	4.97	4.97	4.97	4.97	4.97	4.97	4.97	4.97	4.97	4.97	4.97	4.97
Solids Volume	cm^3	280.323	280.323	280.323	280.323	280.323	280.323	280.323	280.323	280.323	280.323	280.323	280.323	280.323
Void Volume	cm^3	253.621	252.931	252.021	252.021	250.920	249.882	248.301	245.980	244.192	242.615	241.325	239.997	238.298
Water Volume	cm^3	122.463	122.463	247.593	254.363	253.262	252.224	250.643	248.323	246.534	244.958	243.667	242.339	240.640
Void Ratio (e)	-	0.905	0.902	0.899	0.899	0.895	0.891	0.886	0.877	0.871	0.865	0.861	0.856	0.850
Saturation Ratio (Sr)	%	48.29	48.42	98.24	100.93	100.93	100.94	100.94	100.95	100.96	100.97	100.97	100.98	100.98
Effective Confining Stress	kPa					50	100	200	400	600	800	1000	1200	1500
Mean Shear Wave Velocity	m/s					**135.47**	**163.12**	**196.33**	**236.14**	**259.09**	**275.87**	**290.81**	**301.16**	**307.29**
Mean Shear Modulus	Mpa					**56.88**	**82.57**	**119.86**	**173.92**	**209.86**	**238.47**	**265.40**	**285.27**	**297.52**

Photos:

Before Test

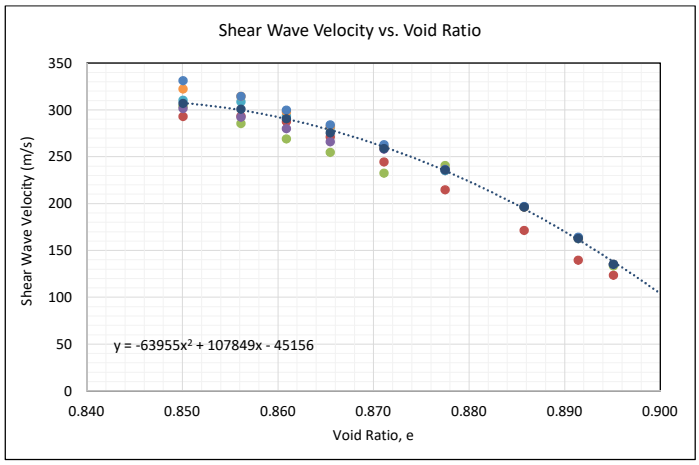
After Test

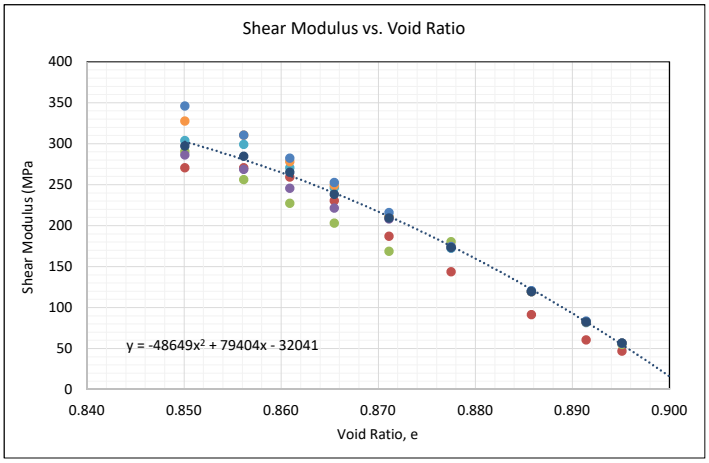



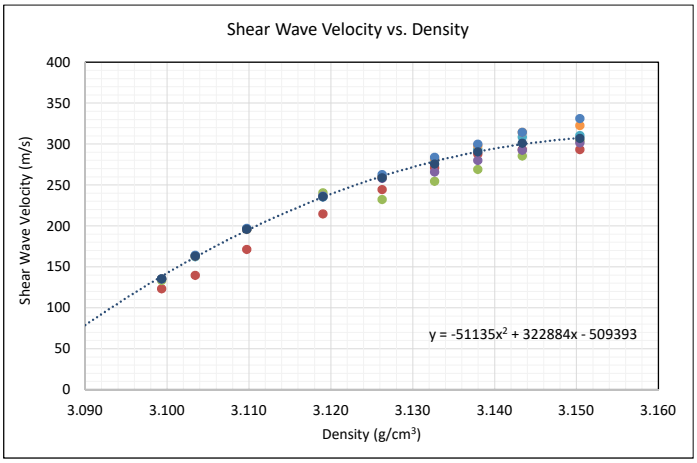
Triaxial Bender Element Test - Charts

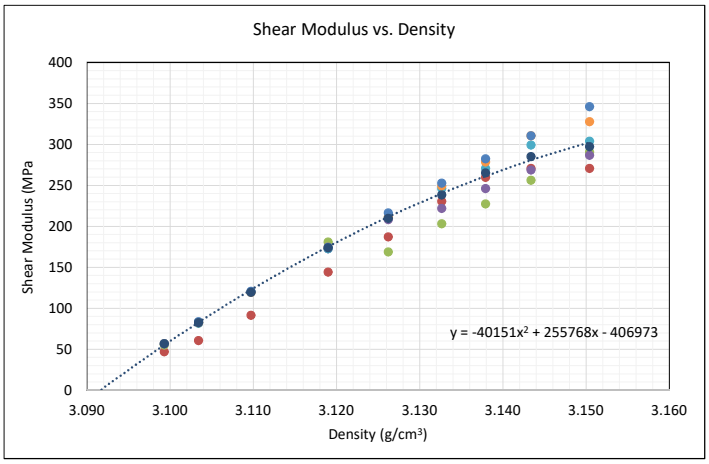
PROJECT NO. : A03355A01
PROJECT :
SAMPLE : Average
TEST NO. : TXBD01 e=0.9

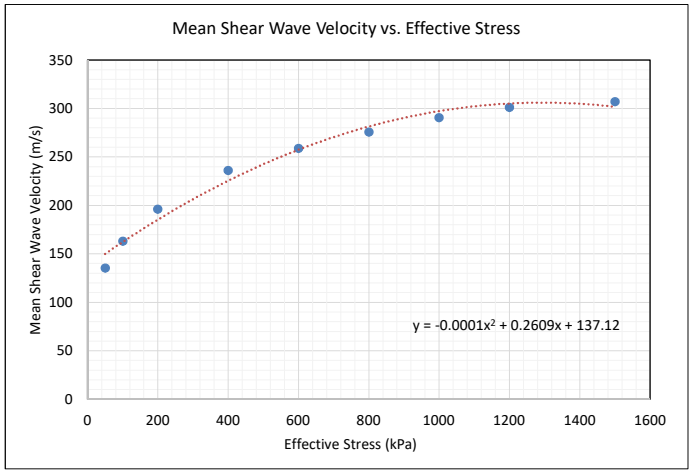
DATE : 2019-08-02
TEST BY: BY
CHECKED BY: JG

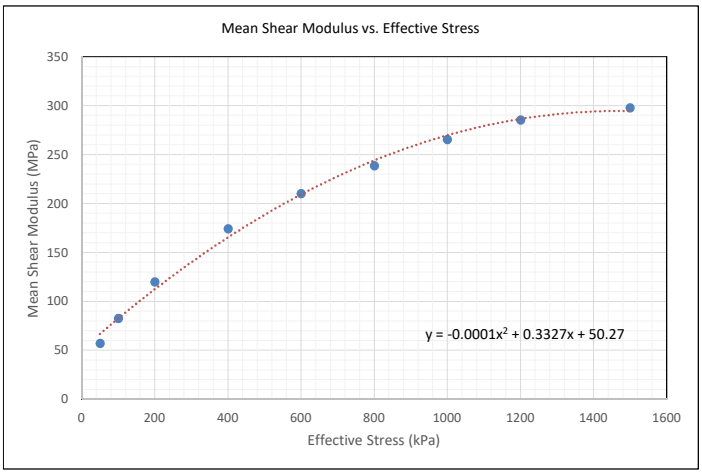












Triaxial Bender Element Test - Summary

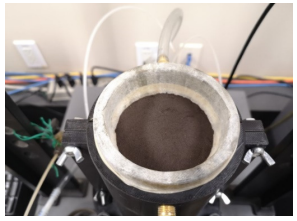
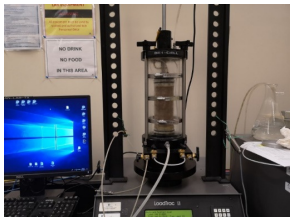
PROJECT NO. A03355A01
PROJECT :
SAMPLE : Average
TEST NO. : TXBD03 e=1.0

DATE : 2019-08-12
TESTED BY: BY
CHECKED BY: JG

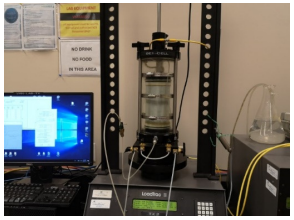
SPECIMEN INFORMATION	UNITS	Initial	Vacuum	Saturation	B value	End 1st Cons	End 2nd Cons	End 3rd Cons	End 4th Cons	End 5th Cons	End 6th Cons	End 7th Cons	End 8th Cons	End 9th Cons
Specimen Height	mm	139.17	138.92	138.92	138.83	138.79	138.66	138.45	138.14	137.89	137.64	137.46	137.27	137.02
Specimen Diameter	mm	69.80	69.66	69.50	69.53	69.49	69.39	69.24	69.04	68.89	68.75	68.64	68.55	68.41
Area	cm^2	38.26	38.11	37.94	37.97	37.93	37.81	37.66	37.44	37.27	37.12	37.00	36.90	36.75
Volume	cm^3	532.533	529.446	527.076	527.076	526.400	524.355	521.365	517.167	513.954	510.891	508.647	506.609	503.610
Wet Weight	g	1386.60	1386.60	1579.20	1587.07	1586.39	1584.35	1581.36	1577.16	1573.95	1570.89	1568.64	1566.60	1563.60
Water Content	%	4.73	4.73	19.28	19.87	19.82	19.67	19.44	19.12	18.88	18.65	18.48	18.33	18.10
Dry Weight	g	1323.98	1323.98	1323.98	1323.98	1323.98	1323.98	1323.98	1323.98	1323.98	1323.98	1323.98	1323.98	1323.98
Wet Density	g/cm^3	2.604	2.619	2.996	3.011	3.014	3.022	3.033	3.050	3.062	3.075	3.084	3.092	3.105
Dry Density	g/cm^3	2.486	2.501	2.512	2.512	2.515	2.525	2.539	2.560	2.576	2.592	2.603	2.613	2.629
Specific Gravity of Solids	-	4.97	4.97	4.97	4.97	4.97	4.97	4.97	4.97	4.97	4.97	4.97	4.97	4.97
Solids Volume	cm^3	266.394	266.394	266.394	266.394	266.394	266.394	266.394	266.394	266.394	266.394	266.394	266.394	266.394
Void Volume	cm^3	266.139	263.052	260.682	260.682	260.007	257.962	254.972	250.773	247.561	244.498	242.253	240.216	237.216
Water Volume	cm^3	62.624	62.624	255.224	263.094	262.418	260.373	257.383	253.185	249.972	246.909	244.665	242.627	239.627
Void Ratio (e)	-	0.999	0.987	0.979	0.979	0.976	0.968	0.957	0.941	0.929	0.918	0.909	0.902	0.890
Saturation Ratio (Sr)	%	23.53	23.81	97.91	100.93	100.93	100.93	100.95	100.96	100.97	100.99	101.00	101.00	101.02
Effective Confining Stress	kPa					50	100	200	400	600	800	1000	1200	1500
Mean Shear Wave Velocity	m/s					**102.44**	**128.59**	**163.83**	**207.36**	**231.49**	**256.52**	**274.66**	**280.67**	**303.55**
Mean Shear Modulus	MPa					**31.62**	**49.97**	**81.41**	**131.13**	**164.10**	**202.33**	**232.65**	**243.60**	**286.08**

Photos:

Before Test

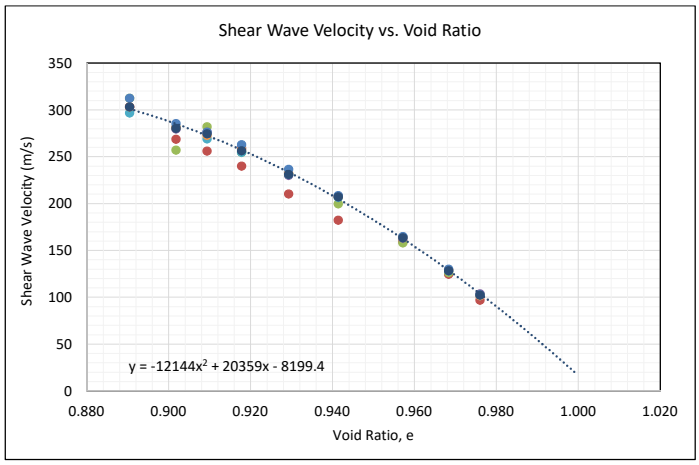



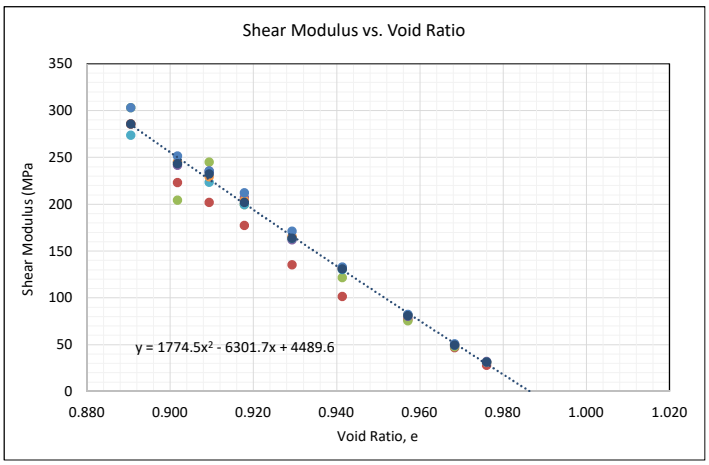
After Test

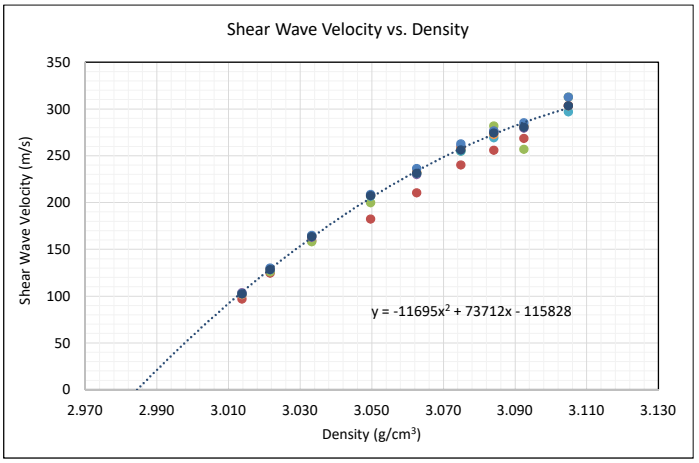


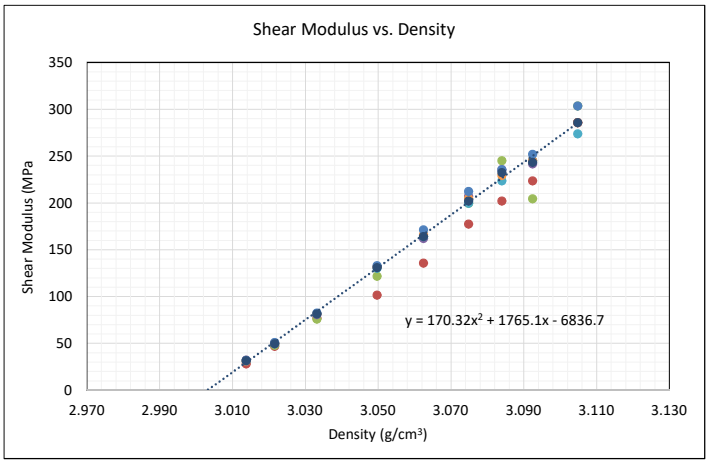

Triaxial Bender Element Test - Charts

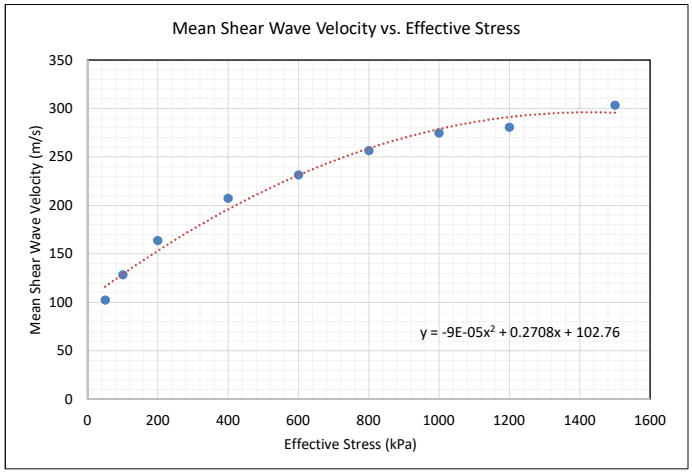
PROJECT NO. :	A03355A01	DATE :	2019-08-12
PROJECT :		TEST BY:	BY
SAMPLE :	Average	CHECKED BY:	JG
TEST NO. :	TXBD03 e=1.0		

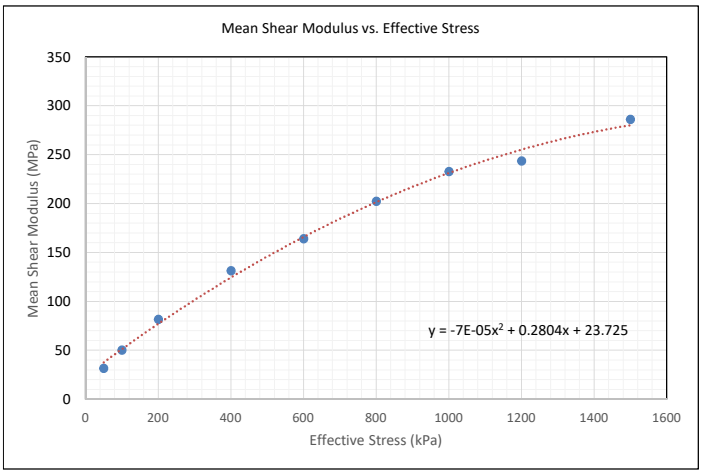












Triaxial Bender Element Test - Summary

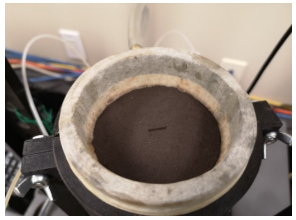
PROJECT NO. A03355A01
PROJECT :
SAMPLE : Fine Gradation
TEST NO. : TXBD04 e=1.1

DATE : 2019-08-19
TESTED BY: BY
CHECKED BY: JG

SPECIMEN INFORMATION	UNITS	Initial	Vacuum	Saturation	B value	End 1st Cons	End 2nd Cons	End 3rd Cons	End 4th Cons	End 5th Cons	End 6th Cons	End 7th Cons	End 8th Cons	End 9th Cons
Specimen Height	mm	138.53	138.2	138.20	138.18	138.18	138.07	137.87	137.52	137.27	137.01	136.83	136.63	136.39
Specimen Diameter	mm	69.80	69.90	69.73	69.73	69.62	69.46	69.27	69.05	68.88	68.76	68.64	68.53	68.40
Area	cm^2	38.26	38.37	38.18	38.19	38.07	37.90	37.69	37.45	37.27	37.13	37.00	36.89	36.74
Volume	cm^3	530.084	530.337	527.693	527.693	525.982	523.238	519.640	514.983	511.560	508.719	506.283	504.042	501.112
Wet Weight	g	1352.17	1352.17	1521.27	1529.28	1527.57	1524.83	1521.23	1516.57	1513.15	1510.31	1507.87	1505.63	1502.70
Water Content	%	7.99	7.99	21.50	22.13	22.00	21.78	21.49	21.12	20.85	20.62	20.42	20.25	20.01
Dry Weight	g	1252.13	1252.13	1252.13	1252.13	1252.13	1252.13	1252.13	1252.13	1252.13	1252.13	1252.13	1252.13	1252.13
Wet Density	g/cm^3	2.551	2.550	2.883	2.898	2.904	2.914	2.927	2.945	2.958	2.969	2.978	2.987	2.999
Dry Density	g/cm^3	2.362	2.361	2.373	2.373	2.381	2.393	2.410	2.431	2.448	2.461	2.473	2.484	2.499
Specific Gravity of Solids	-	4.96	4.96	4.96	4.96	4.96	4.96	4.96	4.96	4.96	4.96	4.96	4.96	4.96
Solids Volume	cm^3	252.445	252.445	252.445	252.445	252.445	252.445	252.445	252.445	252.445	252.445	252.445	252.445	252.445
Void Volume	cm^3	277.639	277.893	275.249	275.249	273.537	270.793	267.196	262.539	259.115	256.274	253.838	251.597	248.667
Water Volume	cm^3	100.045	100.045	269.145	277.157	275.445	272.701	269.104	264.446	261.023	258.182	255.746	253.505	250.575
Void Ratio (e)	-	1.100	1.101	1.090	1.090	1.084	1.073	1.058	1.040	1.026	1.015	1.006	0.997	0.985
Saturation Ratio (Sr)	%	36.03	36.00	97.78	100.69	100.70	100.70	100.71	100.73	100.74	100.74	100.75	100.76	100.77
Effective Confining Stress	kPa					50	100	200	400	600	800	1000	1200	1500
Mean Shear Wave Velocity	m/s					**110.60**	**134.51**	**164.93**	**201.29**	**225.28**	**243.20**	**261.11**	**274.49**	**285.29**
Mean Shear Modulus	MPa					**35.52**	**52.72**	**79.63**	**119.32**	**150.12**	**175.60**	**203.06**	**225.07**	**244.12**

Photos:

Before Test

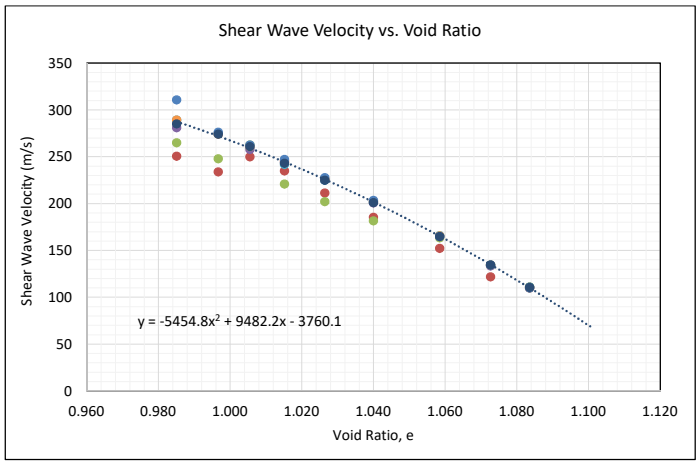


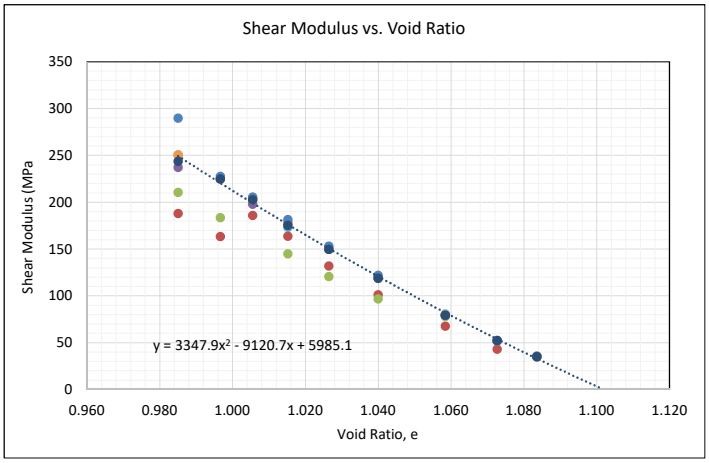

After Test

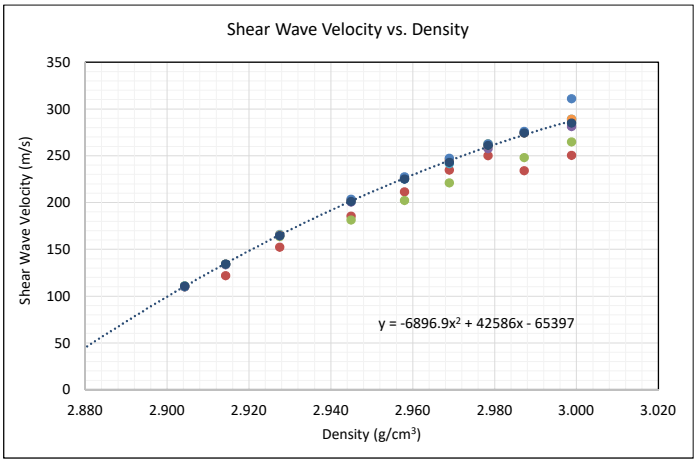


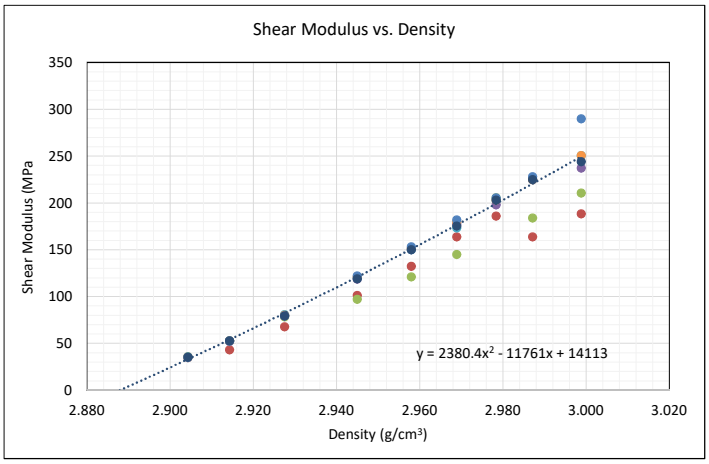

Triaxial Bender Element Test - Charts

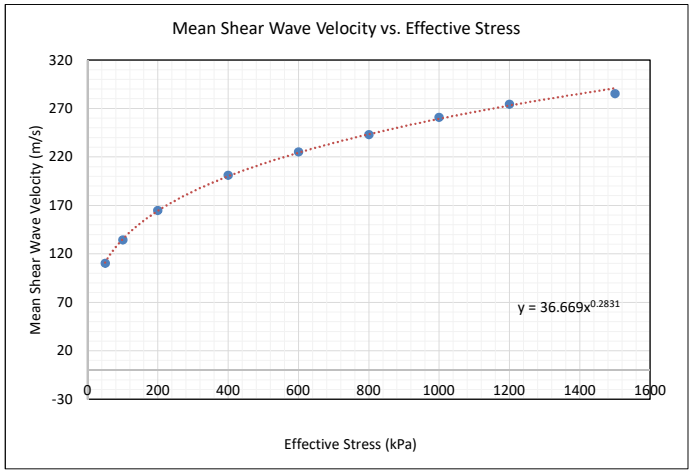
PROJECT NO. :	A03355A01	DATE :	2019-08-19
PROJECT :		TEST BY:	BY
SAMPLE :	Fine Gradation	CHECKED BY:	JG
TEST NO. :	TXBD04 e=1.1		

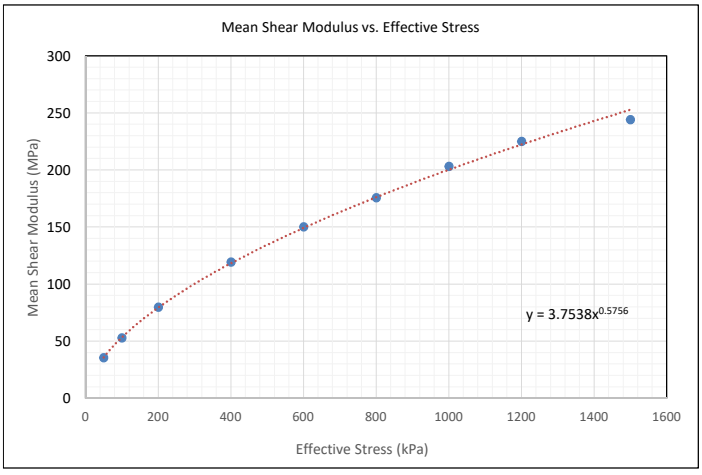












Triaxial Bender Element Test - Summary

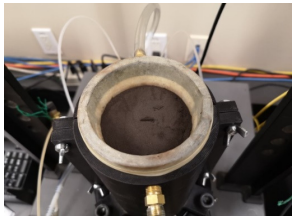
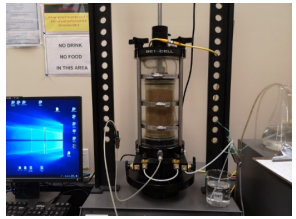
PROJECT NO. A03355A01
PROJECT :
SAMPLE : Fine Gradation
TEST NO. : TXBD05 e=0.9

DATE : 2019-08-22
TESTED BY: BY
CHECKED BY: JG

SPECIMEN INFORMATION	UNITS	Initial	Vacuum	Saturation	B value	End 1st Cons	End 2nd Cons	End 3rd Cons	End 4th Cons	End 5th Cons	End 6th Cons	End 7th Cons	End 8th Cons	End 9th Cons
Specimen Height	mm	139.08	138.72	138.72	138.68	138.62	138.55	138.42	138.31	138.19	138.10	138.01	137.91	137.82
Specimen Diameter	mm	70.15	70.15	70.12	70.13	70.07	70.02	69.96	69.87	69.81	69.75	69.71	69.66	69.60
Area	cm^2	38.65	38.65	38.62	38.63	38.57	38.51	38.44	38.35	38.28	38.21	38.16	38.12	38.04
Volume	cm^3	537.539	536.148	535.691	535.691	534.602	533.554	532.121	530.373	528.964	527.736	526.667	525.683	524.309
Wet Weight	g	1503.34	1503.34	1629.34	1650.20	1649.11	1648.06	1646.63	1644.88	1643.47	1642.24	1641.17	1640.19	1638.81
Water Content	%	7.89	7.89	16.93	18.43	18.35	18.28	18.17	18.05	17.95	17.86	17.78	17.71	17.61
Dry Weight	g	1393.40	1393.40	1393.40	1393.40	1393.40	1393.40	1393.40	1393.40	1393.40	1393.40	1393.40	1393.40	1393.40
Wet Density	g/cm^3	2.797	2.804	3.042	3.081	3.085	3.089	3.094	3.101	3.107	3.112	3.116	3.120	3.126
Dry Density	g/cm^3	2.592	2.599	2.601	2.601	2.606	2.612	2.619	2.627	2.634	2.640	2.646	2.651	2.658
Specific Gravity of Solids	-	4.96	4.96	4.96	4.96	4.96	4.96	4.96	4.96	4.96	4.96	4.96	4.96	4.96
Solids Volume	cm^3	280.928	280.928	280.928	280.928	280.928	280.928	280.928	280.928	280.928	280.928	280.928	280.928	280.928
Void Volume	cm^3	256.611	255.220	254.763	254.763	253.674	252.626	251.193	249.445	248.036	246.809	245.740	244.756	243.381
Water Volume	cm^3	109.939	109.939	235.939	256.795	255.706	254.658	253.225	251.477	250.068	248.841	247.772	246.788	245.413
Void Ratio (e)	-	0.913	0.908	0.907	0.907	0.903	0.899	0.894	0.888	0.883	0.879	0.875	0.871	0.866
Saturation Ratio (Sr)	%	42.84	43.08	92.61	100.80	100.80	100.80	100.81	100.81	100.82	100.82	100.83	100.83	100.83
Effective Confining Stress	kPa					50	100	200	400	600	800	1000	1200	1500
Mean Shear Wave Velocity	m/s					**134.71**	**159.32**	**193.98**	**228.55**	**254.59**	**273.45**	**289.26**	**303.69**	**320.26**
Mean Shear Modulus	MPa					**55.98**	**78.40**	**116.43**	**161.99**	**201.38**	**232.70**	**260.74**	**287.76**	**320.58**

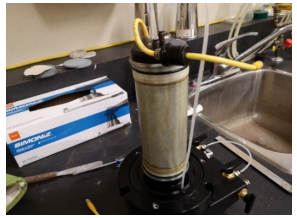
Photos:

Before Test

After Test

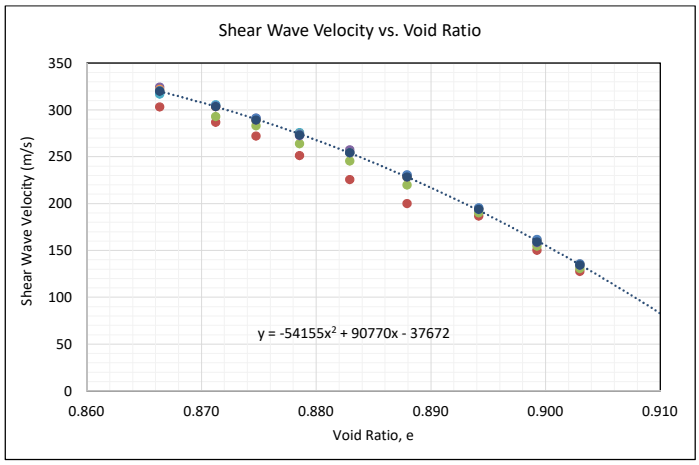


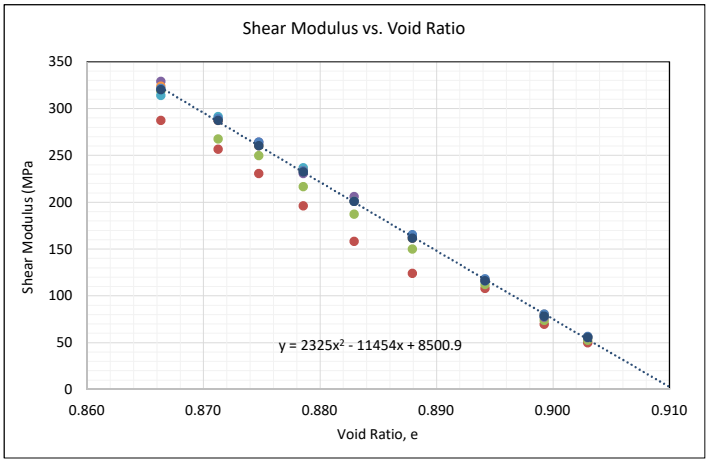


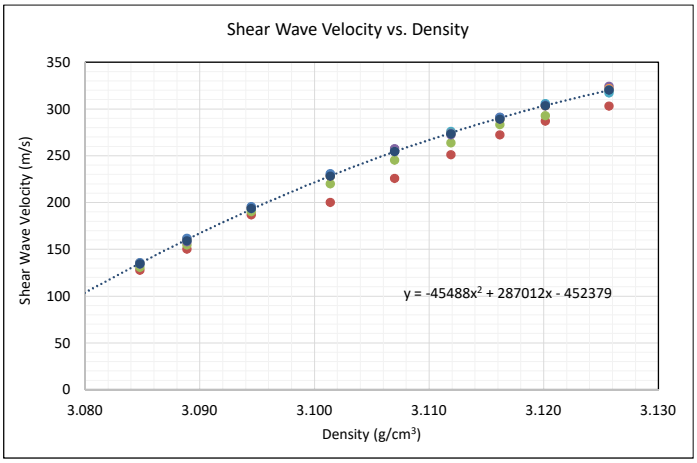
Triaxial Bender Element Test - Charts

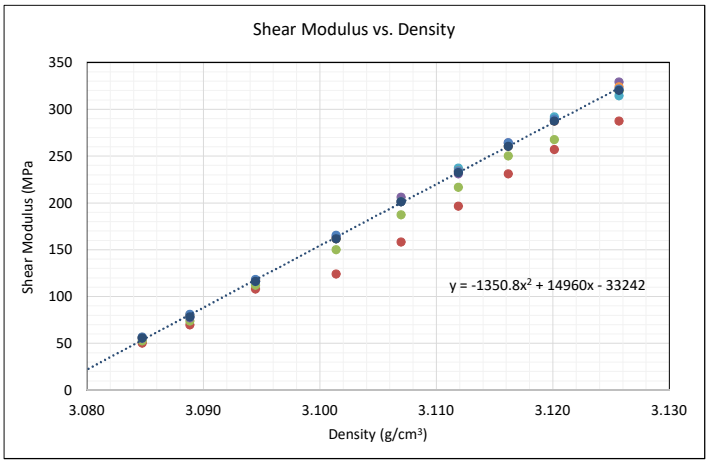
PROJECT NO. : A03355A01
PROJECT :
SAMPLE : Fine Gradation
TEST NO. : TXBD05 e=0.9

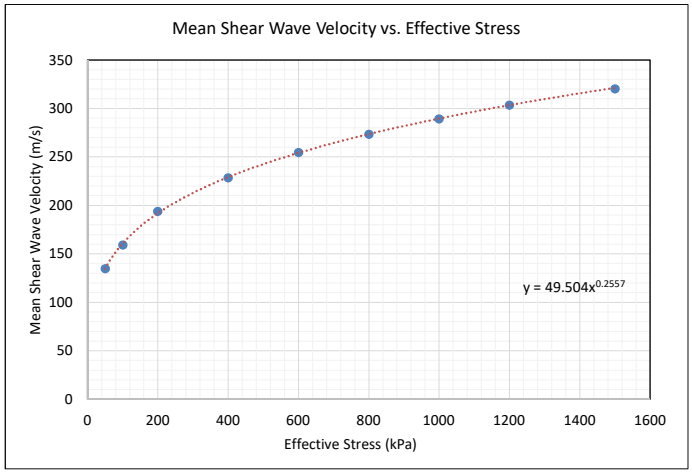
DATE : 2019-08-22
TEST BY: BY
CHECKED BY: JG

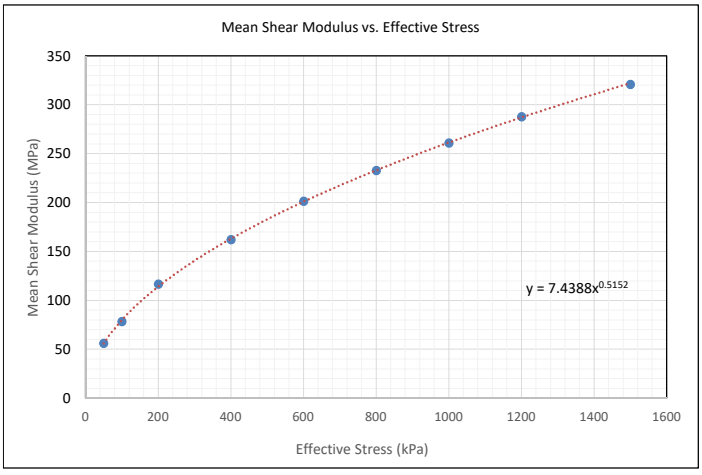












Triaxial Bender Element Test - Summary

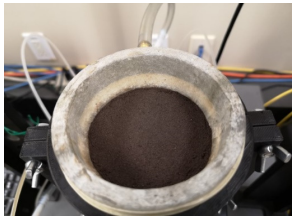
PROJECT NO. A03355A01
PROJECT :
SAMPLE : Coarse
TEST NO. : TXBD06 e=1.1

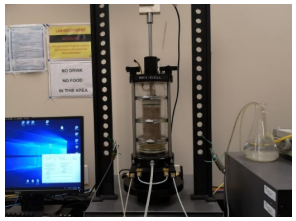
DATE : 2019-08-23
TESTED BY: BY
CHECKED BY: JG

SPECIMEN INFORMATION	UNITS	Initial	Vacuum	Saturation	B value	End 1st Cons	End 2nd Cons	End 3rd Cons	End 4th Cons	End 5th Cons	End 6th Cons	End 7th Cons	End 8th Cons	End 9th Cons
Specimen Height	mm	139.2	138.17	138.17	138.10	137.79	137.43	136.92	136.24	135.72	135.32	134.96	134.62	134.18
Specimen Diameter	mm	69.80	69.86	69.29	69.31	68.94	68.63	68.30	67.93	67.67	67.49	67.33	67.19	67.01
Area	cm^2	38.26	38.33	37.71	37.73	37.32	37.00	36.64	36.25	35.97	35.77	35.61	35.45	35.27
Volume	cm^3	532.648	529.616	521.066	521.066	514.289	508.426	501.648	493.816	488.152	484.081	480.544	477.272	473.280
Wet Weight	g	1342.27	1342.27	1509.57	1512.46	1505.68	1499.82	1493.04	1485.21	1479.55	1475.47	1471.94	1468.67	1464.67
Water Content	%	8.02	8.02	21.48	21.72	21.17	20.70	20.15	19.52	19.07	18.74	18.46	18.19	17.87
Dry Weight	g	1242.61	1242.61	1242.61	1242.61	1242.61	1242.61	1242.61	1242.61	1242.61	1242.61	1242.61	1242.61	1242.61
Wet Density	g/cm^3	2.520	2.534	2.897	2.903	2.928	2.950	2.976	3.008	3.031	3.048	3.063	3.077	3.095
Dry Density	g/cm^3	2.333	2.346	2.385	2.385	2.416	2.444	2.477	2.516	2.546	2.567	2.586	2.604	2.626
Specific Gravity of Solids	-	4.91	4.91	4.91	4.91	4.91	4.91	4.91	4.91	4.91	4.91	4.91	4.91	4.91
Solids Volume	cm^3	253.078	253.078	253.078	253.078	253.078	253.078	253.078	253.078	253.078	253.078	253.078	253.078	253.078
Void Volume	cm^3	279.570	276.538	267.988	267.988	261.211	255.348	248.570	240.738	235.074	231.003	227.467	224.195	220.202
Water Volume	cm^3	99.658	99.658	266.958	269.847	263.070	257.208	250.429	242.597	236.934	232.862	229.326	226.054	222.062
Void Ratio (e)	-	1.105	1.093	1.059	1.059	1.032	1.009	0.982	0.951	0.929	0.913	0.899	0.886	0.870
Saturation Ratio (Sr)	%	35.65	36.04	99.62	100.69	100.71	100.73	100.75	100.77	100.79	100.80	100.82	100.83	100.84
Effective Confining Stress	kPa					50	100	200	400	600	800	1000	1200	1500
Mean Shear Wave Velocity	m/s					**104.77**	**129.61**	**162.32**	**203.98**	**236.33**	**252.16**	**263.61**	**283.79**	**291.98**
Mean Shear Modulus	MPa					**32.13**	**49.56**	**78.41**	**125.14**	**169.28**	**193.81**	**212.93**	**247.83**	**263.95**

Photos:

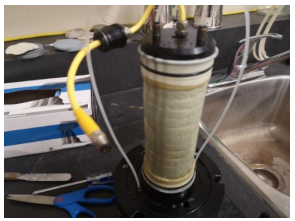
Before Test





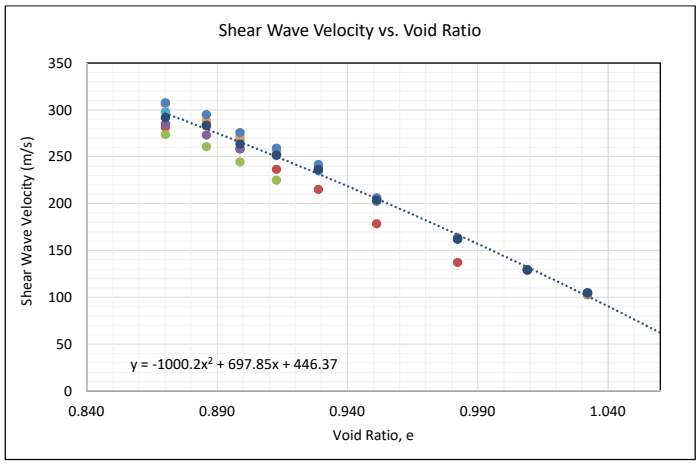
After Test

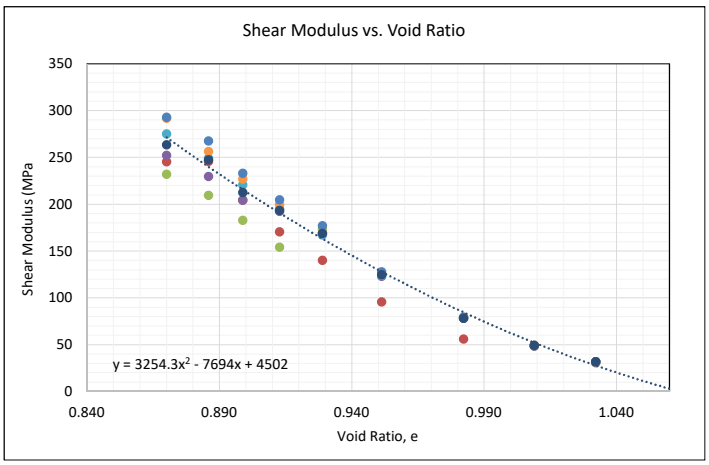


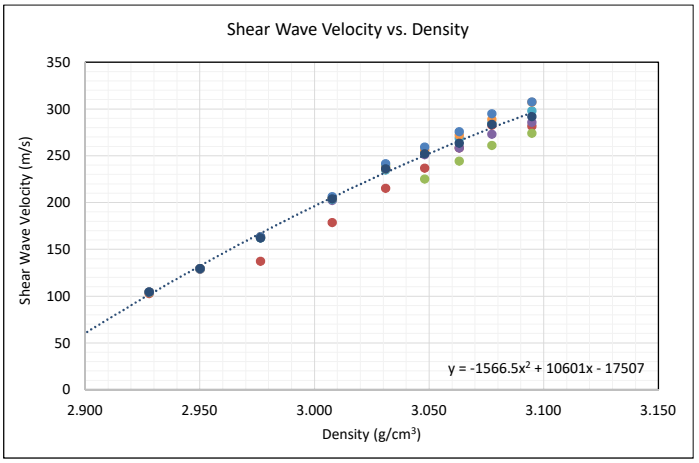


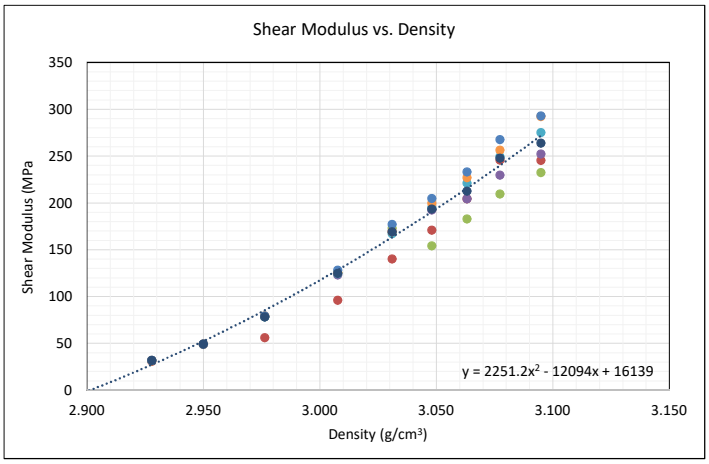
Triaxial Bender Element Test - Charts

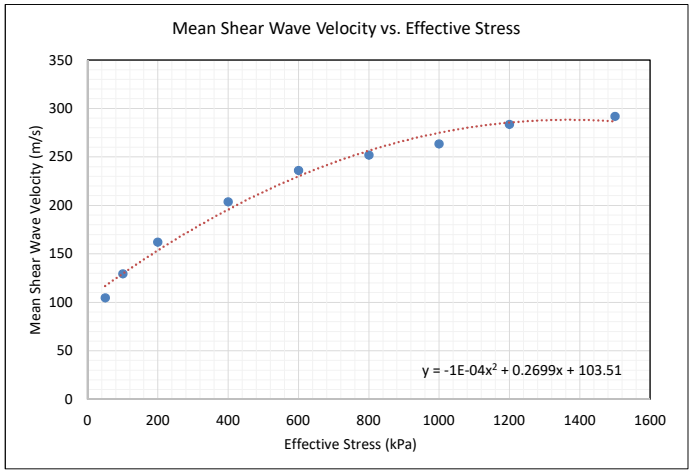
PROJECT NO. :	A03355A01	DATE :	2019-08-23
PROJECT :		TEST BY:	BY
SAMPLE :	Coarse	CHECKED BY:	JG
TEST NO. :	TXBD06 e=1.1		

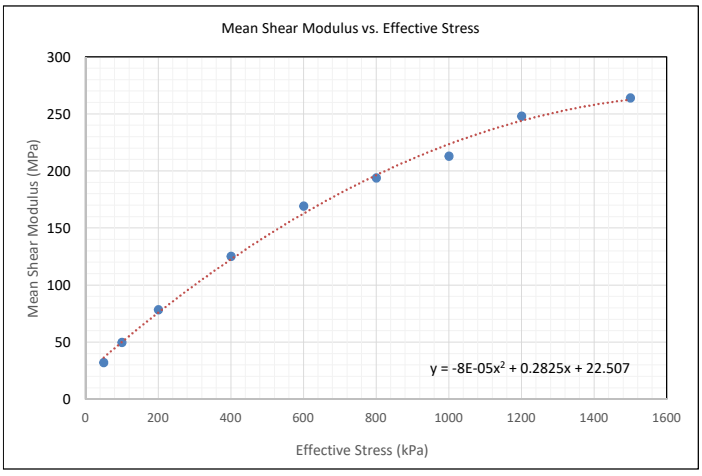












Triaxial Bender Element Test - Summary

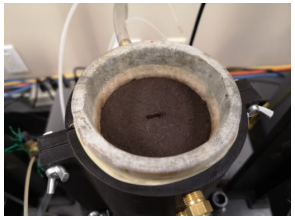
PROJECT NO. A03355A01
PROJECT :
SAMPLE : Coarse Gradation - Batch 3
TEST NO. : TXBD07 e=0.9

DATE : 2019-08-27
TESTED BY: BY
CHECKED BY: JG

SPECIMEN INFORMATION	UNITS	Initial	Vacuum	Saturation	B value	End 1st Cons	End 2nd Cons	End 3rd Cons	End 4th Cons	End 5th Cons	End 6th Cons	End 7th Cons	End 8th Cons	End 9th Cons
Specimen Height	mm	139.06	138.51	138.51	138.45	138.45	138.40	138.27	138.09	137.95	137.77	137.67	137.53	137.36
Specimen Diameter	mm	69.90	70.04	70.04	70.05	69.97	69.89	69.78	69.63	69.51	69.41	69.32	69.24	69.13
Area	cm^2	38.37	38.53	38.53	38.54	38.46	38.36	38.25	38.08	37.95	37.84	37.75	37.66	37.53
Volume	cm^3	533.638	533.658	533.658	533.658	532.420	530.921	528.819	525.819	523.477	521.247	519.624	517.876	515.514
Wet Weight	g	1489.35	1489.35	1620.55	1633.68	1632.44	1630.94	1628.84	1625.84	1623.50	1621.27	1619.65	1617.90	1615.54
Water Content	%	8.00	8.00	17.51	18.47	18.38	18.27	18.12	17.90	17.73	17.57	17.45	17.32	17.15
Dry Weight	g	1379.03	1379.03	1379.03	1379.03	1379.03	1379.03	1379.03	1379.03	1379.03	1379.03	1379.03	1379.03	1379.03
Wet Density	g/cm^3	2.791	2.791	3.037	3.061	3.066	3.072	3.080	3.092	3.101	3.110	3.117	3.124	3.134
Dry Density	g/cm^3	2.584	2.584	2.584	2.584	2.590	2.597	2.608	2.623	2.634	2.646	2.654	2.663	2.675
Specific Gravity of Solids	-	4.91	4.91	4.91	4.91	4.91	4.91	4.91	4.91	4.91	4.91	4.91	4.91	4.91
Solids Volume	cm^3	280.861	280.861	280.861	280.861	280.861	280.861	280.861	280.861	280.861	280.861	280.861	280.861	280.861
Void Volume	cm^3	252.777	252.797	252.797	252.797	251.559	250.060	247.958	244.958	242.616	240.386	238.763	237.015	234.653
Water Volume	cm^3	110.322	110.322	241.522	254.654	253.416	251.917	249.814	246.815	244.473	242.242	240.620	238.872	236.509
Void Ratio (e)	-	0.900	0.900	0.900	0.900	0.896	0.890	0.883	0.872	0.864	0.856	0.850	0.844	0.835
Saturation Ratio (Sr)	%	43.64	43.64	95.54	100.73	100.74	100.74	100.75	100.76	100.77	100.77	100.78	100.78	100.79
Effective Confining Stress	kPa					50	100	200	400	600	800	1000	1200	1500
Mean Shear Wave Velocity	m/s					**130.35**	**158.81**	**195.52**	**239.17**	**267.01**	**291.68**	**307.50**	**325.06**	**339.10**
Mean Shear Modulus	MPa					**52.10**	**77.48**	**117.75**	**176.87**	**221.11**	**264.63**	**294.72**	**330.12**	**360.36**

Photos:

Before Test





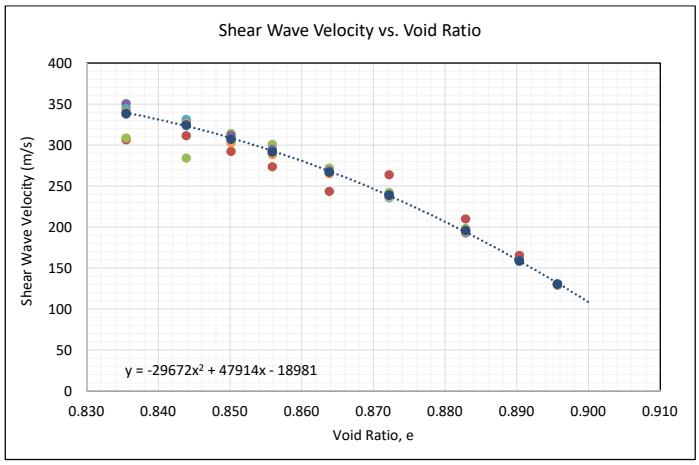
After Test

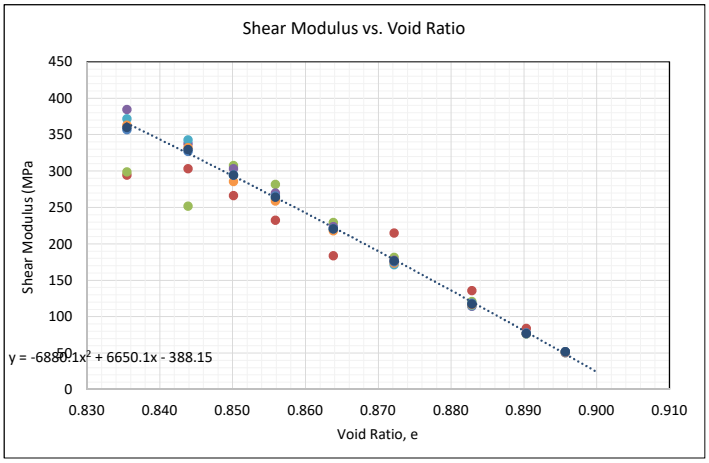


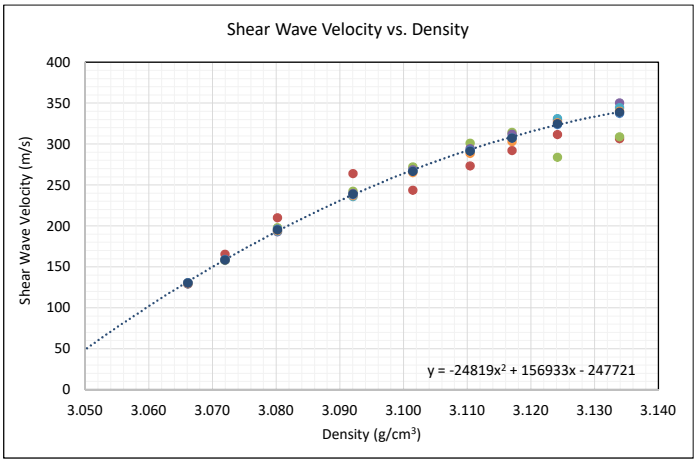


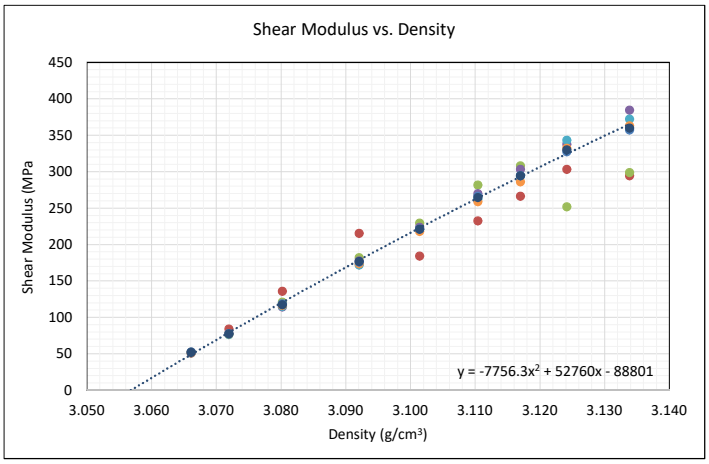
Triaxial Bender Element Test - Charts

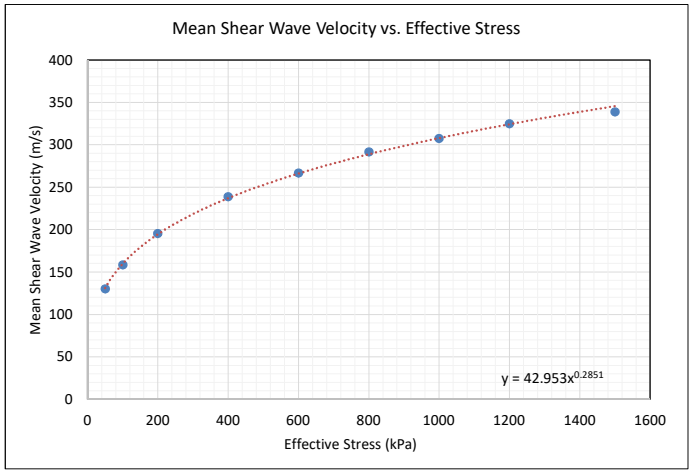
PROJECT NO. :	A03355A01	DATE :	2019-08-27
PROJECT :		TEST BY:	BY
SAMPLE :	Coarse Gradation - Batch 3	CHECKED BY:	JG
TEST NO. :	TXBD07 e=0.9		

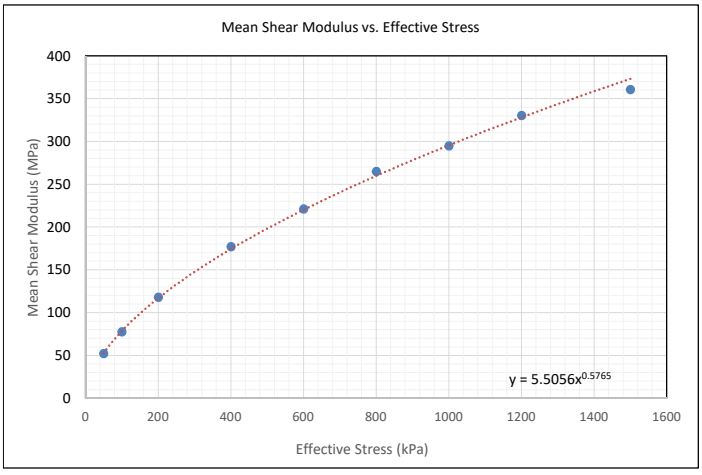












Triaxial Bender Element Test - Summary

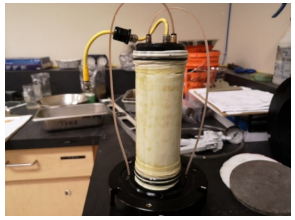
PROJECT NO. A03355A01
PROJECT :
SAMPLE : Average
TEST NO. : TXBE08 e=0.75

DATE : 2019-10-09
TESTED BY: BY / AX
CHECKED BY: JG

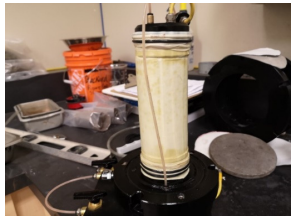
SPECIMEN INFORMATION	UNITS	Initial	Vacuum	Saturation	B value	End 1st Cons	End 2nd Cons	End 3rd Cons	End 4th Cons	End 5th Cons	End 6th Cons	End 7th Cons	End 8th Cons	End 9th Cons
Specimen Height	mm	139.67	139.67	139.67	139.55	139.49	139.42	139.29	139.08	138.96	138.85	138.76	138.68	138.59
Specimen Diameter	mm	70.27	70.27	70.09	70.09	70.05	70.01	69.95	69.89	69.84	69.81	69.78	69.74	69.66
Area	cm^2	38.78	38.78	38.58	38.59	38.54	38.49	38.43	38.37	38.31	38.27	38.24	38.20	38.11
Volume	cm^3	541.668	541.668	538.834	538.464	537.564	536.632	535.307	533.589	532.371	531.395	530.623	529.810	528.112
Wet Weight	g	1640.54	1640.54	1722.64	1753.08	1752.18	1751.25	1749.93	1748.21	1746.99	1746.02	1745.24	1744.43	1742.73
Water Content	%	7.89	7.89	13.29	15.29	15.23	15.17	15.08	14.97	14.89	14.83	14.78	14.72	14.61
Dry Weight	g	1520.57	1520.57	1520.57	1520.57	1520.57	1520.57	1520.57	1520.57	1520.57	1520.57	1520.57	1520.57	1520.57
Wet Density	g/cm^3	3.029	3.029	3.197	3.256	3.259	3.263	3.269	3.276	3.282	3.286	3.289	3.293	3.300
Dry Density	g/cm^3	2.807	2.807	2.822	2.824	2.829	2.834	2.841	2.850	2.856	2.861	2.866	2.870	2.879
Specific Gravity of Solids	-	4.97	4.97	4.97	4.97	4.97	4.97	4.97	4.97	4.97	4.97	4.97	4.97	4.97
Solids Volume	cm^3	305.949	305.949	305.949	305.949	305.949	305.949	305.949	305.949	305.949	305.949	305.949	305.949	305.949
Void Volume	cm^3	235.719	235.719	232.885	232.515	231.615	230.683	229.358	227.639	226.422	225.445	224.674	223.861	222.163
Water Volume	cm^3	119.973	119.973	202.073	232.517	231.617	230.685	229.360	227.642	226.424	225.448	224.677	223.864	222.165
Void Ratio (e)	-	0.770	0.770	0.761	0.760	0.757	0.754	0.750	0.744	0.740	0.737	0.734	0.732	0.726
Saturation Ratio (Sr)	%	50.90	50.90	86.77	100.00	100.00	100.00	100.00	100.00	100.00	100.00	100.00	100.00	100.00
Effective Confining Stress	kPa					50	100	200	400	600	800	1000	1200	1500
Mean Shear Wave Velocity	m/s					**150.10**	**173.97**	**207.36**	**233.85**	**266.81**	**292.36**	**303.71**	**311.34**	**334.56**
Mean Shear Modulus	MPa					**73.44**	**98.77**	**140.57**	**179.66**	**233.63**	**280.85**	**303.39**	**319.17**	**369.39**

Photos:

Before Test



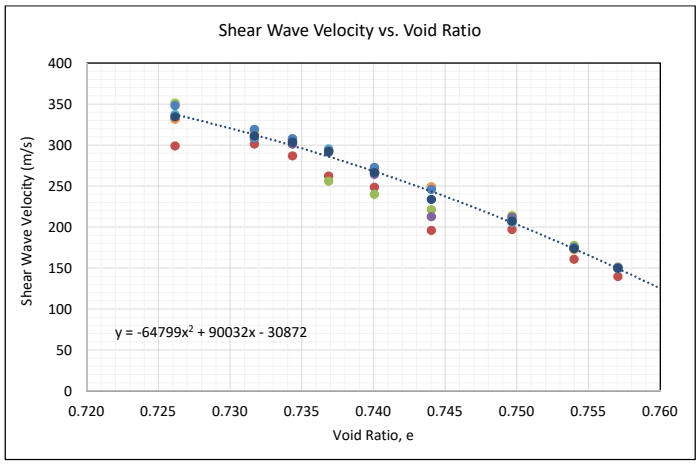
After Test

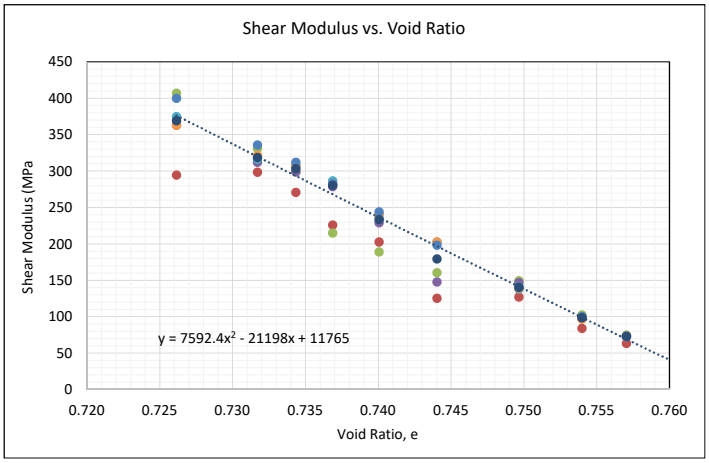


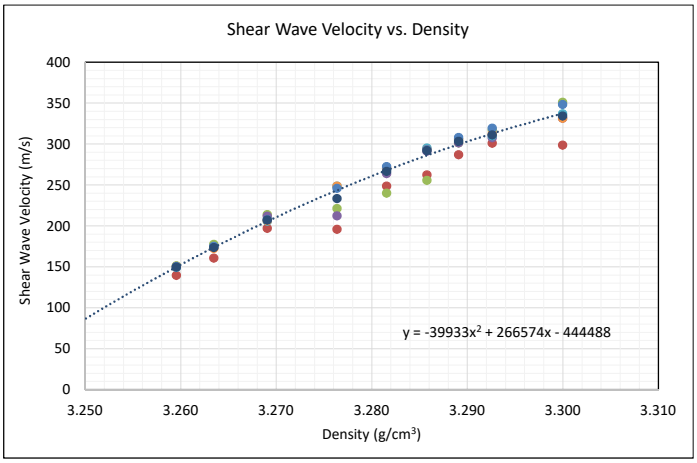
Triaxial Bender Element Test - Charts

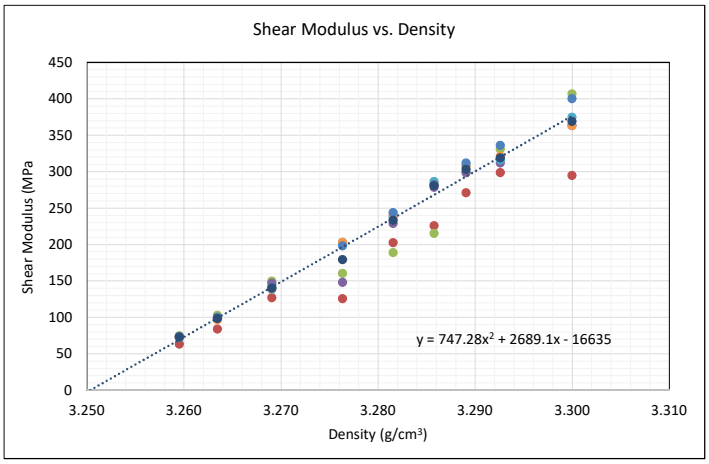
PROJECT NO. : A03355A01
PROJECT :
SAMPLE : Average
TEST NO. : TXBE08 e=0.75

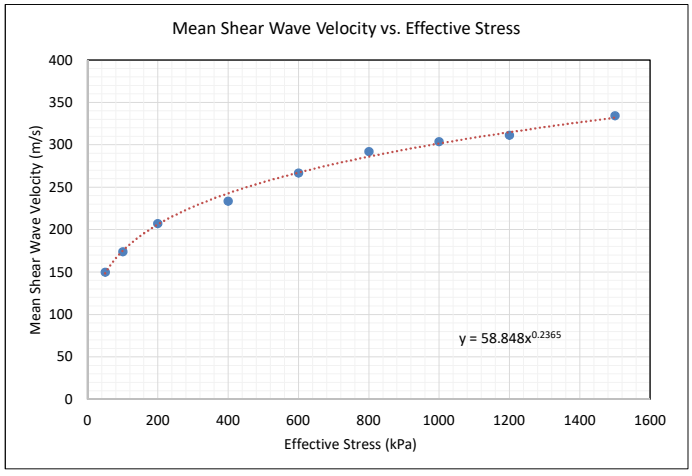
DATE : 2019-10-09
TEST BY: BY / AX
CHECKED BY: JG

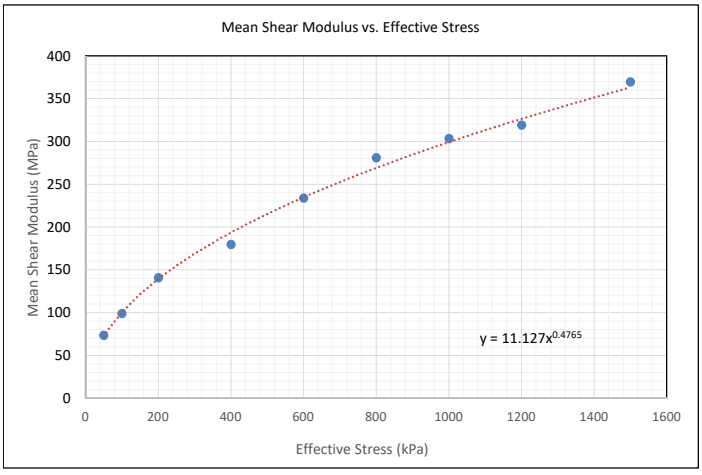












Triaxial Bender Element Test - Summary

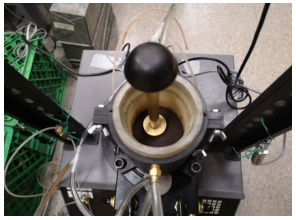
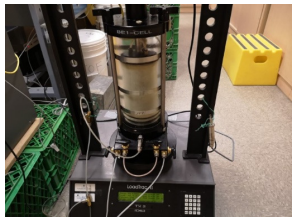
PROJECT NO. A03355A01
PROJECT :
SAMPLE : Coarse
TEST NO. : TXBD09 e=0.7

DATE : 2019-10-31
TESTED BY: BY
CHECKED BY: JG

SPECIMEN INFORMATION	UNITS	Initial	Vacuum	Saturation	B value	End 1st Cons	End 2nd Cons	End 3rd Cons	End 4th Cons	End 5th Cons	End 6th Cons	End 7th Cons	End 8th Cons	End 9th Cons
Specimen Height	mm	139.06	139.06	139.06	138.99	138.96	138.89	138.83	138.71	138.61	138.53	138.45	138.38	138.28
Specimen Diameter	mm	70.11	70.11	70.05	70.07	70.03	70.00	69.94	69.87	69.82	69.79	69.75	69.71	69.67
Area	cm^2	38.61	38.61	38.54	38.56	38.52	38.48	38.42	38.34	38.29	38.25	38.21	38.17	38.12
Volume	cm^3	536.849	536.849	535.899	535.899	535.279	534.506	533.390	531.869	530.766	529.861	528.997	528.195	527.099
Wet Weight	g	1663.85	1663.85	1749.31	1762.51	1761.89	1761.12	1760.00	1758.48	1757.38	1756.47	1755.61	1754.81	1753.71
Water Content	%	8.11	8.11	13.66	14.52	14.48	14.43	14.36	14.26	14.19	14.13	14.07	14.02	13.95
Dry Weight	g	1539.03	1539.03	1539.03	1539.03	1539.03	1539.03	1539.03	1539.03	1539.03	1539.03	1539.03	1539.03	1539.03
Wet Density	g/cm^3	3.099	3.099	3.264	3.289	3.292	3.295	3.300	3.306	3.311	3.315	3.319	3.322	3.327
Dry Density	g/cm^3	2.867	2.867	2.872	2.872	2.875	2.879	2.885	2.894	2.900	2.905	2.909	2.914	2.920
Specific Gravity of Solids	-	4.91	4.91	4.91	4.91	4.91	4.91	4.91	4.91	4.91	4.91	4.91	4.91	4.91
Solids Volume	cm^3	313.449	313.449	313.449	313.449	313.449	313.449	313.449	313.449	313.449	313.449	313.449	313.449	313.449
Void Volume	cm^3	223.400	223.400	222.450	222.450	221.830	221.057	219.941	218.420	217.317	216.412	215.548	214.747	213.650
Water Volume	cm^3	124.816	124.816	210.276	223.476	222.856	222.082	220.966	219.445	218.343	217.437	216.574	215.772	214.676
Void Ratio (e)	-	0.713	0.713	0.710	0.710	0.708	0.705	0.702	0.697	0.693	0.690	0.688	0.685	0.682
Saturation Ratio (Sr)	%	55.87	55.87	94.53	100.46	100.46	100.46	100.47	100.47	100.47	100.47	100.48	100.48	100.48
Effective Confining Stress	kPa					50	100	200	400	600	800	1000	1200	1500
Mean Shear Wave Velocity	m/s					**177.45**	**189.09**	**223.49**	**262.13**	**292.05**	**293.77**	**306.29**	**320.01**	**341.89**
Mean Shear Modulus	MPa					**103.96**	**117.81**	**164.82**	**227.21**	**282.69**	**286.25**	**311.45**	**340.26**	**389.00**

Photos:

Before Test

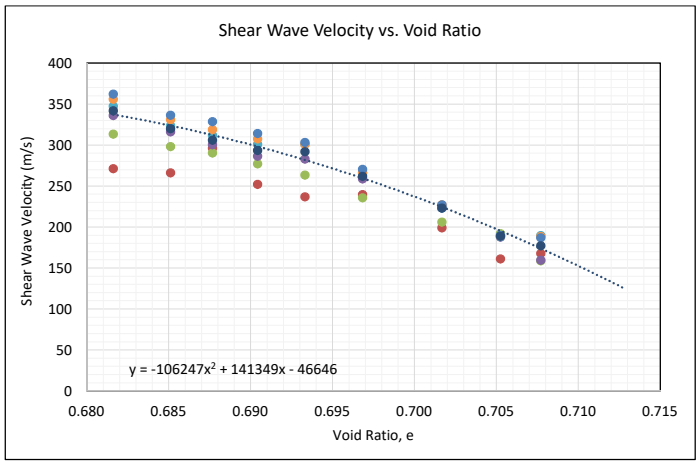
After Test

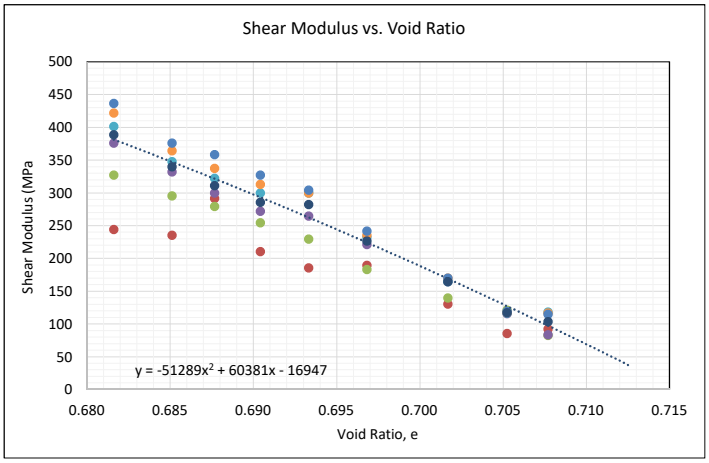


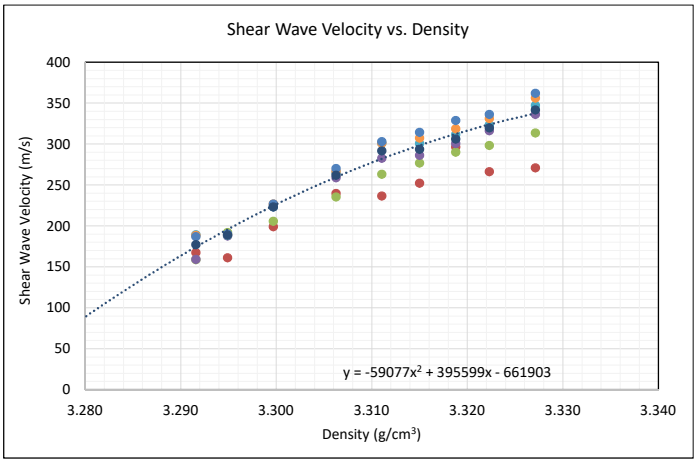

Triaxial Bender Element Test - Charts

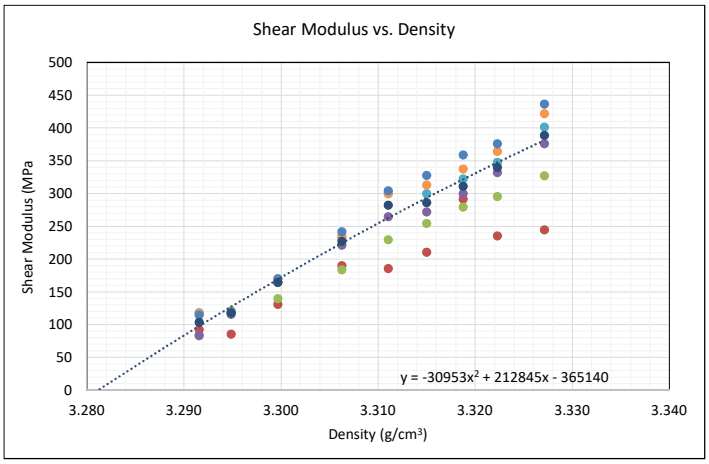
PROJECT NO. : A03355A01
PROJECT :
SAMPLE : Coarse
TEST NO. : TXBD09 e=0.7

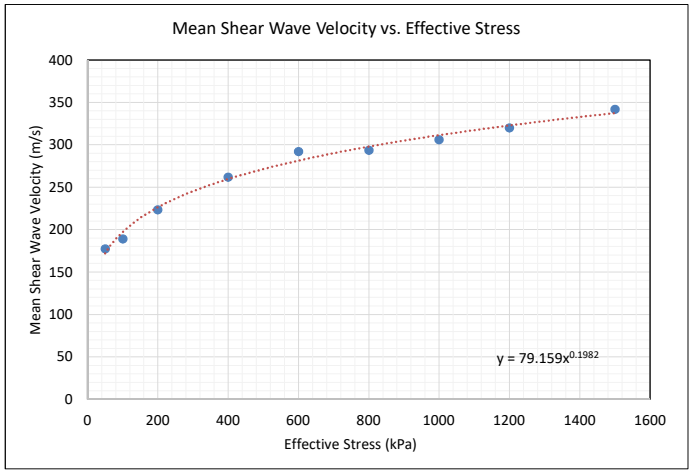
DATE : 2019-10-31
TEST BY: BY
CHECKED BY: JG

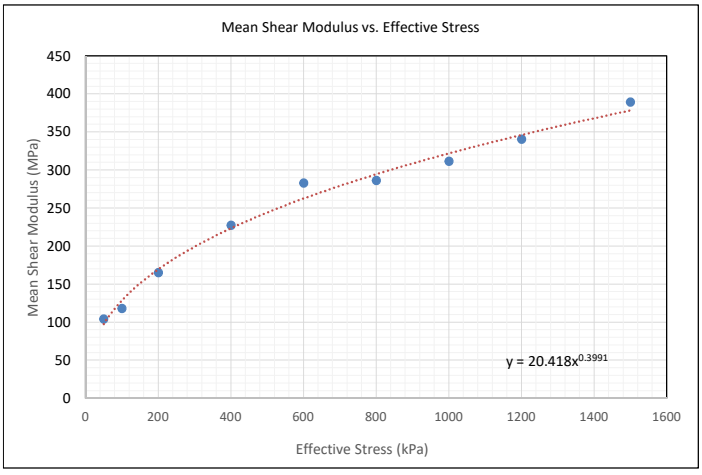












Triaxial Bender Element Test - Summary

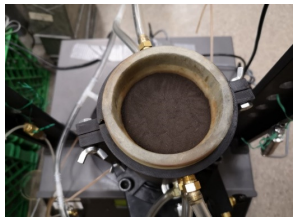
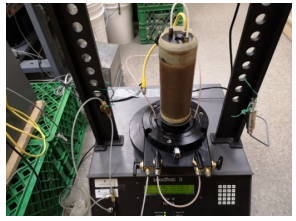
PROJECT NO. A03355A01
PROJECT :
SAMPLE : Fine Gradation
TEST NO. : TXBD10 e=0.7

DATE : 2019-11-03
TESTED BY: BY
CHECKED BY: JG

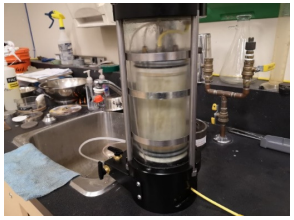
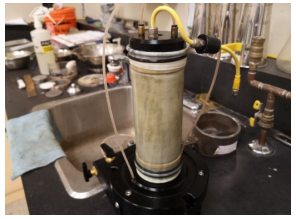
SPECIMEN INFORMATION	UNITS	Initial	Vacuum	Saturation	B value	End 1st Cons	End 2nd Cons	End 3rd Cons	End 4th Cons	End 5th Cons	End 6th Cons	End 7th Cons	End 8th Cons	End 9th Cons
Specimen Height	mm	140.51	140.51	140.51	140.41	140.37	140.31	140.22	140.13	140.04	139.97	139.92	139.86	139.80
Specimen Diameter	mm	70.23	70.23	70.23	70.22	70.18	70.15	70.12	70.07	70.03	70.00	69.97	69.95	69.91
Area	cm^2	38.74	38.74	38.74	38.73	38.68	38.65	38.62	38.56	38.52	38.49	38.46	38.43	38.39
Volume	cm^3	544.305	544.305	544.305	543.805	543.017	542.312	541.494	540.310	539.446	538.707	538.071	537.477	536.664
Wet Weight	g	1681.16	1681.16	1782.96	1787.54	1786.75	1786.05	1785.23	1784.05	1783.18	1782.44	1781.81	1781.22	1780.40
Water Content	%	8.08	8.08	14.62	14.92	14.87	14.82	14.77	14.69	14.64	14.59	14.55	14.51	14.46
Dry Weight	g	1555.48	1555.48	1555.48	1555.48	1555.48	1555.48	1555.48	1555.48	1555.48	1555.48	1555.48	1555.48	1555.48
Wet Density	g/cm^3	3.089	3.089	3.276	3.287	3.290	3.293	3.297	3.302	3.306	3.309	3.311	3.314	3.318
Dry Density	g/cm^3	2.858	2.858	2.858	2.860	2.865	2.868	2.873	2.879	2.883	2.887	2.891	2.894	2.898
Specific Gravity of Solids	-	4.96	4.96	4.96	4.96	4.96	4.96	4.96	4.96	4.96	4.96	4.96	4.96	4.96
Solids Volume	cm^3	313.604	313.604	313.604	313.604	313.604	313.604	313.604	313.604	313.604	313.604	313.604	313.604	313.604
Void Volume	cm^3	230.701	230.701	230.701	230.201	229.412	228.707	227.890	226.706	225.841	225.102	224.467	223.873	223.059
Water Volume	cm^3	125.683	125.683	227.483	232.066	231.277	230.572	229.755	228.571	227.706	226.967	226.332	225.738	224.924
Void Ratio (e)	-	0.736	0.736	0.736	0.734	0.732	0.729	0.727	0.723	0.720	0.718	0.716	0.714	0.711
Saturation Ratio (Sr)	%	54.48	54.48	98.61	100.81	100.81	100.82	100.82	100.82	100.83	100.83	100.83	100.83	100.84
Effective Confining Stress	kPa					50	100	200	400	600	800	1000	1200	1500
Mean Shear Wave Velocity	m/s					**158.81**	**185.57**	**220.87**	**258.04**	**283.57**	**304.66**	**315.80**	**329.14**	**354.89**
Mean Shear Modulus	MPa					**82.99**	**113.42**	**160.84**	**219.86**	**265.80**	**307.12**	**330.27**	**359.16**	**417.83**

Photos:

Before Test

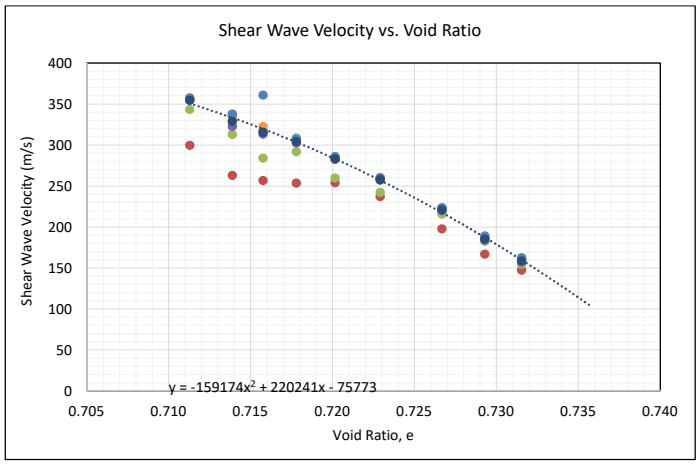
After Test

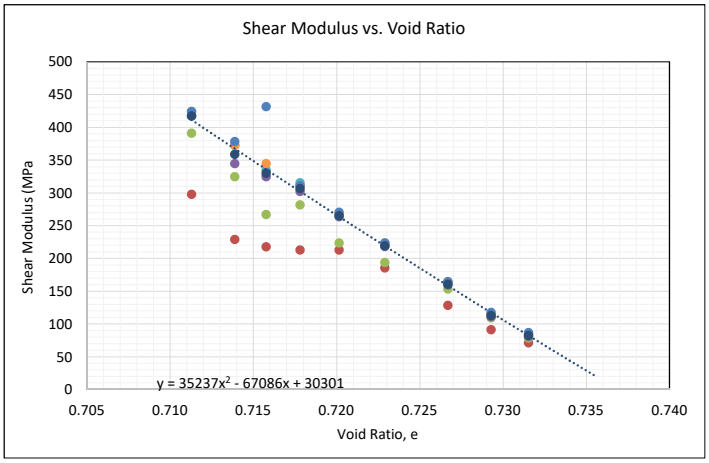



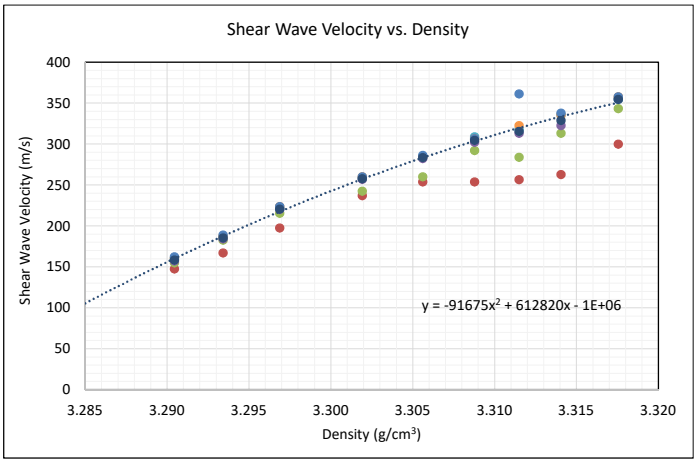
Triaxial Bender Element Test - Charts

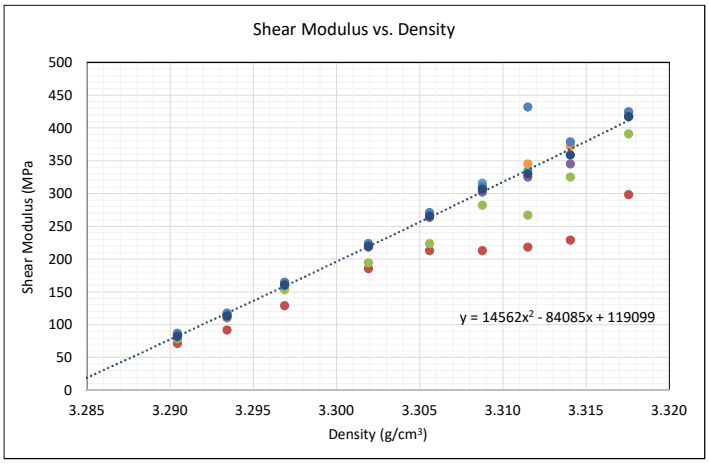
PROJECT NO. : A03355A01
PROJECT :
SAMPLE : Fine Gradation
TEST NO. : TXBD10 e=0.7

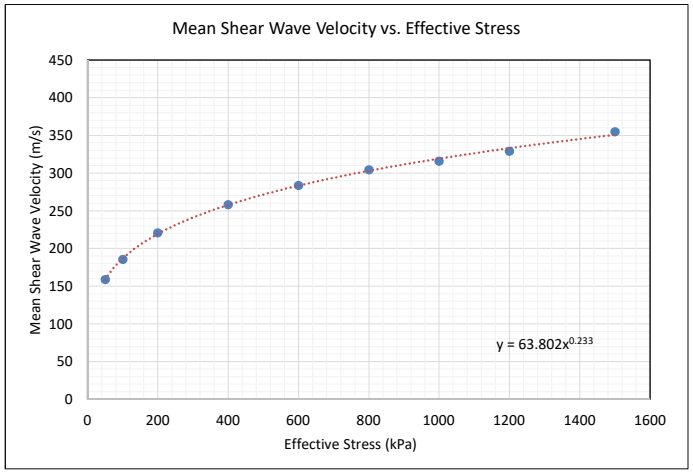
DATE : 2019-11-03
TEST BY: BY
CHECKED BY: JG

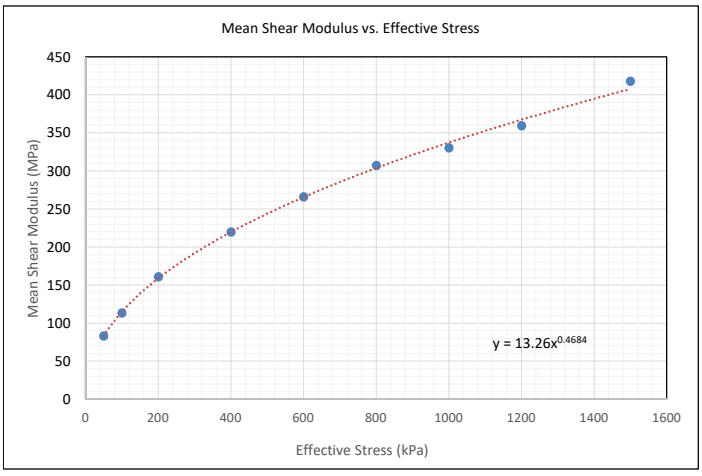




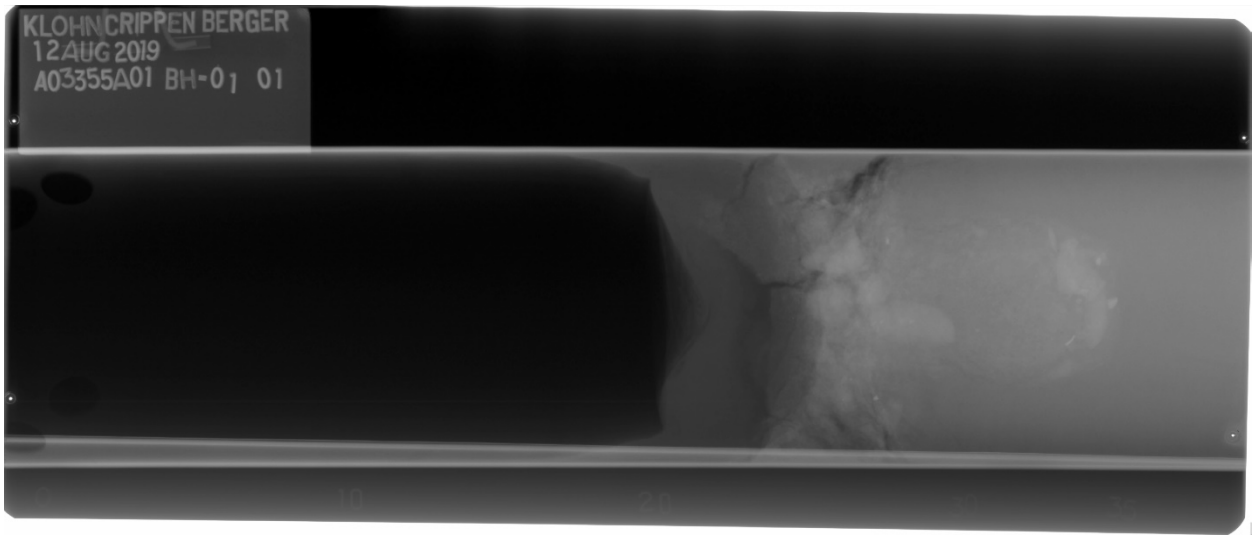


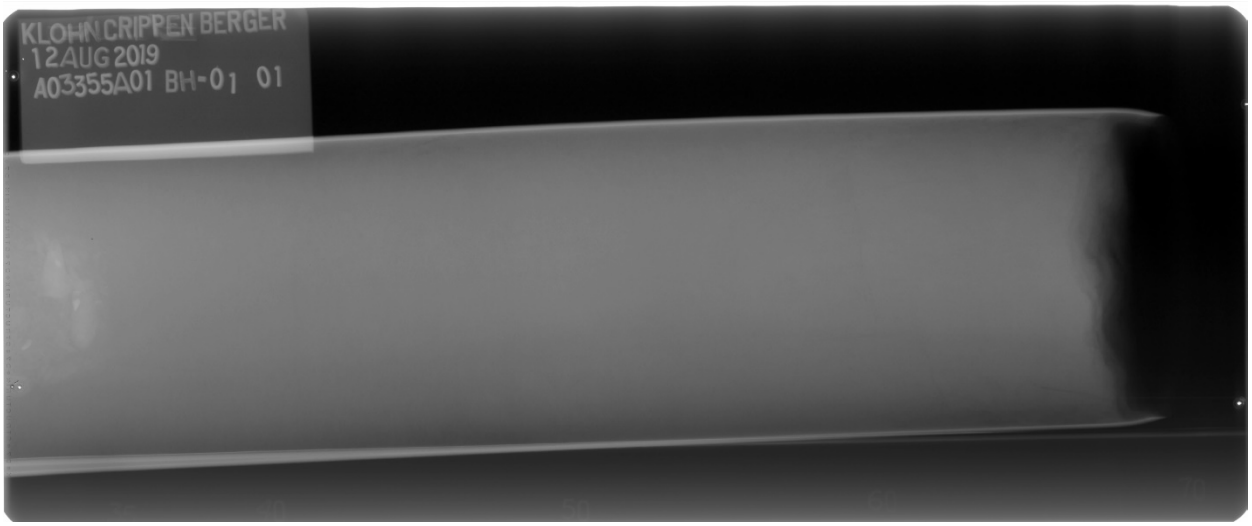


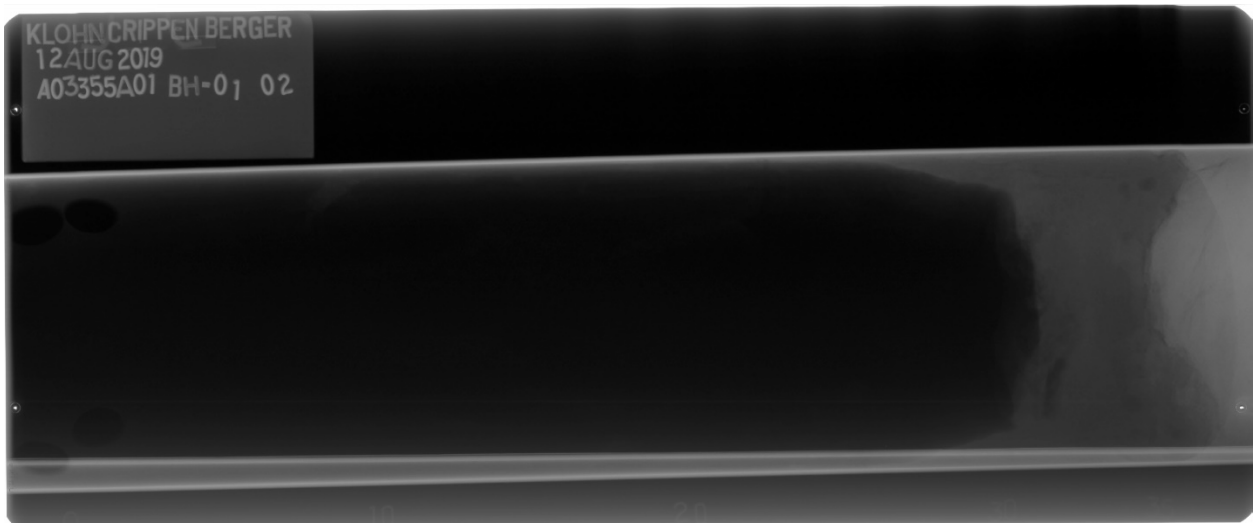




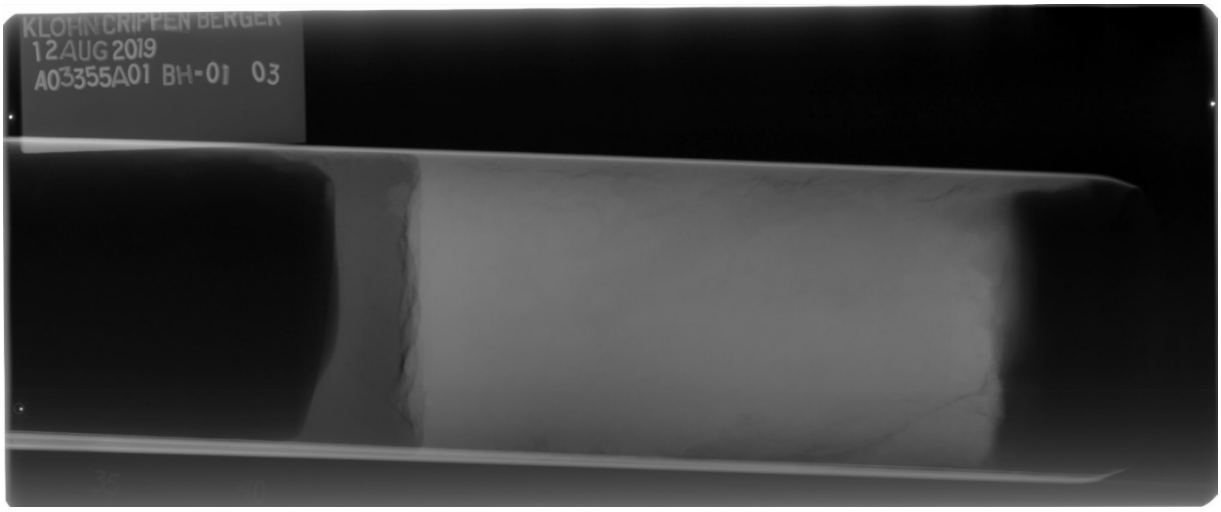
Shelby Tube X-Ray Scans

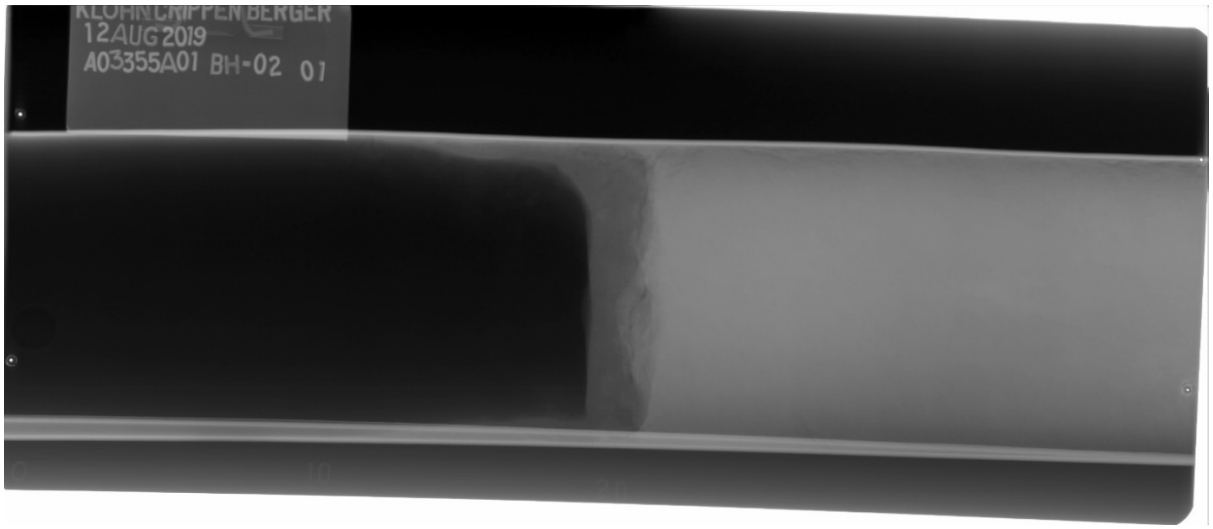

KLOHN CRIPPEN BERGER
12 AUG 2019
A03355A01 BH-01 01

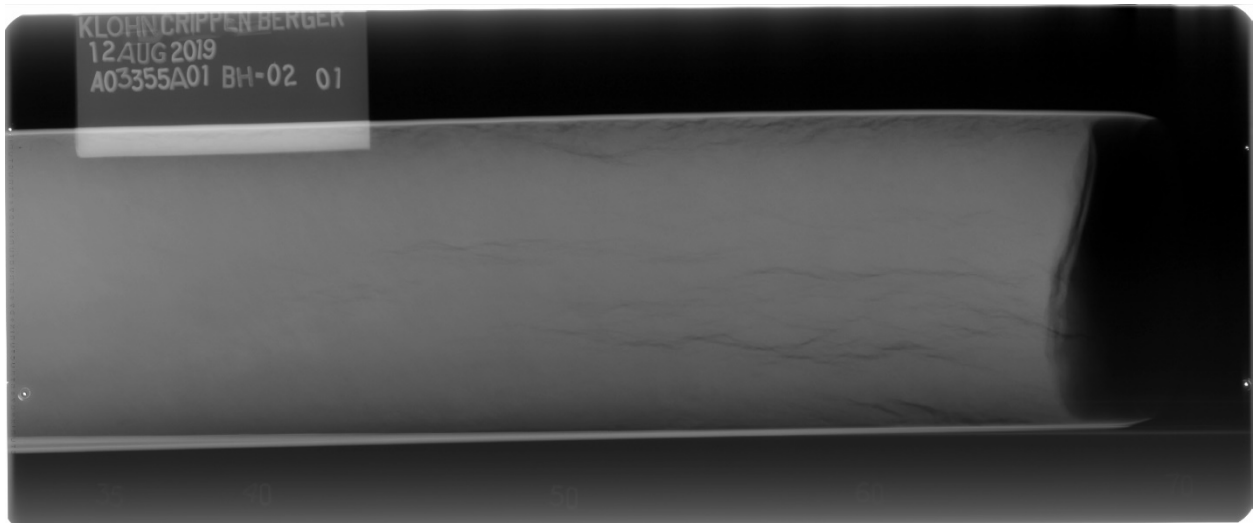

KLOHN CRIPPEN BERGER
12 AUG 2019
A03355A01 BH-01 01

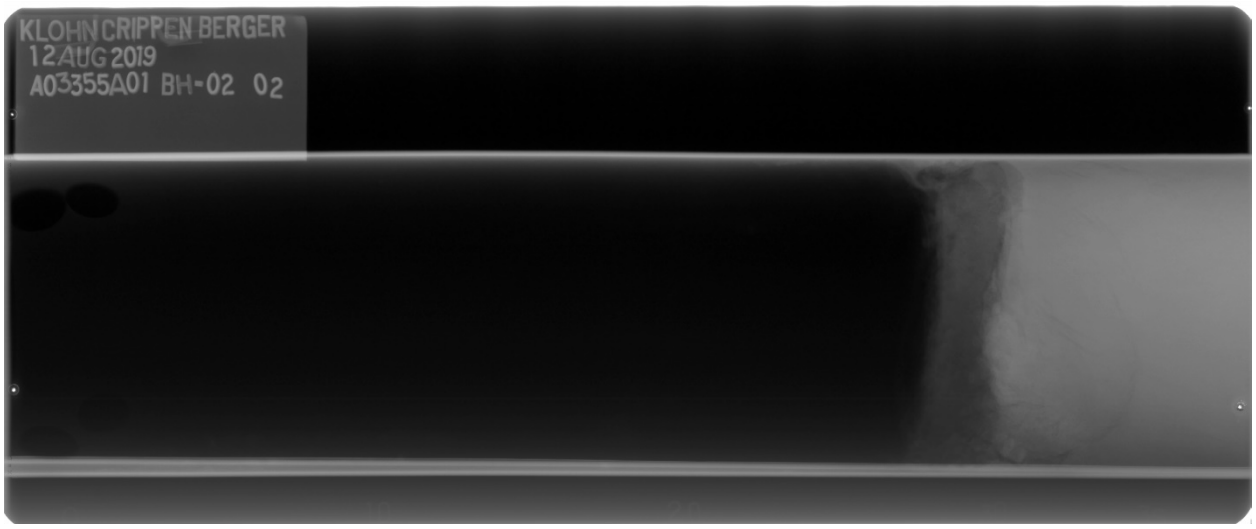

KLOHN CRIPPEN BERGER
12 AUG 2019
A03355A01 BH-01 02


KLOHN CRIPPEN BERGER
12 AUG 2019
A03355A01 BH-01 02

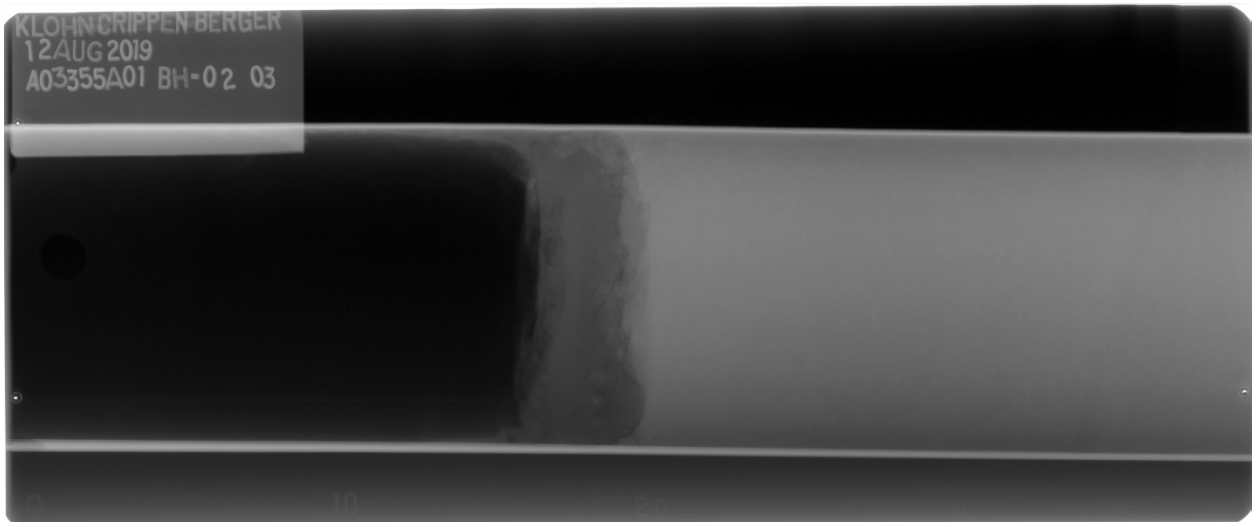

12 AUG 2019
A03355A01 BH-01 03


KLOHN CRIPPEN BERGER
12 AUG 2019
A03355A01 BH-02 01

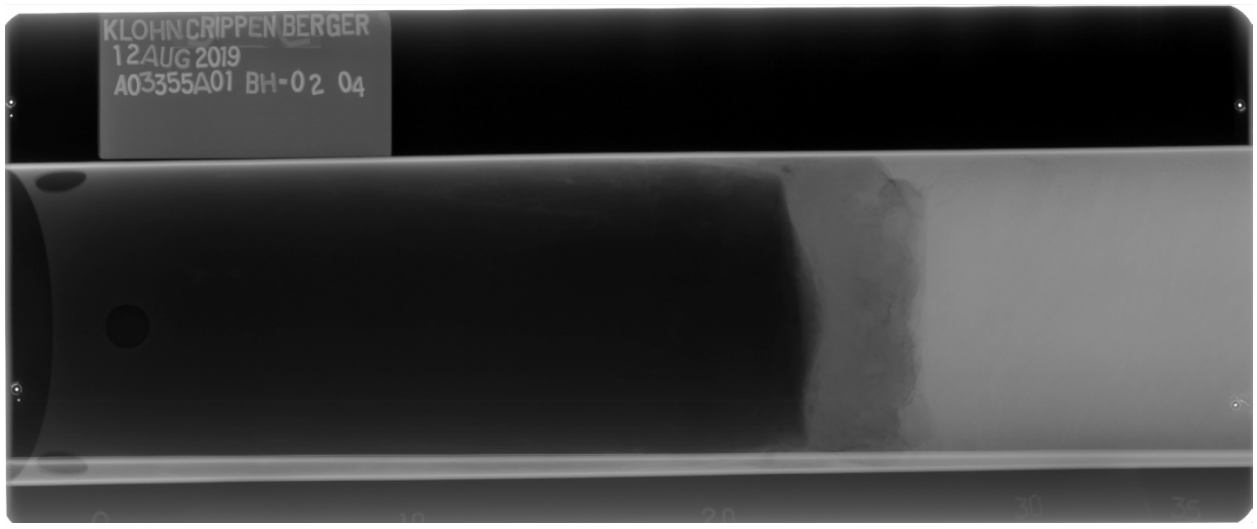

KLOHN CRIPPEN BERGER
12 AUG 2019
A03355A01 BH-02 01

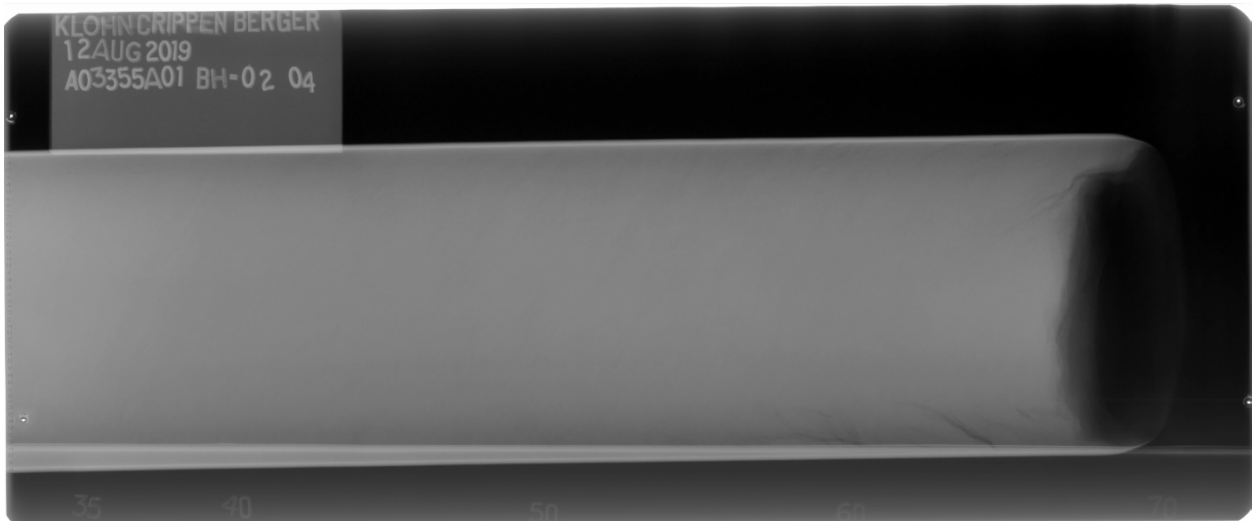

KLOHN CRIPPEN BERGER
12 AUG 2019
A03355A01 BH-02 02

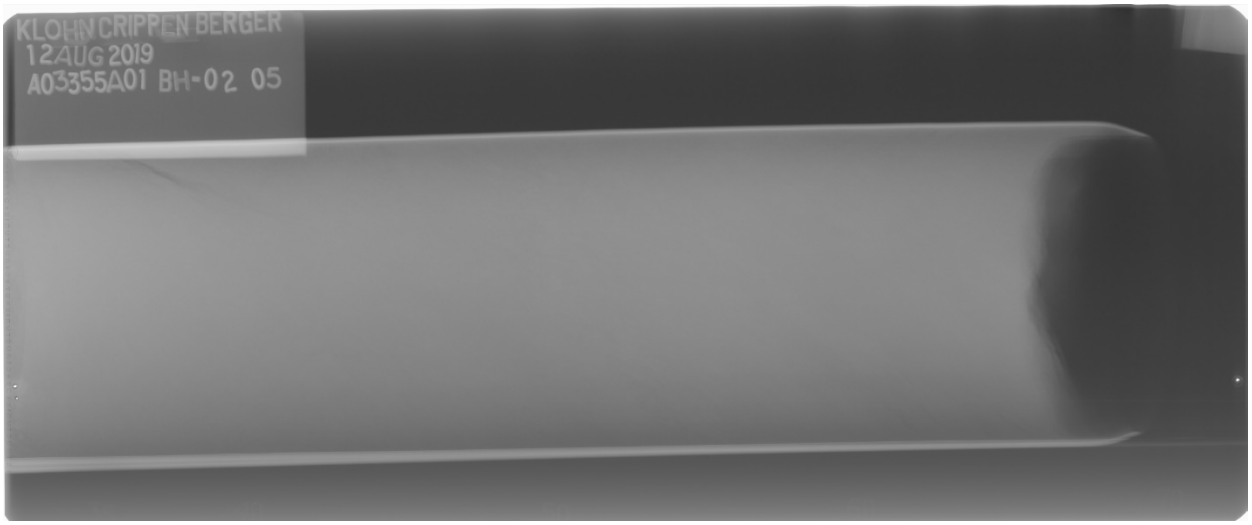

KLOHN CRIPPEN BERGER
12 AUG 2019
A03355A01 BH-02 02

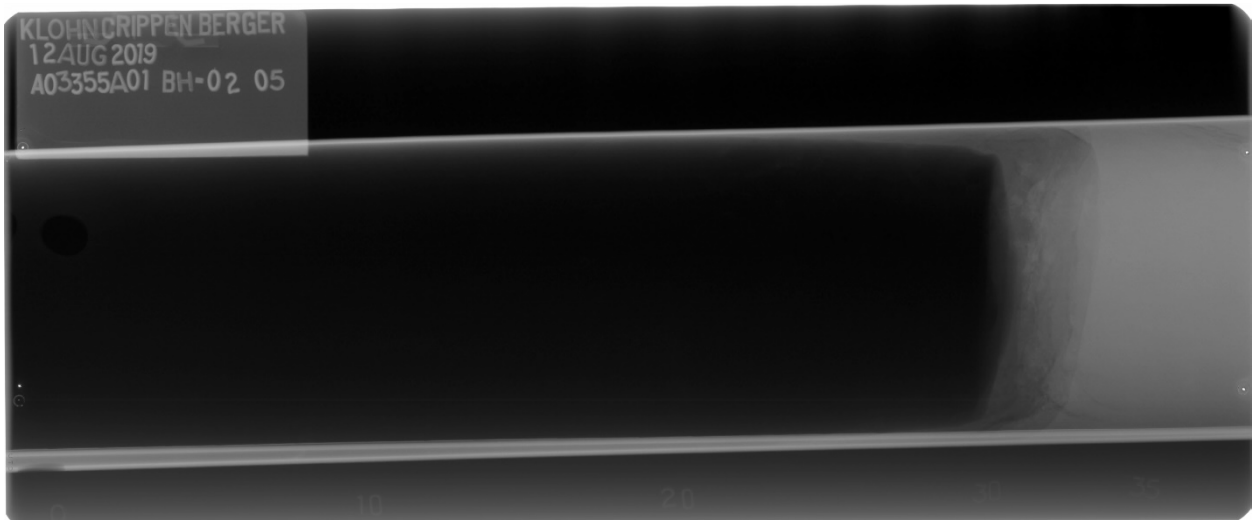

KLOHN CRIPPEN BERGER
12 AUG 2019
A03355A01 BH-02 03

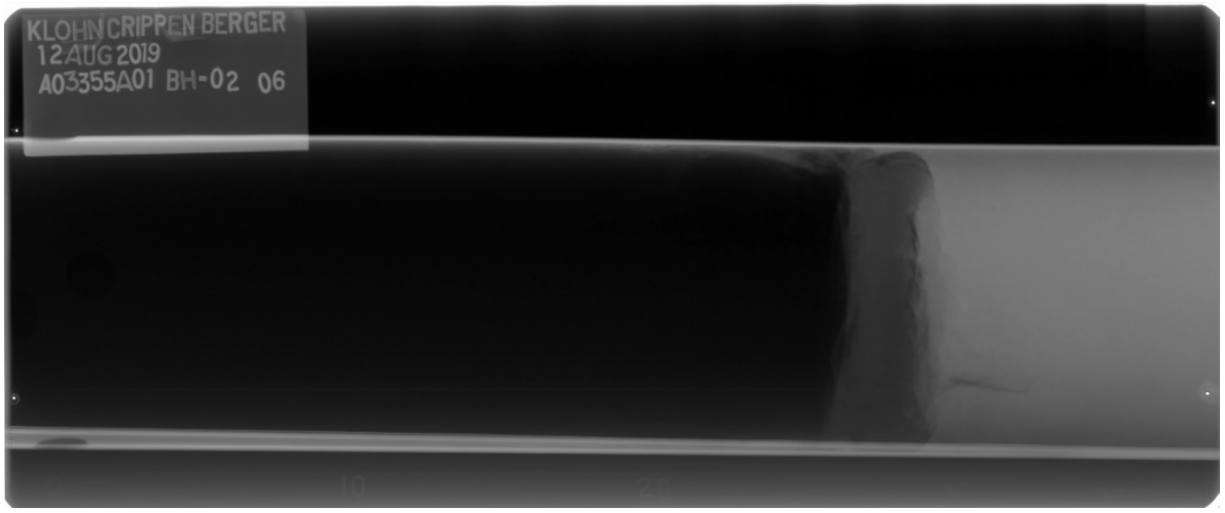

KLOHN CRIPPEN BERGER
12 AUG 2019
A03355A01 BH-02 03


KLOHN CRIPPEN BERGER
12 AUG 2019
A03355A01 BH-02 04


KLOHN CRIPPEN BERGER
12 AUG 2019
A03355A01 BH-02 04

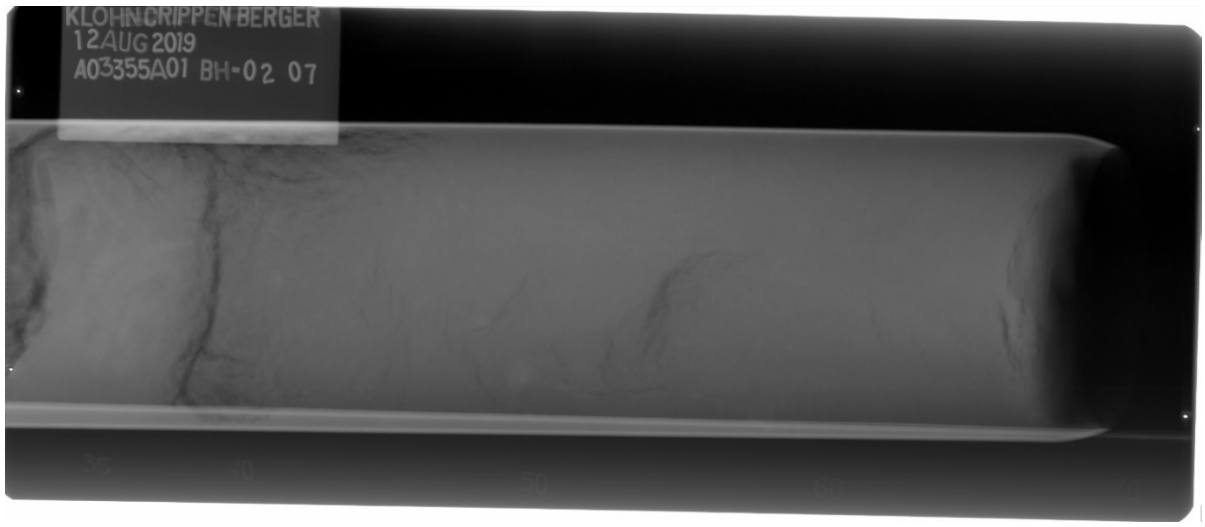

KLOHN CRIPPEN BERGER
12 AUG 2019
A03355A01 BH-02 05

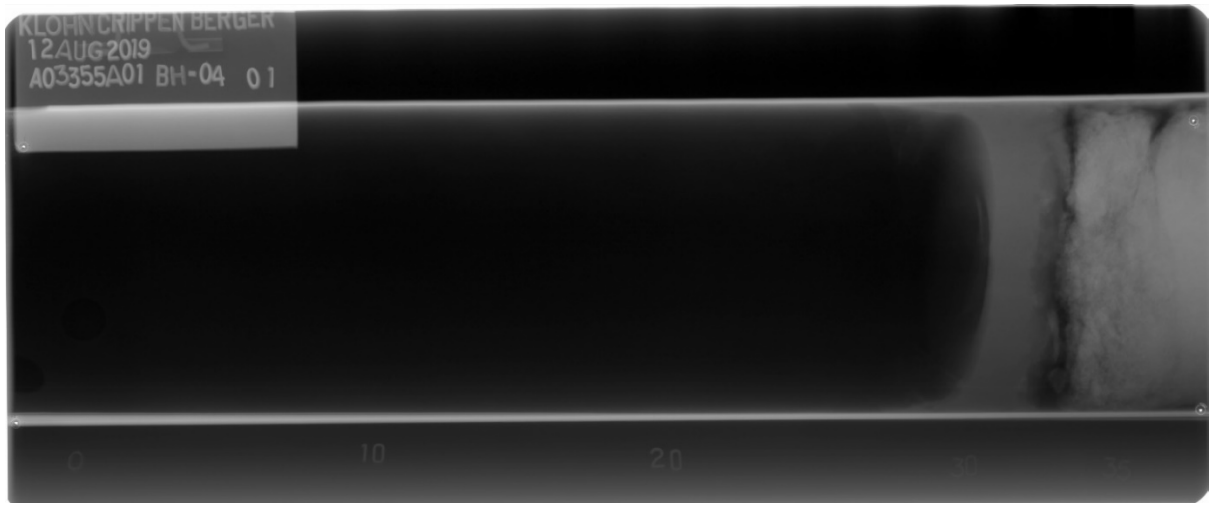

KLOHN CRIPPEN BERGER
12 AUG 2019
A03355A01 BH-02 05


KLOHN CRIPPEN BERGER
12 AUG 2019
A03355A01 BH-02 06

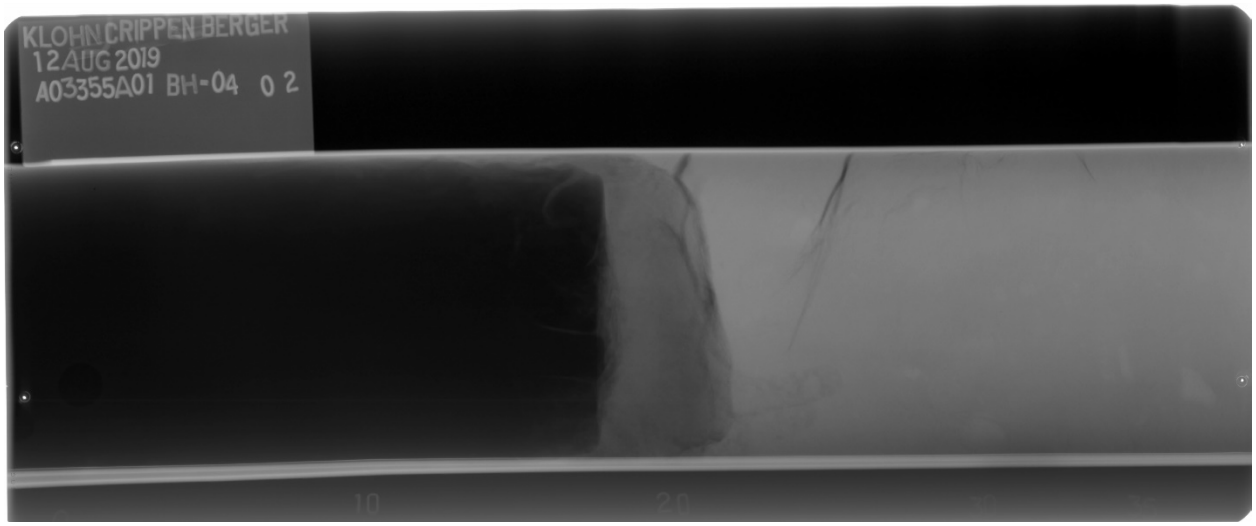

KLOHN CRIPPEN BERGER
12 AUG 2019
A03355A01 BH-02 06


KLOHN CRIPPEN BERGER
12 AUG 2019
A03355A01 BH-02 07


KLOHN CRIPPEN BERGER
12 AUG 2019
A03355A01 BH-02 07


KLOHN CRIPPEN BERGER
12 AUG 2019
A03355A01 BH-04 01


KLOHN CRIPPEN BERGER
12 AUG 2019
A03355A01 BH-04 01


KLOHN CRIPPEN BERGER
12 AUG 2019
A03355A01 BH-04 02


KLOHN CRIPPEN BERGER
12 AUG 2019
A03355A01 BH-04 0 2

Direct Simple Shear Test Results

Static Simple Shear Test

(ASTM D6528)

Project No.:	A03355A01	Borehole ID:	BH01
Project:		Sample ID:	Shelby1
Date:	2019-10-19	Depth:	3.50 m
Test by:	HM	Location:	Brazil
Checked by:	BY	Details:	Trimmed from Shelby Tube

Initial Sample Information		
Specimen Height	mm	23.97
Specimen Diameter	mm	70.01
Area	mm^2	3849.55
Volume	cm^3	92.27
Wet Weight	g	169.39
Water Content	%	35.49
Dry Weight	g	125.02
Wet Density	g/cm^3	1.836
Dry Density	g/cm^3	1.355
Specific Gravity (measured)	-	2.79
Void Ratio (e)	-	1.06
Saturation Ratio (Sr)	%	93.48

Static Shearing (Undrained)		
Initial Vertical Effective Stress	kPa	520
Initial Shear Stress	kPa	0.6
Shearing Rate (Shear Strain Rate)	% / hr	5.00
Peak Shear Strength	kPa	174.62
Ratio of Peak τ/σ'_v	-	0.34
Max. Excess Pore Pressure	kPa	386.33
Max. Shear Strain	%	20.0

FINAL SAMPLE INFORMATION		
Liquid Limit (test sample)		
Plastic Limit (test sample)		
Liquid Limit (shear plane)		
Plastic Limit (shear plane)		
Final Moisture Content	%	36.66
Final Moisture Content (shear plane)	%	
Final Moisture Content (outside shear plane)	%	

CONSOLIDATION	Stage #	1	2	3	4	5			
Vertical Effective Stress	kPa	32	65	130	260	520			
Max Load	kN	0.124	0.249	0.500	1.000	2.001			
Total Height Change	mm	0.18	0.36	0.69	1.20	1.88			
Consolidated Height	mm	23.79	23.61	23.28	22.77	22.09			
Axial Strain *2	%	0.76	1.50	2.89	5.00	7.85			
Duration	min	240	240	320	320	322			

*2 : Axial strain may differ from oedometer test result due to the sample seating system and possible lateral strain caused by the membrane.

Photos:

Before Test





After Test

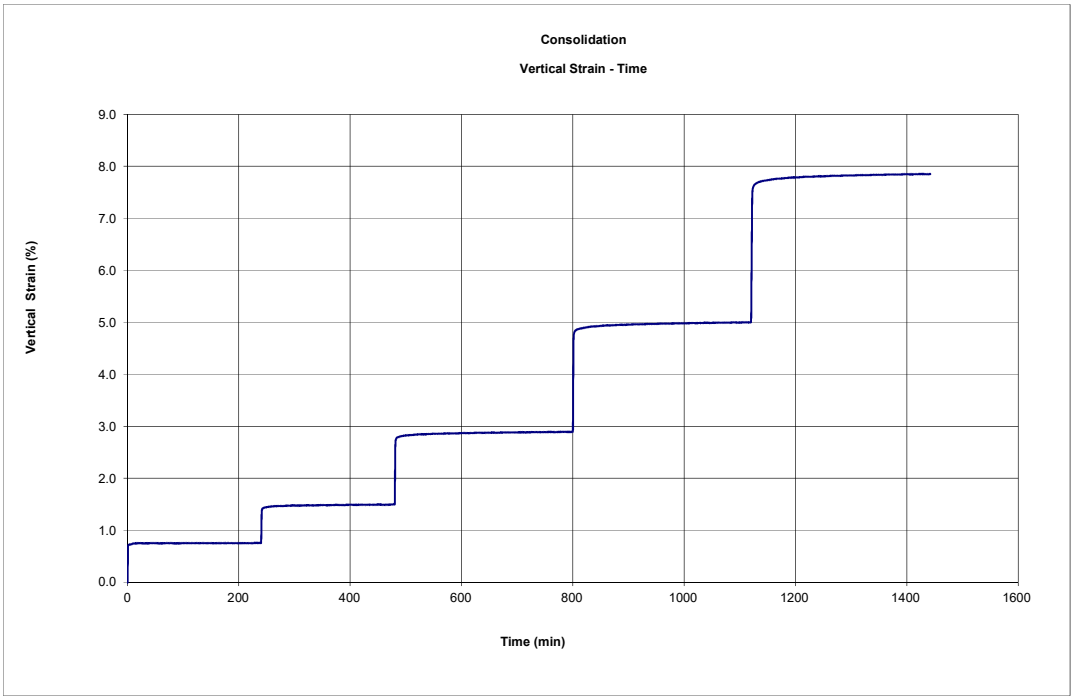


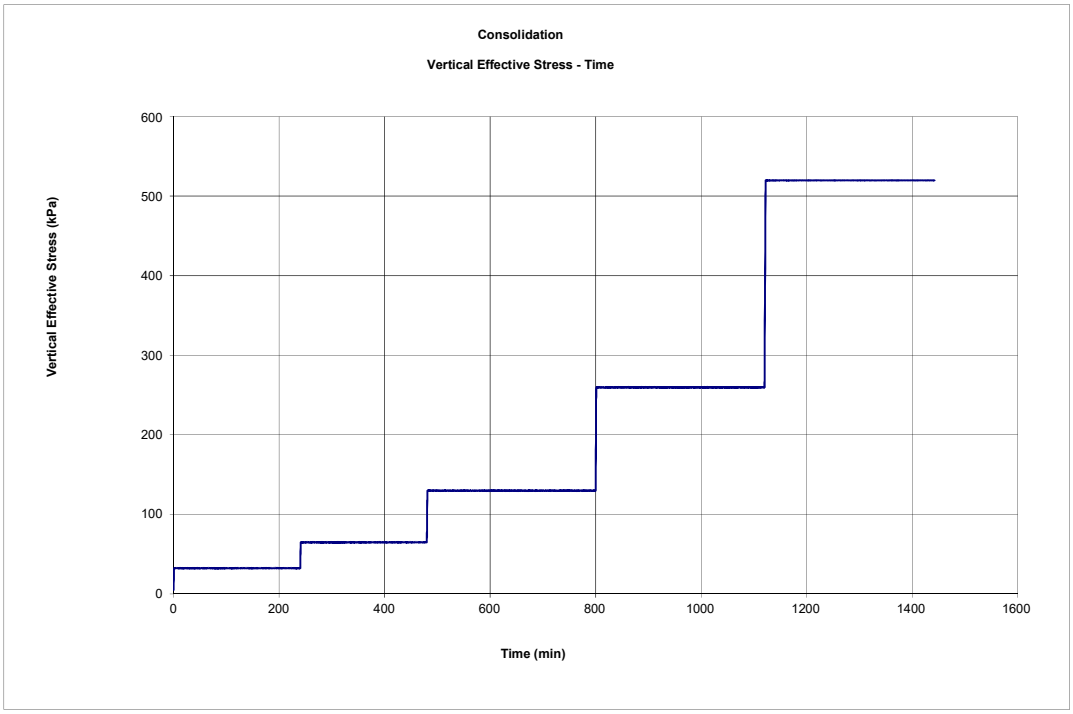


Static Simple Shear Test

(ASTM D6528)

Project No.:	A03355A01	Borehole ID:	BH01
Project:		Sample ID:	Shelby1
Date:	2019-10-19	Depth:	3.50 m
Tested by:	HM	Location:	Brazil
Checked by:	BY	Details:	Trimmed from Shelby Tube

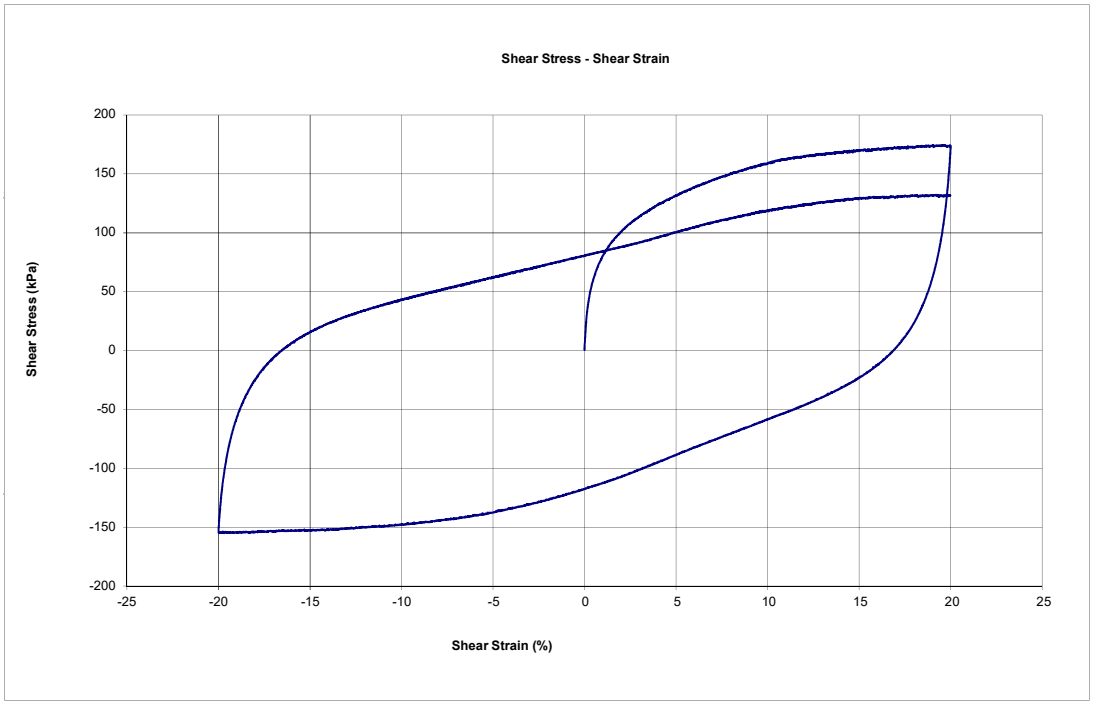


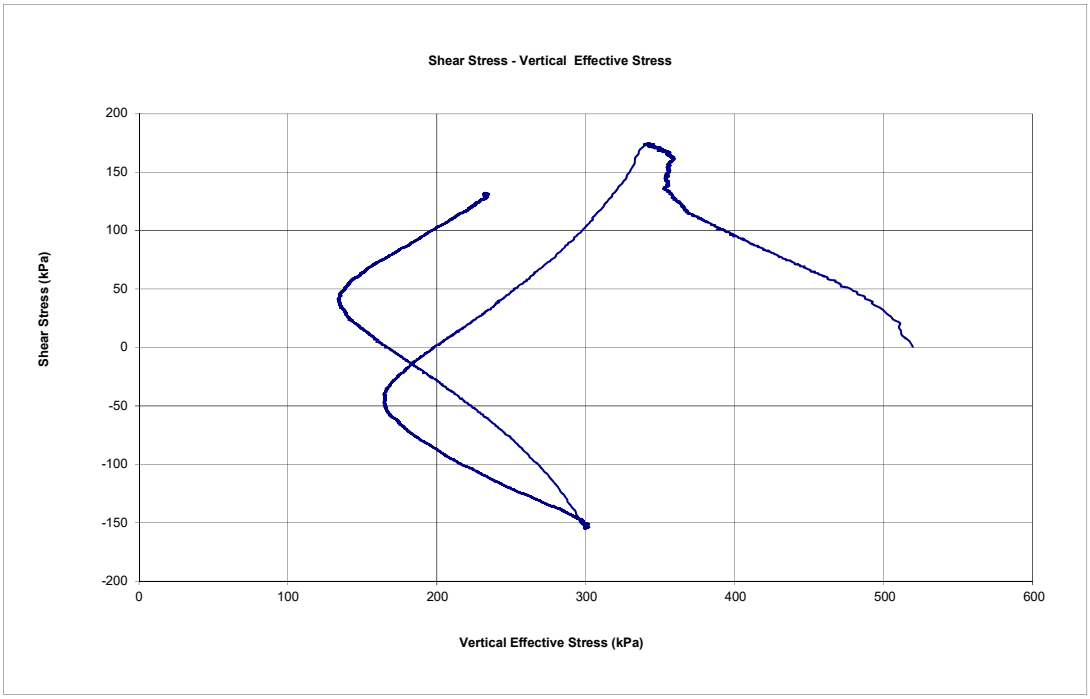


Static Simple Shear Test

(ASTM D6528)

Project No.:	A03355A01	Borehole ID:	BH01
Project:		Sample ID:	Shelby1
Date:	2019-10-19	Depth:	3.50 m
Tested by:	HM	Location:	Brazil
Checked by:	BY	Details:	Trimmed from Shelby Tube

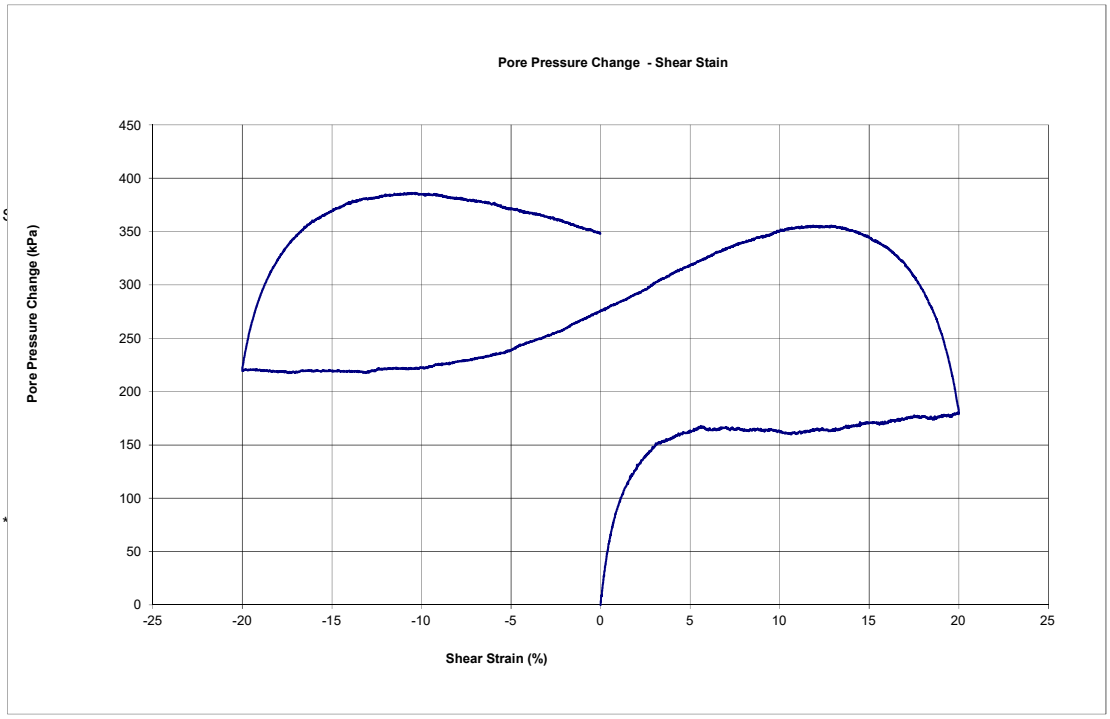


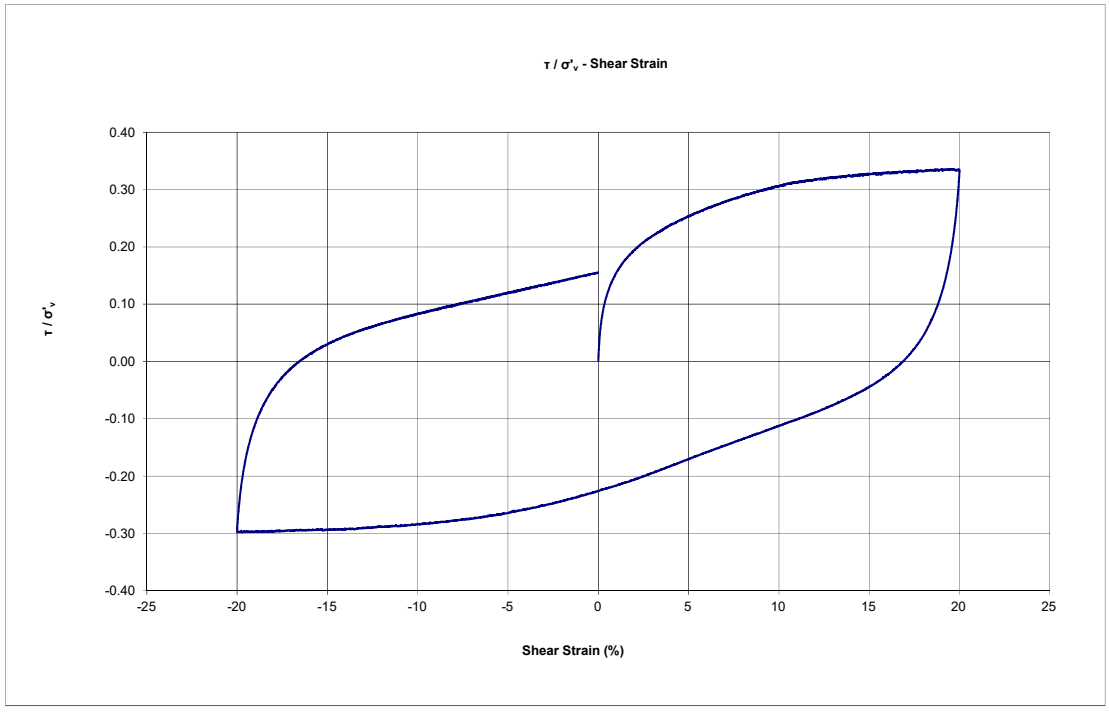


Static Simple Shear Test

(ASTM D6528)

Project No.:	A03355A01	Borehole ID:	BH01
Project:		Sample ID:	Shelby1
Date:	2019-10-19	Depth:	3.50 m
Tested by:	HM	Location:	Brazil
Checked by:	BY	Details:	Trimmed from Shelby Tube





Static Simple Shear Test

(ASTM D6528)

Project No.:	A03355A01	Borehole ID:	BH01
Project:		Sample ID:	Shelby2
Date:	2019-10-17	Depth:	4.50 m
Test by:	HM	Location:	Brazil
Checked by:	BY	Details:	Trimmed from Shelby Tube

Initial Sample Information		
Specimen Height	mm	23.97
Specimen Diameter	mm	70.05
Area	mm^2	3853.95
Volume	cm^3	92.38
Wet Weight	g	161.21
Water Content	%	38.31
Dry Weight	g	116.56
Wet Density	g/cm^3	1.745
Dry Density	g/cm^3	1.262
Specific Gravity (measured)	-	2.79
Void Ratio (e)	-	1.21
Saturation Ratio (Sr)	%	88.24

Static Shearing (Undrained)		
Initial Vertical Effective Stress	kPa	520
Initial Shear Stress	kPa	0.5
Shearing Rate (Shear Strain Rate)	% / hr	5.00
Peak Shear Strength	kPa	184.15
Ratio of Peak τ/σ'_v	-	0.35
Max. Excess Pore Pressure	kPa	406.05
Max. Shear Strain	%	20.0

FINAL SAMPLE INFORMATION		
Liquid Limit (test sample)		
Plastic Limit (test sample)		
Liquid Limit (shear plane)		
Plastic Limit (shear plane)		
Final Moisture Content	%	39.56
Final Moisture Content (shear plane)	%	
Final Moisture Content (outside shear plane)	%	

CONSOLIDATION	Stage #	1	2	3	4	5			
Vertical Effective Stress	kPa	32	65	130	260	520			
Max Load	kN	0.125	0.249	0.500	1.001	2.003			
Total Height Change	mm	0.23	0.40	0.66	1.00	1.60			
Consolidated Height	mm	23.74	23.57	23.31	22.97	22.37			
Axial Strain *2	%	0.97	1.69	2.73	4.17	6.69			
Duration	min	120	180	300	300	299			

*2 : Axial strain may differ from oedometer test result due to the sample seating system and possible lateral strain caused by the membrane.

Photos:

Before Test





After Test

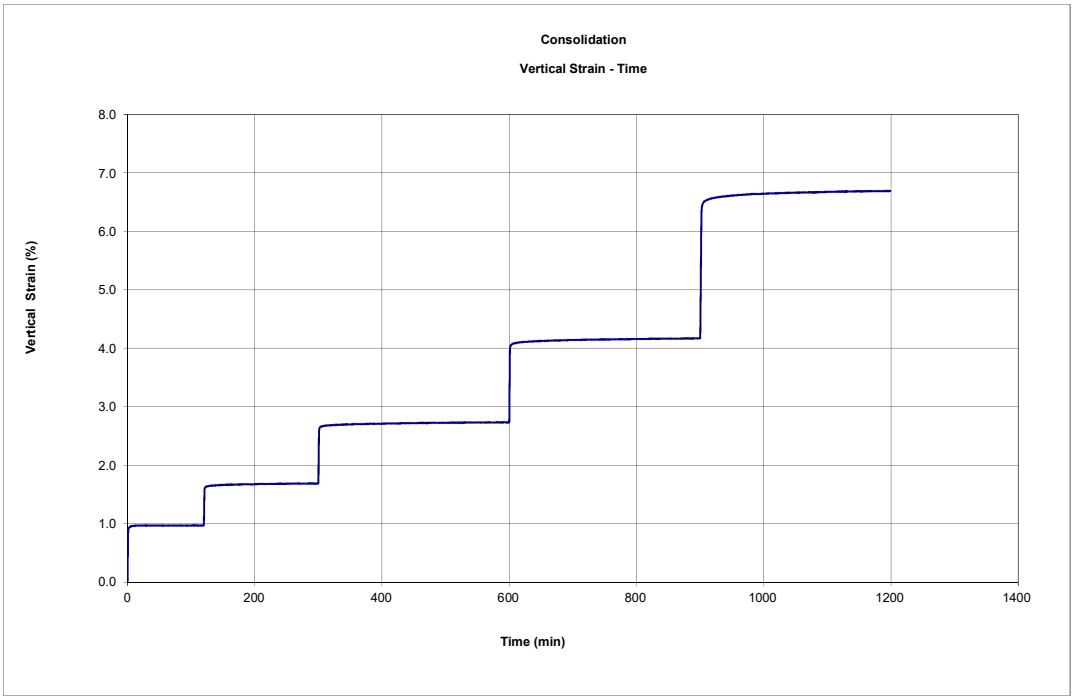


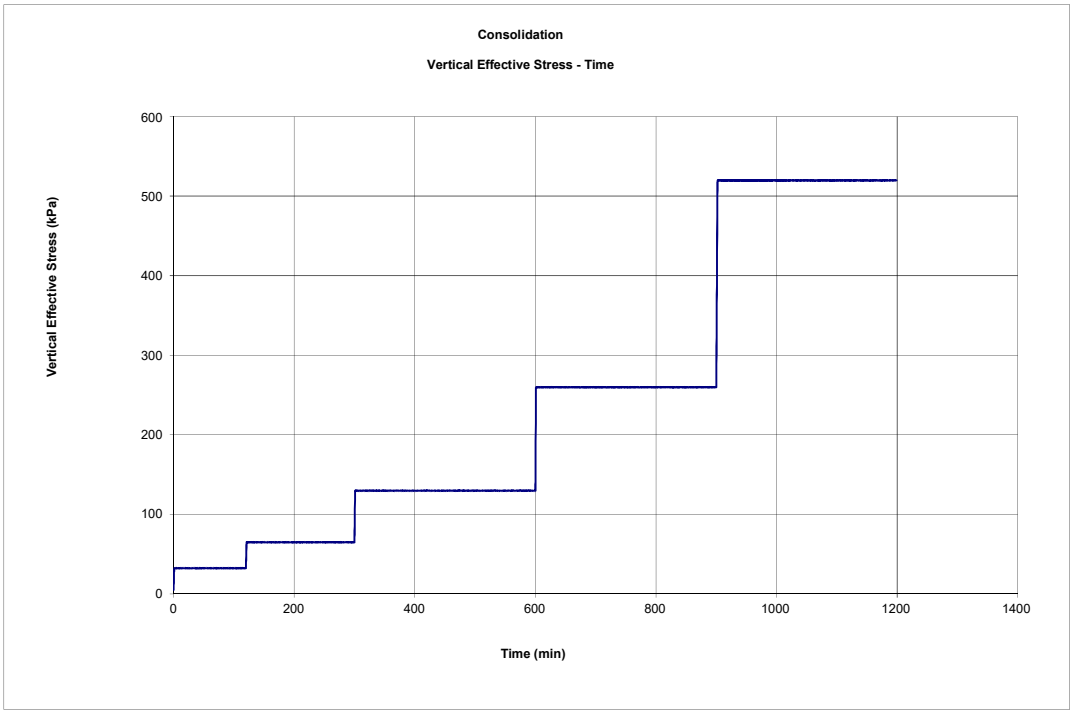


Static Simple Shear Test

(ASTM D6528)

Project No.:	A03355A01	Borehole ID:	BH01
Project:		Sample ID:	Shelby2
Date:	2019-10-17	Depth:	4.50 m
Tested by:	HM	Location:	Brazil
Checked by:	BY	Details:	Trimmed from Shelby Tube

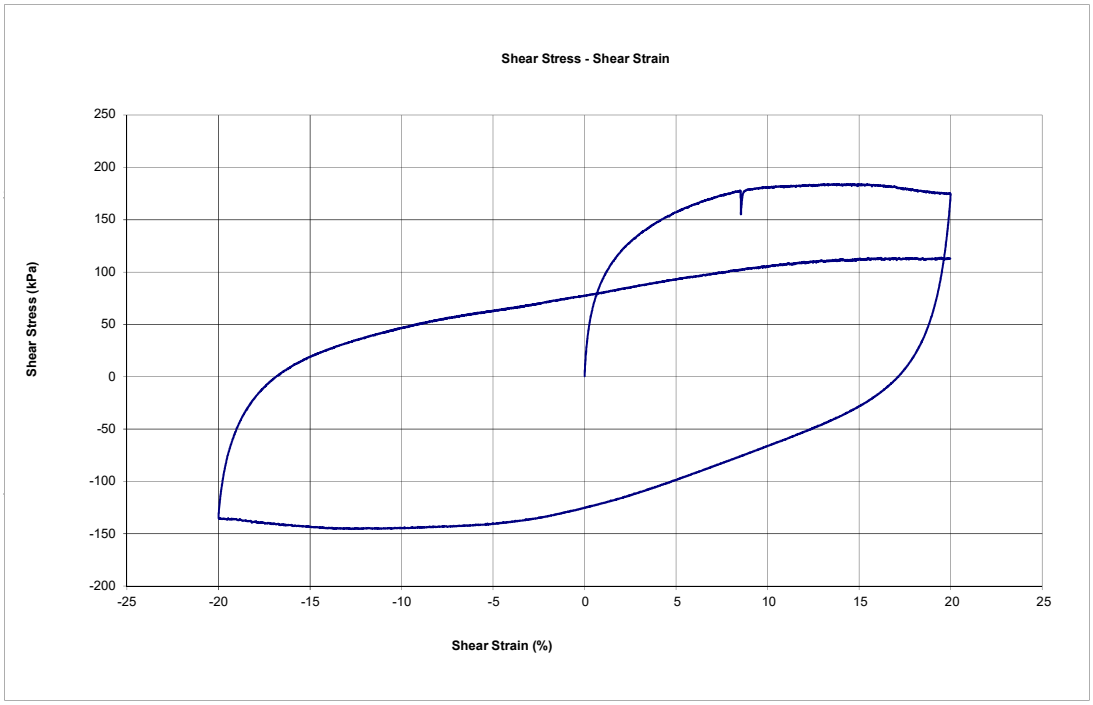


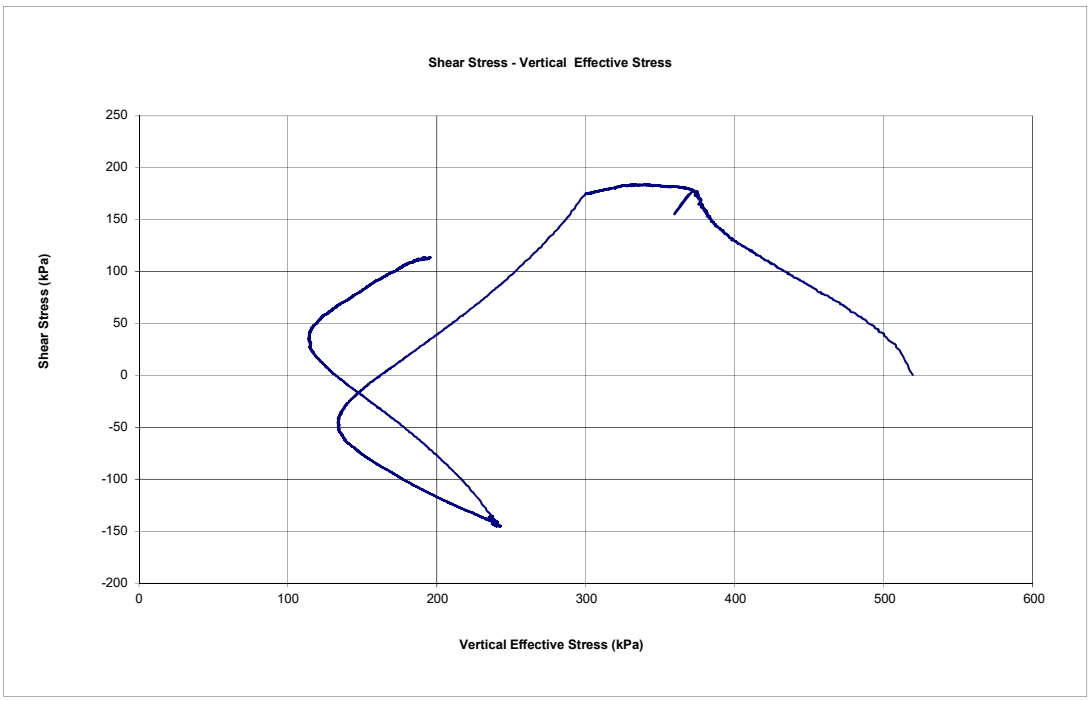


Static Simple Shear Test

(ASTM D6528)

Project No.:	A03355A01	Borehole ID:	BH01
Project:		Sample ID:	Shelby2
Date:	2019-10-17	Depth:	4.50 m
Tested by:	HM	Location:	Brazil
Checked by:	BY	Details:	Trimmed from Shelby Tube

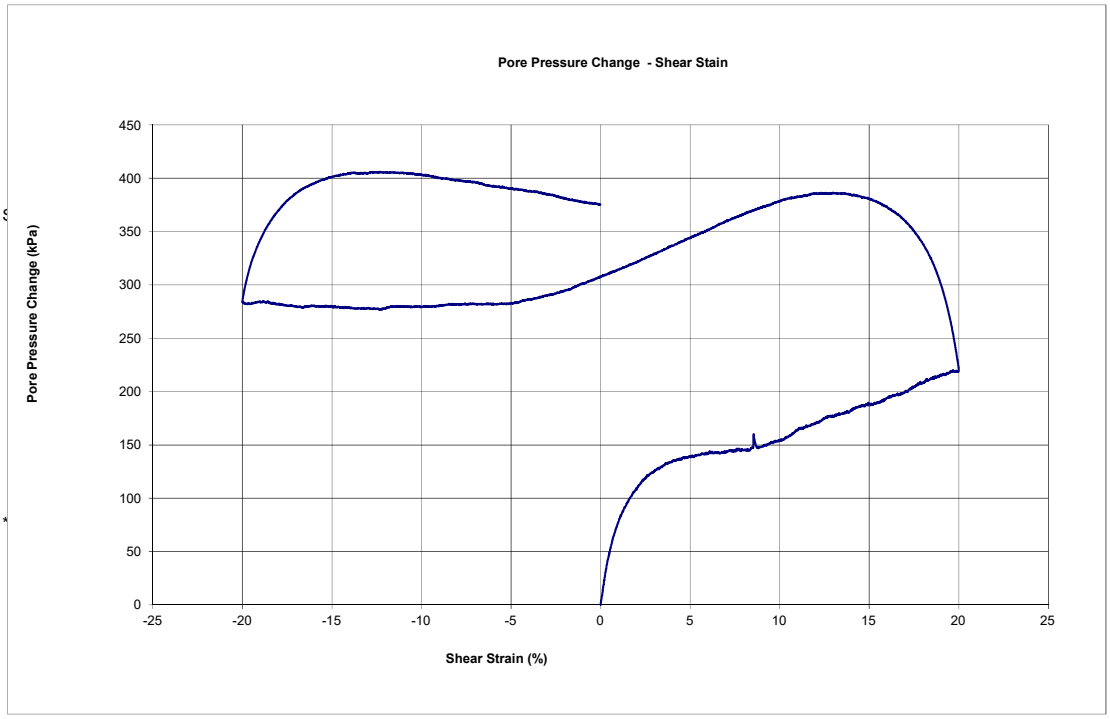


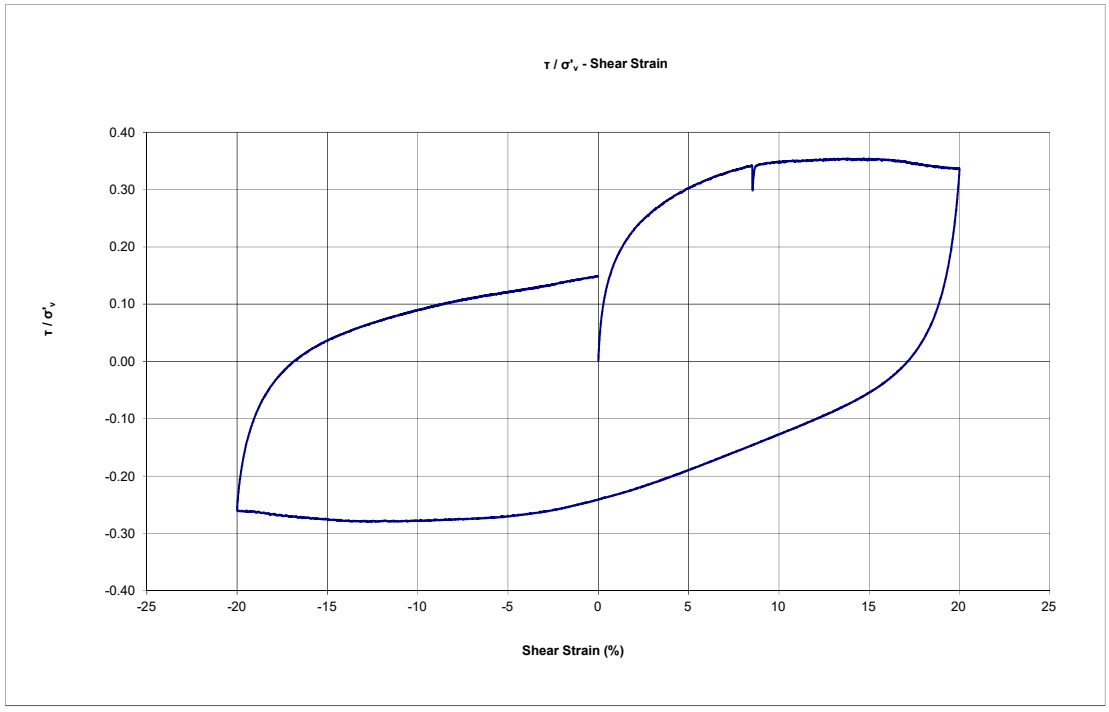


Static Simple Shear Test

(ASTM D6528)

Project No.:	A03355A01	Borehole ID:	BH01
Project:		Sample ID:	Shelby2
Date:	2019-10-17	Depth:	4.50 m
Tested by:	HM	Location:	Brazil
Checked by:	BY	Details:	Trimmed from Shelby Tube





Static Simple Shear Test

(ASTM D6528)

Project No.:	A03355A01	Borehole ID:	BH02
Project:		Sample ID:	Shelby1
Date:	2019-10-17	Depth:	3.50 m
Test by:	HM	Location:	Brazil
Checked by:	BY	Details:	Trimmed from Shelby Tube

Initial Sample Information		
Specimen Height	mm	23.98
Specimen Diameter	mm	70.02
Area	mm^2	3850.65
Volume	cm^3	92.34
Wet Weight	g	160.69
Water Content	%	43.31
Dry Weight	g	112.13
Wet Density	g/cm^3	1.740
Dry Density	g/cm^3	1.214
Specific Gravity (measured)	-	2.81
Void Ratio (e)	-	1.31
Saturation Ratio (Sr)	%	92.61

Static Shearing (Undrained)		
Initial Vertical Effective Stress	kPa	800
Initial Shear Stress	kPa	0.4
Shearing Rate (Shear Strain Rate)	% / hr	5.00
Peak Shear Strength	kPa	221.39
Ratio of Peak τ/σ'_v	-	0.28
Max. Excess Pore Pressure	kPa	656.85
Max. Shear Strain	%	20.0

FINAL SAMPLE INFORMATION		
Liquid Limit (test sample)		
Plastic Limit (test sample)		
Liquid Limit (shear plane)		
Plastic Limit (shear plane)		
Final Moisture Content	%	43.29
Final Moisture Content (shear plane)	%	
Final Moisture Content (outside shear plane)	%	

CONSOLIDATION	Stage #	1	2	3	4	5			
Vertical Effective Stress	kPa	50	100	200	400	800			
Max Load	kN	0.191	0.384	0.769	1.539	3.080			
Total Height Change	mm	0.38	0.62	1.02	1.57	2.40			
Consolidated Height	mm	23.60	23.36	22.96	22.41	21.58			
Axial Strain *2	%	1.57	2.60	4.25	6.56	10.00			
Duration	min	280	280	280	280	393			

*2 : Axial strain may differ from oedometer test result due to the sample seating system and possible lateral strain caused by the membrane.

Photos:

Before Test





After Test

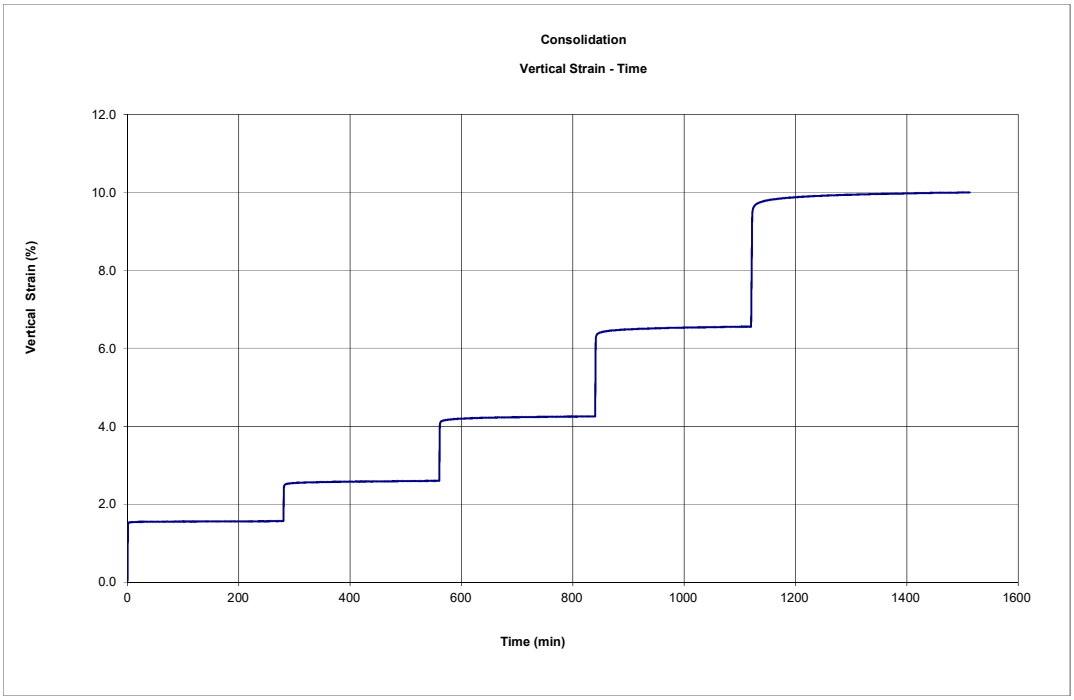


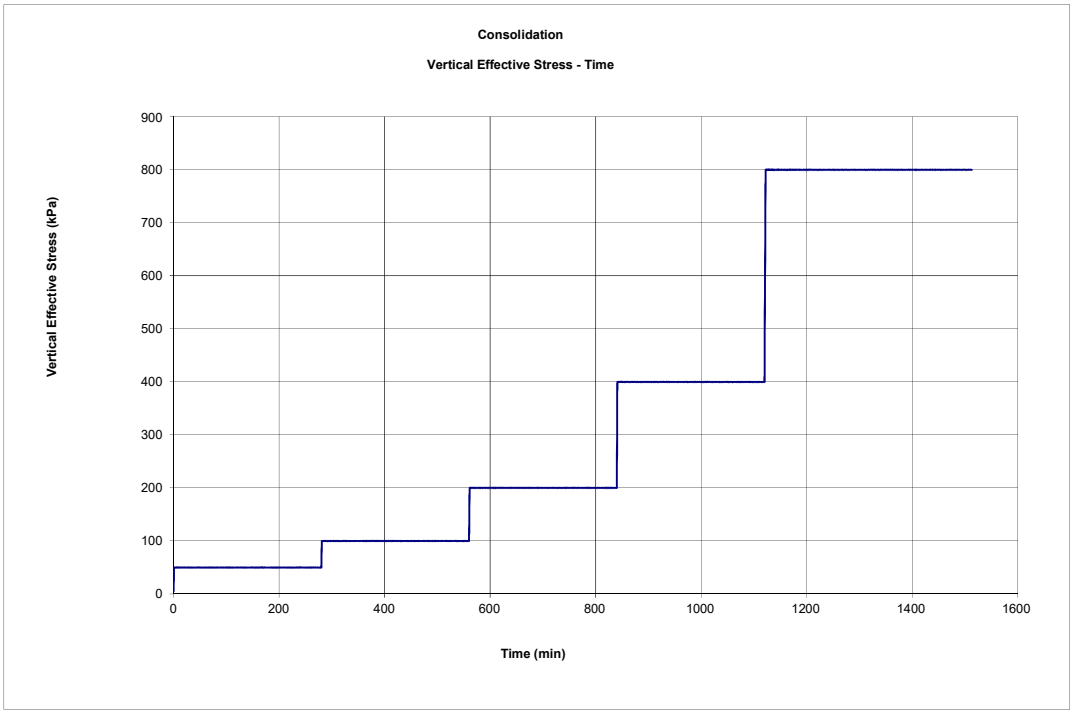


Static Simple Shear Test

(ASTM D6528)

Project No.:	A03355A01	Borehole ID:	BH02
Project:		Sample ID:	Shelby1
Date:	2019-10-17	Depth:	3.50 m
Tested by:	HM	Location:	Brazil
Checked by:	BY	Details:	Trimmed from Shelby Tube

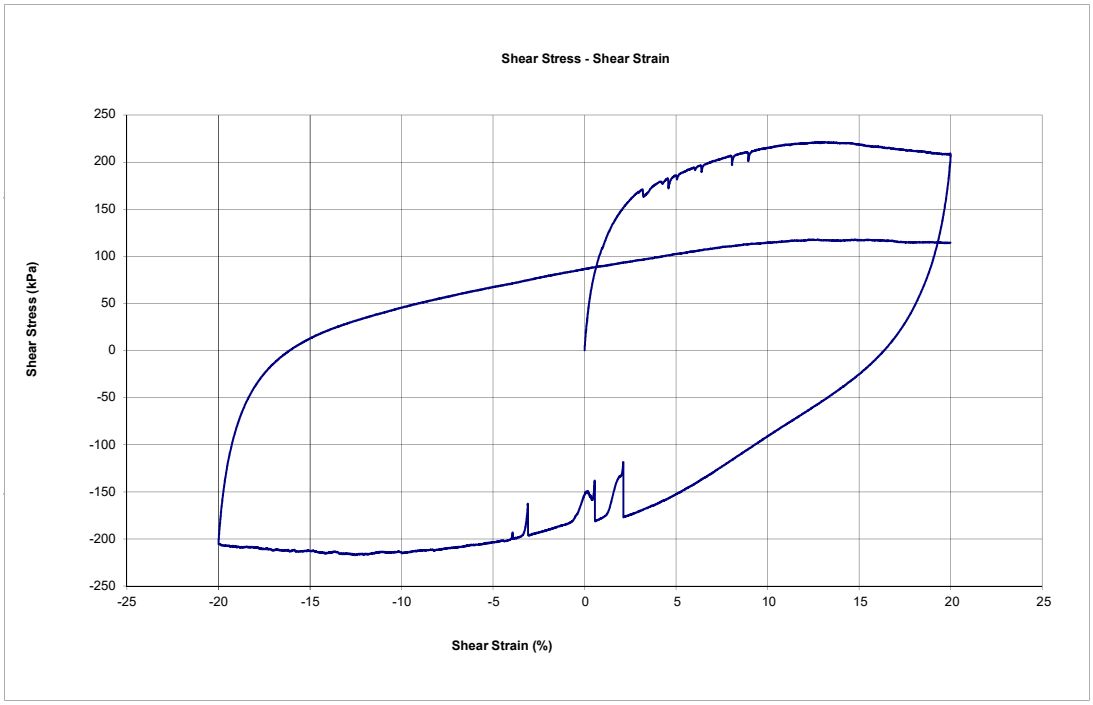


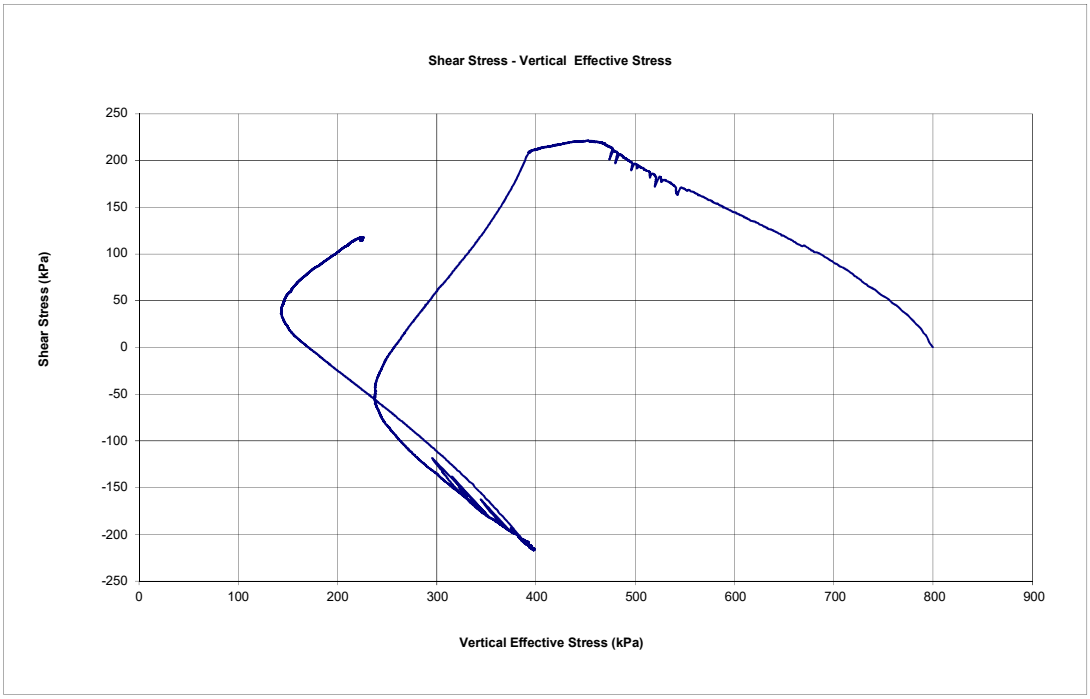


Static Simple Shear Test

(ASTM D6528)

Project No.:	A03355A01	Borehole ID:	BH02
Project:		Sample ID:	Shelby1
Date:	2019-10-17	Depth:	3.50 m
Tested by:	HM	Location:	Brazil
Checked by:	BY	Details:	Trimmed from Shelby Tube

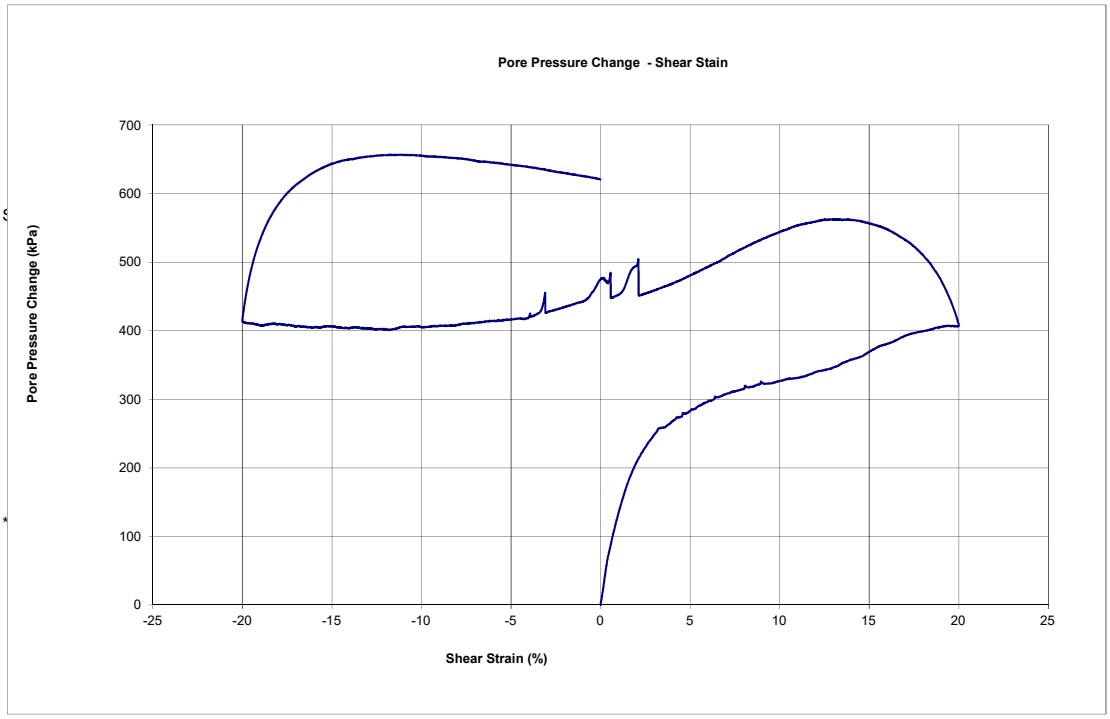


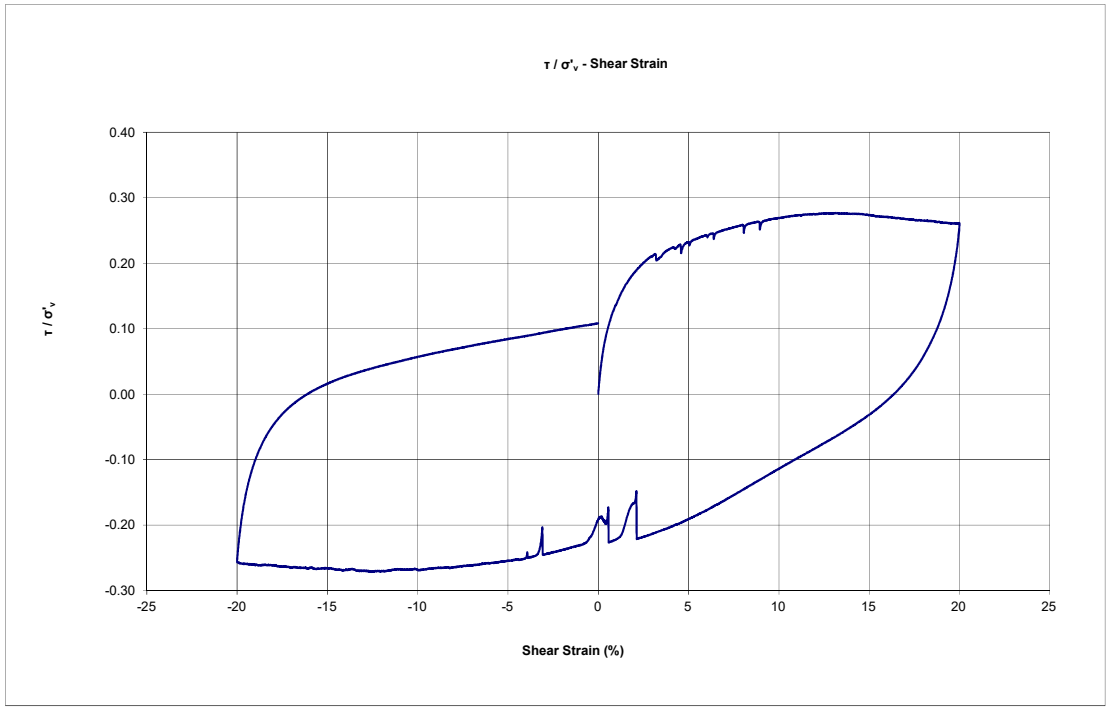


Static Simple Shear Test

(ASTM D6528)

Project No.:	A03355A01	Borehole ID:	BH02
Project:		Sample ID:	Shelby1
Date:	2019-10-17	Depth:	3.50 m
Tested by:	HM	Location:	Brazil
Checked by:	BY	Details:	Trimmed from Shelby Tube





Static Simple Shear Test

(ASTM D6528)

Project No.:	A03355A01	Borehole ID:	BH02
Project:		Sample ID:	Shelby2
Date:	2019-10-10	Depth:	
Test by:	HM	Location:	Brazil
Checked by:	BY	Details:	Trimmed from Shelby Tube

Initial Sample Information		
Specimen Height	mm	24.00
Specimen Diameter	mm	70.03
Area	mm^2	3851.75
Volume	cm^3	92.44
Wet Weight	g	170.83
Water Content	%	29.08
Dry Weight	g	132.34
Wet Density	g/cm^3	1.848
Dry Density	g/cm^3	1.432
Specific Gravity (measured)	-	2.81
Void Ratio (e)	-	0.96
Saturation Ratio (Sr)	%	84.87

Static Shearing (Undrained)		
Initial Vertical Effective Stress	kPa	800
Initial Shear Stress	kPa	0.5
Shearing Rate (Shear Strain Rate)	% / hr	5.00
Peak Shear Strength	kPa	199.00
Ratio of Peak τ/σ'_v	-	0.25
Max. Excess Pore Pressure	kPa	630.05
Max. Shear Strain	%	20.0

FINAL SAMPLE INFORMATION		
Liquid Limit (test sample)		
Plastic Limit (test sample)		
Liquid Limit (shear plane)		
Plastic Limit (shear plane)		
Final Moisture Content	%	29.17
Final Moisture Content (shear plane)	%	
Final Moisture Content (outside shear plane)	%	

CONSOLIDATION	Stage #	1	2	3	4	5			
Vertical Effective Stress	kPa	50	100	200	400	800			
Max Load	kN	0.192	0.384	0.769	1.540	3.081			
Total Height Change	mm	0.22	0.42	0.79	1.33	2.24			
Consolidated Height	mm	23.78	23.58	23.21	22.67	21.77			
Axial Strain *2	%	0.92	1.76	3.27	5.55	9.31			
Duration	min	360	360	360	360	1116			

*2 : Axial strain may differ from oedometer test result due to the sample seating system and possible lateral strain caused by the membrane.

Photos:

Before Test





After Test

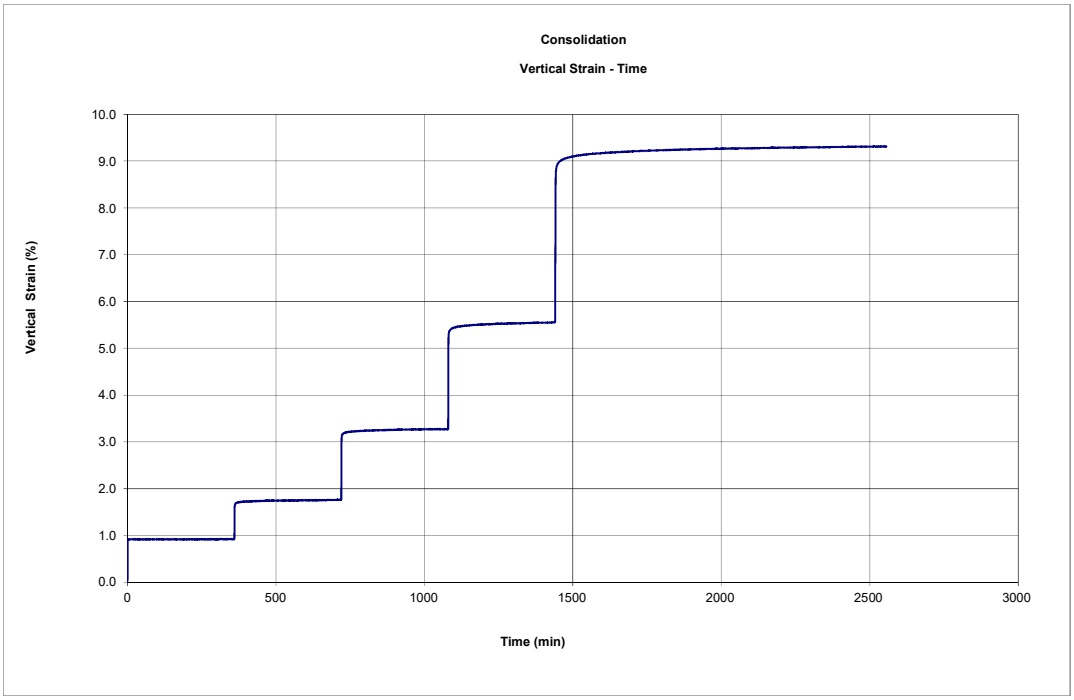


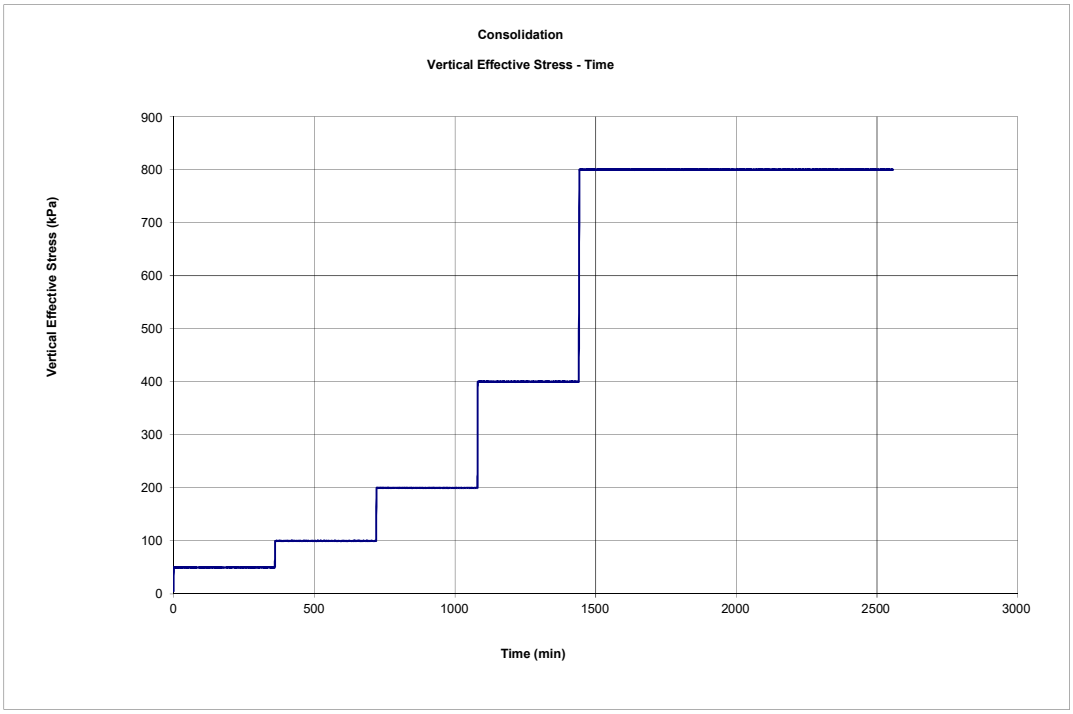


Static Simple Shear Test

(ASTM D6528)

Project No.:	A03355A01	Borehole ID:	BH02
Project:		Sample ID:	Shelby2
Date:	2019-10-10	Depth:	
Tested by:	HM	Location:	Brazil
Checked by:	BY	Details:	Trimmed from Shelby Tube

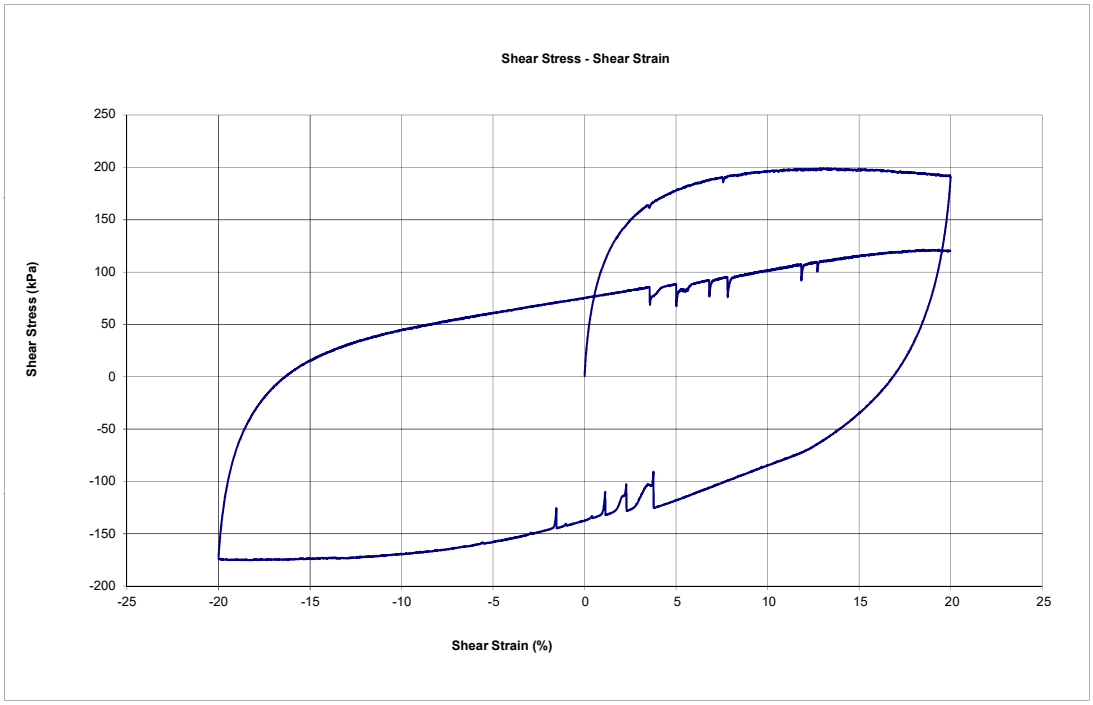


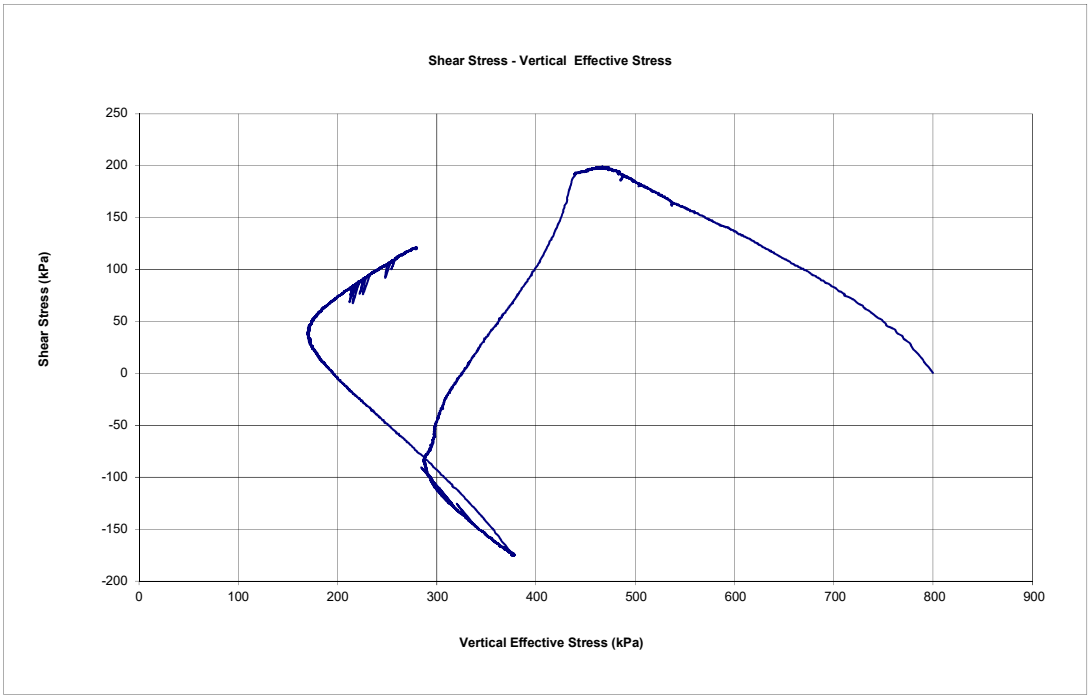


Static Simple Shear Test

(ASTM D6528)

Project No.:	A03355A01	Borehole ID:	BH02
Project:		Sample ID:	Shelby2
Date:	2019-10-10	Depth:	
Tested by:	HM	Location:	Brazil
Checked by:	BY	Details:	Trimmed from Shelby Tube

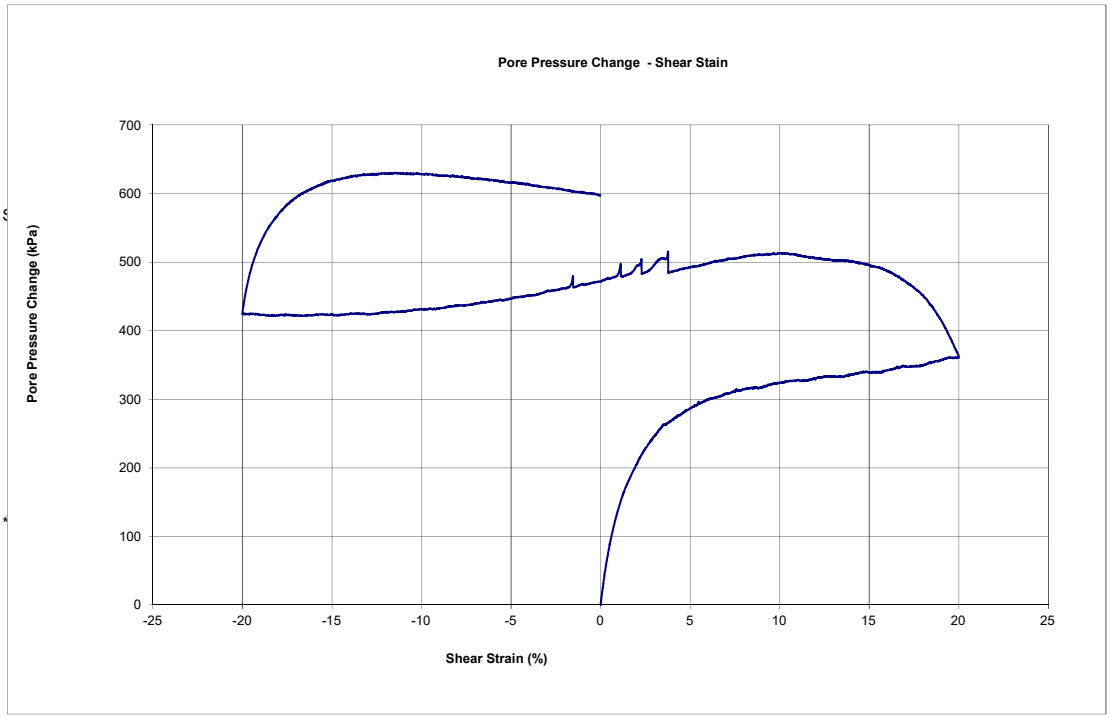


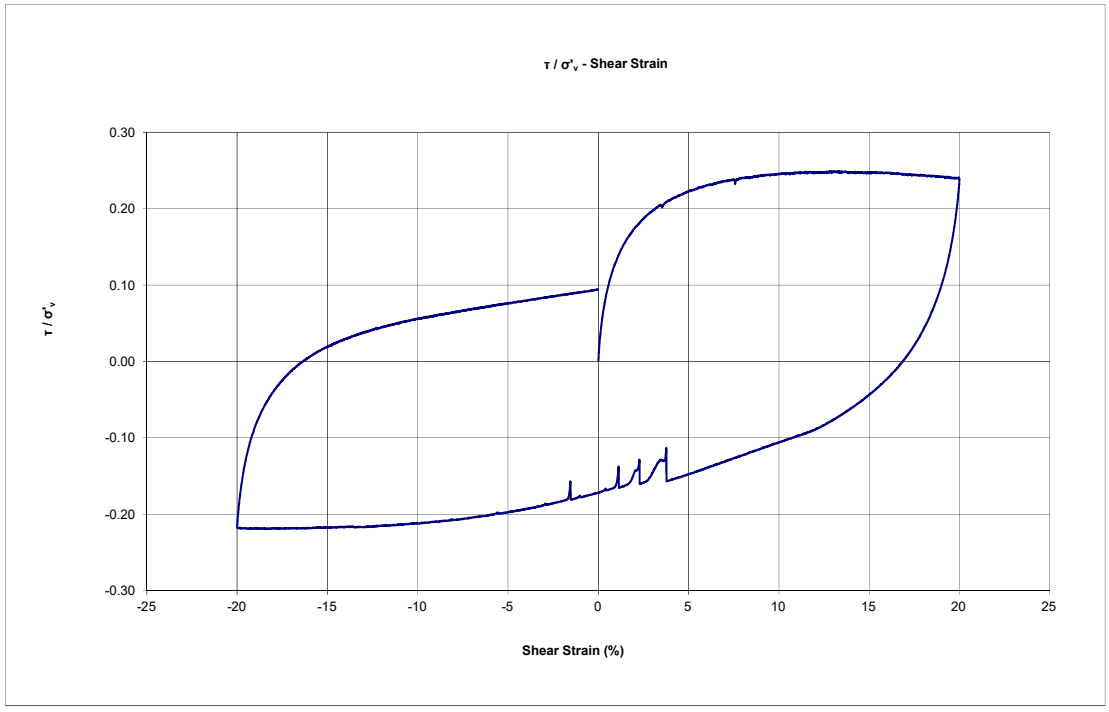


Static Simple Shear Test

(ASTM D6528)

Project No.:	A03355A01	Borehole ID:	BH02
Project:		Sample ID:	Shelby2
Date:	2019-10-10	Depth:	
Tested by:	HM	Location:	Brazil
Checked by:	BY	Details:	Trimmed from Shelby Tube





Static Simple Shear Test

(ASTM D6528)

Project No.:	A03355A01	Borehole ID:	BH04
Project:		Sample ID:	Shelby1
Date:	2019-10-10	Depth:	
Test by:	HM	Location:	Brazil
Checked by:	BY	Details:	Trimmed from Shelby Tube

Initial Sample Information		
Specimen Height	mm	23.98
Specimen Diameter	mm	70.01
Area	mm^2	3849.55
Volume	cm^3	92.31
Wet Weight	g	157.38
Water Content	%	36.13
Dry Weight	g	115.61
Wet Density	g/cm^3	1.705
Dry Density	g/cm^3	1.252
Specific Gravity (measured)	-	2.82
Void Ratio (e)	-	1.25
Saturation Ratio (Sr)	%	81.40

Static Shearing (Undrained)		
Initial Vertical Effective Stress	kPa	350
Initial Shear Stress	kPa	0.6
Shearing Rate (Shear Strain Rate)	% / hr	5.00
Peak Shear Strength	kPa	153.76
Ratio of Peak τ/σ'_v	-	0.44
Max. Excess Pore Pressure	kPa	271.85
Max. Shear Strain	%	20.0

FINAL SAMPLE INFORMATION		
Liquid Limit (test sample)		
Plastic Limit (test sample)		
Liquid Limit (shear plane)		
Plastic Limit (shear plane)		
Final Moisture Content	%	41.67
Final Moisture Content (shear plane)	%	
Final Moisture Content (outside shear plane)	%	

CONSOLIDATION	Stage #	1	2	3	4				
Vertical Effective Stress	kPa	50	100	200	350				
Max Load	kN	0.191	0.384	0.769	1.346				
Total Height Change	mm	0.26	0.46	0.78	1.13				
Consolidated Height	mm	23.72	23.52	23.20	22.85				
Axial Strain *2	%	1.07	1.91	3.24	4.73				
Duration	min	250	360	360	1796				

*2 : Axial strain may differ from oedometer test result due to the sample seating system and possible lateral strain caused by the membrane.

Photos:

Before Test





After Test

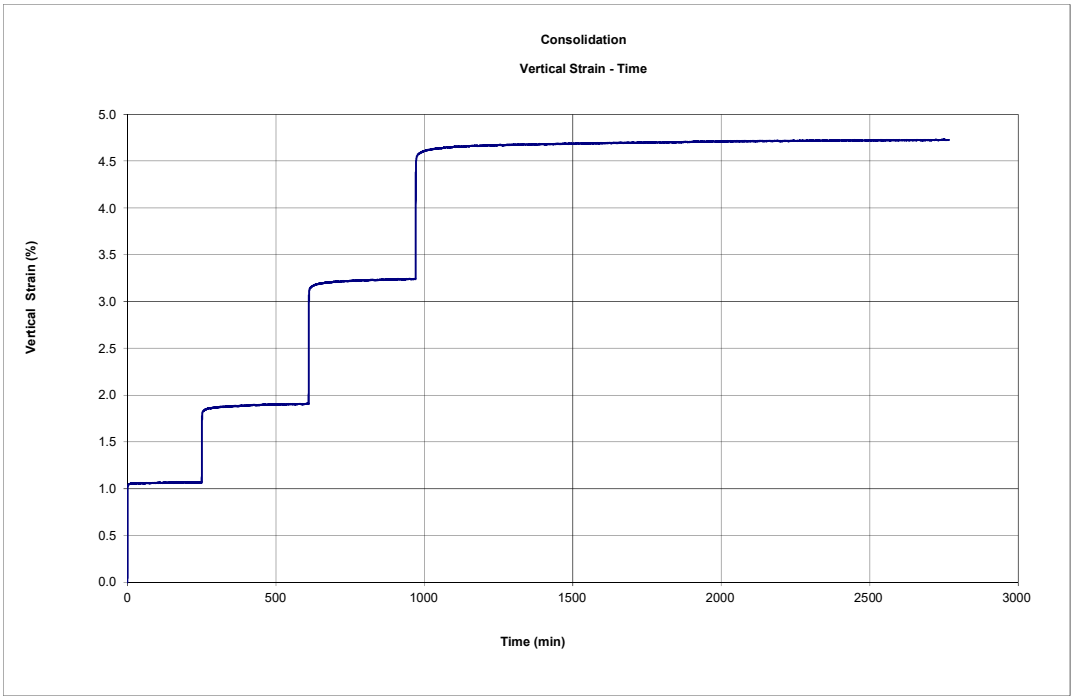


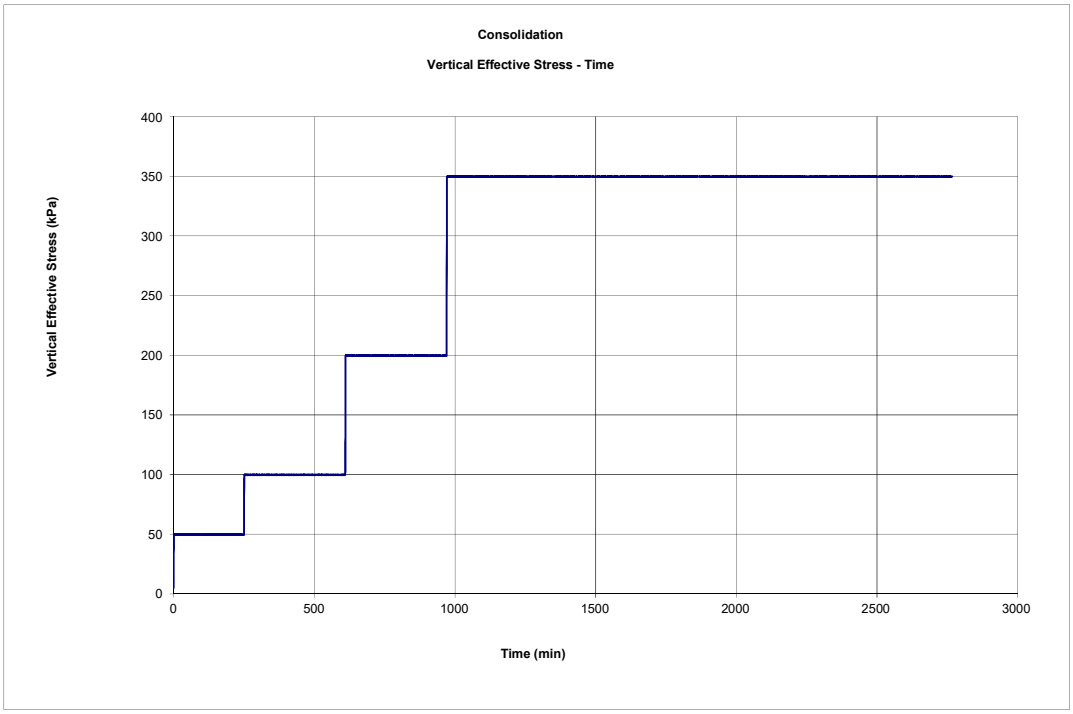


Static Simple Shear Test

(ASTM D6528)

Project No.:	A03355A01	Borehole ID:	BH04
Project:		Sample ID:	Shelby1
Date:	2019-10-10	Depth:	
Tested by:	HM	Location:	Brazil
Checked by:	BY	Details:	Trimmed from Shelby Tube

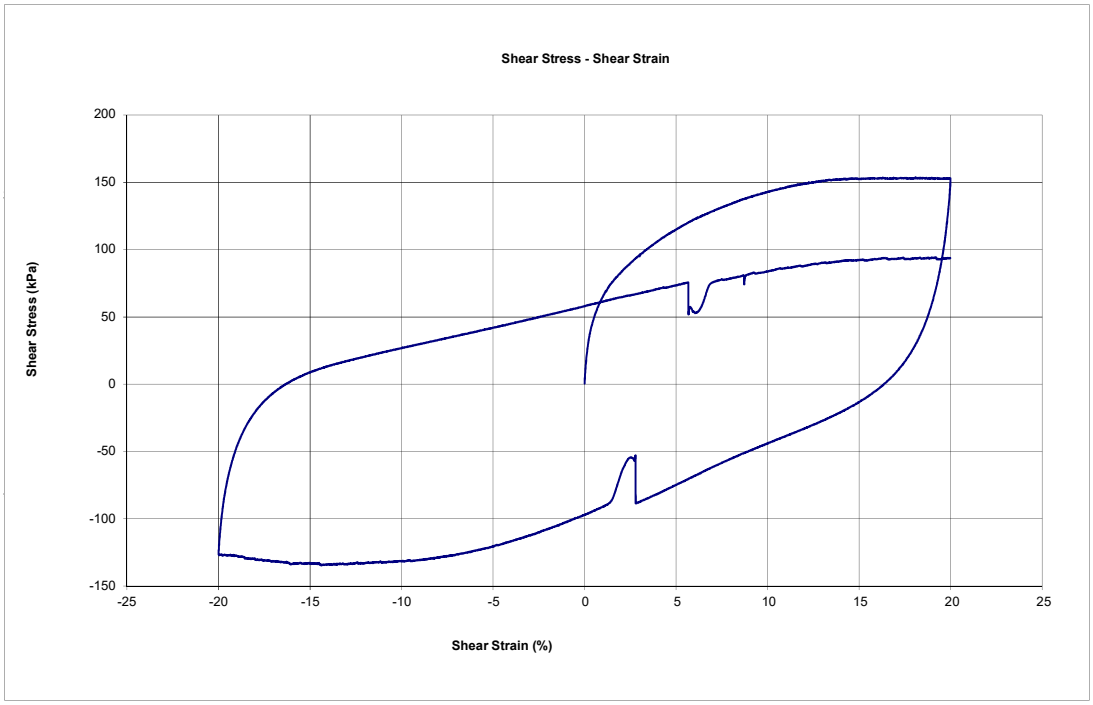


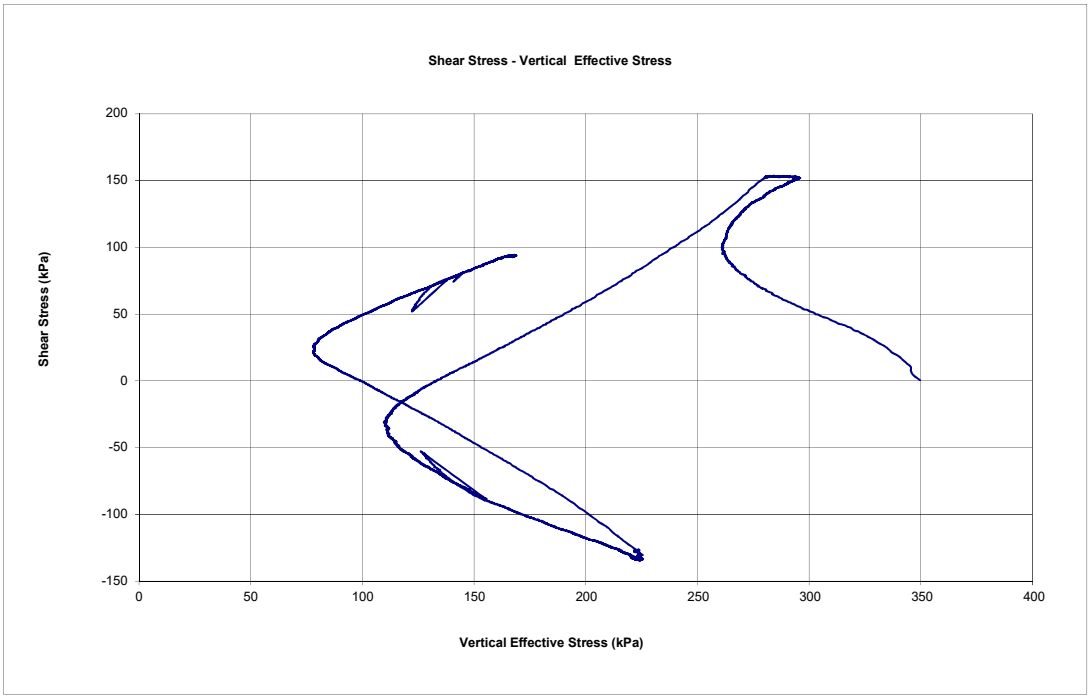


Static Simple Shear Test

(ASTM D6528)

Project No.:	A03355A01	Borehole ID:	BH04
Project:		Sample ID:	Shelby1
Date:	2019-10-10	Depth:	
Tested by:	HM	Location:	Brazil
Checked by:	BY	Details:	Trimmed from Shelby Tube

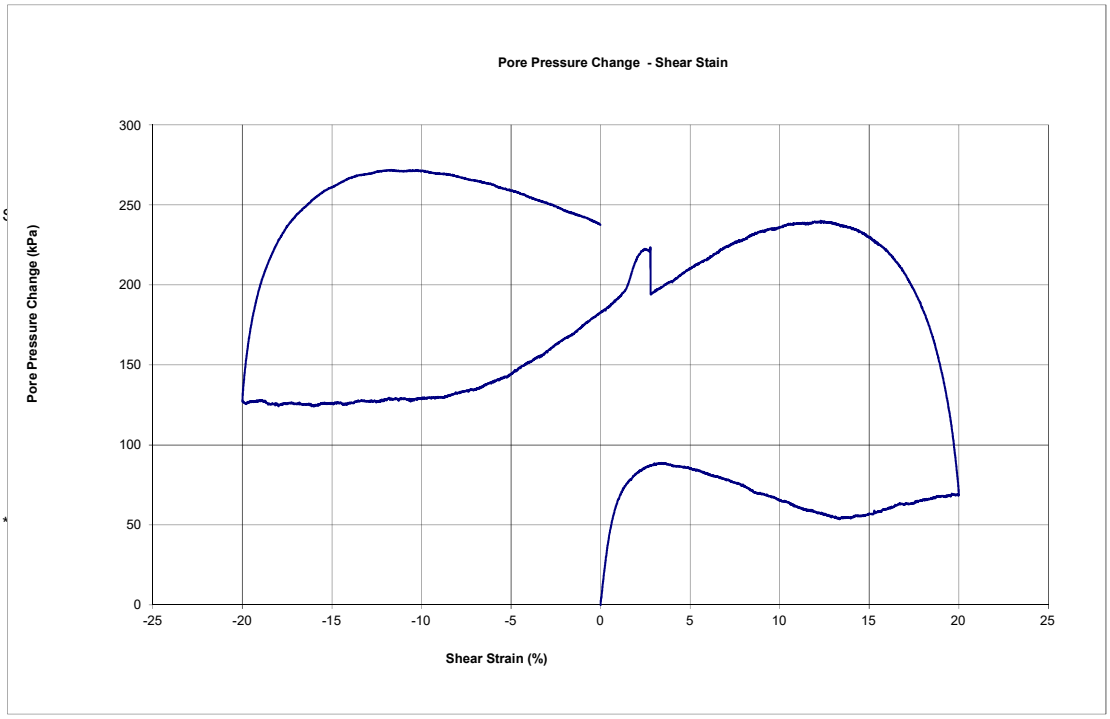


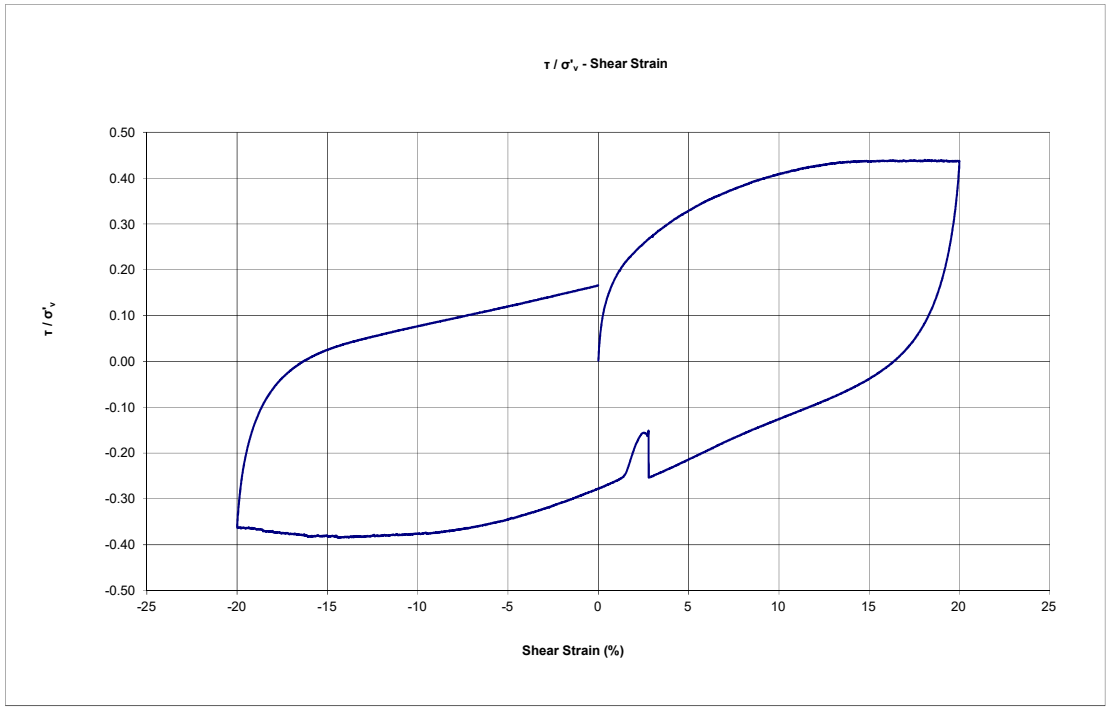


Static Simple Shear Test

(ASTM D6528)

Project No.:	A03355A01	Borehole ID:	BH04
Project:		Sample ID:	Shelby1
Date:	2019-10-10	Depth:	
Tested by:	HM	Location:	Brazil
Checked by:	BY	Details:	Trimmed from Shelby Tube





Static Simple Shear Test

(ASTM D6528)

Project No.:	A03355A01	Borehole ID:	BH04
Project:		Sample ID:	Shelby2
Date:	2019-10-15	Depth:	5.30 m
Test by:	HM	Location:	Brazil
Checked by:	BY	Details:	Trimmed from Shelby Tube

Initial Sample Information		
Specimen Height	mm	23.96
Specimen Diameter	mm	70.03
Area	mm^2	3851.75
Volume	cm^3	92.29
Wet Weight	g	174.17
Water Content	%	30.08
Dry Weight	g	133.89
Wet Density	g/cm^3	1.887
Dry Density	g/cm^3	1.451
Specific Gravity (measured)	-	2.82
Void Ratio (e)	-	0.94
Saturation Ratio (Sr)	%	89.89

Static Shearing (Undrained)		
Initial Vertical Effective Stress	kPa	370
Initial Shear Stress	kPa	0.5
Shearing Rate (Shear Strain Rate)	% / hr	5.00
Peak Shear Strength	kPa	130.56
Ratio of Peak τ/σ'_v	-	0.35
Max. Excess Pore Pressure	kPa	303.29
Max. Shear Strain	%	20.0

FINAL SAMPLE INFORMATION		
Liquid Limit (test sample)		
Plastic Limit (test sample)		
Liquid Limit (shear plane)		
Plastic Limit (shear plane)		
Final Moisture Content	%	29.90
Final Moisture Content (shear plane)	%	
Final Moisture Content (outside shear plane)	%	

CONSOLIDATION	Stage #	1	2	3	4				
Vertical Effective Stress	kPa	50	100	200	370				
Max Load	kN	0.192	0.384	0.769	1.424				
Total Height Change	mm	0.71	1.07	1.56	2.10				
Consolidated Height	mm	23.25	22.89	22.40	21.86				
Axial Strain *2	%	2.94	4.46	6.50	8.75				
Duration	min	360	360	360	591				

*2 : Axial strain may differ from oedometer test result due to the sample seating system and possible lateral strain caused by the membrane.

Photos:

Before Test





After Test

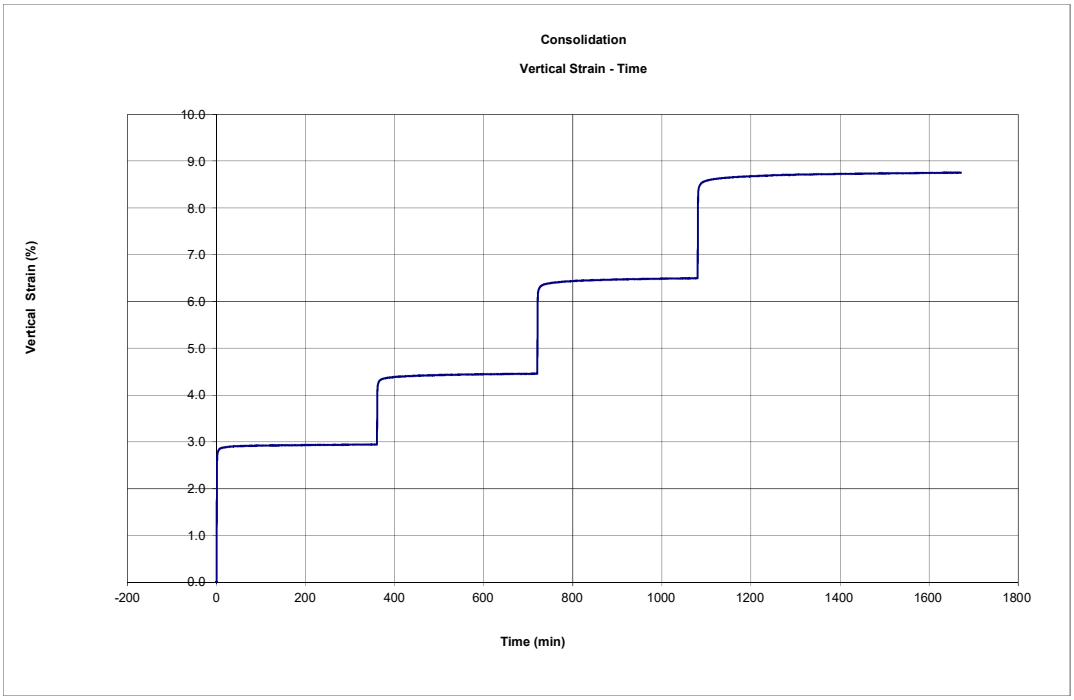


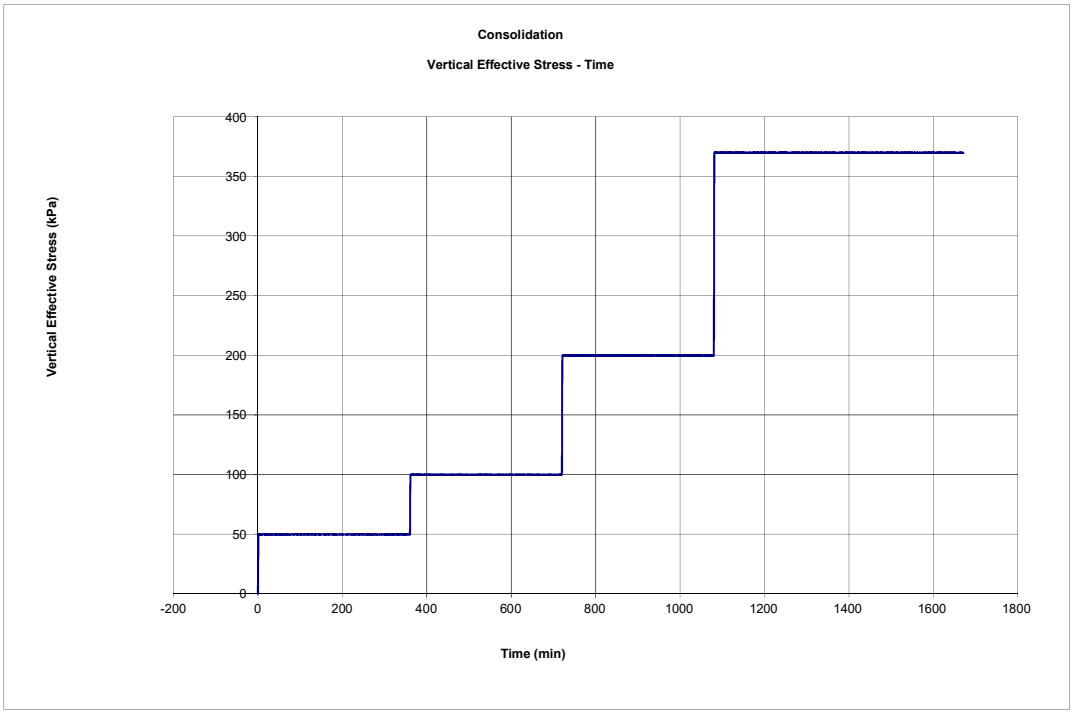


Static Simple Shear Test

(ASTM D6528)

Project No.:	A03355A01	Borehole ID:	BH04
Project:		Sample ID:	Shelby2
Date:	2019-10-15	Depth:	5.30 m
Tested by:	HM	Location:	Brazil
Checked by:	BY	Details:	Trimmed from Shelby Tube

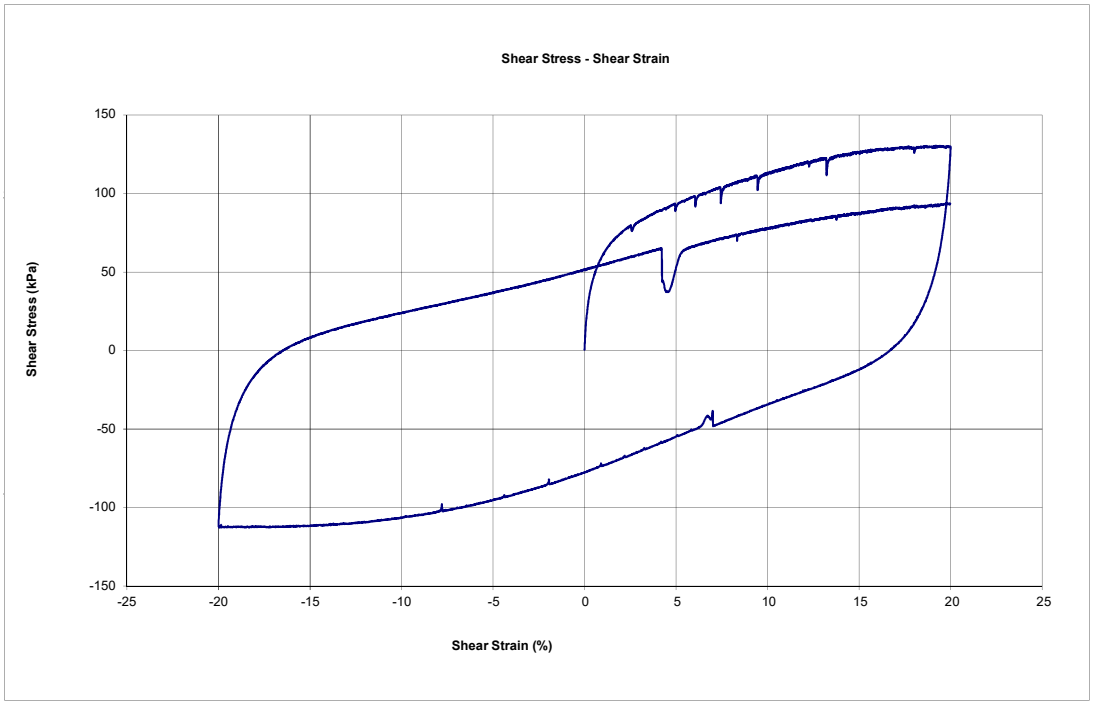


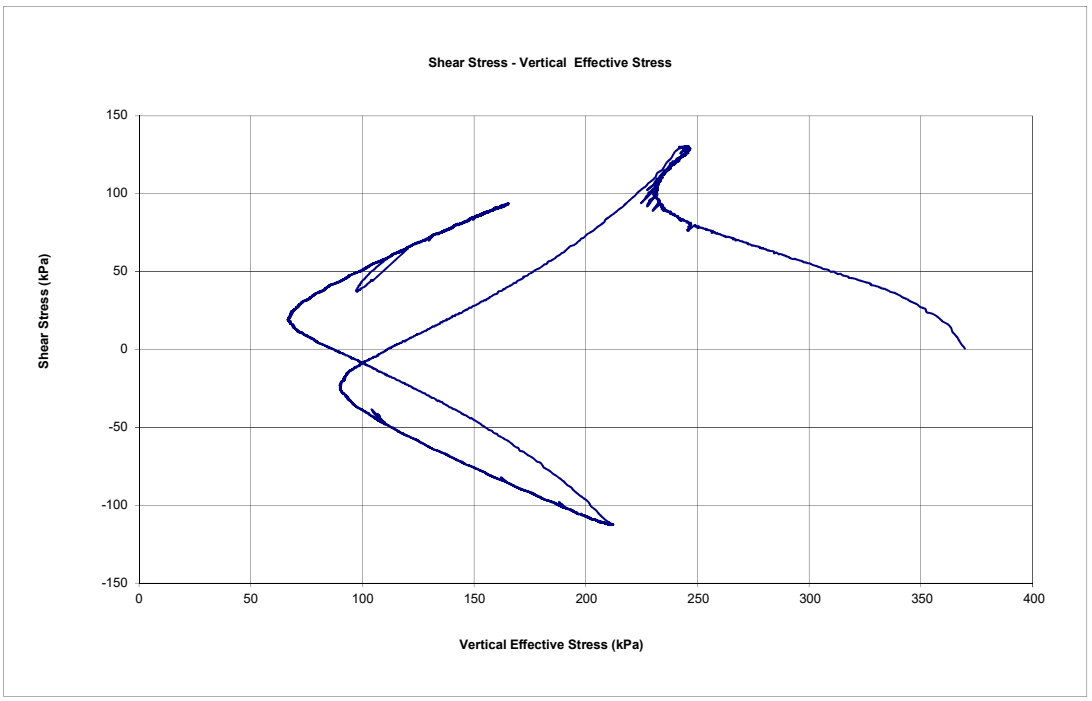


Static Simple Shear Test

(ASTM D6528)

Project No.:	A03355A01	Borehole ID:	BH04
Project:		Sample ID:	Shelby2
Date:	2019-10-15	Depth:	5.30 m
Tested by:	HM	Location:	Brazil
Checked by:	BY	Details:	Trimmed from Shelby Tube

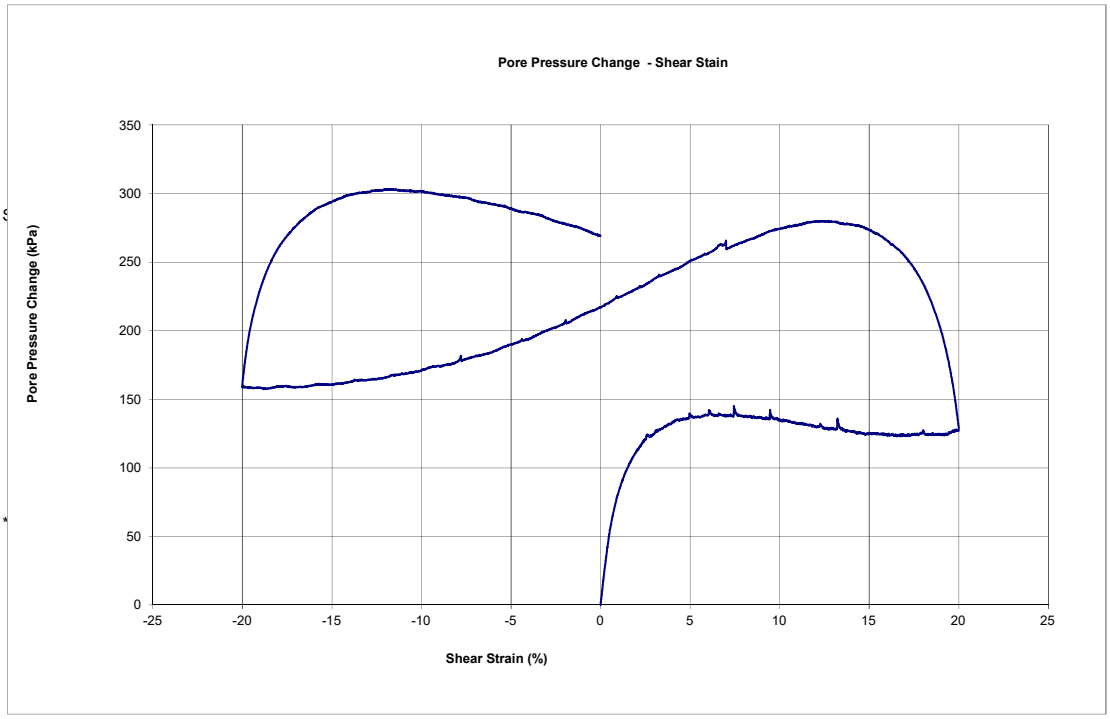


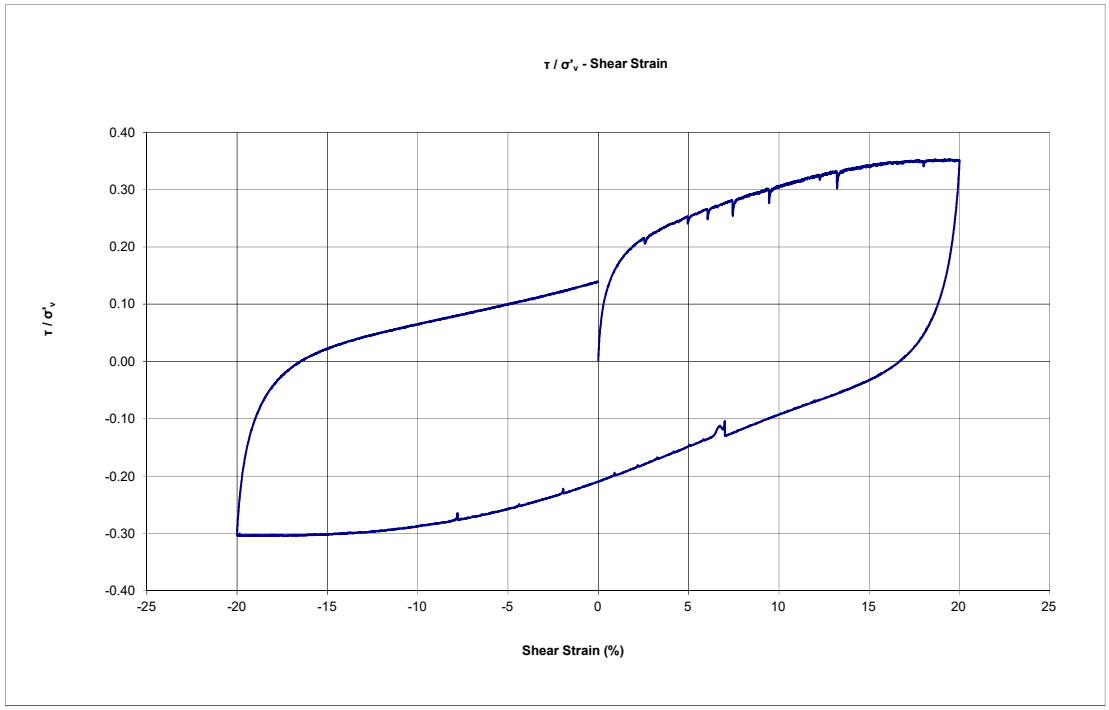


Static Simple Shear Test

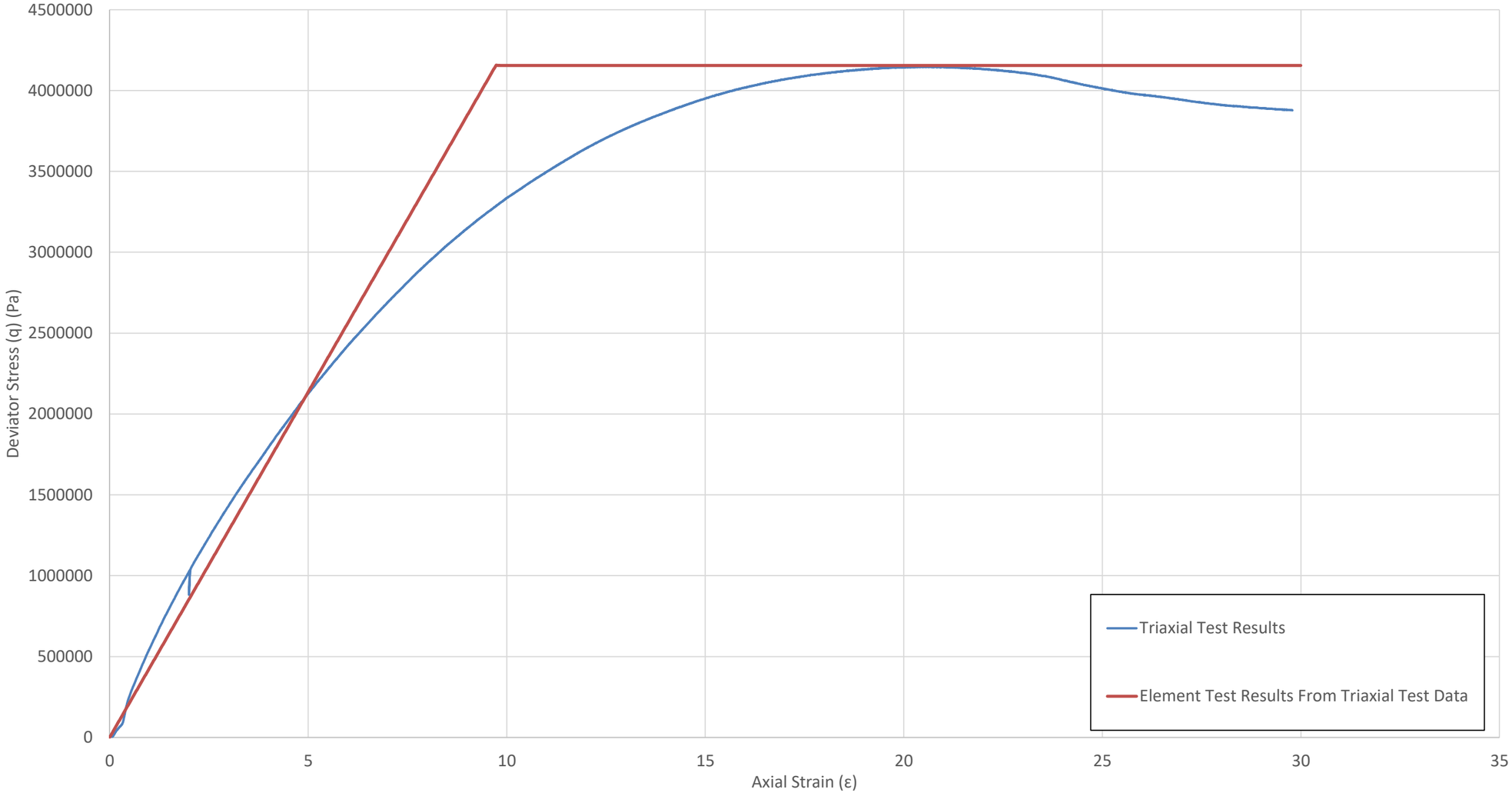
(ASTM D6528)

Project No.:	A03355A01	Borehole ID:	BH04
Project:		Sample ID:	Shelby2
Date:	2019-10-15	Depth:	5.30 m
Tested by:	HM	Location:	Brazil
Checked by:	BY	Details:	Trimmed from Shelby Tube





Mohr-Coulomb Element Tests



NOTES:

AS A MUTUAL PROTECTION TO OUR CLIENT, THE PUBLIC AND OURSELVES, ALL REPORTS AND DRAWINGS ARE SUBMITTED FOR THE CONFIDENTIAL INFORMATION OF OUR CLIENT FOR A SPECIFIC PROJECT AND AUTHORIZATION FOR USE AND/OR PUBLICATION OF DATA STATEMENTS, CONCLUSIONS OR ABSTRACTS FROM OR REGARDING OUR REPORTS AND DRAWINGS IS RESERVED PENDING OUR WRITTEN APPROVAL.

CLIENT

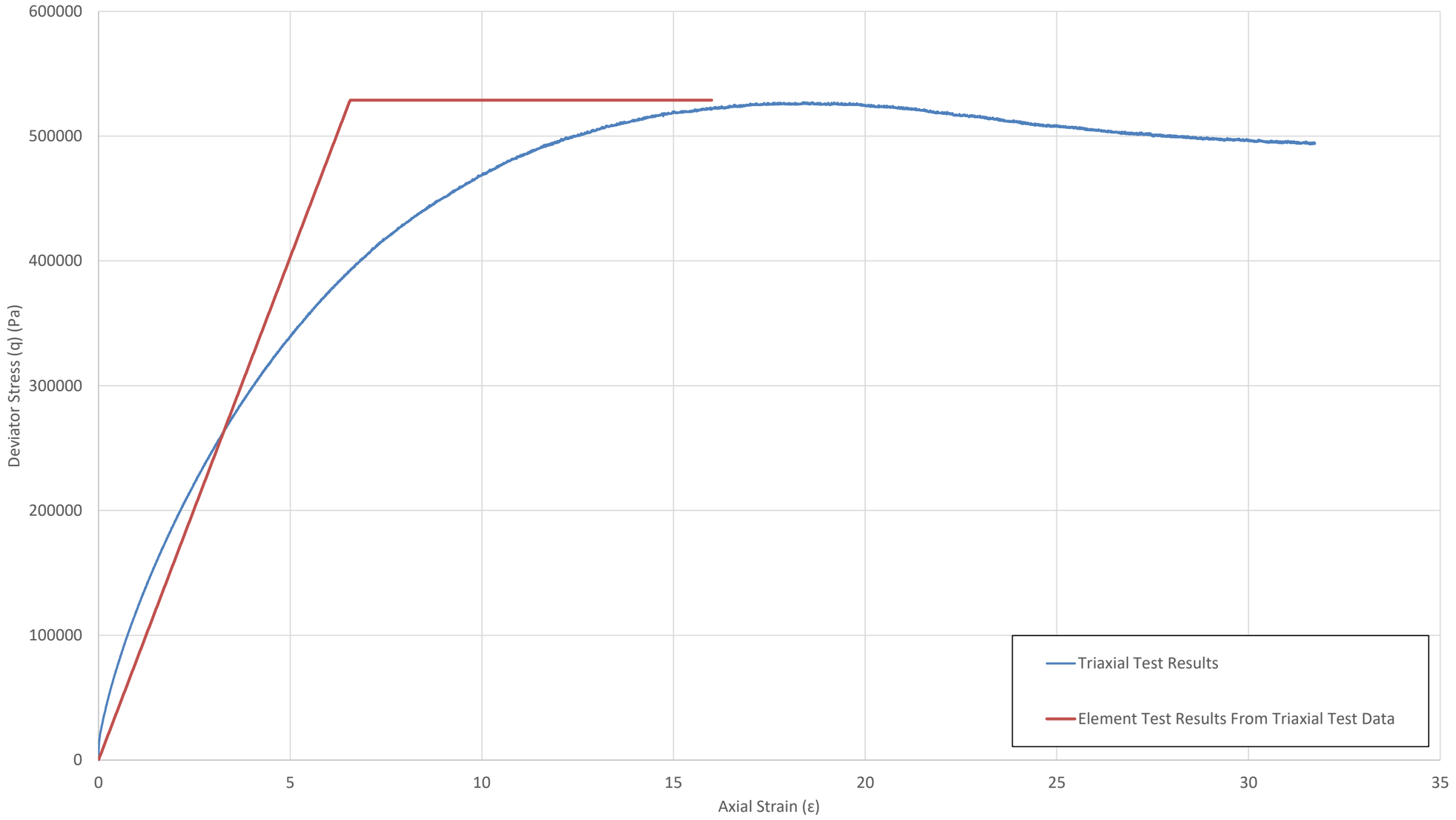
PROJECT

REPORT OF THE EXPERT PANEL ON THE TECHNICAL CAUSES OF THE FAILURE OF FEIJÃO DAM 1

MOHR-COULOMB ELEMENT TEST RESULTS: DRAINED TRIAXIAL COMPRESSION TEST #01

PROJECT No. A03355A01

FIG. No. 01



NOTES:

AS A MUTUAL PROTECTION TO OUR CLIENT, THE PUBLIC AND OURSELVES, ALL REPORTS AND DRAWINGS ARE SUBMITTED FOR THE CONFIDENTIAL INFORMATION OF OUR CLIENT FOR A SPECIFIC PROJECT AND AUTHORIZATION FOR USE AND/OR PUBLICATION OF DATA STATEMENTS, CONCLUSIONS OR ABSTRACTS FROM OR REGARDING OUR REPORTS AND DRAWINGS IS RESERVED PENDING OUR WRITTEN APPROVAL.

CLIENT

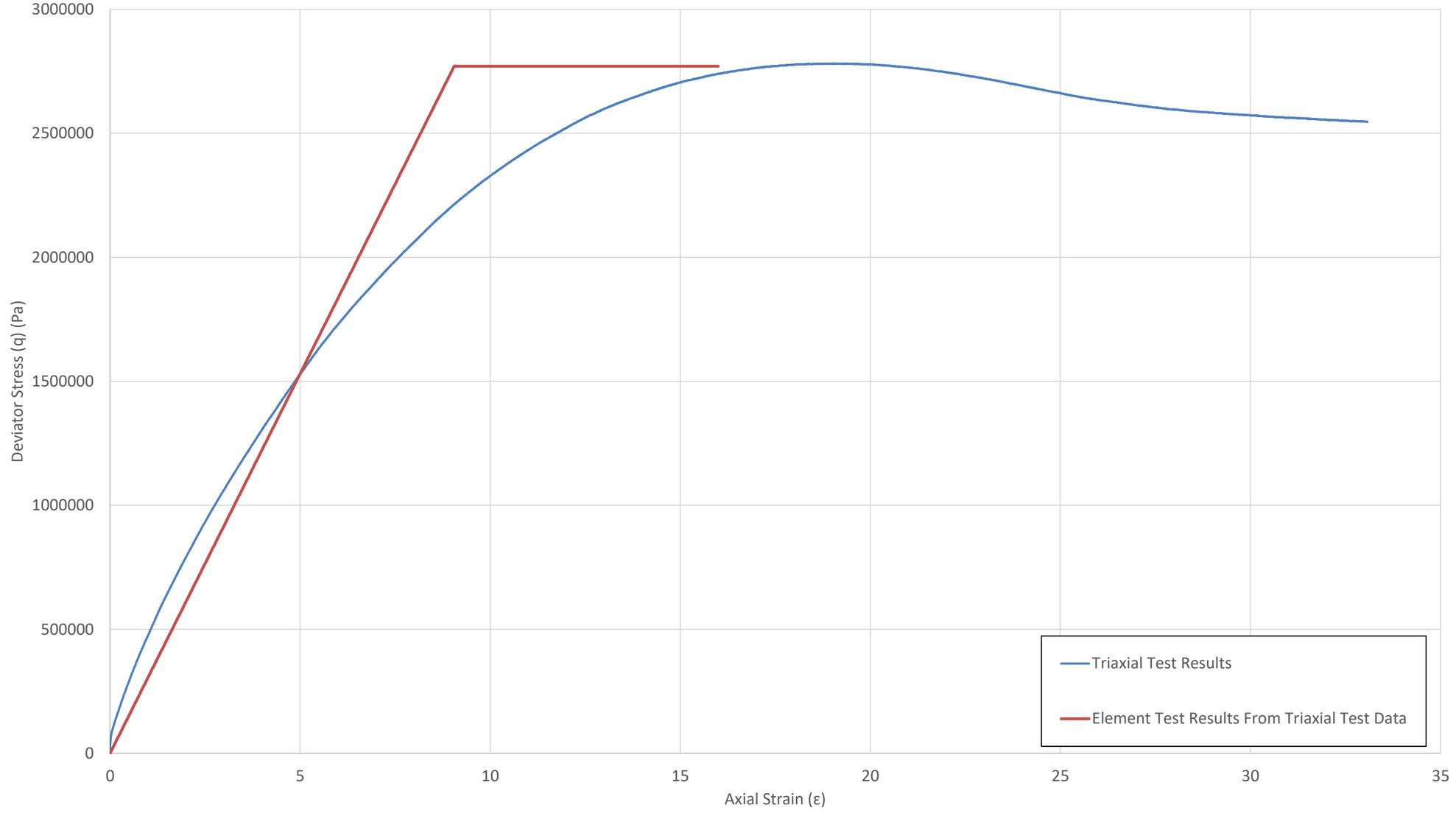
PROJECT

REPORT OF THE EXPERT PANEL ON THE TECHNICAL CAUSES OF THE FAILURE OF FEIJÃO DAM 1

MOHR-COULOMB ELEMENT TEST RESULTS: DRAINED TRIAXIAL COMPRESSION TEST #02

PROJECT No. A03355A01

FIG. No. 02



NOTES:

AS A MUTUAL PROTECTION TO OUR CLIENT, THE PUBLIC AND OURSELVES, ALL REPORTS AND DRAWINGS ARE SUBMITTED FOR THE CONFIDENTIAL INFORMATION OF OUR CLIENT FOR A SPECIFIC PROJECT AND AUTHORIZATION FOR USE AND/OR PUBLICATION OF DATA STATEMENTS, CONCLUSIONS OR ABSTRACTS FROM OR REGARDING OUR REPORTS AND DRAWINGS IS RESERVED PENDING OUR WRITTEN APPROVAL.

CLIENT

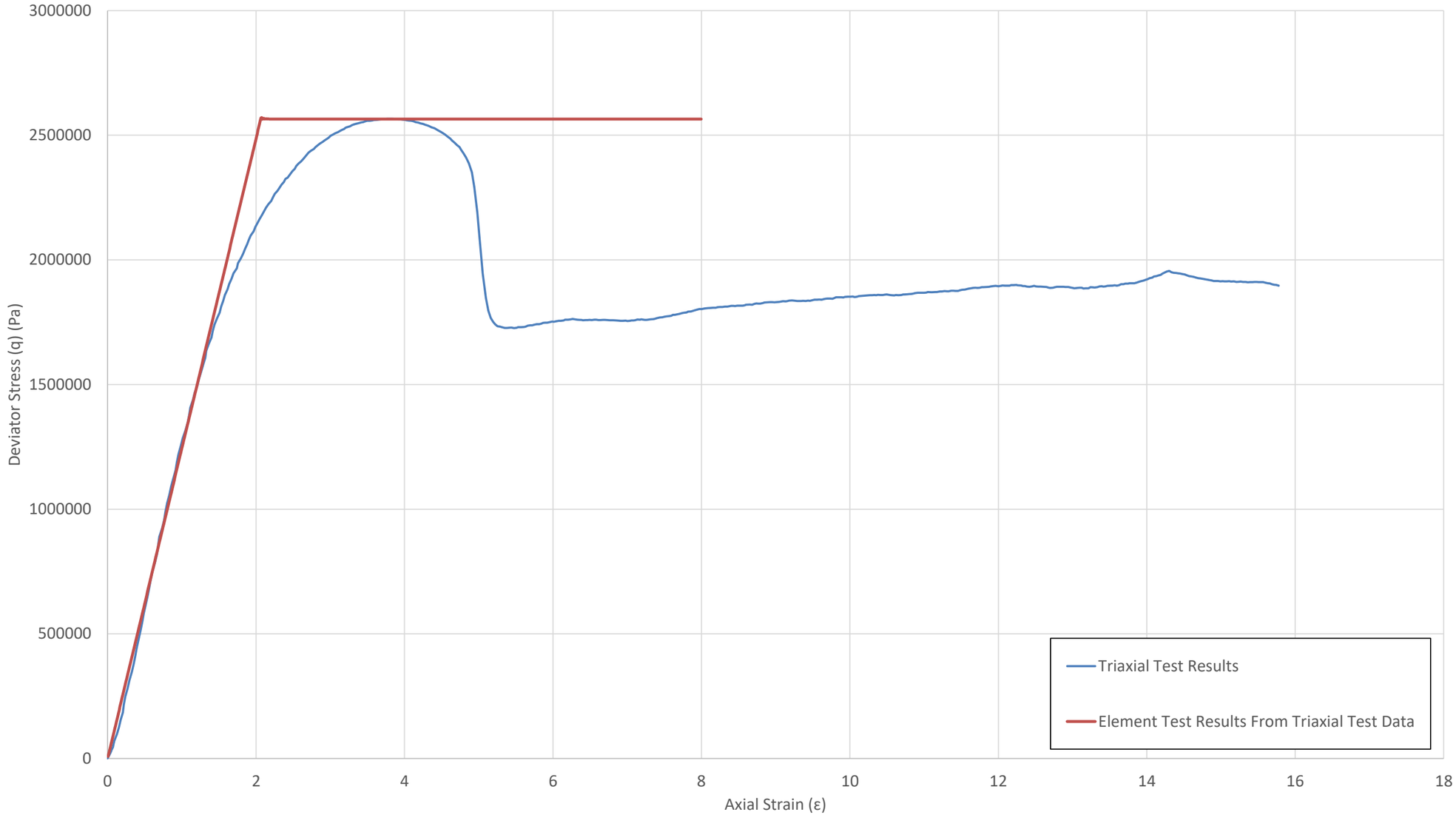
PROJECT

REPORT OF THE EXPERT PANEL ON THE TECHNICAL CAUSES OF THE FAILURE OF FEIJÃO DAM 1

MOHR-COULOMB ELEMENT TEST RESULTS: DRAINED TRIAXIAL COMPRESSION TEST #03

PROJECT No. A03355A01

FIG. No. 03



NOTES:

AS A MUTUAL PROTECTION TO OUR CLIENT, THE PUBLIC AND OURSELVES, ALL REPORTS AND DRAWINGS ARE SUBMITTED FOR THE CONFIDENTIAL INFORMATION OF OUR CLIENT FOR A SPECIFIC PROJECT AND AUTHORIZATION FOR USE AND/OR PUBLICATION OF DATA STATEMENTS, CONCLUSIONS OR ABSTRACTS FROM OR REGARDING OUR REPORTS AND DRAWINGS IS RESERVED PENDING OUR WRITTEN APPROVAL.

CLIENT

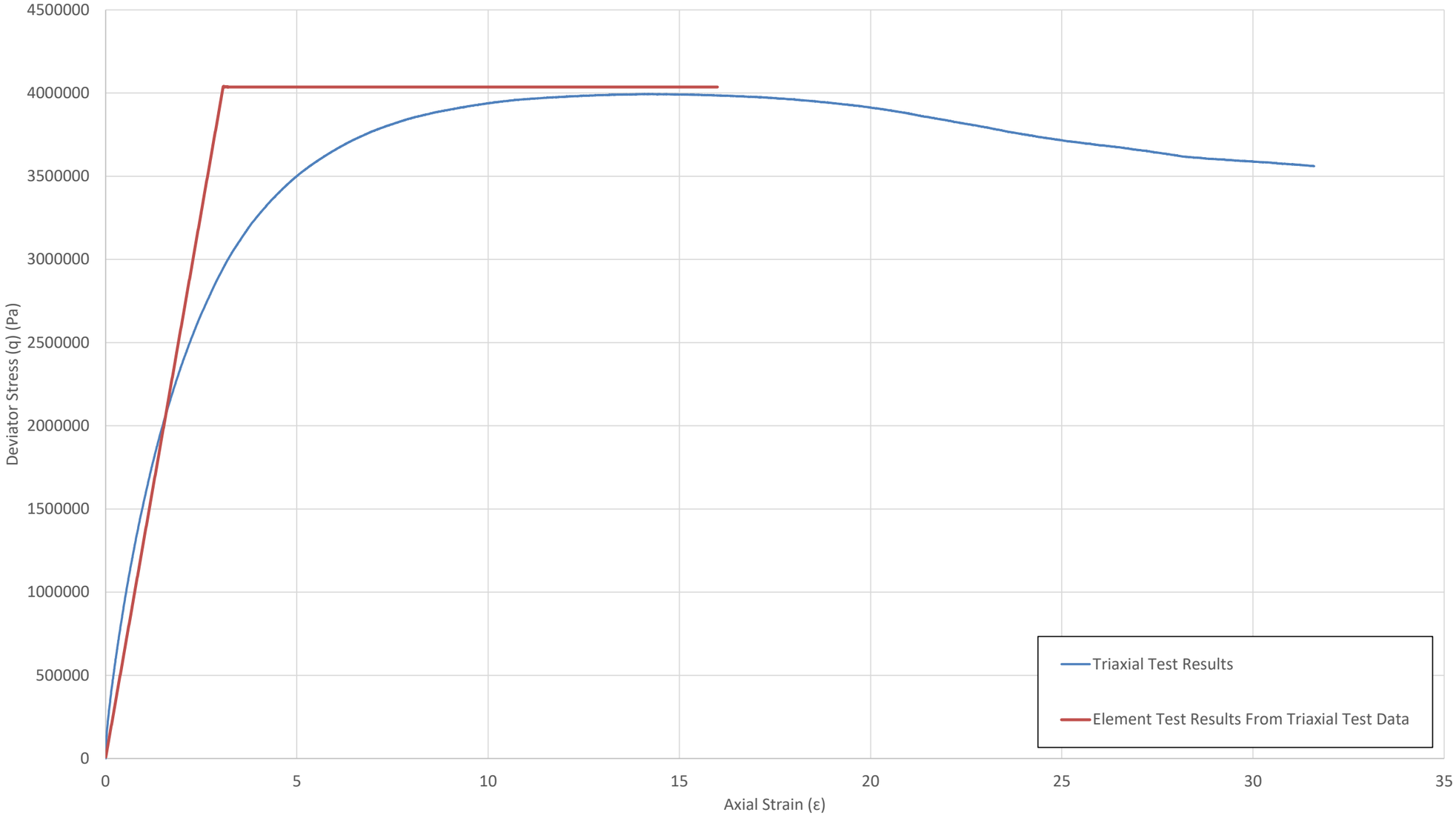
PROJECT

REPORT OF THE EXPERT PANEL ON THE TECHNICAL CAUSES OF THE FAILURE OF FEIJÃO DAM 1

MOHR-COULOMB ELEMENT TEST RESULTS: DRAINED TRIAXIAL COMPRESSION TEST #05

PROJECT No. A03355A01

FIG. No. 04



NOTES:

AS A MUTUAL PROTECTION TO OUR CLIENT, THE PUBLIC AND OURSELVES, ALL REPORTS AND DRAWINGS ARE SUBMITTED FOR THE CONFIDENTIAL INFORMATION OF OUR CLIENT FOR A SPECIFIC PROJECT AND AUTHORIZATION FOR USE AND/OR PUBLICATION OF DATA STATEMENTS, CONCLUSIONS OR ABSTRACTS FROM OR REGARDING OUR REPORTS AND DRAWINGS IS RESERVED PENDING OUR WRITTEN APPROVAL.

CLIENT

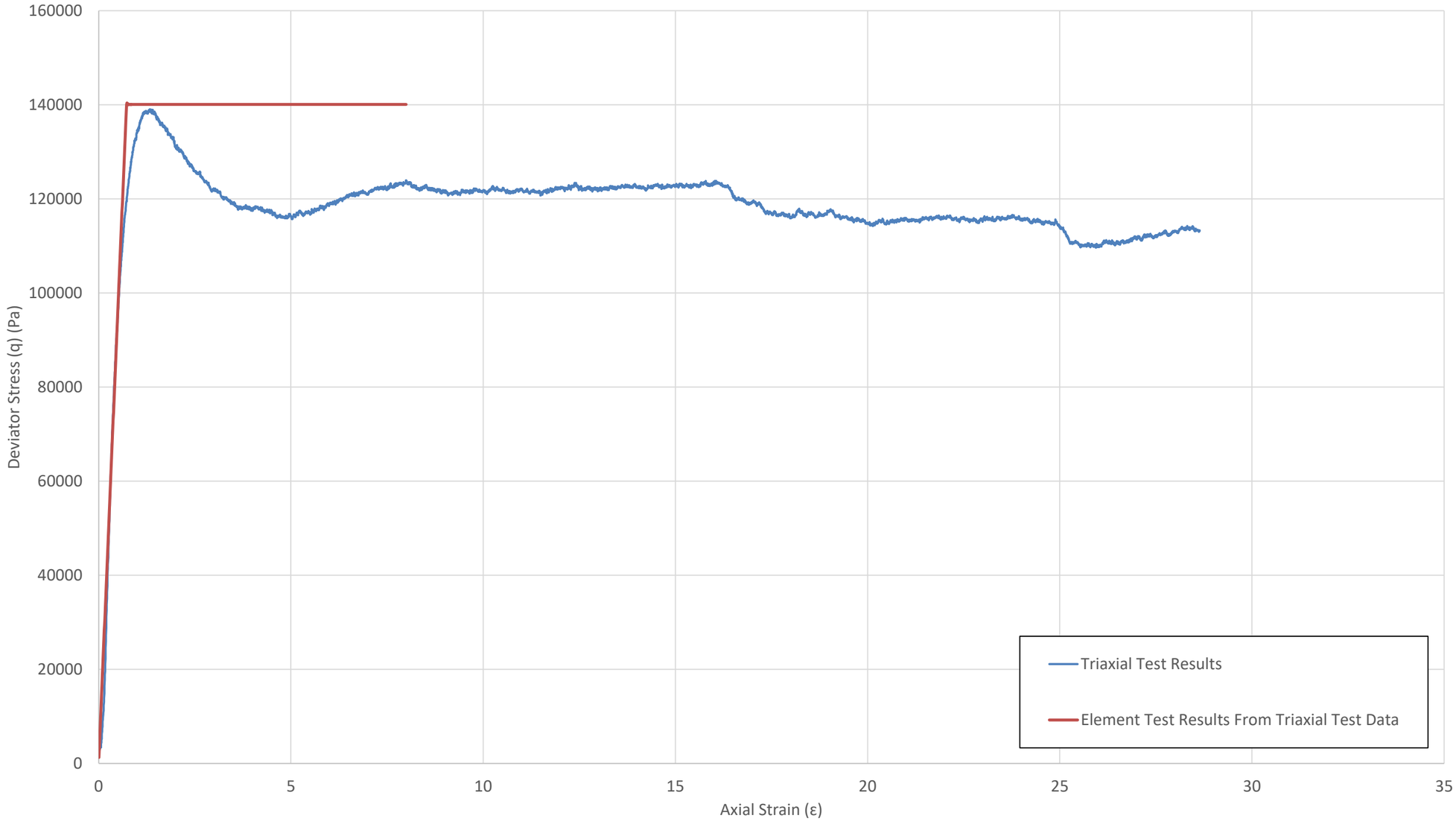
PROJECT

REPORT OF THE EXPERT PANEL ON THE TECHNICAL CAUSES OF THE FAILURE OF FEIJÃO DAM 1

MOHR-COULOMB ELEMENT TEST RESULTS: DRAINED TRIAXIAL COMPRESSION TEST #06

PROJECT No. A03355A01

FIG. No. 05



NOTES:

AS A MUTUAL PROTECTION TO OUR CLIENT, THE PUBLIC AND OURSELVES, ALL REPORTS AND DRAWINGS ARE SUBMITTED FOR THE CONFIDENTIAL INFORMATION OF OUR CLIENT FOR A SPECIFIC PROJECT AND AUTHORIZATION FOR USE AND/OR PUBLICATION OF DATA STATEMENTS, CONCLUSIONS OR ABSTRACTS FROM OR REGARDING OUR REPORTS AND DRAWINGS IS RESERVED PENDING OUR WRITTEN APPROVAL.

CLIENT

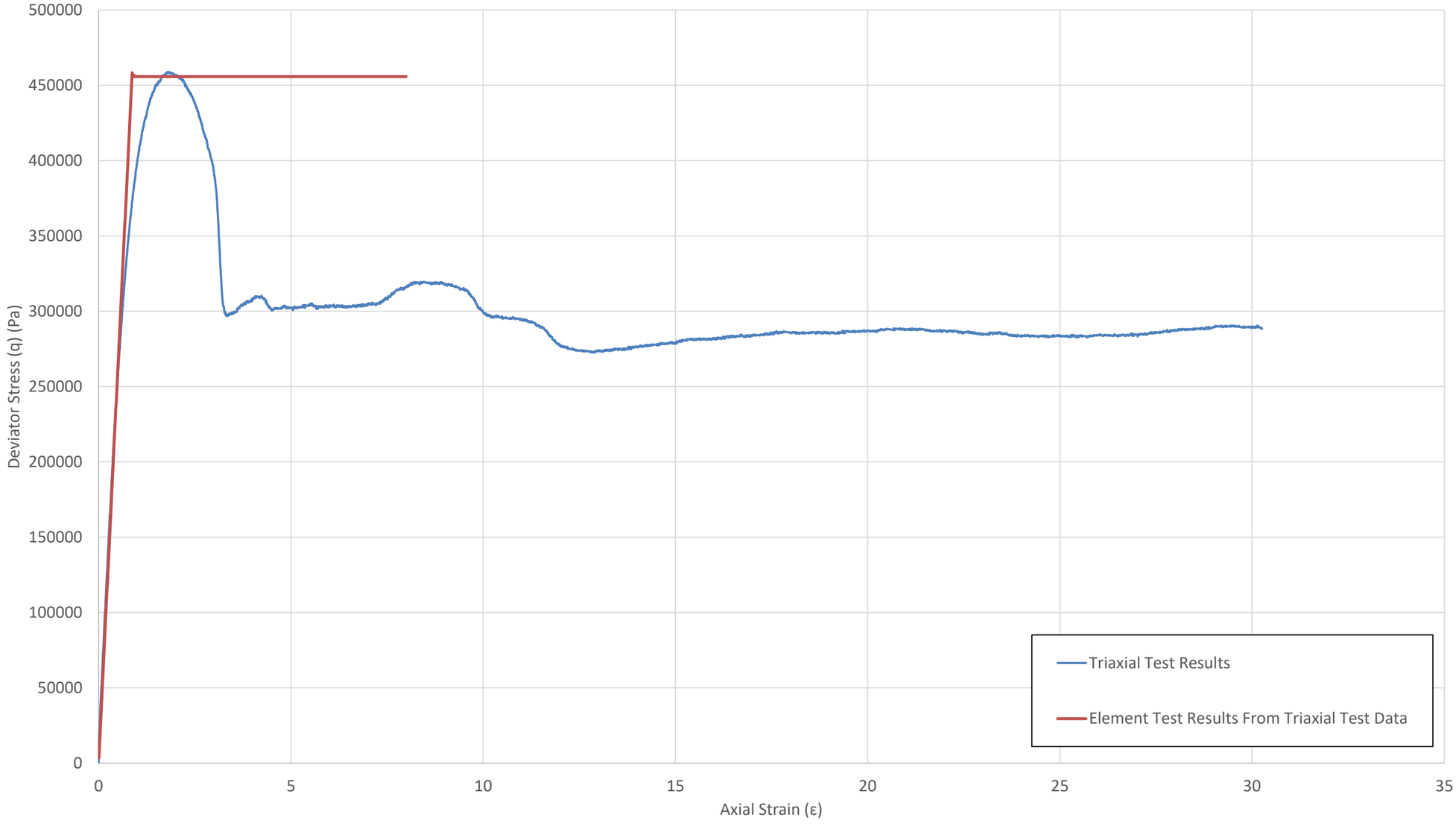
PROJECT

REPORT OF THE EXPERT PANEL ON THE TECHNICAL CAUSES OF THE FAILURE OF FEIJÃO DAM 1

MOHR-COULOMB ELEMENT TEST RESULTS: DRAINED TRIAXIAL COMPRESSION TEST #08

PROJECT No. A03355A01

FIG. No. 06



NOTES:

AS A MUTUAL PROTECTION TO OUR CLIENT, THE PUBLIC AND OURSELVES, ALL REPORTS AND DRAWINGS ARE SUBMITTED FOR THE CONFIDENTIAL INFORMATION OF OUR CLIENT FOR A SPECIFIC PROJECT AND AUTHORIZATION FOR USE AND/OR PUBLICATION OF DATA STATEMENTS, CONCLUSIONS OR ABSTRACTS FROM OR REGARDING OUR REPORTS AND DRAWINGS IS RESERVED PENDING OUR WRITTEN APPROVAL.

CLIENT

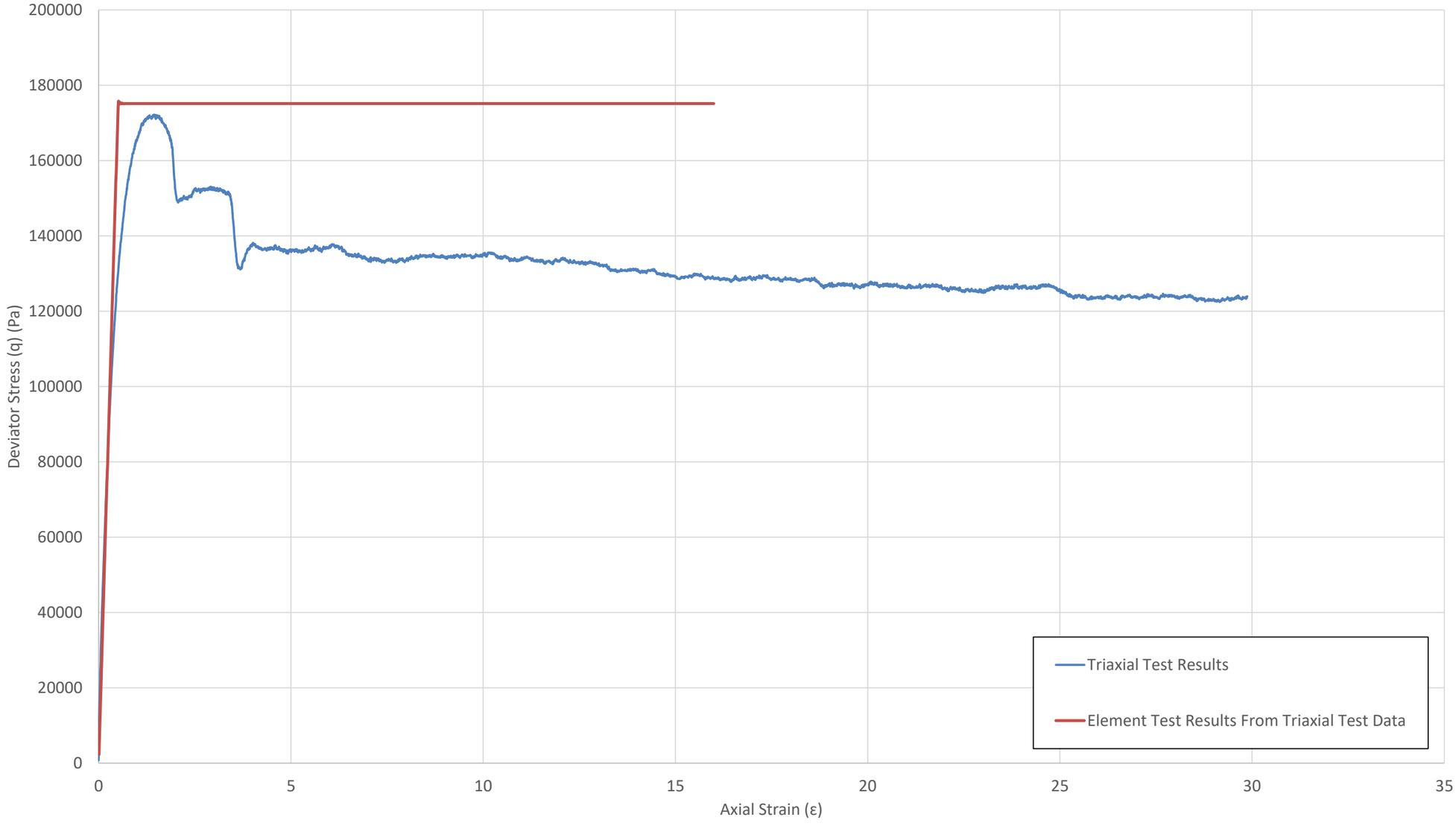
PROJECT

REPORT OF THE EXPERT PANEL ON THE TECHNICAL CAUSES OF THE FAILURE OF FEIJÃO DAM 1

MOHR-COULOMB ELEMENT TEST RESULTS: DRAINED TRIAXIAL COMPRESSION TEST #09

PROJECT No. A03355A01

FIG. No. 07



NOTES:

AS A MUTUAL PROTECTION TO OUR CLIENT, THE PUBLIC AND OURSELVES, ALL REPORTS AND DRAWINGS ARE SUBMITTED FOR THE CONFIDENTIAL INFORMATION OF OUR CLIENT FOR A SPECIFIC PROJECT AND AUTHORIZATION FOR USE AND/OR PUBLICATION OF DATA STATEMENTS, CONCLUSIONS OR ABSTRACTS FROM OR REGARDING OUR REPORTS AND DRAWINGS IS RESERVED PENDING OUR WRITTEN APPROVAL.

CLIENT

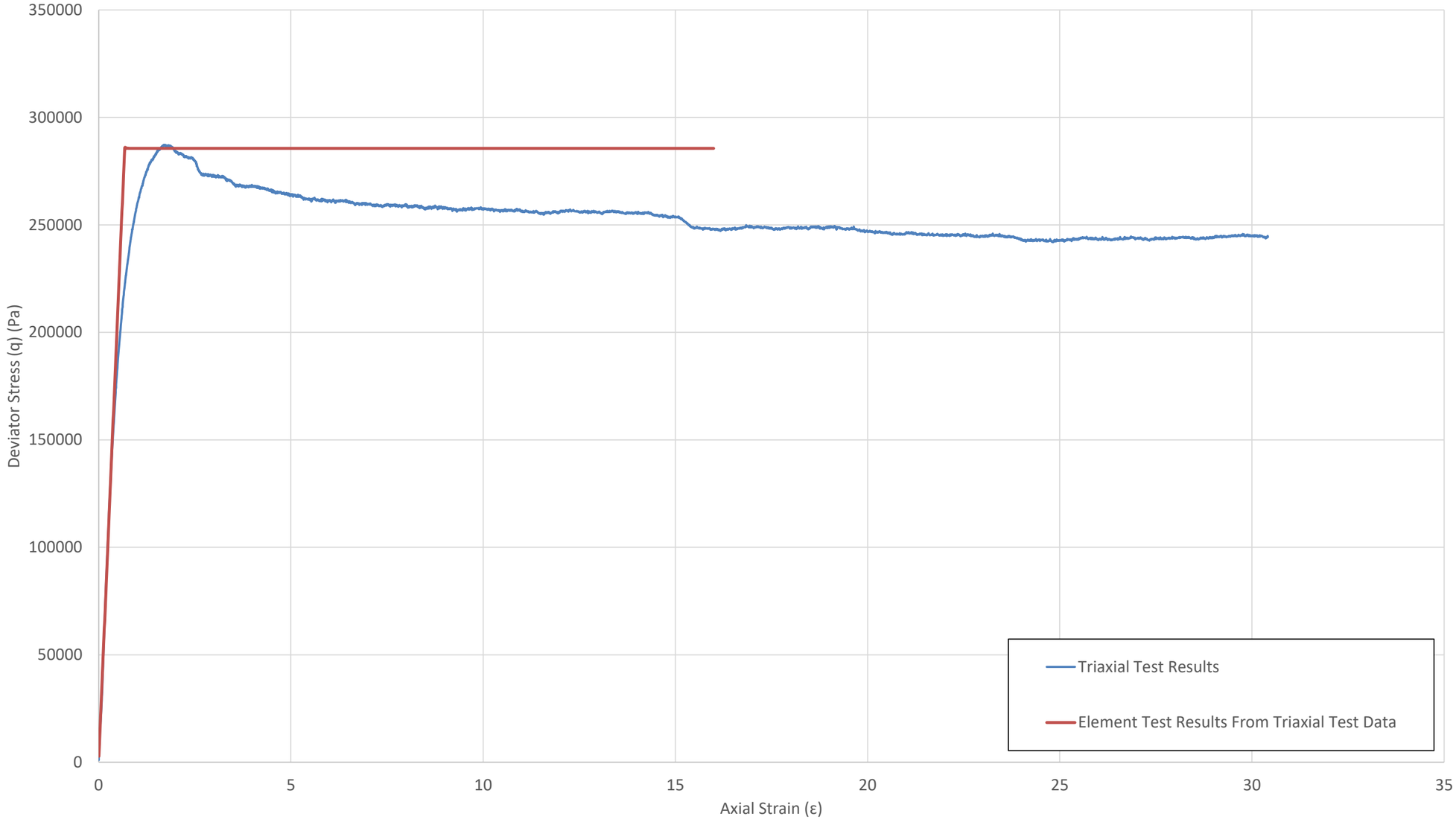
PROJECT

REPORT OF THE EXPERT PANEL ON THE TECHNICAL CAUSES OF THE FAILURE OF FEIJÃO DAM 1

MOHR-COULOMB ELEMENT TEST RESULTS: DRAINED TRIAXIAL COMPRESSION TEST #10

PROJECT No. A03355A01

FIG. No. 08



NOTES:

AS A MUTUAL PROTECTION TO OUR CLIENT, THE PUBLIC AND OURSELVES, ALL REPORTS AND DRAWINGS ARE SUBMITTED FOR THE CONFIDENTIAL INFORMATION OF OUR CLIENT FOR A SPECIFIC PROJECT AND AUTHORIZATION FOR USE AND/OR PUBLICATION OF DATA STATEMENTS, CONCLUSIONS OR ABSTRACTS FROM OR REGARDING OUR REPORTS AND DRAWINGS IS RESERVED PENDING OUR WRITTEN APPROVAL.

CLIENT

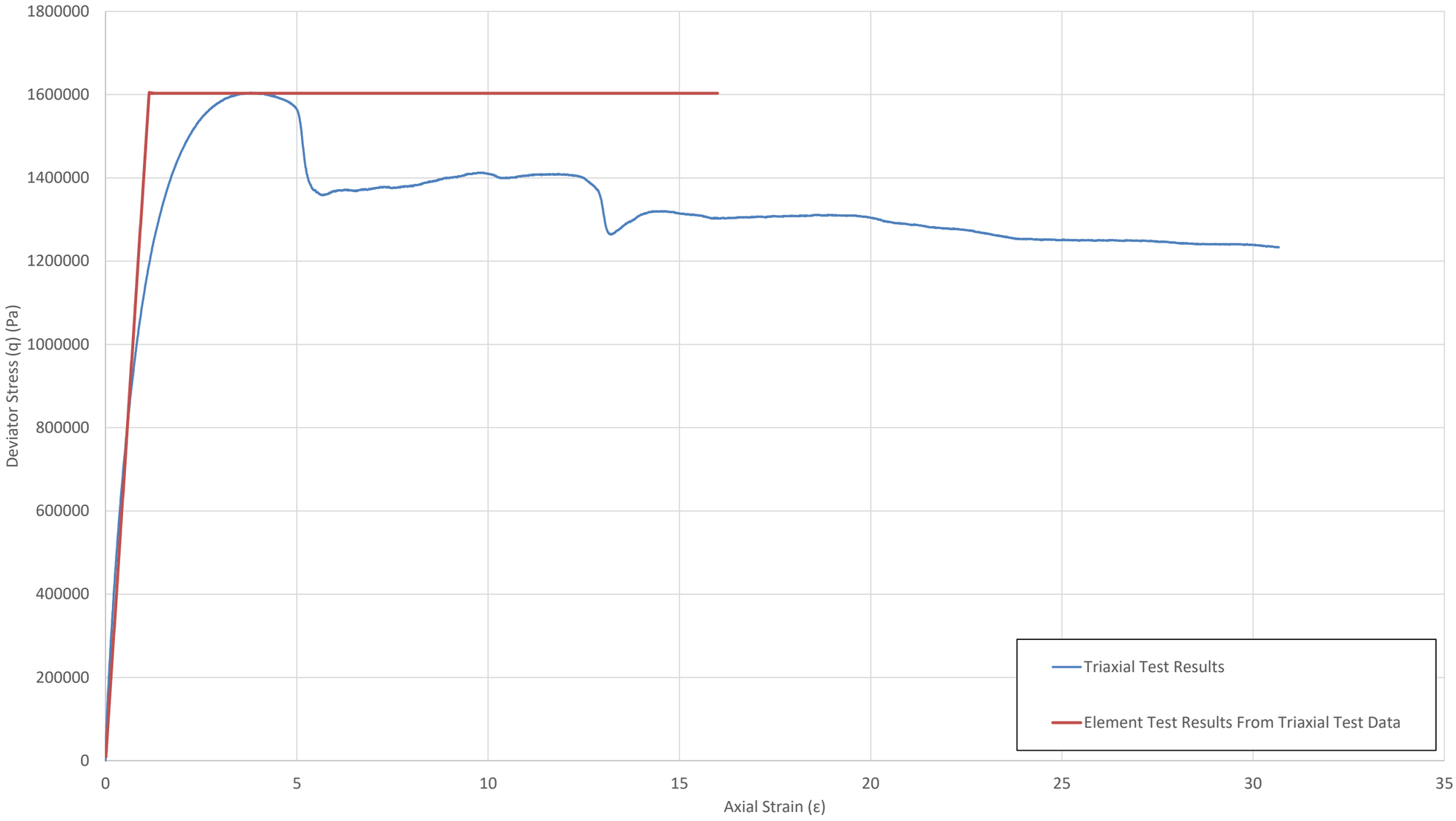
PROJECT

REPORT OF THE EXPERT PANEL ON THE TECHNICAL CAUSES OF THE FAILURE OF FEIJÃO DAM 1

MOHR-COULOMB ELEMENT TEST RESULTS: DRAINED TRIAXIAL COMPRESSION TEST #11

PROJECT No. A03355A01

FIG. No. 09



NOTES:

AS A MUTUAL PROTECTION TO OUR CLIENT, THE PUBLIC AND OURSELVES, ALL REPORTS AND DRAWINGS ARE SUBMITTED FOR THE CONFIDENTIAL INFORMATION OF OUR CLIENT FOR A SPECIFIC PROJECT AND AUTHORIZATION FOR USE AND/OR PUBLICATION OF DATA STATEMENTS, CONCLUSIONS OR ABSTRACTS FROM OR REGARDING OUR REPORTS AND DRAWINGS IS RESERVED PENDING OUR WRITTEN APPROVAL.

CLIENT

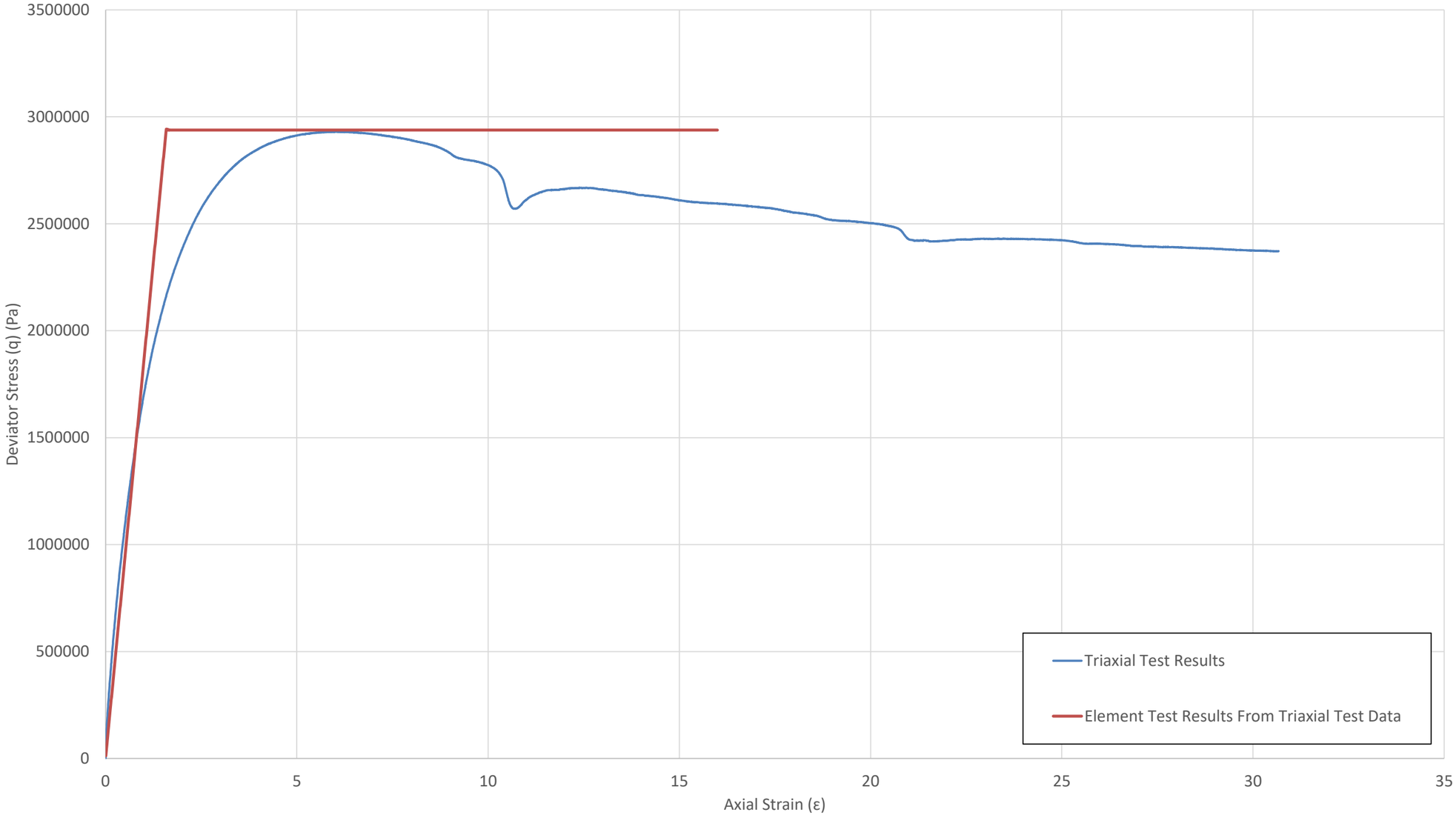
PROJECT

REPORT OF THE EXPERT PANEL ON THE TECHNICAL CAUSES OF THE FAILURE OF FEIJÃO DAM 1

MOHR-COULOMB ELEMENT TEST RESULTS: DRAINED TRIAXIAL COMPRESSION TEST #12

PROJECT No. A03355A01

FIG. No. 10



NOTES:

AS A MUTUAL PROTECTION TO OUR CLIENT, THE PUBLIC AND OURSELVES, ALL REPORTS AND DRAWINGS ARE SUBMITTED FOR THE CONFIDENTIAL INFORMATION OF OUR CLIENT FOR A SPECIFIC PROJECT AND AUTHORIZATION FOR USE AND/OR PUBLICATION OF DATA STATEMENTS, CONCLUSIONS OR ABSTRACTS FROM OR REGARDING OUR REPORTS AND DRAWINGS IS RESERVED PENDING OUR WRITTEN APPROVAL.

CLIENT

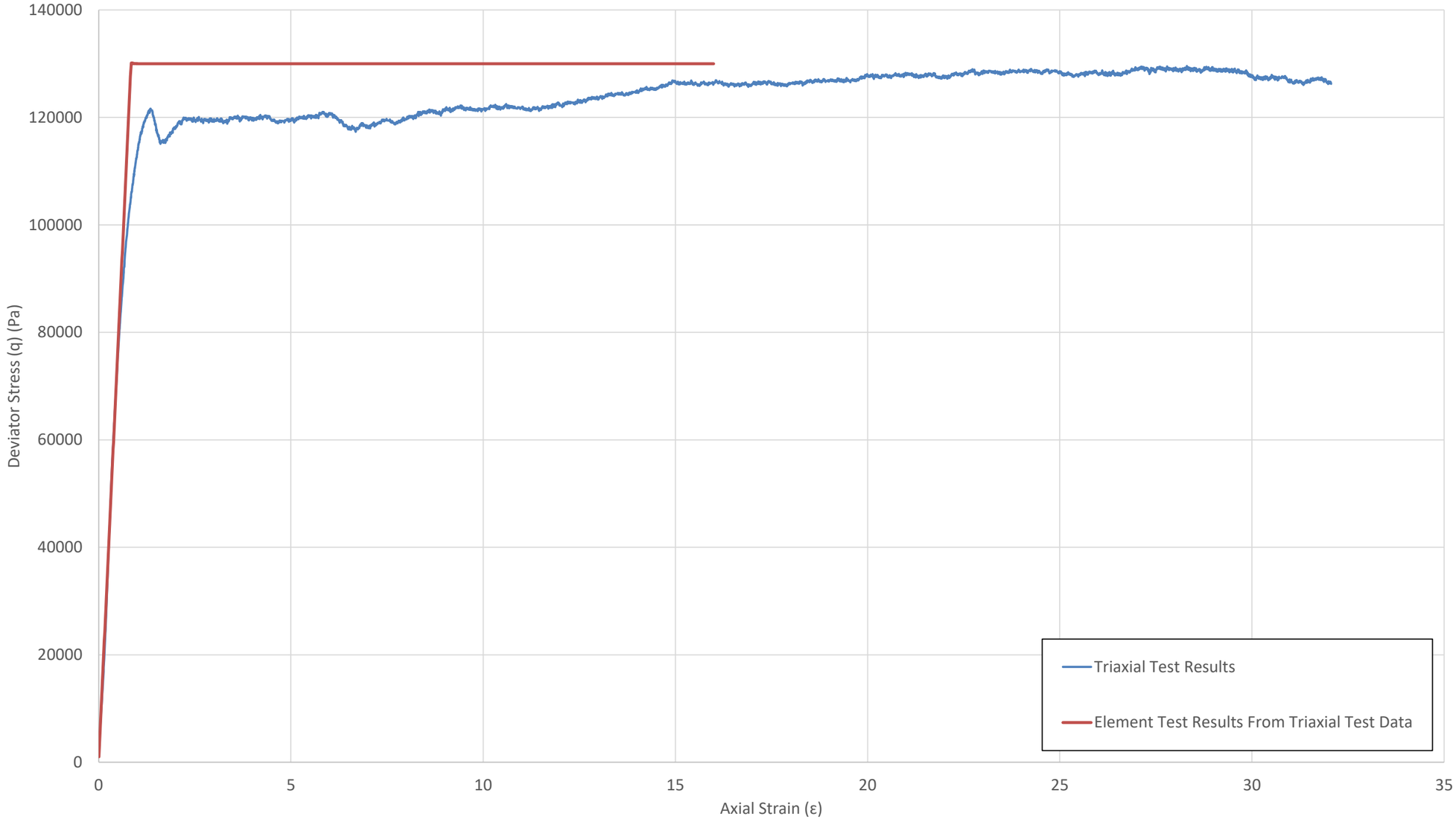
PROJECT

REPORT OF THE EXPERT PANEL ON THE TECHNICAL CAUSES OF THE FAILURE OF FEIJÃO DAM 1

MOHR-COULOMB ELEMENT TEST RESULTS: DRAINED TRIAXIAL COMPRESSION TEST #13

PROJECT No. A03355A01

FIG. No. 11



NOTES:

AS A MUTUAL PROTECTION TO OUR CLIENT, THE PUBLIC AND OURSELVES, ALL REPORTS AND DRAWINGS ARE SUBMITTED FOR THE CONFIDENTIAL INFORMATION OF OUR CLIENT FOR A SPECIFIC PROJECT AND AUTHORIZATION FOR USE AND/OR PUBLICATION OF DATA STATEMENTS, CONCLUSIONS OR ABSTRACTS FROM OR REGARDING OUR REPORTS AND DRAWINGS IS RESERVED PENDING OUR WRITTEN APPROVAL.

CLIENT

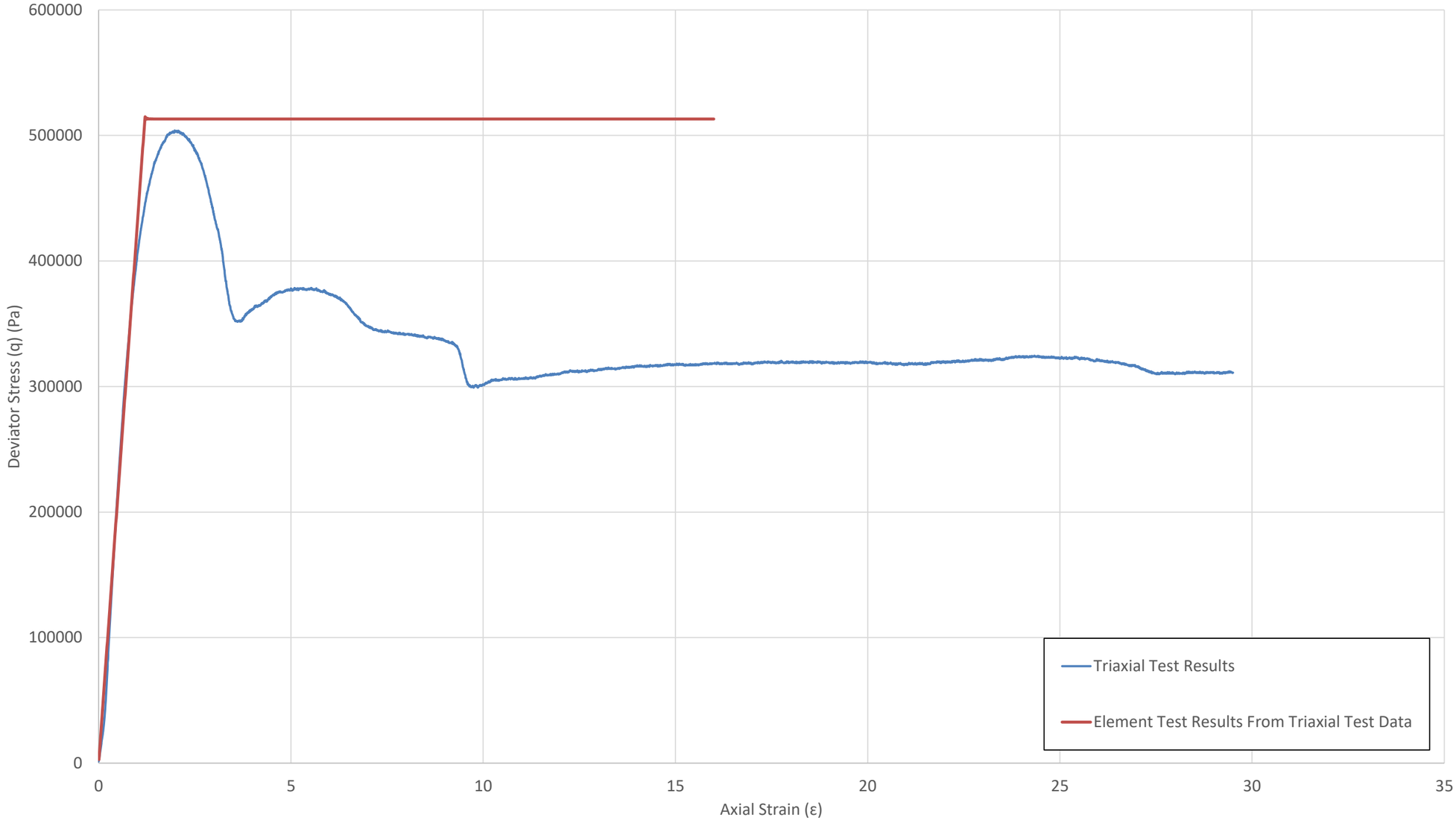
PROJECT

REPORT OF THE EXPERT PANEL ON THE TECHNICAL CAUSES OF THE FAILURE OF FEIJÃO DAM 1

MOHR-COULOMB ELEMENT TEST RESULTS: DRAINED TRIAXIAL COMPRESSION TEST #14

PROJECT No. A03355A01

FIG. No. 12



NOTES:

AS A MUTUAL PROTECTION TO OUR CLIENT, THE PUBLIC AND OURSELVES, ALL REPORTS AND DRAWINGS ARE SUBMITTED FOR THE CONFIDENTIAL INFORMATION OF OUR CLIENT FOR A SPECIFIC PROJECT AND AUTHORIZATION FOR USE AND/OR PUBLICATION OF DATA STATEMENTS, CONCLUSIONS OR ABSTRACTS FROM OR REGARDING OUR REPORTS AND DRAWINGS IS RESERVED PENDING OUR WRITTEN APPROVAL.

CLIENT

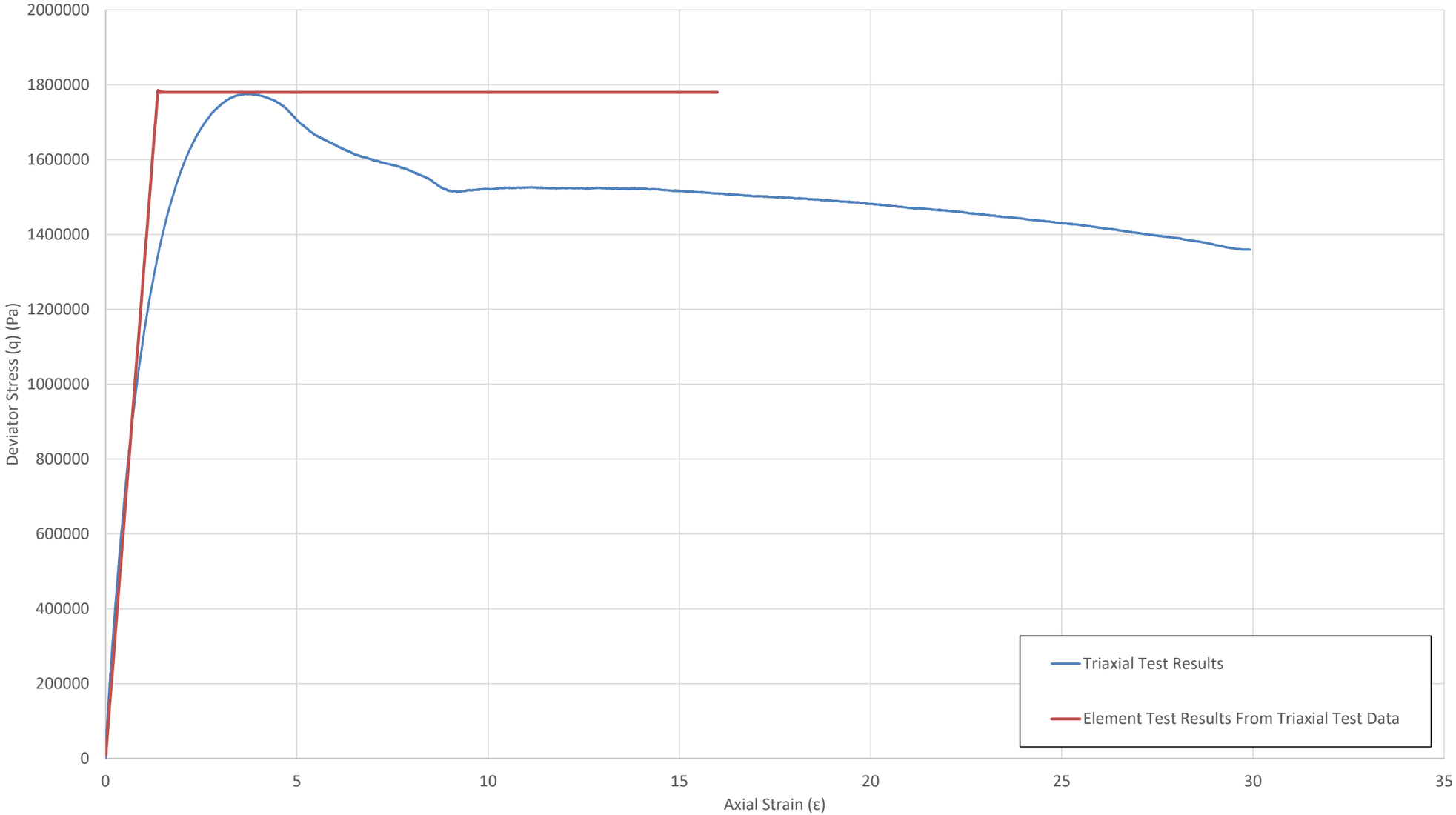
PROJECT

REPORT OF THE EXPERT PANEL ON THE TECHNICAL CAUSES OF THE FAILURE OF FEIJÃO DAM 1

MOHR-COULOMB ELEMENT TEST RESULTS: DRAINED TRIAXIAL COMPRESSION TEST #15

PROJECT No. A03355A01

FIG. No. 13



NOTES:

AS A MUTUAL PROTECTION TO OUR CLIENT, THE PUBLIC AND OURSELVES, ALL REPORTS AND DRAWINGS ARE SUBMITTED FOR THE CONFIDENTIAL INFORMATION OF OUR CLIENT FOR A SPECIFIC PROJECT AND AUTHORIZATION FOR USE AND/OR PUBLICATION OF DATA STATEMENTS, CONCLUSIONS OR ABSTRACTS FROM OR REGARDING OUR REPORTS AND DRAWINGS IS RESERVED PENDING OUR WRITTEN APPROVAL.

CLIENT

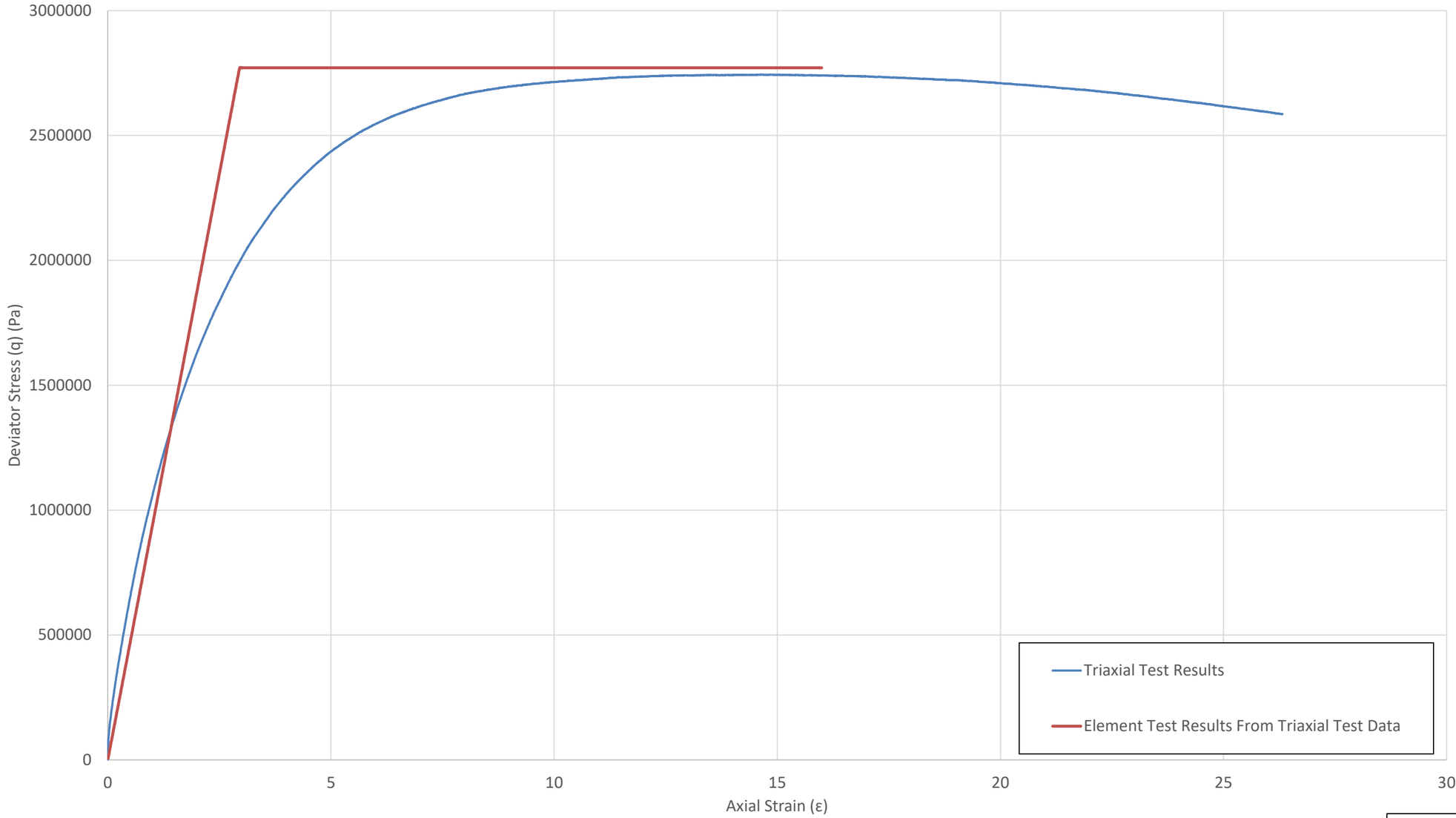
PROJECT

REPORT OF THE EXPERT PANEL ON THE TECHNICAL CAUSES OF THE FAILURE OF FEIJÃO DAM 1

MOHR-COULOMB ELEMENT TEST RESULTS: DRAINED TRIAXIAL COMPRESSION TEST #16

PROJECT No. A03355A01

FIG. No. 14



NOTES:

AS A MUTUAL PROTECTION TO OUR CLIENT, THE PUBLIC AND OURSELVES, ALL REPORTS AND DRAWINGS ARE SUBMITTED FOR THE CONFIDENTIAL INFORMATION OF OUR CLIENT FOR A SPECIFIC PROJECT AND AUTHORIZATION FOR USE AND/OR PUBLICATION OF DATA STATEMENTS, CONCLUSIONS OR ABSTRACTS FROM OR REGARDING OUR REPORTS AND DRAWINGS IS RESERVED PENDING OUR WRITTEN APPROVAL.

CLIENT

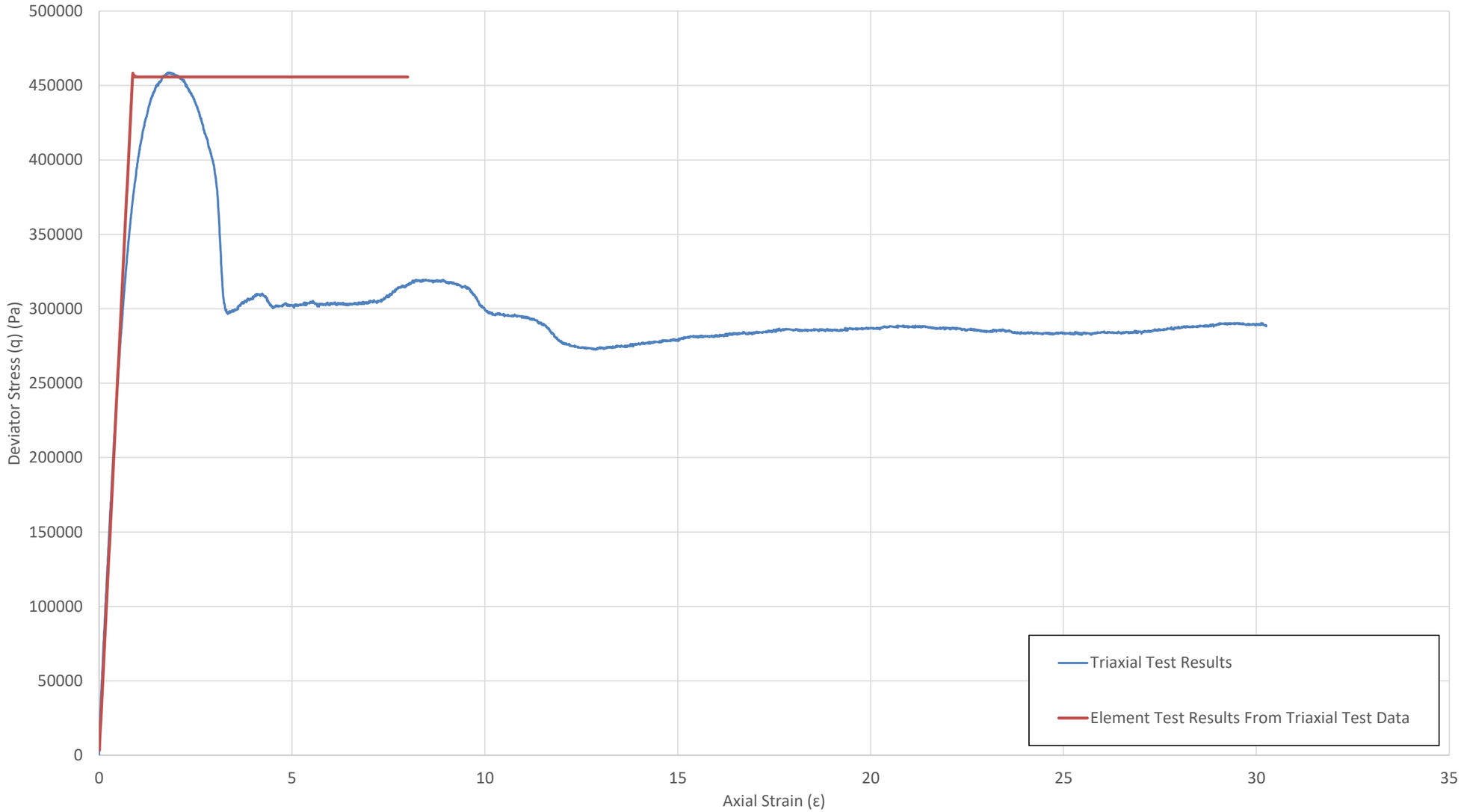
PROJECT

REPORT OF THE EXPERT PANEL ON THE TECHNICAL CAUSES OF THE FAILURE OF FEIJÃO DAM 1

MOHR-COULOMB ELEMENT TEST RESULTS: DRAINED TRIAXIAL COMPRESSION TEST #17

PROJECT No. A03355A01

FIG. No. 15



NOTES:

AS A MUTUAL PROTECTION TO OUR CLIENT, THE PUBLIC AND OURSELVES, ALL REPORTS AND DRAWINGS ARE SUBMITTED FOR THE CONFIDENTIAL INFORMATION OF OUR CLIENT FOR A SPECIFIC PROJECT AND AUTHORIZATION FOR USE AND/OR PUBLICATION OF DATA STATEMENTS, CONCLUSIONS OR ABSTRACTS FROM OR REGARDING OUR REPORTS AND DRAWINGS IS RESERVED PENDING OUR WRITTEN APPROVAL.

CLIENT

PROJECT

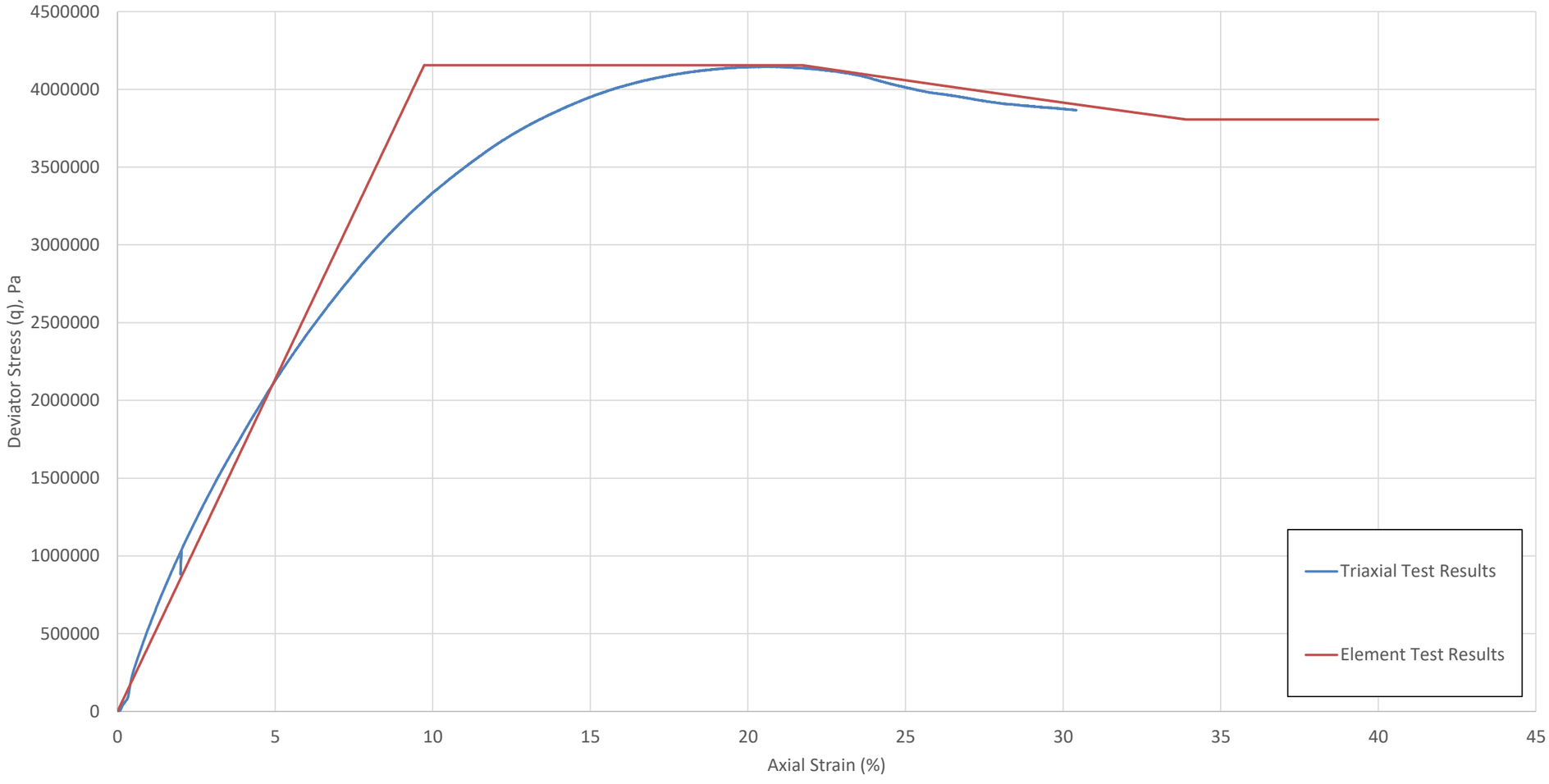
REPORT OF THE EXPERT PANEL ON THE TECHNICAL CAUSES OF THE FAILURE OF FEIJÃO DAM 1

MOHR-COULOMB ELEMENT TEST RESULTS: DRAINED TRIAXIAL COMPRESSION TEST #18

PROJECT No. A03355A01

FIG. No. 16

Strain Weakening Element Tests - Drained



NOTES:

AS A MUTUAL PROTECTION TO OUR CLIENT, THE PUBLIC AND OURSELVES, ALL REPORTS AND DRAWINGS ARE SUBMITTED FOR THE CONFIDENTIAL INFORMATION OF OUR CLIENT FOR A SPECIFIC PROJECT AND AUTHORIZATION FOR USE AND/OR PUBLICATION OF DATA STATEMENTS, CONCLUSIONS OR ABSTRACTS FROM OR REGARDING OUR REPORTS AND DRAWINGS IS RESERVED PENDING OUR WRITTEN APPROVAL.

CLIENT

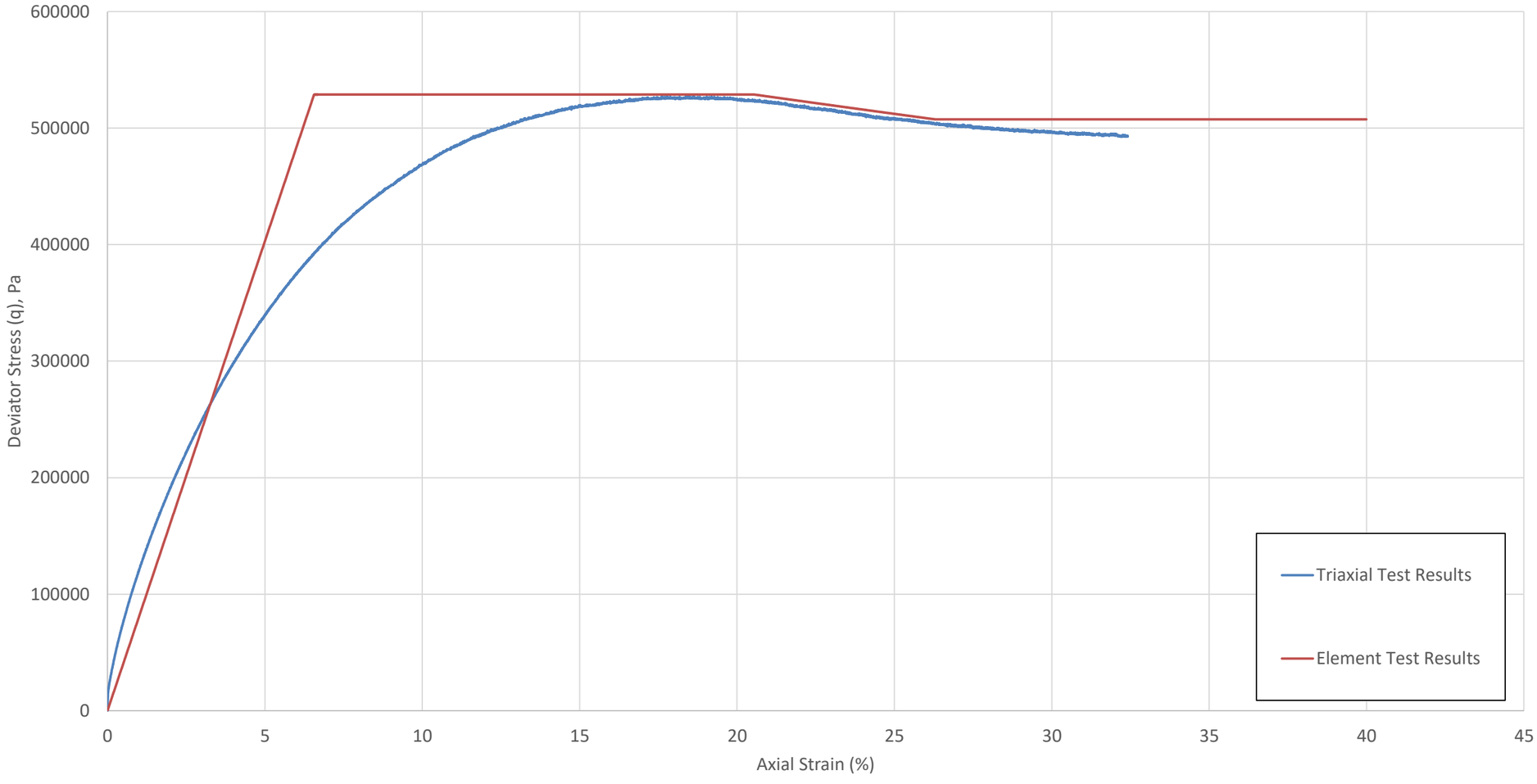
PROJECT

REPORT OF THE EXPERT PANEL ON THE TECHNICAL CAUSES OF THE FAILURE OF FEIJÃO DAM 1

STRAIN WEAKENING ELEMENT TEST RESULTS: DRAINED TRIAXIAL TEST #01

PROJECT No. A03355A01

FIG. No. 17



NOTES:

AS A MUTUAL PROTECTION TO OUR CLIENT, THE PUBLIC AND OURSELVES, ALL REPORTS AND DRAWINGS ARE SUBMITTED FOR THE CONFIDENTIAL INFORMATION OF OUR CLIENT FOR A SPECIFIC PROJECT AND AUTHORIZATION FOR USE AND/OR PUBLICATION OF DATA STATEMENTS, CONCLUSIONS OR ABSTRACTS FROM OR REGARDING OUR REPORTS AND DRAWINGS IS RESERVED PENDING OUR WRITTEN APPROVAL.

CLIENT

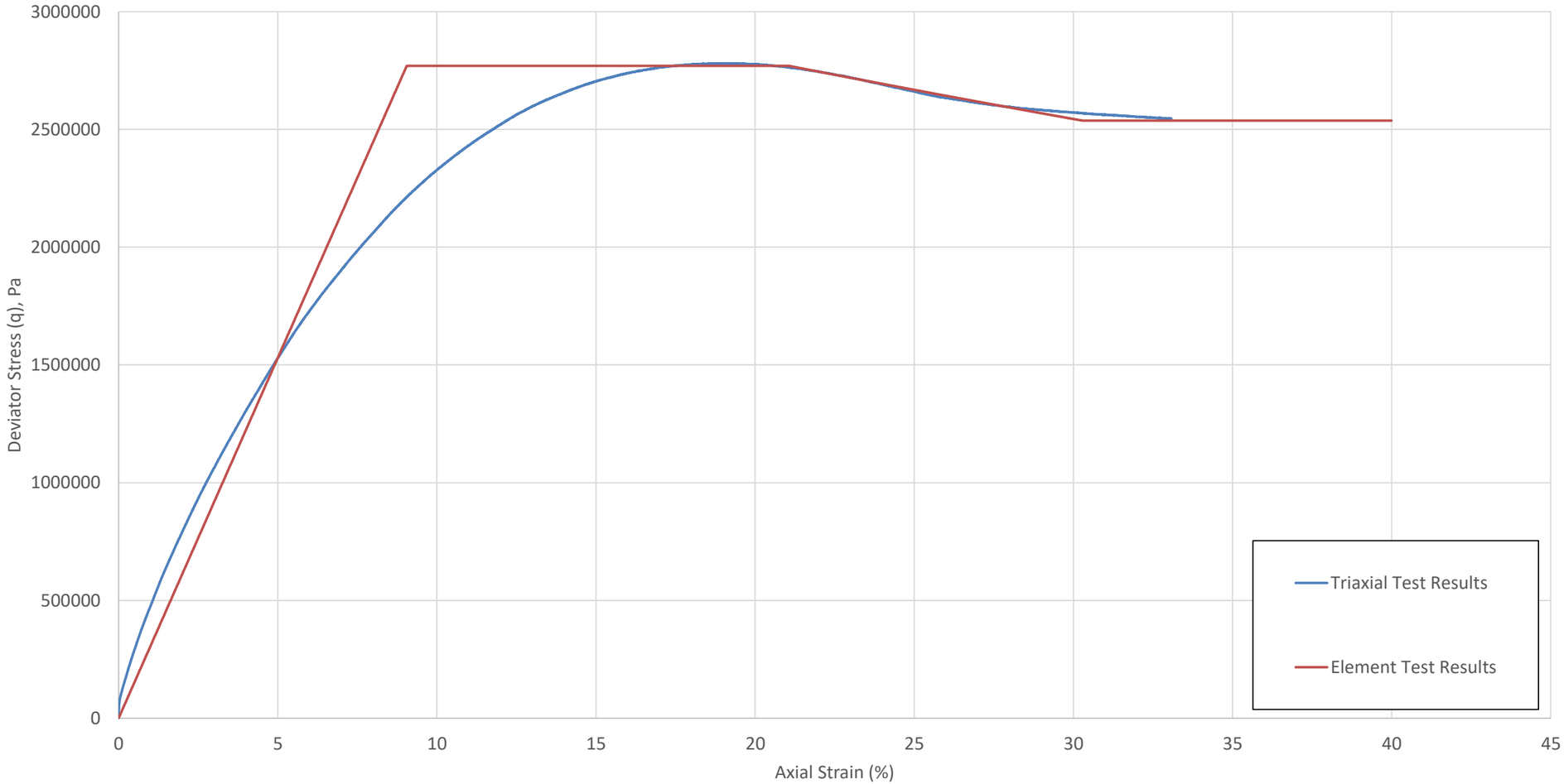
PROJECT

REPORT OF THE EXPERT PANEL ON THE TECHNICAL CAUSES OF THE FAILURE OF FEIJÃO DAM 1

STRAIN WEAKENING ELEMENT TEST RESULTS: DRAINED TRIAXIAL TEST #02

PROJECT No. A03355A01

FIG. No. 18



NOTES:

AS A MUTUAL PROTECTION TO OUR CLIENT, THE PUBLIC AND OURSELVES, ALL REPORTS AND DRAWINGS ARE SUBMITTED FOR THE CONFIDENTIAL INFORMATION OF OUR CLIENT FOR A SPECIFIC PROJECT AND AUTHORIZATION FOR USE AND/OR PUBLICATION OF DATA STATEMENTS, CONCLUSIONS OR ABSTRACTS FROM OR REGARDING OUR REPORTS AND DRAWINGS IS RESERVED PENDING OUR WRITTEN APPROVAL.

CLIENT

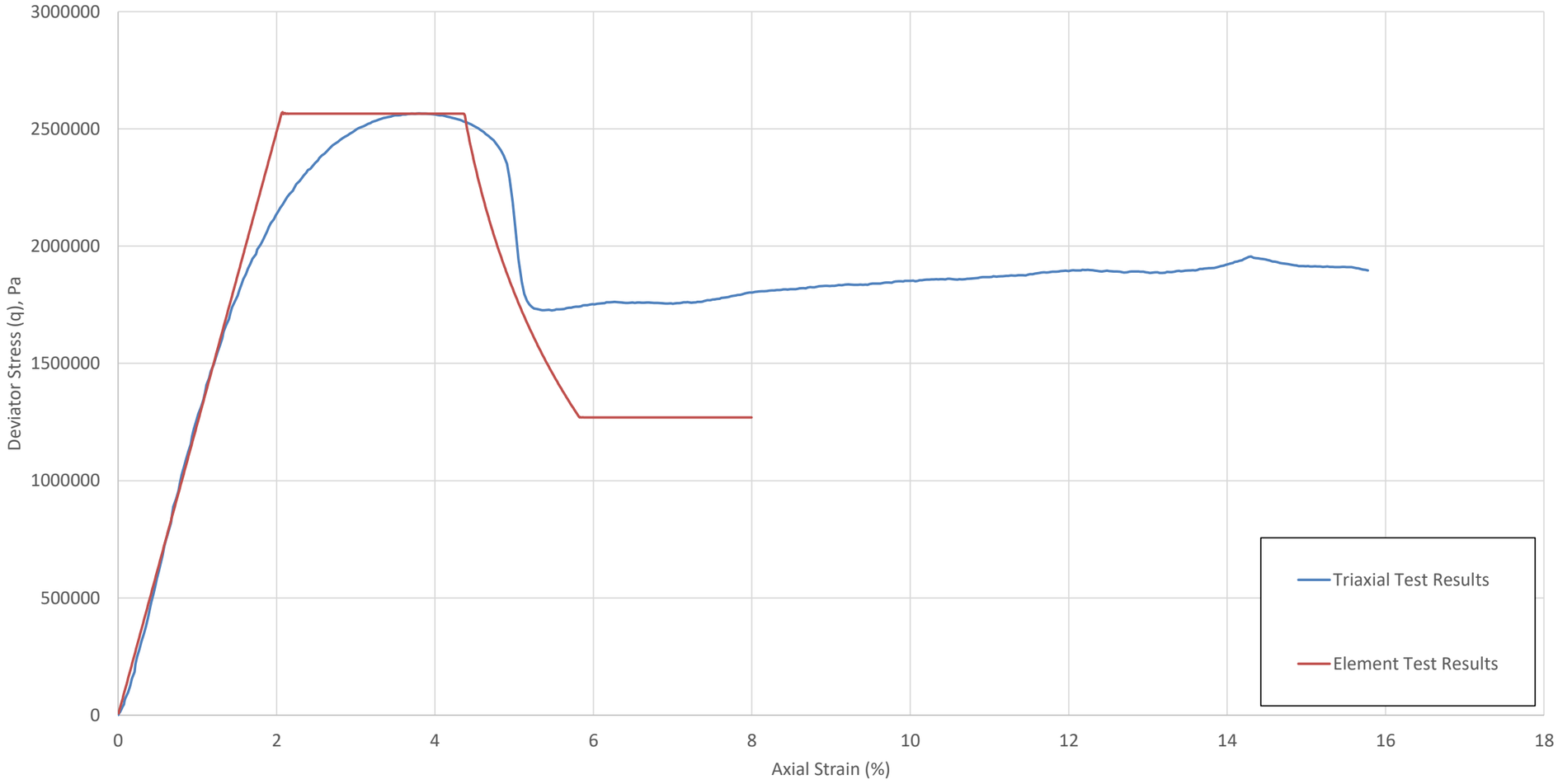
PROJECT

REPORT OF THE EXPERT PANEL ON THE TECHNICAL CAUSES OF THE FAILURE OF FEIJÃO DAM 1

STRAIN WEAKENING ELEMENT TEST RESULTS: DRAINED TRIAXIAL TEST #03

PROJECT No. A03355A01

FIG. No. 19



NOTES:

AS A MUTUAL PROTECTION TO OUR CLIENT, THE PUBLIC AND OURSELVES, ALL REPORTS AND DRAWINGS ARE SUBMITTED FOR THE CONFIDENTIAL INFORMATION OF OUR CLIENT FOR A SPECIFIC PROJECT AND AUTHORIZATION FOR USE AND/OR PUBLICATION OF DATA STATEMENTS, CONCLUSIONS OR ABSTRACTS FROM OR REGARDING OUR REPORTS AND DRAWINGS IS RESERVED PENDING OUR WRITTEN APPROVAL.

CLIENT

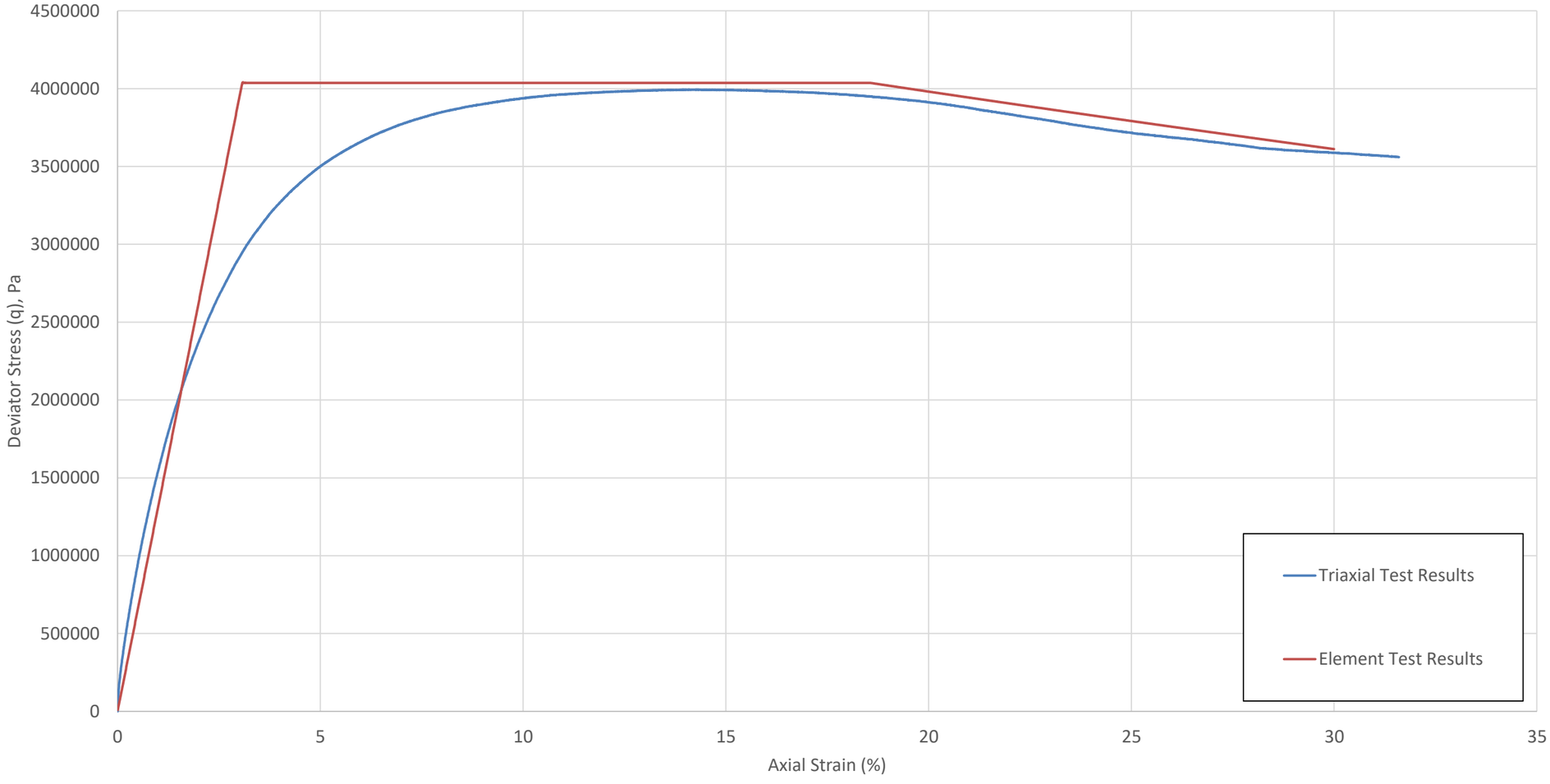
PROJECT

REPORT OF THE EXPERT PANEL ON THE TECHNICAL CAUSES OF THE FAILURE OF FEIJÃO DAM 1

STRAIN WEAKENING ELEMENT TEST RESULTS: DRAINED TRIAXIAL TEST #05

PROJECT No. A03355A01

FIG. No. 20



NOTES:

AS A MUTUAL PROTECTION TO OUR CLIENT, THE PUBLIC AND OURSELVES, ALL REPORTS AND DRAWINGS ARE SUBMITTED FOR THE CONFIDENTIAL INFORMATION OF OUR CLIENT FOR A SPECIFIC PROJECT AND AUTHORIZATION FOR USE AND/OR PUBLICATION OF DATA STATEMENTS, CONCLUSIONS OR ABSTRACTS FROM OR REGARDING OUR REPORTS AND DRAWINGS IS RESERVED PENDING OUR WRITTEN APPROVAL.

CLIENT

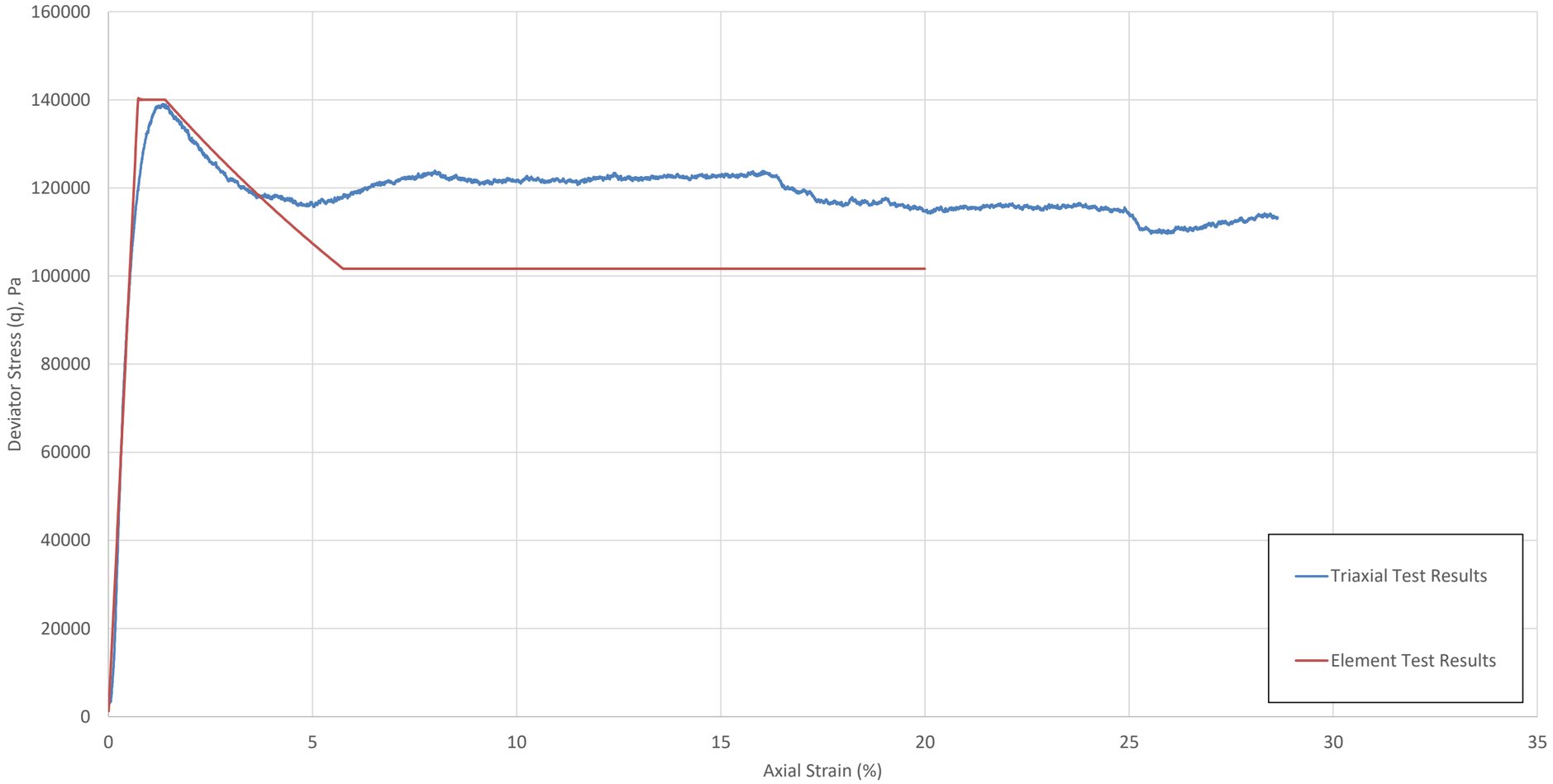
PROJECT

REPORT OF THE EXPERT PANEL ON THE TECHNICAL CAUSES OF THE FAILURE OF FEIJÃO DAM 1

STRAIN WEAKENING ELEMENT TEST RESULTS: DRAINED TRIAXIAL TEST #06

PROJECT No. A03355A01

FIG. No. 21



NOTES:

AS A MUTUAL PROTECTION TO OUR CLIENT, THE PUBLIC AND OURSELVES, ALL REPORTS AND DRAWINGS ARE SUBMITTED FOR THE CONFIDENTIAL INFORMATION OF OUR CLIENT FOR A SPECIFIC PROJECT AND AUTHORIZATION FOR USE AND/OR PUBLICATION OF DATA STATEMENTS, CONCLUSIONS OR ABSTRACTS FROM OR REGARDING OUR REPORTS AND DRAWINGS IS RESERVED PENDING OUR WRITTEN APPROVAL.

CLIENT

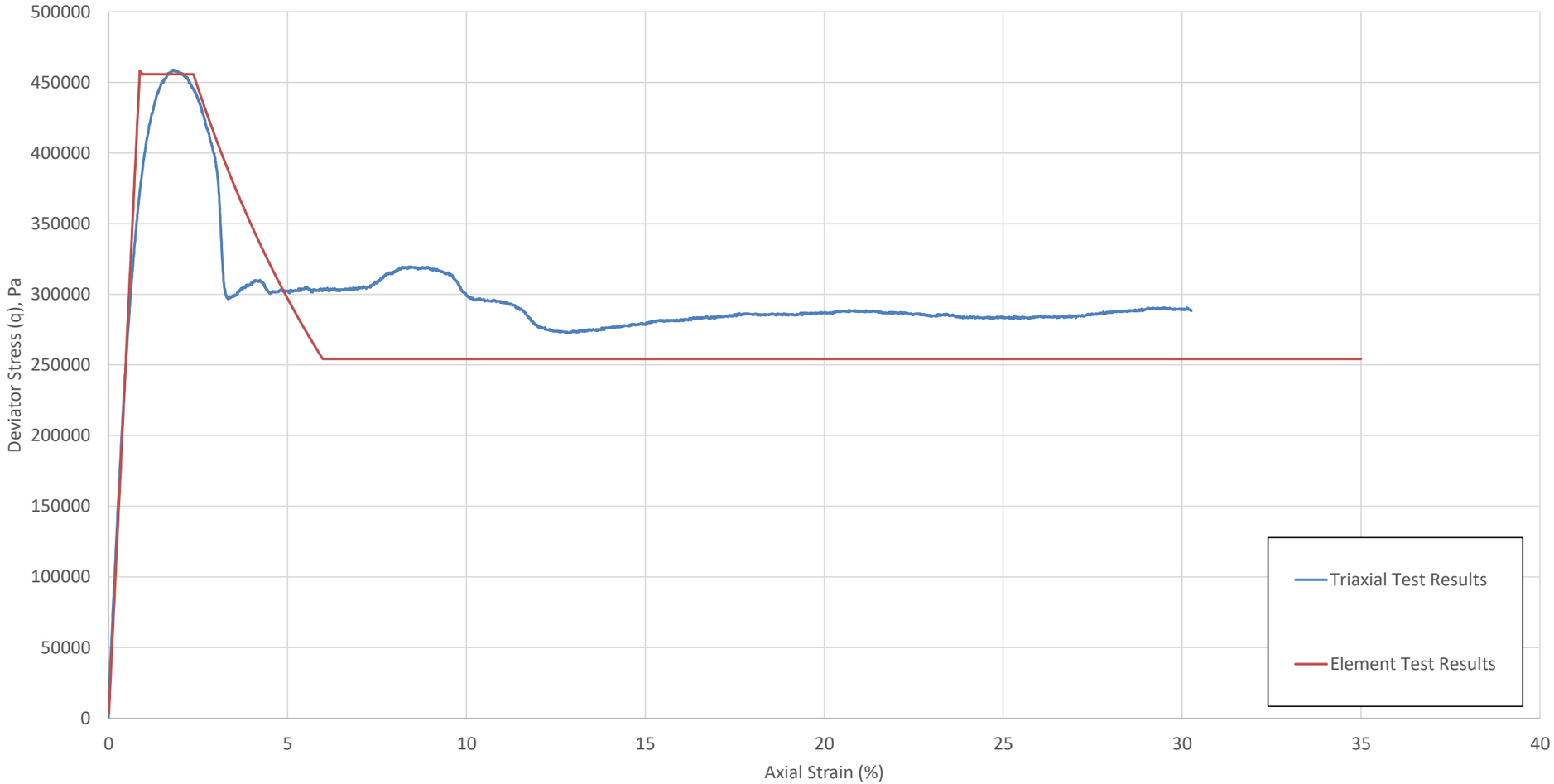
PROJECT

REPORT OF THE EXPERT PANEL ON THE TECHNICAL CAUSES OF THE FAILURE OF FEIJÃO DAM 1

STRAIN WEAKENING ELEMENT TEST RESULTS: DRAINED TRIAXIAL TEST #08

PROJECT No. A03355A01

FIG. No. 22



NOTES:

AS A MUTUAL PROTECTION TO OUR CLIENT, THE PUBLIC AND OURSELVES, ALL REPORTS AND DRAWINGS ARE SUBMITTED FOR THE CONFIDENTIAL INFORMATION OF OUR CLIENT FOR A SPECIFIC PROJECT AND AUTHORIZATION FOR USE AND/OR PUBLICATION OF DATA STATEMENTS, CONCLUSIONS OR ABSTRACTS FROM OR REGARDING OUR REPORTS AND DRAWINGS IS RESERVED PENDING OUR WRITTEN APPROVAL.

CLIENT

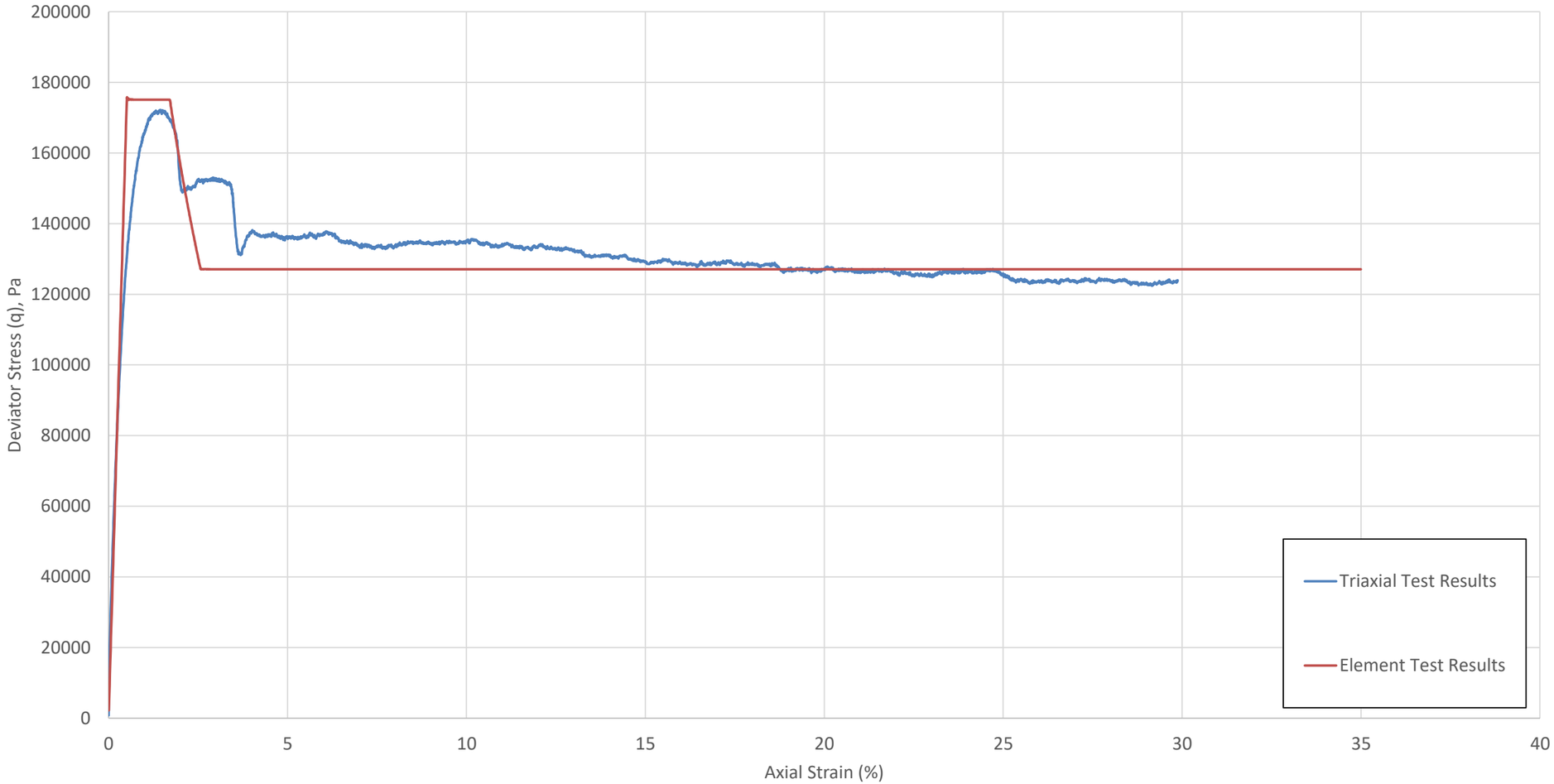
PROJECT

REPORT OF THE EXPERT PANEL ON THE TECHNICAL CAUSES OF THE FAILURE OF FEIJÃO DAM 1

STRAIN WEAKENING ELEMENT TEST RESULTS: DRAINED TRIAXIAL TEST #09

PROJECT No. A03355A01

FIG. No. 23



NOTES:

AS A MUTUAL PROTECTION TO OUR CLIENT, THE PUBLIC AND OURSELVES, ALL REPORTS AND DRAWINGS ARE SUBMITTED FOR THE CONFIDENTIAL INFORMATION OF OUR CLIENT FOR A SPECIFIC PROJECT AND AUTHORIZATION FOR USE AND/OR PUBLICATION OF DATA STATEMENTS, CONCLUSIONS OR ABSTRACTS FROM OR REGARDING OUR REPORTS AND DRAWINGS IS RESERVED PENDING OUR WRITTEN APPROVAL.

CLIENT

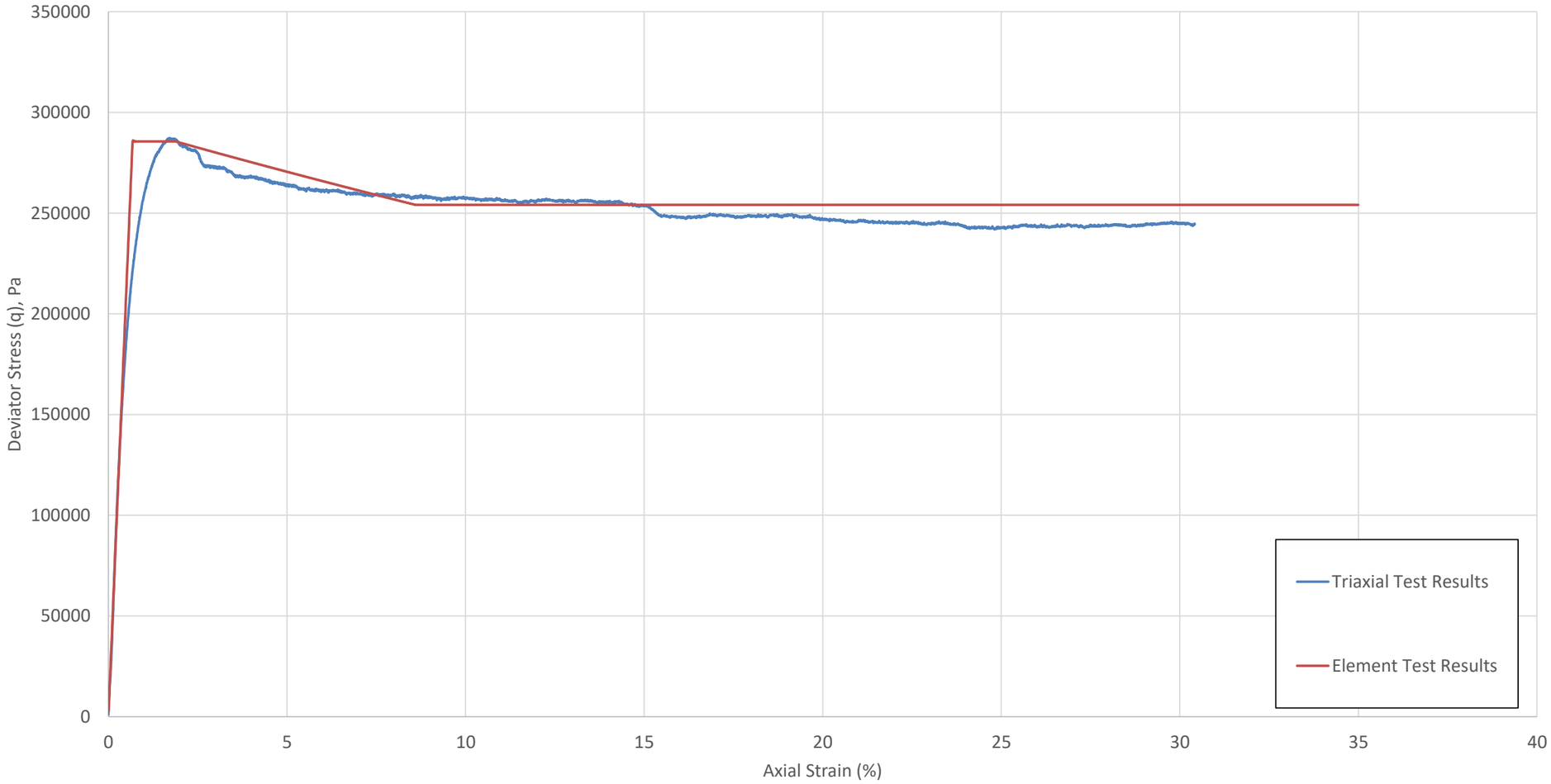
PROJECT

REPORT OF THE EXPERT PANEL ON THE TECHNICAL CAUSES OF THE FAILURE OF FEIJÃO DAM 1

STRAIN WEAKENING ELEMENT TEST RESULTS: DRAINED TRIAXIAL TEST #10

PROJECT No. A03355A01

FIG. No. 24



NOTES:

AS A MUTUAL PROTECTION TO OUR CLIENT, THE PUBLIC AND OURSELVES, ALL REPORTS AND DRAWINGS ARE SUBMITTED FOR THE CONFIDENTIAL INFORMATION OF OUR CLIENT FOR A SPECIFIC PROJECT AND AUTHORIZATION FOR USE AND/OR PUBLICATION OF DATA STATEMENTS, CONCLUSIONS OR ABSTRACTS FROM OR REGARDING OUR REPORTS AND DRAWINGS IS RESERVED PENDING OUR WRITTEN APPROVAL.

CLIENT

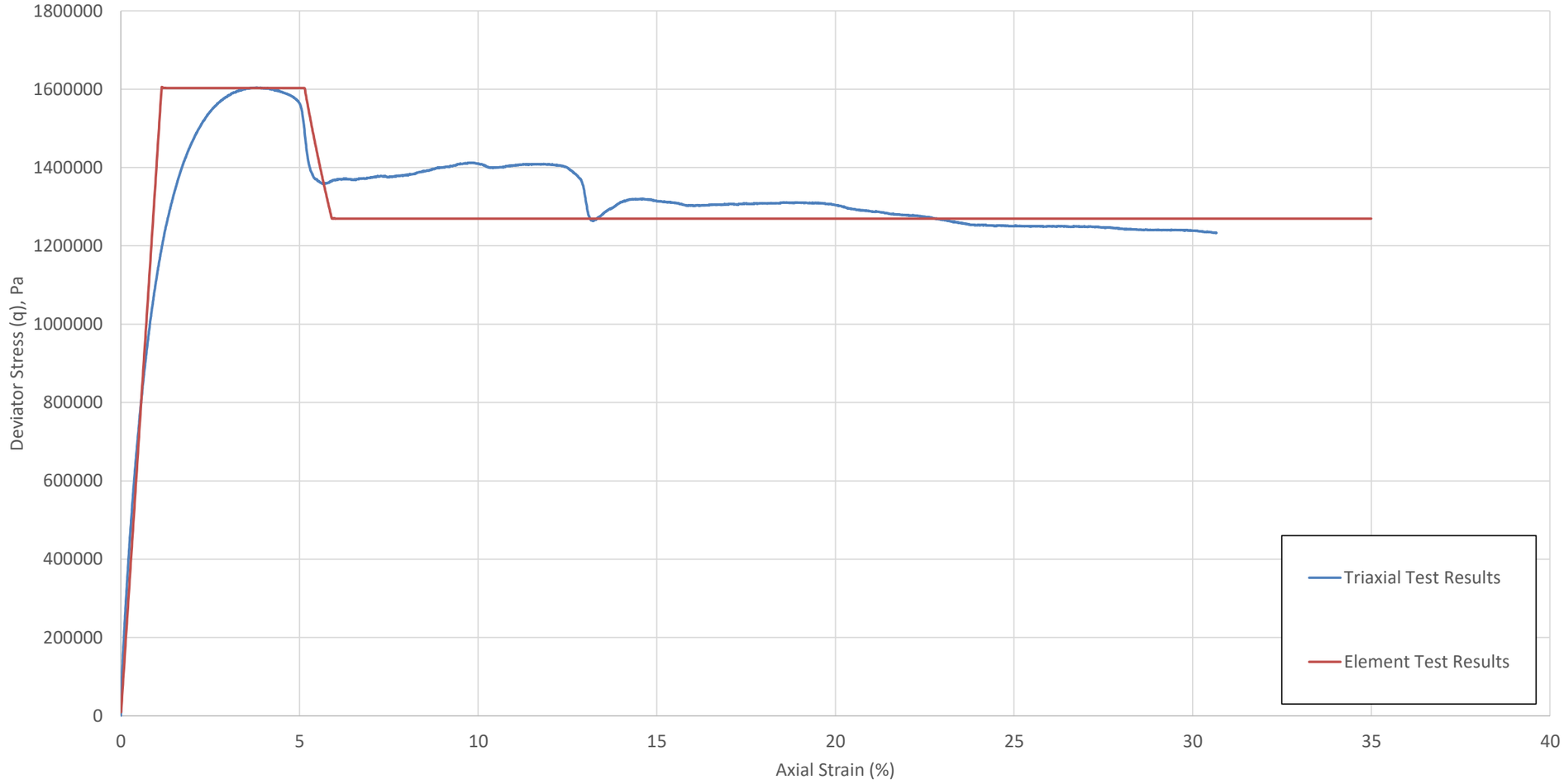
PROJECT

REPORT OF THE EXPERT PANEL ON THE TECHNICAL CAUSES OF THE FAILURE OF FEIJÃO DAM 1

STRAIN WEAKENING ELEMENT TEST RESULTS: DRAINED TRIAXIAL TEST #11

PROJECT No. A03355A01

FIG. No. 25



NOTES:

AS A MUTUAL PROTECTION TO OUR CLIENT, THE PUBLIC AND OURSELVES, ALL REPORTS AND DRAWINGS ARE SUBMITTED FOR THE CONFIDENTIAL INFORMATION OF OUR CLIENT FOR A SPECIFIC PROJECT AND AUTHORIZATION FOR USE AND/OR PUBLICATION OF DATA STATEMENTS, CONCLUSIONS OR ABSTRACTS FROM OR REGARDING OUR REPORTS AND DRAWINGS IS RESERVED PENDING OUR WRITTEN APPROVAL.

CLIENT

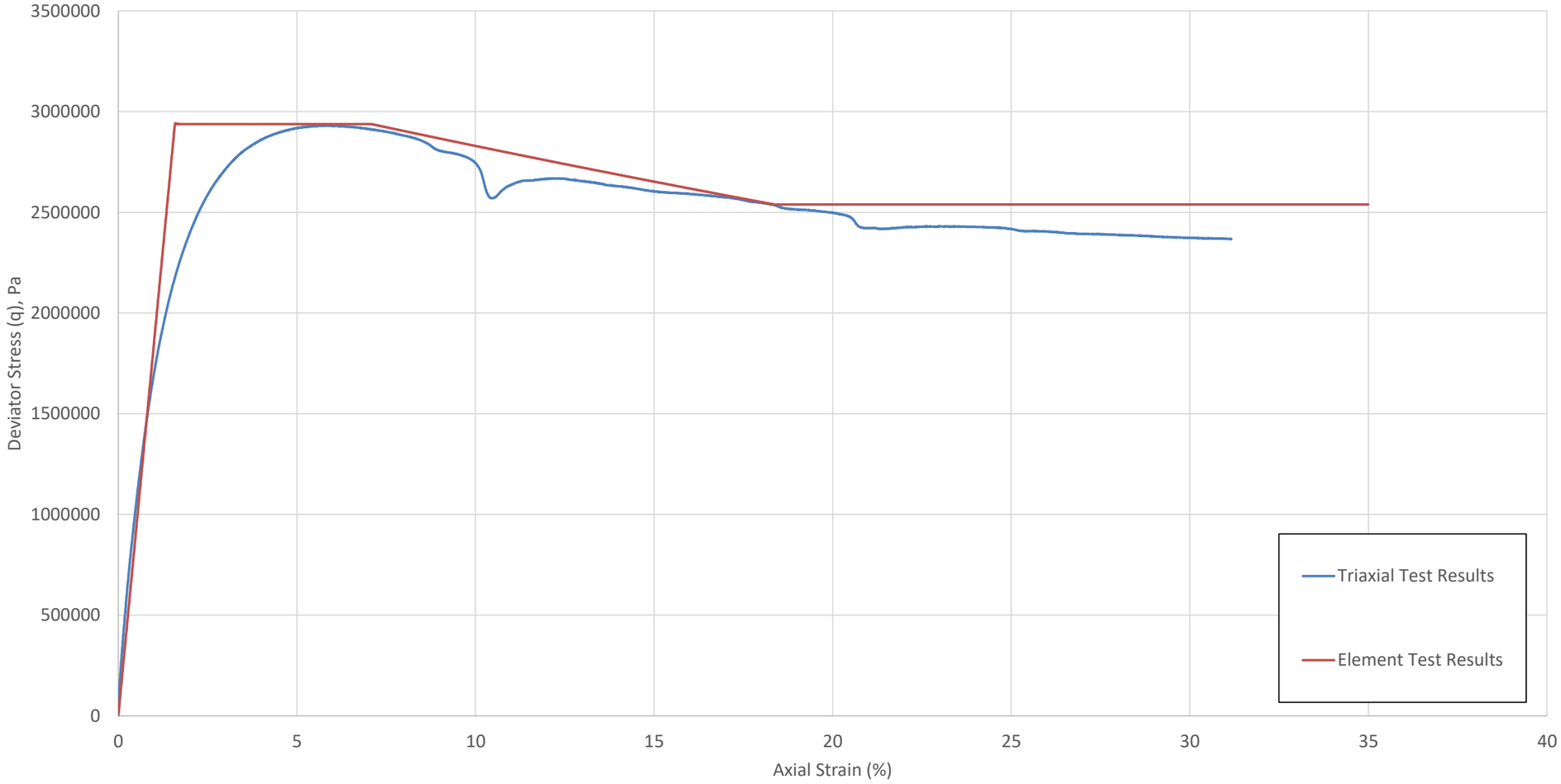
PROJECT

REPORT OF THE EXPERT PANEL ON THE TECHNICAL CAUSES OF THE FAILURE OF FEIJÃO DAM 1

STRAIN WEAKENING ELEMENT TEST RESULTS: DRAINED TRIAXIAL TEST #12

PROJECT No. A03355A01

FIG. No. 26



NOTES:

AS A MUTUAL PROTECTION TO OUR CLIENT, THE PUBLIC AND OURSELVES, ALL REPORTS AND DRAWINGS ARE SUBMITTED FOR THE CONFIDENTIAL INFORMATION OF OUR CLIENT FOR A SPECIFIC PROJECT AND AUTHORIZATION FOR USE AND/OR PUBLICATION OF DATA STATEMENTS, CONCLUSIONS OR ABSTRACTS FROM OR REGARDING OUR REPORTS AND DRAWINGS IS RESERVED PENDING OUR WRITTEN APPROVAL.

CLIENT

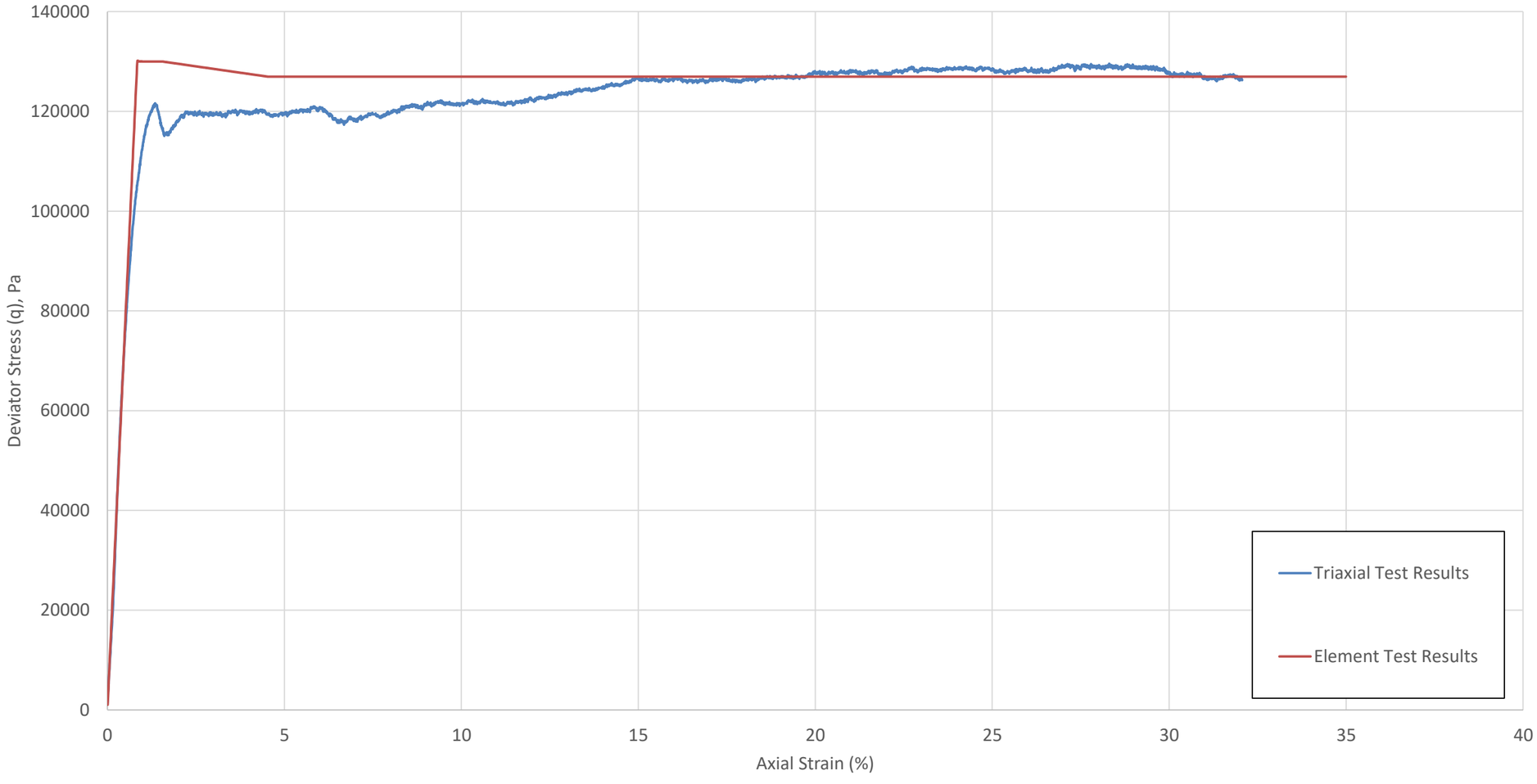
PROJECT

REPORT OF THE EXPERT PANEL ON THE TECHNICAL CAUSES OF THE FAILURE OF FEIJÃO DAM 1

STRAIN WEAKENING ELEMENT TEST RESULTS: DRAINED TRIAXIAL TEST #13

PROJECT No. A03355A01

FIG. No. 27



NOTES:

AS A MUTUAL PROTECTION TO OUR CLIENT, THE PUBLIC AND OURSELVES, ALL REPORTS AND DRAWINGS ARE SUBMITTED FOR THE CONFIDENTIAL INFORMATION OF OUR CLIENT FOR A SPECIFIC PROJECT AND AUTHORIZATION FOR USE AND/OR PUBLICATION OF DATA STATEMENTS, CONCLUSIONS OR ABSTRACTS FROM OR REGARDING OUR REPORTS AND DRAWINGS IS RESERVED PENDING OUR WRITTEN APPROVAL.

CLIENT

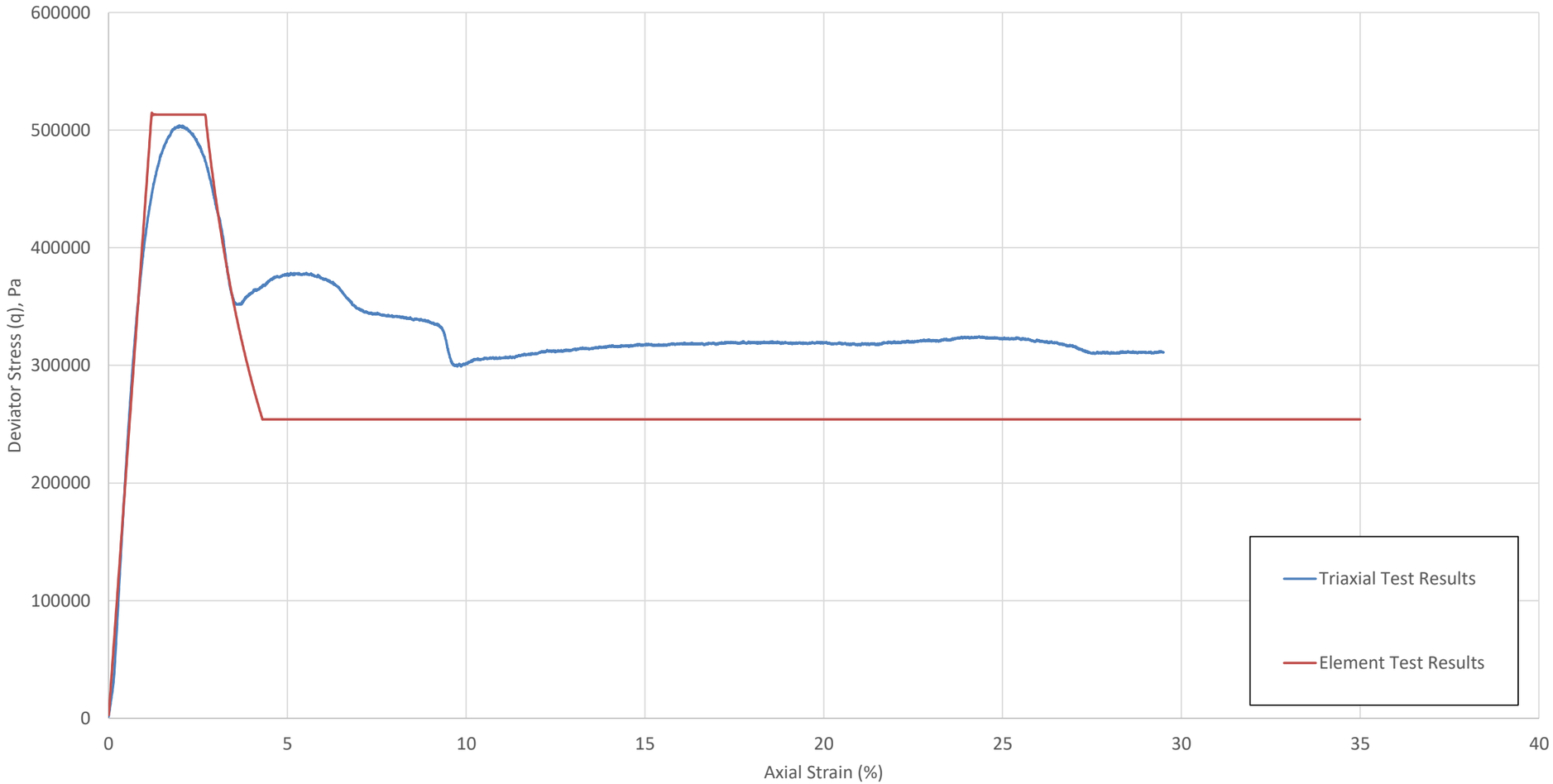
PROJECT

REPORT OF THE EXPERT PANEL ON THE TECHNICAL CAUSES OF THE FAILURE OF FEIJÃO DAM 1

STRAIN WEAKENING ELEMENT TEST RESULTS: DRAINED TRIAXIAL TEST #14

PROJECT No. A03355A01

FIG. No. 28



NOTES:

AS A MUTUAL PROTECTION TO OUR CLIENT, THE PUBLIC AND OURSELVES, ALL REPORTS AND DRAWINGS ARE SUBMITTED FOR THE CONFIDENTIAL INFORMATION OF OUR CLIENT FOR A SPECIFIC PROJECT AND AUTHORIZATION FOR USE AND/OR PUBLICATION OF DATA STATEMENTS, CONCLUSIONS OR ABSTRACTS FROM OR REGARDING OUR REPORTS AND DRAWINGS IS RESERVED PENDING OUR WRITTEN APPROVAL.

CLIENT

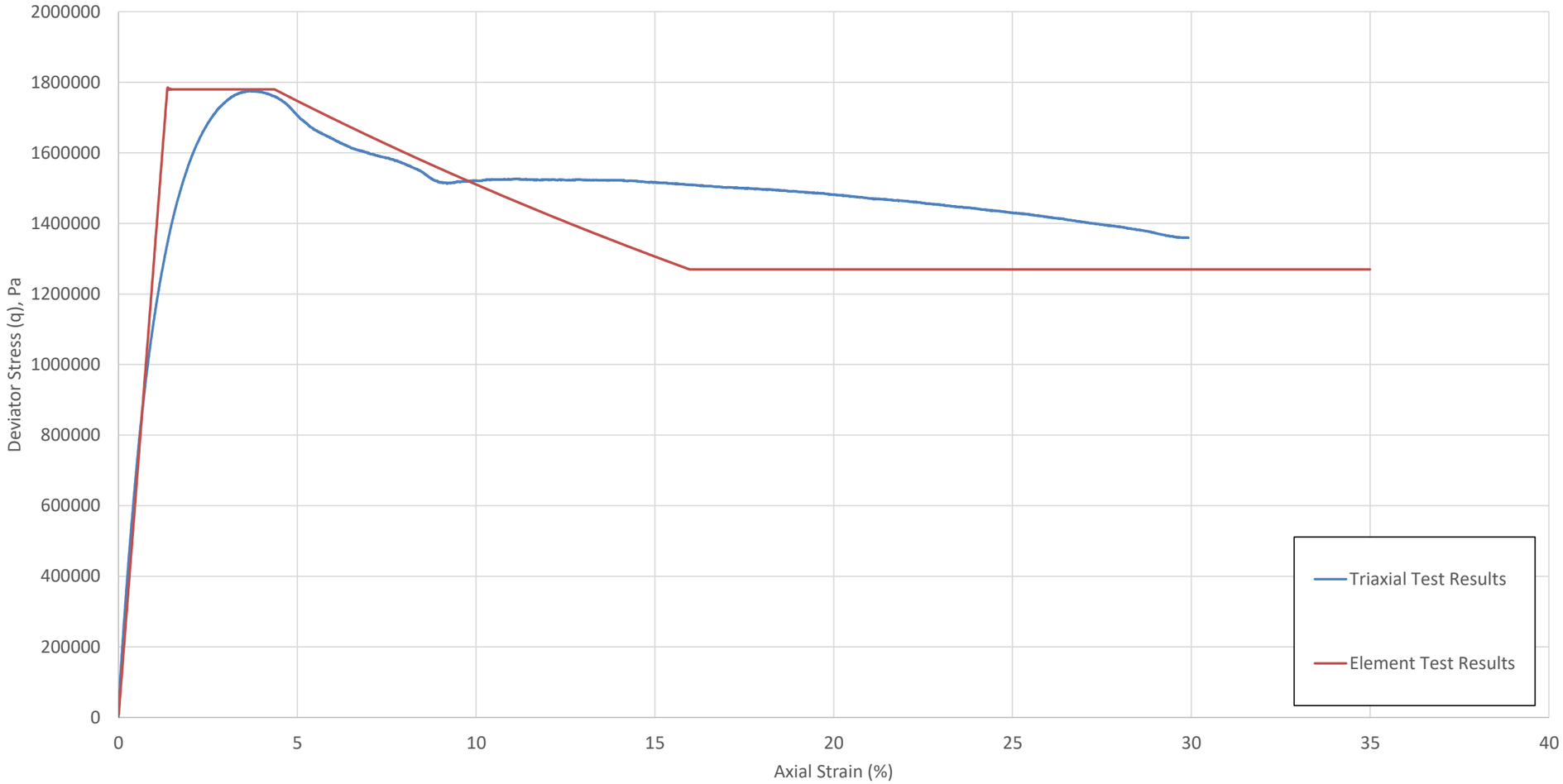
PROJECT

REPORT OF THE EXPERT PANEL ON THE TECHNICAL CAUSES OF THE FAILURE OF FEIJÃO DAM 1

STRAIN WEAKENING ELEMENT TEST RESULTS: DRAINED TRIAXIAL TEST #15

PROJECT No. A03355A01

FIG. No. 29



NOTES:

AS A MUTUAL PROTECTION TO OUR CLIENT, THE PUBLIC AND OURSELVES, ALL REPORTS AND DRAWINGS ARE SUBMITTED FOR THE CONFIDENTIAL INFORMATION OF OUR CLIENT FOR A SPECIFIC PROJECT AND AUTHORIZATION FOR USE AND/OR PUBLICATION OF DATA STATEMENTS, CONCLUSIONS OR ABSTRACTS FROM OR REGARDING OUR REPORTS AND DRAWINGS IS RESERVED PENDING OUR WRITTEN APPROVAL.

CLIENT

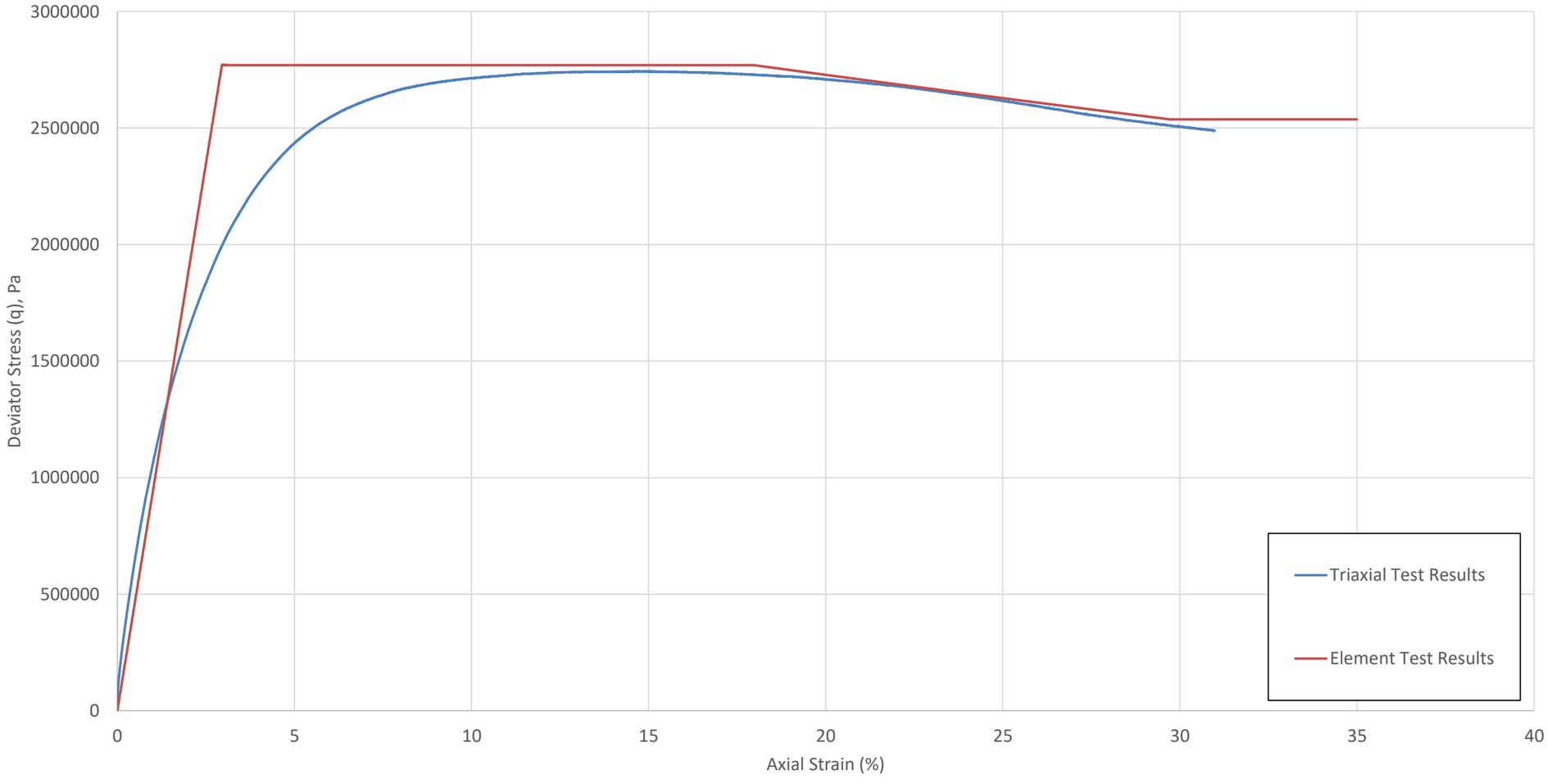
PROJECT

REPORT OF THE EXPERT PANEL ON THE TECHNICAL CAUSES OF THE FAILURE OF FEIJÃO DAM 1

STRAIN WEAKENING ELEMENT TEST RESULTS: DRAINED TRIAXIAL TEST #16

PROJECT No. A03355A01

FIG. No. 30



NOTES:

AS A MUTUAL PROTECTION TO OUR CLIENT, THE PUBLIC AND OURSELVES, ALL REPORTS AND DRAWINGS ARE SUBMITTED FOR THE CONFIDENTIAL INFORMATION OF OUR CLIENT FOR A SPECIFIC PROJECT AND AUTHORIZATION FOR USE AND/OR PUBLICATION OF DATA STATEMENTS, CONCLUSIONS OR ABSTRACTS FROM OR REGARDING OUR REPORTS AND DRAWINGS IS RESERVED PENDING OUR WRITTEN APPROVAL.

CLIENT

PROJECT

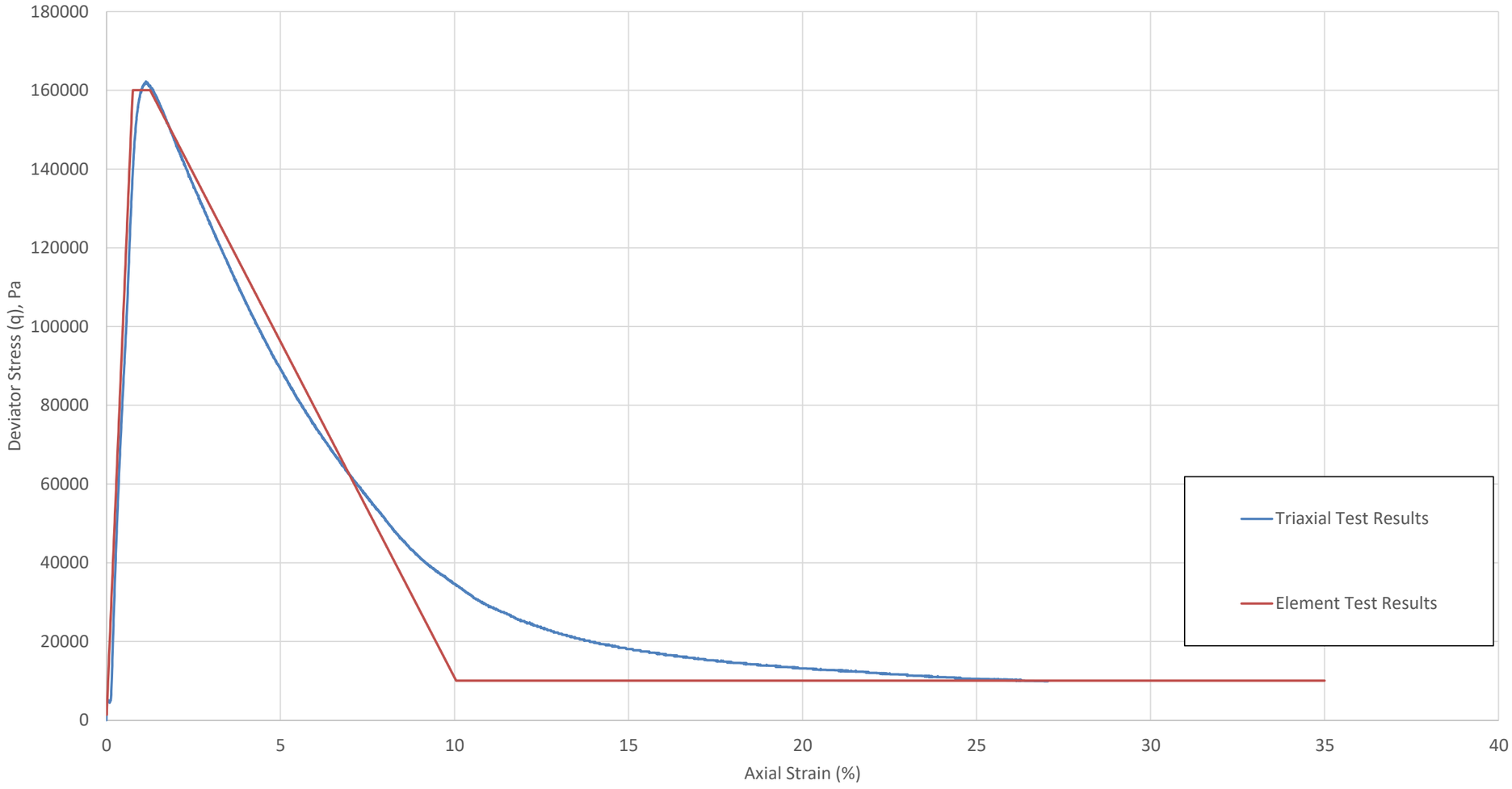
REPORT OF THE EXPERT PANEL ON THE TECHNICAL CAUSES OF THE FAILURE OF FEIJÃO DAM 1

STRAIN WEAKENING ELEMENT TEST RESULTS: DRAINED TRIAXIAL TEST #17

PROJECT No. A03355A01

FIG. No. 31

Strain Weakening Element Tests - Undrained



NOTES:

AS A MUTUAL PROTECTION TO OUR CLIENT, THE PUBLIC AND OURSELVES, ALL REPORTS AND DRAWINGS ARE SUBMITTED FOR THE CONFIDENTIAL INFORMATION OF OUR CLIENT FOR A SPECIFIC PROJECT AND AUTHORIZATION FOR USE AND/OR PUBLICATION OF DATA STATEMENTS, CONCLUSIONS OR ABSTRACTS FROM OR REGARDING OUR REPORTS AND DRAWINGS IS RESERVED PENDING OUR WRITTEN APPROVAL.

CLIENT

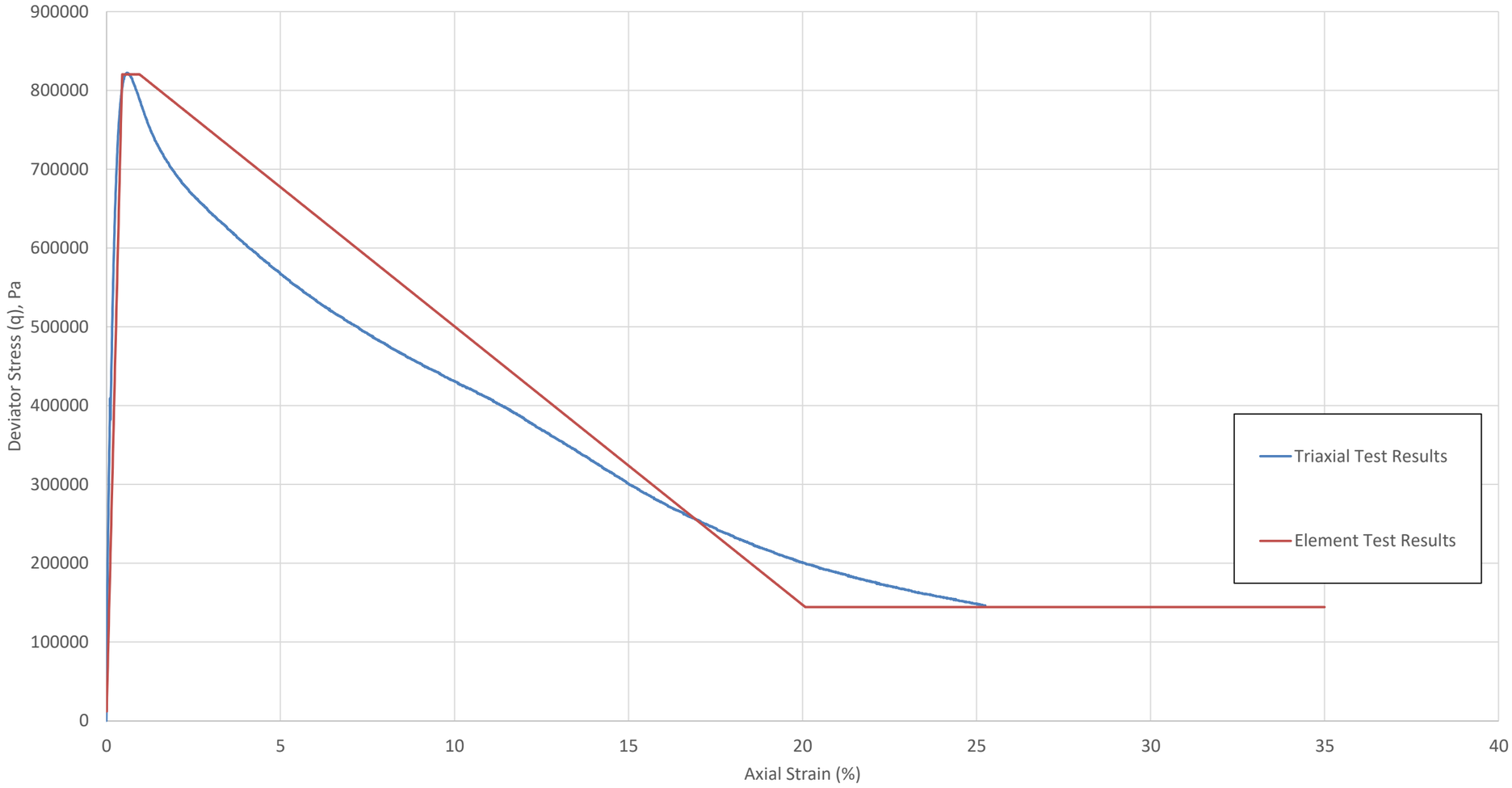
PROJECT

REPORT OF THE EXPERT PANEL ON THE TECHNICAL CAUSES OF THE FAILURE OF FEIJÃO DAM 1

UNDRAINED, STRAIN WEAKENING ELEMENT TEST RESULTS: TRIAXIAL TEST #04

PROJECT No. A03355A01

FIG. No. 32



NOTES:

AS A MUTUAL PROTECTION TO OUR CLIENT, THE PUBLIC AND OURSELVES, ALL REPORTS AND DRAWINGS ARE SUBMITTED FOR THE CONFIDENTIAL INFORMATION OF OUR CLIENT FOR A SPECIFIC PROJECT AND AUTHORIZATION FOR USE AND/OR PUBLICATION OF DATA STATEMENTS, CONCLUSIONS OR ABSTRACTS FROM OR REGARDING OUR REPORTS AND DRAWINGS IS RESERVED PENDING OUR WRITTEN APPROVAL.

CLIENT

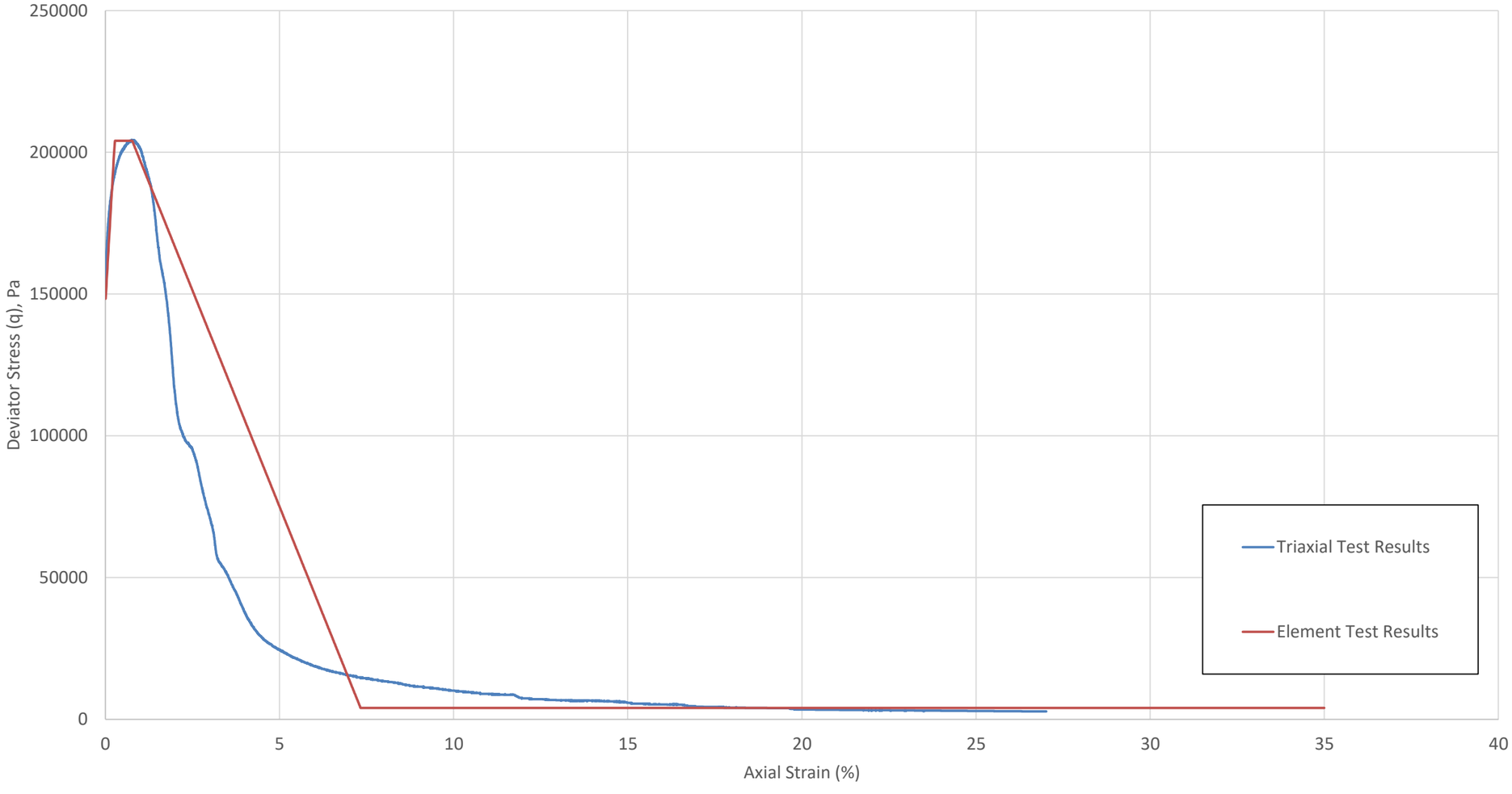
PROJECT

REPORT OF THE EXPERT PANEL ON THE TECHNICAL CAUSES OF THE FAILURE OF FEIJÃO DAM 1

UNDRAINED, STRAIN WEAKENING ELEMENT TEST RESULTS: TRIAXIAL TEST #07

PROJECT No. A03355A01

FIG. No. 33



NOTES:

AS A MUTUAL PROTECTION TO OUR CLIENT, THE PUBLIC AND OURSELVES, ALL REPORTS AND DRAWINGS ARE SUBMITTED FOR THE CONFIDENTIAL INFORMATION OF OUR CLIENT FOR A SPECIFIC PROJECT AND AUTHORIZATION FOR USE AND/OR PUBLICATION OF DATA STATEMENTS, CONCLUSIONS OR ABSTRACTS FROM OR REGARDING OUR REPORTS AND DRAWINGS IS RESERVED PENDING OUR WRITTEN APPROVAL.

CLIENT

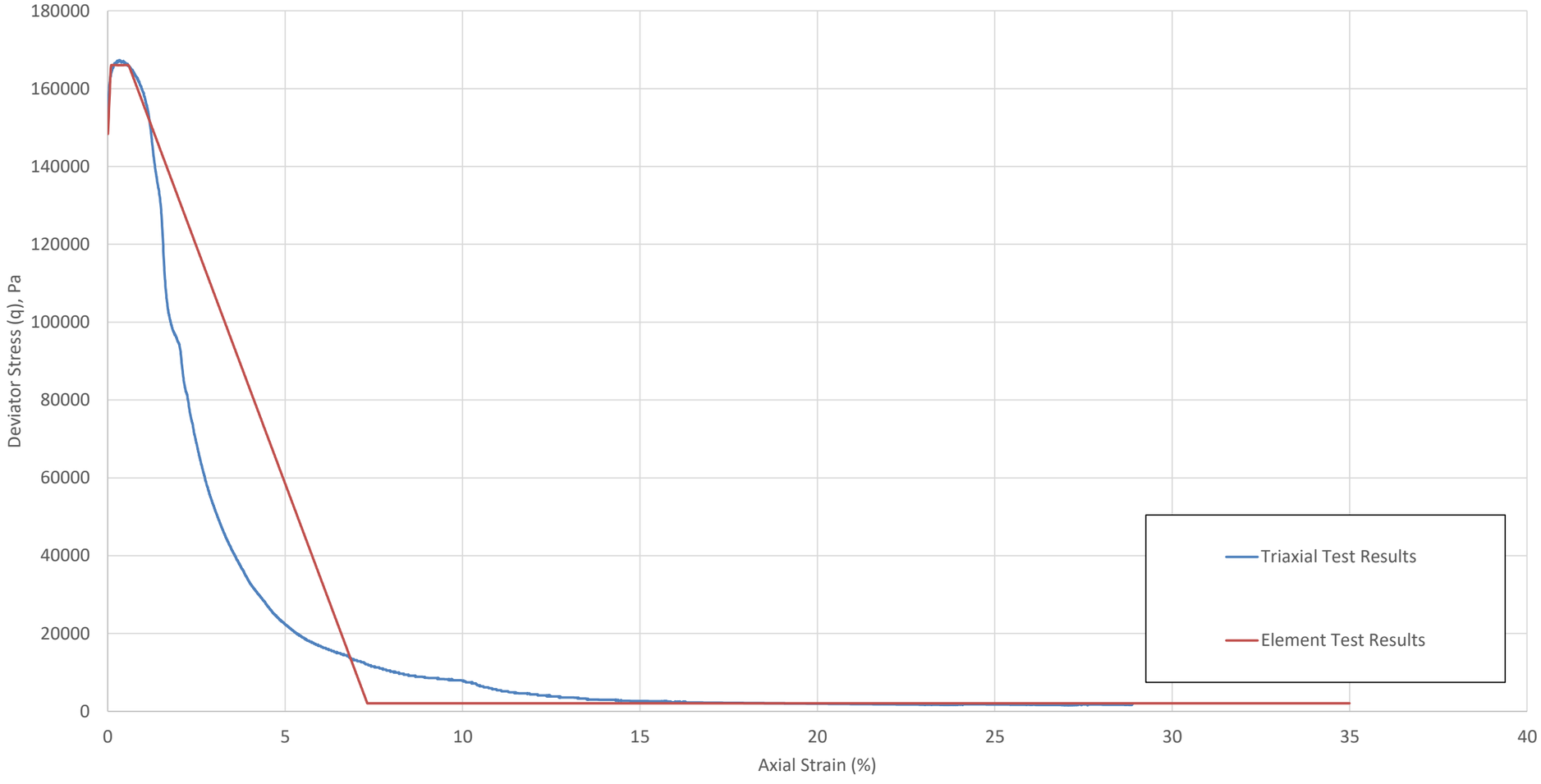
PROJECT

REPORT OF THE EXPERT PANEL ON THE TECHNICAL CAUSES OF THE FAILURE OF FEIJÃO DAM 1

UNDRAINED, STRAIN WEAKENING ELEMENT TEST RESULTS: TRIAXIAL TEST #25

PROJECT No. A03355A01

FIG. No. 34



NOTES:

AS A MUTUAL PROTECTION TO OUR CLIENT, THE PUBLIC AND OURSELVES, ALL REPORTS AND DRAWINGS ARE SUBMITTED FOR THE CONFIDENTIAL INFORMATION OF OUR CLIENT FOR A SPECIFIC PROJECT AND AUTHORIZATION FOR USE AND/OR PUBLICATION OF DATA STATEMENTS, CONCLUSIONS OR ABSTRACTS FROM OR REGARDING OUR REPORTS AND DRAWINGS IS RESERVED PENDING OUR WRITTEN APPROVAL.

CLIENT

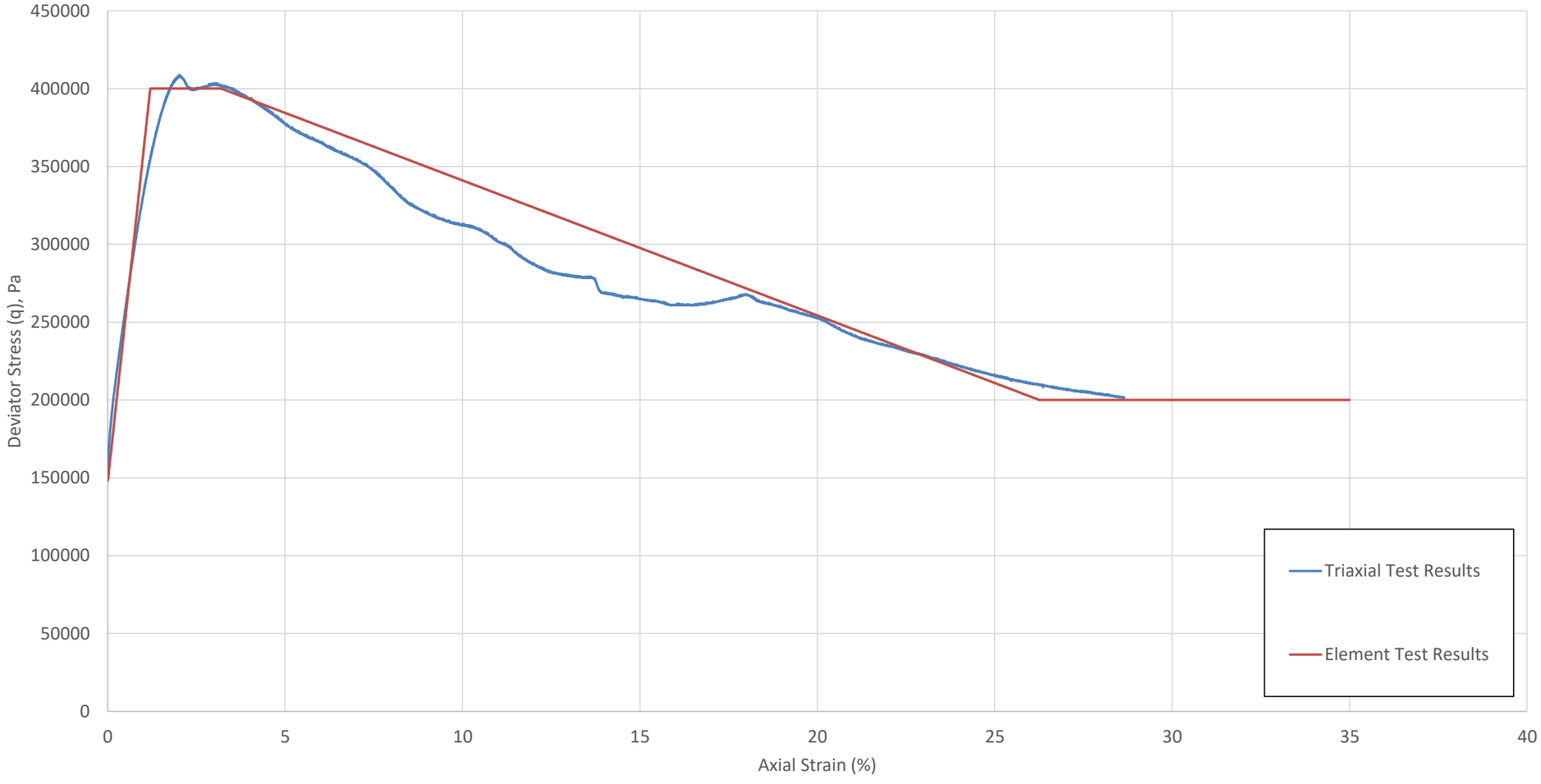
PROJECT

REPORT OF THE EXPERT PANEL ON THE TECHNICAL CAUSES OF THE FAILURE OF FEIJÃO DAM 1

UNDRAINED, STRAIN WEAKENING ELEMENT TEST RESULTS: TRIAXIAL TEST #26

PROJECT No. A03355A01

FIG. No. 35



NOTES:

AS A MUTUAL PROTECTION TO OUR CLIENT, THE PUBLIC AND OURSELVES, ALL REPORTS AND DRAWINGS ARE SUBMITTED FOR THE CONFIDENTIAL INFORMATION OF OUR CLIENT FOR A SPECIFIC PROJECT AND AUTHORIZATION FOR USE AND/OR PUBLICATION OF DATA STATEMENTS, CONCLUSIONS OR ABSTRACTS FROM OR REGARDING OUR REPORTS AND DRAWINGS IS RESERVED PENDING OUR WRITTEN APPROVAL.

CLIENT

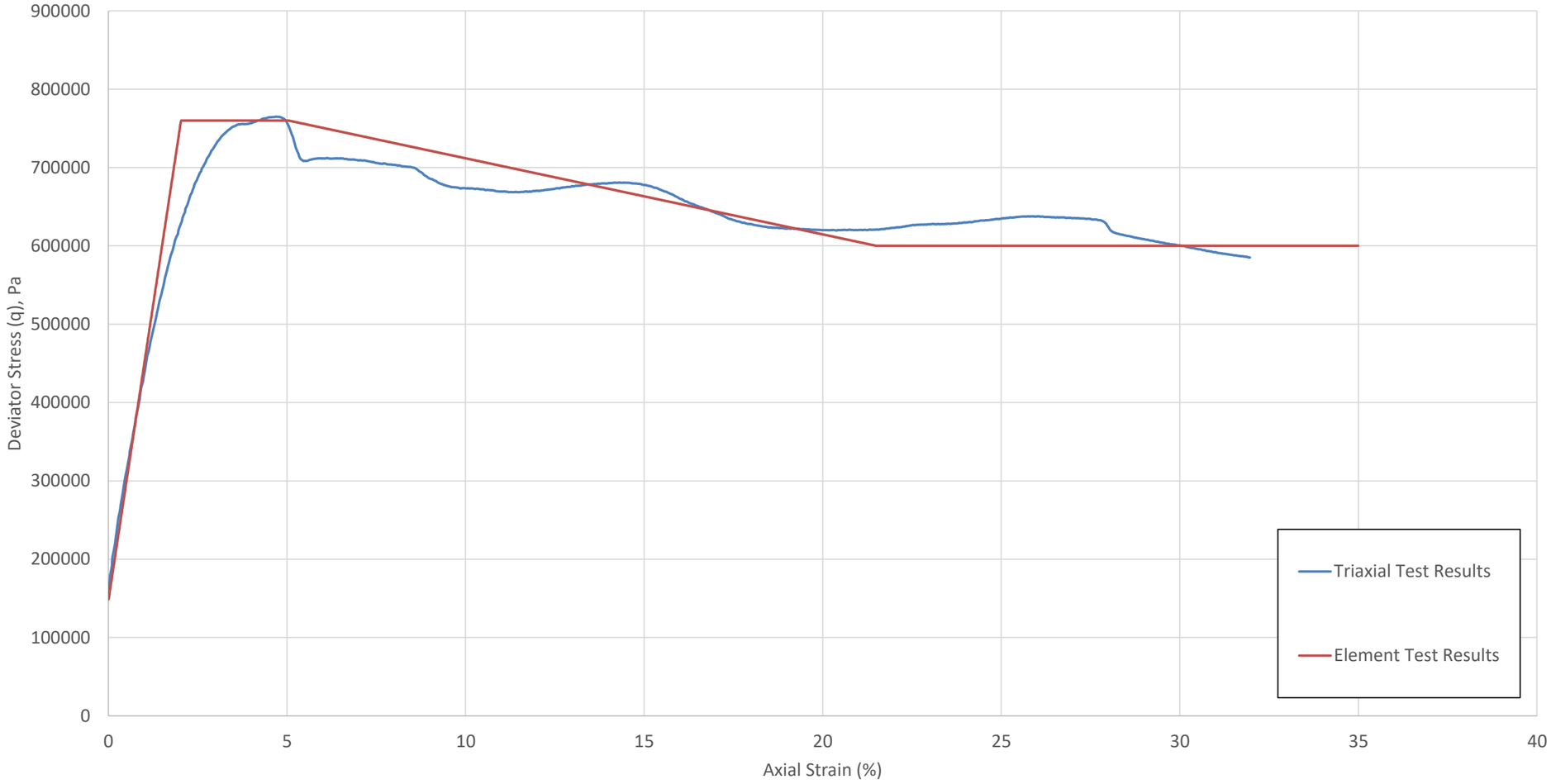
PROJECT

REPORT OF THE EXPERT PANEL ON THE TECHNICAL CAUSES OF THE FAILURE OF FEIJÃO DAM 1

UNDRAINED, STRAIN WEAKENING ELEMENT TEST RESULTS: TRIAXIAL TEST #27

PROJECT No. A03355A01

FIG. No. 36



NOTES:

AS A MUTUAL PROTECTION TO OUR CLIENT, THE PUBLIC AND OURSELVES, ALL REPORTS AND DRAWINGS ARE SUBMITTED FOR THE CONFIDENTIAL INFORMATION OF OUR CLIENT FOR A SPECIFIC PROJECT AND AUTHORIZATION FOR USE AND/OR PUBLICATION OF DATA STATEMENTS, CONCLUSIONS OR ABSTRACTS FROM OR REGARDING OUR REPORTS AND DRAWINGS IS RESERVED PENDING OUR WRITTEN APPROVAL.

CLIENT

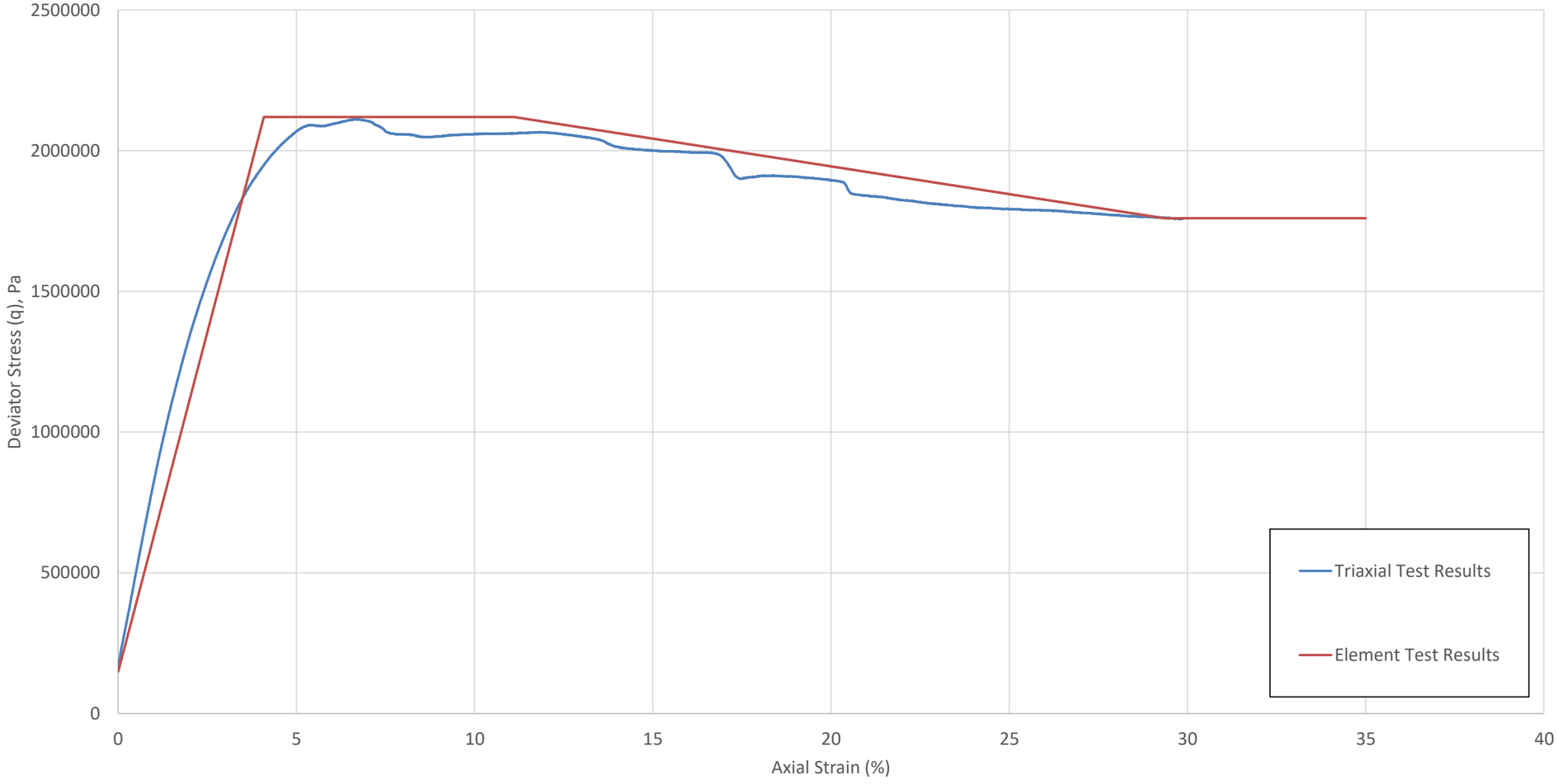
PROJECT

REPORT OF THE EXPERT PANEL ON THE TECHNICAL CAUSES OF THE FAILURE OF FEIJÃO DAM 1

UNDRAINED, STRAIN WEAKENING ELEMENT TEST RESULTS: TRIAXIAL TEST #28

PROJECT No. A03355A01

FIG. No. 37



NOTES:

AS A MUTUAL PROTECTION TO OUR CLIENT, THE PUBLIC AND OURSELVES, ALL REPORTS AND DRAWINGS ARE SUBMITTED FOR THE CONFIDENTIAL INFORMATION OF OUR CLIENT FOR A SPECIFIC PROJECT AND AUTHORIZATION FOR USE AND/OR PUBLICATION OF DATA STATEMENTS, CONCLUSIONS OR ABSTRACTS FROM OR REGARDING OUR REPORTS AND DRAWINGS IS RESERVED PENDING OUR WRITTEN APPROVAL.

CLIENT

PROJECT

REPORT OF THE EXPERT PANEL ON THE TECHNICAL CAUSES OF THE FAILURE OF FEIJÃO DAM 1

UNDRAINED, STRAIN WEAKENING ELEMENT TEST RESULTS: TRIAXIAL TEST #29

PROJECT No. A03355A01

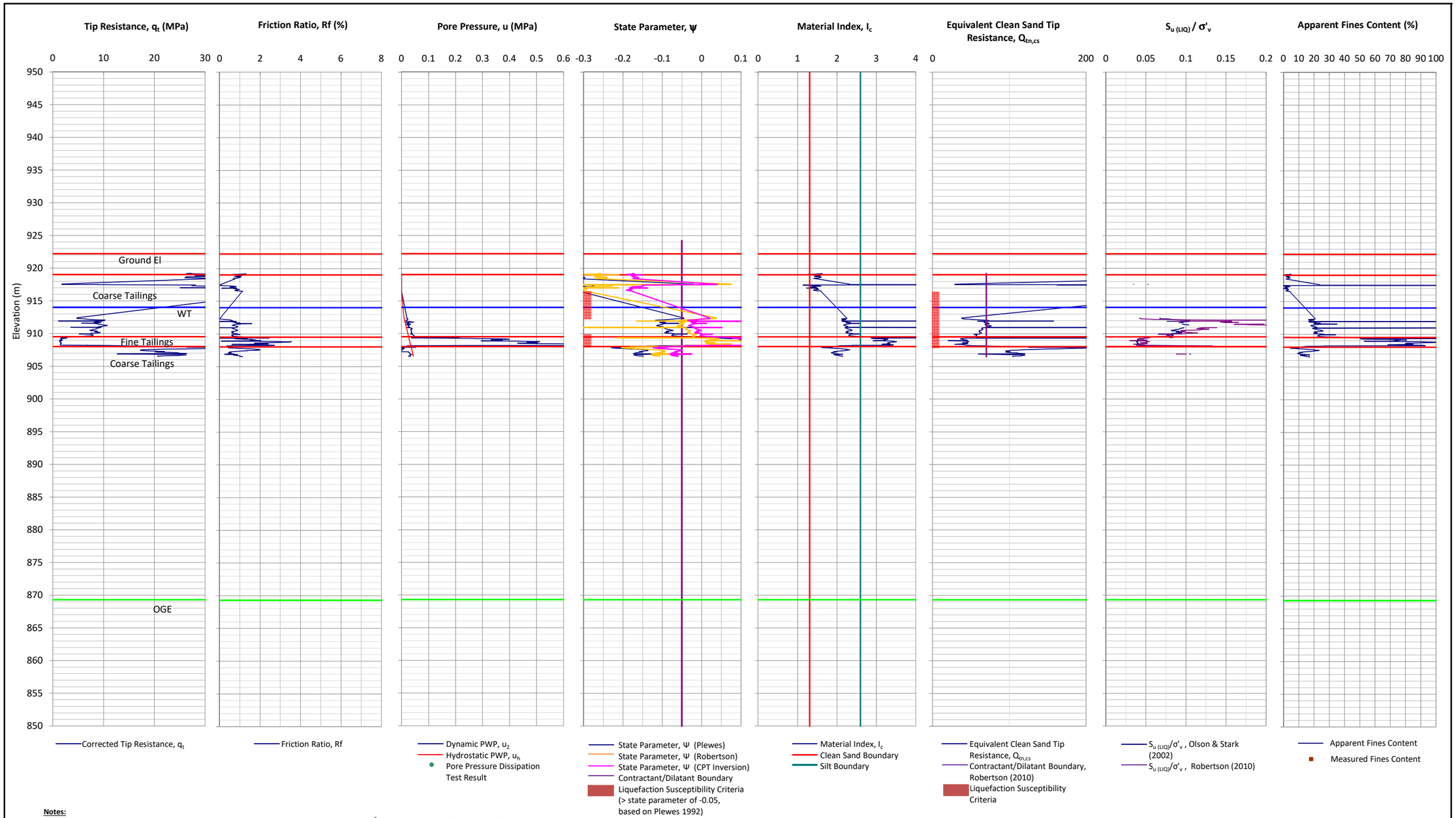
FIG. No. 38

Appendix E

Annex 9 – CPTu Plots, V_s Plots & Histogram

December 2019

CPTu & V_s Plots



Notes:

1. This interpretation is based on the water and soil saturated unit weights γ_w=9.807 kN/m^3, and respective γ_{sat} for each geological unit.
2. The friction ratio Rf is calculated as Rf=f_s/q_t.
3. The hydrostatic pore pressure is calculated using the ground water level (GWL) determined from CPT pore pressure dissipation tests (where available) or dynamic pore pressure.
4. Soil boundary layers (where plotted) are based on KCB interpretation from adjacent borehole logs.
5. The data presented have been plotted to the axis limits. Data may exist beyond the axis limits shown.
6. The Material Index (I_c) boundaries are based on Robertson and Wride (1998).
7. The $Q_{tn,cs}$ contractant/dilatant boundary=70 and is based on Robertson (2010).
8. The State Parameter (Ψ) calculated using Plewes, et al. (1992) and the CPT inversion method is based on an assumed K0 of 0.5.

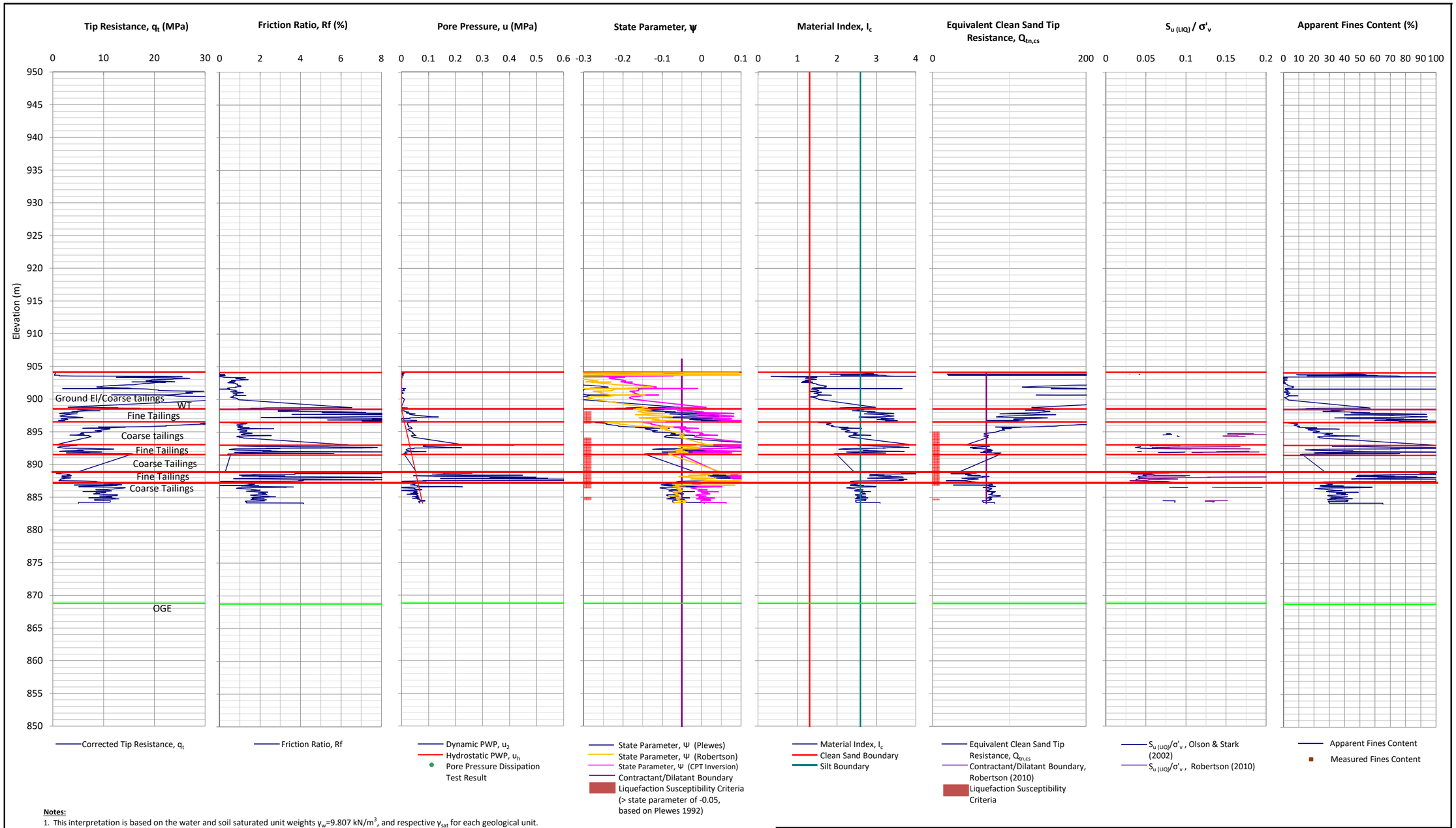
PROJECT: REPORT OF THE EXPERT PANEL ON THE TECHNICAL CAUSES OF THE FAILURE OF FEIJÃO DAM 1

TITLE: CONE PENETRATION TEST CPTU-05-01N_R1

N:7775122.5 E:591862.6 23-Nov-2005

PROJECT NO.: A03355A01

FIGURE NO.: 1



Notes:

1. This interpretation is based on the water and soil saturated unit weights γ_w=9.807 kN/m^3, and respective γ_{sat} for each geological unit.
2. The friction ratio Rf is calculated as Rf=f_s/q_t.
3. The hydrostatic pore pressure is calculated using the ground water level (GWL) determined from CPT pore pressure dissipation tests (where available) or dynamic pore pressure.
4. Soil boundary layers (where plotted) are based on KCB interpretation from adjacent borehole logs.
5. The data presented have been plotted to the axis limits. Data may exist beyond the axis limits shown.
6. The Material Index (I_c) boundaries are based on Robertson and Wride (1998).
7. The $Q_{tn,cs}$ contractant/dilatant boundary=70 and is based on Robertson (2010).
8. The State Parameter (Ψ) is calculated using Plewes, et al. (1992) and the CPT Inversion method is based on an assumed a K0 of 0.5.

AS A MUTUAL PROTECTION TO OUR CLIENT, THE PUBLIC AND OURSELVES, ALL REPORTS AND DRAWINGS ARE SUBMITTED FOR THE CONFIDENTIAL INFORMATION OF OUR CLIENT FOR A SPECIFIC PROJECT AND AUTHORIZATION FOR USE AND/OR PUBLICATION OF DATA STATEMENTS, CONCLUSIONS OR ABSTRACTS FROM OR REWARDING OUR REPORTS AND DRAWINGS IS RESERVED PENDING OUR WRITTEN APPROVAL.

CLIENT

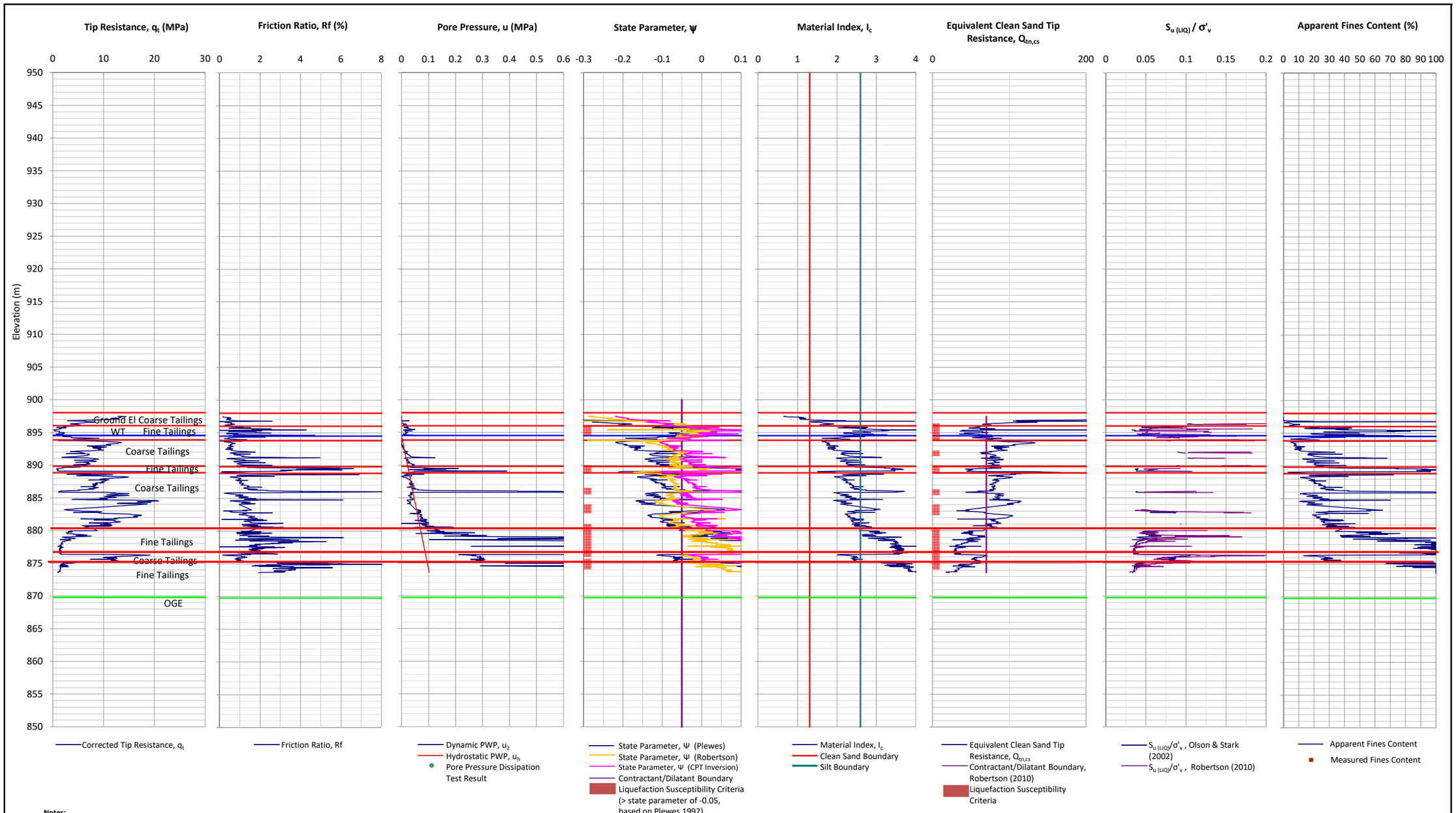
PROJECT: REPORT OF THE EXPERT PANEL ON THE TECHNICAL CAUSES OF THE FAILURE OF FEIJÃO DAM 1

TITLE: CONE PENETRATION TEST CPTU-05-02_R1

N:7775088.2 E:591820.6 28-Oct-2005

PROJECT NO.: A03355A01

FIGURE NO.: 2



Notes:

1. This interpretation is based on the water and soil saturated unit weights γ_w=9.807 kN/m^3, and respective γ_{sat} for each geological unit.
2. The friction ratio Rf is calculated as Rf=f_s/q_t.
3. The hydrostatic pore pressure is calculated using the ground water level (GWL) determined from CPT pore pressure dissipation tests (where available) or dynamic pore pressure.
4. Soil boundary layers (where plotted) are based on KCB interpretation from adjacent borehole logs.
5. The data presented have been plotted to the axis limits. Data may exist beyond the axis limits shown.
6. The Material Index (I_c) boundaries are based on Robertson and Wride (1998).
7. The $Q_{tn,cs}$ contractant/dilatant boundary=70 and is based on Robertson (2010).
8. The State Parameter (Ψ) calculated using Plewes, et al. (1992) and the CPT inversion method is based on an assumed K0 of 0.5.

AS A MUTUAL PROTECTION TO OUR CLIENT, THE PUBLIC AND OURSELVES, ALL REPORTS AND DRAWINGS ARE SUBMITTED FOR THE CONFIDENTIAL INFORMATION OF OUR CLIENT FOR A SPECIFIC PROJECT AND AUTHORIZATION FOR USE AND/OR PUBLICATION OF DATA STATEMENTS, CONCLUSIONS OR ABSTRACTS FROM OR REWARDING OUR REPORTS AND DRAWINGS IS RESERVED PENDING OUR WRITTEN APPROVAL.

CLIENT

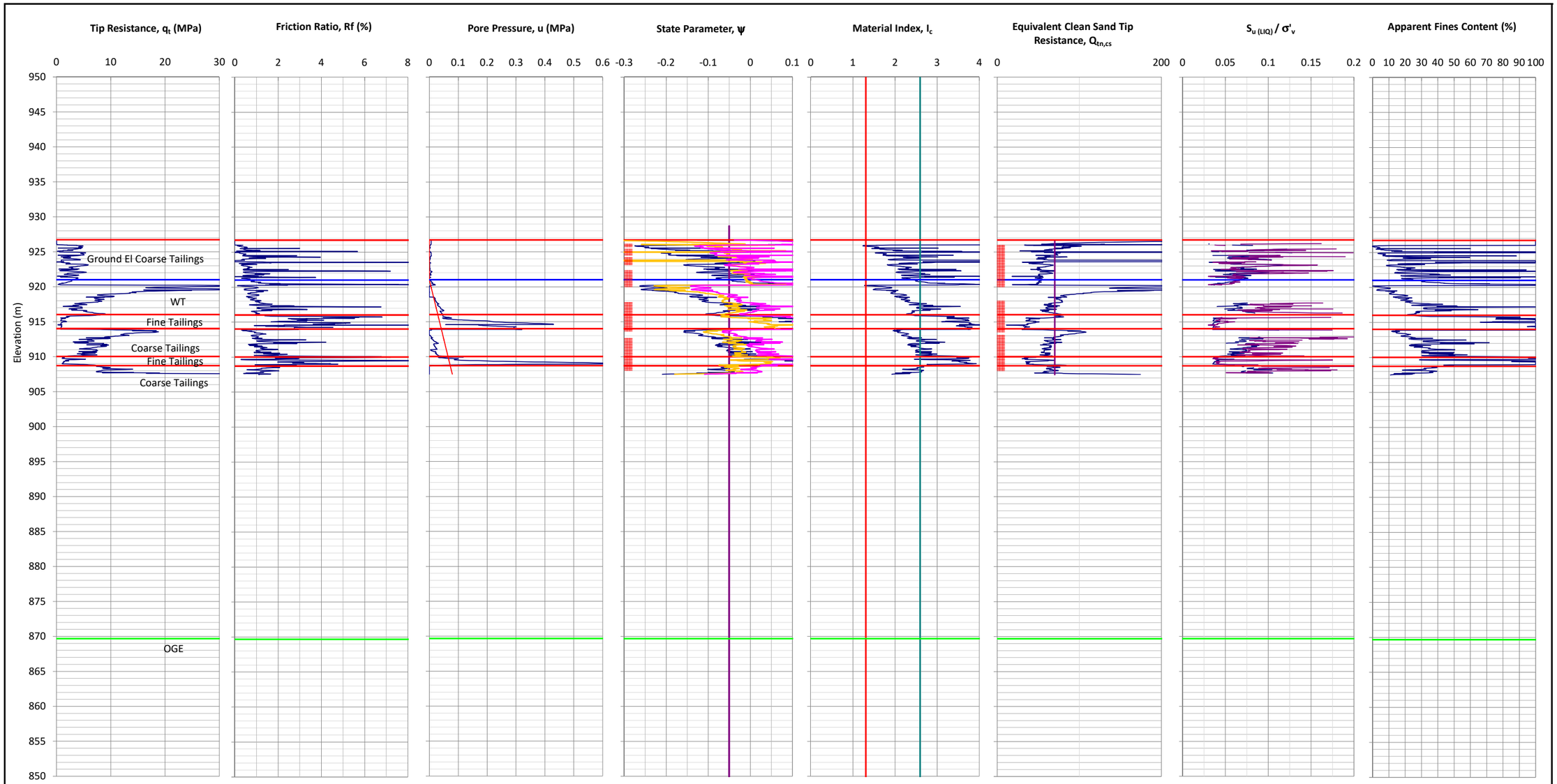
PROJECT: REPORT OF THE EXPERT PANEL ON THE TECHNICAL CAUSES OF THE FAILURE OF FEIJÃO DAM 1

TITLE: CONE PENETRATION TEST CPTU-05-03N_R1

N:7775072.1 E:591803 19-Oct-2005

PROJECT NO.: A03355A01

FIGURE NO.: 3



Notes:

1. This interpretation is based on the water and soil saturated unit weights γ_w=9.807 kN/m^3, and respective γ_{sat} for each geological unit.
2. The friction ratio Rf is calculated as Rf=f_s/q_t.
3. The hydrostatic pore pressure is calculated using the ground water level (GWL) determined from CPT pore pressure dissipation tests (where available) or dynamic pore pressure.
4. Soil boundary layers (where plotted) are based on KCB interpretation from adjacent borehole logs.
5. The data presented have been plotted to the axis limits. Data may exist beyond the axis limits shown.
6. The Material Index (I_c) boundaries are based on Robertson and Wride (1998).
7. The $Q_{tn,cs}$ contractant/dilatant boundary=70 and is based on Robertson (2010).
8. The State Parameter (Ψ) calculated using Plewes, et al. (1992) and the CPT inversion method is based on an assumed K0 of 0.5.

AS A MUTUAL PROTECTION TO OUR CLIENT, THE PUBLIC AND OURSELVES, ALL REPORTS AND DRAWINGS ARE SUBMITTED FOR THE CONFIDENTIAL INFORMATION OF OUR CLIENT FOR A SPECIFIC PROJECT AND AUTHORIZATION FOR USE AND/OR PUBLICATION OF DATA STATEMENTS, CONCLUSIONS OR ABSTRACTS FROM OR REWARDING OUR REPORTS AND DRAWINGS IS RESERVED PENDING OUR WRITTEN APPROVAL.

CLIENT

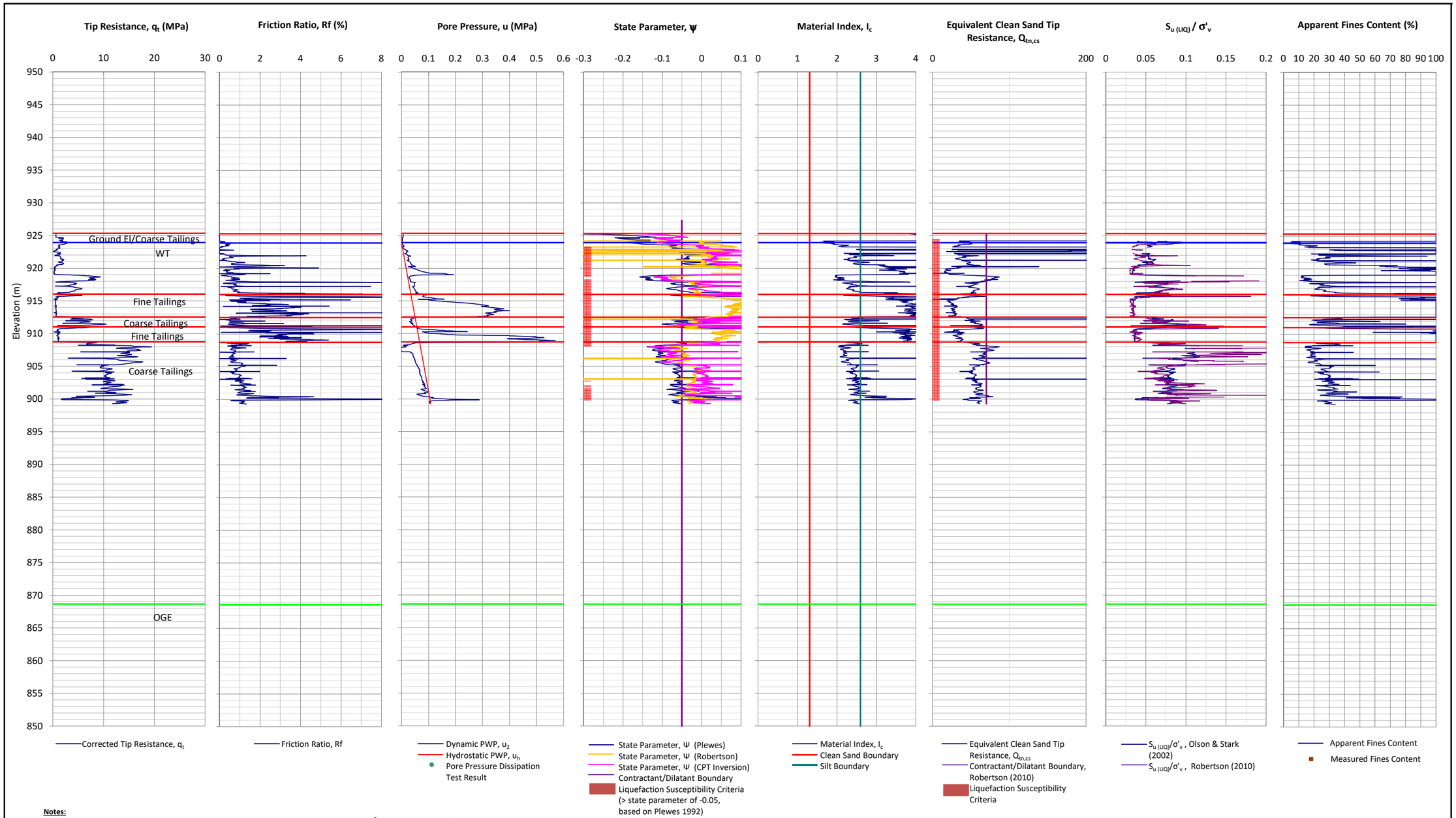
PROJECT: REPORT OF THE EXPERT PANEL ON THE TECHNICAL CAUSES OF THE FAILURE OF FEIJÃO DAM 1

TITLE: CONE PENETRATION TEST CPTU-05-04N_R1

N:7775144.6 E:591899.5 19-Oct-2005

PROJECT NO.: A03355A01

FIGURE NO.: 4



Notes:

1. This interpretation is based on the water and soil saturated unit weights γ_w=9.807 kN/m^3, and respective γ_{sat} for each geological unit.
2. The friction ratio Rf is calculated as Rf=f_s/q_t.
3. The hydrostatic pore pressure is calculated using the ground water level (GWL) determined from CPT pore pressure dissipation tests (where available) or dynamic pore pressure.
4. Soil boundary layers (where plotted) are based on KCB interpretation from adjacent borehole logs.
5. The data presented have been plotted to the axis limits. Data may exist beyond the axis limits shown.
6. The Material Index (I_c) boundaries are based on Robertson and Wride (1998).
7. The $Q_{tn,cs}$ contractant/dilatant boundary=70 and is based on Robertson (2010).
8. The State Parameter (Ψ) calculated using Plewes, et al. (1992) and the CPT inversion method is based on an assumed K0 of 0.5.

AS A MUTUAL PROTECTION TO OUR CLIENT, THE PUBLIC AND OURSELVES, ALL REPORTS AND DRAWINGS ARE SUBMITTED FOR THE CONFIDENTIAL INFORMATION OF OUR CLIENT FOR A SPECIFIC PROJECT AND AUTHORIZATION FOR USE AND/OR PUBLICATION OF DATA STATEMENTS, CONCLUSIONS OR ABSTRACTS FROM OR REWARDING OUR REPORTS AND DRAWINGS IS RESERVED PENDING OUR WRITTEN APPROVAL.

CLIENT

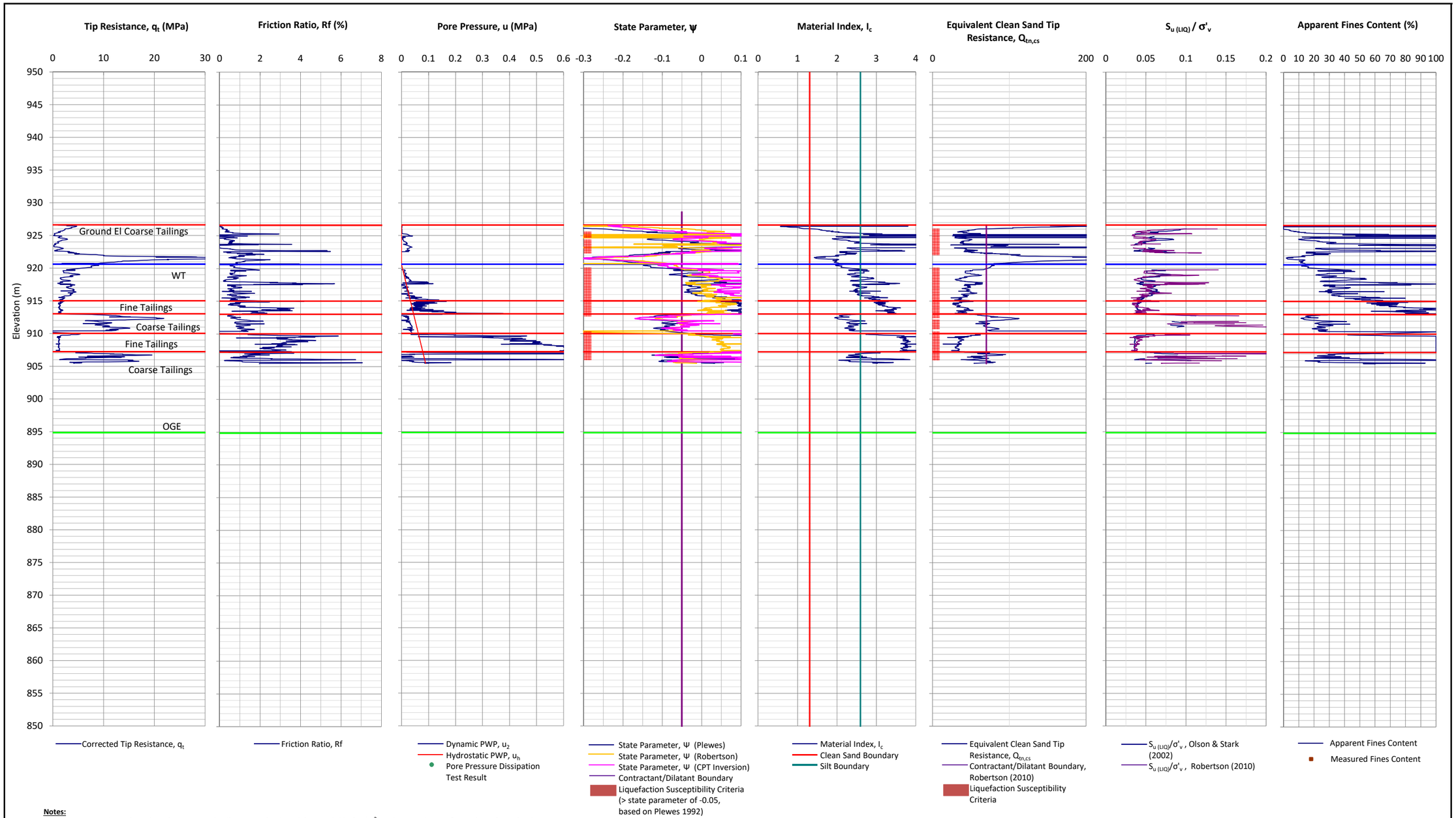
PROJECT: REPORT OF THE EXPERT PANEL ON THE TECHNICAL CAUSES OF THE FAILURE OF FEIJÃO DAM 1

TITLE: CONE PENETRATION TEST CPTU-05-05N_Updated

N:7775166.3 E:591940.5 2005-October-19

PROJECT NO.: A03355A01

FIGURE NO.: 5



Notes:

1. This interpretation is based on the water and soil saturated unit weights γ_w=9.807 kN/m^3, and respective γ_{sat} for each geological unit.
2. The friction ratio Rf is calculated as Rf=f_s/q_t.
3. The hydrostatic pore pressure is calculated using the ground water level (GWL) determined from CPT pore pressure dissipation tests (where available) or dynamic pore pressure.
4. Soil boundary layers (where plotted) are based on KCB interpretation from adjacent borehole logs.
5. The data presented have been plotted to the axis limits. Data may exist beyond the axis limits shown.
6. The Material Index (I_c) boundaries are based on Robertson and Wride (1998).
7. The $Q_{tn,cs}$ contractant/dilatant boundary=70 and is based on Robertson (2010).
8. The State Parameter (Ψ) calculated using Plewes, et al. (1992) and the CPT inversion method is based on an assumed K0 of 0.5.

AS A MUTUAL PROTECTION TO OUR CLIENT, THE PUBLIC AND OURSELVES, ALL REPORTS AND DRAWINGS ARE SUBMITTED FOR THE CONFIDENTIAL INFORMATION OF OUR CLIENT FOR A SPECIFIC PROJECT AND AUTHORIZATION FOR USE AND/OR PUBLICATION OF DATA STATEMENTS, CONCLUSIONS OR ABSTRACTS FROM OR REWARDING OUR REPORTS AND DRAWINGS IS RESERVED PENDING OUR WRITTEN APPROVAL.

CLIENT

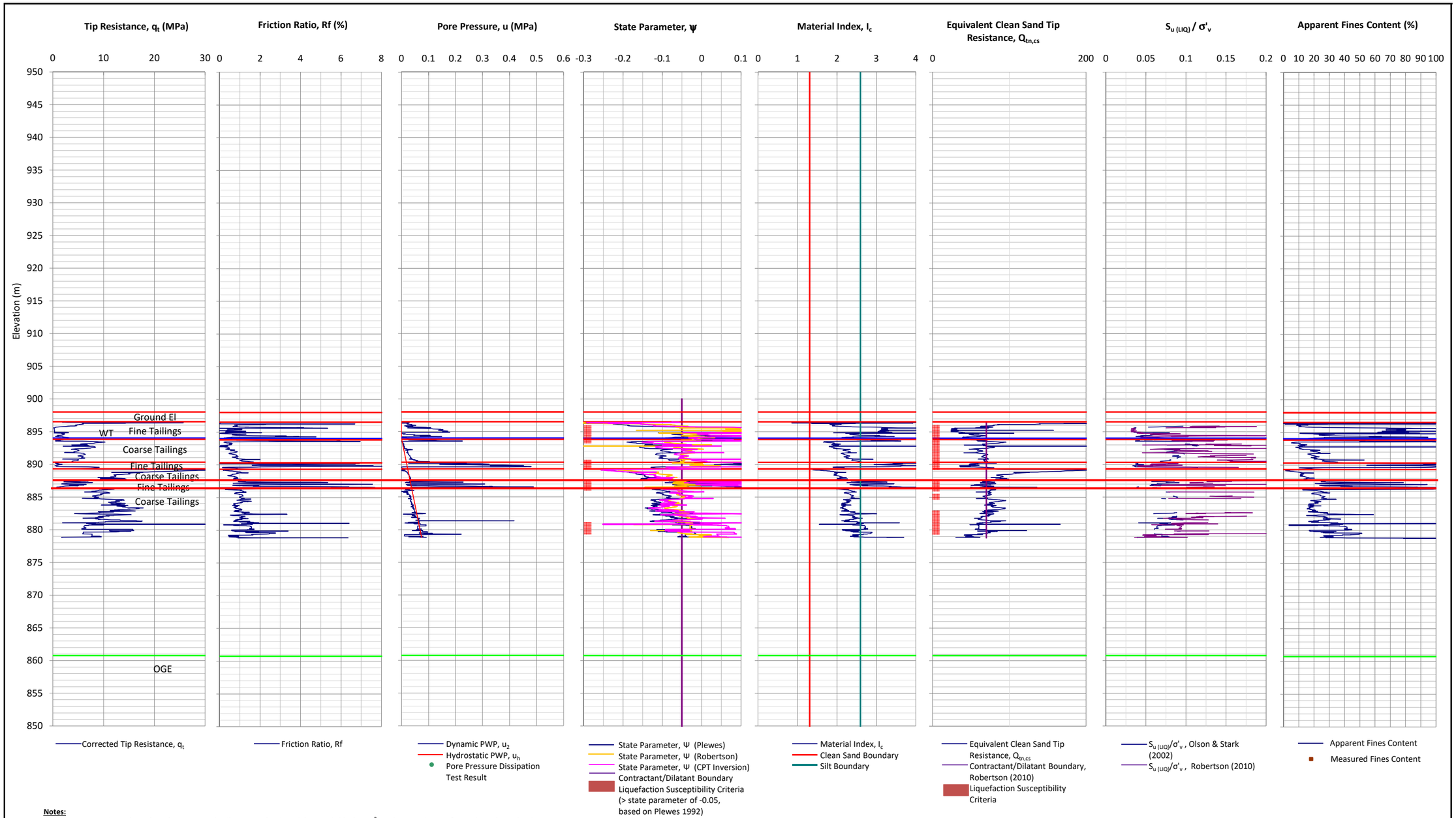
PROJECT: REPORT OF THE EXPERT PANEL ON THE TECHNICAL CAUSES OF THE FAILURE OF FEIJÃO DAM 1

TITLE: CONE PENETRATION TEST CPTU-05-06N_Updated

N:7774886 E:592039.5 2005-November-26

PROJECT NO.: A03355A01

FIGURE NO.: 6



Notes:

1. This interpretation is based on the water and soil saturated unit weights γ_w=9.807 kN/m^3, and respective γ_{sat} for each geological unit.
2. The friction ratio Rf is calculated as Rf=f_s/q_t.
3. The hydrostatic pore pressure is calculated using the ground water level (GWL) determined from CPT pore pressure dissipation tests (where available) or dynamic pore pressure.
4. Soil boundary layers (where plotted) are based on KCB interpretation from adjacent borehole logs.
5. The data presented have been plotted to the axis limits. Data may exist beyond the axis limits shown.
6. The Material Index (I_c) boundaries are based on Robertson and Wride (1998).
7. The $Q_{tn,cs}$ contractant/dilatant boundary=70 and is based on Robertson (2010).
8. The State Parameter (Ψ) calculated using Plewes, et al. (1992) and the CPT inversion method is based on an assumed K0 of 0.5.

AS A MUTUAL PROTECTION TO OUR CLIENT, THE PUBLIC AND OURSELVES, ALL REPORTS AND DRAWINGS ARE SUBMITTED FOR THE CONFIDENTIAL INFORMATION OF OUR CLIENT FOR A SPECIFIC PROJECT AND AUTHORIZATION FOR USE AND/OR PUBLICATION OF DATA STATEMENTS, CONCLUSIONS OR ABSTRACTS FROM OR REWARDING OUR REPORTS AND DRAWINGS IS RESERVED PENDING OUR WRITTEN APPROVAL.

CLIENT

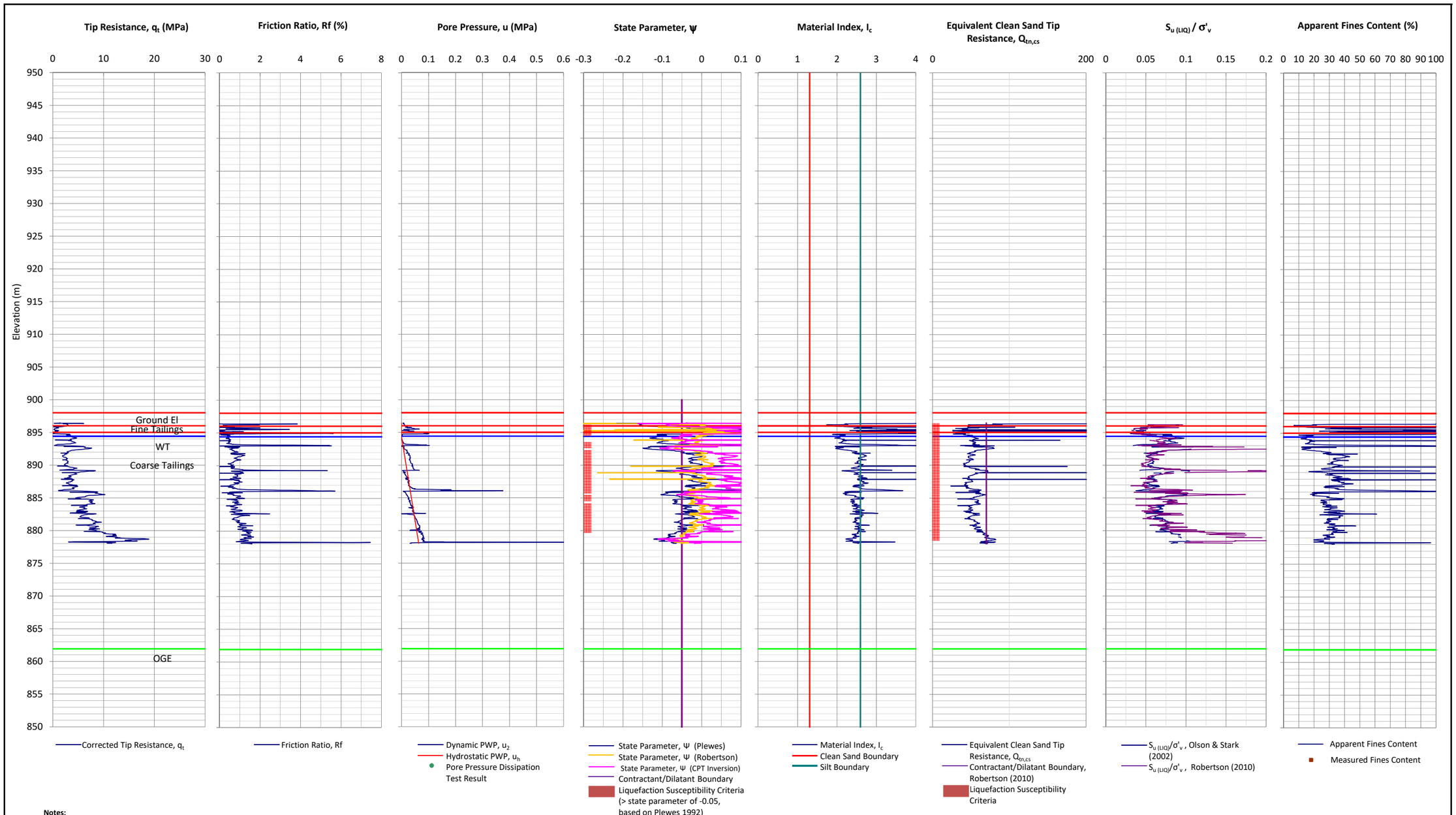
PROJECT: REPORT OF THE EXPERT PANEL ON THE TECHNICAL CAUSES OF THE FAILURE OF FEIJÃO DAM 1

TITLE: CONE PENETRATION TEST CPTU-05-07N_Updated

N:7775013 E:591838.4 2005-November-22

PROJECT NO.: A03355A01

FIGURE NO.: 7



Notes:

1. This interpretation is based on the water and soil saturated unit weights γ_w=9.807 kN/m^3, and respective γ_{sat} for each geological unit.
2. The friction ratio Rf is calculated as Rf=f_s/q_t.
3. The hydrostatic pore pressure is calculated using the ground water level (GWL) determined from CPT pore pressure dissipation tests (where available) or dynamic pore pressure.
4. Soil boundary layers (where plotted) are based on KCB interpretation from adjacent borehole logs.
5. The data presented have been plotted to the axis limits. Data may exist beyond the axis limits shown.
6. The Material Index (I_c) boundaries are based on Robertson and Wride (1998).
7. The $Q_{tn,cs}$ contractant/dilatant boundary=70 and is based on Robertson (2010).
8. The State Parameter (Ψ) calculated using Plewes, et al. (1992) and the CPT inversion method is based on an assumed K0 of 0.5.

AS A MUTUAL PROTECTION TO OUR CLIENT, THE PUBLIC AND OURSELVES, ALL REPORTS AND DRAWINGS ARE SUBMITTED FOR THE CONFIDENTIAL INFORMATION OF OUR CLIENT FOR A SPECIFIC PROJECT AND AUTHORIZATION FOR USE AND/OR PUBLICATION OF DATA STATEMENTS, CONCLUSIONS OR ABSTRACTS FROM OR REWARDING OUR REPORTS AND DRAWINGS IS RESERVED PENDING OUR WRITTEN APPROVAL.

CLIENT

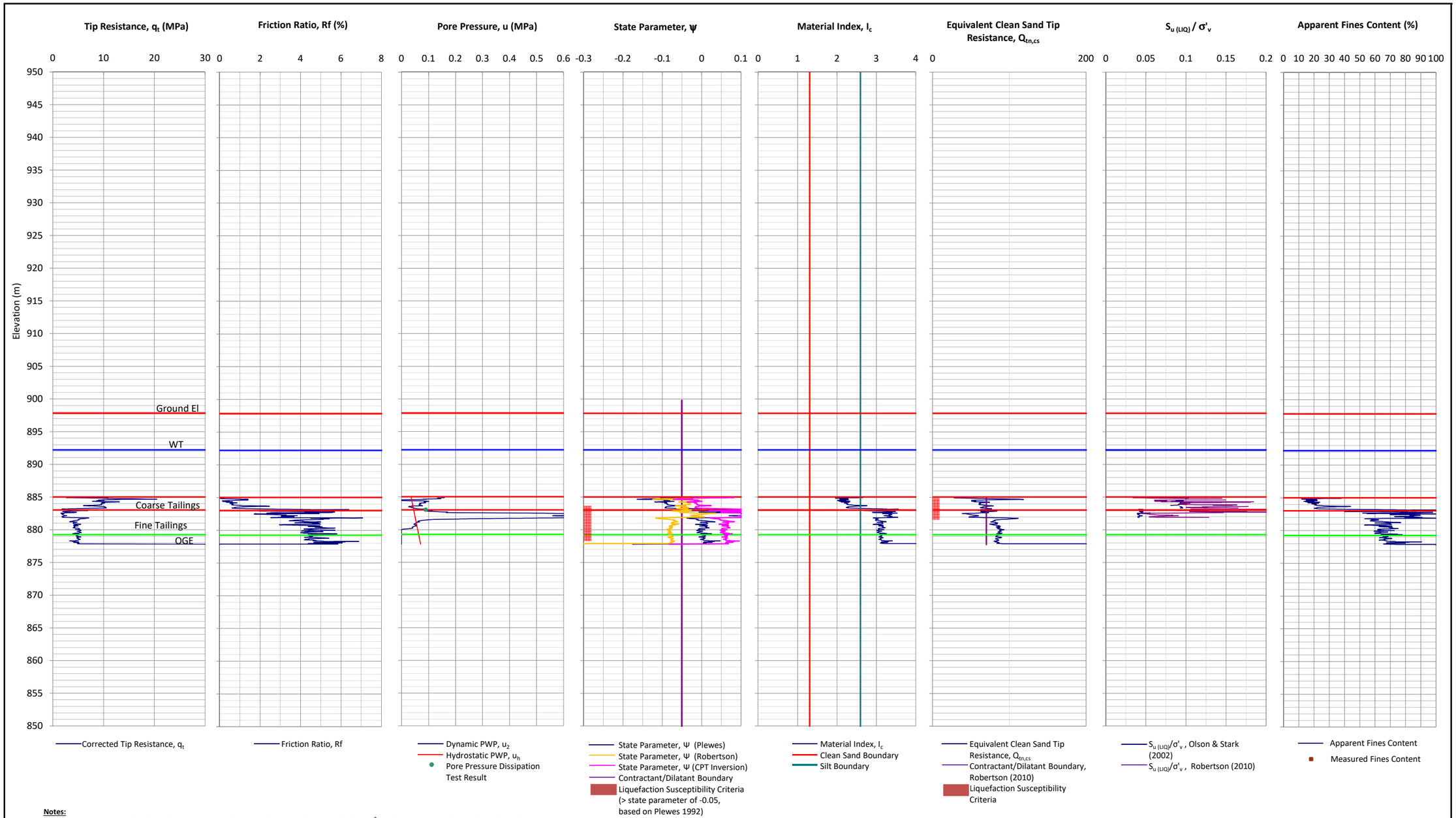
PROJECT: REPORT OF THE EXPERT PANEL ON THE TECHNICAL CAUSES OF THE FAILURE OF FEIJÃO DAM 1

TITLE: CONE PENETRATION TEST CPTU-05-08N_Updated

N:7774948.3 E:591874 2005-November-24

PROJECT NO.: A03355A01

FIGURE NO.: 8



Notes:

1. This interpretation is based on the water and soil saturated unit weights γ_w=9.807 kN/m^3, and respective γ_{sat} for each geological unit.
2. The friction ratio Rf is calculated as Rf=f_s/q_t.
3. The hydrostatic pore pressure is calculated using the ground water level (GWL) determined from CPT pore pressure dissipation tests (where available) or dynamic pore pressure.
4. Soil boundary layers (where plotted) are based on KCB interpretation from adjacent borehole logs.
5. The data presented have been plotted to the axis limits. Data may exist beyond the axis limits shown.
6. The Material Index (I_c) boundaries are based on Robertson and Wride (1998).
7. The $Q_{tn,cs}$ contractant/dilatant boundary=70 and is based on Robertson (2010).
8. The State Parameter (Ψ) calculated using Plewes, et al. (1992) and the CPT inversion method is based on an assumed K0 of 0.5.

AS A MUTUAL PROTECTION TO OUR CLIENT, THE PUBLIC AND OURSELVES, ALL REPORTS AND DRAWINGS ARE SUBMITTED FOR THE CONFIDENTIAL INFORMATION OF OUR CLIENT FOR A SPECIFIC PROJECT AND AUTHORIZATION FOR USE AND/OR PUBLICATION OF DATA STATEMENTS, CONCLUSIONS OR ABSTRACTS FROM OR REWARDING OUR REPORTS AND DRAWINGS IS RESERVED PENDING OUR WRITTEN APPROVAL.

CLIENT

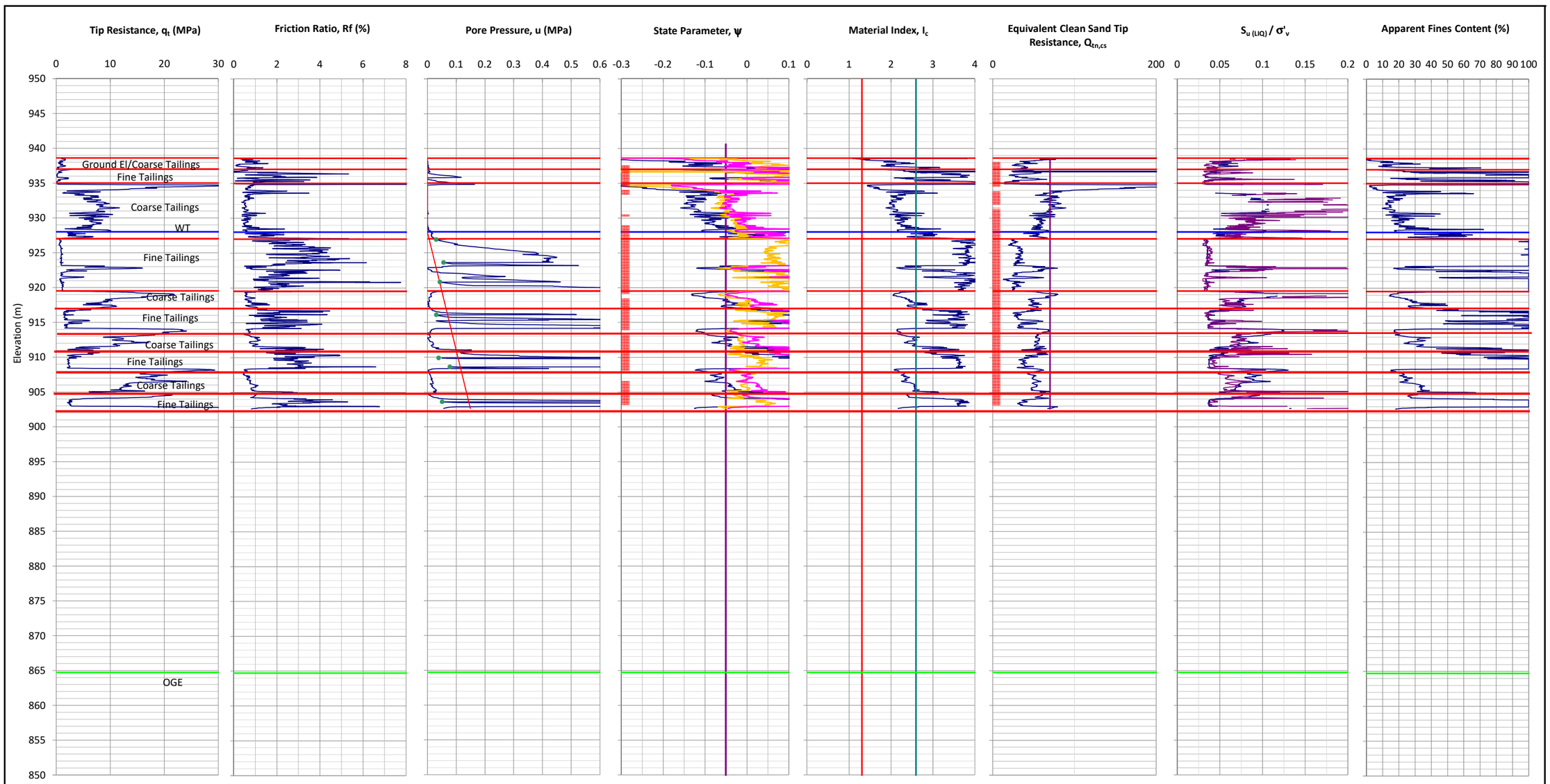
PROJECT: REPORT OF THE EXPERT PANEL ON THE TECHNICAL CAUSES OF THE FAILURE OF FEIJÃO DAM 1

TITLE: CONE PENETRATION TEST CPTU-16-02N_R1

N:7775122.3 E:591774.7 01-Apr-2016

PROJECT NO.: A03355A01

FIGURE NO.: 9



Notes:

1. This interpretation is based on the water and soil saturated unit weights γ_w=9.807 kN/m^3, and respective γ_{sat} for each geological unit.
2. The friction ratio Rf is calculated as Rf=f_s/q_t.
3. The hydrostatic pore pressure is calculated using the ground water level (GWL) determined from CPT pore pressure dissipation tests (where available) or dynamic pore pressure.
4. Soil boundary layers (where plotted) are based on KCB interpretation from adjacent borehole logs.
5. The data presented have been plotted to the axis limits. Data may exist beyond the axis limits shown.
6. The Material Index (I_c) boundaries are based on Robertson and Wride (1998).
7. The $Q_{tn,cs}$ contractant/dilatant boundary=70 and is based on Robertson (2010).
8. The State Parameter (Ψ) calculated using Plewes, et al. (1992) and the CPT inversion method is based on an assumed K0 of 0.5.

AS A MUTUAL PROTECTION TO OUR CLIENT, THE PUBLIC AND OURSELVES, ALL REPORTS AND DRAWINGS ARE SUBMITTED FOR THE CONFIDENTIAL INFORMATION OF OUR CLIENT FOR A SPECIFIC PROJECT AND AUTHORIZATION FOR USE AND/OR PUBLICATION OF DATA STATEMENTS, CONCLUSIONS OR ABSTRACTS FROM OR REWARDING OUR REPORTS AND DRAWINGS IS RESERVED PENDING OUR WRITTEN APPROVAL.

CLIENT

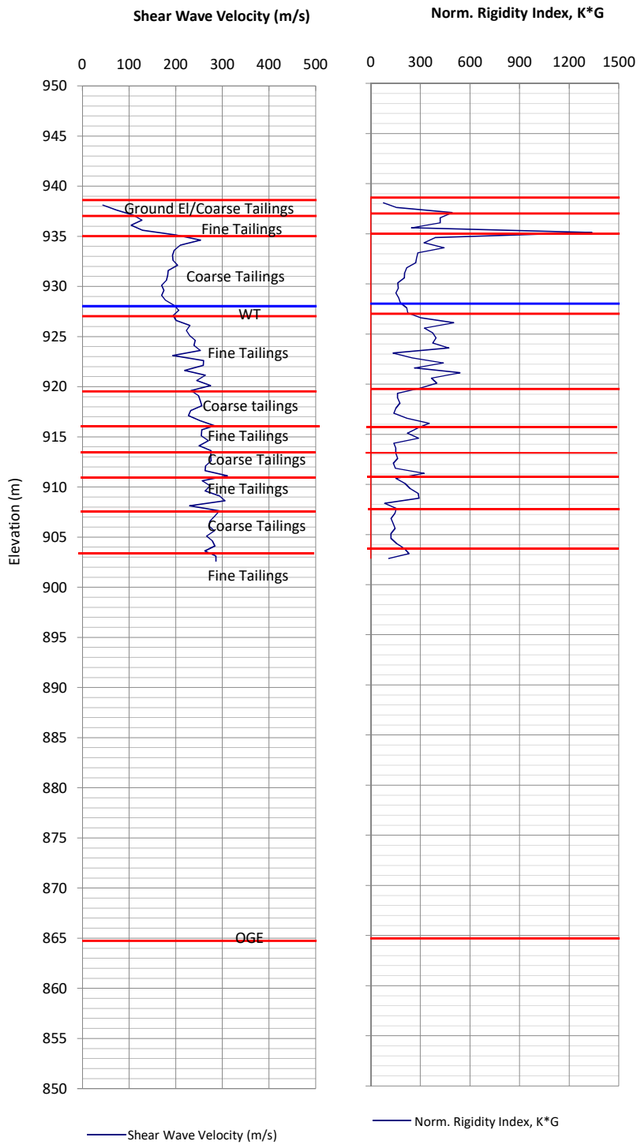
PROJECT: REPORT OF THE EXPERT PANEL ON THE TECHNICAL CAUSES OF THE FAILURE OF FEIJÃO DAM 1

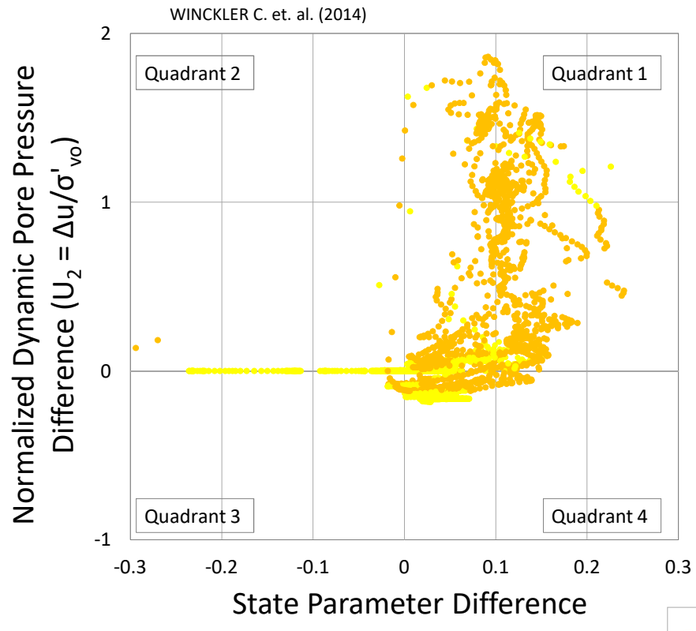
TITLE: CONE PENETRATION TEST CPTU-16-03N-R1

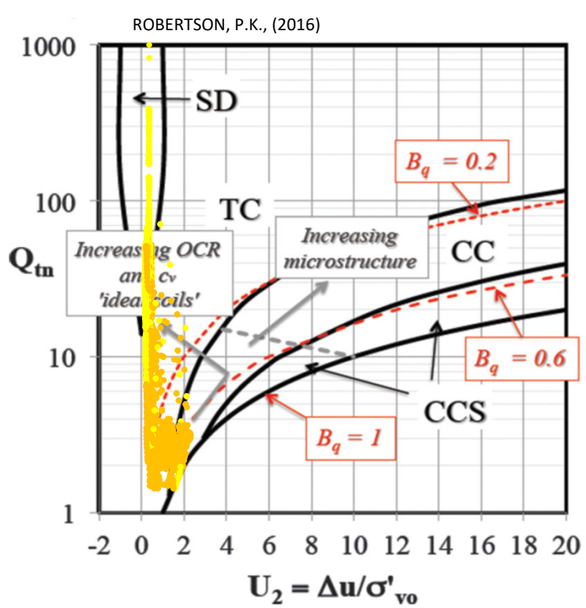
N:7775111.7 E:591977.7 12-Apr-2016

PROJECT NO.: A03355A01

FIGURE NO.: 10

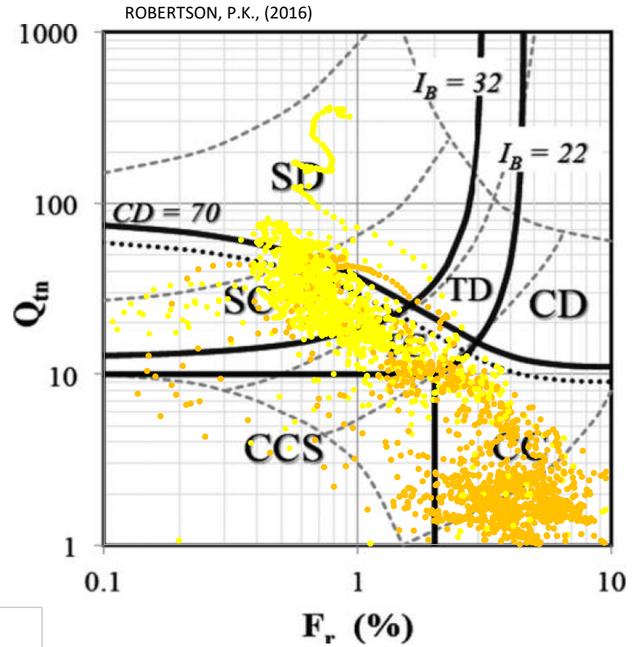


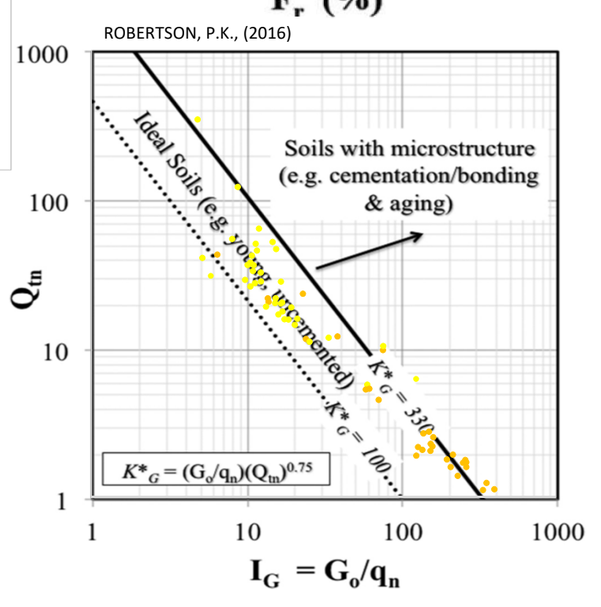




Fine Tailings

Coarse Tailings





Notes:

1. This interpretation is based on the water and soil saturated unit weights γ_w=9.807 kN/m^3, and respective γ_{sat} for each geological unit.
2. The hydrostatic pore pressure is calculated using the ground water level (GWL) determined from CPT pore pressure dissipation tests (where available).
3. Soil boundary layers (where plotted) are based on KCB interpretation from adjacent borehole logs.
4. The data presented have been plotted to the axis limits. Data may exist beyond the axis limits shown.

AS A MUTUAL PROTECTION TO OUR CLIENT, THE PUBLIC AND OURSELVES, ALL REPORTS AND DRAWINGS ARE SUBMITTED FOR THE CONFIDENTIAL INFORMATION OF OUR CLIENT FOR A SPECIFIC PROJECT AND AUTHORIZATION FOR USE AND/OR PUBLICATION OF DATA STATEMENTS, CONCLUSIONS OR ABSTRACTS FROM OR REWARDING OUR REPORTS AND DRAWINGS IS RESERVED PENDING OUR WRITTEN APPROVAL.

CLIENT

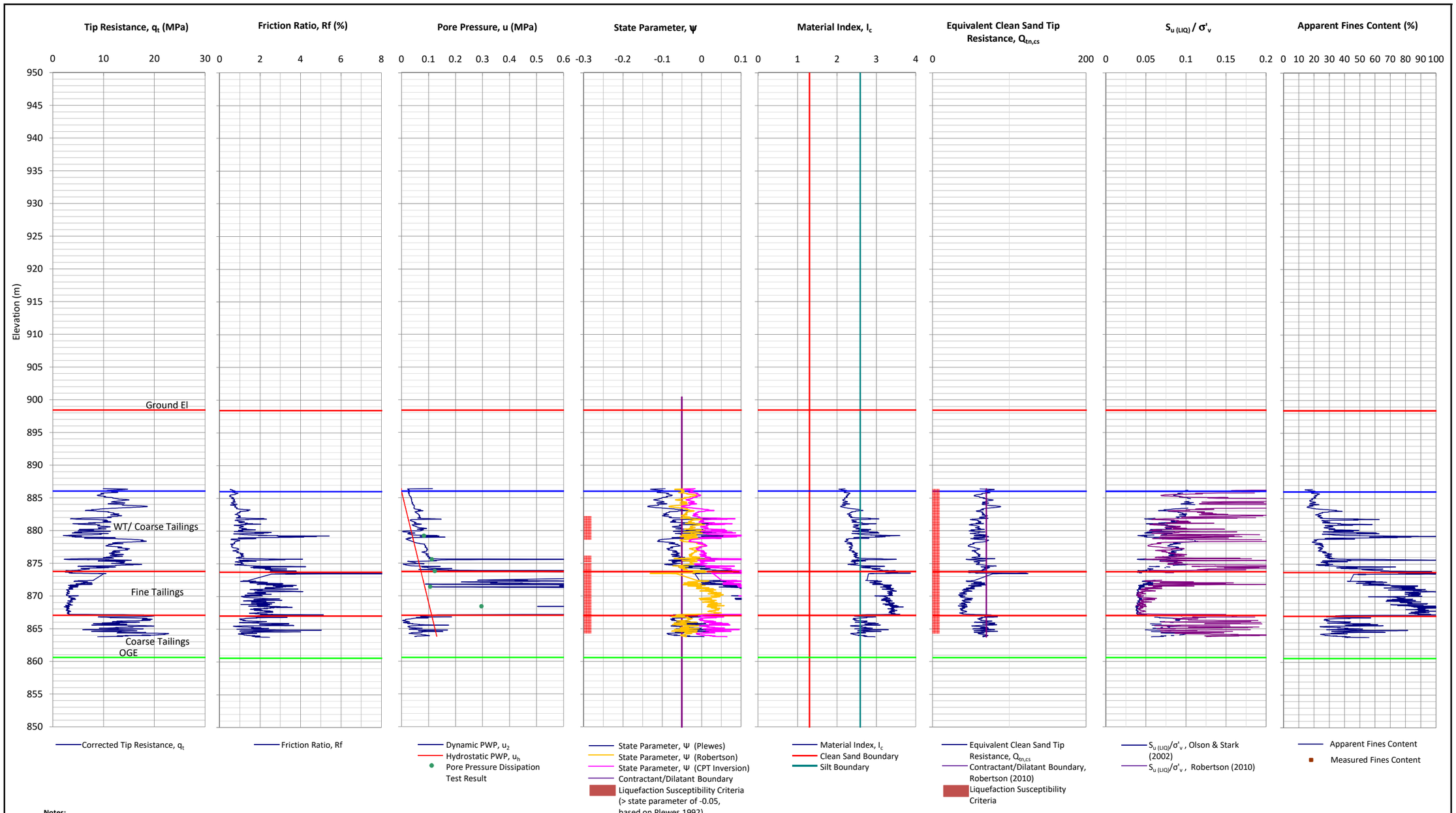
PROJECT: REPORT OF THE EXPERT PANEL ON THE TECHNICAL CAUSES OF THE FAILURE OF FEIJÃO DAM 1

TITLE: V_S/CPT Additional Plots for CPTU-16-03N-R1

N:7775111.7 E:591977.7 12-Apr-2016

PROJECT NO.: A03355A01

FIGURE NO.: 11



Notes:

1. This interpretation is based on the water and soil saturated unit weights γ_w=9.807 kN/m^3, and respective γ_{sat} for each geological unit.
2. The friction ratio Rf is calculated as Rf=f_s/q_t.
3. The hydrostatic pore pressure is calculated using the ground water level (GWL) determined from CPT pore pressure dissipation tests (where available) or dynamic pore pressure.
4. Soil boundary layers (where plotted) are based on KCB interpretation from adjacent borehole logs.
5. The data presented have been plotted to the axis limits. Data may exist beyond the axis limits shown.
6. The Material Index (I_c) boundaries are based on Robertson and Wride (1998).
7. The $Q_{tn,cs}$ contractant/dilatant boundary=70 and is based on Robertson (2010).
8. The State Parameter (Ψ) calculated using Plewes, et al. (1992) and the CPT inversion method is based on an assumed K0 of 0.5.

AS A MUTUAL PROTECTION TO OUR CLIENT, THE PUBLIC AND OURSELVES, ALL REPORTS AND DRAWINGS ARE SUBMITTED FOR THE CONFIDENTIAL INFORMATION OF OUR CLIENT FOR A SPECIFIC PROJECT AND AUTHORIZATION FOR USE AND/OR PUBLICATION OF DATA STATEMENTS, CONCLUSIONS OR ABSTRACTS FROM OR REWARDING OUR REPORTS AND DRAWINGS IS RESERVED PENDING OUR WRITTEN APPROVAL.

CLIENT

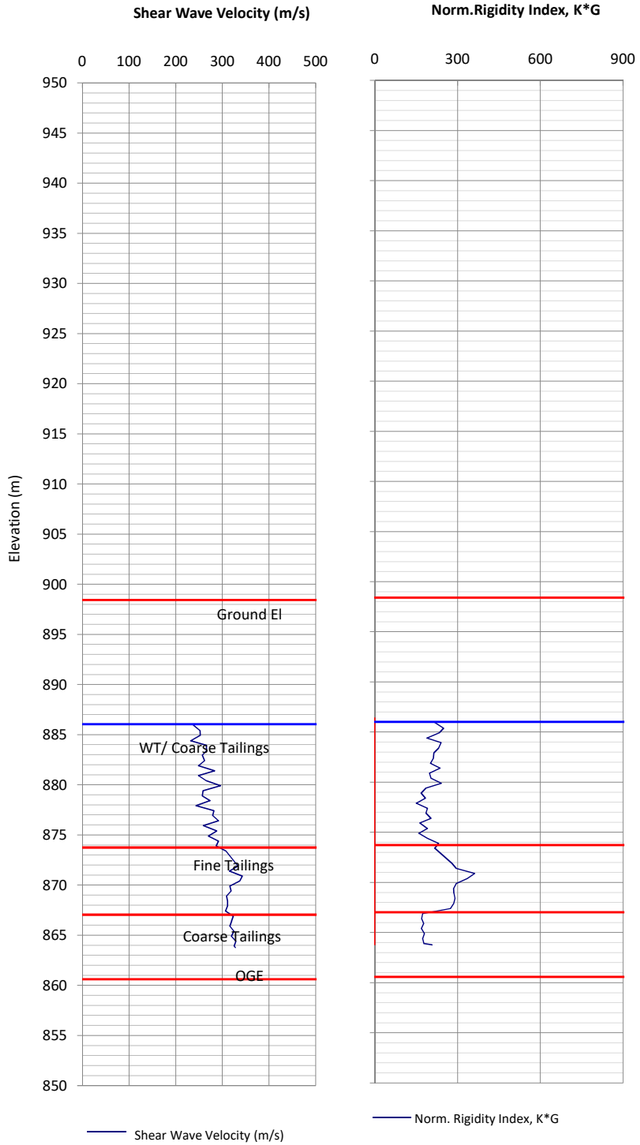
PROJECT: REPORT OF THE EXPERT PANEL ON THE TECHNICAL CAUSES OF THE FAILURE OF FEIJÃO DAM 1

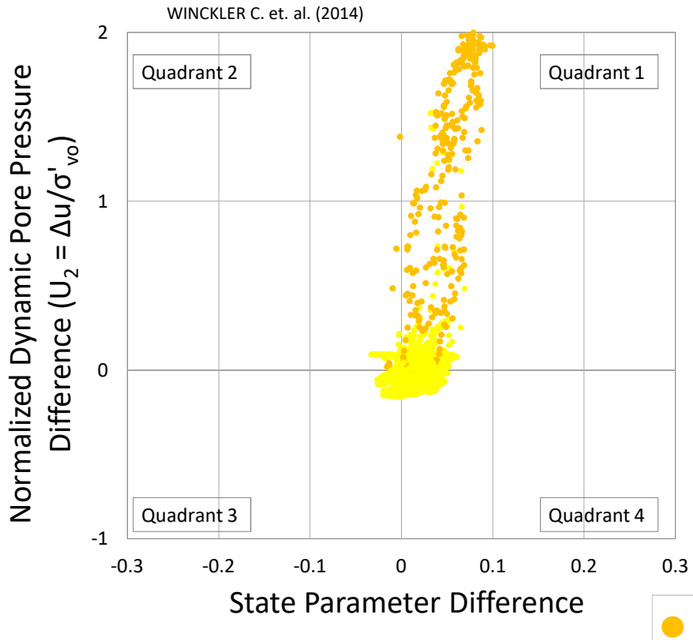
TITLE: CONE PENETRATION TEST CPTU-16-04N_R1

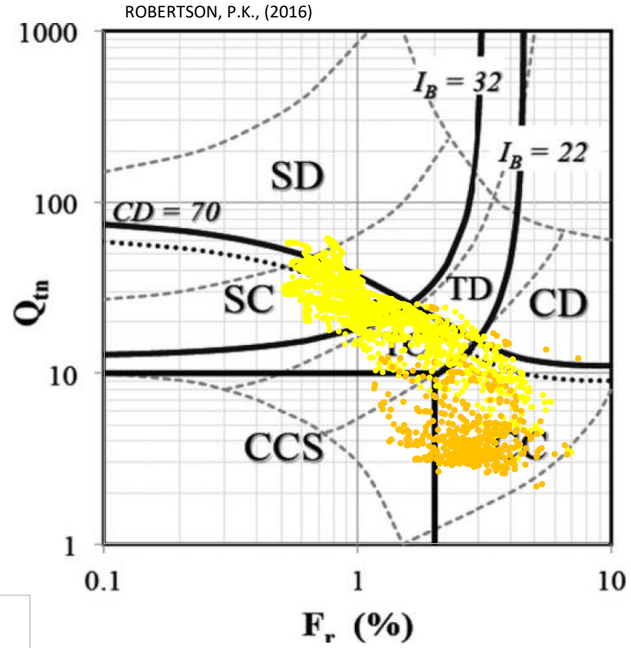
N:7775007.7 E:591838.6 31-Mar-2016

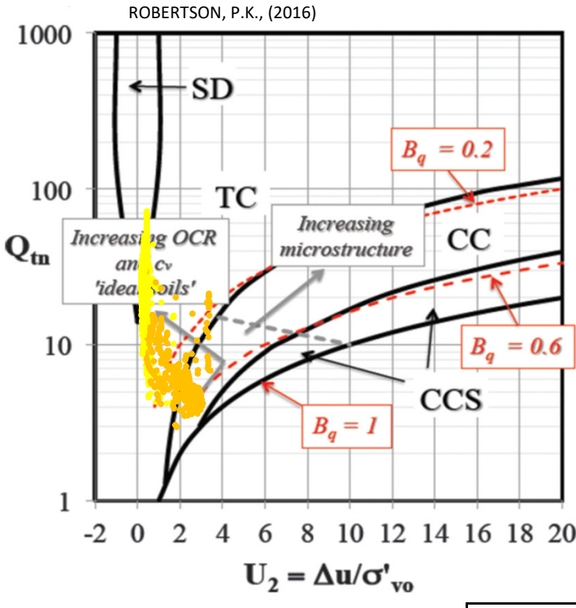
PROJECT NO.: A03355A01

FIGURE NO.: 12



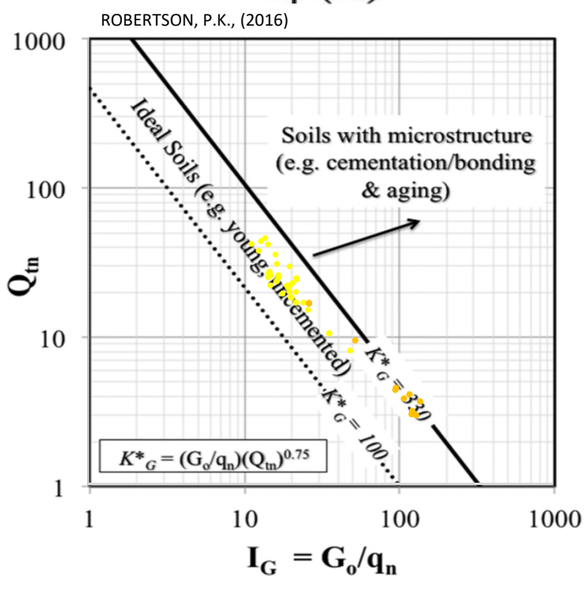






Fine Tailings

Coarse Tailings



Notes:

1. This interpretation is based on the water and soil saturated unit weights γ_w=9.807 kN/m^3, and respective γ_{sat} for each geological unit.
2. The hydrostatic pore pressure is calculated using the ground water level (GWL) determined from CPT pore pressure dissipation tests (where available).
3. Soil boundary layers (where plotted) are based on KCB interpretation from adjacent borehole logs.
4. The data presented have been plotted to the axis limits. Data may exist beyond the axis limits shown.

AS A MUTUAL PROTECTION TO OUR CLIENT, THE PUBLIC AND OURSELVES, ALL REPORTS AND DRAWINGS ARE SUBMITTED FOR THE CONFIDENTIAL INFORMATION OF OUR CLIENT FOR A SPECIFIC PROJECT AND AUTHORIZATION FOR USE AND/OR PUBLICATION OF DATA STATEMENTS, CONCLUSIONS OR ABSTRACTS FROM OR REWARDING OUR REPORTS AND DRAWINGS IS RESERVED PENDING OUR WRITTEN APPROVAL.

CLIENT

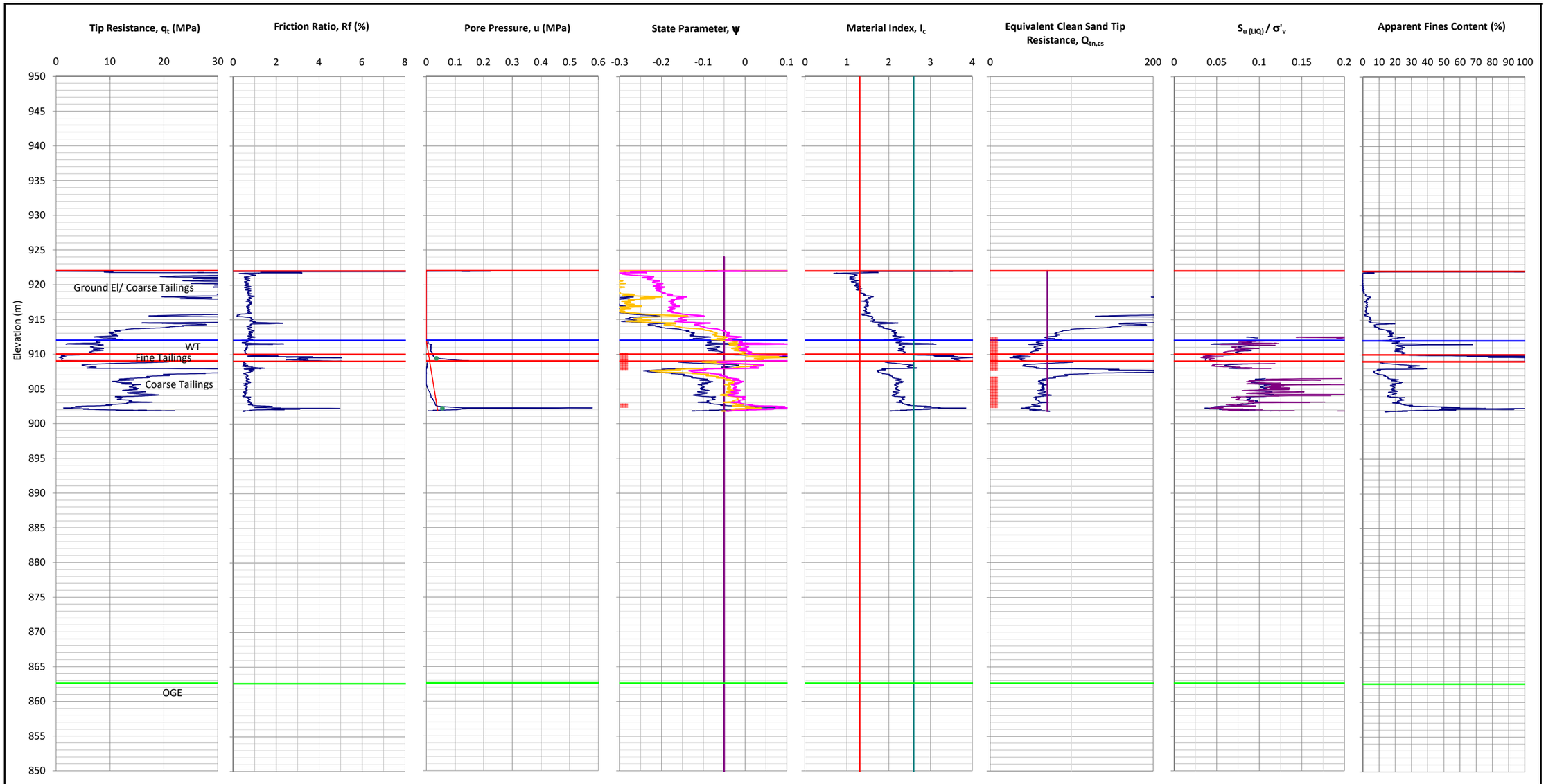
PROJECT: REPORT OF THE EXPERT PANEL ON THE TECHNICAL CAUSES OF THE FAILURE OF FEIJÃO DAM 1

TITLE: V_s/CPT Additional Plots for CPTU-16-04N_R1

N:7775007.7 E:591838.6 31-Mar-2016

PROJECT NO.: A03355A01

FIGURE NO.: 13



Notes:

1. This interpretation is based on the water and soil saturated unit weights γ_w=9.807 kN/m^3, and respective γ_{sat} for each geological unit.
2. The friction ratio Rf is calculated as Rf=f_s/q_t.
3. The hydrostatic pore pressure is calculated using the ground water level (GWL) determined from CPT pore pressure dissipation tests (where available) or dynamic pore pressure.
4. Soil boundary layers (where plotted) are based on KCB interpretation from adjacent borehole logs.
5. The data presented have been plotted to the axis limits. Data may exist beyond the axis limits shown.
6. The Material Index (I_c) boundaries are based on Robertson and Wride (1998).
7. The $Q_{tn,cs}$ contractant/dilatant boundary=70 and is based on Robertson (2010).
8. The State Parameter (Ψ) calculated using Plewes, et al. (1992) and the CPT inversion method is based on an assumed K0 of 0.5.

AS A MUTUAL PROTECTION TO OUR CLIENT, THE PUBLIC AND OURSELVES, ALL REPORTS AND DRAWINGS ARE SUBMITTED FOR THE CONFIDENTIAL INFORMATION OF OUR CLIENT FOR A SPECIFIC PROJECT AND AUTHORIZATION FOR USE AND/OR PUBLICATION OF DATA STATEMENTS, CONCLUSIONS OR ABSTRACTS FROM OR REWARDING OUR REPORTS AND DRAWINGS IS RESERVED PENDING OUR WRITTEN APPROVAL.

CLIENT

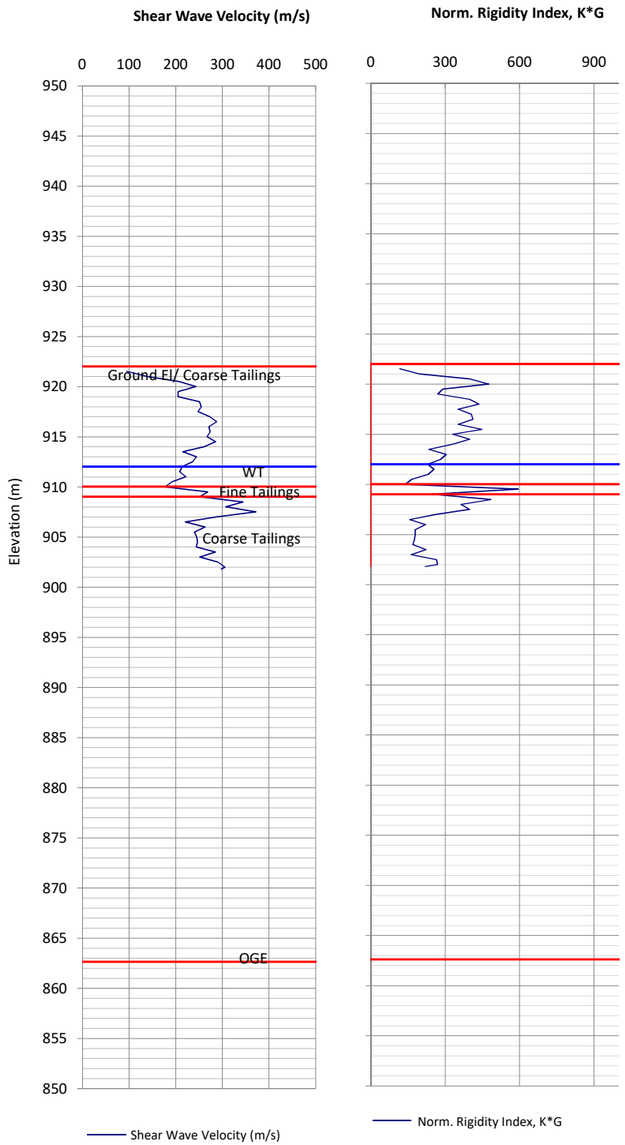
PROJECT: REPORT OF THE EXPERT PANEL ON THE TECHNICAL CAUSES OF THE FAILURE OF FEIJÃO DAM 1

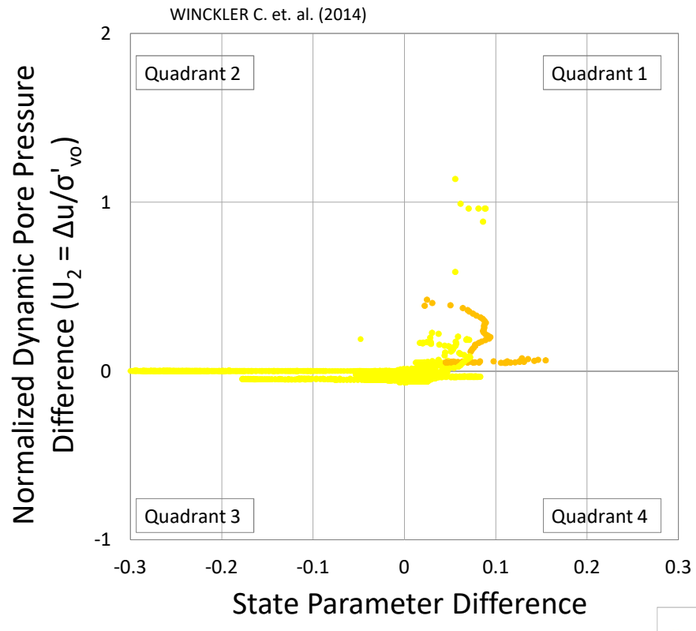
TITLE: CONE PENETRATION TEST CPTU-16-05N_R1

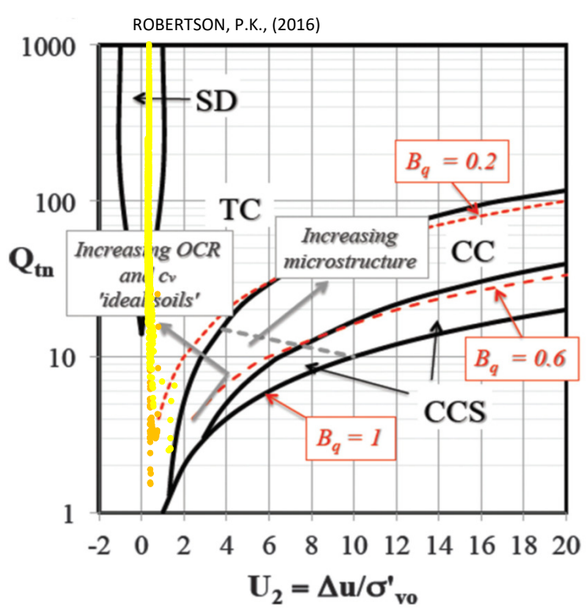
N:7775049.5 E:591901.1 8th April 2016

PROJECT NO.: A03355A01

FIGURE NO.: 14

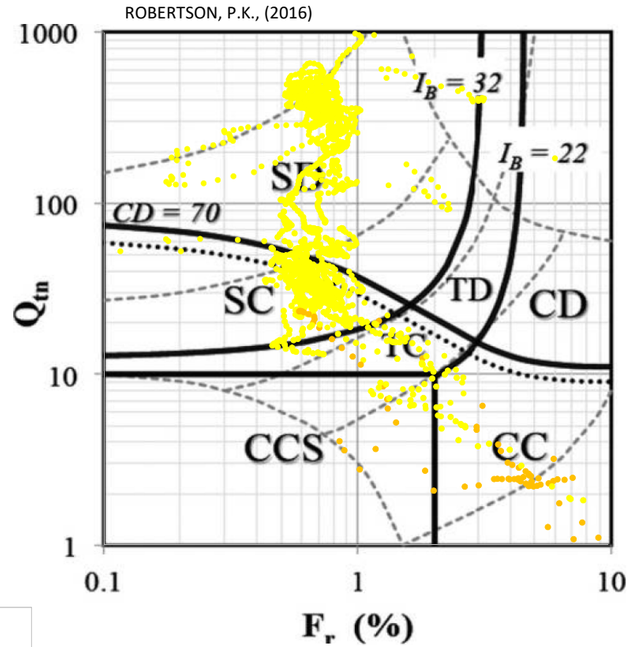


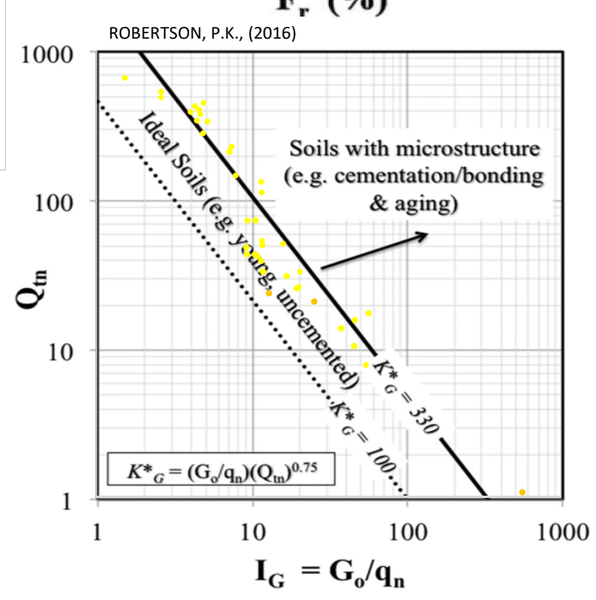




Fine Tailings

Coarse Tailings





Notes:

1. This interpretation is based on the water and soil saturated unit weights γ_w=9.807 kN/m^3, and respective γ_{sat} for each geological unit.
2. The hydrostatic pore pressure is calculated using the ground water level (GWL) determined from CPT pore pressure dissipation tests (where available).
3. Soil boundary layers (where plotted) are based on KCB interpretation from adjacent borehole logs.
4. The data presented have been plotted to the axis limits. Data may exist beyond the axis limits shown.

AS A MUTUAL PROTECTION TO OUR CLIENT, THE PUBLIC AND OURSELVES, ALL REPORTS AND DRAWINGS ARE SUBMITTED FOR THE CONFIDENTIAL INFORMATION OF OUR CLIENT FOR A SPECIFIC PROJECT AND AUTHORIZATION FOR USE AND/OR PUBLICATION OF DATA STATEMENTS, CONCLUSIONS OR ABSTRACTS FROM OR REWARDING OUR REPORTS AND DRAWINGS IS RESERVED PENDING OUR WRITTEN APPROVAL.

CLIENT

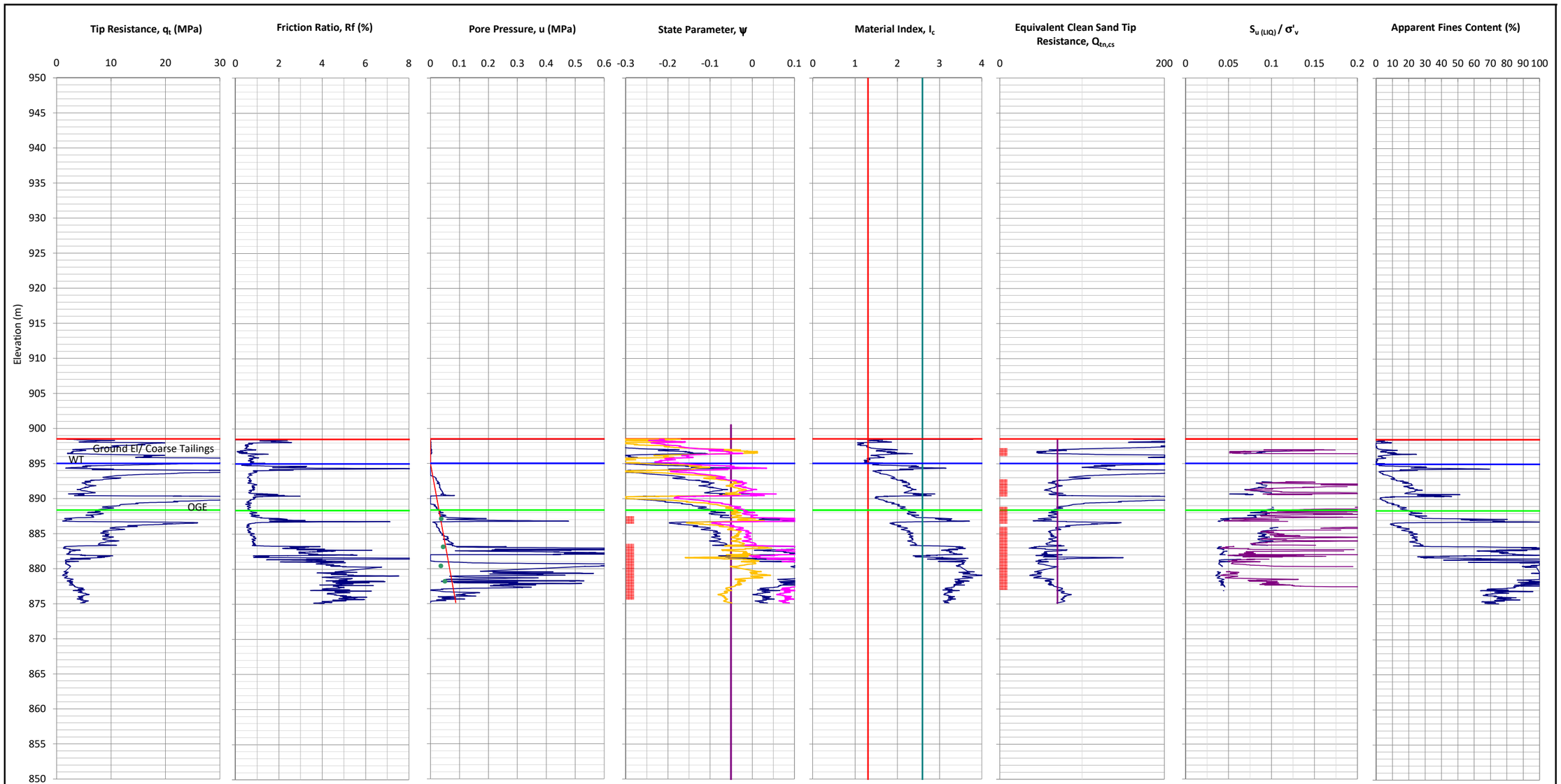
PROJECT: REPORT OF THE EXPERT PANEL ON THE TECHNICAL CAUSES OF THE FAILURE OF FEIJÃO DAM 1

TITLE: V_s/CPT Additional Plots for CPTU-16-05N_R1

N:7775049.5 E:591901.1 8th April 2016

PROJECT NO.: A03355A01

FIGURE NO.: 15



Notes:

1. This interpretation is based on the water and soil saturated unit weights γ_w=9.807 kN/m^3, and respective γ_{sat} for each geological unit.
2. The friction ratio Rf is calculated as Rf=f_s/q_t.
3. The hydrostatic pore pressure is calculated using the ground water level (GWL) determined from CPT pore pressure dissipation tests (where available) or dynamic pore pressure.
4. Soil boundary layers (where plotted) are based on KCB interpretation from adjacent borehole logs.
5. The data presented have been plotted to the axis limits. Data may exist beyond the axis limits shown.
6. The Material Index (I_c) boundaries are based on Robertson and Wride (1998).
7. The $Q_{tn,cs}$ contractant/dilatant boundary=70 and is based on Robertson (2010).
8. The State Parameter (Ψ) calculated using Plewes, et al. (1992) and the CPT inversion method is based on an assumed K0 of 0.5.

AS A MUTUAL PROTECTION TO OUR CLIENT, THE PUBLIC AND OURSELVES, ALL REPORTS AND DRAWINGS ARE SUBMITTED FOR THE CONFIDENTIAL INFORMATION OF OUR CLIENT FOR A SPECIFIC PROJECT AND AUTHORIZATION FOR USE AND/OR PUBLICATION OF DATA STATEMENTS, CONCLUSIONS OR ABSTRACTS FROM OR REWARDING OUR REPORTS AND DRAWINGS IS RESERVED PENDING OUR WRITTEN APPROVAL.

CLIENT

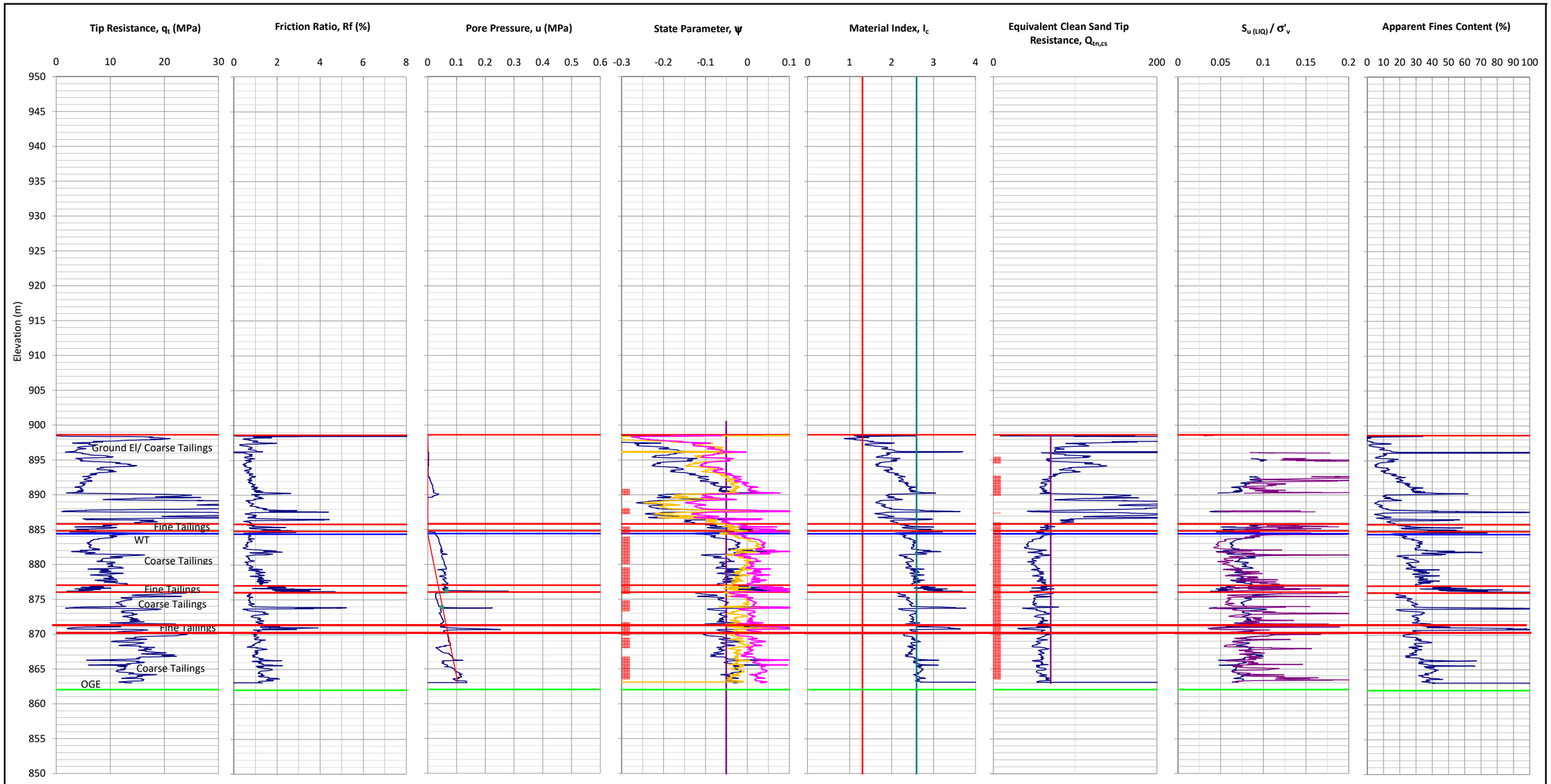
PROJECT: REPORT OF THE EXPERT PANEL ON THE TECHNICAL CAUSES OF THE FAILURE OF FEIJÃO DAM 1

TITLE: CONE PENETRATION TEST CPTU-16-06N_R1

N:7774824.3 E:591940.8 30th March 2016

PROJECT NO.: A03355A01

FIGURE NO.: 16



Notes:

1. This interpretation is based on the water and soil saturated unit weights γ_w=9.807 kN/m^3, and respective γ_{sat} for each geological unit.
2. The friction ratio Rf is calculated as Rf=f_s/q_t.
3. The hydrostatic pore pressure is calculated using the ground water level (GWL) determined from CPT pore pressure dissipation tests (where available) or dynamic pore pressure.
4. Soil boundary layers (where plotted) are based on KCB interpretation from adjacent borehole logs.
5. The data presented have been plotted to the axis limits. Data may exist beyond the axis limits shown.
6. The Material Index (I_c) boundaries are based on Robertson and Wride (1998).
7. The $Q_{tn,cs}$ contractant/dilatant boundary=70 and is based on Robertson (2010).
8. The State Parameter (Ψ) calculated using Plewes, et al. (1992) and the CPT inversion method is based on an assumed K0 of 0.5.

AS A MUTUAL PROTECTION TO OUR CLIENT, THE PUBLIC AND OURSELVES, ALL REPORTS AND DRAWINGS ARE SUBMITTED FOR THE CONFIDENTIAL INFORMATION OF OUR CLIENT FOR A SPECIFIC PROJECT AND AUTHORIZATION FOR USE AND/OR PUBLICATION OF DATA STATEMENTS, CONCLUSIONS OR ABSTRACTS FROM OR REWARDING OUR REPORTS AND DRAWINGS IS RESERVED PENDING OUR WRITTEN APPROVAL.

CLIENT

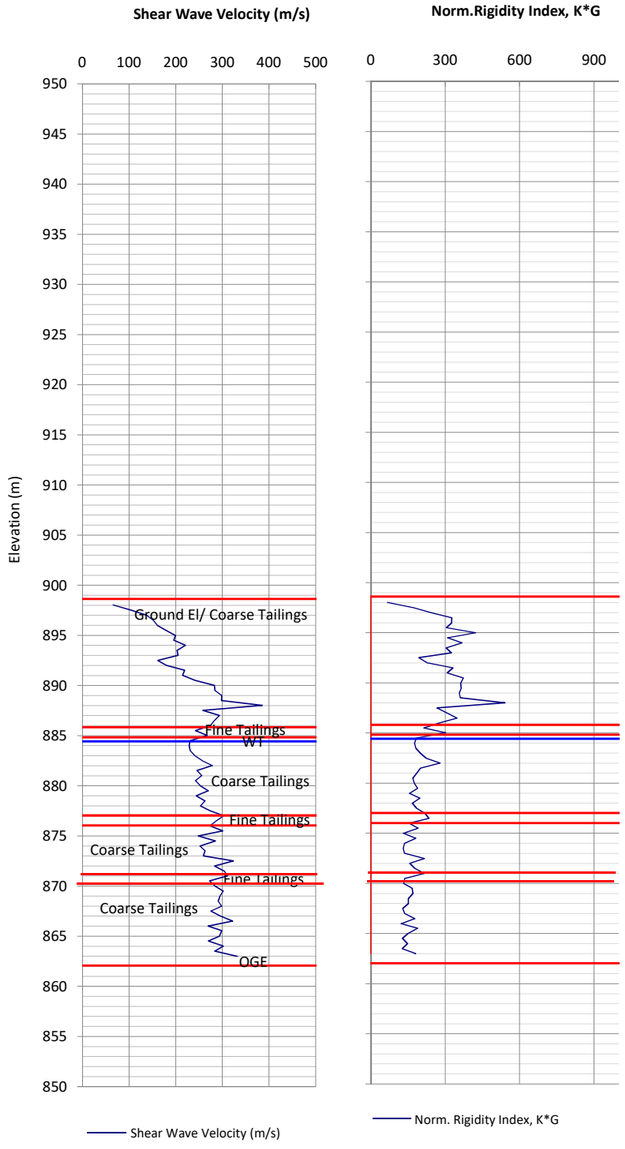
PROJECT: REPORT OF THE EXPERT PANEL ON THE TECHNICAL CAUSES OF THE FAILURE OF FEIJÃO DAM 1

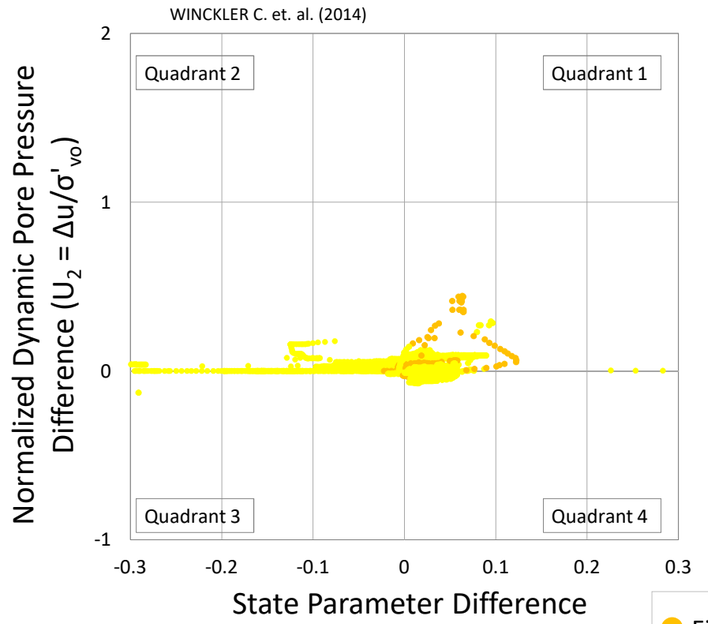
TITLE: CONE PENETRATION TEST CPTU-16-07N_R1

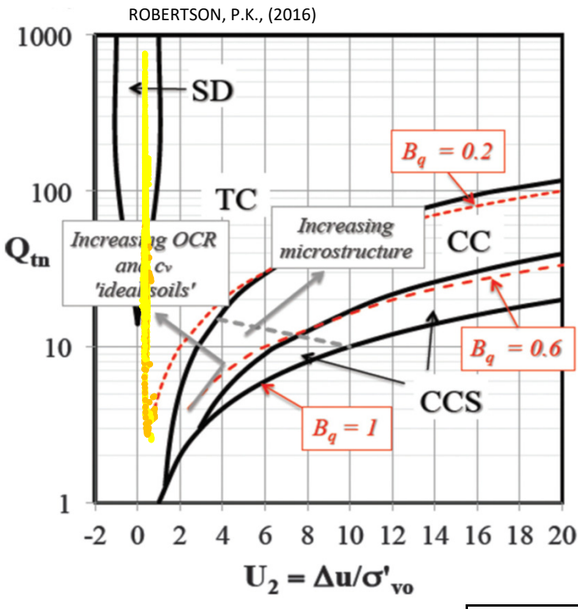
N:7774990.5 E:591801.7 30-Mar-2016

PROJECT NO.: A03355A01

FIGURE NO.: 17

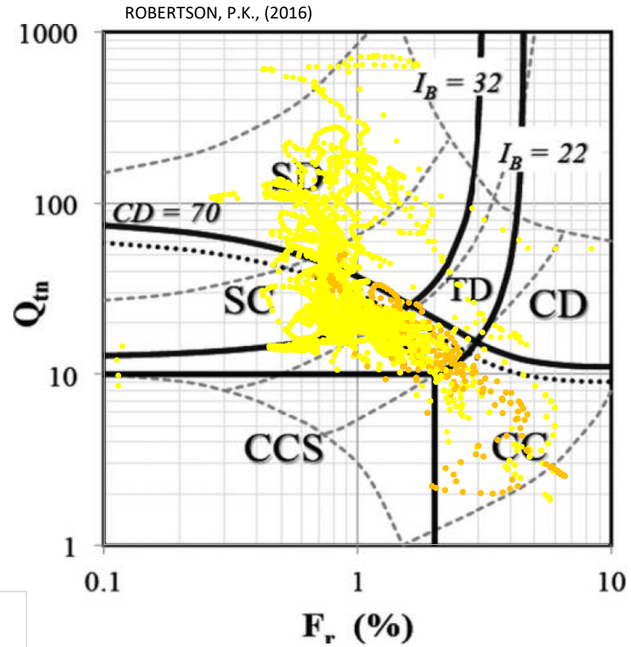


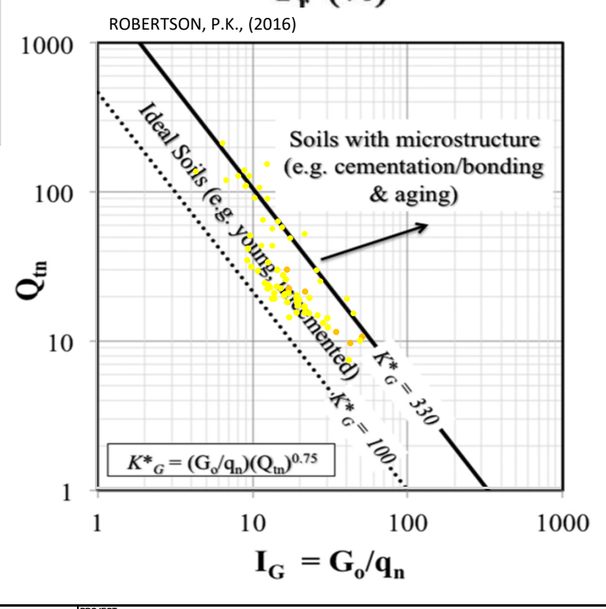




Fine Tailings

Coarse Tailings





Notes:

1. This interpretation is based on the water and soil saturated unit weights γ_w=9.807 kN/m^3, and respective γ_{sat} for each geological unit.
2. The hydrostatic pore pressure is calculated using the ground water level (GWL) determined from CPT pore pressure dissipation tests (where available).
3. Soil boundary layers (where plotted) are based on KCB interpretation from adjacent borehole logs.
4. The data presented have been plotted to the axis limits. Data may exist beyond the axis limits shown.

AS A MUTUAL PROTECTION TO OUR CLIENT, THE PUBLIC AND OURSELVES, ALL REPORTS AND DRAWINGS ARE SUBMITTED FOR THE CONFIDENTIAL INFORMATION OF OUR CLIENT FOR A SPECIFIC PROJECT AND AUTHORIZATION FOR USE AND/OR PUBLICATION OF DATA STATEMENTS, CONCLUSIONS OR ABSTRACTS FROM OR REWARDING OUR REPORTS AND DRAWINGS IS RESERVED PENDING OUR WRITTEN APPROVAL.

CLIENT

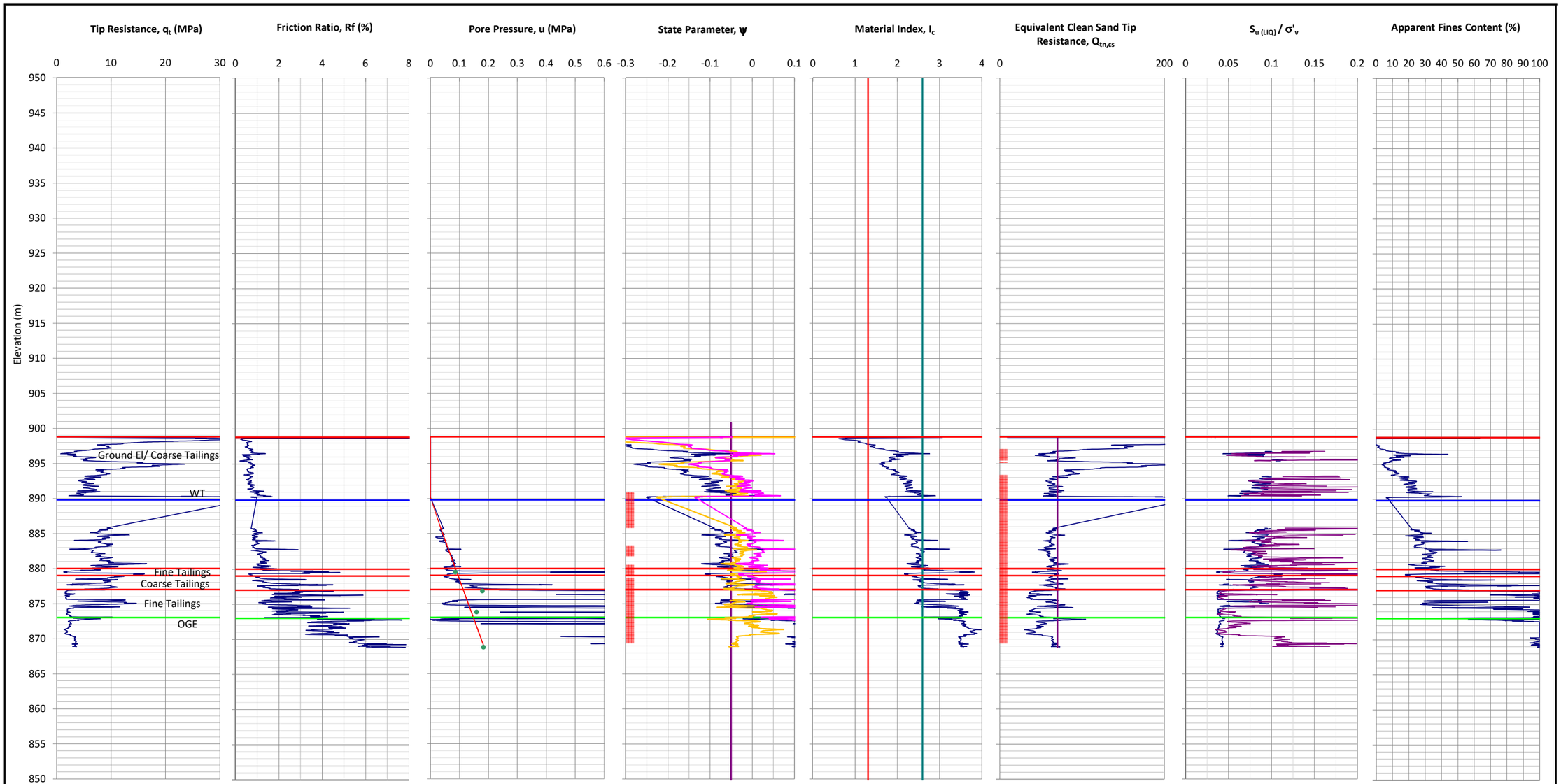
PROJECT: REPORT OF THE EXPERT PANEL ON THE TECHNICAL CAUSES OF THE FAILURE OF FEIJÃO DAM 1

TITLE: V_s/CPT Additional Plots for CPTU-16-07N_R1

N:7774990.5 E:591801.7 30-Mar-2016

PROJECT NO.: A03355A01

FIGURE NO.: 18



Notes:

1. This interpretation is based on the water and soil saturated unit weights γ_w=9.807 kN/m^3, and respective γ_{sat} for each geological unit.
2. The friction ratio Rf is calculated as Rf=f_s/q_t.
3. The hydrostatic pore pressure is calculated using the ground water level (GWL) determined from CPT pore pressure dissipation tests (where available) or dynamic pore pressure.
4. Soil boundary layers (where plotted) are based on KCB interpretation from adjacent borehole logs.
5. The data presented have been plotted to the axis limits. Data may exist beyond the axis limits shown.
6. The Material Index (I_c) boundaries are based on Robertson and Wride (1998).
7. The $Q_{tn,cs}$ contractant/dilatant boundary=70 and is based on Robertson (2010).
8. The State Parameter (Ψ) calculated using Plewes, et al. (1992) and the CPT inversion method is based on an assumed K0 of 0.5.

AS A MUTUAL PROTECTION TO OUR CLIENT, THE PUBLIC AND OURSELVES, ALL REPORTS AND DRAWINGS ARE SUBMITTED FOR THE CONFIDENTIAL INFORMATION OF OUR CLIENT FOR A SPECIFIC PROJECT AND AUTHORIZATION FOR USE AND/OR PUBLICATION OF DATA STATEMENTS, CONCLUSIONS OR ABSTRACTS FROM OR REWARDING OUR REPORTS AND DRAWINGS IS RESERVED PENDING OUR WRITTEN APPROVAL.

CLIENT

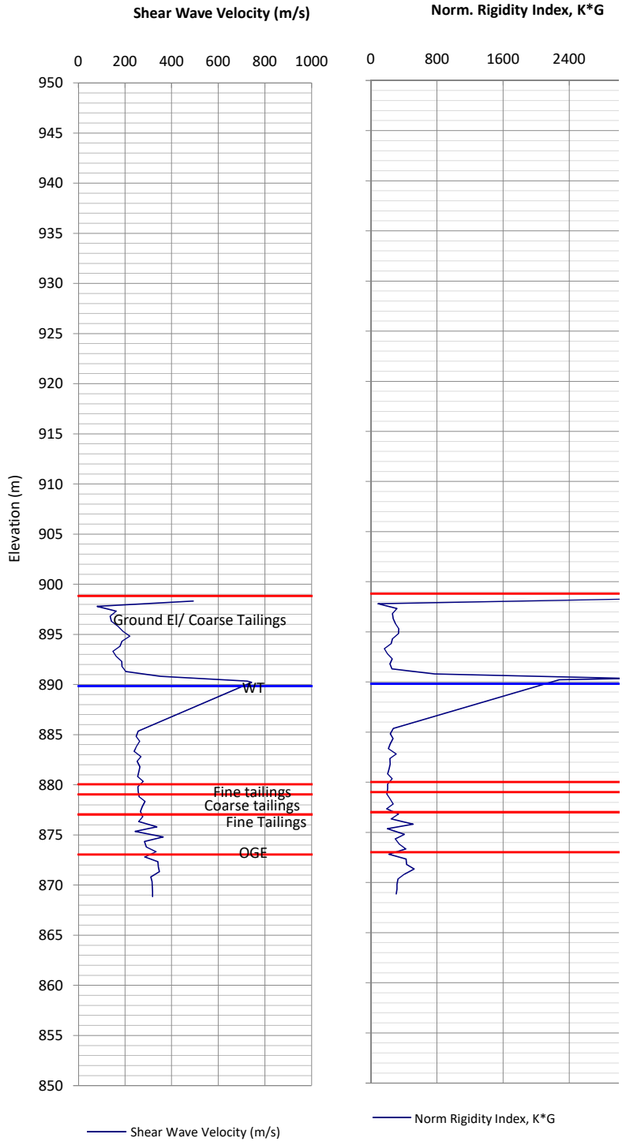
PROJECT: REPORT OF THE EXPERT PANEL ON THE TECHNICAL CAUSES OF THE FAILURE OF FEIJÃO DAM 1

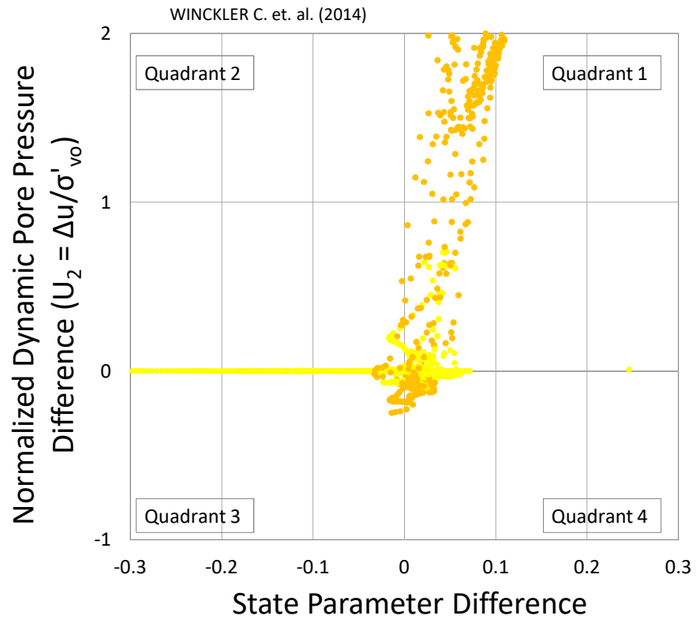
TITLE: CONE PENETRATION TEST CPTU-16-08N_R1

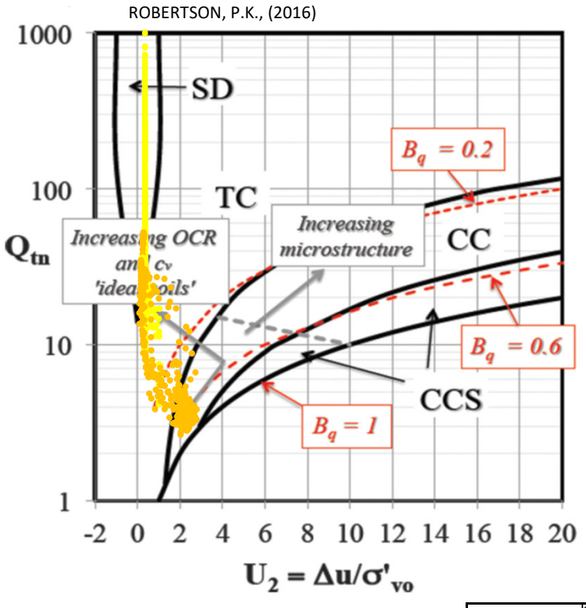
N:7775069.1 E:591776.8 4th April 2016

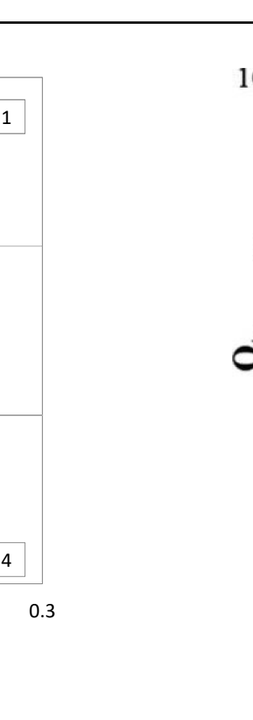
PROJECT NO.: A03355A01

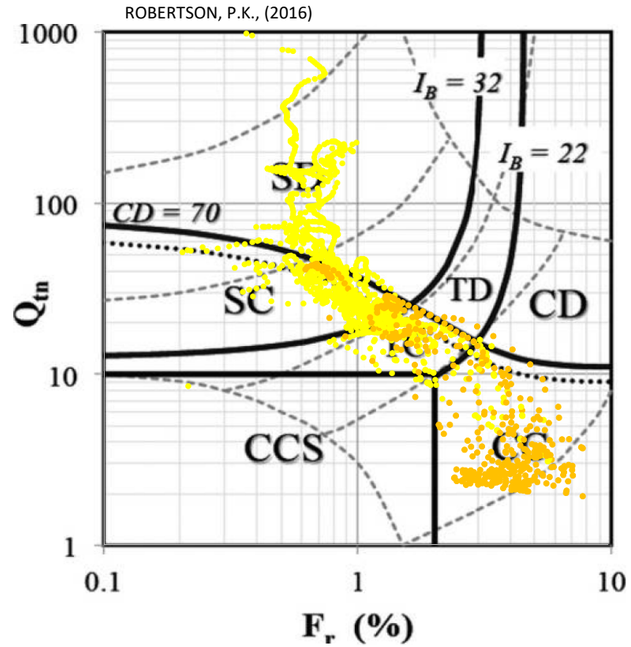
FIGURE NO.: 19











Notes:

1. This interpretation is based on the water and soil saturated unit weights γ_w=9.807 kN/m^3, and respective γ_{sat} for each geological unit.
2. The hydrostatic pore pressure is calculated using the ground water level (GWL) determined from CPT pore pressure dissipation tests (where available).
3. Soil boundary layers (where plotted) are based on KCB interpretation from adjacent borehole logs.
4. The data presented have been plotted to the axis limits. Data may exist beyond the axis limits shown.

AS A MUTUAL PROTECTION TO OUR CLIENT, THE PUBLIC AND OURSELVES, ALL REPORTS AND DRAWINGS ARE SUBMITTED FOR THE CONFIDENTIAL INFORMATION OF OUR CLIENT FOR A SPECIFIC PROJECT AND AUTHORIZATION FOR USE AND/OR PUBLICATION OF DATA STATEMENTS, CONCLUSIONS OR ABSTRACTS FROM OR REWARDING OUR REPORTS AND DRAWINGS IS RESERVED PENDING OUR WRITTEN APPROVAL.

CLIENT

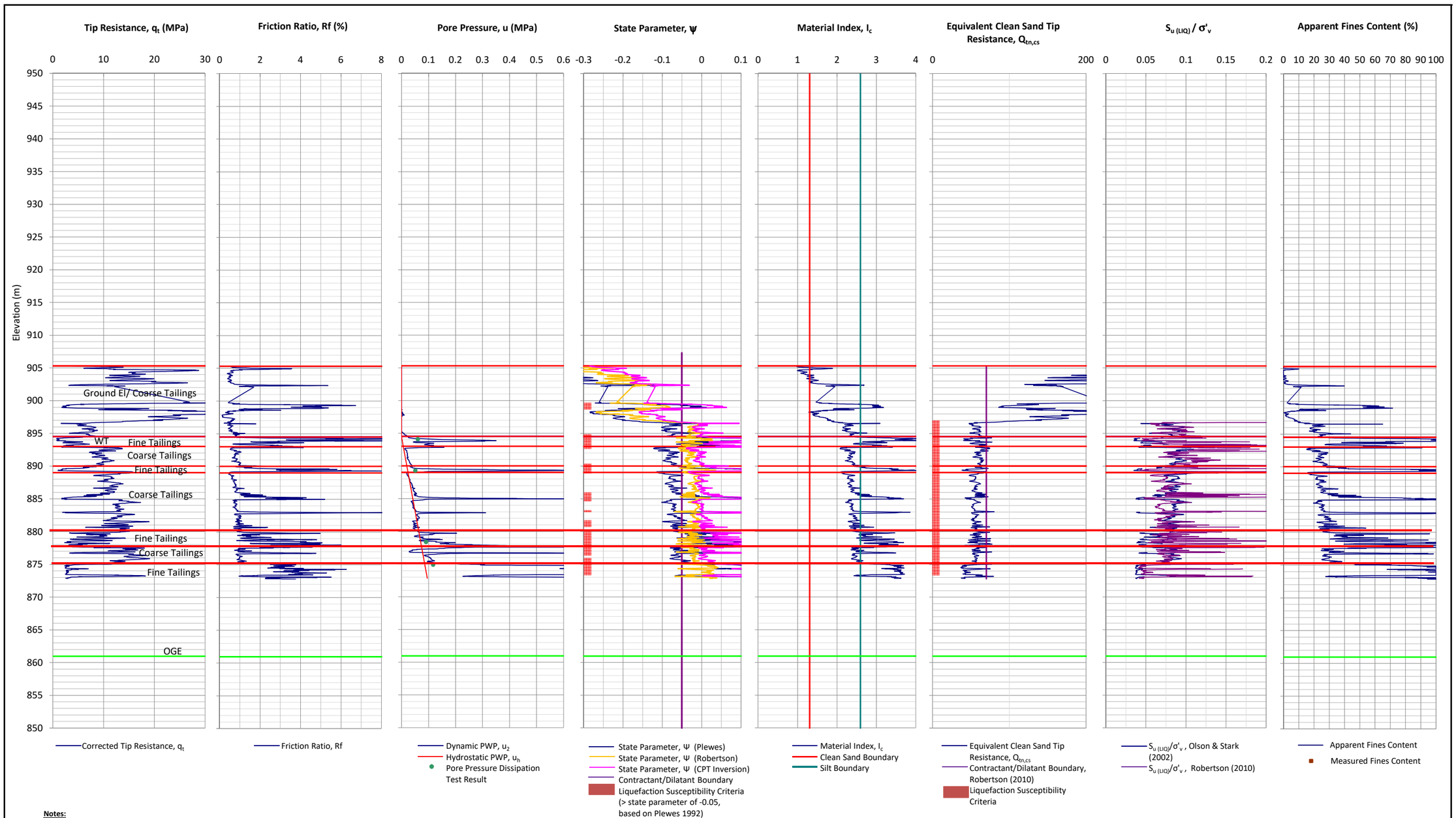
PROJECT: REPORT OF THE EXPERT PANEL ON THE TECHNICAL CAUSES OF THE FAILURE OF FEIJÃO DAM 1

TITLE: V_s/CPT Additional Plots for CPTU-16-08N_R1

N:7775069.1 E:591776.8 4th April 2016

PROJECT NO.: A03355A01

FIGURE NO.: 20



Notes:

1. This interpretation is based on the water and soil saturated unit weights γ_w=9.807 kN/m^3, and respective γ_{sat} for each geological unit.
2. The friction ratio Rf is calculated as Rf=f_s/q_t.
3. The hydrostatic pore pressure is calculated using the ground water level (GWL) determined from CPT pore pressure dissipation tests (where available) or dynamic pore pressure.
4. Soil boundary layers (where plotted) are based on KCB interpretation from adjacent borehole logs.
5. The data presented have been plotted to the axis limits. Data may exist beyond the axis limits shown.
6. The Material Index (I_c) boundaries are based on Robertson and Wride (1998).
7. The $Q_{tn,cs}$ contractant/dilatant boundary=70 and is based on Robertson (2010).
8. The State Parameter (Ψ) calculated using Plewes, et al. (1992) and the CPT inversion method is based on an assumed K0 of 0.5.

AS A MUTUAL PROTECTION TO OUR CLIENT, THE PUBLIC AND OURSELVES, ALL REPORTS AND DRAWINGS ARE SUBMITTED FOR THE CONFIDENTIAL INFORMATION OF OUR CLIENT FOR A SPECIFIC PROJECT AND AUTHORIZATION FOR USE AND/OR PUBLICATION OF DATA STATEMENTS, CONCLUSIONS OR ABSTRACTS FROM OR REMARKING OUR REPORTS AND DRAWINGS IS RESERVED PENDING OUR WRITTEN APPROVAL.

CLIENT

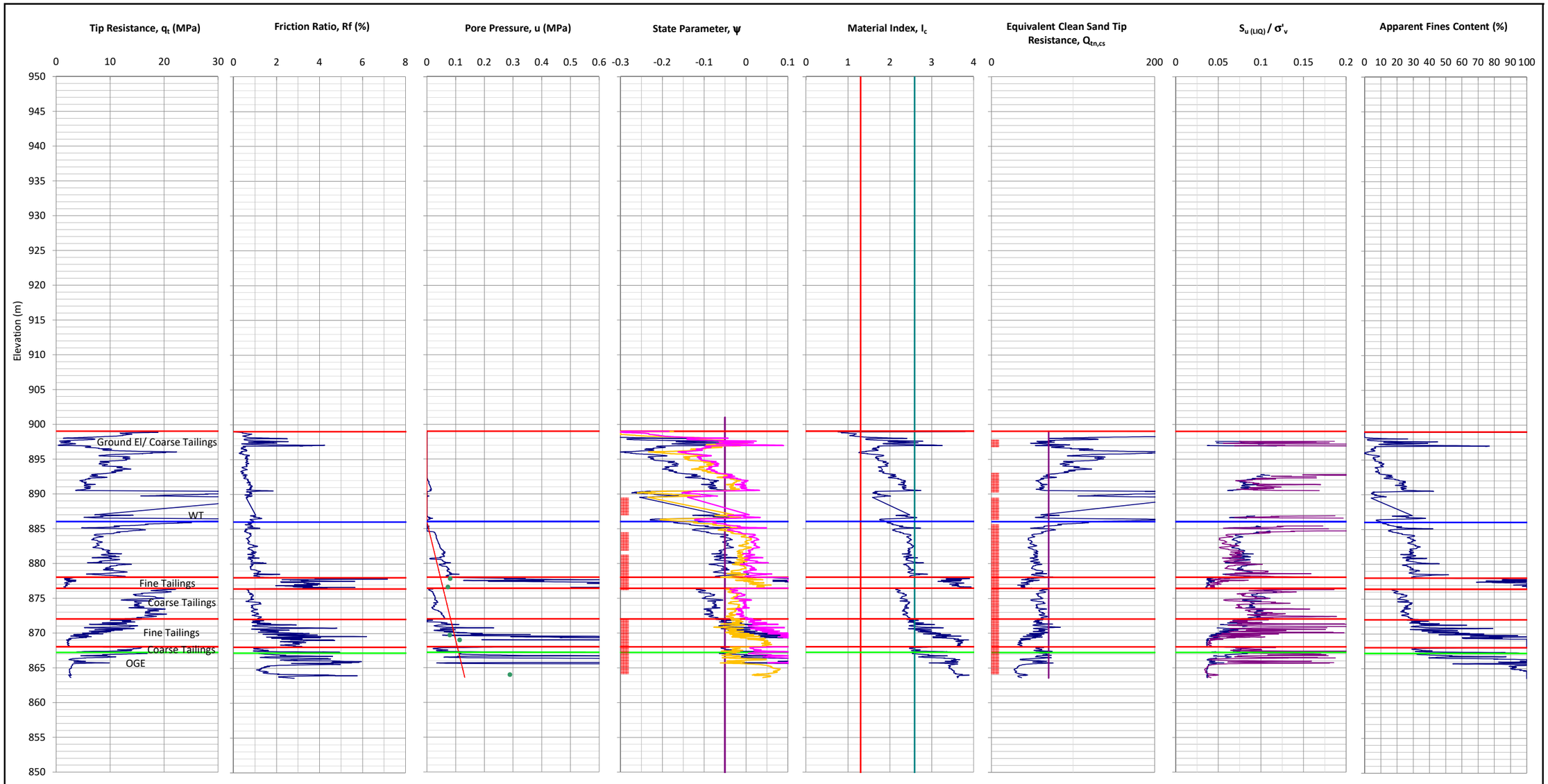
PROJECT: REPORT OF THE EXPERT PANEL ON THE TECHNICAL CAUSES OF THE FAILURE OF FEIJÃO DAM 1

TITLE: CONE PENETRATION TEST CPTU-16-09N_R1

N:7775029.7 E:591850 15th August 2016

PROJECT NO.: A03355A01

FIGURE NO.: 21



Notes:

1. This interpretation is based on the water and soil saturated unit weights γ_w=9.807 kN/m^3, and respective γ_{sat} for each geological unit.
2. The friction ratio Rf is calculated as Rf=f_s/q_t.
3. The hydrostatic pore pressure is calculated using the ground water level (GWL) determined from CPT pore pressure dissipation tests (where available) or dynamic pore pressure.
4. Soil boundary layers (where plotted) are based on KCB interpretation from adjacent borehole logs.
5. The data presented have been plotted to the axis limits. Data may exist beyond the axis limits shown.
6. The Material Index (I_c) boundaries are based on Robertson and Wride (1998).
7. The $Q_{tn,cs}$ contractant/dilatant boundary=70 and is based on Robertson (2010).
8. The State Parameter (Ψ) calculated using Plewes, et al. (1992) and the CPT inversion method is based on an assumed K0 of 0.5.

AS A MUTUAL PROTECTION TO OUR CLIENT, THE PUBLIC AND OURSELVES, ALL REPORTS AND DRAWINGS ARE SUBMITTED FOR THE CONFIDENTIAL INFORMATION OF OUR CLIENT FOR A SPECIFIC PROJECT AND AUTHORIZATION FOR USE AND/OR PUBLICATION OF DATA STATEMENTS, CONCLUSIONS OR ABSTRACTS FROM OR REWARDING OUR REPORTS AND DRAWINGS IS RESERVED PENDING OUR WRITTEN APPROVAL.

CLIENT

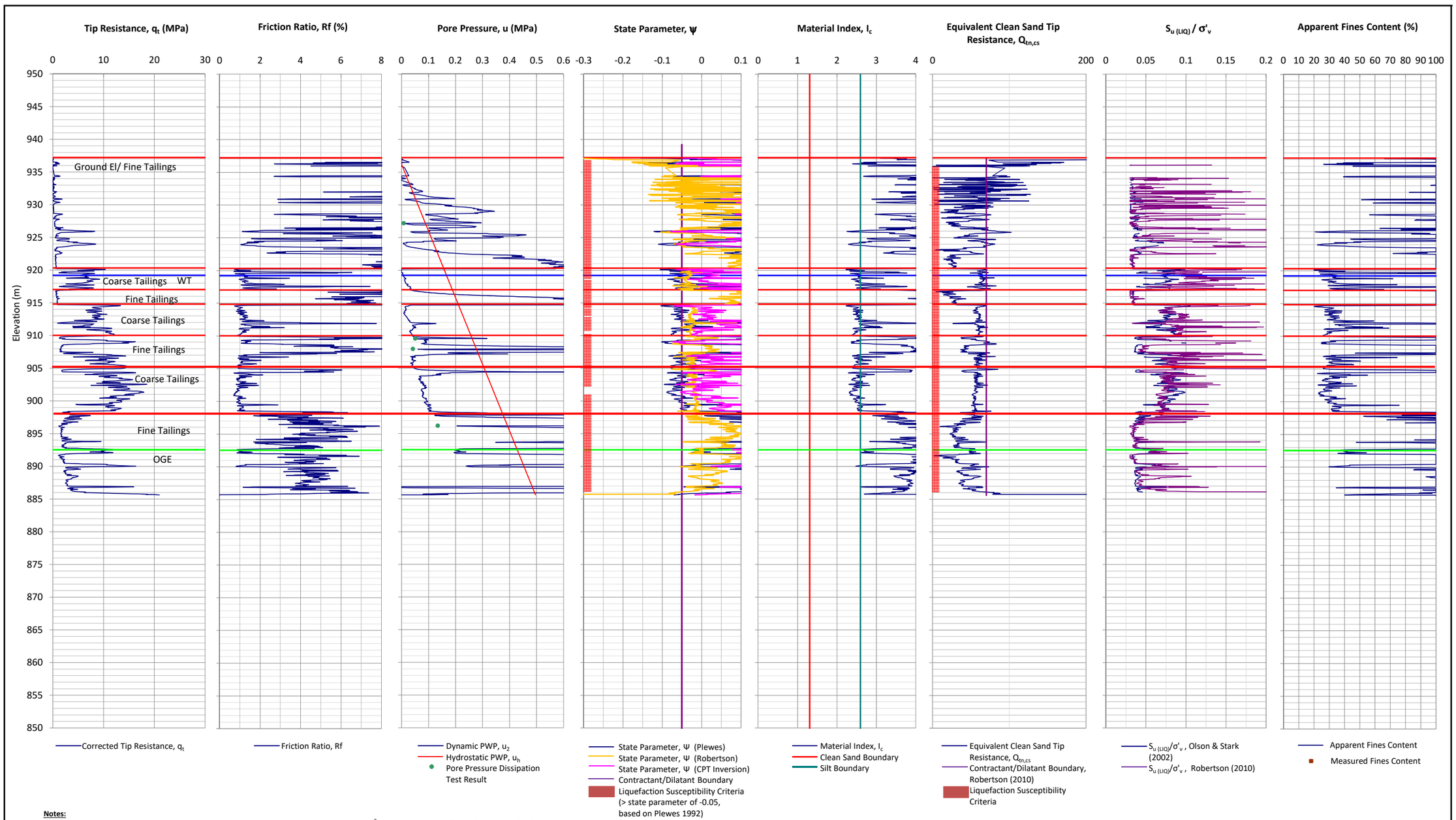
PROJECT: REPORT OF THE EXPERT PANEL ON THE TECHNICAL CAUSES OF THE FAILURE OF FEIJÃO DAM 1

TITLE: CONE PENETRATION TEST CPTU-16-10N_R1

N:7775014.5 E:591782 12-Aug-2016

PROJECT NO.: A03355A01

FIGURE NO.: 22



Notes:

1. This interpretation is based on the water and soil saturated unit weights γ_w=9.807 kN/m^3, and respective γ_{sat} for each geological unit.
2. The friction ratio Rf is calculated as Rf=f_s/q_t.
3. The hydrostatic pore pressure is calculated using the ground water level (GWL) determined from CPT pore pressure dissipation tests (where available) or dynamic pore pressure.
4. Soil boundary layers (where plotted) are based on KCB interpretation from adjacent borehole logs.
5. The data presented have been plotted to the axis limits. Data may exist beyond the axis limits shown.
6. The Material Index (I_c) boundaries are based on Robertson and Wride (1998).
7. The $Q_{tn,cs}$ contractant/dilatant boundary=70 and is based on Robertson (2010).
8. The State Parameter (Ψ) calculated using Plewes, et al. (1992) and the CPT inversion method is based on an assumed K0 of 0.5.

AS A MUTUAL PROTECTION TO OUR CLIENT, THE PUBLIC AND OURSELVES, ALL REPORTS AND DRAWINGS ARE SUBMITTED FOR THE CONFIDENTIAL INFORMATION OF OUR CLIENT FOR A SPECIFIC PROJECT AND AUTHORIZATION FOR USE AND/OR PUBLICATION OF DATA STATEMENTS, CONCLUSIONS OR ABSTRACTS FROM OR REWARDING OUR REPORTS AND DRAWINGS IS RESERVED PENDING OUR WRITTEN APPROVAL.

CLIENT

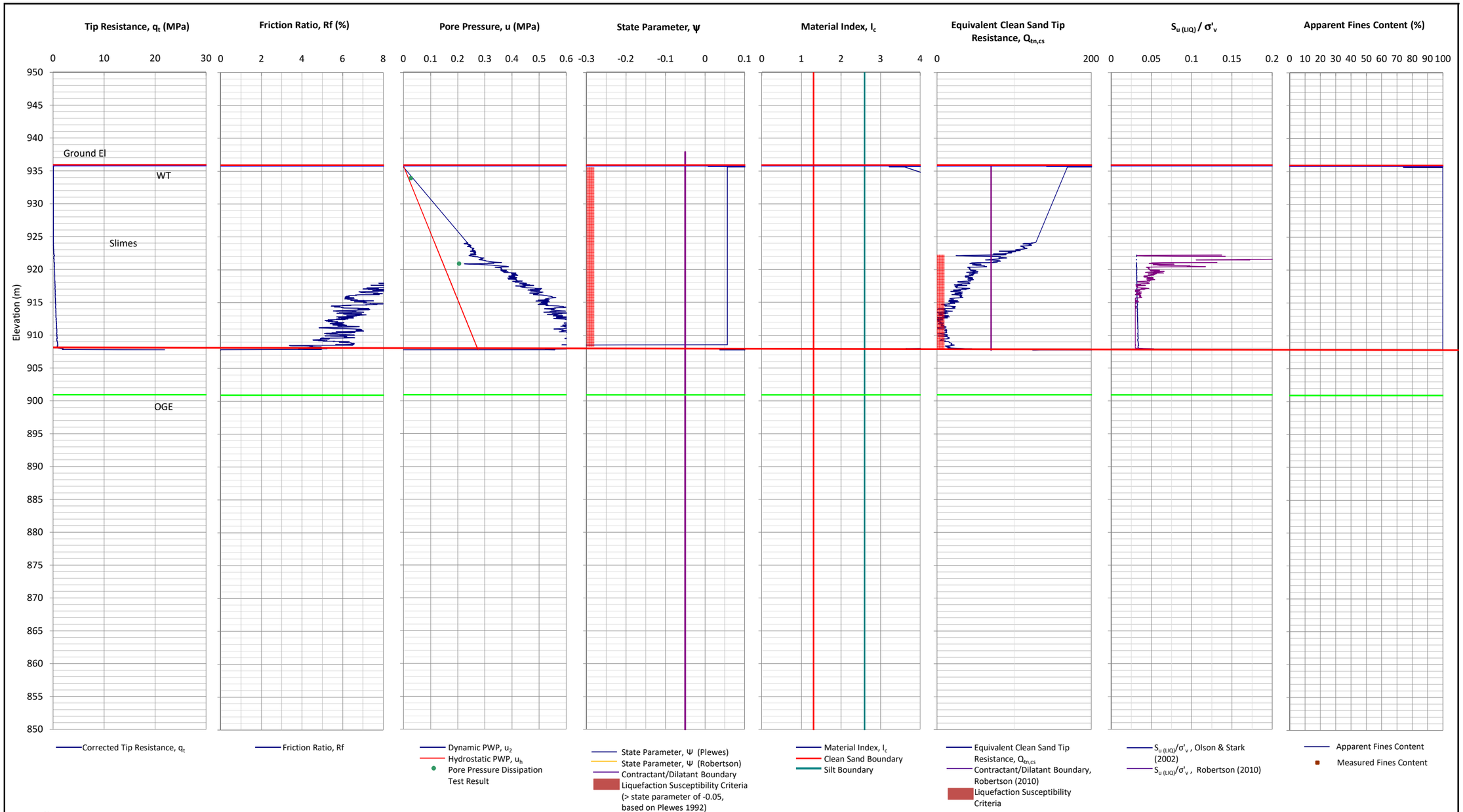
PROJECT: REPORT OF THE EXPERT PANEL ON THE TECHNICAL CAUSES OF THE FAILURE OF FEIJÃO DAM 1

TITLE: CONE PENETRATION TEST B1-CPTU-01_R1

N:7775132.1 E:592215.4 30-Oct-2018

PROJECT NO.: A03355A01

FIGURE NO.: 23



Notes:

1. This interpretation is based on the water and soil saturated unit weights γ_w=9.807 kN/m^3, and respective γ_{sat} for each geological unit.
2. The friction ratio Rf is calculated as Rf=f_s/q_t.
3. The hydrostatic pore pressure is calculated using the ground water level (GWL) determined from CPT pore pressure dissipation tests (where available) or dynamic pore pressure.
4. Soil boundary layers (where plotted) are based on KCB interpretation from adjacent borehole logs.
5. The data presented have been plotted to the axis limits. Data may exist beyond the axis limits shown.
6. The Material Index (I_c) boundaries are based on Robertson and Wride (1998).
7. The $Q_{tn,cs}$ contractant/dilatant boundary=70 and is based on Robertson (2010).
8. The State Parameter (Ψ) is calculated using Plewes, et al. (1992) assuming a K0 of 0.5, and Robertson et al. (2010).

AS A MUTUAL PROTECTION TO OUR CLIENT, THE PUBLIC AND OURSELVES, ALL REPORTS AND DRAWINGS ARE SUBMITTED FOR THE CONFIDENTIAL INFORMATION OF OUR CLIENT FOR A SPECIFIC PROJECT AND AUTHORIZATION FOR USE AND/OR PUBLICATION OF DATA STATEMENTS, CONCLUSIONS OR ABSTRACTS FROM OR REWARDING OUR REPORTS AND DRAWINGS IS RESERVED PENDING OUR WRITTEN APPROVAL.

CLIENT

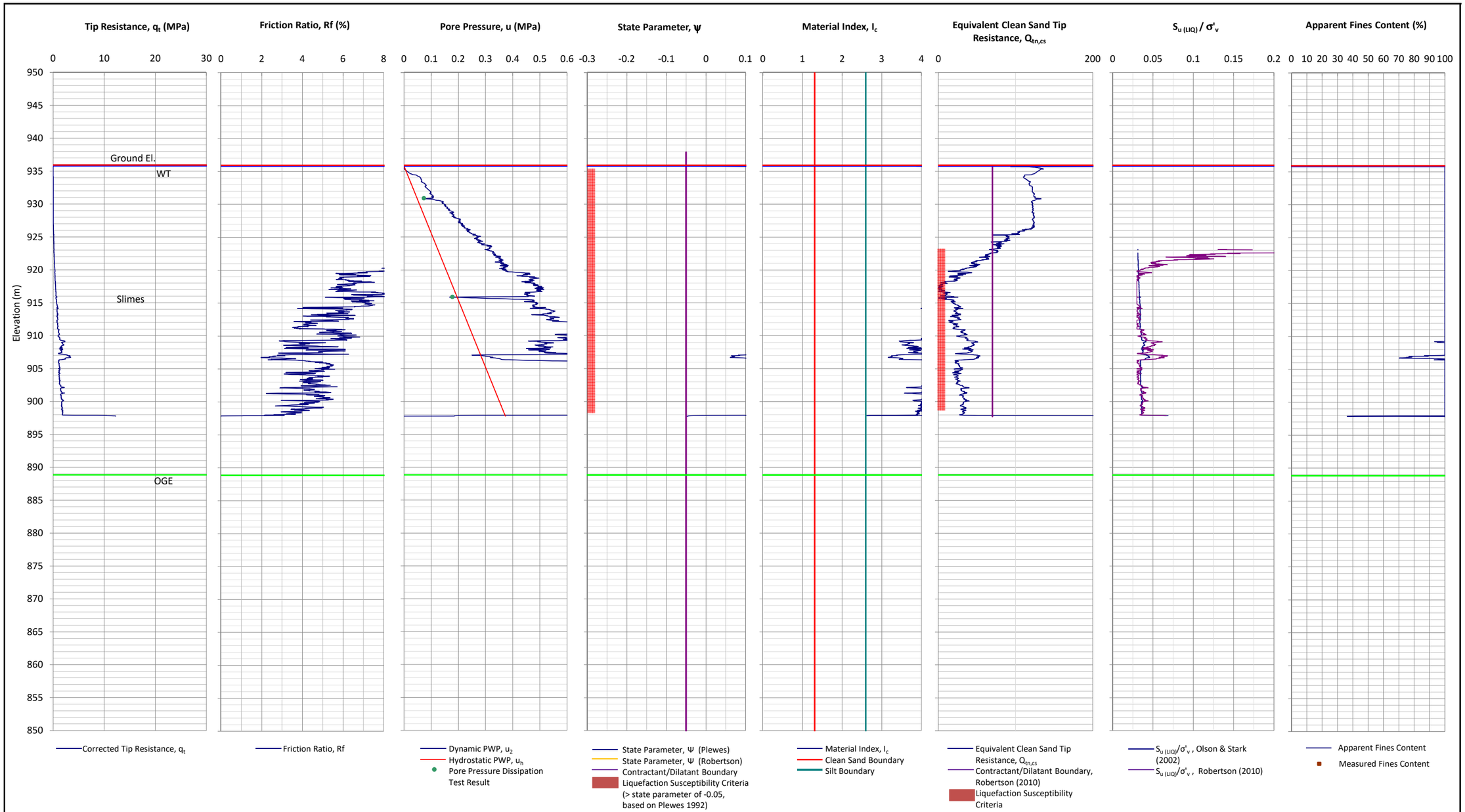
PROJECT: REPORT OF THE EXPERT PANEL ON THE TECHNICAL CAUSES OF THE FAILURE OF FEIJÃO DAM 1

TITLE: CONE PENETRATION TEST B1-CPTU-02M

N:7775204.4 E:592346.8 25th October 2018

PROJECT NO.: A03355A01

FIGURE NO.: 24



Notes:

1. This interpretation is based on the water and soil saturated unit weights γ_w=9.807 kN/m^3, and respective γ_{sat} for each geological unit.
2. The friction ratio Rf is calculated as Rf=f_s/q_t.
3. The hydrostatic pore pressure is calculated using the ground water level (GWL) determined from CPT pore pressure dissipation tests (where available) or dynamic pore pressure.
4. Soil boundary layers (where plotted) are based on KCB interpretation from adjacent borehole logs.
5. The data presented have been plotted to the axis limits. Data may exist beyond the axis limits shown.
6. The Material Index (I_c) boundaries are based on Robertson and Wride (1998).
7. The $Q_{tn,cs}$ contractant/dilatant boundary=70 and is based on Robertson (2010).
8. The State Parameter (Ψ) is calculated using Plewes, et al. (1992) assuming a K0 of 0.5, and Robertson et al. (2010).

AS A MUTUAL PROTECTION TO OUR CLIENT, THE PUBLIC AND OURSELVES, ALL REPORTS AND DRAWINGS ARE SUBMITTED FOR THE CONFIDENTIAL INFORMATION OF OUR CLIENT FOR A SPECIFIC PROJECT AND AUTHORIZATION FOR USE AND/OR PUBLICATION OF DATA STATEMENTS, CONCLUSIONS OR ABSTRACTS FROM OR REWARDING OUR REPORTS AND DRAWINGS IS RESERVED PENDING OUR WRITTEN APPROVAL.

CLIENT

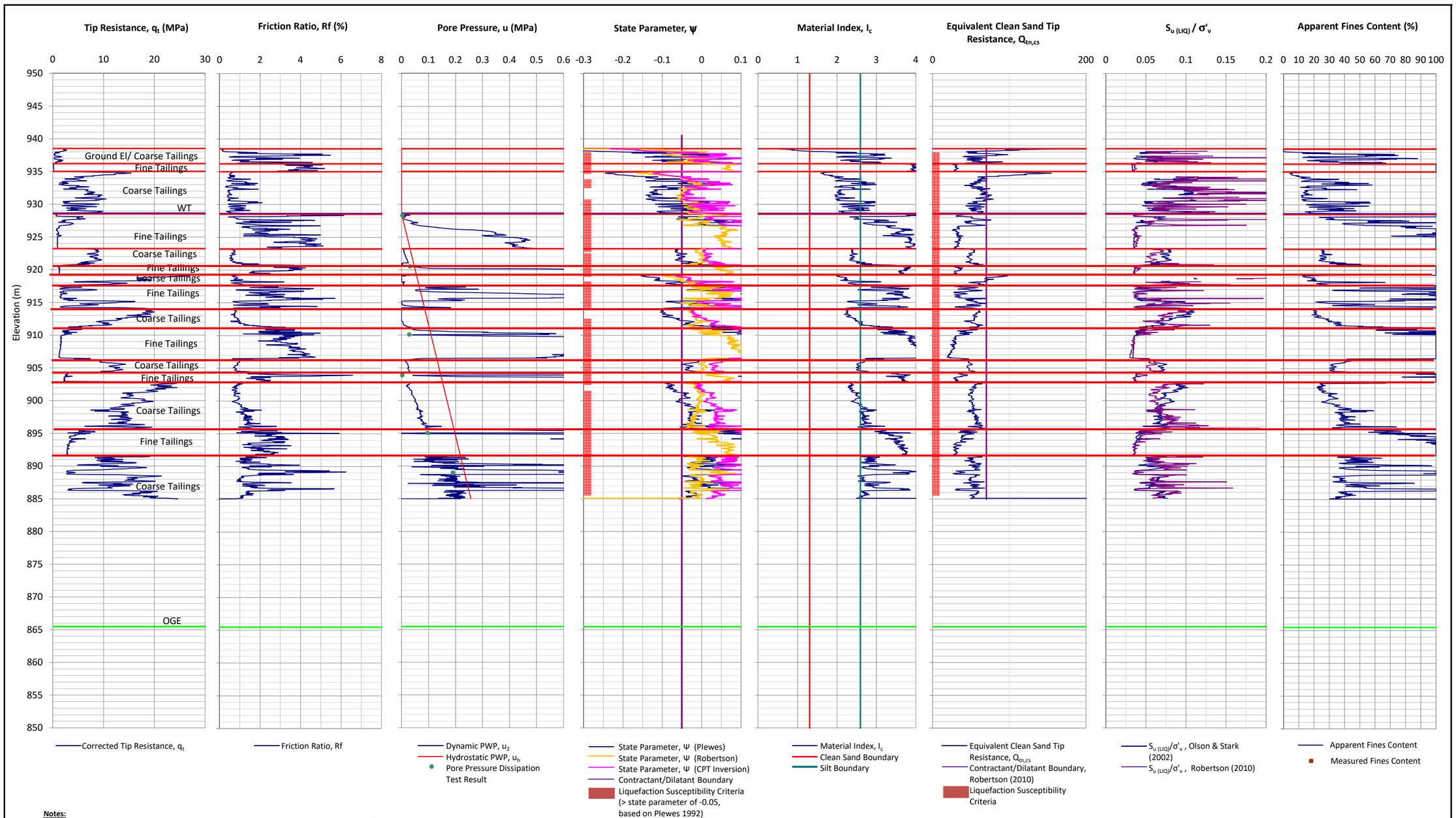
PROJECT: REPORT OF THE EXPERT PANEL ON THE TECHNICAL CAUSES OF THE FAILURE OF FEIJÃO DAM 1

TITLE: CONE PENETRATION TEST B1-CPTU-03_R1

N:7775253.7 E:592234.1 29-Oct-2018

PROJECT NO.: A03355A01

FIGURE NO.: 25



Notes:

1. This interpretation is based on the water and soil saturated unit weights γ_w=9.807 kN/m^3, and respective γ_{sat} for each geological unit.
2. The friction ratio Rf is calculated as Rf=f_s/q_t.
3. The hydrostatic pore pressure is calculated using the ground water level (GWL) determined from CPT pore pressure dissipation tests (where available) or dynamic pore pressure.
4. Soil boundary layers (where plotted) are based on KCB interpretation from adjacent borehole logs.
5. The data presented have been plotted to the axis limits. Data may exist beyond the axis limits shown.
6. The Material Index (I_c) boundaries are based on Robertson and Wride (1998).
7. The $Q_{tn,cs}$ contractant/dilatant boundary=70 and is based on Robertson (2010).
8. The State Parameter (Ψ) calculated using Plewes, et al. (1992) and the CPT inversion method is based on an assumed K0 of 0.5.

AS A MUTUAL PROTECTION TO OUR CLIENT, THE PUBLIC AND OURSELVES, ALL REPORTS AND DRAWINGS ARE SUBMITTED FOR THE CONFIDENTIAL INFORMATION OF OUR CLIENT FOR A SPECIFIC PROJECT AND AUTHORIZATION FOR USE AND/OR PUBLICATION OF DATA STATEMENTS, CONCLUSIONS OR ABSTRACTS FROM OR REWARDING OUR REPORTS AND DRAWINGS IS RESERVED PENDING OUR WRITTEN APPROVAL.

CLIENT

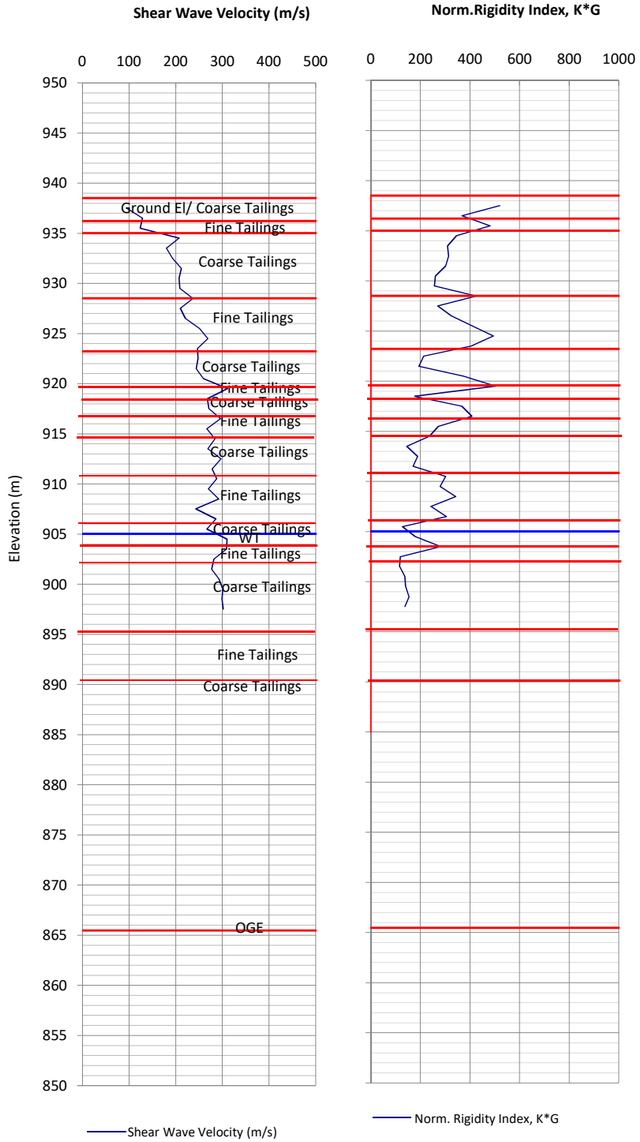
PROJECT: REPORT OF THE EXPERT PANEL ON THE TECHNICAL CAUSES OF THE FAILURE OF FEIJÃO DAM 1

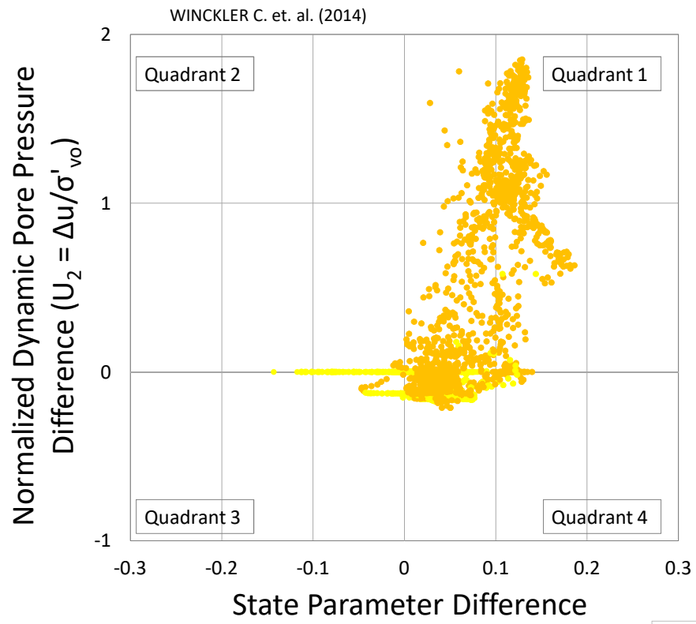
TITLE: CONE PENETRATION TEST CPTU-PZE-1-7-R1

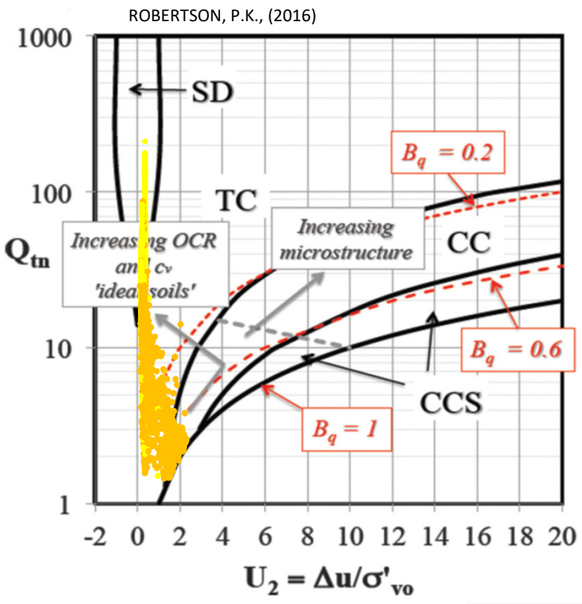
N:7775096 E:591994.9 08/10/2018

PROJECT NO.: A03355A01

FIGURE NO.: 26

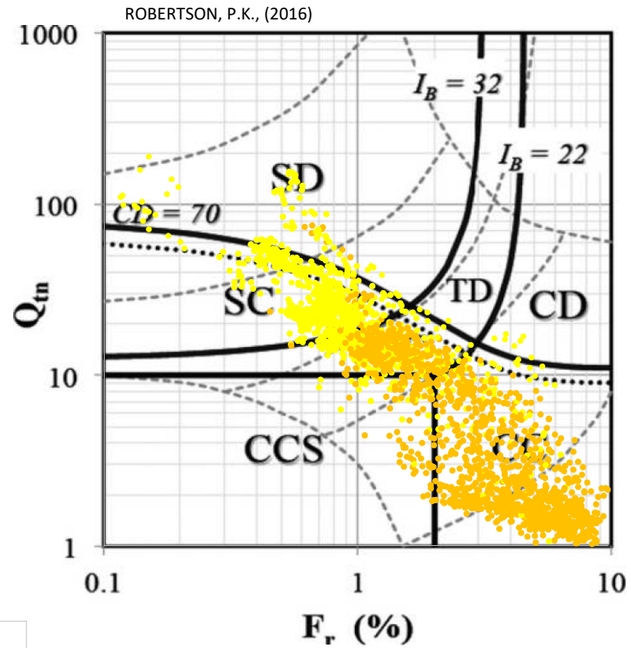


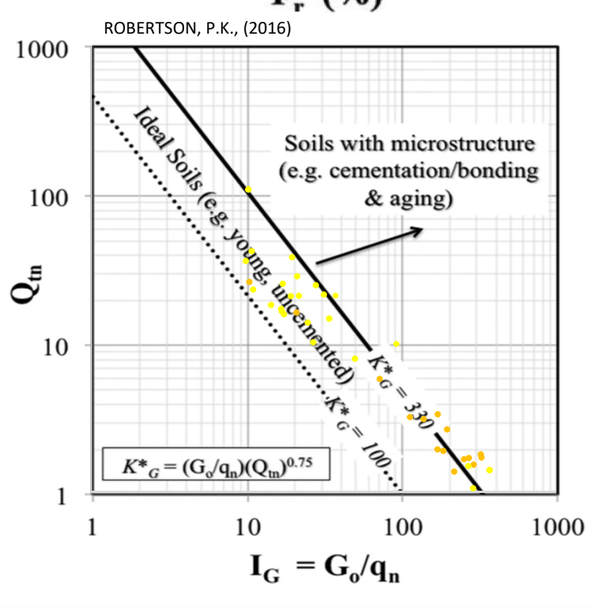




Fine Tailings

Coarse Tailings





Notes:

1. This interpretation is based on the water and soil saturated unit weights γ_w=9.807 kN/m^3, and respective γ_{sat} for each geological unit.
2. The hydrostatic pore pressure is calculated using the ground water level (GWL) determined from CPT pore pressure dissipation tests (where available).
3. Soil boundary layers (where plotted) are based on KCB interpretation from adjacent borehole logs.
4. The data presented have been plotted to the axis limits. Data may exist beyond the axis limits shown.

AS A MUTUAL PROTECTION TO OUR CLIENT, THE PUBLIC AND OURSELVES, ALL REPORTS AND DRAWINGS ARE SUBMITTED FOR THE CONFIDENTIAL INFORMATION OF OUR CLIENT FOR A SPECIFIC PROJECT AND AUTHORIZATION FOR USE AND/OR PUBLICATION OF DATA STATEMENTS, CONCLUSIONS OR ABSTRACTS FROM OR REWARDING OUR REPORTS AND DRAWINGS IS RESERVED PENDING OUR WRITTEN APPROVAL.

CLIENT

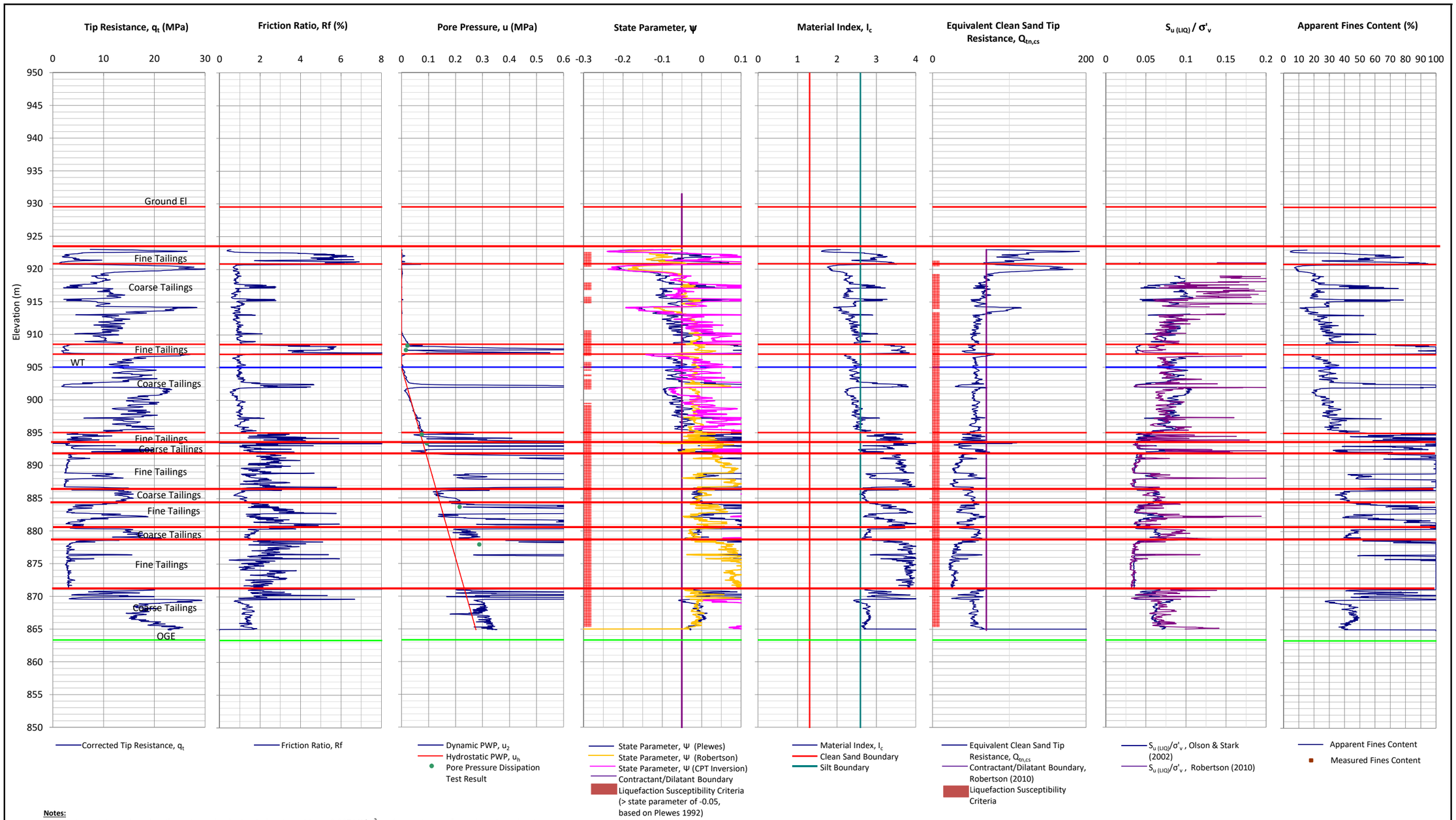
PROJECT: REPORT OF THE EXPERT PANEL ON THE TECHNICAL CAUSES OF THE FAILURE OF FEIJÃO DAM 1

TITLE: V_s/CPT Additional Plots for CPTU-PZE-1-7-R1

N:7775096 E:591994.9 08/10/2018

PROJECT NO.: A03355A01

FIGURE NO.: 27



Notes:

1. This interpretation is based on the water and soil saturated unit weights γ_w=9.807 kN/m^3, and respective γ_{sat} for each geological unit.
2. The friction ratio Rf is calculated as Rf=f_s/q_t.
3. The hydrostatic pore pressure is calculated using the ground water level (GWL) determined from CPT pore pressure dissipation tests (where available) or dynamic pore pressure.
4. Soil boundary layers (where plotted) are based on KCB interpretation from adjacent borehole logs.
5. The data presented have been plotted to the axis limits. Data may exist beyond the axis limits shown.
6. The Material Index (I_c) boundaries are based on Robertson and Wride (1998).
7. The $Q_{tn,cs}$ contractant/dilatant boundary=70 and is based on Robertson (2010).
8. The State Parameter (Ψ) calculated using Plewes, et al. (1992) and the CPT inversion method is based on an assumed K0 of 0.5.

AS A MUTUAL PROTECTION TO OUR CLIENT, THE PUBLIC AND OURSELVES, ALL REPORTS AND DRAWINGS ARE SUBMITTED FOR THE CONFIDENTIAL INFORMATION OF OUR CLIENT FOR A SPECIFIC PROJECT AND AUTHORIZATION FOR USE AND/OR PUBLICATION OF DATA STATEMENTS, CONCLUSIONS OR ABSTRACTS FROM OR REWARDING OUR REPORTS AND DRAWINGS IS RESERVED PENDING OUR WRITTEN APPROVAL.

CLIENT

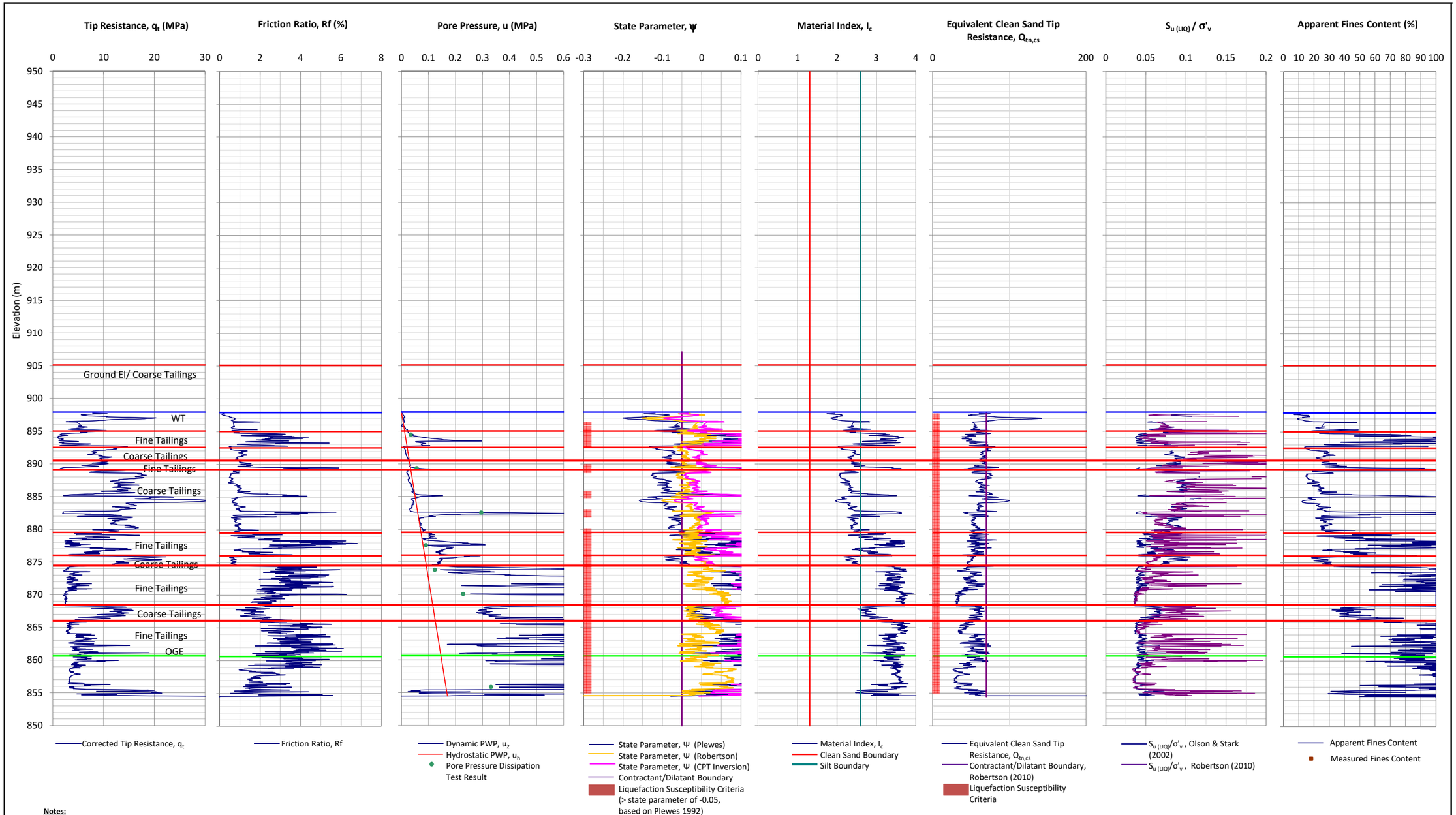
PROJECT: REPORT OF THE EXPERT PANEL ON THE TECHNICAL CAUSES OF THE FAILURE OF FEIJÃO DAM 1

TITLE: CONE PENETRATION TEST CPTU-PZE-09-14N_Updated

N:7775056.4 E:591924.3 2018-October-04

PROJECT NO.: A03355A01

FIGURE NO.: 28



Notes:

1. This interpretation is based on the water and soil saturated unit weights γ_w=9.807 kN/m^3, and respective γ_{sat} for each geological unit.
2. The friction ratio Rf is calculated as Rf=f_s/q_t.
3. The hydrostatic pore pressure is calculated using the ground water level (GWL) determined from CPT pore pressure dissipation tests (where available) or dynamic pore pressure.
4. Soil boundary layers (where plotted) are based on KCB interpretation from adjacent borehole logs.
5. The data presented have been plotted to the axis limits. Data may exist beyond the axis limits shown.
6. The Material Index (I_c) boundaries are based on Robertson and Wride (1998).
7. The $Q_{tn,cs}$ contractant/dilatant boundary=70 and is based on Robertson (2010).
8. The State Parameter (Ψ) calculated using Plewes, et al. (1992) and the CPT inversion method is based on an assumed K0 of 0.5.

AS A MUTUAL PROTECTION TO OUR CLIENT, THE PUBLIC AND OURSELVES, ALL REPORTS AND DRAWINGS ARE SUBMITTED FOR THE CONFIDENTIAL INFORMATION OF OUR CLIENT FOR A SPECIFIC PROJECT AND AUTHORIZATION FOR USE AND/OR PUBLICATION OF DATA STATEMENTS, CONCLUSIONS OR ABSTRACTS FROM OR REWARDING OUR REPORTS AND DRAWINGS IS RESERVED PENDING OUR WRITTEN APPROVAL.

CLIENT

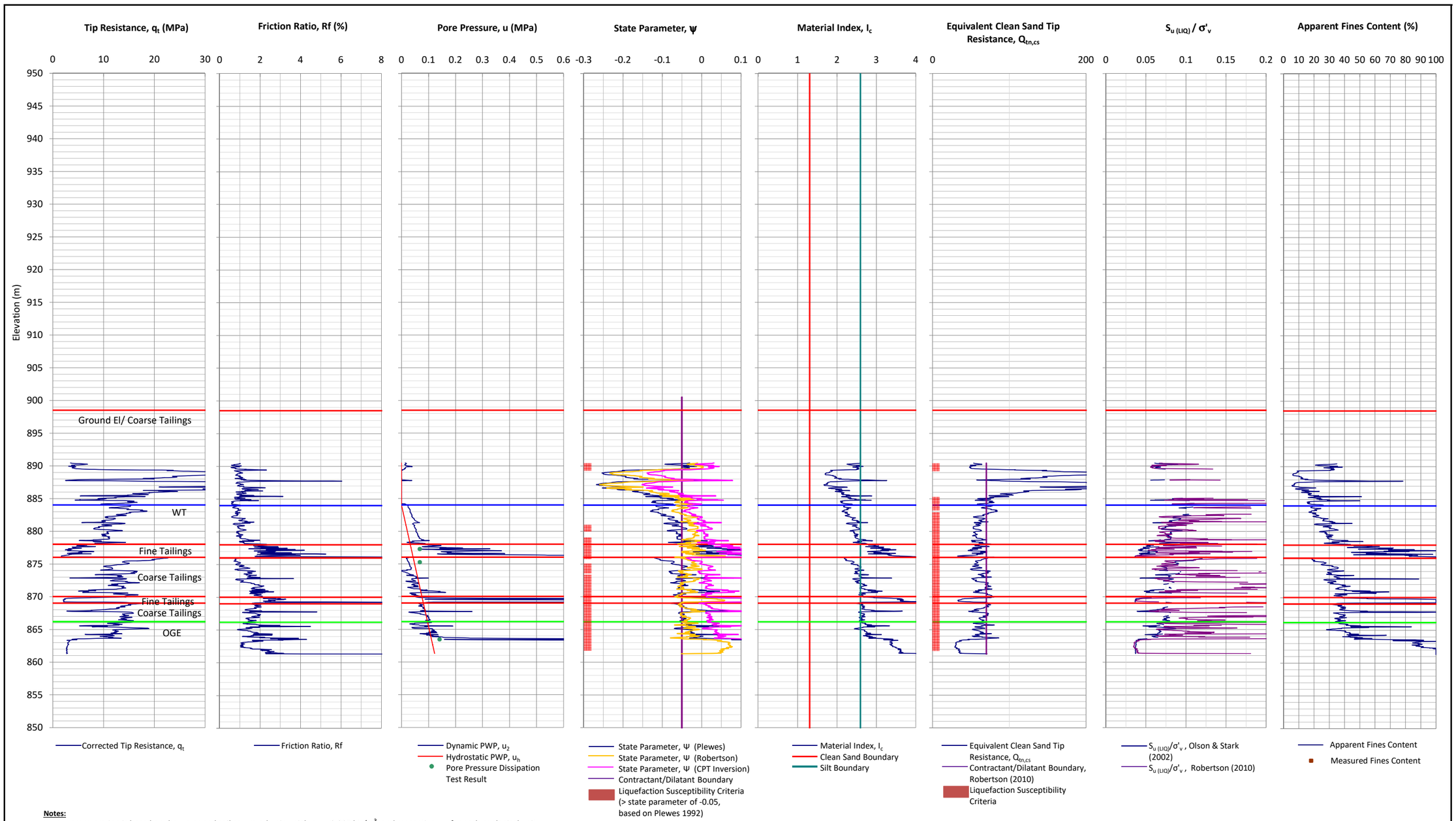
PROJECT: REPORT OF THE EXPERT PANEL ON THE TECHNICAL CAUSES OF THE FAILURE OF FEIJÃO DAM 1

TITLE: CONE PENETRATION TEST CPTU-PZE-15-19N_R1

N:7775018.9 E:591856.5 10/01/2018

PROJECT NO.: A03355A01

FIGURE NO.: 29



Notes:

1. This interpretation is based on the water and soil saturated unit weights γ_w=9.807 kN/m^3, and respective γ_{sat} for each geological unit.
2. The friction ratio Rf is calculated as Rf=f_s/q_t.
3. The hydrostatic pore pressure is calculated using the ground water level (GWL) determined from CPT pore pressure dissipation tests (where available) or dynamic pore pressure.
4. Soil boundary layers (where plotted) are based on KCB interpretation from adjacent borehole logs.
5. The data presented have been plotted to the axis limits. Data may exist beyond the axis limits shown.
6. The Material Index (I_c) boundaries are based on Robertson and Wride (1998).
7. The $Q_{tn,cs}$ contractant/dilatant boundary=70 and is based on Robertson (2010).
8. The State Parameter (Ψ) calculated using Plewes, et al. (1992) and the CPT inversion method is based on an assumed K0 of 0.5.

AS A MUTUAL PROTECTION TO OUR CLIENT, THE PUBLIC AND OURSELVES, ALL REPORTS AND DRAWINGS ARE SUBMITTED FOR THE CONFIDENTIAL INFORMATION OF OUR CLIENT FOR A SPECIFIC PROJECT AND AUTHORIZATION FOR USE AND/OR PUBLICATION OF DATA STATEMENTS, CONCLUSIONS OR ABSTRACTS FROM OR REWARDING OUR REPORTS AND DRAWINGS IS RESERVED PENDING OUR WRITTEN APPROVAL.

CLIENT

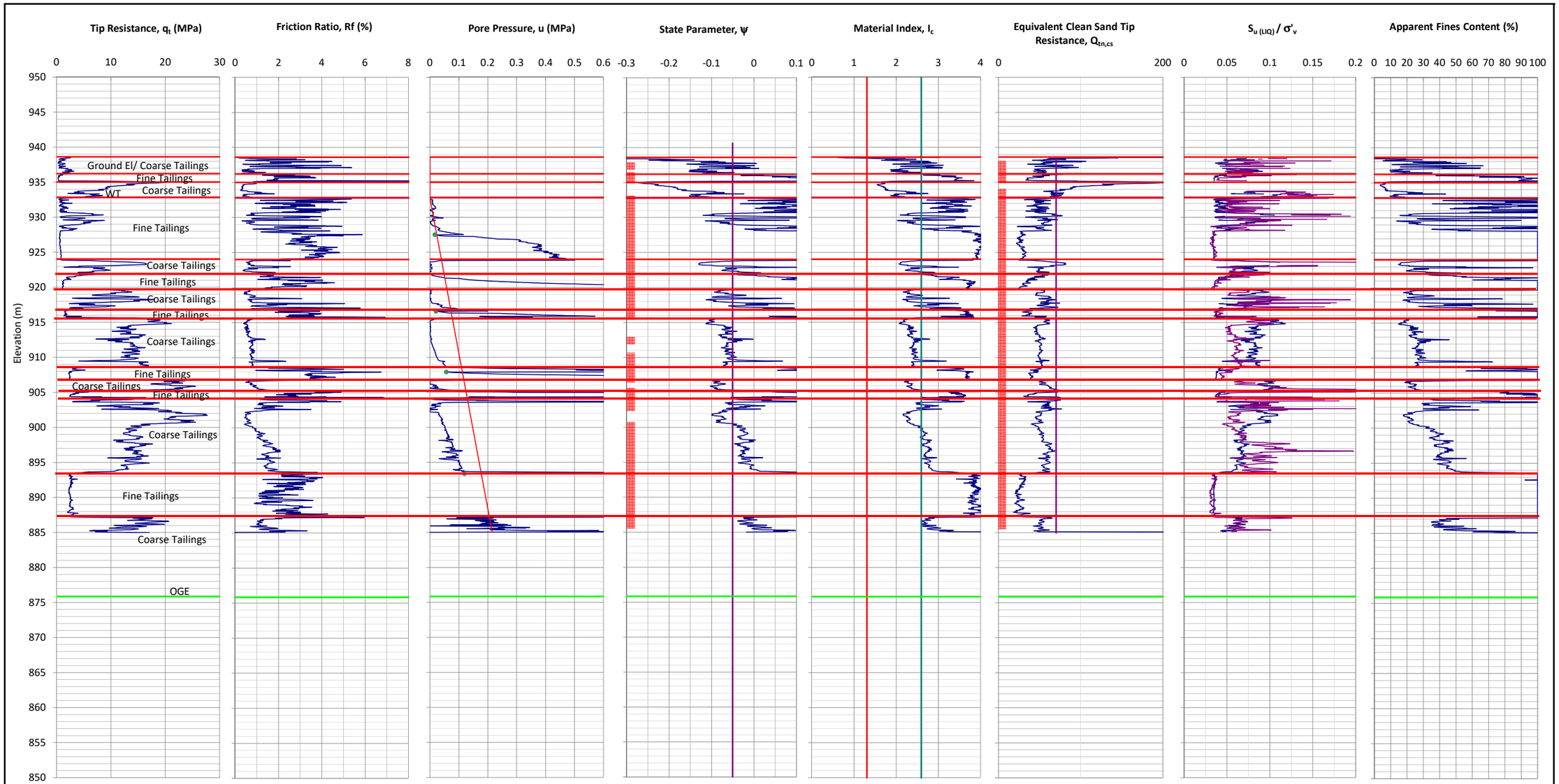
PROJECT: REPORT OF THE EXPERT PANEL ON THE TECHNICAL CAUSES OF THE FAILURE OF FEIJÃO DAM 1

TITLE: CONE PENETRATION TEST CPTU-PZE-20-22N-R1

N:7775010.7 E:591789.6 11/10/2018

PROJECT NO.: A03355A01

FIGURE NO.: 30



Notes:

1. This interpretation is based on the water and soil saturated unit weights γ_w=9.807 kN/m^3, and respective γ_{sat} for each geological unit.
2. The friction ratio Rf is calculated as Rf=f_s/q_t.
3. The hydrostatic pore pressure is calculated using the ground water level (GWL) determined from CPT pore pressure dissipation tests (where available) or dynamic pore pressure.
4. Soil boundary layers (where plotted) are based on KCB interpretation from adjacent borehole logs.
5. The data presented have been plotted to the axis limits. Data may exist beyond the axis limits shown.
6. The Material Index (I_c) boundaries are based on Robertson and Wride (1998).
7. The $Q_{tn,cs}$ contractant/dilatant boundary=70 and is based on Robertson (2010).
8. The State Parameter (Ψ) calculated using Plewes, et al. (1992) and the CPT inversion method is based on an assumed K0 of 0.5.

AS A MUTUAL PROTECTION TO OUR CLIENT, THE PUBLIC AND OURSELVES, ALL REPORTS AND DRAWINGS ARE SUBMITTED FOR THE CONFIDENTIAL INFORMATION OF OUR CLIENT FOR A SPECIFIC PROJECT AND AUTHORIZATION FOR USE AND/OR PUBLICATION OF DATA STATEMENTS, CONCLUSIONS OR ABSTRACTS FROM OR REWARDING OUR REPORTS AND DRAWINGS IS RESERVED PENDING OUR WRITTEN APPROVAL.

CLIENT

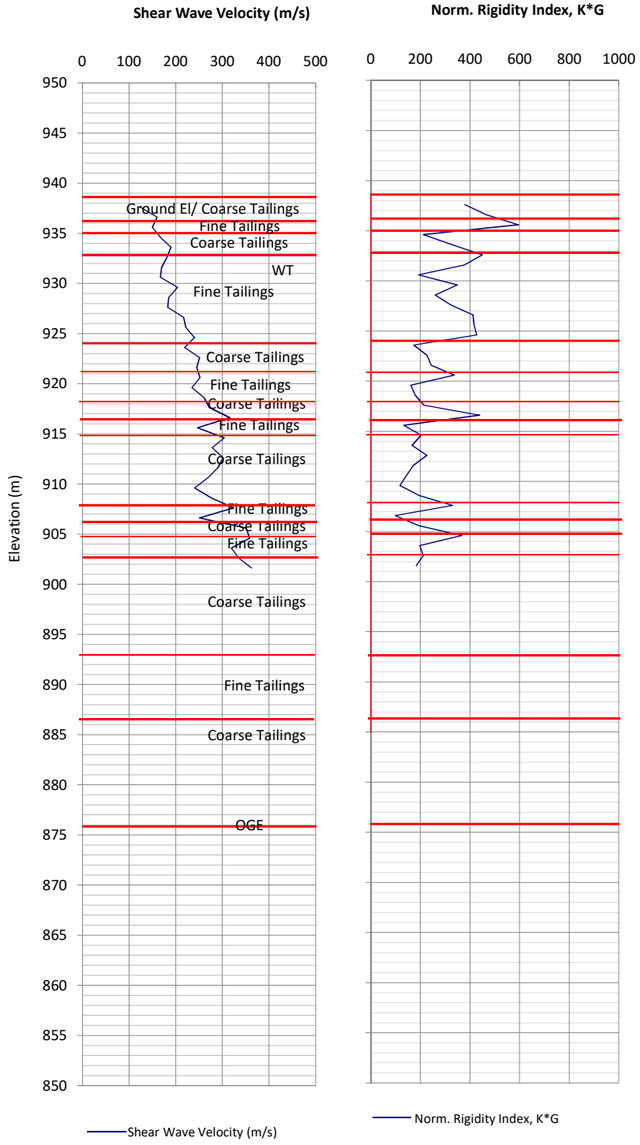
PROJECT: REPORT OF THE EXPERT PANEL ON THE TECHNICAL CAUSES OF THE FAILURE OF FEIJÃO DAM 1

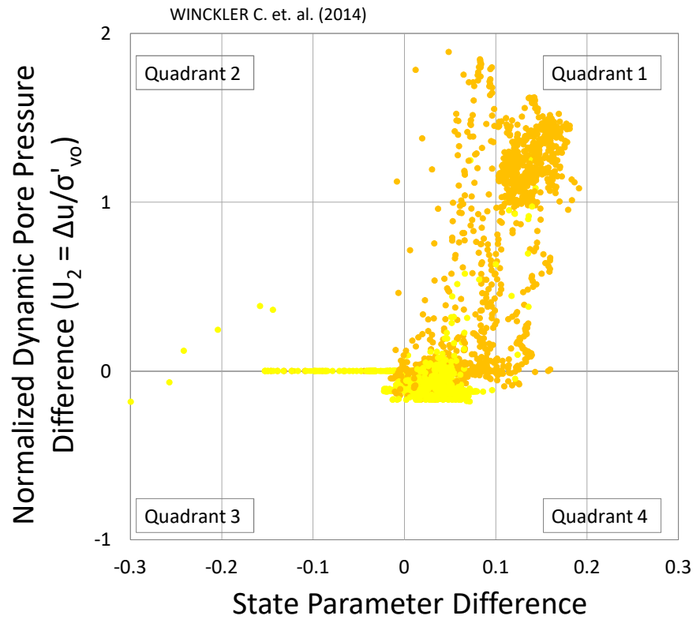
TITLE: CONE PENETRATION TEST CPTU-PZE-23-28N_R1

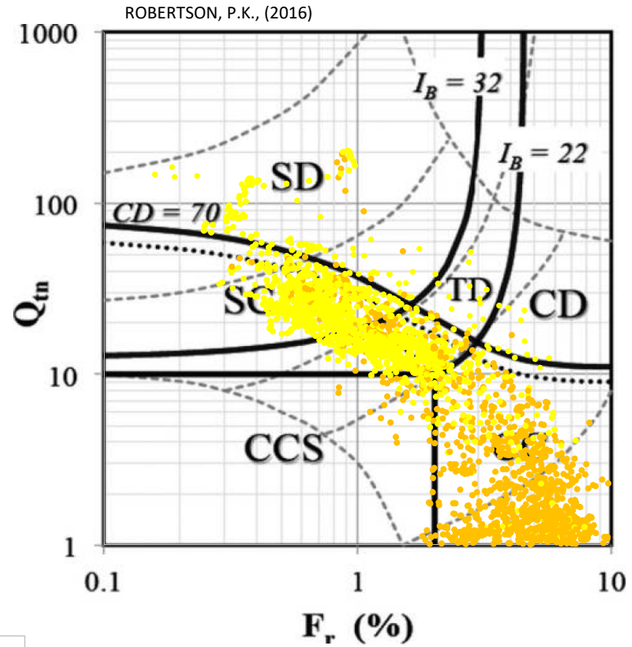
N:7775031 E:592032.5 10/11/2018

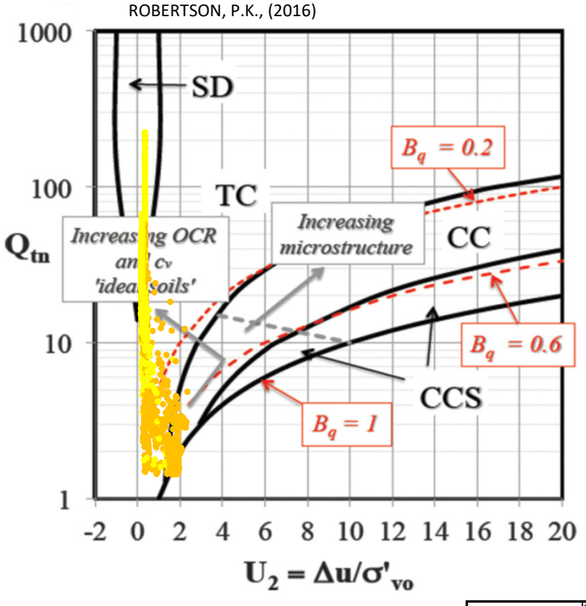
PROJECT NO.: A03355A01

FIGURE NO.: 31



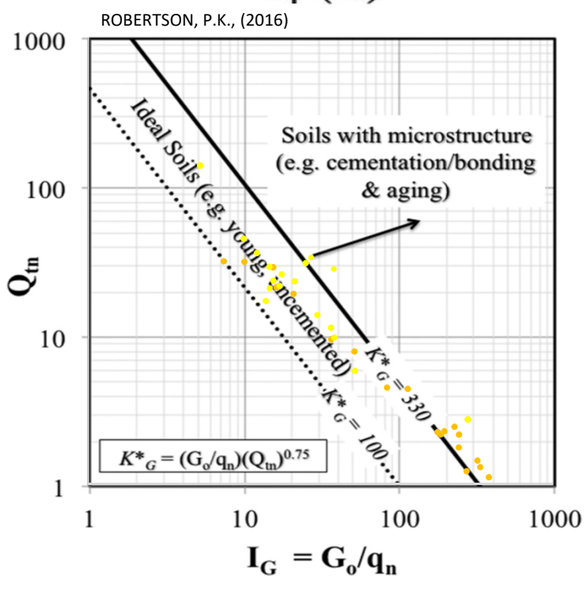






Fine Tailings

Coarse Tailings



Notes:

1. This interpretation is based on the water and soil saturated unit weights γ_w=9.807 kN/m^3, and respective γ_{sat} for each geological unit.
2. The hydrostatic pore pressure is calculated using the ground water level (GWL) determined from CPT pore pressure dissipation tests (where available).
3. Soil boundary layers (where plotted) are based on KCB interpretation from adjacent borehole logs.
4. The data presented have been plotted to the axis limits. Data may exist beyond the axis limits shown.

AS A MUTUAL PROTECTION TO OUR CLIENT, THE PUBLIC AND OURSELVES, ALL REPORTS AND DRAWINGS ARE SUBMITTED FOR THE CONFIDENTIAL INFORMATION OF OUR CLIENT FOR A SPECIFIC PROJECT AND AUTHORIZATION FOR USE AND/OR PUBLICATION OF DATA STATEMENTS, CONCLUSIONS OR ABSTRACTS FROM OR REWARDING OUR REPORTS AND DRAWINGS IS RESERVED PENDING OUR WRITTEN APPROVAL.

CLIENT

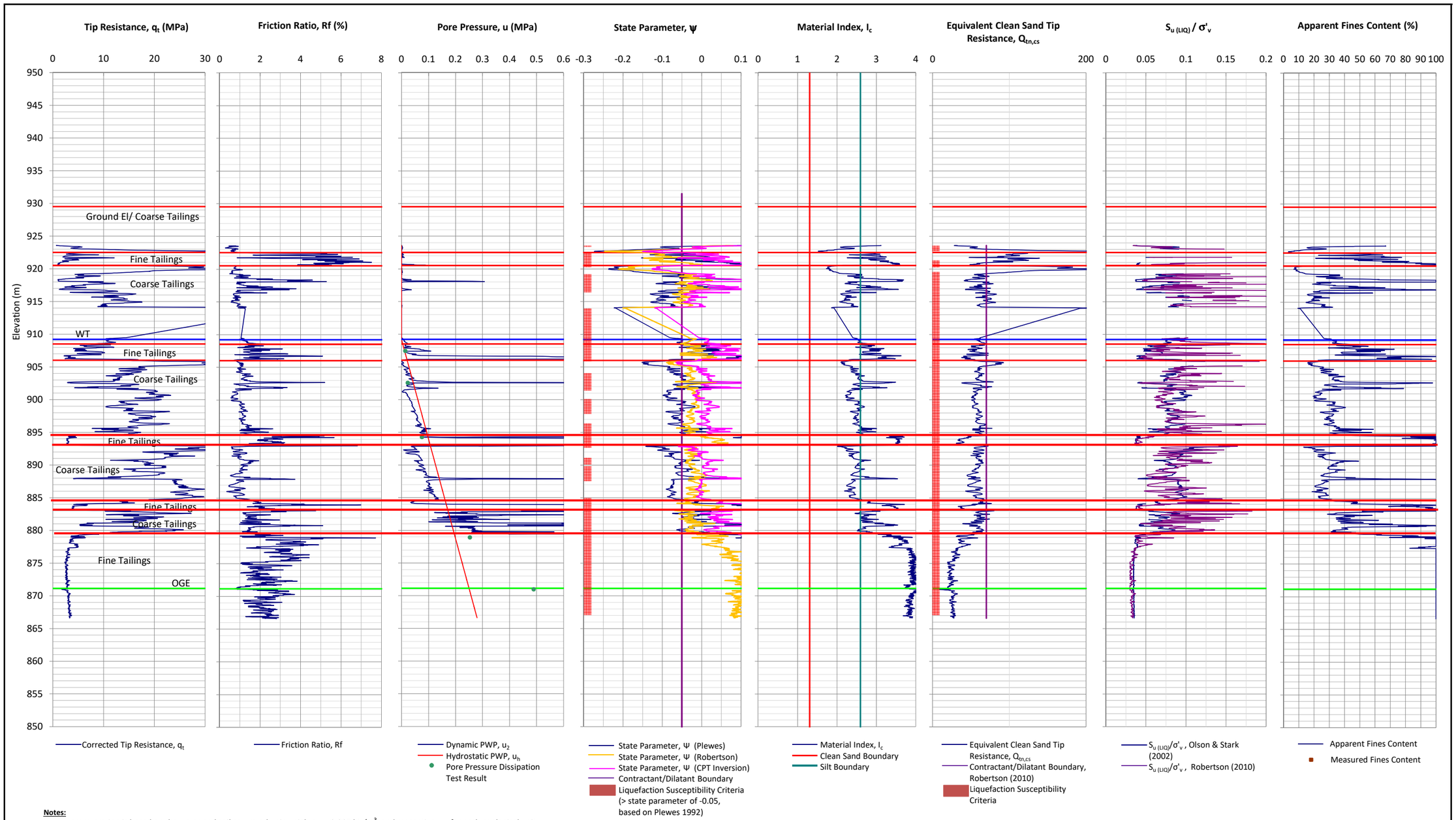
PROJECT: REPORT OF THE EXPERT PANEL ON THE TECHNICAL CAUSES OF THE FAILURE OF FEIJÃO DAM 1

TITLE: V_s/CPT Additional Plots for CPTU-PZE-23-28N_R1

N:7775031 E:592032.5 10/11/2018

PROJECT NO.: A03355A01

FIGURE NO.: 32



Notes:

1. This interpretation is based on the water and soil saturated unit weights γ_w=9.807 kN/m^3, and respective γ_{sat} for each geological unit.
2. The friction ratio Rf is calculated as Rf=f_s/q_t.
3. The hydrostatic pore pressure is calculated using the ground water level (GWL) determined from CPT pore pressure dissipation tests (where available) or dynamic pore pressure.
4. Soil boundary layers (where plotted) are based on KCB interpretation from adjacent borehole logs.
5. The data presented have been plotted to the axis limits. Data may exist beyond the axis limits shown.
6. The Material Index (I_c) boundaries are based on Robertson and Wride (1998).
7. The $Q_{tn,cs}$ contractant/dilatant boundary=70 and is based on Robertson (2010).
8. The State Parameter (Ψ) calculated using Plewes, et al. (1992) and the CPT inversion method is based on an assumed K0 of 0.5.

AS A MUTUAL PROTECTION TO OUR CLIENT, THE PUBLIC AND OURSELVES, ALL REPORTS AND DRAWINGS ARE SUBMITTED FOR THE CONFIDENTIAL INFORMATION OF OUR CLIENT FOR A SPECIFIC PROJECT AND AUTHORIZATION FOR USE AND/OR PUBLICATION OF DATA STATEMENTS, CONCLUSIONS OR ABSTRACTS FROM OR REWARDING OUR REPORTS AND DRAWINGS IS RESERVED PENDING OUR WRITTEN APPROVAL.

CLIENT

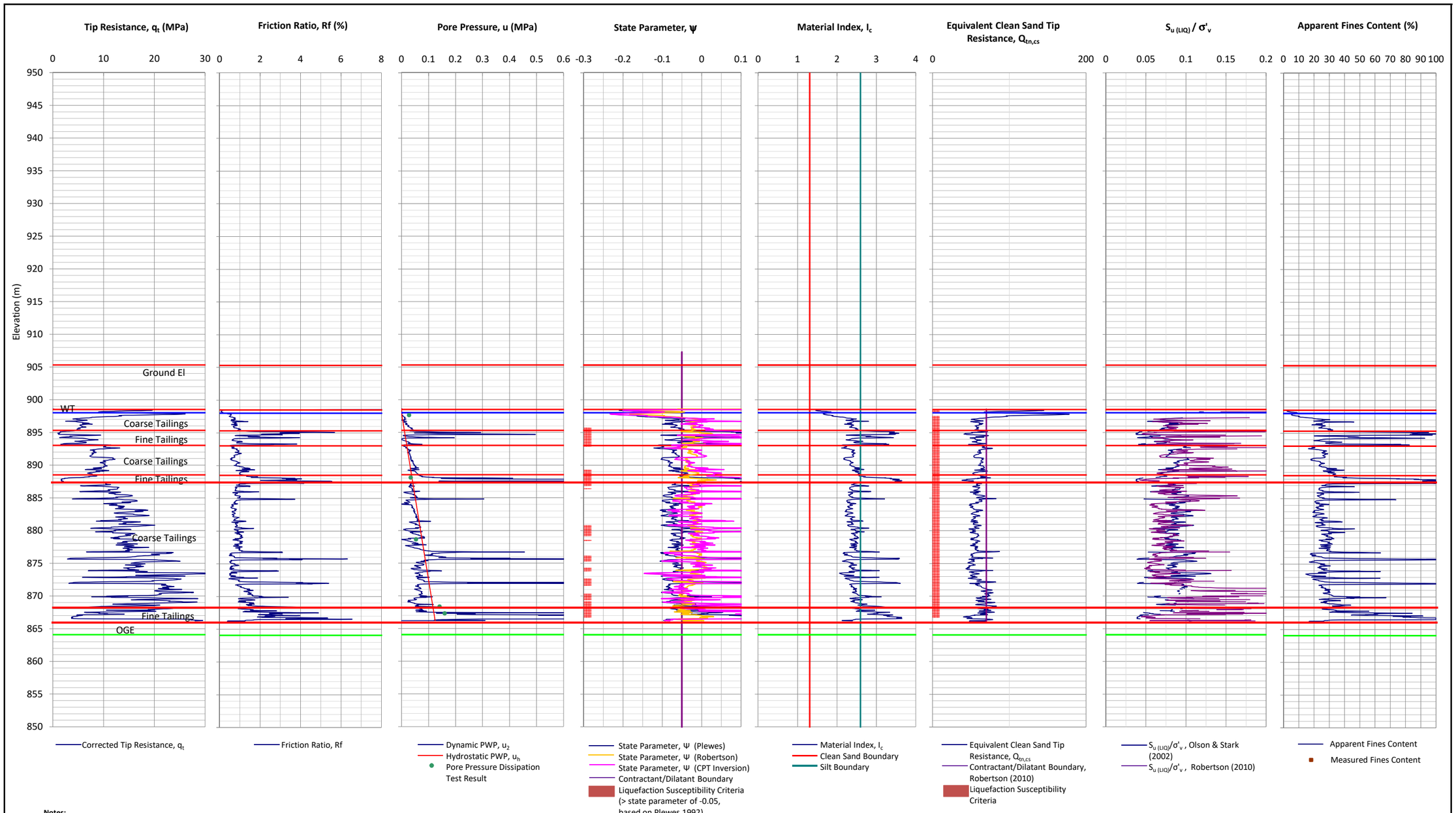
PROJECT: REPORT OF THE EXPERT PANEL ON THE TECHNICAL CAUSES OF THE FAILURE OF FEIJÃO DAM 1

TITLE: CONE PENETRATION TEST CPTU-PZE-29-35N_R1

N:7774991.8 E:591960.6 16/10/2018

PROJECT NO.: A03355A01

FIGURE NO.: 33



Notes:

1. This interpretation is based on the water and soil saturated unit weights γ_w=9.807 kN/m^3, and respective γ_{sat} for each geological unit.
2. The friction ratio Rf is calculated as Rf=f_s/q_t.
3. The hydrostatic pore pressure is calculated using the ground water level (GWL) determined from CPT pore pressure dissipation tests (where available) or dynamic pore pressure.
4. Soil boundary layers (where plotted) are based on KCB interpretation from adjacent borehole logs.
5. The data presented have been plotted to the axis limits. Data may exist beyond the axis limits shown.
6. The Material Index (I_c) boundaries are based on Robertson and Wride (1998).
7. The $Q_{tn,cs}$ contractant/dilatant boundary=70 and is based on Robertson (2010).
8. The State Parameter (Ψ) calculated using Plewes, et al. (1992) and the CPT inversion method is based on an assumed K0 of 0.5.

AS A MUTUAL PROTECTION TO OUR CLIENT, THE PUBLIC AND OURSELVES, ALL REPORTS AND DRAWINGS ARE SUBMITTED FOR THE CONFIDENTIAL INFORMATION OF OUR CLIENT FOR A SPECIFIC PROJECT AND AUTHORIZATION FOR USE AND/OR PUBLICATION OF DATA STATEMENTS, CONCLUSIONS OR ABSTRACTS FROM OR REWARDING OUR REPORTS AND DRAWINGS IS RESERVED PENDING OUR WRITTEN APPROVAL.

CLIENT

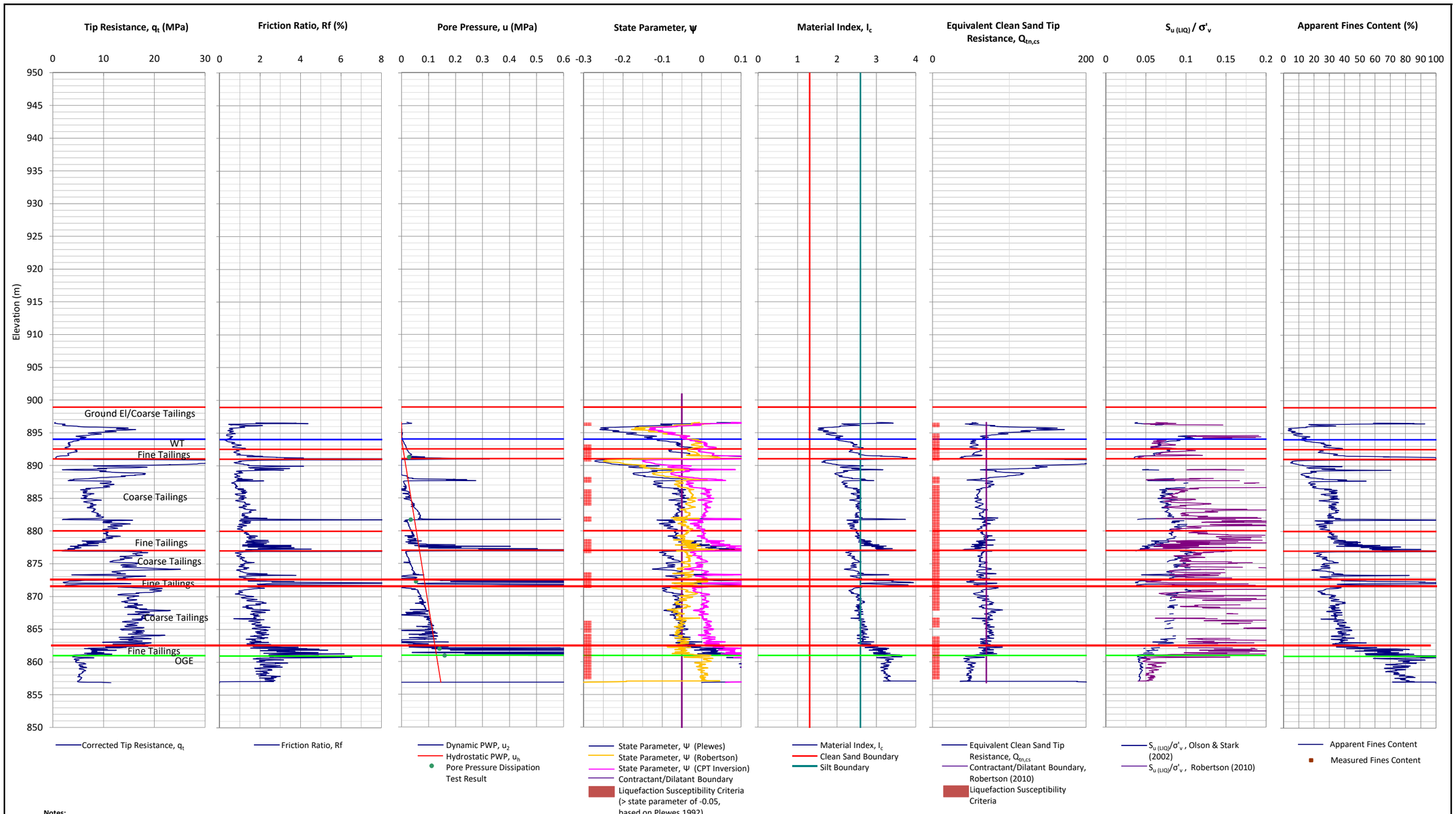
PROJECT: REPORT OF THE EXPERT PANEL ON THE TECHNICAL CAUSES OF THE FAILURE OF FEIJÃO DAM 1

TITLE: CONE PENETRATION TEST CPTU-PZE-36-40N_Updated

N:7774953.8 E:591891.7 2018-August-28

PROJECT NO.: A03355A01

FIGURE NO.: 34



Notes:

1. This interpretation is based on the water and soil saturated unit weights γ_w=9.807 kN/m^3, and respective γ_{sat} for each geological unit.
2. The friction ratio Rf is calculated as Rf=f_s/q_t.
3. The hydrostatic pore pressure is calculated using the ground water level (GWL) determined from CPT pore pressure dissipation tests (where available) or dynamic pore pressure.
4. Soil boundary layers (where plotted) are based on KCB interpretation from adjacent borehole logs.
5. The data presented have been plotted to the axis limits. Data may exist beyond the axis limits shown.
6. The Material Index (I_c) boundaries are based on Robertson and Wride (1998).
7. The $Q_{tn,cs}$ contractant/dilatant boundary=70 and is based on Robertson (2010).
8. The State Parameter (Ψ) calculated using Plewes, et al. (1992) and the CPT inversion method is based on an assumed K0 of 0.5.

AS A MUTUAL PROTECTION TO OUR CLIENT, THE PUBLIC AND OURSELVES, ALL REPORTS AND DRAWINGS ARE SUBMITTED FOR THE CONFIDENTIAL INFORMATION OF OUR CLIENT FOR A SPECIFIC PROJECT AND AUTHORIZATION FOR USE AND/OR PUBLICATION OF DATA STATEMENTS, CONCLUSIONS OR ABSTRACTS FROM OR REWARDING OUR REPORTS AND DRAWINGS IS RESERVED PENDING OUR WRITTEN APPROVAL.

CLIENT

PROJECT: REPORT OF THE EXPERT PANEL ON THE TECHNICAL CAUSES OF THE FAILURE OF FEIJÃO DAM 1

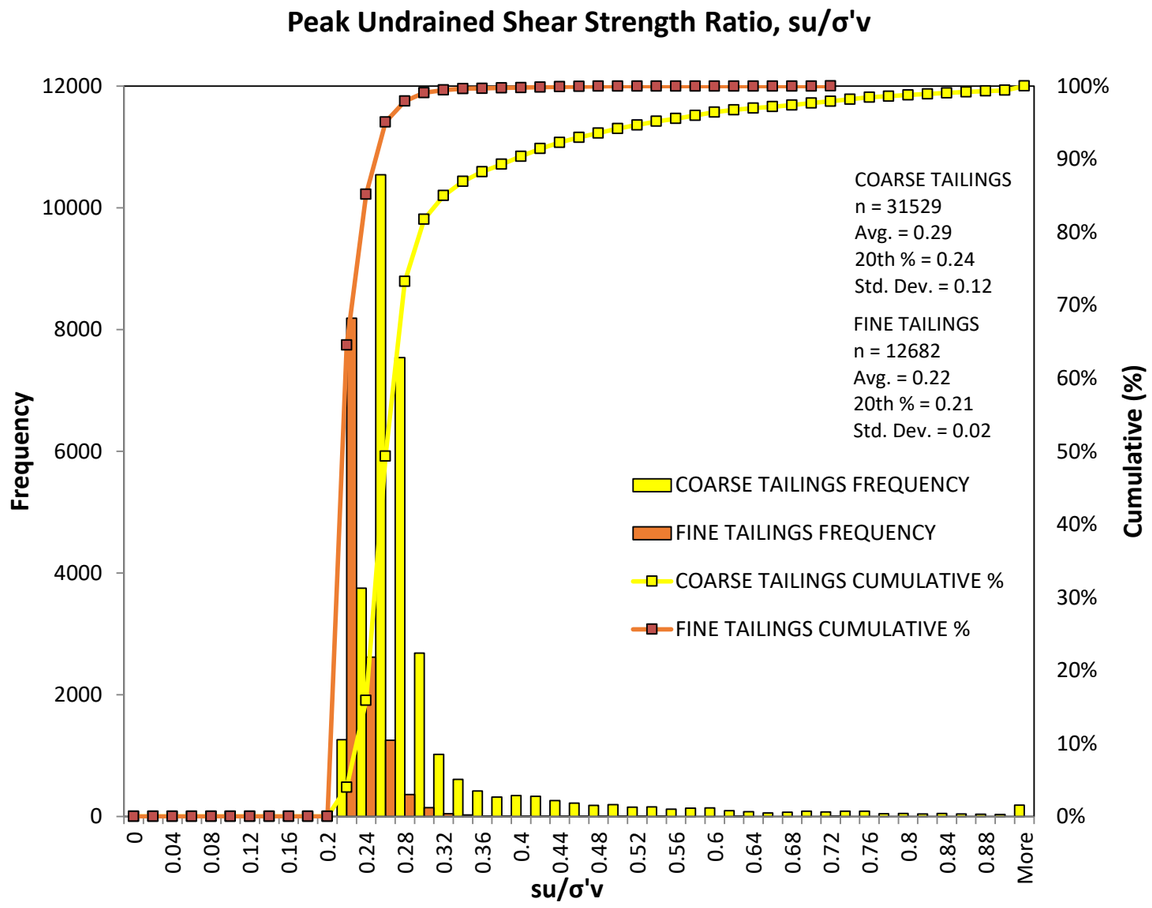
TITLE: CONE PENETRATION TEST CPTU-PZE-41-43N_R1

N:7774931.8 E:591859.6 15/10/2018

PROJECT NO.: A03355A01

FIGURE NO.: 35

Calculated Strength and State Parameter Histograms



NOTES:

AS A MUTUAL PROTECTION TO OUR CLIENT, THE PUBLIC AND OURSELVES, ALL REPORTS AND DRAWINGS ARE SUBMITTED FOR THE CONFIDENTIAL INFORMATION OF OUR CLIENT FOR A SPECIFIC PROJECT AND AUTHORIZATION FOR USE AND/OR PUBLICATION OF DATA STATEMENTS, CONCLUSIONS OR ABSTRACTS FROM OR REGARDING OUR REPORTS AND DRAWINGS IS RESERVED PENDING OUR WRITTEN APPROVAL.

CLIENT

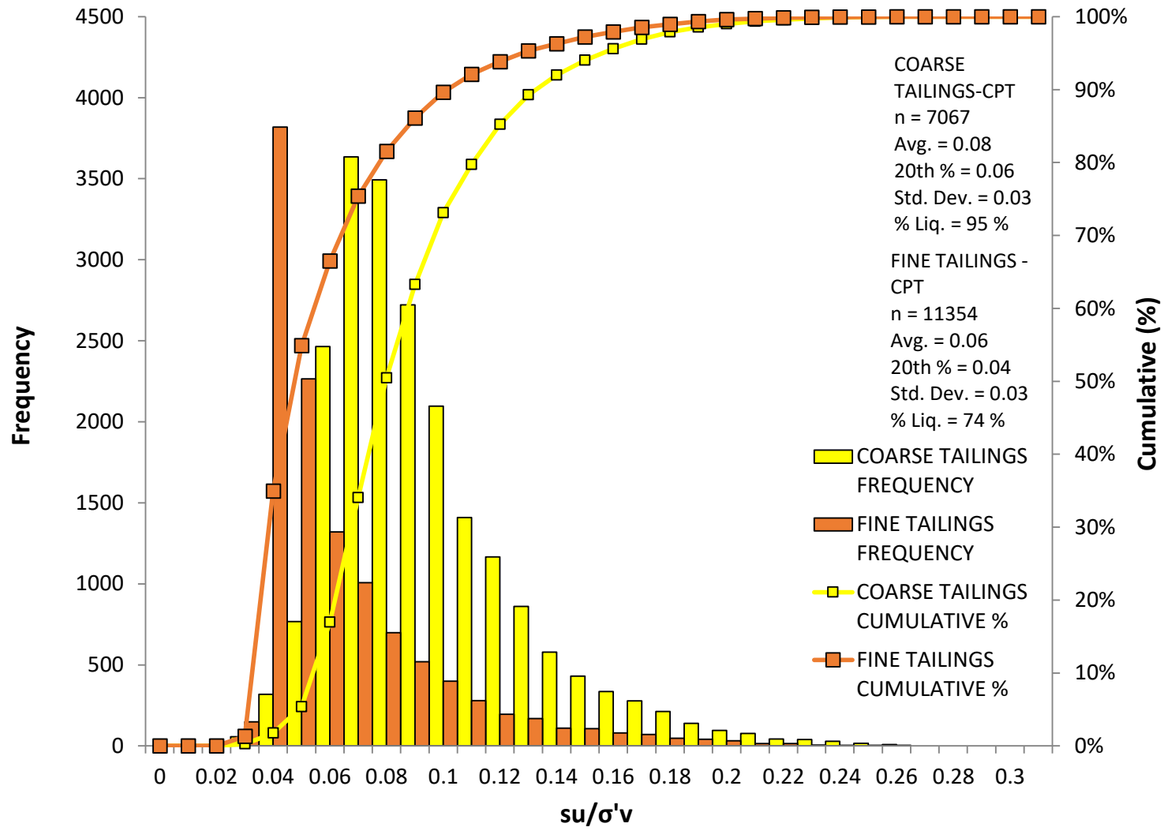
PROJECT: REPORT OF THE EXPERT PANEL ON THE TECHNICAL CAUSES OF THE FAILURE OF FEIJÃO DAM 1

Peak Undrained Shear Strength Ratio for Fine and Coarse Tailings Calculated from CPTu Data

PROJECT No.: A03355A01

FIG. No.: 36

Liquefied Undrained Shear Strength Ratio, su/σ'v
(Robertson, 2010)



NOTES:

AS A MUTUAL PROTECTION TO OUR CLIENT, THE PUBLIC AND OURSELVES, ALL REPORTS AND DRAWINGS ARE SUBMITTED FOR THE CONFIDENTIAL INFORMATION OF OUR CLIENT FOR A SPECIFIC PROJECT AND AUTHORIZATION FOR USE AND/OR PUBLICATION OF DATA STATEMENTS, CONCLUSIONS OR ABSTRACTS FROM OR REGARDING OUR REPORTS AND DRAWINGS IS RESERVED PENDING OUR WRITTEN APPROVAL.

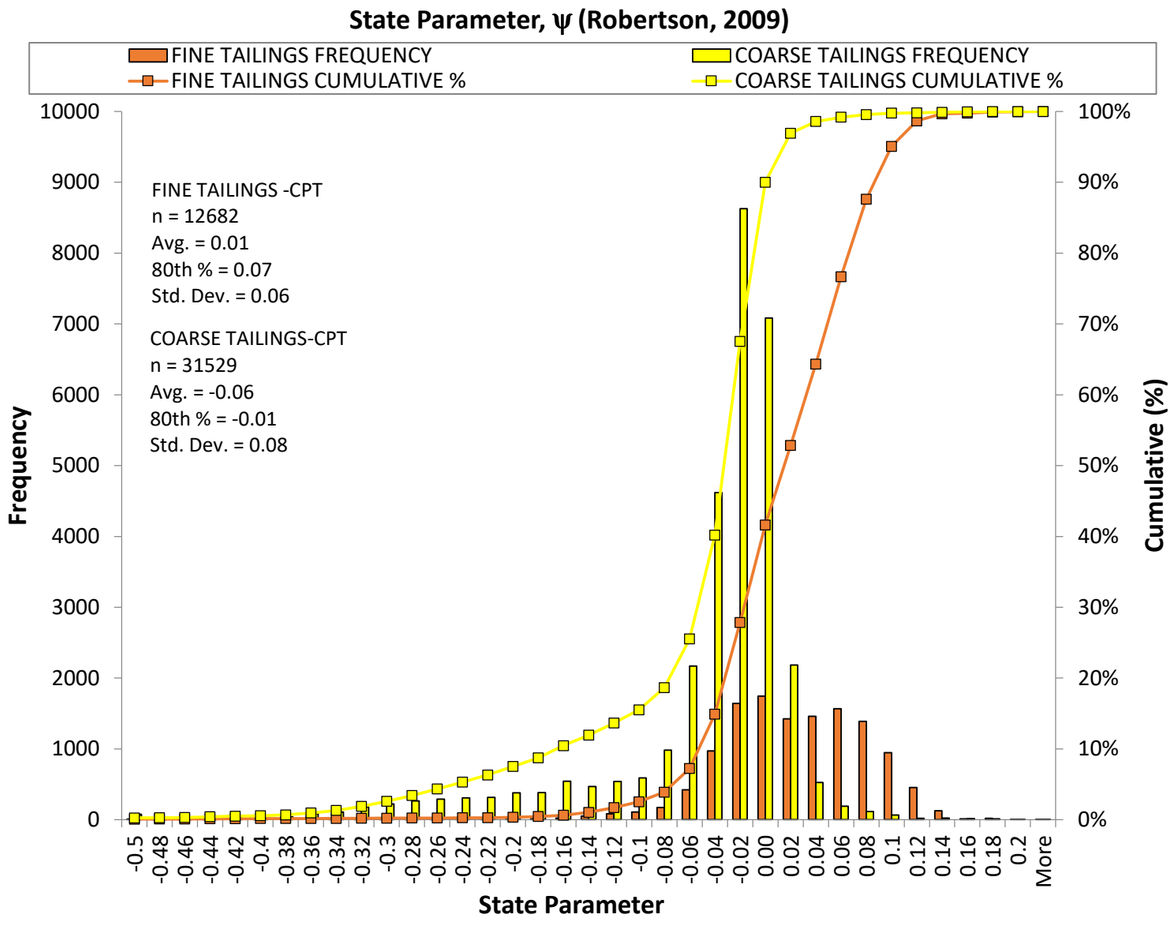
CLIENT

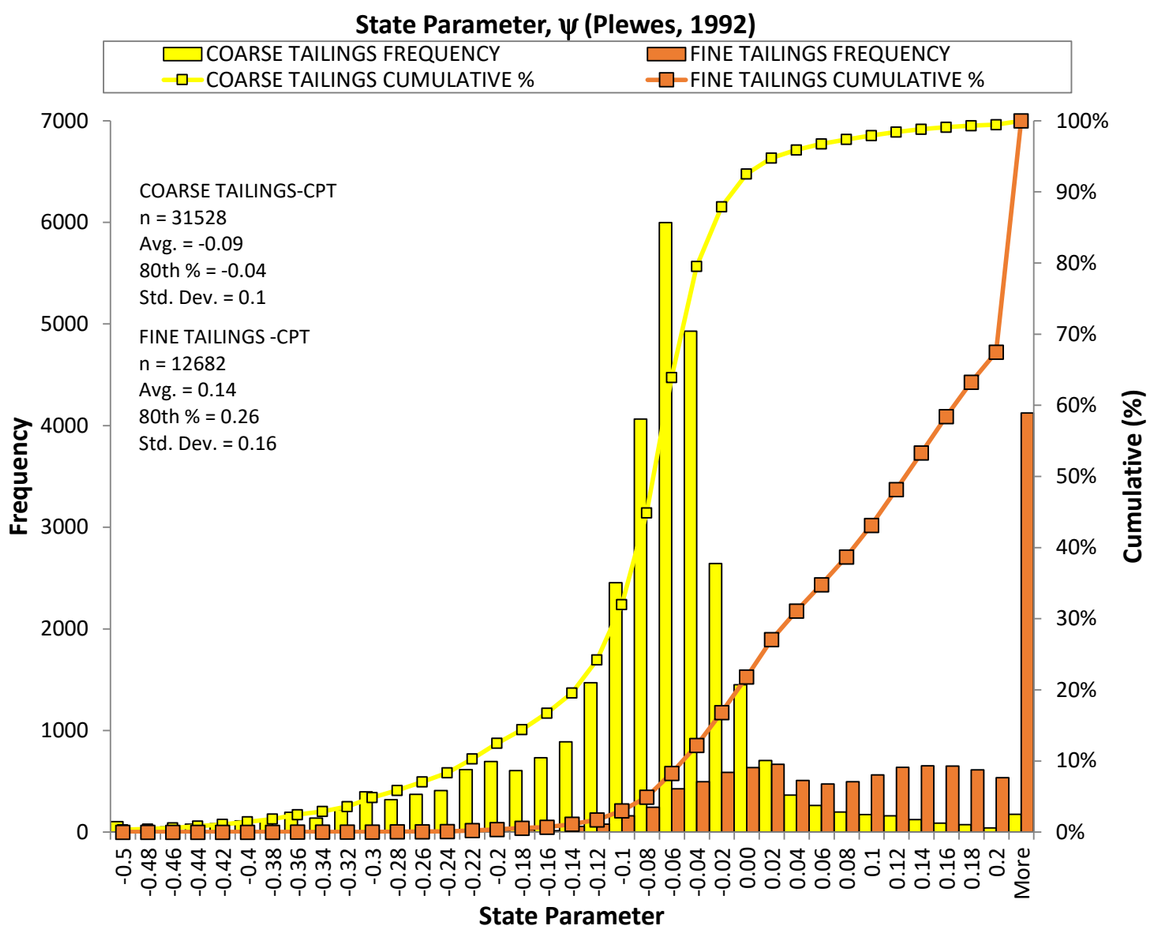
PROJECT: REPORT OF THE EXPERT PANEL ON THE TECHNICAL CAUSES OF THE FAILURE OF FEIJÃO DAM 1

Liquefied Undrained Shear Strength Ratio for Fine and Coarse Tailings Calculated from CPTu Data

PROJECT No.: A03355A01

FIG. No.: 37





NOTES:

AS A MUTUAL PROTECTION TO OUR CLIENT, THE PUBLIC AND OURSELVES, ALL REPORTS AND DRAWINGS ARE SUBMITTED FOR THE CONFIDENTIAL INFORMATION OF OUR CLIENT FOR A SPECIFIC PROJECT AND AUTHORIZATION FOR USE AND/OR PUBLICATION OF DATA STATEMENTS, CONCLUSIONS OR ABSTRACTS FROM OR REGARDING OUR REPORTS AND DRAWINGS IS RESERVED PENDING OUR WRITTEN APPROVAL.

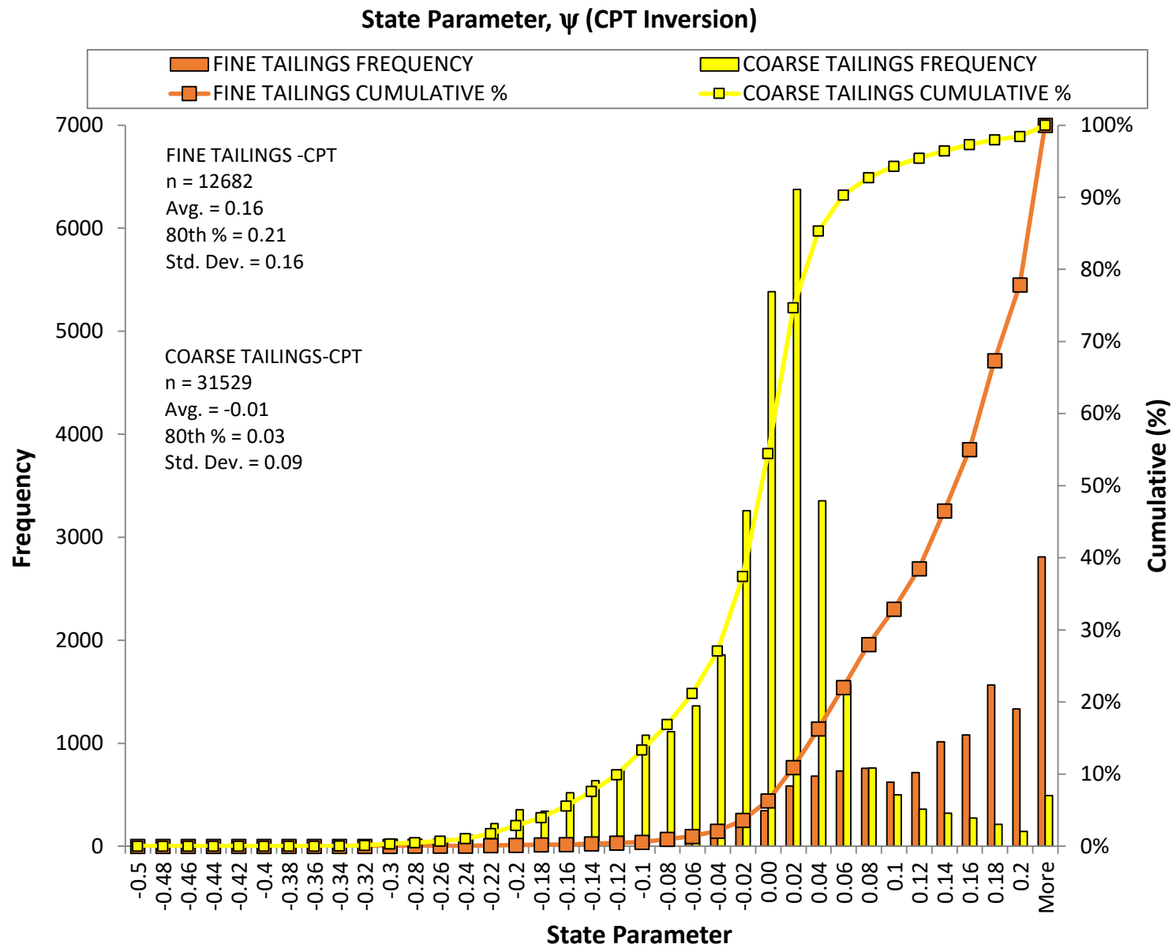
CLIENT

PROJECT: REPORT OF THE EXPERT PANEL ON THE TECHNICAL CAUSES OF THE FAILURE OF FEIJÃO DAM 1

Histograms Plots of State Parameter for Robertson (2009) and Plewes (1992)

PROJECT No.: A03355A01

FIG. No.: 38



NOTES:

AS A MUTUAL PROTECTION TO OUR CLIENT, THE PUBLIC AND OURSELVES, ALL REPORTS AND DRAWINGS ARE SUBMITTED FOR THE CONFIDENTIAL INFORMATION OF OUR CLIENT FOR A SPECIFIC PROJECT AND AUTHORIZATION FOR USE AND/OR PUBLICATION OF DATA STATEMENTS, CONCLUSIONS OR ABSTRACTS FROM OR REGARDING OUR REPORTS AND DRAWINGS IS RESERVED PENDING OUR WRITTEN APPROVAL.

CLIENT

PROJECT: REPORT OF THE EXPERT PANEL ON THE TECHNICAL CAUSES OF THE FAILURE OF FEIJÃO DAM 1

State Parameter Histogram Plot for CPT Inversion Method (Jefferies and Been 2016)

PROJECT No.: A03355A01

FIG. No.: 39